SUMMARY OF SIGNIFICANT RESULTS IN—

- Mineral resources
- Water resources
- Engineering geology and hydrology
- Regional geology
- Principles and processes
- Laboratory and field methods
- Topographic surveys and mapping
- Management of resources on public lands
- Land information and analysis
- Investigations in other countries

LISTS OF—

- Investigations in progress
- Cooperating agencies
- Geological Survey offices

GEOLOGICAL SURVEY RESEARCH 1977

GEOLOGICAL SURVEY PROFESSIONAL PAPER 1050

GEOLOGICAL SURVEY RESEARCH 1977

GEOLOGICAL SURVEY PROFESSIONAL PAPER 1050

A summary of recent significant scientific and economic results accompanied by a list of geologic and hydrologic investigations in progress and a report on the status of topographic mapping

UNITED STATES GOVERNMENT PRINTING OFFICE, WASHINGTON, D.C.: 1977

UNITED STATES DEPARTMENT OF THE INTERIOR

CECIL D. ANDRUS, *Secretary*

GEOLOGICAL SURVEY

W. A. Radlinski, *Acting Director*

Library of Congress catalog-card No. 68-46150

For sale by the Superintendent of Documents, U.S. Government Printing Office
Washington, D.C. 20402
Stock Number 024-001-03054-3

FOREWORD

Most of those who use this volume of the Geological Survey Research Series will come to it primarily to learn about the progress of research in a particular field, or in a group of fields that are closely related. The Geological Survey Research series serves another purpose also—an overview of earth sciences research in progress in the USGS and an indication of the emphasis being given to individual subjects. Few will have the interest or stamina to read Geological Survey Research 1977 from cover to cover, but a few minutes spent on the table of contents will be sufficient to identify the areas that are receiving increased attention.

Because the USGS is a mission-oriented, public service organization, its work responds to the Federal government's perception of public needs. These needs for information about the Earth and its resources and for knowledge of geologic processes and history have been broadening and deepening in recent years in the United States, which has led in turn to expanded investigations in many fields—such as the Outer Continental Shelf, earthquake hazards reduction, geothermal energy, river-quality assessment, and water use, to name only a few of them—in which little or no research was underway only a decade ago.

These trends toward expanded and broadened earth sciences research and factfinding are bound to continue as problems of resource adequacy, environmental quality, and safe use of the land become more complex and difficult, and more critical to the National Welfare.

V. E. McKelvey

V. E. MCKELVEY,
Director

CONTENTS

	Page
Foreword	III
Abbreviations	X
SI units and U.S. customary equivalents	XII
Mineral-resource and mineral-fuel investigations	1
United States and World mineral-resource assessments	1
Mineral-resource assessments of land areas	3
Investigations related to the Wilderness Act	3
Mineral assessment of Indian lands	4
Geologic studies of mining districts and mineral-bearing regions	4
Geochemical and geophysical techniques in resource assessment	9
Regional geochemical and geophysical studies	9
Studies involving iron and manganese oxides	11
Studies involving the use of water, volatiles, or vegetation	12
Geochemical indicators of mineralization	12
Studies involving radioactive material	13
New analytical methods	13
Resource information systems and analysis	14
Resource data bases	14
Resource model studies	15
Energy-related mineral studies	16
Coal resources	16
Oil and gas resources	20
Oil-shale resources	26
Nuclear-fuels resources	26
Geothermal resources	35
Chemical resources	41
Lithium	41
Phosphate	42
Bentonite	43
Regional geologic investigations	45
New England	45
Appalachian Highlands and the Coastal Plain	52
Central region	58
Kentucky	58
Upper Mississippi embayment	59
Lake Superior region	60
Rocky Mountains and Great Plains	61
Stratigraphic studies	61
Igneous studies	64
Tectonic and geophysical studies	64
Basin and range region	67
Mineral-resource studies	67
Stratigraphic and structural studies	68
Igneous rocks	71
Geochronologic studies	71
Pacific Coast region	72
California	72
Oregon	76
Regional geologic investigations—Continued	
Washington	77
Alaska	78
Statewide	78
Northern	79
West-central	81
East-central	82
Southern	82
Southwestern	84
Southeastern	85
Puerto Rico	90
Geologic Maps	92
Water-resource investigations	93
Northeastern region	95
Regional studies	96
Connecticut	96
Delaware	97
Indiana	97
Maryland	97
Massachusetts	98
Michigan	100
Minnesota	100
New Jersey	101
Ohio	101
Pennsylvania	102
Vermont	102
Virginia	102
Wisconsin	102
Southeastern region	102
Florida	103
Georgia	105
Kentucky	106
Mississippi	106
North Carolina	106
Puerto Rico	107
South Carolina	108
Central region	109
Colorado	109
Kansas	112
Louisiana	113
Missouri	113
Montana	113
Nebraska	114
New Mexico	114
North Dakota	115
Oklahoma	116
South Dakota	116
Texas	117
Utah	118
Wyoming	118
Western region	119

Page

Water-resource investigations—Continued
Alaska 119
California 120
Idaho 123
Hawaii 123
Nevada 124
Oregon 124
Washington 124
Special water-resource programs 124
Data coordination, acquisition, and storage 124
National water data exchange 126
Water-data storage systemt 126
Urban water program 127
Water use 127
National water-quality programs 132
Marine geology and coastal hydrology 134
Marine and coastal geology 134
Atlantic coast 134
Gulf coast and Caribbean Sea 138
Pacific coast 140
Alaskan-Arctic investigations 142
Oceanic studies 145
Estuarine and coastal hydrology 147
Gulf coast 147
Atlantic coast 147
Pacific coast 147
Baltic Sea 148
Management of natural resources on Federal and Indian lands 150
Classification and evaluation of mineral lands 150
Classified land 150
Known geologic structures of producing oil and gas fields 151
Known geothermal resource areas 151
Known recoverable coal resource areas 151
Known leasing areas for potassium, phosphate, and sodium 151
Waterpower classification-Preservation of reservoir sites 151
Supervison of mineral leasing 152
Outer Continental Shelf lease sales for oil and gas 152
Cooperation with other Federal agencies 152
Geologic and hydrologic principles, processes, and techniques 153
Experimental geophysics 153
Rock magnetism 153
Geomagnetism 153
Petrophysics 154
Applied geophysical techniques 155
Geochemistry, mineralogy, and petrology 159
Experimental and theoretical geochemistry 159
Crystal chemical studies 164
Mineral studies 165
Volcanic rocks and processes 166
Hawaiian volcano studies 166
Columbia Plateau studies 167
Geochemistry of basaltic rocks 168
Evolution of silicic magma chambers 169
Ancient volcanism in California 170
Uranium in volcanic rocks 170
Plutonic rocks and magmatic processes 171
Metamorphic processes 172
Geochemistry of water and sediments 173
Diagenetic studies 173
Geologic controls on water chemistry 175
Statistical geochemistry and petrology 177

Page

Geologic and hydrologic principles, processes, and techniques—Continued
Isotope and nuclear geochemistry 177
Isotope tracer studies 177
Advances in geochronometry 178
Geothermal systems 181
Sedimentology 183
Impact of high sediment yields 183
Sediment transport and deposition 184
Sediment-measuring techniques 185
Sediment-discharge modeling 185
Sedimentary structures 186
Geology and climate 187
Glaciology 190
Ground-water hydrology 192
Aquifer-model studies 192
Recharge studies 192
Disposal and storage studies 194
Miscellaneous studies 197
Surface-water hydrology 198
Paleontology 200
Mesozoic and Cenozoic studies 200
Paleozoic studies 204
Plant ecology 207
Chemical, physical, and biological characteristics of water 208
Relation between surface water and ground water 210
Evaporation and transpiration 212
Limnology and potamology 212
New hydrologic instruments and techniques 216
Sea-ice studies 217
Analytical methods 217
Analytical chemistry 217
Emission spectroscopy 218
X-ray fluorescence 219
Radio isotope dilution 219
Neutron activation 219
Thin and polished sections 220
Analysis of water 220
Geology and hydrology applied to hazard assessment and environment 222
Earthquake studies 222
Seismicity 222
Earthquake mechanics and prediction studies 223
Earthquake hazards studies 228
Engineering geology 232
Landslide hazards 234
Miscellaneous landslide investigations 234
Regional slope-stability studies 234
Regional geologic hazards that may affect nuclear reactors 236
Environmental aspects of energy 240
Geology and hydrology related to national security 242
Relation of radioactive waste to the geologic environment 243
Relation of radioactive waste to the hydrologic environment 244
Floods 247
Outstanding floods 247
Flood-frequency studies 248
Flood mapping 250
Effects of pollutants on water quality 251
Environmental geochemistry 255
Land subsidence 257
Astrogeology 261

Page

Astrogeology—Continued
Planetary studies ---- 261
Lunar investigations ---- 262
Regional geology ---- 262
Stratigraphy ---- 262
Structure ---- 263
Geochemical and geophysical remote sensing ---- 263
Terrestrial analogs and experimental studies ---- 263
Lunar sample investigations ---- 264
Petrology, mineralogy, and chemistry ---- 264
Isotopic systematics ---- 266
Remote sensing and advanced techniques ---- 268
Earth Resources Observation Systems program ---- 268
Image processing technology ---- 268
Studies using computer-enhanced Landsat data ---- 269
Visual interpretations of Landsat imagers ---- 169
Complementary use of Landsat data and aerial photography ---- 270
Digital analysis of Landsat data ---- 273
Data-collection platforms ---- 273
Data from weather satellites ---- 274
Data from airborne instruments ---- 274
Applications to geologic studies ---- 275
Applications to hydrologic studies ---- 179
Applications to cartographic studies ---- 280
Satellite image maps ---- 280
Hartford 1:250,000-scale image map ---- 281
Parameters for an operational Landsat ---- 281
Landsat mapping and charting of the shallow seas ---- 282
Landsat investigations ---- 282
Nighttime images ---- 282
Space Oblique Mercator projection ---- 283
Land use and environmental impact ---- 284
Multidisciplinary studies in support of land use planning and decisionmaking ---- 284
San Francisco Bay regional studies ---- 284
Colorado Front Range Urban Corridor ---- 284
Geotechnical and geohydrological studies in Fairfax County, Virginia ---- 285
Puget Sound region ESA project ---- 285
Resource and land investigations program ---- 286
Digital systems technology ---- 287
Land use and land cover maps and data and other geographic studies ---- 287
Environmental impact studies ---- 292
Preliminary identification of impacts in EIS's ---- 293
International cooperation in the earth sciences ---- 294
International resources programs ---- 294
Technical assistance and participant training ---- 295
Scope of assistance activities ---- 295
Assistance in remote-sensing applications ---- 295
Assistance to regional organizations ---- 299
Scientific and technical cooperation ---- 300
Scope of cooperation ---- 300
Geologic hazards and disaster response ---- 300
International commissions and representation ---- 301
Resources attache and reporting program ---- 303
International hydrological program and related activities ---- 303
Historical review of hydrologic investigations ---- 304
Summary by countries ---- 304
Argentina ---- 304
Bolivia ---- 304
Brazil ---- 304
Cape Verde ---- 305

Page

International cooperation in the earth sciences—Continued
Ecuador ---- 305
Guatemala ---- 305
India ---- 305
Indonesia ---- 306
Iran ---- 306
Kenya ---- 306
Mexico ---- 306
New Zealand ---- 307
Philippine Islands ---- 307
Saudi Arabia ---- 307
Senegal, Mali, and Mauritania ---- 310
Spain ---- 310
Turkey ---- 310
Venezuela ---- 310
Yemen Arab Republic ---- 310
Yugoslavia ---- 311
Antarctic programs ---- 311
Topographic surveys and mapping ---- 314
Field surveying ---- 314
Inertial positioning system ---- 314
Metal detector evaluation ---- 314
Mapping standards ---- 314
Control ---- 315
Equipment ---- 316
Photogrammetry ---- 316
Camera calibration ---- 316
Analytical aerotriangulation ---- 317
Photogrammetric techniques ---- 317
Nisqually Glacier special map ---- 318
Relative accuracy testing ---- 318
Viking II project ---- 318
Photoimage mapping ---- 318
Orthophoto and satellite products ---- 318
Quad-centered photographs for vertical control ---- 318
Techniques ---- 320
Film mosaicking ---- 320
Quality control ---- 321
Cartography and design ---- 322
Metric mapping ---- 322
Large-scale mapping ---- 322
Intermediate-scale mapping ---- 322
Slope mapping ---- 323
Coastal mapping ---- 323
Special mapping projects ---- 323
Map indexes ---- 324
Pocket maps ---- 324
Drafting media ---- 324
Landsat imagery for 1:250,000-scale mapping ---- 324
The Hotline Oblique Mercator projection applied to Landsat mapping ---- 325
Digital applications ---- 325
Information ---- 326
Geodetic control transfer ---- 326
HP-65 program library ---- 326
Map microfilming ---- 326
Geographic names information system ---- 327
Automated system for locating aerial photography projects ---- 327
EROS user research facility ---- 327
EROS technical memorandums ---- 327
Computer technology ---- 329
Time-sharing systems ---- 329
EPOS Data Center ---- 329

	Page
Computer technology—Continued	
Image processing	329
U.S. Geological Survey publications	331
Publications program	332
Publications issued	332
How to obtain publications	333
Over the counter	333
By mail	333
References cited	335
U.S. Geological Survey offices	350
Headquarters offices	350
Principal field offices	350
Selected field offices in the United States and Puerto Rico	351
Computer Center Division	351
Conservation Division	351
Regional offices	351
Area and district offices	351
U.S. Geological Survey offices—Continued	
Earth Resources Observation Systems program	353
Geologic Division	353
Regional offices	353
Publications Division	353
Regional offices	353
Public Inquiries Offices	354
Distribution Centers	354
Topographic Division	354
Water Resources Division	355
Regional offices	355
District offices	355
Offices in other countries	356
Water Resources Division	356
Investigations in progress in the Geological Survey	357
Indexes	396
Subject index	396
Author index	405

ILLUSTRATIONS

FIGURE 1. Published geologic quadrangle maps (patterned areas) of Kentucky as of March 1, 1977; small squares are 7 1/2-min quadrangles ---- 59
2. Index map of the conterminous United States showing areal subdivisions used in the discussion of water resources ---- 95
3. Map of the United States showing Water Resources Council regions ---- 129
4. Map of the United States showing data on mean concentrations of nitrite nitrogen collected at NASQAN stations during the 1976 water year ---- 133
5. Land use and land cover and associated map sets released to the open file as of December 31, 1976 ---- 289

TABLES

Page

TABLE 1. Summary of data for selected coal samples ---- 18
2. Water withdrawals, sources, and consumption in the United States, 1955–75 ---- 128
3. Water use (excluding that used for hydroelectric power) in 1975 ---- 130
4. Per capita water withdrawals and water consumptions in the eastern and western Water Resources Council regions and the United States, 1975 ---- 130
5. Mineral production, value, and royalty for calendar year 1976 ---- 152
6. Technical assistance to other countries provided by the USGS during January–October 1976 ---- 296
7. Technical and administrative documents issued during the period January through September 1976 as a result of USGS technical and scientific cooperative programs ---- 299

ABBREVIATIONS

A ---- angstrom
ABAG ---- Association of Bay Area Governments
a.c ---- alternating current
A.D. ---- anno Domini
AESOP ---- Automatic Surface Obervation Platforms
AGID ---- Association of Geoscientists for International Development
AIDJEX ---- Arctic Ice Dynamics Joint Experiment
AMRAP ---- Alaska Mineral Resource Assessment Program
ANCSA ---- Alaska Native Claims Settlement Act
AOCS ---- Atlantic Outer Continental Shelf
APD ---- antiphase domain
ARPA ---- Advanced Research Projects Agency
ASL ---- Albuquerque Seismological Laboratory
ASRO ---- Advanced Seismological Research Observatories
atm ---- atmosphere

bbl ---- barrel
BLM ---- Bureau of Land Management
BOD ---- biochemical oxygen demand
B.P ---- before present
Btu ---- British thermal unit

°C ---- degrees Celsius
CAI ---- Color alteration index
cal ---- calorie
CARETS ---- Central Atlantic Regional Ecological Test Site project
CCD ---- Computer Center Division
CCOP ---- U.N. Committee for Coordination of Joint Prospecting for Mineral Resources in Asian Offshore Areas
CCT ---- computer-compatible tape
C/DCP ---- convertible data-collection platforms
CDP ---- common depth point
CENTO ---- Central Treaty Organization
CEQ ---- Council on Environmental Quality
CFRUC ---- Colorado Front Range Urban Corridor Project
CGIS ---- Canada Geographic Information System
cgs ---- Centimeter-gram-second
Ci ---- curie
cm ---- centimeter
COD ---- chemical oxygen demand
COM ---- computer-oriented microform
COST ---- Continent Offshore Stratigraphic Test Group
CPU ---- central processing unit
CRIB ---- Computerized Resource Information Bank
CV ---- characteristic value

d ---- day
d.c ---- direct current
DCS ---- Data-collection system
DEROCS ---- Development of Energy Resources of the Outer Continental Shelf
DMA ---- Defense Mapping Agency
DNPM ---- Departmento Nacional da Produção Mineral
DO ---- dissolved oxygen
DOMES ---- Deep Ocean Mining Environmental Study
DSDP ---- Deep Sea Drilling Project
EIA ---- Environmental Impact Analysis
EIS ---- environmental impact statement
EM ---- electromagnetic (soundings)
EMRIA ---- Energy Mineral Rehabilitation Inventory and Analysis
EPA ---- Environmental Protection Agency
ERDA ---- Energy Research and Development Administration
EROS ---- Earth Resources Observation Systems
ERTS ---- Earth Resources Technology Satellite
ESCAP ---- Economic and Social Commission for Asia and the Pacific Committee on Natural Resources
eV ---- electronvolt

FAO ---- Food and Agriculture Organization
f.l ---- focal length
FLD ---- Fraunhofer line discriminator
FY ---- fiscal year

g ---- gram
GIPSY ---- General Information Processing System
GIRAS ---- Geographic Information Research and Analysis System
GOES ---- Geostationary Operational Environmental Satellite
GRASP ---- Geologic Retrieval and Synopsis Program

h ---- hour
ha ---- hectare
HFU ---- heat-flow unit
HIPLEX ---- High Plains Cooperative Program
hm ---- hectometer
HUD ---- Department of Housing and Urban Development
Hz ---- hertz

IAH ---- International Association of Hydrogeologists
IAHS ---- International Association of Hydrological Scientists
ICAT ---- Inorganic Chemical Analysis Team
IDB ---- Inter-American Development Bank
IDIMS ---- Interactive Display Image Manipulation System
IDOE ---- International Decade of Ocean Exploration
IGCP ---- International Geological Correlation Program
IGU ---- International Geographical Union
IHD ---- International Hydrological Decade
IHP ---- International Hydrological Program
IMW ---- International Map of the World
in ---- inch
IR ---- infrared
ISO ---- International Standardization Organization
IUGS ---- International Union of Geologic Sciences

J ---- joule
JPL ---- Jet Propulsion Laboratory
JTU ---- Jackson turbidity unit

K ---- kelvin
kbar ---- kilobar
KCLA ---- Known Coal Leasing Area
KeV ---- kiloelectronvolt
kg ---- kilogram
KGRA ---- Known Geothermal Resources Area
KGS ---- Known Geologic Structure
kHz ---- kilohertz
kJ ---- kilojoule
km ---- kilometer
KREEP ---- potassium-rare-earth element-phosphorus
kWh ---- kilowatt-hour

L ---- liter
LARS ---- Laboratory for Applications of Remote Sensing
lat ---- latitude
LMF ---- lithic matrix fragments
long ---- longitude

m ---- meter
M ---- magnitude (earthquake)
mcal ---- millicalorie
MEF ---- maximum evident flood
mGal ---- milligal
mi ---- mile
min ---- minute
mg ---- milligram
ml ---- milliliter
mm ---- millimeter
mo ---- month
MPa ---- megapascal
MSS ---- multispectral scanner
MW ---- megawatt
MWe ---- megawatts electrical
m.y. ---- million years
μ ---- micron
μcal ---- microcalorie
μg ---- microgram
μGal ---- microgal
μm ---- micrometer
μmho ---- micromho
μstrain/yr ---- engineering shear

NASA ---- National Aeronautics and Space Administration
NASQAN ---- National Stream Quality Accounting Network
NAWDEX ---- National Water Data Exchange

NCRDS ------ National Coal Resources Data System
NEIS ------ National Earthquake Information Service
NEPA ------ National Environmental Policy Act
ng ------------------------------ nanogram
NLCR -------- nonlinear complex resistivity
NOAA ------ National Oceanic and Atmospheric Administration
NOS ---------------- National Ocean Survey
NPR -------------- Naval Petroleum Reserve
NRA ---------- Nuclear Regulatory Agency
nT ------------------------------ nanotesla
NTIS ------ National Technical Information Service
NTS --------------------- Nevada Test Site

OAS ------ Organization of American States
OCS --------------- Outer Continental Shelf
ohm-m -------------------------- ohm-meter
OIA ------ Office of International Activities
OME -------- Office of Minerals Exploration
ORNL ------ Oak Ridge National Laboratory
OWDC ---- Office of Water-Data Coordination
Ω -------------------------------------- ohm

PAIGH -------- Pan American Institute of Geography and History
PCB -------------- polychlorinated biphenyls
pCi ------------------------------ picocurie
ppb ------------------------ part per billion
ppm ---------------------- part per million
PSRV -------------- pseudo-relative velocity
R ---------------------------------- range
RASS -------- Rock Analysis Storage System
REE --------------------- rare-earth element
RF -------------------------- radio frequency
RMSE -------------- root mean square error
R/V ------------------------ research vessel

s ------------------------------------- second
SFBRS ------ San Francisco Bay Region Environment and Resources Planning Study
SIP ------------ strongly implicit procedure
SLAR ---------- side-looking airborne radar
SMS ----- Synchronous Meteorological Satellite
SOM -------------- Space Oblique Mercator
SP -------------------------- self potential
SRO --------- Seismic Research Observatory

t ------------------------------------- tonne
T ------------------------------- township
TEM ------ transmission electron microscopy
TL --------------------- thermoluminescence
TVA ------------ Tennessee Valley Authority

UNDP -------- U.N. Development Programme
UNESCO ------ United Nations Educational, Scientific and Cultural Organization
USAID ------ U.S. Agency for International Development
USBM --------------- U.S. Bureau of Mines
USDA ------ U.S. Department of Agriculture
USGS -------------- U.S. Geological Survey
USNC/SH ------ United Nations Educational, Scientific and Cultural Organization
USPHS ---------- U.S. Public Health Service
U.S.S.R. -------- Union of Soviet Socialist Republics
UTM -------- Universal Transverse Mercator

V -------------------------------------- volt
VDETS -------- Voice Data Entry Terminal System
VES ------------ Vertical electric soundings
VHRR ------ very high resolution radiometer
VLF -------------------- very low frequency

W ---------------------------------- watt
WMO ----- World Meteorological Organization
WRC -------------- Water Resources Council
WWSSN ------ Worldwide Standardized Seismograph Network

yr ---------------------------------- year

SI UNITS AND U.S. CUSTOMARY EQUIVALENTS

[SI, International System of Units, a modernized metric system of measurement. All values have been rounded to four significant digits except 0.01 bar, which is the exact equivalent of 1 kPa. Use of hectare (ha) as an alternative name for square hectometer (hm^2) is restricted to measurement of land or water areas. Use of liter as a special name for cubic decimeter (dm^3) is restricted to the measurement of liquids and gases; no prefix other than milli should be used with liter. Metric ton (t) as a name for megagram (Mg) should be restricted to commercial usage, and no prefixes should be used with it. Note that the style of meter² rather than square meter has been used for convenience in finding units in this table. Where the units are spelled out in text, Survey style is to use square meter]

SI unit		U.S. customary equivalent	
Length			
millimeter (mm)	=	0.039 37	inch (in)
meter (m)	=	3.281	feet (ft)
	=	1.094	yards (yd)
kilometer (km)	=	0.621 4	mile (mi)
	=	0.540 0	mile, nautical (nmi)
Area			
centimeter² (cm^2)	=	0.155 0	inch² (in^2)
meter² (m^2)	=	10.76	feet² (ft^2)
	=	1.196	yards² (yd^2)
	=	0.000 247 1	acre
hectometer² (hm^2)	=	2.471	acres
	=	0.003 861	section (640 acres or 1 mi^2)
kilometer² (km^2)	=	0.386 1	mile² (mi^2)
Volume			
centimeter³ (cm^3)	=	0.061 02	inch³ (in^3)
decimeter³ (dm^3)	=	61.02	inches³ (in^3)
	=	2.113	pints (pt)
	=	1.057	quarts (qt)
	=	0.264 2	gallon (gal)
	=	0.035 31	foot³ (ft^3)
meter³ (m^3)	=	35.31	feet³ (ft^3)
	=	1.308	yards³ (yd^3)
	=	264.2	gallons (gal)
	=	6.290	barrels (bbl) (petroleum, 1 bbl=42 gal)
	=	0.000 810 7	acre-foot (acre-ft)
hectometer³ (hm^3)	=	810.7	acre-feet (acre-ft)
kilometer³ (km^3)	=	0.239 9	mile³ (mi^3)
Volume per unit time (includes flow)			
decimeter³ per second (dm^3/s)	=	0.035 31	foot³ per second (ft^3/s)
	=	2.119	feet³ per minute (ft^3/min)

SI unit		U.S. customary equivalent	
Volume per unit time (includes flow)—Continued			
	=	15.85	gallons per minute (gal/min)
	=	543.4	barrels per day (bbl/d) (petroleum, 1 bbl=42 gal)
meter³ per second (m^3/s)	=	35.31	feet³ per second (ft^3/s)
	=	15 850	gallons per minute (gal/min)
Mass			
gram (g)	=	0.035 27	ounce avoirdupois (oz avdp)
kilogram (kg)	=	2.205	pounds avoirdupois (lb avdp)
megagram (Mg)	=	1.102	tons, short (2 000 lb)
	=	0.984 2	ton, long (2 240 lb)
Mass per unit volume (includes density)			
kilogram per meter³ (kg/m^3)	=	0.062 43	pound per foot³ (lb/ft^3)
Pressure			
kilopascal (kPa)	=	0.145 0	pound-force per inch² (lbf/in^2)
	=	0.009 869	atmosphere, standard (atm)
	=	0.01	bar
	=	0.296 1	inch of mercury at 60°F (in Hg)
Temperature			
temp kelvin (K)	=	[temp deg Fahrenheit (°F)+459.67]/1.8	
temp deg Celsius (°C)	=	[temp deg Fahrenheit (°F)−32]/1.8	

Any use of trade names and trademarks in this publication is for descriptive purposes only and does not constitute endorsement by the U.S. Geological Survey.

GEOLOGICAL SURVEY RESEARCH 1977

MINERAL-RESOURCE AND MINERAL-FUEL INVESTIGATIONS

UNITED STATES AND WORLD MINERAL-RESOURCE ASSESSMENTS

The study of mineral deposits and the understanding of how they are formed are essential to our continuing ability to find new mineral supplies and to our understanding of the geological limitations placed on mineral availability. During 1976, several studies of mineral-resource availability were completed. Critical imported commodities such as aluminum, chromium, and nickel were given high priority.

Bauxite continues to be major source of aluminum

S. H. Patterson, in a review of the widespread research being done on possible substitutes for bauxite as a source of aluminum, concluded that bauxite will continue to be the major source of the Western World's aluminum. The rocks and materials considered as possible substitutes for bauxite in the United States and other countries include high-alumina clay, igneous-rock alunite, coal-mine waste and washings, shale, dawsonite, and aluminum phosphate rock. Although the cost of bauxite has risen sharply, the high cost of redesigning and constructing plants and the much greater energy required to recover alumina from alternative sources make it likely that bauxite will continue to be the principal raw material.

Bauxite resources in the Andersonville district of Georgia

In a computerized analysis of data generated under a USGS grant to Georgia Southwestern College, N. A. Wright and M. A. Carey (USGS) and H. E. Cofer (Georgia Southwestern College) found that the deposits of kaolin clay and bauxite in the Andersonville district of Georgia are more than adequate to sustain mining at the current rate and for the present uses well into the next century. The kaolin occurs as elongated lenses that are as much as 15 m thick and cover as much as 1,000 ha. The bauxite occurs mainly as smaller lenticular masses of pealike nodules within the larger kaolin deposits. Identified and hypothetical resources of kaolin are estimated to be 680×10^6 t dry. Indicated and inferred reserves of bauxite are about 1.8×10^6 t dry, and hypothetical resources are nearly as large.

The kaolin reserves, which are part of the identified resources, are more than adequate to sustain mining at the present rate for another century. Bauxite and bauxite clay will probably be mined in the district for 25 to 50 years. The kaolin resources in this area are one of the major potential domestic sources of aluminum.

Alunite resource appraisal progress report

R. B. Hall's highly tentative estimate of alunite-ore resources in altered volcanic rock in Arizona, Colorado, Nevada, and Utah indicated a reserve of 336×10^6 t of rock averaging 32 percent alunite, plus a potential resource of $1,479\times10^6$ t of rock containing 10 to 32 percent alunite. Alunitic rock should contain 30 percent alunite or more to be considered ore grade, and the bulk of the remaining rock should be microcrystalline quartz, which is not especially troublesome in the modified Bayer process used to extract alumina from the siliceous aluminous residue after SO_2 and K_2SO_4 have been removed. However, more than a few percent (combined) of phyllosilicate materials such as dickite, kaolinite, halloysite, muscovite (sericite), and pyrophyllite substantially reduces the economic value of the material, since these minerals break down during the caustic leaching phase of processing and introduce silica into the aluminous solution. Costly desilication then is necessary to produce an acceptable cell-grade alumina. An unknown but large proportion of the "potential" resource reported here therefore is not commercially usable with present technology because it contains large amounts of intermixed mica and clay minerals and also because it has a low amount of alunite. A part of the reserve estimated above also is suspect for the same reason, since the mineralogical composition of some deposits has not been precisely determined. There appears to be little doubt that domestic resources of alunitic rock in hydrothermally altered Tertiary volcanic terranes are adequate to support an alumina-from-alunite industry, if it is assumed that the best available alunite ore in the southern Wah Wah Mountains in Beaver County, Utah, can be treated profitably.

Some problems with refractory chromite supply by 1985

A review of the world chromite situation made by T. P. Thayer and B. R. Lipin indicated that supplies of traditional refractory ore will be reduced substantially in the next 10 years. For the last 50 years, American refractory makers have relied on Cuba and the Philippine Islands for high-aluminum chromite, probably 80 percent of all chromite used for refractories. Geologically, high-aluminum deposits are comparatively rare, and the Philippines and Cuba have the largest reserves outside the U.S.S.R. The United States monopolized Cuban production during World War II and, since 1945, has gotten 8.7×10^6 t, or two-thirds of all refractory ore exports, from the Philippines and Cuba. Owing to changes in steel technology, refractory chromite consumption has dropped about 40 percent, to 200,000 to 250,000 t/yr over the last 5 years.

Since 1945, the Coto mine area in the Philippines has shipped more than 12×10^6 t of high-aluminum ore that was recovered from 20×10^6 t of mine-run ore. Most of the ore came from one open-pit mine on a 10×10^6 t orebody. Mining now is essentially all underground, and, in the last 5 years, the concentration ratio of mine-run ore has increased from 1.4:1 to about 2.2:1. Maintaining shipments at 400,000 t/yr and reserves at recent levels until 1985 will require the discovery of 9×10^6 t of ore, all underground. The deposits are of the podiform type, and finding ore on this scale, even in an extraordinarily rich zone, is problematical. It seems most likely that refractory manufacturers will have to rely increasingly on high-iron chromite, which will constitute 99 percent of world resources after 1985.

World nickel resources

A recent survey of world nickel deposits, excluding ocean nodules, conducted by M. P. Foose indicated that identified nickel resources comprise 155×10^6 t of nickel in $19{,}460\times10^6$ t of ore. The ore has an average grade of 0.79 percent. The survey shows that 70 percent of the world's nickel resources occurs in nickel laterites and that 43 percent of the laterite resources occurs on one island, New Caledonia in the South Pacific Ocean. Nickel sulfides constitute the remaining nickel resource. With the exception of the Sudbury Irruptive in Canada and the Penchenga camp at Petsamo in the U.S.S.R., most major economic nickel deposits are associated with ultramafic magmas of the Komatiitic suite.

Identified iron-ore resources of South America assessed

Literature research by Harry Klemic and Margaret Cooper on iron-commodity data showed that the identified iron-ore resources of South America total about 126×10^9 t, more than 15×10^9 t of which are classed as reserves. Most South American iron-ore production is for export markets. In recent years, South American ores have constituted about 50 percent of all U.S. iron-ore imports and about 20 percent of total U.S. iron-ore consumption. These figures indicate the strong interdependence of the United States and South America in iron-ore trade.

Titanium and zircon resources of Pleistocene sand in Adirondack Mountains of New York

E. R. Force determined that Pleistocene delta sands in the Port Leyden quadrangle in the southwestern Adirondack Mountains of New York contain 30×10^6 t of titanium minerals and 2×10^6 t of zircon in wedge-shaped bodies up to 85 m thick (Force, Lipin, and Smith, 1976). Chemical and physical properties of the ilmenite make the deposit subeconomic. Similar deposits are common in the Black River Valley (Waller, 1976).

Zinc distribution in coals in part of the Illinois Basin

High concentrations of epigenetic sphalerite (ZnS) were reported in four major coal seams in the northwestern part of the Illinois Basin (Ruch and others, 1974; Hatch and others, 1976). According to J. C. Cobb (Illinois Geological Survey), the distribution of zinc in the coals is fairly uniform; in areas where the coal is disturbed, however, the distribution may be broader. Large-grid sampling showed the average zinc concentration to be about 0.15 percent for coal across the basin. Other sampling methods demonstrated the epigenetic nature of the sphalerite. Zinc analyses of bench samples ranged from 0.0005 percent to 1.5 percent, and channel samples ranged from 0.005 percent to 0.15 percent of the whole coal. No zinc variations among the seams has been observed.

During mining and cleaning of coal, sphalerite is concentrated in mine slurry and fine-grained gob; occasionally, it is found in the coarse-grained gob. Slurry ponds have been identified in some mines as the principal sites of sphalerite concentration. This sphalerite concentration is dependent on the coal preparation processes used at the mine.

Sphalerite mineralization occurs in clastic dikes as concentric accumulations around a coal nucleus. Sphalerite also occurs in veinlets or cleats normal to bedding. Sphalerite in cleats appears to have grown contemporaneously with cleat dilation. Successive growths occur symmetrically in from cleat walls to a central iron-rich band. The uniformity between the sphalerite characteristics of cleats and those of clastic dikes regardless to the seam suggests that mineralization was continuous and simultaneous in each seam and constant across the district (Cobb and Russell, 1976).

Peat resources in Minnesota

Field reconnaissance by C. C. Cameron of about 185,000 ha of peatlands in western Koochiching County, Minnesota, revealed a spotty distribution of deposits having a thickness greater than 1.5 m, the cutoff point for favorable exploration. Areas containing an estimated 296,000 t of air-dried sphagnum and reed-sedge peat, each with an average thickness of 3.6 m, and areas containing an estimated 475,000 t of reed-sedge and humus peat, each with average thickness of 2.4 m, are interspersed with areas containing a total of 2,640,000 t of reed-sedge and humus peat less than 1.5 m thick.

Patterns, which are observable on recently published orthophoto maps as well as in the field, have been established as guides to peat prospecting in the vast terrane of Glacial Lake Agassiz, in which the thick glacial drift mantle has been reworked by lake action.

The thickest deposits are domes of sphagnum peat over reed-sedge peat located in interstream areas. The domes are bordered by semicircles of glacial moraine or relict lake beaches. Where the domes are some distance from moraine and beach material, they have sharp semicircular boundaries representing a change in vegetation types. All semicircles are convex in a direction up the regional slope. Domes appear on the orthophoto maps as patterns of radiating light and dark streaks. Ground water under hydrostatic head provides water to the peat-forming plants, which take it up by capillarity and form the dome-shaped deposits. Rainwater flows off the dome and down the regional slope through shallow peat covered by marsh and fen vegetation streaked in the direction of flow. Where the water flowing from the dome crosses the direction of regional ground-water flow, the marsh and fen vegetation assumes a lattice pattern. Both patterns mark the position of shallower peat.

MINERAL RESOURCE ASSESSMENTS OF LAND AREAS

INVESTIGATIONS RELATED TO THE WILDERNESS ACT

The Wilderness Act of 1964 directs the Secretary of Agriculture and the Secretary of the Interior to review the suitability of lands being considered for inclusion in the National Wilderness Preservation System. To aid in evaluating the suitability of an area for wilderness inclusion, the USGS and the U.S. Bureau of Mines make mineral-resource assessments of wilderness areas established by the act and wilderness study areas in the national forests as well as in five national game ranges and national monuments on lands held by the Department of the Interior.

Mineral potential of Great Bear Wilderness study area of Montana

Geologic, geochemical, and geophysical studies conducted by M. R. Mudge, R. L. Earhart, and D. D. Rice (USGS) and L. Y. Marks (U.S. Bureau of Mines) indicated that the proposed Great Bear Wilderness has good potential for oil and gas (mainly gas) and a moderate potential for submarginal resources of copper and silver in a belt 40 km long and about 1.6 km wide that is partly within the study area along its western boundary. The eastern part of the study area may contain small submarginal resources of coal.

The area with the best mineral potential lies in the extreme western part of the proposed wilderness, where copper and silver minerals occur in green to light-gray quartzites, siltites, and argillites of the Empire and Spokane Formations between Felix and Hoke Creeks. Although these occurrences are mostly outside of the study area, the downdip projection of the mineralized rocks underlies the westernmost part of the area. Potential disseminated copper sulfide deposits also occur in the Spokane Formation, where selected samples contain more than 2 percent Cu and 70 ppm Ag. The copper content of cross-cutting chip samples ranged from 0.13 percent over 18.3 m to 0.35 percent over 1.8 m and

0.52 percent over 0.61 m. At least 16 copper-bearing occurrences were sampled. Good potential for discovering disseminated copper deposits similar to a deposit outside the area near Hoke Creek exists within the proposed wilderness. The Hoke Creek deposit contains an estimated 635,000 t of 0.15 percent Cu and 3.4 g/t Ag.

Exploratory drilling east of the study area and the discovery of major gas fields in the Canadian portion of the disturbed belt indicated a good potential for gas in the study area. The structure, stratigraphy, and geologic history of gas fields in Canada are similar to those found in the Montana disturbed belt. Tests of gas wells drilled in the 1950's near the study area in Blackleaf Canyon and the East Glacier Park area indicated a production capability of as much as 178.3×10^6 m^3/d of gas from reservoirs in Mississippian and Devonian carbonate rocks.

Stratabound copper-silver deposit in the Scotchman Peak Wilderness study area of Montana

Investigations of mineral resources in the Scotchman Peak Wilderness study area indicated that the eastern half of the area has a moderate to high potential for stratabound deposits of copper and silver, according to D. J. Grimes and R. L. Earhart (1976). The area is in the northwestern Montana copper belt (Harrison, 1972), which contains disseminated copper-silver deposits in quartzite beds of the Revett Formation in the Belt Supergroup of Precambrian age.

The geology and geochemistry of this area compare favorably with those of a large disseminated copper-silver orebody a short distance to the east. High copper and silver values have been found in rock, stream-sediment, and soil samples in an area about 3 km long and about 30 m wide. The anomaly is in the lower part of the Revett Formation and trends parallel to the strike of the strata.

MINERAL ASSESSMENT OF INDIAN LANDS

The USGS and the U.S. Bureau of Mines (USBM), under an agreement with the Bureau of Indian Affairs, are assessing the mineral resources of Indian lands designated as Federal reservations. This program, which began in 1974, consists of two phases of study:

- Phase I—Summary and analysis of available information on the mineral resources of Federal Indian lands.
- Phase II—Field studies to obtain new information on Indian lands where existing information is inadequate to assess the mineral potential.

By October 1976, phase I of the program had resulted in 28 reports covering mineral assessments of 12.2×10^6 ha of Indian lands. On the basis of recommendations made during phase I compilations, phase II studies were started on the Papago Reservation in Arizona (USGS and USBM), the Wind River Reservation in Wasington (USGS), and the Spokane Reservation in Washington (USBM). USGS studies of the Papago Reservation using geologic, geophysical, and geochemical techniques are obtaining information on the potential for discovering porphyry copper deposits. Phase II on the Wind River Reservation studies are in progress in areas having potential for uranium resources.

GEOLOGIC STUDIES OF MINING DISTRICTS AND MINERAL-BEARING REGIONS

Estimates of mineral-resource availability and assessments of the mineral potential of public lands require an ever-increasing knowledge of the nature of mineral deposits—the conditions of their formation and the origin, mode of transport, and concentration of the metals and solutions in ore deposits. During 1976, field and laboratory studies of mineral deposits and districts revealed many facts leading to new concepts in ore genesis and new strategies in mineral exploration.

Mesozoic-Cenozoic metallogenesis of the Western United States

Although the Mesozoic-Cenozoic metallogeny of the Western United States unquestionably resulted from the convergence of the North American continent and Pacific Ocean crust, subduction alone does not adequately explain the distribution of ore deposits according to P. W. Guild. Divergence from a "typical" arc-trench pattern increases from the middle Mesozoic to the late Tertiary and with distance from the continental margins; by latest Mesozoic time, the magmatic-metallogenic province extended irregularly eastward at least 1,500 km from the trench. Lineaments, difficult or impossible to document unequivocally, nevertheless seem to have played some role in localizing mineral belts transverse to plate boundaries. A gross east-west metals zonation lacks the clear-cut divisions evident to the north and south in the Cordillera.

Shallow-dipping or multiple subduction zones have been proposed to account for these features, but mantle convection in a reactivated ensialic back-arc seems to be a more logical explanation for the distinctive "Laramide" metallogeny. It is suggested that small magma pockets were generated episodically by partial fusion of the base of an inhomogeneous continental lithosphere, where deep crustal flaws, many ancient but some perhaps newly created, relieved pressure and provided access to the upper crust. This suggestion does not preclude direct derivation of magma (and metals) from subducting oceanic lithosphere along the magmatic arc.

Metalliferous organic-rich shales in Great Basin

Anomalous metal concentrations of silver, zinc, chromium, and vanadium in certain petroliferous and phosphatic organic-rich beds of Paleozoic marine strata in Nevada and Utah were recognized by G. A. Desborough and F. G. Poole. The concentration and mineralogical residence of these metals and their relation to associated organic material are poorly understood, but preliminary studies indicate that the concentration and distribution of silver, zinc, chromium, and vanadium vary widely in these rocks. Their concentration and mineralogical residence often are found to be independent of bulk chemical composition and bulk mineralogy. Many of the rocks that have anomalously high concentrations of these metals contain mature to immature organic matter and yield as much as 50 g/kg of syncrude oil.

Sedimentary copper deposits associated with glauconite

P. L. Weis reported that anomalously high copper values were found in some lower Paleozoic glauconitic sandstones in southwestern Wisconsin and eastern Tennessee. Mineral separates showed that most of the copper is contained in the glauconite.

These results appear to support the hypothesis that certain sedimentary environments in the United States need to be studied more closely as potential sources of copper and other base metals. The characteristics of those environments include (1) the presence of glauconite; (2) association with sedimentary phosphorite; (3) evidence of volcanic ash in associated sediments; and (4) the presence of evaporites in geographically and stratigraphically nearby sediments.

Gold at Tarkwa, Ghana, not from ancient placer

The gold of the sulfide-free Tarkwa Proterozoic conglomerates of Ghana, like the gold in the pyritic conglomerates of the Witwatersrand in South Africa, is believed by W. B. Myers to have been transported in an aurous sulfide complex and not as placer gold. This inference is sustained by the positive identification of anhydrite by X-ray, mineral-grain, and thin-section study of six samples from the Tarkwa reef. The presence of a primary sulfate mineral intergrown with recrystallized detrital minerals in the 2-billion-year-old Tarkwa conglomerates suggests that the ubiquitous and abundant oval aggregates of hematite were originally pyrite, as were those in the Witwatersrand deposit. The hypothesized oxidation of pyrite to hematite and the concomitant precipitation of gold from an aurous sulfide complex are thought to have occurred in a shallow marine environment as a result of the build-up of oxygen in the Precambrian atmosphere. In the Witwatersrand uranium-gold pyritic conglomerates, which formed in an anoxygenic environment, gold was precipitated by a slow oxidizing reaction resulting from the radioactive decay of uraninite.

Complex hydrologic history of Creede ore deposits in Colorado

Studies of light stable isotope conducted by R. O. Rye, P. M. Bethke, P. B. Barton, Jr., and P. H. Wetlaufer showed that the epithermal silver-lead-zinc-copper ore deposits at Creede, Colo., were deposited from a complex hydrologic system dominated at most times by meteoric waters.

The δD and $\delta^{18}O$ of the hydrothermal fluids responsible for the deposition of various generations of sphalerite, quartz, and carbonate and of sericite and chlorite were determined directly from analysis of fluid inclusions and estimated indirectly from isotopic analysis of the minerals. The $\delta^{13}C$ of the hydrothermal fluids was estimated from data on carbonated rocks. The $\delta^{18}O$ data indicate that the fluids contained a substantial meteoric component during the deposition of sphalerite, quartz, sericite, and chlorite. The carbonate rocks, on the other hand, were deposited from either magmatic waters or waters that equilibrated with country rock at near-magmatic temperatures. The δD data also indicate that two distinct meteoric waters with different recharge areas contributed to the hydrothermal fluids. The $\delta^{13}D$ data indicate that the carbon in the fluids that deposited the carbonate minerals in the veins came from a deep-seated source and not from the sedimentary source from which the large volume of preore travertine deposited in the periphery of the Creede caldera was derived (Steven and Friedman, 1968).

Differences in the isotopic compositions of the fluids correlate with differences in mineralogy but not with depositional sequences, an indication that fluids from different sources occupied the ore zone recurrently.

The existence of meteoric waters of $\delta D = -55$ ppm and $\delta D = -95$ ppm in the same ore deposit has several climatic implications. The difference between these values and those of present-day surface waters ($\delta D = -112$ ppm) suggests that the climate was milder at the time of ore deposition. The difference between the δD values of the two waters suggests that one had a relatively low elevation recharge area, receiving waters dominantly from the Gulf of Mexico, and that the other had a relatively high elevation recharge area, receiving precipitation from the Pacific Ocean. These interpretations are consistent with geologic evidence (Steven and Eaton, 1975) indicating that, at the time of ore deposition (24.6 m.y. B.P.) (Bethke and others, 1976), (1) the Creede area was approximately 1,000 m lower than it is at present; (2) there were no major mountain barriers between the Gulf of Mexico and the Creede district; and (3) there was considerable relief to the north of the district during mineralization.

Compositional variation of carbonates in the Creede vein system of Colorado

P. H. Wetlaufer analyzed, by electron microprobe, carbonate rocks from 44 localities on the Bulldog Mountain, Amethyst, and OH vein systems in the epithermal silver-lead-zinc-copper deposit at Creede, Colo. The overall compositional range falls almost exclusively within the $FeCO_3$-$MnCO_3$ solid-solution series. Carbonate deposition took place during two separate stages in the ore paragenesis.

The earlier manganese-rich carbonate was deposited before the main phase of sulfide and barite deposition and is limited to the southern portions of the vein systems. This rhodochrosite stage shows a limited compositional range, predominantly between 85 and 93 mol percent $MnCO_3$, although some $MnCO_3$ contents as low as 70 mol percent have been measured. All the rhodochrosite has low $CaCO_3$ and $MgCO_3$ contents, which lie between 2 and 8 mol percent, $CaCO_3/MgCO_3$ usually being greater than 4. Textural features are complex because the rhodochrosite appears to have grown frequently as skeletal crystals, to have undergone several stages of leaching and redeposition, and, possibly, to have recrystallized.

The later, predominantly iron-rich carbonate, which is volumetrically minor, was deposited during a major break in sulfide deposition; this carbonate, which occurs in the northern two-thirds of the district, separates the early fine-grained generation and the late coarse-grained generation. This carbonate falls into two compositional groupings:

- Bimodal siderite group. One mode represents a low $CaCO_3$ and $MgCO_3$ (1–4 mole percent of each) siderite, and the other mode represents a relatively higher $CaCO_3$ (6–12 mole percent) and $MgCO_3$ (5–10 mole percent) siderite. The ratio of $CaCO_3$ to $MgCO_3$ is around 1 to 2.
- Manganosiderite group. Compositions range from 30 to 70 mole percent $MnCO_3$ with low $MgCO_3$ (1–4 mole percent) and $CaCO_3$ (1–4 mole percent) contents. The carbonate of this stage occurs as 1- to 2-mm perched rhombs or as infilling in vugs as opposed to the massive, banded, occassionally crystalline textures of the earlier rhodochrosite.

Precambrian sulfide deposits in Gunnison County, Colorado

Precambrian sulfide deposits in the Powderhorn and Gateview quadrangles southwest of Gunnison in Gunnison County, Colorado, occur within a stratigraphic succession that consists largely of metavolcanic rocks. Reconnaissance studies by D. M. Sheridan and W. H. Raymond indicated the following features:

- The deposits are elongate parallel to gradational and interfingering contacts between amphibolite and felsic metavolcanic rocks.
- Groups of deposits appear to be strung out parallel to thin beds of quartzite that probably originated as cherts.
- Sulfides commonly occur in lamine or elongate aggregates parallel to layering and foliation.
- Some specimens of ore observed on dumps of old mines are crudely banded.

These features suggest very strongly that many of the Precambrian sulfide deposits are volcanogenic, a probability that enhances the economic potential of Precambrian rocks in the Gunnison area.

Hydrothermal circulation and fluorspar mineralization at Poncha Hot Springs of Colorado

R. E. Van Alstine reported that the Poncha Hot Springs in Chaffee County, Colorado, provide information on geothermal systems and the genesis of fluorspar deposits because of the hot alkaline waters, travertine deposits, and fluorspar mineralization in major tensional faults, an association that suggests deep hydrothermal circulation. Sodium, silica, bicarbonate, and sulfate (Van Alstine, 1969, p. 35) are the chief constituents of the water, and the high content of fluorine (12 ppm) is noteworthy. The flow at the central sump (elevation about 2,440 m) estimated at various times at 190 to 1,900 L/min, and the temperature is 76°C. Much of the hot water is piped about 6.4 km east to the municipal swimming pool at Salida, Colo.

Travertine at the site is deposited on Precambrian gneiss between two branches of a major east-trending normal fault zone that is mineralized with fluorspar near its intersection with a fluorspar-bearing north-trending fault; the deposits and faults are along the eastern edge of the Rio Grande rift. The travertine is composed chiefly of calcite and manganese oxide; diatoms, chalcedony, opal, limonite, and colorless fluorite are minor constituents. Analyses of the travertine showed 7 percent Ba, 3.35 percent F, and 1 percent W. Samples of the travertine are radioactive, and radium-226 was detected.

Minerals in the complex multistage breccia in the central part of Hicks Dome in Illinois

Samples from drilling in the central fluorite-rich breccias of the Hicks Dome in Illinois were studied by means of X-ray diffraction and microprobe techniques to determine the mineralogy of this fine-grained breccia. The deepest drill hole, the Hamp well (Brown, Emery, and Meyer, 1954; Trace, 1960), was drilled to a depth of 897 m. Its lower part penetrated 487 m of intensely mineralized and brecciated limestone, dolomite, shale, and sandstone and fragments of alkalic igneous rocks. The matrix of the breccia is finely granular (10–100 μm), consists chiefly of carbonates with sericite, and contains abundant purple and white brookite, xenotime, rutile, apatite, a fine-grained beryllium mineral, pyrite, sphalerite, galena, biotite, and sphene. Veinlets of fluorite and calcite 50 to 500 μm thick transect the breccia. Fine-grained bertrandite was identified by J. W. Adams by means of X-ray diffraction in one sample of the Hicks Dome breccia and is probably present in others.

Tungsten and other trace-element distribution at Ivanhoe tungsten mine in Montana

In the Pioneer Mountains of Montana, tungsten mineralization occurs mainly as scheelite in skarns in the Amsden Formation of Pennsylvanian age. The ore-bearing skarn was probably formed from marly beds in the Amsden Formation. Three intrusive rocks are associated with mineralization—a tonalite and a younger granite, both about 70 million years old, and a porphyry sill about 60 million years old. E-an Zen and Jane Hammarstrom collected samples of the marl and the carbonate beds away from contact effects. Neutron activation analyses show that tungsten concentrations are a few parts per million or less in the intrusive and sedimentary rocks and above 1,000 ppm in the ore. The concentration of other elements provides no clue to the possible movement of elements from the intrusive rocks to the skarn except for the major addition of iron to the ore zone. The origin of tungsten in the Amsden Formation thus remains an enigma, as the evidence neither supports nor refutes the hypothesis that the formation became enriched in tungsten through processes of sedimentary concentration.

Geology of the eastern part of the Cuprite mining district of Nevada

Studies by R. P. Ashley in the eastern half of the Cuprite mining district in Esmeralda County, Nevada, indicated a hydrothermally altered area of 10 km^2 that contains volcanic rocks possibly as old as late Oligocene and as young as 6.8 million years. Silicified rocks that are the result of intense acid leaching occupy the central part of the altered area. Most of the remaining altered rocks are opalized, but argillized rocks appear locally near the margins of the altered area. Several sulfur prospects and silica quarries are located along the contact between silicified and opalized rocks, and possible gold prospects are located within the silicified zone. Alunite is abundant locally in the opalite. The alteration and the associated precious-metal mineralization probably are localized along northerly trending faults that are prominent in surrounding unaltered rocks.

Implications of palladium at Iron Canyon, Nevada

Approximately one-half of the 270 samples from the Iron Canyon area, of Lander County, Nevada, analyzed for platinum-group metals, contain measurable amounts of palladium in the 0.001- to 0.02-ppm range, the average being 0.0034 ppm. The rocks include lower Paleozoic sedimentary and volcanic rocks, Tertiary granitic porphyries, and breccia, all of which exhibit various degrees of hydrothermal alteration. Fault-related iron oxides and vein quartz are also present. The area lies astride the outermost fringes of the zone of dispersed alteration visible in outcrops around the middle Tertiary porphyry copper system at Copper Canyon, Nev. At Iron Canyon, the palladium concentrations greater than 0.003 ppm seem to be spatially related to the Butte fault zone, a north-striking fault system active during the time of porphyry-type mineralization. Palladium contents vary directly with those of Hg, As, Sr, Ag, La, and B, as well as with Pb, Au, and Cu in obviously metallized rocks. N. J Page, T. G. Theodore, P. E. Venuti and R. R. Carlson concluded that this relation probably reflects the mobility of palladium during porphyry-type mineralization. However, their study failed to document conclusively the overall introduction of palladium during mineralization. Among the likely sources of palladium are the lower Paleozoic volcanic rocks or fluids equilibrated with magma(s) associated with the middle Tertiary porphyries.

Bedded barite deposits in Nevada

Light-stable isotope studies conducted by R. O. Rye, in collaboration with geologic studies done by D. R. Shawe and F. G. Poole, of the bedded barite deposit at East Northumberland Canyon in the Toquima Range of Nye County, Nevada, corroborated a sedimentary origin for the barite. The conclusions are as follows:

- The $\delta^{34}S$ values of bedded massive-laminated barite in the Slaven Chert from East Northumberland Canyon range from 20.9 to 28.6 permil, most values being near 25 permil, which is typical of Upper Devonian marine sulfate deposits. The Devonian age is indicated by new fossil evidence for the Slaven Chert.
- The fact that the $\delta^{34}S$ values of the massive-laminated barite are constant suggests that changes occurred during diagenesis or that perhaps another source of sulfur was locally involved in barite deposition.
- The initial sedimentary $\delta^{34}S$ values of massive-laminated barite were apparently retained during recrystallization, replacement by silica, and the loss of organic carbon associated with hydrothermal alteration.
- Once the cause of $\delta^{34}S$ variations in massive-laminated barites is determined, it may be possible to use $\delta^{34}S$ as a stratigraphic tool in determining the age of barites in the central barite province.
- Barite rosettes and concretions have $\delta^{34}S$ values ranging from 29.1 to 56.3 permil, the suggestion being that they formed in a closed system either in the restricted basin or within the sediments where bacterial reduction of seawater sulfate occurred.
- The $\delta^{34}S$ values for vein barites in the area are much larger than those for bedded barites but are consistent with the possibility that the sulfur in the veins was derived from bedded barite.
- The $\delta^{18}O$ data on most cherts and carbonates in the bedded barite interval in the Slaven Chert are typical of Devonian marine cherts and carbonate rocks, whereas $\delta^{13}C$ values on the carbonate rocks suggest deposition involving organic matter in a basin that had restricted communication with the carbon reservoir of the open ocean.
- Evidence from conodont color alteration and chert textures indicates that the barite-bearing interval at East Northumberland Canyon was not exposed to prolonged high temperatures or deep burial and that the eugeosynclinal allochthon emplaced during the Antler orogeny was a "thin-skinned" feature that apparently involved only surficial thrusting during emplacement above transitional and migeosynclinal rocks of the Outer Continental Shelf.

Ore controls and mineral zoning in Chloride mining district of New Mexico

According to C. H. Maxwell and A. V. Heyl, ore deposits in the Winston quadrangle of Sierra County, New Mexico, occur for the most part in northwest-trending tension fractures in propylitized andesitic rocks and to a lesser extent in overlying dacites or in Magdalena Group limestone masses that were thrust or slid from the east over andesite tuff. The ore deposits appear to be zoned from sulfide-rich lead, zinc, copper, silver, and chlorite quartz veins in the southern part of the quadrangle to sulfide-poor silver and gold quartz veins in the northern part.

Composition and Curie temperatures of titaniferous magnetite concentrates

Preliminary laboratory studies by Harry Klemic and P. J. Loferski indicated that the Curie temperatures of concentrates of titaniferous magnetite from some deposits in Essex County, New York, are higher than would be expected in synthetic magnetites having an equivalent titanium content. These magnetites, however, also contain elements other than Ti that proxy for Fe, including Al, Mg, V, Cr, and Mn. Other factors, such as intergrowths of pure and impure magnetite on a very fine scale, may interfere with the determination of the Curie temperature of the magnetite concentrates.

Distribution of molybdenum in Puerto Rico porphyry deposits

D. P. Cox and R. E. Learned showed that, in the Tanama and Helecho porphyry copper deposits in Puerto Rico, molybdenum concentrations in soil are higher than those in bedrock but show the same spatial distribution. Soils contain up to 7,000 ppm Mo, whereas the underlying copper ore contains less than 70 ppm Mo. Both soil and bedrock molybdenum are lower in areas of feldspar-stable low-pyrite alteration and higher in areas of intense sericite, pyrite, and clay alteration.

Intrusive center recognized in Keg Mountains of Utah

A previously unrecognized quartz-monzonite porphyry stock was discovered as a result of geologic mapping in the Keg Mountains area of Utah. This stock is apparently the terminal phase of older (Oligocene) volcanic rocks and is partly concealed by one or more sections of younger (Miocene and (or) Pliocene) volcanic rocks. The intrusive body probably marks the eruptive center of the older volcanic rocks and may indicate the part of the Keg Mountains that has the best chance of containing concealed ore deposits.

Exploration guides for native copper in northern Wisconsin

A model, suggested by W. S. White, for native copper mineralization in the Michigan copper district provided geologic guides applicable to exploration in northern Wisconsin. Critical elements of this model are a favorable degree of metamorphism and a hydrologic system that includes a reservoir of buried ground water and channelways to the surface. The existence of a reservoir and channelways, in turn, depends on the distribution of porous fragmental lava and conglomerate in the basin in which the lavas accumulated. Existing geologic data for northern Wisconsin are not adequate for the paleogeographic reconstruction that will be needed to apply the Michigan model, but the most essential data should be obtainable from surface geologic and magnetic mapping supplemented by a limited amount of drilling.

Minerals Discovery Loan Program

The Office of Minerals Exploration (OME), under Public Law 85–701, approved August 21, 1958, is authorized to offer financial assistance to private industry on a participating basis to explore deposits of certain minerals or mineral products. Of the 210 contracts executed in the 17 years of OME's operation, 54 have been certified as successes, having discovered ore reserve valued at about $170 million. Government expenditures for contract support and administrative and technical services have totaled about $9 million.

The OME program has had limited success to date in making significant discoveries of mineral reserves, and various proposals are being considered to improve its effectiveness. Whether an OME-type program is the most effective means of assisting industry in minerals exploration, whether an alternative program should be undertaken, and what the level of government participation should be are questions under consideration. Pending a decision on the future of the program, funds for new exploration contracts have not been requested since FY 1974.

Funds have been requested and received to continue the technical and administrative services required to manage active contracts and to administer completed and certified contracts having continuing obligations for royalty payments on production. Unused funds released from completed prior-year contracts have been used to support contracts awarded since FY 1974.

GEOCHEMICAL AND GEOPHYSICAL TECHNIQUES IN RESOURCE ASSESSMENT

REGIONAL GEOCHEMICAL AND GEOPHYSICAL STUDIES

Possible new mineral occurrences in Alaska

A number of areas of possible new mineral occurrences were outlined during reconnaissance studies in Alaska by G. C. Curtin and R. B. Tripp. Results of potential economic significance include (1) delineation of several possible porphyry copper-molybdenum occurrences in the Tanacross quadrangle; (2) discovery of several localities in the Talkeetna quadrangle where high tin values occur along with high beryllium and tungsten values in stream-sediment and heavy-mineral concentrates; and (3) discovery of several previously unreported gold occurrences in the Seward quadrangle indicated by high gold and tungsten values in stream-sediment and heavy-mineral concentrate samples.

In the Talkeetna quadrangle, the tin occurrences are associated with middle Tertiary granitic rocks of the McKinley sequence (Reed and Lanphere, 1973) and probably are from greisen zones similar to the zone described by Hawley and Clark (1974) in the Upper Chulitna district near the northeastern corner of the Talkeetna quadrangle. In addition, significant amounts of gold are found in heavy-mineral concentrates at several localities in the quadrangle, and some of these occurrences may be similar to those in the Chulitna-Yentna mineral belt on the southern flank of the Alaska Range (Hawley and Clark, 1973). Also, a number of possible base-metal occurrences are outlined in the western half of the Talkeetna quadrangle.

Geochemical anomalies in volcanic rocks in southwestern Oregon

Anomalous concentrations of mercury and other heavy metals were found by J. C. Smith during preliminary reconnaissance sampling in silicic rocks in the Medford 1°×2° quadrangle of Oregon. These rocks are located in the deeply dissected sequence of volcanic rocks of middle-Tertiary age in the western Cascades and are overlain by the largely undissected cones and flows of Pliocene to Holocene age in the High Cascade Range. As much as one-third of the western Cascade sequence was found to consist largely of unfaulted dacite and rhyodacite tuffs and volcaniclastic rocks of intermediate composition in a homoclinal section dipping 15° to 20° east, whereas gently folded basalts and andesite cut by numerous faults previously were thought to make up nearly all of the section.

Ore targets in the Coeur d'Alene district of Idaho

Results of geochemical studies conducted in the Coeur d'Alene district of Idaho by G. B. Gott and J. B. Cathrall indicated that the sequence of events in the formation of the ore deposits was as follows: (1) Formation of northwest-trending mineral belts, (2) intrusion of mineral belts by quartz monzonite, and (3) offsetting of mineral belts by postore faulting. Intrusion of the monzonite stocks caused remobilization and redeposition of ore minerals in a halo surrounding the stocks. Mineral statistics indicate that 85 percent of the Coeur d'Alene ore has come from this halo. Only about one-half of the halo has been prospected.

Geochemical anomalies in the Tooele 1°×2° quadrangle of Utah

Reconnaissance geochemical studies undertaken by W. J. Moore during a mineral-resource appraisal of the Tooele 1°×2° quadrangle of Utah indicated an arsenic-antimony-molybdenum anomaly at Davis Mountain and a lead-zinc-silver anomaly at Wig Mountain. Both anomalies are located in silicified rocks of Late Devonian to Early Mississippian age and may represent leakage of hydrothermal fluids along bedding-plane faults. The silicified zones that contain the geochemical anomalies and an intervening volcanic neck at Little Granite Mountain define a trend parallel to an inferred northwest-trending tear fault that separates lower and middle Paleozoic rocks on the south from thick sequences of Pennsylvanian and Permian rocks on the north.

Geochemical study of the Mineral Butte copper deposit of Arizona

Samples of bedrock and residual soil collected by M. A. Chaffee in the vicinity of the Mineral Butte porphyry copper deposit in Pinal County, Arizona, were analyzed for 39 elements. Of those 39 elements, 7 (Cu, Co, F, Au, Pb, Ag, and Zn) produced anomalies that exhibited generally close spatial relationships to the Mineral Butte deposit as defined by the distribution of copper anomalies. The molybdenum anomalies did not seem to coincide with the copper anomalies.

Samples of leaves and stems collected from four common desert plants growing along stream channels in the region around the Mineral Butte deposit were ashed and analyzed for 38 elements. The deposit was best located by using the copper content of mesquite (*Prosopis juliflora*); the copper contents of blue paloverde (*Cercidium floridum*) and catclaw acacia (*Acacia greggii*), however, were almost as effective.

Geophysical methods as an aid to mineral exploration in southwestern New Mexico

The San Lorenzo fault, previously only inferred, was clearly delineated by J. C. Wynn by using gravity data in the southwestern San Lorenzo quadrangle of New Mexico. This fault has a throw in excess of 3,000 m, downthrown to the east. The Carpenter mining district and a possible caldera (tentatively named Emory Pass), were outlined by gravity stations in the northern and central parts of the San Lorenzo quadrangle.

A strong aeromagnetic anomaly south of the Copper Flats orebody implies that a large buried mass may underlie the andesite field, and the stock may be only an apophysis of this larger mass. Very low frequency-electromagnetic data clearly outline the contact between the Copper Flats monzonite stock and the surrounding andesites and basalts.

Geochemical exploration for copper and nickel in Minnesota

A relatively intense and weakly continuous copper-nickel anomaly in B-horizon soils found by H. V. Alminas appears to be associated with copper-nickel mineralization in the Duluth Complex contact zone of St. Louis and Lake Counties in northeastern Minnesota. The anomaly thus far extends from the western shore of Gabbro Lake some 32 km southwestward to the edge of the sampled area. An additional and subparallel linear anomaly approximately 10 km southeast of the contact zone shows a striking correlation with aeromagnetic and gravity features.

Geochemical anomalies near the Brewer Mine in South Carolina

Henry Bell's preliminary evaluation of contoured geochemical data in the vicinity of the Brewer Mine in Chesterfield County, South Carolina, indicated that, although a strong copper anomaly occurs in the mine area, geochemical anomalies for manganese and cobalt form an arcuate pattern offset to the east beyond the explored area. If this hypothesis is confirmed by additional work, the offset pattern suggests an area for renewed exploration.

STUDIES INVOLVING IRON AND MANGANESE OXIDES

Iron and maganese oxides in stream sediments

In a study of stream sediments from two porphyry copper districts in west-central Puerto Rico, R. E. Learned found that the trace-metal content of the manganese-oxide and amorphous iron-oxide fractions of the sediment afford anomaly-to-background contrasts that are several times higher than "total" trace-metal contents.

The sequential extraction method of T. T. Chao and R. F. Sanzolone, which was applied to the investigation, also determined the trace-metal content of the organic, crystalline iron-oxide, sulfide, and silicate fractions; these fractions, however, provide no enhancement of the ordinary "total" trace-metal contrasts.

Use of Fe-Mn ratios connects silver deposits with porphyry copper deposits

The use of Fe-Mn ratios by K. C. Watts and J. R. Hassemer proved useful for distinguishing pyritic zones in the vicinity of Santa Rita, N. Mex. The geochemical data delineated a northeast-trending zone of high Fe-Mn interpreted as pyritic alteration that extends 6.5 km to the northeast in the same trend as altered dikes and faults in the area. The area is underlain mainly by normally low-iron carbonate rocks. The Fe-Mn pattern bulges and intensifies at the Georgetown silver district, 7.3 km northeast of Santa Rita. The high Fe-Mn ratio is accompanied by northeast-trending strong anomaly patterns in copper, lead, zinc, and silver. Northeastward movement of mineralization solutions and a cogenesis for the Santa Rita copper deposits and the Georgetown silver deposits were inferred.

Weathered halos of iron and manganese oxides outline porphyry copper systems

According to K. C. Watts and J. R. Hassemer, heavy minerals derived from active dry arroyo sediments in New Mexico and analyzed by emission spectrography appear to afford a rapid method of delineating hypogene manganese-oxide haloes that are the distal portion of the porphyry copper-base metal zonation mode. Similarly, iron-oxide zones may indicate zones of intense pyritic alteration where the bedrock is such that mafic minerals are suitably scarce. The pyrite zones are weathered to limonite but show close correlation with strong anomalies in the nonmagnetic (ore mineral) fraction of the concentrated sample; thus, a close spatial association with sulfide mineralization is indicated, perhaps corresponding to the quartz-pyrite-sericite zone of the porphyry-copper alteration model. The manganese-oxide haloes similarly would indicate the propylitic fringe of the porphyry copper model, and, as such, these haloes would be useful in identifying discrete porphyry copper systems, especially where there is no surface exposure of the deposit.

Manganese halo along a fault indicates possible porphyry copper deposit

A weathered, probably hypogene zone of high manganese was traced along the Mimbres fault zone for about 28 km by K. C. Watts and J. R. Hassemer. The pattern begins in the northwest at the Shingle Canyon zinc mine and terminates and broadens in the southeast near the town of Swartz, N. Mex. Metal anomalies are scattered along this zone. The manganese halo departs from the Mimbres fault trend at the Rose copper mine, around which it loops. The area within the manganese halo is a strong aeromagnetic high, which is also enveloped by a molybdenum halo. A similar manganese halo is associated with the Santa Rita porphyry copper deposit to the west. A narrow area of low manganese separates the haloes of high manganese around Santa Rita and around the Rose mine. Metals such as copper show the same pattern as manganese. Therefore, the geochemical and geophysical evidence together indicate a possible buried mineralization porphyry near the Rose mine representing a system that is separate and discrete from Santa Rita, each system being defined by a separate manganese halo.

STUDIES INVOLVING THE USE OF WATER, VOLATILES, OR VEGETATION

Chemical analyses of water and statistical technique define possible molybdenum mineralization

W. R. Miller and W. H. Ficklin (1976) reported a possibly significant geochemical anomaly in the White River National Forest, south of Aspen, Colo., near Hunter Peak. Chemical analyses of waters collected from streams, mine drainages, and springs indicate two areas of mineralization. Copper-zinc mineralization is greatest along Cataract Creek and probably represents small-volume vein-type mineralization. More important is the possible molybdenum mineralization centered west of Hunter Peak. On the basis of a chemical analysis of the waters, the molybdenum mineralization is probably less than 200 m below the surface.

Q-mode factor analysis of the chemical variation of the waters indicates a general zoning pattern. A molybdenum mineralization pattern is centered around Hunter Peak, a copper-zinc mineralization pattern surrounds the molybdenum mineralization pattern, and a pyrite mineralization pattern is pervasive throughout the area but generally surrounds and partly coincides with the copper-zinc mineralization pattern.

Analysis of soil gases from an active geothermal area

Soil-gas samples collected by M. E. Hinkle from soils by means of molecular sieve absorbers buried in the ground over an active geothermal area in the Western States were analyzed by mass spectrometry, gas chromatography, and atomic absorption. Above-average concentrations of helium, carbon oxysulfide, carbon disulfide, and mercury were found in the Roosevelt Hot Springs Known Geothermal Resource Area near Milford, Utah.

Biogeochemical data delineate mineral belts in the Coeur d'Alene district

Vegetation is being used as a sample medium to test the ability of various conifer species to delineate areas of known and suspected mineral belts as revealed by rock and soil samples. Preliminary evaluation of biochemical data in the Coeur d'Alene district of Idaho and Montana by J. B. Cathrall and G. B. Gott delineated, regardless of the species samples, known existing mineral belts and the possible extension of these belts.

GEOCHEMICAL INDICATORS OF MINERALIZATION

Samples characterize different parts of porphyry metal systems

G. J. Neuerburg reported that rock and soil samples are equally useful in flagging areas of mineralized rock and in characterizing porphyry metal systems in Colorado. Soils are enriched in ore elements and depleted in rock elements in comparison with matching rocks, and thus the changes caused by mineralization are magnified. The distribution of metals in soils delineates the distribution of ore minerals, mostly from vein deposits, whereas the distribution of metals in rocks conforms to zones of pervasive hydrothermal alteration that are spatially related to the sites of disseminated porphyry metal deposits.

Use of gold signatures in exploration

J. C. Antweiler and W. L. Campbell reported that gold has a characteristic signature for each of several types of ore deposits, including porphyry copper deposits. The signatures of gold from three porphyry copper deposits (Cala Abajo, Puerto Rico; Butte, Mont.; and Mineral Park, Ariz.) had similar ratios of gold, silver, and copper and similar trace-element contents. Thus, a signature of gold that shows a Au-Ag ratio of about 3 and a Au-Cu ratio ranging from 500 to 2,000 and that is characterized by lead, bismuth, antimony, and zinc may be derived from a porphyry copper. The conditions of formation of several other kinds of ore deposits are likewise reflected in distinctive signatures of gold derived from the deposits. Because gold is associated with a wide variety of ore deposits, determination of its signature may be a useful guide in mineral exploration.

Monazite as a possible indicator of ore deposits

Oolitic dark monazite with an average of 0.31 percent europium oxide (Eu_2O_3) and 0.88 percent thorium oxide (ThO_2) was identified by Sam Rosenblum in panned concentrates from over 60 sites in Alaska and from 9 sources in southwestern Montana where phosphatic beds are thermally metamorphosed by granitic intrusive rocks. Field relations in Montana indicate that dark monazite forms in the outer part of the contact metamorphic zone. Dark monazite was reported in 11 other areas in Africa, Europe, and Asia; the few published analyses are remarkably similar to those for dark monazite in the United States.

Dark monazite has potential as a guide to ore, for, in addition to being an ore of the rare-earth elements (in France), it may indicate phosphatic layers and possible metalliferous veins in a contact zone, especially in poorly known areas. Recent identification of dark monazite in heavy-mineral concentrates from northern Pakistan and the beaches of Bangladesh indicate that these areas are worth exploring for mineral resources. The upper limit of stability (300°C) may be useful to oil-exploration geologists.

STUDIES INVOLVING RADIOACTIVE MATERIAL

Water and stream-sediment samples used in uranium exploration

Correlation and multivariate *R*-mode factor analyses were made on stream-sediment and water samples from Arizona, Colorado, and New Mexico by K. J. Wenrich-Verbeek and D. B. Collins. The minor- and trace-element concentrations in stream sediments are greatly enhanced with decreasing grain size. The strong correlation coefficient for uranium and grain size indicates that, if anomalous concentrations of uranium are not to be overlooked, the sample must not be diluted with the coarse low-uranium fraction; only grain-size fractions less than 90 μm (170 mesh) should be analyzed for uranium. Most elements showed higher concentrations in water samples allowed to remain unfiltered until the time of analysis and particularly high concentrations in samples acidified in this condition. These increases in element concentrations for unfiltered samples are an especially serious problem for turbid water; consequently, the use of filtered samples is recommended to increase sample homogeneity and reproducibility. Uranium in water correlates directly with Ca, Mg, Na, K, Ba, B, Li, and As. It is apparent from this study that uranium in water is most closely related to the alkalies and alkaline earths. Thus, conductivity, which is dependent on the concentration of these major ions, can be used effectively and easily as a control to normalize the uranium values so that the effects of evaporation and dilution, caused by decreased or increased stream discharge, can be minimized. The number of elements that show a positive correlation with uranium in stream sediments is greater than the number that correlate with uranium in stream water. Twenty-one elements show a significant correlation with uranium, although only Th, Nb, Y, P, Ce, Yb, Li, Se, and Mg show strong positive correlations with uranium, whereas silica (SiO_2) shows a strong negative correlation. Because the correlation between uranium and coexisting elements in stream water and uranium and coexisting elements in stream sediments is not as good as might be expected, it is necessary to sample both simultaneously.

Radium as a geochemical guide to uranium deposits

Radium concentrations detected in many mineral springs and some wells exceed equilibrium with the amount of uranium present. Research by R. A. Cadigan and J. K. Felmlee showed that this condition is causd by the greater solubility of radium, in comparison with uranium, in reducing acidic or chloride-rich water. Major-ion and pH analyses of numerous ground waters and some surface waters in Arizona, Colorado, New Mexico, and Utah showed that uranium tends to exceed equilibrium with radium in neutral to slightly alkaline bicarbonate- or sulfate-rich surface water and some ground water (probably oxidizing). However, radium tends to exceed equilibrium with uranium in neutral to slightly acid bicarbonate- or chloride-rich ground water (probably reducing). The large concentrations of radium detected in some mineral springs associated with faults were probably transported from uranium-bearing portions of the underlying fracture system by chloride-rich ground water.

NEW ANALYTICAL METHODS

Copper, zinc, and lead determinations for geochemical exploration

An atomic absorption spectrophotometric method was developed by R. F. Sanzolone and T. T. Chao for determining copper, zinc, and lead in geochemical samples. The sample is digested with HF-HCl-H_2O_2; the final solution for analysis is in 10 percent HCl. Copper and zinc are determined directly by aspirating into an air-acetylene flame. A separate aliquot of the solution is used for determining lead; lead is extracted from the acidic solution in the presence of iodide and ascorbic acid. As much as 40 percent Fe and Ca and 10 percent Al, Mg, or Mn in the sample do not interfere. The method can be applied to the determination of copper, zinc, and lead in a wide range of geological materials, including iron- and manganese-rich calcareous and carbonate samples.

Chemical dissolution of sulfide minerals

Chemical dissolution techniques involving the use of aqua regia, 4N HNO_3, H_2O_2-ascorbic acid, $KClO_3$ + HCl, and $KClO_3$+HCl followed by 4N HNO_3 were applied by T. T. Chao and R. F. Sanzolone to specimens of nine common sulfide minerals (galena, chalcopyrite, cinnabar, molybdenite, orpiment, pyrite, stibnite, sphalerite, and tetrahedrite) mixed individually with a clay loam soil. The resultant decrease in the total sulfur content of the mixture, as determined by the Leco induction furnace, is used to evaluate the effectiveness of each chemical treatment. A combination of KCl_3+HCl followed by 4N HNO_3 boiling gently for 20 minutes has been shown to be very effective in dissolving all the sulfide minerals. This treatment is recommended to dissolve metals residing in sulfide minerals admixed with secondary weathering products as a step in a fractionation scheme whereby metals in soluble and adsorbed forms, and those associated with organic materials and secondary oxides, are first removed by other chemical extractants.

X-ray determination of titanium

An X-ray-fluorescence method was developed by A. E. Hubert and T. T. Chao for determining titanium in geologic materials. A rock or soil sample is decomposed with a mixture of hydrofluoric and sulfuric acids. After evaporation, the residue is dissolved in 5-percent hydrochloric acid. A microliter portion of this solution is dried on a filter-paper circle for X ray. Interferences caused by particle-size variations and absorption of X rays common to the analysis of powder samples have thus been minimized or eliminated. Results obtained on diverse geologic materials compare favorably with accepted values. The range of determination of this method is 0.02 to 10 percent, which covers titanium values both below and above the crustal abundance.

Solvent extraction eliminates interferences and increases sensitivities

Major rock-forming cations, particularly calcium and iron, were found by J. G. Viets to cause enhancement in atomic-absorption determinations of silver, cadmium, bismuth, and lead. Such enhancement may amount to 300 percent when silver or cadmium is determined at the 0.1-ppm level in an acid solution. When background correction by deuterium arc is used, suppression of silver and cadmium values is as great as 60 percent owing to decreased aspirator efficiency caused by the major elements in an acid solution.

A liquid ion-exchange process using Aliquat 336 has been developed; the process will selectively extract Ag, Bi, Cd, Cu, Pb, and Zn from potassium-chlorate hydrochloric-acid-digestion solutions of geologic materials containing potassium iodide in the organic extract without any major element interference. Silver, cadmium, copper, and zinc can be determined at the 0.02-ppm level, and lead and bismuth can be determined at the 0.2-ppm level.

Spectrochemical determination of submicrogram amounts of tungsten

R. W. Leinz and D. J. Grimes reported that the use of spectrochemical techniques for determining submicrogram amounts of tungsten in geologic materials could be very useful in geochemical exploration for concealed tungsten deposits. The low determination limit (0.2 ppm) would also aid in a number of geochemical investigations involving tungsten (for example, source rock, channels of mineralizing solutions, and mobility of tungsten ions in solution).

RESOURCE INFORMATION SYSTEMS AND ANALYSIS

RESOURCE DATA BASES

Computerized Resource Information Bank

The Computerized Resource Information Bank (CRIB) continued to grow in size and use under the direction of J. A. Calkins. In addition to the Tennessee Valley Authority, the U.S. Forest Service, and the U.S. Bureau of Mines, the Bureau of Land Management recently joined CRIB users and contributors. The CRIB file also widened its user community with the implementation of a worldwide CRIB Public User Service through the computer facilities of the University of Oklahoma and the General Electric Company's International Time-sharing Service. Subscribers can now reach the CRIB file by local telephone from 500 cities around the world. Twelve companies presently subscribe to the General Electric CRIB service.

The USGS in-house CRIB operation presently supports 27 batch and time-sharinging terminals in 16 cities on the USGS computer equipment at Reston, Va. This in-house operation supports mainly USGS users and users that have entered into cooperative agreements with the USGS.

Geothermal Data Base

The GEOTHERM geothermal resources file, under the direction of J. A. Swanson, is now fully operational. GEOTHERM was designed to collect and make readily available the increasing amount of data relating to world geothermal resources. The file is a part of the International Geothermal Information Exchange Program, which was initiated at the First Geothermal Implementation Conference, held in New Zealand in 1974.

GEOTHERM contains data on the physical characteristics, geology, geochemistry, and hydrology of geothermal resources. The file is organized into three subtopics: (1) Geothermal fields, (2) geothermal wells, and (3) chemical analyses. Field records contain information on the location, geology, reservoir properties, and reserves of geothermal fields. Geothermal well records contain data on the location, well flow, temperature, pressure, and enthalpy of geothermal drill hole. Chemical analysis records include information on chemical concentrations and collection conditions of geothermal waters.

The GEOTHERM file will be used in an assessment of the geothermal resources of the United States in 1978 as part of the USGS geothermal program. The Division of Geothermal Energy of the Energy Research and Development Administration (ERDA) is initiating an effort to collect and contribute low-temperature geothermal data to GEOTHERM. These data will be used to assist ERDA in evaluating geothermal resources for nonelectric uses.

The information in the file is also available to the public as computer printouts, tabular reports, formatted records for extended computations, and maps.

National Atlas data file

R. A. Weeks, with the assistance of N. A. Wright, established a computer file to be used for updating the mineral-resource maps shown in the National Atlas. The file contains information on the locations and relative sizes of more than 2,100 mining districts and (or) deposits in the United States. Computer generation of maps will allow various subsets of districts to be displayed at a variety of scales and will thus provide a quick means for spot checking the locations of the districts. In addition, computer-derived subsets of districts can be obtained on the basis of commodities or groups of communities, region, State, or range of latitude and longitude for editing or graphic display. The file is presently stored, manipulated, and retrieved from the computer by the Geologic Retrieval and Synopsis Program (GRASP). All retrievals from and manipulations of the file are interactive.

RESOURCE MODEL STUDIES

Resource appraisal and discovery rate models

On the basis of discovery and exploratory drilling-time series data, L. J. Drew developed a method to estimate the distribution of the sizes of deposits remaining to be discovered. The model is based on the area of influence of an exploratory drill hole and does not require assumptions about either the efficiency of exploration or the size of the effective search area. These two quantities are estimated from the data.

Additional studies directed toward an analysis of operator behavior in the exploration process demonstrate that the discovery expectations exhibit several systematic properties. The most significant of these properties is that favorable expectations appear to be sustained by the quantity of oil discovered per time period rather than by the discovery of a specific minimum size of deposit.

Regional resource assessment methods

A new method of regional mineral-resource assessment was developed (Singer, 1975) and applied in the Nabesna (Richter, Singer, and Cox, 1975), Tanacross (Singer, Curtain, and Foster, 1976), and McCarthy (Singer and MacKevett, 1976) quadrangles of Alaska. The method provides an estimate of the number of deposits (both known and undiscovered) in an area. In addition, associated grade and tonnage estimates for the deposits are provided in a probabilistic manner. Because these analyses are important in the decisionmaking process, the criteria used to select favorable areas are also listed.

The effect of not recognizing resource targets with drill holes or samples was analyzed by the area-of-influence method (Singer, 1976). Results suggest that, for circular targets, search effectiveness might be increased by selecting a technique having a high rate of not recognizing targets if the cost per sample drops enough to greatly increase the sample size.

Weighted characteristic analyses

A technique for quantitatively aggregating data on geochemistry, geophysics, geologic attributes, and remote sensing was developed by J. M. Botbol and R. B. McCammon (USGS) and Richard Siding-Larsen (Geological Survey of Norway). The technique requires that data be represented in a Boolian notation—that is, 1's and 0's and a subsequent comparison of aggregated data against a known mine or mineralized (model) area to assess similarity. The development of this methodology, which computes the similarity between the model and any other area, allows for the rapid and quantitative assessment of an area for its resource potential.

The technique was originally applied to geochemical analyses for 11 selected elements in 4,000 rock samples collected in the Coeur d'Alene district of Idaho. Data were modeled and transformed to a binary representation of filtered second-derivative surfaces, where 1 represents a negative second-derivative value and 0 represents all other second-derivative values. Twelve mineral-belt areas were designated as models, and the weighted elemental signature of the aggregated model (that is, all 12 areas) was computed. By using the weighted signature for the aggregate model, each cell of the entire region was compared with the model, and the degree of association was computed. The highest degree of association shows exploration target areas that fall into two groups: (1) Those that conform with prior knowledge and would normally be selected as targets (by means of conventional techniques) and (2) those that fall in areas of limited prior knowledge. All results indicate that the technique performs in a dynamic manner and suggest areas of high resource potential.

Dynamic modeling studies of critical commodities

Two models are being developed by M. S. Hamilton to assess the interrelationships between energy requirements for mineral production and commodity requirements for energy production. The first model assesses the nonfuel raw-material requirements of alternative mixes of energy sources and locates constraints on energy development owing to inadequate mineral supplies. The second model assesses the impact on energy costs of mining lower grade ores, the increased potential for recycling metal owing to higher energy prices, and the changes in material usage owing to the changed energy situation.

ENERGY-RELATED MINERAL STUDIES

Adequate mineral supplies for a sustained economy should be a matter of deep concern, particularly in view of the large quantities of minerals and materials required for energy production and the serious consequences that will follow in the event of deficiencies. The United States' proposed energy independence depends on adequate supplies of nonfuel-mineral raw materials.

Minimum estimates of nonfuel-mineral raw-material requirements (G. H. Goudarzi, L. F. Rooney, and G. L. Shaffer, 1976) for all energy types indicate that concrete and iron are needed in the largest tonnages but that "substantial" quantities of other materials such as aluminum, barite, bentonite, manganese, and nickel must also be available if the Nation's energy goals are to be reached by 1990.

A minimum of about 2.5 billion barrels of oil equivalent may be required to produce 20 selected mineral commodities needed by the energy industries through the next 15 years; 18.5 billion barrels of oil equivalent may be required to produce a supply sufficient to meet the domestic demand for those minerals during the same period. This amount of energy, equal to more than half of the known U.S. recoverable petroleum reserves, is only a fraction of the energy required to produce the 90 or more mineral commodities used in the total economy. Thus, imports of mineral raw materials and semifabricated or processed material also constitute energy imports. Substitution of domestically produced materials for imports will further stress domestic energy production.

Further research conducted by J. H. DeYoung, Jr., into changes in Canada's Federal and Provincial tax laws—studies begun under the Comparative Study of Canadian-United States Resource Programs—showed that declines in mineral exploration activity in Canada, especially in British Columbia, have resulted from some attributes of those laws that could have been avoided. First, the higher taxes imposed on an industry whose prices are set in competitive world markets may result in reduced output and employment by that industry. Second, a gross-profits tax such as the British Columbia Mineral Royalties Act of 1974 may prevent a firm from recovering the average fixed-cost component of the value of total product and thus result in the demise of the firm. Finally, coordination both at different levels of government and between analysts of different physical and social science disciplines is needed to avert unexpected and, in many cases, undesirable effects of policy actions.

COAL RESOURCES

Development of phase II, National Coal Resources Data System

Computer software development for phase II of the National Coal Resources Data System involves the analysis of coal-resources information. The software developed by S. M. Cargill and A. C. Olson produces contour maps on an interactive graphics terminal and on computer-controlled plotting equipment. The software encompasses techniques that simplify the operational burden imposed on the user, reduce the burden placed on the computer resources, and result in minimal response times. The procedures available with this software can be used to perform analysis and mapping tasks that heretofore had been done manually. The system permits the geologist to review and edit his results at various points throughout the procedure.

A set of maps containing geologic and engineering information on the Cache coal bed in the Recluse Model Area of northern Campbell County, Wyoming, were prepared both by computerized modeling and by traditional manual compilation by R. G. Hobbs and E. R. Landis (USGS) and G. B. Schneider (Bureau of Land Management) as an experiment in the presentation of data. The computerized maps fulfill several functions: (1) Data breaks are called to the geologist's attention and (2) the complete computer-generated map forces the geologist to recheck many of his own interpretations and hypotheses.

Participation in interagency EMRIA program

In support of the Energy Minerals Rehabilitation Inventory and Analysis (EMRIA) program administered by the Bureau of Land Management (BLM), many investigational phases of which are conducted by the USGS and the Bureau of Reclamation, E. R. Landis, T. A. Ryer, W. C. Culbertson, D. R. Hatch, M. W. Glenn, W. J. Mapel (USGS) and G. B. Schneider (BLM), made preliminary appraisals of coal quantity and quality for the following reclamation study sites: Bisti West in San Juan County, New Mexico; Foidel Creek in Routt County, Colorado; Red Rim, Sweetwater, and Carbon Counties, Wyoming; Bear Creek in Powder River County, Montana; and Horsenose Butte in Dunn County, North Dakota. Each site was selected because it is representative of conditions within a larger area and because it yields much geologic and engineering information applicable to problems of resource recovery and mined-lands reclamation.

The Bisti West site contains about 74×10^6 t of coal resources with 61 m or less of overburden in a 10.4-km^2 area. A larger area including the site proper—about 15.5 km^2—contains estimated identified resources of about 158×10^6 t, about 62 percent of which is overlain by 61 m or less of overburden. The coal has an apparent rank of subbituminous A. Analyses of 16 core samples from the study area gave the following average values for the coal on an as-received basis: Heat, 18.7×10^6 J/kg; ash, 22.2 percent; and sulfur, 0.5 percent. Analyses of 79 samples of coal from the San Juan River region indicate that the trace-element concentrations are generally below the average for these elements in the continental crust; only the concentrations of selenium and boron are higher by more than an order of magnitude.

The Foidel Creek reclamation study site, almost 11 km^2, is included in a study area of about 130 km^2. Coal is present as two persistent beds in the lower coal-bearing unit of the Williams Fork Formation—the Wadge coal bed, stratigraphically the higher of the two, and the Wolf Creek coal bed, about 52 m below. The Wadge coal bed is as much as 3.7 m thick and contains about 317×10^6 t of resources in the study area. In the site proper, the Wadge coal bed contains about 36×10^6 t of coal, 28×10^6 t of which are beneath overburden 61 m thick or less. The Wolf Creek coal bed locally exceeds 6 m in thickness and contains about 434×10^6 t of resources in the area; the site proper is underlain about 50×10^6 t of Wolf Creek coal.

The Red Rim reclamation study site, an area of about 13 km^2 contains estimated demonstrated coal resources of about 32×10^6 t and inferred resources of about 1.8×10^6 t. The estimated resources are in four closely spaced beds with 61 m of overburden or less; about half the estimated resources are within 30 m of the surface. Seventeen analyses of coal samples from the area indicate that, on an as-received basis, the coal has an average heat value of about 18.8×10^6 J/kg, about 10.4 percent ash, and about 0.4 percent S.

The Bear Creek reclamation study site, an area of about 23 km^2, is underlain by almost 150×10^6 t of coal, all under less than 61 m of overburden. About 144×10^6 t are demonstrated resources, and 80×10^6 t are overlain by less than 30 m of overburden. The coal is in three beds, all of subbituminous C rank. The as-received heating value of the coal ranges from 17.9 to 20.9×10^6 J/kg, the ash content ranges from 3 to 6 percent, and the sulfur content ranges from 0.2 to 0.5 percent.

The Horsenose Butte reclamation study site, an area of about 15.5 km^2, contains estimated demonstrated coal resources of more than 87×10^6 t in four coal beds with 61 m of overburden or less. The Dunn Center coal bed alone contains 65×10^6 t, almost 43×10^6 t of which are overlain by less than 30 m of overburden. The average analysis of 25 samples of Dunn County lignite on an as-received basis is 40.6 percent moisture, 7 percent ash, 0.6 percent S, and a heat value of 14.6×10^6 J/kg.

Coal resources in the Recluse Model Area

The Canyon coal zone in the 518-km^2 Recluse Model Area of northern Campbell County, Wyoming, contains as much as 4.1×10^9 t of coal in a net thickness of 3 m or more, as estimated by E. R. Landis and R. G. Hobbs (USGS) and G. B. Schneider (Bureau of Land Management). Much of this coal might become strippable if the Anderson coal seam, which lies less than 61 m above, and the Dietz coal zone, which intervenes between the Anderson bed and the Canyon coal zone, are surface mined in areas where they contain recoverable resources. In parts of the area, the Canyon coal zone is associated with silty sandstone beds—probably a meander channel sequence—that are very poorly indurated, are aquifers, and contain methane gas. Traditional underground mining of the Canyon coal would be difficult and perhaps wasteful; surface mining or development by in-situ methods might be more practical and economical.

One of two drill holes planned to obtain core samples of coal beds at depths up to 244 m has been completed in the Recluse Model Area. According to Hobbs and Landis, the Cook, Wall, Pawnee, and Cache coal beds contain coal that is recoverable by underground mining or that may be developed by in-situ methods in the area. Prior to completion of the core hole, only the presence and probable thickness of these beds could be interpreted from geophysical well logs.

Coal-bed correlation by tonstein identification

B. F. Bohor contended that the thin widespread partings in coal beds are tonsteins that originated as altered volcanic dust layers. Laboratory and field evidence combine to support this identification (Bohor, Hatch, and Hill, 1976). Because a tonstein originates as fall from airborne volcanic dust, individual partings can be considered as isochronous marker horizons, and their clay-mineral content may be a direct function of the degree of marine influence (salinity) on the depositional environment. The zircon content of tonsteins has been shown to give radiometric dates by the fission-track method.

Bohor identified and traced the Felix coal bed in the Wasatch Formation over an area of more than 2,590 km^2 in the Powder River basin of Wyoming by using the contained tonstein layers for correlation. The study showed that the Felix coal bed at exposures in the Twentymile Butte quadrangle northwest of Gillette, Wyo., is the equivalent of the Arkansas coal zone in the Ulm quadrangle more than 96 km to the northwest. The presence of tonsteins made this correlation feasible in spite of the discontinuity of exposures across the Powder River basin and the changes in the physical character of the coal bed.

Coal-bed characteristics related to ancient environments

Sedimentological studies of coal and related rocks in the Breathitt Formation of Lawrence County, Kentucky, and Wayne County, West Virginia, conducted by R. M. Flores, C. W. Connor, P. T. Hayes, D. E. Ward, and D. J. Sanchez showed that coal beds that formed in the seaward parts of the lower delta plain tend to be persistent and uniform in thickness, whereas coal beds that formed in the upper delta plain or interfluvial swamps are discontinuous but locally thick. Preliminary evaluation of incomplete quality studies indicate that the fluvial coals have lower sulfur contents than the other coals.

Content of selected trace elements in coal

Results of analyses for some 35 to 50 chemical determinations on each of 799 samples of coal from

TABLE 1.—*Summary of data for selected coal samples*

Element	All coal (799 samples), ppm	Anthracite (53 samples), ppm	Bituminous (509 samples), ppm	Subbituminous (183 samples), ppm	Lignite (54 samples), ppm
			Content of element in coal		
As	15	6	25	3	6
F	74	61	77	63	94
Hg	.18	.15	.20	.12	.16
Sb	1.1	.9	1.4	.7	.7
Se	4.1	3.5	4.6	1.3	5.3
Th	4.7	5.4	4.0	3.3	6.3
U	1.8	1.5	1.9	1.3	2.5
			Content of element in ash of coal		
Cd	7.3	1.5	12.3	1.0	3.6
Cu	166	314	190	95	93
Li	142	291	167	61	60
Pb	114	95	151	44	61
Zn	278	151	368	173	114
Ash (percent)	13.3	12.5	13.9	10.8	21.6

28 States were released in open file (Swanson and others, 1976). Most of the samples were taken from operating mines, and about 80 percent were collected by personnel of State Geological Surveys under cooperative arrangements within the USGS. A summary of the data on the samples includes the following average contents, in parts per million, for 12 elements that are of environmental or potential economic importance during the mining and utilization of coal (table 1).

Sulfur in peat and coal

The molecular weight of iron is 55.8, and the molecular weight of sulfur is 32; thus, the ratio of sulfur to iron in pyrite is 64:55.8. According to A. J. Bodenlos, by applying this ratio to the sulfur contained in the pyrite of coal, one can determine the amount of iron tied up in pyrite, and that amount can then be compared to the total iron content in coal. The tabulation shows the average percentages of organic sulfur and sulfur in pyrite and the total iron content of the various ranks of coal, culled from a report on chemical analyses of U.S. coal samples (Swanson and others, 1976, tables 4*A* and 4*C*). The tabulation also shows the calculated iron equivalent of the sulfur in pyrite, the excess iron occurring in some other mineral form, and the percentage of excess iron as compared with the total iron content of these same national averages:

Rank	Organic S, percent	S in pyrite percent	Fe in pyrite, percent
Lignite	0.75	0.68	0.59
Subbituminous	.32	.35	.30
Bituminous	.88	1.70	1.47
Anthracite	.48	.35	.30

Rank	Total Fe, percent	Excess Fe, percent	Percent excess Fe to total Fe
Lignite	2.0	1.41	70
Subbituminous	.52	.22	42
Bituminous	2.2	.73	33
Anthracite	.44	.14	32

Aside from an unknown but relatively small amount of sulfur contained in living plants that since have been altered to coal, the remaining sulfur results from the anaerobic bacterial reduction of sulfate ions to sulfide ions within the original peat-forming swamps. The sulfide ions either combine with iron to form pyrite or become attached to dead organic material and form part of the organic sulfur content of the peat. The tabulation suggests, particularly in high-sulfur coals, that some fraction of the bacteriologically generated sulfide will attach itself to organic material, despite the availability of sufficient iron to react with all the generated sulfide.

The excess of iron in very low sulfur coals, such as those found in some basins of the Rocky Mountain System, may result from a different condition—a paucity of bacteriologically generated sulfide. The organic sulfur content in some of those coals is so low that much or most of it could have accumulated in the original living plant matter. When this organic sulfur is coupled with an accompanying low pyrite content, it would appear that sulfide-ion generation by anaerobes was minimal—or, put in another way, the sulfate content of the original swamp waters was exceedingly low. As a consequence, there may not have been enough sulfide ions available to convert all contained iron to pyrite.

Analysis of the forms of sulfur in peat from different regions confirmed for Z. S. Altschuler and C. S. Zen the idea of a marine source for the excessive sulfur in high-sulfur coals. Peat in the freshwater Everglades region of Florida contains only 0.5 to 1.0 percent S, mostly organic. Saltwater peat in the Everglades and saltmarsh peat of the Louisiana Delta Plain (collected in a cooperative study by personnel from the Coastal Studies Institute of Louisiana State University) contain from 1.0 to 4.5 percent S. The higher values reflect an increase in sulfide sulfur (as in coal). In peat beds from both the freshwater Everglades and the Delta saltmarsh, the sulfide content is greatest, and the organic sulfur content is complementarily less, in the basal zone. This characteristic may be caused by bacterial use of organic matter and the fixation of organic sulfur as sulfide. However, the normal quantities of organic sulfur are inadequate to account for all sulfide in this manner. Bacterial fixation of marine sulfate remains the likeliest source of much of the sulfide.

Peat deposits in the Front Range of Colorado

J. C. Sarnecki reported that, on the eastern slope of the Front Range in Colorado, peat deposits are formed in fens, mires, and carrs (waterlogged woodland communities) along stream valleys, behind glacial moraines, and in nivation basins. The organic matter is mostly reed-sedge peat, formed from sedges (*Carex*), and woody shrubs such as willow (*Salix*) and birch (*Betula*). The fresh peat commonly is brown to yellow-brown, spongy, fibrous material that contains less than 25 percent ash.

The peat deposits are important as soil conditioners and, in their undisturbed state, are environmentally important in controlling floods and maintaining a stable water table. If the water table drops because of natural or artificial causes, the peat dries out and oxidizes, the pH increases, and the plant succession changes as conifers invade the peat swamp. These changes decrease the commercial value and environmental effectiveness of the peat deposit.

Minerals identified in polished coal mounts

R. B. Finkelman's examination of polished mounts of coal from the Waynesburg coal bed in Monongalia County, West Virginia, furnished by R. W. Stanton, revealed the presence of (1) abundant rare-earth-bearing phosphates and silicates, (2) authigenic iron-rich chromite as 1- to 2-μm rims that are always found in the same relative orientation on host quartz grains, (3) nickel silicates and a nickel-bearing iron-rich chromite, (4) relatively large crystals of an olive-green amphibole that are, on the average, 10 times larger than detrital quartz (20 μm), (5) authigenic magnetite octahedra, and (6) a fleck of gold. The accessory minerals may be the key to determining the sources of the trace elements found in the ash of coal.

Gas and leachate from burning culm banks

R. B. Finkelman reported that analysis of the gases collected from a burning culm bank (coal-mine waste dump) near Mather, Pa., indicated the presence of argon and nitrogen in the same proportions found in the atmosphere; oxygen, however, was lower, but the carbon and sulfur dioxides were substantially higher. The leachate from the waste pile contained 20 times more arsenic than other close-by waters. Minerals found on the culm bank included sulfur, mascagnite (ammonium sulfate), thenardite (sodium sulfate), halite (sodium chloride), syngenite (hydrous calcium-potassium sulfate), picromerite (hydrous magnesium-potassium sulfate), and several as yet unidentified phases.

Improved bioelectric cell to treat acid mine water

In his studies on the treatment of acid mine water, F. D. Sisler successfully used several all-glass two-chambered laboratory cells to rapidly neutralize acid waters; mineral-like waxes were a byproduct of the process. Carbon tetrachloride extracts that had been saponified showed infrared spectra closely resembling ceresin. The microorganisms involved in the formation of the waxes were a mixed flora including sulfate reducers, agar liquefiers, and gas producers. Free sulfur was also liberated in the process. This electrochemical device may be useful in explaining natural phenomena involving the formation of hydrocarbons, the production of free sulfur, and the natural leaching processes of ore deposits.

OIL AND GAS RESOURCES

Evaluation of Naval Petroleum Reserve No. 4

A preliminary judgement was made about the probability of occurrence of Prudhoe Bay-type hydrocarbon accumulations in Alaska's Naval Petroleum Reserve No. 4 (NPR–4) on the basis of (1) results of the 1944–53 Pet–4 exploration program, (2) recent investigations by R. D. Carter, C. G. Mull, and K. J. Bird, and (3) the westward projection of eastern North Slope (primarily Prudhoe Bay) data.

The Prudhoe Bay oilfield results from a favorable combination of structural, stratigraphic, and geochemical factors. The most critical factor is the presence of an Early Cretaceous unconformity that superimposes organic-rich Cretaceous source beds over the truncated surfaces of upper Paleozoic and Mesozoic reservoir rocks (Morgridge and Smith, 1972; Jones and Speers, 1976).

The zone of truncation apparently extends northwestward from the Prudhoe Bay area along the northern flank of the Barrow arch. The northern pinchout limit of the most important reservoirs in the Sadlerochit and Lisburne Groups, however, apparently trends generally westward from the area of the Colville River Delta. Well data in the central area of NPR–4 indicate that both groups pinch out down the southern flank of the Barrow arch (Collins and Robinson, 1967). As a result, the Sadlerochit and Lisburne reservoir beds are probably not present in the northern part of NPR–4 or in most of the area of the truncation zone on the northern flank of the Barrow arch. Relatively thick shales of Jurassic age intervene between the best potential reservoir rocks and the rich Cretaceous source beds south and west of Prudhoe Bay. Organic geochemical analyses (Morgridge and Smith, 1972) indicate that the hydrocarbon source potential of the pre-Cretaceous section is less than that of the Cretaceous rocks. These data lessen the possibility of finding giant hydrocarbon accumulations similar to the Prudhoe Bay field in the Sadlerochit or Lisburne Group in much of NPR–4 south of the Barrow arch.

Two on-structure wildcat wells drilled under the supervision of the U.S. Navy at Cape Halkett and East Teshekpuk have been abandoned or suspended as probable dry holes. The lack of success of these wildcats suggests that the best potential petroleum accumulations at NPR–4 may be in stratigraphic traps.

Organic-rich Ordovician inner-arc-basin rocks in central Nevada

The allochthonous Vinini Formation of Ordovician age in central Eureka County, Nevada, was found by F. G. Poole to include thin layers of olive-black shaly mudstone containing as much as 25 percent organic carbon and yielding as much as 5,400 ppm soluble hydrocarbons. The organic matter in these layers is submature and indicates a thermal history of persistent low temperatures. However, these organically immature rocks contain enough hydrocarbons for petroleum generation in other parts of Nevada that have a more favorable thermal regime. The Vinini, which consists principally of marine chert, mudstone, siltstone, and minor sandstone and limestone, is inferred to have been deposited along the eastern side of an Ordovician inner-arc basin west of the Continental Shelf. The formation was subsequently deformed and obducted eastward onto the Outer Continental Shelf as part of the Roberts Mountains allochthon during the Late Devonian and Mississippian Antler orogeny.

Cretaceous(?) to Eocene reservoir and source rocks in eastern Nevada

The Sheep Pass Formation was deposited in Cretaceous(?) and early Tertiary lake systems occupying more than 8,060 km^2 in east-central Nevada. At the Eagle Springs oil field in Railroad Valley, beds in the Sheep Pass Formation serve as reservoir rocks. Analysis of available core indicates that the formation also includes a significant thickness of potential source rock containing in excess of 15 L/t of oil. The Sheep Pass Formation may represent at least two phases of lacustrine sedimentation, separated in the area of the Egan Range by an unconformity. Previously, the entire formation had been considered Eocene in age on the basis of mollusk and ostracode biostratigraphy. T. D. Fouch, however, determined, on the basis of (1) several well-preserved specimens of the Cretaceous(?) ostracode *Cypridea* (*Bisulcocypridea*) *bicostata* from the type section and (2) early Paleocene palynomorphs from a core at the Eagle Springs field, that a Cretaceous(?) to Eocene age is indicated for the first phase of lacustrine sedimentation. The second lacustrine phase, which resulted in deposition of the Sheep Pass(?) Formation, occurred in Eocene and Oligocene(?) time.

The new reconstruction of Cretaceous(?) to early Tertiary depositional systems indicates that lacustrine and alluvial units are present in a band about 48 km wide that extends northeast for a distance of about 168 km. The rocks of the two lacustrine phases crop out in mountain ranges and are present in the subsurface of some of the intervening valleys, where they may contain potential hydrocarbon source rocks and reservoir beds similar to those found at the Eagle Springs oil field.

Petroleum source beds and trace elements in the Phosphoria Formation of Utah and Nevada

The Meade Peak and Retort Phosphatic Shale Members of the Phosphoria Formation (Permian) were found by E. K. Maughan to extend west of the Wasatch Front into northwestern Utah and northeastern Nevada. Their organic-carbon content is similar to the content found in areas east of the Wasatch Front and to the north in eastern Idaho and adjacent parts of Wyoming and Montana. Thus, the content is sufficient to classify the beds in the northeastern Great Basin as probable petroleum source rocks.

Average concentrations of trace elements in the shale members of the Phosphoria Formation in eastern Idaho and adjacent parts of Montana, Utah, and Wyoming, determined semiquantitatively by six-step emission spectrography, are high in Ag (13 ppm), Cr (1,500 ppm), Sr (1,500 ppm), V (1,300 ppm), Y (500 ppm), and Zn (2,100 ppm). The highest trace-element concentrations in the Meade Peak are found along the Idaho-Wyoming State line, whereas the highest concentrations in the Retort are found in southwestern Montana. Concentrations decrease radially from these centers. Presumably, these trace-metal concentrations, like the phosphorites and organic carbon, are genetically related to sapropelic accumulations on the sea floor in areas of upwelling marine currents and biotic efflorescences in the Permian sea.

Favorable areas for Mississippian oil exploration in Utah

The stratigraphy of the depositional interface between the Osagean and lower Meramecian basinal phosphatic shale member at the bottom of the Deseret Limestone and the Woodman Formation on the west and the time-equivalent platform carbonate rocks on the east was being studied in detail by C. A. Sandberg (USGS) and R. C. Gutschick (University of Notre Dame) (1977), with the help of W. J. Sando (USGS). Preliminary analyses suggest that the phosphatic shale may contain about 3 percent organic carbon and that interbedded phosphorites may contain about 1 percent organic carbon. The phosphatic shale basin, which occupies the northern two-thirds of western Utah, is believed to be the source of petroleum that migrated vertically, or laterally updip to the east, into stratigraphically higher reservoir rocks of Late Mississippian age during the Permian or Mesozoic, when the sedimentary overburden became thick enough for hydrocarbon maturation. The regional distribution of conodont color-alteration-index (CAI) values shows that, throughout most of the phosphatic shale basin, the hydrocarbons were overcooked by Tertiary igneous and hydrothermal activity. However, low CAI values ranging from 1 to 2 show that the hydrocarbons remain at optimum maturation in three areas. One of these areas is in western Utah, in the area of the Burbank Hills and the Needle and Confusion Ranges, where petroleum that migrated vertically may still be sought in local structural traps. The other two areas are along the Cordilleran hinge line, where petroleum that migrated updip into Mississippian platform carbonate rocks, as well as into upper Paleozoic rocks, may be sought in stratigraphic and structural traps. These areas are near the southern Pavant Range in central Utah and near Old Laketown Canyon, east of the Bear Range in northern Utah.

Crude oils linked to oil-shale source rocks in Uinta Basin of Utah

Preliminary geochemical studies conducted by D. E. Anders, G. E. Claypool, and P. M. Gerrild on the lacustrine sediments of Tertiary age in the Uinta Basin of Utah showed that the sulfur isotope values of the hydrocarbon deposits—tar sands, crude oils, bituminous veins, and oil shales—consistently decrease in δS^{34} with increasing age and depth of the strata. The crude oils have the widest range of δS^{34} values of any previously studied oils and appear to reflect the sulfur isotope values of the stratigraphic interval from which they were derived. The similarity between the various hydrocarbon fractions in the crude oils and their stratigraphically equivalent oil shales suggests that the oils in the Uinta Basin can be linked to their oil-shale source rocks.

Weathering of organic matter in Phosphoria Formation of Utah

J. L. Clayton and P. J. Swetland made geochemical analyses of core samples of black phosphatic shale collected with the help of E. K. Maughan from an outcrop of the Phosphoria Formation (Permian) on the southern side of the Uinta Mountains in northeastern Utah. These analyses showed that shale from the surface to a depth of 1 m contains as much as 60 percent less organic carbon and 50 percent less soluble hydrocarbons than shale at depths of 1 to 5 m. Because the loss of aromatic hydrocarbons in the upper 1 m is relatively greater than the loss of saturated hydrocarbons, the ratio of saturated hydrocarbons to aromatic hydrocarbons is greater in the upper 1 m than in the 1- to 5-m interval. The upper 1 m also showed an average enrichment in C^{13} of 1.74 ppt relative to the 1- to 5-m interval, whereas the δC^{13} in the saturated hydrocarbons was the same in both intervals. These analyses demonstrate that near-surface weathering can drastically change the organic content and the composition of outcrop samples.

Origin of oil in Denver basin of Colorado

Geochemical analyses done by P. J. Swetland and J. L. Clayton (1976) showed that oils produced from Cretaceous reservoirs in a large part of Colorado's Denver basin are similar, the suggestion being that they were derived from a common source. Analyses of numerous widely distributed subsurface shale samples and surface shale samples, collected under the guidance of L. W. Kitely, indicated that the most likely source beds are geographically restricted to the western side of the basin. This areal restriction suggests that extensive vertical and lateral migration of oil has occurred.

Stratigraphy of possible lower Upper Cretaceous reservoir rocks in Wyoming

A study of outcrops, cores, and well logs by E. A. Merewether, W. A. Cobban, and C. W. Spencer (1976) indicated that the Frontier Formation (lower Upper Cretaceous) in southern Johnson County, Wyoming, was deposited in marine environments during the Cenomanian and Turonian Stages. The Frontier contains abundant marine invertebrate megafossils. The environments range from offshore to tidal beach. Most of the sandstone in the formation probably accumulated on a large wave-dominated delta. The rate of deposition for the Frontier and the lower part of the overlying Cody Shale is probably about 52 m/m.y. Deposition was interrupted during the middle Turonian by erosion, which is represented by a disconformity about 27 m below the top of the Frontier.

The Frontier Formation, which is about 255 m thick, comprises an unnamed basal member composed of interstratified sandstone, siltstone, shale, and bentonite, and the overlying Wall Creek Sandstone Member, which is as much as 21 m thick. Most of the sandstone is quartzose, very fine or fine grained, and moderately or well sorted. The shale is mainly silty and contains mica-illite, mixed-layer clays, chlorite, and kaolinite or montmorillonite.

Stratigraphic traps and source rocks in Powder River basin of Wyoming

General depositional trends of units in so-called "Leo sandstone" in the Lower Pennsylvanian part of the Minnelusa Formation were identified by R. T. Ryder in the eastern Powder River basin. These lenticular sandstone bodies, which are as much as 19 m thick, are locally very porous and closely associated with beds of organic-rich black shale. Consequently, the sandstone bodies may provide reservoirs for stratigraphically trapped oil, as indicated by oil accumulations in the first "Leo sandstone" at the Red Bird and Pine Lodge fields. Many of the reservoir-quality "Leo sandstone" bodies are characterized by relatively low acoustic-impedance values, which contrast with the higher impedance values of adjacent impervious sandstone and carbonate units as determined by R. C. Anderson. Synthetic seismic sections generated with these contrasting acoustic-impedance values suggest that the trap-reservoir interface can be detected with reflected seismic energy.

The organic-rich black-shale units interbedded with the "Leo sandstone" units are progressively truncated toward the north beneath a regional unconformity in the middle part of the Minnelusa Formation. Preliminary studies indicate that the distribution of these potential source beds beneath the unconformity may in part explain the location of the known Minnelusa oilfields in the Powder River basin.

Possible carbonate source rocks in South Florida basin of Florida

Preliminary studies made by J. G. Palacas, J. P. Baysinger, and J. M. Patterson showed that lower Tertiary to Lower Cretaceous rocks in the South Florida basin range in depth from about 1,370 to 4,020 m and consist predominantly of limestone, dolomite, and anhydrite. Preliminary analyses of about 140 core samples indicate that the organic-carbon content ranges widely from 0.05 to 3.2 percent. Most of the rocks contain less than 0.4 percent organic carbon. However, a significant number of carbonate beds with a minimum aggregate thickness of 52 m generally contain 0.5 to 3.2 percent organic carbon and generally lie below a depth of 2,500 m. The relatively high concentrations of apparently indigenous hydrocarbons and the depth of burial suggest that these carbonate beds could be potential source beds of petroleum. Siliceous clastic rocks are virtually absent from the South Florida basin except for a few thin shale interbeds that in aggregate total less than 1 percent of the total rock column. Hence, it is unlikely that these shales could be the sources for the organic carbon found in the carbonate rocks.

Guyana mud accumulation—analog for ancient clastic wedges?

A literature survey and preliminary study made by R. N. Ginsburg (University of Miami) indicated that mud moves northward in giant wave-like banks along 1,500 km of open coast off Guyana in northeastern South America. Thus, it is evident that quite deep-water environments are not necessary for mud deposition. A combination of the Guyana Current and circulation on the inner shelf produces a hydrographic trap for fine sediment. The enormous supply of mud from the Amazon River is the source for this Holocene and Pleistocene accumulation. From descriptions of the sedimentary structures and the fauna and flora of the mud deposits, it is possible to infer a shoaling-upward sequence produced by seaward progradation. The Guyana coastal system may thus demonstrate that some ancient clastic wedges are attenuated deltas of giant rivers.

Possible new deep source of energy

A solubility study done by L. C. Price and L. L. Rumen on crude oil in water as a function of temperature, pressure, and the presence of organic and inorganic gases showed that oil and methane have very high solubilities at temperatures above 275°C. Organic geochemistry studies of deep wells (as much as 9,450 m deep) showed that the generation of hydrocarbons can occur at such depths and that hydrocarbons are thermally stable at much greater depths and higher temperatures than investigators had believed previously. The thermal stability of hydrocarbons was also documented in laboratory cracking experiments. The solubility of oil and methane and the stability of hydrocarbons at high temperatures help substantiate the possible existence of a deep multiple geothermal-oil-gas energy resource. Theoretically, a reservoir of this type, when it was tapped, would produce large quantities of oil and gas dissolved in superheated water.

Rapid evaluation of petroleum source rock

An analytical technique for the rapid, evaluation of petroleum source-rock potential (Claypool and Reed, 1976) was further developed and adapted for proficient laboratory use by G. E. Claypool and J. P. Baysinger. This technique requires only milligram-weight samples, no sample preparation other than rough crushing, and less than 30 minutes of time. The technique, in combination with the conventional organic-carbon determination, reliably estimates organic richness, hydrocarbon generating capacity, type of organic matter, and thermal maturity. The sample is heated in a stream of inert gas at a programmed rate of temperature increase (40°C/min) from room temperature to 700°C. The organic compounds volatilized or pyrolyzed from the sample are quantitatively measured as a function of temperature by means of an organic carbon-specific gas chromatographic detector. Organic richness and hydrocarbon-generating capacity are indicated by the total quantity of volatile and pyrolytic organic compounds produced from the organic matter in the rock. In samples that have a hydrocarbon-generating capacity, the type or quality of the bulk organic matter is indicated by the quantity of organic compounds produced in relation to the total organic matter in the rock as measured by the organic-carbon content. The thermal maturity of the organic matter in shales and coals is indicated by the temperature at which maximum pyrolytic decomposition of the solid organic matter occurs.

Helium surveys for use in petroleum prospecting

Surveys of helium concentrations in the soil gases over three known oilfields were conducted by A. A. Roberts, M. C. Dalziel, and R. L. Brunner to determine the feasibility of using helium surveys as a geochemical prospecting technique. Each field was surveyed by a grid of 80 to 120 sample sites. Preliminary results support the hypothesis that near-surface helium anomalies are indicators of buried petroleum reservoirs and suggest that a helium survey may be a quick, inexpensive, and environmentally nondestructive exploration tool.

The soil-gas survey made over the Garza field in Texas indicated anomalously high helium concentrations (up to twice the background level) over the production area. This field, located on a dome, has produced oil from the Permian at an average depth of 900 m for 40 years and is currently being water flooded.

Another oil and gas field where an associated helium anomaly was observed is the Cement field in the southeastern part of the Anadarko Basin in Oklahoma. The production comes from several zones, including Permian sandstones and Pennsylvanian carbonate and clastic rocks, at depths of 600 to 2,200 m. This helium survey supports the existence of microseepage from the Cement field, as hypothesized by Donovan (1974) on the basis of mineralogic and chemical changes in the outcropping Permian redbeds.

The helium survey of the Red Wing Creek field in North Dakota showed an anomaly in the form of a halo of high helium concentrations extending four-fifths of the way around the field. Such halos are not uncommon in geochemical detection, and, according to Davidson (1963), the better oilfields generally produce halo-type anomalies. This field, which is located on a structure that is suspected to be an astrobleme caused by meteoric impact, produces from the Mississippian at depths of 1,500 to 2,500 m.

Reservoir and source-bed potential of chalks

The patterns of chalk diagenesis related to maximum depths of burial, pore-water chemistry, and primary composition, which were originally established in the North Sea area, were confirmed by P. A. Scholle in the Gulf Coast and Western Interior areas of the United States. In general, a major shift in oxygen-isotope and strontium trace-element values accompanies a burial-related loss of porosity in chalks. However, with a proper understanding of the degree and trend of diagenetic alteration, a combination of carbon and oxygen isotopes can be used to interpret primary depositional environmental conditions. Thus, the study of isotopes can be used to determine the reservoir potential of chalks under various subsurface conditions as well as to provide useful data on variations in the petroleum-source-bed potential of chalks and associated units.

Formation of fine-grained limestones through compaction

Experiments on squeezing cores of Holocene carbonate sediment 10 cm in diameter were conducted by E. A. Shinn, R. B. Halley, J. H. Hudson, and B. H. Lidz (1977). Contrary to widely held geologic opinion, such sediments were found to be susceptible to considerable compaction. Under a load of 141 kg/cm^2, a 50.8-cm length of core was compacted to 11.4 cm—a reduction of about 75 percent. The resultant "rock" contained horsetail-like wisps—termed pseudostylolites or incipient stylolites—identical to those found in ancient limestones. These structures resulted from compaction and rearrangement of organic matter. Burrows were also distorted to produce stuctures such as those found in ancient limestones. Fossils visible to the naked eye were not obviously crushed, although breakage was detectable in thin section. Similar compaction of carbonate sediments by overburden may have been a major factor in the origin of most fine-grained limestones. If compaction did not occur, a dilemma arises: How could a 50- to 70-percent porosity, which is common in recent lime sediments, be filled by carbonate cement to produce a limestone with only a 3- to 5-percent porosity? Although recent sediments show a 50- to 70-percent porosity, their permeability is so low that it would be difficult for enough mineral-rich water to be circulated through them to fill the pores with carbonate cement. Compaction, which reduces porosity to 5 to 15 percent, resolves this dilemma. Conversion of aragonite to calcite, which creates an 8-percent volume increase, is sufficient to further reduce porosity to the 3- to 5-percent range of ancient fine-grained limestones.

Mechanisms of oil and gas seepage

The formation of unusual carbon isotopic compositions, produced by oxidation of hydrocarbons, in replacement carbonate minerals and authigenic cements is well documented for subsea, outcropping, and relatively shallow buried rocks. However, only limited data have been published describing unusual occurrences over producing oilfields or stressing the complex interrelationship between anomalous carbon and oxygen isotopic variations in carbonate materials resulting from long-continued seepage. Recent studies made by T. J. Donovan and M. C. Dalziel of such seepages in carbonate-cemented rocks over oilfields in the Mid-Continent and Rocky Mountain areas of California, and in western Texas indicated that at least three seepage mechanisms are operative:

- Effusion of small to large amounts of gaseous and liquid hydrocarbons from relatively shallow reservoirs through natural avenues of vertical fluid communication such as faults, fractures, and poorly compacted or otherwise inadequate cap rocks.
- Migration of low-molecular-weight hydrocarbons in aqueous solution through capping shales behaving as semipermeable membranes, the driving force being provided either by hydrodynamic pressure or by differences in chemical potential on opposite sides of the membrane.
- Diffusion of gas through cap rocks.

Since any combinations of these three seepage mechanisms may have occurred, their discrimination is based on interpretations of distinctive isotopic and chemical parameters.

Oilspill risk analysis for frontier OCS lease areas

At the request of the Bureau of Land Management, R. A. Smith, J. R. Slack, and T. S. Wyant conducted a series of oilspill risk analyses for the Department of the Interior's proposed lease areas on the Outer Continental Shelf. The studies were made to determine the relative hazards associated with oil and gas development of frontier areas in different regions in order to facilitate final selection of tracts to be offered for sale. To date, five areas have been studied, including the northern and western regions of the Gulf of Alaska and the North, Mid-, and South Atlantic areas (Smith, Slack, and Davis, 1976a, b; Slack and Smith, 1976).

The analyses consist of two parts, the first involving probabilities of spill occurrence and the second dealing with likely trajectories of spills relative to the locations of vulnerable wildlife populations inhabiting the coastal regions. On the basis of estimated quantities of recoverable oil and the anticipated method of transporting oil from production platforms, it is estimated that a total of from two to nine major spills would be expected to occur during the production life of each lease area if all proposed tracts were leased and developed. A major spill is defined as the release of more than 1,000-bbl of oil. The Alaskan areas are expected to experience the greatest spill frequency owing to higher estimated production levels. Spill-frequency estimates are similarly made for individual fields within each lease area and for spills greater than 58 bbl in size.

On the basis of wind and current data provided by the National Oceanographic and Atmospheric Administration, an oilspill trajectory model was constructed to analyze movements of hypothetical oil slicks on a digital map of each area. Short-term patterns in wind variability (3-hour transitions) were described as a first-order Markov process evaluated from weather-station records for the area. Wind transition probability matrices as well as surface-current velocity fields were established separately for all four seasons. The locations of biological resources (for example, migratory waterfowl habitat and shellfish beds) and important recreation areas were digitized in the coordinate system used in spill-trajectory simulations. Probability distributions were then developed giving the likelihood that spills occurring at various locations in the proposed lease areas would impact the resources in question. The locations of wildlife habitats were made seasonally specific so that results of the impact analysis would reflect seasonal correlations between wind and current patterns and the migratory behavior of the species at risk.

By combining oilspill frequency estimates with the trajectory analysis, it is possible to assess the relative oilspill hazards to wildlife populations posed by sale of tracts at different locations in the lease area.

OIL-SHALE RESOURCES

Oil-shale and saline-mineral data base

The oil-shale Fischer assay and saline-mineral data storage and retrieval system, supervised by J. K. Pitman, provided baseline data for evaluating oil-shale recovery methods, areas under litigation, and environmental impact on selected sites. It was also used extensively to provide data used in detailed geologic investigations of oil-shale resources.

Oil-shale distribution in east-central Uinta Basin of Utah

Mapping by C. W. Keighin in the Rainbow, Burnt Timber Canyon, and Cooper Canyon quadrangles in the east-central portion of the Uinta Basin of Utah showed areas containing significant amounts of near-surface oil shales. The near-surface oil shale, probably amenable to removal by surface-mining techniques, is concentrated in the Burnt Timber Canyon and Cooper Canyon quadrangles.

Global oil-shale resources

J. R. Donnell compiled resource data for known oil-shale deposits of the world. Shales that are thicker than 3.1 m and that yielded more than 41.7 L t of oil contain more than 476.9×10^9 L of oil. The oil shales in the Green River Formation of the United States contain approximately two-thirds of the total resource. Large areas of the world are reported to contain oil shale, but most occurrences have not been appraised. There are also presumed to be large undiscovered resources in the world.

Marlstone tongues of Green River Formation

Mapping in the Mount Blaine quadrangle in Garfield County, Colorado, by W. J. Hail showed that four mapped marlstone tongues of the Green River Formation (Eocene) merge southward with the main body of the Parachute Creek Member. The tongues are, in ascending order, the Coughs Creek and Stewart Gulch Tongues and the marlstones at Barnes Ridge and Bull Fork. In general, these units contain appreciable amounts of oil shale only near their merger points with the Parachute Creek Member.

Total sulfur in Colorado oil shale

X-ray fluorescence analyses were performed by J. R. Dyni on portions of two oil-shale drill cores from the Piceance Creek basin in Colorado. In a section approximately 560 m thick, the amount of total sulfur commonly ranges from about 0.5 to 2.5 percent by weight of the whole rock; values locally are as much as 4.9 percent by weight. Most of the sulfur is in the reduced state and is contained in pyrite; small amounts are associated with kerogen. Zones of pyrite enrichment are commonly found just above beds of nahcolite, and nodules of nahcolite are generally rimmed by pyrite. The absence of sulfate evaporite minerals (gypsum and thenardite) and the association of pyrite with nahcolite suggest that sulfur was introduced in the ancient Green River waters as dissolved sulfate ion. The sulfate was subsequently reduced, and some organic matter was oxidized; perhaps reduction was largely effected by sulfate-reducing bacteria. In this redox process, the reduced sulfur formed mostly pyrite, and oxidized organic matter generated large quantities of dissolved bicarbonate ion. The bicarbonate precipitated with available sodium as nahcolite during evaporative stages of the lake; some nahcolite also precipitated as nodules within the homogeneous sediments during basinal dewatering processes. The great abundance of organic matter found in the Piceance Creek basin may account for the effective reduction of all sulfur that was brought into the basin.

NUCLEAR-FUELS RESOURCES

Sand-grain shape and size variations in a braided stream

Quantitative grain-shape and size measurements were made by D. A. Seeland on 32 sand samples from longitudinal and transverse bars in the South Platte and Platte Rivers between Denver, Colo., and Omaha, Nebr., with an electronic image-analysis system. The results of size and shape measurements of 8,000 sand grains showed that, although there is a decrease in maximum gravel size downstream, the sand does not become appreciably finer downstream. Trends of sand-grain shape were somewhat unexpected: Very fine sand does not change in elongation or roundness downstream, medium sand becomes less elongate and rounder downstream, and very coarse sand does not change in elongation but does become more angular downstream.

It was found that fine-grained sand is the most elongate and the roundest of the three sand-sized fractions studied. In contrast, other qualitative shape studies have found fine-grained sand to be most angular. This study suggests that, in ancient sandstones deposited by braided streams, the best paleogeographic inferences would be produced by a study of the medium-sand fraction because these grains become less elongate and rounder downstream.

Some differences between three alkalic complexes in the Wet Mountains of Colorado

At least three separate alkalic complexes of Cambrian age occur in the northern Wet Mountains of Colorado—the Gem Park and McClure Mountain Complexes and the complex at Democrat Creek. Previous USGS work (Parker and Sharp, 1970; Shawe and Parker, 1967) pointed out the similarities between the rocks at Gem Park and and those at McClure Mountain, especially the layered mafic and ultramafic rocks. T. J. Armbrustmacher's preliminary examination of rocks from the complex at Democrat Creek suggested that there are more differences than similarities between these rocks and those of the other complexes, contrary to earlier published accounts (Heinrich and Dahlem, 1966). The ultramafic and mafic rocks at the southern end of the Democrat Creek intrusion, mapped as Precambrian gabbroic gneisses and metamorphosed ultramafic rocks by Brock and Singewald (1968), contain both orthopyroxene and clinopyroxene, which are suggestive of a tholeiitic parentage, unlike the clinopyroxene of alkalic affinities at Gem Park and McClure Mountains. Syenites at Democrat Creek contain fairly abundant modal quartz, whereas the nepheline syenites at McClure Mountain lack modal quartz. In addition, preliminary trace-element data show fundamental differences, such as an average barium content of 2,780 ppm and an average strontium content of 1,670 ppm in McClure Mountain syenites, as compared with an average barium content of 320 ppm and an average strontium content of 80 ppm in syenites at Democrat Creek. Additional data are being evaluated, and a model explaining the relationship of the complex at Democrat Creek to the Gem Park and McClure Mountain Complexes is being prepared.

Ages of Wyoming uranium ores

Preliminary results of U-Pb isotope investigations of ores from the major Wyoming uranium districts gave similar apparent ages for the Shirley Basin, Gas Hills, and Crooks Gap districts. All of the analyzed ore samples from mines in these districts suggest that major ore-forming processes took place before 20 million years ago, most activity occurring before about 28 million years ago. These times are consistent with the uranium sources' being either Oligocene tuffs or Precambrian granites but rule out Love's (1970) suggestion of Pliocene volcanic rocks.

Uraninite zone related to metamorphosed massive sulfide deposit

R. I. Grauch's studies of the Camp Smith-Phillips mine area in Westchester and Putnam Counties, New York, led to the development of a conceptual model for the concentration of uranium in metamorphosed aquagene sedimentary and volcanic rocks. Concentrations and disseminations of uraninite occur in the outer layer of a zoned massive sulfide, in pyroxene-amphibole-quartz-feldspar-apatite pegmatites, and in apatite-bearing zones of magnetite layers within amphibolitic gneisses. The massive sulfide of the Phillips mine is apparently a stratabound body located near the interface of basic and acidic metavolcanic rocks. The uranium-bearing pegmatites and magnetite layers also are located near the interface. It is proposed that, during deposition of the volcanic rocks and minor amounts of nonvolcanic rocks, some mechanism—perhaps the precipitation of apatite—caused the formation of widespread but low-grade concentrations of uranium. This mechanism was presumably operative during the waning stages of massive sulfide formation and the beginning stage of magnetite deposition. During subsequent metamorphism, granulite-grade uraninite was formed. This hypothesis appears to explain other uranium occurrences in the Hudson and Jersey Highland and should have application elsewhere.

Triassic and Jurassic lacustrine basin localizes uranium

Studies of Triassic and Jurassic rocks in the Newark Basin of Pennsylvania and New Jersey by C. E. Turner-Peterson showed that there are uranium deposits in lacustrine black mudstones (Lockatong Formation) and in nearshore sandstones (Stockton Formation) near the black mudstones. The Lockatong was deposited in a reducing alkaline lake, as is indicated by the black color and the presence of pyrite and abundant analcime. The Stockton is also interpreted as having been deposited under reducing conditions (Glaeser, 1966). Destruction of plant debris in sands at the lake margin is attributed to solubilization by alkaline lake waters.

Uranium mineralization in the basin occurred in two stages. First, uranium accumulated in the euxinic central portion of the lake to form widespread low-grade (0.01–0.02 percent) deposits in black mudstones. Alkaline lake and pore waters mobilized organic matter and leached uranium from nearshore sands. Later, organic- and (or) sulfide-bearing pore fluids from black mudstones were injected during compaction into adjacent sandstones of the Stockton Formation and caused uranium and pyrite to precipitate around and near clay clasts. Uranium is believed to have been localized initially on red clay clasts by adsorption of uranyl ions onto hematite, and the availability of iron may account for the localization of pyrite in and near the clasts as well.

A lacustrine interpretation for the Lockatong and most of the Stockton permits construction of a model in which the reductant (from the black mudstones of the Lockatong) and the host sandstone (marginal lacustrine sandstones of the Stockton) are in a close spatial relationship, and movement of great volumes of water for long distances is not required to account for mineralization.

Autunite deposit exposed on Interstate 89

Two parallel roadcuts for Interstate Highway 89 near Lake Sunapee, N.H., exposed oxidized uranium deposits more than 4 m thick that are comparable to those of the Daybreak mine near Spokane, Wash. The Sunapee mineralization occurs mainly in fractures, local fault gouge, and biotitic schlieren in two-mica granite of Devonian age. The granite is somewhat more fractured than correlative rock to the north and south on regional strike but not conspicuously so. In the nearly 10 years since the mineralization was exposed by roadcuts and the water table was lowered, more than 90 percent of the yellow uranium minerals (including autunite, torbernite, and reynardite) have been leached away by vadose ground water. The top of the original water table is believed to have fluctuated within the mineralized zone. It is possible that the uranium minerals have reprecipitated at the lowered (reestablished) water table.

Semipermeable membranes and ore genesis

The vanadium clay minerals of the Colorado Plateau vanadium-uranium deposits appear to be capable of acting as semipermeable membranes. According to C. S. Spirakis, the initial layer of vanadium clay minerals precipitated at a solution interface. Then selective diffusion of anions through the membrane led to a charge imbalance across the membrane. This charge imbalance accelerated the diffusion of H^+ through the membrane, a process that resulted in pH changes on both sides of the growing ore deposit. On one side of the deposit, a basic environment was created, whereas the other side became more acidic. Mineral zones formed in response to the changes in pH on the basic side of the membrane. Bleaching of red mudstones on the acidic side of the deposit was caused by the low pH generated by the membrane. The membrane also provides a means of maintaining the solution interface long enough for the deposit to form.

Uranium, thorium, and rare earths common in Alaskan vein system

A group of en-echelon veins rich in uranium, thorium, and rare-earth elements occurs in a west-northwest-trending fracture system on the eastern flank of Bokan Mountain in Alaska. This vein system lies less than 1 km north of the Cub deposit, the only property in Alaska that has produced uranium. These veins, called the I and L system after claims on their northwestern ends, can be traced for 2.6 km. Geologic studies by M. H. Staatz showed that the veins range in thickness from 0.25 to 152 cm, and, in any one area, there are from one to nine parallel to subparallel veins. These veins, like others in the area, are related to the acmite- and reibeckite-bearing Bokan Mountain Granite. The uranium content of 43 vein samples ranged from 0.005 to 2.8 percent. Thorium and rare-earth contents are also highly variable and range from a few hundredths of a percent to more than 10 percent. The veins also contain abnormal amounts of Ba, Be, Ni, Sr, Sn, and Zr. The mineralogy of the veins is complex; 33 different minerals have been identified, although some occur only locally. Uranium, thorium, and rare-earth minerals include uraninite, brannerite, thorite, allanite, bastnaesite, and xenotime.

Thinning of Fox Hills Formation—a possible guide to uranium mineralization

Geologic studies conducted by H. W. Dodge, Jr., suggested that a relationship exists between areas of thin marine sedimentary rocks of the Fox Hills Formation (Upper Cretaceous) and the uranium mineralization found in the basal portion of the overlying Lance Formation. The Fox Hills Formation is thickest (up to 195 m) in central Niobrara County, Wyoming, where no significant mineralization has been reported. In Crook County, Wyoming, where mineralization is known, the Fox Hills is thin (down to 3 m). It is thought that wedge-shaped Fox Hills aquifer funnels uranium-rich water northward and then upward and laterally into organic-rich (reducing) estuarine, tidal flat, interdistributary bay and fluvial channel deposits of the overlying Lance Formation.

Computer modeling of processes forming uranium roll-type ore

Reaction between oxygenated ore solutions and pyritiferous sandstone results in characteristic alteration zones associated with many uranium deposits in Wyoming. The roll shape of alteration and minor-element zones and the position of ore are explained by the manner in which oxygen is delivered, according to C. G. Warren. Dissolved oxygen is delivered by two different processes: (1) Ground-water movement through the deposit and (2) diffusion toward regions of low concentration. Although fluid transport is generally the more important process, diffusion must be considered because it delivers oxygen to the limbs of the roll and averages out the effects of channelization. A computer-based model for roll deposits permits the rate of flow and diffusion to be evaluated and also evaluates the physical and mineralogical parameters in the formation of deposits with differing geometry.

Chemistry of organic materials associated with uranium ores

Stepwise pyrolysis and gas chromatography were used by J. S. Leventhal to characterize organic materials from the major sandstone uranium deposits. There appear to be four types of material:

- Type 1 is deficient in hydrogen and contains no molecules with more than eight carbon atoms; it has been highly degraded.
- Type 2 contains mainly napthalene, a compound stable to katagenesis, oxidation, and radiation.
- Type 3 is associated with lignites and contains mainly alkanes-alkenes in the range C_{12} to C_{28}.
- Type 4, from mineralized woody material, shows substituted methoxy phenols characteristic of lignite degradation.

The H/C (atomic) ratios of organic materials studied range from approximately 0.3 to 1.5. Samples with high uranium contents often have low H/C ratios.

Uranium in conifer needles

Geochemical and radiometric exploration for uranium in the Northwestern United States is severely hampered by deep weathering and by great variations in soil types. Biogeochemical sampling of needles from Ponderosa pine and Douglas fir trees by J. T. Nash and F. N. Ward in the vicinity of the Midnite uranium mine in Washington demonstrated that this method provides a simple and inexpensive measure of subsurface uranium content. The uranium content of pine-needle ash from trees near the mine ranges from 3 to 200 ppm, in comparison with a background value of about 1 ppm. Values greater than 10 ppm define anomalies above and as much as 300 m from known orebodies.

Thorium veins between Powderhorn and Wet Mountains districts of Colorado

Thorium-bearing veins are sparsely distributed in a few of the inliers of exposed Precambrian rock within a narrow belt between the Powderhorn and Wet Mountains districts of Colorado. On Cochetopa and Razor Creeks, thorium veins occur in sec. 27, T. 47 N., R. 3 E.; secs. 20 and 28, T. 47 N., R. 2 E.; and sec. 3, T. 47 N., R. 2 E. They are as much as 3 m thick and 135 m or more in length in faults or shear zones cutting quartz monzonite of Precambrian X age. A vein near Jacks Creek, in sec. 29, T. 46 N., R. 6 E., contains uranium as well as thorium. Other thorium-bearing deposits are known about 3 km northwest of Sargents and at a locality 2.5 km south of White Pine.

Samples from some veins are relatively low grade, ranging from 50 to 600 ppm Th, but others in the deposit south of White Pine contain as much as 9,000 ppm Th. The scattered concentrations of thorium are of geologic interest because they occur between the 520-million-year alkalic rocks and related thorium deposits of the Wet Mountains and the 570-mililon-year alkalic rocks and related thorium deposits at Powderhorn, 135 km to the west.

Fluvial dispersal patterns of uranium-bearing sandstones in Wyoming

D. A. Seeland found that fluvial dispersal patterns obtained by quantitative measurements of sand-grain shapes and sizes are similar to the patterns obtained by analyzing crossbedding dip directions. This similarity demonstrates the usefulness of textural analysis as a tool for paleogeographic studies.

Quantitative measures of grain shape were found to be particularly accurate indicators of provenance and transport direction. Textural parameters that were measured included maximum grain length, grain elongation, and grain regularity, which is the ratio between area and perimeter squared. These measurements were made on loose sand grains by using an image-analysis system consisting of a microscope, a television scanner, an electronic image analyzer, a small computer, and a plotter.

The sandstones studied are part of the uranium-bearing Eocene fluvial strata of the Wind River and Powder River basins of central and eastern Wyoming. In the Powder River basin, down-basin decreases in sand-grain regularity and elongation are distant and define a paleogeographic framework that almost exactly reproduces the paleogeography obtained from the study of the crossbedding. In contrast, downstream along the Eocene Wind River, in the more linear Wind River basin, trends of grain elongation, regularity, and size are not as well defined, apparently because of sediment contributions from multiple local sources.

Shape factors indicate source areas nearly as well as crossbedding in the Wind River basin and as well as, or better than, crossbedding in the Powder River basin. They provide an alternative to crossbed measurements as indicators of dispersal patterns in fluvial sediments in the subsurface or in areas of poor outcrop.

Uranium residence in granitic rocks

Granitic rocks near the Midnite mine in Stevens County, Washington, and in the St. Francois Mountains of southeastern Missouri are known to contain anomalous amounts of uranium (10–30 ppm), and thus they are likely source rocks for uranium deposits. J. T. Nash's petrographic study of these rocks and of induced fission-track maps of thin sections indicated that more than 80 percent of the uranium is associated with magnetite and that lesser amounts are associated with biotite. The uranium occurs throughout or as rims around magnetite crystals, but its mineralogy has not been established. The fact that most of the uranium is associated with magnetite rather than with refractory minerals such as zircon means that the uranium could be leached easily by hydrothermal or supergene solutions and then could be redeposited in a uranium deposit.

Uranium potential of the Snowy Range Wilderness study area of Wyoming

Geologic studies conducted by R. S. Houston (USGS) and Karl Karlstrom (University of Wyoming) and geochemical studies conducted by W. R. Miller (USGS) indicated that the Snowy Range area of the central Medicine Bow Mountains of Wyoming has good potential for uranium-bearing conglomerate. Radioactive conglomerate is present in feldspathic metaquartzite of the Deep Lake Formation as used by Hills and others (1968) of Precambrian X age in several localities of the north-central Medicine Bow Mountains. These conglomerates are strongly weathered and show evidence of leaching of pyrite; their uranium content is 31 ppm or less. Rocks, water, and stream sediments show no exceptional uranium values, but a pilot geochemical study undertaken by Miller in a key area showed high uranium values in organic material in streams and bogs and exceptionally high radon values in waters from parts of the area near radioactive conglomerate. These high uranium and radon contents suggest that some zone of the conglomerate may be rich in uranium.

Alteration of iron-titanium oxide minerals in uranium-bearing sandstone

Relationships among the iron-titanium oxide and iron sulfide minerals and their alteration products are valuable in interpreting the geochemical histories of roll-type uranium deposits, according to R. L. Reynolds and M. B. Goldhaber. In some deposits, the distribution of these minerals is systematically related to the roll front and thus might be used as an exploration guide. Alteration of iron-titanium oxides in oxidizing environments creates secondary products (hematite) distinct from those produced under reducing conditions (sulfides) Magnetite commonly is totally replaced by sulfide in reduced rock, whereas ilmenite is more resistant to such alteration and is replaced by sulfide only on grain margins. Subsequent oxidation of sulfidized iron-titanium oxides by the processes that formed the uranium roll produces ferric oxide minerals ("limonite") having textures that mimic those of the sulfides.

Radioactive Precambrian conglomerate in the Black Hills

The Estes Conglomerate (middle Precambrian), which crops out in Lawrence County, South Dakota, on the northeastern flank of the Black Hills, contains beds of well-sorted quartz and quartzite-pebble metaconglomerate, estimated to have 5 to 25 percent pyrite in its micaceous matrix. Well-sorted pyritiferous beds and zones in the Estes Conglomerate form distinct radioactive anomalies and are mappable on that basis where they are not covered by deep soil.

Oxidation of pyrite has contributed to the development of zones of deep weathering over radioactive conglomerate, and outcrops are heavily stained and permeated with limonite and hematite. Pyrite is rarely preserved except in deep excavations, such as highway cuts and an abandoned mine that produced gold from radioactive conglomerate. The former presence of pyrite in oxidized outcrops, however, is inferred from abundant pores and vugs, many of which have cubic forms. Analyzed samples of oxidized and leached conglomerate contain up to 40 ppm U and 800 ppm Th.

The middle Precambrian age (probably early middle Precambrian), the pyrite, the radioactivity, and the possible presence of gold, combined with the sedimentological characteristics of the conglomerate, suggests a genetic kinship with deposits at Elliot Lake in Ontario, Canada, and Witwatersrand in South Africa. Estes Conglomerate located below the zone of oxidation and leaching is an attractive prospect for uranium exploration.

Trace elements in Colorado Plateau tabular uranium deposits

Trace-element distributions in tabular uranium deposits determined by R. A. Brooks are very similar to those found in roll-front uranium deposits in Texas and Wyoming. In roll-front uranium deposits, uranium ore lies near the boundary between altered rock and unaltered rock. The altered side is characterized by a concentration of vanadium and selenium, and the unaltered side is characterized by enrichment of molybdenum and mineral carbon. In tabular uranium deposits, megascopic distinction between altered facies and unaltered facies is less obvious, but, typically, vanadium, selenium, and chromium are enriched on one side of the ore and molybdenum and mineral carbon are enriched on the other side. Commonly, but not invariably, there are two subparallel, nearly horizontal zones of uranium enrichment; the trace-element distributions associated with these two zones are commonly mirror images of each other. The vanadium-selenium-chromium zones lie beneath the upper zone and above the lower zone, the molybdenum-mineral carbon enrichments forming an outer rind. The trace-element-distribution pattern is remarkably similar to that found on the altered side of a roll-front deposit at some distance from the ore. The similarity of trace-element distributions suggests that the genetic histories of the two types of deposits are more similar than previous investigations had generally indicated.

Petrology and thorium content of carbonatites in Wet Mountains of Colorado

Carbonatites in the Wet Mountains of Colorado are of two distinctive types, according to T. J. Armbrustmacher. Replacement carbonatites show remanent textures of an originally porphyritic rock with a fine-grained groundmass, similar to lamprophyre dikes of the area, but now consist primarily of carbonate minerals. Primary carbonatites do not show replacement textures; they occur close to or within the alkalic complexes at Gem Park, McClure Mountain, and Democrat Creek, whereas replacement carbonatites have been found as far as 13 km from the nearest known complex. Primary carbonatites contain about 10 times the average amount of total cerium-group rare-earth elements and large average amounts of barium, strontium, lanthanum, and thorium relative to the replacement type. The replacement carbonatites contain larger average amounts of Mg, Ti, Co, Cr, and Ni, elements that tend to be fairly abundant in the lamprophyres.

Genesis of uranium veins in Schwartzwalder mine

Detailed geologic studies of the Schwartzwalder mine and the adjacent area of the Front Range of Colorado by E. J. Young disclosed the presence of Laramide mafic monzonite dikes in the mine area. This finding, along with observations on the epithermal character of vein minerals and wall-rock alteration and the interpretation of sulfur isotope data, suggests a meteoric hydrothermal origin. A model has been developed whereby a small magmatic heat source causes meteoric waters to circulate through nearby sedimentary rocks, leach uranium, and then rise along reactivated Precambrian fault zones to deposit uranium and base metals. This hypothesis suggests that exploration for similar vein-type uranium deposits should focus on contact zones of crystalline and sedimentary rocks having nearby intrusive centers.

Uranium anomaly in the Rio Ojo Caliente

A high uranium value (13 μg/L) found in the water of the Rio Ojo Caliente at La Madera in Rio Arriba County, New Mexico, by K. J. Wenrich-Verbeek and D. B. Collins was further investigated to determine if the stream waters could be used to trace the source of the anomaly. One tributary, Canada de la Cueva, was found to contain 40 μg/L U whereas other tributaries contain less than 3 μg/L U. The source of the anomaly appears to be a hot spring discharging into Canada de la Cueva that contains 60 μg/L U. Thus, surface waters can work successfully as an exploration tool for locating uranium anomalies.

Distal zone of the Cow Springs Sandstone

Careful mapping of the San Rafael Group in the Zith-Tusayan Butte 1 SE quadrangle in Arizona and New Mexico demonstrated that the eolian Cow Springs Sandstone tongues out in a northerly direction into marginal marine sebhka beds of the Summerville Formation at the same stratigraphic horizon and is represented north of the quadrangle only as a few thin, persistent, northerly extending tongues incorporated within the Summerville. Distinct dunes are preserved within some tongues at a few places.

Rocks favorable for uranium in Piceance Basin of Colorado

The Burro Canyon Formation (Lower Cretaceous) of western Colorado is a potential host rock for uranium in the subsurface of the Piceance Basin. Most, if not all, of the physical characteristics considered favorable for the occurrence of uranium-in-sandstone deposits are present in this formation. Studies conducted by L. C. Craig showed that two distinct lobes of thick Burro Canyon sandstone bodies trend northeasterly into the southwestern margin of the Piceance Basin. These lobes may serve to distinguish between more favorable ground and less favorable ground in any exploration of the subsurface of this margin of the basin.

Multiple uranium-copper enrichment zones in breccia pipes

Uranium- and copper-bearing breccia pipes of the western Grand Canyon of Arizona may have a potential for multiple zones of secondary enrichment. Studies conducted by C. G. Bowles showed that the main zone of secondary enrichment underlies the Esplanade surface. In addition, other zones favorable for supergene mineralization are postulated on the basis of geomorphic evidence of canyon widening and geologic evidence of the damming of the Colorado River by lava flows and faults. Several times, dams in the canyon formed lakes that must have recharged previously drained aquifers and reestablished an elevated ground-water table. Stabilization of the ground-water table, either during canyon erosion or, to a lesser degree, following damming of the river, probably created favorable conditions for supergene mineralization.

Uranium deposits related to sedimentary environments

Fred Peterson's basin analysis studies of the Salt Wash Sandstone Member and the lower member of the Morrison Formation in southern Utah indicated that uranium mineralization in the Henry Mountains mineral belt was largely controlled by sedimentary processes. Tabular uranium orebodies occur where there is a close spatial relationship between certain types of lacustrine beds and braided-stream sandstone beds. The particular type of lacustrine deposit that contains uranium consists of laminated or burrowed sandstones and thin, dark gray mudstones containing carbonized plant fragments. Uranium is restricted to areas where this type of lacustrine deposit lies directly above, below, or, in some places, lateral to braided-stream sandstone beds. Uranium is not present where meandering stream sandstone beds and overbank flood-plain deposits separate the lake beds from the braided-stream sandstone or where the lacustrine deposits consist of red beds and gypsum.

These relationships suggest that uranium was transported by oxidized fluids traveling through the braided-stream sandstone beds and was precipitated only where reducing fluids from lacustrine deposits were present. According to this hypothesis, the low Eh waters were present in the formation at the time of deposition rather than brought in at a later time from a considerable distance. Similar relationships between uranium mineralization and depositional processes in other regions suggest that this hypothesis has broad implications for uranium exploration.

Experimental study of pyrite oxidation—implications for uranium-ore formation

Because of the importance of the acid mine drainage problem, previous experimental studies of pyrite oxidation have usually emphasized highly acidic pH conditions. Pyrite oxidation attending the formation of sedimentary roll-type uranium deposits, however, does not occur in this pH range, as is evidenced, for example, by the presence of limonite pseudomorphs after pyrite-marcasite. Accordingly, a study of pyrite oxidation emphasizing the pH range 5 to 9.5 was made. These experiments were conducted at a constant pH, controlled temperature, and constant-oxygen partial pressure. The rate of addition of base necessary to maintain a constant pH was monitored. Samples were withdrawn periodically and analyzed for total sulfur in solution, thiosulfate, and sulfite. Data show that the rate of oxidation at constant-oxygen partial pressure markedly increases with increasing pH, particularly above pH 7. Thiosulfate was found to be an important product during short-term (less than 24 hours) experiments. Sulfite was detected but at a lower concentration than thiosulfate. The results of this study are compatible with the nonbiogenic mechanism of roll-front development previously proposed by Granger and Warren (1969).

Uranium in Triassic rocks in southeastern Utah

Uranium deposits in the Chinle Formation (Upper Triassic) in southeastern Utah are related to specific sedimentary environments. R. D. Lupe reported that rock textures produced by relatively low energy depositional processes appear to have influenced uranium mineralization. The Chinle consists of three fining-upward fluvial-lacustrine sequences, each of which is generally more finely grained than its predecessor. The differences in sediments within each sequence were controlled climatically rather than tectonically because sediment character is similar and transportation trends coincide for each sequence. The fluvial-lacustrine system trended west-northwest from a source east of Moab, Utah, through the San Rafael swell. Uranium minerals are most abundant in the lower part of the lowest sequence in areas where discontinuous distal deposits are overlain by continuous, relatively permeable sandstone deposited in high-energy braided-stream environments. The permeable sandstone acted as conduits for uranium-bearing solutions. Favorable areas for uranium lie on the northern and southern sides of the northwest-trending corridor of predominantly high-energy sediments.

Sulfur isotopes and sulfide petrology elucidate history of roll deposits

Petrologic and sulfur isotope studies conducted by M. B. Goldhaber, R. L. Reynolds, and R. O. Rye characterized the stages of development of a roll-type uranium deposit in the Catahoula Tuff (lower Miocene) of southern Texas. Host-rock preparation in this deposit involved the sulfidization of magnetite and ilmenite by hydrogen sulfide emanating from a fault. Marcasite and pyrite were produced near the fault, and pyrite was produced updip of the fault. The sulfur isotopic composition of the downdip sulfide is about 0 permil, whereas the pyrite further updip is isotopically heavy (+15 permil). Subsequently, oxygenated uranium-bearing ground waters moved downdip and created a redox boundary (roll front). As a result of this process, original iron-disulfide was redistributed (in the absence of hydrogen sulfide) and formed rims around earlier sulfide. The rims are dominantly marcasite near ore, but pyrite rims become more abundant downdip. The stable isotopic composition of this secondary sulfide is extremely light (−25 permil). Sulfate-reducing bacteria were not involved in the origin of this deposit, as organic carbon is everywhere low (<0.1 percent).

Sulfur products of pyrite oxidation

In previous publications, H. C. Granger and C. G. Warren (1969, 1974) stated that limited oxidation of pyrite should yield, on theoretical grounds, either SO_3^{--} or $S_2O_3^{--}$ or both. This theory is in contrast to the frequently cited occurrence of SO (or H_2SO_4) resulting from near-surface weathering of pyrite-bearing rocks and coal. Experiments conducted by Granger and Warren in which air-saturated buffered water is percolated through pyrite-bearing sand and experiments conducted by M. B. Goldhaber in which pyrite is oxidized by bubbling oxygen through pyrite and water at constant pH indicate that, initially, $S_2O_3^{--}$ (plus or minus polythionates) is the dominant aqueous sulfur species formed. These results strongly suggest that SO_4^{--} is not an initial product of the oxidizing systems involved in the formation of roll-type uranium and supergene-enriched sulfide deposits.

Geochemical exploration for uranium in granitic terranes

Uranium typically varies with the thorium and potassium contents of igneous rocks. Because thorium and potassium are not prone to migration under surficial conditions, anomalous concentrations of these elements can be used as a guide to uranium. An evaluation of thorium and potassium results obtained by gamma-ray spectrometry showed that these values should be adequate for exploration purposes (Stuckless and others, 1977). In addition, gamma-ray spectrometry yields RaeU values that can be used as an estimate of uranium contents. Disequilibrium within the upper part of the ^{238}U decay chain may indicate the presence of labile uranium (Stuckless and Ferreira, 1976) and is a criterion for source-rock favorability. Disequilibrium to the extent of 10 percent or more between ^{238}U and ^{226}Ra can be identified by comparing RaeU values with uranium contents obtained by the delayed-neutron technique (Stuckless and others, 1977).

Uranium studies in western Alaska

Reconnaissance petrologic, rádiometric, and geochemical studies were conducted in several parts of western Alaska by T. P. Miller and R. L. Elliott. Attention was focused on this area because of widespread plutonic rocks having above-average uranium and thorium contents and the occurrence of several uranium prospects. Most of the prospects appear to consist of disseminated uranium minerals in intrusive rocks, although vein and pegmatitic deposits may also occur. Dike swarms of aplite and alkaline rocks also appear to be favorable areas for exploration. An association of uranium with fluorite and hematite, with molybdenite, with magnetite, and with unusually large concentrations of allanite was noted in many areas.

A notable mineralized area containing concentrations of uranium, thorium, and rare earths was noted in syenite along the margins of alkaline dikes 24 km northeast of Golovin in the southeastern Seward Peninsula (Miller and others, 1976). Allanite appears to be the principal uranium-, thorium-, and rare-earth-bearing mineral. Grab samples contain as much as 0.15 percent U_3O_8, 1.05 percent ThO_2, and over 2 percent rare earths. The alkaline dikes with which these mineralized rocks are associated are part of a larger dike swarm that crops out over an area of at least 250 km^2 and constitutes a large exploration target.

Mobile helium-detection equipment as a uranium-exploration tool

Helium surveys conducted by G. M. Reimer showed anomalous helium concentrations in soil gas and subsurface water in the vicinity of a known roll-type uranium deposit (Reimer and Otton, 1976). A truck-mobile helium detector (Reimer, 1976) provides rapid quantitative analyses of samples at the field location and can accommodate many variations in the sampling procedure. The results of initial field tests are very encouraging and suggest that helium detection may be at least a useful complementary technique in an integrated geochemical and geophysical uranium-exploration program. The studies also show that helium anomalies occur over known faults.

Depositional environments of the uranium-bearing Cutler Formation of eastern Utah

Deposition of the Cutler Formation in the Lisbon Valley district of San Juan County, Utah, as interpreted by J. A. Campbell (1976), occurred in a transitional area between alluvial fans that formed at the foot of the Uncompahgre Highland to the northeast and a shallow sea to the west and southwest. Depositional environments in this area include (1) fluvial, both braided and meandering; (2) marine, including shallow carbonate, offshore bar, and tidal flat; and, (3) eolian crossbed orientation, which indicates that streams flowed S. 67° W. on the average, marine currents moved sediment S. 36° E. and N. 24° W., and wind transported sand S. 80° E. on the average. Uranium is found in the top 30 to 50 m of the Cutler in arkosic sandstones. Meandering distributarylike streams flowing across flood plains close to sea level, or tidal flats, accompanied by shifting coastal dunes seem to be the setting in which these arkosic sandstones accumulated.

Resistivity study indicates structure of Gettysburg Basin in Pennsylvania

As part of a study of the framework and uranium potential of Triassic and Jurassic basins in the eastern United States, d-c-resistivity soundings made by D. L. Campbell in the Gettysburg Basin of Pennsylvania showed that the western border fault has small displacement and that any major dislocation of the basement would have to be on an unexposed fault inside the basin. In the southwestern part of the basin, the soundings showed the Gettysburg sill, which crops out the length of the basin on the eastern side, to be shallow, thick, and flat lying in the subsurface. In the northeastern part, however, the sill is either missing or deeper than 400 m. Thus, an abrupt subsurface termination or downwarp of the sill is indicated somewhere near Heidlersburg, despite the continuous outcrop of the sill a few kilometers away.

Development of an improved magnetic-susceptibility well-logging system for uranium exploration

A high-sensitivity temperature-stabilized magnetic-susceptibility well-logging system was developed and tested for uranium exploration in sedimentary rocks. It is a well-known fact that altered rocks with low magnetic susceptibility commonly extend updip from roll-front deposits for distances of several thousand meters beyond the limits of roll-type orebodies. This alteration halo constitutes an exploration target many times larger than the uranium orebody itself, so that, if the halo can be detected, the associated uranium deposit can be found with fewer drill holes at wider spacings than would be required otherwise. The magnetic-susceptibility well-logging system is capable of detecting these halos by measuring susceptibilities in the 0- to 100-μcgs range. Typical background values of susceptibility in host sandstones range from 50 to 100 μcgs, whereas halo anomalies range from 0 to 50 μcgs. Reliable detection of these low-level anomalies requires that the drift rate of the measurement system be 20 μcgs/h or less. The USGS system has a drift rate of approximately 10 μcgs/h, which is considerably better than that of available commercial systems.

Electromagnetic methods in uranium exploration

Surface geophysical surveys conducted by B. D. Smith and V. J. Flanigan (Smith and others, 1976; Flanigan, 1976) demonstrated that nonradiometric geophysical methods can be applied to uranium-exploration problems in both crystalline and sedimentary terranes. Two geophysical surveys of sedimentary terranes were conducted in the southern and west-central parts of the Powder River basin of Wyoming. These surveys used total-field-magnetic, very low frequency (VLF), and induced-polarization (IP) methods. The geophysical data suggest that subtle anomalies are associated with uranium roll fronts. A number of general observations were made from the surveys. Negative magnetic anomalies tend to be associated with uranium mineralization. However, these anomalies may be masked, in part, by anomalies caused by the variation of magnetic minerals not controlled or influenced by the processes effecting uranium deposition. IP surveys commonly show uranium mineralization to be bound on one side or on both sides by high resistivity and high IP response. The IP response is probably controlled by the nature and distribution of sulfide and clay minerals. A surprising result of the surveys was the association of tilt angle and (or) apparent-resistivity VLF anomalies caused by shallow (<10 m) sources with deeper uranium mineralization (>50 m).

In crystalline terranes, Turam, Slingram, and VLF electrical methods and the total-field-magnetic method were used to define large-scale geologic features such as faults that can have an important association with uranium mineralizaton. Geophysical surveys at the Schwartzwalder mine in Colorado were successful in defining conductive fault zones. The magnetic-field survey was useful in the geologic mapping of lithologies having different magnetic signatures where exposures are poor or nonexistent.

Uranium in mercury deposits in McDermitt caldera of Nevada and Oregon

The McDermitt caldera on the Nevada-Oregon border contains the Bretz, McDermitt, and Opalite mercury deposits and is one of the major centers of mercury mining in the United States. These deposits are found in sedimentary rocks that are altered to smectite clays and adularia and locally are silicified to opalite. Recent examination of the deposits by J. J. Rytuba revealed that some of the opalite contains uranium in concentrations as great as 520 ppm. Sedimentary rocks outside the caldera are zeolitized to clinoptilolite and erionite and do not contain opalite.

GEOTHERMAL RESOURCES

Geothermal studies on Adak Island, Alaska

Preliminary geothermal studies conducted by T. P. Miller and R. L. Smith on northern Adak Island in Alaska indicated that the Mount Adagdak and Andrew Bay Volcanoes consist chiefly of dacitic andesite domes with SiO_2 contents of up to 61 percent. Potassium-argon age measurements made by G. B. Dalrymple indicated that volcanic activity at Mount Adagdak occurred approximately 0.15 to 0.34 million years ago, whereas Andrew Bay Volcano is about 0.8 million years old. The age range of Moffett Volcano is unknown; an andesitic dome on the eastern side of the volcanic complex, however, yielded an age of less than 0.3 million years.

Geochronology of Mount Drum and Mount Sanford in Wrangell Mountains of Alaska

M. A. Lanphere and G. B. Dalrymple, in cooperation with T. P. Miller, R. L. Smith and D. H. Richter, completed a detailed K-Ar study of Mount Drum and Mount Sanford in the Wrangell Mountains of Alaska. The formation history of Mount Drum, a stratovolcano that rises more than 3,000 m above the surrounding plain, is complex but may be roughly divided into two cycles. Each cycle consisted of an andesitic cone-building phase followed by the emplacement of dacitic domes. The K-Ar dating indicates that first-cycle activity began about 550,000 years ago and lasted less than 100,000 years. This cycle was followed quickly by second-cycle andesitic volcanism and finally by the emplacement of the latest dacitic domes. Second-cycle activity occurred from about 450,000 to 230,000 years ago.

Mount Sanford, a stratovolcano that rises to an elevation of more than 4,800 m is older than Mount Drum and consists primarily of andesitic lavas that were erupted from about 700,000 to 830,000 years ago. Cone building was followed by emplacement of a few dacite and rhyolite domes about 500,000 to 600,000 years ago.

San Francisco volcanic field of Arizona

Geologic mapping and related studies conducted by R. F. Holm, R. B. Moore, G. E. Ulrich, and E. W. Wolfe in the San Francisco volcanic field of northern Arizona indicated that the central part of the field, including the San Francisco Mountain stratovolcano and a 15-km-wide belt west and south of the stratovolcano, are characterized by a striking paucity of alkali-olivine basalt vents. Volcanism in this area has been predominantly andesitic, with differentiated products that range from andesite to rhyolite occurring in both small and large eruptive centers. Basaltic rocks in this association are alkalirich high-alumina basalts rather than the alkaliolivine basalts that are widespread throughout much of the volcanic field. This central andesite zone may imply the existence of a young (probably less than 1 million years old) magma chamber underlying a much larger area than the San Francisco Mountain stratovolcano occupies. Occurrence of a few young alkali-olivine basalt vents in the western part of the zone may indicate local solidification of the magma chamber about 0.5 million years ago. No young alkali-olivine basalts are known in the eastern part of the zone, where the San Francisco Mountain stratovolcano was still being formed about 400,000 years ago. Potassium-argon dating (Damon, Shafiqullah, and Leventhal, 1974; P. E. Damon and M. Shafiqullah, written commun., 1976) of rhyolitic domes and flows on the eastern side of San Francisco Mountain indicates that the magma system was active as recently as 200,000 years ago.

Potential geothermal field in Clear Lake area of California

J. M. Donnelly, F. E. Goff, J. M. Thompson, and B. C. Hearn, Jr. (1976), found that the geochemistry of thermal waters in The Geysers-Clear Lake area of California, in combination with geologic mapping and geophysical data, indicate that a 200°C hot-water system underlies all of the 2.0- to 0.01-million-year-old Clear Lake Volcanics northeast of the Collayomi fault zone, which is probably the northeastern boundary of The Geysers steam field. The 80 or more vents in the volcanic field may act as pipes for water recharge in sufficient volume to prevent the creation of a widespread vapor-dominated system beneath the volcanic field. Although small steam reservoirs could exist locally in favorable structures, their waters are not reaching the surface in any of the springs or wells sampled. Areal distribution of chloride concentrations, which are distinctive for the Great Valley sequence, indicate the subvolcanic extent of the Great Valley sequence on top of Franciscan assemblage. Springs having high chloride contents northeast of Clear Lake, in terrane shown as entirely Franciscan on published maps, suggest the presence of the Great Valley sequence and thus indicate either that the surface exposures are incorrectly identified or that the Great Valley sequence is present at depth, overthrust by Franciscan assemblage.

Geophysical studies of the Coso geothermal area of California

The Coso Mountain area of southern California, the scene of very recent volcanism, is considered to be a major geothermal prospect. In conjunction with exploratory geophysical investigations, the USGS established a 16-station telemetered seismic network at Coso in September 1975. H. M. Iyer, C. S. Weaver, A. M. Pitt, and A. W. Walter reported a very high level of local seismicity during the first 6 months of monitoring, over 2,000 events being located. Although the majority of these events were small ($0 \leq m_L \leq 3$), five events with $m_L > 3.6$ occurred. These larger events were followed by aftershock sequences, which usually lasted from 3 to 10 days. Two earthquake swarms occurred; the largest, on December 12, 1975, consisted of over 500 events in approximately 10 hours. All of the swarm-event locations were accurately determined and were found to be clustered tightly along a fault plane at depths ranging from 4 to 8 km.

The composite results show a complex pattern of activity. Although mapped faults are abundant throughout the area, much of the seismicity cannot be associated easily with specific surface features. The locus of activity exhibited spatial variations over the time scale of a month and shifted abruptly from one distinct area to another. The temporally integrated activity revealed a consistent pattern of epicenters that formed radial "arms" trending away from the center of the volcanic field. The major geothermal area, however, near Coso Hot Springs, appeared to be less active seismically than the surrounding areas. In addition, there were several broad areas having little or no observed activity. Although most of the young faults in the area show normal offsets, the majority of the focal-mechanism plots reveal strike-slip motion, often along nearly vertical planes. Regional north-south compression is consistent with all the fault-plane solutions.

Preliminary results obtained from the inversion of teleseimic residual data in the Coso geothermal area show that the weak *P*-delay anomaly to the south of Coso Hot Springs may be caused by a plug of low-velocity material with roots deep in the crust. Most detailed work will be required to confirm this hypothesis.

Weaver and Walter also reported that a 37-km-long reversed seismic-refraction profile was established in a northeasterly direction across the Coso Hot Springs geothermal area in October 1976. Preliminary results indicate that *P*-wave velocities are between 2.8 and 3.3 km/s in the uppermost crust. A second layer having *P*-wave velocities between 5.5 and 5.7 km/s appears to dip slightly to the southwest toward the Sierra Nevada. This layer is interrupted by a north-south normal fault zone, which contains the Coso Hot Springs. The eastern side of the basement is downdropped relative to the western side across this fault zone, and *P*-wave velocities appear to be lower on the west (5.5 km/s) than they are on the east (5.7 km/s).

D. B. Jackson reported that d-c soundings in the Coso ring structure (Duffield, 1975) show a near-surface conductive layer 250 to 650 m thick overlying a very high resistivity layer of indeterminate thickness in the Devil's Kitchen area. Since the Sierran granitic basement rocks in most of the Coso Range have resistivities less than 200 Ω-m, it seems probable that the near-surface conductive layer is a highly altered impervious layer capping a high-temperature steam zone at depth in the fractured granitic basement rocks. As far as 5 km east of Coso Hot Springs, in what was thought to be an area of granitic rocks covered with a fairly thin mantle of basaltic lava flows, d-c soundings suggest thicknesses of up to 1,500 m of material having resistivities of less than 50 Ω-m. This anomalous area could represent highly fractured rocks containing hot waters, although there are no hot springs present and the only heat-flow value thus far reported from near the west-central part of the area is 3.7 HFU (Upton and others, 1976).

Long Valley caldera in California

The first deep geothermal test well in the Long Valley caldera of eastern California was drilled by the Republic Geothermal Company in May and June of 1976 to a depth of 2,109 m in the east-central part of the caldera. The USGS previously made extensive geologic, hydrologic, geochemical, and geophysical surveys in the caldera, using it as a "type" example of a large caldera-related geothermal system, but lacked deep-drill-hole information by which the various surveys could be "calibrated" (U.S. Geological Survey, 1976a). D. E. White coordinated USGS well-logging surveys and other activities with Republic's drilling activities.

The well penetrated a very thick section of intracaldera welded Bishop Tuff. For geothermal purposes, the well proved disappointing; temperatures did not rise above 100°C, and a broad temperature reversal was found through the middle part (specific data have not yet been released). Although the Republic hole did not reach temperatures high enough for exploitation, it did provide an excellent opportunity to calibrate various geophysical methods used in geothermal evaluation. In the Long Valley environment, electrical methods and seismic noise are so strongly influenced by the shallow regime (<1 km) that the most geothermally significant depths of 1 to 3 km are obscured. Seismic-refraction, passive-teleseismic, self-potential, and geochemical surveys all indicate that geothermal potential is greater in the central resurgent area than it is in the eastern area, which was included in the Bureau of Land Management lease sales.

R. O. Fournier, M. L. Sorey, R. H. Mariner, and A. H. Truesdell reevaluated chemical and isotopic data for thermal and nonthermal waters from the Long Valley region and concluded that an aquifer with 280°C water is present somewhere in the hydrothermal system. The highest previously estimated aquifer temperature was 220°C. These new figures increase the estimated convective heat flow from 4.3×10^7 to 6.6×10^7 cal/s.

Temperatures measured by W. H. Diment and T. C. Urban in seven shallow (<300 m) holes and one deep (2,000 m) hole in the Long Valley caldera indicate a pattern of subsurface temperatures much more intricate than investigators had supposed.

R. A. Bailey's continuing mineralogical and geochemical studies of the volcanic rocks associated with Long Valley caldera suggested that the subjacent magma chamber, which is the heat source of the associated active geothermal system, has been replenished with magma at least twice in postcaldera time. These results confirm in general the conclusions reached by Lachenbruch and others (1976) on the basis of heat-flow studies and are in agreement with evidence obtained from teleseismic *P*-delay studies (Steeples and Pitt, 1976) that the caldera is still partly underlain by molten magma. Analysis of major-, minor-, and trace-element data and rare-earth-element distribution patterns shows that the volcanic rocks fall into three distinct compositonal groups separated by well-defined compositional gaps. Within the groups are second-order compositional trends that can be attributed to subsequent differentiation under oxidizing conditions. The individual groups are interpreted as being generated in a deep source, and the secondary trends are interpreted as being the result of high-level differentiation in the magma chamber. The data imply that, after the magma chamber was formed between 1.9 and 0.9

million years ago and partially emptied 0.7 million years ago by eruption of the Bishop Tuff (Bailey and others, 1976), the chamber was replenished wth new batches of magma 0.6, 0.3, and 0.1 million years ago; this resupplying of additional heat has prolonged the life of the geothermal system as well as its economic potential.

A conceptual model of the hydrothermal system in the Long Valley caldera was developed and analyzed by M. L. Sorey, R. E. Lewis, and F. H. Olmsted on the basis of results from previous geologic, hydrologic, geophysical, and geochemical studies (Muffler and Williams, 1976; Fournier and others, 1976). A hot-water reservoir was assumed to exist in the fractured, densely-welded Bishop Tuff and to be continuous over the area of the caldera at depths of 1 to 3 km. As was indicated by the isotopic contents of caldera waters, water-table altitudes, and the relatively cool temperatures measured in a recently drilled 2 km-deep test hole east of Hot Creek, recharge to the hydrothermal reservoir is simulated around the western and northeastern caldera rims; discharge is simulated along Hot Creek gorge and through the southeastern rim. Modeling results yield estimates of 30 to 350 mD for the effective permeability in a 1 km-thick reservoir. Present-day heat-flow and reservoir temperatures could be sustained for a 35,000-year period of hot-spring discharge with a circulation of 1.5 to 2.5 km and magma at a depth of 6 km under the western half of the caldera; continuous hydrothermal activity over the last 300,000 years requires a circulation of 4 to 5 km. Simulated reservoir temperatures of 50° to 80° C east of Hot Creek are close to measured temperatures in the deep test hole.

Chemical and physical characteristics of low-temperature geothermal systems in Colorado

R. E. Moran coordinated a cooperative study done by the USGS, the Colorado Geological Survey, and the Colorado Department of Natural Resources' Division of Water Resources to evaluate geothermal resources throughout Colorado. All significant hot-spring systems in Colorado were sampled to determine all major and many minor chemical constituents. In addition, subsurface reservoir temperatures at all sites were calculated by using a silicon dioxide model, a sodium-potassium model, a sodium-potassium-calcium model, and mixing-model geothermometers. The data indicate that most of these hydrothermal systems will produce only hot water and that little or no steam generation is possible.

An exploration program using surface-geophysical techniques was initiated in the Upper Arkansas-Northern San Luis Valley region. Preliminary data indicate the presence of a continuous low-resistivity region connecting these two valleys. The presence of this region indicates that the geothermal reservoir, which is evidenced by the hot springs in both valleys, may be continuous under Poncha Pass.

Magma chambers and volcano structure in Hawaii

F. W. Klein used the seismic network on Kilauea Volcano and on the island of Hawaii to obtain accurate locations for local earthquakes. These earthquakes are the key to understanding the seismic deformation of the volcano and the fault systems and stresses related to magma chambers. The seismic network also makes it possible to obtain inversions for the volcano's velocity structure by means of local and teleseismic earthquake sources. Results of inversions indicate that velocities in eruptive centers are higher than those in surrounding regions and that a low-velocity layer exists at the base of the crust under Hawaii.

A detailed seismic survey of Kilauea Iki revealed high microearthquake activity in the lava crust overlying the still-cooling magma body there. This activity is believed to be associated with the contraction of rocks immediately above the melt. By systematically mapping the microearthquake frequency at various positions on the lake flow, one can generally outline the boundary of the magma body.

Very low frequency radio signals from transmitters operated by the U.S. Navy were used as the energy source for mapping the lateral extent of molten rock trapped within Kilauea Iki crater. Transmitter stations located at Lualualei on the island of Oahu and at Jim Creek, Wash., operating at frequencies of 23.4 and 18.6 kHz, respectively, provided signals oriented orthogonally in such a way that the entire perimeter of the lava lake could be mapped effectively. Tilt angle and resistivity measurements at both frequencies were made at each survey station. Resistivity measurements made with the electric field perpendicular to the edge of the conductor were found to be most definitive in interpreting the data with respect to locating the edge of the molten material.

Raft River geothermal area of Idaho

Geophysical, geologic, and hydrologic studies of the Raft River geothermal area in southern Idaho continued in 1976. W. H. Diment and T. C. Urban made temperature measurements in four shallow holes and one deep hole in the Raft River valley. Preliminary results indicate a regional gradient of about 50°C/km and a corresponding heat flow of 2.5 to 2.75 HFU. These holes are apparently outside the zone of high shallow temperatures known to exist in the Raft River valley. Nevertheless, they are valuable in helping to delineate the size of the thermal anomaly in this region.

S. S. Oriel and H. R. Covington examined cuttings, core, and borehole geophysical data from the three deep geothermal exploration holes drilled by the Energy Research and Development Administration near Bridge, Idaho, in the Raft River basin and confirmed that the deep-circulation convective system is controlled by faults and that horizontal water movement is primarily fracture controlled rather than intergranular.

The first two deep exploration holes penetrated a silica cap rock beneath which hot (146°C) water under artesian conditions was encountered in a highly fractured zone. Continued drilling in both holes produced cooler temperatures and fewer fractures below the production zone. The third deep exploration hole encountered few open fractures, but alteration of the rock and healed fractures suggested past or nearby activity. Offset drilling from the third hole produced high-temperature (146°C) water under artesian conditions from fractured zones. Implications are that the geothermal system is self-sealing and that hot (+145°C) water may be found at depths near any young fault within the Raft River basin.

Exploratory drilling for geologic and hydrologic data continued in the Raft River geothermal area during 1976 with the completion of two wells, each approximately 370 m deep. E. G. Crosthwaite reported that flowing water with a surface temperature of 65°C was unexpectedly found at a depth of 45 m in one well. The other well found rhyolitic rock interbedded in sediments shed from a major Basin-and-Range-type fault. The data developed from the drilling program and recent geologic and geophysical investigations are being used to construct digital hydrologic models of both the cold- and the hot-water systems.

Geothermal potential of the Sugar City area of Idaho

Continued geologic mapping and related volcanic studies conducted in the eastern Snake River Plain of Idaho by H. J. Prostka, augmented by interpretation of gravity and hydrologic data, suggested that a large Pliocene caldera complex may be centered beneath the Rexburg Bench, an area of very high heat flow. Hot water in wells near Newdale and the Teton damsite and hot springs at Heise and Canyon Creek all appear to be localized within the caldera ring-fracture zone. Sugar City, located above a subsided and buried part of this zone, is favorably situated for the geothermal-resource development recently proposed for this area. Much additional geologic and geophysical work is needed to better define the extent of the reservoir and the temperature variations within it.

Temperature surveys at 1-m depth in Nevada

Synoptic temperature surveys made at a depth of 1 m in the Soda Lakes and Upsal Hogback areas of the western Carson Desert in Nevada were tested as a reconnaissance method of geothermal exploration by F. H. Olmsted. Correlative data consisted of temperatures and temperature gradients measured in test holes ranging in depth from 10 to 45 m—depths beyond the significant influence of seasonal fluctuations in solar-energy input. The best correlation between temperatures at 1 m and those at 20 m or deeper was obtained where a boiling water table was present at depths of only a few meters, where temperatures and temperature gradients were far above background values, and where corresponding heat flows were hundreds to thousands of times larger than background values. The poorest correlation was found where temperatures and temperature gradients were only slightly to moderately above background values and heat flows were a few times to a few tens of times larger than background values. Large areal variations in geology, topography, depth to the water table, and other perturbing factors greatly limit the effectiveness of 1-m temperature surveys in delineating temperature and heat-flow anomalies at greater depths.

Geothermal assessment of Newberry Volcano in Oregon

Newberry Volcano in central Oregon is a broad shield-shaped volcano with a summit caldera. Its volume equals or exceeds the volumes of the larger stratovolcanos of the nearby Cascade Range. Previous geologic studies (Williams, 1935; Higgins, 1973) have been confined largely to the caldera, where both basalt and rhyolite have erupted in Holocene time. On the basis of limited reconnaissance, the flanks of the volcano have been assumed to be formed of numerous basalt flows, but Holocene ash- and pumice-fall deposits from both Newberry Volcano and Mount Mazama cover much of the flanks to depths of as much as 6 m and obscure older rocks. Geologic mapping by N. S. MacLeod indicated that, although basalt flows are abundant, ash-flow tuffs of intermediate to silicic composition are widespread on the flanks. They are particularly abundant on the eastern and western flanks but may also be widespread on the north and south below younger basalt flows. The large volume of some of the ash-flow-tuff units suggests that some may be related to the initial stage of caldera formation. Rhyolites, which were previously known to occur mainly in the caldera area, are also widespread on the flanks; 12 dome and vent areas have been identified on the flanks. In addition, rhyolite domes and flows of the caldera walls apparently extend at least 4 km outward from the walls, where they form a conspicuous break in slope on the upper flanks of the volcano. The abundance of Quaternary rhyolite surrounding the summit caldera and on the flanks suggests that the volcano may have an even higher geothermal potential than investigators had thought previously and that some of this resource may lie outside the caldera, which has been withdrawn from geothermal development.

Hydrothermal alteration studies of drill core from Yellowstone National Park in Wyoming

T. E. C. Keith, D. E. White, and M. H. Beeson made detailed studies of drill core from research holes Y–7 and Y–8 drilled in the northern part of the Upper Geyser Basin of Yellowstone National Park in Wyoming in 1967 (White and others, 1975). Hole Y–7 is 73.6 m deep, has temperatures up to 143°C and no excess fluid pressure, and thus is outside the present upflow system. Hole Y–8, 130 m southeast of Y–7, is 153.4 m deep, and has temperatures up to 170°C and fluid pressures up to nearly 2.5 b, all of which indicate the direct influence of upflowing fluids. The permeability of the well-sorted obsidian-bearing sands and gravels between the two holes has decreased greatly in response to devitrification, solution, and deposition of hydrothermal minerals, largely in initial pore spaces.

The principal hydrothermal minerals of Y–7 are the high-silica zeolites clinoptilolite and mordenite, the metastable silica minerals opal and cristobalite, and montmorillonite clays. The more intensely altered core of Y–8 includes zones of the same minerals, but, in other prominent zones, quartz and analcime have replaced the less stable clinoptilolite and cristobalite; celaconite is the dominant clay mineral. Below a depth of 27 m in Y–8, hydrothermal potassium-feldspar occurs with analcime and quartz, probably forming from excess potassium in the potassum-rich clinoptilolite. Calcite in Y–8 seems to occur where a rapid upward decrease in fluid overpressure caused localized boiling, loss of CO_2 to vapor with a consequent increase in pH, and conversion of bicarbonate to carbonate in the water.

A detailed study of veinlet mineralogy and paragenesis indicates that first-formed minerals are generally the most soluble and least stable and, in time, are converted into more stable minerals. Major factors influencing the formation of hydrothermal minerals are the abundance and reactivity of obsidian as the dominant unstable starting material, elevated temperature, permeability, silica activity, and fluid composition. During conversion of clinoptilolite-cristobalite to analcime-quartz, much potassium is dissolved (even though it is offset in part by the deposition of potassium-feldspar). The decrease in Na-K in the liquid is the opposite of what would be expected of a high-temperature water cooling and reacting with rocks; this phenomenon demonstrates that the cation geothermometer used so widely in predicting subsurface geothermal-reservoir temperatures must be applied with caution to zeolite-cristobalite mineral assemblages.

The initial lithologies of core from the two drill holes are very similar and indicate high horizontal permeabilities. Thus, present contrasts between the wellhead pressures of the two holes at equivalent depths provide strong evidence for horizontal self-sealing, a process that has important economic consequences in controlling the productive parts of geothermal reservoirs.

Keith and L. J. P. Muffler reported that the ash-flow tuff penetrated by research drill hole Y–5 in Yellowstone National Park has undergone a complex history of crystallization and hydrothermal alteration since its emplacement 600,000 years ago. While the glassy groundmass was cooling down from magnetic temperatures, it underwent either devitrification to alkali feldspar + α-cristobalite $\pm$ tridymite or granophyric crystallization to alkali feldspar + quartz. Associated with the cores of granophyric crystallization are prismatic quartz crystals in miarolitic cavities. Vapor-phase alkali-feldspar, tridymite, magnetite, and sporadic α-cristobalite were deposited in miarolitic and lithophysal cavities and in the void space of pumice fragments. Subsequently, some of the vapor-phase alkali-feldspar crystals were replaced by microcrystalline quartz, and the vapor-phase minerals were frosted by a coating of saccharoidal quartz.

Hydrothermal minerals occur primarily as fillings in cavities and fractures and as alterations of mafic phenocrysts. Chalcedony, the dominant mineral related to the present hydrothermal regime, occurs as microcrystalline material mixed with varying amounts of hematite and (or) goethite. The chalcedony displays intricate layering and banding and was apparently deposited as opal from silica-rich water. Hematite and goethite also occur as replacements for both mafic phenocrysts and vapor-phase magnetite. Other prominent hydrothermal minerals include montmorillonite pyrite, mordenite, calcite, and fluorite. Clinoptilolite, erionite, illite, kaolinite and manganese oxides are sporadic. The hydrothermal minerals show little correlation with temperature, but bladed calcite is restricted to a zone of boiling in the tuff and clearly was deposited when CO_2 was lost during boiling.

Hole Y-5 differs from the other research drill holes in Yellowstone in that it contains common fractures and breccias filled with chalcedony that cannot be interpreted readily as tectonic. It is more likely that they were produced by explosive disruption of the rock caused by a sudden decrease in hydrostatic pressure, perhaps owing to the rapid drainage of an overlying glacial lake. The chalcedony was either deposited very rapidly as a silica floc or else a preexisting floc was moved rapidly into fractures produced during hydrothermal explosion.

CHEMICAL RESOURCES

LITHIUM

Lithium in soils and stream sediments reflects lithium-bearing pegmatites

In the arid environment of Taos County, New Mexico, lithium was detected by W. R. Griffitts in alluvial sediments 1.2 km from known lithium-bearing pegmatites; mineralogic or chemical analyses of panned concentrates detected lithium at even greater distances because of the persistence of spodumene and lepidolite in the sediments. The lithium content of soils is higher above lithium-rich pegmatite than it is elsewhere, even though about 30 m of amphibolite occur between the pegmatite and the soil. Thus, lithium can penetrate metamorphic rocks during staurolite-level metamorphism, and this penetration might indicate deeper pegmatite deposits.

Geophysical characterization of lithium-brine deposits in Clayton Valley of Nevada

Direct-current-resistivity soundings were used by B. D. Smith to explore for lithium-bearing brines and to map the general location of the interface between known brines and fresher water in the Clayton Valley of Nevada. The lithium-rich brine was correlated with a thick sequence of very conductive sediments. Another sequence of conductive sediments, defined by geophysical survey, occurs below the lithium-producing brine and may be a target for future brine production. In addition, electromagnetic soundings with a ground-wire source confirmed the presence of thick sequences of conductive sediments at Willcox, Ariz., and at the so-called "Luke Salt" body near Phoenix, Ariz., that may contain lithium-bearing brines.

Migration and accumulation of lithium in the near-surface environment

C. L. Smith reported that background lithium in Nevada hot springs is as high as or higher than background lithium in ambient-temperature springs. Investigation of a lithium anomaly in two springs, defined by lithium-to-chloride ratios, led to the discovery of high lithium and potassium surface brines currently being generated on the Fish Lake Valley playa in Nevada. Lithium concentration in an exposed 2-m-thick bed of volcanic ash varied from 120 ppm at the top to 650 ppm in the middle to 210 ppm at the bottom. The ash bed is an aquifer for ground water having a lithium concentration of 0.4 ppm.

High-temperature waters consistently high in lithium relative to other constituents

High-temperature waters are consistently high in lithium relative to other constituents and thus are possible source waters for lithium-rich nonmarine evaporites such as the Searles Lake brines and the recently discovered brines in Bolivia.

D. E. White, J. M. Thompson, and R. O. Fournier (1976) found that the relatively dilute thermal waters of Yellowstone Park in Wyoming have an average lithium content of about 3 ppm and a lithium-to-chloride ratio of about 0.01, which is near the upper concentration ratio for natural waters. The calculated discharge of lithium from Yellowstone Park is about 480 t/yr, or 48×10^6 t over the probable minimum duration of 100,000 years. Because of its climatic environment, Yellowstone's lithium is dispersed in river water and eventually in ocean water and associated sediments. But, in an environment favorable for evaporative concentration, such as the Long Valley-Owens River-Searles Lake system of California, and perhaps in a similar system in the Clayton Valley of Nevada, the lithium in high-temperature geothermal waters can become concentrated in commercial deposits.

The Salton Sea geothermal brine (350°C and 26 percent salinity) has about 215 ppm Li, a lithium-to-chloride ratio of 0.0014, and an estimated 1.0×10^6 t

Li in 5 km^3 of brine (White, 1968). This very large potential lithium resource is not yet commercially usable, in spite of its great heat content and other valuable constituents, because of the unsolved chemical problems of corrosion and scaling.

Lithium demand limits exploration

J. D. Vine reported that a new estimate of lithium resources in the United States indicates that about 10 percent of the reserves and identified resources and about 13 percent of the probable future resources are in lithium-rich brines. With the discovery of new brine fields in South America, lithium brines now constitute about two-thirds to three-fourths of the total world resource. Thus, a gradual shift in emphasis to the production of lithium from brines rather than from pegmatites would seem to be indicated. The demand for lithium products, however, has not caught up with industrial capacity, so that industry finds little incentive to explore for lithium-rich brines, rocks, and clays in the United States, even though predictions of future demand far exceed current capacity.

Lithium distribution in Cenozoic alluvium

J. R. Davis (1976) found that alluvium associated with through-flowing streams has the lowest lithium values of any Cenozoic fine-grained alluvial sediments in the Western United States. Holocene and Wisconsinan samples from playas have higher values, and Sangamon and Illinoian(?) sediments from interpluvial playa lakes tend to have the highest values. This trend indicates the importance of restricted surface drainage and dry climatic episodes in the process of concentrating lithium in sediments.

Lithium-rich tin and oil-shale deposits

E. B. Tourtelot reported that samples of granite and vein material from the El Paso tin district of Texas contains as much as 1,300 ppm Li. Tin-bearing rhyolite from the Black Range in New Mexico contains 100 to 200 ppm Li. Samples containing more than 1,000 ppm Li were collected from sections containing oil shale of Oligocene age near Lincoln, Mont., whereas oil-shale sections in the Green River Formation (Eocene) in Wyoming contain 100 to 200 ppm Li.

Lithium occurrences in sedimentary environments

R. G. Bohannon reported that lithium-rich Tertiary rocks are widely exposed in the vicinity of the Muddy Mountains and White basin in Clark County, Nevada. The rocks were deposited in a large basin that contains coarse clastics overlain by carbonates and chemically precipitated rocks. Lithium occurs mostly in the chemical precipitates, probably in the mineral hectorite.

Lithium in flint clays from Pennsylvania and Maryland

Flint clays commonly contain about 1,000 ppm Li (Tourtelot and Meier, 1976). Samples collected by H. A. Tourtelot from Pennsylvania and adjacent Maryland showed both regional and local variations in the lithium contents of megascopically similar materials. Maximum lithium concentrations in the samples ranged from 330 ppm in central Pennsylvania to 2,100 ppm in Clinton County, Pennsylvania.

The mode of occurrence of the lithium is not yet known. Mica-rich flint clay in central Pennsylvania contains relatively small amounts of lithium, the suggestion being that the detrital mica is a dilutant of lithium rather than a source. A spherical nodule of diaspore about 10 cm in diameter from central Pennsylvania consists of an inner core of diaspore (40 ppm Li), a dense inner ring of presumably mixed diaspore and kaolinite (280 ppm Li), an outer ring that appears to be predominantly kaolinite (2,050 ppm Li), and a flint-clay matrix of kaolinite (1,200–1,400 ppm Li). These data suggest that lithium is concentrated either in kaolinite or in a presently unknown mineral by the process that forms the diaspore nodules. Many, but not all, of the flint clays in Pennsylvania having large concentrations of lithium also contain oolites that seem to be diaspore.

PHOSPHATE

California phosphorite

A. E. Roberts reported that phosphorite deposits in the Santa Margarita Formation of late Miocene age in the Cuyama Valley of California are a potential resource for phosphate. The deposits occur in two stratigraphic zones—a lower zone (10 m thick) at the base of the formation and an upper zone (50 m thick) 100 m above the base. The zones generally consist of pelletal sandy siltstones and phosphatic mudstones interbedded with porcelaneous siltstones and diatomaceous shales. The upper zone averages 4.25 percent P_2O_5, and the upper 25 m averages 5.25 percent P_2O_5. The phosphatic grains in the deposits are very fine to medium sand-sized pellets and coarse sand-sized to medium pebble-sized nodules. The pellets are structureless aggregates of microcrystalline carbonate-fluorapatite, and the nodules are microcrystalline aggregates or aggregates of pellets in a phosphatic clay matrix. Most pellets contain varying amounts of detrital material consisting generally of quartz, feldspar, microfossils (diatoms or forams), or shell fragments. Sedimentary structures and faunal assemblages in the phosphatic zones indicate a nearshore shallow-water marine environment having prolonged calm-water conditions interspersed with occasional high-energy-current conditions that winnowed away the fine-grained material and rounded the pellets.

Precambrian phosphorite discovered in Michigan

W. F. Cannon and J. S. Klasner (1976) reported that phosphatic pebbles are widespread in basal units of the Marquette Range Supergroup (about 2 billion years old) in the central part of the northern peninsula of Michigan. At one locality, a conglomeratic bed about 15 m thick averages about 15 percent phosphorous pentoxide (P_2O_5). Many thinner beds are of comparable grade. This occurrence is one of the oldest sedimentary phosphate deposits in the United States and is believed to be the richest deposit in the Precambrian of the United States. Although outcrops in the region are generally scarce, similar but lower grade material has been found at four other localities, the suggestion being that important phosphate deposits may be concealed by the extensive cover of glacial material.

Phosphate resources in southern land-pebble district of Florida

Estimates that deposits of phosphate rock in Florida will be depleted by the year 2000 have caused considerable concern. J. B. Cathcart reported that recent drilling showed that there may be much more minable phosphate in the Hawthorn Formation of southern Florida (Hardee, Manatee, and DeSoto Counties) than investigators had thought previously. In addition, large areas reported to be "barren" are now known to contain potentially minable deposits. Early drilling stopped at the first bed too hard to penetrate with the hand auger. Machine drilling has now proved that possibly economic deposits underlie hard, thin (1–2 m) carbonate lenses stratigraphically above the more massive carbonate "bedrock" of the northern part of the phosphate district in Polk and Hillsborough Counties.

BENTONITE

C. A. Wolfbauer found that bentonites in the Bearpaw Shale (Upper Cretaceous) of northeastern Montana are commonly less than 30 cm thick. Individual beds thicken and thin and are locally absent. Beds are markedly thicker in outcrop than they are in drill core. Most outcropping beds are gypsiferous, and some contain calcareous concretions up to 1 m in diameter. Bentonites in this area have high green-compression strengths and moderate to high dry-compression strengths and are best suited for use in taconite pellets and foundry sand.

REGIONAL GEOLOGIC INVESTIGATIONS

NEW ENGLAND

Deglaciation of the Hamburg quadrangle of Connecticut

Mapping done by R. M. Barker of the surficial geology of the Hamburg quadrangle in southeastern Connecticut (index map, loc. 1) showed that glacial

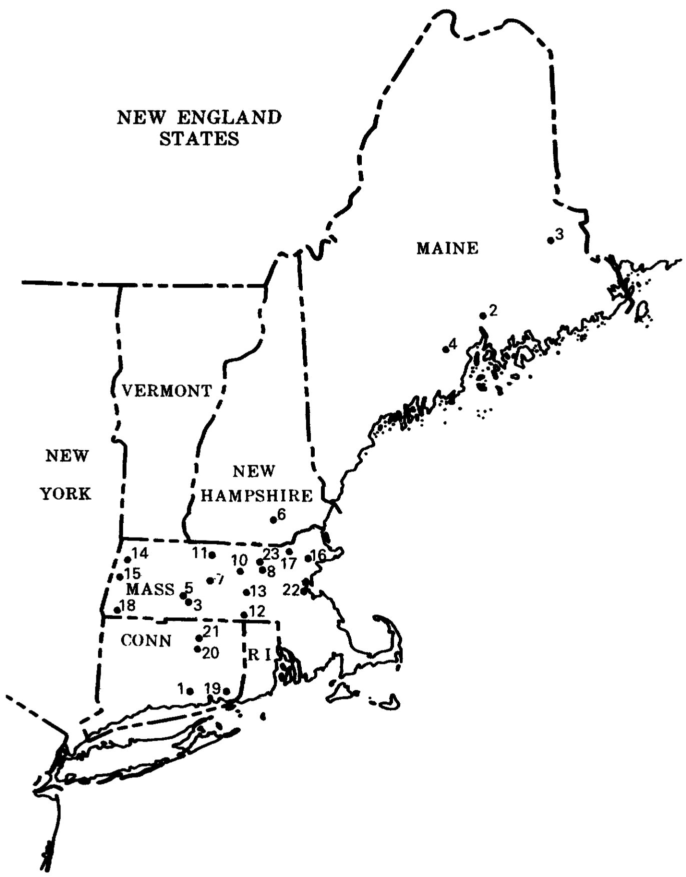

deposition, both directly from ice and by glacial melt waters, was sparse during the latest deglaciation. Evidence of earlier glaciations was not found within the quadrangle. The till cover is thinner and less continuous than normal for New England, and outcropping bedrock is widespread. Stratified drift sequences are mostly short, commonly thin, and of fluvial-ice contact type and consist of coarse-grained materials. Throughout the quadrangle, there was a strong east-to-west component during deglaciation. Several sets of sequences clearly drained east or southeast, while southeasterly or westerly spillways were still choked by ice.

Granitic plutons of New England

The relative compositions of the granitic plutons of New England have been compared with those of the Sierra Nevada batholith on histograms plotting area versus chemical and modal parameters. D. R. Wones demonstrated that New England plutons have a lower color index, less plagioclase, more alkali feldspar, and higher SiO_2 contents than their Sierra Nevadan counterparts. Muscovite-bearing granites are the most common in New England and the least common in the Sierra Nevada. Features such as the regional chemical gradients of K_2O are characteristic of the Sierra Nevada but have not been observed in New England. If the subduction of oceanic crust is related to the Sierra Nevada batholith, as present plate tectonic theories suggest, then the orogenies that led to plutonism in New England must have been substantially different. A combination of rifting followed by or concurrent with continental obduction seems most plausible.

Middle Paleozoic unconformity in Maine

Bedded rocks of the so-called "Bucksport Formation" have been found to lie unconformably on bedded rocks of the so-called "Copeland Schist" and Passagassawakeag Gneiss in Bucksport and Holden, Maine (loc. 2). D. R. Wones, mapping in the Bucksport and Orland quadrangles, found that the older formations are at garnet grade or higher, are pervasively deformed by refolded folds, and are intruded by pegmatite and aplite dikes. The dikes contain zircons, which R. E. Zartman showed by Pb^{206}/Pb^{207} dating to be 420 ± 0.01 million years in age. These dikes do not intrude the "Bucksport Formation," which is at biotite grade and is less complexly folded. The "Bucksport Formation" is intruded by the Mount Waldo and Lucerne plutons, which are 390 and 370 million years in age, respectively (Wones, 1974), and is thought to be equivalent to the Vassalboro and Kellyland Formations. The "Bucksport Formation" also appears to lie unconformably on the Penobscot Formation, although this interpretation is less certain.

Norumbega fault zone in central and eastern Maine

The Norumbega fault zone extends from Brooks to Great Pond, Maine, and probably extends from there to Fredericton in New Brunswick, Canada. D. R. Wones demonstrated that, between Winterport and Great Pond (loc. 3) the zone contains three distinct traces. Mylonite zones and observed slickensides indicate a right-lateral motion for the fault. The blocks included within the fault zone have been subjected to tilting, so that lower Paleozoic metasedimentary rocks ("Copeland Schist") are exposed in one block toward the southwest, whereas the Passagassawakeag Gneiss, which underlies the "Copeland," is exposed in another block to the northeast. Total measured offsets are based on (1) correlations between blocks containing the Passagassawakeag Gneiss, (2) a possible correlation between the granite of Topsfield, Maine (Faul and others, 1963), and the Lucerne pluton, and (3) offsets of the Mississippian-Pennsylvanian boundary in New Brunswick. These correlations indicate about 35 km of right-lateral offset.

Kyanite in schists of the Casco Bay Group in Maine

Identification of kyanite in schists of the Casco Bay Group in the Liberty 15-min quadrangle of Maine (loc. 4) by P. H. Osberg (USGS) corroborated similar reports made by Kost Pankiwskij (Maine Geological Survey). Kyanite appears unaltered in the assemblage quartz+muscovite+biotite+kyanite±garnet. These localities, coupled with those near Portland, Maine, described by Hussey (1971), require a modification to the metamorphic map of New England (Thompson and Norton, 1968). No critical data exist between Portland and the triple-point isobar figured in Thompson and Norton's map; consequently, the triple-point isobar should swing northward to include the kyanite localities in Maine.

Pre-Triassic geology of the Easthampton quadrangle in Massachusetts

Stewart Clark found that, within the Easthampton quadrangle of Massachusetts (loc. 5), the pre-Triassic rocks are mainly medium-grained granodiorite and coarse pegmatite. Local inclusions of country rock are large enough to be separately shown. A plot of schistosity and bedding within these inclusions shows an overall pattern consistent with regional trends in the adjacent Westhampton quadrangle. The emplacement of the granodiorite and pegmatite does not appear to have significantly altered the preemplacement distribution of metasedimentary rocks.

The metasedimentary rocks include rocks that were previously assigned to the Conway Granite and rocks that are lithologically similar to rocks of pre-Silurian age to the west. The rocks tentatively assumed to be pre-Silurian in age include feldspathic schist and hornblende-plagioclase amphibolite.

Elsewhere within the Easthampton quadrangle, the granodiorite is cut by basalt. Inclusions of tonalite in the Belchertown Quartz Monzodiorite have been noted within the granodiorite.

Significance of kettle holes in southern New Hampshire stream terraces

Kettle holes produced by melting of partially or completely buried ice blocks were found by Carl Koteff in postglacial stream terraces cut in deposits of glacial Lakes Merrimack and Hooksett in the Merrimack River valley of southern New Hampshire (loc. 6). The presence of the kettles indicates that buried ice can last for considerable periods of time, perhaps several hundred years. This conclusion is based on very rough estimates for rates of glacier retreat in southern New England of about 400 to 500 m/yr; the glacial lakes were in existence during this time and thus necessarily predate the kettled stream terraces. Although downcutting of more than 30 m by the post-Lake Merrimack river was very rapid in the soft lake sediments, the length of time required for this process also must be added to the lifetime of the buried ice blocks.

Length of Connecticut Valley ice lobe

Detailed mapping of glacial melt-water deposits in the Shutesbury, northern Belchertown, and southern Millers Falls quadrangles of Massachusetts (loc. 7) by J. R. Stone showed that deltaic and lacustrine sediments were deposited in ice-marginal ponds in three major east-west-trending valleys that drain the western edge of the Worcester County plateau. Successively lower delta surfaces are graded to successively lower spillways down each valley and indicate westward shrinking of the Connecticut Valley ice lobe. Upland melt-water channels that supplied sediment to the basins, paleocurrent indicators, and melt-water erosion of successive lake deposits after each lake drained provide evidence that lobation of the ice in the Connecticut Valley extended only a few kilometers south of the upland ice margin.

Geology of the Pepperell and Shirley quadrangles of Massachusetts

The low-grade metamorphic rocks east of the Wekepeke fault system in the Pepperell and Shirley 7½-min quadrangles of Massachusetts (loc. 8) consists of two distal turbidite "flysch" sequences, according to G. R. Robinson, Jr. The rocks have developed a subhorizontal foliation that is commonly axial planar to chevron folding and is probably related to late Acadian west-over-east thrusting.

The Wekepeke system of normal faults forms the western boundary of the low-grade zone. Fault motion postdates regional metamorphism, the intrusion of the Fitchburg Granite, and is probably Mesozoic in age.

Postglacial slide blocks at Mount Tom, Massachusetts

In postglacial time, blocks of Holyoke Basalt have broken loose from steep cliffs on the Mount Tom Range in Massachusetts (loc. 9) and moved west-northwest by sliding or rolling over talus and till-covered bedrock. According to F. D. Larsen, the maximum displacement of any block is 366 m horizontally and 198 m vertically from the nearest outcrop of Holyoke Basalt and 250 m horizontally and 119 m vertically from the toe of the nearest talus. The largest block is $6.1 \times 4.6 \times 4.6$ m and has moved only a few tens of meters from the nearest talus. Elongate slide rocks, the shapes of which are controlled by columnar jointing, are commonly oriented with their long axes directly down the slope. Since damage to surrounding trees has been observed, movement probably took place prior to the growth of the present forest. However, precariously perched joint blocks are common on the cliffs of Mount Tom and constitute a potential geologic hazard, particularly during an earthquake.

Stratigraphic correlation of Ellsworth Schist withdrawn

A structural block exposed north of the Chedabucto fault in the Antigonish Mountains of central Nova Scotia, Canada, is similar in lithology, structure, and geologic history, as described by Benson (1974), to the Ellsworth structural block in eastern coastal Maine. The Browns Mountain Group of Nova Scotia was tentatively correlated with the Ellsworth Schist by D. B. Stewart. Field comparison of these two terranes made in October 1976 failed to yield convincing lithological comparisons, and the tentative correlation is here withdrawn.

Correlation of Paxton Quartz Schist in central Massachusetts

Good regional evidence suggests a correlation of the gray biotite granulites, biotite schists, and calc-silicate granulites of the Paxton Quartz Schist as mapped by Emerson (1917) in central Massachusetts (loc. 10) with various Upper Silurian units in northeastern New England, including the Marid Formation in northwestern Maine, according to Peter Robinson, M. T. Field, and Robert Tucker (University of Massachusetts). Pyrite and pyrrhotite-rich magnesian schist interpreted by Field (1975) to lie at the base of the Paxton in the Ware and North Brookfield quadrangles is correlated on lithic grounds with the Smalls Falls Formation (Silurian?) of northwestern Maine. Southward extension of these two lithic types determined by reconnaissance in the Warren and East Brookfield quadrangles as far south as the Massachusetts Turnpike indicates that much of the Paxton was included by J. S. Pomeroy (written commun., 1976) in the "Upper Gneiss Member of the Hamilton Reservoir Formation," whereas much sulfidic magnesian schist was included in the "Upper Mica Schist Member of the Hamilton Reservoir Formation," where it was not distinguished from more iron-rich schists typical of the Partridge Formation (Middle Ordovician). Northward in the Barre and Templeton quadrangles, the sulfidic magnesian schist and the normal granulite of the Paxton Quartz Schist are separated by a distinctive zone of gray graphitic schist of uncertain correlation.

Subdivision of the Ammonoosuc Volcanics in west-central Massachusetts

A detailed subdivision of the Ammonoosuc Volcanics on the western flank of the Monson Gneiss in the Orange 7½-min quadrangle of Massachusetts (loc. 11) made by Peter Robinson (University of Massachusetts) proved to by a key to local structure. The sequence of units is nearly identical to that found at the southern end of the Keene gneiss dome and similar to that found east of the Warwick dome. The nature of this sequence should enter into any paleogeographic considerations. The Ammonoosuc Volcanics rests on the coarse-grained layered to massive gneiss of the Monson Gneiss in what is believed to be, but cannot yet be proved to be, an unconformity. The basal unit of the Ammonoosuc Volcanics, occurring as a local lens 0 to 9 m thick, is a quartz-granule and quartz-pebble conglomerate with a calcareous matrix of diopside, hornblende, epidote, calcite, and feldspar.

The major mafic lower unit, 61 to 152 m thick, consists of amphibolites, amphibole gneisses, and minor felsic gneiss interpreted to have been basaltic, andesitic, and minor felsic lavas and pyroclastics. Relict pillow structures, agglomerates, and porphyritic textures have been identified at several locations. Mineral assemblages are characterized by various combinations of quartz, feldspar, hornblende, anthophyllite, gedrite, cummingtonite, garnet, biotite, epidote, and diopside. Hornblende-anthophyllite, gedrite-oligoclase, and gedrite-garnet gneisses are particularly characteristic of this unit. Between 3 and 15 m below the top of the mafic lower unit is commonly a calcareous zone 0.9 to 12 m thick consisting of hornblende-calcite, diopside-hornblende-calcite, and biotite-calcite gneiss or calcite marble.

The middle of the formation is marked by a distinctive well-bedded unit 0 to 3 m thick consisting of quartz-garnet-amphibole-magnetite granulite in which the amphibole may be gedrite, cummingtonite, or hornblende. This unit is interpreted to have been ferruginous chert.

The major felsic upper unit, 15 to 152 m thick, consists of various quartz-feldspar-biotite gneisses with minor amphibolites. Most commonly, the felsic gneisses contain muscovite and garnet indicative of a peraluminous parent, but some layers contain hornblende. In this zone are distinctive felsic gneisses with resistant quartz-silimanite nodules. These rocks are considered to have been felsic volcanic rocks that were enriched in alumina by chemical weathering or hydrothermal leaching prior to metamorphism. The felsic upper unit is directly overlain with sharp contact by the metamorphosed marine sulfidic shales of the Partridge Formation, now sillimanite-biotite schists. The Partridge, particularly in its lower part, contains abundant mafic volcanic layers similar to the lower part of the Ammonoosuc Volcanics and also layers of felsic volcanic rocks similar to the adjacent upper part of the Ammonoosuc.

Structure in the Oxford area of Massachusetts

The Lake Char fault, as suggested by earlier work and by Emerson's (1917) map, makes an abrupt bend in the northwestern corner of the Oxford quadrangle of Massachusetts (loc. 12), its trace changing from north-northwest to east-northwest. South of this bend, according to H. R. Dixon, the thickness of rock units in the upper plate is reduced from roughly 5,500 m at the southern border of the quadrangle to about 450 m in a distance of about 6 km. The missing section consists of all of the Quinebaug Formation, with the possible exception of a thin veneer of mylonitic Quinebaug along the fault plane, and all but the uppermost part of the Tatnic Hill Formation. East of the bend of the fault trace, most of this section of rock apparently reappears. Outcrop control of the fault is poor in the northern part of the quadrangle, but the trace of the fault delineated from the few existing outcrops and from boulder evidence is substantiated by aeromagnetic map, on which magnetic trends in the upper plate follow around the fault bend.

The Northbridge Granite Gneiss in the Oxford quadrangle is continuous with and equivalent to the Sterling Plutonic Group of Connecticut and Rhode Island. Varieties of the Sterling that can be mapped in Massachusetts include the equivalents of the upper unit of the Hope Valley Alaskite Gneiss and the underlying Scituate Granite Gneiss. Probably the equivalent of the lowermost part of the Ponaganset Gneiss forms the core of the dome. The Hope Valley equivalent intrudes and is interfolded with the Plainfield Formation, and both have been mylonitized near the Lake Char fault. Lenses of Plainfield can be traced into the dome gneisses, possibly in long attenuated folds, but not across the dome; thus, the correlation of the Plainfield with the Blackstone Group of Rhode Island cannot be subtantiated yet.

Garnets from the Worcester "Coal Mine"

Garnets collected by J. C. Hepburn (USGS) at the Worcester "Coal Mine" site in Massachusetts (loc. 13) from rocks of known Carboniferous age (Grew, Mamay, and Barghoorn, 1970) were analyzed with the electron microprobe. The garnets are small, ranging from 0.2 to 0.7 mm, and occur in a carbonaceous muscovite-quartz phyllite associated with beds of impure meta-anthracite. Analysis reveals that the garnets are zoned, MnO varying from 9.08 percent in the core to 5.59 percent at the rim (David Walker (Harvard University), analyst). The amount of CaO+MnO varies correspondingly from 12.02 to 9.92 percent. Garnet end-member compositions determined from atomic proportions are:

	Core (percent)	Rim (percent)
Almandine	64.2	68.5
Spessartite	22.9	17.3
Pyrope	3.5	3.1
Grossularite	9.4	11.1

The relatively high MnO and MnO+CaO contents of these garnets indicate that the Alleghenian metamorphism in this area probably did not reach the temperatures of the almandine garnet zone.

Thrust faults in northwestern Massachusetts

N. M. Ratcliffe found that green chloritoid-bearing schists of the Greylock Schist on Mount Greylock in the Williamstown and Cheshire quadrangles of Massachusetts (loc. 14) discordantly overlie the Walloomsac Formation (Ordovician) as well as Cambrian and Ordovician units of the Stockbridge Formation. These results differ from Herz's (1958) interpretations, which were based on his work in the Cheshire quadrangle and suggested stratigraphic continuity between the Walloomsac ("Berkshire Schist") and the Greylock Schist. The new findings indicate that the base of the Greylock is a premetamorphic low-angle thrust fault.

Ratcliffe also found a major thrust fault within the Hoosac Formation on Hoosac Mountain in the North Adams quadrangle. The fault separates an upper green (Greylock Schistlike) Hoosac facies from a lower black albitic Hoosac facies that is demonstrably unconformable on the 1-billion-year-old gneisses of the Berkshire massif. The results suggest that the type Hoosac of Hoosac Mountain consists of two or more lithotectonic units (fault slices).

D. B. Potter discovered that the base of the thrust sheet that locally defines the Taconic allochthon of the Brodie Mountain-Potter Mountain Range (loc. 15) in northwestern Massachusetts is a zone of mixed rocks several hundred meters thick. The zone is composed of tabular slivers, hundreds of meters long and a few tens of meters thick, and smaller equant fragments of Taconic sequence and synclinorium sequence rocks (Zen, 1967) imbedded in the autochthonous Walloomsac Formation (Middle and Upper? Ordovician). Contacts between slivers and Walloomsac in this zone are locally silicified and slickensided, but many contacts are clean and show no evidence of faulting. This zone may be a block-in-shale unit formed during emplacement of the thrust sheet in Middle Ordovician time.

Rhythmic laminations in drumlin cores

Recent excavations in Massachusetts drumlins have exposed rhythmically laminated silts and clays in drumlin cores beneath old (drumlin) till. A. V. deForest reported that 2 m of nonfractured and nonfaulted, laterally continuous, alternating light and dark silt and clay laminations, averaging 1 cm thick, are exposed in the eastern flank of a drumlin north of Winning Pond in the Billerica 7½-min quadrangle of Massachusetts (loc. 16). Overlying the rhythmites is dark brown (oxidized) old till 4 to 8 m thick, which is overlain by 2 to 4 m of gray, sandy upper Wisconsinan till. In the Worcester North 7½-min quadrangle, B. D. Stone found a highway cut in the drumlin north of Indian Hill that shows 3 m of laminated silts and clays interbedded with laterally continuous, very thin beds of silty diamicton—a very poorly sorted mixture of clay- to granule-sized particles—and containing angular silt intraclasts. Stone concluded that these diamicton interbeds are gravity-flow deposits laid down intermittently on top of the accumulating suspended-load silts and clays. The laminations and diamicton beds are fractured and sheared along low-angle apparent thrust planes and are overlain by 2 m of oxidized old till in apparent thrust slices.

Similar fractured and sheared silt-clay laminations form the core of a small drumlin north of Route 20 and east of Broad Meadow Brook in the Worcester South quadrangle, where 3 to 5 m of sheared and thrusted gray and brown old till overlie the rhythmites. Sandy upper Wisconsinan till containing discrete old till clasts overlies the sheared old till. The rhythmite cores of all three drumlins may be of similar origin. All three drumlins lie on the western border of major outwash-filled valleys. The stratigraphic and structural relationships indicate that the rhythmites may have been eroded and dragged up from adjacent lowland deposits at the base of an ice sheet and deposited as part of the drumlin cores. Thrust slices of both fresh and previously weathered (Stone and Randall, 1975) old till may have been emplaced at the same time, the indication being that at least part of the deformation and deposition occurred at the base of the late Wisconsinan glacier. Alternatively, the rhythmites may have been deposited and deformed subglacially as drumlin cores.

Geology of the Lowell-Ayer region of Massachusetts

Fieldwork done in the Lowell 7½-min quadrangle of Massachusetts (loc. 17) by R. Z. Gore verified the Tadmuck Brook Schist is separated from the Merrimack Quartzite by the Clinton-Newbury fault zone. The zone of intense cataclasis is very narrow along this segment of the fault, possibly less than 30 m wide.

The Nashoba Formation and the Tadmuck Brook Schist do not appear to be in fault contact in the Ayer 7½-min quadrangle.

The coarse-grained quartz monzonites of the Lowell area are more homogeneous than the presumably equivalent units in Ayer quadrangle.

A major dike in the Tynesboro area, which parallels the regional strike, extends into the town of Ayer where it is approximately 36 m thick. This dike has the appearance of an unaltered "Triassic" dike that postdates all metamorphism. Preliminary optical examination of the potassium feldspars in the country rock immediately adjacent to the dike suggests the presence of a thermal halo. This conclusion is supported by the presence of potassium-feldspar grains whose optical properties suggest a higher temperature structure than that of the regionally prevalent (Gore, 1976) maximum microcline. The dike continues for over 8 km but appears to end abruptly against a locally prominent deflection or kinking of the regional foliation. This dike may offer a small operator a limited local source of high-grade "trap."

Peristerite in low-grade metamorphic rocks

A microprobe study conducted by J. M. Hammarstrom (USGS) showed that many concentrically zoned microporphyroblasts of plagioclase in low-grade (subchloritoid) regionally metamorphosed rocks of the Everett Formation (upper Precambrian? and (or) Lower Cambrian?) of the Taconic allochthon in southwestern Massachusetts (loc. 18) have a core of about An_{10}; the An content increases gradually outward to about An_{20} and then abruptly changes to a rim that is virtually An free. The general result confirms previous microprobe work done on these rocks by E-an Zen (USGS) and A. E. Bence (State University of New York, Stony Brook). The new study, however, is correlated to a detailed transmission electron microscope (TEM) study conducted by G. L. Nord, who found that the high-An zone, whose composition is normally considered to be within the peristerite gap of plagioclase feldspar, is indeed now a peristerite consisting of alternating regions at spacings of about 100 A, presumably resulting from spinodal decomposition of an initially homogeneous phase having the bulk composition indicated by the probe data. Probe data show that a rock of much lower grade contains plagioclase that is nearly pure albite; a rock of slightly lower grade contains zoned plagioclase showing the same gradual outward increase of An but little or no indication of an Ab rim. A rock of somewhat higher grade (just above the chloritoid zone marker) shows an outward increase of An without any sign of an albitic rim. The albite-rimmed plagioclase occurs only in a narrow belt in which other mineral retrogression relationships were also recorded.

Zen (1969) previously interpreted the zoning relation as being due to polyphase metamorphism—an earlier Taconian regional metamorphism on which an Acadian event of slightly lower grade was superimposed and caused the albitic rim. Where the Acadian event was much lower in grade, no mineralogical record is present; where the Acadian event was higher in grade, it alone is recorded. The TEM finding does not contradict this conclusion but does pose the questions of how and why an initially homogenous plagioclase having bulk composition in the peristerite gap was formed. Crawford (1966), on the basis of coexisting discrete plagioclase crystals, proposed that the peristerite solvus has a crest at about An_{10} and in the staurolite zone. Thus, Nord's TEM results could mean initial metastable crystallization between the binodal and coherent spinodal solvi, as Nord, Zen, and Hamarstrom (1976) proposed. Alternatively, however, the stable solvus itself could be at a much lower temperature (maybe 350° to 400° C, judging by the mineral assemblages of Massachusetts); thus, the initial crystallization would have been stable, and the Acadian annealing would have occurred at a temperature within the range of the spinodal solvus.

Petrography of the Preston Gabbro in Connecticut

H. R. Dixon's petrographic study of the Preston Gabbro in the Jewett City 7½ min quadrangle of Connecticut (loc. 19) showed that a zone of diorite to quartz diorite approximately 450 m wide completely surrounds the gabbro, except locally where it is faulted out. Thus, the eastern margin of the gabbro body is not the floor of a laccolithic sill, as Sklar (1958) suggested, but is a fault cutting an antiformal or dome-shaped body. Trondhjemite dikes, which represent an acid differentiate of the gabbro, most commonly occur in the diorite zone or in the adjacent Quinebaug Formation rather than in the gabbro. Since the Preston Gabbro represents a gabbro body differentiated in place, what is presently exposed is only the faulted upper part of a much larger body. The gabbro is, for the most part, a leucogabbro containing more than 50 percent labradorite to bytownite. Mafic to ultramafic varieties have not been found.

A preliminary radiometric age of 420±10 million years was obtained (R. E. Zartman, personal commun., 1976) from zircons in one of the trondhjemite dikes. The trondhjemite analyzed occurs as a dike cutting strongly cataclastic Quinebaug Formation but is not itself cataclastic; in other localities, trondhjemite is cataclastic. The age, therefore, should date the time of intrusion of the gabbro and set minimum and maximum limits on the times of cataclasis—that is, the cataclasis that preceded gabbro and its differentiates.

The Honey Hill fault in eastern Connecticut

According to Wintsch (1976), the Honey Hill fault is a continuous bedding-plane thrust localized in the lower part of the Tatnic Hill Formation that underlies much of eastern Connecticut and that is exposed around the Willimantic Dome. Wintsch's conclusion was based largely on the similarity between deformation in the pelitic rocks of the Tatnic Hill Formation along the Honey Hill fault and in the vicinity of the Lake Char fault and deformation on the dome. This deformation is characterized by large, rotated, deformed blocks and boulders, as well as by small-scale assymetric folding and cataclasis. R. J. Fahey and M. H. Pease, Jr., noted these same features when they were mapping in the South Coventry and Spring Hill 7½-min quadrangles north of the dome. Fahey reexamined exposures of the base of the Tatnic Hill Formation in the Willimantic and Columbia 7½-min quadrangles (loc. 20) and found many occurrences of these tectonically rotated blocks. The blocks may be as large as 100×300×300 m; they are bounded by sheared and slickensided surfaces, and foliation is abruptly truncated at boundaries of blocks. Rocks of the Quinebaug Formation and the Willimantic Gneiss that lie below this chaos zone represent fensters of an older terrane that is exposed south of and beneath the Honey Hill fault as mapped by Dixon and Lundgren (1968). The continuity of a single Honey Hill fault surface as postulated by Wintsch, however, seems unlikely.

Possible intrusion along deep-seated thrusts in eastern Connecticut

The Canterbury Gneiss of eastern Connecticut and its equivalent, the Eastford Gneiss, appeared to M. H. Pease, Jr., and R. J. Fahey to have been emplaced in part within zones of tectonic rifting along which are juxtaposed rocks that may have derived from distant sources. In the Spring Hill and South Coventry 7½-min quadrangles (loc. 21), most exposures of the Canterbury Gneiss lie between rocks of the Southbridge Formation (the Hebron Formation of Dixon and Lundgren (1968)) that belong to the Merrimac synclinorium sequence and rocks of the Tatnic Hill Formation that are not a part of this sequence.

This gneiss is a syntectonic intrusive emplaced at depth under oriented stress that produced penetrative deformation. This deformation is associated with low-angle thrusting in the Spring Hill and South Coventry quadrangles that has juxtaposed the Southbridge rocks against the Tatnic Hill. The intrusive gneiss intertongues with and is interlayered with screens of the Southbridge above and the Tatnic Hill below, with no shearing at the contacts. Emplacement evidently followed tectonic transport and possibly obliterated much of the evidence for shearing between the two formations.

The sketch map of eastern Connecticut (Goldsmith, 1963) (see also Dixon and Lundgren, 1968) shows that the Canterbury everywhere lies near or at the contact between the Tatnic Hill and the Hebron Formations. Perhaps this contact represents a structural break throughout eastern Connecticut rather than a stratigraphic one. Intrusion along a structural zone of weakness is more plausible than intrusion at a stratigraphic horizon.

Late glacial readvance into Boston Basin

Field data and radiocarbon dates now show that a final glacial readvance that brought glacial ice into the Boston Lowland of Massachusetts occurred about 12,000 C–14 years before present, according to C. A. Kaye. This ice appears to have spread from a stable icecap that persisted in the New England interior after ice had vacated the coastal zone (from about 12,000 to 13,000 C–14 years before present). This final glacial readvance entered the Boston Basin through the major valleys of the Charles River and the Mystic Lakes and spread out as broad lobes on the lowlands, which disturbed but did not remove the thick clays that underlay most of this area. One lobe occupied the Back Bay, and another occupied the Fresh Pond area (loc. 22). It is not known how far east this glacial readvance extended.

Possible Cambrian age for the Boston Basin

The probability that the rocks of the Boston Basin of Massachusetts (loc. 22) are all Cambrian in age rather than late Paleozoic (Devonian and Carboniferous) was more firmly established this year, according to C. A. Kaye. Rocks that are lithologically identical to the rocks that bear Cambrian fossils have now been found at many places within the basin. The basin rocks seem to be structurally conformable to the fossiliferous Cambrian (the unconformity, or fault, hypothesized to separate them has not been found in the field), and the Quincy Granite, radiometrically dated as Ordovician in age and clearly intruding fossiliferous Cambrian, is now also seen to intrude basin-type rocks. In addition, rock cores taken from foundation borings in the Revere-Winthrop area and recently studied show the source of the limestone pebbles containing Early Cambrian fossils, described a half-century ago by Clark (1923), to lie within the basin and.to form an integral part of its highly complex sedimentary framework.

Fitchburg pluton and metasedimentary sequence in Fitchburg and Ashby quadrangles of Massachusetts

Plutonic rocks mapped as Fitchburg Granite by Emerson (1917) in the Fitchburg and Ashby 7½-min quadrangles of Massachusetts (loc. 23) were mapped in detail by J. D. Peper. They consist of several early, strongly foliated sills of biotite granite and biotite quartz diorite-granodiorite that are cut by, and form inclusions in, a younger two-mica granite that makes up most of the pluton. The younger granite is identical to granite of Acadian age at Malden Hill near Worcester, Mass. Intrusion of the plutonic rocks superposed a sillimanite-grade north-trending contact aureole across a preexisting northeast-trending regional and andalusite-kyanite isograd, as polymorphic overprinting of aluminosilicate minerals in pelitic schist inclusions indicates. Along the eastern side of the pluton, a unit of biotite granulite and calcareous granulite is conformably overlain by a unit of graded bedded gray schist and quartzite, similar to the sequence Hebron Formation-Scotland Schist of southeastern Connecticut. Coarse granulite in the aureole of the northeastern lobe of the pluton was mapped by Emerson as Paxton Quartz Schist, whereas stratigraphically identical granulite south of the aureole was mapped as Oakdale Quartzite.

Glacial and glaciofluvial sedimentation in east-central Massachusetts

The areal and vertical distributions of coarse-grained glaciofluvial and glacial deltaic deposits in the Worcester-Fitchburg-Shirley area are closely related to the regional deglaciation history of central Massachusetts. Detailed surficial mapping done along the eastern side of the Worcester County Plateau by B. D. Stone demonstrated the progressive retreat of the Wisconsinan ice sheet as a major lobe in the Nashua River valley. Numerous southwest-trending striations and drumlins in the Worcester North and Fitchburg quadrangles indicate active ice retreat on the western side of the Nashua Valley lobe. Metasedimentary gravel clasts derived from the valley east of the Fitchburg-Leominster-Sterling line (loc. 23) were carried southwestward at the front of the receding ice lobe and were laid down as outwash erratics on granite pluton terrane in Worcester, Holden, West Boylston, and Sterling. Ice-contact heads of upland deltaic deposits, as well as major deltas graded to several stages of glacial Lake Nashua, indicate the local northwestward trend of the ice front during lobate retreat. Thick, coarse-grained delta topset beds and interbedded stand-and-gravel forest beds occur in outwash heads in Holden, Sterling, Leominster, and Fitchburg where the ice lobe abutted the upland plateau. Paleocurrent indicators and fining of sediments downstream indicate a southeastward current flow into the deep ice-marginal glacial lake basins.

APPALACHIAN HIGHLANDS AND THE COASTAL PLAIN

Seismic refraction in Charleston area of South Carolina

H. D. Ackermann recorded eight seismic-refraction spreads totaling 22 km in length and also 5 km of multifold high-resolution reflection data northwest of Charleston, S.C. (index map, loc. 1). Preliminary interpretation of the refraction data indicate a large basement feature involving perhaps 1,000 m of vertical offset near Summerville. The nature of this feature is not clear. The reflection data show a Lower Cretaceous section about 700 m thick and consisting of flatlying beds that are not faulted. The base of the Lower Cretaceous section is marked by a large reflection that reproduces numerous multiples that mask any deeper reflections. The character of the reflection sections is constant except in

STATES IN APPALACHIAN HIGHLANDS
AND THE COASTAL PLAINS

the immediate vicinity of Middleton Place, which is the epicenter of a recent magnitude 4 earthquake.

Mineralogy of Clubhouse Crossroads Core Hole No. 1

A continuously cored test hole, located about 40 km west of Charleston, S.C. (loc. 1), was completed. According to B. B. Higgins and G. S. Gohn, Clubhouse Crossroads Core Hole No. 1 penetrated 750 m of Cenozoic and Upper Cretaceous sediments and bottomed at 792 m in 42 m of hydrothermally altered amygdaloidal basalt. The basalt consists of two flows that appear to be subaerial. Trace-element geochemistry done by David Gottfried indicated that the basalt is a quartz-normative tholeiite of the continental extension type, similar in composition to other Mesozoic dolerites in eastern North America. Two whole-rock K-Ar radiometric dates were obtained by R. F. Marvin: 109 ± 4 and 94.8 ± 4.2 million years (late Early Cretaceous and early Late Cretaceous, respectively). Because of the alteration, these ages must be minimum, but, if they are correct, the basalt is significantly younger than the Triassic and Jurassic mafic rocks known to be associated with extensional tectonics in the Eastern United States. The dates are in accord with the early Late Cretaceous age of fossiliferous sediments 3 m above the top of the basalt.

Biostratigraphic studies of the core indicate that there is a sedimentation hiatus of about 10 million years spanning late Eagle Fordian and early Austinian time (Late Cretaceous). This hiatus corresponds to a provenance shift, indicated by heavy-mineral suites, from a dominantly granitic source area to one of regionally metamorphosed pelitic rocks.

The heavy-mineral assemblage in a sample collected at a depth of 455 m from the Black Creek Formation (Upper Cretaceous) is 95 percent andalusite, the remainder being mostly biotite and a trace of cordierite. This assemblage indicates that the sediment source was the hornfels zone of a contact aureole (probably of a dike, sill, or plug) developed in pelitic sediments, and the abundance of andalusite indicates that the source was nearby. In Black Creek time, the coastal plain had a sedimentary cover extending northwestward to the modern Fall Line and probably beyond. The need for a source of contact-metamorphosed sediments within the coastal plain suggests that shallow igneous activity in the general area of the core-hole site occurred as late as Black Creek time. Supporting evidence is diabase 3 m thick that was encountered in an oil test well in Summerville, S. C., 27 m below the elevation of the andalusite-rich sample in the core hole.

X-ray analysis of the clay-size fraction shows that cristobalite and clinoptilolite are common throughout most of the Tertiary sediments but are absent in the Cretaceous. The presence of cristobalite and zeolites in the Tertiary of the Gulf and Atlantic Coastal Plains has been reported by many workers; however, the apparent absence of these minerals in the Upper Cretaceous of the southeastern Atlantic Coastal Plain has not been noted. Although the significance of this finding is still under study, it may prove to be a useful lithostratigraphic tool, particularly in the upper coastal plain of South Carolina where the lithologies of Cretaceous and Tertiary units are similar.

Fault west of Charleston, South Carolina

A fault with a vertical displacement of 38 m at the Eocene-Oligocene time line was found by G. S. Gohn and B. B. Higgins 40 km west-northwest of Charleston, S. C. (loc. 1). The probable strike of the fault plane is E. 25° S., and the dip is high-angle normal or reverse. The fault was located by using the Eocene-Oligocene time line as a marker in two USGS deep test wells and in a number of 30-m-deep auger holes. The time line occurs within the Cooper Marl, and its depth can be determined by means of nannofossils identified by L. M. Bybell, by the absence of clinoptilolite in the Oligocene, and, in some areas, by a lithologic change across the time line.

Computer map aids planners

A technique called computer composite mapping was used to produce a land capability map from which land use planners in Fairfax County, Virginia (loc. 2), made site evaluations. According to J. N. Van Driel, digitized maps showing slope stability, surface-material type, surface water, and vegetation were combined to produce a map that delineated optimum areas in a 4,000-ha site for development of a new town in southern Fairfax County. Using this map and others developed by A. J. Froelich, S. F. Obermeier, and R. H. Johnston, the Fairfax County planning staff was able to evaluate the new town site and suggest alternatives where conflicts existed between the conceptual development plan and actual site conditions.

Post-Miocene weathering beneath the Atlantic Coastal Plain

Crystalline rocks buried beneath Atlantic Coastal Plain sediment in the Washington, D.C., area (loc. 2) commonly have weathering profiles that resemble those of saprolites of the Piedmont, according to M. J. Pavich and S. F. Obermeier. Cuts made along the Metro I–66 route in northern Virginia show a bedrock weathering profile beneath sediments of Cretaceous age and younger. Three lines of evidence indicate that this buried weathering profile has formed in the subsurface and is post-Miocene in age:

- The thickness of the profile, ranging from 2 to 15 m, is a function of the permeability of the overlying material (for example, thinner beneath clays and thicker beneath sands).
- The buried profile shows no evidence of soil formation at its upper surface and, therefore, no evidence of ever having been subaerially exposed.
- Consolidation tests on the cohesive clayey silts in the samples of the weathering profile indicate mechanical equilibrium with the present overburden, whereas consolidation tests on superjacent Cretaceous clays indicate overconsolidation resulting from a thicker pre-upper Miocene overburden.

The post-Miocene age for the buried profile indicates that not all saprolite buried by Cretaceous sediment is pre-Cretaceous in age and is of interest because of its implication about the age of the exposed Piedmont saprollite.

Metamorphic rocks of northernmost Virginia Piedmont

Rocks that have been called Wissahickon Formation or Peters Creek Quartzite in Fairfax County, Virginia (loc. 2), were found by A. A. Drake, Jr., to consist of three different metasedimentary and lesser metavolcaniclastic sequences. At the latitude of the Potomac River, interbedded pelitic schist and graywacke of flyschoid aspect (Wissahickon western sequence of Hopson (1964) crop out from the Triassic-Jurassic(?) border to Cabin John Bridge, where they are in contact with diamictite (the Skyesville Formation as used by Hopson (1964)). These flyschoid rocks appear to have been progressively metamorphosed from the chlorite zone in the west to the sillimanite zone about at Bear Island. The sillimanite-bearing rocks are migmatitic. A short distance east of Sherwin Island, these high-grade rocks are severely sheared and retrogressively metamorphosed to chlorite phyllonites. On the basis of sedimentary structures, this western sequence faces west, is largely overturned, and appears to be physically above the diamictite. These rocks are polydeformed and have polyphase fabrics.

The contact between the western Wissahickon rocks and diamictite has been described by earlier workers to be intergradational. At this latitude, however, where phyllonitic migmatites are in contact with prograde (garnet) diamictite containing clasts, knockers, and rafts of phyllonite, the contact is not intergradational. Only diamictite is exposed eastward along the Potomac to the coastal plain contact. The belt of phyllonized high-grade rocks can be traced southwestward to the Triassic-Jurassic(?) contact near Manassas, Va.

To the south of the Potomac, near Annandale, Va., another sequence of pelitic schist and graywacke crops out. These rocks differ from the western sequence described above, and it has been best determined that they are all at the garnet grade (prograde). Garnet is strongly compositionally controlled in these rocks, and its appearance does not mark an isograd. On the basis of sedimentary structures, this sequence faces east, is largely overturned, and appears to stratigraphically underlie the diamictite. No evidence of intergrading has been seen. These rocks are polydeformed and have polyphase fabrics. Clasts, knockers, and rafts of this sequence occur within the diamictite.

A third metamorphic sequence crops out in a southwest-trending 4-km-wide belt from the coastal plain outlier near Tysons Corner, Va., to the southern boundary of Fairfax County and has been traced by reconnaissance farther south. These rocks, the Clifton Phyllite of Bennison and Milton (1954), consist of metasiltstone and pelitic phyllite that have a fair amount of interbedded felsic and mafic volcaniclastic material. These rocks are probably at biotite grade and have abundant sedimentary structures showing that the sequence faces east. Although the rocks are isoclinally folded, they have polyphase fabrics at only a very few places. These rocks physically underlie the western sequence. The contact may well be an overturned unconformity, but it could be tectonic. The relation of this sequence to the diamictite is not certain at this time. The relation to the sequence near Annandale cannot be determined because of intervening intrusive bodies. No "Clifton Phyllite" has been found within the diamictite.

The exceedingly complex relationships of these rocks are not well understood at this time. An appealing hypothesis (Hopson, 1964) would be that the eastern metamorphic sequence was the base upon which the diamictite was emplaced by submarine sliding; the clasts, knockers, and rafts within the diamictite were ripups picked up during emplacement. The western sequence, visualized as being allochthonous, was emplaced subsequent to high-grade metamorphism and migmatization. The clasts, knockers, and rafts of this sequence were deposited in the diamictite as they spalled from the advancing allochthon. The "Clifton Phyllite" sequence is probably unconformable on the older rocks. Much more work will be required to understand these rocks.

Faults and folds of the coastal plain in northeastern Virginia

A trench across the Dumfries fault of the Stafford fault zone near Stafford, Va. (loc. 3), exposed a high-angle reverse fault juxtaposing Quantico Slate (lower Paleozoic) and Potomac Group (Cretaceous) rocks, according to W. L. Newell, D. C. Prowell, and R. B. Mixon. A system of subsidiary reverse faults and small-scale normal faults disrupt the coastal plain strata adjacent to the main fault. Crosscutting relationships and stratigraphic details indicate that the subsidiary faults in the Cretaceous rocks document a history of episodic deformation, active in part during accumulation of the coastal plain strata. Slickensides and stereo net analysis of the orientation of subsidiary reverse faults, normal faults, and bedding indicate that, through time, faulting consistently included right-lateral separation.

Mixon and Newell reported that four en-echelon northeast-trending structures, including southeast-dipping monoclines and northwest-dipping high-angle reverse faults, have been mapped along the inner edge of the coastal plain in northeastern Virginia—an area generally considered to be undeformed. Although displacements are small (15 to 60 m), the structures markedly affect the present distribution and thickness of coastal plain strata.

Structure contour maps of Cretaceous and Paleocene lithostratigraphic units show that the amount of displacement on the structures increases downward, indicative of recurrent movement. The major deformation occurred in the Cretaceous and middle(?) Tertiary, but some movement in the latest Tertiary or Quaternary is possible. A small (12 cm) offset in upland gravel overlying bedrock (so-called "Fredericksburg" complex) contact has been observed.

The structures, named the Stafford fault system, extend for at least 56 km parallel to the Fall Line and the northeast-trending reach of the Potomac estuary. This relationship supports the hypothesis that the Fall Line and the major river deflections along it have been tectonically influenced.

Antiformal folds in the northeastern Virginia Piedmont

Mapping by Louis Pavlides and K. E. Wier in the Lake Anna West 7½-min quadrangle of Virginia verified the presence of a large northeast-trending antiformal zone (loc. 3). This antiformal terrane occurs along strike to the southwest of a large antiform in the Salem Church quadrangle (Pavlides, 1976) that refolds an earlier synform. In the Lake Anna West quadrangle, the antiformal folds are confined to a terrane of interlayered biotite and hornblende gneisses, amphibolites, foliate granitoid rocks, and lesser amounts of mica schist. This terrane is provisionally assigned to the undivided part of the "Fredericksburg" complex (Pavlides, 1976) and is in discordant contact on its northwestern side with the Quantico Slate that is here a garnetiferous, in part graphitic, mica schist that locally contains kyanite. Whether this contact is an unconformity or a fault has not been resolved by reconnaissance mapping completed thusfar. Reconnaissance mapping of this contact northeastward, however, suggested that it is folded by the antiformal folds within the "Fredericksburg" complex seen in the Lake Anna West quadrangle. The Quantico is also folded by the same antiformal fold generation seen in the Salem Church quadrangle (Pavlides, 1976).

Belair fault zone investigations

The Belair fault zone near Augusta, Ga. (loc. 4), has been mapped for at least 21 km along strike and consists of seven en-echelon reverse fault segments having a total vertical displacement of 30 m. Along the fault zone, phyllite of Precambrian Z age is juxtaposed against Upper Cretaceous sediments by reverse faults. Dissimilar crystalline rocks in contact across the fault zone suggest major strike-slip movement of Paleozoic age or older. The structural configuration of overlying Tertiary sediments that have been eroded away for the most part suggests that they too have been deformed. Studies of the Pleistocene to Holocene history of the fault zone have been focused on three trenches that expose the fault plane, overlying colluvium, a nearby peat bog, and soil horizons developed in the surficial deposits. D. C. Prowell, D. G. Herd, Juergen Reinhardt, W. L. Newell, and E. M. Shoemaker reported that no offsets in the colluvium-Cretaceous sediment contact were observed. Some severely oversteepened alluvial beds within the colluvium on the down block of the fault were noted but are not easily explained by fault movement. Stratigraphic relationships of the surficial materials overlying the Tuscaloosa Formation and the fault plane indicate that the fault movement is greater than 2,000 years old and probably predates 25,000 years.

Late tectonic uplift of Blue Ridge province

J. T. Hack, in compiling data for a study of the Southeastern United States, found physiographic evidence to support the concept that the high relief and altitude of the Blue Ridge province must be the result of some kind of tectonic uplift that probably extended into post-Triassic time. The topography of both the Blue Ridge province and the Piedmont province is typically erosional and is almost entirely in slope. Locally, it is closely adjusted to the resistance of the rocks. On a broad regional scale, however, the two provinces do not conform to differences in rock resistance. Southeast of Hendersonville, N. C. (loc. 5), for example, the Blue Ridge Highland extends southeastward 40 km into rock types characteristic of the Piedmont. In northern North Carolina and Virginia, typical Blue Ridge rock belts extend out into the Piedmont (for example, the Lynchburg Gneiss and the so-called "Blue Ridge" complex).

Both the Blue Ridge and Piedmont provinces contain extensive areas of deep saprolite, but, in the Blue Ridge, saprolite is spotty and confined mostly to areas of low or moderate relief, as exemplified by the Asheville Basin. In the Piedmont, the saprolite probably covers more than 90 percent of the area and averages between 15 and 18 m thick. Thickness correlates with rock type as well as with slope and relief. Within the area studied, it has been shown that either latitude or altitude is directly related to thickness.

The mean topographic relief of 100-km^2 areas is generally between 30 and 60 m in the Piedmont. In the Blue Ridge, it ranges from about 60 to over 600 m.

The great differences between the terranes of these two physiographic regions and the similarities in their geology are evidence of the uplift of one and the relative stability of the other.

Stratigraphic correlation in Atlantic Coastal Plain

The Round Bay 7½-min quadrangle of Maryland (loc. 6) lies near the southern end of the strike transition zone between the clearly delineated outcropping lithologic units of Late Cretaceous and early Tertiary age in the northern part of the Atlantic Coastal Plain in New Jersey and the fewer and less clearly delineated lithologic units in southern Maryland. According to J. P. Minard, this area is farther southwest than any other area in which the Marshalltown and Englishtown Formations are known to crop out. They are represented by thin to feather-edge beds. The Marshalltown crops out continuously and is uniform in its approximate thickness of 1 m, which is to be expected of a probable middle shelf deposit. The Englishtown, however, is present only as thin, irregular remnants, as would be expected of an irregular nearshore beach-lagoonal deposit.

Greenstone conglomerate of the Culpeper Basin in Virginia

A greenstone conglomerate sequence in the Bull Run Formation in the Culpeper Triassic-Jurassic(?) Basin was recognized and mapped from a well-exposed profile of Culpeper City in Culpeper County, Virginia (loc. 7), by K. Y. Lee. This sequence consists of (1) subangular to angular fragments of metamorphosed, green to greenish-gray, epidotized, feldspathic, arenaceous rocks; (2) volcanic rocks; and (3) basic intrusive rocks containing some locally abundant, light-gray to gray and pink, metamorphosed arenaceous rocks, vein quartz, and schist. The unit ranges in thickness from 35 to 1,100 m. It lies above the principal mass of the third basaltic flow and intertongues with the Bull Run sandstone facies and the Balls Bluff Siltstone. The unit consists of several coalescing fans and occurs along the eastern front of the Bull Run Mountains and the southern border of the basin.

Precambrian inlier in the Culpeper Basin of Virginia

An inlier of Precambrian metamorphosed greenstone and feldspathic arenaceous rocks has been discovered in the east-central part of the Culpeper East 7½-min quadrangle in Culpeper County, Virginia (loc. 7). These rocks had formerly been mapped as Triassic sandstones. They are unconformably overlain by greenstone, quartzite conglomerate, and feldspathic sandstone of the Manassas Sandstone on the west, south, and northwest and are cut by intrusive diabase sills on the northeast, east, and southeast. K. Y. Lee believed that this inlier came into existence during monoclinal tilting and synchronous emplacement of diabase sills in the southern portion of the Culpeper Basin.

Western border faults in the Culpeper Basin of Virginia

On the basis of detailed investigations, K. Y. Lee felt that deposition of Triassic and Jurassic? sediments of the Newark Group, including thick wedges of coarse clastics, in the trough-shaped Culpeper Basin of Virginia (loc. 7) was controlled by uplifting of adjacent uplands and downwarping in the basin. Deposition of alluvial fans of the Bull Run Formation along the western border of the basin resulted from uplifting of adjacent uplands and synchronous subsidence in the basin along a series of normal faults. These faults occurred from the western side of the Frederick Valley in Frederick County, Maryland, south to the northern bank of the Robinson River in the Rapidan 7½-min quadrangle in Culpeper County, Virginia. Movement along these faults ceased at the close of Bull Run time, as a sequence of fine to medium sandstones in the uppermost part of the Bull Run indicates. Movement recurred during late monoclinal tilting of the basin. Maximum cumulative displacement along the eastern front of the Bull Run Mountains in Virginia is estimated to be about 5,100 m.

Gold Hill-Silver Hill shear zone in the Lexington-Thomasville area of North Carolina

Reconnaissance mapping done by J. D. Peper in the northeastern corner of the Charlotte 2° quadrangle of North Carolina (loc. 8) suggested that the Gold Hill-Silver Hill shear zone is truncated by a medium-grained post-tectonic granite southwest of High Point, N.C. The shear zone, in the southern part of the Lexington East quadrangle, is a 3-km-wide zone of steeply west dipping slip cleavage developed on the western (overturned) limb of the Silver Valley syncline. Bedding in the slate-belt rocks is transposed into the slip cleavage, and rare, tight asymmetric folds between slip cleavages show a west-over-east sense of movement. The size of mica flakes along the cleavage planes increases from east to west across the zone. To the northeast, the shear zone widens and splays into a northeast-trending fracture cleavage associated with the Silver Valley syncline. Rhyolitic volcanic rocks and mudstones of the Cid Formation are dragged into the shear zone southwest of Thomasville. To the northeast, in the High Point-Thomasville area, phyllites of the shear zone form inclusions and roof pendants in a post-tectonic granite.

Lithostratigraphy of the Oak Grove core

Juergen Reinhardt reported on a stratigraphic test hole—the Oak Grove core—drilled near the southern margin of the Salisbury Embayment on the Northern Neck of Virginia about 45 km east of the Fall Line (loc. 9). The top 24 m was not cored; from 24 to 137.5 m, the core is composed of unconsolidated to partially cemented Tertiary sediments; the remaining 262.5 m consists of unconsolidated Lower Cretaceous sediments. No Upper Cretaceous sediments are present in the core. The hole was logged with gamma-gamma, gamma-ray, neutron, and electrical probes. Subsurface control in adjacent areas and lithologic and palynological data from this core show penetration to be within 30 m of Triassic(?) basement.

Stratigraphic units penetrated by the test hole include (1) upland gravels, undivided (0–2,051 m); (2) Calvert Formation (20.5–60 m); (3) Nanjemoy Formation (60–96 m); (4) Marlboro Clay Member of the Nanjemoy (96–102 m); (5) Aquia Formation (102–137.5 m); and (6) Potomac Group, undivided (137.5–400 m). General lithology and contact relationship are similar to those of the equivalent updip lithostratigraphic units.

The Calvert Formation (Miocene) consists of interbedded illite-vermiculite clays and bioturbated quartz silts. The lower Tertiary bioturbated greensands and illitic clays (Aquia and Nanjemoy) are separated by a massive, slightly burrowed kaolinitic clay (Marlboro). The nature of the sediments, the lack of primary sedimentary structure, and the faunas indicate sedimentation on an open marine shelf well below wave base.

The Lower Cretaceous sediments (Potomac Group) are characterized by alternation of (1) mottled, highly oxidized, and slickensided kaolinitic and illitic clays, (2) laminated carbonaceous silt, and (3) fine to coarse, poorly sorted feldspathic quartz sand. The Lower Cretaceous section contains notable amounts of cristobalite and clinoptilolite in many of its fine-grained units. The overall fine-grained nature of the Potomac Group sediments (Aptian and Albian only in this core), sparse burrows(?) and root structures, and abundant laminated intervals suggest deposition on an alluvial flood plain, probably close to a delta platform.

A major fault system in the Eastern United States

Interpretation and field checking by D. G. Howell (USGS) and R. D. Hatcher (Clemson University) and associates of recent aeromagnetic data suggested the existence of a closely associated series of faults and splays extending from Alabama to Virginia, called the Eastern Piedmont fault system. Characteristic magnetic anomalies were found to be associated with known faults and were used to trace them through covered intervals. The fault system extends northeastward from the Goat Rock fault of Alabama and west-central Georgia, crosses the lower Piedmont of South Carolina, passes beneath a segment of the coastal plain in the Carolinas, flanks the Raleigh belt in North Carolina, and continues into Virginia. From east-central Georgia to Virginia, cataclastic rocks along the faults of the system are bounded to the northwest and southeast by rocks of the Carolina slate belt and form perhaps the most extensive fault system in eastern North America.

New York-Alabama lineament discovered

A northeast-trending magnetic lineament 1,300 km long has been revealed by aeromagnetic mapping in the Appalachian Basin. This lineament is especially well developed on the recently completed aeromagnetic map of West Virginia and has well-defined continuations along strike at least as far south as the northeastern corner of Alabama and as far north as the southern margin of the Adirondack uplift. The magnetic patterns on either side of the lineament indicate a profound contrast in the lithologies of the crystalline basement rocks along a nearly linear discontinuity, which may be a former plate boundary. There is a good correlation with gravity patterns that trend predominantly northeast in the Appalachian Basin on the southeastern side of the lineament, in contrast to the nearly north-trending anomalies of the continental interior on the northwestern side. On the basis of gravity trends, the lineament can be projected southwest across northern Alabama and northeast into the Green Mountains of Vermont. E. R. King and Isidore Zietz named this major crustal feature the New York-Alabama lineament. The lineament appears to mark the southeastern edge of a stable crustal block that controlled later deformation, the more intense Appalachian folding and faulting being tangential to it. Northeast-trending belts of recorded seismic events outline this block on the southeast and also along the northwest in a line connecting New Madrid, Mo., and the St. Lawrence Valley.

CENTRAL REGION

KENTUCKY

Geologic mapping

A USGS-State of Kentucky cooperative project to map all of Kentucky geologically has been in progress since 1960. The maps are printed on recent editions of topographic base maps of quadrangles at 1:24,000 scale and published in the Geologic Quadrangle map series. By March 1, 1977, the project was about 95 percent complete; 587 geologic maps had been printed (fig. 1), another 66 had been approved for publication, and an additional 14 were undergoing review. Fieldwork had been completed in the remaining 42 quadrangles, and the maps were being prepared for review.

The Middlesboro cryptoexplosion structure revisited

Mapping done in the Kayjay quadrangle (index map, loc. 1) by C. L. Rice and E. K. Maughan and in the Middlesboro North quadrangle by Englund, Roen, and De Laney (1964) defined a faulted domal structure in southeastern Kentucky that is roughly the same size as the nearby Middlesboro Basin, interpreted by Englund and Roen (1962) as an ancient meteor-impact scar. The faulted dome is in Pennsylvanian rocks of the Cumberland overthrust block and crosses the border between the Kayjay and the Middlesboro North quadrangles. The center of the structure is about 6.5 km north-northwest of the center of the Middlesboro Basin. Coal beds traced across the structure indicate that the dome has a radius of about 3.2 km and a structural relief of about 180 m.

STATES IN CENTRAL REGION AND GREAT PLAINS

Drill-hole records obtained in the area of the dome show what appears to be an extraordinary thinning of the Pennsylvanian rocks onto the structure; three drill logs from the western flank show that a 240-m section thins as much as 38 in 2.2 km. Since regional thinning could not account for this large amount, part of the doming may have occurred during deposition of the Pennsylvanian rocks.

The movement along the Cumberland overthrust block was estimated by Englund (1968, 1971) to be

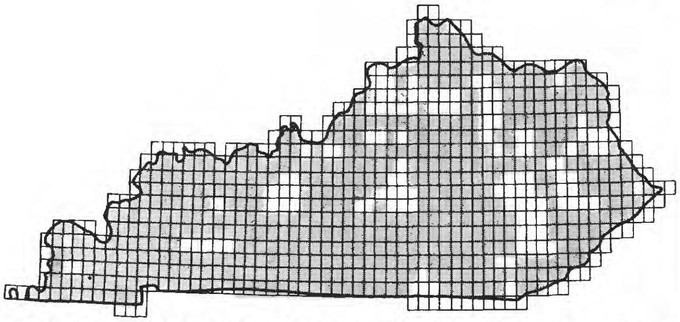

FIGURE 1.—Published geologic quadrangle maps (patterned areas) of Kentucky as of March 1, 1977; small squares are 7½-min quadrangles.

about 6.5 km north-northwestward at its northeastern end and about 18 km north-northwestward at its southwestern end. Thus, the distance between the Middlesboro cryptoexplosion structure and the dome is of about the same magnitude and in the same direction as the movement of the thrust.

These factors suggest the following sequence of events: (1) Doming in Early and Middle Pennsylvanian time; (2) thrusting during the Appalachian orogeny that decapitated the dome and transported the upper part to its present position; and (3) explosion at the original site of the dome that formed the Middlesboro structure. According to this scenario, the Middlesboro structure is of cryptovolcanic origin rather than impact origin.

Regional Pennsylvanian correlations of fusulinid-bearing limestones

Preliminary stratigraphic studies by C. L. Rice and T. M. Kehn and paleontologic studies by R. C. Douglass of newly discovered fusilinid-bearing limestone units in Pennsylvanian formations in eastern and western Kentucky showed the need for major changes in regional correlations. The widespread Magoffin Member of the Breathitt Formation of eastern Kentucky (loc. 2) has long been correlated with the widespread fusilinid-bearing lower and upper limestone units of the Mercer Member of the Pottsville Formation of Ohio and Pennsylvania (Wanless, 1946, p. 145; 1975, p. 39). Recent discoveries of *Profusulinella* in two limestones in eastern Kentucky and one in Ohio show that the Magoffin occurs far below the two Mercer horizons.

In western Kentucky (loc. 3), fusulinids of early Atokan to Des Moinesian age have been collected from outcropping limestones and core material supplied by the Kentucky Geological Survey's extensive drilling project. Douglass showed that these collections represent as many as six different fusulinid horizons and that as many as four different limestones have locally been called or correlated with the Curlew Limestone Member of the Tradewater Formation. The Curlew is an extensive key bed in western Kentucky. Douglass also was able to determine that, of the fusulinid-bearing limestones of Ohio, the type Curlew most nearly resembles the upper limestone unit of the Mercer of Ohio in faunal content.

Useful stratigraphic marker in Upper Devonian shale

A distinctive stratigraphic marker consisting of three greenish-gray shale beds in the upper part of Devonian black shale was found in widely spaced outcrop sections from Tennessee through Kentucky and into southern Ohio by R. C. Kepferle (USGS) and L. J. Provo and P. E. Potter (University of Cincinnati). This marker is easily identified in both outcrop and the subsurface, especially on gamma-ray logs, where the low natural radioactivity of the greenish-gray shale contrasts sharply with the higher radioactivity of the interbedded organic-rich black shale. The bed has been traced in the subsurface throughout most of eastern Kentucky into West Virginia. The marker bed is the so-called "Three Lick" bed, which correlates with the middle unit of the Gassaway Member of the Chattanooga Shale (Conant and Swanson, 1961) in Tennessee and with the lower part of the so-called "Camp Run Member" of the New Albany Shale (Lineback, 1970) in Indiana. Recognizing this key bed is an important step toward establishing the stratigraphy of the Upper Devonian shale sequence throughout the Appalachian Basin.

UPPER MISSISSIPPI EMBAYMENT

Upper Tertiary bedrock terraces in northern Mississippi embayment

Geologic investigations conducted as a part of Kentucky's cooperative mapping program have defined widespread bedrock terraces at altitudes of 128 and 152 m that underlie continental deposits of late Tertiary age—the so-called "Lafayette Formation" —in the Kentucky part of the Mississippi embayment (loc. 4). A continuing investigation by W. W. Olive in the embayment north of latitude 38°15′ N. showed that remnants of these terraces beneath the "Lafayette" are preserved in upland areas within the embayment and in areas marginal to it. Both terraces are developed on rocks ranging from comparatively resistant limestone and chert of Paleozoic age to poorly consolidated, easily eroded sand and clay of Mesozoic and Cenozoic age.

The 152-m terrace is a remarkably flat surface that does not vary in altitude more than 1.5 m above or below the 152-m level over a distance of as much as 56 km parallel to the axis of the embayment. On the other hand, the 128-m terrace, which is less well preserved, has as much as 3 to 4.5 m of local relief and seems to be slightly inclined toward the embayment axis.

At a number of places, the upper surface is traversed by deep, narrow, steep-walled channels incised to near the 128-m terrace level. These channels pass through areas occupied by a buried irregular surface lying midway between the two terraces and merge with the 128-m terrace level. As exposures in gravel quarries indicate, the continental deposits that fill these channels and overlie the 152-m surface represent a single continuum of deposition.

The age of the bedrock terraces is indicated by the age of the sediments on which they are developed and of the continental deposits that overlie them. The youngest sediments truncated by the two terraces contain a pollen assemblage that R. H. Tschudy tentatively assigned to the middle Oligocene. These sediments are part of a stratigraphic sequence no more than 75 m thick that, according to the pollen content, is for the most part Jackson (late Eocene) in age. The Jackson age sediments contain palynomorphs that indicate environments ranging from marine to freshwater. A pollen assemblage from the continental deposits strongly suggests a Pliocene age, according to Tschudy, although he stated that, in the absence of adequate control, it may be as old as Miocene.

Physiographic and stratigraphic relations suggest that the 152-m surface developed as a plane of denudation following deposition of the middle Oligocene(?) sediments when the area was only slightly above sea level. Later, owing to either eustatic change in sea level or epeirogenic uplift, the base level was lowered at least 24 m, and a new epoch of erosion gave rise to the 128-m bedrock surface and the eroded topography below 152-m.

While the 128-m terrace was being eroded and while streams draining into the embayment were deepening their lower courses in adjustment to the new base level, the streams were also alluviating their upper courses. Eventually, alluviation became dominant throughout, and streams began to discharge their loads onto the 128-m surface and to alluviate their courses in all but their headward parts. In time, the thickness of alluvial deposits brought into the northern embayment became so great that the deposits overlapped, spread out over the 152-m terrace, and covered the terrace to a depth of at least 15 m, as present-day thicknesses indicate.

The present altitudes and attitudes of the two terraces indicate further epeirogenic uplift subsequent to the development of the 128-m terrace. If no allowances are made for eustatic change in sea level between the time of development of the 128-m terrace and the present, uplift may have been about 122 m.

Evidence of pre-Pleistocene Mississippi River

Study of the composition of the upper Oligocene(?) to Pliocene gravel that overlies the 128- and 152-m bedrock surfaces in the upper Mississippi embayment (loc. 4) indicated that the gravel was derived largely from Paleozoic sedimentary rocks exposed in areas peripheral to the embayment. Although several suites were identified, they can be classified as belonging to two principal groups: (1) Those east of the Mississippi River, which consist mainly of chert typical of that found in the Fort Payne and Warsaw Formations and St. Louis Limestone of Mississippian age exposed in Kentucky and Tennessee in areas bordering the Tennessee and Ohio Rivers; and (2) those west of the Mississippi River, which consist mainly of chert, sandstone, and quartzite (orthoquartzite and metaquartzite) similar to those found in rocks of Ordovician to Mississippian age exposed along the Mississippi River to the north and in areas within and bordering the embayment in Missouri and Arkansas. The suite west of the Mississippi River also contains rare agate pebbles and very rare reddish metaquartzite pebbles and boulders not found in the eastern suite. According to H. B. Willman (Illinois State Geological Survey) (oral commun., 1976), the agate is similar to that referred to by rock collectors and lapidarists as "Lake Superior agate," which occurs as void fillings in Precambrian volcanic rocks in the Lake Superior region. The reddish quartzite is identical in appearance to the Baraboo Quartzite of Precambrian age at its type locality near Baraboo, Wis. Thus, these two lithologic types strongly suggest a pre-Pleistocene Mississippi River in the midcontinent area, inasmuch as palynological data indicate that the gravel of the northern Mississippi embayment was deposited during late Oligocene(?) to Pliocene time.

LAKE SUPERIOR REGION

Basement rocks in the Lake Superior region

The recognition of two fundamentally different types of Precambrian W (Archean) basement rocks in the Lake Superior region by P. K. Sims and G. B. Morey (Minnesota Geological Survey) (1973) and the subsequent delineation of the boundary between the two terranes in Minnesota (Morey and Sims, 1976) and in northern Wisconsin and Michigan (Sims, 1976a) provided a firm basis for regional synthesis of the early tectonic evolution of this part of the North American craton.

The boundary between the two basement terranes (2,700-million-year-old ensimatic greenstone-granite complexes on the north and 3,000- to 3,500-million-year-old ensialic gneisses on the south) is interpreted as being an ancient suture that probably was welded about 2,700 million years ago, when vast quantities of granite were emplaced into the upper crust. Subsequent to the joining of the two blocks into a coherent continental mass, the tectonic behavior of the two basement terranes was different. The contrast in tectonism was most apparent during Precambrian X time, as published data on the middle Precambrian rock successions indicate, but probably persisted to a lesser degree into the Phanerozoic.

The Precambrian basin, which contains the great iron-formations of the region and the volcanogenic massive sulfide deposits recently discovered in northern Wisconsin (Sims, 1976b), was developed over and along the boundary between the two basement terranes. In the northern part of the basin, which is underlain by greenstone and granite complexes, deposition took place in a stable shelf environment, and the metamorphism and deformation that immediately followed were mild. In contrast, in the southern part of the basin, which is underlain by basement gneisses, the stratigraphic succession records a complete transition from a stable craton to a eugeosynclinal environment, and subsequent metamorphism and deformation were intense.

Studies of the basement rocks as well as of the supracrustal rocks by Sims and Z. E. Peterman (USGS) clearly indicated that the Precambrian W basement gneisses were mobile during Precambrian X time; the mobility of the gneisses is indicated by strongly discordant ages obtained by different radiometric dating techniques and by high initial $^{87}Sr/^{86}Sr$ ratios (Sims and Peterman, 1976) as well as by obvious geologic features discernible in the field, such as gneiss domes and relatively raised fault-bounded gneiss blocks. That the mobility of the gneisses persisted, at least intermittently, into later Precambrian time is indicated by numerous published mineral ages in the range 1,650 to 1,300 million years.

Subdivision of Hemlock Formation

Recently completed geologic mapping of the Ned Lake 15-min quadrangle of Michigan (loc. 5) by M. P. Foose revealed four local units within the Hemlock Formation of Precambrian X age. The lowest observed sequence is composed of amygdaloidal and pillowed flows. These are successively overlain by (1) a sequence of coarse, poorly sorted, angular volcaniclastic rocks and (2) a second sequence of somewhat finer grained, better sorted, and less angular volcaniclastic rocks. This upper volcaniclastic unit contains rare dolomitic marble and slate interbeds. A second sequence of amygdaloidal and pillowed basalts occurs at the top of the formation. Two distinctly different types of intrusions cut the Hemlock: (1) Foliated magnetic amphibolites that may represent intrusive equivalents of some of the extrusive rocks and (2) lenses of massive, equigranular gabbros, which carry some disseminated pyrite and chalcopyrite and may correlate with the Kiernan sills to the south. Abrupt thinning of the Hemlock along strike suggests that the clastic sequences were deposited near major volcanic centers.

ROCKY MOUNTAINS AND GREAT PLAINS

STRATIGRAPHIC STUDIES

Belt and pre-Belt rocks near the Idaho batholith

The high-grade, complexly deformed metamorphic rocks on the northern side of the Idaho batholith have been interpreted as metamorphosed rocks of the Belt Supergroup by many geologists over the past two decades. The lithologic trends of several Belt formations points to a pre-Belt Precambrian source terrane in the area of the high-grade rocks. Scattered samples from some high-grade rocks have given minimum ages of 1,500 million years, which also suggest that pre-Belt rocks are present. But how can one distinguish between high-grade Belt rocks and pre-Belt rocks in the metamorphic complex? Geologic mapping done in Shoshone County, Idaho (index map, loc. 1), by J. E. Harrison indicated that two groups of high-grade rocks occur, at least in that area. The two groups have been tectonically mixed by thrusting, and all contacts between them are tectonic. Both groups contain abundant mica schist and biotite-quartz-plagioclase

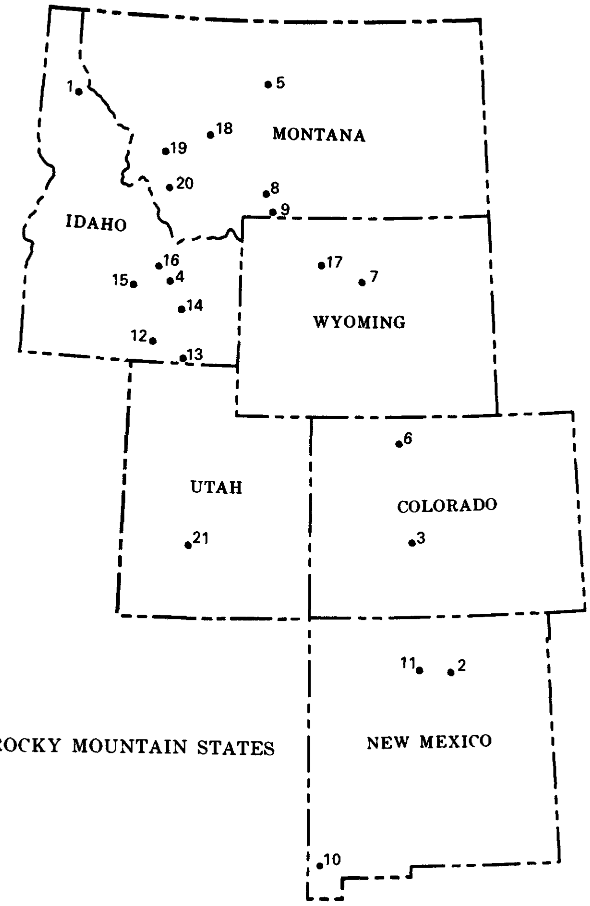

ROCKY MOUNTAIN STATES

gneisses. However, the group that fits expected facies changes and the stratigraphic sequence of Belt rocks contains abundant quartzite or quartz-mica gneiss and sparse interlayers of calc-silicate gneiss and metadiorite, whereas the group that is probably pre-Belt contains only sparse quartzite but abundant amphibolite, anorthosite, migmatite, and porphyroblastic granitic gneisses.

The two-faced Sangre de Cristo Mountains of New Mexico

Recent detailed mapping and stratigraphic studies conducted along the eastern front of the Sangre de Cristo Mountains between Las Vegas and Mora, N. Mex. (loc. 2), indicate that both the Precambrian basement rocks and the overlying Pennsylvanian sedimentary rocks differ considerably from Precambrian and Pennsylvanian rocks in the southern and western parts of the range.

J. M. O'Neill recently subdivided the Precambrian of the eastern area into four mappable rock units. From structurally lowest to highest, they are:

- Quartz-feldspar-mica gneiss containing quartz-rich zones.
- Interlayered quartz-muscovite schist and quartz- and plagioclase-rich amphibolite containing pegmatites.
- Laminated micaceous quartzite containing concordant and discordant amphibolite.
- Complexly mixed quartz-feldspar gneiss, plagioclase amphibolite, metavolcanic(?) rocks, and pink and gray granite gneiss.

None of these rocks contains the diagnostic lithologic components such as (1) thick, gray, translucent quartzite, (2) black, dense phyllite and slate, and (3) quartz metaconglomerate that characterize the Ortega Quartzite and Vadito Formation of Montgomery (1953) in the Picuris and adjacent areas of the western Sangre de Cristo Mountains. Therefore, the structural and stratigraphic relationships of the Precambrian rocks on the eastern and western sides of the mountains are not yet determined.

E. H. Baltz reported that Pennsylvanian rocks in the eastern frontal belt thicken greatly northward from the vicinity of Las Vegas to Mora. At the south, these rocks were deposited on an unstable shelf; at the north, they were deposited in the Rowe-Mora zeugogeosynclinal basin. Mapping of the folded and faulted structure of these rocks, aided by fusulinid and megafossil age determinations, demonstrated that the Sandia Formation and the lower and upper member of the Madera Formation of the shelf can be traced northward through complex changes of facies into the basinal sequence, which may be as much as 1,830 m thick near Mora. The time-related facies framework that is being determined is expected to provide new insight into the paleogeography and facies distribution of Pennsylvanian rocks in the subsurface of the Raton basin east of the Sangre de Cristo Mountains.

Sawatch Quartzite outcrop area extended southward in Colorado

J. C. Olson's discovery of four previously unreported outcrops of Sawatch Quartzite of Late Cambrian age extended the known distribution of that formation in the Sawatch Range of southeasternmost Gunnison County, Colorado, southward as far as Lime Ridge in the Pahlone Peak quadrangle (loc. 3), 10.4 km south of the southernmost previously known outcrop. Poorly exposed remnants of Sawatch Quartzite up to 400 m long and several meters thick occur in secs. 24 and 36, T. 49 N., R. 5 E., and in sec. 31, T. 49 N., R. 6 E., where small patches of the quartzite are preserved on the downthrown side of faults; the southernmost known exposure of Sawatch Quartzite, about 1 m thick, is at the base of the Manitou Dolomite (Ordovician) for a distance of 1 km east of peak 11,636 in the center of the Pahlone Peak quadrangle.

Newly recognized Mississippian rocks in central Idaho

An unnamed slope-forming unit, about 100 m thick and consisting of thin-bedded silty to sandy limestone and some gray mudstone and shale, was differentiated in the southern Lemhi Range of Idaho (loc. 4) by B. A. Skipp and M. H. Hait above the cliff-forming limestone of the Surrett Canyon Formation (Upper Mississippian) and below ridge-forming fine-grained yellow-brown-weathering sandstone assigned to the Lower Pennsylvanian(?) Series. On the basis of present fossil information, W. J. Sando assigned the new unit to the uppermost Mississippian System. Stratigraphic sections of this unit, measured in the southern Pioneer Mountains, the southern Lost River Range, and the southern Lemhi Range and in a thrust block in the southern Beaverhead Mountains, show that black shale and fine-grained sandstone and siltstone increase in volume to the east. Limestone in the unit is mostly silty and aphanitic; beds of bioclastic limestone are more common in the western sections.

Phosphoria Formation discovered in Lemhi Range of Idaho

Mapping done by B. A. Skipp and M. H. Hait in the Tyler Peak quadrangle in the southern Lemhi Range of eastern Butte County, Idaho (loc. 4), disclosed the presence of heretofore unrecognized beds of the Phosphoria Formation (Permian). The Phosphoria is preserved in a large north-trending graben in the center of an anticlinal structure on the eastern flank of the range. The Rex Chert Member of the Phosphoria concordantly overlies Permian dolomite and sandstone. No rocks of Triassic age have yet been recognized in this area.

Depositional environments of the Eagle Sandstone in Montana

On the basis of studies of the Eagle Sandstone (Upper Cretaceous) and associated strata where they crop out along the Missouri River and its tributaries between the town of Virgelle and the mouth of the Judith River (loc. 5) in Chouteau County, Montana, D. D. Rice interpreted the depositional environments represented by these beds, some of which contain shallow accumulations of natural gas.

The Telegraph Creek Formation, underlying the Eagle, accumulated in an offshore transition environment and grades upward into the shoreface, foreshore, and eolian sandstones of the Virgelle Sandstone Member, the basal member of the Eagle. The Virgelle was deposited along an eastward-prograding shoreline and ranges in thickness from 24 to 40 m. The middle member of the Eagle represents coastal plain deposition. In the eastern part of the area, the upper part of this member contains a massive, sheetlike, delta-front sandstone capped by a thin delta-plain unit, which indicates a second progradation during Eagle time. The upper member of the Eagle is a transgressive, delta-destructional sandstone, which marks the beginning of the extensive transgression recorded by the marine shale of the overlying Claggett Formation. In the eastern part of the area, this upper sandstone has the attributes of a shoreface deposit and, in the western part, was deposited on a broad tidal flat. Chert pebbles in the upper member and in the basal Claggett are a lag deposit derived from erosion of channels on the delta plain during the transgression. The combined thickness of the middle and upper members of the Eagle is as much as 55 m.

Natural gas in the Eagle Sandstone in surrounding areas is of biogenic origin and probably was generated in Late Cretaceous time. Although gravity faults, which were formed after the gas was generated, are the primary trapping mechanisms today, the initial control was stratigraphic, and an understanding of depositional environments thus is important. The depositional units recognized in outcrop can be identified in nearby wells; when these identifications are combined with other subsurface data, they can help guide exploration.

Zircons date gravels and flows in Park Range of Colorado

The distribution, origin, and temporal relationships of Tertiary alluvial conglomerates and overlying lavas at Rabbit Ears Peak and Rabbit Ears Pass in southwesternmost Jackson County, Colorado (loc. 6), have been clarified. The prevolcanic conglomerates were believed to be continuous with conglomerates of Eocene and Paleocene age east of Rabbit Ears Peak. New Zircon fission-track dates obtained by C. W. Naeser now show that some of the upper conglomerates and the overlying flows at Rabbit Ears are early Miocene in age. G. L. Snyder mapped intermediate conglomerates, not yet directly dated in this area, and concluded from their distribution that they are alluvial gravels, although some were previously mapped as glacial till(?). One linear body 11.25 km long, 400 m wide, and 50 to 100 m thick along an old abandoned course of Service Creek is especially convincing as an alluvial gravel.

Volcanic ash localities in eastern Big Horn Basin of Wyoming

Beds of volcanic ash were found by M. E. Cooley at three localities along the eastern margin of the Bighorn Basin south of Ten Sleep in Washakie County, Wyoming (loc. 7). The deposits occur in a conspicuous strike valley eroded in the Chugwater (Triassic) and Goose Egg (Triassic and Permian) Formations, which display solution-collapse features resulting from partial solution of gypsum beds in the Goose Egg Formation. Ash in sec. 20, T. 43 N., R. 87 W. is 1.2 m thick and occurs 3 m above Box Elder Creek. It is interbedded with silty sand and silt that form part of a terraced deposit extending from creek level to about 22 m above the creek. Ash in sec. 23, T. 46 N., R. 87 W., is less than 1 m thick, overlies a cemented gravel at least 24 m thick, and is about 30 m above Spring Creek. Ash in sec. 26, T. 46 N., R. 87 W., is 3 to 4 m thick and underlies gravel 4 m thick that caps a terrace about 45 m above Spring Creek. The ash in sec. 26, T. 46 N., R. 87 W., is coarse grained, whereas the other two ash deposits are fine grained. K. L. Pierce suggested that the coarse-grained ash might be a product of the last major "Pearlette" eruption in Yellowstone National Park and that the fine-grained ash might be younger.

IGNEOUS STUDIES

Layered sequence in the Stillwater Complex of Montana

The banded and upper zones of the Stillwater Complex (Precambrian W) in the vicinity of Contact Mountain in Sweetgrass County, Montana (loc. 8), were divided by Kenneth Segerstrom and R. R. Carlson into 10 mappable units, which can be traced along their strike for at least 13 km. The composite section of units in ascending order is:

1. Plagioclase-bronzite cumulate (660 m).
2. Plagioclase–two-pyroxene cumulate (325 m).
3. Plagioclase cumulate (560 m).
4. Mixed zone of plagioclase cumulates, plagioclase-olivine cumulates, and plagioclase-bronzite cumulates (330 m).
5. Predominantly plagioclase–two-pyroxene cumulate (330 m).
6. A group of three units of predominantly plagioclase cumulate, each overlain by plagioclase-olvine and plagioclase-bronzite cumulates (0–295 m).
7. Plagioclase cumulate (650 m).
8. Mixed zone of predominantly plagioclase-olivine cumulate in the lower part and plagioclase-bronzite cumulate in the upper part (60–150 m).
9. Plagioclase–two-pyroxene cumulate with minor plagioclase cumulate at the base (50–330 m).
10. Plagioclase cumulate (exposed thickness of 250–650 m).

Many lithologic changes occur laterally along individual layers, especially in units 4, 5, and 8, but the 10 units are clearly recognized in areas mapped east of the Boulder River. Unit 6 was not found west of the river.

Two intrusive centers near Cooke City, Montana

Petrographic, geochronologic, and chemical studies conducted by J. E. Elliott on intrusive rocks in the Cooke City area of Montana (loc. 9) defined two separate intrusive centers that differ in age, composition alteration, and mineral deposits. Earlier work done by Lovering (1930) suggested that both centers were related in age to each other and to the Absaroka volcanic province. It is now evident that only the southern center is related to the Eocene volcanic rocks of the surrounding region.

The northern center, at Goose Lake, is of Cretaceous age and includes a stock that ranges in composition from syenite to quartz monzonite and dikes and sills of quartz-latite and rhyodacite porphyries. The average composition of the center is probably monzonitic. Late magmatic or postmagmatic hydrothermal activity of Cretaceous age resulted in intensive potassium-feldspar alteration associated with stockwork and disseminated copper mineralization in the center of the exposed portion of the stock. Other metals occur only in minor amounts.

To the south, the main Cooke City center includes intrusive rocks that range in age from about 55 to 40 million years (Paleocene to Eocene) and in composition from diorite or monzodiorite to quartz monzonite. The average composition is probably granodioritic. The oldest rocks are diorite and trachyandesite porphyry, and the youngest are rhyodacite and quartz-latite porphyries. A central zone of pyritic gold-copper and disseminated copper deposits associated with the most intense sericitic and (or) feldspathic alteration is fringed by a zone of lead, zinc, and (or) silver deposits with propylitic alteration.

TECTONIC AND GEOPHYSICAL STUDIES

Tectonic style of southeastern Arizona extends into southwestern New Mexico

Mapping done by H. D. Drewes and C. H. Thorman in part of southwestern New Mexico (Peloncillo, Pyramid, Cedar, Coyote, and Brockman Ranges and other mountain ranges) substantiated the concept that the region (loc. 10) was compressively deformed, like adjacent areas in Arizona, as part of the Cordilleran orogenic belt during the Laramide orogeny. Relicts of a pre-Laramide tectonic history were found, but a substantial post-Laramide volcanic and tectonic history has nearly obscured the earlier features.

The Rio Grande rift of New Mexico

L. E. Cordell interpreted compilations of regional geophysical data as showing that the Rio Grande rift of New Mexico (loc. 11) encompasses uplifts of the southern Rocky Mountains and their southern extensions as well as axial fault blocks. Gravity gradients delineate major faults, which form a gridded or en-echelon pattern over distances on the order of tens of kilometers. Aeromagnetic data show these faults to be alined with basement structural grain—by inference, the rift faults of Neogene age zigzag along preexisting basement cracks.

Disharmonic folds in Sublett Range of southeastern Idaho

R. L. Armstrong (University of British Columbia) found the northern Sublett Range in Cassia County, Idaho (loc. 12), to be a series north-northwest-trending, gently south-southeast-plunging, large upright to westward-overturned folds. The folded strata, of Mississippian to Triassic age in a conformable succession nearly 6 km thick, can be readily correlated to the east with Mississippian to Triassic strata in the adjacent Deep Creek and Black Pine Ranges and beyond. There is no major tectonic duplication of strata; in the large folds, disharmonic style is evident from (1) crumpled layering in the cores of large anticlines and (2) detachment, brecciation, and local thrusting of competent units in the cores of large synclines. Steep strike faults having both normal and reverse displacements disrupt the otherwise simple fold structure of the range. Slaty cleavage in Mississippian black shale and fracture cleavage in Pennsylvanian silty limestone are the only metamorphic features observed. The range was largely buried by Cenozoic ash flows and tuffaceous sediments. It is now being exhumed by fluviatile erosion in its central, higher parts, while the competing process of loess deposition slowly mantles fringing valleys and hills.

Décollement in western fold and thrust belt in southeastern Idaho

The structural style of the Oquirrh Formation (Pennsylvanian and Permian) west and southwest of Malad City, Idaho, (loc. 13), indicated to L. B. Platt (Bryn Mawr College) that these strata have been folded and thrust eastward an unknown distance on a surface within the Manning Canyon Shale of Mississippian and Pennsylvanian age, the unit immediately below the Oquirrh. The thickness of the poorly exposed Manning Canyon Shale is difficut to determine but is reported to be from 80 to 300 m in the western part of the Idaho-Wyoming thrust belt. Some of the variation is stratigraphic, but some may be due to hitherto unrecognized structural complexity at this stratigraphic horizon.

Geophysical model of eastern Snake River Plain in Idaho

A two-dimensional model of the crust along a profile across the eastern Snake River Plain in Idaho (loc. 14) prepared by D. R. Mabey produced gravity, magnetic, and topographic anomalies and was consistent with the known geology. The gravity anomaly requires that the mass producing the broad high over the plain be either deep under the plain or more extensive than the plain. The anomaly cannot be produced by basalt in the upper few kilometers of the crust under the plain. The gravity and topographic anomalies could be produced by a thinning of the crust under the plain, the result being subsidence of the plain and the accumulation of up to 5 km of low-density Cenozoic sedimentary and volcanic rocks in the subsidence. The magnetic anomalies appear to reflect basalt in the near surface, the basalt being more abundant in the central and northern parts of the plain.

Structures beneath Snake River Plain in Idaho

According to B. A. Skipp (1976), the eastward bulge of the Antler highland, defined by the present zero Mississippian isopach, in the vicinity of the Snake River Plain in Idaho (loc. 15) may be in part the result of Paleozoic left-lateral offset along the trans-Idaho discontinuity of Yates (1968) and Cenozoic relative right-lateral offset along a zone postulated to exist beneath the lavas of the Snake River Plain to provide the separating mechanism between major Basin and Range extension south of the plain and relatively minor extension north of the plain.

Lemhi Range "detachment block" is a thrust plate

Two sections of the Jefferson Formation (Devonian) measured by M. H. Hait, Jr. (USGS), and R. D. Hoggan (Ricks College) in the southern Lemhi Range of Idaho (loc. 16) indicated the thrust-plate origin of a slab of rock 10 km wide originally interpreted (Beuttner, 1972) as a gravity block detached from the Lemhi Range. Jefferson strata are 90 m thick in the lower plate (the main Lemhi Range) and 420 m thick in the upper plate. The thrust plate contains a nearly complete, highly folded, Paleozoic section, and its relation to underlying rocks and structures suggests that it moved at least 10 km from the west and crosscut two earlier thrust faults.

Cenozoic tectonics in west-central Montana

In west-central Montana (loc. 18), a series of high-angle faults of late Cenozoic age splays southeast and south from the eastern terminus of the Lewis and Clark line—a zone of vertical tectonic movement. These faults bound grabens such as the Helena, Townsend, and Smith River valleys and, together with faults within the valleys, delineate rhomboid-shaped blocks. M. W. Reynolds interpreted this tectonic pattern as resulting from pull-apart of the crustal block on the southern side of the Lewis and Clark line as that block extends westward relative to the crustal block north of the line. The limit of hot-spring activity in west-central Montana coincides with the limit of Cenozoic faulting; together, these limits define the northeastern extent of the Cordilleran thermotectonic anomaly of Eaton and others (1976).

The Sapphire thrust belt of western Montana

The northern part of western Montana's Sapphire thrust belt (loc. 19), studied by M. R. Klepper and C. A. Wallace, is characterized by a complex zone of imbricate thrusts that is about 30 km wide and trends southeastward at about 110° azimuth from Missoula to Drummond, Mont. The Blackfoot fault mapped by Nelson and Dobell (1961) appears to be the northernmost thrust-fault zone of the Sapphire tectonic block eastward along the crest of the Garnet Range. It has been mapped from north of Bonner Mountain through the Garnet mining district to north of Drummond.

In detail, this northernmost thrust zone is composed of numerous anastomosing fault strands that produced an intricate imbricating pattern in Precambrian and Paleozoic sedimentary rocks. Clastic sedimentary rocks are extensively shattered along thrust faults, fault breccias are generally incoherent, and tight isoclinal folds are generally absent. These features suggest either that there was little confining pressure during thrusting or that there was little lubrication along fracture zones during movement. Facies relationships among Paleozoic and the upper part of Missoula Group (Precambrian) rocks suggest that thrust separation distances between individual strands were probably less than 10 km and were more likely 2 to 5 km.

Because thrusting seems to have disrupted rocks that were previously folded and faulted, younger rocks must have been thrust over older rocks in many small thrust plates.

Fault connections in southwestern Montana

On the basis of knowledge gained in the Pioneer Mountains of southwestern Montana (Vipond Park quadrangle) (loc. 20), E-an Zen reinterpreted segments of thrust or high-angle reverse faults previously mapped in adjacent areas. Zen used the criterion that only Beltian sediments and postfault rocks (batholithic, volcanic, and Tertiary sedimentary) occur on the upper plates, whereas, in the lower plates, upper Precambrian through Mesozoic sedimentary rocks are similar in sequence and facies at most places; he was thus able to connect the Kelly thrust of Myers (1952) in the Argenta mining area across the postfault Pioneer batholith with the high-angle reverse Fourth of July fault (Calbeck, 1975) and then with the Johnson thrust of Fraser and Waldrop (1972). A major loop of the Johnson thrust along the alluvium-filled Big Hole Valley could be a left-lateral offset along a concealed later fault. From Big Hole Valley, the fault trace extends toward the eastern flank of the Anaconda Range and could be related to an east-west fault mapped there by Noel (1956). These faults are similar to those of the Philipsburg and Georgetown thrusts of the Philipsburg Folio (Emmons and Calkins, 1913), but their connection, if any, is unclear. The minimum age of the fault is given by a 75-million-year K-Ar age obtained on biotite from a pluton that cuts the fault in the Johnson segment; a possible minimum age based on poorly preserved plant remains (Myers, 1952) is Judith River, in the 73- to 80-million-year range. A klippe of Beltian rocks in the Vipond Park quadrangle is probably an erosional remnant of the fault system; field evidence suggests that the fault broached the surface and that upper-plate rocks were formerly more extensive in the quadrangle even in late Tertiary or early Quaternary time. If the fault system in the Pioneer Range is indeed genetically related to the Philipsburg thrust, the implication is that the western Pioneer Mountains are tectonically part of the Sapphire tectonic block (Hyndman, Talbot, and Chase, 1975), a rather intriguing possibility. How these faults are related to the major thrust system to the west, called the Medicine Lodge thrust system (Ruppel, 1976), is another topic that needs study.

Mount Belknap caldera in Tushar Mountains of Utah

The Mount Belknap caldera in the Tushar Mountains of northwestern Piute County, Utah (loc. 21), subsided about 18 million years ago in response to the eruption of the highly silicic Joe Lott Tuff. Concurrently, rhyolitic domes and flows were erupted from a separate group of centers near the Sevier River, 15 to 35 km to the east. The lower part of the caldera contains a section of densely welded Joe Lott Tuff at least several hundred meters thick that possibly accumulated in part during subsidence. The remainder of the fill, aggregating nearly 1 km in thickness, consists of huge domes and flows of rhyolite and associated marginal talus and lahar breccias, interspersed with local accumulations of welded tuff identical to that found in the lower part of the caldera fill. Minor local subsidence accompanied the eruption of these flows, but it was no more than a few tens of meters at the most. The large domes and flows overtopped the caldera rim on the northwestern and western sides and shed large quantities of coarse debris into adjacent basins to become part of the immediately succeeding Sevier River Formation.

BASIN AND RANGE REGION

MINERAL-RESOURCE STUDIES

Age of mineralization in the Rochester mining district of northwestern Nevada

Rhyolitic volcanic rocks of the Koipato Group host precious metal and dumortierite (aluminum silicate) deposits in the Rochester mining district of Pershing County, Nevada (index map, loc. 1). The Koipato Group (Lower Triassic) includes the Limerick Greenstone, the (ascending) Rochester Rhyolite, and the Weaver Rhyolite (McKee and Burk, 1972). Numerous dikes, sills, and stocks of rhyolite porphyry and leucogranite intrude the Koipato volcanic pile. Lead-alpha ages of rhyolite porphyry southwest of Unionville, Nev., reported by Wallace, Tatlock, and Silberling (1960), are 230±40 and 290±45 million years. The rhyolite porphyry cuts leucogranite, but locally the contacts are gradational, the suggestion being that they were emplaced coevally. The leucogranite cuts the Rochester Rhyolite but does not intrude the uppermost formation of the group, the Weaver Rhyolite.

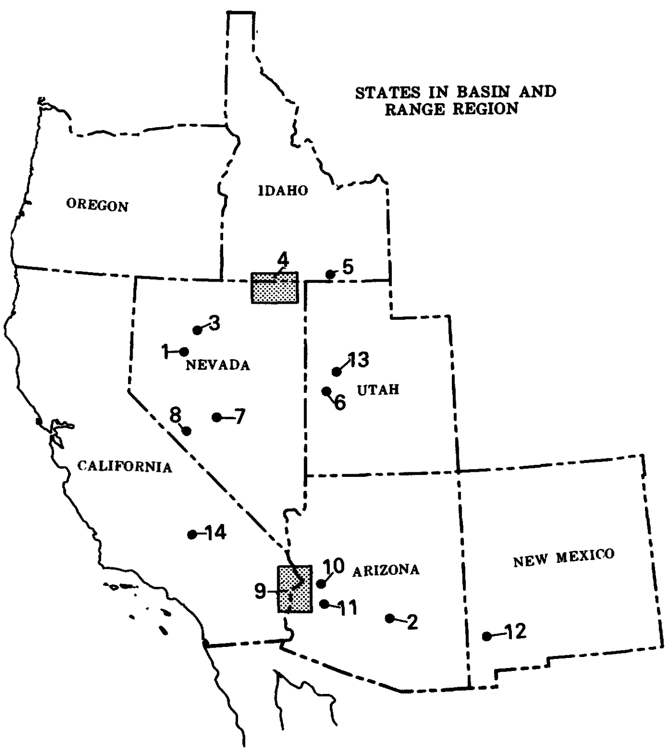

McKee and Burke (1972) reported a zircon fission-track age of 225±30 million years on a welded ash-flow tuff in the Rochester Rhyolite. The isotopic age data indicate a Late Permian-Early Triassic age for the Koipato Group (Geological Society of London, 1964).

Johnson (1976) reported a biotite K-Ar age of 71±3 million years from the Rocky Canyon pluton, a granodiorite to quartz monzonite body that intrudes Triassic strata overlying the Koipato Group 15 km north of Rochester.

At Rochester, the Rochester and Weaver Rhyolites are host rocks for quartz veins that contain silver, gold, and dumortierite. Dumortierite also occurs in sericite-dumortierite-quartz-andalusite schist developed by metasomatism of the Rochester Rhyolite. Four K-Ar ages determined by M. L. Silberman and Peter Vikre on muscovite intergrown with sulfides in these quartz veins and on muscovite from the schist are summarized below:

- Tate prospect (schist), 77.6±2.3 million years.
- Champion mine (sericite and dumortierite in quartz vein), 73.7±2.2 million years.
- Looney mine (sericite in silver-quartz-sulfide vein), 72.5±2.2 million years.
- Nevada Packard mine (sericite in silver-quartz-sulfide vein), 78.8±2.4 million years.

According to Silberman and Vikre, stable isotope data, stratigraphic reconstruction, fluid-inclusion data, and geochemistry strongly suggest that the ores in the Rochester district formed considerably later than Koipato volcanism. The absence of deformation or recrystallization in the vein system supports this hypothesis and leads to the conclusion that the dumortierite and precious-metal mineralization occurred in the Late Cretaceous during a major regional thermal event that may have coincided with the intrusion of the Rocky Canyon pluton to the north.

Precambrian thrusting and Tertiary lead-silver mineralization near Mineral Mountain, Arizona

Recent geologic mapping done by W. J. Keith and T. G. Theodore demonstrated that most of the Mineral Mountain 7½-min quadrangle (loc. 2) of Arizona is underlain by strongly lineated and foliated schists and gneisses of the Pinal Schist of Precambrian X age. The penetrative linear and planar structures in the metamorphic rocks appear to reflect development penecontemporaneous with a major overthrust that juxtaposed two distinct metamorphic terranes some time during Precambrian X and Y time. Diorite, inferred to be correlative with the Madera Diorite of Precambrian X and Y age, does not contain a metamorphic fabric similar to that found in the enclosing schist and gneiss. In addition, Tertiary volcanic rocks crop out prominently throughout the eastern one-third of the quadrangle. They consist of a thick sequence of water-laid tuffs interbedded with and (or) intruded by extrusive rhyolite and quartz-latite flows, dikes, plugs, and sills and a few basalt flows. One of the rhyolitic intrusive masses is particularly interesting in that it shows locally a high degree of vesiculation adjacent to an important north-south lead-silver vein system. Ovoid cavities in the rhyolite seldom exceed 3 mm in length, although a few are as large as 15×10 cm. Vesiculation in the rhyolite may reflect rapid intrusion in a low-pressure environment coupled to an explosive rupturing of the partly crystalline rhyolite and its overburden. Such rupturing may have caused a significant pressure drop in the crystallizing rhyolite and thereby released the volatiles necessary for vesiculation.

STRATIGRAPHIC AND STRUCTURAL STUDIES

Subsidence and thermal history of the Cordilleran miogeocline

In the western part of the upper Precambrian and lower Paleozoic Cordilleran miogeocline in the Western United States, the thickness of strata that accumulated per unit of time is apparently greatest in the older rocks and decreases gradually in the younger rocks, according to J. H. Stewart. The sediments were deposited primarily in shallow marine water, an indication that accumulation is due to subsidence rather than to infilling of an initially deep basin. The rate of accumulation, and thus the rate of subsidence, declines exponentially with a time constant of about 50 million years, an amount similar to subsidence owing to thermal contraction of the lithosphere in oceanic systems and to observed subsidence rates of the Atlantic and Gulf coasts of the United States between Cretaceous and Holocene time. As Sleep (1971) and Sleep and Snell (1976) outlined, subsidence along an Atlantic-type margin should be similar to subsidence in oceanic crust as it spreads away from a midocean ridge. In both cases, the initial thermal event is related to a spreading center. The exponential rate of subsidence in the Cordilleran miogeocline suggests a similar history of thermal contraction following some type of heating event, perhaps related to fragmentation and reshaping of the western margin of the United States by rifting in the late Precambrian.

Ordovician rock temperatures in the Great Basin

A conodont-color-alteration isograd map for Ordovician carbonate rocks in part of the Great Basin was compiled by A. G. Harris, using the technique developed by Epstein, Epstein, and Harris (1977). This map, based on USGS collections from about 100 localities scattered throughout southern Idaho, eastern California, Nevada, and western Utah, shows that (1) Ordovician rocks west of long 116°30′ W. generally have been heated above 250°C; (2) most Ordovician rocks east of long 115°00′ W. have reached maximum temperatures of 100° to 250°C; and (3) most Ordovician rocks in the area between lat 37°30′–42°00′ N. and long 115°00′–116°30′ W. generally have been no hotter than 100°C, with the exception of some Ordovician rocks that were heated to higher temperatures because of their proximity to post-Paleozoic igneous activity.

Aeromagnetic maps of Nevada

The entire State of Nevada, except for a restricted area near the Nevada Test Site in south-central Nevada, is now covered by USGS 1:62,500-, 1:125,000-, or 1:250,000-scale aeromagnetic maps. An aeromagnetic map of Nevada is being prepared for publication. A smaller scale version of the Nevada map was published by J. H. Stewart, W. J. Moore, and Isidore Zietz (1977). These maps have been used in geologic mapping, in explorating for new mineral deposits, and in delineating areas of geothermal potential.

Secondary dolomite in Triassic limestones in northwestern Nevada

Examination by D. H. Whitebread of the Prida and Augusta Mountain Formations (Triassic) in the Dun Glen quadrangle in the East Range of Pershing County, Nevada (loc. 3), revealed a large variation in the amount of secondary dolomite in these formations. At the type locality of the Prida Formation, both formations are composed of limestone, but about 4 km south, near Natchez Pass, the Augusta Mountain Formation is almost completely dolomitized. In exposures 2 to 5 km farther south, a zone of massive dolomite separates Prida limestone from overlying dense laminated dolomite. Whitebread believed that most of the massive dolomite is of hydrothermal origin, whereas Nichols (1974) ascribed its origin to solutions genetically associated with overlying supratidal dolomite.

Interleaved thrust plates of diverse movement in northeastern Nevada

R. R. Coats' analysis of the distribution and direction of movement of late Paleozoic and Mesozoic thrusts in northern Elko County, Nevada (loc. 4), and the ages of the rocks involved revealed that the structural history of the area is more complicated than previous investigators had recognized.

Previous reconstructions indicated that the upper plate of the Roberts Mountains thrust, which consists largely of eugeosynclinal siliceous-assemblage rocks of early Paleozoic age and is regarded as a product of the Antler orogeny (Mississippian to Early Pennsylvanian), extended eastward in the northern part of Elko County almost to long 115°00′ W.

Mapping over the past 10 years has shown that the siliceous facies, east of long 115°45′ W., is tectonically involved with Upper Mississippian, Pennsylvanian, and Permian rocks and was emplaced by thrusting during later orogenies, including the Early Triassic Sonoma orogeny and the middle-Mesozoic Nevadan orogeny. The eugeosynclinal rocks and some of the upper Paleozoic strata of the overlap assemblage were moved, during orogenies subsequent to the Antler, in one of two different directions: (1) Southward or southeastward and (2) eastward. It is hypothesized that the southward movement is the result of two stages of horizontal transport: First, lower Paleozoic eugeosynclinal rocks and upper Paleozoic overlap-assemblage rocks in southwestern Idaho were transported eastward, the Idaho portion of the upper plate being separated from the Nevada portion by a major east-trending right-lateral strike-slip fault; second, parts of the tectonically thickened pile of eugeosynclinal and overlap-assemblage rocks slid southward into northeastern Nevada (Coats and Riva, 1976).

Low-angle faults in the Black Pine Mountains of southeastern Idaho

Low-angle faults form the major structures in the southern half of the Black Pine Mountains in Cassia County, Idaho (loc. 5), where six formations of Devonian to Permian age, recognized by J. F. Smith, have only fault contacts. Younger stratigraphic units are thrust over older units on all faults except one where a Devonian unit is thrust over Mississippian, Pennsylvanian, and Permian strata. Upper Pennsylvanian and Lower Permian calcareous siltstone and sandstone, which are probably part of the Oquirrh Group (upper Paleozoic), make up the highest thrust sheet. Erosion of this thrust sheet and successively lower sheets has opened windows on the rocks below.

Stratigraphy and structure in the House Range of west-central Utah

Geologic mapping done by L. F. Hintze (Brigham Young University) showed that the Cambrian stratigraphic section in the House Range in Millard County, Utah (loc. 6), includes structural complexities and stratigraph variations not heretofore recognized. Attenuation faulting has tectonically thinned the stratigraphic sequence in Death Canyon, the site of some of C. D. Walcott's type sections. Between Marjum Pass and Swasey Peak, uppermost Middle Cambrian strata show rapid facies changes that may represent the transition from a carbonate bank to a shelf setting. The attenuation faulting, newly recognized in the central House Range (Hintze, 1976), seems to have localized alteration and minor mineralization associated with nearby Tertiary volcanism.

Tertiary thrusting near Manhattan, Nevada

A low-angle fault that places older volcanic rocks above younger ones was mapped in the northern part of the Manhattan quadrangle in Nye County, Nevada (loc. 7), by D. R. Shawe. Rocks near the base of a section of gently dipping volcanic rocks at least 800 m thick have been moved on a fault surface dipping 20° to 30° southeast, so that they rest on rocks about 250 m below the top of the volcanic section. Geometric relationships between the fault and the volcanic units suggest that several kilometers of movement may have occurred on the gently dipping fault. Mineralization has occurred locally along the fault. Mineralization at Manhattan, 8 km south of the fault, has been dated at 16 million years before present (Silberman and others, 1975); if mineralization along the low-angle fault correlates with that at Manhattan, the faulting occurred earlier than 16 million years ago; it was no older than 26 million years, the age of the younger volcanic rocks (for example, Silberman and others, 1975). Reconstruction of topography for the interval from 16 to 26 million years ago suggests that relief was inadequate for movement on the low-angle fault to be attributed to gravity sliding. The low-angle fault may have formed as a result of local compression related to right-lateral strike-slip faulting along west-northwest-trending faults within the Walker Lane structural zone, the northern edge of which is near Manhattan.

Mississippian carbonate rocks in southwestern Nevada

Autochthonous marine limestone and dolomitized limestone of Late Mississippian age was recognized by F. G. Poole in Mineral and Esmeralda Counties, Nevada (loc. 8). In the Candelaria Hills and the Monte Cristo Range, the carbonate rocks rest with angular unconformity on strongly deformed allochthonous Ordovician eugeosynclinal rocks and are overlain unconformably by autochthonous medial Diablo Formation (Permian). The shallow subtidal to intertidal carbonate rocks, which are as much as 180 m thick, were deposited on submerged parts of the Antler orogenic belt. Previously, geologists considered this carbonate unit as part of the Diablo Formation.

Major tectonic zone in the eastern Mojave Desert

The presence of a major tectonic belt trending northwest through western Arizona and southeastern California (loc. 9) is suggested by the distribution of Permian and Mesozoic rocks, according to W. J. Carr and D. D. Dickey. The probable correlation of a widespread quartzite in the Arica, Riverside, and Whipple Mountains of California and the Buckskin Mountains of Arizona with the Permian Queantoweap Sandstone of McNair (1951) of the region east of Las Vegas, Nev., supports earlier ideas that the northeastern edge of a major northwest-trending structural zone exists in the Riverside-Big Maria Mountains area of easternmost California. This quartzite, previously correlated with the Coconino Sandstone, appears to resemble the "Queantoweap" more closely. Rocks on the southern side of the Big Maria Mountains are more like typical Supai, Coconino, and Kaibab Formations, as are sections in the Plomosa and Harquahala Mountains to the east and southeast. No Paleozoic rocks are known to occur southwest of this structural zone, and Mesozoic rocks ("Palen" and "McCoy" Formations of local usage and Livingston Hills Formation) are apparently absent northeast of the boundary. One attractive explanation for the distribution of Paleozoic rocks is that a zone of major strike-slip displacement is present along the boundary and roughly coincides with the southwestern edge of the proposed Mojave-Sonoran belt (Carr and Dickey, 1977), a structural zone characterized by a major regional detachment fault.

Cenozoic structure, stratigraphy, and volcanism in west-central Arizona

According to Ivo Lucchitta, the Bill Williams River area in southern Mohave and northern Yuma Counties, Arizona (loc. 10), is located near the northeastern tectonic margin of a region (Mojave-Sonoran belt of Carr and Dickey, (1977)) characterized by Cenozoic terrigenous sedimentary rocks, an assemblage of silicic and mafic volcanic rocks, thrust faults, and closely spaced listric normal faults. The principal sedimentary rocks comprise locally derived arkosic conglomerate and sandstone and a conspicuous monolithologic breccia. The breccia becomes thicker southward toward a thrust system and apparently represents debris shed from the leading edge of advancing thrust plates.

Volcanic rocks interfinger with sedimentary rocks above the breccia. Three volcanic sequences comprise older mafic lavas, silicic rocks, and younger mafic lavas. The older lavas are characterized by quartz xenocrysts and are estimated to range in age from more than 40 to about 20 million years. The silicic rocks are chiefly rhyolite plugs, domes, lava flows, and air-fall tuffs, probably about 20 million years old, according to regional correlation. The silicic vents lie along a N. 79° W.-trending line about 65 km long. The younger mafic lavas, which generally contain large phenocrysts of feldspar and hornblende, probably belong to a widespread group of mesa-forming lavas about 10 million years old.

Other parts of the area are underlain by Tertiary and Quaternary alluvial deposits and by Quaternary pediment and terrace deposits and other surficial material. These deposits reflect the present topography.

Older sedimentary and volcanic rocks are faulted and tilted to the southwest. The main episode of high-angle faulting probably coincided with silicic volcanism. The intricate deformation of the area gives it a distinctive topographic appearance devoid of prominent structural basins and ranges that are common elsewhere—in marked contrast to the north-trending ranges farther north and the group of anomalous northeast-trending ranges immediately south.

Permian rocks in the Harquahala Mountains of southwestern Arizona

Probable stratigraphic equivalents of the Supai-Coconing-Toroweap-Kaibab sequence of northwestern Arizona were recognized by F. G. Poole, P. T. Hayes, W. J. Carr, and D. D. Dickey in the southern Harquahala Mountains of Yuma County, Arizona (loc. 11). Although these beds of fossiliferous limestone and sandstone, siltstone, and gypsum are similar to several Permian facies in northern Arizona, some differences in stratigraphic details prevent precise correlation without further study. The section in the Harquahala Mountains, together with a similar section in the Plomosa Mountains (Miller, 1970) 50 km to the west, provides valuable control points for a regional study of Permian sedimentation and stratigraphy in western Arizona.

IGNEOUS ROCKS

Tyrone laccolith in the Big Burro Mountains of New Mexico

D. C. Hedlund reported that the quartz monzonite of the Tyrone laccolith is only one of a series of structurally controlled rhyolitic and monzonitic intrusions of Tertiary age that are alined along a belt trending N. 35°–40° W. in the eastern part of the Big Burro Mountains in Grant County, New Mexico (loc. 12). Other intrusions include the rhyolite of Saddle Mountain, rhyolite plugs of the Tullock Peak area, rhyolite of the Shrine mine, and the monzonite porphyry of the Twin Peak stock. Several small tonalite and tonalite porphyry intrusions of uncertain age are also present along this belt. Analyses of faults, joints, and dikes in the area indicate two principal zones of structural weakness coincident with the belt. The dominant zone strikes N. 60°–70° E. and coincides in trend with rhyolite dike swarms. A subordinate zone strikes N. 35°–40° W. and coincides in trend with the belt of intrusive rock.

The quartz monzonite of the Tyrone laccolith, dated as 53 million years old by Moorbath, Hurley, and Fairbairn (1967), is believed to be a laccolithic or sheetlike intrusion (Kolessar, 1970). The gently dipping contact of a roof pendant of Precambrian granite and the intrusion (NW¼NE¼ sec. 9, T. 20 S., R. 16 W.) suggests that the upper surface of the intrusive rock is nearly flat. On the basis of drill-hole data obtained in the northeastern part of the intrusion, John Kolessar (written commun., 1976) considered the intrusive rock to have a Precambrian granite floor.

The nearby rhyolite of Saddle Mountain, which appears to be a sheetlike intrusion in Precambrian granite, dips about 30° ENE. Its configuration and contact relation with the surrounding granite suggest similarities to parts of the Tyrone intrusion.

Rhyolite plugs of the Tullock Peak area form outcrops like "beads on a string" and represent bulbous expansions of rhyolite dikes. The rhyolite dike swarms (13–20/km) strike N. 60°–70° E.

Rhyolite of the Shrine mine probably represents an extrusive dome whose outer margins mushroom onto a Precambrian granitic floor. The rhyolite dome is also along a line of rhyolite dike swarms that strike N. 60°–70° E.

The monzonite porphyry of the Twin Peak stock has not been studied but occurs along the same intrusive belt as the Tyrone laccolith. C. H. Hewitt (1959) discovered a large Precambrian migmatite pendant(?) within the Twin Peak intrusion, which suggests that the body has a gently dipping upper surface similar to that of the Tyrone intrusion.

Intrusive center in the Keg Mountains of west-central Utah

A quartz-monzonite porphyry stock was discovered as a result of geologic mapping done by H. T. Morris in the Keg Mountains of Juab County, Utah (loc. 13). This stock is apparently the terminal phase of an older (Oligocene) volcanic series and is partly concealed by younger (Miocene and (or) Pliocene) volcanic rocks. The intrusive body probably marks the eruptive center of the older volcanic series and may indicate an area in the Keg Mountains that has a good chance for containing concealed ore deposits.

GEOCHRONOLOGIC STUDIES

Two isotopic ages were obtained on samples collected by F. G. Poole from the type Mesquite Schist in the El Paso Mountains of Kern County, Cali-

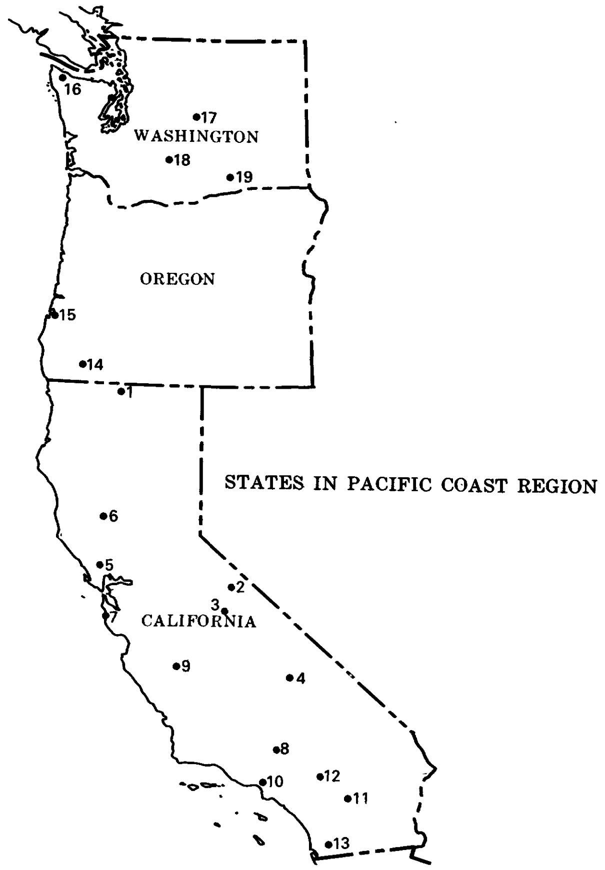

fornia (loc. 14). A muscovite K-Ar age of 168 million years determined by R. F. Marvin apparently records thermal metamorphism related to Jurassic plutonism, whereas whole-rock Rb-Sr dates determined by C. E. Hedge suggest an Ordovician age for the original marine sediments. An Ordovician age for the original Mesquite sediments corroborates Poole's regional correlation with lower Paleozoic inner-arc–basin rocks. Previously, some geologists considered the Mesquite Schist to be late Precambrian in age.

PACIFIC COAST REGION

CALIFORNIA

Mesozoic age of North Fork terrane in Klamath Mountains

Radiolaria were used for dating ancient oceanic crust and time of plate convergence in the southern Klamath Mountains of California (index map, loc. 1) by W. P. Irwin and D. L. Jones (USGS) and E. A. Pessagno, Jr. (University of Texas, Dallas). The North Fork terrane includes one of several ophiolite belts in the province, along with associated ribbon chert, siliceous tuff, other volcanic rocks, and minor limestone. These rocks have been considered Permian in age on the basis of fusulinids found in the limestone. However, the North Fork terrane, where it has been sampled along a transect near the latitude of Hayfork, now has been found to be mainly Mesozoic in age rather than Paleozoic. There the chert and tuff yield abundant radiolaria that indicate a range in age from Late Triassic(?) to Middle Jurassic(?). Some of the tuff contains a radiolarian fauna similar to the fauna found in some Franciscan cherts. The pods of Permian limestone may be exotic blocks derived from an older terrane. On the basis of the age of the radiolaria and other regional relations, the time of convergence of the North Fork terrane with Devonian metamorphic rocks to the east now is thought to have been Late Jurassic. This research is in an early stage, but the preliminary results clearly have far-reaching implications for the paleotectonic history of the western California region.

Period of activity along the Melones fault in California

For many years, geologists have recognized that a major tectonic feature in the western Sierra Nevada of California (loc. 2) is a great system of regional faults that extends over hundreds of kilometers. One of the longest of these faults, the Melones, is marked by tectonic mélange and numerous occurrences of alpine-type serpentinite and gabbro and may be the suture line for an east-dipping subduction zone that juxtaposed volcanic and flysch rocks of Jurassic age against a continental mass of rocks of Paleozoic age and older. B. A. Morgan III completed mapping a section across the western Sierra Nevada and investigated about 100 km of the Melones fault between Sonora and Mariposa, Calif. When detailed information on small intrusive rocks in the area is used in conjunction with isotopic dates (U-Pb on zircon obtained by T. W. Stern), rather definite limits can be placed on the time of activity of the Melones fault. East of Moccasin, Calif., the Melones fault disrupts a small diorite stock dated at 162 million years. Data from the 1,000-m-deep Eagle Shamut mine several kilometers north of Moccasin suggest that the fault may disrupt at depth a small diorite pluton dated at 148 million years. Near Mariposa, rocks near and in the fault zone that have been contact metamorphosed by the igneous complex near Guadalupe to a hornfels apparently have not been broken by the Melones fault. A new zircon sample taken from the upper part of this complex has been dated at 140 million years a date very similar to one of 136 million years based on K-Ar in biotite. These dates bracket the time of activity of the fault in the area as being between 162 and 140 million years a possible tighter bracket would be 148 to 140 million years. This span of activity is remarkably short and may account for only a small part of the total time of deformation associated with the Nevadan orogeny. Underthrusting of the continent by an east-dipping subduction zone probably continued after 140 million years ago, but the site of thrusting and deformation may have migrated westward to the Great Valley and ultimately to the California Coast Ranges some 80 km west of the Melones fault.

Mesozoic metavolcanic rocks of the Bean Canyon roof pendant in southern Sierra Nevada

R. J. Fleck (USGS) and G. A. Davis (University of Southern California) completed a study of the geochronology and structure of a roof pendant in the southernmost Sierra Nevada-northern Mojave region at Bean Canyon, Calif. (loc. 3). Samples of dacitic metavolcanic rocks dated by the Rb-Sr method yield ages averaging about 150 million years. Granitic rocks of the Sierra Nevada batholith immediately north of the pendant dated by the K-Ar method yield concordant biotite and hornblende ages of about 81 million years (Evernden and Kistler, 1970). Considered as a whole, the sample set indicates either open-system behavior of rubidium and (or) strontium or significant variation (0.7079–0.7096) in initial $^{87}Sr/^{86}Sr$ ratios. Samples collected from the same stratigraphic horizons appear to have been in isotopic equilibrium since Late Jurassic time. The variation in initial ratio, however, permits the interpretation that the rocks were originally comagmatic, formed more than 150 million years ago, and were subjected to local metamorphic homogenization of strontium isotopic systems at about 150 million years. The isotopic systems have remained closed since that time, however, in most of the units, although the pendant suffered significant contact metamorphism during the 81-million-year intrusive event. The metavolcanic rocks and associated metasedimentary rocks are tectonically interlayered with a thick ultramafic sheet, probably by thrust faulting. Because the only geologic event recorded in the rocks other than the batholithic intrusion at 81 million years is the presumed overthrusting, the 150-million-year age must represent either the time of volcanism or the time of thrusting. Unfortunately, the data do not permit a unique solution.

Chronology of Miocene volcanism in the Owlshead Mountains of California

Geologic mapping and K-Ar age studies conducted by R. J. Fleck (USGS) and G. A. Davis (University of Southern California) in the Owlshead Mountains in the southwestern Death Valley area of California (loc. 4) revealed a surprisingly condensed chronology of Miocene volcanism, block faulting, erosion, and gravity sliding. Miocene lahars, pyroclastic rocks, and andesitic to basaltic lava flows were deposited between the Owl and Lost Lake playas on a granitic basement that had more than 100 m of relief. Basement rocks resemble the Teutonia Quartz Monzonite of the northeastern Mojave Desert and yield comparable K-Ar ages of biotite (95×10^6 years). Closely similar sequences of Miocene strata are contained in three major sheetlike allochthons that lie discordantly on one another, on their autochthonous counterparts, and on the granitic basement. The allochthons, interpreted as gravity-driven slide sheets, cover a minimum area of 30 km^2 and have minimum northeastward displacements of 10 km.

Well-exposed field relationships in the central Owlshead Mountains support the following sequence of events: (1) Accumulation of flow and volcaniclastic deposits with at least one intervening period of tilting and erosion; (2) minor east-west block faulting; (3) north-south block faulting, the fault blocks being tilted west; (4) erosion; (5) gravity sliding; (6) northeast-southwest high-angle faulting; (7) erosion; (8) renewed gravity sliding; and (9) hypabyssal intrusion across the base of slide sheet. Potassium-argon age determinations of allochthonous and autochthonous volcanic (1) and hypabyssal (9) units show that this complex geologic history was confined to a 2-million years period between 12 and 14 million years ago. In contrast, the period from 12 million years to the present has seen tectonic stability and only minimal erosion of the 12-million-year-old landscape.

New major thrust fault in California Coast Ranges

E. H. Bailey, M. C. Blake, Jr., and R. J. McLaughlin found evidence in regional structural relationships for a previously unrecognized east-dipping thrust fault of regional extent west of Healdsburg, Calif. (loc. 5). This thrust separates Upper Cretaceous and lower Tertiary rocks of the Franciscan coastal belt from older Upper Jurassic and Upper Cretaceous Franciscan rocks on the northeast. This "Coastal Belt thrust" is structurally below the Coast

Range thrust of Bailey, Blake, and Jones (1970), although the two thrusts appear to converge toward the west. Hypothetically, the Coastal Belt thrust represents the early Tertiary stage of a west-stepping subduction zone that operated between Late Jurassic and early Tertiary time.

Age relations above and below Coast Range ophiolite

Investigations conducted by R. J. McLaughlin (USGS) and E. A. Pessagno (University of Texas, Dallas) in The Geysers-Clear Lake area of northern California (loc. 6) showed that an Upper Jurassic ophiolite and depositionally overlying Tithonian to Valanginian strata of the Great Valley sequence rest on deformed and metamorphosed Cenomanian rocks of the Franciscan assemblage. These relations clearly demonstrate the validity of the Coast Range thrust and suggest that the Great Valley sequence was not deposited on a tectonically active shelf of older Franciscan rocks, as Maxwell (1974) had postulated. Contact relations of the ophiolite and the overlying Great Valley sequence in The Geysers-Clear Lake area suggest that more than 305 m of the ophiolite may have been eroded locally during late Kimmeridgian to middle Tithonian time. However, other local differences in the ophiolite cannot be explained by differential erosion and must be due to original lateral differences in composition of the ophiolite sheet, differential removal of ophiolite units by shearing during subduction, or postsubduction faulting related to uplift.

A composite section of the ophiolite indicates the following units in ascending order: (1) 1,212 m of sheared ultramafic rocks; (2) 636 m of cumulate gabbro; (3) 455 m of semiconcordant diabase dikes; and (4) more than 455 m of pillow basalt, tuff, pillow breccia, basalt-diabase breccia, and tuffaceous chert of late Kimmeridgian Age.

Lateral movement on San Gregorio fault

Regional geologic studies conducted by J. C. Clark and E. E. Brabb indicated that the onshore trace of the San Gregorio fault extends from coastal exposures east of Año Nuevo Point northwestward for 27 km to the coast near San Gregorio, Calif. (loc. 7). This fault has juxtaposed two major tectonic blocks with markedly different stratigraphic sequences, the suggestion being that the fault has extensive lateral displacement.

In the Pigeon Point block southwest of the San Gregorio fault, porphyritic silicic rocks may form part of the basement; they are overlain by at least 2,600 m of clastic strata of Late Cretaceous age. Cretaceous strata are not present in the La Honda and Ben Lomond blocks northeast of the fault where more than 10,000 m of Paleocene to Pliocene rocks rests on a pre-Tertiary granitic basement. Paleocene and Eocene rocks are not present in the Pigeon Point block. Oligocene (Zemorrian) and middle Miocene (Relizian and Luisian) strata occur in both tectonic blocks, but they differ in lithology, fauna, and bathymetry on opposite sides. A thick upper Miocene to lower Pliocene mudstone section in the La Honda and Ben Lomond blocks is missing west of the fault.

Cordilleran miogeosyncline—an unlikely parent for Salinian block metamorphic rocks

D. C. Ross's analysis of the preintrusive metamorphic rocks of the Salinian block (loc. 8) suggested an original sedimentary section composed dominantly of thinly bedded, fine- to medium-grained siliceous clastic rocks in which coarse-grained rocks and pure quartzite were quite rare. Marble, although eye catching and locally abundant, is nevertheless subordinate and mixed with other lithologies when large blocks of basement are examined.

Tradition and word of mouth have long suggested that the rocks of the Salinian block came from the area of the Cordilleran miogeosyncline. Yet the pure massive quartzites in the upper Precambrian and lower Paleozoic, the thick pure carbonate units throughout the section, and the coarse clastic rocks in the overlap rocks of the upper Paleozoic in western Nevada and eastern California do not appear to have counterparts in the Salinian block. Present data therefore indicate that investigators must look elsewhere for a parent terrane for the Salinian block metasedimentary rocks.

Late Cenozoic climatic history of central California

Work done by D. E. Marchand indicated that the uppermost Tertiary and Quaternary nonmarine deposits of the eastern San Joaquin Valley (loc. 9) of California record a long history of cyclical deposition, land stability and soil formation, and erosional incision. Present evidence suggests seven major pre-Sangamon and eight post-Sangamon episodes of terrace and alluvial fan aggradation, most, if not all, of which can be related to climatic oscillations. The alluvial-lacustrine sequence of the San Joaquin Valley can be correlated, although not directly, with glacial events in the adjacent Sierra Nevada and potentially with estuarine deposits in and beneath the San Joaquin-Sacramento Delta and San Francisco Bay.

Surface mapping shows that the Laguna Formation contains upper Pliocene fluvial granitic sediment lithologically identical to that found in the Pleistocene glaciogenic Turlock Lake, Riverbank, and Modesto Formation of Davis and Hall (1958). A strongly developed paleosol within the Laguna indicates at least two periods of alluviation, possibly correlative with the Deadman Pass and McGee Glaciations of the Sierra Nevada and with lake beds (K-Ar age, 2.3 million years) on the eastern side of Owens Valley, Calif. The lower unit of Davis and Hall's Turlock Lake Formation, probably equivalent to the Sherwin Glaciation of the Sierra Nevada, was deposited during a paleomagnetically reversed epoch that may include one normal (Jaramillo(?)) event. The upper unit of the Turlock Lake, which is probably correlative with the Hobart Glaciation of the northern Sierra Nevada and possibly with the Kansan Glaciation of the midcontinent region, contains pumiceous ash having a K-Ar age of 0.6 million years. Davis and Hall's Riverbank Formation, which is perhaps equivalent to the Illinoian of the Midwest, represents three separate outwash events that are found, on the basis of soil development, to be substantially younger than their Turlock Lake Formation but older than the Sangamon Interglaciation. The Wisconsin is represented by up to six phases of alluvial fan deposition (Davis and Hall's Modesto Formation), four of them in Tioga (late Wisconsin) time. The brief episodes of late Holocene aggradation are also recognized.

The stratigraphic sequence in the San Joaquin Valley subsurface, preserved through continuous valley subsidence throughout Cenozoic time, may represent the most nearly complete Quaternary record in western North America. Near the eastern basin margin, alluvial units are separated by unconformities and buried paleosols. No major unconformities, however, have been recognized in the 1,000-m Quaternary sequence of reduced sediments along the valley axis; deposition here is thus shown to have been continuous or very nearly so, although it varied markedly in rate. Radiometric ages demonstrate the contemporaneity of basin lakes with outwash fans and hence with climatic oscillations. At least eight major lacustrine units have been identified—five of them are 600,000 years and younger, and three of them are older. The dated pumice lies conformably on the Corcoran Clay Member of the Tulare Formation (Davis and Hall's Turlock Lake), the thickest and most extensive of the subsurface lacustrine deposits. The youngest lacustrine clay is bracketed by carbon-14 ages of about 9,000 and 27,000 years and may itself represent three or more minor lake fluctuations.

The late Cenozoic nonmarine climatic record from the San Joaquin Valley is thus unusually long and complete; can be tied to a glacial record in a major middle-latitude mountain range; shows potential for correlation with a marine estuarine sequence; bears a striking resemblance to long records from deep-sea cores and other sources; and supports the hypothesis of major climatic cycles of approximately 100,000 years.

Geotechnical data problems in Los Angeles

J. C. Tinsley found that, although a large quantity of geologic and geotechnical data are available for certain sectors of the Los Angeles Basin of California (loc. 10), their applicability often may be limited severely because the data were collected during specialized studies conducted at certain sites for specific purposes. For example, vast amounts of geotechnical data are available from shallow boreholes (depths generally less than 20 m) used to collect samples for estimating foundation conditions prior to design and construction of buildings. Such data have limited application to the selection of tunnel alinements, tunnel design criteria, and tunnel boring conditions because tunnels in this area would almost certainly be deeper than 20 m. Also, much data relevant to tunneling conditions typically are not collected during the geologic and geotechnical studies performed for foundation investigations.

Dating deformational structures in sediments to determine earthquake recurrence intervals

J. D. Sims examined outcrops of sediments of ancient Lake Cahuilla in the Coachella Valley of California (loc. 11). The upper 4 to 5 m of these deposits represents the time between 300 and 200 years before present. The deposits near Mecca, Calif., reveal soft sediment deformational structures similar to those found in other areas (Sims, 1975). Further work may yield an earthquake history and recurrence interval for the southern part of the area of aseismic uplift described by Castle, Church, and Elliott (1976).

Cores from Hidden Lake in Alaska contain about 4.5 m of olive-black, organic-rich sediments overlying $>$1.5 m of gray, rhythmically laminated glaciolacustrine sediments. Glaciers retreated from the Hidden Lake area about 10,000 years before present. Thus, the upper 4.5 m of this core represents most, if not all, of Holocene time. The lower 1.5 m of this core contains varved sediments similar to those being deposited in the present-day Skilak Lake nearby. The upper parts of cores from Hidden Lake contain abundant ash beds and carbonaceous material that will be used to correlate with and date deformational structures in cores from Skilak Lake.

Offsets along Mojave Desert faults

Potassium-argon dating of granitic rocks in the eastern Transverse Ranges and southern Mojave Desert of California (loc. 12) done by D. M. Morton and F. K. Miller indicated that such dating may provide a precise quantitative estimate of offsets along five major strike-slip faults in the Mojave Desert. From east to west, the five subparallel northwest-trending faults are the Helendale, the Lenwood, the Camprock, the Calico-Mesquite, and the Pisgah. The average length of the faults is about 75 km, and all have exhibited historic seismicity or have very youthful primary fault features developed along them in young alluvial material.

All of the granitic rocks in the eastern Transverse Ranges and the southernmost Mojave Desert yield cooling ages that reflect the general cooling history of the region and may approach the true emplacement age for only a few of the youngest plutons. Surrounding this zone of relatively uniform cooling ages is a well-defined zone of discordant ages, outside of which the granitic rocks appear to yield concordant K-Ar ages that are probably close to emplacement ages. This well-defined zone of discordant ages is offset by the strike-slip faults on the Mojave Desert. Preliminary results indicate that the Helendale fault may offset the zone in a right-lateral sense about 8 km, and the Lenwood fault offsets it about 15 km. Closely spaced samples collected in the zone of discordance on both sides of all five faults are being dated now and should provide relatively precise measurements of offset across all the faults.

Mafic plutonic rocks of two ages in Peninsular Ranges batholith of California

V. R. Todd mapped two distinctive groups of mafic plutonic rocks in the Peninsular Ranges batholith of south-central San Diego County, California (loc. 13). The first group consists of a variety of gabbroic rocks that are correlated by most workers with the San Marcos Gabbro (Cretaceous) of northern San Diego County. These gabbroic rocks are the oldest plutonic rocks in this part of the Peninsular Ranges batholith. They are cut by granitic plutons that have divided them into a number of large bodies (3 to 7 km across), most of which form prominent peaks.

The mafic rocks of the second group, chiefly quartz-bearing biotite-hornblende diorite with lesser amounts of gabbro, are among the youngest plutons in this part of the batholith. They are about half the size of the older mafic bodies and for the most part were emplaced along preexisting plutonic contacts. A widespread system of metadiabase dikes is related to the younger mafic plutons.

Contacts between granitic plutons and mafic plutonic rocks of both early and late suites are complex, and age relations are locally ambiguous. Contacts are typically synplutonic—that is, plutons have been diked along their margins by the rocks into which they were emplaced. Rock textures suggest that mafic and granitic plutons were hot and mobile simultaneously during batholithic emplacement.

Both suites of mafic rocks have tectonite fabrics that are concordant with the regional synkinematic fabric shared by all plutonic and metamorphic rocks in this part of the batholith.

OREGON

Southwestern Oregon greenstone

M. G. Johnson's study of greenstone in the north-central part of the Medford 2° quadrangle of Oregon (loc. 14) resulted in the recognition of two disparate metavolcanic sequences containing seven distinctive lithofacies that have lateral continuity of at least 27 km and provide a key to correlation in the Rogue Formation to the south. The sequences were thrust westward over the Dothan Formation and are themselves broken by a major thrust fault. The western sequence, predominantly pyroxene-bearing pryoclastic rocks, is more mineralized in base metals than the eastern sequence, which is predominantly hornblende-bearing tuffs and flows. The thrust fault that separates the two sequences is mineralized, but the highest concentration of anomalous base metals is in a subsidiary thrust sheet in rocks of the westernmost lithofacies. This block is also the host for the Silver Peak massive sulfide deposit mined in the early part of the century.

Complicated late Mesozoic paleogeography in southwestern Oregon

Mapping done by M. C. Blake, Jr., in the southern part of the Coos Bay 2° quadrangle of Oregon (loc.

15) resulted in the recognition of four distinctive fault-bounded terranes of late Mesozoic age. The westernmost terrane is underlain by the Otter Formation (Upper Jurassic, Tithonian), which is largely quartz-poor volcanic sandstone and subordinate andesite. Overlying this unit, along a major east-dipping thrust fault, are lithic graywacke and shale plus abundant greenstone and chert of the Dothan Formation (also containing Tithonian fossils). To the east, these western Dothan rocks are in high-angle fault contact with another Dothan unit characterized largely by quartzofeldspathic graywacke containing latest Jurassic (Tithonian) to Early Cretaceous fossils. Structurally overlying the eastern Dothan belt is a thrust sheet of sandstone, mudstone, and conglomerate of the Myrtle Group, which again contains fossils of latest Jurassic (Tithonian) to Early Cretaceous age. The Myrtle sediments appear to rest on a dismembered ophiolite sequence, and serpentinized ultramafic rocks occur as fault slices in the other three belts. No satisfactory paleogeographic reconstruction has yet emerged, but the Otter Point Formation appears to be a good candidate for an island arc.

WASHINGTON

Tertiary tectonic framework in northwestern Olympic Peninsula

Detailed geologic mapping done in the northwesternmost part of the Olympic Peninsula (loc. 16) south of the Calawah fault in Washington by P. D. Snavely, Jr., J. E. Pearl, and A. R. Niem indicated that folded and thrust-faulted strata of late Eocene and early Oligocene(?) age overlie a lower to middle Eocene mélange "basement." In most places, the contact between the mélange and younger rocks is faulted, but, in several places, upper Eocene strata rest depositionally on the mélange.

The tectonic fabric of the mélange is commonly near vertical and strikes northward, whereas the younger beds have lower dips. The mélange appears to consist of imbricate thrust slices that have been rotated to near vertical by continuous compressive stresses, which are interpreted as being related to the eastward underthrusting of the Pacific (Farallon) plate beneath the American plate. The orientation of drag folds in thin-bedded siltstone units between some thrust slices supports predominant east-west compression and westward tectonic transport of the landward-dipping thrusts in the autochthonous plate.

The accretionary prism of imbricated lower to middle Eocene sediments formed the basement upon which outer-shelf sediments were deposited during late Eocene to middle Miocene time. Renewed underthrusting in late middle Miocene time intensely deformed these strata and probably initiated diapirism of the mélange.

Revision of Swauk stratigraphy and age

Mapping done in the Wenatchee 2° quadrangle of Washington (loc. 17) by R. W. Tabor and V. A. Frizzell detailed some important lower Tertiary stratigraphy. In its type area, the Swauk Formation consists of thin-bedded and crossbedded, dark-gray, lithic and feldspathic sandstone, shale, and conglomerate. A mafic tuff interbed, probably a tongue of Foster's (1960) Silver Pass Volcanics has a zircon fission-track age of 49 ± 5 million years (C. W Naeser, written commun., 1976).

West of the type area, folded sandstone of the Swauk Formation and overlying but partly interbedded Foster's Silver Pass Volcanics are overlain unconformably by Teanaway Basalt. Ages of zircons from two tuffs in Foster's Silver Pass Volcanics are about 53 ± 5 and 51 ± 5 million years (J. A. Vance, written commun., 1976). The Teanaway is succeeded conformably by arkose of the Roslyn Formation.

East of the type area, the Swauk in general becomes more shaly upward, but includes tongues of poorly sorted arkose of Roslyn aspect eastward and in the uppermost part.

East of the Leavenworth fault and within the Chiwaukum graben, the predominantly arkosic sandstone contains a tuff interbed that has been dated at 44×10^6 years. Correlation of this arkose with the Roslyn is supported by a thin, conformable, nearly basal layer of basalt breccia, probably an eastern tongue of the Teanaway.

Tabular bodies of monolithologic granodiorite breccia and conglomerate and serpentinite fanglomerate parallel faults marking the southern end of the Leavenworth fault zone and indicate contemporaneous deposition and uplift along the Leavenworth fault during late Swauk and early Roslyn time.

Revision of lower Pleistocene glacial sequence in Wenatchee and Yakima Valleys of Washington

Mapping done by R. B. Waitt, Jr., of Quaternary deposits in the Wenatchee (loc. 17) and Yakima (loc. 18) River Valleys changed the correlation of the oldest glaciogenic units in each valley. In Yakima Valley, the "Thorp till" now appears to be much younger than the "Thorp outwash" of Porter (1976). In Wenatchee Valley, the "Chumstick" drift of Long and Porter (1968) and Porter (1969) is spurious, Page (1939) having been essentially correct in the mapping of his "Peshastin" drift. The revised, nonformalized rock-stratigraphic terminology is:

Yakima Valley	*Wenatchee Valley*
"Lakedale" drift (5 members).	"Leavenworth" drift (5 members).
"Kittitas" drift (2 members).	"Peshastin" drift (1 member).
"Lookout Mountain" drift (1 member).	"Boundary Butte" drift (1 member).

Faults along the Olympic-Wallowa lineament in south-central Washington

Mapping done by D. A. Swanson and T. L. Wright along the eastern extension of the Horse Heaven Hills and in the Wallula Gap area of Washington (loc. 19) revealed abundant evidence for west-northwest-trending faults. These faults lie along and help define the Olympic-Wallowa lineament, a controversial topographic lineament that extends across the entire State. The faults are recognized by offset stratigraphy and linear belts of tectonic breccia. Some workers have considered the breccia to be blow breccia, but the breccias cut across stratigraphy and thus must have a tectonic origin. Vertical offsets of several tens of meters are common along the faults. Aeromagnetic evidence is consistent with left-lateral strike-slip displacement within the fault zone. Recognition of the Olympic-Wallowa lineament as at least partially fault controlled reopens the question of whether the lineament reflects a major throughgoing strucure of regional significance.

ALASKA

Significant new scientific and economic geologic information has been obtained from many field and topical investigations conducted in Alaska during the past year. Discussions of the findings are grouped under seven subdivisions corresponding to six major geographic regions and a general statewide category. Outlines of the regions and locations of the study areas are shown on the accompanying index map of Alaska.

STATEWIDE

Alaska Mineral Resource Assessment Program enters third year with dual objectives

The year 1976 witnessed a surge of public and private concern about the classification, allocation, and development of Alaska's vast lands and mineral resources. In response to this concern, the Alaska Mineral Resource Assessment Program (AMRAP), administered by H. C. Berg, set two closely coordinated and interdependent objectives designed specifically to furnish information about Alaska's lands.

One objective, based on a 1:250,000-scale ($1° \times 3°$) quadrangle format, is a systematic statewide assessment of terranes having high economic mineral potential. With current levels of staffing and funding the deadline for achieving this goal is 1984. The other objective, based on a 1:1,000,000-scale map format, is a synoptic mineral appraisal of the 33.8×10^6 ha that are proposed for classification as National Interest (d–2) lands under the Alaska Native Claims Settlement Act (ANCSA). The obective, informally termed RAMRAP (Regional Alaska Mineral Resource Assessment Program), is scheduled for completion by early 1978, about a year in advance of the December 1978 deadline for final congressional action on ANCSA.

This multidisciplinary program is being carried out mainly by geologists and subprofessionals in the Alaskan Geology Branch in collaboration with specialists from other branches and subactivities in the Geologic Division. In addition, several geoscientists from the Alaska Division of Geological and Geophysical Surveys, the University of Alaska, and the Bureau of Mines also are participants.

As of January 1, 1977, sytematic resource assessments had been completed in eight $1° \times 3°$ quadrangles and were underway in five others. These quadrangles aggregate approximately 14.8×10^6 ha, 3.3×10^6 ha of which have been proposed for National Interest (d–2) lands. These systematic resource assessments have resulted in the publication of more than 36 topical research reports on the geology, geochemistry, geophysics, and mineral resourses of Alaska. In addition, new potential resources of molybdenum, chromite, gold, and tin have been discovered in the Talkeetna quadrangle; significant increases in the sizes of copper resouces have been recognized in the Ketchikan and Talkeetna Mountains quadrangle; and a potentially economic porphyry molybdenum deposit was discovered near Burroughs Bay in the Ketchikan quadrangle. This last deposit was staked by commercial interests in 1976.

Metamorphic facies map of Alaska

A metamorphic facies map of Alaska at a scale of 1:2,500,000 is planned as a contribution to a Map of the Metamorphic Belts of the World (sponsored by the Commission for the Geological Map of the

World of the International Geological Congress and the International Union of Geological Sciences) and as a joint USGS-Alaska Division of Geological and Geophysical Surveys publication. The map will show metamorphic facies, facies groups, facies series, selected isograds, and granitic rock bodies according to the metamorphic facies map explanation suggested by the International Union of Geological Sciences (Zwart and others, 1967). D. A. Brew reported that progress to date includes preliminary compilation and review of regional metamorphic facies maps at 1:1,000,000 scale for all of the State, coding of background metamorphic mineral-locality information, and beginning the final combination of 1:1,000,000-scale regional maps.

NORTHERN

Galena at Galena Creek

A brief inspection of rocks near Galena Creek in the southeastern Brooks Range by W. P. Brosgé (USGS) and James Barker (Bureau of Mines) showed that the creek is well named. Galena Creek (index map, loc. 1) is on the southern flank of Bear Mountain, an anticlinal dome of lower Paleozoic and possibly older rocks that are intruded by small bodies of rhyolite. Gray-green phyllite, phyllitic sandstone and greenstone, and fine-grained quartzite in the core of the dome are overlain by a thick conglomerate of probable Devonian age that forms most of the mountain. The rhyolite occurs mainly in the older rocks, but one dike intrudes Devonian conglomerate on the western flank of the mountain, and another intrudes the overlying Mississippian shale on the eastern flank. Reconnaissance mapping and sampling done 10 years ago revealed anomalous amounts of lead and zinc in the streams draining the southern flank of Bear Mountain, as well as abundant galena in quartz veins at the contacts of some rhyolite dikes. Lead and zinc concentrations were highest in Galena Creek and its two neighboring streams, where as much as 500 ppm Pb and 380 ppm Zn were found in sediments in the main valleys and 1,500 ppm Pb and 360 ppm Zn were found in sedi-

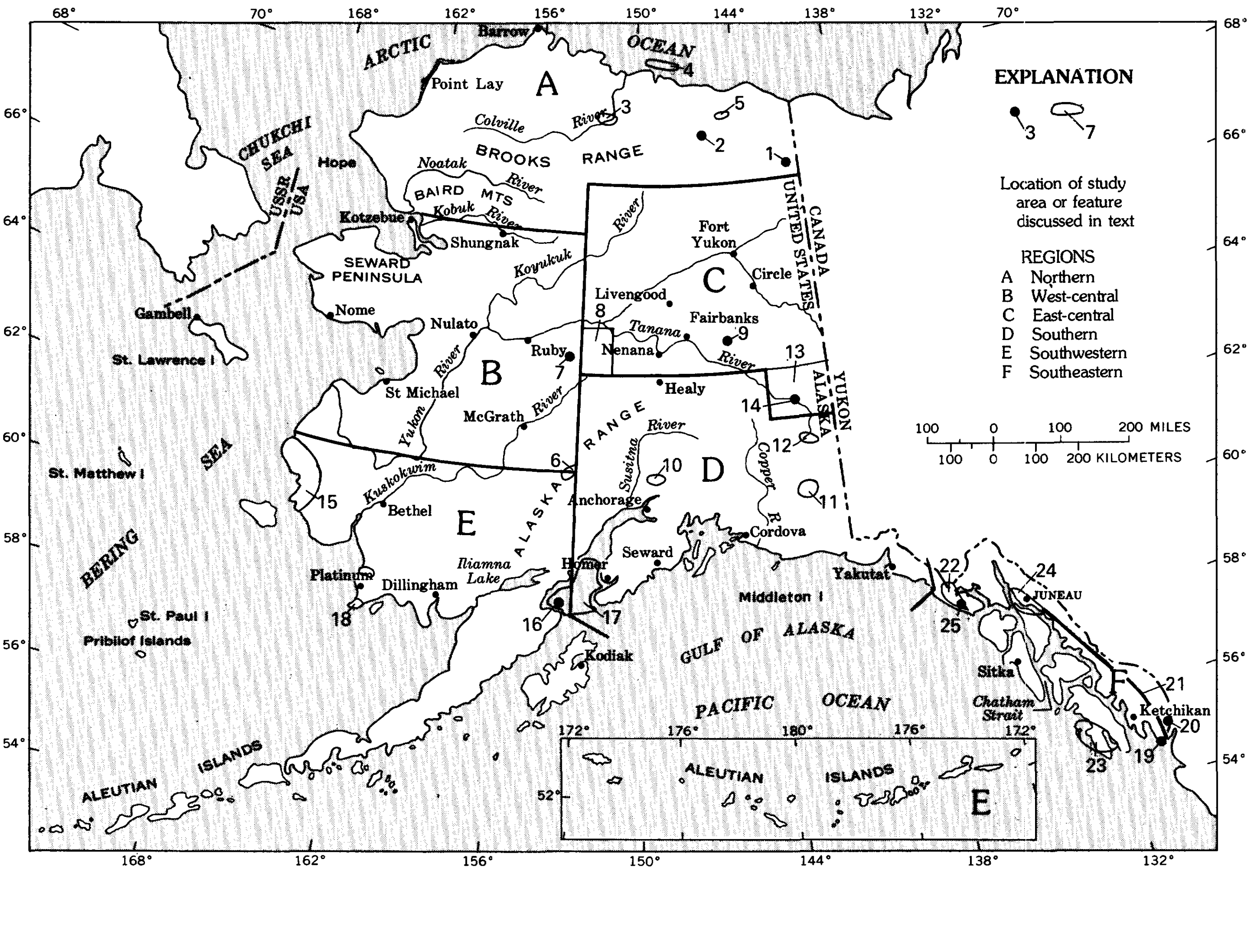

ments from one small tributary. These streams drain the core of the anticline where most of the rhyolite occurs and where it invades only the oldest rocks. Because observations had been limited, it was thought that mineralization was restricted to large veins at the rhyolite contacts. However, a traverse of one of the phyllitic sandstone ridges having a longitudinal dike along its western face showed that mineralization is pervasive in the country rock across the ridge crest in a zone at least 200 wide and 750 long. Galena occurs in tiny veinlets, with or without quartz along foliation and small fractures in the fine-grained phyllitic sandstone and in the minor amounts of intercalated greenstone. No galena was found in the rhyolite, and no anomalous amounts of lead have been found in the few analyses done on other Bear Mountain rhyolites, so it is uncertain whether the lead was introduced by the rhyolite or was indigenous to the host rocks. However, the fact that lead anomalies occur in gossan soil on the dike in Devonian conglomerate on the western flank of the dome and in soil on a fault zone within Devonian conglomerate on the northern flank indicates that the mineralization is younger than that of the lower Paleozoic phyllite.

Carboniferous volcanic rocks in northeastern Alaska

Mafic volcanic and volcaniclastic rocks were discovered on the northern flank of the northeastern Brooks Range. Necessarily hasty field observations indicated that the sequence overlies the Lisburne Group and is Permian in age. These rocks, which crop out on both the northern and southern sides of the Ivishak River Valley in the southern corner of the Sagavanirktok A–2 quadrangle (loc. 2), were visited by W. P. Brosgé, R. L. Detterman, J. T. Dutro, Jr., and H. N. Reiser.

The sequence includes flows, tuffs, coarse volcaniclastic rocks, and tuffaceous limestone and is interbedded with and overlain by Lisburne limestones. Total thickness varies and is estimated to be from 100 to 200 m. A single brachiopod collected from tuffaceous limestone in the volcanic sequence appears to be Late Mississippian in age and indicates that the mafic volcanic rocks are definitely Carboniferous and correlate with the Alapah Limestone.

New Permian to Triassic section in northeastern Brooks Range

A unusually thick and fossiliferous sequence of Permian and Triassic rocks in the Sadlerochit Group was investigated by J. T. Dutro, Jr., and R. L. Detterman on a tributary of the Ivishak River in the southeastern part of the Sagavanirktok quadrangle (loc. 2). The Echooka Formation, about 270 thick, disconformably overlies Lisburne carbonate rocks and is overlain by at least 360 m of the Ivishak Formation. These two formations are about 25 percent thicker here than they are at Flood Creek 15 km to the southwest, and thus this sequence of Sadlerochit strata is the thickest known in northern Alaska.

The Joe Creek Member of the Echooka consists of about 120 m of sandy limestone, siliceous and calcareous sandstone, and siltstone containing Early Permian shelly faunas, including the brachiopod genera *Yakovlevia, Waagenoconcha, Linoproductus, Cancrinella, Thamnosia, Timaniella?, Spiriferella,* and *Attenuatella.* These fossils represent some part of Zone F of Bamber and Waterhouse (1971) and are correlated with the upper Leonardian and Road Canyon of western Texas.

The Ikiakpaurak Member of the Echooka is about 150 m thick and contains a brachiopod coquina bed (mainly *Kuvelousia*) near its base. This represents Zone G and is most likely a upper Guadalupian and Capitan equivalent (Kazanian).

Although few fossils were seen at this locality, the Ivishak Formation has yielded Early Triassic fossils in nearby areas. *Ophiceras commune* Spath and *Claraia stachei* Bittner identified from the lower part of the Ivishak Formation by N. J. Silberling, indicate a late Griesbachian Age.

Reservoir characteristics of sandstones of the Nanushuk and Colville Groups

Physical and biogenic sedimentary structures and paleontology indicated that selected sandstones of Nanushuk and Colville Groups (Cretaceous) in the Umiat oilfield (loc. 3) were deposited in a shallow-water nearshore marine environment—in the foreshore, upper shoreface, lower shoreface, and upper offshore—according to J. E. Fox, C. L. Jochim, P. W. Lambert, D. W. Niven, J. K. Pitman, and C. H. Wu. Sandstones of the Nanushuk Group are very fine to fine-grained litharenites composed mainly of quartz, chert, and low-grade metamorphic rock fragments. Sandstones of the Colville Group also are very fine to fine-grained litharenites but contain abundant volcanic rock fragments (andesite) and plagioclase in addition to quartz, chert, and low-grade metamorphic rock fragments. Some sandstones of both groups are thoroughly cemented with calcite. The porosity and permeability of many of the sandstones of the Nanushuk Group, the principal producing formation in the oilfield, appear to be inversely proportional to the content of phyllite rock fragments. The soft phyllite fragments and the phyllosilicate fragments abraded from them tend to be squeezed and packed into primary intergranular pores. The poor porosity and permeability of sandstones of the Colville Group appear to be due mainly to a high content of authigenic clay minerals filling intergranular pores. Clay minerals in the sandstones include illite, chlorite, montmorillonite-chlorite, and kaolinite. In sandstones of both groups, porosity and permeability tend to increase with increasing grain size.

The weighted average porosities and permeabilities determined from core and well-log analyses for sandstones in the various formations are as follows:

Formation	Average porosity, percent	Average permeability, md
Grandstand Formation:		
Lower	15.1	58.6
Upper	15.6	167.0
Chandler Formation, Killik Tongue	16.4	96.2
Ninuluk Formation	12.6	10.7
Seabee Formaton	11.5	3.1
Prince Creek Formation, Tuluvak Tongue	14.6	3.9

The formation water is mostly fresh—about 5,000 ppm dissolved solids—with a resistivity of 1.6 ohm-m at 13°C.

Extensive permafrost on the continental shelf of the Beaufort Sea

Results of the Prudhoe Bay drilling program (loc. 4) indicated that brine-soaked permafrost extends at least 15 km offshore beneath water depths of 15 m or more. Furthermore, according to D. M. Hopkins, strongly negative temperature gradients in every drill hole demonstrate that colder, ice-bonded permafrost exists at depths in the 50- to 100-m range.

Ferruginous bauxite deposit in northern Alaska

Mapping done by H. N. Reiser and W. P. Brosgé in the northeastern Brooks Range revealed the occurence of small deposits of diaspore and pyrophyllite. The outcrops are slightly metamorphosed "pocket-type" deposits of ferruginous bauxite developed on a pre-Mississippian angular unconformity in northeastern Alaska. S. H. Patterson postulated that the diaspore and the pyrophyllite are derived from original boehmite and gibbsite, respectively. The pyrophyllitic quartzite previously reported in the area (Reed and Hemley, 1966) probably originated in the same way. Four rapid-rock chemical analyses of the diaspore-bearing rocks from two localities within the Mount Michelson quadrangle (loc. 5) (lat 69° 22.5′ N., long 145° 41.5′ W., and lat 69° 27′ N., long 144° 27′ W.) have average percentages as follows: SiO_2, 18.73; Al_2O_3, 35.00; Fe_2O_3, 7.38; FeO, 22.25; MgO, 1.57; CaO, 0.64; Na_2O, 0.01; K_2O, 0.74; H_2O^+, 10.25; H_2O^-, 0.40; TiO_2, 2.65; P_2O_5, 0.32; MnO, 0.18; and CO_2, 0.21 (sum, 100.33).

WEST-CENTRAL

Continental margin facies in Alaska Range points to new petroleum target areas

The lower Ordovician through Upper Silurian sequence of graptolitic shale, chert, sandstone, and limestone in the Terra Cotta Mountains of the Alaska Range (loc. 6), studied by Michael Churkin, Jr., B. L. Reed, Claire Carter, and G. R. Winkler, represents an ancient continental margin succession of hemipelagic sediments and turbidites deposited immediately seaward of bioclastic limestone, including reefs north of the Alaska Range, that represents a continental shelf. If large-scale displacement of lower Paleozoic facies has not occurred across western extensions of the Denali fault system, then shoreline and shelf facies may be present in lower Paleozoic rocks that are now concealed in the Minchumina Basin and other basins north of the Alaska Range—this concept is useful in exploring for petroleum and other commodities that are known to occur along ancient continental margins.

Pre-Ordovician unconformity in central Alaska

The common belief that major unconformity exists at the base of the Paleozoic section in central Alaska is based at least in part on observations made by H. M. Eakin (1918) in the Telsitna River area of the northern Kuskokwim Mountains (loc. 7). At this classic locality, fossiliferous Ordovician carbonate rocks structurally overlie a metamorphic complex composed of mica schist and quartzite. Eakin described the contact as an angular unconformity and assigned the metamorphic complex a pre-Ordovician age. Reexamination of the Telsitna locality by W. W. Patton, Jr., J. T. Dutro, Jr., and R. M. Chapman strongly suggested, however, that the contact is a thrust fault rather than an unconformity. Along the contact, slivers and blocks of the carbonate rocks are tectonically mixed with the metamorphic rocks, and, at the base of the Paleozoic sequence, the carbonate rocks are heavily sheared and brecciated. The presence of a thrust along the contact does not disprove the presence of an unconformity, but, at present, the age of the metamorphic rocks is uncertain, and the possibility that the carbonate and metamorphic terranes have been juxtaposed by large-scale lateral transport cannot be ruled out.

EAST-CENTRAL

Geochemical anomalies in bedrock of Kantishna River quadrangle

Seventy-five bedrock samples were collected for geochemical analysis in the western half of the Kantishna River quadrangle (loc. 8) by R. M. Chapman and W. W. Patton, Jr. A preliminary evaluation of the analytical data for selected elements shows anomalous amounts of one or more of the following elements in 49 of the 75 samples: Ag, 0.7–20 ppm; As, 300–1,000 ppm; B, 300–10,000 ppm; Be, 7–20 ppm; Bi, 7–30 ppm; Cu, 150–700 ppm; Hg, 0.12–10 ppm; Li, 100–1,000 ppm; Mo, 10 ppm; Pb, 70–1,000 ppm; Sb, 200 ppm; Sn, 10–200 ppm; V, 500–1,000 ppm; and Zn, 300–2,000 ppm. These anomalous values are conservatively interpreted from imspection of the data and from comparisons with amounts used in several Alaskan geochemical surveys and in various tables of crustal abundances of elements.

A number of Ag, As, B, Bi, Li, and Sn anomalies and a few Be, Cu, Mo, Pb, V, and Zn anomalies occur in 14 of the 16 samples from a 50-km^2 area at the head of the Cosna River. The samples are from iron-stained, low-grade metasedimentary rocks, some of which are slightly hornfelsed and contain tourmaline and andalusite, and from numerous associated small rhyolitic dikes and quartz veins. A granitic body at shallow depth may be inferred from this geologic setting. Additional geological and geochemical exploration in this area is warranted in view of the anomalous abundances of several metallic elements, the favorable setting for mineral deposits, and the reports that some prospecting was done in the area many years ago.

Occurrence of kyanite in the Big Delta C–4 quadrangle

Schists that crop out on the northern side of an area of sillimanite gneiss in the Big Delta C–4 quadrangle (loc. 9) contain kyanite, according to H. L. Foster. Kyanite had not been found previously in the Big Delta quadrangle except in the Eilson deep test hole at a depth of 2,504 m. Kyanite is also rare elsewhere in the Yukon-Tanana Upland, probably partly because of the quartzitic composition of the metamorphosed sediments but perhaps also because sediments metamorphosed deeply enough in the crust to form kyanite rarely are exposed.

SOUTHERN

Cretaceous age for the Arkose Ridge Formation

Reconnaissance geologic mapping done in the southwestern Talkeetna Mountains (loc. 10) by Béla Csejtey, Jr., and W. H. Nelson indicated that the granitic rocks in the Little Susitna River drainage, adjacent to the reportedly Arkose Ridge Formation of Paleocene age (Detterman and others, 1976), are not of just one age but include Jurassic quartz diorite and Upper Cretaceous tonalite. Although the Arkose Ridge Formation unconformably overlies the Jurassic quartz diorite and related metamorphic rocks, it appears to be intruded by the Upper Cretaceous tonalite. The contact between the Arkose Ridge and the tonalite is nowhere exposed, but the two units occur on opposite sides of the Little Susitna Valley about 1 km apart, separated by glacial deposits. There is no evidence in the area that the tonalite and the Arkose Ridge are in fault contact. Close to the tonalite, the Arkose Ridge is extremely indurated but becomes rather friable a few kilometers away. Petrographic characteristics of the tonalite suggest that it was emplaced in the lower part of the epizone and thus required a minimum of 5 to 7 km of roof. Potassium-argon age determinations on three biotite-hornblende mineral pairs from the tonalite (M. A. Lanphere, written commun., 1976) yielded concordant Cretaceous ages of 67.3 to 72.5 million years. If it is assumed that the Arkose Ridge is of Paleocene age, the present spatial proximity of the Arkose Ridge rocks to the tonalite would necessitate a somewhat unlikely rapid rate of unroofing for the tonalite. Thus, field evidence strongly suggests that the Arkose Ridge is older than, and was intruded by, the tonalite and that the Arkose Ridge in part, made up the necessary roof for the tonalite pluton.

To substantiate the apparent intrusive relationship, several thin sections of Arkose Ridge rocks taken about 1 km from exposed tonalite were examined for contact metamorphic effects by Csejtey and G. D. Eberlein. Most of the sections examined showed in-place growth of secondary fine-grained biotite and (or) muscovite and chlorite—minerals that require some heat for crystallization in the absence of a directed fabric. A thin section of an Arkose Ridge sample taken several kilometers from the tonalite showed no development of secondary biotite, muscovite, or chlorite.

Thus, field and petrographic evidence strongly suggest that the Arkose Ridge is older than about 70 million years and is an integral part of the Matanuska Formation (Lower and Upper Cretaceous). Such an age assignment for Arkose Ridge is attractive because it greatly simplifies the interpretation of the tectonic history of both the southern Talkeetna Mountains and the Matanuska Valley.

Mineralogy and stable isotope geochemistry of massive copper sulfide deposits at Kennecott

R. W. Potter II and M. L. Silberman (USGS) are carrying on a detailed study of the Kennecott massive sulfide deposits near McCarthy (loc. 11). Arie Nissenbaum (Weizmann Institute of Science, Rehovot, Israel) and Alan Matthews (Hebrew University, Jerusalem, Israel) are providing stable isotope analyses of carbonate and silicate minerals from rocks within and near the ore deposits. Preliminary results indicated that the Kennecott massive sulfide deposits were originally deposited in a sebkha environment at low temperature. The deposits were initially a pyrite-chalcopyrite-bornite-covellite-luzonite assemblage, which implies a low formation temperature. Textural evidence suggests that complex multistage processes were responsible for replacing the original assemblage with chalcocite-djurlite-dignenite-anilite-blaubleibender covellite-covellite. This assemblage indicates a formation temperature below 93°C. Fluid inclusions from calcite veins containing sulfides have homogenization temperatures of 50°C and salinites of 15 percent. Isotopic analyses of carbonate rocks from the Chitistone Limestone (Upper Triassic) (host rock for the deposits) indicate depletion of O^{18} but not of C^{13}. Unaltered Chitistone Limestone has a δO^{18} (standard mean ocean water) value of +20 to +26 ppt and a δC^{13} value of +1.5 to +4.1 ppt. Recrystallized limestone near the ore deposit is further depleted in O^{18} (+17–+22 ppt) but has the same δC^{13} value as unaltered limestone. Sulfide containing vein calcite has a δO^{18} value of +9 to +18 ppt and a δC^{13} value of +0.4 to +2.7 ppt. Quartz-epidote-copper veins in the Nikolai Greenstone, which underlies the Chitistone Limestone, have a δO^{18} value for epidote of +4 to +5 ppt and a δO^{18} value for quartz of +15 to +16 ppt; the large fractionation implies a low formation temperature. The δO^{18} values of chlorite, hornblende, and feldspars from nearby Tertiary igneous rocks in the range +6 to +12 ppt are characteristic of igneous minerals that have undergone exchange with fluids enriched in O^{18}, such as formation waters from sedimentary rocks like those found near Kennecott. The mineralogy, isotope data, and geometry of the orebodies indicate a sabkha, origin which was later modified by remobilization due to the action of oxidizing, saline, cool fluids probably having a significant nonmeteoric component generated by igneous activity in the Mesozoic or perhaps the late Cenozoic.

Ages of disseminated copper and molybdenum deposits in the eastern Alaska Range

Alteration and mineralization ages of disseminated copper mineralization associated with granitic rocks of the Nabesna and Klein Creek plutons (loc. 12) were obtained by K-Ar analyses of hydrothermal biotite, muscovite, potassium-feldspar, amphibole, and chlorite. Copper mineralization ages from Baultoff, Horsfeld, Carl Creek, and Ptarmigan Creek in the Klein Creek batholith range from 107 to 118 million years, and the mineralization from Orange Hill in the Nabesna pluton is 110 million years. Molybdenum-bearing quartz porphyries and veins at Orange Hill yield K-Ar ages ranging from 104 to 108 million years. Previously reported biotite and hornblende ages from unmineralized parts of the Nabesna and Klein Creek plutons are 108 to 117 and 113 to 114 million years, respectively. The age data suggested to M. L. Silberman, J. L. Morton, D. C. Cox, and D. H. Richter that major copper mineralization occurred during emplacement and crystallization of these plutons. Molybdenite mineralization at Orange Hill is related to late-state quartz porphyries, which form part of the Nabesna pluton. Two younger stages of igneous intrusion and mineralization-alteration occurred within the Nabesna pluton. A major pluton containing disseminated chalcopyrite was emplaced at the center fork of Bond Creek 81 to 90 million years ago. At the eastern fork of Bond Creek, trondhjemitic dikes and intrusions and a silicic breccia pipe containing disseminated pyrite and molybdenite were emplaced 22 million years ago.

Chlorite, which replaces hydrothermal or igneous biotite at Carl Creek, Baultoff, and the eastern Fork of Bond Creek, yielded K-Ar ages that agree with ages of hydrothermal potassium-feldspar, muscovite, and biotite from the same rocks. The data suggest that, at least in some areas, chlorite may be useful in determining the age of disseminated copper deposits by the K-Ar method.

Till of possible pre-Delta age in the Tanana Valley near Tok

Eight to 10 meters of massive sandy till are exposed in a general pit along the Alaskan Highway, 8 km east of Tok (loc. 13). The till occupies an area of roughly 6 km^2 and is bordered by modern alluvium of the Tok and Tanana Rivers and by gravels presumed to be equivalent in age to the Donnelly Glaciation. The surface of the till stands a few meters above the surrounding terrain but does not exhibit morainal topography, and large boulders are not exposed. The glacial origin of the deposit is apparent only because construction excavations reveal internally the unstratified character of the materials and the presence of boulders up to at least 1.5 m in diameter.

Till of equivalent age once must have covered a large area in the vicinity of Tok, but it has since been either buried by gravels of the Tok fan or removed by erosion prior to deposition of the Tok fan. L. D. Carter and J. P. Galloway concluded that most of the gravels of the Tok fan were deposited during the Delta Glaciation. If so, the till described above must be pre-Delta in age.

Geochemical sample media in the Tanacross quadrangle

To help determine the mineral potential of the Tanacross quadrangle (loc. 14), geochemical sampling included the collection of several different sample media at each locality. In the maturely dissected areas of the quadrangle (part of the Yukon-Tanana Upland), it was demonstrated that mineral occurrences are defined by a combination of sample media more completely than they are by any single type of sample. However, oxide residue is the most useful single sample medium for identifying base-metal occurrences. Heavy-mineral concentrates are most useful for detecting localities of tin and tungsten mineralization and for delineating anomalous distributions of some other metals such as bismuth. Streambank sod and aquatic bryophytes are somewhat less useful than the oxide residue, but they can provide supporting geochemical data.

In the Alaska Range, where mechanical weathering is the primary destructive process, stream sediments reflect the mineralogy of the bedrock in the drainage basins; therefore, minus-80-mesh stream sediments and heavy-mineral concentrates are adequate for defining areas of mineral potential.

Porphyry copper potential in the Tanacross quadrangle

Compilation and interpretation of geologic, aeromagnetic, geochemical, and satellite data obtained in the Tanacross quadrangle (loc. 14) by D. A. Singer, H. L. Foster, and G. C. Curtin indicated several areas worthy of being explored further for copper deposits.

Known porphyry copper deposits all appear to be genetically related to Tertiary felsic volcanic or hypabyssal rocks. The limited amount of drilling done by industry in the quadrangle suggests that the copper and molybdenum contents of the deposits are low in comparison with those of deposits in the conterminous United States. Although porphyry deposits are the only type of copper and molybdenum deposits known to occur in the Tanacross quadrangle, other copper-bearing deposits, such as massive sulfide veins and skarns, could also occur on the margins of the volcanic or hypabyssal rocks.

SOUTHWESTERN

History of the Yukon River Delta

W. R. Dupre (USGS) established that the southern part of the coalescent deltas of the Yukon and Kuskokwim Rivers (loc. 15) formed during Wisconsin time, probably on the order of 14,000 to 18,000 years ago. The southern side of the channel leading to this part of the Yukon-Kuskokwim Delta, near Nelson Island, is adjoined by a row of dunes and blocked by younger dunes adjoining the southern side of a younger Yukon River Channel that leads past Cape Romanzof toward a submerged deltaic deposit dated by J. S. Creager and H. J. Knebel (University of Washington) as about 14,000 years old. Delta lobes to the north and south were occupied during most of Holocene time, and the outlet of the Yukon River shifted to its present position at the northern edge of the delta complex only about 1,200 years ago.

Volcanic hazards in lower Cook Inlet

A violent eruption of Augustine Volcano (loc. 16) in January 1976 followed by only 12 years a previous major eruption (Detterman, 1968). This interval represents a significant reduction in the periodic 28- to 35- year eruptive cycle recorded for the volcano during historic times (Coats, 1950). A further reduction in the cycle, which R. L. Detterman considered likely, could present a serious environmental hazard to petroleum exploration in lower Cook Inlet as well as to shipping and shore installations in adjacent areas.

Reservoir and source-rock parameters in lower Cook Inlet

Reservoir and source-rock parameters of lower Cook Inlet stratigraphic units were studied by I. F. Palmer, J. G. Bolm, J. C. Wills, L. B. Magoon, III, and R. M. Egbert (USGS) and W. M. Lyle and J. A. Morehouse (Alaska Division of Geological and Geophysical Surveys). Potential reservoir sandstones have low porosity and permeability owing to original tight packing and subsequent zeolitization. Thermal-alteration-index determinations indicate that the basin is mature enough to have generated hydrocarbons. Extracted soluble hydrocarbons are present in moderate amounts and indicate source-rock capability. The petroleum potential of the lower Cook Inlet Outer Continental Shelf area (loc. 17) is considered to be fair to good.

Blue amphiboles in southwestern Alaska

Blue amphiboles were found recently by J. M. Hoare and W. L. Coonrad in highly tectonized rock at five localities in southwestern Alaska (loc. 18). Two localities are in the Goodnews B–7 and B–8 quadrangles; the others are 90 km to the south, across the regional trend of the rocks, in the Hagemeister Island C–5 and C–6 quadrangles. There is no known connection between the northern and southern localities. In the Hagemeister quadrangles, the blue amphiboles are closely associated with a metamorphosed and dismembered ophiolite complex. The amphiboles are in altered, moderately foliated volcanogenic rocks that also contain chlorite, pumpellyite, and actinolite. The two northern localities are in completely recrystallized quartz-chlorite schist and crenulated calcareous schist that contains detrital quartz and clinopyroxene. All of the blue amphibole localities are in, or on the projected trend of, previously recognized fault zones. The fault zones trend northeast, dip south, and show northwestward tectonic transport. The fault zones probably extend to subcrustal depths because they also contain two or more sheared serpentine bodies. The serpentine bodies are interpreted as rootless tectonic blocks because (1) they are rather small; (2) they are moderately or intensely sheared; (3) one of them is in fault contact with limestone; and (4) they are in, or very near, large fault zones. The origin of the serpentine is presumably in the mantle. The isolated bodies are probably tectonically emplaced pieces of serpentinized peridotite that were intruded into the fault zones.

The fundamental tectonic identity of the rocks in the Goodnews and Hagemeister Island quadrangles is not yet completely understood, but the association of blue amphiboles and serpentinized periodotite in these highly tectonized rocks permits the inference that they have been produced at zones of active plate convergence.

SOUTHEASTERN

Metamorphosed Alexander terrane trondhjemite in Coast Range plutonic and metamorphic complex

Recent fieldwork done, by R. D. Koch, R. L. Elliot, J. G. Smith, and H. C. Berg in the area between Foggy Bay and Cape Fox in the Prince Rupert D–3 quadrangle of southern southeastern Alaska (loc. 19) showed that an elongate body of rock originally mapped as greenschist (Wright and Wright, 1908; Buddington and Chapin, 1929) is instead a sheared trondhjemite pluton, informally referred to as the Cape Fox pluton. This body is exposed over an elliptical area 9×19 km along the western margin of the plutonic and metamorphic complex in the Coast Range. Despite its inclusion in the Coast Range complex, the Cape Fox pluton may be part of the older Alexander terrane, which lies in a roughly parallel belt to the west (Berg, Jones, and Richter, 1972).

Geologic settings.—The plutonic and metamorphic complex in the Coast Range is a linear belt that extends 1,700 km along the Pacific coast from British Columbia through southeastern Alaska into Yukon Territory (Douglas and others, 1970; Hutchison, 1970; Roddick and Hutchinson, 1974). Within the Ketchikan and Prince Rupert quadrangles, the complex forms three north-trending irregular belts (Elliott, Smith, and Hudson, 1976; Berg and others, 1977). The easternmost belt lies just west of Portland Canal and consists predominantly of discrete granodiorite and quartz monzonite plutons. A central belt of high-grade paragneiss and foliated plutonic rocks is flanked on the west by a third, heterogeneous belt of phyllite, pelitic schist, greenschist, amphibolite, minor marble, and subordinate plutonic rocks. In the Ketchikan region, K-Ar dating indicates that the Coast Range complex formed mainly during two major metomorphic and intrusive episodes 80 and 50 million years ago. (Smith, 1975).

The Alexander terrane is an irregular belt of allochthonous sedimentary, volcanic, and metamorphic rocks that extends for 1,000 km along the Pacific coast from Dixon Entrance to the Wrangell Mountains (Berg, Jones, and Richter, 1972). The oldest fossil-bearing rocks in the terrane are Lower Ordovician graptolitic shales, but intrusive relations and a thick underlying section of undated beds suggest that the stratigraphy extends into the Cambrian and probably into the Precambrian. The youngest fossil-bearing rocks assigned to the Alexander terrane are Late Triassic in age. The terrane is cut by granitic plutons ranging in age from Precambrian(?) to Cenozoic. The southern half of the terrane includes several trondhjemite plutons that are of Silurian age or older. The largest of these trondhjemite plutons is the Annette pluton on Annette Island (Berg, 1972), which is 400 million years old or older.

Cape Fox pluton.—The Cape Fox pluton was originally a medium-grained hypidiomorphic granular biotite trondhjemite. Potassium-feldspar was completely absent, or present only in small amounts, and biotite was the only original mafic mineral. Most of the pluton was sheared and altered during regional metamorphism that produced cataclastic, commonly semischistose rocks. The granitic texture was, in places, completely destroyed. The degree of deformation and alteration is not uniform areally, and variation is apparent even at outcrop scale. Portions of some outcrops are now chlorite-epidote-muscovite-plagioclase-quartz schist and strongly resemble greenschist. Most outcrops are characterized by abundant angular quartz porphyroblasts. The southeastern margin of the pluton is a band of quartz-mica schist 1 km wide that was produced by cataclasis and structural intercalation of the pluton with the adjacent metavolcanic and metapelitic rocks.

The Cape Fox pluton and the surrounding country rocks are inferred to have been regionally metamorphosed during the 80-million-year-old Coast Range metamorphic event. This age is based in part on a partially reset biotite K-Ar date of 67 million years obtained on a sample of schist collected 12 km north of the pluton. Comparison of this date with a pattern of reset ages to the north (Smith, 1975) suggests a metamorphic age of 80 million years for this schist. A granodiorite stock near Sykes Lake, 25 km north of the Cape Fox pluton, has a distinct thermal aureole that overprints the surrounding regionally metamorphosed schists. The pluton yielded discordant K-Ar dates, but the hornblende date of 78 million years indicates that a significant regional metamorphic event occurred at least 80 million years ago.

The likelihood that the Cape Fox pluton and the surrounding rocks were regionally metamorphosed before 80 million years ago suggests that this pluton may correlate with other pre-80-million-year-old trondhjemite plutons in southern southeastern Alaska. The only such plutons known in the region are parts of the Alexander terrane. Petrographic, modal, and chemical evidence suggests a possible correlation with the Annette pluton of Silurian age or older, a trondhjemite stock on Annette Island 40 km to the northwest. If this correlation is correct, it will mark the first documented occurrence of Alexander terrane rocks in the Coast Range plutonic and metamorphic complex.

Investigations of the Wilson Arm molybdenite deposit

The Wilson Arm molybdenite deposit in the Ketchikan B–2 quadrangle (loc. 20) was visited briefly by T. L. Hudson, R. L. Elliott, J. G. Smith, and R. D. Koch to study and sample the intrusive rocks associated with the mineralization. Field examination confirmed that the two felsic stocks in the area are composite hypabyssal bodies separated at the surface by a narrow septum of gneiss. The stocks are oval in plan and sharply discordant with the enclosing metamorphic and plutonic rocks. The contact zone is commonly a complex irregular network of pegmatite, aplite, and porphyry dikes and sills. Lamprophyre dikes crosscut all intrusive phases and mineralized zones along a consistent northeastern trend, but locally they have been slightly displaced by small cross faults. A preliminary report by Elliott, Smith, and Hudson (1976) summarized many aspects of the general geology the setting of the stocks that were known.

Both stocks contain many textural facies. The southern stock includes biotite-quartz porphyry, biotite-quartz-feldspar porphyry, and seriate fine-to-medium-grained biotite granite. The porphyritic rocks commonly have an aplitic groundmass; irregular pods and veins of quartz-feldspar pegmatite are relatively abundant in some parts of the southern stock. The principal mineralization occurs in the northern stock, which includes fine-grained equigranular biotite granodiorite(?), fine-grained equigranular biotite granite, and a variety of porphyrytic rocks with a groundmass that is locally aphanitic but generally fine grained and aplitic.

Molybdenite-quartz veins and molybdenite fracture coatings occur over large areas of the northern stock, and pyrite is nearly ubiquitous in and around the stock. The pyrite occurs as disseminated euhedra in porphyritic rocks, in veinlets cutting both molybdenite-bearing and molybdenite-free rocks, and as disseminations in country rocks adjacent to the stock. Amphibolite observed near the southern contact of the northern stock is particularly pyrite-rich. The ubiquitous pyrite of the northern stock contrasts sharply with the pyrite-free nature of the southern stock, which appears to be nonmineralized over most of its area. Chlorite commonly occurs along fractures in many molybdenite- and (or) pyrite-bearing rocks of the northern stock.

Samples of the different phases and mineralized parts of the stocks have been collected, and the objectives of present laboratory work are to describe the petrology, determine the major- and trace-element chemistry, and obtain the K-Ar ages of the intrusive complexes. These data will define the general characteristics of the host rocks for the important Wilson Arm molybdenite deposit and assist in identifying rocks and mineralized zones elsewhere in southeastern Alaska.

The Coast Range "megalineament"

The Coast Range "megalineament" (loc. 21) is a nearly continuous, prominent topographic and structural feature that extends southeastward for about 550 km from where it joins the Chatham Strait-Lynn Canal fault north of Berners Bay to where it leaves southeastern Alaska in Tongass Passage near the mouth of Pearse Canal. (It probably extends still farther southeastward into British Columbia along Work Channel and Chatham Sound-Grenville Channel.)

The megalineament is generally a zone a few hundred meters to 10 km wide in which closely spaced joints, foliation, compositional layering, and small faults parallel the megalineament trend. The zone usually occurs in topographic depressions apparently caused by glacial erosion of the less resistant rocks of the zone.

Studies conducted in the Juneau area and in the Tracy Arm-Fords Terror Wilderness study area by D. A. Brew and A. B. Ford indicated that the megalineament (1) is at least locally the site of small lateral and vertical separations on the order of 1 km; (2) is itself probably not a major discontinuity; (3) may be located near older premetamorphism and preintrusion discontinuities; (4) is consistently associated with steep gradients of both the gravity and the magnetic fields; and (5) may reflect the presence at depth of the western contact of the dominant intrusive rocks and gneisses of the Coast Range plutonic and metamorphic complex.

Newly discovered granitic and gabbroic bodies in Glacier Bay National Monument

Available geologic information on the Fairweather Range (Brew and Ovenshine, 1974; MacKevett and others, 1971; Rossman, 1963a, b; Plafker and MacKevett, 1970) is fragmentary. D. A. Brew, B. R. Johnson, C. J. Nutt, Donald Grybeck, and A. B. Ford (1977) conducted brief investigations into the mineral-resource potential of the range (loc. 22) as a factor bearing on its suitability for wilderness designation. Their studies added significantly to knowledge about the occurrence of granitic and gabbroic bodies in this remote, rugged, and nearly inaccessible area.

Rossman (1963a) mapped a few diorite and quartz diorite bodies between the southern peaks of the Fairweather Range and Cross Sound. Recent work has refined Rossman's mapping considerably. There are two groups of intrusions, each characterized by a different typical lithology and age. The older group consists mostly of poorly foliated to well-foliated biotite-horneblende quartz diorite of inferred Tertiary or Cretaceous age; the younger group includes commonly foliated garnet-biotite granodiorite and slightly foliated garnet-muscovite-biotite granite, both of inferred Tertiary age. The younger group in particular has associated aureoles of andalusite-quartz-plagioclase-biotite hornfels.

In the upper reaches of Lituya Glacier, about 5 km northwest of the northernmost exposures of the Mount Crillon-La Perouse layered gabbro body (Rossman, 1963b), is a newly discovered, crudely layered gabbro body that is not yet completely mapped. The body is relatively inaccessible because of extremely rugged topography. The body may be only partially unroofed; the contact on the western side, extends northward for about 7 km to within about 11 km of the southernmost exposures of the poorly understood Mount Fairweather layered gabbro body (Plafker and MacKevett, 1970). There is as yet no control on the eastern contact of the newly discovered body. Where it has been studied to date, the Lituya Glacier body consists of layers 0.5 to 1 m thick of coarse-grained pyroxene-hornblende gabbro and pyroxene gabbro with discontinuous layers of pyroxenite 2 cm thick and hornblendite 10 cm thick.

Paleozoic or Precambrian age of rocks in Glacier Bay National Monument

Several inconsistent but generally converging lines of evidence suggested to D. A. Brew, R. A. Loney, R. W. Kistler, S. C. Grommé, and Mitsunobu Tatsumoto that the rocks in the high part of the Fairweather Range (loc. 22), which heretofore have been interpreted to be either no older than late Paleozoic (Rossman, 1963a; Brew, Loney, and Muffler, 1966; MacKevett and others, 1971; Brew and Ovenshine, 1974) or, by distant lithologic correlation, middle Paleozoic (Hudson, Plafker, and Lanphere, 1977; Brew and others, 1976), may be as old as Precambrian. This hypothesis has significance for the paleotectonic analysis of the northeastern rim of the Pacific Ocean.

The oldest rocks in the high part of the Fairweather Range are an apparently thick, complexly folded sequence of metamorphosed graywacke and shale. Few, if any, carbonate units are present; no fossils have been reported. Associated with the metagraywackes and metashales are a few kilometer-long, thin lenses of metavolcanic rocks that to the west and southwest become the dominant rock type. These rocks have been correlated by Rossman (1963a) and Brew (Brew, Loney, and Muffler, 1966; MacKevett and others, 1971; Souther, Brew, and Okulitch, 1976) with very sparsely fossiliferous rock units of Triassic through Early Cretaceous age on Chichagof Island to the south. Plafker and others (1976) and Hudson, Plafker, and Lanphere (1977), on the other hand, have correlated the same units with rocks in the Yakutat area, which, because they are intruded by plutons of late Paleozoic age, are inferred to be at least as old as middle Paleozoic.

There is thus no clear, direct evidence for the age of metasedimentary and metavolcanic rocks in the high part of the Fairweather Range. The rocks are, however, intruded by a variety of plutons. In Glacier Bay National Monument, the oldest rocks that give consistent mineral ages are middle Tertiary in age; they are unfoliated leucocratic biotite granites and granodiorites. An apparently slightly older foliated granodiorite pluton in the Fairweather Range gives discordant mineral-pair ages that probably represent the revision of an emplacement age of no older than middle-Cretaceous. The oldest plutons recognized in the Yakutat area are apparently late Paleozoic.

The critical plutons in the Fairweather Range are the layered gabbros, the largest of which are the Mount Fairweather (Plafker and MacKevett, 1970), the Lituya Glacier, and the Mount Crillon-La Perouse (Rossman, 1963b) bodies. The Mount Crillon-La Perouse body, the largest, is apparently at least 9,000 m thick and is about 27×13 km in plan view. All of these thick layered bodies appear to have developed contact aureoles in the metasedimentary and metavolcanic host rocks, as the younger granitic intrusions have.

There is only one known good analog of these layered bodies elsewhere in the world—the Axelgold intrusion of British Columbia (Irvine, 1975), which is considered to be middle Cretaceous in age and which intrudes upper Paleozoic rocks. The Jabal Shayi intrusion in Saudi Arabia (Coleman, Ghent, and Fleck, 1973), which intrudes Precambrian rocks and which is itself Precambrian in age, is also a possible analog. The Mount Crillon-La Perouse body differs from these bodies in one significant way, however; it has a large copper-nickel-platinum deposit associated with it (Cornwall, 1966; MacKevett and others, 1971). Throughout the world, most of the large known nickel deposits that are associated with mafic and (or) ultramafic rocks occur in the Precambrian (Naldrett and Cabri, 1976).

The Mount Crillon-La Perouse body appears to have a relatively simple relationship to the surrounding rocks and to nearby younger intrusions; this relationship together with lithologic correlations with rock units of Mesozoic age on northern Baranof Island, led to an initial interpretation that the body was Tertiary (Brew, Loney, and Muffler, 1966). Radiometric study shows that this apparent simplicity is misleading. Potassium-argon dates of biotite, hornblende, pyroxene, and plagioclase from the body range from 36 to 250 million years. Of eight specimens dated, no two had the same date. Even though this study does not yield an age of emplacement for the body, it does demonstrate that the unit has undergone a complex metamorphic history that was not apparent from the geologic studies. Further radiometric studies using other isotopes are underway. Preliminary results indicate that rocks from the body have extremely low $^{87}Sr/^{86}Sr$ isotopic ratios, like those of oceanic basalts rather than those of continental crustal rocks; thus, a relatively primitive nature is suggested.

Paleomagnetic study of rocks from the Mount Crillon-La Perouse body likewise indicates a complicated history. Preliminary and incomplete results are compatible with a Precambrian age.

None of these lines of reasoning—field relations, associated sulfide deposits, radiometric data, isotopic data, or paleomagnetic data—points clearly to an age of emplacement for the Mount Crillon-La Perouse body and associated bodies or to an age for the host rocks. Most of these studies are internally inconsistent, and most are not clearly consistent with one another. Taken together, however, they indicate a complexity and a general situation that are best explained by a Paleozoic or older age of emplacement for the layered gabbros and a similarly older age for the host rocks. The hypothesis of an older Paleozoic or Precambrian age for both must be considered seriously.

If the rocks in the high part of the Fairweather Range are early Paleozoic or Precambrian in age, then the early history of the Alexander terrane (Berg, Jones, and Richter, 1972) becomes even more complex. Rocks of probable Precambrian age occur in the Wales Group on Prince of Wales Island to the south. The high Fairweather Range country rocks do not appear to correlate lithologically or structurally with the highly mixed metavolcanic, metasedimentary, and metacarbonate rocks of the Wales Group, the suggestion being that, if a Precambrian age is assumed, more than one basement terrane may be present. Likewise, the lithologies of the high Fairweather Range rocks do not correspond to those of the recently recognized Ordovician rocks nearby in Yukon Territory (Reed and Monger, 1975) or with the older Paleozoic sections on Prince of Wales Island (Eberlein and Churkin, 1970) or elsewhere in Glacier Bay National Monument (Rossman, 1963a).

Subdivision of Ordovician and Silurian time scale using accumulation rates of graptolitic shales

If radiometric data on the age of graptolite zones in the Esquibel Island section of southern Alaska (loc. 23) are used, it is possible to suggest preliminary age assignments for Middle and Upper Ordovician zones in other parts of the North American Cordillera, including the unusually complete Trail Creek zonation in Idaho. Calculations made by Michael Churkin, Jr., Claire Carter, and B. R. Johnson indicated an average accumulation rate of 4 ± 1 m/m.y. based on careful measurements of graptolite zone thicknesses. This figure falls within the 2- to 5-m/m.y. range for deposition rates of modern abyssal clays and siliceous oozes, which they believed to be the closest analog for ancient black graptolitic siliceous shale and chert sequences.

Suggested plate tectonic model for development of ancient borderland terranes of North American Cordillera

The inability to correlate the lower Paleozoic and Precambrian rocks of southeastern Alaska, perhaps best understood in the Craig area (loc. 23), with other sequences of the North American Cordillera supports the view that such sequences are allochthonous with respect to the North American continent. G. D. Eberlein and Michael Churkin, Jr., formulated a new plate tectonic interpretation of the allochthonous sequences that suggests that at least six lithospheric microcontinental plates and volcanic arcs may be represented by ancient rocks in southeastern Alaska and by similar rocks in other borderland terranes ranging as far south as northern Californa. These terranes moved outboard and inboard during the late Paleozoic and early Mesozoic to accommodate a succession of marginal ocean basins that opened and closed behind migrating arcs. This episode was followed by large-scale northwestward drift in the late Mesozoic and Cenozoic.

Radiometric age of the *Monograptus cyphus* zone

M. A. Lanphere, Michael Churkin, Jr., and G. D. Eberlein completed a K-Ar study of an Early Silurian datum on Esquibel Island (loc. 23), where a continuous succession of graptolite faunas occurs across the Ordovician-Silurian boundary. The uppermost graptolite zone in this succession is the *Monograptus cyphus* zone of the lower Silurian. Immediately above the graptolite succession is a sedimentary breccia containing pyrogenic hornblende that yielded an $^{40}Ar/^{39}Ar$ age of 433 ± 3 million years. This result provides a minimum age for the *Monograptus cyphus* zone. The ancient shales resemble in many ways modern deep-sea pelagic sediments on which accumulation rates of 2 to 5 m/m.y. have been estimated. When the hornblende K-Ar age and these sediment accumulation rates are used, an age of 435 to 437 million years is estimated for the Ordovician boundary.

Revised age assignment of Karheen Formation on eastern Heceta Island

Conodont studies conducted by Norman Savage (University of Oregon) indicated that the Karheen Formation at USGS locality 2689 on eastern Heceta Island (loc. 22) contains faunas indicative of an early Praguian (middle Early Devonian) Age. The same conodonts occur in the Port St. Nicholas section of the Karheen Formation, 44 km to the southeast, directly beneath shale that contains *Monograptus yukonensis, Monograptus craigensis,* and *Monograptus pacificus,* indicatively of a late Siegenian to early Emsian (Praguian) Age.

Metamorphic zonation pattern truncated by Coast Range batholithic complex in northern southeastern Alaska

The synkinematic Barrovian metamorphic belt along the western side of the Coast Range batholithic complex near Juneau (loc. 24) includes rocks ranging from subgreenschist facies to garnet-, staurolite-, kyanite-, and stillimanite-bearing mica schists of the amphibolite facies. The metamorphic zonation pattern is known in detail (Ford and Brew, 1973, 1977a; Brew and Ford, 1977). The parent rocks are late Paleozoic to late Mesozoic in age and consist of basalt, shale, graywacke, sandstone, and calcareous sediments. The age of the metomorphism is probably late Cretaceous or early Tertiary (Forbes and Engels, 1970).

The western margin of the batholithic complex consists of some mica schist mixed with an assortment of gneisses, including some discrete bodies of homogeneous quartz dioritic to granodioritic orthogneiss, which A. B. Ford and D. A. Brew interpreted to be early phases of the batholith that were emplaced and solidified during a late stage of the metamorphism after temperatures declined but before deformation ceased. The Mount Juneau pluton, for example, lies east of the schist belt southeast of Juneau but to the north cuts westward across the metamorphic belt as far as the garnet isograd. The pluton is discordant to and has no apparent effect on the regional metamorphic zonation, but its well-developed foliation parallels that in the schists.

This same situation exists northwest of Juneau, where almost the entire metamorphic sequence is truncated by a 60-km-long transgressive batholithic contact. Apparently, the early phases of intrusive activity over a broad area accompanied a late stage of regional metamorphism.

Chemical nature of greenstone near Juneau indicates tholeiitic ocean-floor volcanism

Metamorphic mafic volcanic rocks of Cretaceous age are widely distributed along the apparent eastern age of an upper Mesozoic sedimentary basin in northern southeastern Alaska (loc. 24). These rocks were studied by A. B. Ford and D. A. Brew, who found them to be dominantly metamorphosed tuff and breccia, with some metaflow rocks and fossiliferous marine metasedimentary rocks; they estimated the volcanic pile to have been 1,000 to 3,000 m thick. The tectonic setting of the volcanism is uncertain, largely because of the presence of the Alexander microplate to the west.

Major- and trace-element geochemistry of 28 analyzed samples shows that (1) the greenstones are compositionally basaltic; (2) olivine and hypersthene are present in CIPW norms, indicative of an undersaturated olivine tholeiite composition; and (3) the criteria of Pearce (1975) for titanium-zirconium-yttrium ratios suggest ocean-floor volcanism, with some possibility of volcanic-arc origin.

The rocks are chemically unlike the upper Mesozoic meta-andesites of the Ketchikan area (Berg, Jones, and Richter, 1972) and differ from the synchronous alkali olivine basalt of the nearby Berners Bay area (Irvine, 1973). The tectonic meaning of this diversity is uncertain, but it is possible that systematic lateral variations along strike of this group of rocks are related to significantly different tectonic-volcanogenic processes adjacent to the Alexander microplate in the Cretaceous (Ford and Brew, 1977b).

La Perouse gabbro and associated sulfide deposits

R. A. Loney, G. R. Himmelberg, and G. K. Czamanske continued their detailed field and laboratory study of the La Perouse layered gabbro intrusion (loc. 25). The body is located in the southern Fairweather Range and was previously mapped in reconnaissance by Rossman (1963b). The intrusion is an asymmetrical basin that is roughly elliptical in plan and consists of inward-dipping layers bounded by steep contacts. The body underlies an area of approximately 375 km^2 and has an exposed stratigraphic thickness of approximately 10,000 m. The exposed part of the intrusion consists dominantly of olivine gabbro, and noritic gabbro. Ultramafic rocks, interlayered with olivine gabbro, are known to occur only in the vicinity of two nunataks in the Brady Glacier about 5 km southeast of the main exposures of the intrusion. These rocks represent the basal zone of the intrusion. Layering and textural characteristics indicate that the intrusion originated by cumulus processes. Preliminary data suggest that the intrusion has undergone only limited chemical differentiation, like the Axelgold layered gabbro in British Columbia (Irvine, 1975).

Marginally economic concentrations of nickel-copper sulfides have been established by diamond drilling in the vicinty of the Brady Glacier nunataks by Newmont Exploration, Ltd. Mineralization is predominantly in the form of disseminated sulfide minerals, but several massive sulfide pods crop out in one of the nunataks, and massive sulfide lenses are common in the drill core. Predominant sulfide phases are pyrrhotite, pentlandite, and chalcopyrite.

PUERTO RICO

Role of spilite in the origin of amphibolite in western Puerto Rico

Mattson (1960, 1973) suggested that amphibolite associated with and included as blocks within serpentinite in western Puerto Rico was derived from the regional metamorphism of tholeiitic oceanic crust and that spilite may have been an intermediate step in this process. A geologic study done by A. F. Curet and R. D. Krushensky of a large mass of spilite enclosed in serpentinite in the core of the Las Mesas-Fraile anticline in western Puerto Rico indicated a chilled contact of the spilite against the enclosing serpentinite. The prespilite basaltic rock is therefore intrusive into and younger than the serpentinite. The difference between the metamorphic grade of the spilite (zeolite facies) and that of a nearby large mass of amphibolite (hornblende hornfels facies) also enclosed in the serpentinite suggests that this particular spilite was never subjected to a regional metamorphism high enough to have produced amphibolite-grade rocks.

Source of the Daguao Formation of eastern Puerto Rico

A detailed field study of the Naguabo quadrangle in eastern Puerto Rico by J. W. M'Gonigle showed that two hypabyssal stocks of andesitic breccia, each roughly circular in plan view and about 500 m across, intrude the Daguao Formation (Lower Cretaceous). These stocks are generally epidotized and consist of clasts of porphyritic andesite (plagioclase and clinopyroxene) as much as 15 cm across in a matrix of smaller lithic clasts of the same type. Clasts in tuff breccia and autoclastic breccia flows of the Daguao Formation appear texturally and mineralogically identical to lithic clasts in the breccia stocks. Therefore, it is thought that these stocks were volcanic necks or conduits that supplied much of the andesitic breccia comprising the Daguao Formation.

Unconformity between Late Cretaceous and early Tertiary in western Puerto Rico—a concept rejected

Geologic mapping done in western-central Puerto Rico by R. D. Krushensky suggested that evidence previously thought to indicate the presence of a major unconformity between rocks of Late Cretaceous and Eocene age is invalid because it was based on the misidentification of a fault breccia as a stratigraphic unit, the miscorrelation of two formations, and insufficiently extensive areal mapping.

Mattson (1966) described a transgressive basal conglomerate, later named the Miromar Formation (Glover and Mattson, 1967), that marked a major unconformity between rocks of the underlying Achiote Conglomerate of Late Cretaceous age and rocks of the overlying Cuevas Limestone of early Tertiary age (Mattson, 1968a; Glover, 1971). Mapping in the Ponce quadrangle (Krushensky and Monroe, 1975), however, indicated that the "Miramar" is actually a slickenside-riddled breccia composed of angular clasts of porphyritic andesite from the underlying Achiote Conglomerate or mudstone of the Maravillas Formation, algal calcarenite from overlying allochthons of the Cuevas Limestone, and a clay matrix. This breccia is identical in the field and in continuous outcrop with "megabreccia" mapped in the Rio Descalabrado quadrangle (Glover and Mattson, 1973). Both breccias are related in origin to gravity gliding of the Cuevas, and both are here considered fault breccia.

Farther west in the Monte Guilarte quadrangle and surrounding quadrangles, geologic mapping indicated, according to Krushensky and A. F. Curet, that the rock mapped as the Robles Formation in the Adjuntas and Bayaney quadrangles (Mattson, 1968b; Nelson and Tobisch, 1968) is lithologically distinct from the Robles in the type area (Pease and Briggs, 1960); it is, however, identical to the lithologically distinctive Maricao Basalt both in the type area (McIntyre, Aaron, and Tobisch, 1970; McIntyre, 1975) and as mapped in the Monte Guilarte quadrangle. The absence of a thick sequence of lower through Upper Cretaceous rocks above the Maricao—the "Robles' of the Adjuntas and Bayaney quadrangles—is therefore invalid as evidence for an uncornformity, since the Maricao is Late Cretaceous in age.

Mapping in the Monte Guilarte quadrangle also indicated that the Yauco, Lago Garzas, and Maricao Formations, known to be of Late Cretaceous age in widespread areas, are interbedded with one another and with the Anón Formation, known in the type area to be of Eocene age (Mattison, 1968a; 1967). The Anón in the south-central part of the Monte Guilarte quadrangle is overlain by the Maricao and interbedded with the Yauco Formation; there the Yauco contains Foraminifera of middle Campanian through late Maestrichtian Age. In the Maricao quadrangle (McIntyre, 1975), the Mal Paso Formation, an interbedded lithofacies of the Lago Garzas and Anón Formations, contains fossils of early Eocene age. The Lago Garzas is at least in part of Eocene age, and the Anón is in part of Late Cretaceous age.

The recognition of the "Miramar Formation" as a fault breccia and of the "Robles Formation" of the Aduntas and Bayaney quadrangles as the Maricao; the conformable interbedding of the Yauco, Lago Garzas, Maricao, and Anón Formations; and the Late Cretaceous through early Tertiary fossils contained in the interbedded lithofacies suggest that deposition in western-central Puerto Rico was continuous from the Late Cretaceous through the Eocene.

GEOLOGIC MAPS

Geologic map of Wyoming, scale 1 : 500,000, J. D. Love, compiler.

A new geologic map of Wyoming is being compiled in cooperation with the Geological Survey of Wyoming. Sixteen 2° sheets at a scale of 1 : 250,000 on topographic bases will be published first in black and white as USGS miscellaneous Field Studies maps and then scribed and published in color by the Wyoming Geological Survey in the State Survey map series. Finally, the USGS will publish a single map in color at a scale of 1 : 500,000.

Geologic map of Colorado, scale 1 : 500,000, O. L. Tweto, compiler.

A new geologic map of Colorado, begun in 1971, was published in 1976 in a preliminary black-and-white version (Tweto, 1976). The map is plotted on a modern base that shows highways and 500-ft contours; the final full-color sheet is in preparation.

Geologic map of Alaska, scale 1 : 2,500,000, H. M. Beikman, compiler.

The geologic map of Alaska was published in a preliminary black-and-white version at a scale of 1 : 1,000,000 in five segments (Beikman, 1974a, b; 1975a, b, Beikman and Lathram, 1976). It will be published as a single multicolor map showing the bathymetry of adjacent sea bottoms.

Quaternary map of the conterminous United States, scale 1 : 1,000,000, G. M. Richmond, editor.

The Quaternary map of the conterminous United States is being compiled in cooperation with various State geological survey and university personnel. Surficial deposits will be shown as well as Quaternary volcanic rocks, Quaternary structures, and submarine deposits. The initial compilations, now in progress in 32 States, will be on 50 sheets of the International Map of the World (IMW) series at a scale of 1 : 1,000,000; only selected maps at this scale will be published. The final product will be a two-sheet map in color at a scale of 1 : 2,500,000.

WATER-RESOURCE INVESTIGATIONS

The USGS conducts investigations, surveys, and research on the occurrence, quality, quantity, distribution, use, movement, and availability of the Nation's surface- and ground-water resources. This work includes (1) investigations of floods and droughts and their magnitude, frequency, and relation to climate and physiographic factors; (2) evaluations of available waters in river basins and ground-water provinces, including assessments of water requirements for industrial, domestic, and agricultural purposes; (3) determinations of the chemical, physical, and biological characteristics of water resources and the relation of water quality and suspended-sediment load to various parts of the hydrologic cycle; and (4) studies of the interrelation of the water supply with climate, topography, vegetation, soils, and urbanization. One of the USGS's most important activities is the systematic collection, analysis, and interpretation of data for evaluating the Nation's water resources. These data are computer processed for storage, retrieval, and dissemination of water information.

The USGS is responsible for coordinating national network and special water-data-acquisition activities and maintaining a central catalog of water information for use by Federal agencies and other interested parties.

Research is conducted to improve the scientific basis of investigations in hydraulics, hydrology, instrumentation, and the chemical, physical, and biological characteristics of water.

Subjects currently under investigation or researched recently by the USGS include the following: (1) Properties of water—geochemistry, temperature, and water chemistry; (2) drainage, runoff, and watersheds—flood plains, floods, frozen ground, playas, and storm runoff; (3) evaporation, meteorology, and precipitation—droughts, evapotranspiration, glaciers, glaciology, ice and icing, snow, and transpiration; (4) flow, hydraulics, and streams—availability of water, base flow, channel morphology, culverts, drainage, floodflow formulas, flood hazards, flood-inundation maps, fluid mechanics, gaging, geomorphology, highway drainage, hydraulic engineering, hydrodynamics, low flow, measurement of streamflow and time of travel under ice, acid mine drainage, overland flow, river basins, rivers, seepage, storm drainage, stratified flow, streamflow, stream classification, and water problems of the coal industry; (5) ground water—aquifers, artesian aquifers, artificial recharge, availability, carbonate-rock hydrology, connate water, core sampling, dispersion of contaminants, earthquake effects, electric-analog-model studies, flow, geochemistry, geochronology, geophysical logging, hot springs, hydraulics, hydrogeology, hydrologic properties, interpretations, investigations, levels, mapping, nuclear-explosion effects, nuclear-waste disposal, piezometric maps, pollution, pumping and pumpage rates, quality, quantity, radiocarbon dating, research, resistivity studies, saltwater intrusion, springs, subsidence of land, test-well drilling, thermal water, use of water, use of isotopes in investigations, waste disposal, and wells; (6) soil water—soil moisture, soil-water movement, and soil-water relationships; (7) lakes and reservoirs—biology and ecology, eutrophication, impoundments, lake levels, lake basins, limnology, ponds, and stratification; (8) water and plants—phreatophyte control, plant-water relationships, and tree rings; (9) erosion, sedimentation, and sediments—reservoir sedimentation, reservoir siltation, siltation, sediment control, and sediment transport; (10) quality of water—biological and ecological aspects of water chemistry, brine, chemical analysis, geochemistry, inorganic constituents, kinetics, radioactivity in water, salinity, solutes and solutions, and trace elements; (11) estuarine problems—biological and ecological problems, brackish water, distribution of sediments and wastes, tidal studies, transient flow, and upstream movement of saltwater; (12) water use—agricultural use, aluminum industry, copper industry, evaporation control, evapotranspiration control, hydroelectric use, industrial use, municipal use, petroleum industry, pulp and paper industry, rayon- and acetate-fiber industry, styrene-butadiene industry, surface- and ground- and waste-water use, synthetic-rubber industry, and water requirements; (13) agriculture, irrigation, and pesticides—movement in streams and ground water of pesticides, water requirements, and water spreading; (14) water management—flood control, management of ground- and surface-water resources, and use of models; (15) water-pollution effects, water-pollution sources, and water quality—agricultural sources of pollution, detergents in water, effect of pollutants on aquatic life, industrial wastes, movement of pesticides and other pollutants in streams and ground water, pesticides in water, pollutant identification, radioactive rainout, saline-water intrusion, source of pollutants, temperature, and thermal pollution; (16) waste disposal—radioactive-waste disposal and waste-water disposal; (17) planning and water-resource development—development of ground- and surface-water resources, flood forecasting, river-basin planning, water budgets, and water supply; (18) water law; (19) environments—antarctic regions, arctic regions, arid lands, deltas, deserts, karst terranes, swamps, urban areas, and wetlands; (20) water-resource studies—appraisals, computer applications in water research, data processing, evaluation, hydrologic data, infrared application, instrumentation for hydrologic studies and resource research, interpretations, investigations, mapping of ground water, model studies, processing, publication, remote sensing, reports, research, stochastic hydrology, techniques for hydrologic studies and resource research, and telemetry; (21) corrosion—well casings; and (22) water cycle.

A significant part of USGS water-resource activities is providing scientific and technical assistance to other Federal agencies. When USGS interests are related to the interests of other agencies, USGS assistance contributes to the efficiency of their programs and encourages the maintenance of high standards of technical accomplishment.

The USGS develops ground- and surface-water technology and the technologies necessary for dealing with (1) the chemical, physical, and biological properties of water and (2) the interrelation of these water-quality properties within the environment.

During FY 1977, data on streamflow were collected at 7,564 continuous-record discharge stations and at 8,736 lake- and reservoir-level sites and partial-record streamflow stations. About 12,500 maps of flood-prone areas in all States and Puerto Rico have been completed to date, and about 900 pamphlets covering areas susceptible to flooding have been published. Studies of the quality of surface water were expanded; there were 5,173 water-quality stations in the United States and in outlying areas where surface water was analyzed by the USGS. Parameters measured include selected major cations and anions, specific conductance or dissolved solids, and pH. Other parameters, measured as needed, include trace elements, phosphorus and nitrogen compounds, detergents, pesticides, radioactivity, phenols, BOD, and coliform bacteria. Streamflow and water-temperature records were collected at 4,067 of the water-quality stations. Sediment data were obtained at 1,222 locations.

Annually, about 500 USGS scientists report participation in areal water-resource studies and research on hydrologic principles, processes, and techniques. There is a total of 1,988 active water-resource projects; 673 of the studies in progress are classified as research projects. Of the current water-resource studies, 147 are related to urban hydrology problems.

In FY 1977, 546 areal appraisal studies were carried out. Maximum and mean areas of the studies were 3.077 million square kilometers and 79,720 km^2, respectively. Total areal appraisal funding was about $28 million. Ground-water studies have been made or are currently in progress for about two-thirds of the Nation. Scheduled measurements of ground-water levels were made in about 28,000 wells, and periodic measurements were made in many thousands of other wells. Studies of saline-water aquifers, particularly as a medium for the disposal of waste products, are becoming increasingly important, as are hydrologic principles governing the occurrence of brackish water in estuaries. Land subsidence owing to ground-water depletion and the possibilities for induced ground-water recharge are under investigation in areas where the land surface has settled significantly. The effects of coal-mining activities on both ground- and surface-water resources are being intensively studied.

The use of computers—in research studies of hydrologic systems, in expanding data-storage systems, and in quantifying many aspects of water-resource studies—continued to increase during FY 1977. Records of about 310,000 station-years of streamflow acquired at about 10,000 regular streamflow stations are sorted on magnetic tape, and data on about 440,000 wells and springs have been entered in a new automated system for storage and retrieval of ground-water data. Digital-computer techniques are used to some extent in almost all of the research projects, and new techniques and programs are being developed continually.

The principal publications devoted to basic hydrologic data are the following series of USGS water-supply papers: (1) "Surface-Water Supply of the United States," (2) "Quality of Surface Waters of the

United States," and (3) "Ground-Water Levels in the United States." In addition to these basic-data reports, other series of water-supply papers describe (1) the magnitude and frequency of floods for the entire country, (2) floods by drainage-basin areas, and (3) noteworthy floods for each year.

Requests for data on water use in the United States and in relatively small areas increased in 1976. The need to develop energy sources of various kinds in areas where industrial development has been nonexistent or minimal requires estimates of future water requirements in these areas and evaluation of the adequacy of water resources to meet the demand. Studies are underway to improve methods for expanding the scope, intensity, and accuracy of water-use investigations.

Investigations describing the occurrence of water as a natural resource are given in the following sections for the four regions of the United States (fig. 2) used since 1973 by the USGS for administering the water-resource program.

NORTHEASTERN REGION

Flows of some Minnesota streams during 1976 were less than those expected on an average of once in 50 years. Using data from 100 continuous-record stations not significantly affected by regulation, USGS investigators compared the 7-day 10-year low flows for 1976 with those for other years. Although the 1976 flows at 20 of the 100 stations were at or below previously recorded minimums, the flows of large rivers generally remained above the critical low flows of the 1930's. During 1976, the 7-day low flow of the lower reach of the Mississippi River was that expected on an average of once in 20 years, the 7-day low flow of the lower Minnesota River was that expected once in 10 years, the 7-day low flow of the St. Croix River was that expected once in 5 years, and the 7-day low flow of the Red River of the North was that expected once in 2 years.

The storm of February 2, 1976, along the Maine coast caused a surge up the Penobscot River, which resulted in the flooding of part of Bangor. The flood elevation was 5.3 m above mean sea level, the third highest level since 1846. Flood damage in Bangor was reported to exceed $2 million. Apparently, no deaths were caused by the storm.

Relatively fresh ground water was found in continental shelf sediments during test drilling off the coasts of several Northeastern States. Apparently, fresh ground water occurs as far as 100 km offshore.

FIGURE 2.—Index map of the conterminous United States showing areal subdivisions used in the discussion of water resources.

The water presumably is residual ground water from Pleistocene time when the sea level was lower.

The Silurian Salina Formation (or Group) is being evaluated as a repository for high-level radioactive-waste material in Michigan, New York, and Ohio. Potential associated hydrologic hazards are being carefully investigated.

The possibility that land subsidence is being caused by ground-water withdrawal in the coastal plain areas of the Northeast is being studied. Geodetic measurements suggested such an association in parts of Delaware, Maryland, New Jersey, and Virginia.

REGIONAL STUDIES

A mathematical model was developed by T. S. Wyant, R. A. Smith, and J. R. Slack to predict the movement of an oilspill at sea. This model was used after an oilspill resulted from the breakup of the tanker *Argo Merchant* in December 1976. Preliminary model runs made during and immediately after the breakup used observed wind velocities as input data and simulated the slick movement during the first days and weeks after the accident; the computed slick trajectory agreed closely with observed movement. Predictive runs were then made by using various assumed wind and current conditions as input data, the objective being to predict the future trajectory of the slick and the probability that it would reach shore. Computed probabilities ranged from 0.07 to 0.24. Similar predictive runs were made for possible subsequent oil releases from remaining fragments of the ship's hull. The analysis showed that, if new oil slicks should form as the result of further breakup of the hull, the probability of their reaching land would range from 0.08 to 0.92, depending on the time of the release and the assumed wind and current conditions.

The model was modified to allow for a long-term prediction of the movement of the oil slick within the Gulf Stream. Results of this analysis suggested that the slick would move generally northeastward, toward the British Isles. However, because of uncertainty as to the effect of long-term weathering on the oil slick, predictions over this length of time were highly speculative.

CONNECTICUT

Water-quality assessment of the Farm River basin

David Grason made a preliminary analysis of the quality of stream water in the Farm River basin in south-central Connecticut. Samples collected at different seasons in 1975 and 1976 showed that the chemical and bacteriological quality of the main stem deteriorates downstream from Totoket. The degradation is attributable in part to contributions from Burrs Brook, which receives water imported into the basin by an aqueduct. Burrs Brook water is high in pH and concentrations of bacteria, bicarbonate, magnesium, organic carbon, dissolved solids, and sulfate. The other tributaries to the Farm River have no significant impact on main-stem water quality. Stream degradation is significantly greater downstream from Foxon. Diversion in Foxon reduces the dilution capacity of flow in the more highly developed lower part of the basin. Total coliform bacteria, iron, organic carbon, and phosphorus concentrations rise sharply at Foxon and remain high downstream.

Stratified-drift aquifer in the Pootatuck River valley

F. P. Haeni's study of 15 test holes and 8 seismic refraction lines, supplemented by data from older drillers' logs, showed that the saturated thickness of stratified drift along the Pootatuck River in southwestern Connecticut consists of sand and gravel with a maximum thickness of 30 m. Twelve split-spoon samples collected from the streambed of the Pootatuck River showed unexpectedly uniform material consisting of sand and gravel, with less than 10 percent silt and clay along a 6.4-km reach. Laboratory tests determined that two of the streambed samples had vertical hydraulic conductivities of 0.4 and 1.2 m/d.

Long-term yields estimated for stratified-drift aquifers in Quinnipiac River basin

Using a FORTRAN language analytical model, D. L. Mazzaferro evaluated 14 areas favorable for ground-water development in the Quinnipiac River basin of Connecticut. Estimated long-term yields from these areas ranged from 0.04 to 0.7 m^3/s. The model also indicated that potential long-term yields of individual wells in the main valley may exceed 0.07 m^3/s.

Drainage-area maps for land use planning

R. L. Melvin and M. P. Thomas reported that the USGS, in cooperation with the Connecticut Department of Environmental Protection, compiled 21 drainage-area maps of Connecticut. The 1:24,000-scale maps will be used in resource management, environmental engineering, and land use planning.

Ground-water availability in Farmington

Preliminary analyses of data from 7 seismic profiles, 25 test borings, and 17 observation wells by

D. L. Mazzaferro revealed an area favorable for ground-water development southeast of River Glen, in the town of Farmington, Conn., where the saturated thickness of sand and gravel exceeds 30 m. Farther southeast, saturated thickness may exceed 107 m, but data indicate that the materials in this area are generally finer grained.

DELAWARE

A digital model was developed by P. P. Leahy to simulate the effects of increased pumpage on the Piney Point aquifer in Kent County, Delaware. The model was calibrated by using pumpage records from 1970 to 1975. Calibration involved comparisons of (1) simulated and interpreted potentiometric surfaces and (2) simulated and observed hydrographs for three observation wells. At 18 control points in Delaware, the mean error between the simulated and observed water levels was -0.67 m, with a standard deviation of ±1.46 m.

The calibrated digital model was used to predict water levels that will result from three different development plans. The model simulated 25 years of pumpage estimates, and the results were shown in a series of maps and hydrographs. The model predicted the following:

- Under the 1975 stress of 0.12 m^3/s, water will stabilize at a minimum level of 46 m below mean sea level at the center of the Dover cone of depression and leave approximately 42 m of available drawdown to the top of the aquifer.
- Proposed withdrawals of 0.26 m^3/s, mainly in the Dover area, will dewater updip areas of the aquifer.
- If the aquifer is developed downdip (southwest of Dover), a withdrawal of 0.24 m^3/s will result in a stabilized minimum water level of 82 m below mean sea level at the center of the Dover cone and leave about 6 m of available drawdown to the top of the aquifer.

INDIANA

Digital model for simulating the movement of leachate

R. A. Pettijohn used a solute-transport digital model to simulate the movement of leachate through the sand-and-gravel aquifer underlying a landfill at Indianapolis, Ind. The difference between the concentration of dissolved solids in native ground water and that in ground water from below the landfill was used to estimate leachate content. Field data and model analyses indicated that the movement of leachate through the sand-and-gravel aquifer is toward two industrial well fields located less than 1.6 km from the landfill. The results from the model simulation indicated that the observed leachate concentrations are approximately in equilibrium for the distribution and rate of industrial pumpage in 1977. Model results also indicated that it took approximately 3 years for concentrations to reach steady state within the flow pattern from the landfill to the industrial well field.

Saline ground water near Vincennes

R. J. Shedlock reported the discovery of moderately saline ground water (specific conductance as much as 14,000 μmho/cm at 25°C) near the municipal well field in Vincennes, Ind., in the valley-train aquifer of the Wabash River alluvium. Water with a chloride concentration of as much as 4,000 mg/L is found in the bottom 2 m of the aquifer. The saline water constitutes a narrow plume that extends from the well field to a point 1.6 km west of the well field. The plume has been drawn toward the well field by the cone of depression caused by pumping and has prevented the city from using two new wells, one in the plume and one near the plume. Nearby abandoned oil wells may be the source of the saline water.

Lineament mapping in limestone terrane

Jennings County is in the eastern karst region of Indiana. The karst has developed on limestone and shale of Silurian and Devonian age. T. K. Greeman reported that dependable ground-water supplies are not easily located within this area.

Surface lineaments in limestone may reflect the pattern of subsurface joints and faults, which may be conduits for the movement of ground water. Such lineaments are being mapped from aerial phographs. The maps should aid in locating adequate supplies of ground water.

MARYLAND

Model compares predicted demands with availability of ground water

A digital model was developed by F. K. Mack and R. J. Mandle to help evaluate the availability of water from the Magothy aquifer in the coastal plain of Maryland. The model was used to determine whether predicted water needs in the year 2000 in specific places will be satisfied by local well fields. Simulations indicated that there will be adequate supplies only in some places. The availability of water from the Magothy aquifer at a specific site is directly related to transmissivity and available drawdown at the site. Yields of wells will be greater in eastern Anne Arundel and northern Calvert

Counties, where transmissivity and available drawdown are greatest. A lack of available drawdown, low transmissivity, and the proximity of negative hydrologic boundaries severely limit the availability of water from the Magothy in the southern and western parts of the project area.

Two-dimensional model of the Piney Point aquifer

A digital model of the Piney Point (Eocene) aquifer in Maryland is being calibrated by J. F. Williams. The Piney Point aquifer, composed of medium to very fine sand, underlies both southern and eastern Maryland (Delmarva Peninsula), more than 10,000 km^2 of the State. A large cone of depression centered over Cambridge seems to be nearing steady-state conditions after a water-level decline of more than 33 m. Transmissivity ranges from about 5 to 560 m^2/d. The hydraulic conductivity of the upper confining bed seems to differ by 3 to 4 orders of magnitude in a general north-south direction, the lowest values (3×10^{-10} cm/s) being in the northern part of the study area. In order to gather data to calibrate the model, the USGS installed 17 observation wells ranging in depth from 60 to 183 m. Initial model runs indicated that a large quantity of water is leaking into the aquifer through adjacent confining beds.

Mainland and offshore data on the Manokin aquifer and overlying confining beds

Using acoustical profiles and data from an offshore core hole, J. M. Weigle mapped the Manokin aquifer along an 11-km section seaward of Ocean City, Md. Cores were taken from the principal confining beds in the offshore test hole and also in a test well drilled at Ocean City. Water squeezed from cores at both test sites had similar salinity profiles—water in the upper 50 m was relatively saline, and water below 50 m was relatively fresh (less than 1,000 mg/L of dissolved solids). At Ocean City, water pumped from the aquifer material was consistently fresher than water from the confining beds. Since no water was obtained from the aquifers at the offshore site, it is not known whether this same relationship holds there.

Saltwater monitoring of the Manokin aquifer at Ocean City

Seasonably variable chloride content of water in the Manokin aquifer in the Ocean City area of Maryland was reported by J. M. Weigle. Results of monitoring wells indicated that chloride content is proportional to rates of withdrawal; they are highest in summer and lowest in winter. Although it fluctuates seasonally, the chloride content of water from observation wells in the lower part of the Manokin has been increasing from year to year. These observations, together with the presence of a thick underlying confining bed with very low vertical hydraulic conductivity, suggest that the toe of the saltwater interface in the Manokin occurs beneath Ocean City and that the interface is moving slowly landward in response to withdrawal of ground water.

MASSACHUSETTS

Ground-water exploration on Cape Cod

A test hole drilled about 30 m from the shore of Cape Cod Bay at Dennis, Mass., penetrated 96 m of unconsolidated sediments saturated with freshwater, according to D. R. LeBlanc and J. H. Guswa. Piezometers at depths of 46 and 89 m showed water levels that ranged from 3 to 4 m above mean sea level through the tidal cycle. These piezometers were located 12 and 55 m below a 6-m-thick confining layer of very fine sand, silt, and clay. A piezometer installed previously at a depth of 26 m, 3 m above the confining layer, showed water levels that ranged from 1 to 2 m above mean sea level through the tidal cycle. A piezometer at a depth of 5 m at this same location showed a water level of 3.6 m above sea level that was unaffected by tides.

Analyses of the results of an aquifer test in Orleans, Mass., indicated that medium to coarse sand at a depth of 17 to 20 m has a hydraulic conductivity of approximately 91 m/d. A further analysis, made by using a digital radial flow model of the test results, indicated that the upper 11 m of the aquifer has a lateral to vertical hydraulic conductivity ratio of about 2:1.

Assessment of ground water in the Shawsheen River basin

Sand-and-gravel aquifers capable of supplying 6 to 19 L/s of water to individual wells occur within the unconsolidated deposits in the Shawsheen River basin in northeastern Massachusetts, according to F. B. Gay and D. F. Delaney. The aquifers generally coincide with watercourses and are from 0.8 to 1.6 km wide and from 3 to 6 km long. Zones within these aquifers have enough volume and transmissivity to sustain yields in excess of 19 L/s to individual wells and, for the most part, have been developed to yield much of their total capacity.

Ground-water quality is generally good throughout the basin, and the water is suitable for most uses. However, in many places, iron and manganese exceed 0.3 and 0.05 mg/L, respectively. Iron and manganese problems are most often reported for wells in or near swamps.

Analyses of base-flow measurements for streams over 1 mi^2 (2.59 km^2) show that the annual minimum 7-day mean flows range from 0 to 1.22 $(dm^3/s)/km^2$ at 10-year recurrence intervals. Variations in the annual minimum 7-day mean flows at the 10-year recurrence interval per unit of drainage area are caused by diversions from pumping wells and differences in water storage and hydraulic conductivity of the unconsolidated deposits that these streams drain.

Water resources of Nantucket Island

Analyses of samples collected by E. H. Walker during the past year showed that water on Nantucket Island, Mass., is of excellent quality. Dissolved-solids concentrations in ground water average about 80 mg/L. The principal dissolved constituents are chloride and sodium, which average about 25 and 14 mg/L, respectively. Bicarbonate, calcium, and sulfate are present in lower concentrations. The water tends to be slightly acidic—pH averaged less than 6.5 for 14 of 17 measurements. Iron content averaged 0.3 mg/L. Some wells close to the shore tap brackish water at shallow depths.

Water in the few brooks that drain swampy areas contains 50 to 60 mg/L of dissolved solids, mainly sodium and chloride. The brook water is highly acidic (pH ranges from 3.6 to 5.5) and is a tea-brown color owing to humic acids generated in the swamps. Samples of bottom sediment from two brooks had 23 and 180 ppb of DDD and 53 and 90 ppb of DDT, although these substances were last used in 1966 for mosquito control.

Water in the inland ponds is fresh and low in dissolved solids. The ponds along the eastern and southern shores of Nantucket are brackish to salty, owing to saltwater blown inland during storms and to the ponds' being opened to the ocean to lower their water levels in the spring.

Results of deep drilling in Martha's Vineyard

D. F. Delaney reported that preliminary results of drilling a 260-m-deep test well near the center of Martha's Vineyard, Mass., as part of an evaluation of the island's water resources indicated that only the top 52 m of saturated deposits (from the water table to 58 m below land surface) contain materials with sufficient permeability to be considered aquifers.

Preliminary analyses of cores (Ray Hall, oral commun., 1977) indicated that the test hole penetrated glacial outwash composed of silty sand and clay of Pleistocene age to depths of 46 m and penetrated pale-green sand and olive-green silt and clay of marine origin and Tertiary age from depths of 46 to 73 m. Tertiary deposits are underlain by clay and sand beds of Cretaceous age to a depth of 251 m. Red-brown sandstone, probably of Triassic age, was penetrated from depths of 251 to 262 m (the bottom of the test hole).

Two aquifers in the upper 52 m of saturated Pleistocene and Tertiary deposits extend from the water table, 6 m below land surface, to a depth of 58 m. The upper water-table aquifer is about 24 m thick and is composed of sand and gravel. A sequence of silty sand and clay 8 m thick separates this upper aquifer from an underlying sand aquifer, which extends from depths of 38 to 58 m.

Core samples collected at 3-m intervals were examined for lithology and squeezed for field analyses of salinity. Salinity of water samples squeezed from cores and pumped from the test hole indicated that freshwater extends from the water table to a depth of 158 m. There is a gradual increase in salinity below the 158-m depth amounting to 3.9 ppt at a depth of 226 m. Seawater salinity near the island is 33 ppt (H. B. Bigelow and Mary Sears, 1935).

Analyses of water pumped from wells in the upper aquifer indicated that the chemical quality of the water meets the minimum standards for drinking water recommended by the EPA (National Academy of Sciences, 1973). Analyses of water pumped from wells tapping the lower sand aquifer, however, indicated that iron concentration in water from the 47-m depth is greater than 3 mg/L, and that from the 56-m depth is greater than 5 mg/L; the EPA standard for concentration of iron in drinking water is 0.3 mg/L.

Appraisal of ground-water quality on Cape Cod

F. B. Gay and M. H. Frimpter reported that a reconnaissance of ground-water quality on Cape Cod, Mass., indicated that the water is low in dissolved solids, soft, and slightly acidic. In the 15 Cape Cod towns, domestic water is discharged to the aquifer through septic systems and cesspools. Municipal sewerage systems discharge treated waste water through filter beds to the aquifer, and solid waste is placed in landfills in recharge areas.

Chemical analyses showed that samples collected from 72 wells had mean concentrations of dissolved solids of 71 mg/L, hardness of 21 mg/L, sodium of 13 mg/L, chloride of 22 mg/L, and nitrate-nitrogen of 0.54 mg/L; pH ranged from 4.2 to 7.3. Values of nitrate-nitrogen greater than 0.20 mg/L suggested contamination of wells by waste disposal or other human activities.

Water from organic sediment deposits contains hydrogen sulfide and, probably, methane. The gases are generated in marsh deposits buried by windblown sand. Water containing iron in excess of 0.3

mg/L was found in 29 of 73 samples. The iron is found where ground water is in a reducing environment, notably where the organic content of the aquifer is high.

MICHIGAN

A study conducted by T. R. Cummings to determine the relationship of agricultural land use practices to the erosion of chemical and physical materials in the Upper St. Joseph River basin of Michigan established baseline conditions against which future changes can be judged. In cooperation with the Michigan Department of Agriculture, 42 sites in the 303-km^2 drainage basin were sampled continually or periodically. Data indicated a strong correlation between surface runoff, the loads of various forms of nitrogen and phosphorus transported, suspended-sediment loads, and the use of land in small subbasins.

MINNESOTA

Ground water in Park Rapids area

An evaluation of the water-supply potential of a 2,000-km^2 surficial outwash aquifer in the Park Rapids area of Minnesota is being completed by J. O. Helgesen. Well yields probably will exceed 60 L/s in about 15 percent of the area, mostly in the northern half. The surficial aquifer in much of the southern part of the area is too thin to yield more than about 6 L/s to individual wells. An analysis of the natural aquifer system, aided by a digital computer model, indicated that long-term recharge, mostly from precipitation, averages 9 m^3/s. About 95 percent of that total is discharged from the aquifer to streams and lakes, and about 5 percent is evaporated and transpired. Current ground-water development does not affect the water budget significantly. Completion of the model analysis will define the aquifer's long-term potential as a water source by simulating aquifer response to selected hypothetical pumping patterns.

Effects of copper and nickel mining on surface and ground water in northeastern Minnesota

Streamflow in 1976 was monitored at 12 record gaging stations and 10 periodic measurement sites in northeastern Minnesota. According to P. G. Olcott and D. W. Ericson, flow in several streams varied widely. Floodflow in the Stony River, for example, exceeded the 25-year recurrence interval in April, yet the September flow was less than the 99-percentile on the daily duration curve and was almost a 20-year event on the 7-consecutive-day low-flow-frequency curve. New minimum flows of record were observed on several streams, and many of the small streams ceased to flow in late summer. These flows and minimum flows measured during a 3-day low-flow survey at 90 sites indicated a lack of basin storage in much of the area where thin till overlies crystalline bedrock.

In August 1976, a flow of 0.04 m^3/s was moving out of the Dunka River through outwash sand and gravel into a nearby taconite mine. At least two other streams had losing stretches owing to taconite mining. A reservoir was contributing flow through seepage to two streams in the area.

Ground water is available in moderate to large quantities from thick outwash deposits in much of the Embarrass and Dunka River basins. Several other small outwash deposits will locally yield small to moderate amounts of water to wells, but, in the remainder of the area, yields from the thin clayey till or crystalline bedrock are negligible.

Water in shallow aquifers is soft to moderately hard and generally contains copper, nickel, and other trace metals in concentrations of only a few micrograms per liter. Saline water having extremely high concentrations of calcium, magnesium, sodium, and chloride has been encountered at depth in mine exploration holes in the Precambrian Duluth Complex. However, the water is confined to small fracture systems and has not been found in significant quantities.

Ground water in central Minnesota

Increasing amounts of ground water are being used for irrigation in sand-plain areas of Benton, Sherburne, Stearns, and Wright Counties in central Minnesota, where large-yield wells have been completed in unconfined surficial outwash aquifers. According to G. F. Lindholm, test augering indicated that, locally, the upper sand beds are as thick as 30 m, although in several areas they are too thin to support large-yield wells. Where the unconfined aquifer is inadequate, confined drift or bedrock aquifers are possible sources of irrigation water. Cambrian sandstones underlying the drift in the eastern part of the study area are reliable sources of large quantities of water. Granite underlies the drift in the rest of the study area, and drift aquifers are the only possible sources there of large water supplies.

Red-clay sediment and water-quality evaluation

E. G. Giacomini reported that three gaging stations with sediment samplers were established in the Elim Creek, Skunk Creek, and Deer Creek basins of Minnesota. Stage-discharge relationships were established for the Elim Creek and Skunk Creek stations, and sediment samples were analyzed.

Results of water-quality analyses done by G. A. Payne showed the water to be a calcium bicarbonate type. Total organic carbon content ranged from 6.1 to 23 mg/L, similar to that of other streams in northeastern Minnesota. None of the minor elements exceeded concentrations recommended for public water supplies.

An investigation is underway to determine the relationship of the slumping of hillsides at gullies, road cuts, and streams in the "red clay" area to vertical-pressure differences of the area's ground water. R. J. Wolf established three piezometer nests in an east-west line crossing Skunk Creek; two nests were on upland areas, and one was in the creek valley. In the eastern upland area, the potential exists for upward ground-water movement, and, possibly, for lateral ground-water movement toward the creek in the western area. In the valley, the potential exists for upward movement, but indications are that the upward movement would be seasonal.

Minnesota streamflows approach record lows

The flows of some Minnesota streams during 1976 were less than those expected on an average of once in 50 years. Using data from 100 continuous-record stations not significantly affected by regulation, K. L. Lindskov compared the 7-day 10-year low flows for 1976 with those of other water years. Streams in northeastern Minnesota, among them the Pigeon River, experienced flows lower than those expected once in 50 years. Streamflows in the central and southwestern parts of the State were as low as those expected once in 20 years, whereas flows in the northwestern and southeastern areas were not significantly below normal. Although the 1976 flows at 20 of the 100 stations were at or below previously recorded minimums, the largest rivers generally maintained flows above the critical low flows of the 1930's. During 1976, the lower reach of the Mississippi River experienced low flows expected once in 20 years. However, the 7-day low flow of 27 m^3/s, from September 8 to 14, 1976, of the Mississippi River at St. Paul is comparable to the low flow of 21 m^3/s in 1934. The lower Minnesota and St. Croix Rivers and the Red River of the North experienced low flows expected once in 10, 5, and 2 years, respectively.

Surface resistivity aids in delimiting Buffalo aquifer

Preliminary interpretation of test holes and surface-resistivity traverses to delimit the Buffalo aquifer in Clay and Wilken Counties in Minnesota showed the aquifer to be more than 48 km long, according to R. J. Wolf. Test holes showed that the northern part of the Buffalo aquifer extends from near land surface to a depth of about 46 m. An east-west resistivity traverse near Dilworth showed that the sand-and-gravel aquifer extends from 0.3 km west of County Road 11 to 0.4 km east of South Branch Buffalo River, a total width of 3.2 km; it also showed a channel carved into the basement rock to depths of 80 to 150 m. In the southern part, test drilling showed that the aquifer extends from the land surface to depths of 14 to 20 m. A 14-km resistivity traverse near Wolverton indicated that the western half of the section is predominantly clay and that the eastern half is predominantly sand with some clay. Thus, the Buffalo aquifer may be 7 km wide in the southern part. Depth to basement along the 14-km traverse ranges from 150 to 250 m, and the basement slope from north to south averages 2.7 m/km.

NEW JERSEY

To qualify and quantify the nonpoint source contaminants in storm runoff from Willingboro, a planned residential community in southern New Jersey, J. C. Schornick and D. K. Fishel selected sample-collection sites where the residential area could be subsampled to avoid agricultural input from upstream. Five storm and three background samples were collected and analyzed for as many as 65 parameters. Analyses of samples included both the suspended and dissolved phases. Results indicated that, although contaminant concentrations peak during storms, the peaks are short lived, and concentrations of contaminants seldom exceed the limits recommended by the USPHS for drinking water. The only significant exception is the fecal coliform bacteria count.

OHIO

In a study of the glacial-outwash aquifer in the Miami River basin of Ohio, K. F. Evans collected and analyzed water samples from 98 sites to determine their inorganic and organic parameters in the first half of 1976. The aquifer is heavily pumped, and natural recharge is supplemented by artificial recharge. Analyses of samples indicated locally high iron concentrations of up to 5.6 mg/L, ammonia nitrogen (as N) concentrations as high as 11 mg/L, nitrate-nitrogen (as N) concentrations as high as 9.8 mg/L, total organic-carbon concentrations as high as 71 mg/L, and dissolved-solids concentrations as high as 1,260 mg/L.

Over the entire study area, the water tends to be very hard and high in dissolved solids; in general, ground water in the vicinity of major industrial centers appears to be slightly higher in dissolved substances than ground water elsewhere in the study area.

A comparison of present and past chemical analyses for certain sites indicated that some changes in water quality have occurred at a few sites.

PENNSYLVANIA

Preliminary results of water-quality studies conducted in the Tioga River basin of Pennsylvania by J. R. Ward showed that the Tioga River receives acid mine drainage near Blossburg from both strip- and deep-mined areas. Alkaline water from numerous tributaries, however, helps to neutralize the acid so that, at a distance of 61 km downstream from Blossburg, the river can support a diverse population of aquatic life.

VERMONT

Near Rutland, Vt., along the western flank of the Green Mountains, unconsolidated sand-and-gravel deposits form aquifers capable of meeting some municipal water demands. North-south-trending structurally controlled stream valleys contain mostly silt and clay from the damming of glacial melt waters as glacial ice receded northward down the valleys. According to R. E. Willey, high-capacity wells could be developed in coarse-grained ice-contact and glaciofluvial deposits in the major valleys and in what may be a lake spillway draining westward.

VIRGINIA

H. T. Hopkins and S. M. Rogers determined, on the basis of historical and recent water-quality data for the area north of the James River, that the position of the freshwater-saline water interface in the Atlantic Coastal Plain of Virginia agrees with that reported by Sanford (1913). South of the James River, heavy pumpage has caused the interface to move westward to an area near the Virginia-North Carolina border.

WISCONSIN

Ground-water quality good in Wisconsin

The chemical quality of Wisconsin's ground water is generally very good throughout the State, according to S. M. Hindall. However, in some areas, concentrations of various constituents in ground water are high enough to cause problems. Iron, manganese, and nitrate are the constituents most commonly found in concentrations that exceed the maximum concentrations recommended for drinking water; others, such as high dissolved-solids, trace-element, and phenol concentrations, however, may present problems in some areas.

Proposed operation plan for Chippewa Flowage feasible

A proposal to stabilize the water level on Wisconsin's Chippewa Flowage and to limit seasonal water-level fluctuations to 0.6 m was investigated by W. R. Krug and found to be feasible. The proposal's additional limitation—that discharge from the flowage be maintained at between 1.6 and 200 m^3/s—would occasionally require the water level to fluctuate more than 0.6 m. About once in 5 years, floods would require the upper limit of the water level to be exceeded slightly, and occasional winter low flows would require the lower limit of the water level to be exceeded.

SOUTHEASTERN REGION

During the past year, emphasis continued to be placed on water-management studies throughout the southeastern region. Studies in Florida involved investigations of known aquifer systems to obtain data that will be used by water-management groups; the delineation of new ground-water sources was also of major interest. Contrary to popular belief, the Piedmont Province of Georgia may be an important source of ground water; preliminary studies indicated that wells with relatively large yields can be developed in contact zones between different rock types. Abandoned coal mines in eastern Kentucky appear to be potential sources of good-quality water.

Environmental problems in the southeastern region also received a great deal of attention. In the Albemarle-Pamlico Peninsula of North Carolina, about 3,000 km^2 of swampland will have been cleared and drained by 1980, owing to large-scale farming activities; a regional lowering of the water table and changes in streamflow and evapotranspiration are anticipated. In Florida, the effects of sewage effluent and solid-waste disposal on ground-water quality continued to be of major interest; initial tests were made on several deep-well sewage-effluent storage systems. On the southern coast of Puerto Rico, a study is underway to determine the potential benefits or deleterious effects of using sewage effluent to irrigate the water-short alluvial plain.

FLORIDA

Chloride concentration increases with depth of penetration in Suwannee Limestone

Water samples collected from wells tapping the Oligocene Suwannee Limestone in Florida's upper Ochlockonee River basin showed that chloride concentrations increased significantly with sampling depth, according to C. A. Pascale. For example, chloride concentrations increased from 85 mg/L at a depth of 120 m (the top of the Suwannee) to 1,000 mg/L at a depth of 180 m in an irrigation well in the western part of the basin and from 150 mg/L at a depth of 130 m to 750 mg/L at a depth of 180 m in a municipal well in the central part of the basin.

Water resources of northwestern Florida adequate until the year 2020

J. E. Dysart reported that 16 counties in northwestern Florida apparently will have adequate water until the year 2020. In the four westernmost counties, the sand-and-gravel aquifer and the streams can provide 96 to 158 m^3/s of water. Streams in the remaining 12 counties can provide about 250 m^3/s, and the Floridan aquifer can provide about 10 m^3/s. Generally, water of quality suitable for most purposes is available throughout the area, although water in some streams and in the sand-and-gravel aquifer is acidic and locally contains excessive iron. Water in the upper part of the Floridan aquifer is generally fresh, although it becomes saline at depth and in some coastal areas.

The quantity of water available in the study area is about 356 to 418 m^3/s, and projected needs for the year 2020 range from 110 to 181 m^3/s.

Sewage-effluent disposal by spray irrigation in Tallahassee

One month after spray irrigation of sewage effluent was discontinued in Tallahassee, Fla. (July 1974), ground water in the upper limestone immediately beneath the application site showed considerable chemical recovery; the total nitrogen concentration dropped from 18 to 8.8 mg/L in 1 month and continued to decrease until the effluent was again applied in April 1976.

It appears that the rate of movement of the effluent plume decreases with distance. As L. J. Slack (1975) previously reported, the effluent plume moved about 550 m in 9 months. During the past 3½ years, the plume has not moved the additional 670 m to the nearest downgradient observation well, unless it is moving below the zone sampled, according to Slack.

Supplemental ground water for Jacksonville

L. V. Causey reported that preliminary results from pumping tests indicated that the shallow aquifers in the Jacksonville area of Florida are important supplemental sources of freshwater. The water meets USPHS drinking-water standards except at a few sites where concentrations of iron exceed 0.3 mg/L. At 13 sites, test wells 51 mm in diameter were drilled into the semiconfined to confined rock aquifer to depths ranging from 14 to 70 m; water levels ranged from 1 to 4.5 m below land surface; and estimated maximum yields ranged from 1.3 to 12.6 L/s. Wells drilled into the surficial sand aquifer at each site ranged from 3 to 8 m in depth; water levels ranged from 0.3 to 3 m below land surface; and yields seldom exceeded 0.6 L/s.

Computer model of Floridan aquifer in northeastern Florida

The latest computer runs of a detailed finite-difference computer model of the Floridan aquifer in northeastern Florida, designed by G. W. Leve and G. G. Phelps, indicated that this model is nearly calibrated. Although no predictions have yet been made with the model, preliminary results indicated that the hydraulic conductivity of the overlying beds confining the Floridan aquifer varies widely and is greater in many areas than investigators had supposed. Analyzing the complex leakage relationships between the Floridan aquifer and the confining beds has been the most difficult problem in calibrating the computer model.

Test drilling (coring) into the confining beds was completed, and the cores were analyzed. Laboratory values of the hydraulic conductivity k' of the confining beds, values determined from pumping tests, and values estimated from the computer model for one site were:

Method	k', m/d
Pumping test	1.12×10^{-2}
Computer model	9.14×10^{-4}
Laboratory analysis:	
Marl	2.98×10^{-3}
Clay	1.88×10^{-5}
Clay	2.98×10^{-5}

Differences in the values are probably explained by the fact that pumping tests and estimates from modeling yielded a composite value for the entire overburden, whereas laboratory analyses gave separate values for the different lithologic components of the confining layers.

Information about the hydraulic conductivity of the confining layers is useful in estimating the amount of recharge contributed to the aquifer by leakage through these confining beds. Hydrologic budgets indicate that about 0.95 to 1.14 hm^3/d is being withdrawn from the aquifer in the Jacksonville area, and only about 0.076 hm^3/d flows into the area from the principal recharge area. Rough calculations show that, if there were a deficiency of 0.87 to 1.06 hm^3/d, water levels in Jacksonville would drop approximately 1 to 2 m/yr. Measured water-level declines of about 0.5 m/yr indicate that additional recharge must come from leakage through the confining beds.

Geohydrology of Tamiami Formation in Hendry County

A test-drilling program in a 470-km^2 area of western Hendry County, Florida, was undertaken by T. H. O'Donnell to locate and evaluate potential sources of potable water in the lower Pliocene Tamiami Formation. Two water-bearing zones were encountered. A 3- to 7.5-m thick limestone occurring at depths between 45 and 60 m was encountered throughout all but the eastern edge of the study area. Yields of 250-mm-diameter wells that tap this zone are as much as 50 L/s. A second zone of medium to coarse quartz sand and gravel ranges in thickness from 6 to 15 m and occurs at depths between 75 and 90 m along the eastern edge of the study area. The 200-mm-diameter wells that tap this zone yield as much as 32 L/s. Concentrations of dissolved solids in both zones range from 300 to 900 mg/L.

Potential for using a shallow aquifer system by means of connector wells

The shallow aquifer system underlying the 3,238-km^2 upper Peace and eastern Alafia River basins in central Florida consists of an unconfined surficial sand aquifer and an underlying confined limestone aquifer. Over most of the area, the shallow aquifer system is hydraulically separated from the underlying Floridan aquifer by sand and clay confining beds.

C. B. Hutchinson reported that the shallow aquifer system could be developed by means of withdrawal wells tapping the Floridan aquifer and gravity-flow connector wells between the shallow aquifer system and the Floridan aquifer. About 2,400 km^2 of the surficial aquifer and about 2,600 km^2 of the limestone aquifer are suitable for such development.

Waste-injection zone identified

J. J. Hickey reported that detailed hydrogeologic analyses of the McKay Creek test-injection site in Pinellas County, Florida, identified a potential waste-injection zone in dolomite at a depth of 296 to 311 m. The capability of this zone to accept and contain injected waste effluent was established by an 83-hour withdrawal test at 264 L/s and a 2-month injection test at 44 L/s. The interface between freshwater and saltwater is estimated to be 85 m below land surface.

Water supplies from the Withlacoochee and Weeki Wachee Rivers

W. C. Sinclair reported that a diversion of 5.7 m^3/s from the Withlacoochee River near Dunnellon, Fla., is feasible on a perennial basis. Saltwater encroachment in the lower Withlacoochee River may increase during periods of extreme low flow (discharge less than 14 m^3/s).

Analyses of the frequency of the annual low flow of the Weeki Wachee River indicated that diversions of one-third of the minimum flow could not be sustained over a 5-year recurrence interval without depleting the river below the average annual minimum.

Saltwater intrusion in Citrus and Hernando Counties

Chloride concentration is increasing in water from wells near the coast in Citrus and Hernando Counties in west-central Florida. L. R. Mills and P. D. Ryder reported that the greatest increases in chloride concentrations are occurring in urban areas of the two counties. The major causes of the increased chloride concentrations are construction of canals to provide access to the gulf, deficient rainfall over the past decade, and increased ground-water pumpage. Saltwater intrusion extends farther inland in Citrus County than it does in Hernando County because urbanization and resultant ground-water pumpage are greater in Citrus County.

Water resources of St. Lucie County

Increasing urbanization and agricultural activities in St. Lucie County, Florida, have increased stresses on the water resources of the Canal-23, Canal-24, and Canal-25 basins, according to W. L. Miller. Surplus water from extensive irrigation by more than 1,000 wells with highly mineralized water from the artesian Floridan aquifer and heavy applications of fertilizers and pesticides have increased contaminants and mineral concentrations in the area's surface water and shallow aquifer system. Increased water demands in coastal urban areas may cause saltwater intrusion in municipal well fields tapping the shallow aquifer system.

Water resources of Palm Beach County

Investigations conducted by H. G. Rodis, L. F. Land, W. B. Scott, and J. J. Schneider (Rodis and Land, 1976; Scott, Land, and Rodis, 1977) indicated that the shallow aquifer in Palm Beach County supplies more than 90 percent of all drinking water and much of the water used by industry and agriculture in the eastern part of this Florida county. In most of the county, the aquifer consists of sand, sandstone, limestone, and shell or mixtures of these materials. An elongated north-south-trending area several kilometers inland from the coast is composed of cavity-riddled sandy limestone. This part of the shallow aquifer, approximately 5 km wide and extending almost the entire length of the county, offers excellent potential for development of future ground-water supplies.

In recent years, ground-water levels in parts of the county have been lowered as a result of large ground-water withdrawals and drainage, and, as a consequence, saltwater has made some inland advances into the shallow aquifer. The growing problem of saltwater intrusion is generally the factor limiting well-field development along the coastal area.

The concentration of dissolved solids in water from the shallow aquifer in the eastern part of the county is generally less than 500 mg/L. These concentrations tend to increase with depth toward the east. Potable-water supplies from the shallow aquifer are very limited in the western half of the county.

Movement of leachates to ground water in Broward County

Analyses of water samples from test wells drilled adjacent to percolation ponds at five sewage-treatment plants in Broward County, Florida, indicated some movement of leachates from the ponds into the ground water, according to H. W. Bearden. Sodium, chloride, and nutrients appeared to be the best indicators. Analyses of samples taken at the Davie landfill indicated that some contamination of ground water occurred in an area near the sludge-disposal pit.

Search for water in the Florida Keys

Geophysical data from a 650-m-deep test well at Marathon in the lower Florida Keys suggested that there is brackish artesian water between depths of 290 and 380 m and at 530 m, according to F. W. Meyer. The Florida Keys Aqueduct Authority is interested in the upper brackish zone as a possible source of brackish water for desalting by a reverse-osmosis process.

On nearby Big Pine Key, C. E. Hanson has begun a study to determine the maximum sustainable water yield from a lens of freshwater that is a major source of water for the island. Seasonal horizontal and vertical chloride gradients are being monitored to determine the boundaries and volume of available potable water. It appears that the shape and thickness of the freshwater lens is influenced by the Ghyben-Herzberg relationship, the stratification of limestone in the aquifer, and the dredging of finger canals in the aquifer.

GEORGIA

Quality of ground water from Cretaceous aquifers in Georgia

Cretaceous formations in the Georgia coastal plain are exposed south of the Fall Line where they overlap the crystalline rocks of the Piedmont province. According to L. D. Pollard and R. C. Vorhis, water near the surface in the recharge (exposed) area is typically low in dissolved solids and pH. As the water moves downgradient, dissolved-solids concentration and pH increase, and the water becomes enriched in sodium and bicarbonate ions. With increased depth from the surface or distance downdip from the outcrop, the water has increasingly higher concentrations of sodium and chloride ions. Freshwater with a chloride concentration of less than 250 mg/L can be obtained from Cretaceous aquifers 100 to 190 km downdip from the outcrop area to depths ranging from 300 to 750 m below sea level.

Quality and availability of ground water in Georgia

A study of ground-water quality conducted by L. D. Pollard and C. W. Cressler showed that most of Georgia's ground water is suitable for agricultural, industrial, and public supplies. The Coastal Plain province, where yields range from 3 to 315 L/s, has the greatest potential for ground-water development. In the Valley and Ridge province, the Cumberland Plateau, and the Piedmont province, yields are as large as 63 L/s but generally are from 0.6 to 3 L/s.

Quality of storm runoff in the Atlanta area

J. B. McConnell reported that concentrations of total nitrogen, phosphorus, and organic carbon varied less than twofold during a November 1976 storm-runoff event at most measurement sites in the Atlanta urban area of Georgia. The overall concentration range of all storm-runoff samples collected was 0.55 to 5.3 mg/L of total nitrogen, 0.08 to 1.0 mg/L of total phosphorus, and 4.7 to 14 mg/L of total organic carbon. The greatest concentrations were measured at combined sewer overflow sites. In the Chattahoochee River, a major receiving stream in the area, nutrient concentrations were significantly higher downstream of the Atlanta urban area.

Lead and zinc were the most abundant trace metals detected; concentrations ranged from 8 to 80 mg/L and from 10 to 150 mg/L, respectively. At all sites sampled, pesticide concentrations were below the detection limit, and DO concentrations were at or near saturation values.

High-yield wells in the Atlanta area

Because of their low permeability, the crystalline rocks of Georgia's greater Atlanta region have the reputation of furnishing only small quantities (0.1 to 2.0 L/s) of ground water to wells, according to C. W. Cressler. As a result, many engineering firms and consultants consider wells to be impractical sources of industrial and public water supplies. Thus, the economic growth of the part of the metropolitan Atlanta area not served by public water systems has been limited.

Contrary to popular belief, a large number of wells in the Atlanta metropolitan area yield between 6.3 and 30 L/s. A study of 30 such well sites revealed that a few wells derive water from zones of fracture concentration, but most tap permeable contact zones between rock types of contrasting characters. The largest yields come from contacts between quartzite and amphibolite or gneiss, granite or gneiss and amphibolite, granite or gneiss and schist, and amphibolite and schist. By determining the exact locations and attitudes of such contact zones and by selecting sites in topographic settings that favor recharge, it should be possible to develop well supplies of 5 to 30 L/s throughout much of the Atlanta area.

Low-flow analyses of regulated streams

R. F. Carter found that obtaining accurate results from analyses of low flows of streams below major reservoirs in Georgia requires omission of records for the first few years of reservoir operations. Characteristically, during the first few years of operation, a large hydroelectric reservoir requires much testing and adjustment and produces downstream flow conditions that are quite different from the standardized regimen of flow in later years.

Minicomputer for processing ground-water data

Several programs written for desk-top computer-plotters by D. N. Ku and R. E. Krause were used to process historic data and to maintain current data on ground-water levels, water quality, and precipitation in Georgia. Although various types of graphs and tables are the principal output, polynomial-regression plots also can be made. The use of these programs has made reports much more timely and of "publication" quality.

KENTUCKY

Significant quantities of relatively good quality water are available from abandoned coal mines in Johnson and Martin Counties, Kentucky, according to D. S. Mull (USGS) and Steve Cordiviola (Kentucky Geological Survey). Drift mines that have been abandoned for 30 to 40 years yield as much as 48 L/s of water. Water from several mines has less than 250 mg/L of total dissolved solids; sulfate and iron concentrations are as low as 34 and 0.03 mg/L, respectively.

MISSISSIPPI

Scour at bridges on Mississippi highways created maintenance problems for more than 30 years, according to K. V. Wilson, who developed case histories at 40 sites for a Federal Highway Administration research project. Ten of the sites were along channels that were altered by the U.S. Army Corps of Engineers or the Soil Conservation Service. Countermeasures to correct scour problems included using earthen-spur dikes, masonry-spur dikes, riprap, timber-pile jetties, steel-pile jetties, timber-pile retards, and car-body retards and planting willow trees. Some bridge foundations were reinforced, some bridges were lengthened, and, on occasion, some bridges were reconstructed. Many of the countermeasures failed, but many survived floods larger than those that had created scour problems. Earthen-spur dikes were found to be quite effective in causing the scour to be located at the upstream ends of the dikes rather than near bridge abutments.

NORTH CAROLINA

Hydrologic effects of land clearing and drainage, Albemarle-Pamlico Peninsula

C. C. Daniel reported that a USGS cooperative study with the North Carolina Department of Natural and Economic Resources is underway to determine the hydrologic effects of land clearing and drainage on the 4,900-km^2 Albemarle-Pamlico Peninsula in eastern North Carolina. Although farming in the region began in colonial times, land clearing has only recently become so extensive and occurred at such a rate that the effects of this activity upon the hydrology of the region have become a major concern. In the years prior to 1959, less than 520 km^2 of land had been cleared and placed under cultivation. By 1973, approximately 1,100 km^2 were under cultivation, and, on the basis of the preliminary plans of large corporate farms, more than 2,000 km^2 will be cleared and drained for intensive farming and livestock production by 1980.

This rapid development provides an opportunity to compare the hydrologies of cleared and uncleared areas and to observe the changes that occur in hydrologic characteristics and water quality during the conversion of areas from a natural state to a completely developed state. The emphasis during development has been to remove excess water by digging canals and grading the land surface. Land clearing and drainage also have resulted in a regional lowering of the water table, changes in stream (canal) runoff, and, possibly, changes in evapotranspiration losses.

According to Daniel, preliminary results of a study of a forested site northeast of Pungo Lake showed that construction of drainage canals, a minimum of 402 m apart, lowered ground-water levels in an organic muck soil by several meters. Subsidence due to drying of these muck soils was also observed along canal banks. Analyses of water samples from the surrounding canals showed that the water is low in dissolved solids, high in organic constituents, and acidic; pH values of samples collected during 1976 ranged from 3.6 to 5.6.

Water budget of a small coastal plain watershed

A water-budget study of a small coastal plain watershed in eastern North Carolina showed that the area's precipitation is accounted for by overland runoff (17 percent), base runoff (20 percent), ground-water outflow (2 percent), and evapotranspiration (61 percent). The investigation was designed to determine changes in the hydrologic regime of and changes in the surface-water quality of Creeping Swamp (Beaufort, Craven, and Pitt Counties) that would be caused by stream channelization. According to M. D. Winner, Jr., and C. E. Simmons (1977), hydrologic data were collected for 4 years at six sites in the project area before the plans for channelizing Creeping Swamp were cancelled. The study indicated that the greatest decline in ground-water levels caused by channelization would have occurred near the stream, and the decline would have diminished as distance from the stream increased. It is believed that dry periods in this area are not long enough to allow the effects of channelization to reach the ground-water divide before the aquifer is recharged. Channelization also would have resulted in a decrease in overland runoff and an increase in the amount of water reaching Creeping Swamp through the ground-water system, although there would have been little, if any, change in the total annual runoff. Because the concentrations of some chemical constituents in ground water are greater than those in surface water in the area, there would have been a general increase in these constituents in surface water after channelization.

PUERTO RICO

Artesian water-pressure drop in the Montebello Limestone aquifer

Water pressures in the Montebello Limestone aquifer in Puerto Rico have diminished owing to a high rate of water withdrawal and, possibly, damage to the aquifer, according to J. E. Heisel and J. R. Gonzalez. The Montebello Limestone Member of the Tertiary Cibao Formation was hailed as a valuable and extensive aquifer when artesian pressures were discovered there in 1968. In 1976, there were 11 wells tapping this aquifer; 4 of these wells also tapped another deeper artesian aquifer. The four dual completion wells were designed and installed so that the aquifers would be kept hydraulically separate. Eight of the 11 wells are in an area 4.0×6.4 km. Head drops in wells tapping the Montebello range from 76 m in the center of the area to 22 m in a well remote from the area of major withdrawals.

The well that had a head loss of 22 m had a specific capacity of 0.027 (L/s)/m at a flow rate of 11 L/s in August 1972, but the same well had a specific capacity of 0.035 (L/s)/m at a flow rate of 11 L/s when it was retested in June 1975.

The well that had a head loss of 76 m had specific capacities of 2.2 (L/s)/m in July 1973 and 2.1 (L/s)/m in March 1975, an indication that a change in specific capacity did not take place in all parts of the aquifer. Pressure in this well dropped 16 m in 1 month. (The same type of dramatic change occurred to a lesser extent in other deep wells.) The well continues to lose pressure even though no withdrawals are being made from it, and all nearby wells have a higher pressure. The continued loss of pressure indicates that there is a discharge from the well, probably to the water-table aquifer in the vicinity of this well, which is completed in the two artesian aquifers. It is evident that there is no leakage between the two artesian aquifers—pressures in the deeper artesian aquifer are not affected at the well and remain higher than those in the Montebello.

Sewage effluent for irrigation and recharge near Fort Allen

A study of the use of secondary treated sewage effluent for irrigation and ground-water recharge is being made by J. R. Díaz at Fort Allen on Puerto Rico's southern coastal plain. Two test plots—a circular plot 30 m in diameter planted to Guinea grass and a rectangular plot 27×37 m planted to sugarcane—are being used. Effluent is applied by gun sprinkler to the Guinea grass and by furrow flooding to the sugarcane. From mid-September through December 1976, 100 mm of effluent was applied each week. During that time, rainfall totaled 270 mm, 244 mm of which fell in September and October. Twenty suction lysimeters were installed in the unsaturated zone at depths ranging from 1 to 3 m below land surface, but, by the end of December, water had been recovered from only one lysimeter at a depth of 1 m. The chemical quality of the recovered water was similar to that of the sewage effluent. Initial results of the investigation suggested that most of the water applied is being returned to the atmosphere as evapotranspiration, and the remainder is being retained as soil moisture at depths of less than 1 m.

SOUTH CAROLINA

L. R. Hayes reported that test drilling in South Carolina's Colleton and Hampton Counties showed that the limestone aquifer present in Beaufort, Hampton, and Jasper Counties is not present or is very different in lithologic character in Colleton County, which lies to the north of the other three counties. This limestone aquifer crops out in the northwestern part of Hampton County and in places appears to have been eroded away. Geohydrologic data indicate that significant local recharge to the limestone aquifer is taking place in the northwestern part of Hampton County and in parts of Beaufort County.

The limestone dips in a southeastern direction and is about 35 m below land surface in the vicinity of Hilton Head, S.C., but exceeds depths of 60 m in southern Jasper County near the South Carolina-Georgia State line. Yields to wells are less than 0.6 L/s in the outcrop area of the aquifer but exceed 60 L/s in southern Jasper County and in the vicinity of Hilton Head.

Ground-water withdrawals in Colleton County are mainly from lower Tertiary sediments that occur at depths of about 100 m in the northern part of the county and at depths of 200 m in the southern part of the county. The city of Walterboro in Colleton County has two wells open to sediments of Late Cretaceous age (at depths of about 500 m) that supply a natural flow of 75 L/s of good-quality water. Near Brickyard Point in Beaufort County, a limestone unit about 235 m below land surface may be a source of potable water.

CENTRAL REGION

Hydrologic studies related to energy development and environmental problems were again strongly emphasized in the central region. Long-established programs for the collection and publication of diverse water-resource data continued. Intensive water-resource investigations related to coal and oil-shale development continued in Colorado, Montana, New Mexico, North Dakota, Oklahoma, Utah, and Wyoming.

The program for monitoring the water resources of major Federal coal-lease areas was augmented by the addition in six States of more than 70 streamflow and surface-water-quality measuring sites and about 200 ground-water-observation wells. This augmented monitoring program is to be operated by consulting and engineering firms under contract to the USGS.

A regional study of the hydraulic and hydrologic characteristics of the Mississippian Madison Limestone aquifer system in the Powder River basin of Montana, North Dakota, South Dakota, and Wyoming was advanced by the completion of a deep test well in northeastern Wyoming at about 1,500 m below land surface. A second deep test well, started in southeastern Montana during the year, is expected to be completed at a depth of nearly 3,500 m.

Water-quality studies in the coal areas of Colorado, Iowa, Montana, New Mexico, North Dakota, Oklahoma, Utah, and Wyoming continued throughout the year. Many of these studies were designed to define existing water-quality conditions prior to mining; however, some of the studies were designed to provide information on factors that control the quality of surface and ground water. These energy-related water-quality investigations included studies of sediment, bed material, and water chemistry. Studies of the aquatic biota in relation to physical and chemical water-quality changes were initiated in Colorado and Utah.

The quality of water draining urban areas received attention in several States in the central region, especially Colorado, Missouri, and Texas. In Joplin, Mo., a study to determine the quality of water draining mine-tailing piles was completed. The study covered not only the concentrations of specific chemical constituents but also their concentrations in relation to runoff volume. Chemical-equilibrium modeling techniques were used in the mine-tailing study to better understand surface water-ground water relationships.

Algal production, geochemistry, and seasonal changes in chemical and thermal regimes were studied in lakes and reservoirs in Utah and Wyoming.

Throughout the region additional flood-prone areas were mapped. HUD type-15 flood-insurance studies were made at many sites during the year.

Flood-frequency studies were completed in Colorado, Louisiana, Nebraska, Oklahoma, Texas, and Wyoming. Programs to study scour in rivers at and near bridges continued in Arkansas, Kansas, and New Mexico.

Anomalous changes in the stage-discharge relationship of the Mississippi River near St. Louis, Mo., are being investigated cooperatively with the U.S. Army Corps of Engineers. Recent flooding produced some of the highest stages of record, discharges being identified with a flood-recurrence interval estimated to be only 10 to 25 years. Methods of measurements used in the late 1800's are being compared with modern-day methods to determine whether differences exist that would explain the unusually high flood stages.

Channel-geometry studies were continued in several States in the central region; one special study of channel geometry in the entire Missouri River basin was completed, and a comprehensive report was prepared.

Special studies were made of the disastrous flood of July 31–August 1, 1976, on the Big Thompson River in central Colorado. As much as 30 cm of rain fell in a period of 5 hours; the resulting flood caused the deaths of at least 139 persons and property damage of about $16.5 million. Summary reports were issued, and work was begun on a comprehensive report in cooperation with other Federal agencies.

Ground-water studies emphasized the evaluation of sources to supplement drought-related low streamflows. Studies of ground water in stream valleys as supplemental supplies and of the relationship between ground- and surface-water flow are underway in Iowa and South Dakota. Mathematical models were used in studies to define ground-water flow systems in the Houston area of Texas, in the Roswell basin of New Mexico, and in the Ogallala aquifer of western Oklahoma, western Nebraska, and eastern Colorado.

COLORADO

Water-level changes in the northern High Plains of Colorado

Water-level-change maps for 1964–76 and 1972–76 of the northern High Plains of Colorado, prepared by R. G. Borman and T. J. Major, showed that the rate of water-level declines has increased. Changes ranged from a maximum rise of 4.9 m for both periods to a maximum decline of 12 m from 1964 to 1976 and a maximum decline of 9.8 m from 1972 to 1976. Areas where the aquifer is thin and where little irrigation pumpage occurred generally had water-level rises of less than 2.4 m. Areas where substantial irrigation pumpage occurred generally had maximum declines of 4.9 m from 1964 to 1976 and 2.4 m from 1972 to 1976.

Surface-water-quality inventory in northwestern Colorado

Currently, a water-quality investigation of northwestern Colorado is being conducted by L. J. Britton to determine present water-quality conditions in streams and, in some instances, to identify local water-quality problems and goals for a six-county area. Because the study area is undergoing increased population growth and tourism, a water-quality management program has become imperative.

Chemical and biological analyses of samples collected from 83 sites during the spring and summer of 1976 indicated that surface water in the region generally is suitable for most uses. Trace-metal concentrations that exceed USPHS drinking-water standards were found in some streams where there is mining activity. DO concentrations were greater than 6 mg/L and saturated in all streams except those in Jackson County, where undersaturated conditions occurred. Total coliform bacteria ranged from less than 1 to 1,000 colonies/100 mL in water from the Fraser River below Tabernash in Grand County.

Effects of the proposed Narrows Reservoir on the adjacent aquifer

A. W. Burns and J. B. Weeks (1976) used a digital model to estimate the effects of the proposed Narrows Reservoir on the alluvial aquifer adjacent to the South Platte River near Fort Morgan, Colo. Changes in ground-water discharge to the river caused by the proposed reservoir were estimated, steady-state conditions being assumed. The proposed reservoir was simulated for two different reservoir-pool altitudes. For the conditions simulated, the principal effects of the proposed reservoir on the ground-water system would be an increase in water-table altitude in the aquifer and a redistribution of ground-water discharge to the South Platte River.

The results of the model study indicated that the proposed reservoir would cause water-level changes in the aquifer between Fort Morgan and the proposed dam. The change in water level at Fort Morgan would be less than 0.3 m for the two reservoir conditions simulated. No significant change in the ground-water system would occur downstream from Fort Morgan. Ground-water discharge to the South Platte River would be decreased at the reservoir site and increased downstream from the proposed reservoir. The model study indicated that ground-water discharge would decrease by 0.68 m^3/s above the proposed dam and increase by 0.68 m^3/s below the proposed dam for steady-state conditions with the reservoir-pool altitude at 1,342 m. Ground-water discharge would decrease by 0.31 m^3/s above the posed dam and increase by 0.68 m^3/s below the proposed dam for steady-state conditions with the reservoir-pool altitude at 1,342 m. Ground-water

Chemical quality of storm runoff in the western Denver area affected by man's activities

The USGS has monitored the quality of urban storm runoff from a 25-ha basin containing multifamily housing and office buildings in the western Denver metropolitan area of Colorado since March 1976. Data collected to date indicate that man's activities play an important role in the chemical quality of storm runoff from this area.

S. R. Ellis's preliminary evaluation of chemical data from storm runoff collected on September 14, 1976, indicated that the average total nitrogen (as N) was as much as four times greater than previously determined levels. Both dissolved orthophosphate and total phosphate were as much as five times greater than previously determined levels. On September 13, 1976, lawns of the multifamily housing units were fertilized; the housing manager reported that an inspection of the lawns on September 15 indicated that most of the fertilizer had been removed by the September 14 storm, and the lawns had to be fertilized again.

This type of activity can have an important influence on the chemical quality of storm runoff. To prevent errors in the mathematical models used to determine the chemical quality of storm runoff, man's activities must be considered.

Water quality of the Colorado River in the Grand Junction area

T. R. Ford reported that preliminary results of a waste-load assimilation study of the Colorado River in the Grand Junction area of Colorado between Palisade and Fruita, made during the fall of 1976, indicated that present waste loads are not significantly affecting water quality in the river. The lack of significant water-quality changes is a result of effluent discharges that are relatively small in comparison with the discharge of the Colorado River.

Availability and quality of ground water in the Eagle-Vail and Gunnison-Crested Butte areas

T. F. Giles collected hydrologic and geologic data in and near the Eagle-Vail and Gunnison-Crested Butte areas of Colorado in order to determine the availability and chemical characteristics of ground water.

Water quality from aquifers in part of the Eagle River valley between Eagle and Vail is variable and dependent on rock type. In general, water from aquifers in the alluvium, the Cretaceous Dakota Sandstone, the Permian and Triassic State Bridge Formation, and Precambrian metamorphic rocks is of good quality and can be used with little treatment for municipal, industrial, and domestic purposes. Water developed from aquifers in the Cretaceous Benton and Niobrara Formations, the Pierre Shale, and the Pennsylvanian Eagle Valley Evaporite often contains chemical constituents such as sulfate, dissolved solids, and selenium in concentrations that exceed USPHS standards for drinking water.

Water from aquifers in the Gunnison-Crested Butte area is generally of good quality, with the exception of water from deep (122–518 m) wells completed in the Dakota Sandstone and the Jurassic Morrison and Entrada Formations. Dissolved-solids concentrations in these formations range from 300 to 1,200 mg/L.

Shallow water table in Upper Arkansas River valley

K. E. Goddard found that the Upper Arkansas River valley in central Colorado has a water table only 1 to 5 m below land surface in many areas. Seepage from streams and recharge from irrigation maintain the shallow water table in the thick alluvial aquifer. Discharge from the aquifer results in major areas of springs along the Arkansas River, particularly in the area north of Browns Canyon and near Salida. In the vicinity of Salida, discharge of springs is approximately 3,000 L/s during the late summer.

Water quality in Jefferson County

D. C. Hall analyzed water samples from 11 of the wells in fractured crystalline rock in Jefferson County, Colorado, for 19 water-quality parameters to test for seasonal changes. Only four parameters—silicon dioxide, dissolved magnesium, dissolved orthophosphate, and temperature—were found to change significantly on the basis of an analysis of variance (0.05 level of significance). Temperature showed a seasonal trend, being 0.5° to 1.0°C higher during warm sampling periods. It is not clear whether the other three parameters reflect a seasonal trend, a long-time trend, or differences in sampling or analysis procedures between sampling periods. Generally, however, there do not appear to be significant seasonal water-quality changes in the fractured-crystalline-rock aquifer.

Eleven trace elements were studied in ground-water samples obtained from 26 wells in the aquifer. Most trace-element concentrations were below the USPHS recommended limits for drinking water. The concentrations of iron exceeded 0.3 mg/L in 6 wells, manganese exceeded 0.05 mg/L in 8 wells, and zinc exceeded 5 mg/L in 2 wells. The high concentrations of these elements are thought to be caused by the construction and plumbing associated with each of the 26 wells.

Radiochemical analyses were made on water from the 26 wells in the fractured-crystalline-rock aquifer. Gross-alpha radiation ranged from less than 0.9 to 147 pCi/L. Gross-beta radiation ranged from 1.5 to 28 pCi/L. Strontium-90 was determined in one sample (with gross-beta radiation of 19 pCi/L) and found to be less than the detection limit of 0.1 pCi/L. Radium-226 radiation in 22 samples ranged from 0.06 to 1.3 pCi/L. Uranium concentrations in 14 samples ranged from 1.3 to 86 μg/L (0.9–60 pCi/L).

Water quality in Boulder County

D. C. Hall, E. L. Boyd, and D. L. Cain collected ground-water samples from springs, domestic wells, irrigation wells, and stock wells in Boulder County, Colorado, for chemical and biological analyses. Of the 570 ground-water samples collected, 154 samples contained two or more coliform bacteria colonies per 100 mL. The percentage of samples containing coliform bacteria was higher in water samples from the plains (34 percent) than it was in those from the mountains (18 percent). Fecal-coliform bacteria (one or more colonies per 100 mL) were found in 51 samples, and the percentage of samples containing fecal-coliform bacteria was higher in the plains (11 percent) than it was in the mountains (6 percent). Nitrate (as N) concentrations were above 10 mg/L in 2 percent of all of the ground-water samples. Fewer than 1 percent of the samples contained more than 250 mg/L of chloride.

Hydrology of the Arapahoe aquifer in the Englewood-Castle Rock area

According to D. E. Hillier, R. E. Brogden, and P. A. Schneider, Jr. (1977), aggregate-sand thickness in the Arapahoe aquifer ranges from less than 30 m in the northwestern part of the Englewood-Castle Rock area of Colorado to 170 m in the central part. The greatest aggregate-sand thickness occurs in a northeast-trending band from near Louviers to east of Interstate Highway 25. Two types of water—calcium bicarbonate and sodium bicarbonate—are found in the aquifer in most of the study area. Calcium sulfate or sodium sulfate water occurs in the northwestern part of the area. In some wells, concentrations of dissolved solids, fluoride, iron, manganese, and sulfate exceed the limits recommended by the Colorado Department of Health for drinking water. Hardness may be a problem, depending on the use of the water.

The configuration of the potentiometric surface and the resulting flow system for 1975 were significantly different than for 1965. Ground-water flow was principally to the north and northwest in 1965 and principally to the northwest in 1975. The potentiometric surface declined throughout the area from 1965 to 1975. Declines of 60 to 90 m have occurred in the central part of the area. The decline of the potentiometric surface indicates that the aquifer is being "mined" (withdrawals exceed recharge). Most wells that flowed in 1965 had ceased flowing by 1975. Only one flowing well, which had an estimated flow of 0.2 L/s, was observed during the study.

Shallow ground water in the Front Range urban corridor

D. E. Hillier, P. A. Schneider, Jr., and E. C. Hutchison investigated the quality of water, the depth of water, and the altitude of the water table in the terrace and alluvial deposits and dune sand in an area of increasing population and industrial growth along the Front Range between Fort Collins and Colorado Springs, Colo.

Preliminary results of more than 300 chemical analyses indicated that concentrations of arsenic, iron, manganese, selenium, chloride, dissolved solids, fluoride, nitrate, and sulfate locally exceed Federal and State standards for drinking water. Water quality is poorest along the South Platte River north of Denver and along Jimmy Camp Creek near Colorado Springs where farmland is extensively irrigated. Dissolved-solids concentrations are as much as 7,600 mg/L in the terrace deposits along the South Platte River.

In some areas, the depth to water is less than 3 m and may affect building construction. The water table fluctuates annually in response to the amount of precipitation and streamflow and to irrigation practices. However, no long-term declines have been observed.

Contaminated wells found in northeastern Park County

Preliminary data collected by J. M. Klein, K. E. Goddard, and R. K. Livingston in Park and Teller Counties in Colorado indicated that the most widely used aquifer in the study area is fractured Precambrian rock in Park County. Well yields from the Precambrian aquifer are low, ranging from 0.02 to 1.3 L/s; an average well yields from 0.03 to 0.06 L/s. An estimated 20 hm^3 of recoverable ground water is present in the fractured Precambrian aquifer in Park County.

Of the 67 wells sampled in northeastern Park County, 21 wells contained water with nitrate concentrations greater than 5 mg/L, and 4 wells contained water with nitrate concentrations greater than 20 mg/L. The highest nitrate concentration determined was 75 mg/L. Bacterial contamination was found in 20 wells, the total coliform being as much as 2,000 colonies/100 mL. Chemical degradation of ground water was most pronounced in areas of high-density housing, particularly the Highland Park and Harris Park areas, where lot sizes are generally less than 0.8 ha.

Water-resource appraisal of the Wet Mountain Valley

Colorado's Wet Mountain Valley in western Custer and southwestern Fremont Counties is an intermontane trough filled to a depth of at least 2,000 m with unconsolidated deposits. C. J. Londquist and R. K. Livingston reported that the depth to water is less than 3 m in a 119-km^2 area underlain by basin-fill material in the central part of the valley. An estimated 1,850 hm^3 of recoverable water is stored in the basin-fill material. Well yields range from more than 3 L/s in the central part of the basin-fill aquifer to less than 0.6 L/s in the mountainous areas.

Streamflow in the area is typical of that of a high mountain valley; most streamflow occurs during the snowmelt period of June and July. Runoff, measured at seven sites during 1975 and 1976, ranged from less than 0.001 to 0.017 $(m^3/s)/km^2$ and is a function of site altitude.

A generalized water budget for the southern part of the basin-fill area indicated that 73 percent of the water entering the basin-fill aquifer is from direct precipitation and that the remaining 27 percent is from surface inflow. Evapotranspiration accounts for 86 percent of the water leaving the basin-fill aquifer, and surface outflow accounts for the remaining 14 percent. With few exceptions, both surface and ground water can be used for drinking and irrigation.

Erosion reduced by replacing sagebrush with grass

The hydrologic effects of replacing sagebrush cover with grass cover on rangeland were studied by G. C. Lusby from 1965 to 1973 at a site in west-central Colorado. Runoff and sediment yield from four small sagebrush-covered watersheds were measured for 3 years, after which time two of the watersheds were plowed and seeded to bluebunch wheatgrass. Measurements were then continued for an additional 6 years. Usable forage on the two seeded watersheds increased about 300 percent after replanting to grass, and the size of barren interspaces between plants was reduced proportionately. A reduction in annual runoff of approximately 14 percent resulted from a reduction in summer runoff of 65 percent and an increase in runoff from snowmelt of 12 percent. Sediment yield from the two seeded watersheds was reduced about 88 percent; most of this reduction was related to the decrease in runoff from summer rainstorms.

Spring-water flow in the Piceance Creek basin

The majority of springs in Colorado's Piceance Creek basin are associated with the Eocene Uinta Formation and marlstone tongues of the Parachute Creek Member of the Eocene Green River Formation that are within the Uinta Formation. The remainder of the springs issue either from outcrops of the Parachute Creek Member of the Green River Formation or from the Parachute Creek Member through faults and fractures in the overlying Uinta Formation. Within the Uinta Formation, the majority of springs have their source in silty sandstone beds. A comparison of spring locations with a fracture map and aerial photographs of the Piceance Creek basin by G. J. Saulnier, Jr., indicated that the majority of springs occur on or near faults and fractures. A few of the springs that discharge water from deep aquifers were identified by using water-quality and temperature data.

Discharge rates of the 90 springs investigated ranged from less than 3 L/s to more than 200 L/s. Sixty of the springs had discharge rates of less than 30 L/s, 24 of the springs had discharge rates between 30 and 80 L/s, and 6 of the springs had discharge rates greater than 80 L/s. Spring hydrographs indicated that the discharge of springs is directly related to recharge due to snowmelt in the highlands in the western and southern parts of the Piceance Creek basin. The time of discharge peaks appeared to be directly related to the distance from the recharge area.

KANSAS

Streamflow modeling in western Kansas

Preliminary results of streamflow studies conducted in western Kansas indicated that the average flow of some streams is decreasing. P. R. Jordan reported that flows of Beaver Creek and South Fork Solomon River have decreased in relation to a given amount of rainfall, as simple rainfall-runoff relationships and detailed mathematical modeling indicate. Changes in farming practices appeared to have had a major influence on the decrease in streamflow.

Critical depletion of Ogallala aquifer near Marienthal

Kansas Groundwater Management District No. 1 designated a 32-km^2 area in Wichita County, north of Marienthal, as a critical area in which the Ogallala Formation has been significantly dewatered. E. D.

Gutentag reported that ground-water withdrawals for irrigation have reduced the saturated thickness of the Ogallala between 30 and 50 percent since 1950.

LOUISIANA

Appraisal of ground-water resources in Washington Parish

H. L. Case III reported that the principal aquifer (the "1500-foot" sand) tapped by the city of Bogalusa, La., pinches out near the city's southern limits. Water levels in wells in this sand declined at an average rate of about 0.5 m/yr from 1967 to 1976, but the rate of decline has increased to about 1.2 m/yr since 1975. The water is of good quality and has an iron concentration of about 30 μg/L, which increases northward; at Varnado, about 11 km north of Bogalusa, the iron concentration is about 900 μ g/L. Two aquifers in the Bogalusa area have been mapped, but additional test-drilling and sampling are needed to provide hydrologic and water-quality data.

Water levels in wells about 820 m deep tapping the Franklinton aquifer are declining about 0.46 m/yr. In the fall of 1976, water levels in wells in the shallow aquifer ranged from about 41.4 m below land surface in the northeastern part of Washington Parish to about 2.4 m above land surface in the Bogue Chitto flood plain in the southwestern part of the parish.

Seasonal water-quality changes in the Red River alluvial aquifer

M. S. Whitfield, Jr., observed that the mineral concentrations in approximately one-half of the 540 wells sampled in the Red River alluvial aquifer of Louisiana undergo noticeable seasonal changes owing to recharge by precipitation. The greatest changes occur in the shallow part of the aquifer. Concentrations of calcium, magnesium, iron, chloride, and sulfate change quickly in response to recharge. Concentrations of these ions were reduced about 60 percent in an observation well near Natchitoches after 360 mm of rain fell in 9 days in May 1975. Recharge conditions are ideal in this area because surface drainage is slow and surface water infiltrates only a few meters of fine surficial material before it reaches the aquifer.

Chemical analyses of water from wells screened in the Red River alluvial aquifer show some of the water-quality changes that have occurred in the alluvium since samples were first collected in 1931. A decrease in chloride concentration ranging from 10 to 100 percent has occurred in water from many wells in Caddo, Bossier, and Red River Parishes. This decrease in chloride is attributed to the discontinuation of most saltwater-disposal pits (formerly used to dispose of oilfield brines), to the dilution of the resulting saltwater bodies by infiltration of precipitation, and to inflow from adjacent aquifers.

Terrace aquifer in central Louisiana contaminated by chloride

In the area of the Nebo Oil Field in Louisiana's southern La Salle Parish, the water in the shallow terrace aquifer of Pleistocene age has an anomalously high concentration of chloride and other chemical constituents. After studying the terrace aquifer, J. L. Snider concluded that the contamination is associated with oil production; possibly, it is related to the disposal of saltwater in pits or wells. Normal chloride concentrations in the terrace aquifer range from less than 5 to about 40 mg/L, but chloride concentrations in the terrace aquifer in the anomalous area range from about 300 to 2,300 mg/L.

MISSOURI

L. F. Emmett and R. R. Luckey reported yields as high as 0.16 m^3/s from wells open to 305 m of Cambrian and Ordovician dolomite in the Springfield area of southwestern Missouri. These wells yield good-quality water with 55 m of drawdown in 56 hours. The dolomite is separated from 27 m of overlying Mississippian limestone by 1.5 to 24 m of dolomitic shale, which retards the exchange of water between the limestone and the dolomite.

A significant portion of the 0.35 m^3/s of water presently being withdrawn from the dolomite is derived from the overlying limestone. A digital model of the aquifer indicated that an additional withdrawal of 0.44 m^3/s from existing wells would result in a water-level decline of as much as 120 m near the primary point of withdrawal.

MONTANA

Ground-water-resource study of part of Flathead Indian Reservation

Well data collected near Ronan, Mont., by A. J. Boettcher during a hydrologic study of part of the Flathead Indian Reservation indicated the existence of a shallow (less than 30 m) aquifer and a deep aquifer. In the rest of the area, only one aquifer exists in the first 150 to 185 m of the glacial deposits. The shallow water-table aquifer is recharged by an irrigation canal and springs, whereas the deeper artesian aquifer is recharged by runoff from the adjacent Mission Mountains.

The shallow aquifer provides an adequate source of water to wells for domestic and stock uses, and the deep aquifer provides water to wells for irrigation and public supplies. Many wells tapping the artesian aquifer flow; heads of 45 m above land surface have been measured. Some of the flowing wells discharge at rates in excess of 13 L/s.

Evaluation of hydrologic factors in reclamation potential of coal lands in southeastern Montana

J. D. Stoner and W. R. Hotchkiss conducted a study of the reclamation potential of strippable coal deposits on 104 km^2 of the Pumpkin Creek coalfield 16 km northeast of Broadus, Mont. Fifteen test holes were drilled through the 9.5-m-thick Sawyer coal, which comprises one unit of the Tongue River Member of the Paleocene Fort Union Formation. Water in coal was encountered in only three of the test holes, none of which produced more than 0.1 L/s. One test hole on the western side of the area, near Pumpkin Creek, penetrated about 18 m of sandstone below the coal and produced about 1 L/s. Major constituents in water from existing wells were generally sodium and sulfate, but one well contained magnesium calcium bicarbonate water; dissolved solids ranged from 300 to 4,300 mg/L.

About 25 stock reservoirs, each of which is 4 ha or less in area, provide some inflow to the ground-water reservoir. Intermittent surface-water outflow occurs through Mizpah Creek and Pumpkin Creek to the east and west, respectively.

NEBRASKA

Ground-water-quality atlas of Nebraska

R. A. Engberg prepared a ground-water-quality atlas of Nebraska in which all available water-quality data for the State are shown on a series of maps. These maps will aid planners and managers in identifying existing and potential water-quality problem areas. Dissolved-solids concentrations in water from the Nebraska sandhills are generally less than 200 mg/L; silica concentrations approach 60 mg/L. Dissolved-solids concentrations in water from Pleistocene or Tertiary deposits outside the sandhills are generally less than 500 mg/L, except in localized areas affected by infiltration of more highly mineralized water derived from surface sources. Water from older deposits is extremely variable in quality.

Farming practice may contribute to ground-water recharge in southwestern Nebraska

E. G. Lappala reported that, since the 1930's, water-level rises of as much as 6 m have occurred in an area of southwestern Nebraska that is not extensively irrigated. The area covers parts of Lincoln, Perkins, and Keith Counties and extends westward into Colorado. More than 6.2×10^8 m^3 of water was added to ground-water storage in the Ogallala aquifer from 1952 to 1975. Trend analyses of climatic records from 1925 to 1975 showed no significant increase in precipitation available for recharge. The water-level rises are attributed to increased recharge from areas in which "wheat-fallow" agriculture (half of the land is fallow and half is planted in wheat) is practiced. More than 75 percent of the affected area is farmland, about 80 percent of which is farmed under the "wheat-fallow" system.

Ground-water recharge in interfluvial areas near McCook attributed to canal leakage

As part of a study conducted by E. G. Lappala and P. F. Hemphill to assess the availability of ground water to augment declining surface-water supplies, previously unpublished water-level rises of as much as 12 m from 1950 to 1975 were documented. The rises cover an area of 120 km^2 in southwestern Nebraska in the interfluvial areas on both sides of the Republican River near McCook. The ground-water rises are the result of leakage from canals, deep percolation of irrigation water, and reservoir stages that are higher than the predevelopment stream levels controlling ground-water discharge. Lappala and Hemphill estimated that water added to storage from 1950 to 1975 was about 130 hm^3, and ground-water discharge to the Republican River between Trenton and McCook increased by about 5 to 10 percent.

NEW MEXICO

Hydrology of the San Juan River valley

The San Juan River gains about 3 m^3/s during winter months in the 110-km reach between Navajo Dam and Shiprock, N. Mex. This contribution includes irrigation return flow and flow from bedrock units. According to F. P. Lyford, the dissolved-solids concentration of the ground-water contribution is about 2,000 mg/L and causes degradation of water quality downstream in the San Juan River. Major constituents in the ground water are sodium, chloride, and sulfate. Changes in the ground-water contribution will probably occur in the future as a result of increased irrigated acreage and the development of coal and uranium resources.

Hydrogeology of northwestern New Mexico

The Morrison Formation of Jurassic age is the major aquifer in northwestern New Mexico. Transmissivity ranges from less than 5 to 40 m^2/d. A potentiometric surface map prepared by F. P. Lyford and Peter Frenzel shows that water moves from topographically high areas on the edge of the basin toward the San Juan River near Four Corners and toward the Rio Puerco south of Cuba, N. Mex. Ground-water contributions to these rivers are small and probably not detectable by streamflow-measuring techniques. In places, the potentiometric surface is 210 m or more above the land surface, an indication that some water may move vertically to shallower geologic units or to the land surface. In a large part of McKinley and San Juan Counties, water from the Morrison aquifer is potable. Withdrawals of water from the Morrison aquifer will greatly increase as uranium mining expands. Modeling showed that mine dewatering will substantially affect the potentiometric surface but will have relatively little effect on ground-water discharge to streams.

Other aquifers in the study area are the Gallup Sandstone of Cretaceous age and the Ojo Alamo Sandstone of Paleocene age. The transmissivity of these units generally does not exceed 20 m^2/d. Sandstones of Jurassic age below the Morrison Formation also may be aquifers.

Hydrologic characteristics of Gallup Sandstone

The city of Gallup, N. Mex., derives much of its municipal water supply from wells developed in the Gallup Sandstone at the Yah-ta-hey well field, 13 km north of Gallup. A month-long aquifer test was conducted in this well field by J. S. McLean during late January and early February 1976. The results of the aquifer test, which were affected by interference from nearby domestic wells and by multiple-aquifer completion of the observation wells, showed a transmissivity range of 30 to 40 m^2/d and a storage coefficient of 10^{-4}.

Water quality and sediment in the Chaco River basin

Water-resource information was collected by Kim Ong from a network of surface- and ground-water sites along the Chaco River and selected tributaries in northwestern New Mexico to determine existing conditions, particularly with respect to water quality, before coal or uranium is mined in parts of the basin. Many chemical constituents were analyzed with emphasis on constituents (nutrients, trace metals, and radiochemicals) important to water-quality standards. Two continuously recording stream-gaging stations were established on the Chaco River. Also, because of the unpredictable flow in the arroyos, special samplers were designed and spaced in the channel cross section to capture flows at various stages. High suspended-sediment concentrations, ranging from 2,000 to 200,000 mg/L, were found. Principal dissolved constituents in surface-water or shallow ground-water supplies were sodium, sulfate, and bicarbonate. Trace elements other than boron, iron, and fluoride were not found in significant concentrations.

Definition of "shallow aquifer" in Roswell basin

The "shallow aquifer" of the Roswell ground-water basin in New Mexico generally is considered to be composed of sand-and-gravel beds of Holocene, Pleistocene, and, possibly, Pliocene age; these beds are referred to locally as "valley fill." G. E. Welder's recent studies of the shallow-water zones indicated that the "shallow aquifer" locally also includes 15 to 60 m of the underlying Permian rock along a 2- to 5-km-wide zone in the eastern part of the basin between Roswell and Hagerman. This zone coincides with solution and collapse features that were mapped at the base of the "valley fill" and the top of the Permian San Andres Formation, which is separated from the "valley fill" by about 90 to 210 m of Permian sandstone, siltstone, claystone, and gypsum.

NORTH DAKOTA

Movement and quality of ground water in southwestern North Dakota counties

L. O. Anna reported that recent test drilling in southwestern North Dakota provided additional data for identifying major aquifer systems in the area. The lower Ludlow aquifer in the Paleocene Fort Union Formation is a very fine-grained sandstone to medium-grained sandstone with a constant transmissivity of 20 m^2/d. The lower Tongue River aquifer in the Fort Union has a variable transmissivity caused by changes in both thickness and permeability; the transmissivity ranges from less than 1 to 40 m^2/d. Water quality is also variable, the dissolved-solids content averaging 1,500 mg/L.

Recent head measurements of flowing wells along the Little Missouri River indicated that ground-water levels in the Fox Hills and lower Ludlow aquifers decline about 0.5 to 1.5 m/yr and create major cones of depression.

Valley aquifer discovered in western Dickey County

C. A. Armstrong reported that an unnamed aquifer was discovered about 11 km west of Oakes in Dickey County, North Dakota. The aquifer is about 21 km long, 3 km wide, and as much as 12 m thick. The aquifer occupies an abandoned James River valley that was formed at a time when the river flowed more than 12 m above its present flood plain. The material forming the central part of the aquifer generally is a gravelly coarse sand, but lenses of silt, clay, and fine sand are present. Estimates of well yield range from about 0.2 L/s in thin parts of the aquifer to about 50 L/s in thick parts of the aquifer.

Analyses of samples from the aquifer showed that the water is a very hard, calcium sulfate or sodium sulfate type in the northern and central parts of the aquifer; it is a sodium sulfate or sodium bicarbonate type in the southern part of the aquifer and near the aquifer's edges. Dissolved-solids concentrations in five water samples ranged from 710 to 1,440 mg/L. Sodium-adsorption ratios ranged from 0.5 to 4.9.

Hydrology of strippable lignite deposits

W. F. Horak found diverse hydrologic conditions among several lignite-deposit areas in western North Dakota. In many areas, the strippable beds serve as the principal source of ground water. In other areas, the shallow lignite beds are above the zone of saturation. Poorly consolidated sands of variable thickness are commonly interbedded with the predominant clay and silt of the Paleocene strata. Where sands are saturated, they are used locally for water supplies. Flow in the shallow lignite and sand aquifers is controlled mainly by local topography. Perched water conditions are evident throughout the area of study.

Dissolved-solids concentrations in lignite aquifers are slightly higher than those in sand aquifers (respective medians, 1,700 and 1,300 mg/L). The relative ionic compositions of the two types of aquifers are very similar. Sodium is generally the predominant cation, and the anionic makeup usually is divided evenly between sulfate and bicarbonate.

Buried glaciofluvial aquifer near Zeeland

R. L. Klausing reported that test drilling revealed the presence of a buried glaciofluvial aquifer about 4 km east of Zeeland in McIntosh County in south-central North Dakota. The aquifer, which has not been delineated completely, is at least 10 km long and about 3 km wide. The aquifer, which consists of intermixed sand and gravel, has an average thickness of about 7 m. Preliminary data from an aquifer test indicated that wells penetrating the aquifer will yield about 22 L/s. Analyses of 13 water samples from the aquifer showed that the water is predominantly a sodium-calcium bicarbonate type and that dissolved-solids concentrations are generally less than 1,000 mg/L.

Geologic structure and hydrologic conditions of the Souris River valley

P. G. Randich reported that test drilling in McHenry County, North Dakota, showed a synclinal structure underlying and conforming to the southeastern loop of the present Souris River valley. Test holes that penetrated the lower Tertiary and Upper Cretaceous sedimentary rocks down to the Pierre Shale indicated that preglacial geomorphogeny influenced the eastern course of the Souris River drainage in North Dakota. All geologic formations in this part of the State usually dip northwestward toward the Williston Basin except in this localized area of structural folding.

Water levels in wells developed in the Fox Hills and Hell Creek aquifers showed an upward vertical gradient toward the Cannonball (in the Fort Union Formation) and glacial-drift aquifers. The chemical quality of ground water in these aquifers ranges from a sodium chloride type in the deeper Fox Hills aquifer to a sodium sulfate or sodium bicarbonate type in the shallower Hell Creek, Cannonball, and Tongue River aquifers.

OKLAHOMA

The Pennsylvanian Vamoosa Formation underlies several counties in a broad north-trending band across central Oklahoma. Ground water in the Vamoosa aquifer occurs under both confined and unconfined conditions. J. J. D'Lugosz reported that about 8,600 hm^3 of the 74,000 hm^3 of water stored in the Vamoosa aquifer probably is recoverable. Recharge to the aquifer is approximately 4.5 percent of the annual rainfall, or 123 hm^3/yr. The amount of water withdrawn annually is one-twentieth of the amount of water recharged to the aquifer. Therefore, ground water is discharged to the major streams and most of their tributaries. Sand-thickness maps were constructed for both the unconfined and the confined areas. In some areas, the interface between potable water and saltwater is rising in the aquifer. Water-quality data show that saltwater injection has degraded the water quality in most of these areas.

SOUTH DAKOTA

Extensive aquifers found in Clark County

Glacial aquifers in lacustrine and outwash deposits underlie most of Clark County, 2,528 km^2 of rolling to hilly glacial-till plains in northeastern South Dakota. L. J. Hamilton (USGS) and C. M. Christensen (South Dakota Geological Survey) used information from about 400 test holes and 600 wells to determine that the thickness of the aquifers averages about 15 m in many areas but is as much as 50 m in other areas. Water from the aquifers is mostly a very hard, calcium sulfate type. Total dissolved solids range from 400 mg/L in a well 6 m deep to 2,560 mg/L in a well 160 m deep.

The Grand aquifer in north-central South Dakota

Glacial aquifers, mostly outwash sand and gravel, underlie about one-third of Edmunds, Faulk, and McPherson Counties in north-central South Dakota. L. J. Hamilton (USGS) and C. M. Christensen (South Dakota Geological Survey) used information from about 400 test holes and 2,000 wells to locate the aquifers. The largest and most extensive of these, the Grand aquifer, extends northwestward through an area of 930 km^2 in a branching channel that averages about 6 km in width. The channel is incised in shale bedrock at depths ranging from 45 m in the southeast to 180 m in the northwest. The thickness of the aquifer averages about 15 m, but, locally, where it is composed of five thick beds of sand and gravel, it is as much as 53 m thick. Wells capable of yielding more than 30 L/s can be obtained throughout a 340-km^2 area. Water from the aquifers has dissolved-solids concentrations that average 1,000 mg/L but range from 260 to 3,350 mg/L.

Major glacial-outwash aquifer in western Miner County

The Floyd aquifer, previously mapped in Beadle and Sanborn Counties, also occurs in western Miner County in southeastern South Dakota. According to Jack Kume, this major glacial-outwash aquifer has the potential to supply large-capacity wells such as those needed for irrigation. At the present time, however, only a few irrigation wells tap the aquifer.

In Miner County, the aquifer is under artesian conditions; it consists of 5 to 36 m of saturated sand and gravel at depths of 5 to 30 m below land surface. In 1976, depth to water in wells tapping the aquifer was 7 to 12 m below land surface.

Major glacial-outwash aquifer in buried channel of ancestral Grand River

The Grand aquifer, previously mapped in Edmunds, Faulk, and McPherson Counties and equivalent to the deep glacial aquifer mapped in Campbell County, was mapped in northwestern Walworth County in north-central South Dakota. The aquifer occurs in the glacial-drift-covered channel of the preglacial Grand River.

This major glacial-outwash aquifer has the potential to supply water to large-capacity wells such as those used for irrigation. Current development of the aquifer in Walworth County includes several municipal water-supply wells.

Studies by Jack Kume indicated that, in Walworth County, the aquifer is under artesian conditions and consists of 1 to 16 m of saturated sand and gravel at depths of 16 to 63 m below land surface. In 1976, the depth to water in wells tapping the aquifer ranged from 7 to 19 m below land surface.

TEXAS

Stratigraphic and hydrogeologic relationships established for coastal plain of Texas

A series of 12 sections along the strike and dip of strata was prepared by E. T. Baker, Jr., to illustrate the stratigraphic and hydrogeologic framework of a large part of the coastal plain of Texas from the Sabine River to the Rio Grande. A relationship between stratigraphic units and hydrogeologic units was thus established statewide. Units ranging in age from Paleocene to Holocene were delineated on the sections. Each of the 11 dip sections is about 160 km long, and the strike section is about 800 km long. The sections, which are based on electrical logs, show correlations that extend from the outcrops of the units to maximum depths of 2,316 m below sea level. Selected faunal positions and locations of water having less than 3,000 mg/L of dissolved solids are shown also.

Availability of ground water in the westernmost basins of Texas

J. S. Gates, D. E. White, W. D. Stanley, and H. D. Ackermann used data from a well and spring inventory, geophysical surveys, and four deep test holes to evaluate ground water in the basins west of the Pecos River drainage of Texas. Almost 30 km^3 of freshwater is estimated to occur in basin fill. Of this amount, about 15 km^3 is in El Paso County, 14 km^3 is in the Hueco Bolson, and 0.7 km^3 is in the lower Mesilla Valley. Significant amounts of fresh ground water also occur at Wildhorse, Michigan, and Lobo Flats and probably occur at Ryan Flats and between Lobo and Ryan Flats in the Salt Basin. Significant quantities of fresh ground water possibly occur in Red Light Draw, in the southeastern Presidio Bolson, and in the Green River valley.

In addition, about 8.6 km^3 of slightly saline water is estimated to be present in the basin fill of westernmost Texas, including that present in the Rio Grande alluvium of the Hueco Bolson and lower Mesilla Valley and in the Permian Capitan Limestone in the northern Salt Basin.

Pore structure of Edwards Limestone in southern Texas

According to R. W. Maclay and T. A. Small (1976), the pore structure of the Cretaceous Edwards Limestone in southern Texas is a complex maze of different sizes and types of voids that may or may not be interconnected. The types of pores that are commonly interconnected include interparticle and intercrystalline voids, fractures, and solution channels. The types of pores that are poorly connected or not connected include molds, intraparticle voids, and some vugs.

The predominant types of pores within the saline zone of the Edwards aquifer include the intercrystalline pore space of dolomites and the interparticle porosity of grainstones. The total porosity within the saline zone is relatively high, but the intrinsic permeability is relatively low. The predominant types of pores within the freshwater zone of the Edwards aquifer are secondary—included are fractures, solution channels, and vugs. Cementation and recrystallization of the rocks within the freshwater zone have resulted in a reduction of intercrystalline and interparticle porosity and a lower total porosity.

Although total porosity is reduced in the freshwater zone, intrinsic permeability is very high because of well-connected secondary porosity. Much of the storage capacity of the Edwards aquifer probably can be attributed to the smaller, interconnected pore spaces within the rock matrix. A lesser amount of storage occurs in the larger secondary openings (Maclay and Small, 1976).

UTAH

Spanish Valley ground-water model

Using available data, J. H. Eychaner constructed a digital-computer simulation model to determine the effects of a proposed scheme for artificial recharge in Spanish Valley near Moab, Utah. The results indicated that artificial recharge during periods of high runoff can provide enough water to permit an increase of as much as 150 percent in ground-water withdrawal.

Water quality in Dirty Devil River basin

J. C. Mundorff obtained data on the general chemical characteristics of surface water at approximately 100 stream sites throughout the 12,000-km^2 Dirty Devil River basin of southeastern Utah. These data showed very large increases in dissolved-solids concentrations downstream from areas of major diversions and irrigation in the upper parts of the Muddy Creek and Fremont River basins. The calcium-bicarbonate-type runoff from the mountains upstream from these areas generally had dissolved-solids concentrations of less than 300 mg/L. The depleted flow, which is mainly irrigation return flow and seepage downstream from the major irrigated areas, had dissolved-solids concentrations as high as 6,660 mg/L and sulfate concentrations as high as 4,000 mg/L in Muddy Creek downstream from diversions and irrigation. Dissolved-solids concentrations as high as 2,940 mg/L and sulfate concentrations as high as 1,500 mg/L were observed in downstream reaches of the Fremont River.

Coal-mining impact on streamflow in Wasatch Plateau

Analyses of stream-gaging records having concurrent periods of record in adjacent drainage basins in the Wasatch Plateau of Utah showed good correlations of low flows of mountain streams during the fall months. Standard errors of estimate for stations near canyon mouths ranged from about 10 to 20 percent. On the basis of these relationships, K. M. Waddell concluded that the effects of coal mining on the base flows of streams can be evaluated by using data from partial-record stream-gaging stations.

WYOMING

Hydrology of Arikaree Formation

M. A. Crist estimated that the average annual recharge to the Arikaree Formation of early Miocene age in an area of about 2,600 km^2 in southern Niobrara and northern Goshen Counties in Wyoming is 29.6 hm^3 from streams and precipitation. Accumulative pumpage from public-supply and irrigation wells was estimated at 59.2 hm^3 from 1938 through 1972 and 47.7 hm^3 from 1973 through 1975. Through 1972, pumping had not caused any noticeable decrease in natural discharge.

A digital model was developed to simulate the ground-water system in the Arikaree Formation. The model can be used to indicate which areas are best suited for increased development by irrigation wells.

Test drilling of Madison aquifer

E. M. Cushing reported that a 1,323-m test hole was completed as part of a regional evaluation of the geology, hydrology, and geochemistry of the Madison aquifer in Wyoming. Madison Test Well No. 1, in sec. 15, T. 57 N., R. 65 W., in Crook County was completed in the Precambrian in October 1976. Twenty-two cores, ranging in age from Jurassic to Precambrian, were taken at selected intervals. Core recovery was 186 m out of 197.5 m attempted. Sixteen drill-stem and packer tests were attempted in formations ranging in age from Jurassic to Cambrian. Geophysical logs available include electric, induction electric, gamma, guard, neutron, acoustic, density, three-dimensional velocity, temperature, and caliper. The well is cased into the top of the Madison aquifer at a depth of 707 m below land surface. The open-hole part of the well begins about 12 m below the top of the Madison and ends about 18 m below the top of the Precambrian. Water from the open-hole part of the well has a head of 330 kPa. It flowed, without development work, at a rate of 15.8 L/s through a 50.8-mm valve with a head loss of 110 kPa. The temperature of the water at land surface is about 49°C.

Further development, testing, and geophysical logging of the test hole are scheduled for calendar year 1977, and another test well is to be drilled in Custer County, Montana.

WESTERN REGION

The catastrophic failure of the Teton Dam in Idaho on June 5, 1976, resulted in floodflow rates estimated to be as great as 3.9 million cubic meters per minute in the canyon a short distance downstream from the dam. The flood caused 11 fatalities and hundreds of millions of dollars in property damage. Teams of USGS hydrologists and topographers documented the areas flooded in a series of maps.

Because of rapid modernization in the Trust Territory of the Pacific Islands, the USGS was requested to help in the collection and interpretation of information on island water resources. In addition, the USGS provided technical guidance in drilling and testing 22 wells on Moen in the Truk Islands and selected sites for 5 wells on Saipan in the Mariana Island group.

Several continuing studies in the western region were directed toward understanding the hydrology of geothermal areas. So far, geothermal energy has shown more promise as an alternative energy source in the West than it has in any other part of the country. A report on the Long Valley caldera geothermal area of eastern California estimated aquifer temperatures to be between 180° and 280°C at depths of 1 to 3 km. The heat flow is on the order of 6.9×10^7 cal/s, and the ground-water flux through the hydrothermal reservoir is 190 to 300 kg/s. A digital model in three dimensions was prepared for the hydrothermal system.

The interagency Geothermal Environmental Advisory Panel, based in Menlo Park, Calif., completed guidelines for acquiring baseline environmental data on Federal geothermal leaselands.

As the trans-Alaska pipeline neared completion, USGS hydrologists continued to collect data on streams along its route and began studies necessary for the postconstruction period. A survey was made of the numerous and extensive icings (aufeis) that develop along the pipeline corridor each winter and cause disruptions in road travel. Data are being collected to provide background information for assessing the effects of an oilspill or other event that can adversely affect streams and lakes.

USGS glaciologists reported that Columbia Glacier near Valdez, Alaska, may be entering a decades-long drastic retreat from its present terminus on a shoal 2 or 3 km from land. If that retreat occurs, it is likely to result in the calving of icebergs that are larger and more numerous than those that the glacier currently discharges into shipping lanes leading to Valdez, the southern terminus of the trans-Alaska pipeline. These estimates are based on a study of aerial photographs taken over a period of many years, on field observations, on histories of physically comparable Alaskan glaciers whose retreats have been observed, and on soundings made adjacent to the ice face of the glacier from a remotely controlled small boat. This work is being done in cooperation with the U.S. Coast Guard.

USGS scientists are studying the movement of chemicals in the subsurface near Visalia, Calif., as part of a continuing project to determine the occurrence, movement, and disposition of organic materials in water. The chemicals in the Visalia area were discharged to the ground by leakage from a tank used to dip utility poles in a preservative solution containing creosote before 1968 and, since then, pentachlorophenol. Both substances have been found in the ground water. Information is being obtained on the extent of contamination and on methods whereby the contamination can be contained and ultimately eliminated.

In Washington, near the crest of Mount Baker, the intense fumarolic activity that caused concern in 1975 diminished appreciably in 1976, but it was still higher than it had been in most earlier years of observation. The 1975 pH range in Boulder Creek was 3.5 to 4.2 units, but, in 1976, the range was from 4.5 to 5.5 units. However, the volume of acid discharged into Baker Lake by Boulder Creek has not been large enough to contaminate the lake beyond a small area at the mouth of the creek.

Throughout the western region, collection of hydrologic data, pursuit of problem-oriented projects, and basic hydrologic research continued. The noteworthy shifts in emphasis, perhaps, were in project goals and in cooperating agencies. There is a growing concern with the environmental consequences of actions, and this trend shows no signs of stopping. Consequently, the need for personnel having competence in water-quality studies, including aquatic biology, has caused a gradual change in the composition of the work force; the spectrum of special skills is broader than that present even 10 years ago.

ALASKA

Fairbanks water-resource study

A 3-year water-resource study of the Fairbanks North Star Borough of Alaska was initiated by G. L. Nelson (USGS) in the early part of 1975. Water levels measured in a deep observation well on a ridge directly north of Fairbanks were interpreted to indicate a steady decline of the water table during the past 2 years. This decline may have been caused by a concurrent increase in the number of wells in the uplands. However, there was a decrease in precipitation during this period.

Arsenic concentrations of up to 10,000 $\mu g/L$ were found recently in water from wells west of Fairbanks by Dorothy Wilcox (University of Alaska). Arsenic concentrations of up to 300 $\mu g/L$ were found in the uplands and in the lowlands bordering the ridges around Fairbanks. The wells that have high arsenic concentrations are sporadically distributed. The source of the arsenic may be mineralized bedrock.

Surface-water data from Alaskan coal-resource areas

D. R. Scully, D. E. Donaldson, and G. L. Nelson collected water-discharge, suspended-sediment, and water-quality data on streams in three areas of Alaska to delineate the present hydrologic conditions in areas with known coal-development potential. In 1976, data were collected at seven sites in the Beluga coal area in south-central Alaska. A recording station was installed on the Chuitna River near Tyonek to obtain continuous river-stage and temperature data. Computed unit-area discharge in the Beluga area ranged from 3 to 130 $(L/s)/km^2$; a unit-area flood peak of about 350 $(L/s)/km^2$ was recorded on the Chuitna River on September 20, 1976. Measured suspended-sediment concentrations ranged from 1 to 420 mg/L. Low concentrations of dissolved solids were indicated by a range in measured specific conductance from 20 to 80 μmho; the range in pH was 6.5 to 7.5.

Streamflow and ground-water relationship in Ship Creek

L. D. Patrick, G. W. Freethey, and G. S. Anderson analyzed hydrologic test data for the shallow unconfined aquifer in lower Ship Creek at Anchorage, Alaska. They concluded that significant quantities of ground water can be developed from the sand-and-gravel aquifer to augment surface-water supplies for a proposed fish hatchery. Practically all of the ground water that will be pumped will be derived ultimately from Ship Creek streamflow.

Water resources of Alaska's North Slope

Abundant surface water of excellent quality for most uses exists on the North Slope of Alaska, but, because of continuous and deep permafrost, ground-water resources are negligible except at springs, according to G. L. Nelson. During the winter, lakes and streams are almost completely frozen, and potable water supplies are found only in deep pools, in streams that head in the mountains, and in a few deep (>2 m) lakes.

Flow in all streams and flow through their underlying thaw bulbs, or taliks, generally cease by midwinter each year; there is water only in deep isolated pools and in the deep, disconnected segments of the underlying thaw bulbs. This cessation of flow is indicated by the cessation of aufeis (probably brackish water) formation. The rate of ice thickening on the surface of pools and lakes can be reduced significantly by rerouting access roads and by insulating the surfaces of the pools. Greater amounts of water thus will be available during the late winter. Artificial storage in tanks, surface reservoirs, or brackish to saline aquifers may be adequate to assure year-round supplies.

Winter hydrologic reconnaissance of a western Arctic area

A hydrologic reconnaissance of the western Arctic area in Alaska between Kotzebue and the Colville River was made in April 1976 by C. E. Sloan, J. C. Meckel, J. M. Childers, and J. W. Nauman. The locations of nine springs and their associated icings in the vicinity of Kotzebue were determined by an examination of Landsat images. Discharge from the springs ranged from less than 0.04 to 0.37 m^3/s and averaged about 0.20 m^3/s. Except for Kavrorak Spring (near Kivalina), which was slightly brackish, the water quality of the spring was excellent for drinking and other uses.

No spings or icings were evident on the Landsat images of the area north of Point Hope, and none were found in the field.

No streamflow could be found or measured in any of the streams between Point Hope and Point Barrow, although pools of water under ice were found in several of the larger streams.

Teshekpuk Lake, the third largest lake in Alaska, is about 6 m deep near the center, where it was sampled. Eight other lakes sampled in this area were about 2 m deep.

CALIFORNIA

Water-level declines at Twentynine Palms Marine Corps Base

Water levels of five supply wells at the Marine Corps Base in Twentynine Palms, Calif., have declined an average of 11 m in the past 10 years. According to D. H. Schaefer, this decline is associated with (1) the proximity of a major fault, (2) the close spacing of the wells, and (3) the large volume of water extracted (3.2 hm^3 in 1975). By 1980, the increase (projected) of water consumption on the base to 3.7 hm^3 and the present rate of water-level decline will result in a drop of the pumping water levels in the wells to below present pump settings.

As part of the geohydrologic evaluation of the Surprise Spring subbasin, three test holes were drilled in an area northwest of the present well field. This area promises to be a good location for drilling three new supply wells. The additional wells will take some of the stress off the existing well field and reduce the water-level decline. Usable ground-water storage was estimated to be about 700 hm^3 in the subbasin.

Areal and temporal water-quality variations in the San Lorenzo River basin

California's San Lorenzo River basin is experiencing rapid urbanization, which is placing heavy demands on the water resources and waste-water disposal capabilities of the basin. Water-quality data from previous studies have not been adequate to define baseline conditions or to assess sources of degradation. The objectives of a study conducted by M. A. Sylvester and K. J. Covay were to determine areal and temporal variations in water quality and to identify problem reaches in the basin.

Calcium bicarbonate water was found throughout the basin. On the basis of the magnitude of dissolved constituents in the basin water, the basin can be divided into three water-quality areas, which generally correspond to the major geologic divisions of the basin. The most pronounced change in water quality occurs during storms when streamflows, turbidities, fecal coliform counts, and organic nitrogen, phosphorus, and potassium concentrations increase markedly and most dissolved-constituent concentrations decrease.

An intensive diel survey was made to determine if oxygen-demanding wastes were present and causing nighttime DO to be depressed below the State standard of 7.0 mg/L. Oxygen-demanding wastes do not appear to be a problem in the basin; in 5-day tests, BOD_5 values were usually less than 3 mg/L, and no significant nighttime DO depletion was noticed.

Reconnaissance sampling for benthic invertebrates provided data on the composition and stability of the benthic community. During the rainy season from October to May, the diversity of benthic invertebrates was reduced at one of the two stations as a result of repeated scouring and aggradation of the streambed.

Chemical quality of ground water in the central Sacramento Valley

R. P. Fogelman (1976) documented the chemical character of native ground water in California's Sacramento Valley prior to water-level declines caused by extensive pumping for irrigation or, in some parts of the area, by possible extensive use of imported surface water. The study area included about 3,100 km^2 in the central Sacramento Valley adjacent to the Sacramento River from Knights Landing to Los Molinos, Calif. Because of recent agricultural development in the area, land previously used for dry farming and grazing is being irrigated.

Analyses of water samples from 209 wells showed that most of the area is underlain by ground water of a quality suitable for most agricultural and domestic uses.

Typically, the water in the area has dissolved-solids concentrations ranging from 100 to 700 mg/L. The general water type for the area is a transitional (with calcium, magnesium, and sodium) bicarbonate water that contains negligible amounts of toxic or phytotoxic trace elements.

Migration of the Sacramento River

Rates and processes of lateral erosion were studied by James Brice for the middle Sacramento River between Chico Landing and Colusa, Calif., a river distance of about 80 km along which the river is bordered by valuable agricultural land. The study was based on comparisons of maps made during the period 1867–1949 and on aerial photographs made during the period 1924–74.

Meander loops migrate by downstream translation in a direction nearly perpendicular to the loop axes. Loops are cut off by straight or diagonal chutes across the meander neck rather than by gradual closure of the neck. The sinuosity of the river gradually decreased from a value of 1.56 in 1896 to 1.35 in 1974. The morphology and curvature of meander loops cut off before settlement indicate that the river was more stable in 1896, as well as more sinuous. The subsequent morphologic changes are attributed mainly to the clearing of riparian vegetation and the effects of levees in reducing the area of overflow. The bank-erosion rate, as measured by the shift of the channel centerline between successive times of survey, was 0.458 ha/yr per kilometer of stream for the period 1896–1974. Before 1948, cumulative bank erosion increased at about the same rate as cumulative discharge above mean annual, but it has increased at a lesser rate since 1948, probably because of flow regulation by the Shasta Reservoir.

Model to predict aquifer response to artificial-recharge program for the upper Santa Ana River valley

A digital-computer two-layer ground-water model was developed for a 315-km^2 area of the upper Santa

Ana River valley in California. The model simulates head response to natural and manmade stresses in a hydraulically connected multiaquifer alluvial basin about 450 m thick.

According to W. F. Hardt and C. B. Hutchinson, the importation of water for recharge in the upper part of the basin could cause artesian heads to rise once again above the land surface in the lower part of the basin near the city of San Bernardino. Although the area is now urbanized, it was historically the site of marshlands caused by flowing wells and waterlogged soils.

The model was deemed calibrated for steady-state and transient conditions when model-computed hydraulic heads matched those observed in the field. Model predictions indicated the locations where artificial recharge must be controlled if high water levels are to be kept from damaging the urbanized area. The use of the model, as a part of a comprehensive water-management program, will also aid in determining the effects of redistributing pumpage and of optimizing a hydrogeologic monitoring program.

Well-response model for Bunker Hill ground-water basin

A well-response model was developed by T. J. Durbin and C. O. Morgan for wells in the confined area of the Bunker Hill ground-water basin near San Bernardino, Calif. In the usual application of modeling techniques to quantitative ground-water analysis, the focus of the model is on the ground-water basin as a whole. In this study, the focus of the model was on a particular well. The model is a mechanism for transforming input to an imperfectly understood ground-water basin into a water-level hydrograph for a well. The transformation relationship is the two-dimensional equation of ground-water flow, which is solved numerically by the Galerkin finite-element method. The aquifer parameters that occur in the equation were treated as coefficients in a nonlinear regression analysis.

Hydrologic and solute transport models of Upper Coachella Valley

According to L. A. Swain, water levels declined more than 30 m in some areas of California's Upper Coachella Valley from 1936 to 1974. To offset this decline, recharge of water from the Colorado River Aqueduct to the basin was begun in 1973. The recharge water has a dissolved-solids concentration of from 600 to 800 mg/L. The ground water in the recharge area has a dissolved-solids concentration of about 210 mg/L.

Projections from a finite-element hydrologic model of the basin indicated that, without recharge, the water level in the Palm Springs area will decline 61 m between 1974 and 2000 but that, with artificial recharge, the water levels in the Palm Springs area will decline only 9 m during the same period.

Projections from a finite-element solute-transport model indicated that the artificial-recharge plume (bounded by the 300-mg/L line) will move only 1.6 km downgradient from the recharge ponds by 1981, and it will move 7 km by the year 2000.

Ground-water modeling of Salinas Valley

Finite-element digital flow models for the Salinas Valley of California were calibrated by comparing monthly water levels and river flows with observed values, according to T. J. Durbin, G. W. Kapple, and J. R. Freckleton. A two-dimensional model was developed for the entire valley, and a three-dimensional model was developed for the confined portion of the valley near Monterey Bay. Pumpage was calculated from electric-power consumption records. Transmissivity and storage-coefficient values were estimated initially from sand-clay contents and refined later during the calibration process.

Leakage from the Salinas River, the principal source of aquifer recharge, was computed by a function involving exponential river flows and used implicitly in the model. Tributary streamflows and infiltration quantities were calculated by a rainfall-runoff correlation process and an infiltration equation. Most of the computed water levels and river flows were within 10 percent of observed values.

Fresh ground-water basin in the Merced area

R. W. Page reported that the fresh ground-water basin in the Merced area of California is about 370 m thick. Five aquifers occur in the basin—the Mehrten Formation (Miocene and Pliocene), a confined aquifer, an intermediate aquifer, a shallow aquifer, and a probably unconfined aquifer. Recharge to the aquifers is from ground-water flow, leakage from other aquifers, and irrigation water that moves downward into the shallow aquifer. Discharge of ground water occurs by leakage, seepage into streams, evaporation, transpiration from crops, and pumpage. Chemical analyses indicated that ground-water quality is good and that a particular chemical type of water is not unique to a particular geologic unit or aquifer.

Overdraft in Koehn Lake area

J. H. Koehler estimated recharge to the ground water from percolation of surface runoff and from underflow from 1958 to 1976 at about 18.2 hm^3/yr in the Koehn Lake area of California. The annual consumptive use ranged from 22.8 hm^3 in 1960 to 74.0 hm^3 in 1976. The overdraft has caused a large pumping depression southwest of Koehn Lake. As the ground-water gradient toward the pumping depression increases, the probability that the freshwater will be degraded by the saline water under Koehn Lake increases.

HAWAII

K. J. Takasaki's appraisal of the ground-water resources of Hawaii indicated that ground water is a better potential source for additional future water supplies than surface water. In 1975, ground water supplied 44 percent of the water used, and surface water supplied 56 percent; in the years ahead, however, these percentages will likely be reversed. Approximately 10 percent of the water is required for self-supplied industrial uses, and 70 percent is used for agricultural purposes.

Rainfall is the principal source of ground-water recharge. Local mean annual rainfall ranges from less than 510 to more than 7,600 mm. Ground-water recharge has been estimated at about 9.08 km^3/yr (285 m^3/s) or about 30 percent of the rainfall.

Most fresh ground water in the region is stored in the underground space below sea level in porous lava flows, much of it in basal-water bodies floating on heavier saline ground water intruded from the sea.

Ground-water problems in the region generally can be subdivided into three categories: (1) Areas of inadequate information where the major problems are related to the geologic framework and climatic parameters; (2) hydrologic problems where the major difficulties are related to the quality and the quality impairment of ground water and its quantification in both time and space; and (3) institutional areas where the major problems are in management and monitoring related to State and Federal statutes, including rights and allocations.

IDAHO

Water resources of the upper Henrys Fork basin above Ashton

The USGS, in cooperation with the Idaho Department of Water Resources, completed a 2-year investigation of the upper Henrys Fork basin.

R. L. Whitehead reported that volcanic rocks and alluvium comprise most of the basin's aquifer materials. Ground water moves through topographic subbasin divides, but most of it leaves the basin as surface flow. Large springs and ground-water accretion sustain flows in many of the basin's streams.

About 1.28×10^9 m^3 of surface water flows out of the basin annually. This amount represents about 53 percent of the basin's estimated 860 mm of annual precipitation. The high yield is greatly influenced by permeable volcanic ash flows.

The basin's water quality is generally excellent, as samples from about 60 sites indicate, but there are exceptions. Specific conductance values ranged from less than 100 to about 300 μmho, except in some ground water sampled near Ashton, where values ranged to 800 μmho.

Ground-water resources of the Mountain Home plateau

Agricultural development of the ground-water resources of the Mountain Home plateau in Idaho has caused water-level declines in several areas. A 1-year study conducted by H. W. Young showed declines of nearly 9 m since 1967.

An inventory of 260 wells in the plateau indicated that ground water occurs under water-table conditions; the most productive aquifers occur in the basalts of the Bruneau Formation and the terrace deposits of the Pleistocene Idaho Group. Ground-water-level fluctuations in the plateau respond chiefly to surface-water irrigation and pumpage for ground-water irrigation.

Sources of recharge to the ground-water systems are Boise River drainage water, precipitation in the adjacent mountains, and precipitation on outcrops of the Miocene Idavada Volcanics, both within and outside the drainage divide.

Ground water-surface water relationships in the Silver Creek area

J. A. Moreland studied ground water-surface water relationships in the Silver Creek area of Blaine County, Idaho, as part of a comprehensive investigation of the area's water resources. Ground-water withdrawals calculated for 1975 totaled about 20 hm^3 of pumped ground water and 15 hm^3 of ground water extracted through flowing wells. Shallow test holes were drilled and cased to define the extent and effectiveness of confining layers in the southern part of the valley. Water-level fluctuations monitored in almost 75 wells showed seasonal variations of 12 m in the northern part of the area and less than 1.5 m in some wells in the southern part of the area. Most of the flow in Silver Creek rises from springs discharging from the shallow aquifer near the edge of the confining member. Only a small amount of discharge to the creek is attributable to upward movement of water through the confining member. Discharge from the artesian aquifer near Stanton Crossing may contribute a significant part of the spring flow that feeds the Big Wood River.

NEVADA

Residential development along the northwestern shore of Topaz Lake has been limited by the Nevada State Board of Health in response to concern about the effects of septic-tank effluents on the quality of individual domestic water supplies and the lake. Existing hydrologic and water-quality data were compiled by J. R. Harrill and J. O. Nowlin (1976) (Nowlin, 1976) to provide a base against which to measure the effects of future development. The current site inventory includes data for 52 wells, 2 springs, the lake, and a tributary stream. Most domestic wells are finished in one or more of the confined alluvial aquifers that are upgradient from and apparently hydraulically connected to the lake. Ground waters are of a calcium-bicarbonate type; the upgradient waters have higher concentrations of sulfate and dissolved solids than waters near the lake. The waters generally meet drinking-water standards, with the exception of one well yielding water with high arsenic (>300 μg/L). Background concentrations of nitrate-nitrogen are generally less than 1.5 mg/L, except in five wells that produce water with 3.0 to 11 mg/L. Concentrations of dissolved organic carbon at 10 sites ranged from 0 to 0.1 mg/L.

OREGON

Ground water near Winston

Wells near Winston in southeastern Oregon produce water of variable quality and quantity, but most of the water is adequate for domestic supplies. According to J. H. Robison and C. A. Collins, total dissolved-solids concentrations generally range from about 50 to 500 mg/L, although water with dissolved-solids concentrations as high as several thousand milligrams per liter is found in places. The area's wells, which are an average of about 30 m in depth, produce from less than 0.1 to about 2.5 L/s of water from Eocene and pre-Tertiary rocks.

Ground-water quality in the Dallas-Monmouth area of the west-central Willamette Valley

Eocene marine-rock formations contain brackish ground water at depth throughout the Dallas-Monmouth area of Oregon on the western edge of the Willamette Valley. In the foothills of the Coast Range, brackish water apparently occurs at shallower depths beneath valleys than it does beneath uplands. A study by J. B. Gonthier indicated that this relationship is less apparent in the eastern part of the area where the topography is more subdued. Observed specific conductivity of ground water in the study area ranged from less than 50 to more than 16,000 μmho/cm at 25°C.

WASHINGTON

Hydrology of the Pullman-Moscow basin

R. A. Barker developed a digital model of the primary aquifer system in the Pullman-Moscow basin. The basin comprises about 660 km^2 in southeastern Washington and northern Idaho in which ground-water levels in the primary basalt aquifer have declined about 24 m since 1900. Pumpage in 1975 of about 8 hm^3 supported both irrigation and public supplies.

Model simulation showed that vertical leakage from upper unconfined aquifers is the most important source of recharge to the primary aquifer system within the basin; flux simulated for 1975 was about 6 hm^3. The calibrated storage coefficient for the primary aquifer ranges from 0.005 to 0.006, and the calibrated transmissivity ranges from 26 to 8,560 m^2/d.

Simulation runs for the period 1975–2000 predicted an additional water-level decline of 9 to 10 m for that period if pumpage rates are doubled. However, if 1975 pumpage rates are tripled, the projected decline from 1975 to 2000 is as much as 17 m.

Design of a streamflow-data network

A statistical procedure that evaluates the improvement in accuracy of streamflow-parameter estimates was used by W. L. Haushild and M. E. Moss in the design of the streamflow-data networks for Washington. Results indicated that there would be no improvement in the ability to transfer information from gaged to ungaged sites by means of regional regression analyses if the existing streamflow-data base were extended either by adding new gaging stations or by extending the existing records. Therefore, the streamflow data networks in Washington will be comprised of stations used for the following purposes: (1) definition of long-term trends, (2) current-purpose data, and (3) collection of data for inter-station transfer of information by correlation analysis.

SPECIAL WATER-RESOURCE PROGRAMS

DATA COORDINATION, ACQUISITION, AND STORAGE

OFFICE OF WATER-DATA COORDINATION

The Office of Water Data Coordination (OWDC) has a continuing responsibility to implement Office of Management and Budget (OMB) guidelines for the coordination of certain water-data-acquisition activities by Federal agencies. During FY 1977, progress was made in several major areas of OWDC's coordination programs: (1) Field-level coordination and planning, (2) compilation of the "Catalog of Information on Water Data" (3) preparation of a series of nationally consistent hydrologic unit maps, and (4) recommendations regarding methods of coordinating activities.

The "Federal Plan for the Acquisition of Water Data, Fiscal Year 1977," which documents the FY 1977 field-level coordination effort, was distributed in March 1977. In addition to a region-by-region summarization of 21 regional plans, several important activities related to the coordination effort are reported in this document. These related coordination activities include the current status of implementation of the National Water Data Exchange (NAWDEX), the stream-quality and stream-quantity components of the Level I accounting element of the National Water Data Network, the National Water Quality Surveillance System of EPA, and the water-data-acquisition activities of several USGS divisions.

The computer file of the "Catalog of Information on Water Data" has been updated through 1976, and the sections on streamflow and stream stage, surface-water quality, ground-water quality, and areal investigations and miscellaneous activities were also updated and added to the catalog. Short-term data activities (station activities with less than 3 years of continuous record) of all participating agencies were included in the catalog for the first time.

There is an increasing need for information on the water resources of areas where urban and industrial growth is continuing in coastal regions. To help meet this need, a special section of the four-volume "Catalog of Information on Water Data" lists water-data-acquisition activities in coastal and estuarine counties, including those around the Great Lakes.

Most of the chapters in OWDC's new "National Handbook on Recommended Methods for Water Data Acquisition" have been completed. In addition to categories (surface water, ground water, chemical and biological quality of water, automatic monitors, and fluvial sediment) covered in the 1972 preliminary edition, the new handbook includes chapters on soil moisture, basin characteristics, evaporation and transpiration, snow and ice, and hydrometeorological observations. In February 1976, the U.S. Bureau of Standards designated the Coordinating Council for Water Data Acquisition Methods (the steering committee for the "recommended-methods" effort) as the Federal Interagency Metric Panel for Hydrology. This body is responsible for recommending metric units, precision and accuracy limits, conversion factors, and conversions of equipment for hydrologic measuments.

Publication of the USGS State Hydrologic Unit Map series was completed in May 1977. The series, sold and distributed by the USGS, consists of 47 separate maps (1:500,000 scale) of the 50 States and Puerto Rico that show a numerically digitized hierarchy of hydrologic units that are basically hydrographic in nature. These units range in areal extent from the regions and subregions designated by the U.S. Water Resources Council for use in its national assessments to the accounting units of the National Water Data Network and the cataloging units used for the "Catalog of Information on Water Data."

Digitized data are being acquired for all of the hydrologic-unit boundaries for each State within the conterminous United States. These data will be used to (1) compute drainage areas for all hydrologic units, (2) plot hydrologic-unit boundaries on other maps, and (3) identify hydrologic-unit code assignments for stations by computer search, using known latitude and longitude coordinates of a site.

The first joint meeting of the Advisory Committee on Water Data for Public Use (non-Federal) and the Interagency Advisory Committee on Water Data (Federal) was held in Denver, Colo., from November 30 to December 2, 1976. The meeting was cochaired by the Director and the Chief Hydrologist of the USGS and was attended by more than 100 members and observers. The following items were included in the meeting agenda: (1) A review of the progress made over the past year in the implementation of OMB guidelines; (2) reports of the first meeting of the newly impaneled Federal interagency working groups on needs for data on the quality of precipitation and the water quality of small watersheds and on improved communications; (3) reports of progress on the implementation of NAWDEX and the development and refinement of the transmission of water data via satellite data-relay systems; (4) a working-group session to review the USGS's pilot river-quality assessments; (5) a working-group session to consider the preparation of the "National Handbook of Recommended Methods"; and (6) a working-group session to consider ways and means of improving communications between agencies that collect water data and agencies that use water data. The meeting agenda also included a tour of the recently dedicated USGS National Water Quality Laboratory in Denver.

NATIONAL WATER DATA EXCHANGE

The National Water Data Exchange (NAWDEX) was established to assist users of water data in the identification, location, and acquisition of needed data. NAWDEX consists of water-oriented organizations throughout all levels of Federal, State, and local governments, as well as private organizations that work together to make their water data readily and conveniently available. Membership in NAWDEX is voluntary and open to any water-oriented organization that wishes to take an active role in NAWDEX activities. There are no dues or fees associated with membership.

The central management of NAWDEX is provided by a Program Office located at the USGS National Center in Reston, Va. It has the responsibility for coordinating all operational activities within the program. A network of 51 Local Assistance Centers (LAC's) in the offices of NAWDEX members provides local and convenient access to NAWDEX and its services; there are LAC's in 45 States and Puerto Rico. (A list of LAC's and their locations may be obtained from the NAWDEX Program Office.) Most centers are equipped with computer terminals and thereby provide an extensive telecommunication network for access to the computerized directory and indexes maintained by the NAWDEX Program Office.

Identification of sources of water data

The NAWDEX Program Office maintains a computerized "Water Data Sources Directory." This directory identifies organizations that collect water data, locations within these organizations from which data may be obtained, the geographic areas in which water data are collected by these organizations, the types of water data collected, alternate sources for acquiring the organization's data, and the media in which the data are available.

Nationwide indexing of water data

A computerized "Master Water Data Index" identifies individual sites for which water data are available, the locations of these sites, the organizations collecting the data, the hydrologic discipline represented by the data, the periods of record, water-data parameters, the frequency of measurement of the parameters, and the media in which the data are available. These data are collected by 21 Federal agencies and more than 300 non-Federal organizations.

Data search assistance

Through its "Water Data Sources Directory," its "Master Water Data Index," and other indexes and reference sources made available by its participating members, NAWDEX assists its users in locating data of special interest. These data include water data in computerized form and in published and unpublished forms. Data search assistance may be obtained from the NAWDEX Program Office or from any of the LAC's.

WATER-DATA STORAGE SYSTEM

The USGS uses a digital computer to process, store, retrieve, and display water-resource data. The computer is also used in water-resource studies that require capabilities in statistical and analytical techniques, graphical display and map presentation of data, and mathematical modeling of hydrologic systems. The computer system consists of a central computer located in Reston, Va., and remote terminal facilities located in 45 States.

Data on daily discharge, collected by the USGS and cooperating Federal and State agencies at about 10,000 regular streamflow stations, are stored on magnetic tape. The volume of data holdings is equivalent to about 310,000 station years of record. More than 80 percent of all streamflow data collected under this program is covered. The data are stored in discrete units containing figures for daily water discharge for each gaging station and for each year of record; thus, the data are compatible with a variety of statistical programs for analysis on the basis of calendar years, water years, climatic years, or any other period desired.

An automated system for storage and retrieval of surface-water-quality data has been in use since 1959. All data collected since then, plus selected long-term historical records, have been entered into the system. The system contains the following types of data: (1) Chemical and physical analyses of surface water, (2) suspended sediment, (3) water temperature, (4) specific conductance, and (5) multi-item data collected by digital monitors. The results of about 1 million analyses are stored in the file.

A new automated system for storage and retrieval of ground-water data has been introduced. The Ground-Water Site Inventory data base operates under a proprietary data-base management system that allows data retrieval on the basis of about 30 key parameters. Information in the new file includes data on location, physical characteristics, construction history, geohydrology, aquifer characteristics, field quality determinations, and water levels and withdrawals for wells, springs, or other sources of ground water. By the end of February 1977, records of about 440,000 wells and springs had been converted from the old punchcard format and entered into the new system.

URBAN WATER PROGRAM

The USGS urban-hydrology program includes studies of the relation of rainfall to runoff, to sediment transport, to the chemical and biological quality of the runoff, and to ground-water recharge under various types and degrees of land development. The program's objective is to provide generalized relations for estimating the hydrologic changes caused by urbanization.

Hydrologic modeling

To provide preliminary criteria for the design of storm-drainage facilities in the Memphis area of Tennessee, C. W. Boning developed a regression model to synthesize annual peak flows for small streams. The model, developed from data on 57 flood peaks at 20 gaging stations, expresses discharge as a function of drainage area, the percentage of the area that is impervious, and maximum 2-hour rainfall. Model error is about 25 percent. A test of the predictive accuracy of the model using data on 45 additional peaks, some of which occurred at gaging stations not used in model development, indicated that the model has a standard error of prediction of about 35 percent. The model is being used to develop flood-frequency curves for basins of various sizes and various percentages of imperviousness. The ultimate objective of the project is to use a rainfall-runoff model, calibrated for streams in the area, to make more accurate predictions of flood frequency.

J. M. Knott and D. R. Dawdy used a modified version of the USGS rainfall-runoff model to study the hydrology and water quality of the Calabazas Creek basin in California. The model is a hybrid of (1) the antecedent-moisture and infiltration components of the previous model and (2) a routing component based on the motion of a kinematic wave in uniform channels receiving lateral and upstream flows. Because the model incorporates many physical characteristics of the basin in the simulation of storm events (slope, roughness, channel dimensions, basin dimensions, and proportion of impervious area), discharge hydrographs can be generated for any stream coordinates in the basin. The model also can generate discharge hydrographs for adjacent basins if rainfall, soil infiltration, and basin characteristics are known. The model has been modified to permit (1) simulation of storm runoff for a basin that contains two different soil types and (2) Thiessen adjustment of rainfall input data to vary rainfall data throughout the basin.

High peak flows created by long-term, low-intensity storms

Peak runoff in the Portland area of Oregon appears to be influenced more by long, sustained rains than by high rainfall intensities. Whereas extremely small basins with drainage areas of less than 1.0 km^2 and with a high percentage of impervious area tend to respond readily to the high-intensity rainfall, the largest peak flows in most basins occur after rains of long duration. According to Antonius Laenen, rainfall intensities in the Portland area are lower than those in many parts of the United States, and intensities of 2.5 mm/h have been exceeded only twice in 80 years at the Portland weather station. Rainfall intensities of 0.8 mm in 5 minutes have been exceeded only three times in 80 years.

Ground-water pollution potential from landfill site

L. L. Dearborn's analyses of hydrologic and water-quality data from the Merrill Field landfill (solid-waste disposal) site at Anchorage, Alaska, indicated that, although drawdown caused by pumping has created a potential for downward movement of polluted shallow ground water, the underlying public-supply aquifers are not immediately endangered. The water table in the area is at very shallow depths, and natural artesian levels were higher than the land surface when landfill operations began in 1950. The water-quality data show that the leachate has apparently moved only a very short distance. Although aquifer test data from a nearby well indicated areal leakage rates as great as 6 mm/d, vertical hydraulic conductivities determined from core samples at a test well within the landfill were very low (0.02 mm/d).

WATER USE

Estimated use of water in the United States in 1975

C. R. Murray and E. B. Reeves reported that the Hydrologic Review Group of the USGS Water Resources Division, in cooperation with the Division's district offices, surveyed water use for 1975 in order to update the 1970 water-use data report (Murray and Reeves, 1972). Some of the preliminary water-use data for 1975 are shown in tables 2, 3, and 4.

Table 2 shows populations, water withdrawals for each of the water-use categories, quantities of water derived from various sources, water consumption (water removed from the water environment and not available for reuse), and water used for hydroelectric power production in the United States from 1955 to 1975. Percentage changes for each of these items from 1970 to 1975 are also shown.

About 1,600 hm^3/d, equivalent to about 7.32 m^3/d per person, was withdrawn for uses other than the generation of hydroelectric power. About 360 hm^3/d

TABLE 2.—*Water withdrawals, sources, and consumption in the United States, 1955-75*

[Partial figures may not add to total because of independent rounding]

	1955	1960	1965	1970	1975	Percent change, 1970–75
Total population (millions)	164.0	179.3	193.8	203.2	215.0	+ 5
Withdrawals (hm^3/d):						
Public supplies	64	79	91	100	110	+10
Rural domestic and livestock	14	14	15	17	18	+ 6
Irrigation	420	420	450	490	530	+ 8
Thermoelectric power	270	420	490	640	740	+16
Other self-supplied industrial	150	140	170	180	170	- 6
Total	920	1,100	1,200	1,400	1,600	+14
Sources from which water was withdrawn (hm^3/d):						
Ground water:						
Fresh	180	190	230	260	320	+24
Saline	2.5	1.4	1.8	3.8	4.4	+16
Surface water:						
Fresh	680	720	790	950	1,000	+ 5
Saline	68	120	160	200	240	+20
Reclaimed sewage	0.76	0.38	2.6	1.9	1.9	+ 0
Consumption (hm^3/d)	[1]	230	290	330[2]	360[2]	+10
Water used for hydroelectric power (hm^3/d)	5,700	7,600	8,700	10,600	12,600	+19

[1] Data not available.
[2] Freshwater only.

(23 percent) of the freshwater withdrawn was consumed, a per capita consumption of about 1.66 m^3/d. About 12,600 hm^3/d (58.6 m^3/d per person) was withdrawn for hydroelectric-power generation.

Water withdrawn for industrial uses (including water used for thermoelectric-power production) was about 910 hm^3/d (4.2 m^3/d per person), of which about 645 m^3/d was freshwater and about 265 hm^3/d was saline water. Irrigation withdrawals accounted for about 530 hm^3/d (2.5 m^3/d per person), public-supply uses required 110 hm^3/d, and rural domestic and livestock uses were about 18 hm^3/d. Ground water furnished about 19.6 percent of all water (both fresh and saline) withdrawn and accounted for 23.7 percent of freshwater withdrawals. Rounded figures indicate that 58 percent of the water withdrawn was used by industry, 34 percent was used for irrigation, 7 percent was used for public supplies, and 1 percent was used for rural domestic and livestock purposes.

Irrigation consumption was 302 hm^3/d, 83 percent of the 362 hm^3/d of freshwater consumed. Public supplies consumed 25 hm^3/d (7 percent of total consumption), industry consumed 23 hm^3/d (6 percent of total consumption), and rural domestic and livestock uses consumed 13 hm^3/d (4 percent of total consumption).

Estimates of water withdrawals by sources and of freshwater consumed in each of the Water Resources Council (WRC) regions (fig. 3) are shown in table 3.

Table 4 shows average per capita water withdrawals and average per capita freshwater consumption in the 9 eastern WRC regions, the 9 western WRC regions, and the 50 States, Puerto Rico, and the Virgin Islands. It also shows the per capita use for (1) public supplies, (2) total withdrawal uses, and (3) withdrawal uses plus hydroelectric-power use.

About 93 percent of the 530 hm^3/d of water withdrawn for irrigation was withdrawn in the 9 western regions, which approximately correspond to the 17 Western States. About 57 percent of the water withdrawn for irrigation in the United States was consumed. About 86 percent of the 645 hm^3/d of self-supplied industrial water was withdrawn in the 9 eastern regions, which approximately correspond to the 31 Eastern States. Only about 3 percent of the total freshwater and saline water withdrawn by industry was consumed. Consumption by thermoelectric powerplants amounted to about 0.86 percent of

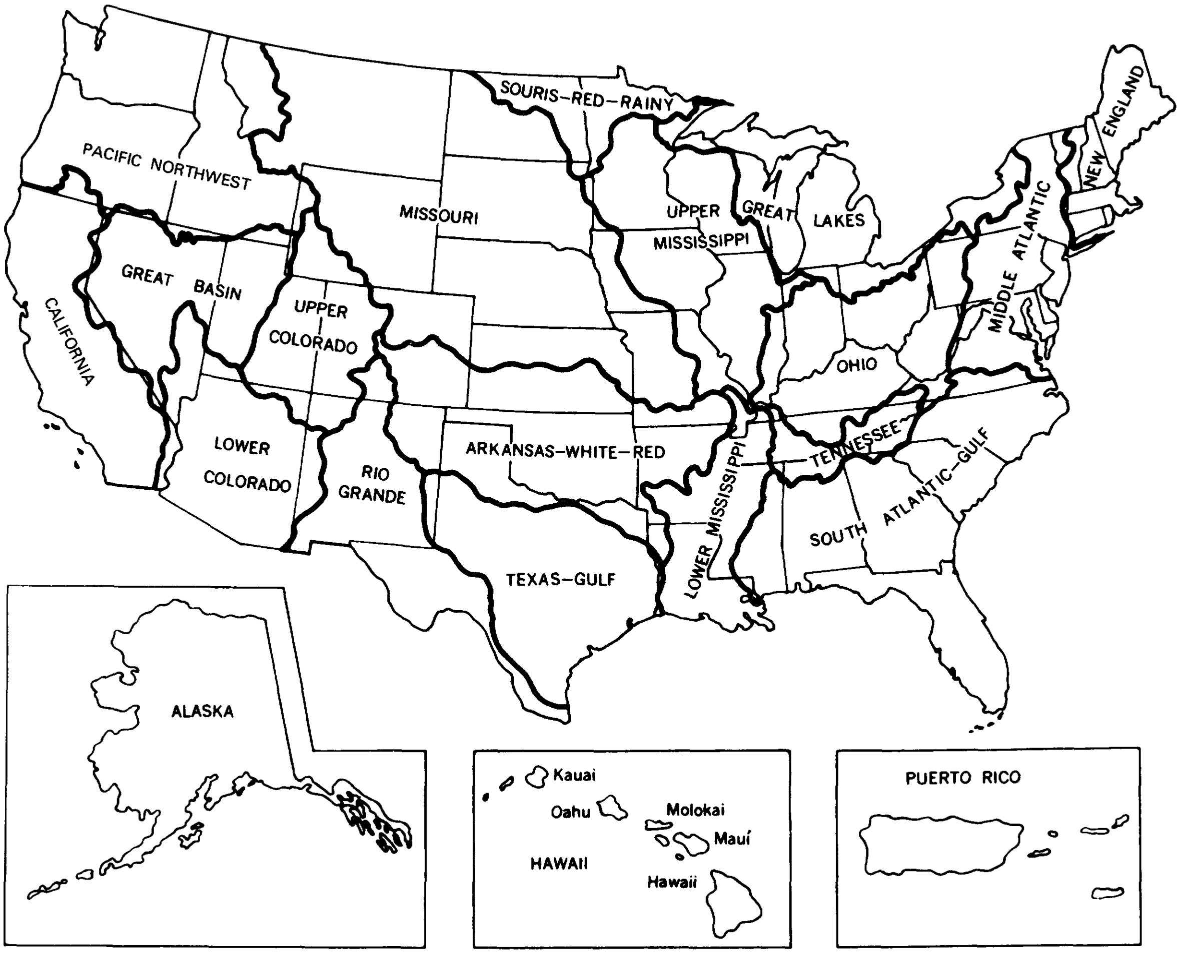

FIGURE 3.—Map of the United States showing Water Resources Council regions.

withdrawals, and water consumed by other industries was about 11 percent of withdrawals.

About 36.6 hm³/d (0.72 m³/d per person), 46 percent of which was ground water, was withdrawn in the nine western regions for public supplies in 1975; about 72.9 hm³/d (0.60 m³/d per person), about 31 percent of which was ground water, was withdrawn for public supplies in the nine eastern regions. Consumption of water in 1975 for public supplies in the West was 13.4 hm³/d, or about 37 percent of withdrawals; the consumptive use for public supplies in the East was 11.5 hm³/d, or 16 percent of withdrawals. Per capita consumption was 0.26 m³/d in the western regions and 0.10 m³/d in the eastern regions.

Public-supply withdrawals used for residential purposes in the West cause a greater draft on the supply then they do in the East. In the arid West, the large quantities of water used for the irrigation of lawns increase both per capita withdrawals and per capita consumption. Water delivered for domestic and public uses and water-system losses in 1975 accounted for 74 percent, or 27.3 hm³/d (0.54 m³/d per person), of the public-supply withdrawals in the nine western regions but for only 66 percent, or 48.2 hm³/d (0.40 m³/d per person), of the public-supply withdrawals in the more populous eastern regions. About 9.51 hm³/d (0.19 m³/d per person) from public supplies was used by commerce and industry in the West, and about 24.6 hm³/d (0.20 m³/d per person) was so used in the East.

Ground water (fresh and saline) withdrawn in 1975 for industrial uses (excluding thermoelectric power production) was about 16.7 hm³/d in the nine western regions and about 23.1 hm³/d in the nine eastern regions; fresh ground water accounted for 15.0 hm³/d in the West and 21.1 hm³/d in the East. Excluding water used by thermoelectric powerplants, ground water amounted to 44 percent of all water withdrawals for industry in the West and 18 percent of water withdrawals for industry in the East. However, ground water furnished 60 percent of the freshwater withdrawals for industrial uses

TABLE 3.—*Water use (excluding that used for hydroelectric power) in 1975*

[Quantities are shown to three significant figures unless they are less than unity]

Water Resources Council region	Freshwater withdrawn (hm³/d) Ground water	Surface water	Waste-water	All freshwater	Saline water withdrawn[1] (hm³/d)	Freshwater consumed (hm³/d)
New England	2.29	18.9	0	21.2	40.8	1.53
Mid-Atlantic	10.2	83.5	0.56	94.3	102	5.90
South Atlantic-Gulf	20.7	91.9	0	113	52.7	14.2
Great Lakes	4.46	132	0	136	1.51	3.61
Ohio	6.61	127	0	134	.08	4.57
Tennessee	1.03	39.7	0	40.8	0	1.07
Upper Mississippi	8.95	62.2	0	71.2	.06	3.03
Lower Mississippi	18.4	45.8	0	64.2	1.13	20.8
Souris-Red-Rainy	.33	1.02	0	1.35	0	.35
Missouri Basin	39.5	93	.30	133	.14	55.6
Arkansas-White-Red	33.4	22.7	.01	56.1	.55	34.2
Texas-Gulf	27.3	41.7	.12	69.1	19.4	29.4
Rio Grande	8.77	11.6	.08	20.5	.02	13.1
Upper Colorado	.47	14.9	0	15.4	.07	6.22
Lower Colorado	20.2	13.1	.25	33.6	0	24.7
Great Basin	5.35	20.4	.04	25.8	.69	13.5
Pacific Northwest	27.8	96.9	.03	125	.15	40.0
California	72.5	83.0	.61	156	37.6	86.8
Alaska	.17	.60	0	.77	0	.02
Hawaii	3.36	2.54	0	5.09	3.70	2.26
Caribbean	.69	1.91	0	2.60	12.2	.88
Total	312	1,000	2.00	1,320	273	362

[1] Water containing 1,000 mg/L or more dissolved solids, for industrial purposes.

(excluding thermoelectric power) in the West and 18 percent in the East.

Comparisons of the preliminary 1975 water-use data and the 1970 water-use data indicated that the proportion of water withdrawn for irrigation decreased 1 percent and that the percentage of water consumption for each major category of water used, in comparison with total consumption, was nearly the same in 1975 as it was in 1970. Consumption for irrigation decreased 1 percent, and consumption by industry increased 1 percent. However, percentages of increased use were not as great from 1970 to 1975 as they had been from 1965 to 1970; irrigation, however, showed over 8-percent increases during both 5-year periods. The 5-percent increase in population during each of the 5-year periods was reflected in

TABLE 4.—*Per capita water withdrawals and water consumptions in the eastern and western Water Resources Council regions and the United States, 1975*

Area	Public supplies: Population served (millions)	Public supplies: All uses (m³/d)	Public supplies: Domestic and public uses only[1] (m³/d)	Total population (millions)	All withdrawal uses: Excluding water power (m³/d)	All withdrawal uses: Including water power (m³/d)	Freshwater consumed, all off-channel uses (m³/d)
WRC regions:							
Eastern (9)	121.072	0.60	0.40	148.414	5.88	42.42	0.37
Western (9)	50.810	.72	.54	61.317	11.17	128.	4.95
50 States, D.C., P.R. and V.I.	175.199	.64	.44	217.483	7.32	65.05	1.66

[1] Includes water losses in systems.

increased water use. In 1975, the only category of water use that had not increased at a rate exceeding the rate of population growth was self-supplied industrial use (excluding thermoelectric power use), which decreased 6 percent; however, industrial use (including thermoelectric power use) increased 12½ percent.

The quantity of water withdrawn from fresh surface-water supplies increased only 5 percent from 1970 to 1975. To meet the increased demand for water, increases of 24 percent in fresh ground-water withdrawals and 20 percent in saline surface-water withdrawals were necessary. The 5-percent increase in fresh surface-water withdrawals was accompanied, however, by a 19-percent increase in its in-channel use for hydroelectric power development, an increase attributed to the increased cost of fossil and nuclear fuels.

Water use in thermoelectric powerplant cooling

One of the largest water-consuming activities in the Nation is the cooling of thermoelectric powerplants. The basic technologies now used are once-through cooling, ponds, and evaporative cooling towers. All of these cooling methods involve evaporation, a consumptive use of water. In the case of ponds and towers, a consumptive use is easily determined as the difference between withdrawal and discharge. For once-through cooling, however, withdrawal and discharge are equal; all of the evaporation takes place in a natural water body. R. M. Hirsch developed a steady-state numerical model of evaporative losses for laterally and vertically mixed rivers. The theoretical basis for the model was a heat-balance study of rivers and canals made by H. E. Jobson (1973). The model demonstrates that evaporation accounts for between 25 and 80 percent of the cooling load. (The remainder of the heat is lost through conduction and back radiation.) The 25-percent value is for very cold (about 0°C) water temperatures and calm winds, whereas the 80-percent value is for high (about 35°C) temperatures and high windspeeds (about 7 m/s). Model results (in cubic meters of water per second per megawatt of heat flux) are given in terms of a few essential parameters—natural water temperature, initial temperature rise due to thermal load, windspeed, and atmospheric pressure.

Hirsch also developed a similar model of evaporation in a cooling-pond system, and the results (in cubic meters of water per second per megawatt of heat flux) are expressed in terms of natural water temperature, heat load per unit pond area, windspeed, and atmospheric pressure.

By integrating the results of each of these models over the range of climatic conditions typical for the Yampa River basin of Colorado, estimates of annual consumption for a 2,000-MW powerplant were developed. Annual consumption was estimated at 16.5 hm^3 for once-through cooling and 35 hm^3 for ponds. Apparently, in this environment, once-through cooling consumes only about 40 percent as much water as cooling towers, whereas ponds consume 86 percent as much water as cooling towers.

Water consumed by coal mining and power production

F. A. Kilpatrick and G. H. Davis (1976) reported that water consumed (water no longer available for reuse) by surface coal mining is 17 L/t, whereas water consumed by underground coal mining is 63 L/t. Also, there is a 33-L/t waste-disposal requirement for each type of mining. In the arid and semiarid West, an additional 67 L/t is consumed by vegetation established on reclaimed surface-mine spoils.

Total water consumption for coal mining in the United States is about 43 hm^3 per year or about twice the amount of water consumed by a single coal-fired 2,000-MW thermoelectric powerplant. Water consumed by coal-fired powerplants is about 18,500 m^3/yr for each megawatt of capacity; if wet scrubbers are required for air-pollution control, water consumption increases 20 percent.

On a comparable energy-output basis, coal-gasification and coal-liquefaction processes consume from about 25 to 100 percent as much water as a coal-fired powerplant, depending on the amount of air cooling used in a powerplant.

Irrigation water use increasing in southeastern Missouri

A study of the Mississippi River Embayment in southeastern Missouri is being made by R. R. Luckey to determine the amount of ground water available for irrigation in the area. There are presently more than 3,500 irrigation wells in the 10,000-km^2 area, and this number is increasing at a rate of more than 10 percent/yr. The principal crops include rice, soybeans, corn, cotton, and small grains. Synoptic water-level measurements made in approximately 800 wells in the spring and fall of 1976 indicated that there is no long-term decline in water levels despite continuing development for irrigation. Similar water-level-measurement programs were carried out in 1956 and 1965.

The irrigation wells are developed in 15 to 50 m of alluvium and will yield from 0.03 to over 0.20 m^3/s. Water-use data collected as part of this project indicated that, during 1976, from 600 to 1,200 mm of supplemental water was needed to irrigate the rice crop, whereas the corn crop required from 50 to 100 mm.

Water use in Nevada in 1975

During 1975, about 4,860 hm^3 of water (excluding that used for hydroelectric power) was withdrawn in Nevada, according to J. O. Nowlin and J. R. Harrill. About 3,920 hm^3 was supplied by surface-water sources, and the remaining 950 hm^3 was supplied by ground water (well pumpage and spring diversions). About 1,200 hm^3 of the water withdrawn was consumed. Total withdrawals (including water used for hydroelectric power) increased from about 5,670 hm^3 in 1970 to about 6,090 hm^3 in 1975. This change was primarily due to increased use of imported Colorado River water and to increased ground-water pumpage for irrigation.

NATIONAL WATER-QUALITY PROGRAMS

Yampa River basin water-quality study

A river-quality assessment study is being conducted to investigate the potential environmental effects of developing coal resources in the Yampa River basin of northwestern Colorado and south-central Wyoming (T. D. Steele, D. P. Bauer, D. A. Wentz, and J. W. Warner, 1976; T. D. Steele, I. C. James II, and D. P. Bauer, 1976; R. M. Eddy, 1976). Steele (1976) defined water-quality conditions at 82 sites in the basin. Three sites were found to have high concentrations of Cu, Fe, Mn, Pb, and V in water and Cr and Fe in bottom sediments. On the basis of benthic-invertebrate samples, three other sites had diversity indices of less than 1. At 33 sites, iron concentrations exceeded the maximum recommended by the USPHS for drinking water.

A waste-assimilative capacity study of the Yampa River between Steamboat Springs and Hayden, Colo., determined nutrient concentrations resulting from discharge of treated wastes. Steele estimated that future nonionized ammonia concentrations may exceed by a factor of 2 to 3 a proposed stream standard of 0.02 mg/L. Field data for this analysis indicated an inverse relationship between variations in nutrient concentrations and diversity indices at sampled sites.

Preliminary solute-transport modeling of the ground water in an intensively mined area of the basin indicated that conservative solutes—waterborne salts and trace metals from overburden waste piles—will reach the Yampa River through subsurface flow within 60 years.

National Stream Quality Accounting Network

The USGS's National Stream Quality Accounting Network (NASQAN) provides a uniform assessment of the quality of U.S. rivers. At each of 345 NASQAN stations, the USGS monitors volume of streamflow, water temperature, specific conductance, pH, pollution-indicator bacteria, 14 common inorganic constituents, 11 trace elements in both total and dissolved forms, 3 forms of major biological nutrients, concentrations and sizes of suspended sediments, numbers and types of phytoplankton (floating algae), and organic carbon. In addition, samples for analyses of about 20 pesticide compounds are collected quarterly at 153 selected NASQAN stations, and 51 stations are sampled for radiochemical analyses.

NASQAN is an accounting network designed so that the stations measure the quantity and quality of water flowing from nearly all of the 350 hydrologic units designated by the U.S. Water Resources Council. Consequently, maps of the United States can be constructed with the accounting units colored or shaded to represent the quality of the water leaving the units; figure 4, which represents concentrations of nitrite plus nitrate nitrogen, is an example of one of these maps. According to the map, the highest concentrations of nitrogen occur in agricultural regions of the country. (These high nitrogen concentrations probably result from the use of artificial fertilizers and erodible soils.) The lowest concentrations of nitrogen occur in forested regions, in some desert regions, and in sparsely populated areas.

R. O. Hawkinson, J. F. Ficke, and L. G. Saindon (1977) used NASQAN data to describe the quality of U.S. rivers during the 1974 water year. Similar reports are being prepared for the 1975 and 1976 water years. Maps of the type shown in figure 4 are used in the annual environmental-quality reports of the Council on Environmental Quality and are of value for many other kinds of assessments of national resources.

Central Laboratories System

The Central Laboratories System expanded the types of analytical services available to water-resource projects during 1977. According to W. A. Beetem, about 8 percent of the laboratories' manpower was reassigned to programs involving custom analyses of chemicals affecting the environments. The Albany Central Laboratory's work on inorganic analyses was reassigned to the Atlanta and Denver Central Laboratories, and the Albany Central Laboratory was closed. To better respond to the Federal programs related to examining concentra-

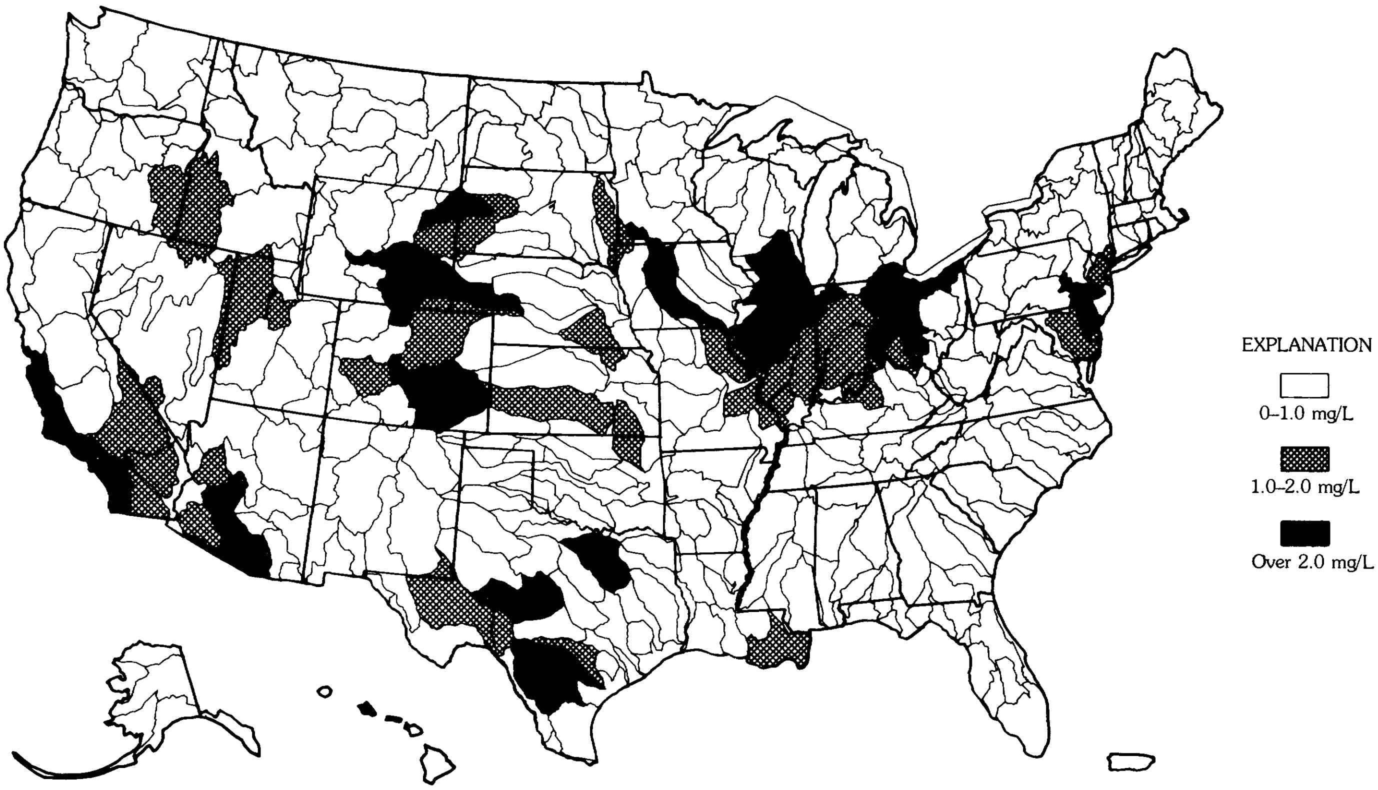

FIGURE 4.—Map of the United States showing data on mean concentrations of nitrite plus nitrate nitrogen collected at NASQAN stations during the 1976 water year. (Prepared in cooperation with the Council on Environmental Quality.)

tions of trace metals and trace organics in water, the Atlanta Central Laboratory was enlarged. The analyses workload for 1977 increased about 12 percent over that for 1976.

MARINE GEOLOGY AND COASTAL HYDROLOGY

MARINE AND COASTAL GEOLOGY

ATLANTIC COAST

Structural and geophysical studies of the Atlantic Continental Margin

Analysis of 770 km of multichannel reflection data collected over Georges Bank and adjacent areas revealed the presence of deeper block-faulted basins under the main part of the Georges Bank basin. According to J. S. Schlee, the main basin contains up to 8 km of presumed Jurassic and younger sedimentary rocks as a broad seaward-thickening accumulation; most of the section is inferred to be Jurassic in age. The underlying fault basins are areally restricted and contain an unknown thickness of presumed Triassic and older sediments. They are probably the equivalent of similar fault basins already described in the southern Gulf of Maine.

Three features that may have petroleum possibilities are a zone of marked acoustic contrast in the western part of the basin at a depth of 4.9 km, a faint diapir within a block-fault basin under the northern edge of the bank, and a broad warp (with acoustic contrast) in the south-central part of the basin.

J. C. Behrendt, K. D. Klitgord, J. A. Grow, and J. S. Schlee noted that depth-to-basement estimates for the continental shelf and slope north of Cape Hatteras obtained by using both the USGS aeromagnetic survey and the USGS common-depth-point multichannel seismic-reflection lines were in close agreement. They reveal not only the major troughs—the Baltimore Canyon Trough and the Georges Bank Trough—but also a series of smaller troughs south of New England. The Long Island platform appears to comprise a series of ridges and troughs oriented along N. 25° E. Martha's Vineyard and Nantucket, Mass., sit on one of these ridges, separated by a deep trough filled with Jurassic (Triassic?) sediments. South of the Long Island platform (just north of and beneath the east coast magnetic anomaly) is another deep narrow trough that connects the Baltimore Canyon Trough with the Georges Bank Trough. South of Cape Hatteras, there appears to be yet another deep trough extending from the cape to the Blake Plateau. This trough is located between the "Brunswick" anomaly along the coast and the East Coast magnetic anomaly further seaward.

Investigations of the oceanic crust between Bermuda and the Atlantic margin have yielded a pattern of sea-floor-spreading magnetic anomalies and fracture zones remarkably consistent with those found along the African margin. The use of seismic-reflection and aeromagnetic data show that these fracture zones continue onto the Atlantic Continental Shelf and should permit an accurate reconstruction of the initial fit of Africa to North America. The apparent close coincidence between the locations of the fracture zones and the limits of the numerous basins located along the margin suggests a causal link between them. The major seismic activity along the coast also appears to be associated with the fracture zones.

The magnetic and seismic data obtained along the continental slope reveal a ridgelike structure along almost the entire margin. This feature generally is located beneath the East Coast magnetic anomaly but is too weakly magnetized to be the major source of the anomaly. The "ridge" lies at a depth of 7 to 8 km and probably is at the seaward edge of the deep basins that lie along the continental margin between the Blake Plateau and Georges Bank. The ridge may be a carbonate structure or possibly may be volcanic. It is possible that the East Coast magnetic anomaly is primarily an edge effect between the flat-lying sediments in the deep (12–14 km) trough just landward of the anomaly and the oceanic crust just seaward of the anomaly.

Approximately 39,000 km of new marine gravity data were collected off the Atlantic Continental Margin. A free-air gravity anomaly map of the data north of Cape Hatteras (Grow and others, 1976) reveals abrupt changes in mean field values or transverse trends at several discreet locations along the Atlantic Continental Margin. J. A. Grow noted that the major transition zones are east of Norfolk, Va., the Delaware Bay, and Atlantic City, N.J., and south of Martha's Vineyard. The transition zones, like the magnetic anomalies, reflect deep fractures in the continental crust that appear to extend beneath the continental slope and rise. These zones were also probably the loci of initial fracture zones formed when Africa and North America separated during the Jurassic.

The major sedimentary basins used for resource studies and basement configuration are outlined by the free-air gravity anomalies. Thick Mesozoic basins are characterized by broad free-air anomaly lows. The transition zones may indicate regions of weak crust and latent earthquake potential.

According to W. P. Dillon, a deep angular unconformity beneath the Blake Plateau in the southern Atlantic region shows an abrupt deepening towards the south along an extension of the trend of the Blake Spur fracture zone, which was determined by K. D. Klitgord from offsets of ocean-opening magnetic stripes in the deep sea. The strata that were eroded to form the unconformity probably were laid down in troughs and deep zones formed by Triassic rifting and during Jurassic continental drift. Apparently, sediments laid down early in the formation of the continental margin were uplifted and eroded, probably in Jurassic time, and this eroded surface was covered by a high-velocity material that may be volcanic rock. At roughly the same time, faults on the fracture zone extension apparently were reactivated. Thus, a minor tectonic interval, probably of Jurassic age, has been inferred in the rocks beneath the Blake Plateau. This interval might be correlated with a radical change in spreading rate at the end of Jurassic time.

Stratigraphic coring of the Atlantic Continental Shelf and Slope

The USGS carried out a 60-day program of core drilling on the shelf and upper slope of the eastern United States aboard the D/V *GLOMAR CONCEPTION*. The coring penetrated as much as 310 m below the sea floor at 19 sites along the continental margin from Georgia to Georges Bank off New England in water depths ranging from 20 to 300 m; 1,020 m of material were recovered in 380 cores ranging in age from Late Cretaceous to Holocene. A preliminary summary of the results of the Atlantic Margin Coring Project has been released (Hathaway and others, 1976), and specific findings of some of the investigations are reported elsewhere in this volume.

Late Mesozoic and Cenozoic development of inner shelf off Massachusetts

Interpretation of high-resolution subbottom profiling data by C. J. O'Hara, R. N. Oldale and J. M. Robb defined the late Tertiary to Holocene history of Buzzards Bay, Vineyard Sound, and eastern Rhode Island Sound off Massachusetts. They found that the deepest unconformity, of late Tertiary to early Pleistocene age, delineates an inner lowland underlain nearshore by pre-Mesozoic crystalline and sedimentary rock of the Fall Zone and offshore by unconsolidated to semiconsolidated coastal plain sediments of Cretaceous to early Pleistocene age. The coastal plain deposits underlie a cuesta that extends from Long Island Sound to the eastern part of Georges Bank in the Gulf of Maine. Paleodrainage patterns indicate southward-flowing streams on the Fall Zone surface and northward-flowing streams on the inface slope of the cuesta. The stream valleys appear to be tributary to a much larger subsequent stream, and the regional slope of the Fall Zone surface suggests that this stream probably flowed westward to a water gap in the cuesta. Two glacial drifts overlie the coastal plain strata. The lower drift may be of pre-Sangamon age and may correlate with the older drift deposits on Martha's Vineyard and Long Island. The upper drift is inferred to be of late Wisconsin age and to correlate with end moraines and outwash deposits of southern New England, Block Island, and Long Island. The older drift and coastal plain deposits are locally folded and faulted and may represent the offshore equivalent of the ice-disturbed sediments of Gay Head at Martha's Vineyard. Prior to the postglacial rise of sea level, the glacial drift and older deposits were subject to subaerial fluvial erosion, which developed three distinct drainage systems all flowing southwestward. Radiocarbon dates from freshwater peats indicate that complete margin submergence of this region took place no earlier than 5,000 years ago. Fluvial, estuarine, and marine deposits blanket this youngest unconformity.

Environmental conditions of the Georges Bank area

Movement of bottom sediment as sand waves, mainly in response to high waves and strong tidal and storm-driven currents, probably constitutes the main hazard to petroleum exploration and development. D. W. Folger, Bradford Butman, and M. H. Bothner found, however, that the surface of the thick (80 m) layer of sand overlying the bank moves in a broad spectrum of sand waves even during relatively calm weather. Sediment apparently is widely distributed throughout the water column over the bank during heavy weather. Internal waves may account for some resuspension of sediment in the area, but most resuspension is probably due to tides, winter northeastern storms, and fall hurricanes. Seston varies both in composition and in concentration in relation to season and weather conditions. A reconnaissance seismic survey of the area suggests that faulting does not constitute a major hazard.

Geological studies on the COST No. B-2 well in the Mid-Atlantic Outer Continental Shelf area

Until recently, all information on the stratigraphic framework of the U.S. Atlantic Outer Continental Shelf (AOCS) had come from onshore wells, offshore bottom sampling or shallow coring, geophysical surveys, and extrapolation from Canadian offshore wells. However, the first deep stratigraphic test well was drilled on the AOCS by Ocean Production Company, which acted as operator for a group of 31 petroleum companies, the Continental Offshore Stratigraphic Test (COST) Group. This hole, designated the COST No. B-2 well, was drilled on the outer part of the AOCS about 146 km east of Atlantic City, N.J.

Much basic lithologic and stratigraphic data, mostly derived from industry reports, has been released (Smith and others, 1976), and this study and other USGS studies on the well samples and on related geophysical data have been summarized (Scholle, 1977).

The well was drilled on the eastern flank of the Baltimore Canyon Trough to a total depth of 4,810 m. E. C. Rhodehamel and P. A. Scholle stated that it penetrated a section composed almost entirely of sand and shale and subordinate amounts of limestone, coal, and lignite. Biostratigraphic studies by C. W. Poag, P. C. Valentine, R. A. Scott, and E. I. Robbins showed that the uppermost 1,500 m is of Tertiary and Quaternary age and was deposited in nonmarine to deep marine environments. The Upper Cretaceous section is about 900 m thick and is of dominantly shallow marine origin. The basal 2,400 m of sediment was tentatively determined to be entirely of Early Cretaceous age, the basal sediments being dated as Berriasian. This Lower Cretaceous section is primarily nonmarine to very shallow marine in origin.

Examination of cores, well cuttings, and electric logs shows that thick potential reservoir sands are found through much of the section. However, porosity and permeability decrease strikingly in the deeper parts of the Lower Cretaceous section as a result of compaction and cementation. Most of the sands are quite feldspathic, and progressive decomposition of feldspar stimulates the formation of authigenic clay and silica.

E. I. Robbins, G. E. Claypool, C. M. Lubeck, J. P. Baysinger, and T. G. Ging reported that studies of color alteration of visible organic matter, organic geochemistry, and vitrinite reflectance show that, although many units have high organic-carbon contents, moderately low geothermal gradients may have retarded thermal maturation. This hypothesis, in conjunction with the scarcity of marine-derived organic matter in the lower part of the section, suggests a relatively low potential for the generation of liquid hydrocarbons. However, the overall combination of source beds, reservoirs, seals, structures, and thermal gradients may be favorable for the generation and entrapment of natural gas. Geophysical studies conducted by D. J. Taylor, R. E. Mattick, and K. C. Bayer showed the presence of reservoir rocks, seals, and trapping structures with a significant potential for entrapment of either natural gas or petroleum that was generated deeper in the basin and then migrated either laterally or vertically. In addition, "bright-spot" studies suggest the possibility of at least one substantial gas accumulation.

An earlier estimate (before drilling of the COST No. B-2 well) of an 85-percent marginal probability of finding hydrocarbons in commercially recoverable quantities remained substantially unchanged. Mattick, Scholle, O. W. Girard, Jr., J. A. Grow, and J. S. Schlee interpreted common-depth-point reflection records to show a Lower Cretaceous shelf-edge carbonate complex beneath the slope. Reef, back-reef, and fore-reef facies beneath the slope are considered to be potential reservoirs; possible analogs are the carbonate reef trends of the El Abra and Tamaulipas Formations of Mexico and the Edwards Limestone of Texas. However, there are radical differences between the hydrocarbon production of the Mexican Unit and that of the Texas unit owing largely to the degree of exposure to subaerial diagenesis. These differences pose problems in the prediction of the reservoir properties of equivalent Atlantic margin reefs because their diagenetic history is largely unknown.

Environmental conditions of the Mid-Atlantic Continental Shelf

Studies conducted off the Middle Atlantic States by H. J. Knebel, D. W. Folger, Bradford Butman, M. H. Bothner, and W. P. Dillon included long-term observations of sediment movement made by deploying tripod systems. Bottom-current and time-lapse camera observations show that vigorous bottom-water flow (40-50 cm/s) at depths greater than 60 m is caused largely by the passage of strong winter storms during which sand ripples form rapidly and marked changes are noted in bottom turbidity. Wave-generated currents are especially important in determining initial sediment motion. Mean currents during storms are primarily parallel to the coast and may transport suspended matter as much as 30 km along the shore. Flow to both the northeast and the southwest was observed during winter storms.

During the summer months, internal waves, which may be important in the transport of suspended bottom material, are present. The internal waves generally occur in distinct packets of 2 to 10 waves; these packets have periods on the order of 15 minutes, which appear to correlate with the semidiurnal tide.

Studies of high-resolution seismic-reflection profiles and sediment samples show that the surficial sand sheet at the sea floor is of Holocene age and ranges in thickness from 0 to 20 m; the ancestral Delaware River valley trends southeastward from the mouth of Delaware Bay to the head of Wilmington Canyon; and shallow faults with a throw of about 1.5 m offset sediments to within 7 m of the sea floor near the edge of the continental shelf off New Jersey.

Studies of the natural variability of hydrocarbons in sediments of the Mid-Atlantic Continental Shelf were conducted by R. E. Miller and D. M. Schultz in conjunction with environmental assessment studies made by the Bureau of Land Management. In 150 surface-sediment samples, the aliphatic (straight chain) hydrocarbons occur in very low concentrations, generally less than 5 mg/g of sediment. The aliphatics are dominated by two major components: (1) A "triplet" in the $n\text{-}C_{20}$ to $n\text{-}C_{21}$ region, and (2) the long-chain odd-carbon wax ester hydrocarbons in $n\text{-}C_{25}$, $n\text{-}C_{27}$, $n\text{-}C_{29}$, and $n\text{-}C_{31}$. Only a trace of aromatics was detected in a few of the sediments. The odd-to-even ratio of the normal alkanes and the "triplet" and long-chain odd-carbon wax ester hydrocarbons suggest that these aromatics occur naturally and are not caused by man's activities. Miller and Schultz also analyzed samples from stratigraphic cores collected onboard the *GLOMAR CONCEPTION*. They found methane concentrations ranging from less than 100 ppm to more than 400×10^3 ppm. In several coreholes, significant amounts of ethane and propane were detected (Hathaway and others, 1976). The highest concentrations of methane, ethane, and propane were found in sediments of Pleistocene age from the upper continental slope. Hole 6021-C, 139 km east of Atlantic City, N.J., was drilled in about 300 m of water. Cores contained concentrations of methane in excess of 290×10^3 ppm over a 200-m-sediment section and concentrations of ethane that increased relative to concentrations of methane with increasing core depth. Leakage of light hydrocarbons from deeper sediments may, in part, account for this relationship. The high gas content may cause instability in the upper continental slope sediments and thereby lead to unstable foundation conditions for offshore platform structures.

Interstitial water studies made aboard the *GLOMAR CONCEPTION* by F. T. Manheim, F. A. Kohout, M. H. Bothner, and Robert Schoen indicated that a lens of relatively fresh water (salinities less than 3 ppt) extends beneath the continental shelf as much as 111 km seaward from the New Jersey coast. Water of about 1 ppt salinity was found beneath the shelf more than 13 km off Ocean City, Md., and Barnegat Inlet, N.J. (Hathaway and others, 1976).

Accuracy of bathymetric chart comparisons—a case study

Bathymetric charts of the same location made on different dates have often been compared to yield measurements of the net erosion and accretion of the sea floor. These measurements have been used for a variety of purposes, including coastal sediment budget studies and design criteria for pipelines and offshore structures. The reliability of the derived measures, however, has more often than not been ignored. A case study was undertaken by A. H. Sallenger to describe useful techniques whereby the accuracy of a given comparison can be ascertained.

A comparison of charts (smooth sheets) from surveys made in 1852 and 1933 off the eastern shore of Virginia indicated that the ridge and swale topography (a common morphological component of the central east coast inner shelf) had become better developed between the two dates. The ridges had grown in height, and the swales had been more deeply eroded. This response of the ridges and swales agrees with one of the dominant hypotheses on the dynamics of these features—that helical cells confined between ridges scour the swales and deposit sediment on the ridges. Before the indicated changes and the evident correlation can be accepted, however, the accuracy of the comparison must be considered.

The vertical and horizontal precision of soundings can be determined by analyzing the vertical differences indicated at sounding-line crossings. A confidence interval on horizontal and vertical precision can be determined by measuring the differences at each line crossing and computing the standard deviation for each chart. Horizontal errors caused by distortion of the charts should be determined.

The interpolation error can be obtained by analyzing compared depth profiles. The depth differences are obtained where soundings occur at the same or approximately the same horizontal location on each profile. The probable amount of real change is the quantity by which the derived vertical errors are exceeded. The depth differences at points where interpolations are necessary are then measured. The interpolation error amounts to that part of the depth difference that exceeds the vertical errors plus the local real change.

The application of these techniques to the comparison of the ridge and swale topography shown on the Virginia charts results in an error of ±1.9 m at the 95-percent level owing to horizontal and vertical precision. There was no measurable distortion error. At points where the soundings of one chart overlay the soundings of the other, the depth differences (in the region of ridge and swale) are less than this error. In view of these results, the indicated changes over the ridge and swale topography cannot be considered accurate.

Shallow structure of the South Atlantic Continental Shelf

High-resolution reflection records reveal a number of regionally correlatable erosional unconformities within Cenozoic sediments of the South Atlantic Continental Shelf. The identity of those unconformities has been established in wells tied into the seismic net. Faulting and slumping revealed on the reflection lines are not on a scale that appears to constitute a hazard to drilling for oil and gas.

Preliminary analysis of the core data indicates that the upper 5 m or so of sandy shelf sediment is Holocene in age and overlies a patchy crust capping finer grained sediments.

W. P. Dillon (USGS) and D. W. Edsall (U.S. Naval Academy) reported that 19 northwest-southeast traverses were made with a minisparker across the continental shelf, the Florida-Hatteras Slope, and the western part of the Blake Plateau between latitude 30° and 34° N. Two northeast southwest traverses were run as tielines, one across the shelf just west of the shelf break and the other across the Blake Plateau near the southeastern end of each traverse. The acoustic-stratigraphic sequences observed on the minisparker records were dated by extrapolation of ages assigned to various vibracore and piston-core samples and to cores from two holes (6002 and 6004) drilled for the USGS by the *GLOMAR CONCEPTION* (Hathaway and others, 1976). The continental shelf and slope formed by upbuilding and outbuilding on a sequence of Upper Cretaceous and Paleocene sediments. Sediments of Eocene and Oligocene age generally are absent. Miocene, Pliocene, and Pleistocene sediments are restricted to the shelf and slope south of 32°30′ N. To the north, they are also present on the Blake Plateau. The records clearly show the formation of the shelf and slope in a stable area, where dynamic equilibrium has been reached between sediment supply and the erosional activities of the Gulf Stream and its predecessors. North of 32°30′ N., depth decreases noticeably to the top of the Paleocene sequence. The decrease in depth coincides with an abrupt change in the strike of erosional channels cut into the Paleocene sequence. The channels are filled with Miocene sediments, which are overlain by Pliocene, Pleistocene, and Holocene sediments. The Upper Cretaceous and Paleocene sediments apparently were deformed to a platform that was shallow enough to deflect currents, so that sediments of Miocene, Pliocene, and Pleistocene age could accumulate on the plateau north of 32°30′ N.

GULF COAST AND CARIBBEAN SEA

Gulf of Mexico Continental Slope—a petroleum frontier

The continental slope of the northern Gulf of Mexico is the seaward face of the petroleum-rich gulf coast basin and includes all of the steeply sloping sea floor from the shelf edge (200 m) to the abyssal plain (3,200 m). The structural grain and hummocky topography of the slope are controlled primarily by salt tectonics, and almost the entire province is underlain by gigantic salt stocks and pillowlike swells. Basinal areas between salt domes commonly contain as much as 3.5 km of sediments, most of which are muddy slump deposits with infrequent turbidite sand zones. Despite the apparently low incidence of turbidite sands encountered in exploratory drilling on the upper slope, R. G. Martin suggested that sands of reservoir quality could conceivably be present in intraslope basins, especially in Pleistocene strata that accumulated when shorelines and sediment sources were close to the present shelf edge. Prospects in the upper slope province include strata of Pliocene and Pleistocene age in the area seaward of the Mississippi Delta and mainly Pleistocene age elsewhere. Potential reservoirs are expected in regressive wedges of neritic sand and in turbidite accumulations and localized along zones of shelf-edge growth faults and on the flanks of salt structures.

Future production of hydrocarbons from the Gulf of Mexico Upper Continental Slope appears likely. The greatly increased cost of operating in deep water beyond the shelf is doubtlessly an inhibiting factor, but recent discoveries of major hydrocarbon accumulations in the upper slope off the Mississippi Delta suggest the budding of a petroleum frontier in the Gulf of Mexico.

Common-depth-point seismic survey in Gulf of Mexico

The Geophysics Laboratory of the University of Texas Marine-Science Institute at Galveston conducted a 8,154-km multichannel seismic survey in the Gulf of Mexico. The survey was partly supported by a research grant from the USGS. Twelvefold common-depth-point data were collected along twin parallel tracks from the Florida platform in the eastern Gulf of Mexico to the Mexican shelf near Tampico, and from the Texas shelf to the Banco de Campeche off the Yucatan Peninsula. Additionally, a pair of twelvefold lines were recorded from the Sigsbee Knolls to the continental shelf adjacent to the petroleum-rich State of Tobasco in southern Mexico. Important tectonic features such as the Sigsbee, Campeche, and Florida Escarpments, the Campeche Knolls, and the Mexico Ridges were surveyed along detailed grids where 24-channel data were recorded. The data are being studied by university, company, and USGS scientists. R. G. Martin reported that general results of the studies so far include the finding of additional salt diapirs north of the Campeche Escarpment, which indicate that the Sigsbee Knolls salt province extends more than 60 km eastward of its previously interpreted limits. A deep reflection event marks the top of Jurassic salt in the Sigsbee Knolls region, and the event can be traced to the edges of the deep gulf basin, where it is lost beneath thick continental slope deposits beyond the limits of seismic penetration. Seismic-stratigraphic and velocity evidence show that strata of Cretaceous age and older lie relatively undeformed beneath the Mexican fold zone, the suggestion being that the Mexican Ridges formed in response to downslope movement and plastic deformation of shales of probable early Tertiary age.

Studies of bottom stability in the northern Gulf of Mexico

L. E. Garrison and J. S. Booth compiled a preliminary map of potential geologic hazards on the upper continental slope of the northern Gulf of Mexico by using more than 17,700 km of high-resolution sparker records. The map reveals widespread areas of shelf-edge slumping, shallow faulting, shallow gas-charged zones, and mud flows just at or below the shelf break throughout the region. More detailed seismic surveys were then made of 15 of the apparently unstable areas, and piston cores were taken at selected sites within these areas. Sedimentological and geotechnical analyses of the cores and surface geologic maps of the areas investigated indicate that most of the features studied are relicts from former low sea levels. Sediment carried across the exposed shelf by Pleistocene rivers accumulated rapidly in the shallow waters as deltaic deposits on the present upper slope. Slumps and slides were common when the growing sediment slopes became oversteepened. Since the Holocene rise of sea level, most of the river-transported sediment has been trapped in coastal bays and lagoons or on the shallow inner shelf, and depositional rates on the upper slope have been greatly diminished. Some upper slope areas still contain unstable sediments, however, especially where the Mississippi Delta extends across the shelf and pours sediment onto the upper slope. Mud flows, slumps, shallow faults, and gas-charged zones may be found in these areas. Gas from leaking reservoirs may charge the shallow sediments in other slope areas and prove hazardous to drilling or boring operations. In areas of rugged topography, sediment on the flanks of diapiric uplifts must be considered potentially hazardous until more information becomes available.

Bottom-motion response to wave pressures

Field measurements of bottom oscillations and wave characteristics were made by J. N. Suhayda in a study of the interaction of fine-grained sediments and surface waves. The results of the experiments indicate that bottom motions under wave action show well-defined periodic features. Bottom oscillations on the order of 2.5 cm in amplitude occurred for seas having a significant wave height of about 1 m and a period of 5 seconds. The bottom appears to undergo an elastic wave response to changing bottom pressure and is depressed under a surface wave crest. Comparisons of wave-height measurements indicate that bottom pressures are not predicted by linear theory for a rigid bottom. Pressures were larger than predicted by up to 35 percent in many cases. Under the range of bottom pressures measured, bottom displacement varied linearly with bottom pressure. The wave energy lost to the bottom was found to be an order of magnitude greater than the energy lost to bottom friction.

Thus, it appears that direct measurement of the sea-floor oscillations accompanying storm-wave conditions is feasible with present techniques and can provide useful information to define the characteristics of bottom motion. These results suggest that cyclic testing for softening of soils based upon several cycles of forcing (2–10), separated in time by quiet intervals of 10 to 20 wave periods, may be more representative of the natural situation than tests of equal-amplitude waves run over 10 to 100 cycles. Further, design-wave heights in muddy regions actually may be reduced inshore of shelf areas having soft clay areas.

Environmental studies on the south Texas shelf

Marine geologic investigations of the south Texas Outer Continental Shelf were carried out by H. L. Berryhill, Jr., C. W. Holmes, G. L. Shideler, and Gary Hill. Shideler found that turbidity through the water column is highly seasonal and is greatest in the spring. Patterns of turbidity suggest two regimes of water movement over the shelf. On the inner shelf, suspended sediments are carried generally southward and are spread in fanlike fashion over the entire southern part of the shelf from the northwest; on the outer shelf, however, clear, deep gulf water, almost free of suspended sediments, loops or spreads over the northeastern part of the shelf. The Pb^{210} dating done by Holmes on the undisturbed upper few centimeters of sediments in cores indicated local rates of deposition of as much as 5 mm/yr for midshelf areas. A synthesis of the investigations indicates that two well-defined regimes for the south Texas shelf will be pertinent in assessing the impact of petroleum development. The inner shelf is characterized by (1) high continental runoff in the spring, including encroachment of Mississippi River water; (2) high nutrient levels; (3) high biological activity for most types of organisms; and (4) increases in the contents of some trace metals related to the runoff and the biological activity. The outer shelf is characterized by (1) a looping or spreading of deeper gulf water in all seasons; (2) increased nutrients in the water but generally low biological activity for all organisms except microzooplankton; (3) downfaulting of the continental terrace with possible escape of natural gas along the faults; and (4) localized slumping of surficial sediments along the shelf edge.

Suspended sediments of Corpus Christi Bay in Texas

Suspended sediments of the Corpus Christi Bay estuary of Texas were studied during a flood tide in the months of May, June, and August. G. L. Shideler and Frances Firek reported that quasi-synoptic water samples and vertical light transmissivity-temperature profiles were obtained at seven monitoring stations along the axial trend of the bay. The water-column transmissivity generally indicated an increasing turbidity gradient with depth at individual stations; stations near the bay's tidal inlet generally exhibited the lowest turbidity and thus reflect relatively transparent oceanic tidal floodwater. Gravimetric analyses indicated that the monthly ranges of sediment concentrations were 6.0 to 164.0 mg/L in May, 15.2 to 59.6 mg/L in June, and 0.4 to 41.2 mg/L in August. Vertical temperature profiles generally indicated isothermal conditions at each station, which apparently reflect the shallowness of the bay and mixing by local winds. Sediments are composed primarily of inorganic silt-clay particles but contain a subordinate phytoplankton fraction dominated by diatoms.

Corals as climatic and environmental indicators in southern Florida and Dry Tortugas

E. A. Shinn, R. B. Halley, J. H. Hudson, and B. H. Lidz reported that X-radiograph analysis of corals from various modern environments suggests that the width of bands (which is equal to annual growth rate) may be a useful indicator of both water depth and temperature. This information, in addition to being useful for environmental analyses in modern reefs, may also help determine water depth and temperatures in Pleistocene coral deposits in southern Florida (Hudson and others, 1976a, b). Shinn and his colleagues also discovered by drilling that the reefs at the Dry Tortugas (Fort Jefferson National Monument) have never contained *Acropora palmata*. This discovery has significant environmental implications, for it clearly indicates that the absence of the coral on the present reef is not due to the activities of man, such as the construction of Fort Jefferson. The absence of *A. palmata,* thought to be caused by low winter water temperatures, may explain why this species is also absent from the Key Largo Limestone (Pleistocene). In the past, this absence was thought to indicate that Key Largo was a patch reef.

Puerto Rican offshore sand resources

Preliminary investigation of Puerto Rico's major offshore potential sand deposits suggests that extracting sand from at least some of them would not significantly affect the island's severely eroded coastline. Novel sand-movement maps for two of the sand areas, made by Jose Muniz and Nelson Espinell, used the technique of algebraic addition of contoured soundings used on two bathymetric surveys made 60 years apart by the National Ocean Survey (formerly Coast and Geodetic Survey). The maps show that the sand in a field of sand waves seaward of Bahia Sucia is apparently being swept seaward around the rocky southwestern tip of Puerto Rico. Stakes have been set in the sand-wave field by scuba divers to permit precise measurement of sand movement. Off the northwestern tip of Vieques Island, the maps show sand accumulation in a protected shallow-water area well away from land.

PACIFIC COAST

Pre-Neogene sedimentary rocks found on Santa Catalina Island

Miocene volcanic and sedimentary rocks on Santa Catalina Island were reinvestigated by J. G. Vedder and D. G. Howell to aid interpretation of the geology along the submergent Santa Cruz-Catalina Ridge. Work done on the island revealed heretofore unrecognized stratigraphic relations and ages that are critical in reconstructing regional paleogeography and tectonism. In the northwestern part of the island near the isthmus, a sequence of interlayered schist breccia lenses, volcaniclastic beds, and pyroxene andesite flows, flanks, and partly drapes over a large dacite dome. These rocks, in turn, are overlain by interbedded diatomaceous shale, lapilli tuff, and basaltic andesite flows. Fossil mollusks, calcareous phytoplankton, benthic foraminifers, and diatoms indicate that the sedimentary sequence accumulated in a shallow (< 200 m) marine environment during a short span of provincial middle to late Miocene time. Unpublished K-Ar dates on the volcanic rocks range from approximately 12 to 15 million years. At the southeastern end of the island, a thick zone of greenschist breccia is pervasively intruded by dacitic rocks that presumably are offshoots from the approximately 19-million-year-old quartz diorite porphyry pluton; although these relations were previously recognized, underlying variegated sandstone and mudstone beds and an interbedded marine sandstone, siltstone, and conglomerate unit have not been described. These underlying strata resemble elements in nonmarine Oligocene(?) and marine Upper Cretaceous formations of the Santa Monica Mountains and eastern Los Angeles basin of California. The nearest known occurrence of similar rocks is in surface and subsurface sections in the San Joaquin Hills nearly 50 km to the northeast. Formerly, it was believed that pre-lower Miocene sedimentary rocks were not present anywhere along the Santa Cruz-Catalina Ridge, and paleogeographic interpretations reflected this concept. The new findings require substantial revision of previous tectonic reconstructions.

Investigation of bottom boundary layers and sediment transport on continental shelves

A self-contained tripod-mounted instrument package for studying the bottom boundary layer and sediment-transport processes on the continental margin was developed and field tested by D. A. Cacchione and D. E. Drake. The system consists of five current-velocity sensors mounted in a vertical array within 2 m of the sea floor; a quartz crystal pressure transducer; four thermistors; a light transmission and scattering sensor; a 35-mm-camera system capable of taking 800 pictures; and an acoustic release system for tripod recovery. The tripod has been designed to operate unattended for as long as 3 months at depths up to 300 m. Rates and intervals of sensor sampling can be programmed to provide statistically reliable evaluations of the flow field induced by high-frequency surface waves and lower frequency forcing mechanisms.

Initial field tests were successfully completed off San Diego, Calif. and Nome, Alaska. Preliminary current and temperature data from the San Diego experiment (Cacchione and others, 1976) show that the internal barotropic and baroclinic tides propagate past the experimental site as surgelike periodic features characterized by intense horizontal thermal gradients. These tides are followed by a cluster of relatively large amplitude (1 to 3 m), higher frequency internal waves.

Underwater television monitoring of the sea floor in the vicinity of a transmissiometer and pressure and temperature sensors indicated a strong correlation between surface waves and bedload transport. Decreases in near-bottom visibility, as measured by the underwater television and the transmissometer, were related to the passage of the internal surge. Specifically, low light transmission was strongly correlated with temperature increases caused by passage of the internal wave trough near the sea floor.

Shallow structures of the Oregon-Washington shelf

High-resolution profiles obtained on the Oregon and Washington Outer Continental Shelf during the cruise of the SP *Lee* provide significant new information on the shallow structures of the shelf. P. D. Snavely, Jr., reported that numerous north-trending normal faults offset all but the recent sea-floor sediments on the inner shelf off central Oregon. These faults probably correlate with a set of north-trending faults mapped along the coast by Snavely and others (1976). Onland, these faults offset strata of middle Miocene age but do not cut the marine terrace deposits. On the Washington inner shelf off Grays Harbor, a trap-door-type fault offsets the sea floor and has a throw of about 20 m. Recent faults also are associated with several of the large shale diapirs traversed during the cruise. One diapir, acting as a piston, lifted the sea-floor sediments some 10 to 20 m above its roof. Broad marginal synclines are often associated with the shale diapirs, but strata turn up rapidly along the flanks of the diapirs. Numerous growth faults are found on the flanks of the shale diapirs. A line across a broad anticline located on the outer shelf off the central Oregon coast contains a horizontal reflector that cut across the gently folded strata. This reflector may be a gas phase, or clathrates, trapped near the crest of this anticline.

Deep-sea Navy Fan of southern California

W. R. Normark and G. R. Hess used a deeply towed geophysical instrument package to survey the deep-sea Navy Fan in the San Clemente Basin of southern California. The study revealed a radial pattern of shallow distributary channels formed at the terminus of the prominent leveed fan valley of the upper fan. Scours, resembling flute marks but measuring 10 to hundreds of meters across, have formed in sandy sediments on the middle fan. Bottom photographs reveal a fairly uniform sediment cover over the entire fan, but the acoustic reflectivity of the surficial sediments and sediment distribution data from cores show that surface sand is more common in southern distributaries than it is in northern ones, the suggestion being that the locus of deposition has shifted.

Depositional environment of an upper Miocene sand in Santa Cruz Mountains of California

Extensive channeling, thick sets of crossbedded sand and gravel, undirectional current structure, and marine fossils characterize the tidal-current-dominated Santa Margarita Sandstone (upper Miocene) in the Santa Cruz Mountains of California, according to Larry Phillips. The preserved channel may be as wide as 2 km and may contain an erosional base with thick lag deposits of shells or gravel. Large-scale (to 8 m) crossbedded sand and gravel may fill the channels as unidirectional crossbedded sets. Migration of the channel with lateral accretion of the channel wall or migration of tidal-current ridges account for much of the depositional sequences of the channel-fill sediments. Extensive bioturbation and the presence of marine vertebrates and echinoids indicate a marine origin for the crossbedded sands. A west-to-southwest current direction dominates much of the depositional structures. Current reversals with east-to-northeast directions occur locally on channel lag gravels or on the southern side of topographic ridges. A depositional environment dominated by shallow marine, high-energy tidal currents characterizes much of the history of the Santa Margarita Sandstone. Displacement back along the San Andreas fault further suggests that the Santa Margarita represents a seaway connection between the Pacific Ocean and the late Miocene sea that occupied the present San Joaquin Valley.

Distinguishing sorting and source effects in beach-sand mineralogy

Using elemental analyses of titanium and chromium in magnetite from beaches rich in black sands appears to be a statistically valid means of distinguishing between sorting and source effects on the southwestern Oregon coast. Gretchen Luepke found that the ratio of titanium to chromium in the magnetic fraction of a sample is for the most part independent of the relative location of the sample along a beach and also is independent of the percentage of heavy minerals or magnetite within the sample.

Hydrocarbons in sediments of Willapa Bay, Washington

Willapa Bay is an estuary on the relatively unpopulated and unindustrialized southwestern coast of Washington. K. A. Kvenvolden, J. B. Rapp, and H. E. Clifton have been studying hydrocarbons in the silty muds of this bay as a measure of man's impact on this generally pristine region.

Complex mixtures of hydrocarbons, attributed to petroleum-derived products, are concentrated in sediments near Raymond on the Willapa River and probably come from surface runoff and sewage effluent. The complex mixture is less evident on the northern side of the bay near the mouth of the river and is barely detectable in sediments from the southern portions of the bay. The data define a baseline for evaluating the impacts of possible future petroleum-related development affecting this part of the coastline.

Tidal point bar sequences in Willapa Bay, Washington

Tidal point bars are an important depositional component in an estuary. Studies conducted by H. E. Clifton and others showed that the sedimentary facies in tidal point bars are characterized by distinctive vertical sequences and consistent lateral trends. Grain texture strongly controls the character of physical and biological structures. In the subtidal environment, grain size decreases both laterally upslope and longitudinally upriver. In the intertidal environments, grain size depends dominantly on the amount of expended wave energy. A complete vertical sequence shows, in upward progression, channel-bottom deposits (characterized by intense bioturbation and the development of lag deposits); accretionary bank deposits (generally well bedded); tidal creek deposits (finely laminated cross-stratified mud); tide flat deposits (intensely bioturbated or, if bound by algae, broadly and horizontally stratified); and supratidal flats (finely,more or less evenly laminated muds containing abundant rootlets). The nature of the vertical sequence changes systematically as a function of grain-size differences. Numerous examples of tidal point bar sequences in the Pleistocene terrace deposits bordering Willapa Bay validate this general sedimentary model.

ALASKAN-ARCTIC INVESTIGATIONS

Slope instability related to tectonics in western Gulf of Alaska

Lower Cook Inlet in Alaska has high tidal currents that average 6 to 7 km/s and normally reach a peak of 11 to 15 km/s. The bottom has an average depth of about 60 to 70 m in the central part of the inlet at the latitude of Homer and deepens toward the south. Several types of bedforms, such as sand waves, dunes, ripples, sand ribbons, and lag deposits, form a microtopography on the otherwise smooth sea floor. Each bedform type covers a small field normally a few hundred to a few thousand meters wide and usually several kilometers long parallel to the tidal-flow direction. High-resolution seismic systems, side-scan sonar, and bottom television were used by A. H. Bouma and M. A. Hampton to detect locations and to study some of the characteristics of these bedforms. They observed large sand waves with wavelengths in places over 300 m and wave heights up to 10 m. Fields of ebb- or flood-oriented asymmetric bedforms often grade into more symmetrical shapes. Several orders of smaller sand waves and dunes cover the flanks of the very large bedforms. Normally, the crest directions of both size groups are parallel, but deviations up to 90° have been observed. Local deviations may occur where smaller forms approach the crests of the larger sand waves.

Bottom-television observations revealed active bedload transport in a northerly direction on the crests and midflanks of southerly asymmetric large sand waves. In their troughs, no transport could be observed. Movement of bedload occurs by small ripples.

Although the asymmetry of the large bedforms suggests that migration has taken place in the ebb or flood directions, the very low surface angles (2.5° to 8°) of these bedforms do not indicate regular movements. It is probable that the large bedforms are relict features or migrate only under severe conditions, whereas active sand transport by ripples and smaller sand waves and dunes moves bedload back and forth with the tides. An understanding of such movements is essential for determining design criteria for offshore installations and for benthic faunal studies.

The uppermost continental slope in the western Gulf of Alaska, from southern Albatross Bank to Portlock Bank, includes two broad areas where large rotational slumps occur and one intervening area where they are absent. The large slumps involve sediment a few hundred meters thick. The areas where large slumps are present show evidence for active near-surface folding and consequent steepening of slopes, which apparently is the ultimate control on slumping. No evidence for similar active steepening was found in the area containing no large rotational slumps, where slope gradients are relatively gentle.

Thin debris slides, which differ fundamentally from the larger rotational slumps and involve sediment only a few tens of meters thick, occur in all three areas on slopes that are not necessarily actively steepening. These slides probably are stratigraphically controlled, the failure occurring along a weak subsurface stratum.

Strong earthquakes and the related accelerations probably are responsible for the actual triggering of many of the large and small slumps. As long as the tectonic setting remains as it is today, future large-scale rotational slumping should remain confined to the two broad areas in which it presently exists. However, the shallow debris slides might occur in any of the three areas.

Structural features of the Bering Sea Outer Continental Shelf

Over 5,000 km of geophysical data including multichannel seismic-reflection profiles were collected in the Bering Sea. M. S. Marlow, A. K. Cooper, D. W. Scholl and K. A. Bailey reported that these data revealed the existence of a new subshelf basin called the Amak Basin near the Alaska Peninsula. This elongate graben is alined with the St. George and Sanak Basins and is filled with more than 5 km of sedimentary layers. In nearby Bristol Bay basin, a number of large slump structures that cut the basin fill were discovered. These structures may be environmental hazards to future exploratory drilling, especially close to the Alaska Peninsula. Anticlinally deformed Mesozoic rocks exposed on the Alaska Peninsula can be traced offshore beneath the shelf over 200 km west of the peninsula.

A geophysical line near Siberia over the Navarin Basin revealed large folded and truncated beds within the basin fill. Numerous high-amplitude reflectors and associated velocity "pulldowns" were also detected and may be indicative of hydrocarbon accumulations. Sediment thickness in the basin exceeds 15,000 m.

Mantle refractions from airgun seismic data

A preliminary interpretation by A. K. Cooper and J. R. Childs of sonobuoy refraction measurements made in the Aleutian Basin in the Bering Sea showed that it is possible to record refraction arrivals from the crust-mantle boundary by using a rapidly fired (18 second) sound source consisting of a tuned array of variable-power airguns (total power of 21,750 cm^3). Mantle-refraction arrivals were observed on several sonobuoy records collected exclusively from deep (13,800 m) water areas underlain by thick accumulations of flat-lying sedimentary rock (3-5 km thick). Previous attempts at recording mantle-refraction arrivals in the Aleutian Basin (Ludwig and others, 1971) have been accomplished only by using two-ship dynamite-shooting techniques. The ability to record deep-earth refraction arrivals (from 15-km depths) by using rapid-fire airguns offers a faster and more economical method for obtaining information on deep crustal structure in deep-water geologic environments.

Littoral drift directions along the Bering Sea coast

The pattern of littoral drift along the Bering Sea coast from Bering Strait to the tip of the Alaska Peninsula was interpreted from geomorphic evidence by R. E. Hunter, A. H. Sallenger, Jr., and W. R. Dupre. The kinds of features used as evidence included (1) bays of hooked planform, (2) shoreline offsets at headlands, (3) spits, (4) patterns of beach ridges, (5) barrier islands of tapering planform, (6) deflected stream mouths and tidal inlets, (7) shoreline offsets at stream mouths and tidal inlets, and (8) nearshore bars oriented obliquely to shore. Convergence points of the littoral drift system tend to occur within embayments, and divergence points tend to occur at headlands. The drift directions, dominantly to the north and the east, can be explained by waves approaching from the southwest, and local deviations from this pattern can be explained by refraction of the main wave trains as they approach shore.

Complex topography on a shelf in northwestern Alaska

C. H. Nelson, D. A. Cacchione, M. E. Field, D. E. Drake and Tor Nilsen found that linear sand shoals 15 to 30 km long, 3 to 7 km wide, and 5 to 15 km high occur near the Bering Straits in Alaska. These sand bodies are all constructional, but they apparently represent an interplay of sedimentary processes related to past transgressive shoreline history and present strong, northward-flowing currents. Ridge crests coincide with depths of ancient submerged beaches elsewhere in the northern Bering Sea. However, sand waves and current and oscillation ripples demonstrate active modification by the present current regime. Other sand bodies as much as 50 km long, 10 km wide, and 10 to 20 m high appear to have been caused by secondary (leeward side) circulation systems induced by the presence of King Island and the promontory of Cape Prince of Wales.

Current measurements and observations of the shoal crests made by underwater television demonstrate active bedload movement in oscillation sand ripples; current speeds measure 20 to 30 cm/s. Water samples taken 2 m above the shoal contain abundant terrigenous coarse silt and locally very fine sand. Asymmetrical sand waves (height about 2 m, wavelength about 15 m) superimposed on the linear shoals are generally alined normal to the mean (northward) bottom currents, but these bedforms are probably active only during periods of intensified flow caused by storms.

The studies suggest that these large linear sand ridges have been generated by three major processes: (1) Deposition from interrupted current flow leeward of islands and peninsulas; (2) initial formation as spits at shoreline stillstands during transgressions; and (3) accumulation mainly as modern sand-wave fields modifying ancient constructional features.

Beaufort Sea nearshore studies

Satellite imagery, together with a variety of ice and seabed data, including side-scan sonar, high-resolution seismic-reflection data, and precisely controlled bathymetric surveys, was used by Erk Reimnitz, L. J. Toimil, and P. W. Barnes to study the zonation of sea ice in relation to shelf dynamics, bottom morphology, and geologic processes on the Beaufort Sea Continental Shelf.

During the early winter, the location of the boundary between undeformed fast ice and the westward drifting polar pack ice is controlled by major coastal promontories. Pronounced linear pressure and shear ridges, as well as hummock fields, form along the boundary and are stabilized by grounding, generally between the 10- to 20-m isobaths. Slippage along this boundary occurs intermittently at or seaward of the grounded ridges and forms new grounded-ridge systems in a widening zone—the stamukhi zone—which by later winter may extend out to the 40-m isobath. The stamukhi zone protects the inner shelf and coast from pack-ice forces.

There is a causal relationship between the spatial distribution of major ice-ridge systems and the offshore shoals downdrift of major coastal promontories. Ice has forced the shoals to migrate shoreward over distances of up to 400 m in the last 25 years. The sea floor seaward of such shoals, within the stamukhi zone, shows a high density of ice gouges, a great depth of incision, and a high degree of disruption of internal sedimentary structures. The concentration of large-scale ice deformation and intense sea-floor disruption in the stamukhi zone indicates that a considerable amount of the available marine energy is expended here during winter. The inner shelf and coast, where the relatively undeformed fast ice grows, are sheltered.

Properly placed artificial structures similar to offshore shoals should be able to withstand the forces of the ice, should serve to modify the observed ice zonation, and might be used to make the inner-shelf environment less hostile to man's endeavors.

Studies conducted near Prudhoe Bay by Barnes, Reimnitz, and G. L. Smith suggested a coastal erosion rate of 1 to 2 m/yr. The entrance channel to the bay also has apparently migrated shoreward at a similar rate, at least since 1950, and possibly experiences seasonal erosion and infilling; the erosion is due to flow restrictions accompanying the growth of the ice cover, and the infilling is the result of dominant northeasterly summer winds. The onshore movement of a nearby barrier island is additional evidence for the relatively rapid retreat of coastal and nearshore morphologic features along this section of the Alaskan arctic coast.

OCEANIC STUDIES

Nodule and sediment distribution and chemistry in North Pacific Ocean

J. L. Bischoff and D. Z. Piper reported that sediment and nodules from the North Pacific Ocean were collected by box coring in an area of about 25 km^2 at Site C as part of continuing USGS participation in NOAA's Deep Ocean Mining Environmental Study (DOMES). The area is located at lat 15°01′ N, long 126°00′ W. Cores collected in this past year's study were more closely spaced than those collected previously from the three DOMES sites. The samples, together with stereo bottom photographs from the same area, were used to estimate nodule abundance. Nodules are observed on the top of three abyssal hills more frequently than they are within channels between the hills. Within these channels, however, nodules tend to be relatively large, usually greater than 4 cm in diameter. Owing to their greater size, nodules within the channels represent a deposit that is approximately 50 percent larger per unit area than the deposits on the tops of abyssal hills.

Metalliferous sediment, observed previously in a single core from this area, was observed within 15 cm of the surface in five additional cores. All of these cores are from the western slope of an abyssal hill. Results of high-resolution seismic studies indicate that near-surface sediment associated with this sediment may be as old as Miocene. In 3.5-kHz records, the surface sediment appears as a series of opaque reflectors, which are overlain elsewhere in this area by a layer of transparent sediment of possible Pliocene and Pleistocene age.

Nodules recently acquired by the USGS from the Summa Corporation were collected in the vicinity of lat 30° N., long 140°–175° W. Analyses of several nodules showed that the elemental composition of their interiors differs from that of the outermost layers. If nodules grow as slowly as radiometric measurements indicate (1–10 mm/m.y.) and if they are rafted from one oceanic bottom environment to another owing to movement of the Pacific plate in response to plate tectonics, then these compositional variations within individual nodules may be related to movement of the sea floor. For example, these nodules would have been closer to the equator during the initial stage of growth, possibly in the area of lat 10°–15° N. Nodules currently forming at this lower latitude are characterized by relatively high Mn-Fe ratios and high nickel and copper concentrations.

Experiments on seawater-basalt interaction are continuing in order to assess the role of heated seawater in the transport of heavy metals found in the metalliferous sediments. Recent results indicate that, when the water-to-rock ratio exceeds 50:1, metal solubility is significantly enhanced. High metal solubility is apparently caused by the acidic nature of heated seawater, which is maintained when not enough rock is present to act as a neutralizer.

Cyclic deposition off northwest Africa

Some of the results of studies related to Leg 41 of the *Glomar Challenger* Deep Sea Drilling Project (DSDP) were reported by J. V. Gardner and W. E. Dean, Jr. Cycles of $CaCo_3$ and clay found in sediments of Eocene to middle Miocene age of the Sierra Leone Rise (DSDP Site 366) are interpreted as resulting from cyclic variations in the dissolution of $CaCO_3$, possibly aided by the influx of terrigenous material. These cycles have periods that range from 7,000 to 21,000 years for chalk-siliceous limestone cycles of Eocene age to 29,000 to 50,000 years for chalk-marl cycles of late Eocene to middle Miocene age. Gardner (1975; Gardner and Hays, 1976) found that these periods are similar to periods reported for climatically induced dissolution cycles in Pleistocene carbonate sediments in the same area. It is thus suggested that variations in the Earth's orbital movement, believed to be the main driving forces for climatic change in the Pleistocene, extended back into at least the Tertiary.

Cyclic interbeds of green and black clay or shale, red and green clay or shale, and white and black limestone and marlstone, ranging in age from Late Jurassic to Eocene in the Cape Verde Basin (DSDP Site 367), appear to be the result of variations in the rate of influx of organic material, largely of terrigenous origin. All of these organic-rich organic-poor cycles have periods on the order of 50,000 years and, like the carbonate dissolution cycles on the Sierra Leone Rise, may reflect climatic changes induced by variations in the Earth's orbital geometry.

Barite rosettes and lenses are common in highly organic Lower Cretaceous sediments at DSDP Sites 369 and 370 along the continental margin of northwest Africa (Dean and Schreiber, 1976). The barite occurs immediately below major unconformities and is associated with marked increases in interstitial water salinities. The barite is interpreted as having formed diagenetically under oxidizing or slightly reducing conditions in sediments exposed at the sediment-water interface for long periods of time during pauses in sedimentation. The main source of barium was oxidation of organic material. Three possible sources of sulfate include (1) downward diffusion of overlying seawater sulfate to replace sulfate consumed by barite formation and (or) sulfate reduction, (2) oxidation of pyrite, and (3) upward diffusion of sulfate from solution of Jurassic evaporite deposits underlying both sites.

Pliocene silicoflagellate correlation of Hess Rise and Walvis Ridge

Hess Rise in the Pacific Ocean (DSDP Site 310, lat 37° N.) and Walvis Ridge in the Atlantic Ocean (DSDP Site 362, lat 19° S.) have rich siliceous and calcareous phytoplankton assemblages of Pliocene and Quaternary age. Both sites are near boundaries between tropical and temperate water masses. J. D. Bukry reported that 8,000 silicoflagellate specimens demonstrate distinct similarities in ranges and abundances for the two sites. The disappearance of *Mesocena circulus* and *Distephanus boliviensis jimlingii* mark the Pliocene-Pleistocene boundary at both sites. *Dictyocha brevispina* disappears in the late Pliocene, and *D. stapedia stapedia* evolves through the Pliocene and becomes a dominant taxon in the Quaternary. Although silicoflagellate assemblages typically show strong paleoecologic influences, the synchroneity of events between sites 310 and 362, calibrated by the more cosmopolitan calcareous nannoplankton, indicates that transoceanic correlation by silicoflagellates can be important in similar paleoecologic settings.

North Atlantic Paleocene silicoflagellates

Deep-sea drilling of the "J-anomaly" ridge at site DSDP 384 south of the Grand Banks recovered the first joint calcareous nannoplankton- and silicoflagellate-bearing sediment of Paleocene age from the North Atlantic area. This association permits a definite regional correlation and new age assignment for the noncalcareous "Eocene diatomite" beds at Fur and Mors in Denmark. The silicoflagellate guide fossils, *Corbisema disymmetrica communis, Dictyocha elongata,* and *Naviculopsis danica,* reported from Denmark are frequent to abundant at DSDP 384. J. D. Bukry reported that the abundant and diverse calcareous nannoplankton assemblages associated with these fossils at DSDP 384 belong to the upper Paleocene *Discoaster mohleri* Zone and *D. nobilis* Zone. This evidence suggests recognition of a more extensive Paleocene section in Denmark.

Geochronology of DSDP basalts from the Ninetyeast Ridge

The Ninetyeast Ridge is a prominent volcanic lineament in the eastern Indian Ocean whose geomorphology suggests that it was formed in a shallow marine or subaerial environment. This linear feature rises just south of its intersection with the Broken Ridge at 33° S. and extends slightly east of north close to the 90th meridian, a distance of about 4,500 km, before disappearing beneath the sediments of the Bengal Fan. R. A. Duncan measured ages on basalts collected by the DSDP at five sites on or near the Ninetyeast Ridge by means of conventional K-Ar and $^{40}Ar/^{39}Ar$ techniques. The basalt ages increase from about 40 million years in the southern sites to about 85 million years in the northern sites. This pattern may be modeled by the northward passage of the Indian plate away from a stationary source of volcanism near Kerguelen Island from Late Cretaceous to Tertiary time.

Methane hydrate in the sea floor

The evidence for the existence of clathrate hydrate of methane in sea-floor sediments and the conditions of its formation were reevaluated by D. J. Milton. Recently published statements that the bulk of organic carbon in sea-floor sediments is trapped as methane hydrate were shown to be based on an incorrect value for the solubility of methane in water in equilibrium with hydrate. Nevertheless, geophysical and deep-sea-drilling results strongly suggest that hydrate exists in some areas.

Holocene rates of reef growth at Eniwetak Atoll

A drill hole cored to a depth of 23 m near the reef edge at Eniwetak Atoll in the Marshall Islands, with nearly complete recovery, provides evidence for rates of reef growth following the Holocene rise of sea level, according to J. I. Tracey, Jr. (USGS), and E. R. Goter (Rensselaer Polytechnic Institute). Hole PAR-16, drilled by the Department of Defense in 1972, was located about 50 m from the reef crest on a reef-flat pavement 0.2 m below mean tide level. The Holocene section overlies a Pleistocene unconformity at a depth of 8.5 m and consists of a lower constructional coral-algal unit (8.5 to 3.2 m) dominated by in-situ algal-encrusted massive and branching corals 15 to 30 cm in length and infilled by poorly cemented, poorly sorted detritus. This unit is overlain (3.2 m to surface) by a more fragmental or conglomeratic unit containing smaller corals in place, numerous coral and algal fragments, foraminifers, and shells well cemented by aragonite and magnesium-calcite marine cements; near the top, the unit is overlain by algal and coral laminate growth. The following radiocarbon dates were obtained:

Sample	Depth (m)	C^{14} age (years B.P.)
I–8038	0.3	2,120±85
I–8039	1.8	3,675±95
I–8040	2.6	6,030±115
I–8041	3.6	6,705±115
I–8042	7.9	7,145±115

B. J. Szabo reported uranium-series dates of 7,900±500 years for the coral at 7.9 m and 132,000±4,000 years for a coral 1.2 m below the unconformity at 8.5 m. These ages are revised from preliminary dates reported earlier (U.S. Geological Survey, 1975, p. 164). The radiocarbon dates, which are not corrected for variations in atmospheric carbon or for the presence of younger marine carbonate cement, show a rapid rate of growth of the early Holocene reef (from 8.5 to 3.2 m) of about 10 mm/yr, followed by much slower growth and accumulation ranging from 0.3 to 1.5 mm/yr and averaging about 0.5 mm/yr. The slower vertical growth marks the reef-flat or pavement-building stage, which began about 6,500 years ago when sea level was about 2.5 m lower than it is at present at Eniwetak. The average rate of vertical growth was about 2 mm/yr and compares with that inferred from other evidence by Tracey and Ladd (1974). The rapid growth during initial stages, 6,000 to 7,000 radiocarbon years ago, is comparable to rates deduced by Chappell and Polach (1976) for Huon Peninsula in New Guinea and by Macintyre and Glynn (1976) for Galeta Point in Panama.

ESTUARINE AND COASTAL HYDROLOGY

GULF COAST

A major waterway construction project which is planned for approximately 56 km of ship channel in Florida's Tampa Bay, includes an 11-km reach in Hillsborough Bay. Shipping lanes are to be deepened and widened by means of hydraulic dredging. Open-water disposal of material will result in the creation of several large spoil islands, which must be located in areas where their adverse effects on bay environment will be minimal. C. R. Goodwin (1977) reported that a digital, hydrodynamic model was used to simulate circulation and flushing patterns in Hillsborough Bay under alternative spoil-island configuration plans. Each plan represents a different configuration for the islands to be created from the dredged material. Simulated circulation and flushing patterns were evaluated. Model results indicated that circulation within Hillsborough Bay will be significantly increased through proper spoil-island configuration. Improvement of overall flushing characteristics of the bay (interchange between Tampa and Hillsborough Bays), however, was minimal for the alternative plans tested.

ATLANTIC COAST

F. A. Johnson reported that fresh surface-water flow in South Carolina's Intercoastal Waterway is contributed by only one major tributary, the Waccamaw River, which divides at mile 375, where two-thirds of the river flows southward. The one-third that flows northward takes about 6 days to reach Little River Inlet. The saltwater-interface position at high tide is largely controlled by the amount of northward flow of the Waccamaw River, which, in turn, is probably governed by the amount of backwater caused by the Pee Dee River through Bull Creek. The interface at high-slack tide changes position by only several kilometers between low and high freshwater inflow and usually remains within 10 to 16 km of Little River Inlet. Apparently, the water above the interface is of good quality and suitable for most uses.

PACIFIC COAST

Bedform dynamics in San Francisco Bay

Bed configurations in San Francisco Bay were plotted by D. M. Rubin and D. S. McCulloch (1976) as a function of depth, sediment-grain size, and flow velocity. In the bay, as in flumes, these parameters were found to determine quantitatively bedforms that are in equilibrium. Data from the bay and published data from flume experiments were combined to determine equilibrium bed configurations for depths of 0.1 to 100 m, grain sizes of 0.04 to 3.0 mm, and flow velocities of 10 to 250 cm/s. Sand-wave amplitude is a function of the same parameters. The larger sand waves (approximately 20 percent of the flow depth) occur under conditions that plot near the center of the sand-wave stability field.

Clay-mineral variability in the suspended sediments of San Francisco Bay

H. J. Knebel, T. J. Conomos, and J. A. Commeau (1977) made semiquantitative determinations of the clay-mineral composition of nearls synoptic, surface suspended-sediment samples collected seasonally throughout the San Francisco Bay system. The relative amounts of chlorite plus kaolinite are generally highest in the northern reach of the system, whereas illite is dominant in the southern reach. The proportion of montmorillonite is low throughout the bay. Time-series and replicate samples collected at individual stations show that the difference in clay-mineral contents of the reaches is real and reflects a change in the source of clay-mineral particles within the bay. The Sacramento-San Joaquin River system supplies the northern reach, whereas most clay-mineral particles come from resuspension by waves and tidal currents in the southern reach. Analyses of bottom sediments and the spatial variability in the northern reach suggest that the relationship between the abundance and the sources of clay minerals may, in turn, be a function of particle size. This study demonstrates the usefulness of suspended clay minerals in interpreting sediment-dispersal patterns in estuaries.

Numerical simulation of dissolved silica in San Francisco Bay

D. H. Peterson (USGS), J. F. Festa (NOAA), and T. J. Conomos (USGS) (1977) described a two-dimensional (vertical) steady-state numerical model that simulates water circulation and dissolved-silica distributions and applied the model to the northern San Francisco Bay. The model (1) describes the strong influence of river inflow on estuarine circulation and, in turn, on the biologically modulated silica concentration and (2) shows how rates of silica uptake relate to silica supply and mixing rates in modifying a conservative behavior. Longitudinal silica distributions determined by biological uptake (assuming both vertically uniform and vertically decreasing uptake situations) show that rates of 1 to 10 μ g at L^{-1} d^{-1} are sufficient to depress silica (SiO_2) concentrations at river inflows of 100 to 400 m^3/s, respectively, and that the higher rates appear ineffective at inflows above 400 m^3/s. The simulations further indicate that higher silica utilization in the null zone is not essential to strongly depress silica concentrations there. Advective water-replacement times at river inflows of 400, 200, and 100 m^3/s are computed to be less than 25, 45, and 75 days, respectively, for a 120-km estuary-river system.

Infaunal biomass and production on a San Francisco Bay mudflat

F. H. Nichols (1977a) estimated the biomass distribution and animal productivity of all common macrofaunal (>0.5 mm) invertebrate species on the broad intertidal mudflats adjacent to *Spartina-Salicornia* salt marshes in the southern San Francisco Bay. Total specimen numbers (mean of four seasons) varied between 53,000 and 155,000/m^2 at three stations along a 154-m intertidal transect normal to the marsh edge, but there were large seasonal variations. Infaunal biomass (mean of four seasons) varied from 13 to 24 g ash-free dry weight/m^2 without large seasonal variations. The bivalves *Gemma gemma* and *Macoma balthica* together accounted for most (72 to 85 percent) of this biomass. Minimum rates of annual productivity, estimated by using a factor relating production to biomass (4.5×mean annual biomass) as well as size-frequency data, varied from 53 to 110 g m^{-2} yr^{-1}, or at least 25 g carbon m^{-2} yr^{-1}. This high secondary productivity, supporting a large shorebird community, is probably maintained by (1) tidal transport of detritus from the salt marsh, especially following winter dieoff of the higher marsh plants; (2) continuous resuspension of surface sediment, benthic diatoms, and detritus through tide and wind wave action; (3) the presence of a diatom layer on the mud surface throughout much of the year; and (4) the presence of plankton, treated sewage, and riverborne particulate matter in the water column.

Holocene estuarine sedimentation in Tillamook Estuary of Oregon

A coring program and an acoustic subbottom survey to determine modern and Holocene sediment sources and sediment-deposition rates in the estuary at Tillamook, Oreg., were completed by J. L. Glenn. With the exception of near-surface sediments associated with the spit across the estuary mouth and with the modern inlet through the spit, rivers entering the estuary from the nearby Coast Range were the major sources of Holocene and modern fill; transport of sediments from the marine source through the modern inlet and into the estuary is apparently a fairly recent occurrence. Deposition rates generally were high in the early Holocene, moderate in the middle Holocene, and increasing in late Holocene and prehistorical time. Sedimentation in the Tillamook Estuary is apparently a complex function of (1) relative sea-level rise, (2) changes in climate that may have resulted in varying rates of river-sediment supply, and (3) agricultural and forestry practices.

BALTIC SEA

Influence of fair weather on a benthic community in Kiel Bay

F. H. Nichols (1977b) studied the influence of unusual periods of warm, calm weather on the benthic fauna in Western Germany's Kiel Bay, an appendage of the western Baltic Sea. Kiel Bay is a relatively shallow estuarine system influenced primarily by water-mass exchange with the North Sea and runoff from the land. However, it is subject to increased eutrophication as water temperature, salinity, and waste input gradually increase and runoff decreases. In summer, bottom waters become isolated from the surface by establishment of a strong pycnocline. In European waters, during recent hot summers (particularly 1973 and 1975), surface sediments and the overlying water below 20 m became anoxic and almost totally destroyed the benthic fauna that is normally part of the food supply for the commercially exploited bottom fish. There is reduced production of these food organisms on an annual basis. Such conditions, if they worsen, might affect man's harvest of fish in this region.

MANAGEMENT OF NATURAL RESOURCES ON FEDERAL AND INDIAN LANDS

The Conservation Division is responsible for carrying out the USGS's role in managing the mineral and water resources on Federal and Indian lands, including the Outer Continental Shelf; that role includes, in particular, the conservation, evaluation, and development of the leasable mineral resources and waterpower potential of these areas. Primary functions are (1) mapping and evaluation of mineral lands; (2) delineation and preservation of potential public-land reservoir and waterpower sites; (3) promotion of orderly development, conservation, and proper use of mineral resources on Federal lands under lease; (4) supervision of mineral operations in a manner that will assure protection of the environment and the realization of a fair value from the sale of leases and that will obtain satisfactory royalties on mineral production; and (5) cooperation with other agencies in the management of Federal mineral and water resources.

CLASSIFICATION AND EVALUATION OF MINERAL LANDS

The organic act creating the USGS gave the Director the responsibility of classifying and evaluating the mineral resources of public-domain lands. There are about 101 million ha of land for which estimates of the magnitude of leasable mineral occurrences have been only partially made. Such appraisals are needed so that the rights to valuable minerals can be retained in the event that the land surface is disposed of and so that the extent of U.S. mineral resources can be determined. Estimates are based on data acquired through field mapping and the study of available geologic reports, in addition to spot checks and investigations made in response to the needs of other Government agencies. As an aid in this assessment of certain minerals, guidelines have been prepared setting forth limits of thickness, quality, depth, and extent of a mineral occurrence that are necessary before land is considered mineral land.

CLASSIFIED LAND

Mineral-land classification complements the leasing provisions of the mineral-leasing laws by reserving to the Government, in disposals of public land, the title to energy resources such as coal, oil, gas, oil shale, asphalt, and bituminous rock and fertilizer and industrial minerals such as phosphate, potash, sodium minerals, and sulfur.

These reserved minerals on public lands are subject to development by private industry under the provisions of the Mineral Leasing Act of 1920. All minerals in acquired lands and on the Outer Continental Shelf are subject to development under comparable acts.

As a result of USGS investigations, large areas of Federal land have been formally classified as mineral land. At the end of calendar year 1976, more than 17 million ha of land had been formally classified, and an additional 947 million ha had been designated prospectively valuable for a leasable mineral:

Commodity	Formally classified lands, ha		Prospectively valuable lands, ha	
	During calendar year 1976	Total at end of calendar year 1976	During calendar year 1976	Total at end of calendar yar 1976
Asphaltic materials	0	0	0	7,262,766
Coal	12,866	16,815,760	0	141,966,842
Geothermal resources	0	0	369,058	41,583,457
Oil and gas	0	1,714	0	597,337,153
Oil shale	0	0	0	5,815,256
Phosphate	0	166,459	1,052	12,383,571
Sodium	0	252,950	69,624	108,303,594

KNOWN GEOLOGIC STRUCTURES OF PRODUCING OIL AND GAS FIELDS

Under the provisions of the Mineral Leasing Act of 1920, the Secretary of the Interior is authorized to grant to any applicant qualified under the act a noncompetitive lease to prospect for oil and gas on any part of the mineral estate of the United States that is not within any Known Geologic Structure (KGS) of a producing oil or gas field. Lands within such known structures are competitively leased to the highest bidder. During calendar year 1976, 105,903 ha of onshore Federal land was determined to be in KGS's—the total at the end of the year was more than 7 million ha.

KNOWN GEOTHERMAL RESOURCE AREAS

The Geothermal Steam Act of 1970 provides for development by private industry of federally owned geothermal resources through competitive and noncompetitive leasing. During calendar year 1976, 52,895 ha was included in Known Geothermal Resources Areas (KGRA) and brought the total to 1,296,151 ha.

KNOWN RECOVERABLE COAL RESOURCE AREAS

The Federal Coal Leasing Amendments Act of 1975 provides for the development of federally owned coal lands by private industry through competitive lease and authorizes the Secretary of the Interior to designate Known Recoverable Coal Resource Areas (KRCRA). During calendar year 1976, 1,433,337 ha of coal land was included in KRCRA's and brought the total to 5,187,723 ha.

KNOWN LEASING AREAS FOR POTASSIUM, PHOSPHATE, AND SODIUM

During calendar year 1976, 28,212 ha was added to Known Potassium Leasing Areas, for a year-end total of 174,545 ha. Known Phosphate Leasing Areas were increased by 9,629 ha for a total of 27,012 ha. The total of 116,515 ha in Known Sodium Leasing Areas remained unchanged during 1976.

WATERPOWER CLASSIFICATION—PRESERVATION OF RESERVOIR SITES

Suitable sites for water-resource development are valuable natural resources that should be protected to assure that they will be available when they are needed. The waterpower classification program is conducted to identify, evaluate, and protect from disposal and injurious uses those Federal lands located in sites having significant potential for future development. USGS engineers review maps, serial photographs, and streamflow records to determine potential dam and reservoir sites. Topographic, engineering, and geologic studies are made of the identified sites to determine whether the potential value warrants formal classification of affected Federal lands. These resource studies provide the land-administering agencies with information that is basic to management decisions on land disposal and multiple use. Previous classifications are reviewed as additional data become available and as funds permit. If the sites are no longer considered suitable for development, the classification of the affected Federal lands is revoked. If the lands are not reserved for other purposes, they are returned to the unencumbered public domain for possible disposition or other use. During calendar year 1976, about 4,000 ha of previously classified lands in four Western States was released, and reviews of classifications were conducted in eight river basins in the Western States and Alaska.

During calendar year 1976, USGS engineers studied several of the most favorable pumped-storage sites affecting Federal lands in California, Idaho, and Oregon. There is an increasing trend to develop pumped-storage hydroelectric projects, which convert low-cost off-peak energy produced by fossil- or nuclear-fueled thermal plants to high-value peaking energy available during periods of greatest demand.

SUPERVISION OF MINERAL LEASING

Supervision of competitive and noncompetitive leasing activities for the development and recovery of leasable minerals in deposits on Federal and Indian lands is a function of the USGS, delegated by the Secretary of the Interior. It includes (1) geologic and engineering examination of applied-for lands to determine whether a lease or a permit is appropriately applicable, (2) approval of operating plans, (3) inspection of operations to insure compliance with regulations and approved methods, and (4) verification of production and the collection of royalties (see table 5).

Before recommending a lease or a permit, USGS engineers and geologists consider its possible effects on the environment. Of major concern are the esthetic value of scenic and historic sites, the preservation of fish and wildlife and their breeding areas, and the prevention of land erosion, flooding, air pollution, and the release of toxic chemicals and

TABLE 5.—*Mineral production, value, and royalty for calendar year 1976*

Lands	Oil (tonnes)	Gas (1,000 m³)	Gas liquids (liters)	Other[1] (tonnes)	Value (dollars)	Royalty (dollars)
Public	22,039,263	29,083,252	1,467,231,090	43,751,709	2,413,624,739	246,971,130
Acquired	833,254	882,423	15,117,157	1,053,392	203,359,195	13,881,470
Indian	3,728,396	3,583,584	164,669,130	25,527,138	591,191,244	58,282,963
Military	42,149	617,489	64,577,841	----------	14,214,420	2,274,961
Outer Continental Shelf	43,413,714	101,836,568	7,271,546,813	----------	4,402,439,996	699,424,790
Naval Petroleum Reserve No. 2	116,109	63,069	30,060,155	----------	12,434,705	1,346,888
Total	70,172,885	136,066,385	9,013,202,186	70,332,239	7,637,264,299	1,022,182,202

[1] All minerals except petroleum products; includes coal, potassium, sodium minerals, and so forth.

dangerous materials. Consideration is also given to the amount and kind of mining-land reclamation that will be required.

OUTER CONTINENTAL SHELF LEASE SALES FOR OIL AND GAS

Four sales of Federal Outer Continental Shelf (OCS) leases for oil and gas were held in calendar year 1976. Two sales held in February and November 1976 in the Gulf of Mexico OCS offered 381,301 ha for lease. High bids totaling $555,125,455 were accepted for 137,388 ha in 77 tracts. In August 1976, 354,816 ha was offered for lease in the Mid-Atlantic OCS. High bids totaling $1,127,936,425 were accepted for 214,272 ha in 93 tracts. The first lease sale in the Frontier OCS area of the Gulf of Alaska, held in April 1976, offered 408,134 ha. High bids totaling $599,836,587 were accepted for 165,543 ha in 76 tracts. USGS geologists, geophysicists, and engineers evaluated each tract offered to insure that the Government received fair market value.

COOPERATION WITH OTHER FEDERAL AGENCIES

The USGS acts as a consultant to other Federal agencies in land-disposal cases. In response to their requests, the USGS determines the mineral character and water-resource-development potential of specific tracts of Federal lands under their supervision that are proposed for sale, exchange, or other disposal. About 3,400 such reports were made during calendar year 1976.

GEOLOGIC AND HYDROLOGIC PRINCIPLES, PROCESSES, AND TECHNIQUES

EXPERIMENTAL GEOPHYSICS

ROCK MAGNETISM

Paleomagnetic anomaly in Pleistocene Lake Russell sediments

The Pleistocene glacially derived sediments of ancient Lake Russell that occur in the vicinity of Mono Lake in California are known to record a brief period of anomalous behavior of the geomagnetic field, termed an excursion. J. C. Liddicoat reinvestigated this locality and found that the angular departure of the paleomagnetic direction from the normal value is 65° and that the maximum amplitude of the entire oscillation is 85°, much greater than investigators had thought previously. The excursion is recorded faithfully at several sites in the same sedimentary rock formation and now is seen to be large enough to be used as a stratigraphic marker. Radiocarbon dates place the excursion at 24,600 years before present and indicate its total duration to be about 1,000 years. During the excursion, the geomagnetic field intensity apparently diminished by about 60 percent. The details of the changes in paleomagnetic direction can be interpreted to mean that both eastward and westward movements of the nondipole part of the geomagnetic field occurred, in contrast to the westward movement observed historically. Mathematical models of the excursion suggest that it was caused by abnormally large foci of the nondipole field.

Paleomagnetism of the Great Valley sequence in Sacramento Valley of California

Paleomagnetic samples from five localities within the Great Valley sequence in the Sacramento Valley of California were studied by E. A. Mankinen. The samples range in age from Late Jurassic to Late Cretaceous and span a total thickness of approximately 15,000 m. Audiofrequency demagnetization experiments show that the remanence of these sediments was acquired after the sequence was folded. A mean paleomagnetic pole position determined from the demagnetized samples is not significantly different from known Cretaceous poles of North America, an indication that the sequence must have been folded and remagnetized during the Late Cretaceous.

Large-scale displacement of the Nikolai Greenstone Triassic in McCarthy, Alaska

Paleomagnetic results obtained by J. W. Hillhouse and R. R. Doell from the Nikolai Greenstone (Middle and (or) Upper Triassic), near McCarthy, Alaska, indicated that these basalts originated at a paleolatitude near 15° N. The mean Nikolai paleolatitude lies approximately 27° (3,000 km) south of the Triassic latitude predicted for McCarthy, on the basis of paleomagnetic data for continental North America. The Nikolai paleomagnetic pole is at lat 2.2° N., long 146.1° E., with a statistical uncertainty of ±4.8° as determined from 50 flows sampled at five sites. Geologic and paleomagnetic evidence indicates that the Nikolai is allochthonous to Alaska and that, together with associated formations on Baranof, Chichagof, Queen Charlotte, and Vancouver Islands, it is part of a now disrupted equatorial terrane.

GEOMAGNETISM

Geomagnetic secular variation

L. R. Alldredge completed a study of geomagnetic variations having periods from 13 to 30 years. He concluded that these variations must come from sources internal to the Earth. The variations could not be explained by the westward drift of a core dynamo with a detailed fine structure. Hydromagnetic waves in the core offered a better explanation. The amplitude of variations having a period of 25 years is as large as 60 nT, which is approximately six times the amplitude of variations having a period of 15 years. This type of information is useful in estimating deep mantle conductivity.

Main field, long-wavelength anomalies

According to J. C. Cain, the partial transfer of energy from the dipole (n=1) to the higher order modes represented by wave numbers n=2, 3, and 4 has been verified in preliminary analysis of secular change since 1920. The partition of the surface field between core and crustal source functions has been found to occur gradually from n=9 to n=13, the energy in n=8 being anomalously low. The features represented by $n > 22$ are clearly crustal and show interesting, but incompletely explained, correlations with crustal development.

Current loop models of the geomagnetic field

N. W. Peddie developed computer algorithms that yield the value of the magnetic field vector at any point owing to an arbitrary system of dipoles and circular current loops. Using an evenly distributed set of approximately 400 representative values of the geomagnetic field vector and modern techniques of nonlinear optimization, Peddie modeled the static geomagnetic field with systems of up to six unconstrained dipoles and current loops. The behavior of these systems in time is being analyzed and applied to the problem of secular variation. In particular, tests are being made to determine whether the extrapolation of such systems forward in time provides a prediction of the geomagnetic field that is significantly improved over that which can be obtained from the linear or quadratic extrapolation of spherical harmonic coefficients, the technique in current use for modeling secular variation for world charts and reference field models such as the International Geomagnetic Reference Field.

Geomagnetic observatories

According to J. D. Wood, geomagnetic observatory operations were continued at Barrow, Sitka, and College, Alaska; Guam in the Mariana Islands; Newport, Wash.; Boulder, Colo.; Fredericksburg, Va.; and San Juan, P.R. Observations at Castle Rock, Calif., were suspended. Conventional photographic recording magnetographs are operated at all of the observatories except Barrow; digitally recording fluxgate magnetometers are now in operation at Barrow and five other observatories. R. J. Main, Jr., was responsible for processing the photographic data and determining magnetic indices and special effects before results were released for dissemination through World Data Center A. Programs for processing the digital data were developed by L. R. Wilson, and digital data for some observatories are now being furnished to the World Data Center for distribution.

Repeat magnetic surveys

Measurements of the absolute values of the components of the Earth's magnetic field are acquired periodically at more than 200 repeat stations scattered throughout the conterminous United States, Alaska, and the Pacific islands. According to J. D. Wood, processing of the data collected from 20 stations in Alaska in 1975 was completed, and thg data were used to help determine the secular changes for Alaska for the past decade.

Magnetic charts of the United States, 1975.0

Publication of the entire series of national magnetic charts of the United States was completed in December 1976. The charts in this series are Map I-912 (Peddie, Jones, and Fabiano, 1976), Map I-913 (Fabiano and Jones, 1976), Map I-914 (Jones and Fabiano, 1976), and Map I-915 (Fabiano, Peddie, and Jones, 1976). In an evaluation of the charts, E. B. Fabiano found the overall root-mean-square of the deviations to be on the order of 200 nT in the main-field components of the horizontal, vertical, and total intensity and 5 nT/yr in the annual change rates. Although elementary least squares functions appear to be adequate for smoothed representations of the magnetic vector field in the United States, additional refinements for improved accuracy would not be significantly meaningful without additions of new survey measurements to the existing data base, 60 percent of which consists of surveys made prior to 1950.

PETROPHYSICS

Establishment of petrophysics laboratory

A petrophysics laboratory was established in Denver to measure the electrical, magnetic, and optical properties of geologic materials in a variety of environments. These data can be used to interpret in-hole, ground, airborne and satellite geophysical measurements. Current capabilities include (1) matrix characterization (specific gravity, bulk density, porosity, specific surface area, and cation exchange capacity); (2) automated electrical properties (complex resistivity and complex dielectric constant) as a function of frequency from 10^{-5} to 10^{10} Hz, current density ($\mu 10^{-8}$ A/cm^2), water content (10^{-9} torr to saturation), temperature (-30° to 1,700°C), pressure (to 10 kb), explicitly controlled pH and Eh; (3) magnetic susceptibility and remanence; and (4) spectral transmittance, reflectance, and emittance from 0.18 to 50 μm.

Nonlinearity in complex resistivity of permafrost clay confirmed

Studies conducted by G. R. Olhoeft confirmed the existence of substantial nonlinearity in the current voltage of the complex resistivity of montmorillonite from +21° to −31°C. The nonlinearity is attributed to the absorption-desorption process of cation exchange and is one of the primary mechanisms responsible for the large induced polarization responses sometimes observed in non-sulfide-bearing permafrost.

Nonlinear complex resistivity used in geophysical exploration techniques

The technique of nonlinear complex resistivity (NLCR) is being used by G. R. Olhoeft to study the interfacial electrochemical mechanisms that determine induced polarization and other geophysical exploration techniques on the basis of electrical properties. The power of the NLCR technique is in its sensitivity to specific chemical reactions. NLCR uses the nonlinear current-voltage variations of the complex resistivity with frequency and harmonics, current density, and chemistry (pH, Eh, pX) to explain the interactions between aqueous solutions and sulfide- or uranium-bearing rock. Olhoeft's studies indicated that the NLCR technique will be useful in situ to delineate chemical variations in a mine site and thus will help tailor solution mining techniques to that particular site.

Large-scale magnetic anomalies over burned coal seams

Studies conducted by D. E. Watson on the magnetic properties of sediments baked by burning coal seams show that:

- The chemical nature of the combustion that occurs during the natural burning of coal seams can be determined by analyzing the resultant thermochemical alteration of the magnetic mineral in the overburden. This information provides (1) an understanding of the conditions required to improve in situ gasification and (2) data for developing a technique for locating the burning front during gasification or coal-mine fires.
- It is possible to classify the qualify of burned clinkers by relating it to the magnetic anomaly produced during the baking process. This procedure will provide remote evaluation of clinker hardness and thus determine its suitability for roadbed use or for determining where to place a road through the clinker with least effort.

Spectral signatures of particular minerals

On the basis of spectral reflectance measurements made from 0.4 to 2.5 μm on several hundred well-characterized particulate mineral samples, G. R. Hunt generated a spectral signature diagram that summarizes the diagnostic information available and identifies the source process for each band as being due to electronic processes, such as crystal field effects, charge transfer, color centers, or transitions to the conduction band, or to vibrational overtone or combination processes. The diagram provides a ready reference for the interpretation of visible and near-infrared features that typically appear in remotely sensed data.

Infrared spectral behavior of finely particulate solids

Transmission and emission spectra of clouds and layers of fine particulate solids recorded in the 6.5- to 35- μm region by G. R. Hunt demonstrated that (1) the behavior of layers of particles constitutes a good analog for the behavior of a cloud of particles; (2) individual micron-sized particles emit most where they absorb most; (3) as the particle size is increased, the emission features reverse polarity and the spectrum approaches that obtained from a polished plate of the material; and (4) as the particle-layer thickness increases, radiative interaction becomes increasingly important, so that the emission maximum shifts from the strongest features to weaker ones or produces a maximum at the Christiansen wavelength. These results are of particular importance for studies of lunar and planetary regoliths as well as of atmospheric aerosol layers and dust storms.

APPLIED GEOPHYSICAL TECHNIQUES

Gravity variations at Kilauea Volcano

Repeated high-precision gravity measurements made near the summit of Kilauea Volcano in Hawaii revealed temporal variations of gravity associated with the deflation of the volcano that followed the earthquake and eruption of November 29, 1975 (Tilling and others, 1976). Gravity differences with respect to a base station located on the southern flank of Mauna Loa Volcano in Hawaii were measured at 18 sites within 5 km of Kilauea Crater. The original survey, conducted between November 10 and 23, 1975, was repeated during the 2 weeks following the earthquake. Standard errors of the gravity differences measured during both surveys average about 5 μ Gal. The results of these two surveys indicate that the gravity at sites near the summit of Kilauea Volcano increased with respect to gravity at sites located away from the summit. The pattern of gravity increase at the summit sites is roughly radially symmetrical about the geodetically determined locus of the deflation, which is located approximately 1 km southeast of Kilauea Crater and has a half width of 2.2 km. Gravity increases at three sites along the eastern rift zone are approximately 110 μGal. Gravity at the summit sites changed smoothly during the 2 weeks following the earthquake, whereas gravity changes at the rift sites were restricted to the first 36 hours following the earthquake. The gravity changes correlate closely with elevation changes that occurred between level surveys conducted on September 22, 1975, and January 8, 1976. The relation between gravity change and elevation change (-1.70±0.07 μGal/cm) shows that the local mass distribution beneath the summit of Kilauea Volcano changed during the time between the surveys. Mass balance calculations indicate that the volume of subsidence is too small to account for the gravity changes, presumably because some magma moved away from the summit area without complete collapse of the resulting voids.

Geophysical characteristics of uranium deposits

Studies conducted in Texas and Wyoming uranium districts showed that induced polarization, magnetic susceptibility, and resistivity anomalies are associated with sedimentary uranium deposits. J. J. Daniels attributed these anomalies to variations in pyrite, magnetite, clays, and calcite cement across the roll front. Induced polarization and resistivity anomalies were detected between drill holes up to 300 m apart with hole-to-hole measurements. Although conventional logging measurements in single drill holes also showed induced polarization and resistivity anomalies, hole-to-hole measurements greatly increased the range of detection of exploration targets.

Gravity exploration for gold-bearing gravels

A study was made by H. W. Oliver to test the feasibility of applying gravity surveying to the determination of bedrock configurations beneath gold-bearing Tertiary gravels in the northern Sierra Nevada of California. Small gravity lows of 0.8 and 1.4 mGal occur over deposits of Tertiary gravels at Badger Hill and North Columbia, respectively. The maximum thicknesses of gravels at the two localities, as determined by drilling, are about 60 m at Badger Hill and 140 m at North Columbia. Comparisons of drilled depths of bedrock and models interpreted from gravity data indicate that the gravity method may be used to determine the general form of bedrock configurations beneath the exposed gravels by using a density contrast of -0.27 g/cm^3 between the gravels and the bedrock. Gravity data obtained over the bedrock surrounding the Tertiary gravels is required to determine the isolation of these gravel-associated anomalies from those caused by intrabedrock density contrasts. Gravity anomalies of -0.5 to -2 mGal were detected over channels buried by 60 to 200 m of upper Tertiary volcanic rock, but the anomalies are difficult to distinguish from those caused by other sources.

Detection of underground conductors

Scale-model studies conducted by F. C. Frischknecht and J. C. Wynn showed that grounded conductors such as rails or pipelines can be detected at depths as great as 100 to 200 m by using low-frequency loop-loop electromagnetic studies. Dipole-dipole resistivity measurements are potentially useful in locating the same sorts of targets, although the array must be alined approximately parallel to the strike of the source. Experiments made with partially insulated conductors demonstrated that the grounding impedance between the conductor and the Earth is the most critical parameter governing the response. R. D. Watts' analysis of electromagnetic scattering in a plane wave field caused by buried pipes, wires, or rails revealed that these conductors are detectable if they are shallower than one-fourth of the skin depth at the measurement frequency. Although the conductors' depth and position can be determined readily, their size cannot. The results of these studies are useful in evaluating the effects of surface cultural features on geoelectric measurements, as well as in locating objects in underground workings.

Electrical properties of oil shale

D. L. Campbell and G. R. Olhoeft completed preliminary multifrequency laboratory measurements of the electrical properties of a suite of oil-shale samples from the Piceance Basin in Colorado. The data indicate that the presence of kerogen in wet marls greatly increases direct current resistivity, introduces substantial anisotropy, and causes a frequency dependence above 10 to 100 Hz. The magnitude of these effects is maximum for intermediate grades of oil shale. The conductivity of oil shale has a substantial dielectric component, which should be taken into account in interpreting electromagnetic soundings from the region.

Gravity surveys in coal exploration

Results of high-precision (±0.02-mGal Bouguer anomaly values) gravity surveys conducted by W. P. Hasbrouck in North Dakota and Colorado indicated that (1) the sharp edge of a thick coal bed near the surface is reflected in the gravity data, (2) glacial channels (in North Dakota, these ancient streams are known to have cutout coal seams) can also be found by gravity measurements; and (3) the existence of minor faulting, as well as abrupt changes in thickness of shallow lignite deposits, is apparent on gravity profiles.

Nuclear borehole sonde for uranium exploration

F. E. Senftle constructed and tested a borehole sonde (1.7 m long and 7.3 cm in diameter) by using a 200-m^2 planar intrinsic germanium detector mounted in a cryostat cooled by removable canisters of frozen propane. The sonde is especially useful in measuring X-ray and low-energy gamma-ray spectra (40 to 400 keV). Laboratory tests in an artificial borehole indicate that the sonde can be used to make in-situ uranium analyses in boreholes irrespective of the state of equilibrium in the uranium series. Both natural gamma-ray and neutron-activation gamma-ray spectra have been measured with the sonde. Although the neutron-activation technique yields greater sensitivity, improvements being made in the resolution and efficiency of intrinsic germanium detectors suggest that it will soon be possible to use a similar sonde in the passive mode for measuring uranium in a borehole down to about 0.1 percent with acceptable accuracy. If a similar detector and neutron activation are used, the sonde can be used to measure uranium down to 0.01 percent.

Geomagnetic soundings

The Coso Range in California and Adak Island in Alaska were the sites of two geomagnetic sounding studies. Preliminary analysis of the Coso Range records indicated that the conductivity effect of the Pacific Ocean is detected in the study region and that detailed modeling and data processing will be required to interpret the electrical conductivity structure of the area. Geomagnetic and telluric observations made on Adak Island showed a large change in electrical conductivity across the island from the resistive southern island to a very conductive, young, northern portion that includes Mount Adagdak.

D. V. Fitterman developed a processing system for handling geomagnetic sounding data recorded with the USGS's digital geomagnetic array. Data, which are recorded on magnetic cassettes, are transcribed on nine-track magnetic tape and then plotted. The processing system is capable of reporting data breaks, selectively extracting data segments, plotting selected data segments, and low-pass-filtering data. The system is implemented on a dedicated minicomputer system to provide low-cost data-processing capability.

Deep-well seismic measurements in petroleum exploration

Investigations by A. H. Balch, M. W. Lee, and R. T. Ryder suggested that many diagnostic rock properties relevant to finding petroleum can be measured by a seismometer locked in a well. The method, called vertical seismic profiling, involves lowering a special geophone into a well on a conventional logging cable, energizing a seismic source at the surface, and measuring the resultant wave field in the Earth. In this manner, important acoustic properties of the subsurface rock layers, some of which may be related to the presence or absence of petroleum, are measured. In addition, the method enables the geophysicist to better interpret surface seismic data by tracing reflected events from the surface down to their origin. Preliminary results from wells in the eastern Powder River basin of Wyoming suggest that the spectrum of waves reflected by porous rock horizons may differ significantly from that reflected by nonporous rock horizons.

Controlled-source electromagnetic measurements

A controlled-source frequency-domain electromagnetic system was developed recently by F. C. Frischknecht, J. A. Bradley, and C. M. Mitchell and tested in the geothermal area of Idaho's Raft River Valley. Data obtained by W. L. Anderson were inverted to determine the geoelectrical section down to depths greater than one-half the source-receiver separation, or up to 1 km. Results compare favorably with those obtained by Schlumberger sounding methods, and the controlled-source electromagnetic method should be useful in geothermal investigations and in other investigations, particularly in regions where Schlumberger array configurations are physically difficult to set up.

Gravity and magnetic modeling

A computer program developed by J. W. Cady to calculate the magnetic or gravity fields of prisms with polygonal cross sections and finite lengths has an optional least squares solutions for magnetization or density of a body. The operating ease of the program is comparable to that of the Talwani-type two-dimensional modeling programs, but it addresses the more realistic problem of bodies of finite length. The program includes a least squares option that permits optimum fitting of a modeled body to the measured magnetic or gravity values and also allows a body to be subdivided so that its uniformity along strike can be examined. The program is computationally very fast and has immediate display of graphical output.

Gamma-ray measurements in northeastern Washington

J. A. Pitkin made truck-borne gamma-ray spectrometry measurements in the area of the Togo Formation in northeastern Washington, including the Midnite mine and the Mount Spokane alaskites. Apparent concentrations of the radioelements potassium, uranium, and thorium were computed from the field data to determine the surface extent of uranium mineralization in the areas surveyed. Initial results show only large anomalous concentrations of uranium in areas of known mineralization. Subtle changes in concentration may be related to hitherto unknown mineralization.

Interpretation of airborne gamma-ray data

A special imaging technique that presents airborne gamma-ray data as a color image was developed by J. S. Duval. This technique was applied to data from a survey flown near Freer, Tex., and the resulting image enhances the differences between geologic materials so that terrace deposits, alluvium from different sources, and very similar geologic units can be distinguished. Additionally, the image shows subtle colorations that seem to be related to the presence of a favorable environment for uranium deposition. One of these color areas coincides with the area of the ARCO Clay West leach site. Using the same gamma-ray data, histograms for uranium, thorium, and potassium in mapped geologic units were calculated in order to investigate the hypothesis that the shape of the histograms might indicate whether a geologic formation was favorable for the occurrence of uranium mineralization. Results in this test area suggest that an oddly shaped histogram reflects the complexity of the geologic unit rather than special geochemical properties that might be related to potential uranium mineralization.

Schlumberger soundings near Fallon, Nevada

Thirty-one Schlumberger soundings were made near Fallon, Nev., by A. A. R. Zohdy and R. J. Bisdorf to estimate and delineate the volume of fill containing fresh ground water and to map the lateral extent and thickness of a series of basalt flows that are the principle aquifer in the area. The results indicated that it is possible to map the basalt aquifer and to delineate areas where the sedimentary rocks are primarily composed of clays and (or) saturated with salty ground water. It was found that the basalt aquifer extends over an area of approximately 35 km^2 and that its maximum thickness is as much as 500 m. The depth to the electric basement of high-resistivity rocks was also determined to be between 2.5 and 3.5 km.

Geophysical studies in Bob Marshall Wilderness area in Montana

M. D. Kleinkopf interpreted aeromagnetic and gravity data from the Bob Marshall Wilderness area of Montana to provide information about the structural framework and distribution of several areas of near-surface crystalline rocks. In evaluating the petroleum potential of the wilderness area, gravity data provide constraints on the depth and configuration of the top of the Mississippian as an aid in constructing geologic cross sections. It is speculated that the northeasterly trends in the geophysical data may reflect broad arching or fault zones that could have influenced the entrapment of petroleum deposits.

Crustal blocks in Central America

J. E. Case's analyses of regional Bouguer gravity anomalies indicated that nuclear Central America may include two blocks of "continental" crust whose thickness is as great as 45 km. The northern block, characterized by Bouguer anomalies of -100 to -150 mGal (Bowin, 1976), extends from southern Mexico across central Guatemala and into central Honduras (Case and Donnelly, 1976). A 40-km crust was indicated by studies of the aftershocks of the 1976 Guatemala earthquake (Langer and others, 1976). The basement of Guatemala and northern Honduras is known to include Precambrian and Paleozoic metamorphic and igneous rocks. A second prominent negative anomaly occurs in northern Costa Rica where Bouguer gravity values are as low as -75 mGal. Matumoto, Ohtake, and Latham (1976) reported that the crustal thickness of the central volcanic province of Costa Rica is about 43 km. Although basement rocks are not exposed in north-central Costa Rica, the combined seismic and gravitational evidence indicates that a block of continental crust is probably present at depth. In contrast, Bouguer anomalies near Managua, Nicaragua, ranging from -15 to +40 mGal are suggestive of "oceanic" or transitional crust. In studies of the aftershocks of the 1972 Managua earthquake, Brown, Ward, and Plafker (1973), Langer and others (1974), and Ward and others (1974) assumed a crust of about 25 km consistent with mean Bouguer anomalies of about zero. If nuclear Central America was attached to the craton of northern South America, as some investigators postulate, these blocks have a net displacement azimuth of 300° to 308° with respect to a fixed South America and net displacement rates of about 0.9 to 1.5 cm/yr during the past 150 million years.

Magnetization of Mount Shasta

Aeromagnetic data were collected over Mount Shasta, California, and the surrounding terrain as part of a resource appraisal of the Mount Shasta Wilderness study area. R. J. Blakely applied inverse methods to these data in order to assess the bulk properties of the magnetic source. Blakely's experiments were of two types: (1) A calculation of the intensity and direction of magnetization using a linear least square method that Blakely recently developed. Each method assumes that the top of the source corresponds to the surface of the volcano and that the magnetization is uniform. The results of these experiments can be interpreted in two general ways: (1) Either the western flank of Mount Shasta is substantially more magnetic than the rest of the volcano, or (2) the Curie-point isotherm rises to relatively shallow depths beneath the summit and eastern flank. Both observations satisfy gravity data (LaFehr, 1965). The second interpretation, however, is also supported by surface manifestations of geothermal activity. Moreover, recent geologic studies conducted by R. L. Christiansen showed that the summit is silicic in nature and less than 3,000 years in age, which suggests that it may be underlain by a shallow magma chamber.

Geophysical discovery of caldera in northwestern Nevada

Gravity data reported by Donald Plouff, S. L. Robbins, and K. D. Holden (1976) were used to delineate a previously unreported caldera located about 70 km southwest of Denio, Nev., in the Charles Sheldon Antelope Range. The site of the probable caldera is marked by a 16×25-km 18-mGal gravity minimum and by a nearly coincident 230-gamma magnetic minimum (U.S. Geological Survey, 1972). A smaller 8×19-km 13-mGal gravity minimum, centered 23 km to the northeast of the larger gravity anomaly, also may indicate the presence of a caldera. A preliminary interpretation of the data based on a density contrast of 0.2 g/cm^3 indicates that the mass anomaly associated with the larger caldera may extend to a depth of 2.5 km beneath the surface.

Potential geothermal source on Adak Island, Alaska

Gravity, magnetotelluric, audiomagnetotelluric, self-potential, and telluric traverse surveys on Adak Island, Alaska, showed that a large, low-density, conductive body exists at a depth of not over 1 km under the southern flank of Mount Adagdak, an extinct volcano. These data were interpreted by D. B. Hoover as an indication of a shallow geothermal reservoir under this part of Adak Island.

Self-potential related to soil moisture

A serious noise problem in self-potential measurements related to varying soil-moisture content, called capillary pressure potential, is related to Donnan systems and the capillary effect potential. D. B. Hoover reported that, given some simplifying assumptions, the potential can be shown to be given by

$$E_{CP} = K\left(\frac{\sigma P_C}{\gamma\lambda C}\right),$$

where K is a constant, σ is the specific surface conductance, λ is equivalent conductance, C is the concentration of the pore fluid, and P_C is the capillary pressure. This equation predicts, for unsaturated materials such as soil at the surface, a potential that varies with the percent of water saturation or elevation above the free-water interface. Some topographic variations of self-potential can be explained by this mechanism.

Geoelectric structure of Kilauea Iki lava lake

Schlumberger vertical electric soundings (VES) and horizontal loop-loop electromagnetic (EM) soundings supplemented by very low frequency (VLF) measurements were made by C. J. Zablocki to determine the geoelectric structure of Kilauea Iki lava lake in Hawaii. The VES results showed a liquid-water zone formed by condensed steam above the hot, dry, and highly resistive basalt that lies immediately above the ionically conductive melt. VLF impedance measurements indicated a lower resistivity for the western zone than the galvanic VES measurements indicated, and this variance probably results from frequency dependent electrical properties. Inversion and analysis of the EM sounding data indicated a conductivity-thickness product for the melt zone to be between 6.0 and 7.2 mho. The lateral boundaries of the existing molten lava in Kilauea Iki lava lake were delineated by using VLF and turam profiling techniques. Analysis of all data sets showed that the surface projection of the molten edge can be defined within ±30 m, except toward the western edge where it appears to be thinner and irregular.

GEOCHEMISTRY, MINERALOGY, AND PETROLOGY

EXPERIMENTAL AND THEORETICAL GEOCHEMISTRY

National Center for the Thermodynamic Data of Minerals

The USGS has established a National Center for the Thermodynamic Data of Minerals in Reston, Va., in cooperation with the Office of Standard Reference Data of the National Bureau of Standards under the National Standard Reference Data System. The aim of the center is to acquire and provide, on a continuing basis, critically evaluated descriptions of the thermodynamic properties of minerals and other geologic materials over the ranges of temperature, pressure, and composition observed in the geological environment.

The center's staff will place primary emphasis on coverage of the numerical data needed to understand the geological environment and to use its resources. Specifically, the center will develop critically evaluated data on the properties of all naturally occurring solid phases of chemical end-members of bases and aqueous ions. The evaluated results will be published in the "Journal of Physical and Chemical Reference Data," the publications of the USGS, and other appropriate outlets to achieve the maximum distribution to interested users.

The initial staff of the National Center for the Thermodynamic Data of Minerals is headed by John L. Haas, Jr. Other members of the USGS serve as consultants to the center for their particular specialties.

Heat capacities of minerals

The heat capacities of corundum, periclase, anorthite, $CaAl_2Si_2O_8$ glass, muscovite, pyrophyllite, $KAlSi_3O_8$ glass, grossular, and $NaAlSi_3O_8$ glass were determined to an accuracy of ±1.0 percent by differential scanning calorimetry between 350 and 1,000 K. These results were combined with existing low-temperature heat capacity and entropy data and fitted by least squares to the following equations:

$$C_P^\circ \text{ (anorthite)}=516.83-0.09249T-1408500T^{-2}-4588.5T^{-1/2}+4.188\times10^{-5}T^2 \quad (298-1850\text{ K})$$

$$C_P^\circ \text{ (CaAl}_2\text{Si}_2\text{O}_8\text{ glass)}=375.17+0.03197T-2814700T^{-2}-24594T^{-1/2} \quad (298-1500\text{ K})$$

$$C_P^\circ \text{ (muscovite)}=917.67-0.08111T+2834100T^{-2}-10348T^{-1/2} \quad (298-1000\text{ K})$$

$$C_P^\circ \text{ (pyrophyllite)}=746.75-0.05354T-7578T^{-1/2}+1.986\times10^{-5}T^2 \quad (298-800\text{ K})$$

$$C_P^\circ \text{ KAlSi}_3\text{O}_8\text{ glass)}=684.69-0.1481T+3527700T^{-2}-8182^{-1/2}+3.305\times10^{-5}T^2 \quad (298-1200\text{ K})$$

$$C_P^\circ \text{ (grossular)}=1529.3-0.6990T+7442600T^{-2}-18943T^{-1/2}+2.530\times10^{-4}T^2 \quad (298-1200\text{ K})$$

$$C_P^\circ \text{ (NaAlSi}_3\text{O}_8\text{ glass)}=917.95-0.3824T+5279600T^{-2}-11511T^{-1/2}+1.474\times10^{-4}T^2 \quad (298-1200\text{ K})$$

These equations are constrained to join smoothly between 300 and 375 K with more accurate C_P° values previously determined by low-temperature adiabatic calorimetry. Calorimetric data for muscovite, pyrophyllite, and grossular were combined with data from recent equilibrium studies to derive improved values for $\Delta G^\circ_{f,198}$ for muscovite, pyrophyllite, and grossular.

Thermodynamic data of 2M_1 muscovite

E-an Zen concluded that the calculation of thermochemical data on minerals based on reversed hydrothermal phase-equilibrium studies should be made on the basis of values of temperature, pressure, and fugacity of volatiles at the actual reversal limits rather than at some average values; such a procedure would allow meaningful computation of errors and lead to discrimination of different types of errors. This approach and hydrothermal data published recently by Chatterjee and Johannes (1974) and Day (1973) can be used to compute a standard Gibbs free energy of formation of $2M_1$ muscovite from the elements of -5598.4 ±2.9 kJ $\geqslant G_f^\circ(298,1) \geqslant$ -5600.1 ± -5600.1 ±3.1 kJ. This value is nearly identical to recent calorimetric determinations made by Robie, Hemingway, and Wilson (1976), provided that a zero-point entropy of 18.7 J/mol K owing to the complete and ideal mixing of tetrahedral aluminum and silicon is assumed. Since $2M_1$ muscovite is known through structural determinations of tetrahedral O-M bond length to show no site preference, a random distribution of aluminum and silicon is suggested. The thermochemical calculations provide an independent verification of this inference.

Stability of phlogopite

Phlogopite reacts with diopside and quartz to form tremolite and sanidine at 750 °C between 200 and 350 bars of total pressure. D. R. Wones and F. C. W. Dodge found this reaction to be insensitive to H_2O pressure. The phlogopite-pyroxene-quartz assemblage, found in both volcanic and intrusive rocks where H_2O activities are low and $KASi_3O_8$ activities are high, is favored by iron. Amphibole-potassium feldspar assemblages are common in rocks where H_2O and $NaFeSi_2O_6$ activities are high and $KASi_3O_8$ activity is relatively low. The iron-free phlogopite-quartz-diopside assemblage is rare because it requires high temperatures combined with H_2O pressures in the range of 200 to 2,000 bars in an Na_2O-free environment. This assemblage has been reported from regional metamorphic terranes of granulite facies and contact aureoles of shallow plutons.

Chlorite-sulfide phase relations

Sulfide orebodies as variable as metamorphic copper ores (Ducktown, Tenn.), hydrothermal base-metal deposits (Creede, Colo.), and volcanogenic copper-nickel ores (Tilt Cove, Newfoundland) all contain sulfide ores and chlorite within the gangue. Metamorphosed black shales also contain complex assemblages of sulfides and chlorites. R. K. Popp synthesized a suite of chlorites of varying iron, magnesium, and aluminum contents to equilibrate with sulfide assemblages. Early results indicate that 7-A phases tend to persist in the iron-rich region and that the aluminum and silicon contents of the chlorites are variable at different conditions of pressure, temperature, and composition.

Solubility of amorphous silica at high temperatures and pressures

R. O. Fournier and J. J. Rowe developed equations describing the solubility of amorphous silica in pure water over a wide range of temperatures and pressures up to 380°C and 1,034 bars from the results of laboratory experiments that used both vitreous and gelatinous silica as starting materials. The solubility at the vapor pressure of the solution, from 0°C to 250°C, is given by the equation

$$\log C = \frac{-731}{T} + 4.52,$$

where C is the silica concentration in milligrams per kilogram, and T is absolute temperature. At a constant pressure of 1,034 bars, the solubility of amorphous silica from 0°C to 380°C is given by the equation

$$\log C = \frac{-810}{T} + 4.82.$$

The differential heat of solution $\Delta\bar{H}$ is 3.71 ± 0.05 Kcal/mol, and the differential eutropy $\Delta\bar{S}$ is 13.9 ± 0.05 cal/mol.

Experimental evidence for iron-silicic acid complexes

In exploratory experiments, the solubility of (1) Quartz in K_2SO_4-$KHSO_4$ solutions, (2) the oxide pair magnetite+hematite in K_2SO_4-$KHSO_4$ solutions, and (3) quartz+magnetite+hematite in K_2SO_4-$KHSO_4$ solutions were measured at 250°C and at the vapor pressure of the solution. Analyses of samples taken over a period from 1 day to several months after the beginning of the experiment showed that the presence of ferrous iron, derived from the solution of the iron oxides, both affects the rate at which quartz is dissolved and increases the solubility of quartz. Iron oxides are more soluble in the presence of quartz. These results lead to the conclusion that the behavior of silicic acid (probably H_4SiO_4) is similar to that of phosphoric acid (H_3PO_4) or sulfuric acid (H_2SO_4) in aqueous solutions at room temperature. Only at elevated temperatures, where the solubility of quartz is high, is the liquid nature of silicic acid significant. These data show that quartz solubility is a function of the type and concentration of cations in the solution, as well as of the temperature and density of the solution.

New technique for analysis of fluid inclusions

In a joint effort with G. J. Rosasco (National Bureau of Standards), Edwin Roedder (USGS), and J. H. Simmom (Catholic University) reported that laser-excited Raman spectroscopy has been successfully applied to the identification and partial analysis of solid, liquid, and gaseous phases in fluid inclusions in minerals. The procedure will not solve all the problems of analysis of fluid inclusions, but some unique features make it very useful. In particular, the measurement is performed in situ, it is nondestructive, and it can produce qualitative and quantitative data, some of which cannot be obtained otherwise, for samples as small as 10^{-9} g. It has been proved useful in the detection and measurement of the following variables in fluid inclusions: H_2O (as a brine); CO_2 (liquid and gas); CH_4 (gas); CO_2, $HCO^-{}_3$, CO_3^{2-}, and SO_4^{2-} (in water solutions); N_2 and CH_4 (in CO_2 fluid); CH_4 vapor pressure; ^{13}C to ^{12}C ratios in liquid CO_2; and some daughter phases. The original equipment described by Rosasco, Roedder, and Simmons (1975) had rather stringent sample requirements (relatively large, clear inclusions were needed) that seriously limited its usefulness. In a subsequent development, Rosasco and Roedder (1976) described a new instrument that permits measurement of backscattered Raman radiation. This development reduced the sample required by three orders of magnitude, so that most ordinary fluid inclusions now can be analyzed for those polynuclear constituents that have strong Raman spectra. This technique is particularly well suited for the one aspect of fluid inclusion analysis most intractable by previous methods—the sulfur species present. Normal microchemical analytical procedures seldom extend to the submicrogram (10^{-6}g) range of total sulfur and generally cannot discriminate between the various sulfur ions present in this range. The new Raman technique permits estimation of quantities of SO_4^{2-} in the 10^{-11}-g range, and, although it has not yet been verified with actual inclusions, it should have a sensitivity for HS^- in the same range.

Sulfur compounds in fluid associated with porphyry copper deposits

Fluid inclusions trapped in the minerals of porphyry copper deposits provide information on the nature of the fluids responsible for ore deposition. Throughout the world, prophyry copper deposits characteristically show inclusions containing very high concentrations of soluble salts such as NaCl and KCl (as much as 60 weight percent) (Roedder, 1971). These fluids (actually hydrosaline melts) were trapped at high temperatures, and, when they cooled to surface temperature, they precipitated crystals of these various salts, called daughter minerals. When they are reheated in the laboratory, these daughter minerals normally redissolve in the inclusion fluids. One perplexing problem has been the presence of a crystal phase in these inclusions. On the basis of rather meager data, the crystal phase is thought to be anhydrite, which does not redissolve when it is reheated. Although anhydrite is unusual in that it normally shows retrograde solubility, this characteristic does not explain how it came to be present in the inclusions.

Recent work by Rosasco and Roedder (1976) resulted in the first unambiguous identification of these crystals as anhydrite. Even though it is only 5 μm in size, one of these crystals from the porphyry copper deposit at Bingham, Utah, yielded nine lines in the Raman spectrum characteristic of the SO_4^{2-} group in the anhydrite structure. The liquid solution surrounding the crystal also showed a Raman line at 980 cm^{-1}, characteristic of the SO_4^{2-} ion in water solution.

The only feasible mechanism that has been suggested to explain the origin of the anhydrite crystals involves the leakage of hydrogen out of the inclusions (Roedder and Skinner, 1968). If the fluids surrounding the host quartz crystals became more oxidizing than they were at the time the inclusion was trapped, hydrogen (from dissociation of water molecules) would tend to diffuse out of the inclusion and leave behind the equivalent oxygen and thus cause the autoxidation of original S^{--} ion present in solution to SO_4^{2-} and the precipitation of anhydrite. Original ferrous iron ions in solution would similarly be oxidized to ferric and hence could yield the crystals of hematite found in the inclusions of many porphyry copper deposits; these crystals also do not dissolve on reheating.

Thus, these phases in the inclusions of porphyry copper deposits seem to require that the later fluids bathing these deposits must be relatively oxidizing but still hot enough to permit diffusion of hydrogen through the host mineral. This change in state of oxidation may well signify a basic change in the circulation of the ore fluids and permit more oxygen-rich surface waters to permeate the orebodies. It is important to note, however, that the anhydrite and hematite phases in these inclusions are typical only of porphyry copper deposits and hence may signify a basic difference between the ore-forming conditions of such deposits and most other types of metal deposits. They may provide an even more diagnostic exploration tool for porphyry copper deposits than the presence of fluid inclusions with extremely high salinities.

Modeling of high-pressure processes

Two approaches to understanding the petrogenesis of igneous rock were applied to the so-called Ice Harbor basalts of the Columbia River Basalt Group. The "Ice Harbor" unit consists of four distance chemical types—"Basin City" (BC), "Ice Harbor 1" (IH1), "Ice Harbor 1 upper flow" (IH1u), and "Ice Harbor 2" (IH2). On the basis of least squares computer modeling of the chemistry, T. L. Wright and R. L. Helz showed that none of these chemical types are related by phenocryst (that is, low pressure) fractionation but may be related at higher pressures by the following processes: (1) Fractionation at moderate pressure (IH1→IH1u), (2) different degrees of partial melting of a very similar source rock (BC as opposed to IH1u), and (3) comparable degrees of melting of slightly different source (BC as opposed to IH1).

In order to test these relations, Helz conducted high-pressure melting experiments on all four compositions. Since the predictions made on the basis of least squares calculations are confirmed in every case by the melting studies, Helz and Wright concluded that mass balance calculations can be used to model moderate- to high-pressure processes relating magmas that cannot be related by fractionation of observed phenocrysts. Interpretations of such calculations are an adequate substitute for extensive experimental work, and the calculations can be used to distinguish partial melting from fractionation and to place constraints on the nature of the mantle source rock and the degree of partial melting involved. Helz and Wright extended these sorts of calculations to other Columbia River basalts, deep-sea basalts, and Hawaiian tholeiites. The results so far are compatible with the data available for these samples.

Effect of chromium on spinel crystallization

B. R. Lipin extended his previous studies by adding small amounts of Cr_2O_3 (2.0 and 0.5 weight percent) to the Fe/Fe+Mg = 0.41 composition plane of the system $CaAl_2Si_2O_8$-(Mg, Fe)$_2SiO_4$-SiO_2. Under reducing conditions in the 2-percent Cr_2O_3 runs, spinel is the liquidus phase in all mixtures studied, and the spinel extends over almost the entire liquidus surface. In the 0.5-percent Cr_2O_3 system, the spinel field is remarkably similar to that in the chromium-free system. The partitioning of chromium between the liquid and the crystalline silicates olivine and orthopyroxene is the same within analytical uncertainties as it is in the 2-percent Cr_2O_3 runs reported by Huebner, Lipin, and Wiggins (1976). Although there is good indirect evidence for the presence of Cr^{2+} in the experimental liquid and silicates, the compositions of the spinels (Mg, Fe) (Cr^{3+}, Al)$_2O_4$ show no indication of Cr^{2+}, in accord with crystal-chemical considerations. Because of the relatively large size and the large octahedral site preference energy of Cr^{2+}, it is an unlikely occupant of the tetrahedral spinel site. However, because of its electronic configuration, Cr^{2+} is subject to Jahn-Teller distortions so extreme that it will not substitute in the octahedral spinel site. Thus, Cr^{2+} is an extremely unlikely constituent of a spinel.

Since Cr^{2+} is not accepted into the spinels, chromium cannot be depleted simply by spinel crystallization from a liquid in which chromium is predominantly divalent. This discovery possibly explains the retention of chromium in reduced residual liquid of the lunar-wide magma. In contrast, chromium in terrestrial magmas is predominantly trivalent and is rapidly depleted by spinel crystallization under these more oxidizing conditions.

Chromium partitioning between crystals and melts

J. S. Huebner, B. R. Lipin, and L. B. Wiggins determined the distribution of chromium (D_{Cr}) between crystalline silicates, olivine and pyroxenes) and melts at oxygen fugacity values near those of lunar rocks (more reducing than the iron-wüstite assemblage) for a wide range of bulk compositions. D_{Cr} is the weight percent of Cr_2O_3 in crystals divided by the weight percent of Cr_2O_3 in melt. The range of values of D_{Cr} for olivine is from to 0.6 to 1.3 (average, 0.9), and for pyroxene the range is from 1.6 to 3.5 (average, 2.5). The D_{Cr} shows no obvious dependence on any experimental parameter. Arguments based on composition indicate that most of the chromium in olivine is present as octahedrally coordinated Cr^{2+} and also as Cr^{3+} charge compensated by tetrahedral Al^{3+}. Chromium has great potential as a petrogenetic indicator of parental relationships between magma and crystals. Several currently popular lunar petrogenetic models propose magma-residuum pairs that, on the basis of the distribution of chromium, cannot be related by simple phase-equilibrium processes.

Oxygen fugacity of the mantle environment

The intrinsic oxygen fugacities of minerals of mantle origin were directly determined by the solid electrolyte method. On the basis of these results, Motoaki Sata concluded that the minerals probably formed in a reducing environment where graphite was stable. In some samples, the presence of submicroscopic graphite trapped within a mineral was indicated by a slow downward shift of f_{O_2} at temperatures above 1,100°C. Considering other factors such as the common occurrence of graphite or diamond in kimberlite-type nodules, Sato interpreted the predominance of CO_2 in fluid inclusions trapped in mantle-derived minerals, the low solubility of CO_2 relative to that of H_2O in magmatic melts, and the lack of other suitable f_{O_2} controlling buffer systems in the observed f_{O_2} region as indicating that the f_{O_2} of the upper mantle is essentially buffered by the graphite-CO_2 system. At deeper horizons, where the pressure is in excess of about 40 kbar, Sato postulated that the diamond-magnesite buffer would control f_{O_2}. According to this model, the f_{CO_2} of a basaltic magma should first decrease as the magma ascnds and then increase as hydrogen begins to escape rapidly somewhere in the crust.

Oxygen fugacity values of the Skaergaard intrusive

Measurements made by Motoaki Sato (USGS) and Mariano Valenza (University of Palermo) of the f_{O_2} values of bulk rock samples, mineral separates, and simulated liquids of various horizons of the Skaergaard intrusive body in Greenland demonstrated that the f_{O_2} of the Skaergaard magma never reached that of the quartz-fayalite-magnetite assemblage but stayed below the f_{O_2} of the magnetite-wustite assemblage, except during the crystallization of the Upper Zone *a*. This is contrary to previous estimates based on the magnetite-ilmenite methods or on ideal solid-solution models. The f_{O_2} of the magma during the crystallization of the Lower Zone horizons was close to that of the wustite nonassemblage and probably under the control of the graphite-CO_2 equilibria. In fact, some of the Lower Zone samples showed autoreduction above 1,100°C, a reasonably reliable sign of the presence of submicroscopic graphite. Sometime during the crystallization of the Lower Zone, graphite was probably exhausted by the combined oxidation effect of hydrogen escape (which favors the reaction $C+2H_2O=2H_2+CO_2$) and the relative enrichment of Fe^{3+} in magma caused by the crystallization of olivine and pyroxene (which favors the reaction $C+2Fe_2O_3=4FeO+CO_2$). The relative f_{C_2} of the magma began to rise at this point. By the time the Upper Zone *a* horizion had crystallized, the increased stability and crystallization of the magnetite-ulvospinel phase began depleting the magma of Fe^{3+} relative to Fe^{2+}, and the relative f_{O_2} began falling. The results obtained with the Skaergaard intrusive sequence appear to show several important points:

- The possible persistence of graphite in magma from the mantle up to the crustal environment.
- The complexity of the mechanism of the control of magmatic f_{O_2}.
- The significant role played by volatile-forming elements in influencing the oxidation state of magma.
- The limitation of the reliability of the magnetite-ilmenite method, particularly when the magnetite and ilmenite were produced by subsolidus unmixing.
- The possible role of carbon and hydrogen in dehydrating magma, a process that might eventually have induced the Skaergaard magma to absorb meteoric water in the late stage of crystallization.

CRYSTAL CHEMICAL STUDIES

Crystal structure of scandium-lithium protoenstatite

H. T. Evans, Jr., and J. A. Konnert completed a structure study of scandium- and lithium-rich protoenstatite synthesized by Jun Ito (University of Chicago). They measured 1,520 intensities with the automatic diffractometer by using Mo K α radiation, and then Evans and Konnert used this data set for a crystal structure refinement. When a model was used in which scandium and lithium were randomly distributed over the M(1) and M(2) sites, refinement stopped at a reliability index of R=0.13. When all the scandium was placed in M(1) and all the lithium in M(2), R was reduced to 0.09. When the formula $(Mc_{1-x}Sc_x)(Mg_{1-x}Li_x)Si_2O_6$ was assumed and x allowed to vary in the least squares analysis, R reached a final value of 0.043 with x=0.228(9).

The M(1) site $(Mg_{0.77}Sc_{0.23})$ has a fairly regular octahedral coordination with M-O bond lengths 2.005, 2.071, 2.200 A (2 each, ±0.002 A). The M(2) site has four oxygen atoms at the corners of a nearly regular octahedron at 2.063, 2.066, 2.365 A. The Si-O bonds are 1.648 and 1.656 to the chain-linking oxygen atoms and 1.619 and 1.585 A to the unlinked atoms. The space group symmetry shows no indication of departure from the centrosymmetric ***Pbcn***. Several weak, forbidden *hk0*, *0kl*, and *h0l* reflections were observed with the crystal in rational alinement with the azimuth goniometer axis, but these disappeared completely when the crystal was tilted about 5°, and thus proved that these reflections are caused by double diffraction.

Cation distribution in lunar orthopyroxene as an indicator of thermal history

J. S. Huebner has concluded that the site occupancy refinement (by H. T. Evans, Jr., and J. A. Konnert) of orthopyroxene from lunar anorthosite 15415 indicates the high degree of cation order expected of pyroxenes subjected to Apollonian metamorphism at lower than 500-600°C. There is no evidence for a subsequent thermal event of sufficient intensity to disorder the pyroxene. On the basis of previous laboratory studies of argon-release patterns of lunar plagioclase and disorder-order kinetics of terrestrial pyroxenes, the reported isotopic age (3.9-4.1 AE) may be attributed to cessation of metamorphism, perhaps caused by excavation by meteorite impact.

Magnetic susceptibility in erbium and ytterbium-doped zircon

Magnetic susceptibility measurements have been made by F. E. Senftle, A. N. Thorpe, and C. C. Alexander for both erbium and ytterbium-doped ($\sim 10^3$ ppm) zircon single crystals with the magnetic field perpendicular and parallel to the [001] axis. Large susceptibility anisotropies were found in both cases. The observed anisotropies of ytterbium-doped $ZrSiO_4$ indicate small populations of ytterbium ions (~ 19 percent) at the tetragonal sites. The susceptibility of this phase would be nearly isotropic if the ytterbium ions occupied only the zirconium positions. When erbium occupies the zirconium sites, their data indicate that the first excited state is paramagnetic with g_x=9 and $g_y \sim 5$ at 20 cm^{-1} above the ground state ($g_x \sim 0$, $g_y \sim 15$). The first excited state is quite similar to the ground states observed for Er^{3+} in many other crystal structures.

Crystal structure of ulexite

The crystal structure of ulexite, $NaCa\text{-}B_5O_6(OH)_6 \cdot 5H_2O$, has been refined by J. R. Clark (in collaboration with Subrata Ghose and Che'ng Wan, University of Washington) to R=0.046 using block-diagonal least squares methods and 4,911 reflections collected on a single-crystal diffractometer. The refined cell constants are: triclinic $P\bar{1}$, a=8.816(3), b=12.870(7), c=6.678(1) A, α =90.36(2)°, β =109.05(2)°, γ =104.98(4)°, V=688.43 A^3, Z=2, ρ (calc.)=1.955 g/cm^3. The structure contains isolated pentaborate-type polyanions composed of two triangles and three tetrahedra (5:2 Δ +3T), plus edge-sharing chains of sodium octahedra and of calcium polyhedra, all cross-linked by polyanion and water molecule bonds to the sodium and calcium cations and by a network of hydrogen bonds. All 16 hydrogen atoms were located and all form hydrogen bonds. Average bond distances (A) are: B-O tetrahedral 1.475 triangular 1.367, Na-O 2.421, Ca-O 2.484, O-H 0.80, H . . . O 2.08, O-H . . . O 2.844. The octahedral and polyhedral chains run parallel to c, the fiber-axis optical direction, and are considered responsible for the unusual light-transmission characteristics of ulexite.

Crystal chemistry of hydrated borate minerals

A reexamination of Christ's rules (Christ, 1970) that govern the formation of polyions in hydrated borate minerals has been made by C. L. Christ and J. R. Clark. Since 1960 a large number of structure determinations for such minerals have been reported. As a result the old rules have been modified and expanded. The 1976 rules are summarized as follows:

- Boron will link either three oxygen atoms to form a triangle or four oxygen atoms to form a tetrahedron.
- Polynuclear anions are formed by corner sharing only of boron-oxygen triangles and tetrahedra in such a manner that a compact insular group results.
- In the hydrated borates, protonable oxygen atoms will be protonated in the following sequence: (1) Available protons are first assigned to free O^{2-} ions to convert these to free OH^- ions, (2) additional protons are assigned to tet rahedral oxygen ions in the borate ion, (3) protons are next assigned to triangular oxygen ions in the borate ion, and (4) any remaining protons are assigned to free OH^- ions to form H_2O molecules.
- The hydrated insular groups may polymerize in various ways by splitting out water; this process may be accompanied by the breaking of boron-oxygen bonds within the polyanion framework.
- Complex borate polyanions may be modified by attachment of an individual side group, such as (but not limited to) an extra borate tetrahedron, an extra borate triangle, two linked triangles, or an arsenate tetrahedron.
- Isolated $B(OH)_3$ groups, or polymers of these, may exist in the presence of other anions.

MINERAL STUDIES

Zoned chromium, iron-spinel from Alaska

Zoned spinel of unusual composition and morphology has been found by G. K. Czamanske in massive pyrrhotite-chalcopyrite-pentlandite ore from the La Perouse layered gabbro intrusion in the Fairweather Range, southeastern Alaska. The spinel grains show continuous zoning from cores with up to 53 weight percent Cr_2O_3 to rims with less than 11 weight percent Cr_2O_3. Their composition is exceptional because they contain less than 0.32 weight percent MgO and less than 0.10 weight percent Al_2O_3 and TiO_2. Also notable are the concentrations of MnO and V_2O_3, which reach 4.73 and 4.50 weight percent, respectively, in the cores. The spinel is thought to have crystallized at low oxygen fugacity and at temperatures above 900°C, directly from a sulfide melt that separated by immiscibility from the gabbroic parental magma.

A new calcium tantalum-niobium oxide

M. E. Mrose and E. E. Foord (Stanford University) have completed the characterization and description of rynersonite, a new species isostructural with synthetic $CaTa_2O_6$, from the Himalaya pegmatite-aplite dike system, Mesa Grande district, San Diego County, California. The new mineral mynersonite occurs as creamy-white to reddish pink felted masses of fibrous to lath-like crystals. Individual laths average less than 0.5 mm in length and 0.05 mm in thickness. Electron diffraction patterns established that the laths are elongated along a and flattened on (010). Hardness of rynersonite is about 4-½; it has an earthy luster—a white streak—and an uneven fracture. Rynersonite also is biaxial positive (+) with moderate 2V; it has indices of refraction that are >2.05 and a birefringence of about 0.14; Z=a, light straw yellow.

Reddish-pink rynersonite is orthorhombic, space group $Pmnb$, with a=7.505(1) A, b=11.063(2) A, c=5.370(1) A, Z=4, D_x=6.394, D_m=6.402. The six strongest lines of the X-ray pattern (d, in A; intensity, hkl) include 3.038 *100* 031, 4.835 *91* 011, 2.964 *91* 211, 3.754 *71* 200, 2.683 *50* 002, 2.359 *50* 231. Heating in air for 20 hours at 550°C, 800°C, and 1,050°C produced no changes in cell dimensions or structure. Electron microprobe analyses indicate a range of composition from $Ca(Ta_{1.76}Nb_{0.24})O_6$ to $Ca(Ta_{1.21}Nb_{0.77})O_6$. Rynersonite formed as an alteration product of stibiocolumbite-stibiotantalite crystals and is intimately associated with minor amounts of antimonian microlite and fersmite, $Ca(Nb,Ta)_2O_6$.

The mineral is named for Eugene B. Rynerson and Buel F. Rynerson, and their father, the late Fred J.

Rynerson, in recognition of their lifelong interest in mining the gem-bearing pegmatites in Mesa Grande, California.

Cooling history of lunar plagioclase

G. L. Nord has found that plagioclase in the slowly cooled lunar troctolite 76535 contains abundant rows of inclusions oriented parallel to [301], [$\bar{1}$01] and [010]. The inclusions are shown by transmission electron microscopy, electron diffraction and X-ray energy analysis to consist mainly of augite, pigeonite, orthopyroxene, pores, and an unidentified phase that is preferentially thinned out during sample preparation. A minor inclusion is nickel-iron metal. The pyroxenes are interpreted to have exsolved from plagioclase in the solid state.

The size of antiphase domains induced by the $I1 \rightarrow P\bar{1}$ transition in plagioclase is more similar to that for the cooling rate through Tc (~600°C) of a basalt than to that of a deep-seated plutonic rock. Thus, it is suggested that rock 76535 cooled slowly and continuously from crystallization (4.6 AE) to some temperature between 810°C and 600°C at which time it was excavated (4.0 AE) and cooled quickly through the anorthite $I\bar{1} \rightarrow P\bar{1}$ transition.

VOLCANIC ROCKS AND PROCESSES

HAWAIIAN VOLCANO STUDIES

Ground deformation during the November 29, 1975, earthquake

The existence of a regional geodimeter network and an extensive series of level lines within the area affected by the November 29, 1975, earthquake, the largest in Hawaii in more than 100 years, has presented an unusual opportunity to document in detail the nature of associated ground deformation. The changes are the largest ever observed in the Kilauea area, with individual geodimeter lines changing by as much as 5.8 m and with vertical elevation changes of as much as 1.2 m occurring across level lines. The fact that the dominant motions were downward and seaward supports interpretation of the earthquake as related to large-scale slumping of the south flank of Kilauea Volcano. The geologic record indicates that the ground deformation pattern has occurred repeatedly in the past, that it is an integral part of the growth of Kilauea Volcano, and that it undoubtedly will occur again in the future.

Electrical self-potential monitoring across the upper East Rift indicated that magma moved from Kilauea Summit to a point or points within the fissure system of the East Rift at the time of the November 29, 1975, earthquake and again during short periods in June and July of 1975. The flow of magma within the East Rift has been confirmed by newly created self-potential anomalies measured in the lower East Rift area and most notably by developing "hot spots" at, and between, Heiheiahulu and Puu Kauka.

Aftershock activity from the November 29, 1975, earthquake continued through most of 1976 over a large part of the south flank of Kilauea. The aftershock pattern was interrupted on June 21-22, 1976, when a swarm of nearly 3,000 events occurred near Mauna Ulu and Pauahi areas and again on July 14-15, 1976, when a burst of nearly 1,000 events occurred in the Mauna Ulu vicinity.

Mauna Loa continues to inflate

Geodimeter and dry tilt surveys have shown that Mauna Loa Volcano has continued to inflate, building toward an eruption expected within two years. The center of this inflation has been shown to be slightly south of Mokuaweoweo caldera, in contrast to earlier, incomplete observations, which suggested an inflation center within the caldera.

In cooperation with several military agencies, testing of various types of explosives have been conducted to learn the optimum means of disrupting lava flow supply channels. Contingency plans have been developed for use of large explosive devices if certain types of Mauna Loa eruptions should threaten populated areas of Hawaii Island.

Complexity and hazards of Hawaiian shield volcanoes

According to R. T. Holcomb (1976), Hawaiian shield volcanoes are, in at least three ways, more complex than commonly thought:

- Calderas form and fill repeatedly as shields grow; they are not restricted to the end of growth. Both Mauna Loa and Kilauea have rapidly filling calderas but no sign of senescence, and each had at least one older caldera completely filled before the present one formed.
- Eruptions during tholeiitic shield growth change in frequency, extent, duration, flow types, and chemistry over periods of decades and more. Changes are repetitive, perhaps cyclical, and possibly related to repeated formation of calderas, which provide clues to the existence of old calderas otherwise obliterated by larger younger collapses.
- Large-scale slumping occurs throughout the lives of shields.

Slumping after the end of shield growth may remove half the subaerial edifice (Waianae, Koolau); before the end of growth, it can produce a younger shield banked against remnants of an older one (Wailau, Lanai). Slumping can modify patterns of volcanism by changing orientations of rift zones (Mauna Loa southwestern rift) of pirating magma from one volcano to build another (Kilauea), and thereby aid migration of volcanism. It thus contributes not only to destruction of volcanoes but to their construction as well.

These complexities imply particular hazards; still-growing shields will have further caldera collapses and explosive eruptions. Some areas of few recent eruptions will have more frequent and extensive eruptions in the future. Large areas of both active and inactive shields will subside and be flooded owing to slumping of unbuttressed flanks.

Revised age, Midway Volcano, Hawaiian volcanic chain

Midway Islands are part of a coral atoll that caps Midway Volcano, which rises nearly 5,000 m above the surrounding sea floor. In 1965, two drill holes penetrated the coral cap and bottomed in tholeiitic basalt flows, and provided samples of the volcano for study. Because of its position west of Hawaii, the age of Midway is of critical importance to hypotheses concerning the origin of the Hawaiian volcanic chain. Estimates of the age of the volcano, however, have ranged from pre-Miocene, based on fossils from the ancient coral reef, to 18 million years, based on K-Ar measurements on altered tholeiitic lavas.

G. B. Dalrymple and M. A. Lanphere, in cooperation with D. A. Clague (Middlebury College) have made new conventional and $^{40}Ar/^{39}Ar$ technique K-Ar measurements on samples of the altered tholeiitic lavas and on pebbles of alkalic basalt from a basalt conglomerate that overlies the lava flows. The K-Ar ages of two fresh Hawaiite pebbles show that Midway had evolved past the tholeiitic shield-building stage and had formed an alkalic cap 27.0 $\pm$ 0.6 million years ago. Incremental $^{40}Ar/^{39}Ar$ heating experiments on samples from the altered tholeiitic flows give age spectra and isochrons diagnostic of disturbed systems, which demonstrates that the previously published age of 18 million years on these samples is too young by about 10 million years. Electron microprobe examination of the altered tholeiitic basalts indicate that the anomalously young ages are due to montmorillonitic clays, formed by alteration in seawater, which contain a significant proportion of the potassium in these rocks.

COLUMBIA PLATEAU STUDIES

Duration and volume of Columbia River basalt volcanism

More than 200,000 km^3 of flood basalt, constituting the Columbia River Basalt Group in Washington, Oregon, and Idaho were erupted on the Columbia Plateau during middle and late Miocene time. K-Ar dates recently obtained and published by E. H. McKee indicate that this volcanism took place during a 10-million-year period from about 16 to 6 million years ago. D. A. Swanson and T. L. Wright have calculated that probably more than 99 percent of this lava, comprising the so-called Imnaha basalt flow, the Picture Gorge Basalt, and lower and middle parts of the Yakima Basalt, was erupted between about 16 and 13.5 million years ago. Eruptions occurred every few thousand years during this time, with probably no hiatus longer than 100,000 years, as determined from the number of flows present and the complete geologic and magnetostratigraphic record comprising seven different polarity intervals. After about 13.5 million years ago, eruptions became increasingly less frequent, and volcaniclastic and epiclastic deposits commonly separate flows. The four youngest sequences of flows—the "Pomona," "Elephant Mountain," "Ice Harbor," and "Lower Monumental"—are about 12, 10.5, 8.5, and 6 million years old, respectively. These four units, all of which locally fill deep canyons eroded in older flows, have progressively smaller volumes: "Pomona," about 625 cubic kilometers; "Elephant Mountain," 250 km^3; "Ice Harbor," 10 km^3; and "Lower Monumental," 5 km^3. The pattern of rapid, almost continuous, emplacement of basalt followed by a much longer period of episodic eruption suggests a major initial melting event followed by several relatively minor melting events spread over a 7-million-year period. The locus of volcanism on the plateau shows no progressive change in location within the 16 to 6-million-year interval, in contrast to patterns in southeast Oregon and the Snake River Plain.

Invasive sills near Wenatchee, Washington

Fifteen years ago, Hoyt (1961) described a 120-m-thick sill of Yakima Basalt intruding fine-grained sedimentary deposits at Rock Island Dam near Wenatchee, Washington. The sill, which Hoyt named the Hammond sill, has a glassy chilled upper contact with the siltstones and fine sandstones, and dikelike offshoots connect it with one or more satellite sills 10 to 20 m higher in the sedimentary section. Hoyt concluded that the sill is a true sill, that is, one in which magma intruded the sedimentary deposits from depth.

Field observations and mapping by D. A. Swanson and G. R. Byerly indicate that the Hammond sill and other similar bodies in the area are not sills in the usual sense but are "invasive sills" formed when lava pours into a basin containing a thick deposit of poorly consolidated, low-density sediments. The lava invades these sediments and hydraulically jacks up the deposit as more and more lava continues to pour into the basin.

Evidence comes from pillow-palagonite and hyaloclastite complexes on top of the sill grading laterally into peperites and deformed sediments that in turn grade laterally into the virtually undisturbed deposits. Direction-of-flow indicators show movement toward the basin, not away from it. The upper major sill grades laterally into a thick complex zone of lava flows, some peperites, and foreset-bedded lava deltas that must have formed on the surface. Feeder dikes and doming of overlying flows are lacking. Many of the pillow fragments associated with the sills are rather flat and have thick glass selvages on both sides, similar to fragments commonly dredged from the sea floor, which clearly indicates water ingress into hollow pillows before breakup.

One invasive sill on the Columbia Plateau may have economic significance. Diatomite in the Frenchman Coulee area is mined from a deposit thought to lie depositionally on lava flows of the Roza Member of the Yakima Basalt. Observations by Swanson and Byerly, however, indicate that the Roza is invasive into the diatomite, which actually was being deposited when the Roza was erupted. Exploration to extend the mining operations has heretofore concentrated on the post-Roza sediments. It seems possible that commercial diatomite equivalent to that currently being mined may occur beneath the Roza, where the flows failed to invade and lift it up.

GEOCHEMISTRY OF BASALTIC ROCKS

Sulfide globules in Mid-Atlantic Ridge basalts

G. K. Czamanske, using the electron microprobe, has determined the bulk composition of immiscible sulfide globules in the glass phase of 25 fresh submarine basalt samples collected by J. G. Moore from the Mid-Atlantic Ridge. Twenty-three samples represent a spectrum of primitive through differentiated tholeiites from the FAMOUS dive area, north of the Azores; two are differentiated basalts from the Rejkjanes Ridge, south of Iceland. The analyzed globules range in diameter from 11 to 223 μm. On the average, they constitute only 0.002 volume percent of the rocks and contain less than 1.5 percent of the sulfur. Compositions of the globules change with differentiation as measured by iron/(iron + magnesium) or TiO_2 content of the host glass. Globules in glass containing 0.66 to 1.0 weight percent TiO_2 typically contain 20 to 26 weight percent nickel + copper and have an average atomic nickel to copper ratio of 1.6. With differentiation toward 1.6 weight percent TiO_2, nickel + copper content of the globules falls to less than 10 weight percent and atomic nickel to copper ratio falls to 0.4.

Sulfur content of the host glasses shows a strong correlation with FeO content; the sulfur content increases from 840 ppm to 1,370 ppm as FeO content increases from 8.0 to 12.6 weight percent. Reference to experimental studies shows that this relationship is consistent with sulfur saturation of the host glass at liquidus temperatures. Crustal fractionation is considered to be the dominant factor in keeping the differentiating melt at sulfur saturation.

The sulfide globules may have persisted in the basaltic melt from its place of formation by partial melting in the mantle, or they may have exsolved from the melt as it became sulfur-saturated in a high-level magma chamber. Globule abundance and composition indicates adjustment to the composition of the melt in which they were trapped. Material balance calculations suggest that one-third of the copper and commensurate amounts of sulfur, nickel, and iron have settled from the magma as immiscible globules.

The sulfide globules contain less than 4 weight percent magnetite, compatible with low oxygen fugacity in the magma. Three sulfide phases coexisted in the globules at about 600°C: monosulfide solid solution, intermediate solid solution; and pentlandite. At lower temperatures the intermediate solid solution has broken down and the monosulfide solid solution has exsolved a second generation of pentlandite.

Chemical changes in Watchung Basalt New Jersey

Pearce and Cann (1973) and Pearce, Gorman, and Birkett (1975) presented chemical criteria using Ti, Zr, Y, Sr, and Nb contents and K_2O to TiO_2 to P_2O_5 ratios that purportedly are useful in distinguishing the tectonic settings of basaltic rocks. Application of these chemical criteria by G. T. Faust to the Watchung Basalt and the Palisade Diabase of New Jersey yields spurious or unequivocal tectonic settings. Although the potassium contents of the Watchung and Palisade rocks have been enriched by lowgrade metamorphism, the trace element contents appear to be essentially unmodified, and the failure of the chemical criteria as tectonic indicators seems to cast some doubt on their applicability to altered rocks.

Hydrothermal alteration of ophiolites

Secondary mineral assemblages in mafic rocks from the Miocene ophiolite of the southeastern Red Sea Coastal Plain, Saudi Arabia, and from the Semail ophiolite, Oman, studied by R. G. Coleman, indicate sub-sea floor hydrothermal metamorphism under conditions transitional from zeolite facies, through prehnite-pumpellyite and greenschist facies, to lower amphibolite facies of metamorphism, at probable temperatures of about 150° to 400°C. The retention of primary igneous textures is characteristic of these rocks and distinguishes this type of metamorphism from regional dynamothermal metamorphism. Typical mineral assemblages in greenschist-facies rocks include chlorite, albite, epidote, actinolite, and sphene. At lower grades zeolites, albite, sphene, prehnite, and rare pumpellyite occur. At grades transitional to amphibolite facies, plagioclase (An_{45-60}) is stable and may retain igneous zoning; clinopyroxene is totally replaced by fibrous blue-green to green amphibole (uralite). In the Omani rocks, zeolite facies assemblages are confined to basaltic rocks; diabase ranges from prehnite-pumpellyite to lower amphibolite facies, and gabbro displays upper greenschist to lower amphibolite-facies mineralogies. A similar pattern of alteration is observed in the ophiolite of Saudi Arabia; however, the grade of metamorphism generally does not exceed the greenschist facies. Chemically, the lower grade rocks diverge most strongly from their presumed original compositions. Marked changes in CaO, Na_2O and MgO contents reflect a high degree of chemical mobility and exchange with hydrothermal fluids. The higher grade rocks do not exhibit this extensive metasomatism.

EVOLUTION OF SILICIC MAGMA CHAMBERS

Thermal and chemical evolution of high level silicic magma chambers

Studies by H. R. Shaw and R. L. Smith (USGS) and Wes Hildreth (University of California) indicate that chemical gradients form in the upper 1 to 2 km of high-level silicic magma chambers without significant crystallization during at least 100,000 years prior to eruptions that produce voluminous ash flow sheets. Low phenocryst contents, temperature gradients based on iron-titanium oxide data, and evidence for shallow depth indicate that natural convection exists within these chambers during their pre-eruptive evolution but is suppressed within the upper 1 to 2 km at a late stage to preserve the observed chemical and phenocryst gradients. A mechanism of thermogravitational chemical separation in the liquid state coupled with boundary layer convection and diffusional exchange across these layers is derived to explain this evolution. As convection and exchange progress, light fractions are gradually accumulated at the top of the chamber, and the convection boundary layer is gradually displaced downward as the buoyant fraction increases. Although many parameters are uncertain, calculations based on the theory of thermogravitational separation columns are consistent with major and trace element enrichment factors observed in the Bishop Tuff, California (Hildreth, 1976) and the Bandelier Tuff, New Mexico (Smith and Bailey, 1966) that represent the contents of magma chambers of Long Valley and Valles calderas, respectively.

Chemical evolution of Long Valley magma chamber, California

R. A. Bailey's studies of preliminary results of mineralogical and chemical studies of the silicic volcanic rocks of Long Valley caldera, Mono County, Calif., indicate that four distinct "batches" of magma, separated by well-defined compositional gaps, occupied the magma chamber during its pre- and post-caldera evolution. Each magma batch is represented by a paired sequence of aphyric to sparsely porphyritic rocks and younger coarsely porphyritic rocks. With increasing silica content, the batches show a progressive increase in FeO (total)/FeO(total)+MgO, typical of calc-alkaline differentiation trends (Nockolds, 1947). However, within each batch, the coarsely porphyritic rocks show a secondary trend of decreasing FeO(total)/FeO(total)+MgO with increasing silica, typical of trends defined by Osborne (1959). Preliminary interpretation of these contrasting trends is that the interbatch calc-alkaline trend was produced during generation of the individual batches, either by fractional fusion at depth or by some other differentiation process during rise of the magma to shallow levels in the crust; and that the secondary intrabatch trends were produced by differentiation under oxidizing conditions within the shallow magma chamber.

Marked europium depletion in the more silicic batches and decreasing depletion in the less silicic batches indicates that plagioclase fractionation was important during generation of the successive batches, but little or no change in europium depletion *within* the batches indicates that plagioclase fractionation did not occur during high-level differentiation of the individual batches. This interpretation is corroborated by a marked change in strontium content accompanying the interbatch trends and by little or no change accompanying the intrabatch trends.

Magmatic cycles in the Coso Range, California

The Coso Range of southeast California is underlain principally by Mesozoic granitic rocks that are partly veneered by upper Cenozoic volcanic rocks. Field mapping by W. A. Duffield and C. R.

Bacon and K–Ar dating by G. B. Dalrymple have tentatitvely identified two cycles of volcanism during the late Cenozoic. The older cycle began about 4 million years ago with eruption of many basalt flows, the oldest volcanic rocks at Coso, and ended about 3 million years ago with explosive eruption of rhyodacite. Some andesitic to dacitic lavas, as well as basalt, were extruded during middle parts of the cycle. The younger cycle, like the older, was initiated by eruption of basalt and culminated with extrusion of 37 rhyolite domes. No rocks of intermediate compositions are associated with this cycle. The oldest dated lava that may represent the onset of the younger cycle gave a K–Ar age of about 2 million years, but older basaltic units, as yet undated, may be somewhat older. Most of the rhyolite domes are younger than 150,000 years, with some extruded as recently as a few tens of thousands of years ago. Both cycles are characterized by an evolution from basaltic to rhyolitic compositions, although in detail the older cycle is more complex.

ANCIENT VOLCANISM IN CALIFORNIA

Early Cretaceous volcanism in the Sierra Nevada

A small (3 km^2) composite pluton, the granodiorite of Rush Creek and the quartz monzonite of Billy Lake, exposed along the southern edge of the Mono Craters Quadrangle (Kistler, 1966) in the east central Sierra Nevada has been dated by R. W. Kistler by the rubidium-strontium whole-rock technique. The pluton has been deformed by the latter of two deformations that folded volcanic rocks intruded by the pluton. The age of the pluton therefore provides an upper limit for the first deformation and a lower limit for the second deformation.

The deformed composite pluton is 99.1 ± 7.2 million years old, and its initial $^{87}Sr/^{86}Sr$ is $0.7048_8 \pm 0.0001_7$. The deformed pluton is intruded by undeformed granitic rocks 83 million years old. Thus, the first deformation is older than 99 million years, and the second deformation is between 99 and 83 million years old (middle Cretaceous).

The age and initial $^{87}Sr/^{86}Sr$ of the composite pluton are identical to those of a 1-km thick section of Lower Cretaceous metamorphosed volcanic rocks exposed about 5 km away. Correlation of these volcanic and plutonic units suggests that the pluton is the eroded vent area for the volcanic pile. A geologic cross section through the area suggests that the eruptive center was a dacite-rhyodacite stratovolcano. This pluton is the first demonstrable Mesozoic volcanic source area in the Sierra Nevada.

Devonian island-arc volcanism, West Shasta district

Devonian rocks of the West Shasta district in California include the Copley Greenstone and the largely overlying Balaklala Rhyolite. These units are intruded by the so-called Mule Mountain Rhyolite (trondhjemite). Geochemical results by Fred Barker, H. T. Millard, Jr., and R. J. Knight show that the Copley ranges in silica content from 54 to 63 percent, has low concentrations of potassium and rubidium, has lanthanum contents 5 to 11 times and lutecium contents 8 to 17 times that of chondrites, and probably is a fractionate of low-potassium or island-arc tholeiite. The Balaklala Rhyolite is a low-potassium, high-silica dacite, has had its original concentrations of potassium, rubidium, and strontium disturbed by diagenesis and low-rank metamorphism, shows lathanum 7 to 8 times and lutecium 13 to 23 times that of chondrites, and is an arc-type dacite like that of Saipan. These results thus confirm earlier workers' designation of the Copley and Balaklala as island-arc volcanic rocks.

The "Mule Mountain" trondhjemite is nearly identical in major- and minor-element composition to the least siliceous sample of Balaklala Rhyolite. Thus "Mule Mountain," even though not directly dated by radio-metric techniques, probably is a plutonic equivalent of the Balaklala and is not of Mesozoic age, as supposed by earlier workers.

URANIUM IN VOLCANIC ROCKS

Uranium in tuffaceous aquifer rocks, Nevada

Uranium abundance and distribution have been measured in about 50 rhyolite core samples collected by R. A. Zielinski at the Nevada Test Site, Nye County, Nev. Samples were of peralkaline Grouse Canyon Member of the Belted Range Tuff and were chosen to represent various degrees of welding, devitrification, and alteration. Uranium abundances ranged from 2.6 to 9.0 ppm and were remarkably constant within individual flow units. Local remobilization of uranium resulting from crystallization and (or) alteration was evident from study of fission track maps of polished thin sections. Uranium distribution was homogeneous in obsidian and glassy groundmass but was localized in many "hot spots" in devitrified lavas. Areas most susceptible to attack by groundwaters such as microfractures and pumice fragments contained uraniferous secondary oxides of iron and manganese. Contacts of flattened pumice fragments and groundmass commonly were areas of uranium concentration.

Dating of secondary silica: a guide to uranium mobility

As part of a geochemical investigation in the Shirley Basin, Wyoming, samples of cryptocrystalline silica present as fracture fillings in tuffaceous sandstone have been dated by lead-uranium isotopic systematics. The fracture fillings, originally described by E. N. Harshman (1972), consist of grey translucent silica and occur as bands, 1-5 cm wide, in basal members of the White River Formation (Oligocene). The majority of bands follow fractures that closely parallel bedding, although some small bands crosscut bedding at angles up to 90°. Fission track maps of samples collected by R. A. Zielinski revealed a homogeneous distribution of uranium with concentrations greater than 200 ppm. Tentative interpretation is that groundwater percolated downward through glassy tuff of the White River Formation and dissolved silica and uranium until supersaturation of silica caused coprecipitation of silica and uranium in basal tuff. To investigate the timing of such a process, a 1-cm-wide band was crushed to a coarseness that allowed hand picking of inclusion-free material. U-Pb isotopic analysis of this material by K. R. Ludwig gave a discordant apparent ($^{207}Pb/^{235}U$) age of 18.8 ±.7 million years and a uranium content of 242 ppm. The age discordance is typical of many geologic materials and is likely caused by leakage of members of the ^{238}U-decay series. If such is the case, Pb^{207}/U^{235} age represents a best estimate of the minimum age of the silica bands. Maximum age is that of the host rock, which is 32.4 ±2.6 million years (determined by C. W. Naeser, who used fission track measurements of zircon separates from tuff collected about 5 m above the band). Minimum ages of 24 ± 3 to > 35 million years, previously determined by K. R. Ludwig (in press) for nearby uranium deposits found in Eocene sandstone of the Wind River Formation, permit some uranium contribution from the postulated leaching of tuffs. Tighter correlation of dates for ore formation and nearby uranium migration should be possible for samples of uraniferous secondary silica and uranium ores that occur in the same host rock.

PLUTONIC ROCKS AND MAGMATIC PROCESSES

Evolution of a tin-granite complex and associated Seward Peninsula, Alaska

The Upper Cretaceous biotite granite complex of the Serpentine Hot Springs area of Alaska, recently studied by T. L. Hudson, like several similar granitic complexes in the region, is spatially and genetically associated with tin mineralization. This complex is an epizonal composite stock that contains several sequentially developed textural facies. Compositional variations through the facies sequence define an early crystallization stage characterized by salic compositions (SiO_2 = 73 to 77 percent, CaO < 1 percent), a transition to an intermediate stage characterized by less salic compositions (SiO_2 = 71 percent, CaO ≥ 1.5 percent), and a late crystallization stage that marks a distinct shift back to more salic compositions (SiO_2 = 75 to 77 percent, CaO < 0.75 percent). Whole-rock and biotite trace-element analyses show that the late shift to more salic compositions marks the evolution of a residual volatile-rich magma system enriched in such elements as lithium and tin. Some distinctive compositional characteristics of the entire complex are the high average Na_2O/K_2O ratio, the overall enrichment in such trace elements as Be, Li, Nb, Pb, Sn, and Zn, and the high initial $^{87}Sr/^{86}Sr$ ratios. These relations indicate that the tin-granite magma was initially strongly fractionated and probably produced by crystallization of a parent batholith partially melted from old sialic crust. Final crystallization of the tin-granite magma in an epizonal environment was marked by the escape of a tin-rich aqueous phase along high-angle faults. These faults are probably related to dynamic adjustments that accompanied late-stage crystallization of the stock; they are the principal controls to tin and associated mineralization.

Partial fusion on granite by basalt in the Sierra Nevada

Partially fused granite adjacent to a 100-m diameter basalt plug near Tuolumne Meadows in the central Sierra Nevada has been studied by F. C. Dodge and L. C. Calk. The granite has not been altered at distances greater than 3.5 m from the plug; however, within this distance trace amounts of glass occur along fractures and grain boundaries, biotite changes from dark olive to dark reddish brown, and optic axial angles decrease toward the contact.

As much as 20 percent by volume of glass occurs in a reentrant and in inclusions within the plug. Two partially fused samples have been studied in detail. SiO_2 is clearly depleted relative to unfused granite in both samples, whereas K_2O is depleted in one but not significantly changed in the other. Al_2O_3, total Fe, MgO, H_2O, and possibly Na_2O show apparent increases in both samples; other constituents show no significant changes. Relative chemistry suggests that as much as 30 weight percent of the original material may have been lost, probably by mass migration of glass rather than by chemical diffusion from the partially fused rock. SiO_2 content of the presently included glass is greater than that in its partially fused host; Al_2O_3, total Fe, and CaO are less, and MgO, Na_2O, and K_2O are less in one sample but greater in the other. If initial compositions are assumed to have been the same, compositions of the glasses can be related to trends of fractional partial fusion of the original rock.

Granitic rocks of Yosemite National Park, California

Recently completed geologic mapping by D. L. Peck of the Merced Peak and Yosemite quadrangles, which cover the southern third of Yosemite National Park, reveals the area to be underlain predominantly by Cretaceous plutonic rocks in more than 50 individual bodies ranging in composition from quartz diorite to leucogranite. Field relations and radiometric dating by R. W. Kistler and T. W. Stern show that almost all of the granitic bodies belong to four plutonic associations, each of which is composed of granitoid rocks of similar age and lithology. The oldest association, which underlies the western border of the park, has been provisionally dated at about 115 million years; it consists of hornblende tonalite and biotite granodiorite, which is called, in part, the granodiorite of the Gateway by Calkins (1930). The second association, which forms an adjoining north-northwest-trending belt on the east, has been provisionally dated at about 100 million years; it consists of coarse-grained, porphyritic biotite granodiorite and granite and includes the El Capitan and Taft Granites. The next younger association, exposed farther east in the Sierra Nevada, is composed of nearly contemporaneous metavolcanic rocks, subvolcanic domes, and granitoid plutons, which have yielded ages in the range of 95 to 100 million years. The metavolcanic rocks, which are preserved in screens and pendants near Merced Peak, are chiefly derived from massive rhyodacitic and rhyolitic tuffs. These are intruded by two stocks or domes of fine-grained granite porphyry, one of which (the granite of Red Peak) apparently intruded water-saturated wall rocks at shallow depth, as shown by widely distributed pyrite and miarolitic cavities. The metavolcanic rocks and granite porphyries are in turn intimately intruded by medium-grained biotite granodiorite of the Jackass Lakes pluton. The granite porphyry bodies are interpreted to be the degassed fillings of subvolcanic cupolas atop a larger chamber now represented by the Jackass Lake pluton. This complex of metavolcanic rocks is intruded by slightly younger compound plutons of the same association centered on the Buena Vista Crest and Washburn Lake; these are zoned from margins of quartz diorite and mafic granodiorite to small cores of fine-grained granite and granite porphyry that may record later volcanism. The youngest association comprises several concentrically zoned plutons near the crest of the Sierra Nevada, including the classic Tuolumne Intrusive Series of Calkins (1930). Many K-Ar analyses of biotite and hornblende from these bodies range from 80 to 90 million years. Considering the duration of intrusion and solidification of each association, probably 5 to 10 million years, and the uncertainty of radiometric dating, the associations appear to reflect nearly continuous igneous activity in this part of the Sierra Nevada batholith from 115 to 80 million years ago.

METAMORPHIC PROCESSES

P_{total} versus P_{H_2O} in metamorphism

The importance of total pressure relative to P_{H_2O} is a major consideration in metamorphic processes. Past discussions of this problem in the literature have been incomplete and perhaps obscure to many readers. J. J. Hemley has pointed out the relationship

$$G^*_{H_2O\ equil.} - G^*_{H_2O\ unknown} = (P_{total} - P_{H_2O\ equil.})\Delta Vs,$$

where G* is the free energy of formation of water at P_{H_2O} and T, relative to the elements at 298°C, 1 bar, Δ Vs is the volume change of reaction for the solid phases, and the subscript *equil.* refers to any point on a univariant P_{H_2O}-T mineral dehydration curve for the system under consideration. By using this equation and the tabulations for the face energy of formation of water, any given P_{H_2O}-T petrogenetic net is easily recalculated for different values of P_{total}. For precise work, compressibility and thermal expansion of the solids may be incorporated. New invariant points are not produced, however, nor the topology of the *PT* net modified. These calculations are very important for any experimental or theoretical metamorphic study as the shift in P_{H_2O}-T curves, and the consequent migration of invariant points may render a given reaction curve or invariant point either more accessible or less accessible geologically and thereby critically alter potential geologic interpretations.

Petrology and age of the Belchertown pluton, Massachusetts

The Belchertown pluton in west-central Massachusetts that intrudes lower to middle Paleozoic strata in the Bronson Hill anticlinorium has been studied by G. W. Leo (USGS) and L. D. Ashwal, (Princeton University). On the south and east sides, the Belchertown pluton is quasi-concordant with the surrounding country rock. On the north side, the pluton cuts irregularly across a series of early Acadian recumbent folds. Gravity and aeromagnetic models suggest a relatively thin (about 1 km), disc-shaped mass with a deeper root in the southeast portion, consistent with a funnel-shaped (lopolithic) intrusion or with the eroded remnant of a more extensive sub-horizontal sheet preserved by downfolding.

The pluton has a small core of essentially unmetamorphosed, two-pyroxene biotite quartz monzodiorite. The primary oxide assemblage of magnetite-titanohematite suggests a very high oxygen fugacity during magmatic crystallization. Outward from the unmetamorphosed core, the rocks of the pluton grade to pyroxene-free, hornblende-biotite-epidote gneiss that has foliations and lineations parallel to those in the adjacent metamorphosed country rock. Petrographic evidence and bulk rock analyses of the pluton indicate that mineralogical changes from unaltered core to marginal gneiss were essentially isochemical except for water and reflect progressive hydration accompanying regional metamorphism. Detailed structural studies show that hydration of marginal gneiss was facilitated by influx of fluid along cataclastic shear zones in solidified quartz monzodiorite.

A U-Pb zircon age determination from the least altered quartz monzodiorite of 380 $\pm$5 million years is in excellent agreement with ages from several other plutons in the region that also cut across early fold structures. All of these plutons have in turn been deformed and metamorphosed in the later stages of the Acadian orogeny.

Stability relations of antigorite and chrysotile

A controversial and poorly understood aspect of the origin of serpentinites is the stability relationship of antigorite and chrysotile. On the basis of the idealized structural formula for antigorite ($Mg_{2.825}Si_2O_5(OH)_{3.65}$) and thermodynamic data derived from earlier experimental studies, J. J. Hemley has calculated the transition temperatures for the reactions: 0.117 talc+1.766 chrysotile=2 antigorite and chrysotile=antigorite+0.175 brucite at approximately 180°C and 325°C, respectively, at 1 kbar. These temperatures define a range of stable coexistence for chrysotile and antigorite of approximately 145°C, with the presence of brucite extending, and that of talc diminishing, the temperature stability limit of chrysotile. The uncertainty in the temperatures is largely due to the unusual sensitivity of the calculations to errors and uncertainties in the thermodynamic data, and, in fact, is sufficient to eliminate substantially a field of stability for chrysotile. However, in agreement with geologic field relations, a stability field is suggested at these low, but geologically reasonable temperatures, with higher temperature, higher aqueous silica activity, and probably higher total pressure favoring the stability of antigorite relative to chrysotile.

GEOCHEMISTRY OF WATER AND SEDIMENTS

DIAGENETIC STUDIES

Geochemistry of volcanic sediment in an alkaline lake

A study of sediment provenance and initial interaction of water with volcanics at saline, alkaline Lake Abert in south-central Oregon was carried out by B. F. Jones and R. G. Deike by means of separation of particle-sized fractions, followed by optical, X-ray, and cation chemical analyses of the fine (75–150 μm) sand. The mineral distribution showed that: (1) Sediments at the south end of the lake contain very little calcite, despite supersaturated solutions, and increase in abundance northward; (2) plagioclase feldspar, pyroxene, and magnetite detritus are most abundant near areas dominated by holocrystalline basalts; (3) lithic matrix fragments (LMF), chiefly from cryptocrystalline pyroclastics, are most abundant near Chewaucan River inflow to the south and the steep slopes of Abert Rim to the east; (4) diatom frustules are most common in and near dilute inflow; (5) glass shards are plentiful and uncorroded at depth in midlake and playa cores; (6) olivene, although common in some source rocks, is only rarely found in the lake sediments; and (7) other minerals are present in very minor amounts. The positive correlation between the amount of LMF in the fine-sand fraction and the quantity of clay, which may compose more than 50 percent of the sediment and is primarily mixed-layer smectite/illite, suggests LMF alteration as a prime source of fine material. The highly irregular zeolite distribution and the association of the zeolite with fresh glass shards suggest that zeolite formation precedes deposition in the lake. Sediment fine-sand fractions account for solute losses of calcium and silica in calcite and diatoms, whereas the somewhat higher magnesium content of cryptocrystalline LMF and the association of LMF with clay content suggest reactions between lake waters and submicroscopic sediment.

Sedimentary diagenesis related to marine ferromanganese deposits

On the basis of transition-metal analyses of the northeastern equatorial Pacific Ocean pelagic sediment interstitial water and associated sedimentary material, Edward Callender and R. J. Shedlock (USGS), C. J. Bowser (University of Wisconsin) postulated that manganese is efficiently trapped within surficial oxidized sediment. However, copper, which is associated predominantly with biogenic carrier phases, is diagenetically remobilized within surficial sediment. A significant fraction of the remobilized copper diffuses across the depositional interface into deep ocean water while some of the remainder is incorporated into manganese micronodules that are forming in surficial sediment. Interstitial water and associated sediment-chemistry data suggest that the diagenetic mobilization process for copper is more intense in red-brown clay sediments than in siliceous-ooze sediments.

Distribution coefficients for zinc and cadmium in stream water and seawater

V. C. Kennedy and G. W. Zellweger found that addition of 110 mg/L of suspended sediment to stream water of pH 8 containing 2 μg/L of cadmium and 10 μg/L of zinc in solution permitted the determination of the distribution coefficient (K_d of these metals between sediment and solution. K_d is defined for this study as the ratio of the metal taken up by the sediment (mg/kg) to the metal concentration in solution (mg/L) after addition and equilibration for 6 hours. The K_d under the conditions described was 5,800 for cadmium and was 30,000 for zinc. When a similar experiment was conducted in seawater at pH 7.9 and a suspended-sediment concentration of 400 mg/L, the K_d for cadmium was less than 300 and was 3,000 for zinc. These data suggest that substantial desorption of cadmium and zinc occurs when freshwater sediments enter the marine environment. Such desorption has been observed by others when studying the effect of seawater on radioactive zinc held in river sediments. Both the water and sediments used in the experiments described here were taken from the Mattole River, a clean coastal stream in northern California.

A biogenic-chemical stratified-lake model

A model proposed by G. A. Desborough involves biogenic-magnesium enrichment, a stratified-lake environment, and authigenic growth of minerals that led to the development of oil shale in the lacustrine Green River Formation. The chemistry and mineralogy of Ca-Mg-Fe carbonates and other minerals in oil shale are consistent with an authigenic origin. The higher content of magnesium with respect to calcium in kerogen-rich rocks is probably due to the preferential concentration of magnesium with respect to calcium by blue-green algae whose remains, after accumulating on the lake bottom, released these cations. These elements were available for incorporation in Ca-Mg-Fe carbonates that crystallized in lake-bottom muds, while degradation of admixed algal material led to the development of kerogen. In modern lacustrine environments, primary and secondary Ca-Mg-Fe carbonate development and stability in terms of geologic time are consistent with authigenic development of the Ca-Mg-Fe carbonates present in Green River Formation oil shale. Iron is a significant component of these rhombohedral carbonate assemblages in oil shale and thus limits interpretations of origin of oil shale in the context of $CaCO_3$-$MgCO_3$ equilibria.

The variable composition and variety of Ca-Mg-Fe carbonates in oil shale also prohibit interpretations in terms of $CaCO_3$-$MgCO_3$ equilibrium diagrams. Similarly, inferences regarding the chemical composition and structure of these carbonates lead to misinterpretations owing to either a lack of adequate chemical data or to a misunderstanding of crystallographic parameters.

Greater amounts of mineral matter in time-stratigraphic intervals in the depositional center of the Piceance Creek basin, compared to the basin's margins, strongly suggest that authigenic mineral development is more important than detrital accumulation of minerals in the rich oil-shale sequences.

Fluid inclusion evidence on the environments of sedimentary diagenesis

Most sedimentary diagenesis involves recrystallization or overgrowths on original minerals or the growth of new phases. E. W. Roedder has shown that this new growth may trap fluid as inclusions that provide data not only on the nature, composition, pressure, and density of the fluids present during diagenesis but also particularly on the temperature at which the host crystals grew. As most optical methods of study require inclusions >1 to 2 μm in diameter, fine-grained products of diagenesis, in the 10 to 20 μm range, seldom provide useful material. The possibilities of finding inclusions of useful size increase with the size of the host crystal. In spite of these limitations, reasonably valid quantitative or qualitative physical and chemical data, both new and from the literature, have been obtained on inclusions from the following specific diagenetic environments: (1) Crystal-lined geodes, vugs, and veins in sediments; (2) Mississippi Valley-type ore deposits; (3) carbonate and quartz cements in detrital rocks; (4) saline and sulfur deposits; (5) petroleum reservoir rocks; and (6) sphalerite in bituminous coalbeds.

Most inclusion temperatures in these and other similar environments range from 25°C to 150°C, and the fluids are generally strongly saline brines that commonly contain petroleum and up to tens of atmospheres of methane-rich gas. Homogenization temperatures of inclusions in some Mississippi Valley-type ore deposits are higher than 150°C but seldom exceed 200°C. It is concluded that hot, strongly saline fluids have moved through many if not most sediments at some time in their history and that at least part of the diagenetic changes seen have been caused by such fluids.

Origin of natural gas associated with shales

I. A. Breger's and Marta Drasnow's study of peat derived from sawgrass in the Florida Everglades showed that degradation of cellulose is retarded where there is an increase in the quartz-sand content of the peat. Inasmuch as anaerobic decomposition of cellulose leads to the formation of methane, this observation suggests that burial of cellulose from plant debris in a mineral-rich environment may eventually lead to the later formation of methane under conditions where it can be trapped and retained in sediment. This may explain the association of natural gas with the Devonian shales of the southeastern United States where the organic matter in the shale, the kerogen, has been shown to be related to coal.

GEOLOGIC CONTROLS ON WATER CHEMISTRY

Ion-ratio maps used to define ground-water-flow systems

Ion-ratio maps prepared by R. W. Lee from preliminary ground-water-quality data on aquifers above the Pierre Shale in southeastern Montana indicated that the ground-water regimen consists of two distinct geochemical systems. The geochemical gradients observed on the ion-ratio maps corroborated concepts of S. E. Slagle and B. D. Lewis that the flow of water at shallow depths (less than about 75 m) is characterized by flow from recharge areas near topographic divides to discharge areas in drainages. The ion-ratio gradients delineated the cellular fabric of the shallow ground-water system, which coincided with the topographic contours. Water quality varied from the primary constituents $Mg^{++} > Ca^{++} \geqslant Na^{+}$ and $HCO_3^{-} \geqslant SO_4^{--}$ of low dissolved-solids concentrations (500 mg/L) near the recharge areas to predominantly Na^{+} and SO_4^{--} of moderately high dissolved-solids concentrations (3,500–4,000 mg/L) near the drainages or discharge areas.

Water in deep aquifers (below about 75 m) was really more uniform in chemical composition and was dominated by Na^{+} and HCO_3^{-} of 1,500 to 2,000 mg/L dissolved solids. This consistency of chemical composition led to the concept of a regional flow system for the deep ground water.

The concept of a shallow ground-water system, at depths of less than 75 m, defined and localized by topography to form a cell-like fabric overlying a deeper regional ground-water-flow system, at depths greater than about 75 m and characterized by upward flow or discharge to shallower aquifers, was incorporated into a digital model of ground water above the Pierre Shale in the Powder River basin.

Tuffaceous rocks in southern Nevada

The results of an extensive ground-water geochemical sampling program at the Nevada Test Site and adjacent areas provided an opportunity to investigate kinetic and equilibrium mechanisms controlling the chemistry of ground water associated with Tertiary rhyolitic tuffs. A. F. White reported that a comparison of the quality of this water with the quality of ground-water related to crystalline rocks of similar bulk composition, and also with the results of laboratory dissolution and exchange studies, suggested that the predominantly sodium bicarbonate ground water, high in dissolved silica, is primarily the result of hydrolysis and dissolution of the vitric phase of the tuff. Apparently, this results from the greater reactivity of the vitric phase and the larger surface areas associated with greater interstitial porosity. Ground-water geochemistry is also controlled by aqueous solubility and by formation of secondary phases, including amorphous silica, montmorillonite, and a number of sodium-rich zeolites. In areas of shallow ground water, evapotranspiration further increases dissolved solids and permits the precipitation of calcite and fluorite.

Geochemical kinetics

A matrix of aqueous reactions to determine reaction path, kinetic-rate constant and its dependence on reactant concentration, temperature, and surface-to-volume ratio were carried out on a single-phase (solid) system, vitric material from the Miocene Rainier Mesa Member of the Timber Mountain Tuff. H. C. Claassen and A. F. White reported that initial behavior of this system can be represented by a simple diffusion model; however, high surface-to-volume ratios produce measurable deviations from the simple model. These deviations are probably caused by changes in the Gouy electrical double layer that result from greater solution concentrations. The temperature dependence of reaction rate was found to obey the Arrhenius equation. Some results of these experiments were used to aid in defining a complex ground-water system in southern Nevada.

Preliminary experiments with a multiphase (solid) system indicated results similar to those shown by the single-phase system. In addition, the reaction path defined by laboratory experiments appeared to be identical to that deduced from random sampling of water quality in a lithologically homogeneous and hydrologically isolated model-study area.

Decomposition of organic compounds in ground water

M. J. Baedecker and William Back (USGS) are working informally with Michael Apgar and Ron Stoufer (Delaware Division of Environmental Control) to determine the effects of organic compounds and inorganic constituents on controlling chemical reactions. They have tentatively concluded that organic compounds decompose rapidly as leachate mixes with oxygenated ground water. Carbon-13 measurements by E. G. Spiker showed that the resultant HCO_3^- is exceedingly heavy (up to about +16 per mil). Gas analyses by D. W. Fisher, along with other chemical and hydrologic data, permitted the delineation of an oxygen deficient zone, a transition zone, and an oxygenated zone.

Geopressured geothermal waters

Y. K. Kharaka, Edward Callender, and W. W. Carothers (1977) reported that detailed chemical and isotopic analyses of 54 formation water samples from 11 oilfields and gasfields in Texas showed that (1) the salinity of water in the geopressured zone may range from about 20,000 to 70,000 mg/L dissolved solids, higher than previously believed; (2) samples from many gas wells yield low salinities not representative of the true salinity of formation water because they are diluted by condensed water vapor produced with natural gas—chemical geothermometers can be used to identify the diluted samples; (3) organic acid anions contribute significantly to the measured alkalinites (W. W. Carothers, 1976); and (4) the concentrations of problem components, H_2S and silica, are low, and the concentrations of toxic components, such as boron and ammonia, are moderately high. Subsurface injection is probably the only acceptable method of disposal of spent geothermal waters.

Warm springs of South Island, New Zealand

Studies of South Island, New Zealand, warm springs by Ivan Barnes, in cooperation with the New Zealand Department of Scientific and Industrial Research, showed appropriate potentials to dissolve albite and calcite and to precipitate laumontite. Zeolite-facies metamorphism apparently may occur at temperatures as low as 40°C and does not require deep burial.

Adsorption of lead by streambed sediment

Behavior of the silt-size fraction (2-74-μm diameter) of bed sediment from Colma Creek in San Mateo County, California, toward lead and other cations was studied in simulated natural water in a laboratory. A computer model developed by D. W. Brown (1976), which uses Langmuir isotherm adsorption constants obtained from the laboratory study, predicted distribution of lead between solution and adsorbed forms. Agreement between predicted and measured dissolved lead in test solution was generally within a few tenths of a log unit over a wide range of concentrations of competing ions. The adsorption affinity of the ions present was $PbOH^+ > H^+ > Pb^{+2} > Ca^{+2} > K^+ > Mg^{+2} > Na^+$.

Solubility of natural fluorite

D. W. Brown and C. E. Roberson (1977) determined the solubility of samples of natural fluorite (from Rosiclare, Ill., and Modoc, Ontario, Canada) at 25°C in dilute sodium perchlorate solutions. After 3 years of equilibration, a solubility product (extrapolated to zero ionic strength) of $10^{-10.58\pm.17}$ was obtained. This value is more nearly in accord with solubilities observed in natural water than most previously published solubility products for fluorite.

Using a fluoride ion-specific electrode, C. E. Roberson and R. B. Barnes (1977) determined the equilibrium constant for the reaction, $Si(OH)_4aq^+6F^- \pm 4H^+ = SiF_6^{-2} + 4H_2$, to be $10^{30.18}$. Other silicon fluoride complexes did not occur in important amounts. Condensates of some volcanic gases from Kilauea, Hawaii, contained substantial amounts of the complex. In most acidic natural water, aluminum and iron are more important than silicon in complexing fluoride.

Chemical rock weathering in forested watersheds

In a 2-year study of water quality in the Redwood Creek and Mill Creek drainage basins of California, W. L. Bradford and R. T. Iwatsubo found a relationship between rates of chemical weathering and kinds of land cover. Evidence suggests that calcium bicarbonate in the stream water is produced by chemical weathering of the Franciscan Formation underlying the basins, but the chlorides are transported inland from the ocean as dry fallout and spray and in rain. Exposure of the surface soil to the elements, either by logging or by natural causes such as sparse vegetation, seems to cause faster chemical weathering, which causes water type to be calcium bicarbonate. Logging accelerates chemical weathering most in tributary watersheds with regoliths derived from sandstone and least in regoliths derived from schist; rapid weathering can occur in a schistose-based watershed if soil disruption is extensive.

STATISTICAL GEOCHEMISTRY AND PETROLOGY

Geochemical Correlations

J. O. Kork has examined the Chayes-Kruskal procedure for testing correlations between proportions (Chayes and Kruskal, 1966). The Chayes-Kruskal procedure uses a linear approximation to the actual closure transformation to provide a null value, P_{ij}, against which an observed correlation coefficient, r_{ij}, can be tested. It has been suggested that a significant difference between P_{ij} and r_{ij} would indicate a nonzero covariance relationship between the *i*th and *j*th open variables. The linear approximation to the closure transformation has been described in terms of a matrix equation, and examination of the solution set of that equation has shown that estimation of, or even the identification of, significant nonzero open correlations is essentially impossible even if the number of variables and the sample size are large.

Computer simulation of compositional data

A computer program, CORRAN, has been prepared by A. T. Miesch to generate matrices of random numbers with any reasonably specified intercolumn correlations and will be useful in simulating geochemical and petrologic data. The columns of the matrices may have any specified means and variances and may be either normally or lognormally distributed. The intercolumn correlations are specified either by entering a correlation matrix or a factor matrix. If a correlation matrix is entered, the program checks for Gramian properties and rejects the matrix if they are not present. CORRAN has been especially useful in investigations of the effects of the constant sum (Chayes, 1960) on correlations observed among compositional variables.

Geochemical anomalies

An anomaly in geochemical exploration is generally regarded as a data value or group of values that departs significantly from other values that comprise the geochemical background. In practice, the values or the sampling locality averages are conceptually ordered by magnitude, and an examination is made to identify gaps—that is, large differences between adjacent averages in the ordered array—that may separate background and anomalous values. The problem is in recognizing a significant gap when it occurs. A. T. Miesch (1976) has investigated the problem by computer simulation inasmuch as existing statistical theory that is precisely applicable to the problem could not be found. The simulation experiments are used to estimate values of C_p, which can be used in the expression $g=C_p s_x$, where g is the maximum gap to be expected (at probability p) if there are actually no differences among the samples or the sampling localities and s_x is the standard error of the values or the averages. If there are only 2 values or averages (unlikely in exploration geochemistry), C_p is equal to $t\sqrt{2}$ (where t is Student's t) and g is equal to the conventional least significant difference. When more than two averages are considered, the values of C_p and g are considerably smaller.

Extended *Q*-mode factor analysis

A. T. Miesch has continued investigations of the application of an extended form of *Q*-mode factor analysis to igneous petrology. When the compositions of the lavas of Paricutin Volcano, as given by Wilcox (1954), are represented as vectors in seven-dimensional space (representing the seven major oxides, SiO_2, Al_2O_3, FeO, MgO, CaO, Na_2O, and K_2O) the vectors cluster about three planes that are interpreted to represent three distinct periods of magmatic differentiation. The first period extended from February 1943 to April 1947, the second period extended from April 1947 to November 1947, and the third period extended from November 1947 to February 1952. The compositional changes in the magma during the first period can be approximated by subtracting a mixture of plagioclase and olivine. Those changes during the second period can be approximated by subtracting a mixture of plagioclase and pyroxene and those during the final period can be approximated by either a combination of both these processes or by the assimilation of granitic material as proposed by Wilcox (1954). The methods used in the investigation have been described in Miesch (1976) and in other reports cited therein.

ISOTOPE AND NUCLEAR GEOCHEMISTRY

ISOTOPE TRACER STUDIES

Isotopic evidence for the source of hot spring deposits, Yellowstone National Park

B. R. Doe and J. F. Whelan (USGS) and W. P. Leeman (Oregon State University) studied the radiogenic isotopes of lead and strontium, as well as the light stable isotopes of carbon, oxygen and hydrogen/deuterium in hot spring deposits of Yellowstone National Park in the Western United States. The isotopic compositions contain a sedimentary component for hot spring deposits both outside and within the limits of the caldera. Either there is long lateral migration of water from outside the caldera where sediments are present, or there are sediments buried at depth under the volcanic rocks filling the caldera. The more likely interpretation is that sediments are present at depth within the caldera because most of the precipitation in the area is within the confines of the caldera and the hot spring water is determined to be meteoric. The study confirms previous suppositions that the hot spring waters within the caldera interact with sediments. These were based on the presence of travertine (calcium carbonate), which is difficult to derive from siliceous volcanic rocks.

Isotopic composition of lead in oceanic basalts

Mitsunobu Tatsumoto evaluated basalt genesis and mantle evolution based on new data for (1) the lead isotopic compositions and uranium, thorium, and lead concentrations of basalts from the Island of Hawaii; (2) redetermined lead isotopic compositions of some abyssal tholeiites; and (3) the uranium, thorium, and lead concentrations of altered and fresh abyssal basalts. The Th/U ratios of abyssal and Japanese tholeiites are distinctly lower than those of tholeiites and alkali basalts from other areas, possibly reflecting a mantle source that is depleted in large-ion lithophile elements. Thus, a model for mantle evolution is proposed in which Th/U ratios in the depleted zone have decreased to about 2, U/Pb ratios have increased, and plots of $^{207}Pb/^{204}Pb$ versus $^{206}Pb/^{204}Pb$ show an apparent isochron slope of about one billion years.

The lead isotopic composition of basalts from the Island of Hawaii are distinct for each of the five volcanoes. Within each volcano, the lead of tholeiites is similar to that of alkali basalts, which suggests they are of the same source or closely related ones. An interaction between partially melted material of the asthenosphere (hot plume?) and the lithosphere is suggested to explain the trend in the lead isotopic compositions of Hawaiian basalts.

Lead isotope composition of minerals from basalt from Leg 34 of the Deep Sea Drilling Program

D. M. Unruh and Mitsunobu Tatsumoto completed a study of lead, uranium, and thorium in mineral separates from basalts and in sediments obtained from the Nazca Plate by Leg 34 of the Deep Sea Drilling Project. Owing to analytical difficulties (low lead concentrations and relatively high blanks), detailed lead isotopic studies on mineral separates from oceanic basalts have not previously been reported.

The two most striking features of the basalts are (1) the homogeneity of the lead isotopic composition in the whole rocks when corrected for in situ decay of uranium and thorium (corrected for 15 million years of decay at Site 319 and 40 million years of decay at Site 321) and (2) the very distinct lead isotopic compositions of the pyroxene separates compared to those of other mineral separates (magnetites, plagioclases, and smectites) and whole rocks. These features suggest that partial melting of one or more primary sources produced isotopically homogeneous melts in the interval from 15 to 40 million years ago, but the pyroxenes retained distinct isotopic identities for a long time. Calculations for a four-stage model indicate that the lead of the pyroxenes evolved for at least the last 3 billion years in an environment that was higher in $^{238}U/^{204}Pb$ than that for the whole rocks and other mineral separates. These pyroxenes are not thought to have been carried from the mantle source area for the basalts because diffusion rates for lead and uranium at mantle temperatures are probably too high to allow isotopic heterogeneity to persist. It is thought that the lead isotopic composition of the magmas changed during ascent by reacting with wall rocks of the conduit after crystallization of the pyroxene. The lead isotopic composition of the pyroxenes indicates that differentiation within the mantle began prior to 3 billion years ago and contradicts the apparent "mantle isochron" age of 1.6 billion years that has recently been emphasized by Brooks and others (1976) based on strontium and lead isotopes in abyssal basalts.

ADVANCES IN GEOCHRONOMETRY

Dating of kimberlite diatreme in Albany County, Wyoming

Zircons recovered from the kimberlitic matrix of a diatreme, collected by M. E. McCallum (Colorado State University), were dated by C. W. Naeser (USGS). These zircons gave a fission-track age of 377 ± 8 million years. This Devonian age is compatible with the age previously estimated from geologic reasoning. Previous attempts to date these diatremes through the use of apatite (fission track) and biotite (potassium-argon) had produced ages that were geologically impossible.

Long-lived mineralization at Climax, Colorado

W. E. Hall and Irving Friedman separated two samples of hydrothermal sericite from the Climax molybdenum deposit for K-Ar dating to test if the time span of mineralization could be determined. They were pessimistic that it could be determined because of resetting of ages to that of the latest stage of mineralization. One sericite sample was separated from an alteration zone associated with quartz-molybdenite mineralization of the upper molybdenite orebody; the other was a sericite sample associated with the late barren stage of mineralization.

J. D. Obradovich determined this time span to be approximately 4.5 million years. The upper orebody mineralization was 29.8 ± 0.40 million years ago while the late barren mineralization was 25.3 ± 0.34 million years ago.

Thermoluminescence dating of silicic volcanic rocks

R. J. May has completed preliminary development of a thermoluminescence (TL) dating technique for silicic volcanic rocks by using a sanidine from rhyolite domes and flows of known age from the Inyo Craters, Long Valley, and Coso Mountains areas of California. The estimated age limits of the method are from about 750 to at least 100,000 years B.P. The TL data are quantified as the ratio of the 300°C natural TL to 250°C artificial TL peak heights; the artificial TL is produced by a standardized exposure to X-radiation. Both natural and artificial TL are measured within a narrow bandwidth encompassing the 4,500°A feldspar emission peak. Each TL ratio is additionally normalized for its calculated annual natural radiation dose rate.

The TL ratios for the dated samples increase at a predictable, approximately linear rate with age; the equation for the best-fit line through a plot of the TL ratios versus known age constitutes an age equation that can be used to assign relative ages to other samples of similar composition. The method has been used to establish preliminary TL ages for several previously undated sanidine-bearing rhyolite domes of the Mono Craters in California. The ages range from 8,000 to about 45,000 years B.P. and have an estimated precision of ± 5 percent.

Ancient sialic terrane identified near Watersmeet, Michigan

Radiometric dating and geologic studies of gneisses in the western part of northern Michigan by Z. E. Peterman, R. E. Zartman, and P. K. Sims (1976) have identified an ancient sialic terrane that formed more than 3,400 million years ago. An antiformal structure in the Watersmeet area of Michigan contains a core of tonalitic to granitic gneiss that is surrounded by folded and metamorphosed Precambrian X graywackes. The gneiss is cataclastically deformed and recrystallized, and geochronologic data reflect the effects of severe tectonic and thermal events. Whole-rock Rb–Sr data are highly disturbed, but data for samples from two localities define secondary isochrons of about 1,800 million years (Sims and Peterman, 1976). A substantially older age of the gneiss is indicated by high initial $^{87}Sr/^{86}Sr$ ratios of 0.773 and 0.717 for the two isochrons. These high initial ratios resulted from local redistribution of previously generated radiogenic ^{87}Sr during the major period of cataclasis and recrystallization. Metamorphism of adjacent Precambrian X rocks occurred synchronously with the reactivation and mobilization of the gneiss as suggested by an 1,810 million years isochron obtained on four whole-rock samples of graywacke immediately adjacent to the gneiss along the northern contact.

U–Pb data obtained on zircon separated from the gneisses also reflect the complex geologic history but clearly place the time of primary crystallization at 3,400 million years or more. Three size fractions of zircon from one sample and a single size fraction from a second sample, all from tonalitic augen gneiss, have $^{207}Pb/^{206}Pb$ ages ranging from 3,310 to 3,410 million years, and a primary age of 3,600 million years is suggested by the defined chord. Zircon from a compositionally similar but much more thoroughly deformed and recrystallized phase of the gneiss yields $^{206}Pb/^{238}U$, $^{207}Pb/^{235}U$, and $^{207}Pb/^{206}Pb$ ages that are concordant at 1,760 million years. This lower age agrees with the whole-rock and mineral Rb–Sr ages and apparently indicates total resetting or perhaps even crystallization of the zircon during this metamorphic event. Data for three zircon fractions from a leucocratic phase of the gneiss plot on a chord that intersects concordia at about 2,600 million years. These data may indicate the presence of granitic intrusions that were emplaced in the older gneisses during the Algoman orogeny. About 20 km northwest of the gneiss at Watersmeet, the 2,710-million-year old Puritan Quartz Monzonite and Precambrian W metavolcanic and metasedimentary rocks form a greenstone-granite terrane that evolved in an ensimatic environment.

$^{230}Th/^{234}U$ dating of travertine and caliche rinds

In search for a tool for determining late Quarternary fault histories, J. N. Rosholt has been investigating an isochron technique as a means of estimating the $^{230}Th/^{234}U$ age of selected forms of caliche and travertine deposits. Both of these materials contain a significant ^{232}Th content that is attributed to silicate mineral-bearing detritus that cannot be separated completely from the carbonate fraction to be dated. The presence of ^{232}Th requires that a correction be made for an initial contaminating ^{230}Th component before the ^{230}Th growth component can be calculated. The most suitable technique appears to be dissolution of the samples with dilute nitric acid after heat treatment ($CaCO_3$ converted to CaO at 900°C) and cooling. A soluble fraction and a residual fraction are obtained after dissolution of the CaO and analyses of ^{238}U, ^{234}U, ^{230}Th, and ^{232}Th are required in each fraction. Dissolution of $CaCO_3$ with acetic acid did not prove suitable for samples with relatively high uranium concentration in the carbonate fraction because of apparent adsorption of uranium on residual components with formation of organic compounds from decomposition of acetic acid.

A single isochron plot, based on $^{230}Th/^{232}Th$ versus $^{234}U/^{232}Th$ values determined in soluble fraction, residual fraction, and total rock, is used to calculate the age of the carbonate fraction. The slope of the isochron represents a $^{230}Th/^{234}U$ value in which the ^{230}Th is the growth component produced from the total ^{234}U content of the sample. The intercept of the isochron with the $^{230}Th/^{232}Th$ axis represents the $^{230}Th_0e^{-\lambda t}$ component of the initial ^{230}Th contaminant. The apparent age is calculated from the $^{230}Th/^{234}U$ ratio represented by the slope of the isochron. Applying these techniques to travertine from the Yellowstone Park area supplied by L. J. P. Muffler, a Terrace Mountain travertine that predates the Pinedale Glaciation dates at 20,000 ± 5,000 years. Near Arco, Idaho, the soil on faulted fan gravels has stratified caliche rinds on the undersides of stones furnished by K. L. Pierce. Results indicate that $^{230}Th/^{234}U$ ages increase with increasing stratigraphic age of the rinds, 133,000 ± 30,000 years for the inner rind, 67,000 ± 10,000 years for the middle rind, and 17,000 ± 5,000 years for the outer rind.

Lead isotopes indicate two distinct sources for the ores in the Gold Hill mining district, Utah

The Gold Hill mining district of Utah is situated near the Nevada border at lat. 40°10′. A hitherto unsuspected dichotomy between the northern and southern parts of this district has been revealed by a new study by J. S. Stacey. The Gold Hill stock is shown to comprise two intrusive bodies of quite different ages. K-Ar measurements on biotite give ages of 38 ± 2 million years for the northern body and 152 ± 5 million years for the southern one. Rb-Sr measurements yield initial $^{87}Sr/^{86}Sr$ values of 0.715 ± 0.001 and 0.709 ± 0.001 for the north and south, respectively.

Measurements of the isotopic composition of feldspar lead from the same intrusive rocks confirm the north-south grouping. Feldspar lead from the northern stock is homogeneous and comparatively unradiogenic [$^{206}Pb/^{204}Pb$=18.66–18.71]. Galena data from nearby small deposits exhibit a linear trend on the $^{207}Pb/^{204}Pb$–$^{206}Pb/^{204}Pb$ plot and indicate a probable derivation from 1,650-million-years basement rocks such as are exposed in the Wasatch Mountains 128 km to the east. The lead from these galenas is not directly related to lead from the feldspars in the northern stock, nor is the lead related to the lead in the southern part of the district.

In the south, lead from both ores and igneous rocks is quite homogeneous and rather radiogeneic [$^{206}Pb/^{204}Pb$=19.39–19.73]. These data are similar to those in Nevada and suggest magma derivation from the thick sequence of miogeosynclinal sediments extending westward from Gold Hill.

Samarium-neodymium chronology of extra-terrestrial material

Noboru Nakamura (Colorado School of Mines) and Mitsunobu Tatsumoto have successfully begun to use ^{147}Sm–^{143}Nd chronology. The method has an advantage in that both parent and daughter elements are rare-earth elements and the Sm-Nd clock is therefore not expected to be reset easily by metamorphism. On the other hand, the ^{147}Sm half-life is 1.06×10^{11} years and, owing to similar chemistry, the Sm-Nd fractionation is small among rock-forming minerals; therefore, the method is suitable only for old rocks, in order to find the initial formation age. By using the ^{147}Sm–^{143}Nd chronology method, the oldest component (norite, 77215) of Boulder 7, Apollo 17, has been determined to be 4.37 ± 0.07 billion years old. The determination was made from a mineral isochron consisting of plagioclase and pyroxenes. The age agrees with the Rb-Sr mineral isochron age of 4.36 ± 0.04 billion years that is obtained simultaneously for the same mineral fractions. However, the U-Pb mineral isochron age, which is 3.75 billion years; (Nunes, Tatsumoto, and Unruh, 1974) and the ^{39}Ar–^{40}Ar whole-rock age, which is 4.0 billion years (Stettler and others, 1974), for the rock are considerably younger than those determined by the Sm-Nd and Rb-Sr methods. Since other components of the Boulder 7 shows younger Rb-Sr and U-Pb ages of approximately 3.75 billion years, it is interpreted that the Sm-Nd and Rb-Sr clocks of the norite breccia 77215 were not reset by one or more younger metamorphic (impact) event(s); whereas, the U-Pb clock was mostly, if not completely, reset and the K-Ar clock was reset halfway.

The method was further applied on the eucrite Pasamonte in order to investigate the relative susceptibilities of Sm-Nd, Rb-Sr, and U-Th-Pb methods to metamorphic events as well as to determine the age of the meteorite and its history.

It was found that Sm-Nd system of Pasamonte appeared not to be disturbed by later metamorphic events and indicated the initial formation age, whereas the Rb-Sr and U-Pb systems were very much disturbed by the metamorphic events. The U-Pb systematics are, however, very useful because they indicate that at least two metamorphic events have affected Pasamonte. The Sm-Nd data of mineral separates and whole-rock samples plotted on a Sm-Nd evolution diagram define an internal isochron that corresponds to a 4.58 ± 0.08 billion years age, whereas the Rb-Sr data plotted on a Rb-Sr evolution diagram show a large spread and do not define an isochron. The U-Pb data plotted on a U-Pb concordia diagram indicated a lead enrichment on plagioclase but a lead loss from the pyroxene component.

These results indicate that the parent body of Pasamonte initially formed at approximately 4.57 billion years and underwent at least two metamorphic events; an early event (brecciation?) probably occurred within the first 100-200 million years after formation, and a recent event that occurred about 100 million years (collision?) apparently did not disturb the Sm-Nd system significantly. But the Rb-Sr and U-Pb systems were severely disturbed.

Geochronology in the western Sierra Nevada

When T. W. Stern and B. A. Morgan combined radiometric dating with recent geologic mapping and paleontological data, they improved the chronology assigned to the deformation and plutonium of rocks in the western Sierra Nevada between Sonora and Mariposa, Calif. The large pyroxene diorite 1 km east of Sonora is dated at 259 million years; the pluton forcibly intrudes and contact metamorphoses the interfolded slaty rocks and andesitic volcanic rocks of the Calaveras Formation. The Calaveras rocks are abruptly truncated by the Melones fault. West of the fault, a small pluton at Chinese Camp, dated at 190 million years, intrudes both a complex of alpine-type ultramafic rocks and the unconformably overlying Penon Blanco Volcanics. These ultramafic and volcanic rocks are faulted in a set of imbricate slabs into the Mariposa Formation and Upper Jurassic turbidite and volcanic sequence containing Oxfordian and Kimmeridgian fossils. The Penon Blanco, Mariposa, and related rocks all compose the footwall of an east-dipping subduction zone; the suture line is now marked by a narrow (usually less than 1 km wide) tectonic melange forming the Melones fault. The Melones fault disrupts a small diorite stock dated at 162 million years that intrudes the Calaveras Formation east of Moccasin. The upper section of the igneous complex in the Guadalupe Mountain pluton, dated at 140 million years, intrudes and contact metamorphoses the Mariposa Formation forming an extensive hornfels zone. Emplacement of this complex apparently postdates major deformation along the Melones fault.

GEOTHERMAL SYSTEMS

Passive seismic exploration for geothermal systems

P. A. Reasenberg reports that a sophisticated seismic data acquisition and analysis system to aid in geophysical investigations of geothermal areas has been developed. The data analysis system includes a minicomputer capable of performing both interactive graphic data presentations and advanced numerical analysis programs. The results of system tests to date indicate that high-quality seismic data is produced by the system.

Two-phase, finite-difference modeling of geothermal reservoirs

J. W. Mercer and C. R. Faust applied a two-dimensional, two-phase, areal finite-difference model to the Wairakei, New Zealand, geothermal reservoir. Preliminary results indicate that a vertically uniform saturation assumption is inadequate. The theoretical and numerical models were therefore extended to include the concept of vertical equilibrium. Furthermore, the model was extended to a three-dimensional capability. Because three-dimensional problems are so time consuming, much work was necessary to improve the model's efficiency in problem solving data preparation. For example, an alternative diagonal ordering scheme was programmed. Also, various techniques were examined for solving non-linear problems by using Galerkin and collocation finite-element methods.

Modeling hydraulic fractures in shallow geothermal fields

Models for hydraulic fracturing must take into account the presence of the Earth's surface when the fracture length is longer than its depth. G. R. Holzhausen and C. Y. King developed a hydraulic fracture model that explains the effect of the surface when the fracture is parallel to the surface. The model can be used to describe hydraulic fracturing in shallow geothermal fields, in quarries, and in mining operations.

The effects of vertical flow on temperature distribution in geothermal reservoirs

In recent analyses of geothermal systems under exploitation it has been suggested that large quantities of cold water are entering the reservoir by flowing down from the surface and then horizontally into the reservoir because of decreased reservoir pressures. It has also been suggested that decreased reservoir pressures should increase these downward flows above their pre-exploitation levels. In order to estimate the effects of vertical flow on the temperature distribution, Manuel Nathenson obtained analytical solutions for two idealized problems. In both problems the initial condition is a linear temperature increase with depth, and the flow starts at time equal to zero. In the first problem, the flow is through a semi-confining layer with temperature fixed at the top and bottom of the layer. In the second problem, the flow is into a half space with the surface temperature fixed. Results indicate that if the augmented recharge takes place over restricted areas, measured temperatures in monitor wells should be able to indicate the amount of recharge after a few years.

Modeling vapor-dominated geothermal systems

A numerical model of steam transport through a porous medium was developed by A. F. Moench (1976a) and applied to a hypothetical geothermal reservoir in order to explain observed production characteristics. The physical system was idealized as a vertical column of porous or highly fractured rock initially filled with a mixture of steam and liquid water under high pressure. Analysis involves evaluation of pressure, temperature, and liquid-water saturation distributions when steam is withdrawn at either constant discharge or constant pressure. Computation of the temperature-, pressure-, and discharge-versus-time relationships provide an aid to estimating reservoir life and productivity.

In reports by A. F. Moench (1976a, 1976b), some of the physical phenomena that may occur in vapor-dominated geothermal reservoirs are examined. It is found that (1) movement in the liquid phase can be neglected at low liquid-water saturations, (2) energy changes owing to adiabatic expansion of the steam can be significant in regions where the steam is superheated, (3) conductive heat transport process can result in increasing temperature of produced steam, and (4) effects owing to the weight of the steam column can be neglected.

Geothermal well logging

A. E. Hess and G. B. Leon have developed and tested a high temperature probe for in-hole spectrometry. W. S. Keys logged with the probe in a geothermal well at Marysville, Montana. Data collected with this probe suggest that there has been significant redistribution of gamma-emitting radioisotopes in the Uranium decay series. Redistribution of radioisotopes occurred during the last 6 months of 1976 in the vicinity of a cased-off fracture zone that is a major source of hot water. Studies of several other geothermal reservoirs suggest that the distribution of radioisotopes is related to lithology and movement of hydrothermal solutions. Borehole gamma spectrometry may also provide data related to the generation of radon gas.

An improved high temperature acoustic televiewer has been utilized to determine the location of natural and hydraulically induced fractures in geothermal wells at Raft River, Idaho; Marysville, Montana; Long Valley, California; and Los Alamos, New Mexico. The probe was operated at a maximum depth of 3,039 m and maximum temperature of approximately 200°C in the Los Alamos well where a complex, vertical hydraulically induced fracture was recorded.

Model for predicting thermodynamic properties of complex brines

J. R. Haas, Jr., and R. W. Potter II developed methods for calculating the vapor pressure and volumetric properties of complex brines. The vapor pressure may be calculated from the boiling point and freezing point of the solution while the volumetric properties may be calculated from the volumetric properties of the binary components. These parameters may in turn be used to erect a PVTX grid from which the thermodynamic properties may be extracted.

If the brine has a freezing point, a boiling point, and volumetric properties similar to a solution with known thermodynamic properties, the thermodynamic properties of the known solution can be used to represent those of the geothermal brine. NaCl solutions are the only ones whose thermodynamic properties are known in the P-T range of geothermal interest. Experimental studies confirmed that most synthetic brines in the system Na-K-Ca-Mg-Cl-SO_4-Br have boiling and freezing points that correspond to more concentrated NCl solutions. The volumetric properties were found to be essentially the same (i.e., the density was ± 0.001 g/cm^3 to ± 0.007 g/cm^3 of the NaCl solution). Hence, from the freezing point depression and boiling point elevation of the brine, one can estimate the thermodynamic properties by using the measured NaCl equivalents and Haas' equation of state.

Elastic wave velocities in granite at elevated temperature and pressure

R. M. Stewart and Louis Peselnick determined *P* and *S* elastic wave velocities for dry Westerly granite to 300°C and 7 kbar. Compressional transducers were used for sample 1. Simultaneous measurement of *P* and *S* velocities for sample 2 were obtained by using shear transducers having a small compressional component. The velocities, temperature derivatives, and pressure derivatives at 25°C and 4 kb are shown in the table below.

Sample	V (km/sec)	$(\partial V/\partial T)p$ (m/sec/°C)	$(\partial V/\partial T)t$ (m/sec/kb)	Mode
1	6.33	−.42	22	*P*
2	6.24	−.60	36	*P*
2	3.59	−.27	18	*S*

These results agree with previously reported work at room temperature, but the pressure and temperature derivatives of the velocities show considerable variation in the literature. As a consequence, estimates of the critical thermal gradients may vary by nearly an order of magnitude for dry granitic crust.

Effects of subsurface boiling and dilution on the isotopic compositions of thermal waters

Isotope studies of geothermal systems have generally emphasized deep circulation of meteoric water, demonstrated by constancy of deuterium contents, and an "oxygen isotope shift" to higher oxygen-18 contents produced by water-rock reaction. However, subsurface boiling in high-temperature systems and dilution may cause deuterium and oxygen-18 contents of hot-spring and recharge waters to differ significantly.

A. H. Truesdell, Manuel Nathenson, and R. O. Rye report that using thermodynamic and isotope fractionation data for water and steam, the differences in chloride, oxygen-18, and deuterium between surface and deep thermal waters have been calculated for *single-stage* steam separation (in which steam remains mixed with water and separates near a single temperature) and *continuous* steam separation (in which steam is separated as it is formed). Although changes in chloride concentration resulting from these processes are nearly identical, isotopic changes differ greatly. Single-stage steam separation from 250°C to 95°C results in increases in Cl, $10^3 \ln \Delta^{18}O$, and $10^3 \ln \Delta D$ ($\Delta = [(10^3 + \delta_{surf})/(10^3 + \delta_{deep})]$) of 1.44 times, 1.75°/oo, and 9.1°/oo, respectively, whereas continuous steam separation results in increases of 1.41 times, 1.05°/oo, and 3.1°/oo. Because of these effects, deuterium contents of hot springs may be substantially higher th in recharging water, and part of the observed oxygen isotope shift may be due to boiling.

These calculations have been applied to the deuterium and chloride compositions of hot spring and shallow drillhole waters of Norris, Lower, and Shoshone Geyser Basins in Yellowstone National Park, Wyoming. The diverse compositions observed could result from boiling with *multiple-stage* (intermediate between single-stage and continuous) steam separation of mixtures of a single deep thermal water (360°C, 310 ppm Cl, -149°/oo δ D) with cold dilute (5°C, 2 ppm Cl) meteoric waters differing in deuterium according to locality (Norris, -142°/oo; Lower, -144°/oo; Shoshone, -133°/oo). The source of recharge to the deep thermal water must be precipitation remote from the geyser basins or ancient precipitation from a colder period.

SEDIMENTOLOGY

Sedimentology, the study of sediment and sedimentary rock, encompasses investigations of principles and processes of sedimentation and includes development of new techniques and methods of study. Sedimentological studies in the USGS are directed toward (1) the solution of water-resource problems and (2) the destermination of the genesis of sediment and the application of this knowledge to sedimentary rocks to gain a more precise interpretation of their depositional environments. Many USGS studies involving sedimentology have applications to other topics such as water-resource investigations, marine, economic, and engineering geology, and to regional stratigraphic and structural studies; these studies are presented elsewhere in this volume under their appropriate headings.

Studies of fluvial sedimentation are directed toward the solution of water-resource problems involving water-sediment mixtures. Sediment is being considered more and more as a pollutant. Inorganic and organic sediment, transported by streams to sites where deposition takes place, carries major quantities of sorbed toxic metals, pesticides, herbicides, and other organic constituents that accelerate the eutrophication of lakes and reservoirs. A knowledge of erosion processes, the movement of sediment in rivers and streams, and the deposition of sediment in stream channels and reservoirs is of great economic importance to the Nation.

IMPACT OF HIGH SEDIMENT YIELDS

Sedimentation in Coon Creek Valley, Wisconsin

Coon Creek drains a severely eroded area typical of rather intensely used agricultural lands in the Driftless Area of the southwestern part of Wisconsin. The stream was first studied by V. E. McKelvey (USGS) (1939) and S. C. Happ (University of Wisconsin) in 1938-39, and the old data were recently reprocessed by Happ. Between about 1850 and 1938, a net total of about 1.97×10^7 m^3 (5.2×10^4 m^3/km^2) of alluvium was deposited in the valleys—an annual rate of about 6.0×10^2 m^3/km^2. Recent measurements in Coon Creek by S. W. Trimble (1976) and S. C. Happ showed that between 1938 and 1975 sedimentation continued, but at about half the previous rate. It is also evident that the present rate may be less than 10 percent of the high rates of the 1920's and 1930's. This decrease is primarily attributed to changes in land use and land treatment.

This study indicates that the extraordinarily high rates of erosion and sedimentation occurring caused by man's disturbance of the land can be greatly mitigated. The study also supports the theory that much, if not most, eroded material may be deposited in the valleys and therefore is not measured at conventional suspended-sediment-load monitoring stations. Conversely, a considerable part of the stream-sediment load may be attributable to recent erosion of tributary channels rather than to upland erosion. Thus, stream-sediment loads may be dubious indicators of upland processes even when the stream-sediment-load data have been acquired over a period of more than a century.

Effects of mining debris on San Francisco Bay, California

According to George Porterfield, total suspended- and bottom-sediment discharge from California streams to San Francisco Bay averaged 13,500 Mg per day (approximately 4.9 hm^3/yr), from 1957-66. These data verify G. K. Gilbert's (1917) projections of the quantity and rate of movement of mining debris in the San Joaquin and Sacramento Rivers. Gilbert suggested that in the 50 years following 1914, the effects of mining debris on these streams would end and that the annual sediment-discharge rate would drop from 28 hm^3 (the 1849–1914 rate) to 6 hm^3.

Sediment yield from a coal strip-mining area in Wyoming

L. M. Shown, R. F. Hadley, and B. H. Ringen found that sediment yield of a small basin, part of which had been surface mined during 1949-55 and not rehabilitated, is about eight times greater than sediment yield of an adjacent unmined basin. Both basins, which are near Sheridan, Wyo., have small reservoirs constructed 25 years ago on main channels. Measurements of sediment deposition in the reservoirs showed that the average annual sediment yield from the 0.83-km^2 basin where only 0.21 km^2 had been mined was 114.3 m^3/km^2, and the average annual sediment yield from the 0.49-km^2 unmined basin was 14.3 m^3/km^2. Most of the sediment from the mined basin comes from nearly barren high walls and rough-graded spoils. Ungraded spoil areas contribute little or no sediment because overland flow drains to closed depressions between spoil rows. Therefore, sediment yield could be expected to be considerably more if all of the area had been rough graded to allow exterior drainage.

Effect of highway construction on a small area in Pennsylvania

R. E. Helm reported that highway construction on an approximately 0.4-km^2 area adjacent to the upper Schuylkill River of Pennsylvania caused annual sediment loads to increase from 90 to 108 Mg/km^2 at a downstream measuring site with a drainage area of 70 km^2. The primary method used for controlling sediment movement was prompt seeding and mulching of cut and fill areas in the construction zone.

SEDIMENT TRANSPORT AND DEPOSITION

Amazon River sediment study

During the high-water season (June and July) of 1976, R. H. Meade, Jr., and C. F. Nordin, Jr., measured the suspended-sediment load at five sections across the main stem of the Amazon River between Iquitos, Peru, and Óbidos, Brazil. Measurements were made from the research vessel *Alpha Helix* (operated for the National Science Foundation by Scripps Institution of Oceanography) with a specially designed instrumental array that included a sonic sounder, a current-velocity meter, and a suspended-sediment point sampler.

The suspended-sediment load decreased and increased irregularly because of losses of sediment to the flood plain and contributions from tributaries, whereas the concentration of suspended sediment downstream decreased fairly steadily. The suspended-sediment load at Obidos on June 15 (measured during the period of greatest water discharge since the record flood of 1953) was on the order of 3×10^6 Gg per day.

Degradation downstream of Cochiti Dam, New Mexico

J. D. Dewey reported that sand and pea gravel moved in notable quantities from the channel in the 13-km reach from New Mexico's Cochiti Dam to its confluence with Galisteo Creek. A sand wave moved from the dam through the reach within a few weeks. After passage of the sand wave, sand removed from the somewhat armored bed dispersed into the flow without producing bed forms. Pea gravel from the dam required about 2 years to reach the confluence with Galisteo Creek. Most of the pea gravel was transported along the bed in the form of dunes.

Stream power

W. W. Emmett (1976) reported that when sediment with a large range in size occurs in a river, large particles may inhibit the motion of small particles and suppress transport rates below those predicted, which confirms the fact that bedload transport in natural rivers is related to a predictable proportion of available stream power. Generalized relations of bedload-transport rate as a function of unit stream power also have been inferred for cases of no constraint on the availability or mobility of sediment (L. B. Leopold and W. W. Emmett, 1976).

Deposition in Fox Chain-of-Lakes, Illinois

T. P. Brabets reported that the average annual suspended-sediment load transported to the Fox Chain-of-Lakes in Illinois is 31 Tg, of which 15 Tg are from the Fox River, 13 Tg are from Nippersink Creek, and 3 Tg are from Squaw Creek. Assuming negligible impact from unmeasured bedload, 100-percent trap efficiency, and an average deposition unit weight of 0.8 Mg/m^3, the average rate of total accumulation throughout the Chain-of-Lakes is 1.5 mm/yr.

Chemistry of deposited sediments and biological uptake of contaminants

Sediment has been found to be the most active sink of trace contaminants in aquatic ecosystems. A lack of correlation between trace-metal concentrations in sediments and metal concentrations in sediment-ingesting animals has suggested that metals may be permanently sequestered in sediments. However, laboratory studies by S. N. Luoma and E. A. Jenne (1976) showed that this lack of correlation results from a failure to consider the physical and (or) chemical state of the metal in the sediments. Uptake of metals by clams ingesting contaminated sediment may vary as much as 1,000 percent among chemically different sediment types. Improved chemical-extraction techniques specifically designed to determine the form of the sediment-bound metal should facilitate a correlation of environmental metal concentrations with biological effects of those metals.

Organic carbon on bottom materials in Susquehanna River

For the second successive year, bed-material samples were collected from 25 sites in the Susquehanna River basin for chemical and particle-size analyses. Most of the sediment collected was sand or larger material, according to J. R. Ritter. The results of the chemical analyses suggest that organic carbon may be attached to the surface of the sand as a coating. The sediment was also analyzed for 12 types of pesticide residues, inorganic and organic nitrogen and carbon, and 15 metals. Throughout the basin, the changes in concentrations of organic carbon in sediments between 1975 and 1976 seem to be related to changes in organic nitrogen concentrations, but in the lower part of the basin the organic carbon changes may also be related to changes in PCB concentrations.

SEDIMENT-MEASURING TECHNIQUES

Suspended solids

In order to measure the concentration of suspended solids in water, N. J. Asting, M. C. Goldberg, and E. R. Weiner (1976) solved the Fraunhofer diffraction equation to obtain intensities that were ratioed at various theoretical angles of observation and correlated to the experimental dispersion spectra obtained from laser-induced particle scattering. Observations of scattering intensity were made at the extreme forward angles, usually below 12°. It was found that monodisperse systems generally vary by 20 percent from a calculated particle-size value and exhibit the expected size distribution in ranges from 0.1 to 0.5 μm. The results are independent of particle density or refractive index.

Bedload sampler

Laboratory tests of a new pit-type sampler developed by D. W. Hubbell and H. H. Stevens, Jr., demonstrated that self-burial of the sampler in a sand bed is entirely feasible. They found, however, that use of a motor-driven mechanism to effect the burial process unduly complicated handling of the sampler.

Turbidity recording

J. F. Truhlar, Jr. (1976), in a cooperative study with the Pennsylvania Department of Transportation, achieved a good correlation between daily mean discharge-weighted turbidity and daily mean discharge-weighted suspended-sediment concentration. Turbidity is monitored continuously along with the water discharge. During periods when there are insufficient suspended-sediment data (a large percentage of the time on small streams), the daily mean discharge-weighted suspended-sediment concentration is determined from the turbidity-sediment correlations and used with daily mean water discharge to calculate daily sediment discharge.

SEDIMENT-DISCHARGE MODELING

Modified Einstein procedure

H. H. Stevens, Jr., revised an existing computer program for computing total sediment discharge by using the modified Einstein procedure. The revision eliminates extraneous parts of the original program, uses more rapid and efficient subroutines, and improves the ability to use several options.

A computer program, MODEIN, was developed by D. E. Burkham, C. G. Kroll, and George Porterfield (1976) to compute total sediment discharge according to the current usage of the modified Einstein procedure. The model uses the same data as that normally required for computation (B. R. Colby and C. H. Hembree, 1955).

Highway-construction sites

An equation to predict sediment discharge from highway-construction sites was developed by L. A. Reed, J. R. Ward, and K. L. Wetzel. The equation includes factors for the effectiveness of sediment-control devices, such as seeding, mulching, onstream ponds, offstream ponds, and rock dams in reducing sediment discharge. Equations were also developed to predict base flow, storm runoff, and natural sediment discharges. Inputs to the equations are precipitation, construction area, drainage-basin area, season, days between storm events, types of sediment control, area protected by each type of sediment control, and type of soil.

Wisconsin streams

S. M. Hindall (1976), in a USGS cooperative study with the State of Wisconsin, developed regression equations for the four major geographic provinces of Wisconsin to predict sediment yields at any location on 95 percent of the State's streams. The equations relate sediment yield to the physical factors, such as topography, soils, land use, stream hydraulics, and climate, that control sediment movement into and through the streams.

Arid regions

R. F. Hadley and L. M. Shown (1976) made a qualitative analysis of the relation between erosion and sediment yield in arid regions. For a given amount of gross erosion, stream-channel characteristics, diversity of land forms, and flood-plain development are important factors in determining the conveyance of eroded sediment to and through a channel system. Most streams in arid regions have dry sandy channels that characteristically cause a decrease in streamflow and an increase in sediment concentration in the downstream direction. Therefore, routing of sediment through a channel system is a complex problem because of the independent response of tributaries to input by individual storm events. A quantitative analysis of a sediment-yield problem would require data on the processes and rates of transport from hillsides to stream channels and the residence times of the sediment at intermediate points.

SEDIMENTARY STRUCTURES

Stratigraphy model for shallow-water deposits

The stratigraphy of a complex series of red beds and carbonate rocks (the Supai Group of Pennsylvanian and Permian age and the Hermit Shale of Permian age) in northwestern Arizona was studied by E. D. McKee. Correlation of 34 detailed measured sections was made possible by establishing a sequence of key beds on the basis of lithology and the age of intervening strata on the basis of invertebrate fossils found there. As a result, characteristic features of the paleogeography, isopach trends, lithofacies patterns, and other stratigraphic data pertinent to an interpretation of the environment of deposition were established. A model was developed for application to the exploration of subsurface deposits of a shallow-water marine and continental type formed in a semiarid region.

Point-bar sequences in ephemeral streams

Point-bar sequences in the ephemeral Rio Puerco of New Mexico differ markedly from those in perennial streams, according to R. G. Shepherd (1976). Upper flow regime and eolian processes are of major importance, and the abundant trough-crossbedding and fining-upward sequences that characterize the classic point-bar sequences of perennial streams are notably rare on active Rio Puerco point bars. The vertical sequence of a typical Rio Puerco point bar includes the following four distinctive zones:

- The *thalweg* zone conveys the lowest flows and contains flat-laminae sets beneath ripples with mud drapes. Mud balls and beds of eolian sand are common.
- The *sheet-bar* zone is flooded yearly and marked by a deflationary surface. Contorted bedding is common and wedges of eolian sand accumulate in the lee of erosional scarps.
- The *chute* zone contains swale-fill structures in channels scoured by pattern-controlling discharges that flood the tops of point bars and may result in chute cutoffs. (Neck cutoffs also are common.)
- The *brush-dune* zone, the highest zone, has a hummocky surface caused by fluvial and eolian deposition in the lees of brushy obstacles (mostly salt cedar). Stratification is disturbed by exposure and bioturbation.

Dependent on bend curvature and stage of development, one or more zones can be volumetrically insignificant. Point-bar deposits can exceed 4 m in thickness, whereas individual zones can exceed 3 m. Ephemeral-stream point-bar sequences constitute an important element of valley-fill sedimentation in the Rio Puerco type of alluvial environment.

GEOLOGY AND CLIMATE

A geologist's perception of climate differs from that of the meteorologist, since a geologist is motivated not by day-to-day changes in weather, nor generally by small-scale atmospheric variations measurable over periods of only a few years, but instead he seeks to comprehend the longer-term effects of climate on the Earth's surface. That is, the geologist perceives climate in terms of its effects on terrestrial processes. The time scale of the geologist can be as short as a single climatic event such as the geologic hazards provoked by a hurricane, but more generally the geologist's time scale embraces intervals long enough to leave a lasting geologic record. This can be a matter of decades or a period measured in millions of years. Indeed, the climatic implications of ancient eolian sandstones, evaporite deposits, coral reefs, and beds of coal have long been used in reconstructing climates of the past. The proximity of the Quarternary Period, however, and the detailed history that can be deciphered from its geologic record, make the study of Quaternary climate especially rewarding. This comparatively precise knowledge of climate provides perspective on the magnitude, duration, frequency, and impacts of the Earth's response to climatic inputs, as well as accurate information on the former geography of climatic patterns. Such a perspective is essential in seeking to obtain optimum use of land and water resources, now and in the future.

Many USGS studies that involve the effects of climate, ancient and contemporary, pertain to topics discussed elsewhere in this volume. The results described below are representative of the range of this research.

Fossils at Clear Lake, California

The Pleistocene and Holocene climate at Clear Lake in Lake County, Calif., in the northern Coast Range, was investigated by identifying fossil plants and by interpreting features of growth on fish scales.

The fossil plants came from outcrops that represent an uplifted arm of the former lake. Pine cones collected by M. J. Rymer from the upper part of a sequence of lake deposits south of Kelseyville were determined by J. A. Wolfe to be a subalpine species of foxtail pine, now disjunct between the southern Sierra Nevada and the northern Coast ranges. Further collecting by Wolfe produced a diverse flora representative of a glacial period, probably Illinoian. The present distribution of these plants implies that the mean annual temperature was then about 7°C cooler than now and that the precipitation was slightly greater than now. The lower part of the sequence so far has produced leaves of only the California sycamore, a species now restricted to the warm valleys in central California. Pollen analysis by Wolfe indicated that the lower part, as shown by the sycamore leaves, indeed represents a warm period, probably of Yarmouth (interglacial) age.

A core from Clear Lake yielded scales of Tule perch, for which the patterns of growth probably reflect changes in climate in the northern Coast Range. The analysis of the growth was described by R. W. Castell (Simon Frazer University, British Columbia) and by D. P. Adam and J. D. Sims (USGS) (Castell, Adams, and Sims, 1977). Because the growth rate of this fish depends on temperature, it was inferred that changes in growth characteristics over the past 11,000 years implied depressed temperatures 10,000 to 9,000 years before the present, a steady increase in effective temperature during the early and middle Holocene, reaching a peak between about 4,000 and 2,800 years before the present, and a decline thereafter.

Past and future climate on Black Mesa, Arizona

Extrapolating from a chronology of climatic change for Black Mesa, on the Navajo Indian Reservation, T. N. V. Karlstrom speculated that the present interval of drought may reach a turning point in about the year 1990, resulting in an abrupt recovery to wetter conditions within 50 years. The climatic chronology extends back to 800 B.C. and exhibits repeated cycles of drought (or, alternately, wetness) each lasting an average of 550 years, with many shorter climatic fluctuations of lesser amplitude that lasted approximately 50 years, 100 years, or as long as 275 years. The chronology was derived from geologic evidence of alluvial deposition, erosion, and soil formation, and from tree-ring records established for the American Southwest. Additional tree-ring records, particularly for juniper forests that were buried by buildup of alluvial deposits, were obtained by Jeffrey Dean (University of Arizona). Other dates in the chronology came from carbon-14 ages and from archaeological findings. Further, the coincidence of prehistoric cultural adaptations on Black Mesa with times of drought suggested to Karlstrom that past changes in the physical environment played a significant role in the timing and direction of prehistoric migration and adaptive change to environmental stress. Archaeologists with knowledge of Black Mesa generally have agreed with this interpretation and have further pointed out the important effects of population pressures and other social factors (Gumerman and Euler, 1976).

Arroyo cutting in New Mexico

Arroyos have been forming in the American Southwest since the 1880's, which is a circumstance seemingly initiated and perpetuated by the prevailing arid and semiarid climate. Under this climate the dense ground cover needed to promote infiltration of rainfall cannot develop, and the resulting sudden runoff causes floods and erosion. Such erosion and its associated runoff were measured by H. E. Malde and A. G. Scott for the period from 1970 to 1975 at two arroyos near Santa Fe, Cañada de la Cueva and Pueblo Cañon (Melde and Scott, 1976). Erosion was measured by Malde by repeated surveys of channel floors, cross sections, and headcuts, and by repeated photographs taken as stereopairs. Rainfall and discharge were measured simultaneously in 5-minute intervals by Scott, who used dual digital recorders at a gaging station on Cañada de la Cueva (drainage area 4.64 km^2). Discharge was as much as 18.2 m^3/s from rainfall of 25.2 mm. The maximum 15-minute intensity for this storm was 64.0 mm/hr, and runoff was 7.9 mm. The flood peak arrived in 20 minutes, by which time 80 percent of the rain had fallen, and the flow subsided to a tenth of its maximum in less than an hour. This storm at Pueblo Cañon (drainage area 13.3 km^2 above the place of measurement) resulted in an estimated discharge of 140 m^3/s, and features produced by hail on the channel floor suggested that the duration of flow could have been as brief as 30 minutes. Observed increments of headward cutting at Cañada de la Cueva ranged from 0.28 m for 1.8 mm of runoff to 4.9 m for 12 mm of runoff. Aggregate cutting in 5 years was as much as 13.7 m, resulting in erosion of 570 m^3 of alluvium. Headward cutting near the mouth of Pueblo Cañon was observed in increments of 10.3, 14.6, and 20.7 m, for an aggregate of 45.6 m, as measured from 1971 to 1974. This cutting removed 1,770 m^3 of alluvium.

Sedimentary record of San Joaquin Valley

The San Joaquin Valley in central California has preserved a virtually continuous record of continental sediments as much as 1,000 m thick, perhaps the most complete in western North America, according to D. E. Marchand. In this respect, the sedimentary record bears a striking resemblance to the long records in ocean cores. The stratigraphy supports an hypothesis of major climatic cycles of approximately 100,000 years duration, in that lake and stream deposits can be correlated with glacial events in the Sierra Nevada and, potentially, with estuarine deposits beneath the San Joaquin-Sacramento Delta and in San Francisco Bay. Radiometric ages demonstrated that some former lakes were contemporaneous with outwash fans and, hence, with climatic oscillations. At least eight major lacustrine units have been identified, three of them being older than 600,000 years, one being associated with pumiceous volcanic ash dated at 600,000 years by the potassium-argon method, and four being younger. The youngest lacustrine clay is bracketed by carbon-14 ages of about 9,000 and 27,000 years.

Erosion rates shown by growth rings in tree roots

P. E. Carrara found that growth rings in tree roots of the Piceance Basin of western Colorado indicate differences in erosion rates during the last 800 years, presumably because of climatic change. To determine the rates of erosion, annual growth rings in roots exposed by hillslope erosion were examined. Twenty root sections of either pinyon pine or juniper were collected from each of three sites. Their ages ranged from 84 to 771 years. Erosion rates were then calculated, based on the height of the root above ground and its age. The average rates measured at the three sites were 0.65 mm/yr, 0.57 mm/yr, and 0.42 mm/yr. These represent minimum rates because the original thickness of soil above a root cannot be known. The exposed roots were found nearly exclusively on south-facing slopes, demonstrating that erosion of such slopes is much faster than on north-facing slopes. The measurements further indicated an inverse relation between tree age and erosion rates, thus suggesting that tree age may be controlled by local erosion. Slopes that face southwest appeared to erode at the highest rates and also to have the youngest trees (average age 286 years). Preliminary analysis suggested that erosion rates from 200 to 300 years ago were higher than for any other 100-year interval during the last 800 years. Carrara concluded that the changes in erosion rates probably were caused by variations in climate.

Growth bands of corals

A research team at Miami Beach, Florida, discovered that climatic information can be read from bands deposited by corals during the annual growth of their skeletons. Studying certain coral species mainly from reefs off the Florida Keys, J. H. Hudson found that the bands can be counted to provide an exact chronology. Some dense bands, called stress bands, are thicker and darker than other annual bands. The times of formation of the stress bands were correlated with air temperatures and other weather phenomena recorded at Key West, for which the records date back to 1873 (Hudson, Shinn, Halley, and Lidz, 1976). The correlation showed that stress bands formed during unusually cold winters. This inference was then confirmed by oxygen isotope analyses of bands that grew during winter and summer and at times of stress. Stress bands were observed in all individual corals in the study area for the winters of 1941-42, 1957-58, 1963-64, and 1969-70. The winter of 1969 and 1970 was cold enough to kill most corals at the reef studied. Furthermore, many stress bands formed during the same years as El Nino, which created climatically induced shift in ocean currents off Peru that affects the enormous anchovy and sardine fisheries there. A core from a coral head 3 m high, which has annual bands back to the year 1620, is now being studied.

Deuterium in Pleistocene precipitation

The ratio of deuterium to hydrogen (D/H) in hydrated saline minerals that are found in Pleistocene deposits of Searles Lake, San Bernardino and Inyo Counties, California, was used by G. I. Smith and Irving Friedman to interpret upper air temperatures and the trajectories of storm tracks when these saline minerals were formed. The minerals provide samples of "fossil" water from which the D/H ratio of saline waters in the former lake can be estimated. This ratio, when corrected for changes that occurred during evaporation and crystallization, expresses the D/H ratio in the snow and rain that characterized the former climate of the area. Samples of the modern snow and rain in the principal area that provided water for Searles Lake, namely the eastern slopes of the Sierra Nevada, showed that the D/H ratio is chiefly controlled by upper air temperatures and the path of storms. Preliminary analysis of D/H ratios for the saline minerals indicated that the Pleistocene precipitation had average values isotopically lighter than at present, but that these values were within the present range of variation observed during and between individual storms. This finding is interpreted to mean that Pleistocene storm tracks and upper air temperatures were not drastically different from present, but that the number of cold and isotopically light storms was greater.

Climate and glaciers

Glaciers reflect the former climate by storing samples of "fossil" precipitation and by expanding and shrinking in response to climatic change. The role of climate in the history of a glacier is evaluated by seeking to understand how precipitation is added to the glacier and by observing how changes in thickness relate to changes in rate of ice deformation and the speed of movement. In the northern Cascades of Washington, M. F. Meier and his associates studied the recent and long-term behavior of several glaciers, concentrating on Nisqually Glacier and South Cascade Glacier.

Nisqually Glacier began to thicken in 1945 after many years of thinning, perhaps in response to a worldwide cooling trend that began in the mid-1940's. During the following decade, the glacier thickened 50 percent, and the speed of flow increased from 10 meters to over 120 meters per year at one place of measurement. The wave of thickening traveled rapidly down the glacier and caused the terminus to advance 520 m from 1953 to 1966. A second wave of thickening is now causing another period of advance.

Similar results were observed for South Cascade Glacier. Numerical modeling by W. V. Tangborn of the net mass balance of glaciers in the region, including South Cascade Glacier, showed that snow accumulation and summer cloudiness increased from 1945 to 1975, and melting correspondingly decreased. His analysis was based on measurements of glaciers and records of low-altitude precipitation, temperature, and streamflow for the years since 1885. Summer cloudiness especially increased from 1952 to 1975. Also, measurements of the surface of South Cascade Glacier by R. M. Krimmel in 1970 and 1976 showed an average gain in thickness of 4.5 m. Krimmel also observed the increase by making annual measurements of residual snow and ice ablation. These recent changes in South Cascade Glacier are of interest in the light of geological records. Carbon-14 dating, tree rings, and lichens have indicated that South Cascade Glacier attained its present size about 5,000 years ago. Its greatest extent was reached during the 16th Century in response to an increase in snow accumulation (or decrease in melting) of only 0.9 m, as compared with the average accumulation of the last 20 years. This is a small value compared with recent year-to-year fluctuations.

Subglacially precipitated calcite

The isotopes of oxygen and carbon in calcite that formed where Pleistocene glaciers moved across calcareous bedrock in Glacier National Park, Montana, have been studied by B. B. Hanshaw (USGS) and Bernard Hallet (Stanford University). The carbon isotope values were nearly the same as those of calcite in the bedrock, a finding that supported the conclusion that the subglacial calcite is a chemical precipitate derived from the bedrock, but the oxygen isotope values were unrelated to values for the bedrock calcite. Hanshaw and Hallet inferred that the oxygen isotope values of the subglacial calcite reflect the isotopic composition of former glaciers—an hypothesis that has interesting paleoclimatic implications. That is, because the glaciers were necessarily formed from precipitation taken from the oceans, further study of subglacial precipitates may be an indirect means of measuring the oxygen isotope composition of Pleistocene oceans, if suitable corrections can be made for atmospheric phenomena, and if oceanic sources of former storms can be determined. The results would provide a basis for correcting the paleotemperature scale obtained from oxygen isotopic analyses of foraminifera. Hallet (1976) described the process by which the subglacial calcite is formed. As a glacier moves across calcareous bedrock, carbonate minerals are dissolved on the stoss side of bedrock obstacles and are then chemically precipitated as patchy white calcite on the lee side by the freezing of melt water.

Weathering rinds

The thickness of weathering rinds on andesitic and basaltic stones was interpreted by S. M. Colman and K. L. Pierce to provide an approximate climatic chronology for the western United States, as expressed by terminal moraines of mountain glaciers. Rind thickness appeared to be a logarithmic function of time, based on many other weathering studies and on a sequence of terminal moraines at West Yellowstone, Montana. The Yellowstone sequence was dated by the potassium-argon and obsidian hydration methods. By using the relation of rind thickness to time determined at West Yellowstone, a similar relation was derived for the weathering of stones in terminal moraines at several other areas. For this purpose, a terminal moraine thought to correlate with a moraine at West Yellowstone, which had been dated at 140,000 years before the present, was used for calibration. The younger moraines at these areas then fell into three age groups: 75,000 to 60,000 years, 45,000 to 35,000 years, and 20,000 to 13,000 years before the present. However, a complete record of these moraines was rarely preserved in a single locality. From these results, Colman and Pierce concluded that the chronology of the terminal moraines is consistent with the climate chronology inferred from the oxygen-isotope record in ocean cores.

GLACIOLOGY

Although considerable work is underway in studies of seasonal snow cover by USGS scientists, most glaciological research is directed toward glacier studies. In 1976 the glacier-research program focused on one difficult subject of major scientific interest—how water within and under a glacier couples the glacier to the underlying bedrock—and two subjects of considerable practical interest—calving and surging glaciers. In addition, the number of climate-related activities has increased in recent years.

Fluctuations of U.S. glaciers from 1970 to 1975

Data on the fluctuations of 114 U.S. glaciers over the 5-year period 1970–75 were compiled by C. S. Brown. Terminus studies gave the following typical results: (1) Thirteen glaciers in the Colorado Front Range are stationary; (2) 20 of the Northern Cascades Range glaciers of Washington (primarily glaciers on Mount Baker and Mount Rainier) are advancing, 1 is stationary, 2 are retreating, and 1 is indeterminate; and (3) in Alaska, 27 glaciers are advancing, 23 are stationary, 25 are retreating (2 of these are surge-type glaciers), and 1 is oscillating. These data were part of the U.S. contribution to the Permanent Service on the Fluctuations of Glaciers (Zürich).

Mass change of South Cascade Glacier, Washington, between 1970 and 1976

In September 1970, the altitudes of approximately 100 precisely located points on the surface of South Cascade Glacier of Washington were determined. The altitudes of the same horizontal locations were again determined in September 1976 by R. M. Krimmel. The change in surface level integrated over area is the volume change of the glacier for this time interval. The glacier has gained an average of 4.5 m since 1970; before 1970 the glacier had been shrinking. Eighty percent of the glacier area showed an increase in volume, with a maximum increase of about 8 m in the upper basin; the maximum decrease on the lower glacier was 14 m. The mass increase was also observed by annual measurements of residual snow and ice ablation (net balance). Results of these independent methods are consistent. The recent mass increase of South Cascade Glacier is typical of most of the glaciers in the northern Cascade Range of Washington. Many of the glaciers are now advancing in response to the mass increase. The results of this investigation do not necessarily indicate a climatic reversal but rather only a short-term trend.

Stability of Columbia Glacier, Alaska, terminus

Columbia Glacier is the only remaining ocean-calving glacier in Alaska that has not undergone a massive retreat during the last several thousand years. Research on its stability and potential for retreat by Austin Post (1975) indicated that a major retreat of the glacier could cause greatly increased production of icebergs and thereby create a threat to tankers entering or leaving Port Valdez. A precision-survey net at Columbia Glacier was established in 1974, and the height of the glacier was measured. In 1976, L. R. Mayo and D. C. Trabant remeasured the glacier's height and extended the survey net an additional 10 km upglacier. These measurements showed that from 1974 to 1976 Columbia Glacier became 12 m thinner; from 5 to 15 km above the terminus, it thinned 1.5 to 4.0 m, and from 15 to 30 km above the terminus, it thinned 0.3 to 1.0 m. This thinning measurably decreased the stability of Columbia Glacier, and its potential for iceberg production has increased.

Iceberg drift from Columbia Glacier, Alaska

Daily reports on sizes and locations of icebergs from Alaska's Columbia Glacier that were supplied by officers of an Alaskan ferry and a tourist vessel were compiled by Austin Post. These data, together with aerial photography, showed that icebergs were released in large numbers by the glacier in July and August, 1976, and that many icebergs 10 m or more in length, as well as many hundreds of smaller fragments, drifted into the tanker lanes in Valdez Arm. These exceptionally large iceberg releases resulted in a retreat of about 1 km of nearly half of the 4-km-wide glacier terminus discharging into Columbia Bay. These releases have occurred most years since 1969 and are consistent with the measurements made by L. R. Mayo and D. C. Trabant, which indicated that the lower glacier is getting thinner.

Calving rate of Portage Glacier, Alaska

L. R. Mayo predicted that the Portage Glacier of Alaska, a glacier that is a tourist attraction, will continue to calve so rapidly that by the year 2020 the terminus will recede from view of the site of the visitor's center. Even a substantial change in climate is unlikely to change this pronounced retreat because the rapid calving of icebergs from the glacier terminus is controlled by the 170-m-deep water of Portage Lake rather than by the flow of ice down the glacier.

Changes in mass velocity and volume of Black Rapids Glacier, Alaska

Alaska's Black Rapids Glacier is a 47-km-long surging glacier which is presently in a quiescent phase. A program was begun in 1972 to obtain data on the buildup of the glacier as it approaches surge conditions as input to existing or proposed surging models. A comparison by L. R. Mayo of 1971 glacier-surface altitudes with glacier-surface altitudes shown on a 1950 map indicated an ice buildup of 50 m in a region 10 to 25 km below the glacier head. This mass buildup is surge related and is below the normal equilibrium line of the glacier. According to R. M. Krimmel, the present ice velocity ranges from 70 m/yr at a distance of 12 km from the glacier head to less than 10 m/yr near the terminus.

Radar soundings of the Black Rapids Glacier were made in March 1976 to determine the amount of ice that will surge into the Delta River valley. The glacier has eroded the Denali fault trench to a level lower than the level of the Delta River valley. The ice in the fault trench is 550 m thick near the glacier terminus and is thicker upglacier. Assuming that the glacier will move 8.5 km in the fault trench as it did during three previous surges, 6.7 km^3 of ice will surge into the Delta River valley within the next 1 or 2 decades.

Measurements of thickness of temperate glaciers

Radio-echo sounding to determine the thickness of a glacier, a technique that has been used successfully on "cold" (no liquid water present) glaciers, can now be used on temperate (wet) glaciers as well, according to R. W. Watts and A. T. England. Previously, scattering from water-filled voids within the ice rapidly diminished below frequencies of about 10 MHz, but a sounder which transmits a pulse with a center frequency of from 1.4 to 5 MHz and a duration of about 1 cycle was demonstrated on the South Cascade Glacier of Washington and, later, on the Columbia Glacier of Alaska where ice thicknesses of up to 1,300 m were measured. The receiver is untuned; the signal is displayed directly on an oscilloscope as a function of time. Resolution is approximately 10 m in ice thickness. The entire system can be easily transported by one person.

More recently, this system was used by S. M. Hodge to make a detailed bedrock map of South Cascade Glacier and to obtain several transverse profiles on Nisqually, Black Rapids, and Gulkana Glaciers. Results agreed with those obtained by borehole drilling, but depths measured on three glaciers seemed to be consistently deeper (up to 50 percent) than depths determined by gravity measurements. This may be due to underestimation of the regional gravity field.

Inventory of surging glaciers in the Pamirs of the U.S.S.R.

Landsat imagery was used by R. M. Krimmel to compile an inventory of surging glaciers in the

Pamirs of the U.S.S.R. Surging glaciers were found only in the northwestern part of a four-image mosaic. The primary criterion used to identify surging glaciers was the appearance of medial moraines. When loops are seen, irregular flow is indicated.

Russian glaciologists indicated that only about 25 percent of the surging glaciers can be successfully identified by using Landsat images exclusively; thus, ground observations are required. Nevertheless, remotely sensed images are very valuable for inventorying glaciers and identifying surge-type glaciers.

GROUND-WATER HYDROLOGY

Research in ground-water hydrology by the USGS reflects the increasing need for a better understanding of ground-water systems and for developing and applying new methods of study to improve the management of ground water, one of our most valuable resources.

During the past year, old techniques were refined and new solutions were adopted for two- and three-dimensional ground-water-flow models. A computer technique capable of processing extremely large three-dimensional models was developed. A hybrid digital-analog system for modeling three-dimensional multiaquifer flow was completed, and a digital model that describes spatial variations of hydraulic conductivity in an alluvial fan by simulating the depositional processes involved was tested.

Problems relating to recharge, both natural and artificial, received much attention during the year. Ground-water recharge and discharge of an unconfined aquifer overlying a geothermal reservoir were evaluated by steady-state simulation analyses. Hydrologic variables indicating the interrelationship of percentage of paving and the amount of available recharge water to an aquifer were incorporated in a conceptual model. In addition, field tests showed that high infiltration rates in ponding basins receiving sewage effluents can be stabilized by maintaining constant and adequate chlorine treatment.

Problems of disposal of waste liquids, storage of freshwater, and geohydrologic relationship of saline water and freshwater continued to be subjects for intensive study. The effects of industrial-waste injection and of waste-water irrigation were observed and evaluated. Storage of freshwater in saline-water aquifers as a technique for effective water management was reported to have high potential in some areas, according to field tests and model studies.

Deep-injection-recovery tests indicated a recovery of as much as 50 percent of injected freshwater before chloride concentration exceeded 250 mg/L; the residence time of the water underground was at least 54 days.

Continuing experiments in Florida showed that a properly constructed connector well can conduct water from a shallow aquifer to recharge a deep aquifer, provided the potentiometric surface in the deep aquifer is lower than that in the shallow aquifer.

The geohydrologic relationship between saline water and freshwater in stream-aquifer systems was investigated, and saline ground-water flow from a solution-collapse zone was traced.

Other studies included geophysical and geochemical investigations, new applications of borehole geophysics and tracer techniques, lithologic and stratigraphic assessments of aquifer development through local weathering, test drilling in preglacial river valleys, studies showing that considerable interflow exists between Arkansas basins separated by Crowleys Ridge, heretofore thought to be a barrier, and an appraisal of the ground-water resources of the lower Mississippi region where, reportedly, only one-third of the available supply is being used.

AQUIFER-MODEL STUDIES

Direct solution algorithm for two-dimensional ground-water-flow simulator

S. P. Larson reported that a direct-solution technique which uses the *D*4 (alternating diagonal) ordering scheme (H. S. Price and H. K. Coats, 1974) was coded for the two-dimensional ground-water flow simulator (P. C. Trescott, G. F. Pinder, and S. P. Larson, 1976). By using *D*4 ordering, the work required for direct solution can be only one-fourth that required for standard ordering.

The computer code was constructed as a substitute for the LSOR (line-successive overrelaxation) algorithm currently in the simulator. Preliminary tests indicated that simulations involving more than 3,000 unknowns can be solved by this method using 756 K bytes of core storage on an IBM 370/155 computer. The work required to solve a problem of this size is roughly equivalent to 13 iterations of the strongly implicit procedure. This method is very competitive with iterative techniques for problems commonly encountered in ground-water modeling, and potential difficulties inherent in iterative methods (selection of iteration parameters and convergence) are virtually eliminated.

Mathematical simulation of hydrogeologic systems

A new nonlinear least-squares solution for the hydrogeologic parameters, sources, sinks, and boundary fluxes contained in the equations approximately governing two-dimensional or radial, steady-state, ground-water motion was developed by R. L. Cooley in which a linearization and iteration procedure is applied to the finite element discretization of the problem. Techniques involved (1) using an iteration parameter to interpolate or extrapolate the changes in computed parameters and head distribution at each iteration, and (2) conditioning of the least-squares coefficient matrix through use of ridge-regression techniques were proven to induce convergence of the procedure for virtually all problems.

A methodology was developed for assessing the reliability and significance of the computed parameters and for assessing the reliability of heads predicted using new sources, sinks, or flux boundary conditions. These procedures were applied to two field problems—a small-scale cross section in the Hula basin in Israel, and a large-scale area problem in Truckee Meadows, Nev.

A new method for solving matrix equations where the matrix is positive definite was also derived and tested. This procedure, which was developed by T. A. Manteuffel and Cooley, uses approximate factorization of the matrix in combination with the genralized conjugate gradient method. The new process was found to be ideal for solving large sparse systems of equations such as those generated by finite-element methods. For these types of equations, the new method was often at least twice as fast as the conjugate gradient method.

A finite-element computer program for solution of general linear unsteady-state ground-water-flow problems was developed. All boundary conditions, sources, and sinks can be arbitrary functions of time, and permeability (or transmissivity) can be anisotropic with the principal directions varying from element to element.

Application of three-dimensional flow model to extremely large models

Recent computer techniques applied by D. R. Posson and G. A. Hearne to the three-dimensional strongly implicit procedure (SIP) ground-water-flow model developed by P. C. Trescott (1975) and S. P. Larson (P.C. Trescott and S.P. Larson, 1976), resulted in the capability to process extremely large models economically. The New Mexico model, conceptually derived from the HULL computer program written by Daniel Matuska (U.S. Air Force Weapons Laboratory, Albuquerque, N. Mex.), has been applied to numerous hydrologic models ranging in size from 800 to 161,000 nodes.

Larger models are processed by segmenting the node data arrays into slices that fit into available memory. The slices, in three dimensions, are passed efficiently through the program from directly addressable mass-storage devices until each SIP iteration is complete. In addition, considerable changes were incorporated to facilitate the logistics of array initialization, restarting a problem, and generating selective output listings and graphics.

Hydrologic models in many layers, previously simplified owing to computer-size restrictions, can now be processed. Although the SIP algorithm for flow problems is the only numerical scheme now online, the general technique can be easily applied to any layered, gridded implicit, or explicit model that is constrained by computer-memory size problems.

Hybrid computational system for multiaquifer problems

S. M. Longwill completed a general-purpose hybrid computing system for use in modeling multiaquifer flow problems. Flow including vertical flow, in as many as five aquifers can be simulated by the system. Small-circuit modules representing the aquifer characteristics of transmissivity and storage serve as the primary building blocks for the system. These modules are inserted in jacks mounted on the main circuit board to create resistor-capacitor networks that simulate the actual aquifer properties. Components representing vertical flow are mounted on removable patch boards. This enables either individual components or the entire panel of components to be quickly replaced. Inflow and outflow to the system can be programed by mounting components on special pluggable modules that can then be patched to individual nodes. A crossbar scanner and appropriate electronic conversion equipment linked to a minicomputer provide the means for automatically controlling the system.

Development of digital simulation model of alluvial-fan deposition

Improvements and tests were made on a digital model (W. E. Price, Jr., 1976) that describes spatial variations in hydraulic conductivity of water-bearing beds of an alluvial fan by simulating the processes of deposition on the fan. According to Price changes were made in the algorithm of the model, new features were added to the model, and verification of some aspects of the model operation was completed.

Simulation by the model was improved by changing the method of calculating debris-flow movement and by strengthening the correlation between the probability of flow movement in a given direction and the land-surface gradient in that direction. New features added to the model provided for a variable surface of initial deposition and for generating different initial sequences of random numbers. Qualitative tests confirmed that the model properly similates two characteristics of flow on the fan surface: (1) Flows move in a relatively straight path down the fan in response to the land-surface gradient, and (2) the direction of flow switches in a random manner about the apex of the fan.

RECHARGE STUDIES

Simulation of an unconfined aquifer overlying a geothermal reservoir

About 520 km^2 of a semiarid agricultural and rangeland area in the southern part of the Raft River Valley in south-central Idaho and northwestern Utah, including the known geothermal-resource area near Bridge, Idaho, was modeled numerically by W. D. Nichols to evaluate the hydrodynamics of the unconfined aquifer. A steady-state simulation analysis based on 1952 water levels suggested that (1) recharge to the unconfined aquifer is on the order of 78 hm^3/yr, (2) ground-water discharge through evapotranspiration by phreatophytes is greater than previously estimated, and (3) the major source of recharge may be upward leakage of deep infiltration from adjacent subbasins within the Raft River basin. A transient simulation analysis suggested that aquifer transmissivity does not exceed about 720 m^2/d.

These analyses, together with available field evidence, strongly suggested that there is no significant interconnection between the unconfined aquifer and the geothermal reservoir. The two aquifers are indirectly connected by vertical leakage through intervening thick confining beds with low hydraulic conductivity. Limited direct interconnection is indicated by several warm and hot wells in the Bridge area, but their occurrence is localized and probably results from the penetration of a virtually sealed fracture system of limited extent through which hot water is circulating.

Effects of paving on recharge to Floridan aquifer

The percentage of paving that can occur in Floridan aquifer recharge areas in east-central Florida and not reduce the net recharge to the Floridan aquifer is a function of many variables that include rainfall, depth to water table, depth to potentiometric surface of the Floridan, evaporation from paved areas, evapotranspiration from unpaved areas, runoff, pattern of paving, and leakance coefficient of the confining beds. C. H. Tibbals developed and coupled equations that incorporate those variables to produce a conceptual model that indicates relative amounts of water available for recharge and percentage of unpaved area under which increased Floridan aquifer recharge rates must occur. An assumption inherent in the use of the conceptual model is that excess water from the paved areas is placed in the nonartesian aquifer in the unpaved area, allowing the water table to build up and thus increase the hydraulic-head difference between the nonartesian and Floridan aquifers, thereby driving water across the confining beds at an increased rate compensating for the reduced area (caused by paving) under which recharge actually occurs. This model cannot be used as a basis for engineering design; its purpose is to show approximate mathematical interrelations of rainfall, runoff, evapotranspiration, percentage of paving, Floridan aquifer recharge, and to aid in estimating approximate amounts of water available for Floridan aquifer recharge before and after paving. The percentages of paving calculated for four examples range from 86.8 to 3.6 percent.

Basin recharge with tertiary treated effluent

Tests where 1,260 m^3/m^2 of treated sewage effluent were added to a ponding basin in outwash sand and gravel showed that clogging reduced the infiltration rate in the top 0.3 m of material. Although clogging was most intense in the upper few millimeters, clogging below this depth is also a factor to be considered in the selection of basin-management practices. Surface treatment during drying periods was only partially effective in restoring infiltration. Removal of the surface crust, followed by raking, restored the infiltration rate to about one-fifth of the initial rate of 130 cm/h. Removal of the upper 7 cm, followed by replacement with clean sand and gravel, restored the rate to about two-fifths of the initial rate.

According to R. C. Prill and E. T. Oaksford, chlorination of sewage effluent was a requirement for maintaining high infiltration rates. Pronounced drops in infiltration rate occurred when the chlorine supply was cut off, but stabilization in rate usually occurred when the supply was returned. The *Eh* of the effluent proved to be a valuable parameter for evaluating the effectiveness of the chlorine treatment.

DISPOSAL AND STORAGE STUDIES

Storage of liquids in saline-water aquifers

Changes in water levels of two wells installed in 1974 for observation of the combined regional hydraulic effects of two subsurface waste-liquid injection systems in northwestern Florida compared closely with changes predicted by application of a mathematical model of the hydrogeologic system, according to G. L. Faulkner and C. A. Pascale. Agreement of these observations (made over a period of nearly 3 years) with earlier estimates increases the degree of confidence associated with the ability to predict response of the hydrogeologic system to stresses imposed on it by injection of waste fluids.

In Mulberry, Fla., injection since 1972 of more than 1.1 hm^3 of a high-chloride acidic industrial-waste liquid into carbonate rocks has resulted in dissolution of the host rock. Caliper and sonar logging of the injection well indicated development of a cavity around the well between 1,326 and 1,356 m below land surface, according to W. E. Wilson. The cavity has a maximum diameter of 7.0 m and an average diameter of 4.9 m.

At another acid-waste injection site near Belle Glade, Fla., data collected during 1973-75 indicated that remedial actions taken by the operator to confine the acid waste to the receiving zone were unsuccessful, according to D. J. McKenzie (1976). The waste appeared in a monitor well whose bottom is about 30 m above the 456 to 683 m injection zone. Plans call for relocating the injection zone at a depth interval centered about 900 m.

Cyclic storage of freshwater in saline-water aquifers under optimum hydrogeologic conditions has high potential in Florida as a technique for water management. G. L. Faulkner (1976) reported that usable subsurface space is plentiful in a limestone-dolomite sequence, 100- to 1,000-m thick, consisting of porous (30 percent) and moderately to highly transmissive (1,000 to 125,000 m^2/d) zones separated vertically by beds of very low hydraulic conductivity. Field tests indicated that the zones with the best potential for recovery are storage zones in the lower part rather than zones in the higher part of the transmissivity range.

Modeling cyclic storage of water in aquifers

The temporary storage of freshwater in saltwater aquifers can be an effective means of water management in some areas. Designing an efficient system for the cyclic storage of water in aquifers and testing its feasibility require the ability to predict the effect of cyclic injection and withdrawal on both flow and water quality in the aquifer. L. F. Konikow and D. B. Grove demonstrated that if the physical and chemical properties of an aquifer, its native fluid, and its injected fluid can be described adequately, accurate predictions for effects in complex aquifers can be made using a deterministic, three-dimensional, transient, finite-difference model that solves simultaneously flow, temperature, and solute-transport equations. The general model used in this study is described and documented in detail in a report by INTERCOMP Resource Development and Engineering, Inc. (1976).

Results of injection-recovery tests promising

Two injection-recovery tests in a deep artesian aquifer at Miami, Fla., were completed successfully, according to F. W. Meyer. For the first test, 159,000 m^3 of freshwater was injected, and a volume equivalent to 38 percent of the injected water was recovered before the chloride concentration exceeded 250 mg/L. For the second test, 322,000 m^3 of freshwater was injected. After a residence time of at least 54 days, a volume equivalent to 50 percent of the injected water was recovered before the chloride concentration exceeded 250 mg/L.

Connector-well experiment in Orange County, Florida

An experimental connector well, screened in the shallow sand aquifer, finished with open hole in the Floridan (artesian) aquifer, and cased through the confining layer between the two aquifers, is providing information on the nature and function of the shallow aquifer in eastern Orange County as related to connector-well operation. Because the potentiometric surface of the shallow aquifer is about 14 m higher than the potentiometric surface of the Floridan aquifer, gravity draws water from the shallow aquifer down to the Floridan aquifer through the well connecting the two aquifers. Continuous flow measurements during a 12-month period show that the well discharges an average of slightly more than 3.2 L/s, varying seasonally. Observation wells showed that, except for seasonal variations, water levels within the area of influence have reached steady state within measurable limits. Vertical anisotropy in the shallow aquifer results in predominately horizontal flow toward the connector well, except very close to the well where drawdown of the free-water surface becomes very steep. The vertical anisotropy is apparently caused by the shape and arrangement of the sand grains comprising the shallow aquifer, rather than by distinct confining layers of different lithology. Transmissivity of the shallow aquifer at the site was calculated to be 55 m^2/d. Extensive dewatering of wetlands in eastern Orange County by connector wells alone is unlikely. Nevertheless, large amounts of water could be channeled to the Floridan aquifer by connector wells. According to P. W. Bush, results of this connector-well experiment imply that water is being captured in the vicinity of the connector well.

MISCELLANEOUS STUDIES

Saline-water and freshwater relationship in stream-aquifer systems

The geohydrologic relationship between saline water in Permian rocks and freshwater in stream-aquifer systems of central Kansas is being determined from water-level measurements in a series of observation wells in a northerly trending solution-collapse zone along the eastern margin of the Hutchinson Salt Member of the Wellington Formation. According to A. J. Gogel, preliminary indications are that the potentiometric surface of saline water in the solution zone is at nearly the same altitude as the water table in the overlying freshwater aquifer southwest of Buhler and west of Belle Plaine, Kans.

J. B. Gillespie reported that six observation wells were installed in a solution-collapse zone underlying the Smoky Hill Valley from Lindsborg to Salina, Kans. Cavities also were found in gypsum beds of the lower part of the Wellington Formation east of Salina. Six observation wells were installed in the gypsum-cavity zone that underlies the Smoky Hill Valley from Salina to Solomon, Kans. The potentiometric surface of this saltwater aquifer in the Wellington Formation slopes northward from Lindsborg to Salina and eastward from Salina to Solomon. Thus, saline ground water flows northerly from near Lindsborg to Salina in the solution-collapse zone, then easterly through the gypsum-cavity zone, and then discharges to the Smoky Hill River near the confluence of the Solomon River near Solomon.

Borehole geophysics applied to ground-water hydrology

D. E. Eggers wrote computer programs for the determination of compressional and shear-wave velocities from digitized full acoustic waveform logs. The Borehole Geophysics Research project determined how acoustic velocities are related to the porosity and lithology of aquifers and adjacent rocks. In addition, borehole gamma spectra were used to provide new information on several ground-water reservoirs.

W. S. Keys reported a change in the relative concentration of uranium and thorium at the base of the freshwater zone in a well at Valdosta, Ga. Uranium concentration is relatively high and thorium concentration is low in the freshwater aquifers. In the underlying saline-water aquifers, uranium concentration is much lower and thorium concentration is apparently higher.

Using inhole spectra, Eggers made preliminary calculations of thorium concentrations in a well in North Conway, N.H. The average thorium concentration for the upper 340 m of the Conway Granite of Mesozori age penetrated by this well is approximately 30 mg/kg, and the average thorium concentration for the depth interval 344 to 700 m is approximately 60 mg/kg. Keys and T. A. Taylor ran gamma spectra in a well near Raleigh, N.C. The data showed that all of the radioactive anomalies were due to an increase in uranium content except one that was due to thorium content.

Borehole traverses made in a municipal well in Albany, Georgia

Current-meter traverses made in Albany, Ga., in one of the city's production wells which taps four water-bearing zones, indicated that more than 90 percent of the well's yield is from uppermost screened intervals tapping middle to lower Eocene sands. R. E. Krause noted that this yield pattern may be in contrast to that of other wells in the area which are also screened in Eocene sands, open hole in Paleocene limestone, and screened in upper Cretaceous sands. Relative yields from the various screened intervals did not vary appreciably, even when the discharge was doubled during a second traverse. Borehole flow in the well under nonpumping conditions was downward while eight similarly constructed production wells in the area were being pumped.

Tracer studies for aquifer evaluation in Nevada

R. J. Sun selected a site with five wells, 20 to 36 cm in diameter, in the Amargosa Desert in Nye County, Nevada, for an investigation of the single-well tracer method of aquifer evaluation. Depths of the wells, that penetrated fractured dolomite (Bonanza King Formation) and limestone (Canara Formation) of Cambrian age, ranged from 200 to 300 m. Hydraulic tests made in each well indicated that a thin layer of highly fractured dolomite was the water-producing zone. A 4-day pumping test was made in May 1976 to determine hydraulic parameters of the aquifer.

After the 4-day pumping test, a two-well tracer study was made in September and October 1976. During the tracer study, the downgradient well was used as a pumping well while the upgradient well was used as an injection well. A 10-cm-diameter, 120-m long plastic pipe was used to connect the upgradient and downgradient wells. Water was pumped from the downgradient well at a constant rate of 1.9×10^{-2} m^3/s, and the water was injected through the injection well via the 10-cm-diameter plastic pipe.

To reach the condition of stability, the system was stressed for 1 day by pumping and injection. After the system was stabilized, a slug of tracers was injected into the aquifer; tritium and ammonium bromide were used as tracers and injected simultaneously. After the tracers were injected, water samples were collected from the pumping well and from three observation wells. Laboratory analyses of the samples will define the movement and distribution of the tracers.

D. I. Leap completed a long-term drift-tracer test using sulfur-35 as a tracer in a well at the Nevada Test Site. Results show a bimodal breakthrough curve that is believed to reflect porosity and dispersivity differences in two distinct aquifers penetrated by the well.

A two-well recirculating test was performed at a tracer calibration site in the Amargosa Desert in Nye County, Nevada. Leap employed tritium and ammonium bromide together in an effort to compare radioactive and nonradioactive tracers *in situ* in fractured rocks. Preliminary results indicated that the bromide ion is an efficient tracer whose breakthrough curve very closely resembles that of tritium.

Differential aquifer development within Fort Payne Chert

The Fort Payne Chert of Early Mississippian (Osagean) age has been locally modified through weathering into a prolific artesian aquifer along the eastern Highland Rim of central Tennessee. Wells tapping this aquifer produce as much as 2,250 L/min.

According to M. S. Moran, the shallow aquifer can be divided into two zones. Uppermost is a highly permeable chert-rubble zone hydraulically linked to a lower zone of interconnected solution cavities within bedrock. Gravel-sized chert in the rubble zone, at depths as great as 25 m, gradationally decreases in size into the clay-sized chert of the upper confining bed. The lower confining bed is the Chattanooga Shale of Late Devonian and Early Mississippian age.

To determine the stratigraphic occurrence and nature of the development of the aquifer within the Fort Payne Chert, hand specimens, geophysical well logs, and thin sections were used to assess the lithology and stratigraphy of the formation. Fresh samples were artifically weathered under laboratory conditions, which simulated accelerated natural processes acting on the southeastern Highland Rim area of Tennessee.

Results indicated that the aquifer was developed in weathered bedrock near the base of the Fort Payne Chert. The parent lithology of the chert-rubble part of the aquifer is silicified dolowackestone. The lower part of the aquifer was developed within preferentially weathered, silicified, and nonsilicified dolosiltstone.

Test drilling in preglacial river valleys of the Albany area of New York

R. M. Waller reported that the USGS in cooperation with the New York State Geological Survey, which provided seismic profiles for some site locations, drilled 22 test holes in the area of preglacial river valleys in Albany and Saratoga Counties, New York. Known water-bearing sand and gravel beneath a thick areawide clay-silt deposit was encountered in about one-third of the tests. Drilling and logging data indicated that yields of 0.2 to about 10 m^3/min for screened and developed wells may be feasible in selected areas. Waller concluded that test drilling with mud rotary-drilling equipment in conjunction with geophysical logging is an efficient means of locating discontinuous sand and gravel aquifers in buried valleys, and preliminary use of seismic profiles can narrow the field of exploration.

Liquid-waste disposal, Arbuckle Group, Kansas

The Arbuckle Group of Cambrian and Ordovician age is a freshwater aquifer in southeastern Kansas. The rocks are an important hydrocarbon reservoir in central and south-central Kansas and are used for disposal of large quantities of brine and industrial waste throughout most of the State. The potentiometric surfaces of the Arbuckle Group and the overlying Lansing and Kansas City Groups (Pennsylvanian age) are being determined as part of a study of general regional geohydrology of the Arbuckle. According to A. J. Gogel, preliminary indications are that the hydraulic head of the Arbuckle is lower than the head in the overlying rocks in spite of the large amount of liquid waste being injected.

Effects of waste-water irrigation on ground-water flow

Treated effluents in the Muskegon County, Michigan, waste-water system are now being applied by spray irrigation on 2,200 ha of field corn. Irrigation water not lost to evapotranspiration seeps into the ground and is collected by 113 km of drainage tile and then discharged to streams. Digital-model studies of the waste-water system by W. B. Fleck and M. G. McDonald verified the effectiveness of the drainage tiles. The three-dimensional finite-difference model developed by P. C. Trescott (1975) was used to simulate the two aquifer systems in the area. Results indicate that the waste-water system generally creates a ground-water sink where the tile is buried below the ground-water table. In areas where the tile is above the water table and in areas where there is no tile, irrigation of 7.6 cm/week causes ground-water mounding that may extend as much as 1.5 km from the area being irrigated. The model also indicates that excess precipitation in 1974–75 was the principal cause of a high water table in areas near the treatment site.

Ground-water flow breaches Crowleys Ridge, Arkansas

Crowleys Ridge, an erosional remnant in northeastern Arkansas, forms a prominent drainage divide between the Cache and L'Anguille River basins and the St. Francis River basin. The ridge is underlain largely by clay and sand formations of Tertiary age. Quaternary alluvium underlying the basins contains a thick, permeable sand-and-gravel aquifer that wedges out against the ridge. Heavy pumping from the alluvial aquifer for rice irrigation on the Cache-L'Anguille side of the ridge has caused an extensive potentiometric depression adjacent to part of the ridge. Pumping from the alluvial aquifer on the St. Francis side of the ridge is comparatively light; consequently, a steep hydraulic gradient has been created through the ridge toward the potentiometric depression.

Previous concepts of the hydrology of Crowleys Ridge held that the ridge functioned mostly as a barrier to ground-water movement between the Cache and L'Anguille River basins and the St. Francis River basin. Recent data compiled by M. E. Broom indicated that considerable basin interflow occurs along the ridge where the alluvial aquifers wedge out against the sandy Claiborne Group in Craighead, Cross, and Poinsett Counties.

Large amount of ground water available in lower Mississippi region

J. E. Terry, Jr., R. L. Hosman, and C. T. Bryant reported that an appraisal of the ground-water resources of parts of Arkansas, Illinois, Kentucky, Louisiana, Mississippi, Missouri, and Tennessee, in the lower Mississippi region, indicated that about 24 km^3 of fresh ground water is available annually. Regionally, only about one-third of this available supply is being utilized. By adequately planning for the regional effects of ground-water development and related activities, more benefit can be obtained from ground water. Most of the region is within the Gulf Coastal Plain, and two or more productive sand and gravel aquifers of post-Cretaceous age are available almost anywhere within the region.

Salty ground water is available in large quantities in the region; the quantity of saltwater available is several times that of freshwater.

SURFACE-WATER HYDROLOGY

The objectives of research in surface-water hydrology are (1) to define the magnitude and variation of streamflow in time and space, under both natural and manmade conditions, (2) to understand the flow process in stream channels and estuaries, and (3) to define the rates of movement and dissipation of pollutants in streams.

Flow and channel processes

A. P. Jackman (USGS) and R. D. Noble (University of Wyoming) (1976) devised a low-cost data-collection scheme for assessing the stream-temperature regime of a small basin. Incoming radiation, air temperature, windspeed, streamflow, traveltime, and water temperature were measured for 3 summer months in the Mattole River basin of California. Water temperature was monitored by portable, battety-powered cassette-recording devices. Analyses of these data indicated that incoming radiation and average channel depth are the two important variables controlling transient-stream temperatures in this mountainous basin.

R. E. Fish and Nobuhiro Yotsukura (1976) found that the temperature of water released from the bottom of Cannonsville Reservoir in the Delaware River basin during the summer months increases about 13°C by the time it reaches an ambient level about 105 km downstream. Variations of temperature with distance can be predicted by an exponential equation with a constant surface-heat-exchange coefficient.

The radioactive- and modified-tracer techniques for measuring reaeration coefficients were compared by R. E. Rathbun and R. S. Grant in experiments on Black Earth and Badfish Creeks near Madison, Wis. Coefficients obtained on Black Earth Creek agreed closely; results from the modified-tracer method ranged from 7 percent less to 30 percent greater than results from the radioactive-tracer technique. Unsteady flow complicated interpretation of the results for Badfish Creek; flow was steady for the radioactive-technique run but unsteady for the modified-tracer technique run. By using computed values for dye loss and discharge increase, the modified-tracer technique results ranged from 8 percent less to 62 percent greater than those obtained by the radioactive-tracer technique.

In another study, Rathbun, using 19 equations from the literature, computed reaeration coefficients for five streams and compared the results with coefficients measured by the radioactive-tracer technique. The standard error of estimate and the normalized mean percentage error were used as criteria for comparisons. No single equation was best for all streams. Calculated coefficients generally were greater than measured values.

K. L. Lindskov measured the times of travel and dispersion on 82 km of the Mississippi River and on

63 km of the Minnesota River in Minnesota's Twin Cities metropolitan area from July to September 1976. Fluorescent dye was used to simulate the movement of water-borne wastes. Results will be used in a water-quality model for waste-management planning. Flow in the reaches studied is regulated for navigation by four locks and dams. Time-concentration curves were defined at 19 locations and lateral dispersion was measured at 3 of these. River flows during the study were lower than the minimum flows expected once in 10 years. Travel-times were 365 hours for the 82-km reach of the Mississippi River and 305 hours for the 63-km reach of the Minnesota River. Mean velocities for individual subreaches ranged from 0.1 to 2.2 km/h. Barge traffic speeded up lateral dispersion of the dye. On the basis of these measurements, and for comparable streamflow, a slug of pollutant entering the Mississippi River in the vicinity of the Twin Cities' Metro Waste Treatment Plant would reach Hastings (34 km downstream) 146 hours later, and the dispersed pollutant would take 200 hours to pass that point.

Channel erosion at 28 sites along the trans-Alaskan pipeline route is being documented by P. F. Doyle and J. M. Childers. Ten gaging stations, established in the early 1970's, provided current hydrologic data useful in this and other studies. Methods of surveillance of channel behavior included field surveys, photogrammetric surveys, and photograph comparisons. Relatively little erosion has occurred at most of the channel-erosion sites since the 1975 surveys. Some channel changes occurred owing to pipeline construction. A break-out flood from a glacier-dammed lake was observed, and its effects at the Tazlina River pipeline crossing site were noted. The Tsina River also had a similar break-out flood in 1976.

The minimum-variance theory proposed by W. B. Langbein (1964) predicts the approximate rate at which mean velocity, mean depth, and water-surface width change with discharge at a cross section on an alluvial stream. Research by G. P. Williams showed that the major variables to use with the theory are mean velocity, mean depth, water-surface width, bed shear, friction factor, slope, and stream power.

Open-channel hydraulics

In a study of the procedures for computing backwater and discharge at width constrictions of heavily vegetated flood plains, V. R. Schneider, J. W. Board, B. E. Colson, F. N. Lee, and L. A. Druffel (1977) showed that the energy loss computed in the approach reach was too low. A method of estimating the average-flow path in the approach was devised to increase the computed energy loss. By using this flow-path distance, the mean errors were reduced from 29 percent to 1 percent in computing backwater and from 21 percent to 3 percent in computing discharge.

J. T. Armbruster generated 17 years of streamflow data at five sites downstream from Raystown Lake on the Juniata River of Pennsylvania, by using a flow-routing technique developed by T. N. Keefer and R. S. McQuivey (1974). The multiple-linearization flow-routing model performed well at all flow levels. Flows were simulated to evaluate the effects of Raystown Lake, a newly constructed reservoir, on the low-flow characteristics downstream. Operation of the reservoir will cause significant increases in low flows.

Flood characteristics in semiarid regions

Scarcity of streamflow and precipitation records and the lack of a good relation between flood characteristics and drainage area severely limit the reliability with which flood characteristics at ungaged sites in semiarid regions can be estimated by conventional techniques. D. O. Moore (1976) developed a method for computing the 10-year flood of an ungaged stream in Nevada by using basin areas within each of several elevation zones. Because hydrologic conditions in northern Nevada differ from those in southern Nevada, an estimating relation was derived for each part of the State. These relations appear to give satisfactory results in areas having large topographic relief, but they are not applicable to flatter lowland areas.

Another method of estimating flood characteristics of ungaged streams is by use of channel width. This method is applicable in all hydrologic regimes, but it is especially useful in semiarid and arid regions. A disadvantage is that a channel measurement must be obtained at each site where the relation is to be applied. However, a site visit is not required if channel widths are measured at many sites in a basin and the flood characteristics defined at these sites are plotted on a map. With that map, the user can estimate flood characteristics at other sites by interpolation. H. C. Riggs and W. A. Harenberg (1976) demonstrated this method in southwestern Idaho where conventional methods are not applicable.

Computer applications

Chintu Lai (USGS) and Chen-Lung Chen (Utah State University) are applying the computer simulation of two-dimensional unsteady flows by the method of characteristics to unsteady flow over a flood plain. They found that the original two-dimensional interpolation scheme that truncated the Taylor series according to the homogeneity of the order of partial derivatives did not meet the collocation condition and therefore was often unstable. A further numerical study indicated that this defect can be remedied by expanding each derivative term in the Taylor series into difference terms, then collecting the like terms, and finally arranging them according to the family of difference terms expressible by the given grid points. The resulting interpolation formulae should yield continuous and stable interpolated values with the exact function value at each grid point. This technique can be applied to various grid points in the 2-D grid system, such as interior, edge, corner, and reentrant corner points, for better flow simulation.

J. F. Turner, Jr., calibrated a modified version of the Georgia Tech Watershed Model at five gaged locations on the Hillsborough, Alafia, and Anclote Rivers of west-central Florida. Four years of rainfall, runoff, and evapotranspiration data were used. The modeled watersheds ranged in size from about 180 to 1,700 km^2. Calibration results were evaluated by regression analyses of (1) observed and synthesized flood peaks and volumes of flood events used in the calibration, and (2) observed annual flood-peak discharges and comparable discharges synthesized from rainfall records from 1950 to 1972 for two sites. Standard errors of estimate for peaks ranged from 17 to 36 percent for the calibration period and from 30 to 42 percent for the period 1950–72.

J. O. Shearman completed documentation of a computer program for stepbackwater and floodway analyses. He also developed a method of handling supercritical flows in stepbackwater analyses.

L. F. Land completed a computer program to compute the water exchange between a flowing stream and a hydraulically connected aquifer.

M. E. Jennings completed flow-sediment and vegetation trend modeling studies in the Atchafalaya River basin of Louisiana.

Low flows

In an extensive analysis of the minimum flows of North Carolina streams, R. C. Heath and N. M. Jackson, Jr., found a close correlation between flows and the major bedrock zones of the piedmont and mountain physiographic provinces. The largest minimum flows occur in the southwestern part of the State, an area underlain by sedimentary and metasedimentary rocks. On the other hand, streams draining only areas underlain by Triassic rocks have no flow at intervals averaging 10 or fewer years. Minimum flows in the Coastal Plain province depend on the extent of channelization.

H. C. Riggs (1976) described the dominant factors influencing the magnitude of minimum streamflows and provided some guidelines for estimating the effects of basin changes on minimum flows.

Flood-frequency analyses

Different analysts often produce different flood-frequency curves from the same basic data. One reason is that the curves may be defined either with or without an expected-probability adjustment. D. M. Thomas (1976) explained various aspects of flood-frequency analysis and showed the attributes and limitations of frequency curves with and without the expected-probability adjustment.

PALEONTOLOGY

Research by paleontologists of the USGS involves biostratigraphic, paleoecologic, taxonomic, and phylogenetic studies in a wide variety of plant and animal groups. The results of this research are applied to specific geologic problems related to the USGS program of geologic mapping, resource investigation, and to providing a biostratigraphic framework for synthesis of the geologic history of North America and the surrounding oceans. Some of the significant results of paleontological research attained during the past year, many of them as yet unpublished, are summarized in this section by major geologic age and area. Many additional paleontologic studies are carried out by paleontologists of the USGS in cooperation with USGS colleagues. The results of these investigations are ordinarily reported under the section "Geological, Geophysical, and Mineral-Resource Investigation."

MESOZOIC AND CENOZOIC STUDIES

Porosity in late Miocene reefs, southern Spain

Seacliff exposures studied by A. K. Armstrong, P. D. Snavely, Jr., and W. O. Addicott, 40 km east of Almeria, southeastern Spain, contain late Miocene reefs and patch reefs formed of milleporids, Scleractinia, calcareous algae, and Mollusca. The reef cores are up to 65 m thick, and several hundred meters wide. Forereef talus beds extend to 1,300 m and 40 m thick. The reefs and reef breccias are composed of calcitic dolomite. The reefs rest on volcanic rocks that have a K-Ar date of 11.5 million years and in turn are overlain by the Vicar Formation (Upper Miocene).

The porosity and permeability of the reef cores and forereef breccia beds are:

- Primary porosity by (a) boring clams in the Scleractinia coral heads, cemented reef rocks and breccias; (b) intraparticle porosity within the milleporids, corals, *Halimeda* plates, vermetid worm tubes; (c) interparticle porosity between bioclastic fragments and broken reef breccia.
- Post-depositional porosity, which is moldic porosity formed by the solution of aragonitic material such as molluscan, milleporid, and Scleractinia coral fragments. Resulting pores range from a few micrometers to 30 cm. Extensive intercrystalline porosity formed by the dolomitization of calcium carbonate bioclasts and micritic matrix. Dolomite rhombs are 10 to 30 μm.

Some porosity reduction has occurred by incomplete and partial sparry calcite infilling of interparticular, moldic, and intercrystalline voids.

The high porosity and permeability of these reefs make them important targets for petroleum exploration in the western Mediterranean off southern Spain.

Age of Sarten Sandstone and Colorado Formation, Luna County, New Mexico

The Sarten Sandstone in the Cooks Range, Luna County, New Mexico, has long been assigned an Early Cretaceous age (Albian) based on marine molluscan fossils from the middle of the formation collected by N. H. Darton in 1916. Molluscan fossils collected from the top of the Sarten Sandstone in 1976 by S. C. Hook (New Mexico Bureau of Mines and Mineral Resources), E. R. Landis, and W. A. Cobban (both of the USGS) suggest a Late Cretaceous age (early Cenomanian) for this part of the formation. The Sarten Sandstone is overlain disconformably by the Colorado Formation of Late Cretaceous age. Fossil mollusks collected by Hook, Landis, and Cobban from a 1.5-m bed of sandstone at the base of the Colorado reveal a late Cenomanian Age for this part. In terms of the ammonite sequence and formations in the central Great Plains area, the lower part of the Colorado Formation is about the age of the *Dunreganoceras pondi* Zone in the basal part of the Greenhorn Formation of the Great Plains region.

Early Eocene age rocks in Elbert County, Colorado

Rock samples submitted to R. H. Tschudy by P. E. Soister yielded specimens of the fossil pollen genera *Platycarya* and *Intratriporopollenites*. These fossils have not been observed in rocks older or younger than Eocene. In the Powder River basin of Montana and Wyoming with the first appearance of the genera approximately coincides with the first appearance of Eocene vertebrate fossils (Tschudy, 1976). The find of palynomorphs of Eocene age indicates that some of the rocks in Elbert County are younger than previously thought. No other Eocene fossils have been found in this area.

Age of Kootenai Formation, Glacier County, Montana

The Kootenai Formation in the Sweetgrass Arch area of northwestern Montana has long been considered to be of Early Cretaceous age. The lower part of the formation is made up of three members, the basal Cut Bank Sandstone, the middle Sunburst Sandstone and the upper Moulton. The Cut Bank is separated from underlying well-dated Jurassic rocks by a regional unconformity. The Cut Bank was assigned an Early Cretaceous age by Bertram and Erdmann (1935). Erdmann and Davis (1939), Blixt (1941), and Cobban (1945; 1955). This placement was based largely upon lithologic criteria as no fossils indicative of age had been found in the basal part of the Kootenai Formation. More recently, Weimer (1959), on the basis of well log correlations, included the Cut Bank as a facies of the Swift Formation (Middle and Upper Jurassic). He further indicated that the overlying Sunburst Sandstone member should be included in the Morrison Formation (Upper Jurassic).

Dark gray shale samples from the gradational interval at the top of the Cut Bank Sandstone Member have been collected by D. D. Rice. R. H. Tschudy examined these for palynomorphs and found good, though somewhat corroded specimens. The fossils found indicate that the samples are no older than Barremian and no younger than middle Albian. Thus, the palynomorph suite supports the correlation of the lower part of the Kootenai with the lower part of the Blairmore Group of southern Canada and confirms the Early Cretaceous age originally assigned to the formation.

Chitistone Limestone (Triassic), Alaska

Recent investigations by A. K. Armstrong and E. M. MacKevett, Jr., show that sabkha deposits were important in the genesis of Kennecott-type copper ore. Massive chalcocite-rich lodes at Kennecott and nearby deposits formed in the lower 110 m of Chitistone Limestone (Upper Triassic). The Chitistone and superimposed Upper Triassic and Jurassic sedimentary rocks formed in a marine basin on and surrounded by Nikolai Greenstone, a thick, extensive, largely subaerial succession of tholeiitic basalt with intrinsically high copper content. The lowermost 110 m of the Chitistone contains three incomplete upward-shoaling lime and cyclic sequences that each consist of shallow subtidal limestone grading upward to intertidal stromatolitic fine-grained dolomite. The youngest cycle contains well-developed sabkha features and dolomitic pisolitic and laminate crust caliches and underlies shallow-marine limestone. The ore deposits are related to the youngest supratidal sequence. This carbonate sequence represents a regional sabkha facies that developed between 90–110 m above the Nikolai Greenstone. This facies, which contained abundant gypsum-anhydrite, was exposed to vadose weathering that leached much gypsum-anhydrite and developed a vuggy zone interbedded with porous dolomitic calich zones. Subsequent marine deposition capped the porous zone with an impermeable seal.

The youngest sabkha horizon served as a permeable conduit for the ore-forming solution and was instrumental in localizing the major Kennecott-type ores.

Pleistocene climates at Clear Lake, California

In connection with his fieldwork for Earthquake Hazards around Clear Lake, M. J. Rymer has been investigating Pleistocene deposits that represent an uplifted arm of the lake. The upper part of these deposits south of Kelseyville produced several pine cones, which were submitted to J. A. Wolfe for determination. The cones represent foxtail pine, which is a subalpine species now disjunct between the southern Sierra Nevada and northern part of the Coast Ranges. Further collecting produced a diverse flora indicating that the enclosing sediments represent a glacial period, probably Illinoian. The present distribution of the vegetational types indicates that mean annual temperature during the Illinoian was probably about 7°C lower than it is now and that precipitation was slightly higher than it is now. The lower part of these Pleistocene deposits have so far produced leaves of only the California sycamore, but this species is now restricted in central California to the warm valleys. Pollen analysis by Wolfe of samples from the lower and upper part of the deposits have shown that the lower part, as indicated by the sycamore, was indeed a warm period, probably of Yarmouth (interglacial) age. Further paleobotanical work should produce a detailed record of climatic change from an interglacial into a glacial period.

Planktonic foraminifers from the type San Lorenzo Formation

A study of planktonic foraminifers from the upper part of the Butano Sandstone and type San Lorenzo Formation, Santa Cruz Mountains, California, has been completed by R. Z. Poore. The study that forms part of a joint effort by Poore and E. E. Brabb reveals that the middle Eocene–late Eocene boundary of international usage occurs within the Twobar Shale Member of the type San Lorenzo Formation. As previous studies have shown that the Twobar is referable to the upper zone (*Amphimorphina jenkinsi* Zone) of the Narizian provincial benthic foraminiferal stage, the results of this study, when combined with those of Poore (1976), indicate that most of the "late Eocene" Narizian Stage of the Pacific Coast is of middle Eocene age.

Age of Skonun Formation of British Columbia, Canada

New collections of marine invertebrates from the Skonun Formation, Queen Charlotte Islands, British Columbia, show that this unit is of provincial late Miocene age. Exposures of nearshore marine and nonmarine sandstone exposed along the north coast of Graham Islands (lat 54° N.), examined by W. O. Addicott, and P. D. Snavely, Jr., contain a fauna of 25 species indicative of correlation with the Wishkahan Stage (early late Miocene) of western Washington. Correlative strata occur near Icy Point, Alaska (lat 58°N.) and along Bogachiel River in western Washington (lat 48° N.). The depositional environment of the Skonun, as deduced from molluscan assemblages, varied from shallow marine to brackish water. Lignite- and pollen-bearing strata indicate nonmarine deposition throughout much of the formation.

Upper Oligocene strata in North Carolina

Examination of benthic and planktonic foraminifers by T. G. Gibson from "Silverdale-age" beds in eastern North Carolina has led to the conclusion that they are of late Oligocene age. The "Silverdale beds" generally have been considered of questionable early Miocene age. The late Oligocene age of the beds examined correlates them with the Chickasawhay-Paynes Hammock transgression in the eastern Gulf Coast region and, thus, provides evidence of this transgression on the Atlantic Coastal Plain as far north as central North Carolina. North of the New Bern high area Oligocene strata are not present on the Carolina Coastal Plain even though the area was a basin during the Miocene through the Pleistocene indicating considerable Oligocene and younger tectonic activity.

Upper Oligocene rocks in the Virginia Coastal Plain

Upper Oligocene rocks (Chickasawhayan stage) have been found outcropping about 20 km east of Richmond, Va., by B. W. Blackwelder and L. W. Ward. Oligocene rocks have not been previously reported from the Virginia Coastal Plain. On the basis of the contained mollusks, these rocks may be correlated with parts of the Cooper Formation in South Carolina. These Oligocene beds are underlain by glauconitic Eocene sands and are overlain by Miocene (diatomaceous clayey sands of the Calvert Formation) or younger beds. The Oligocene beds are light-gray, shelly, slightly clayey, slightly glauconitic, partially leached quartzose sandstones. Some beds of these upper Oligocene deposits may have been included in the subsurface Chicakahominy Formation that has been considered to be late Eocene in age. Prominent mollusks in these Oligocene beds include *Anomia ruffini* (Conrad), *Pecten tricenarius* Conrad, and *Pecten dispalatus* Conrad. Although these mollusks were named from this area of Virginia and figured in 1845, their importance and the significance of the localities was not previously understood. Recognition of upper Oligocene beds in Virginia contributes significantly to interpretation of the structural and tectonic history of the Virginia Coastal Plain.

Late Cretaceous dinoflagellates from northern New Jersey

The Monmouth Group (Campanian to Maestrichtian) at Atlantic Highlands, Monmouth County, N.J., has yielded 91 species of dinoflagellates from the families Cymnodiniaceae, Peridiniaceae, and Gonyaulacaceae; three genera and 20 species are considered new. Paleoecological determinations by F. E. May based on species diversity, relative frequency, and dominance suggest that the Mount Laurel Sand and Sandy Hook Member of the Red Bank Sand were deposited in nearshore gulf to inner shelf conditions, whereas the Navesink Formation appears to have been deposited in inner to outer shelf conditions. The Campanian-Maestrichtian boundary, based on dinoflagellates, appears to lie within the uppermost part of the Mount Laurel or basal part of the Navesink. Based on comparison with dinoflagellate assemblages from the type Maestrichtian of Holland, the Navesink and lower part of the Red Bank (Sandy Hook Member) are considered tó be early Maestrichtian in age.

Cenomanian mollusks from Martha's Vineyard, Massachusetts

Shaler (1889) reported the occurrence of Cretaceous fossilbearing sandstone nodules in glacially disturbed deposits on Martha's Vineyard, Massachusetts. Subsequently, Stephenson (1936, p. 367) considered them to be assignable to beds coeval with the Matawan Group (Campanian) of New Jersey.

Examination of collections submitted by C. A. Kaye from Martha's Vineyard plus re-examination of the older Survey collections examined by Stephenson has led N. F. Sohl to conclude that the mollusks are Cenomanian rather than Campanian in age and correlate with the Raritan Formation of New Jersey and the Woodbine Formation of Texas rather than the Matawan Group. These correlations are based upon the co-occurrence in these units of such species as *Exogyra columbella* Meek, *Anomia ponticulana* Stephenson, *Brachidontes filisculptus* (Cragin) and *Voysa eulessana* Stephenson.

The fossils are found in concretionary masses separable into two lithologic types:

- Sandstone concretions with an abundance of such epifaunal bivalves as *Brachydontes, Anomia, Crassostrea* and *Exogyra,* and cerithiid gastropods such as, *Voysa* and *Laevicerithuim.* The assemblage suggests lagoonal or estuarine conditions of somewhat reduced salinity.
- Sideritic nodules with a lesser diversity of mollusks, primarily, *Crassostrea, Anomia, Plicatula,* and *Brachidontes.* This assemblage appears to represent even more brackish and marginal marine conditions than the assemblage of the sandstone concretions.

Of special note is the occurrence of rare specimens of the gastropod *Actaeonella* a genus normally associated with tropical to subtropical warm water faunas of the Cretaceous. Its presence suggests that the northward paleolatitudinal extent of warm waters along the eastern seaboard was greater during the Cenomanian than for subsequent time intervals of the Late Cretaceous.

Late Cretaceous calcareous nannoplankton from Texas

The calcareous nannoplankton rank with the planktonic foraminifers, radiolaria, ammonites, and other pelagic groups of fossils as outstanding biostratigraphic indices. Their cosmopolitan nature, rapid floral change during Mesozoic and Cenozoic time, great diversity, and extreme abundance in the smallest of samples make them superb biostratigraphic indicators for developing detailed systems of zonation applicable to the worldwide correlation of marine strata. C. C. Smith has recently completed an investigation of the calcareous nannoplankton floras from the upper parts of the Eagle Ford Group and lower parts of the Austin Group (late Turonian to early Santonian) throughout Texas. Detailed studies of the calcareous nannoplankton from these beds has resulted in the recognition of a new nannoplankton zone, the *Lucianorhabdus cayeuxii* Zone, within the lower portions of the Austin Group. The base of this new zone is defined by the initial (earliest) appearance of *Cylindralithus asymmetricus* Bukry, *Kamptnerius magnificus* Deflandre, and *Lucianorhabdus cayeuxii* Deflandre, while the top of the zone is marked by the initial (earliest) appearance of *Tetrali-*

thus obscurus Deflandre. The upper and lower limits of this relatively thin biostratigraphic zone are believed to be coincident with the boundaries of the European Coniacian Stage. These studies have also documented the presence of discontinuous patches of Coniacian strata, 4 to 20 m in thickness, which are present along the erosional unconformity between the Eagle Ford and Austin Groups. Prior to these studies, strata of Coniacian Age were unknown within the north-central and northeast Texas areas.

PALEOZOIC STUDIES

Early Paleozoic pelecypods

New information about the Late Ordovician pelecypod *Coralldomus* Whitfield, shows clearly that it was a facultative borer, and provides the oldest documented record of this mode of life in the class Pelecypoda (Pojeta and Palmer, 1976).

The finding of markedly anteriorly elongated pelecypods with taxodont teeth and the ligament on the short end of the shell indicates that the solemyids arose from the paleotaxodonts in the early Middle Ordovician. The new specimens are from Tennessee and Estonia. Solemyids have previously been placed in a subclass of their own; they should now be united with the paleotaxodonts.

Examination by John Pojeta, Jr., of all of the better preserved Ordovician paleotaxodont pelecypods at American and Australian museums, as well as some material from Great Britain, France, and Sweden, combined with a thorough search of the literature, shows that there are about 30 useful generic names for this subclass in the Ordovician. At present seven genera are known to occur in the Lower Ordovician, 24 occur in the Middle Ordovician, and 18 are known from the Upper Ordovician. Suites of genera should prove useful in dating rocks biostratigraphically.

Cambrian-Ordovician boundary in North America

Historically, recognition of the Cambrian-Ordovician boundary in the United States has been difficult because of strong biofacies differences between North American platform carbonate rocks and the black shales, silts, and subordinate carbonaceous limestones of the classic type area of Europe and related facies in the Maritime Provinces of Canada. The Cambrian-Ordovician boundary in the United States usually has been placed at the boundary between the *Saukia* Zone (Trempealeauan Stage) and the overlying *Missisquoia* Zone (lowermost Canadian Series). However, the evidence for this assignment has been meager and the placement therefore has been somewhat arbitrary.

Trilobites identified by M. E. Taylor (USGS) and conodonts identified by Ed Landing (University of Michigan) show that the earliest known occurrence of *Cordylodus proavus* Müller, is within the uppermost Cambrian *Acerocare* Zone at St. John, New Brunswick. The horizon is locally 7 m below Tremadocian beds containing the graptolite *Dictyonema*. *Cordylodus proavus* is widespread in North America beginning at the base of the *Corbinia apopsis* Subzone of the *Saukia* Zone. At some localities in the United States, the *Missisquoia* Zone contains the rare Tremadocian trilobites *Jujuyaspis* and *Parabolinella*. These occurrences plus the new conodont data suggest that the *Saukia-Missisquoia* Zone boundary may coincide approximately with the Upper Cambrian-Tremadocian boundary in New Brunswick and Europe.

A working group of the Commission on Stratigraphy, IUGS, is currently evaluating several proposals for standardization of the position of the Cambrian-Ordovician boundary. One proposal is to recognize the base of the Tremadocian Stage as the base of the Ordovician System. The new faunal data from New Brunswick suggest that the proposal has considerable merit because trilobites, conodonts, and graptolites can be used to correlate lower Tremadocian rock equivalents in the major regions of the world, and the proposal would not require major adjustment in position of the systemic boundary as it has been traditionally recognized in North American stratigraphic literature.

Land snails are land snails

A study of late Paleozoic land snails from the nonmarine Monongahela and Dunkard Groups in the Appalachian Basin by E. L. Yochelson (USGS) and Alan Solem (Field Museum of Natural History) showed fossils which were drifted into shallow ponds, a well-known phenomenon today. The study included a systematic review of these collections, plus others from Illinois and Indiana, and classic collections from Nova Scotia made 125 years ago by Sir William Dawson. The fossils from Nova Scotia are the earliest known land snails. Of the eight known living orders of land snails, three appeared simultaneously. SEM study of the microsculpture on the shell provided critical detail for assignment to lower levels. Most of the 10 known species can be assigned to extant families. Invasion of the terrestrial habitat was the dramatic evolutionary event for these snails. Once that was accomplished the land snails were exceedingly conservative. As a consequence, they appear to have a limited potential for stratigraphic utility in the late Paleozoic. However, they provide data for paleoecologic interpretation. Further, the occurrence of common genera in Europe and North America is another line of evidence that might suggest that no Atlantic Ocean was present during that time.

Silurian and Devonian coral biostratigraphy

Charles W. Merriam studied Paleozoic stratigraphy and paleontology of Great Basin rocks for four decades. This culminated in 1973–74 with the publication of four USGS papers on the systematics and biostratigraphy of Silurian and Devonian rugose corals in the area. Merriam described 12 coral zones, basing his age assignments almost entirely on a comparison of the Great Basin corals with those known from other areas of the world. He died in 1974 before completing work on the Late Devonian corals and while only beginning to relate his coral zones to zones based on other biologic groups.

W. A. Oliver, Jr. (USGS), and J. G. Johnson (Oregon State University) have analyzed the relationships of the coral zones to zones based on brachiopods, conodonts, and graptolites. They assign three of Merriam's zones to the Silurian, six to the Early Devonian, and three to the Middle Devonian. Merriam designated two additional (higher) zones, but did not describe the included corals. Oliver has partly filled this gap by preparing lists of Great Basin rugose coral genera of Late Devonian age, thus he has completed the synthesis and correlation of the coral succession in a major North American area.

Fusulinids of the Oquirrh Group, Utah

H. T. Morris, R. C. Douglas, and R. W. Kopf have divided the Oquirrh Group (Pennsylvanian and Permain) into four formations of which the upper three units contain fusulinids. The West Canyon Limestone (Lower Pennsylvanian, Morrowan) is overlain by the Butterfield Peaks Formation (Middle Pennsylvanian, Atokan? and Des Moinesian) with fusulinids including *Millerella* sp., *Pseudostaffella?* sp., *Fusulinella* sp., *Wedekindellina* spp., and *Beedeina* spp. The next higher unit is the Bingham Mine Formation (Upper Pennsylvanian, Missourian) with fusulinids including *Bartramella* sp., *Eowaeringella* sp., *Triticites* spp., and *Pseudofusulinella* sp. The upper unit is the new Furner Valley Limestone of Late Pennsylvanian and Early Permian (Missourian to Wolfcampian) age with fusulinids including *Triticites* spp., *Kansanella* sp., *Pseudofusulinella* sp., *Schwagerina* spp., *Pseudofusulina* sp., *Schubertella* sp., and *Pseudoschwagerina* sp.

Fusulinids of the Furner Valley Limestone, Utah

The upper part of the Oquirrh Group in the East Tintic Mountains in Utah has been named the Furner Valley Limestone. Fusulinids, studied by R. C. Douglass are present at many horizons through the carbonate rocks that constitute nearly 90 percent of the unit. Late Pennsylvanian fusulinids are present in the lower beds of the unit, and the upper beds carry an abundant fauna of Early Permian fusulinids. The Permian fusulinids compare favorably with those described by Thompson (Thompson, 1954) from unnamed Permian beds in the Wasatch Mountains of Utah. *Triticites* is represented by forms like *T. cellamagnus* and is succeeded by several species of *Schwagerina* in addition to *Pseudofusulina, Schubertella,* and *Pseudoschwagerina.*

Late Ordovician Bryozoa in Kentucky

In continuing studies of the stratigraphic distribution of fossil faunas in the Upper Ordovician rocks of Kentucky, O. L. Karklins identified bryozoans from a 109 m thick section in roadcuts along U.S. Highway 42, about 4.3 km east of Bedford in Trimble County, northeastern Kentucky. The bryozoan faunule in the Bedford section consists of approximately 33 taxa, most of which are trepostome species. *Hallopora* cf. *H. rugosa* (Milne-Edwards and Haime) is abundant in the lower half of the section, *H.* cf. *H. andrewsi* (Nicholson) occurs abundantly in the lower two thirds and *Bythopora* aff. *B. dendrina* (James) and *Batostomella gracilis* (Nicholson) are common in the upper two thirds of the section. These species together with others suggest a Maysvillian Age for the lower half of the Bedford section.

Gortanipora bassleri (Nickles) and *Rhombotrypa quadrata* (Rominger), however, occur near the top of the section and both are considered to be typical of Richmondian Age strata. Their presence suggests that bryozoans in the upper half of the Bedford section probably represent a transitional faunule between Maysvillian and Richmondian Ages as understood in the area around Cincinnati, Ohio, and in adjacent areas in Kentucky.

Pennsylvanian and Permian biostratigraphy, south central New Mexico

J. T. Dutro, Jr., and E. L. Yochelson reassessed extensive fossil collections from Pennsylvanian and Permian rocks in the Robledo and Dona Ana Mountains and vicinity. The reassessment resulted in biostratigraphic refinement and revised paleoecological interpretations. The Hueco collections are of Wolfcampian age, and those from the San Andres are post-Wolfcampanian. Fossils from the Bursum Formation suggest an early Wolfcampian equivalence and a collection from the "Tularosa clay pit" appears to be latest Pennsylvanian. Brachiopods from beds assigned to the Missourian and Virgilian Series are long-ranging forms that indicate only a post-Des Moinesian age. Diversified Des Moinesian assemblages verify correlations with that mid-Continent series and brachiopods from the "Derry series" suggest Atokan correlations.

A mollusk-rich assemblage, with abundant small gastropods suggests a slightly hypersaline environment for the upper part of the Hueco and San Andres Limestones. A diversified fauna with a wide variety of mollusks, from the "Tularosa clay pit," probably represents a normal benthic mollusk-rich environment. Sublittoral conditions are inferred for the pelecypod-rich silty Abo Sandstone. Brachiopod shell beds that contain many specimens of only one or two genera occur throughout the sequence and probably are transported, size-sorted gravels. A single occurrence of a coral biostrome in beds of Des Moines age indicates shallow, warm, non-turbulent water. A black shale assemblage in the "Derry series" suggests deeper water and poorly aerated conditions. There are four main subtypes of brachiopod-rich assemblages, each of which could reflect minor variations in depth, temperature, salinity or substrate condition. The shallow benthic "normal marine" assemblages are encountered throughout the sequence.

Mississippian microfacies Lisburne Group, Endicott Mountains, Alaska

Investigations by A. K. Armstrong (USGS) and B. L. Mamet (University of Montreal) show that deeper water limestones and chert facies of the lower part (Mississippian) of the Lisburne Group are exposed in a sequence of allochthonous thrust sheets in the Endicott Mountains, central Brooks Range. The Alapah Mountain section is north, and the John River and Rumbling Mountain sections are to the south. In the Alapah Mountain section, which is about 1,100 m thick, carbonate sedimentation began on a shallow marine platform, then subsidence outpaced carbonate production. Deeper water carbonate beds were deposited and also were overlain by shallow-water sediments. The shallow marine lower limestones, about 300 m thick, are echinoderm-brachiopod-bryozoan wackestone and packstone. These are in contact with a slope facies that consists of about 89 m of thin dark-gray argillaceous pellet-echinoderm-bryozoan wackestone and packstone. In gradational contact are the starved basin or deeper water facies, about 300 m thick, composed of dark-gray to black thin-bedded dolomite and black radiolarian-spiculitic argillaceous phosphatic chert. These grade upward into shelf carbonate sediments about 400 m thick.

The John River section, which is 430 m thick, is composed of deeper water, starved basin sediments, black and brown shale and siltstone, thin-bedded argillaceous spiculitic lime mudstone, phosphatic packstone, and radiolarian black chert.

The incomplete Rumbling Mountain section, which is 545 m thick, is the lateral equivalent of the lower and middle parts of the Alapah Mountain section.

Foraminifers of Zones 7 (middle Tournaisian), 9 (upper Tournaisian), 10 and 11 (lower Visean), 12 and 13 (middle Visean), 16_{inf} and 16_{sup} (upper Visean), 17 and 18 (lower Namurian) have been identified. The base of the Rumbling Mountain section displays the *Chernyshinella* Zone, the oldest Carboniferous foraminiferal assemblage known from Arctic Alaska. The zone has been reported previously in the upper part of the Banff Formation and in the lowermost part of the Pekisko Formation in the Canadian Cordillera.

Devonian-Mississippian boundary in Fitchville Formation, Utah

The long-standing controversy regarding age assignment and depositional continuity of the Fitchville Formation has been resolved by 23 conodont collections and 13 coral collections madg by C. A. Sandberg and W. J. Sardo (USGS) and R. C. Gutschick (University of Notre Dame), at the type locality on Fitchville Ridge in the East Tintic Mountains, near Eureka, Utah. Collections were from closely spaced intervals in the lower 45 m of the Fitchville and upper 9 m of the underlying Pinyon Peak Limestone. The Devonian-Mississippian contact was found to be an unconformity at 33.6 m above the base of the Fitchville or 0.8 m below the top of the "white limestone of Crane" (Morris and Lovering, 1961, p. 85). On the basis of conodonts, the entire fossiliferous part of the Pinyon Peak and at least the basal 3.7 m of the Fitchville are assigned to the uppermost Devonian (upper Famennian) Upper *Polygnathus styriacus* Zone. Limestones between 11.0 and 32.2 m above the base of the Fitchville are assigned to the overlying upper Famennian Lower *Bispathodus costatus* Zone. Five collections from the next higher 1.4 m yielded only sparse Devonian faunas that may be assignable to higher parts of the *B. costatus* Zone. Directly above the unconformity, large diverse faunas of the basal part of the Mississippian *Siphonodella sulcata* Zone were recovered in the interval from 33.6 to 34.4 m. The next higher zone, the *S. duplicata* Zone, was not found; either it is represented by rocks thinner than the sampled interval, or a second unconformity is indicated by the sandstone at the base of the "blue shaly limestone of Crane" (Morris and Lovering, 1961, p. 85) at 34.4 to 34.8 m. The highest conodont collections, from 36.3 to 45.0 m above the base of the formation, yielded the middle Kinderhookian *S. sandbergi* Zone. Coral faunas from the Pinyon Peak and lower 29.0 m of the Fitchville are contained in the Devonian Upper *P. styriacus* and Lower *B. costatus* and Lower *B. costatus* Zones and are comparable to coral faunas of the Etroeungt Limestone in Belgium. They include advanced clisiophyllid and caninoid corals similar to forms that occur in the Visean (Meramecian equivalent) in Belgium, but generally do not occur in Kinderhookian, Osagean, or Meramecian rocks in North America.

PLANT ECOLOGY

Plant-nutrient dynamics in forested watersheds

In a 2-year study of water quality in the Redwood Creek and Mill Creek drainage basins, W. L. Bradford and R. T. Iwatsubo determined some effects of watershed logging on the occurrence of plant nutrients in surface waters.

The plant nutrients and plant-derived materials—kjeldahl nitrogen, ammonia, dissolved phosphorus, and dissolved organic carbon—apparently accumulate in the soil during the dry season and are washed out as the rainy season progresses. Little of these materials reaches the water table probably because of adsorption on the soil; as a result, little appears in base flow during the dry season. Nitrates seem to be fixed in the soil during the rainy season by nitrogen-fixing plants. Nitrates are fixed in excess of plant requirements in logged watersheds probably because trees are not present to assimilate the fixed nitrates, whereas in forested watersheds, trees assimilate nitrate as it is produced. Nitrate concentrations, therefore, increase in streams from logged watersheds and decrease in streams from forested watersheds as the rainy season progresses. Little nitrate appears in the base flow.

Botany of central Florida Everglades freshwater peat

C. S. Zen and Z. S. Altschuler studied the botany of freshwater peat in the central Florida Everglades from thin sections of a transect of cores taken at 3.2-km intervals along the Tamiami Trail. The dominant readily identifiable plant species are sawgrass (*Mariscus jamaicensis* (Crantz) Birtton) and water lily (*Nymphaea* spp.). In the Everglades today, *Nymphaea* prevails in areas that are more continuously and deeply flooded. *Mariscus* is found in seasonally dry areas and under relatively shallow water, although *Mariscus* stands are commonly flooded by 30-60 cm of water during the wet season. No consistent zonation of plant species exists within the cores or in any basinwide bed of either species. This may be because the coexisting habitats in this eminently flat domain displaced and succeeded each other with only slight changes of surface or water levels. The apparent lack of systematic zonation may also have been affected by differential compaction. Sawgrass is the dominant plant type in the top 5 cm of each core, probably reflecting the shallow-water conditions caused by canal construction and draining since the turn of the century.

Change in tree-trunk wood dates alluvial deposition

According to R. S. Sigafoos, a change in the physical characteristics of the wood in the buried part of a large cottonwood tree growing on the flood plain of Redwood Creek in California indicates the time when alluvium was first deposited on a part of that flood plain. From 1964–76, 1.5 m of alluvium was deposited at the site. The annual rings that have grown since 1964 have significantly fewer vessels per unit area than the annual rings that grew before 1964. The younger buried wood is more like root wood than stem wood.

Dendroclimatic studies in the Great Dismal Swamp

Dendroclimatic investigations in the Great Dismal Swamp of Virginia and North Carolina by R. L. Phipps and D. L. Ierley have shown a positive correlation between early summer precipitation and size of loblolly pine-tree rings formed prior to drainage-ditch construction. Growth subsequent to ditch construction seemed limited as much by temperature as by precipitation; prior growth and climate accounted for 65 to 70 percent of the yearly ring-width variance.

Results of C. P. Baker's hydroecological investigations suggested that the primary effect of ditch construction is the interruption of surface sheet flow. Poor correlation between tree growth and precipitation after ditch construction may indicate that precipitation is a less important factor in limiting growth than [and may be the result of] reduced surface flow across the study area.

L. H. Applegate's companion study of Virginia's Lake Drummond, which showed a correlation between early summer water levels of the lake and tree-ring size of bald cypress trees growing in the lake, permitted an approximation of past early summer lake levels. Apparently, the factors that cause increased evaporation from the lake also cause greater internal water stress in the trees and thus results in decreased tree-ring growth.

CHEMICAL, PHYSICAL, AND BIOLOGICAL CHARACTERISTICS OF WATER

Natural radioactivity in thermal waters

Radioactive hot springs issue from a fault zone in crystalline rock of the Boulder batholith at Alhambra in southwestern Montana. According to R. B. Leonard, the discharge contains high concentrations of radon, and the gross alpha activity and the concentration of radium-226 far exceed maximums recommended for drinking water by the EPA in the July 9, 1976, *Federal Register*. Part of the discharge is diverted for space heating and domestic use. The radioactive thermal waters (59.9°C) are sodium bicarbonate type, saturated with respect to calcium carbonate.

Local surface water and shallow ground water are calcium bicarbonate type and exhibit low background radioactivity. Mixed waters (17.7°C) were found in a shallow (30-m-deep) well drilled about 0.5 km east of the fault zone to provide an alternative domestic water supply. The temperature, percent sodium, and radioactivity of the water increase with depth; radioactivity, although higher than normal background, is below the maximum recommended by the EPA.

Radioactive water, chemically similar to the discharge of the hot springs, flows under artesian head from a fracture at a depth of about 100 m from a well 0.4 km west of the springs. The water seems to have been conductively cooled during migration through a nearly horizontal fracture from the fault zone to the well bore. Despite the lower temperature (30°C), the minimum subsurface temperature calculated from chemical geothermometry is higher than the 111°C temperature calculated for the springs.

Samples from most of the major hot springs in southwestern Montana have been analyzed for gross alpha and beta activity. The high level of radioactivity at Alhambra appears to be related to dissolution of radioactive elements from local siliceous uranium deposits by ascending thermal waters, and it is not a normal characteristic of hot springs from fractured crystalline rock in Montana.

Computer model of the distribution of saline waters in the Piceance Creek basin of Colorado

S. G. Robson and G. J. Saulnier, Jr., reported that a reevaluation of ground-water data collected in the Piceance Creek basin of Colorado and interim results of uncalibrated two-layer, two-dimensional solute-transport models, suggested that significant changes in dissolved-solids concentration may occur vertically in either the upper or the lower aquifer in the basin. The occurrence of saline water in some wells and springs is thought to be caused by the mixing of waters of greatly different quality and not representative of the average water quality in the aquifer. Maps showing the thickness and elevation of the top or bottom of each of various geologic units in the aquifer system were prepared for use in a three-dimensional model that will show the effects of variation in dissolved-solids concentration with depth in the aquifer. The maps indicate that the alinement of Piceance Creek corresponds to the alinement of the primary structural trough in the Green River Formation. Initial solutions to three-dimensional flow equations made by the model were in good agreement with field data.

Dissolved gases in Appalachian warm springs

D. W. Fisher, F. J. Pearson, Jr., and J. C. Chemerys found small amounts of dissolved helium in one or more samples from each of six thermal springs and two hot water wells in carbonate rocks in the Appalachian Mountains. Dissolved helium can be an indicator of an α -emitting radioactive heat source. Only one of four sampled thermal springs issuing from silica rocks in the Appalachians contained a detectable amount ($\geq 0.1\ \mu$ g/L) of dissolved helium.

Pearson and L. N. Plummer observed that laboratory analyses of dissolved CO_2 may be preferable to pH determinations made in the field for carbonate equilibrium studies; carbonate-ion activity calculations are highly sensitive to errors in pH determinations that may result from outgassing of CO_2 during the pH measurement process.

A generalized structural model of humic acid

R. L. Wershaw, E. J. Pickney, and S. E. Booker (1977) developed a generalized model for humic acid that should provide a basis for the modeling of chemical interactions between humic materials and other organic and inorganic components in natural water systems. Humic acid is modeled as a hierarchy of structural elements. At the lowest level in this hierarchy are simple phenolic, quinonic, and benzene carboxylic acid groups that are covalently bonded together into small particles. Particles of similar chemical structure are linked together by weak bonds to form "homogeneous" aggregates, and two or more different types of aggregates can be linked together to form mixed aggregates. Complexes of humic acid and clay minerals are also formed.

Distribution of organic materials in water

M. C. Goldberg (1976) reported that most small organic molecules in surface waters of the United States come from industrial, urban, or agricultural sources. Agricultural materials, particularly chlorinated pesticides and herbicides, were examined to determine concentration ranges within which the characteristic interactions of these solutes could be defined. Chlorinated hydrocarbon concentrations in bottom sediments at selected locations ranged from 5 ng/kg to 3.5 μg/kg, and ranged from 5 ng/L to 0.06 μg/L in water. Herbicide concentrations in water ranged from 5 ng/L to 1.5 μg/L for the same samples. Total organic carbon concentrations at these locations ranged from less than 0.1 to 42 mg/L.

By measuring surface activity of minerals that are ubiquitous in the environment, it was established that organic soil matter, mainly humic acid components, stabilizes organic moities such as dodecylguanidine acetate, even in salt concentrations as high as 10^5 mg/L. Kaolinite clay stabilizes the organic molecules equally as well as organic soil in low salt concentrations (10^{-3} mg/L) but not at high ionic strengths. Quartz exhibits very low stabilizing properties and, as in the case of soil organic material and kaolinite clays, undergoes changes in stability as a function of ionic strength.

Evaluation of surface-water-quality data for management

S. P. Larson, W. B. Mann IV, and T. D. Steele (USGS), and R. H. Susag (Twin Cities Metropolitan Sewer Board) (1976), in an evaluation of surface-water-quality data, demonstrated that infrequent (monthly) data are not particularly significant with respect to DO and BOD from a control- or operating-decision basis. Continuous measurements or intensified sampling are useful only during critical periods of low-flow or high-temperature conditions when water quality is most affected by pollution-control strategies, such as bypassing certain levels of wastewater treatment. Continuous measurements may be warranted only at critical stream sections during critical periods. Periodic sampling can provide a basis for making decisions regarding sampling locations and measurement-frequency schedules.

This evaluation also demonstrated the insensitivity of the stream system to many external forces. The physical size (in terms of flow volume) of the upper Mississippi River in the study area is such that changes in pollution-control strategies for most waste dischargers have no observable effect on water-quality measurements, and only the loads from major waste sources, or the cumulative effect over time of loads from many sources, is significant.

Modeling chemical-quality and temperature of Wyoming streams

L. L. DeLong developed a three-variable regression model that describes dissolved-solids concentrations of streamflow in the Green River basin of Wyoming with better accuracy than previous two-variable regression models. Magnitude of discharge and a harmonic function that accounts for seasonal differences are independent variables of the model. Adding harmonic function to regression resulted in standard errors of estimate of from 10 to 15 percent, whereas standard errors of from 20 to 50 percent were obtained when discharge alone was regressed against dissolved-solids concentration.

A study of the water resources in a potential coal strip-mine area in the Great Divide Basin of Wyoming resulted in an improved understanding of the nature of water quality of plains streams. L. R. Larson defined the dissolved-solids concentration of a plains stream by means of a three-variable regression model that uses discharge and time of year as independent variables. The highest dissolved-solids concentration occurs during early spring when the basin and channel are flushed by the first flows of snowmelt. Subsequent flows have significantly lower dissolved-solids concentrations. After the flushing action is complete, the dissolved-solids concentration varies as a logarithmic function of discharge.

H. W. Lowham analyzed water temperatures in the Green River basin of Wyoming to determine stream-temperature characteristics on a regional basis. Continuous and periodic water-temperature data were analyzed by using a simple harmonic curve-fitting procedure. Regional values of the harmonic coefficients were then analyzed by regression using basin and climatic variables. Results of the regional analysis can be used to predict stream temperatures at unsampled sites.

Relationship between water-quality parameters during periods of storm runoff near Portland, Oregon

No simple correlation exists between water-quality parameters during periods of urban storm runoff from small drainage basins in the Portland, Oreg., metropolitan area. An evaluation by S. W. McKenzie indicated that response time of several water-quality parameters differed during a period of storm runoff. For example, in Tryon Creek, peak suspended-sediment concentration of 600 mg/L and peak BOD of 20 mg/L occurred well before peak turbidity of 260 JTU; suspended sediment peaked before BOD. This variation in response time resulted in "loop" correlations between water-quality parameters similar to a "loop" stage-discharge rating at a stream-gaging station. Because of these "loop" correlations, the relationship between two parameters defined by a single set of samples is influenced by the time of sampling.

Physical, chemical, and biological relationships of four ponds in a Wyoming coal strip-mine area

D. J. Wangsness studied physical, chemical, and biological differences between natural pond ecosystems and pond ecosystems in an abandoned coal strip-mine area in north-central Wyoming. Ponds in the mined area had higher major-ion concentrations that fluctuated more than those in the natural ponds that were used as a control. Because of high concentrations of suspended sediment in ponds in the mined areas, light did not penetrate to as great a depth there as it did in ponds in unmined areas. DO concentrations decreased with depth in the ponds in the mined area; this was probably caused by oxidation of sulfides in the bottom waters and by oxidation of settling organic matter such as phytoplankton.

Even though the strip-mined area was abandoned 20 years ago, a stable littoral zone still has not developed in the ponds in that area. The lack of an extensive aquatic habitat and the substantial seasonal fluctuations of the chemical environment have resulted in a biological community in the mined area that is less stable and less diverse than the biologic community in the natural ponds not affected by mining.

Nitrification in acidic streams

Four characteristically acidic streams in southern New Jersey were investigated by J. C. Schornick and N. M. Ram to determine the effect of secondary sewage effluent on nitrification in the receiving water. Seven factors—pH, water temperature, DO, BOD, neutralization, nitrogen species, and nitrifying bacteria—were evaluated to determine the nitrification potential of the streams. Because each stream had a unique distribution of conditions, it was possible to qualitatively rank the streams in the order of their potential for nitrification. Haystack Brook apparently has a greater potential for nitrification than the other streams, and nitrification does not occur to any perceivable degree in Landing Creek. Nitrification occurs in Hammonton Creek and Squankum Branch, but the relative extent of nitrification in each could not be assessed. Although these streams are acidic, acidity does not appear to be an exclusive factor that determines the occurrence of nitrification.

Isolation of iron-releasing bacteria

G. G. Ehrlich and E. M. Godsy studied Fe^{+2} release from hydrated iron (III) oxides under anoxic conditions. Sand-iron hydroxide mixtures in glass columns were saturated with nutrient media, inoculated with mixed bacterial cultures, and allowed to stand 7-10 days. Ferrous iron concentrations of 100 to 200 mg/L were obtained if effluent pH was 5 or less. If pH was greater than 5, Fe^{+2} concentrations were 20 mg/L or less. Fe^{+3} was not found in effluents.

Several bacterial species possessing iron-releasing activity were isolated. Fe^{+2} concentrations of 20 mg/L at pH 5.5 were obtained with a saccharolytic *Clostridium* sp. No single species could match Fe^{+2} concentrations produced by mixed cultures, however. A two-membered system consisting of a *Streptococcus* sp. and a strain of *Klebsiella pneumoniae* released 12 mg/L of Fe^{+2} at pH 3.9. Individually, the streptococci showed negligible iron-release at pH 3.9; the *Klebsiella* sp. released only 1 mg/L of Fe^{+2} at pH 6.5.

RELATION BETWEEN SURFACE WATER AND GROUND WATER

Modeling interaction of lakes and ground water

Two-dimensional, cross-section modeling studies of the interaction of lakes and ground water showed that seepage of water to and from lakes is controlled by the continuity of a local-flow-system boundary beneath the lake. T. C. Winter (1976) determined that the configuration and continuity of a divide is controlled by the configuration of the water table in the vicinity of the lake and by the hydraulic conductivity contrasts within the ground-water reservoir. Continuation of this type of analysis, by using a three-dimensional ground-water-flow model, showed that the stagnation zone associated with the local-flow-system boundary can be mapped in three-dimensions, as can streamlines of regional flow systems passing beneath the local system. In the case of lakes that lose water to the ground-water system, three-dimensional simulation makes it possible to map the areal extent of a lakebed through which outflow seepage occurs. These new findings allow for optimum placement of wells to determine the interrelationship of lakes and ground water and for a better understanding of the quality of water in wells near lakes.

Lake-aquifer connection in Florida

The existence of a hydraulic connection between Lake Tsala Apopka in Citrus County, Florida, and the underlying Floridan limestone aquifer was shown by A. T. Rutledge. Lake Tsala Apopka is a series of shallow, interconnected lakes, ponds, swamps, and marshes that slope northward at 9.5×10^{-3} m/km. Open water is characteristic along the western side of the lake, whereas marshes and swamps cover most of the eastern part of the lake. Generally, the difference between the lake's surface or water table and the potentiometric surface of the Floridan aquifer is less than 1.5 m. At its highest point, the potentiometric surface is less than 0.03 m lower than the water table.

Lake-level fluctuations differ among lake types

Lake-level fluctuation is closely related to lake type, according to R. P. Novitzki and R. W. Devaul. A preliminary analysis, based on long-term records for 33 Wisconsin lakes, showed that levels of ground-water flow-through lakes (usually having no inlet or outlet, and supported by the local ground-water system) typically fluctuated from 1 m to more than 3 m during 30 years of record. During the same period, levels of ground-water discharge lakes (usually having a permanent outlet, small inlets, and functioning as a discharge point for a local ground-water system) typically fluctuated less than 1 m. Fluctuations of levels of surface-water flow-through lakes (having major inlet and outlet streams) were generally greater than those of ground-water discharge lakes, but less than those of ground-water flow-through lakes.

Ground-water budget for Lake Wingra Marsh, Wisconsin

H. L. Young prepared a ground-water budget for a 9.8-ha segment of marsh bordering Lake Wingra in Wisconsin as part of a nutrient-transport investigation by the Water Chemistry Department of the University of Wisconsin-at-Madison. The marsh segment is bounded by two small spring-fed creeks that flow to the lake. A storm sewer that drains a 6.1-km^2 residential area empties into the upper part of the marsh. The storm water spreads onto the marsh and flows to the boundary creeks and Lake Wingra.

The water budget was prepared for a 12-month period that included the very dry summer of 1976. Precipitation was 561 mm, or 5.5×10^4 m^3 of water on the marsh, and the storm-sewer discharge was 98.5×10^4 m^3, a total surface-water input of 104×10^4 m^3. Recharge to ground water was 5.9×10^4 m^3, or 5.6 percent of the surface input. Ground water moving upward into the marsh was 1.8×10^4 m^3. Lateral discharge of ground water to the boundary creeks and the lake was 4.8×10^4 m^3. Ground water lost to evapotranspiration and to replenish soil-moisture losses was 3.6×10^4 m^3. A net loss from ground-water storage of 1.0×10^4 m^3 occurred because of insufficient precipitation.

Hydrology of the Nevin Wetland, Wisconsin

The Nevin Wetland is a ground-water discharge area, according to R. P. Novitzki. A study of the wetland and its basin near Madison, Wis., showed that the wetland receives approximately 90 percent of its water supply as ground-water inflow, 6 percent as direct precipitation, and 4 percent as surface runoff from the upland part of the basin. The ground water is from a local shallow-aquifer system comprised of glacial drift and shallow sandstone and seems to be relatively independent of the deeper sandstone aquifer that provides the public water supply for the Madison area. Preliminary results indicated that there is some reduction in nutrients (total nitrogen and total phosphorus) in the water as it passes through the wetland.

Digital model of the Arikaree aquifer, Wyoming

Large supplies of ground water may be available from about 3,900 km^2 of the unconfined Arikaree sandstone aquifer in the Sweetwater River basin of central Wyoming. W. B. Borchert used a digital model to simulate the flow system in the Arikaree aquifer and its relation to the Sweetwater River. The steady-state hydraulic heads calculated by the preliminary model were within 15 m of the observed heads at about 98 percent of the nodes. The model-computed leakage from the Arikaree aquifer to the Sweetwater River was within 13 percent of the leakage estimated from gain and loss studies. Results from this preliminary model will be used to evaluate the feasibility of developing a comprehensive digital model of the area.

Tracer experiment in the Missouri Ozarks

In the Lebanon area of Missouri, manmade changes have been imposed on the hydrologic system by the addition of treated municipal wastes into a losing reach of Dry Auglaize Creek in the Grandglaize Creek basin. Using rhodamine-WT dye (20-percent solution), John Skelton conducted a ground-water tracing experiment which showed that the treatment plant effluent travels underground through the carbonate-rock terrane in a northwesterly direction and resurges in Sweet Blue and Hahatonka Springs in the adjacent Niangua River basin; the springs are located approximately 22.5 and 29 km from the dye-injection point, respectively. Computed average velocities, assuming straight-line travel through the system, are about 0.8 km/d to

Sweet Blue Spring and 0.5 km/d to Hahatonka Spring.

EVAPORATION AND TRANSPIRATION

Evaporation from water surfaces and the combined evaporation and transpiration (evapotranspiration) from vegetation on land surfaces play a major role in hydrology. The processes return an average of about 70 percent of the incident precipitation in the conterminous United States to the atmosphere. Moreover, changes in land use, such as irrigation development, reforestation, and urbanization, can substantially change the amount of evapotranspiration and thus affect the availability of water for other uses. Consequently, knowledge of evapotranspiration under various land-use and climatic conditions is needed for planning purposes.

Most of the significant evaporation and transpiration data obtained during the past year were from water-budget studies of relatively small basins or plots.

Evapotranspiration from a small stream basin

Average annual evapotranspiration from Spring Creek basin in central Louisiana is about 1,000 mm/yr, according to J. E. Rogers. This determination was made by subtracting the average annual discharge of Spring Creek per unit area, measured near Glenmora during 1957–68, from the average annual rainfall, as determined at two stations near the basin. This water-budget estimate of evapotranspiration is valid because (1) the ground-water divide in the terrace aquifer, the surficial aquifer, nearly coincided with the drainage divide for Spring Creek basin; (2) there was essentially no exchange of water between the terrace aquifer and underlying geologic units; (3) there was little ground water withdrawn during the period, as it predates development of a municipal well field; (4) net changes in ground-water storage were small over the 12-year period; and (5) there was little ground-water underflow past the stream-gaging station. Thus, rainfall that infiltrated the terrace aquifer was ultimately discharged to Spring Creek, and all water leaving the basin, except for that lost to evapotranspiration, was measured at the gaging station.

Errors in water-budget evapotranspiration estimates

Errors in water-budget evapotranspiration rates from plots ranging in size from 560 to 930 ha in the Gila River flood plain of Arizona for a given 14-day period could be as much as ±59 percent of the evapotranspiration before clearing of phreatophytes, and as much as ±113 percent after clearing. According to R. L. Hanson and D. R. Dawdy (1976), the principal sources of error were in the stream-inflow and stream-outflow components and in estimates of changes in soil-moisture storage. However, streamflow and its associated measurement errors generally were small during the summer months when evapotranspiration was high. Moreover, computed possible errors due to each component of the water budget provided a means of selecting periods for which the evapotranspiration estimate was valid. Thus, it was demonstrated that reliable estimates of summer evapotranspiration can be obtained and that significant differences occurred in evapotranspiration owing to clearing of phreatophytes.

LIMNOLOGY AND POTAMOLOGY

The sciences of limnology and potamology comprise the scientific study of inland waters and the interactions between the environment and the organisms within those waters. Limnology is often defined as the study of standing waters, and potamology is defined as the study of running waters. Usage varies, however, and the term "limnology" frequently includes all inland waters. Research during the past year was directed toward both streams and lakes. Many lakes exhibited summer thermal stratification. Such lakes are separated into three horizontal strata as a consequence of solar heating and wind mixing. The uppermost warm and well-mixed layer, the epilimnion, overlies an intermediate layer, the metalimnion, wherein temperature decreases sharply with depth. Below these layers, at the lake bottom, lies a cold, dense, stagnant layer, the hypolimnion. The well-lighted epilimnion is characterized by the occurrence of photosynthesis; whereas in the hypolimnion, decomposition of sedimented organic material dominates.

Lake reconnaissance

Lake-reconnaissance surveys provide baseline information, identify problems for more intensive investigation, and form a basis for regional classification of lakes.

G. C. Bortleson and N. P. Dion developed a method for comparing and characterizing lakes in Washington on the basis of water quality. The method can be used as an aid in establishing priorities among lakes for lake-rehabilitation efforts. To simplify such comparisons, a characteristic value (CV) was developed by using a principal-component analysis for each of

617 lakes in Washington. Only 3 of the 14 water-quality parameters measured were used in this analysis because the principal component of the 3 parameters accounted for 63 percent of the variance in the correlation matrix. The three parameters were Secchi-disc visibility, concentration of total phosphorus, and concentration of total organic nitrogen. The significance of the derived CV's was evaluated by regression of chlorophyll-*a* concentration against CV. The resulting standard error of estimate of ±1.8 μg/L of chlorophyll *a* indicated that CV can be a useful index in assessing relative water-quality and trophic conditions of lakes.

Dissolved oxygen depletion in lakes and reservoirs

J. T. Turk studied six lakes in Westchester County, New York, in areas that have widely varying land-use patterns in order to determine the extent of oxygen depletion, algal production, toxic materials, and septic-waste contamination. Lakes Katonah, Kitchawan, Lincolndale, Mohegan, Peach, and Trinity exhibited lack of oxygen in near-bottom water during the summer months; algal populations consisted principally of blue-green algae and were not significantly different from the other lakes. Lakes Katonah and Lincolndale had arsenic concentrations of up to 55 and 15 μg/L, respectively. In all lakes except Kitchawan and Trinity, calculated septic-waste loadings of nitrogen and phosphorus exceeded precipitation loadings of new nitrogen and phosphorus.

L. R. Frost, Jr., reported that DO profiles of New Hampshire's Lake Winnisquam indicate zones of production, respiration, and mixing. Nitrogen and phosphorus data indicate that the lake is sufficiently enriched to support a large algal population. Several parameters were considered to be indicators of the trophic condition of the lake and of the response of the lake to diversion and upgrading of sewage inputs, but the parameter found to be most indicative of the overall condition of the lake was the rate of decrease in the hypolimnetic DO concentration. The rate is higher in the lower basin of the lake than in the upper basin of the lake. Bottom-material samples show that copper (from copper sulfate algicides) and phosphorus have accumulated in the bottom sediments. Nitrogen concentrations found in the bottom materials were not unlike those found in relatively nonproductive lakes of Maine.

Anaerobic or near-anaerobic conditions occur perennially in the deep hypolimnetic water of Utah's Flaming Gorge Reservoir near the dam owing to lack of circulation with overlying water. According to E. L. Bolke, the depth and narrowness of the reservoir basin probably inhibit mixing, and the position of the lowest gate on the dam does not allow for displacement of dead storage. Near-anaerobic conditions also occur annually in the upstream part of the reservoir near the confluence of Blacks Fork and the Green River. Oxygen depletion begins in early summer in the bottom water as the reservoir begins to stratify owing to the decomposition of naturally occurring organic material or other pollutants brought in by Blacks Fork and the Green River. Stratification controls the movement of the low-oxygen water through the reservoir because the inflowing water seeks its own density level as it enters the reservoir. In the early summer months, low-oxygen water moves as interflow through the reservoir, but as cool water enters the reservoir in the fall, it wedges under the warmer reservoir water and moves as underflow. Eventually, cooling of the reservoir from the surface increases the density during the fall turnover and the anaerobic conditions are destroyed.

Simulation model for predicting lake temperatures

D. E. Ford (U.S. Army Corps of Engineers) (1976) developed a simulation model for predicting daily variations of temperature in a dimictic lake with density stratification. The model is based on a system of energy equations and a stability criterion on vertical mixing. Necessary meteorologic, morphometric, and disc transparency data were collected in 1974–75 from six small lakes near Minneapolis, Minn. Predictions of the model for the onset of stratification, surface temperature, hypolimnetic temperature, and mixing-layer depth are in good or excellent agreement with the data.

Macronutrient concentrations in surface water on Sanibel Island, Florida

A study of macronutrient concentrations in real-estate ponds and drainage canals within the interior wetlands area of Sanibel Island, Fla., was undertaken by T. H. O'Donnell. The concentration of nitrogen ranged from 1 to 12 mg/L; more than 90 percent of the nitrogen occurred in organic form. The concentration of phosphorus ranged from 0.01 to 4.0 mg/L; the orthophosphate component constituted a variable proportion of the total phosphorus. The concentration of organic carbon ranged from 10 to 150 mg/L. In terms of macronutrients, there are three surface-water categories: (1) Low macronutrient concentration, (2) high nitrogen and low phosphorus concentrations, and (3) high macronutrient concentration. Low macronutrient concentrations occur in water bodies that have large aquatic-plant biomasses because of their nutrient uptake. Most of the surface-water bodies on the island that were dredged prior to 1975 are in this category. High-nitrogen, low-phosphorus concentrations occur in recently dredged ponds that have large phytoplankton biomasses. High macronutrient concentrations occur in water in which there is infiltration of sewage effluent that has been discharged into holding ponds.

Mississippi River water-quality investigations

Low discharge in the Mississippi River during the summer and fall of 1976 resulted in the upstream movement of saltwater from the Gulf of Mexico to approximately 96 km above Head of Passes, according to F. C. Wells. During September, the saltwater moved at an average rate of approximately 1.4 km/d. The leading edge of the saltwater wedge was very well defined. Chloride concentrations typically increased from approximately 100 mg/L to over 5,000 mg/L within a 1.5-m change in depth. Downstream from the leading edge, the freshwater-saltwater interface was less distinct; the slight mixing action that occurred at the interface caused a gradual increase in chloride concentrations near the surface of the river downstream from the interface.

Approximately 35 genera of benthic invertebrates from 4 sampling locations on the lower Mississippi River between St. Francisville, La., (river mile 266) and Venice, La., (river mile 11) were identified. The dominant benthic invertebrates were *Corbicula*, an asiatic clam; Tubificidae, aquatic earthworms; Chironomidae, midge larva; *Tortopus*, an ephemerid-type mayfly; and *Corophium*, a euryhaline amphipod.

Assessment of the aquatic biology of Redwood Creek and Mill Creek drainage basins in Redwood National Park, California

The downstream areas of the Redwood Creek and Mill Creek drainage basins are located in Redwood National Park in California. The areas upslope and upstream from the park boundaries have been and are currently being subjected to timber harvest. R. T. Iwatsubo and R. C. Averett began a 2-year study in September 1973 to describe the aquatic ecosystem of these basins and to assess the impact of land-use activities, upslope and upstream from the park boundaries, on the aquatic biota in the park.

The biological data that were collected included data on bacteria, benthic invertebrates, fish, periphyton, phytoplankton, and seston. Results of the study indicated that the aquatic productivity of the Redwood Creek and Mill Creek drainage basins is low. Bacterial densities were low, except in samples collected from Prairie Creek, a tributary to Redwood Creek. Activities associated with a State park, a county fish hatchery, a grazing plot, a lumber mill, and scattered residential areas probably caused fecal-coliform- and fecal-streptococcal bacteria densities to be higher in Prairie Creek. Preliminary analyses of the benthic-invertebrate data indicated a diverse benthic fauna that varies considerably between streams and stream sections. Seven species of fish that were captured during the study represented species typical of northern California coastal streams. Because of the extremely large natural variation in fish populations from year to year in this area, the impact of land-use activities and the impact of the March 18, 1975, flood on the fish population were difficult to assess.

Periphyton and phytoplankton communities were diverse and dominated by diatoms. The productivity of periphyton and phytoplankton was low and primarily limited by insolation. The periphyton-biomass data indicated that road construction and logging-debris removal directly from the stream channel caused the rate of inorganic material deposition to greatly exceed the rate of periphyton production. Seston concentrations were extremely variable between and within each station sampled and were influenced seasonally by the aquatic productivity at each station and the amount of allochthonous material from the terrestrial ecosystem. During two storms, seston samples were collected at nearly hourly intervals from Harry Wier Creek (in a drainage basin that was being logged) and Little Lost Man Creek (in a control drainage basin). The results indicated that larger and sharper peak concentrations of organic seston were flushed from the logged drainage basin than from the control drainage basin.

Aquatic biology of the upper Salmon River area in Idaho

A study of the relationship between physical and chemical properties of streams and their biological communities is being conducted by K. V. Slack and L. J. Tilley in the upper drainage basin of the Salmon River in south-central Idaho. The western side of the East Fork Salmon River, the area of study, is generally mountainous with forested slopes; the eastern side is drier and consists of a high, dissected plateau where sagebrush and other semiarid vegetation predominate. W. W. Emmett (1975) described the channels and waters of the area. The East Fork and its western tributaries are lower in specific conductance, seston, and relative amounts of fine sediment in streambeds than the eastern tributaries are. In a preliminary study of a ubiquitous aquatic-insect group, the Chironomidae, L. J. Tilley found 16,801 individuals representing 78 taxa in dip-net samples from 27 sites on 13 streams during low flow. Chironomid larvae averaged 16 taxa and 1,156 individuals per site in the tributaries draining the drier eastern side of the basin compared to 11 taxa and 525 individuals per site to the East Fork and its western tributaries. Because of their abundance, variety, and range in environmental requirements, Chironomids show increasing promise as useful indicators of water quality.

Distribution and abundance of benthic organisms in the Sacramento River, California

The Sacramento River was studied by the California Department of Water Resources in 1960-61 to provide guidelines for maintaining adequate levels of water quality. In 1972-73, R. C. Averett, L. J. Britton, and R. F. Ferreira assessed the water-quality of the Sacramento River to determine what changes in water quality might have taken place since 1961.

A comparison of data showed no clearly defined differences between the benthic-organism samples collected in 1960-61 and those collected in 1972-73. Downstream changes in benthic-organism composition were consistent with the changes that occur in substrate type. The 1972-73 data showed variable patterns in monthly changes of benthic organisms at each site. Generally, the mean number of taxa per square meter and the diversity index for all sampling periods were higher in the upper reach than in the lower reach of the Sacramento River.

Succession and relative rates of periphyton growth on artificial substrates

L. J. Britton, R. F. Ferreira, and R. J. Hoffman collected periphyton samples every 3 or 4 days during two 1-month periods from a number of artificial substrates at three sites on the Sacramento and Feather Rivers of California. The artificial substrates showed the typical sigmoid growth curve of periphyton at each site, and peak similarity between phytoplankton and periphyton occurring after 1 week of exposure. Analyses of some of the data indicated that large amounts of periphyton may have been sloughed off the artificial substrates because of suspended-sediment impact, and thereby contributed to the phytoplankton population of the river.

Effects of stream relocation on aquatic habitat

A study of the effects of stream relocation at Canyon Slough along a part of the trans-Alaska pipeline route was conducted by J. W. Nauman, D. R. Kernodle, and C. E. Sloan to determine if the relocated streambed was colonized by benthic organisms similar to those in the natural streambed. Inasmuch as Canyon Slough is a salmon-spawning stream, indirect evaluation of conditions for salmon-spawning beds could be made by comparing the benthic faunas in the stream.

Drifting benthic invertebrates were collected during 1-hour driftnet samplings. The nets were installed in midchannel at two locations, one in the natural stream channel and one about 2 km downstream in the relocated channel. The total number of genera and midge genera, as well as species diversity, were higher in the new channel than in the natural channel upstream of the relocation. However, there were fewer individuals collected per unit volume of flow in the new channel than in the natural channel.

Two midge genera (in larval stages), *Cricitopus* sp. and *Diamesa* sp., were not found at the natural stream site but were abundant in the relocated channel; the difference may have been due to the fact that the nutrient level in the water of the relocated channel had not yet increased to match that of the natural channel. These initial results indicated (1) that the relocated stream was colonized by a benthic community somewhat more diverse than that in the natural channel and (2) that the new streambed area should provide an adequate spawning substrate.

Streamflow preferred by salmon for spawning and rearing

C. H. Swift III determined stream discharges and streambed areas preferred by 5 species of salmon for spawning and rearing at 84 study reaches on 28 streams in Washington. In the streams studied, preferred spawning discharges ranged from 2.2 to 200 m^3/s for Chinook salmon, 0.3 to 130 m^3/s for Sockeye and Coho salmon, and 0.4 to 230 m^3/s for Pink and Chum salmon. Those discharges represent ranges of approximately 0.3 to 11 times the median monthly mean discharges for September and October and 0.1 to 6 times the median monthly mean discharges for November and December (the months when spawning is greatest in the study streams). Discharges preferred for salmon rearing ranged from 0.1 to 79 m^3/s, about 0.7 to 4 times the median monthly mean discharge for September when low flows are usually most limiting to the rearing capacity of the streams. Peak-unit spawnable area (maximum area per square meter of channel length that has preferred water depths and velocities) was similar for the five salmon species and ranged from 0.2 to 52 m^2. In order that estimates of those discharges and areas could be made for ungaged sites, Swift developed equations of relationships with toe-of-bank channel widths (3.4 to 167 m) and basin drainage areas (9.0 to 3,990 km^2); minimum standard errors of estimate for the equations were 40 percent for preferred spawning discharges, 57 percent for preferred rearing discharges, and 27 percent for peak-unit spawnable area.

Quantification of aquatic ecosystems

M. J. Sebetich, V. C. Kennedy, and S. M. Zand used a 10-m-long, portable, flow-through, Plexiglas flume to study the effects of controlled variables on periphyton. The periphyton community was effectively isolated from higher trophic levels in the stream, and its response to selected nutrients was measured throughout the flume.

S. M. Zand (1976) evaluated the water-quality diversity index to determine its shortcomings when it is used to classify the quality of water bodies. Zand demonstrated the differences between the Shannon and Brillouin formulas, described the units involved, and proposed alternative indices. He suggested that the diversity index be used as part of a diversity matrix formed by incorporating other indices and variables relevant to aquatic ecosystems.

Effects of recent volcanic activity on Baker Lake, Washington

Increased volcanic activity on Mount Baker, Washington, that began in March 1975, represents the greatest known activity of a Cascade Range volcano since eruptions at Lassen Peak, California, during 1914–17. G. C. Bortleson reported that the most undesirable natural results that have been observed after 1 year of increased volcanic activity are an increase in local atmospheric pollution and a decrease in the quality of some local water resources, including Baker Lake.

Boulder Creek, which drains only about 5 percent of the total drainage area of Baker Lake, carried sizable but variable loads of acid and dissolved minerals into the lake during 1975. Sulfurous gases and fumarole dust from Sherman Crater are the main sources of these materials, which are brought into upper Boulder Creek by meltwater from the crater. In September 1973, before the increased volcanic activity, Boulder Creek water had a pH of 6.0 to 6.6, whereas after the increase, the pH was as low as 3.5. Most nearby streams had pH values of about 7. On April 29, 1975, the dissolved sulfate concentration of Boulder Creek water was 6 to 29 times greater than that of nearby creeks or of Baker River; total iron concentration was 18 to 53 times greater than that of nearby creeks. By dilution, chemical neutralization, and buffering of the acid-rich Boulder Creek water, Baker Lake probably could assimilate indefinitely the acid loads measured during 1975. The greatest opportunity for water from Boulder Creek to persist as a layer and extend farthest before mixing with the other reservoir water occurs when Baker Lake is strongly stratified and Boulder Creek flow rate is large in relation to other feedwater.

Diel fluctuations of water quality described for Bear Creek in Jackson County, Oregon

Diel (24-hour period) variations of DO and pH were observed at selected sites in Bear Creek in Jackson County, Oregon. S. W. McKenzie reported that DO at one site ranged from a low of 84-percent saturation in the early morning to a high of 141-percent saturation in the afternoon. At that site, pH ranged from a low of 7.5 to a high of 9.4. Oregon Department of Environmental Quality standards for Bear Creek allow a maximum pH of 8.5 and a minimum DO content of 90-percent saturation. Because of diel variation, the time of sampling could determine whether or not the DO and pH meet those standards.

Low pH in a southern New Jersey stream

Fishkills in Oyster Creek, near Waretown, N.J., are attributed to rapid drops in pH from normal levels to levels of 3.5 to 3.7. These drops occur during periodic flushing of the surrounding swamp, but they are not necessarily directly related to rainfall. The time interval between rains seems to be more important than the amount of rain. Although the normal pH of the stream is about 4.2 and that of the swamp water is about 3.8, there are significant fluctuations above and below these values; and there appears to be a relationship between the swamp pH and the stream pH. The primary cause of the low stream pH is the flushing of weakly acidic organic matter into a poorly buffered receiving stream. The oxidation of sulfides to sulfates may also be a contributing factor to the low pH of the swamp water.

NEW HYDROLOGIC INSTRUMENTS AND TECHNIQUES

A standard rating was developed by V. R. Schneider and G. F. Smoot (1976) for the Price pygmy current meter that, if implemented, would eliminate the need for a central repair facility and for individual calibrations without sacrificing accuracy of current-meter measurements. Standard errors of the standard rating ranged from 4.5 percent at 0.076 m/s to 1 percent at 0.91 m/s.

E. H. Cordes reported that convertible data-collection platforms (C/DCP) were deployed at 10 existing surface and ground-water stations in southern Florida. Each station monitors stage and rainfall and is equipped with an independent timer and a battery on a digital recorder to provide backup should the C/DCP fail. All equipment is housed in a double-walled rock-filled shelter that will withstand abuse by most types of firearms.

Studies by W. W. Emmett, L. A. Druffel, V. R. Schneider, and J. V. Skinner (1976) showed that the hydraulic efficiency of the 7.62-cm and 15.24-cm Helley-Smith bedload samplers is approximately 1.54 for the range of flow conditions tested. Their efficiencies can be regulated by changing the exit-entrance area ratio of the nozzles; the efficiency for a nozzle with a 7.62-cm opening increased from 1.06 to 1.54 as the ratio increased from 1.00 to 2.62. When the ratio is greater than 2.62, but less than 3.22, the efficiency remains constant. The sample bag can be filled to 40-percent of capacity without reducing efficiency.

J. V. Skinner and J. P. Beverage (USGS) and D. A. Benson (U.S. Army Corps of Engineers) completed designs of several new suspended-sediment samplers and accessories for samplers. The group converted all sediment samplers to ½-L capacity in order to facilitate the collection of large-volume samples for both sediment and chemical analyses. A few 1-L-capacity models are available. A point-integrating sampler was designed to operate at depths to 80 m and velocities of up to 3 m/s. The group also reported the development of a small light-weight power supply to operate point-integrating samplers. This capacitive-discharge supply can operate a sampler about 200 times on one set of batteries.

D. C. Signor designed a small-diameter compressed-gas-actuated sampling pump. The pump is less than 50 mm in diameter and is suitable for use in well casings of 50 mm or more in diameter. The gas does not come in contact with the sampler; therefore, compressed air may be used without fear of sample contamination. Pump operation time on a bottle of compressed gas is dependent upon the pumping head and the pumping rate. Tests have shown, however, that for a pumping head of 33 m, 7.6 m of submergence, a pumping rate of 240 cm^3/min, and a pump-operating pressure of 5.6 kg/cm^2, a standard-size compressed-gas bottle with an initial pressure of 126.6 kg/cm^2 provides more than 48 hours of continuous operation.

SEA-ICE STUDIES

Aircraft and spacecraft observations of Arctic Sea ice

W. J. Campbell (USGS), Per Gloersen, T. T. Wilheit, T. C. Chang, and H. J. Zwally (NASA-Goddard Space Flight Center) used microwave imagery from NASA aircraft and Nimbus-5 and -6 satellites to study the variation in the distribution of sea ice in the North American sector of the Arctic Ocean. An algorithm was developed that permits the determination of the parameters sea-ice concentration (C), sea-ice surface temperature (T_{ice}), and fraction of multiyear ice (F), by using a combination of data from the three channels on the Nimbus-5 and -6 microwave imagers at wavelengths of 0.8 and 1.55 cm, and both polarizations at 0.81 cm. Both this analysis and 1.55-cm data collected by the NASA Convair-990 Airborne Laboratory indicated that the fraction of multiyear sea ice is considerably higher in the eastern Beaufort Sea and Arctic Ocean off Banks Island than it is to the west.

AIDJEX

W. J. Campbell reported that the fourth and final set of remote-sensing aircraft flights for the AIDJEX Main Experiment was made in April 1974. The NASA Convair-990 Airborne Laboratory collected infrared, passive microwave, side-looking radar, scatterometer, and photographic data over the AIDJEX triangle of manned camps and data buoys. Simultaneously, surface data were collected from selected test sites in the triangle. Aircraft and surface data on pack ice in the Beaufort Sea were collected for all seasons of the year for the main experiment. These data are being reduced and analyzed and applied to numerical models of the Beaufort Sea pack ice.

Antarctic sea-ice model

The structure of a numerical model of the dynamics of Antarctic sea ice was designed by W. J. Campbell, L. A. Rasmussen, and C. H. Ling. The wind-stress component, which converts synoptic surface-pressure data to the stress on the ice, has been completed. The model is for use with passive microwave imagery from the electronically scanning microwave radiometer and scanning multichannel microwave radiometer sensors carried by Nimbus satellites.

ANALYTICAL METHODS

ANALYTICAL CHEMISTRY

Determination of trivalent manganese in the presence of divalent iron

A spectrophotometric method for the determination of milligram amounts of trivalent manganese in the presence of divalent iron, trivalent iron, and divalent manganese was developed by J. W. Marinenko (1976). Powdered samples were dissolved by heating in concentrated phosphoric acid in the presence of iodic acid. Trivalent manganese in phosphoric acid was determined spectrophotometrically following the extraction of iodine with carbon tetrachloride.

Comparison of analytical techniques for uranium, thorium, and potassium

J. S. Stuckless, H. T. Millard, Jr., C. M. Bunker, C. A. Bush, and Claude Huffman, Jr., compared various analytical techniques for uranium, thorium, and potassium. Geochemical exploration for uranium requires accurate and precise determinations of low-level concentrations. Several different methods and four treatments of the fluorometric method were used to analyze for uranium in granitic rocks. In addition, four methods for thorium and three for potassium, two elements that are usually associated with uranium in igneous rocks, were also applied. The results showed that commonly used techniques for thorium and potassium are adequately precise and accurate, but that many techniques used for uranium determinations lack the precision and accuracy required for reliable geochemical exploration.

Uranium and thorium values were evaluated by comparing them to the obtained by isotope dilution using mass spectrometry. The delayed neutron technique and isotope dilution along with the use of spectrometry both yielded results that were accurate within 5 percent. Equivalent uranium (eU) by total $\beta - \gamma$ count for samples that contained < 100 ppm uranium were 70 to 400 percent too high. Radium equivalent uranium (RaeU) values obtained by sealed-can γ-ray spectrometry were as much as 100 percent greater than uranium values, but most were 15 to 20 percent lower than uranium values. Fluorometric values were strongly dependent on the sample treatment and were at best marginally accurate or precise enough for detailed interpretation.

The combination of delayed neutrons for uranium and γ-ray spectrometry for RaeU, thorium, and potassium provide the best data for geochemical exploration for uranium in granitic rocks. The combination of γ-ray spectrometry and γ spectrometry is the best approach for detailed studies on a few specific samples. Carefully done fluorometric analyses is sufficient for mineralized rocks and ores.

EMISSION SPECTROSCOPY

Determination of lithium, cesium, and rubidium at the parts per million level

A quantitative emission spectrographic technique for the determination of lithium, cesium, and rubidium was developed by R. E. Mays and J. L. Seeley. The method was designed to cover all concentrations down to 1 ppm, by using intensity values rather than line-width measurements. Application of the technique was successful in the analysis of high lithium content (0.1–0.5 percent) biotite separates, as well as to lower lithium-containing materials such as synthetic quartz samples and the USGS rock standards *AGV*-1, *BCR*-1, *G*-2, and *GSP*-1. A strong correlation between X-ray rubidium results and those determined via this method was demonstrated.

Determination of Sb, As, Bi, Cd, Se, Tl, Ta, and Zn at the part per million level

Chris Heropoulos and J. L. Seeley have developed an emission spectrographic analytical procedure for antimony, arsenic, bismuth, cadmium, selenium, tellurium, thallium, and zinc in sulfide minerals and rocks down to 0.5–1 ppm. The methodology includes use of a short wavelength radiation sensitive emulsion, with sample preparation limited to dilution with graphite. Optimum excitation conditions, exposure time, and sample charge have been established. Application of the technique has been made to a suite of stibnites, to hydrothermal deposits, and to ore genesis studies involving possible hydrothermal transport.

Standardization and quality control programs for minicomputer-based emission spectrographic analysis

C. P. Thomas has expanded the program library by adding standardization programs that greatly reduce the hours spent examining spectral lines for their analytical usefulness. The new programs tabulate transmittances, intensities, location of spectral lines and interfering lines, and analytical concentrations from all the spectra on standard plates. The computer calculates first and second degree coefficients for the analytical curve (Ln *I* versus Ln *C*). It evaluates the curve based on concentration range, goodness of fit, and slope. It suggests concentration limits such that a signal to noise ratio of 2 is maintained. If necessary the curve is refitted in the suggested range. A summary sheet containing the wavelengths, ranges, coefficients, and computer evaluation of all the analytical lines is presented.

Other programs allow analyses of natural rock reference materials to be used to improve analytical line finding and interference corrections.

Quality control has been improved by routinely including spectra of several standard reference materials on each spectrogram. The accuracy with which these rocks are analyzed is monitored, along with the effective arc temperatures and electron pressures.

X-RAY FLUORESCENCE

Sample preparation for trace element analysis of silicate rocks

A modified method of preparing silicate rock samples for automated X-ray fluorescence trace element analysis was developed by B. W. King, L. F. Espos, and B. P. Fabbi. Samples previously prepared with a high proportion of cellulose sample to binder (1:1) were found to deteriorate when irradiated with new high intensity X-ray tubes. The deterioration affected the precision and accuracy of analysis owing to a non-uniform concentration of the sample during analysis.

By reducing the amount of binder to 15 percent, less than 1 percent change in X-ray intensity has been observed after 10 hours of sample irradiation. The method now has greater precision and sensitivity for the elements Na, P, S, Cl, K, Sc, Ti, V, Cr, Ni, Zr, Rb, Sr, Y, Zr, and Ba.

Glass disc fusion method to prepare silicate rocks for X-ray fluorescence analysis

A glass disc fusion method for silicate rock analysis has been developed by B. P. Fabbi and H. N. Elsheimer (1976). One gram of sample is mixed with 6 grams of lithium tetraborate ($Li_2B_4O_7$) and 1.5 grams of lithium nitrate ($LiNO_3$). An automatic fusion device is used to prepare the glass discs for automated X-ray fluorescence analysis. The device is unique in that it mixes the sample melt during fusion, controls the temperature and time of fusion, and casts the cooled melt into glass discs. There are several advantages of this method over those previously used by Survey laboratories. The method is four times faster, precision and accuracy are twice as good, sampling errors are significantly reduced, and sensitivity is improved for all analyses, which includes SiO_2, Al_2O_3, total Fe as Fe_2O_3, MgO, CaO, K_2O, TiO_2, P_2O_5, and MnO.

RADIO ISOTOPE DILUTION

Trace element fractionation during magmatic crystallization

L. P. Greenland and E. Y. Campbell (1977) used radio isotope dilution and atomic absorption techniques to study the variation of chalcophilic elements through a drill core from the Great Lake in Tasmania. Two periods of sulfide crystallization were demonstrated. The initial period effectively removed gold and tellurium from the magma while leaving sufficient selenium and copper to be concentrated in the subsequent crystallization. Thallium was concentrated in residual magmas throughout crystallization, whereas indium was carried in mafic silicates.

Rapid determination of chlorine

L. P. Greenland and E. Y. Campbell devised a procedure to determine chlorine rapidly by decomposing 200-mg rock samples with hydrofluoric acid in a Teflon bomb at ~200°. A specific-ion electrode was used to measure chlorine activity directly in the bomb after dilution with water. The bomb technique gave a rapid decomposition and a small final volume that made high sensitivity possible. Ions which make silver complex are too low in abundance to give serious ion electrode interference in most rocks.

Accuracy and precision were studied by an analysis of variance of data from seven USGS standard rocks and by comparison with results from a similar study by using a common spectrophotometric technique. Results of the two techniques were in good agreement, and thus the much greater speed and simplicity of the specificion method were obtained without sacrificing analytical quality.

NEUTRON ACTIVATION

Epithermal neutron activation as a supplement to thermal irradiation

A study by P. A. Baedecker and J. J. Rowe of the use of thermal and epithermal neutron activation analysis with data collection by Ge(Li) and Planar detector systems showed that the epithermal irradiation supplements the thermal irradiation procedure by permitting the determination of Ni, Sr, Mo and U and improves the sensitivity and accuracy for the determination of , Rb, Sb, Cs, Ba, Gd, Tb, Tm, Yb, Hf, Ta and Th. Employing the planar detector to make use of the X-ray peaks associated with electron capture or internal conversion processes improved the determination of Mo, Ba, Ce, Nd, Sm, Yb, Hf, Ta, U, Se, Gd and Tm.

The epithermal irradiation technique was also studied by Rowe for application to coal analysis. It was found that from a total of 30 elements studied, the epithermal technique appeared advantageous for the determination of Ni, Ga, As, Se, Br, Rb, Sr, Zr, Mo, In, Sb, Cs, Ba, Sm, Ho, Hf, Ta, W, Th and U.

Chromium in rocks and minerals in the southern California batholith

F. O. Simon and C. L. Rollinson (University of Maryland) (1976) determined chromium by neutron-activation analysis in a suite of rocks and minerals from the southern California batholith and showed that chromium was concentrated in the mafic differentiates, which decreases as the more felsic rocks are approached. This trend was evident for samples of the Woodson Mountain Granodiorite from a single differentiated stock.

The distribution of chromium in the minerals from the rocks of the southern California batholith showed that it was depleted in the magma during the course of crystallization. The data indicated that the minerals were in equilibrium with the magma during crystallization and that the distribution coefficient (Cr in biotite/Cr in hornblende) is correlated with differentiation indices, which indicated either temperature or compositional dependence. The average distribution coefficient (Cr in biotite/Cr in hornblende) was 1.18, which compared favorably with the average values found by other investigators for other suites.

Characterization of organic materials in organic-rich rocks

Preliminary qualitative studies by G. A. Desborough show the following: (1) In addition to N, C, and O, heavier elements such as F, P, Ca, Ti, V, Cr, and Fe may be present in concentrations between 0.0X and X.0 weight percent. (2) Sample current-image and X-ray-image studies reveal the shape, size, texture, mineral relationships, and homogeneity of individual particulate organics, and the distribution and relative abundance of elements heavier than nitrogen. Many samples contain two complexly intergrown organics in what appears to be a single phase by light microscopy. (3) Virtually all samples examined contain two or more types of organics which can be distinguished by either sample current image analysis or elemental analysis, or both. (4) The relative volatility, pyrolyzability, or refractiveness can be estimated by observing the decomposition due to electron beam bombardment. (5) Particles, fragments, or grains of the organics greater than about 2 micrometers in the minimum dimension can be successfully studied with the electron optical techniques available on the electron microprobe. Optimum working magnifications range from about 100–2,000X.

THIN AND POLISHED SECTIONS

Semi-automated thin section preparation

Robert Shely has developed a semi-automated thin-section preparation procedure that is a major improvement over previous methods. A twin-bladed saw cuts parallel-sided rock slabs of uniform thickness at twice the speed of previous saws. Only the ends of the specimen require shaping. Lapping is done with 21 specimens at a time on a 38 cm Crane lapping machine that provides absolutely uniform flatness to all specimens. This has cut lapping time to one tenth of previous procedure. For cementing it was found that only 2 cements Petropoxy 154 and Yale C.I.B.A. with refractive index of 1.540 were suitable. Mounting was done on a jig that accepts 10 samples at a time, by using a pressure equalizer block with spring-activated pressure rods. An unmeasurable thin film of cement remained between the specimens and the glass support. The samples were then sawed in a vacuum chuck cut-off saw to produce a mounted slab 150–200 μm thick, which completely eliminated grinding.

The specimens are finished down to 30 μm, 18 at a time on an LP30 machine. The machine has three diamond check rings with six samples on each ring. The chucks are rotated on a moving lap wheel, and when the diamond rings touch the discs surface, the finishing operation is completed.

ANALYSIS OF WATER

Determination of mercury

A completely automated atomic-absorption method for determining dissolved organic and inorganic mercury in water was evaluated by M. J. Fishman. Organic mercury compounds, if present, are decomposed by hot (95°C) digestion with potassium dichromate and potassium persulfate in sulfuric acid solution. The mercuric ions are then reduced to the elemental state with stannous chloride, the mercury is subsequently removed from solution by aeration, then it is passed through a cell positioned in the light path of a spectrometer, and its absorbence is measured. Twenty samples per hour can be analyzed by using 10 mL of water. As little as 0.1 μg/L of mercury can be determined.

Determination of cyanide

An automated colorimetric method for determining dissolved cyanide was evaluated by D. E. Erdmann. The method is based on the chlorination of cyanide with chloramine-T and the subsequent reaction with pyridine-barbituric acid reagent. Only simple cyanides are detected. To determine both simple and complex cyanides, the method incorporates an ultraviolet digestion-plus-distillation step to break down the complexes to simple cyanides. Distillation also removes certain interferences. Twenty samples per hour can be analyzed for cyanide concentrations between 10 and 300 μg/L.

Volatile organohalides

A method for the determination of volatile organohalides in water and treated sewage effluents was developed by D. F. Goerlitz (1976). The compounds are stripped from solution by a gas purge and are collected on a short porous-polymer chromatographic column. The organohalides are determined by program-temperature gas chromatography employing specific halide detection.

Separation of organic solutes from water

The analytical techniques used to concentrate, separate, and classify natural organic solutes in water (J. A. Leenheer and E. W. D. Huffman, Jr., 1976) were scaled up and applied to aqueous-process wastes from oil-shale retorting operations so that gram-sized quantities of these waste organic solutes could be isolated for further study. According to J. A. Leenheer, this large-scale separation was necessary for the study of the sorption of these waste organic solutes on processed shale, soil, and sediment after disposal of the aqueous-process wastes. The goal of this research is to supply analytical methodology that can be used to provide the sorption parameters needed in organic-solute transport models of wastes in surface and ground waters.

Remote sensing of dissolved solutes

A limited capability to remotely sense dissolved solutes in water has been documented by investigators who used methods that involved analyzing the Raman-scattered light returned from a water bulk by a special sensor mounted in a low-flying aircraft. Laboratory studies of the resolution and sensitivities of this sensor were conducted by M. C. Goldberg and E. R. Weiner (USGS) and Kirk Cunningham (Denver University) (1977). With the use of a high-powered laser-light source, the Raman-scattered light from eight solutes in a water sample was analyzed as a function of counting time, light intensity, and solute concentration to determine both the resolution and the sensitivity of detection for each solute.

Calculations indicated that the sensitivity limit is set by the intensity of the water signal in the 860 to $1,400^{-}cm^{-1}$ (wave frequency) region. The data also show that, at a signal-to-noise level of 2 and a counting time of 1,000 s, the following sensitivities can be predicted: phosphoric acid (H_3PO_4), 6.3 mg/L; biphosphate (HPO_4), 6 mg/L; carbonate (CO_3), 4 mg/L; acetic acid (CH_3COOH), 10 mg/L; bicarbonate (HCO_3), 6.3 mg/L; nitrate (NO_3), 2 mg/L; acetate, 10 mg/L; and sulfate (SO_4), 2.5 mg/L.

It is possible to increase the detection sensitivity beyond these limits by several techniques, such as compensation of the laser-power fluctuation, larger light-gathering optics, or optical multichannel light readout.

GEOLOGY AND HYDROLOGY APPLIED TO HAZARD ASSESSMENT AND ENVIRONMENT

EARTHQUAKE STUDIES

SEISMICITY

The National Earthquake Information Service (NEIS) in Golden, Colo., occupies an esteemed position within the international scientific community. It is the foremost source of data on recent earthquake activity around the world. Last year, as part of its program to monitor global seismicity, the NEIS determined the location and magnitude of approximately 6,000 earthquakes. Of these, approximately 1,500 were large enough to cause damage in populated areas. The NEIS program to monitor earthquakes throughout the world can be viewed as an information-gathering and analysis procedure. Input data in the form of arrival times and amplitudes recorded at cooperative seismograph stations throughout the world are sent to Golden where they are machine processed to obtain output composed of earthquake origin times, locations, magnitudes, and associated station observations. These results are then disseminated to seismologists, engineers, government agencies, and other interested parties throughout the world.

According to J. S. Derr, the NEIS early alert service, which operates on a 24-hour basis, issued over 50 earthquake bulletins last year. These bulletins concern potentially destructive shocks overseas or somewhat smaller U.S. quakes that may have caused damage. Because of the breakdown in communications following a major earthquake, these bulletins often provide disaster relief organizations, public safety agencies, and the news media with the only factual information available for a considerable period of time after the shock.

Through cooperation with universities and other agencies and the installation of new equipment, an effort has been made to lower the detection threshold of U.S. earthquakes. To assure uniform treatment of the data, J. H. Minsch was assigned the task of overseeing the collection and processing of data associated with all U.S. events. Stations in New York, New Jersey, and California were added to the U.S. seismic network of telemetered seismograph stations, according to M. A. Carlson. This system is composed of widely dispersed seismometers that transmit signals over telephone lines to Golden, where they are displayed visually. The network, which now extends from coast to coast and border to border, gives NEIS the capability of responding rapidly to earthquakes within the conterminous United States.

In conjunction with university seismological centers, the USGS established a network to investigate the northeastern United States. P. W. Pomeroy was selected to direct this network, which is now operational. Origin times, locations, and magnitudes of all events within this regional network are published in the "Bulletin of Seismicity of the Northeastern United States."

The NEIS carried out surveys of the damage done by and felt areas of 93 earthquakes in the conterminous United States last year, according to C. W. Stover. These intensity surveys, which permit recent instrumentally recorded shocks to be compared with historic earthquakes, are valuable in engineering seismology and risk analysis. The basic data needed to delineate the severity and extent of ground shaking accompanying an earthquake are obtained by means of a postal questionnaire canvass carried out by means of modern data-processing techniques. The results of the questionnaire canvass and maps showing the areal distribution of intensities are published in the quarterly circular "Earthquakes in the United States."

The Albuquerque Seismological Laboratory (ASL) has become a recognized leader in efforts to upgrade instrument and recording systems used at seismograph stations. The ASL continued to provide the technical and logistical support necessary to keep the Worldwide Standardized Seismograph Network (WWSSN) operational (C. E. Cran). At present, this 15-year-old network is composed of 85 foreign stations and 31 domestic stations. Each observatory consists of matched, three-component, long-period, and short-period instruments. Paper seismograms recorded at the stations are sent to Golden for quality control (R. P. McCarthy) and forwarded to the National Oceanic and Atmospheric Administration (NOAA) data center at Boulder, Colo., for film reduction. Researchers from all over the world may order exact copies of the WWSSN records from NOAA at moderate cost.

According to H. M. Butler, the ASL has completed cooperative arrangements with the host countries for 12 Seismic Research Observatories (SRO). Six of these very sensitive seismograph systems have been installed and are operational at the following locations: Wellington, New Zealand; Taipei, Taiwan; Guam, Marianas Islands; Mashhad, Iran; Narrogin, Australia; and Albuquerque, New Mexico. The SRO system features analog and digital recording and a dynamic range of six orders of amplitude over a wide band of frequency. The digitally recorded output of the systems can be used as input to computers for spectral analysis and particle-motion studies. Approval has also been obtained for four advanced Seismological Research Observatories; these systems have been installed at Charters Towers, Australia, and La Paz, Bolivia.

The NEIS research group has made studies of the relationships between seismicity and tectonics in selected regions. W. J. Spence investigated the mechanics of the movement between the Pacific plate and the North American plate in the Aleutian Islands. He pointed out that normal faulting, which is initiated in the trench or pretrench rise, is carried, escalatorlike, down the Pacific plate as it descends beneath the North American plate. He suggested that the downward movement of the Pacific plate may be associated with earthquakes or fault creep on zones of weakness along these existing normal faults. Spence and W. J. Person found that the February 4, 1976, Guatemala earthquake, which killed over 23,000 people, occurred in a zone of anomalously low seismicity between the Caribbean and North American plates. Their findings show that such earthquakes are repeated about every 200 years in this zone.

EARTHQUAKE MECHANICS AND PREDICTION STUDIES

Nonscientific earthquake predictions

In view of the numerous nonscientific earthquake predictions that now appear in the media, R. N. Hunter initiated a study to separate fact from fallacy in the earthquake-prediction field. His objective is to offset the possible harmful effects of an accidentally correct prediction. Hunter has begun a file of predictions made by a variety of individuals, whose roles vary from scientist to psychic. He has also written a computer program to evaluate the relative value of each prediction based on the probability that an earthquake with the specified magnitude will occur within the stated time and space window. An analysis of the 171 predictions that have been entered into his file from 32 sources indicates that none of the predictions have achieved a high enough score to merit consideration.

Seismic studies for prediction

Fault behavior along a 9-km zone of the Calaveras fault southeast of San Jose, Calif., has been described by a simple model similar to the spring-driven frictional models used in laboratory simulations of stick slip. On the basis of this model, Bufe, Harsh, and Burford (1977) successfully predicted a magnitude 3.2 earthquake that occurred in the zone on December 8, 1976. The earthquake occurred within 3 km of the predicted hypocenter and within 24 days of the target date, which was January 1, 1977. On the basis of seismicity over the past 15 years, the probability of an earthquake of magnitude 3 or greater occurring within 24 days of any randomly selected date is only 10 percent for this zone.

J. D. Byerlee summarized recent laboratory results of possible importance to earthquake prediction:

- The attenuation of *P* and *S* waves during the deformation of rock can either increase or decrease depending on the particle motion with respect to the principal stress directions.
- Oblique slip in fault zones may precede sudden slip between the gouge zone and the country rock.
- The *b* values may decrease before sudden slip on faults even if the rock is dry.
- The Lomnitz creep law is followed during the deformation of sandstone and granite at high pressure.

On the basis of laboratory data and some Chinese results, changes in the ratio of *P* to *S* amplitudes look promising as a diagnostic tool for identifying foreshocks. A. G. Lindh and C. E. Mantis measured *P* and *S* amplitudes for a uniform set of about 25 small foreshocks and 100 aftershocks of the magnitude 5.7 Oroville, Calif., earthquake. They found that:

- The ratio of *P* to *S* waves at Station KPK (20 km east of Oroville) changes dramatically at the time of the main event. The ratio of *P* amp to *S* amp changes from ~ 2.0 to ~ 0.4. (Unfortunately, the sense of change is the opposite of that predicted by D. A. Lockner and J. D. Byerlee's laboratory results.)

- The main event at Oroville was preceded by 3 hours by a magnitude 4.7 foreshock that was followed by numerous small events. Amplitude ratios for these events scattered widely (from 3.0 to 0.1), unlike the earlier foreshocks or the aftershocks of the main event.
- A preliminary interpretation of all the amplitudes measured so far indicates that a small change in the dip of the fault plane was observed for very small earthquakes near the hypocenter of the main event. This change could be interpreted as a local change in the orientation of the principal stress axes in the hypocentral volume.

The data suggest that *P* and *S* amplitudes may contain informaion relevant to prediction and maybe even be a short-term precursor.

An examination of arrival-time residuals recorded on the Hawaiian network before the magnitude 7.2 Kalapana earthquake of November 1975 failed to show any precursory anomaly, but examination for possible precursory effects is continuing (Ellsworth, 1976).

Earthquake precursors

A USGS radon monitoring network in central California recorded a large anomaly in radon emanation that coincided with the occurrence of a magnitude 4.3 earthquake nearby. This earthquake occurred on March 17, 1976, and was located 25 km east of Hollister. According to C. Y. King, the recorded radon emanation began to increase significantly above the average preearthquake level 5 weeks before the quake. It reached a peak value, which is 130 percent or 5 standard deviations above the average level, immediately before the quake. Since then, the radon emanation has gradually decreased to below average values. The radon change may reflect an annual cycle, but similar changes were not recorded at two control stations in Los Altos, which is about 100 km northwest of the network, where the weather conditions were similar.

Arrays of relatively inexpensive tilt, strain, and magnetic instruments, installed along active faults in western United States, are being used to provide details on both seismic and aseismic (creep) fault failure. Of particular interest is the detailed fault-mechanics sequence that results in earthquakes. Preliminary results, summarized by M. J. Johnston, are:

- Precursive slip, seen most clearly before earthquakes of $M > 4$, dominates the earthquake process.
- Surface expression of aseismic slip (creep) does not appear to be associated with large-scale strain-field changes.
- Change in crustal stress fields, as inferred from magnetic measurements, can apparently have a scale exceeding several tens of kilometers.

W. D. Stuart devised a statistical technique for the computer recognition of precursory anomalies from telemetered tilt data from the San Andreas fault in northern California. Anomalies are characterized by abrupt changes of slope between two nearly linear tilt trends. If a simple theoretical model for the dependence of tilt-anomaly amplitude on earthquake distance, depth, and magnitude is assumed, analysis shows that about 80 percent of all suitably located earthquakes could have been anticipated. On the other hand, about half of the identified anomalies were false alarms.

Abrupt increases in local fault-creep rates were recorded at several creepmeter sites along the San Andreas fault between San Juan Bautista and Bear Valley, Calif., during a sequence of moderate earthquakes ($4.0 \leq M_L \leq 5.0$) lasting from December 1971 through January 1973. The onset times for increased creep rate at all but one site closely correspond to the time of the nearest moderate shock. The creepmeter records also seem to show a depressed creep rate for periods of several months to a few years prior to the moderate earthquakes, but this feature is difficult to prove because most of the continuous instrumental records are too short to cover anomaly onset times or to establish reliable, independent, long-term average rates. Comparisons of the short-term rates with values independently determined from measurements of older offset structures at Melendy Ranch (25 mm/yr) and the Almaden Cienega Winery (12.3 mm/yr), and at San Juan Bautista (12 mm/yr) demonstrate that the short-term results are reasonably consistent (20.8, 12.9, and 9.0 mm/yr, respectively). The close match (or lower instrumental rate) at three sites firmly supports the idea that the preearthquake creep rates were anomalously low, according to R. O. Burford. The longer winery record also clearly shows an onset of lowered creep rate 16± 1.5 months prior to the first shock in the sequence (December 29, 1971, $M_L = 4.0$, 8 km, southeast of winery at a depth of 6 km).

Tiltmeter, strainmeter, water-well and creepmeter records from a densely instrumented section of the San Andreas fault near the Almaden Cienega Winery, south of Hollister, Calif., at the times of several creep events were studied, and theoretical models were found that fit the observed data well. These studies, conducted by C. E. Mortensen, conclude that a relatively shallow propagating source best explains the observations.

Crustal stress

Stress measurements made in wells near the San Andreas fault in California and near Charleston, S. C., were reported by J. H. Healy and M. D. Zoback. The measurement in central California (50 km northwest along the San Andreas from Parkfield) shows the region to be subjected to high horizontal compressive stresses. The maximum compressive stress appears to be at an azimuth of N. 15° E. and the results imply that motion on northwest-trending thrust faults might be expected to occur at very shallow depths in the crust, that is, several hundred meters. The region in South Carolina appears to be under considerably less compressive stress. The maximum compression appears to occur at an azimuth of N. 51° E., relative extension occurring normal to that direction (the least horizontal stress is less than the overburden stress at 200 m). These results suggest the tendency for earthquakes in the area to be either of the strike-slip type on north-northeast- or east-southeast-striking faults or of the normal type on northeast-striking fault planes.

M. D. Zoback's theoretical analysis of hydraulic fracture growth showed the relative importance of the parameters controlling propagation. The analysis illustrates the importance of the value of the least principal stress, for example, in attempting to predict the necessary pressures, flow rates, and procedures used in field operations. The analysis also proved valuable in interpreting field data from both energy-stimulation hydraulic-fracturing operations and hydrofrac operations for determining in-situ stress.

W. S. Keys completed a preliminary study of hydraulic fracturing tests on the western side of the San Andreas fault near Pancho Rico, Calif. The acoustic televiewer was used to locate and determine the orientation of hydraulically induced and natural fractures in an attempt to determine the state of stress in this area. Hydraulic fracturing was only partly successful; thus, a statistically meaningful sample was not produced. The dip of induced fractures, however, was steeper than that of natural fractures, and the strike appeared to be random. In contrast, 93 natural fractures had a mean dip of 58.3°, with a standard deviation of only 1.64. Most of the natural fractures fell into two groups that dipped in opposite directions and were subparallel to the fault. The predominant dip direction was about S. 75° W.

Experimental results reported by M. D. Wood indicated, with exceptions, that a tilt signal associated with fracturing caused by mass transport at depths of at least 2 km can be detected at the surface. The azimuth and the extent of the fracture, as well as average velocity of fracture-tip propagation, were determined.

Crustal deformation

In southern California, an array of tiltmeters was installed near Tejon Pass, and the existing arrays along the San Gabriel and San Jacinto faults were extended to the east and the south. These new instruments may provide important data regarding the reported Palmdale uplift. Speculation concerning the origin and tectonic significance of the uplift continue.

Careful analysis by W. H. Prescott and J. C. Savage (1976) of the deformation of a triangulation network along the San Andreas fault near Palmdale, surveyed several times since 1932, suggested that the 200-mm uplift that occurred at Palmdale in 1961–62 was not accompanied by an anomalous strain accumulation. This result is supported by early geodimeter measurements made from 1959 to 1963. This evidence appears to be inconsistent with the 1961–62 thrusting episode postulated by W. R. Thatcher, who concluded on the basis of triangulation alone that unusual horizontal crustal deformation accompanied the development of the uplift. During this time, according to Thatcher (1976), compressive strains were oriented roughly normal to the San Andreas fault tending to lock it, the suggestion being that the uplift produced little, if any, shear-strain accumulation across this fault. On the other hand, orientation of the anomalous shear straining is consistent with strain accumulation across north-dipping range-front thrusts like the San Fernando fault. Thus, the uplift was interpreted as a short epoch of rapid strain accumulation on these frontal faults.

Although these geodetic data alone cannot be used to estimate when these accumulated strains will be relieved by earthquakes, observation of an unusual sequence of tilts prior to the 1971 San Fernando earthquake (M=6.4) offers some promise for precursor modeling. Data are adequately explained by a model of progressive updip propagation of aseismic slip toward the 1971 epicentral region. Both data and model suggest a viable geodetic precursor monitoring scheme which is now being implemented in the southern California uplift region.

Gravity measurements made before and after the destructive Guatemala earthquake of February 4, 1976, were used by R. C. Jachens to search for vertical deformation associated with the earthquake. Gravity measurements made in and around Guatemala, originally at various times between 1961 and 1972 were repeated during March 1976. Gravity increases on the order of 30 to 70 μGal were found at Sanarate, El Progresso, and Zacapa and along a closely spaced profile extending north from Zacapa. These sites all lie south of the Motagua fault, which displayed predominately left-lateral strike-slip movement during the earthquake and aftershock sequence (Plafker, 1976). Gravity at seven sites north of the fault and extending from about the longitude of Zacapa east to Puerto Barrios was found to have remained constant between 1969 and 1976. The gravity changes are interpreted as resulting from vertical displacement of tectonic origin rather than from fluctuations in the ground-water level or compaction of the alluvium. If the Bouguer relation between gravity change and elevation change of -2 μGal/cm is used, these results suggest that an area south of the Motagua fault about 100 km long and more than 10 km wide in some places was displaced downward by as much as 35 cm. The sense of the vertical deformation suggested by the gravity observations is in agreement with vertical displacements on the Motagua fault system during the past 40,000 years as deduced from studies of stream terraces (Schwartz, 1976). Repeat measurements at stations of the Latin American Primary Gravity Network in Guatemala and northern Honduras indicate that, with the possible exception of the station at Guatemala City, the network was not affected by the earthquake.

Ground-tilt data indicating that Fuego Volcano in Guatemala is inflating began in May 1975 and continued through 1975, according to D. H. Harlow. Along with intermittent periods of high-frequency tremor recorded on seismograph records, these data suggest that the volcano may erupt in the near future. Although it is not yet possible to predict the exact time or violence of an eruption, these data are important to future forecasting efforts and to a better understanding of the mechanics of eruptive processes.

Comparisons of precise leveling done on Middleton Island in the Gulf of Alaska in 1966, 1974, and 1975 indicate that, since the 1964 earthquake, the island has been tilting down to the northwest at a rate of 5.0+0.8 μrad/yr (Prescott and Lisowski, 1976). The direction of tilt is normal to the axis of the Aleutian Trench, 50 km to the southeast. The data are inadequate to determine if the rate has been constant since the earthquake. A simple model for slip on the near-surface projection of the fault surface that ruptured in 1964 suggests that on the order of 2.5m/yr of slip would be required to account for the observed tilt.

Crust and upper mantle structure

During the past year, refinements have been made in the inversion of *P*-arrival times and seismic-ray tracing. Initial results have been published (Aki and Lee, 1976; Engdahl and Lee, 1976). Various methods for generalized inversion were investigated, and the method of singular value decomposition proved to be extremely valuable in understanding the relationship between model and data spaces.

A seismic-refraction experiment conducted during July 1976 produced two 60-km-long reversed profiles centered on the aftershock region of the August 1, 1975, magnitude 5.9 Oroville, Calif., earthquake. One profile trends to the north-northwest parallel with the Sierra Nevada foothills greenstone belt. The other crosses the greenstone belt from the Great Valley on the south-southwest to the granitic terrane of the Sierra Nevada on the east-northeast. Preliminary analysis of the traveltime curves by M. A. Spieth indicate that the *P*-wave velocities of the crystalline basement in the greenstone belt are 6.0 km/s within about 0.3 km of the surface and increase to about 6.5 km/s at depths between 2 to 4 km.

Seismic and petrographic properties were determined by Louis Peselnick and R. M. Stewart for two Iherzolite xenoliths found in a basalt pipe cutting the Sierra Nevada batholith 1.5 km northwest of Big Creek in Fresno County, California. With respect to the batholith model of Bateman and Eaton (1967, fig. 4), these xenoliths would have originated at depths exceeding 45 km below sea level.

P velocities were determined as a function of pressure and temperature to 9kb and 260°C. Calculations show the xenoliths to have an anisotropy of 0.5 to 0.6 km/s at upper mantle pressure-temperature conditions under the Sierra Nevada. The maximum and minimum *P* velocities are 8.4 ± 0.1 and 7.85 ± 0.12 km/s. The observed seismic refraction P_n of 7.9 km/s (Bateman and Eaton, 1967) is nearly parallel to the long axis of the batholith, approximately in the same direction as the minimum V_p in the oceanic upper mantle off California (Raitt and others, 1969, 1969) and near Hawaii (Morris, Rait, and Shore, 1969). These results make it tempting to speculate that large-scale upper mantle anisotropy exists under the Sierra Nevada possibly as a consequence of the subduction of oceanic lithosphere during Mesozoic time (Hamilton, 1969).

The first study of the effects of a solid-state phase change on the creep properties of a rock-forming mineral was completed by S. H. Kirby. A dramatic difference in the activation energy for creep was detected in α- and β-quartz. The evidence suggests that the phase change affects creep rates through its effect on the rates of diffusion of water dissolved in the quartz structure. Since flow cannot occur under the conditions of these experiments without inpure water, these observations may provide the key to the water-weakening process.

Preliminary results of a study of crustal and upper mantle structure in the Mojave Desert and Transverse Ranges of California were summarized by G. S. Fuis:

- A relatively high intrinsic velocity of about 8.4 km/s is seen in the uppermost mantle beneath the central part of the Mojave network. Elsewhere in southern California, uppermost mantle velocities are around 7.8 km/s.
- A shallow "trough" is apparent on the Moho in the central part of the Mojave network. This trough plunges shallowly to the northwest. Crustal thicknesses vary from 20 km on the edges of the trough in the Imperial Valley and 26 km near the Colorado River, to over 30 km in the deepest part of the trough near Barstow, Calif.
- A "ridge" of relatively high velocity (8.3 km/s) material was discovered in the upper mantle in the vicinity of the Transverse Ranges. This ridge is overlain by lower velocity (7.8 km/s) material. It trends east-northeast and underlies the San Gabriel Mountains and the desert ranges north of the San Bernardino Mountains. It crosses the deep projection of the San Andreas fault without significant offset (Hadley and Kanamori, 1976).

A portable cassette recording system with memory designed by J. R. Van Schaack is capable of recording up to 10 seismic refraction shots at predetermined times. The system will automatically turn on, calibrate itself, and record for a period of up to 16 minutes at each preselected recording time.

Seismicity

Earthquake swarms are common in areas of recent volcanism and geothermal activity. A model by D. P. Hill that may apply to many such areas consists of the following concepts: (1) Clusters of magma-filled dikes exist within brittle volumes of the crust, (2) dikes within a cluster are systematically oriented with their long dimension in the direction of the greatest principal regional stress, and (3) a sequence of shear failures (an earthquake swarm) occur along a system of conjugate fault planes joining enhelon offset dike tips at oblique angles. This model accounts for commonly observed geometric relationships between surface faulting patterns and the distribution and focal mechanisms of events in many swarm sequences. If this model is correct, it suggests that heat sources for geothermal reservoirs in volcanic regions may be magma-filled dikes within volumes defined by the hypocentral distribution of earthquakes in a swarm sequence.

A "first-generation" totally automatic computer-based system for recognizing and locating earthquakes within 100-sensor seismic network in central California is operational. During the past year, a "second-generation" earthquake recognition algorithm was developed and tested by R. V. Allen. This algorithm presently analyzes one seismic trace. It has been tested extensively with recorded data consisting of earthquake swarms, aftershock sequences, and data from very noisy stations. It correctly recognizes, times, and analyzes 60 to 80 percent of the events normally timed by hand methods in routine operation of the central California seismic network. This algorithm is less prone to make "false picks" than the algorithm currently in operational use.

The center for the reduction of earthquake hazards in Nicaragua has been operating for almost 2 years, according to D. H. Harlow. Early results led to the identification of several active faults in western Nicaragua that are potential sources of large earthquakes similar to the earthquake that destroyed Managua, Nicaragua, on December 23, 1972. Results from data collected during the last year show that these zones continue to be seismically active, but the level of activity at specific zones often varies with time. The shallow seismic activity west of San Cristobal Volcano decreased from the high level observed during 1975. In the vicinity of Concepcion Volcano, however, shallow seismic activity increased from an occasional earthquake to from 3 to 25 events per day. This activity began in late September 1975 and was continuing 3 months later at the end of December. During the last week of December 1976 and the first week of January 1977, three minor felt earthquakes were located in and near Managua. These events, which had a magnitude of roughly 3, were the first felt earthquakes since the aftershock activity following the Managua earthquake died down in early 1974. The earthquakes occurred as single events with no recorded aftershock, and each appears to be located on a different fault in the highly faulted zone that characterizes the geologic setting of Managua. Thus, these results are leading to a better understanding of the location and occurrence of shallow seismic activity in western Nicaragua.

The six-station seismic network near Guatemala City was installed 11 months before the Guatemalan earthquake of February 4, 1976. Results from this net show that only 11 percent of all regional earthquakes could have originated on the Motagua fault. These results are consistent with seismicity determined with a single low-gain seismograph in Guatemala during the preceding 30 years. The majority of regional earthquakes occur on the Benioff zone that dips northeastward beneath Guatemala. Thus, the seismic zone that produced the most destructive earthquake in the recent history of Guatemala has exhibited a level of seismicity over the last 30 years that is lower than the prominent seismic activity that occurs on the deep seismic zone (Harlow, 1976). The six-station seismic network is located approximately 25 km south of the western terminus of observed fault displacement on the Motagua fault. Observed secondary faulting occurs inside the net, which is roughly coincident with the region of highest damage and casualties. The 30-km distance between the secondary faulting and the main fault is the longest ever documented for secondary faults associated with strike-slip faulting and, therefore, is of considerable scientific interest (Plafker, Bonilla, and Bonis, 1976). Preliminary results from more than 700 aftershocks suggest that an 1,800-km^2 area of the Guatemalan highlands west of Guatemala City is almost completely fractured by a series of separate and interconnected faults. These results support theories that this section of the crust is being torn apart by normal faults as a result of the prevailing strike-slip motion along the Motagua fault (Plafker, 1976).

EARTHQUAKE HAZARDS STUDIES

Fault activity and earthquake hazards

Diverse geologic investigations including field studies of stratigraphy and structure, studies of scarp morphology, exploratory trenches, and interpretation of aerial photographs—and the integration of these studies with the results of geophysical studies—have delineated active and potentially active faults and zones of faulting in many areas of the United States and have led to increased understanding of crustal deformation in areas of previously known active faulting.

E. J. Helley and D. G. Herd, in an analysis of faulted topography in the San Francisco Bay region of California, found evidence for several previously unrecognized active faults and reported that the pattern of deformation in some known fault zones (such as the Rogers Creek and Maacama faults) are more complex than previous mapping suggests. Major northwest-trending faults in the bay region are connected by north-trending, right-stepping en-echelon zones of subsidiary faulting.

According to M. M. Clark, normal faults in Quaternary alluvium within the Coachella Valley in southern California are probably related to movement on the nearby San Andreas fault. Clark found hundreds of closely spaced faults with lengths as great as 1 km and with scarp heights ranging from less than 1 dm to more than 10 m. The faults most commonly offset previously undisturbed alluvium and have no consistent topographic displacement. Among the older subdued scarps observed by Clark are some with rejuvenated segments less than 1 m high at their bases. Multiple episodes of activity are also shown by progressively larger displacements in deposits of increasingly older ages adjacent to some faults. Displacements of young channel deposits demonstrate that some of these movements are of Holocene age. Orientation of the faults indicates east-west extension and north-south compression; these stresses are compatible with right-lateral displacements in the San Andreas fault zone, which passes within 5 km of the scarps.

Mapping by R. V. Sharp in the Imperial Valley of southern California delineated several fault segments of Holocene age. Sharp believed these previously unrecognized scarps, whose left-stepping en-echelon pattern indicates right lateral movements on a fault at depth, to be on a southward-curving active extension of the San Andreas fault. This inference is supported by coincident earthquake epicenters and appropriate measurements of crustal strain. The crustal model proposed by Sharp has the San Andreas fault curving in the area north of the Salton Sea and joining with the Imperial or Brawley fault zones in the central part of the valley.

Sharp also found that surface fractures resulting from 1975 movement along the Brawley fault zone coincide closely with a zone of preexisting fault features of Holocene age. Aerial photographs taken in 1937 by the U.S. Department of Agriculture recorded these features; much of this evidence, however, has since been obliterated by agricultural activity. Several separate strands within the Brawley fault zone moved at the surface in 1975 in a left-stepping en-echelon pattern. The preexisting scarps noted by Sharp indicate that movement has been occurring on a fault at depth with right-lateral displacement. The scarps are tectonic in origin and are not the result of shaking or compaction in alluvium.

The lowest of the emergent marine terraces found along the west coast of the United States were generally formed during the last major (Sangamon) interglacial epoch, but dating of terrace remnants by K. R. Lajoie and several coworkers indicated that they may not be closely equivalent in absolute age. Oxygen isotope analysis and an experimental dating method based on changes through time in the structure of fossil amino acid were used by Lajoie, who found these remnants to range from 125,000 to 85,000 years old. Variations in the ratio of oxygen isotopes may result in part from a general cooling trend during the Sangamon. Differences in the rates of regional tectonic deformation presumably account for much of the disparity seen in the times of terrace emergence, but other factors such as crustal uplift in the Puget Sound region of Washington caused by the unloading of glacial ice had lesser effects on terrace deformation. Older, higher Pleistocene terrace remnants were found to record a longer deformational history generally consistent with that of Sangamon to recent time.

Regional mapping by R. C. Bucknam in northwestern Utah showed that fault scarps postdating probable upper Pleistocene alluvial deposits occur along the eastern side of the Wasatch Plateau in Joes Valley, which is east of the generally accepted margin of active normal faulting in the Basin and Range province. Several of the scarps display evidence of recurrent movement.

Investigations conducted in the Rio Grande rift zone of central New Mexico by E. H. Baltz showed that the tilting of large fault blocks and the uplift of marginal mountain ranges have been important mechanisms in the late Cenozoic deformation of the central portion of the rift. Baltz observed stratigraphic evidence of fault recurrence at two localities near Albuquerque and reported that cumulative vertical displacements of as much as 80 m have occurred on several major fault zones during the last million years. The tectonic processes that produce these features are presumed to be still operating in the region; fault displacements and earthquakes can occur throughout the area of the rift, even in those parts where historic seismicity is low.

Recent seismic activity in the Helena region of Montana, including two magnitude 6 earthquakes in 1935, has probably occurred along a normal fault that R. G. Schmidt traced for 30 km across the region. Vertical displacements of bedrock along the fault northwest of Helena are as large as 2,000 m. Another short segment of comparable fault displacements is recognized to the southeast of Helena, and Schmidt inferred that the two segments are part of a single structure that is largely covered by Cenozoic deposits near the city.

A fault scarp along the base of the Lost River Range north of Mackay, Idaho, probably resulted in part from movements within the last several thousand years. W. E. Scott and M. H. Hait, Jr., investigated stratigraphic relationships along the zone of faulting and in trench exposures across the fault. Moraines and outwash fans deposited during the last major glacial advance in the region (Pinedalian) were offset by faulting after soil profiles had developed on them in Holocene time. Exploratory trenches exposed volcanic ash in the fill of a graben along the fault, and this ash may have been derived from the explosive eruption of Mount Mazama in Oregon about 6,600 years ago. Scott and Hait suggested that a single seismic event during the last few thousand years produced scarps as high as 3m on the 35-km long zone that they studied.

Two zones of faulting that are perhaps only several hundred years old were discovered by L. D. Cress in the Curlew Valley of Idaho. One zone is evidenced by about 18 km of intermittently exposed scarps on a northeastern trend between Holbrook and Stone. Pleistocene deposits of Lake Bonneville have been downdropped along this zone as much as 24 m during the last 25,000 years. A second shorter zone of northwest-trending faulting was traced for a short distance north of the town of Holbrook. Faulting in this zone also offset Lake Bonneville sediments. Shorelines of the Provo high lake stand are tilted toward the center of Curlew Valley near the surface ruptures. Earthquakes in 1973, 1975, and 1976 were alined along the longer of the two zones.

R. P. Holcomb's surveys of Pleistocene and Holocene basaltic lava ponds in the central Snake River Plain of Idaho demonstrated that some older ponds have been tilted since they were formed; this discovery indicates that the plain has been warped in recent geologic time and suggests that it may be undergoing continued warping despite a low level of present seismicity. The pattern of warping may be related to other structural features. For example, ponded lava in the vicinity of the Great Rift National Landmark is tilted toward the rift by amounts that can be correlated with the age of the lava. The Great Rift thus appears to have been an active feature through much of Quaternary time.

M. F. Kane and T. G. Hildenbrand compiled simple Bouguer gravity and total-field aeromagnetic maps for the northern Mississippi embayment that reveal several similarly shaped anomalies ranging up to 37mGal and 1,200 gammas, respectively, associated with shallow mafic or ultramafic plutons. Spectral analysis of both gravity and magnetic anomalies indicates that these intrusive bodies are dense and highly magnetic, possess a complex shape, and extend laterally for appreciable distances. Earthquakes in this region of moderate seismicity are concentrated between the plutons, and, in one instance, an arcuate pattern of seismicity extends around an edge of one of the plutons. The pattern of seismicity strongly suggests that the plutons influence the state of stress in the northern Mississippi embayment. A model is suggested whereby stress is concentrated near the margins of plutons in much the same way that stress concentrations occur near the margins of defects or holes in plates under stress.

A synthesis of existing geodetic data made by R. O. Castle documented episodic and apparently aseismic uplift in southern California that began about 1960 and has since spread eastward from the intersection of the Garlock and San Andreas faults to at least Cajon Pass and Barstow. The uplift above the 0.15-m contour occupies an area of at least 12,000 km^2.

Earthquake studies in Guatemala

The Guatemalan earthquake of February 4, 1976, had a magnitude of 7.5 and was felt over an area of at least 100,000 km^2. The earthquake was generated by left-lateral displacement on the Motagua fault and was accompanied by displacements on other subsidiary faults. At least 23,000 people were killed; more than 77,000 were injured. Numerous landslides disrupted communication lines and added to the damage caused by seismic shaking. A preliminary estimate of material losses was about $1,100 million. USGS Professional paper 1002, edited by A. F. Espinosa (USGS) (1976), contains 10 papers describing the tectonic setting and seismicity of Guatemala, the mechanism of faulting, aftershock activity, surface faulting, landsliding, intensity of shaking, casualties and damage, and engineering implications for future design and construction.

According to R. V. Sharp, R. C. Bucknam, and George Plafker (USGS), surface displacements occurred along at least 230 km of the Motagua fault during the earthquake of February 4, 1976. Aftershocks were distributed along about 300 km of the fault length. The nearly east-west trace of surface rupture was smoothly linear and displayed only a few irregularities and en-echelon discontinuities. Left-lateral components of slip were as large as 340 cm. The largest displacement was about 40 km from the western end of the surface ruptures and about 170 km west of the main shock epicenter. The average lateral component of slip was about 108 cm. The largest vertical component of displacement was about 37 cm; the sense of this displacement was inconsistant along the trace of surface rupture. Additional displacements following those of the main event were documented at four localities near the middle of the surface rupture. As much as 20 percent of the total displacement was the result of this afterslip. Artificial exposures revealed that en-echelon surface cracks merged at shallow depths into nearly planar slip surfaces and that these surfaces had sustained movements in previous faulting events. Further work by Bucknam showed that afterslip continued for at least 9 months following the main earthquake and that it locally accounts for nearly half of the total surface displacement.

Secondary faulting as far as 35 km from the Motagua fault was discovered by M. G. Bonilla (USGS), S. B. Bonis (Instituto Geografico Nacional), and S. C. Widhelm (Department of Geology, Stanford University). This faulting apparently also produced earthquakes, at least one of which was large enough to cause damage. Scarps, displaced bedding, and other evidence indicates that the secondary movements occurred on preexisting faults, and seismic records show that small earthquakes were occurring on or near these faults prior to the earthquake of February 4, 1976.

More than 10,000 seismically induced slope failures occurred during the Guatemala earthquake, according to E. L. Harp and G. F. Wieczorek, (USGS). Most landslide masses had small volumes (less than 15,000 m^3) and occurred in Pleistocene pumice deposits. The location and morphology of the landslides were largely controlled by preexisting fractures in the deposits. Tensional spalling where seismic waves were reflected at free faces on steep canyon walls is believed to have been the manner by which the landslides were generated. Older landslide masses remained relatively stable during the earthquake.

Earthquake damage maps were prepared for Guatemala City by Raul Husid (USGS) as an initial step toward the seismic zonation of the city.

Seismic network studies

An examination of hypocentral data from the USGS seismographic network in south-central Alaska by J. C. Lahr revealed an interesting contrast in the distribution of earthquakes throughout the region. A pattern of uniform temporal and spatial seismicity in the Cook Inlet area grades into episodic activity in the Prince William Sound area. The entire region is underlain by a Benioff zone that marks the boundary between the American plate and the subducted Pacific plate. In the east, beneath Prince William Sound, where the westward dip of the Benioff zone is shallow and the American plate lithosphere and the Pacific plate lithosphere are in extensive contact, classical main shock-aftershock earthquake sequences are found, particularly in the upper plate. In the west, where the dip of the Benioff zone steepens and the Pacific lithosphere plunges into the asthenosphere beneath Cook Inlet, earthquakes with magnitudes up to 6 have occurred with no evidence of aftershock activity. Shallow seismic activity, which is quite high in the east, dies out to the west except for occasional swarms of earthquakes related to the active volcanoes on the western side of Cook Inlet. This contrast in seismicity may reflect the difference between stress accumulation and release in the shallow, rigid lithosphere caused by plate motion and stresses caused by the changing thermal regime within the plunging lithospheric slab.

Since September 1974, the USGS has monitored seismic activity along the Gulf of Alaska region from Cordova to Yakutat Bay. According to Lahr, very difficult environmental factors—including the very rugged Chugach Mountain terrain, the vast ice-covered areas of the Bering and Malaspina Glaciers, extremely heavy coastal snowfall, low temperatures, and high winds—made continuous year-round recording of seismic data next to impossible. However, new techniques have been developed each year to combat these problems. Seismic activity has continued to be most notable along the Chugach Mountains between Cordova and Yakutat, marked concentrations occurring in the vicinity of Mount St. Elias and Mount Steller. There has also been substantial activity around the Icy Bay area.

The most important finding that has emerged from the South Carolina seismographic network is that seismicity in the State appears to be concentrated in discrete source areas rather than distributed over a linear zone, as had previously been hypothesized. The most important of these areas, according to A. C. Tarr, is northwest of Charleston near Middleton Place and is probably the source of earthquakes that have been felt persistently in Summerville since the Charleston earthquake of 1886. The largest and best-located shocks are about 7 to 14 km deep, almost directly below Middleton Place. The fault-plane solution for one of the Middleton Place events suggests that the crust in the source area is undergoing compression in a northeastern to southwestern direction.

Tarr's analysis of seismic data recorded by the Puerto Rican seismographic network since November 1975 confirmed several earlier findings: (1) Seismic activity on the Puerto Rico-Virgin Islands platform is characterized by numerous, small, crustal earthquakes that are not as yet obviously correlated with mapped faults; and (2) activity around the platform is characterized by larger shocks that can be associated with physiographic features such as the Mona Canyon and offsets in bathymetric contours of the south wall of the Puerto Rico trench. An inclined seismic zone under Puerto Rico dips approximately 45° to the south from the Puerto Rico Trench.

Recent work by A. M. Rogers showed a diffuse and low level of seismicity in the Central Basin Platform in Texas. During the 1-year monitoring period, about 100 events were detected, and 30 were located. The largest events were three felt earthquakes of about magnitude 3.7 or less. A swarm of about 70 events occurred in April and May of 1976. Events are occurring both within and outside the net. The area of seismicity appears much broader than was suspected originally.

Ground-motion investigations

The general theory of viscoelasticity predicts that the physical characteristics of seismic waves transmitted across a soil-soil, a soil-bedrock, or a crust-mantle boundary differ significantly from those that have been considered previously in the seismological literature. Numerical results obtained by R. D. Borcherdt suggested that the new set of physical characteristics must be taken into account to explain seismic observations in soils. For teleseismic experiments, the numerical results suggest that the differences in velocity, attenuation, and energy flux are of sufficient magnitude only for measuring rays near critical and wide-angle reflections in field experiments.

R. M. Hazlewood completed a seismic refraction study to determine the depth and the configuration of the bedrock surface in the southern San Francisco Bay region of California. The data from 85 reversed profiles ranging in length from 800 to 2,400 m. were compiled on a "green-line" base and published at a scale of 1:62,500. The configuration of the bedrock surface was shown to be considerably different from what had been inferred from gravity data. The data were used to question the existence of the Palo Alto fault and the northern extension of the Silver Creek fault inferred from gravity data. The data provide a new basis for geologic interpretations and seismic hazard evaluations in the region.

An investigation of seismic velocities in the San Francisco Bay region was conducted by J. F. Gibbs, T. E. Fumal, and R. D. Borcherdt. Seismic velocity and geologic logs were measured at 59 sites. At each site, seismic traveltimes were determined at 2.5 intervals in drill holes to a depth of 30 m. Geologic logs were compiled for each site from drill hole cuttings, undisturbed samples, and penetrometer samples. Soil units found to have distinctly different seismic velocities were silty clay-clay (< 4 blows/ft), silty clay-clay (4 to 20 blows/ft), silty clay-clay (> 20 blows/ft), sandy clay-silts, sands (< 40 blows/ft), sand (> 40 blows/ft), and gravels. Seismically distinct rock units were found to be igneous-sedimentary (hard, close to very close fracture spacing), sedimentary (hard to firm, moderate, wider fracture spacing), and igneous (hard, close to moderate fracture spacing). These correlations provide an improved data base for seismic zonation of the San Francisco Bay region and a data base for extrapolation of results to other metropolitan areas with significant earthquake hazards.

R. D. Nason used new understanding of seismic intensities to evaluate the strength of seismic shaking in the 1906 San Francisco earthquake at more than 200 localities on the basis of detailed published descriptions. It appears that the strength of the seismic shaking was the same adjacent to the fault as it was at distances of up to 30 km. The most intense shaking occurred at Fort Bragg, 11 km from the fault. The shaking caused damage as much as 65 km from the fault. The pattern shows that the decrease of shaking intensity with distance from the fault was less then investigators had thought previously and that there was no concentration of shaking adjacent to the fault.

A. F. Espinosa, Raul Husid, and S. T. Algermissen studied the intensity distribution of the October 3, 1974, earthquake in Lima, Peru. Modified Mercalli intensity questionnaires gathered in the field were used to rate the intensity in metropolitan Lima. This study revealed an intensity amplification in the La Molina, Barranco, and La Campina districts and in a very localized area in downtown Lima. An isoseismal map showing areas in Lima that experienced Mercallie intensity V through XI was constructed.

W. W. Hays studied ground-motion data from a nuclear explosion recorded on a 20-station seismic array deployed in the Salt Lake Valley area of Utah. The seismic stations were located on rock in the adjacent mountains and on various types of surficial soil in the valley. Preliminary analysis of the data indicates that there is a significant difference in the levels of ground response. The stations located on soil exhibited levels of ground motion much higher than those of stations located on rock.

Eight nuclear events from the Nevada Test Site were recorded at 53 stations in Los Angeles Basin by using a three-component wide-band seismograph. Data gathered by A. M. Rogers showed that (1) ground response was higher on Holocene soils than it was on Pleistocene soils, (spectral ratios relative to rock of 4.1 and 1.9, respectively); (2) response on clay-silt soils tended to be higher than that on sandy soils; and (3) response was higher on soils with high void ratios. Comparison of ground-motion-response ratios for these nuclear events and for earthquakes at three stations indicated the nuclear ratios are 30 to 50 percent higher than the earthquake ratios. The response to nuclear explosions observed in Compton was higher than that observed in Long Beach and correlates well with S. H. Wood's observations of damage done to the two areas during a 1933 earthquake.

Analysis of seismic risk

S. T. Algermissen and D. M. Perkins prepared a preliminary probabilistic map of ground accelerations in rock associated with earthquake activity in the contiguous United States. This map indicates that maximum accelerations (about 0.8 g in rock) in the most seismically active areas of California are about 8 times as great as those estimated for the more active seismic areas of the eastern United States (about 0.1 g in rock) for a 50-year exposure time at the 90-percent probability level. This map is being used as input by the Applied Technology Council for the preparation of new model earthquake-resistant design provisions for building codes.

R. K. McGuire examined a method for estimating seismic risk that accounts for the uncertainties in seismicity and defines seismic source areas. Using this method to establish design intensities avoids the sensitivity of deterministic methods to the seismotectonic provinces embraced and to the seismic history observed. The results obtained by using this method are sensitive to the largest event that is assumed possible. The seismic history available for the United States is not adequate to establish this event on a statistical basis; thus, the importance of geophysical and geological investigations for estimating maximum possible events emphasized.

ENGINEERING GEOLOGY

Research in geology related to tunneling

Maps of surface and near-surface geologic conditions of a 141-km^2 area of metropolitan Los Angeles, Calif., were prepared at a scale of 1:12,000 by R. F. Yerkes as an aid in determining the feasibility of constructing tunnels for a mass-transit subway system. The maps also show recently active faults, locations of epicenters of historic earthquakes, depth to and configuration of the buried bedrock surface, depth to the ground-water table, and the locations of about 900 wells and boreholes for which subsurface information is available. Geologic structure sections along possible tunnel alinements were prepared and described from the maps and the borehole data. The study emphasizes areas of difficult or hazardous tunneling conditions, and the poor quality, unreliability, and irregular distribution of existing subsurface data on geotechnical-hydrologic properties, particularly the distribution of near-surface boulders and various petroleum deposits.

Maps showing the hydrostatic head of water in relation to the top of the St. Peter Sandstone in the Minneapolis-St. Paul area of Minnesota prepared by R. F. Norvitch and E. L. Madsen. These maps are useful in determining the feasibility of possible tunnel alinements in the Twin Cities metropolitan area, particularly in regard to the need for dewatering procedures, the amount of water that might be encountered, and the possibility of water under artesian pressure conditions.

Research in soils engineering

Liquefaction-induced ground failures that occur during earthquakes are confined to specific geologic settings, according to investigations made by T. L. Youd and S. M. Hoose. An analysis of published earthquake reports indicates that shallow, saturated, Holocene fluvial, deltaic, and eolian deposits and poorly compacted artificial sand fills have the highest susceptibilities to liquefaction and ground failure; somewhat smaller susceptibilities are present in Holocene alluvial-fan, alluvial-plain, beach, terrace, and playa deposits. Pleistocene sand deposits are generally even less susceptible, and glacial till, clay-rich, and pre-Pleistocene deposits are usually immune to liquefaction. The studies also show that there is a maximum distance beyond which liquefaction is not likely to occur for an earthquake of a given magnitude. This distance ranges from essentially zero for magnitudes less than 5 (no liquefaction) to epicentral distances as great as 500 km for magnitudes greater than 8.

On the basis of data gathered from eight borings in the southern San Francisco Bay shore area of California, R. C. Wilson determined that each of the three Quaternary formations—bay mud, Holocene alluvium, and Pleistocene alluvium—has a characteristic set of ASTM soil types, geotechnical properties, and seismic velocities (measured by R. E. Warrick). The bay mud consists of soft, normally consolidated estuarine elastic silts (MH) and fat clays (CH) with an average shear wave velocity of 80 m/s. The Holocene alluvium consists of well-graded sands (SW) and gravels (GW) deposited in alluvial fans, interbedded with poorly graded fluvial channel sands (SP) and stiff, over-consolidated, nonplastic silts (ML) and lean clays (CL) deposited on flood plains between fans with an average shear-wave velocity of 280 m/s. The Pleistocene alluvium is also composed of well-graded sands and gravels from alluvial fans but has a higher degree of consolidation than the Holocene fan deposits, and a higher shear-wave velocity of 550 m/s. These findings will assist in defining mappable ground-response units for seismic zonation.

Research in slope stability

A detailed seismic study of a landslide in the Wasatch Formation 16 km south of Sheridan, Wyo., by C. H. Miller, A. F. Chleborad, and W. F. Ebaugh, indicated that the slide may be part of a zone of weathered material common throughout the Sheridan-Buffalo area. Preliminary analyses of core samples from the landslide indicates that the failure zone, which is less than 7 m deep, involves both weathered bedrock and colluvium consisting of variable amounts of clay and silt with a few thin beds of sand and carbonaceous shale. The change from disturbed to undisturbed material that occurs at the base of the weathered zone also is marked by a change in the natural moisture content, from generally above the plastic limit to generally below, and by an increase in soil shear strength as determined by pocket penetrometer tests. The weathered and disturbed zone has low seismic velocity and a shear strength 5 to 10 times less than that of the underlying layer as determined by seismic measurements.

Factors that influence the stability of highwalls in open-pit mines in the western Powder River basin include rebound of overconsolidated rocks, desiccation, pore-water pressure, orientation and spacing of fractures, and strength and deformation properties of the rocks and coals. Many of these factors and properties were included in finite-element and limit-equilibrium analyses of stability of a typical highwall in the study area by W. Z. Savage, W. K. Smith, and F. T. Lee. Safety factors calculated by these methods are less than 1.0 when the highwall has been degraded by fracturing associated with desiccation and rebound of overconsolidated rocks. Because of the time dependent nature of these degradation processes, postmining failures are common and can be critical if mining is delayed, and then resumed after a period of several months. Such time-dependent instability of final highwalls should be one of the parameters considered in the reclamation of strip-mined lands.

Research in geologic hazards

Approximately 900 physical-property tests were performed by E. E. McGregor on 250 core samples from the Fort Union Formation in the field at the Recluse Model Study Site in Wyoming, and the Bear Creek Study Site in Montana. With only a few exceptions, index tests indicate that compressive and tensile strengths of the rock samples are low. Some of the rocks were so weak that they could not be tested as rocks and had to be considered as soils. These data and the physical properties data, such as Atterberg limits and gradation (grain-size distribution), suggest the need for careful design of coal-mining operations to assure stability in slopes, open-mine faces, and open-pit floors.

The Wasatch Formation underlying Buffalo, Wyo., was cored to a depth of 133 m, and various physical property tests were performed on the core samples under the direction of R. A. Farrow. Results of testing show the coal to be the most competent material present. Sandstones and claystones, even at depth, are weakly indurated and almost without cohesive strength. Artesian flow from the weak sandstone near the surface may cause serious stability problems for highwalls in open-pit mines that may be opened in the unit, and, in addition, loss of artesian pressure might affect the flow from local domestic water wells.

Initial engineering geologic mapping and sampling in and near Buffalo, Wyo., by H. E. Simpson and Ernest Dobrovolny indicated that geologic hazards in that area probably consist of (1) stream flooding caused by cloudbursts, (2) surface subsidence related to a pre-1912 underground coal mine, and (3) local landsliding along the right (southern) valley wall of Clear Creek.

Magnetic, gravity, electromagnetic, and seismic surveys were carried out over abandoned underground coal mines in the Sheridan, Wyo., and Bighorn, Mont., areas of the Powder River basin by C. H. Miller and F. W. Osterwald to test the feasibility of locating the mine workings from the surface. The seismic method may help to delineate abandoned openings in detail, whereas the other three methods show only apparent trends.

Research in field measurement techniques

A new technique developed by W. F. Ebaugh, H. W. Olsen, and J. B. Bennetti, Jr., reduced unwanted voids in annular sand packs surrounding inclinometer casings installed in boreholes. The technique involves generating a quick condition in the annulus sand owing to upward water seepage. Simple end fittings direct water down the inside of the casing, out at the bottom in an upward direction, and through the annulus to the surface. Field experience indicates that shovel-placed annular sand packs decrease in volume by about 10 percent after becoming quick and that the inclinometer casing becomes firmly seated in the borehole.

LANDSLIDE HAZARDS

MISCELLANEOUS LANDSLIDE INVESTIGATIONS

Landslide in Manti Canyon, Utah

A large landslide located in an area of extensive inactive landslide deposits in Manti Canyon, Utah, was being studied by R. L. Schuster, R. B. Johnson, Fred Taylor, and R. W. Fleming (USGS), and E. P. Olson (U.S. Forest Service). Initial movement in the landslide resulted from a rockslide at the crown, which reactivated rapid movement in 15 million m^3 of landslide debris. The landslide disrupted the Manti water-supply pipeline, forced the shutdown of a small hydroelectric plant, and supplied excessive amounts of silt to irrigation ditches and irrigated fields. Although the landslide occurred 6 km from the nearest permanent dwellings, it caused more than $2 million in damages.

Environmental study of the Big Fork-Avon area of Montana

Timber cutting on both Federal and private lands is one of the major industries in the Big Fork-Avon area of Montana. Landslides along access roads in this area were studied by I. J. Witkind. Virtually all of these roads were constructed, in part, across a thick layer of till. Because the topography is steep, most of the roads cling to hillsides. The inner edge (cut slope) of the road is flanked by a till wall, and the outer edge (sill slope) drops off into a till valley. During dry periods, the till is firm and stable and causes no problems. But when it is wet, the till becomes unstable and tends to slide. Although a few of the landslides are large enough to take out a section of a road, most are small and probably do not exceed 10 m^3 in volume. The small landslides commonly block the drainage ditch along the cut slope of a road. Water accumulates behind the slide and, becuase it is unable to top the slide, eventually flows obliquely downslope across the road. In a very short time, the sill slope of the road begins to fray. If the small landslide blocking the ditch is not removed, the access road is broken, and all traffic is halted.

The small slides are more prevalent in some types of till than in others. As yet, however, it has not been possible to determine the physical characteristics of one till deposit that cause it to slide more readily than another.

REGIONAL SLOPE-STABILITY STUDIES

Large-scale gravitational spreading in Crested Butte area of Colorado

Crested Butte, a large, isolated laccolithic mountain in south-central Colorado, was examined in the field by D. H. Radbruch-Hall and D. J. Varnes. The butte, consisting of about 600 m of porphyry resting on Mancos Shale, is about 5×7 km in area and rises more than 1,000 m above the surrounding valleys. All of the sedimentary cover that once arched over the laccolith has been stripped away. The remaining porphyry mass contains several sets of joints, the most prominent of which is a set that trends northwestward, more or less along the longer axis of the laccolith, and dips to the southwest, very steeply in the western part and more gently in the eastern part. The whole mountain appears to have broken into slices and spread, owing to lateral flow of the underlying shale. Many of the differential movements took place on the principal joint set referred to above and resulted in numerous large ridges and trenches in the porphyry that trend parallel to the long axis of the mountain. The eastern flank of the mountain mass is broken by many uphill-facing scarps. The deformation resembles that at Dolores Peak in southwestern Colorado, which was studied last year.

The northern flank of Crested Butte has been under active development as a ski resort; extensive construction has been completed, and more is planned. Inasmuch as the lower flanks of the butte are mantled by almost continuous landslide debris from slumps and earthflows in the shale, the area has been studied by the Colorado State Geological Survey to evaluate the slope-stability hazard. The laccolith may still be spreading and squeezing shale out around its base, and this action may contribute to the active earthflows and slumps that have affected construction on the lower slopes.

A simplified elastic-plastic finite-element model was analyzed by W. Z. Savage to study the mechanics of the gravitational spreading exhibited by Dolores Peak and Crested Butte. A two-dimensional model consisting of a triangular mass of strong elastic-plastic material (porphyry) representing the laccolith on a base of weak elastic-plastic material representing shale was examined. An analysis was made of the stresses and displacements in the mass as it deformed under its own weight.

The analysis revealed large tensile stresses in the porphyry just above the contact with the shale, as well as large shear stresses along the contact. Both of these features were attributed to extension of the porphyry just above the contact with the shale. as well as large shear stresses along the contact. Both of these features were attributed to extension of the porphyry in response to lateral flow of the relatively

Large-scale gravitational spreading of mountain ridges in the Stillwater Complex of Montana

A very large area of gravitational slope deformation (sackung) in the Stillwater Complex of Montana was examined in the field by Kenneth Segerstrom, R. R. Carlson, and D. H. Radbruch-Hall. The Stillwater Complex is a well-known, basic, layered intrusive rock of Precambrian age, but the northern part of the complex has never been mapped in detail. The few sackung trenches that appear on existing maps are shown as faults.

At its northwestern end, the complex is exposed in a high northwest-trending ridge known as Contact Mountain. Here the layering strikes northwestward and is in general inclined toward the northeast. A steep slope more than 1,220 m high (the northeastern wall of the valley of the Boulder River) bounds the ridge on the southwest, and slopes nearly as high but less steep bound it on the northeast. The sackung features in the intrusive lie on the top and the southwestern side of the ridge. Most of the sackung features trend northwestward, in the same direction as a prominent joint system that is approximately parallel to the layering; this trend indicates that the gravitational movement took advantage of inherent weaknesses in the material underlying the slope. In other places, however, the scarps and trenches cut slightly across the layering, subparallel to slopes that cross the layering but approximately parallel to a lesser joint or minor fault system. It is, therefore, apparent that these features are not everywhere directly associated with the layering but use only the joints parallel to the layering, where its strike is parallel to a contour on the steep southwest-facing slope. The trenches are within a very large landslide, approximately 2 km from crest to toe and 3 km wide, that has moved off Contact Mountain southwestward into the valley of Boulder River. The movement extended to the back (northeastern side) of the ridge, and thus involved the crest; and so the uppermost scarp is on the northeastern side of the ridge, facing uphill toward the southwest. This scarp forms the northeastern boundary of a graben on top of the ridge.

The existence of a graben implies that the top of the ridge dropped down as the southwest-facing slope bulged out. As movement proceeded, reverse slippage took place along the major joint system that parallels the layering, the rock below the plane of slippage moving upward relative to the one above it and forming uphill-facing (or antislope) scarps on the mountainside. These scarps, with trenches behind them, are then also the lower walls of the joints and dip northeastward into the mountainside. The scarps do not extend beyond the lateral boundaries of the displaced mass, and there is no indication that they are tectonic in origin rather than gravitational.

The area has been glaciated, and postglacial landslides of all kinds are common throughout the Beartooth Mountains. The Contact Mountain landslide, in particular, with its associated sackung features, undoubtedly formed after glaciers that occupied the valley of Boulder River had retreated and left the oversteepened slope unsupported. Although the trenches are in bedrock, the ridges that bound them on the downhill side are capped in places by remnants of glacial till.

Types of slope failure characteristic of different topography

Tentative results from detailed field mapping in the Franciscan terrane of Marin County, California, by S. D. Ellen and others revealed marked contrasts between the types of slope failure characteristic of the extremely rugged topographic areas previously mapped from 1:80,000-scale aerial photographs. Steep terrane with regular sidehill drainages (hard topography) was characterized by debris flows generated from soil slips in granular colluvial soils. This type of movement is rapid and occurs suddenly, without warning, and thus poses hazards to life and property by impact. However, hazardous areas within hard topography are limited largely to canyon bottoms and fans at mouths of canyons, and the timing of these events can be predicted, at least crudely, by using measurements of rainfall intensity and saturation of surficial soils (Campbell, 1975). In contrast, gently sloping terrane with irregular or poorly developed sidehill drainages (soft topography) was characterized by shallow, slow-moving slumps and earthflows in clayey surficial materials. This type of failure is less regularly distributed within the soft topography, and poses hazard largely by relatively slow distortion of structures bearing on the sliding material. The timing of this type of movement is less predictable since it has an indirect relation to periods of rainfall.

Rocky Mountain landslide inventory

A preliminary inventory of landslides in the regional coal environmental impact study area, in the northern Powder River basin of southeastern Montana, was made by R. B. Colton during three flights between Billings and Broadus. Many small landslide areas that were observed were estimated to underlie less than 5 percent of the area.

Aerial reconnaissance revealed many large landslide and rockfall areas in and around the southern Utah coal fields. As a result of this preliminary inventory and an open-file compilation, it was estimated that less than 5 percent of the area west of the Hurricane fault zone is underlain by landslide and rockfall deposits. East of the Hurricane fault zone, as much as 15 percent of the area may be underlain by landslide deposits. Landslides are a major environmental problem in areas in the eastern half of the Cedar City 2° quadrangle, in the western half of the Escalante quadrangle, and in an arcuate belt 209 km long (the Book Cliffs) in the Price 2° quadrangle, where the coal-bearing Straight Cliffs Formation and Mesaverde Group are underlain by the Tropic Shale and the Mancos Shale, respectively.

Observations made during the November 1976 reconnaissance flights along the Hurricane fault zone and in the western part of the Price 2° quadrangle suggested that the great uplift east of the Hurricane and Wasatch fault zones and east and west of the Joes Valley fault zone produced conditions ideal for large-scale landsliding. It was postulated that earthquakes possibly might have triggered some of the landsliding observed along the fault zone.

Landslide investigation in northern Appalachians

Investigations of the incidence of and susceptibility to landsliding in the Valley and Ridge area of the northern Appalachian Mountains were conducted by W. E. Davies, R. L. Hackman, A. B. Olsen, P. J. Ruane, and G. C. Ohlmacher. The dominant form of slope failure was the debris avalanche. Areas highly susceptible to landsliding were identified where the dip slope of the rocks and the surface slope are of similar magnitude and direction. The landslide deposits are thin, generally less than 2 m thick, and consist of round stones ranging up to cobble size in a clay-silt or clay-sand matrix.

Debris avalanches in valleys generally seem to be multiple events having a spacing of 50 years or more between slides. Debris avalanches on other parts of mountain flanks were probably single events having a spacing of centuries. The difference in time generally reflects the rate of accumulation of weathered material. Evidence of old debris avalanches was common at the lower extremities of small, shallow, steep valleys, but evidence of old debris avalanches on other parts of mountains was difficult to identify. Debris avalanche areas are generally stable under normal precipitation but may be activated during periods of short-duration high-intensity rainfall.

REGIONAL GEOLOGIC HAZARDS THAT MAY AFFECT NUCLEAR REACTORS

Quaternary faults—Western United States

D. E. Marchand, D. E. Stuart-Alexander (USGS), and others made trench examinations along the complex Foothills fault zone east of the Sacramento Valley of California; together with the work of consultants, their examinations demonstrated displacements of upper Tertiary and some Quaternary units indicative of continuing late Cenozoic movements along the fault zone, a conclusion consistent with the slight surface rupture that accompanied the M=6 Oroville earthquake of August 1975.

In southern California, three fault zones with probable Quaternary displacement recognized by V. R. Todd and W. C. Hoggatt (USGS) suggested that at least the eastern third of the southern Santa Ana block is broken by faults that splay southward from the southern end of the right-lateral part of the Elsinore fault zone. The faults follow the metamorphic grain of the rocks and vertically displace sheeted plutonic complexes. At least some faults in each zone have young topographic expression and locally appear to cut colluvium. Additional faults cutting upper Quaternary sediments have been found along the southeastern trend of the Elsinore fault zone at the eastern margin of the Santa Ana block. These faults appear as short breaks with vertical displacement and are not throughgoing ruptures.

Study of aerial photographs and reconnaissance field checking in southern Mendocino County, California, by E. H. Pampeyan (USGS) revealed a zone of geomorphic features indicative of late Quaternary faulting. This zone is marked by sag ponds, closed depressions, linear scarps and ridges in Pleistocene(?) gravels, and stream channels that show right-lateral offset. The zone appears to extend discontinuously more than 65 km northwestward from south of Hopland at least as far as Willits. At its south end, this zone appears to join the previously mapped Maacama fault zone. Near Ukiah, midway between Hopland and Willits, E. C. Winterhalder (Harding-Lawson Assoc., Inc.) recognized, from previous site studies, ground-water barriers and fault gouge in Pleistocene (?) gravels, as well as scarps, sag ponds, and linear features in this same zone. Many of the geomorphic features noted in the reconnaissance study are as fresh looking as similar features in the San Andreas fault zone, the suggestion being that they may have been formed as recently as Holocene time. Further work will be necessary to verify the total extent, continuity, and origin of these geomorphic features.

In the Wenatchee region of Washington, R. B. Waitt, Jr. (USGS), found evidence for Quaternary movement on three east-trending faults in the northern Kititas Valley. These faults offset 3.7 million-year-old alluvium but do not affect alluvium correlated with the 0.13- to 0.14-million-year-old glaciation of the region. The faults are probably reverse, suggestive of north-south compression, and their southeastward en-echelon trend may reflect right-lateral strain on the Olympic-Wallowa lineament. To the north, in contrast, R. W. Tabor and Waitt (USGS) and J. T. Whetten (University of Washington) found no evidence for Quaternary faulting along the major Entiat and Leavenworth faults that bound the north-trending Chiwaukum graben. Some uncertainty remains about these faults, however, for a major earthquake may have occurred in the area in 1872. The youngest demonstrated offset on the Entiat fault is post-42 million years, and on the Leavenworth fault the offset is post-15 million years; 13,000-year-old glacial deposits are not offset by the Entiat fault.

The Gila Bend lineament, a feature of complex structural origin in Arizona, includes a 1.25-km-long scarp of probable fault origin, according to an aerial photograph study by Richard Van Horn.

Mapping and preliminary analysis by M. A. Kuntz suggest that basalt volcanism and extensional faulting have recurred at approximately 10,000-year intervals along the Arco rift zone in the Snake River Plain of Idaho. This 15-km-wide zone extends 50 km southeastward from the northern margin of the Snake River Plain at Arco to near Atomic City. It is the locus of extensional faults, graben, basalt volcanoes, and a rhyolite dome. The two youngest basalt flows are 10,500 and 12,000 C-14 years old, and at least 10 other flows are judged to be less than 50,000 years old. Flows near the northeastern end of the zone, estimated to be 40,000 ± 20,000 years old, are offset by many extensional faults that have as much as 8 m of vertical displacement. The Arco rift zone appears to be an extension of Basin and Range structure onto the Snake River Plain. Other rift zones on the Plain may have been formed the same way.

Cenozoic faults—Atlantic Coastal Plain

The four down-to-the-coast reverse faults of the Stafford fault zone that reach the coast in Virginia (Mixon and Newell, 1976) displace upland gravels of uncertain, possibly late Miocene and Pliocene age. As yet, no offsets have been found in Quaternary deposits. The zone has an aggregate vertical offset of 120 m, a length of at least 50 km, and is alined with some and parallel to other faulted Triassic and Jurassic basins and older structures.

Reconnaissance mapping in Virginia reveals no clear offset of the distinctive Eocene Marlboro Clay Member of the Nanjemoy Formation across the Brandywine structure (limit of recognition about 3 m), despite its similarities to the nearby Stafford fault zone. Quaternary structural control by the Brandywine structure is suggested by anomalous terrace heights, transition over the structure from fluvial to estuarine terrace sediments, and peculiar bends in the Rappahannock River.

A detailed multidisciplinary study of part of the Belair fault zone in northeastern Georgia invalidated preliminary conclusions (Prowell, O'Connor, and Rubin, 1975) of Holocene offset. Currently demonstrable offsets are Cretaceous to probable Tertiary, but the possibility of late Cenozoic movements is as yet unresolved.

Modern vertical movements—Eastern United States

Careful study by P. T. Lyttle and D. S. Wright of repeated first-order level surveys along 3,500 km of level lines in parts of nine States on the eastern seaboard indicated that, within the past 45 years, significant real vertical movements have occurred within the past 45 years. These movements are in the range of 1 to 5 mm/yr along 50- to 100-km. Separate profiles tend to show remarkable similarity within the same geomorphic or geologic province. Reversals in the direction of vertical movement are commonly indicated where several surveys have been repeated along a single line, and thus cyclic movement is suggested. Long-term extrapolation of the modern rates of vertical movement seems unreasonable because landforms do not corroborate differential vertical changes within 100 km that would be as much as 1 km/200,000 years; episodic and (or) cyclic movements therefore seem required.

Wright demonstrated a 17-cm error in the first-order Macon-Savannah survey line in Georgia run by the U.S. Coast and Geodetic Survey in 1917, which has served as a principal reference line for subsequent surveying in the region. Discovery of the error obviated the necessity of geologically evaluating this apparent modern offset that was on strike with a Cenozoic fault.

Uranium-series dating of caliche rinds

Study of faulted fan gravels north of the Idaho National Engineering Laboratory (previously the National Reactor Testing Station) by K. L. Pierce, together with an isotope geochemistry study by J. N. Rosholt, Jr., yielded promising results using a new application of uranium-series dating. The fan, a calcic soil with stratified caliche rinds on boulders, is cut by a fault with 12 m of total displacement. These caliche layers can be separated into three distinct units: outer (youngest), middle, and inner (oldest). Rosholt determined the uranium-series ages on the three stratigraphic units of the rinds by means of a new technique that accounts for detrital contamination by silicate soil particles. The outer rinds dated 17,500 ± 5,000 years; the middle dated 67,000 ± 10,000 years; and the inner dated 133,000 ± 30,000 years. These ages appear reasonable for they are consistent with independent controls on age. The following evidence provides controls for evaluating the dates: (1) The fan surface is on the order of 100,000 years old based on the age of the ash, and (2) the caliche layers should increase in age from outer layer to inner layer; the youngest layer is on the order of tens of thousands of years, for it is similar in appearance and thickness to rinds on nearby glacial outwash.

Amino-acid dating of Quaternary fossils

Relative and absolute dating of late Quaternary fossils from amino-acid enantiomeric ratios is feasible and geologically practical, according to work by K. R. Lajoie (USGS) and J. F. Wehmiller (University of Delaware). The technique is extremely useful for correlation purposes and provides reliable age estimates back to about one million years. Systematic generic effects on the observed rates of racemization do exist, an observation previously made only for foraminifera from deep-sea sediments. Of six molluscan genera studied in detail from 10 localities along the west coast, *Protothaca, Saxidomus,* and *Tivela* seem to form a slow group; *Macoma, Tegula,* and *Epilucina* form a faster group in which the enantiomeric ratios are 30 to 50 percent greater. Geologic results of this work include recognition of marine terraces of post-Sangamon age at Goleta, Calif., and Cape Blanco, Ore. Apparent amino-acid ages of selected mollusks from these localities are about 30,000 to 40,000 years and suggest that previous young radiometric dates (C-14 and Th-230) are valid and that terraces younger than the predominant low Sangamon terraces do exist along the west coast.

Soil development and age—California Great Valley

Several field and laboratory parameters were demonstrated to be potentially useful indices of soil age by D. E. Marchand and J. W. Harden. Many field soil parameters such as Munsell hue and chroma, pH, and horizon thickness correlate very well with time. Laboratory data useful as age indices include free-iron oxides, clay, calcium carbonate, bulk density, base saturation, organic carbon, carbon-nitrogen ratios, cation exchange capacity, conductivity, and sodium; the first six variables listed are much more valuable indicators than the last four. Most parameters, when they are plotted against linear time, yield curves that show a rapid initial increase for about 20,000 years; a more gradual increase with time follows, and finally a constant value or steady state is reached. The time required for attainment of the constant value varies with the parameter: about 100,000 years or less for bulk density; about 500,000 years for B-horizon thickness, depth to loose, fresh parent material, and clay concentration; and 1 million years or more for color, pH, and total clay in the profile. All changes beyond about 500,000 years, however, take place very slowly so that it is possible to use soils to discriminate only those deposits that differ in age by several hundred thousand years. Extreme care in site selection and sampling is crucial if soil data are to be used for correlation or semiquantitative dating of Quaternary deposits.

These parameters have been tested in the northern San Joaquin Valley of California on soils of varying profile development that formed on uneroded alluvial surfaces of modern to late Pliocene age. The relative ages of these soils can be demonstrated from independent geologic evidence; some absolute age control is also available. The soils of the northeastern San Joaquin Valley can be grouped into four chronosequences on the basis of parent material and drainage history: (1) Sandy, well-drained alluvium; (2) finer grained, stratified granitic basin and interfluvial deposits with a history of impeded drainage; (3) sandy, well-drained andesitic alluvium; and (4) finer grained andesitic basin and interfluvial deposits. Soils have formed more rapidly on andesitic aluvium than they have on granitic alluvium. Soils developed under conditions of impeded drainage show thinner but more pronounced B horizons than well-drained soils of the same age formed on the same parent material. Properties of well-drained soils show gradual downward changes over a considerable vertical span.

Aseismic faulting

Modern surface faulting near Pichaco, Ariz., was recognized by T. L. Holzer and B. E. Lofgren (USGS) and S. N. Davis (Indiana State University) demonstrated to be causally related to withdrawal of ground water. The successful application of dislocation theory to the records of repeated level surveys along closely spaced bench marks across the Picacho fault suggests a means of distinguishing tectonic faulting from faulting driven by fluid extraction. In contrast, large tension cracks in alluvial basins, termed earth fissures by Holzer and Davis, are due to shrinkage caused by the decline of the water table, rather than to distortion caused by land subsidence, as investigators had thought previously. Fissures in central Arizona, Las Vegas Valley in Nevada, and San Joaquin Valley in California are best associated directly with water-table declines rather than with subsidence; they extend deep into the alluvial section and can be demonstrated from field relations to propagate upward toward the ground surface rather than downward.

Field mapping and photointerpretation by E. R. Verbeek demonstrated that surface faults are common features of the Texas Gulf Coast and form a regional pattern dominated by northeast-trending complex graben that crudely parallel the coast and a generally subordinate fault system that crosses the graben at high angles. This pattern has been carefully documented in several areas, and many of the faults are evident on high-altitude images. Many of the faults exhibit surface scarps that range from 10 cm to 1.5 m high in upper Quaternary deposits, and some of these faults have displaced streets, houses, and other modern structures. The occurrence of modern faulting in the Houston-Galveston subsidence bowl is well known, but Verbeek recognized modern faulting well beyond the obvious limits of subsidence. Although ground-water withdrawal in the Houston region is probably responsible for accelerated surface-fault movements as well as for the general ground subsidence there, the proof that some faults break modern structures in areas of little or no surface subsidence suggests that a natural potential for modern surface faulting may exist throughout the Texas Gulf Coast region.

Volcanic hazards

A preliminary appraisal of volvanic hazards in the 48 conterminous States (Mullineaux, 1976) indicated that large-scale ash fall, pyroclastic flow, and mudflow hazards are almost entirely restricted to areas downwind and downvalley from the Cascade Range volcanoes. Minor ash fall, lava flow, and pyroclastic flow hazards are widely but sparsely distributed throughout the Western United States. Catastrophic ash flows from a few widely spaced centers are possible, and their effects would be widespread, but such eruptions are of very low frequency. As a result of his studies on the thickness and distribution of the large postglacial tephra layer Yn from Mount St. Helens, D. R. Mullineaux found that the potential thicknesses of volcanic ash from similar Cascade Range volcanoes are greater than previous investigators has thought. New data indicate that representative maximum thicknesses of layer Yn at distances of more than 50 km from the volcano are mostly 25 to 50 percent greater than the best previous data had indicated. Thus, tephra presents a somewhat more severe and extensive hazard to power reactors than previously thought.

Rock stress in foundation design

Preliminary in-situ stress determinations made in and adjacent to 10×10×5-m block of Barre Granite in the Wetmore and Morse quarry near Barre, Vt., by T. C. Nichols, Jr., F. T. Lee, W. Z. Savage, D. R. Miller, and G. R. Terry, demonstrate the existence of near-surface strain energy large enough to cause measurable surface deformations when the block is quarried. Moreover, concentrations of near-surface strain energy have created enough elastic and time dependent deformations to cause visible rock failures and floor heaving in the quarry. Further deformation measurements indicate that there are time-dependent deformations that cannot be explained by present thermal strains. The magnitude of observed deformations, both instantaneous and with time, are large enough to be of concern in foundation design (Nichols and Savage, 1976).

ENVIRONMENTAL ASPECTS OF ENERGY

Studies of the environmental aspects of energy are designed to provide geologic information concerning the actual and potential effects on the environment that result from energy-resource development. Investigations in 16 states included (1) bedrock and surficial geologic mapping, (2) engineering geologic and geotechnical studies, (3) climatic constraints to mined-land reclamation, (4) geochemical baseline studies of plants and surficial materials, (5) computerized mapping of elements that influence reclamation potential, (6) inventories by several States of lands disturbed by mining, and (7) production of an energy resources map of Colorado.

Mapping potential for reclamation of surface-mined lands

D. W. Moore developed a system for combining several single-factor maps by using a computer to produce a map showing the relative potential for successful reclamation of surface-mined lands. The study area was a 500 km^2 area underlain by strippable coal near Gillette, Wyo. The map is being prepared at a scale of 1:100,000 and shows good, fair, and poor potential for reclamation for individual 8-ha land parcels. Reclamation potential is the likelihood of establishing a set of desired physical conditions for several environmental factors after surface mining. That likelihood is predicted on the basis of reclamation research results and published resource maps from governmental and private sources. The reclamation potential is the sum of the likelihoods of successful reclamation of six environmental factors: (1) Ground-water quality, (2) surface-water quantity, (3) land use, (4) revegetation characteristics, (5) wildlife habitat, and (6) scenic values. The resultant map can be used to identify sites that may be adversely affected by surface mining and thus should be considered in the mine plan. Also, the map can help to indicate a sequence of mining whereby reclamation is first achieved in areas having the greatest reclamation potential.

Evaluating nonmineral resources in regions of strippable coal

Previously unquantified nonmineral resources were evaluated, and a map of their relative values was made by D. W. Moore and J. M. Boyles (1976) for the Gap 7½-min quadrangle in northeastern Wyoming. The mapped area is underlain by strippable coal and is in a region where several surface mines are planned or are beginning operations. The method used to make the map implements section 102(B) of the National Environmental Policy Act of 1969 in that it shows the relative value of nonmineral resources so that they may be considered in decisions concerning the recovery of mineral resources by surface mining. Resources that were evaluated include (1) scenic values, (2) wildlife habitat, (3) ground-water quality, (4) surface-water quantity, (5) rangeland carrying capacity, and (6) land use. Values of classes of natural differences of these resources were ranked on a scale of 0 to 9, where 0 is least valuable and 9 is most valuable, according to the following criteria: (1) value to man's livelihood (2) intrinsic value as part of the total ecosystem, and (3) esthetic value. The ranking scores were added to get an overall environmental score. The sum was divided into four classes of environmental value ranging from very high through low. This map can be used to weigh the value of nonmineral resources against mineral resources in undertakings requiring large-scale environmental disturbance.

Kaiparowits coal-basin studies

Studies conducted by K. A. Sargent in the Kaiparowits Plateau of southern Utah showed that in the center of the basin, where coal appears to be thickest, the availability of ground water for possible future power generation and mining is low, transportation routes are difficult to establish and maintain, and the depth of coal is locally greater than 610 m. Sufficient ground water from a deep source (Navajo Sandstone) may be available for mining but not for large-scale power generation. The only large source of surface water is Lake Powell. Investigations in progress in the Kaiparowits Plateau include geologic, hydrologic, and engineering-geologic studies. A folio of maps of the area is being prepared.

Molybdenosis—a potential problem in ruminants ranging over coal-mine spoils

Although no incidence of molybdenosis has been reported for cattle or sheep grazing over coal-mine spoils, the potential for this nutritional disease does exist, according to evidence reported by J. A. Erdman and R. J. Ebens (1976). Altered physical and geochemical properties of normal soils caused by the addition of coal-mine spoils and the concern that such changes may prove harmful to livestock ranging on the reclaimed land led to the examination of the element composition of sweetclover and associated spoil materials from eight selected coal mines in the northern part of the Great Plains province. Molybdenum-induced copper deficiency has been well documented in both cattle and sheep where copper-to-molybdenum ratios of greater than 5:1 were found in the herbage. The copper-to-molybdenum ratios in sweetclover from the mine-spoil areas in this study ranged from 0.4:1 to 6.5:1, which are within the ranges reported to cause molybdenosis. It appears that the molybdenum contents of sweetclover growing on some coal-mine spoil banks may be high enough to induce metabolic imbalances in cattle, sheep, and possibly native ruminants at subclinical (if not acute) levels, if the animals were assumed to feed predominantly on this legume. Proper management of reclaimed areas, however, could effectively reduce this hazard.

Geochemistry of trace elements related to coal usage and disposal

Peter Zubovic made detailed geochemical studies of fly ash from six coal-fired powerplants. His data show that where they exist in the coal fuel, more than 90 percent of the volatile elements mercury, chlorine, iodine, and sulphur are emitted from the plants when they are released by burning. Other volatile elements show the following losses:

Element	*Percent*
As	0–74
Br	43–96
F	0–88
Sb	0–98
Se	0–65

The emission of these elements is controlled largely by their concentration on the fly-ash particles that pass through entrapment mechanisms used by the plants. The principal rock-forming elements such as silicon, aluminum, iron, and others are about equally distributed in the fly ash and bottom ash. Elements that are known to be organically associated in coal generally are found in higher concentrations in the fly ash. Some of these elements have been shown by other investigators to be highly concentrated on the smaller fly-ash particles. Such elements would have a higher percentage of their input discharged to the atmosphere.

Higher fly ash-to-bottom ash ratios for many elements appear to be related to the original ash content of the coal. The higher ratios of low-ash coals indicate an enrichment of the elements in fly ash, probably the result of the greater amount of organic association of the elements in low-ash coals.

Because of the variability of the trace-element content of coal and the use of coals from different beds and, in some cases, from different regions in a powerplant, significant differences in trace-element emissions can result from day to day. Thus, a single sampling of a powerplant gives valid results only for the coal blend used at that time.

Powder River basin remotely sensed

A grant to the University of Wyoming helped finance a study to provide information on land use, surface features, and vegetation on a regional scale for the Wyoming portion of the Powder River basin. These data, based chiefly on interpretation of remote-sensing imagery, will contribute significantly to a series of basin overview maps that are being prepared by the USGS to assist in evaluating the long-term environmental effects of large-scale energy-resource development throughout this coal-rich region. The mapping was coordinated closely with contemporaneous USGS field investigations in several parts of the Powder River basin. The study was directed by the principal investigator, R. J. Marrs (University of Wyoming).

New energy-resources map of Colorado

D. A. Myers and J. A. Sharps were the principal USGS compilers of the composite map of the State of Colorado (Colorado Geological Survey and U.S. Geological Survey, 1977), which shows the distribution of energy resources (coal, oil and gas, and uranium) and the locations of energy-related transportation and distribution systems. The Colorado Geological Survey participated in this study by furnishing certain component parts of the map, including locations of energy-resource mines and related energy-conversion and distribution facilities and information on producing horizons and production figures on oil and gas fields. Colorado Geological Survey personnel also assisted in reviewing and processing the final map product, which was published by the USGS. The map is designed to be used for statewide and regional planning for all levels of human involvement.

Foreign mining methods assessed

Horst Ueblacker (Consulting Geologist of Lakewood, Colo.) under contract to the USGS, prepared an interpretive report on surface-mining activities, reclamation practices, environmental planning, and laws and regulations governing mining, reclamation, and environmental assessment in foreign countries. Based on a comprehensive review and analysis of pertinent scientific and technological reference materials, the report provides a basis for comparing similar matters in the United States and abroad and constitutes a reservoir of data that can be drawn upon as environmental geologic and related studies are undertaken in the Nation's energy lands. The report presently is in draft form and is being prepared by the USGS.

Climatic constraints to mined-land reclamation

T. J. Toy (University of Denver) was given a USGS grant to study annual precipitation and evapotranspiration rates and to develop a more comprehensive and reliable basis for measuring the amount of water available to rehabilitate lands disturbed by surface mining across the Powder River basin. Climatological data from approximately 25 weather stations within the basin and surrounding areas were assembled and processed, and basinwide maps showing average annual precipitation and standard error of the mean were constructed. Estimates also were made of evapotranspiration rates, and appropriate maps were prepared from these data. The combined data are used for estimating the water availability for various kinds of plant communities and for determining the potential needs for artificial irrigation in revegetating surface-mine spoils.

GEOLOGY AND HYDROLOGY RELATED TO NATIONAL SECURITY

The USGS, through interagency agreements with the Energy Research and Development Administration (ERDA) and the Department of Defense (DOD), investigates the geologic and hydrologic environment of each site within the Nevada Test Site (NTS) where underground nuclear explosions are conducted. In addition, the USGS compiles geologic and hydrologic information pertaining to underground nuclear explosions conducted within the Soviet Union. Geologic and hydrologic data are needed to assess the safety, engineering feasibility, and environmental effects of nuclear explosions. The USGS does research on specialized techniques needed to acquire geophysical and hydrologic data at nuclear-explosion sites; some of the results of this research are summarized below.

At the Cambric site, where a low-yield explosion was detonated more than 10 years ago below the static water level, 560,000 m^3 of water were pumped from a well 100 m away from the point of the explosion. Tritium was detected in the pumped water at a concentration of about 1pCi/L. Assuming radial isotropy, W. W. Dudley, Jr., calculated a minimum effective porosity of about 0.2, a value thought to be too high for the coarse but poorly sorted alluvium in which the explosion was emplaced. Consequently, anisotropy with respect to flow of water in the alluvium is suspected.

At the Startwort site, a reentry hole into the explosion cavity was destroyed by a nearby explosion. However, some 3 years after the Startwort explosion, the temperature of the ground water in the cavity had dropped below boiling, and the cavity filling was accelerating. Final tritium concentrations were 2.5×10^8 pCi/L.

At the Almendro site, the temperatures in the cavity region are still about 200°C some 4 years after the explosion, and ground water is not infiltrating the cavity region. Water samples from a reentry hole contain concentrations of 3.6×10^8 pCi/L.

At the Cheshire site, a reentry hole was completed as a hydrologic test hole below the cavity region, and a few water samples have been obtained from a zone below the point of detonation. Small amounts of tritium have been detected in these samples.

At the Faultless explosion site in central Nevada, hydrologic monitoring of the ground-water infill into the explosion cavity has been in progress since the explosion was detonated in 1968. G. A. Dinwiddie reported that the water level rises in the collapsed alluvium overlying the explosion at a rate of 0.1 m/d. This rate has remained approximately constant during the year, and the water level is still more than 400 m below the local water table. The concentration of tritium in water samples removed from a depth of 790 m increased by two orders of magnitude during the past year.

Dudley, W. C. Ballance, and V. M. Glanzman studied changes in the hydrologic properties of the rocks at the site of the Cannikin nuclear explosion detonated 1,791 m beneath Amchitka Island in Alaska in 1971. The explosion created a subsidence lake that captured the local surface-water drainage and created a permeable collapse zone over the explosion so that the hydraulic head of the lake level is applied to rocks as deep as 1,800 m. These rocks have low transmissivities, and their effective porosities are extremely low, probably on the order of 10^{-4}. Dudley and his coworkers suggested that active ground-water flow may now be deep enough to begin flushing radioactive water away from the explosion cavity.

G. C. Doty and Dudley investigated water wells in Las Vegas, Nev., that were alleged to have been damaged by ground motion resulting from nuclear explosions at NTS. They concluded that land subsidence induced by ground-water pumping is the primary cause of well failure. Surface subsidence of about 1 m is common in areas from which most well-damage claims have been filed. At other places in southern Nevada and adjacent California, decreased in head resulting from sustained pumping are suspected to have initiated consolidation of fine-grained alluvial strata and release of poor-quality water to nearby wells.

W. L. Ellis and his associates used three techniques to measure in-situ stress in the rocks beneath Ranier Mesa at NTS at depths of about 400 m: (1) The overcore method, (2) hydraulic fracturing, and (3) vibrating-wire stressmeters. In-situ stress data are used to design tunnels and underground experiments related to nuclear tests. Explosion-induced residual stresses are believed to be significant with regard to the effective containment of underground nuclear explosions. Preexplosion and postexplosion measurements of rock stresses are being used to obtain quantitative data concerning explosion-induced stresses. The few field data obtained to date agree well with predictions based on computational models or rock behavior under explosion conditions.

R. D. Carroll and M. J. Cunningham used a variety of energy sources to generate seismic shear waves in the tuffs beneath Rainier Mesa: (1) Primer cord mounted on aluminum plates buried in ditches, (2) standard dynamite in shot holes, and (3) a 272-kg weight drop. The volcanic tuff of Rainier Mesa is a strong supporter of SV-type shear-wave energy. The clearest shear-wave signatures are generated by the weight drop; those generated by the primer-cored source are next clearest. However, geophysical logs of the full-wave acoustic type show little or no shear-wave energy in drill holes that penetrate the tuffs beneath Ranier Mesa.

The United States and the Soviet Union negotiated a treaty in 1975 governing the conduct of underground nuclear explosions for peaceful purposes. This treaty provides that, under certain conditions, the country conducting a peaceful nuclear explosion will allow teams from the other country to be present at the site to verify certain aspects of the project. One of these teams will have as its objective verifying the geology of the project site. The USGS was assigned by ERDA the lead role in designing, training, and fielding a geologic team to make on-site verification of the geology of peaceful Soviet nuclear-explosion sites. Twelve USGS geologists participated in orientation and training courses for the team. In addition, the USGS conducted two seminars at NTS to familiarize geologists from both USGS and ERDA laboratories with geologic activities related to underground nuclear explosions.

The geology of several areas in the Soviet Union where underground nuclear explosions have occurred was studied by Jack Rachlin and his associates. Salih Faizi compiled geologic maps, stratigraphic sections, and other relevant geologic information for the areas of the Soviet tests based on published scientific literature. Using this basic information, together with information provided by the Soviets at international meetings and other materials, P. J. Ruane, W. J. Dempsey, Selma Bonham, and Rachlin analyzed the explosions in a series of classified reports. This work included computational analyses and comparisons with nuclear explosions conducted by the United States.

RELATION OF RADIOACTIVE WASTE TO THE GEOLOGIC ENVIRONMENT

A national effort to find suitable repositories in deep geologic formations for radioactive wastes from military operations and the nuclear fuel cycle was continued by the Energy Research and Development Agency (ERDA). Investigations over a broad spectrum of the Earth sciences are now underway to find solutions to this pressing problem.

There is currently considerable uncertainty as to what form the waste will have and how much there will be. Solid highly radioactive waste from the military program will total an estimated 450,000 t by the early 1980's (Willrich, 1976). Spent commercial nuclear fuel is currently being kept in temporary storage. It must either be disposed of, placed in long-term storage, or reprocessed. Reprocessing of spent reactor fuel will result in significant amounts of high and low-level radioactive wastes (Blomeke and Kee, 1976) which, like the spent fuel itself, must be sequestered from the biosphere for millions of years.

Potential Waste Isolation Pilot Plant (WIPP) site in southeastern New Mexico

Reconnaissance studies conducted by C. L. Jones, M. E. Cooley, and G. O. Bachman (1973) were used by ERDA to select a site for a pilot repository for military radioactive wastes in the bedded salt of the Salado Formation in southeastern New Mexico. Exploration of this site is more advanced than that for any waste repository under consideration. Recent geologic studies concentrated on determining the extent of potash deposits beneath the site of the proposed Waste Isolation Pilot Plant. A series of 21 core holes was drilled and logged. A determination of the economic value and recoverability of the resources will be made by the U.S. Bureau of Mines.

Twenty low-level seismic events have been detected in part of the Central Basin Platform 50 km from the New Mexico site under a seismic monitoring program coordinated by A. M. Rogers. These events may be related to water flooding of oilfields in this area.

Paradox Basin of Utah

Part of the Salt Valley anticline northwest of Arches National Park in Grand County, Utah, is being studied for underground storage of radioactive waste in salt. Field studies by L. M. Gard, Jr., R. P. Snyder, located a small area along the collapsed axis of the anticline, where the salt core lies about 245 m below the ground surface, that merits intensive subsurface study as a potentially suitable site for waste storage (Gard, 1976).

Reprocessing of existing seismic data indicates that the low frequencies and coarse spacing of shots and receivers used in the petroleum industry are not appropriate for mapping the thin, complexly folded intersalt layers. A ray-path model computer study by A. H. Balch indicates that the high salt velocity and the complex structure cause a divergent lens effect; thus, relatively few rays penetrate the salt. It is concluded that the seismic sources and receivers must be placed in the salt to minimize this effect.

Subsurface data evaluated by R. J. Hite indicate that the salt mass averages about 87 percent halite. The maximum penetration of pure halite rock in the Salt Valley anticline is 400 m, and numerous wells intersect 155 m or more of uninterrupted halite. All drill holes in this area show the salt mass to be complexly folded and faulted.

Region of the Pierre Shale

G. R. Schurr studied the large region of occurrence of the Pierre Shale in the Western Interior by subsurface methods to delineate areas that may be suitable for radioactive waste repositories. Data from 550 wells were used in the first phase of the study. Three potential study areas were located: (1) On the southeastern side of the Williston Basin in South Dakota, (2) on the eastern margin of the Denver Basin in Colorado, and (3) on the eastern margin of the Williston Basin in North Dakota. These areas share the following characteristics:

- Depth to the base of the Pierre is 300 to 1,000 m.
- The formation is greater than 300 m thick.
- Overburden thickness is less than 150m.
- There are fewer than 100 oil and gas wells within cells that are 15 min. in both lititude and longitude.
- There are no sandstone interbeds.
- There are no major structural features.

Potential repositories in the Eleana Formation at the Nevada Test Site

The Nevada Test Site, which is a weapons-testing area for ERDA snd the Department of Defense, is currently being studied to determine its suitability for active waste disposal. The USGS has conducted detailed geologic studies of the site for over 20 years and has the lead role in evaluating the site from the waste-management viewpoint.

D. L. Hoover found that the upper part of unit J of the Eleana Formation at the Nevada Test Site contains clay-rich argillite that may be favorable for a waste repository. Geologic mapping and a 914 m drill hole indicate that a thickness of 600 m of argillite is present in the Syncline Ridge area. The area was intensely deformed during Paleozoic and Mesozoic time but appears to have been unfaulted during the Tertiary and Holocene in an area of about 50 km^2.

RELATION OF RADIOACTIVE WASTE TO THE HYDROLOGIC ENVIRONMENT

One of the few unresolved problems facing the nuclear-power industry in the United States is the management of radioactive-waste material generated in the nuclear-fuel cycle. The present waste-management concept envisions emplacement of solidified radioactive-waste material at several locations with varying hydrogeologic environments. The USGS is assisting ERDA in identifying potential hazards to hydrogeological environments at existing disposal sites in several regions and at potential disposal-site areas.

The migration of waste nuclides from selected disposal sites will be by erosional processes or ground water. The processes and principles of waste migration are being investigated at field locations in Idaho, Illinois, Kentucky, Nevada, New York, South Carolina, and Tennessee and in USGS regional laboratories.

Hydrogeologic investigation of the Maxey Flats radioactive-waste storage site

H. H. Zehner reported that the USGS's 5-year study, of the hydrogeology of the Maxey Flats radioactive-waste storage site in Kentucky has the following two primary objectives:

- The hydrogeologic conditions at the Maxey Flats site, such as the positions of water tables in several fractured aquitards underlying the site, aquitard testing of the saturated zones, and the quality of both ground water and water that has

accumulated in the burial trenches, will be determined.
- The hydrogeologic criteria for selecting future radioactive waste-burial sites in areas underlain by fractured aquitards will be established.

In the summer of 1976, four wells were drilled and completed to various depths at a location about 300 m from the burial area. Hydrologic data and water samples were collected from these wells.

Eighteen samples of water were obtained from trenches on the burial site. These samples are being analyzed by scientists at Brookhaven National Laboratory in New York for organic, inorganic (nonisotopic), and radionuclide chemical constituents.

Evaluation of radioactive-waste burial in coastal sediments

At the low-level radioactive-waste burial site in Barnwell County, South Carolina, test-drilling data indicated that four discrete aquifer units can be differentiated in the upper 160 m of coastal sediments. According to J. M. Cahill, these units are differentiated on the basis of hydraulic head, quality of water, and range in hydraulic conductivity. The upper unit is composed of Miocene sediments and has a hydraulic conductivity of about 10^{-2} m/d. The next two units are Eocene sediments that contain thick lenses of medium to coarse sand, and wells tapping these units yield from moderate to large amounts of water. The lower unit is composed of Upper Cretaceous sediments, and large amounts of water can be obtained from this aquifer.

It is believed that any radioactive contaminants that may reach the saturated zone beneath the burial grounds will affect only the upper two units. This belief is based on the assumption that a spring located about 0.8 km south of the burial grounds will act as a source of discharge before contaminants can migrate to lower depths. Efforts are now being directed toward verifying this assumption.

Radioactive-waste landfill in New York

A. D. Randall and D. E. Prudic reported that core samples collected from test holes drilled in 1975 through glacial till near the other than high-level radioactive-waste disposal trenches at West Valley, N.Y., were analyzed radiometrically for tritium. The Radiological Sciences Laboratory of the New York State Department of Health analyzed about 170 cores collected at depths of 1 to 15 m from holes between 2 and 5 m from the calculated position of 8-m-deep trench walls. Tritium activity of 1 to 10^{-4} μCi/mL near land surface generally declined rapidly with depth to between 1×10^{-5} and 2×10^{-7} μCi/mL. The higher values were in an area where trench-water seepage occurred early in 1975. In three holes, cores from a narrow zone deeper than 8 m indicated that tritium activity was more than an order of magnitude greater than it was in cores farther up the hole and thereby suggested lateral flow of water from the burial trenches through the till, perhaps chiefly along silt lenses in the till.

Spectral gamma logs were run by W. S. Keys in seven of the holes near the trenches; activity of cesium and (or) cobalt isotopes was detected in four holes, but all were at shallow depths, within back-filled cover material, and all but one were above the highest water level reached in nearby trenches. This information suggests that lateral migration of radioisotopes away from the burial trenches has been very limited. This theory is consistent with the results of earlier test drilling (Duckworth, Jump, and Knight, 1974) and with water-level measurements made by Prudic in 1975–76, which suggested predominantly downward flow.

Gamma spectrometry in radioactive-waste investigations

W. S. Keys, T. A. Taylor, and J. B. Foster identified cobalt-60 behind the casing of a monitoring well drilled near a trench at the solid low-level radioactive-waste disposal site at Sheffield, Ill.

D. E. Eggers developed computer programs for gain shift, spectral stripping, and quantitative analyses of in-hole gamma spectra. Eggers (1976) published the results of quantitative analyses of borehole spectra made at Maxey Flats, Ky., where concentrations of 2 to 95 pCi/g were calculated for contaminated shale behind the well casing. Detection limits for this method are on the order of 0.2 pCi/g or 8 parts in 10^{17} in terms of mass concentration for cobalt-60.

Radioactive burial ground in Idaho studied

Ten wells were drilled at the Idaho National Engineering Laboratory's radioactive-waste burial ground to determine hydrogeologic conditions, to detect migrating radionuclides, and to monitor the hydrologic system. According to J. T. Barraclough (J. T. Barraclough, J. B. Robertson, and V. J. Janzer, 1976), the subsurface rocks are principally basalt. Wind- and water-deposited sediments occur at the surface and in two principal beds at about 34 and 73 m below the land surface. The water table in the Snake River Plain aquifer is at a depth of 177 m.

Trace amounts of radioactivity were detected in about half of the samples from the subsurface sedimentary layers beneath the burial ground. This radioactivity could have been carried downward by infiltrating water that made contact with buried waste, or it could have been introduced artificially during drilling and sampling. Radionuclide constituents from the burial ground have not migrated into the underlying Snake River Plain aquifer, and radionuclides are not expected to migrate to the aquifer in detectable concentrations if the percolation of water through the burial ground is minimized. Additional drilling is underway to provide more subsurface information.

Computer model simulates radioactive waste seepage from ponding

With the aid of a computer model, J. B. Robertson (1976) analyzed subsurface migration of radioactive and chemical wastes from a disposal pond at the Idaho National Engineering Laboratory. The model simulated the fate of solutes that seep downward from disposal ponds into a large perched groundwater body, laterally through the perched-water zone, and then downward through the perching layer and underlying unsaturated zone to the regional Snake River Plain aquifer. Although waste tritium and chloride reached the aquifer several years ago, the model analyses suggested that the more easily adsorbed solutes, such as cesium-137 and strontium-90, would not reach the aquifer in detectable concentrations within 150 years under the conditions assumed. These results imply that some precautions will be necessary in disposing of radioactive waste at the facility.

Ground-water movement at radioactive-waste disposal site in Illinois

Tritium concentrations in wells about 0.4 km downgradient from a radioactive waste-disposal site at Argonne National Laboratory in Illinois fluctuate in a cyclic manner corresponding to high groundwater levels at the disposal site. In a geohydrologic study being conducted by M. G. Sherill, annual concentrations of tritium are being observed over a 4- to 5-month period that roughly corresponds to the period when ground-water levels are in or near the base of the disposal fill during recharge in the spring season.

Disposal of radioactive waste by grout injection after hydraulic fracturing of shales

As injection of liquid waste at the U.S. Army's Rocky Mountain Arsenal well near Denver, Colo., from 1962 through 1965 appears to have triggered earthquakes, the USGS is evaluating the practicability of a hydraulic fracturing and grout-injection method planned by ERDA at Melton Valley, Tenn., within the Oak Ridge National Laboratory (ORNL) reservation.

R. J. Sun (1976) determined the conditions necessary for producing earthquakes by fluid injection through wells and by reservoir construction: (1) The underlying rock must be stressed to the verge of fracturing by tectonic stresses and (or) be on the verge of sliding on preexisting fault planes; (2) the area must have one or more potentially active fault(s); and (3) there must be an increase of pore pressure in the rock caused by fluid injection or seepage from reservoir(s). The disposal of radioactive wastes in shale by hydraulic fracturing and grout injection has different effects than the injection of fluid. The injected grout is in its liquid phase only during the injection period and is confined in the hydraulically induced bedding-plane fractures. The grout is allowed to solidify under pressure after termination of the injection. After solidification, the grout becomes an integral part of the shale.

Sun noted the following significant characteristics of the disposal method at the ORNL site:

- Owing to the low permeability of shale, the high viscosity of the injection grout, and the solidification of grout after injection, pore pressure in the shale beyond the region of induced fractures does not increase.
- The selected injection site is free of local faults and of major interconnected joints and fractures.
- Owing to low tensile strength along shale bedding planes, the energy needed to induce bedding-plane fractures is small.

In view of the fact that at the proposed ORNL site there is (1) no increase in pore pressure in shale (which is the triggering force for earthquakes), (2) no increase in pore pressure produced by the disposal method, and (3) no association with potentially active fault(s), it is apparent that neither the site nor the disposal method has the characteristics for triggering earthquakes during and after grout injections.

Hydrologic aspects of nuclear-waste storage in Louisiana salt domes

The initial phase of a study of the geohydrologic aspects of storing radioactive wastes in northern Louisiana salt domes was completed by the USGS in cooperation with ERDA. R. L. Hosman found that the hydrology around a salt dome can be highly complex, and many factors must be considered in anticipation of possible contaminant leakage. The regional hydrology of the salt-dome basin can be fairly well described, but almost all of the data now available pertain to the freshwater-bearing parts of the major aquifer systems. Additional data are needed to complete the regional picture and to enable determination of the geohydrology at specific domes. The possible hydrologic effects of heat from the waste were considered for temperatures up to 400°C; the warming of saturated brine in contact with the salt could increase the solvency of the salt and possibly trigger a cycle of dissolution of the dome. It was found that, if a waste chamber is located at least 300 m from any perimeter of a dome, radioactive decay will begin to cool the heat source before temperatures can rise significantly at the outer edges of the dome. A digital model was used to determine flow directions and velocities in the Sparta Sand, the major aquifer in the area. Flow paths and traveltimes of water moving past several selected domes to points of withdrawal (major pumping centers) were plotted in an effort to visualize possible routes that might be taken by an escaped contaminant.

Potential waste-disposal sites in the Pierre Shale

G. W. Shurr (USGS Oil and Gas Resources, Denver, Colo.) is studying the Pierre Shale of Cretaceous age, which is distributed over more than half a million square kilometers of the Great Plains, as a host medium for long-term radioactive-waste isolation. Initial studies of well-log data and literature have identified three areas of the Pierre Shale that require more detailed investigation. In these areas, which lie in Colorado, North Dakota, and South Dakota, the Pierre Shale has less than 152 m of overburden, is more than 305 m thick, contains no sandstones, has no major structural features, and has a shale base from 305 to 915 m deep. Investigations in these areas will identify smaller areas that are potential waste-disposal site areas.

FLOODS

Three major categories of floods studied by the USGS are (1) measurement of stage and discharge, (2) definition of the relation between the magnitude of floods and their frequency of occurrence, and (3) delineation of the extent of inundation of flood plains by specific floods or by floods having specific recurrence intervals.

OUTSTANDING FLOODS

Maine coastal flood of February 2, 1976

R. A. Morill reported that a major business section of Bangor, Maine's second largest city, was flooded by water up to 3.66 m deep on February 2, 1976. Morrill reported that the flood elevation was 5.32 m above National Geodetic Vertical Datum of 1929 (NGVD) at the Washington Street Bridge over the Kenduskeag River and was the third highest known flood elevation since 1846. The flood, which was caused by an ocean surge coming up the Penobscot River, was the first documented major flood of this type in Bangor.

Flood in southeastern Idaho resulting from Teton Dam failure

Major flooding struck suddenly on June 5, 1976, in southeastern Idaho along the Teton River, Henrys Fork, and part of the upper Snake River downstream from Henrys Fork when the Teton Dam on the Teton River near Newdale failed at 11:57 a.m. H. A. Ray reported that the reservoir behind the 93-m-high earthfill dam contained 309 hm^3 of water at that time. In the next 143 minutes, approximately 213 hm^3 of water drained through the breach. Nearly 480 km^2 of land was inundated. The resultant peak discharge was about 65,000 m^3/s. About 303 hm^3 of water rampaged along a 241-km reach of the upper Snake River, causing 11 deaths and damages estimated as high as $1 billion. American Falls Reservoir, which has a capacity of about 1,600 hm^3, easily contained the flood volume.

Effects of the flood were detected in a number of ground-water wells located in or near the flooded area and adjacent to the Teton Reservoir. Water samples were collected at five regular stream-gaging stations for analyses of chemical constituents, and additional water samples were collected to determine the amounts of insecticides, herbicides, total organic carbon, nutrients, minor elements, fecal and total coliforms, and suspended and stream-bottom sediments in the floodwaters. Water samples were collected from about 30 wells within the inundated area for both chemical and bacteriological analyses.

A series of 17 Hydrologic Investigation Atlases—"Teton Dam flood of June 1976, Idaho" (HA-565 to HA-581)—was completed for rapid release to the public and many interested agencies. Each atlas delineates the flood boundaries for a particular 7½-min topographic map and shows the locations and elevations of high-water marks.

W. E. Scott reported that a new channel of the Teton River, formed in the 7-km-long canyon below the dam, was defined by a series of sand to exceptionally coarse gravel bars deposited downstream from bedrock projections. The largest boulder known to have been moved by the flood was of welded ash-flow tuff eroded from the canyon wall. The boulder measured 11×8×4 m (approximate weight, 810×10^3 kg). At the mouth of the canyon, a wall of floodwater as high as 5 m spread out over low-relief areas. Several sections of agricultural land were destroyed by erosion of thin loess from basalt or gravel, and (or) by deposition of thick gravel. Downstream areas in the vicinity of Rexburg were inundated by water several meters deep. Erosion was localized on features, such as road embankments, irrigation canals, and terrace scarps, that promoted increased flow turbulence. Eroded gravel was usually deposited as thin sheets (< 0.3 m deep) within a 100 m of its source. A layer of thin (< 0.2 m deep) silt and fine sand was widely deposited over the flooded area, primarily in diked fields and other areas of slack water.

In geologic perspective, the occurrence of flooding will be evidenced only by the extremely large boulders that were deposited locally in the canyon.

Big Thompson River flood of July 31-August 1, 1976

R. U. Grozier and J. F. McCain (USGS) and L. F. Lang and D. C. Merriman (Colorado Water Conservation Board) (1976) reported that severe thunderstorms during the evening of July 31, 1976, in the Big Thompson River basin resulted in a devastating flood on the Big Thompson River and its tributaries between Estes Park and Loveland, Colo. As much as 300 mm of rainfall was measured. Larimer County officials reported that 139 lives were lost and that property damage was $16.5 million.

Streams started to rise about 7:00 p.m. The first reported damage occurred about 7:30 p.m. along U.S. Highway 34, about 12 km east of Estes Park. Peak stages on the Big Thompson River occurred at 8:00 p.m. at Glen Comfort, 8:30 p.m. at Waltonia, 9:00 p.m. at Drake, 9:30 p.m. at Loveland powerplant, and about 11:00 p.m. at the mouth of the canyon, about 13 km west of Loveland.

On the North Fork Big Thompson River, the flood resulted from heavy rainfall centered within a few kilometers of Glen Haven. Extreme flood runoff occurred in the area extending from the basin divide on the south to about 6.4 northeast of Glen Haven.

The peak stage on the Big Thompson River just downstream from Drake occurred before the peak from the North Fork arrived at Drake. No apparent reduction in discharge occurred as the flood peak moved through the 11.7-km reach of channel between Drake and the canyon mouth. East of the canyon mouth, the Big Thompson River valley widens rapidly. The peak discharge of 883 m^3/s on the Big Thompson River at the gaging station at the mouth of the canyon near Drake was reduced to about 70.8 m^3/s by valley storage and overflow into many reservoirs near LaSalle, about 60 km to the east.

R. R. Shroba and P. W. Schmidt reported that, in the upper part of the canyon, sheet erosion, gullying, and landsliding were widespread on moderate (5°) to steep (40°) slopes. Tributary gulches, scoured to bedrock during the storm, contributed significant amounts of sand- to boulder-sized material that built fans into the main stream and locally aggraded the channel. In tributary gulches where precipitation was less, surficial deposits were mobilized and redeposited as debris flows and boulder jams.

Along the river in the lower part of the canyon, gravel bars with boulders as large as 4 m in diameter were deposited at inside bends and slightly expanded reaches having gradients of about 20 to 30 m/km. Sheets of fine to medium sand were deposited where the gradient decreased to less than 10 m/km.

Many homes along the river were damaged or destroyed by the impact of floating and saltating debris, and many homes were washed downstream. Major sections of U.S. Highway 34 and several homes were destroyed by lateral stream cutting.

FLOOD-FREQUENCY STUDIES

Flood-frequency relations for small rural streams in Alabama

D. A. Olin and R. H. Bingham developed equations for estimating magnitudes of floods for 2-, 5-, 10-, 25-, 50, and 100-year recurrence intervals on natural rural streams in Alabama with drainage areas of 2.6 to 38.8 km^2. One equation for each recurrence interval applies statewide. The equations were developed from multiple-regression analysis of observed streamflow data (8–24 years) collected at gaging stations and synthetic streamflow data generated by a calibrated rainfall-runoff model. The regression analysis indicated that drainage area and main-channel slope are the most significant basin characteristics affecting flood frequency. These characteristics generally can be determined from topographic maps.

Flood-frequency relations for streams in Arizona

R. H. Roeske used a multiple-regression analysis to develop relations for estimating the magnitude and frequency of floods on natural streams. Equations were developed to estimate the magnitude of the 2-, 5-, 10-, 25-, 50-, and 100-year floods. Preliminary results indicated that four sets of equations based on the mean elevation of the basins improve the relations. The elevation breaks are at 1,070, 1,680, and 2,260 m. The significant parameters in the equations are drainage area and mean annual precipitation. The standard error of estimate ranges from −58 to +140 percent.

Stage of 100-year flood in Lucerne Valley of California

A study of the flood hydrology of the Lucerne Valley of California was undertaken by M. W. Busby to develop the 100-year stage for Lucerne Lake. Synthetic hydrologic techniques were used because no adequate hydrologic of meteorologic data were available for the basin. The 100-year flood stage was estimated to be at an elevation of 899 m above National Geodetic Vertical Datum of 1929.

Effects of Tatum Sawgrass dikes on flood-frequency relations of Myakka River in Florida

K. M. Hammett, J. F. Turner, Jr., and W. R. Murphy, Jr., completed a flood-hazard evaluation study of the Myakka River, a coastal stream that drains a 1,400-km^2 area in southwestern Florida. A large surface depression, Tatum Sawgrass, is located in the upper basin. Under natural conditions, Tatum Sawgrass served as a flood detention area for Myakka River floods. A dike system constructed across the mouth of Tatum Sawgrass restricted use of the depression as a floodwater-overflow storage area for the Myakka River.

Natural-condition areal flood-frequency relations were developed in a multiple-regression analysis of flow and basin-parameter data for the Myakka River and 20 other nearby basins. A modified Puls method was used to route flood hydrographs through the Tatum Sawgrass area, with and without dikes in place, to determine the change in peak discharge caused by dikes. Flood heights were determiend for natural- and diked-condition recurrence-interval flood-peak discharges by using the USGS step-backwater computer program.

Diked-condition flood heights for 1974 were used in constructing 2-, 2.33-, 5-, 10-, 25-, 50-, 100-, 200-, and 500-year recurrence-interval flood profiles for the nontidal part of the 72-km Myakka River study reach. Results of the study indicated that diking increased flood-peak discharges by as much as 27 percent and increased flood heights by as much as 0.3 m near the downstream end of the reach.

Techniques for estimating magnitude and frequency of floods on small streams in Illinois

G. W. Curtis reported that a technique for estimating flood magnitudes and frequencies on rural streams in Illinois is applicable to all drainage areas greater than 0.05 km^2. Recurrence intervals from 2 to 100 years can be estimated by using the technique.

Data from 242 streamflow gaging stations were used to develop the technique. Eighty-seven stations had drainage areas of less than 25 km^2, and records for 54 of these small areas were extended in time by using the USGS rainfall-runoff model. Flood-frequency curves were developed from all gaged sites by using the log-Pearson type III frequency distribution. Floodflow characteristics from the station frequency curves were related to drainage-basin characteristics by using multiple-regression analyses to develop regionwide relationships. Drainage area, mean channel slope, and rainfall intensity proved to be the significant independent variables. Estimating equations were developed for predicting flood magnitudes (dependent variables) for recurrence intervals of 2, 5, 10, 25, 50, and 100 years. A factor was provided for each of four areas in Illinois to adjust predicted flood magnitudes for regional influences.

Floodflow characteristics of small streams in Massachusetts

S. W. Wandle, Jr., reported that flood peaks on rural, unregulated streams in Massachusetts can best be defined by dividing the State into eastern and western flood-frequency regions. Multiple-regression techniques were used to develop the relationship between a set of basin and climatic characteristics and a set of flood peaks at 113 gaging stations. Station flood peaks were computed by using the guidelines recommended by the U.S. Water Resources Council (1976).

The regression equations related peak discharges with 0.5, 0.2, 0.1, 0.04, 0.02, 0.01, and 0.002 exceedance probabilities to drainage area and main-channel slope in the eastern river basins and to drainage area, area of lakes and ponds, and mean annual precipitation in the western river basins. Standard errors of estimate were 42 to 70 percent for the eastern region and 32 to 68 percent for the western region, an improvement of about 10 percent over the 1974 estimating relations (C. G. Johnson and G. D. Tasker, 1974).

Flood-frequency relations at ungaged sites on streams in Minnesota

L. C. Guetzkow reported that techniques were developed for estimating flood characteristics at ungaged sites on Minnesota streams. Multiple-regression analyses provided equations for estimating floods of various recurrence intervals on streams that were unaffected by regulation, diversion, or urbanization. Eight hydrologic regions were defined for the State, each of which had unique regression equations relating flood-magnitude to basin characteristics. Flood-frequency data at gaged sites and graphs relating flood magnitude to drainage-area size for the main stems of the Minnesota River, the Mississippi River, and the Red River of the North were developed. Basin characteristics found to be most significant in flood-frequency relations were drainage area, main-channel slope, and basin storage.

Depths of floods of selected frequency in rigid-boundary channels

D. E. Burkham reported a simplified technique for determining depths of *T*-year floods (floods of selected recurrence intervals) in natural channels (channels not significantly affected by regulation or urbanization) having channel-control conditions and rigid boundaries (channels having a low probability of change that would significantly affect the hydraulic characteristics of a *T*-year discharge. The technique requires that the discharge of the *T*-year flood in the reach of interest be known. In addition, a channel-shape factor, width at a reference depth, channel-bottom slope (or water-surface slope), and Manning's roughness factor *n* are needed.

Flood-hydrograph synthesis and peak-discharge reduction in Colorado River basin

J. H. Eychaner (1976) used hydrographs of 364 floods at 18 continuous-record gaging stations in the Colorado River basin in southern Utah to define a relationship between flood volume and peak discharge. The results, in the form of a mean dimensionless hydrograph, can be used to define synthetic hydrographs for design flood peaks for drainage areas of 13 to 780 km^2 and peak discharges of less than 200 m^3/s. A short method was developed to estimate the reduction in peak discharge that would occur if part of the floodwater were stored temporarily behind a highway embankment. Culvert- and bridge-capacity reduction of 25 percent can be achieved by storing 4 percent of the flood volume.

FLOOD MAPPING

Flood-prone areas in Cave Creek quadrangle of Arizona

Flood-hazard zones that represent definable and homogeneous potential flood hazards closely correspond to landforms. Mountain fronts, bedrock areas, and alluvial slopes have distinct potential flood hazards. H. W. Hjalmarson (1977) delineated these landforms on a map to define potential flood-hazard zones. Potential flood hazards along the mountain fronts are defined channels, where flow velocities are high, and steep slopes, where sheetflow, landslides, and rolling boulders occur. In bedrock areas, potential flood hazards are due to flow confined to channels and narrow flood plains that occupy lowlands between defined ridges. Potential flood hazards on the alluvial slopes are due to floodflow that spreads out adjacent to small channels. Many well-defined channels that leave the mountain fronts and bedrock areas branch and rebranch into unstable distributary on slightly dissected alluvial slopes.

Flood-flow capacity of Sacramento River between Ordbend and Glenn, California

R. G. Simpson (1976) determined the adequacy of a 13.6-km reach of the Sacramento River north of Glenn, Calif., to carry floodflows. Maps, profiles, cross sections, and stage-discharge relationships for flooding expected to occur from flows up to 5,950 m^3/s are shown in Simpson's report.

Flood-prone areas in Palmer Lake, Colorado

R. D. Jarrett investigated the existence and severity of flood hazards in the town of Palmer Lake, Colo. For the 100-year flood on streams in the community, flood-prone areas range in width from 30 to 250 m and include 12 percent of the area within the town's corporate limits. Steep stream slopes cause hazardous velocities on all streams, and mean velocities on Monument Creek reach 4 m/s. Depths of floodwaters are as much as 4.6 m and overtop all but one road crossing in the community.

Adjustment of Manning's roughness coefficient for predicting floodflows in urban areas

H. R. Hejl, Jr., devised a technique for determining the value of Manning's roughness coefficient in flooded urban areas by adjusting verified roughness coefficients for natural conditions on the basis of the density of buildings on a flood plain. Urban roughness coefficients were calculated to emulate the water-surface profiles to within 0.06 m for depths of flow less than 0.6 m and within ± 10 percent for depths between 0.6 and 2 m. The method is particularly useful in studies made to predict flooding hazards in urban areas.

Flood-prone areas in Twin Cities metropolitan area of Minnesota

L. C. Guetzkow, G. H. Carlson, K. T. Gunard, and C. W. Saboe, completed comprehensive flood studies in 12 communities in Minnesota in a continuing series of investigations to develop data for all main-stem river corridors in the seven-county Twin Cities metropolitan area. Flood-frequency analyses, flood profiles, flood inundation maps, and floodway evaluations were made, and flow-frequency estimates were coordinated at 65 sites.

Accuracy of flood-prone area maps

D. E. Burkham appraised the accuracy of flood-prone mapping for rigid-boundary channels. The probable nationwide average standard errors of estimate in percent of depth for 100-year flood-boundary elevations, obtained by three general methods, are 21.2, 22.9, and 26.0.

Maps of flood-prone areas

Areas inundated by the 100-year flood are outlined on topographic maps as part of the National Program for Managing Flood Losses. The objective of this program is to rapidly inform cities and towns of the general extent of their potential flood problems. According to G. W. Edelen, Jr., nearly 12,500 such maps have been completed for all of the States, the District of Columbia, and Puerto Rico.

The maps identify the flood-prone areas of most of the already developed parts of the Nation as well as those parts being developed. Flood-hazard maps are used extensively to meet local planning needs and to meet the objectives of the National Flood Insurance Act of 1968 and the National Disaster Protection Act of 1973.

Basin and climatic characteristics that can be used to define flood discharges of selected recurrence intervals at ungaged sites on unregulated streams were defined in 31 States.

Inundation maps of Teton Dam area of Idaho

Maps showing areas inundated by the June 5, 1976, Teton Dam flood in Idaho, together with maximum water-surface elevations, were published as Hydrologic Investigations Atlases for the Rose quadrangle (J. H. Bartells and L. L. Hubbard, 1976a); the Blackfoot quadrangle (Bartells and Hubbard, 1976b); the Moody quadrangle (W. A. Harenberg and B. B. Bigelow, 1976a); the Rexburg quadrangle (Harenberg and Bigelow, 1976b); the Firth quadrangle (Hubbard and Bartells, 19769a); the Moreland quadrangle (Hubbard and Bartells, 1970b); the Pingree quadrangle (Hubbard and Bartells, 1976c); the Woodville quadrangle (H. F. Matthai and H. A. Ray, 1976); the Deer Parks quadrangle (H. A. Ray, C. M. Bennett, and A. W. Records, 1976); the Rigby quadrangle (Ray and Bigelow, 1976a); the Lewisville quadrangle (Ray and Bigelow, 1976b); the Idaho Falls North quadrangle (Ray and Matthai, 1976a); the Idaho Falls South quadrangle (Ray and Matthai, 1976b); the Newdale quadrangle (H. A. Ray, H. F. Matthai, and C. A. Thomas, 1976); the Parker quadrangle (Thomas and Ray, 1976); the Menan Buttes quadrangle (Thomas, Ray, and Harenberg, 1976); and the St. Anthony quadrangle (Thomas, Ray, and Matthai, 1976).

EFFECTS OF POLLUTANTS ON WATER QUALITY

Underground disposal of liquid industrial wastes

C. A. Pascale (1975) investigated two underground waste injection systems in western Florida, one near Pensacola and the other near Milton, in which liquid industrial wastes are being injected into a confined saline-water-filled limestone aquifer of low transmissivity. The injection sites are about 13.7 km apart. More than 48 million cubic meters of acidic industrial waste have been injected at the site near Pensacola since 1963. (D. A. Goolsby, 1971, 1972; J. B. Foster and D. A. Goolsby, 1972; G. L. Faulkner and C. P. Pascale, 1975). In 1977, injection rates averaged about 150 L/s, and wellhead pressures at the two injection wells averaged 12.4 kg/cm^2. The pressure at two deep monitor wells, 3.1 km north and 2.4 km south of the injection site, averaged 8.3 and 8.6 kg/cm^2, respectively. At the injection site, pressure in a shallow monitor well in the artesian aquifer immediately above the 67-m-thick confining bed averaged about 0.82 kg/cm^2 and continued to decline slightly.

Bicarbonate and dissolved organic carbon concentrations at the southern monitor well have continued to increase since the arrival of dilute waste at the well in mid-1973. Alkalinity (reported as bicarbonate) has increased from a background level of 270 mg/L to 640 mg/L, and it has increased about 100 mg/L during the past year. Dissolved organic carbon has increased from a background level of about 3 mg/L to 53 mg/L and it has increased 13 mg/L during the past year. Methane gas concentration also has increased—from 48 mg/L in February 1976 to 70 mg/L in August 1976. No changes in water chemistry were detected at the northern monitor well or at the shallow monitor well at the injection site.

Injection began at the site near Milton in June 1975, and more than 1.7 million cubic meters of treated industrial waste have been injected. This new deep-well waste-injection system uses the same injection zone as the similar system near Pensacola. In 1977, the injection rate averaged 35 L/s, and wellhead pressure at the injection well averaged 6.7 kg/cm^2 above the preinjection potentiometric surface. The pressure at three deep monitor wells in the injection zone 2.5 km northeast, 0.31 km southwest, and 0.47 km south of the injection well averaged 1.5, 2.5, and 3.2 kg/cm^2, respectively. At the injection site, the water level in a shallow monitor well in the artesian aquifer immediately above the 65-m-thick confining layer remained unchanged and averaged 18.6 m below land surface. Increases in bicarbonate and dissolved organic-carbon concentrations occurred in February 1976 at the monitor well closest to the injection well. The bicarbonate concentration was 465 mg/L in February 1976, 75 mg/L above background; by December 1976, the bicarbonate concentration had increased to 1,270 mg/L. Dissolved organic carbon increased from 5 mg/L in February 1976 to 47 mg/L in December 1976.

Effects of mining on water quality

Colorado.—The Argo Tunnel in Idaho Springs, Colo., is 6.69 km long and intersects about 26 sulfide ore veins. Water flowing from this abandoned drainage tunnel enters Clear Creek and significantly deteriorates water quality in the stream. Discharge, water temperature, and specific conductance of the drainage have been monitored continuously since January 1976. Data collected through November 1976 by D. A. Wentz show very little variation in flow 10-16 L/s) and a relatively constant temperature of about 16°C. Specific conductance was about 3,400 μmho/cm at 25°C in January, dropped to about 3,100 μ mho/cm by early March, and, except for a minimum of about 2,900 μ mho/cm in August, has remained fairly constant since that time.

Monthly analyses of other constituents show the following ranges: DO, 1.4 to 1.7 mg/L, pH, 2.9 to 3.0; total Sb, to μg/L; total As, 100 to 180 μ g/L; total Ba, 0 to 200 μg/L; total Cd, 140 to 170 μg/L; total Cr, 0 to 30 μg/L; total Cu, 5,400 to 6,500 μg/L; total Fe, 170,000 to 200,000 μg/L; total Pb, < 100 to 160 μg/L; total Li, 30 to 50 μg/L; total Mn, 80,000 to 110,000 μg/L; total Hg, 0 to .2 μ g/L; total Mo, 0 to 2 μg/L; total Se, 0 μg/L, total Ag, 0 to 60 μg/L, and total Zn, 40,000 to 49,000 μg/L. Most trace elements are greater than 90 percent dissolved; only lead (20-30 percent dissolved) and silver (0 percent dissolved) deviate from this generalization. Dissolved trace-element concentrations do not seem to correlate significantly with specific conductance.

Kansas.—The quality of water in the principal streams of Crawford and Cherokee Counties in southeastern Kansas has been adversely affected by extensive strip and shaft mining for coal, lead, and zinc. A. M. Diaz and C. D. Albert obtained field and laboratory data in April 1976 from a reconnaissance of 50 low-flow sites on Cow Creek (drainage area approximately 440 km^2), Cherry Creek (drainage area approximately 230 km^2), and Lightning Creek (drainage area approximately 650 km^2).

Data from the reconnaissance indicate that, at low flow, the water is generally alkaline (pH >7). However, pH values of 3.5 were observed at sites where seepage from abandoned mine shafts is highly localized. Oxidation of pyrite yields high concentrations of sulfate to the ground waters and the surface waters in the area. In the coal-mined area, the concentration of sulfate ion (SO_4) ranged from 110 to 3,000 mg/L. Historical data, and data observed in parts of the study area that are unaffected by mining activities, indicate that the pH of streams draining areas that have not been mined is generally alkaline and that the concentrations of sulfate ion are generally less than 100 mg/L.

Ohio.—C. G. Angelo and C. L. Terbeek conducted a study in eastern Ohio to determine the effects of mining on water quality in four small drainage basins, each of which was representative of a basin with (1) an active strip mine, (2) a reclaimed strip mine, (3) an abandoned strip mine, or (4) an abandoned underground mine. The main stream in each basin was sampled at several points to determine downstream changes in water quality. All tributaries were traced to their sources and were sampled to determine their relationships to downstream changes in the main streams.

Headwater streams were unaffected by mine drainage, and waters generally had pH values above 6.0 and specific-conductance values of less than 650. The streams became acidic downstream with the addition of acid tributaries issuing from abandoned mines. By contrast, the two basins containing reclaimed and active strip mines produced no acid drainage whatsoever, although streams in the reclaimed basin were very high in sulfate (usually over 2,000 mg/L).

Oklahoma-Kansas.—Onsite measurements of pH, specific conductance, and water temperature made by S. J. Playton and R. E. Davis showed that water in seven mine shafts in northeastern Oklahoma and southeastern Kansas is stratified; pH decreased and specific conductance and water temperature increased as sampling depth increased. Concentrations of chemical constituents, such as dissolved solids, total and dissolved metals, and dissolved sulfate, also tended to increase as sampling depth increased. Water in the mine shafts is unsuitable for most uses without treatment. High concentrations of toxic metals, such as cadmium and lead, that cannot be effectively removed preclude use of the water for public supply.

Pennsylvania.—D. J. Growitz and M. M. Beard reported that data from a recent mass-sampling program conducted in the four anthracite coal fields of northeastern Pennsylvania indicate that the average daily discharge of mine drainage is to about 25.5 m^{3}s. The average acid load (to pH 7 as H SO_4) is approximately 270 t/d, and the average dissolved-iron load is about 68 t/d. More than 80 percent of the total mine drainage and acid load is discharged to the Susquehanna River basin; the remaining flow enters the Delaware River basin. Most of the mine drainage comes from abandoned mine workings.

Washington.—F. A. Packard studied the effect of drainage from a coal strip mine and stockpile on the quality of water in Hanaford Creek near Centralia, Wash. Results of the study are based on chemical analyses of grab samples obtained daily from sites upstream and downstream of the points of effluent discharges from the mine since 1970 and from the stockpile since 1971. Time-trend analyses of the average monthly differences between simultaneous upstream and downstream measurements show no significant increases or decreases in pH, alkalinity, DO saturation, or water temperature of the mine effluent. Turbidity from mine effluent also has not increased or decreased significantly since control of siltation-pond operation was improved in 1971. Owing to mine effluents, however, the conductivity of creek water has increased significantly since 1970 in proportion to the amount of land disturbed each year. Similar time-trend analyses of data obtained upstream and downstream from the coal-stockpile drainage showed no significant change in DO saturation, water temperature, pH, or net acidity. However, the analyses indicated that stockpile drainage may be causing some increases in conductivity, turbidity, and total iron; the increases in turbidity and total iron are attributed to the design of the flocculation ponds.

Effects of the trans-Alaska pipeline on water quality

In 1976, J. W. Nauman, C. E. Sloan, and D. R. Kernodle (Nauman and Kernodle, 1975) studied three streams along the trans-Alaska pipeline corridor to evaluate the effects of fuel-oil leaks on water quality and benthic invertebrates. Streams affected by leaks were Jim River at Prospect Camp, Unnamed Creek at Galbraith Lake Camp, and Happy Creek at Happy Valley Camp.

Drifting benthic invertebrates were collected with drift nets installed for 1 hour above and below the oilspill sites. Species diversity was lower at the downstream site in each stream. The diversity reductions were from 2.96 to 2.39 at Jim River, from 1.26 to 1.06 at Unnamed Creek, and from 2.43 to 1.86 at Happy Creek. There was also a reduction in the total number of taxa collected at each downstream site. However, little difference was apparent in the composition of the benthic community.

Although a surface oil sheen was visible at each downstream site, no oil was detected on samples collected below the surface by using the freon extraction method for oil and grease. However, oil and grease were detected in the streambed material. Oil concentrations ranged from 0.1 to 1.6 mg/kg in Jim River, from 0.1 to 9.7 mg/kg at Unnamed Creek, and from 0.1 to 24.7 mg/kg in Happy Creek. Although these concentrations of oil in sediment were relatively low, they suggested that fuel-oil contamination from the initial leak and continued seepage into these streams had reduced the benthic-invertebrate population immediately downstream from the area of fuel-oil leaks in these three streams. Furthermore, the diversity of benthic organisms below the seep area had not reached its preseepage level, an indication that the oil is a continuing detriment to the benthic community.

Sloan and Nauman studied the effects of ditching and backfilling operations during emplacement of the buried Alaska oil-pipeline crossing of the Salcha River between Fairbanks and Big Delta from March 9 to March 28, 1976. Turbidity values upstream of the crossing during this period ranged from 2 to 4 JTU. Downstream, during ditching operations, measured turbidity ranged from 29 to 95 JTU; during backfilling operations, turbidity reached a high of 200 JTU. Streamflow discharge during this period was about $2.8 m^3/s$.

Forty-two benthic-invertebrate drift samples were collected at three sites located 134 m upstream and 137 and 442 m downstream from the pipeline crossing from March 14 to 27, 1976, during ditching and backfilling operations. Drifting invertebrates collected at the station 137 m downstream from the crossing were fewer than those collected at the upstream station, and nets installed at the station farthest downstream retained many more organisms than nets at the other two stations. The numbers of drifting invertebrates under ice were substantially greater at night than during the day at all stations.

Artificial substrates were installed at the same sites on March 26 and retrieved on April 16; another set was installed on May 26 and retrieved on October 8. Although these samples have not yet been analyzed, cursory inspection indicates that the benthic-community structure was not significantly changed, in the long term, by the pipeline operations.

Modeling organics solutes in ground water

J. B. Robertson and D. F. Goerlitz used numerical modeling techniques to study a small area of an alluvial aquifer system in central California that has been contaminated by toxic pentachlorophenol (PCP), a biocidal wood preservative. Preliminary results indicated that this compound migrates in the local ground water as a relatively conservative anion. PCP was not measurably adsorbed on the aquifer material under near-natural chemical conditions. However, significant adsorption occurred in shallower soils containing higher amounts of organic material. Supportive studies by G. G. Ehrlich indicated that, although PCP is biodegradable under aerobic conditions, it is apparently not biodegradable under the anaerobic conditions that probably occur in the aquifer.

Separation of organic solutes from water

J. A. Leenherr (USGS) and E. W. D. Huffman, Jr. (Huffman Laboratories, Inc.) (1976), modified the analytical techniques used to concentrate, separate, and classify natural organic solutes in water and applied them to aqueous-process wastes from oil-shale retorting operations so that gram-sized quantities of these waste organic solutes could be isolated for further study. A large-scale separation was necessary to study the sorption of the waste organic solutes on processed shale, soil, and sediment after disposal of the aqueous-process wastes. This analytical methodology will be used to provide the sorption parameters needed in organic-solute transport models of wastes in surface and ground waters.

Landfill leachate migration

H. C. Mattraw, Jr., J. E. Hull, and Howard Klein studied a 24-year-old solid-waste disposal facility in the northwestern part of Miami, Fla. The facility is located about 1.5 km west of a major Dade County municipal well field and overlies the Biscayne aquifer, a highly permeable, solution-riddled limestone aquifer that transports leachates eastward from the landfill at a rate of 0.8 m/d. Data acquired from nine multidepth ground-water samplings made between August 1973 and July 1975 identified the leachate characteristics and the conservative components that most readily migrated downgradient.

Downgradient from the facility, concentrations of sodium, chloride, ammonia, and dissolved solids decreased with depth in response to advective and convective dispersion, and leachates also were diluted by rainfall infiltrating the permeable aquifer. At a distance of approximately 0.8 km, the combined effects of dispersion and dilution caused the conservative leachate components to approach steady-state concentrations for the period covered by the nine samplings. Heavy metals, pesticides, and other constituents were filtered or adsorbed by the aquifer materials, or were precipitated near the disposal site.

Effect of sludge application on ground-water quality

According to William Kam, the land application of anaerobic-digested domestic sludge with 5 percent solids is being tested to determine its effects on ground-water quality in New Jersey. Three different soil-type sites were subdivided into 12 plots of 0.1 ha each. During three growing seasons, each plot received a different application of sludge at annual rates ranging from about 22,000 to 90,000 kg/ha. After the three growing seasons, contamination of the shallow ground water was occurring under each of the plots and downgradient from the plots. Ground-water monitoring by means of "skim" samples and multiple-depth samples showed that specific conductance fluctuated from a background of less than 45 μmho/cm to about 1,300 μmho/cm for a plot where sludge application was 90,000 kg/ha, to about 1,100 μmho/cm for a plot where sludge application was 45,000 kg/ha, and to about 460 μmho/cm for a plot where sludge application was 22,400 kg/ha. Nitrate and nitrogen concentration fluctuated from a background of about 5 mg/L or less to a high of 100 mg/L for a plot where sludge application was 45,000 kg/ha, and to 38 mg/L for a plot where sludge application was 22,400 kg/ha. Total organic-carbon concentration fluctuated irregularly from a background of about 3 mg/L or less to a high of 42 mg/L for a plot where sludge application was 90,000 kg/ha, to 26 mg/L for a plot where a sludge application was 45,000 kg/ha, and to 50 mg/L for a plot where sludge application was 22,400 kg/ha. Chloride concentration fluctuated from a background of less than 40 mg/L to a high of 300 mg/L for a plot where sludge application was 90,000 kg/ha, to 366 mg/L for a plot where sludge application was 45,000 kg/ha, and to 110 mg/L for a plot where sludge application was 22,400 kg/ha.

Urban water quality

Tests for the presence of 23 different insecticides, herbicides, and industrial compounds in the water and bottom sediment of Sugar Creek downstream from the Bloomington-Normal sewage-treatment plant in Illinois, resulted in 9 positive and 14 negative determinations, according to B. J. Prugh, Jr. The compounds found included chlordane, dieldrin, and heptachlor epoxides, in addition to PCB and polychlorinated napthalenes. The pesticides are apparently coming from nonpoint-source agricultural runoff above the urban area; the industrial compounds appear to be entering the creek from unknown sources above the sanitary plant and through the plant outfall. The concentrations of dissolved iron and manganese in the creek below the sanitary treatment plant are lower than the normal background levels of other streams in this part of Illinois; the boron concentration was found to be higher than that in other streams.

Abatement of nitrate contamination

High concentrations of dissolved nitrate in the ground water in the Redlands area of California threaten public water supplies. Dissolved nitrate-nitrogen concentrations in water from wells, which frequently exceed 10 mg/L, are attributed to the historic application of excessive quantities of commercial nitrogen fertilizer on citrus crops. J. M. Klein reported that USGS investigators made an appraisal of the hydrologic system in the vicinity of an important public-supply well field. Such an appraisal will aid in an attempt to reduce the concentration of dissolved nitrate pumped from a large-capacity well (233 L/s). Chemical and physical data obtained from a series of independent pumping tests concluded in the well field and conceptual models developed by L. A. Eccles and W. F. Hardt in previous investigations showed that the highest concentrations of dissolved nitrate are in an upper zone of saturation. Therefore, when a packer was installed at a depth to coincide with a thick clay deposit and the pump was reset below the packer, the dissolved nitrate concentration in water produced from the well was reduced from 20 to 4 mg/L, while the well yield was reduced only 30 percent.

Variations in water quality result from land use, climate, and physiography in the Susquehanna River basin

On the basis of preliminary results of statistical analyses of 94 drainages in the Susquehanna River basin in New York, Pennsylvania, and Maryland, D. J. Lystrom found that variations in some water-quality parameters can be explained by multiple linear-regression techniques. This methodology relates water-quality parameters to land use and climatic and physiographic characteristics. Results of multiple-regression analyses indicated that total dissolved-solids loads and average concentrations of total nitrogen are significantly affected by urbanization and agriculture. The multiple-regression equations can be used to estimate background water quality by hypothetically setting man-affected basin variables (percent of urbanization and agriculture) at zero. Preliminary analyses showed that total dissolved-solids loads and average total-nitrogen concentrations observed for developed basins are several times greater than estimates of background values.

Quality of water in the Red River of Louisiana

The upper Red River drainage basin in Louisiana contains extensive natural salt deposits. The salt deposits and brine releases from petroleum operations have served as major sources of sodium and chloride contamination. R. F. Martien reported that the effects of abatement techniques put into practice in the early 1960's can be seen in water-quality changes in the lower Red River at Hosston, La. From 1958 to 1967, the sodium and chloride concentrations were equal to or less than 68 mg/L and 105 mg/L, respectively, 50 percent of the time. From 1968 to 1975, concentrations of sodium and chloride were equal to or less than 42 mg/L and 72 mg/L, respectively, 50 percent of the time, a significant reduction from the earlier period.

Chloride concentrations in ground water in Massachusetts

L. R. Frost, Jr., and S. J. Pollock reported that chloride concentrations, caused by applications of sodium and calcium chlorides to highways, were observed in ground water at various distances from the edges of highways at sites having different geologies, hydrologies, and highway drainage features. At Chelmsford, Mass., a site in sand and gravel deposits with little diversion of highway runoff had an average chloride concentration (1975–76) of 219 mg/L approximately 305 m from the edge of the highway. At Wayland, Mass., a site in sand deposits where there were curbings and a raised shoulder, average chloride concentrations (1972–76) declined from 220 mg/L at 14 m from the edge of the highway to 15 mg/L at 35 m from the edge of the highway. At Andover, Mass., a site in glacial till with no diversion of highway runoff on the downgradient side of the highway, average chloride concentrations (1971–75) declined from 211 mg/L at 69 m from the edge of the highway to 71 mg/L at 102 m from the edge of the highway. The effect of geology seems to be significant—high concentrations of chloride occur at greater distances from the edges of highways in the more permeable materials.

Chloride-and nitrate-ion concentrations mapped in a valley-floor glacial aquifer near Cortland, New York

Ground-water investigations conducted by William Buller, W. J. Nichols, and J. F. Harsh revealed that near Cortland, N.Y., there are anomalous areas with high chloride concentrations in the valley-floor aquifer. Chloride concentrations in these areas range from 40 to 70 mg/L., about three times higher than the average background concentration in the aquifer. Although road salt is thought to be the major source of the chloride, one anomalous area is associated with a housing development serviced by septic-tank systems. Another anomalous area may result from leakage from municipal sewer lines, road salting, and septic-tank effluent. Nitrate concentrations are moderately elevated in the ground water; they range from 2 to 5 mg/L and appear to be caused by nitrogen compounds used in farming and lawn fertilizing and by sewage effluent. Apparently, in wet years, input and outflow of chloride and nitrate are about equal.

ENVIRONMENTAL GEOCHEMISTRY

Geochemical survey of the western energy regions

Three years of work in the coal-bearing regions of the northern Great Plains and Rocky Mountains resulted in the provisional establishment of regionally useful geochemical baselines in 17 near-surface ("landscape") materials (Connor, Keith, and Anderson, 1976; Tidball and Ebens, 1976; U.S. Geological Survey, 1976b). These results are based on 25 independent field studies of regional scope in the Powder River basin, the northern Great Plains, and the oil-shale region of Colorado, Wyoming, and Utah. Baselines were established for as many as 45 elements in rocks, soils, sediments, waters, and plants, although the element suite varies from material to material and only partial data are currently available from many of the studies.

The materials studied in the Powder River basin include sandstone and shale of the Fort Union Formation, surface and subsurface soil, sediments of the Powder River, and sagebrush, lichen, and grass. Rocks of the Fort Union, surface and subsurface soil, and stream sediments were also collected in the northern Great Plains, as were wheat and shallow ground water. In the oil-shale region, soils were collected from Colorado, stream sediments from Colorado and Utah, and sagebrush from Wyoming.

Adjuncts to this regional work included attempts to measure geochemical change in landscapes disturbed by activities related to energy production. J. A. Erdman and R. J. Ebens examined the geochemistry of spoil material at eight strip-mined areas (both reclaimed and abandoned) in the northern Great Plains and found that the average concentration of a number of elements (including F, Hg, U, Li, and Th) nearly equals or exceeds the probable maximum concentration expected in nearby native surface soil at one or more of the mined areas studied. The geochemical impact observed on vegetation growing on mined spoils includes average copper-to-molybdenum ratios in sweetclover of 1.5 in comparison with an optimum for forage of 7 or more and increased concentrations of Cd, Co, F, U, and Zn in wheatgrass in comparison with controls. In addition, B. M. Anderson, J. J. Connor, J. R. Keith, and L. P. Gough demonstrated vegetation impacts around two coal-fired electric generating plants. These effects include elevated concentrations of selenium in both sagebrush and lichen near the Dave Johnston powerplant in Wyoming and in grass near the Four Corners powerplant in New Mexico. Also, strontium was elevated in all three vegetation types at "close-in" sampline sites, and iron was elevated in lichen and in grass at the "close-in" sites.

Oil-shale geochemistry

W. E. Dean (USGS) estimated abundances for 27 major, minor, and trace elements in oil shale of the Green River Formation of Colorado, Wyoming, and Utah (U.S. Geological Survey, 1976b, p. 48–56). The estimates were based on examination of more than 700 analyses drawn from a variety of sources, many of them unpublished. Primary emphasis in this compilation was placed on seven elements (Cd, As, Sb, Hg, Se, F, and B) that have been the focus of attention in predevelopment baseline environmental assessments in the prototype oil-shale lease areas of Colorado and Utah.

In addition, Dean and C. D. Ringrose and R. W. Klusman (Colorado School of Mines) established provisional geochemical baselines for 37 major, minor, and trace elements in soils of the Piceance Creek basin, a major oil-shale area of western Colorado (U.S. Geological Survey, 1976b, p. 101–111). Five elements (Fe, Be, Cu, Li, and Zn) exhibit statistically significant regional trends across the basin, increasing from north to south. Comparisons of element concentrations in these soils with concentrations in oil shale suggest that oil shale tends to contain substantially higher concentrations of As, Hg, and Se and slightly higher concentrations of F, Li, and Mo. This suggests that any land reclamation in the Piceance Creek basin using spent shale or overburden as fill could induce an increase in several of the potentially toxic trace elements in the near-surface environment.

Urban geochemistry

H. A. Tourtelot, in a continuing study of trace-metal accumulations in urban areas, found that higher concentrations of As, Cu, Pb, Hg, Sn, and Zn appear to be consistently associated with areas in which commercial and technological activities are most intense. Although explicit technological sources for these elements cannot be explicitly recognized yet, technologically produced metal-bearing particulate matter and normally occurring particulate matter onto which aerosols can be adsorbed may be the chief mechanism of transport. Washout by rain and snow carry the particulate matter to the ground where it becomes incorporated in the surficial material. Thus local meteorological patterns have certainly influenced the distribution of these metals.

In another urban-oriented study, J. A. Erdman and H. A. Tourtelot (1976) investigated the geochemical impact of using liquid sewage sludge in agricultural practices. Sludge from the Metropolitan Denver Sewage Disposal District No. 1 was added to a Truckton loamy sand near Watkins, Colo., at rates equivalent to 0, 44, 90, and 123 t/ha (dry-weight basis) to assess its effect on dryland production and the element composition of hard winter wheat (*Triticum aestivum* L. cv. Wichita). Yields from the 1974 crop increased significantly ($p < 0.05$), from from 1,132 L/ha for the control plots to 1,915 L/ha for each group of treatment plots; also, a highly significant increase ($p < 0.01$) in the protein content resulted from the sludge additions. The mean for the control plots was 12.7 percent protein, and the mean for the treated plots was >15.2 percent. These obvious benefits must be weighed, however, against highly significant increases in the amounts of cadmium, nickel, and zinc in the grain. Concentrations of these heavy metals in all samples from the treated plots exceeded the central 95-percent expected ranges, which were based on a suite of 12 wheat samples collected across the northern Great Plains. Manganese and selenium also increased significantly in samples from the sludge plots, but the concentrations of selenium were within the range expected in wheat. An additional geochemical impact was a highly significant increase in the amounts of mercury, silver, copper, and zinc and a decrease in pH in soils from the treated plots.

Vertical variation in saprolite

G. W. Leo, M. J. Pavich, and S. F. Obermeier are conducting a study of saprolite overlying Piedmont rocks including pelitic schist, metagraywacke, granite, diabase, and serpentinite in Fairfax County, Virginia. Sampling was done by core drilling to produce relatively undisturbed and complete samples from surface to fresh bedrock, and investigations covered petrography, texture, clay mineralogy, and chemistry in addition to engineering properties such as shear strength and compressibility.

Geochemical changes in each rock type follow generally predictable trends from fresh rock to soil profile. All rocks show relative losses of sodium, calcium, magnesium, and ferrous iron and an increase in water; the exception is serpentinite, in which calcium and sodium increase and water decreases. Chemical variations are most pronounced and regular for mafic and ultramafic rocks and least pronounced for schist and metagraywacke. Clay minerals in granite, schist, and metagraywacke saprolite are kaolinite, dioctahedral vermiculite, interlayered micavermiculite, and minor illite. Gibbsite is locally developed near the surface in schist saprolite.

Standard-penetration test data for the upper 7 m of saprolite over schist and metagraywacke suggest alterations between stronger and weaker horizons that probably reflect variable lithology, including quartz lenses. Results for granite saprolite are more consistent but indicate lower strength. The engineering behavior of diabase saprolite is controlled by a dense, plastic, near-surface clay layer (montmorillonite and kaolinite) overlying gruslike weathered rock; the engineering behavior of serpentinite is controlled by a very thin weathering profile.

LAND SUBSIDENCE

Studies by C. R. Dunrud on the effects of subsidence, including coal-mine subsidence in Utah, Colorado, and Wyoming, and a recent reconnaissance study of subsidence caused by solution mining of salt in eastern Texas, indicated that a comprehensive subsidence program is needed within the USGS to effectively respond to geologic hazards included under the Disaster Relief Act of 1974 (Public Law 93-288). The slow lowering or sudden collapse of land surface into cavities or voids created by natural or artificial means and the tensile, compressive, and shear deformations produced by flexure of rocks and soils in response to downwarping constitute a potential hazard to the environment and, in some cases, to life and property.

The sudden subsidence of a street in Grand Saline, Tex., on April 27, 1976, into an abandoned solution salt-mine cavity created during the period 1924–49 and the solution mine subsidences near Hutchinson, Kans., on October 21, 1974, and near Detroit, Mich., in early 1971 are recent examples of types of subsidence that can be hazards to life and property if they should occur beneath structures occupied by people. Pits and cracks caused by subsidence above mine cavities in various mining regions of the United States, solution cavities in karst regions, the effects of fluid removal, and hydrocompaction of rock or unconsolidated material commonly are environmental hazards and, in some cases, could be hazardous to life.

Environmental consequences of open-pit and underground mining

Results of coal-mine deformation studies conducted in the western Powder River basin by C. R. Dunrud and F. W. Osterwald revealed that the effects of past underground room-and-pillar mining were more damaging to the environment and much less productive than current surface-mining activities with adequate land-restoration practices. Surface subsidence features, such as depressions, pits, tension cracks, and compression bulges, as well as underground fires, are a continuing threat to the environment and to land values above mines that were abandoned 25 to 50 years ago. In addition, only 10 to 25 percent of the coal was extracted because the coal beds were too thick to mine with available mining methods. In contrast, surface-mining activities in weak rocks less than 60 m thick commonly extract at least 90 percent of the resource and provide for a more effective and timely restoration of the mined lands than underground mining.

Land subsidence continues in the Houston-Galveston area of Texas

The importation of large supplies of surface water from Lake Livingston has been delayed and subsidence continues in the area between Houston and Galveston as artesian pressures continue to decline, according to R. K. Gabrysch. During 1977, it is expected that deliveries of surface water will be made to all major industries using ground water in the southern part of Harris County. A decrease in ground-water production of about 350 m^3/s, which will allow as much as 35 m of recovery in water levels, is anticipated in the center of the large cone of depression. The possible use of tide gages for monitoring subsidence in the coastal areas is being investigated by the USGS in cooperation with the Harris-Galveston Coastal Subsidence District and the Texas Water Development Board.

Sergio Garza reported that a theoretical investigation of the feasibility of artificially recharging the ground-water reservoir in order to stop subsidence at the NASA Johnson Space Center southeast of Houston has been completed. Hydrologic digital models were developed to determine the quantities of recharge water needed by using a model of the ground-water basin already available. The land surface at the space center was about 4 to 6 m above mean sea level in 1974 and is sinking at an annual rate of more than 0.06 m. Assuming that the regional stresses will remain constant after 1980, Garza estimated that 1 m of local subsidence at the space center can be prevented by an effective and feasible well-injection program. Also, about 0.5 m of local subsidence can be prevented if surface-water importation significantly reduces ground-water pumping.

Compaction measured at Baton Rouge, Louisiana

Three free-pipe extensometers have been installed at a site near the center of pumping and land subsidence at Baton Rouge, La., according to C. D. Whiteman, Jr. The extensometers were designed to continuously record compaction to depths of 254, 518, and 913 m. During the first year of operation, both compaction and rebound were measured. Net compaction for the three depth intervals was 0.013, 0.016, and 0.022 m, respectively.

Semiquantitative analyses of 21 clay samples from the depth interval of 137 to 930 m at the recorder site and 16 clay samples from the depth interval of 125 to 818 m at a site about 5 km to the south indicated that the clays of this area consist predominantly of mixed-layer clays and montmorillonite with minor amounts of kaolinite and illite. The samples also contained an average of about 30 percent fine-grained quartz and minor amounts of potassium and plagioclase feldspars.

Subsidence in New York related to ground-water discharge

Circular areas of land subsidence associated with vents of upwelling, sediment-laden freshwater in the Finger Lakes region of central New York State were investigated by R. M. Waller. Subsidence depressions as large as 100 m in diameter occur along Onondaga Creek in a glaciated valley underlain primarily by proglacial lake deposits. Discharge from the vents varies in time and location and apparently results from water released when the deposits compact. Although subsidence began only in recent years, landowners report that venting has occurred for at least 50 years. Subsidence scarps, some of which are more than 1 m high, are common. A buried petroleum pipeline that has been exposed in the creek bottom in the last 2 years gives evidence of local subsidence in the area.

Solution-type mining of salt from depths greater than 350 m has continued for many years about 3 km upvalley from the areas of subsidence. Also, an abandoned 90-year-old brine well field, with numerous sinkholes and collapse pits, in hummocky terrain resembling glacial kame-and-kettle topography is directly upvalley. Although water discharging from the vents is fresh and the distance between the vents and the mining operations is great, it is possible that the mining operations are causing the subsidence; hydraulic stresses in the saturated glacial deposits can be transmitted considerable distances and may be responsible for the subsidence features.

Hydrogeologic changes in subsidence area of San Joaquin Valley of California

After 40 years of ground-water overdraft, canal imports have generally reversed subsidence trends in most of the San Joaquin Valley of California, according to B. E, Lofgren. In 1976, artesian heads had recovered toward presubsidence levels, and subsidence rates had decreased from an earlier maximum of 0.5 m/yr to near zero in much of the valley. However, increasing irrigation demands, particularly during years of deficient precipitation, pose the threat of increased pumping and another cycle of widespread land subsidence. Because of significant hydrogeologic changes during the 1930-70 overdraft period, the ground-water basin will respond differently during a second cycle of overdraft.

Many permanent changes have occurred in the San Joaquin Valley as a direct result of the 1930–70 ground-water overdraft. The most obvious changes relate directly to the effects of surface subsidence, such as disrupted gradients of natural streams, canals, and drainages.

Other changes, which are less obvious, affect the characteristics of the subsurface ground-water reservoir (Lofgren, 1977). The following three changes are especially important:

- Because of high ground-water levels in 1976, little or no subsidence should occur during a second period of drawdown until pumping levels approach their former lows and preconsolidation stresses are again exceeded.
- When the compressible deposits of the aquifer systems are preconsolidated, both the compressibility and the storage coefficient of the aquifer systems are in the elastic range of stressing rather than in the inelastic or virgin range of prior times. For this reason, water levels will decline much more rapidly during a second cycle of overdraft for a given rate of pumping—possibly 10 to 50 times as fast.
- Because water of compaction is a one-time mining of pore water from the compressible aquifer system, this supply is not available during a second extended period of drawdown. During 40 years of overdraft on the western side of the San Joaquin Valley, the volume of subsidence (water of compaction) was roughly one-third of the total pumpage.

Application of a subsidence model

A one-dimensional mathematical model that calculates idealized aquifer-system compaction and expansion was applied to observed water-level fluctuations at six sites in the Santa Clara Valley of California by D. C. Helm (1977). The simulation of observed compaction and expansion of the confined-aquifer system at these sites was good to excellent. Using independently prescribed values at each site for (1) total cumulative thickness of fine-grained interbeds within the confined-aquifer system, (2) weighted-average thickness of these interbeds, (3) initial distribution of preconsolidation pressure, and (4) average recoverable vertical compressibility of the skeletal matrix, Helm estimated model values for vertical components of hydraulic conductivity, (K') and nonrecoverable compressibility (S'_{skv}) by trial-and-error fitting of calculated compaction history to observed compaction history. Estimated values for K' ranged from 1.7×10^{-7} to 3.8×10^{-6} m/d; those for S'_{skv} ranged from 4.6×10^{-4} to 4.3×10^{-3} m^{-1}. Helm (1976) found that although simulation improved greatly when model parameter values were allowed to vary as functions of calculated preconsolidation pressure, he concluded that constant values for two sites in the Santa Clara Valley can be used for at least 50 years.

Future compaction (subsidence) can be predicted for a prescribed stress history (projected water-level fluctuations) by using carefully corroborated model parameter values. Subsidence of as much as 4 m occurred in the Santa Clara Valley from 1916 to 1970. Water levels started rising during the mid-1960's, and, by the late 1960's, subsidence rates had diminished to near zero. According to the subsidence model, if water levels at the sites studied are returned to and held at their mid-1960 historical lows, additional residual subsidence of as much as 3.1 m can be expected. The degree of confidence of prediction depends on the appropriateness (uniqueness) of estimated model parameter values (Helm, 1977).

Land subsidence stopped by artesian-head recovery in Santa Clara Valley of California

After 50 years of declining ground-water levels and widespread subsidence in the Santa Clara Valley of California, artesian water levels began a rapid recovery in 1966, according to J. F. Poland. From 1916 to 1966, generally deficient rainfall and runoff in the San Jose area was accompanied by a fourfold increase in ground-water withdrawals. In response, the artesian head declined 55 to 75 m, and the land surface subsided as much as 4 m. Subsidence affected an area of about 650 km^2 in the southern part of the valley.

For several sites in the valley, compaction records were plotted against the change in artesian head to provide field-based stress-strain diagrams. These plots indicated that, in the elastic range of stress, the component of average specific storage contributed by deformation of the aquifer-system skeleton (or parts thereof) ranges from 6.6×10^{-6} to 16×10^{-6}m^{-1}. Extensometers furnished proof that the rise in artesian head in the confined aquifers was large enough to equal or exceed the excess pore pressures in the aquitards, and thus compaction and subsidence had stopped. Subsidence will recur in the future if the artesian head is drawn down appreciably below the 1974 level.

Subsidence in the Savannah area of Georgia

G. H. Davis and H. B. Counts (USGS) and S. R. Holdahl (NOAA) (1977) reported that land subsidence in downtown Savannah, Ga., is continuing at the rate of 4 mm/yr despite a cessation, since 1963, of artesian-head decline. Moreover, the subsidence bowl is spreading outward from the Savannah area. New releveling data confirm that the subsidence is being caused by the slow drainage of poorly permeable beds in the Tertiary limestone aquifer system and the overlying Hawthorne Formation (Miocene). Apparently, a threshold stress equivalent to 15 m of head decline is required to produce major subsidence in the Savannah area.

Faulting caused by ground-water extraction

According to T. L. Holzer and B. E. Lofgren (USGS) and S. N. Davis (University of Arizona), an active normal fault with more than 0.4 m of offset and a trace exceeding 11 km in length has formed since 1961 near Picacho, Ariz., because of ground-water overdraft. The fault crosses Interstate Highway 10 on the eastern margin of the Eloy-Picacho subsidence bowl where as much as 3.5 m of subsidence, which resulted from ground-water-level declines locally exceeding 90 m, has occurred since 1934. Faulting is restricted to the alluvial basin.

Although earth fissures related to pumping overdraft occur in numerous areas of Arizona, California, Nevada, and Utah, the Picacho fault is the only area where measurable vertical offsets have been recognized. The association of this modern surface feature with a subsurface bedrock fault has not yet been demonstrated. Precise measurements of horizontal and vertical displacements across about 25 fissures, principally in central Arizona, are continuing.

A major recovery of artesian head from 1966 to 1975 was due to several causes:

- The average precipitation was 13 percent above normal.
- Imports of surface water to the valley increased from 77.7 hm^3 in 1965–66 to 182 hm^3 in 1974–75.
- Average yearly pumpage decreased 19 percent from 228 hm^3 in 1960–65 to 185 hm^3 in 1970–75.

Furthermore, from 1970 to 1975 an average of 51.3 hm^3 of imported water was diverted yearly to stream channels for direct recharge to the ground-water reservoir. In effect, this recharge reduced the net yearly withdrawal to roughly 133 hm^3, 42 percent below the average gross pumpage of 1960–65. Measurements of compaction of the confined aquifer system obtained from extensometers demonstrated the marked decrease in compaction rate that followed. In San Jose, annual compaction decreased from 30 cm in 1961 to 7.3 cm in 1967 and to 0.3 cm in 1973. Net expansion (land-surface rebound) of 0.6 cm occurred in 1974 (J. F. Poland, 1977).

ASTROGEOLOGY

PLANETARY STUDIES

In 1976, man for the first time placed a spacecraft on Mars. Viking 1 landed July 20, and Viking 2 landed on September 3. USGS personnel were involved in many phases of the mission in both operational and scientific roles. During the search for landing sites at the start of the mission, maps were made of potential sites, data was derived on terrain, radar data of the surface was interpreted, and the scientific merits of different sites were evaluated. After landing, in addition to participating in scientific data analysis, USGS personnel helped in choosing rock and soil samples by providing information about the physical properties of near-surface materials based on photogrammetric evidence.

The first landing was on the western slopes of the large depression Chryse Planitia (22.47° N., 48.0° W.), and the second landing was on the level plains of Utopia Planitia (47.89° N., 225.86° W.) almost 8,000 km east of the first landing site. E. C. Morris (USGS), a member of the lander imaging team, reported that the cameras mounted on the two Viking Mars landers took more than 1,000 detailed photographs that show the Martian surface at both landing sites to be a rocky, boulder-strewn, reddish-orange desert. Many of the rocks that litter the surface at both sites seem to be vesicular and could have been produced either by volcanic processes or by hypervelocity impacts of meteorites. Impact and eolian processes are evident at both sites.

Both lander sites appear to be similar block-strewn landscapes, but, in detail, certain differences show that the small-scale features of these areas exhibit considerable variety and are not everywhere the same. The lander 1 site has an undulating surface with a relief of several meters and locally exposed bedrock. Also present is a spectacular field of dunes or drifts of fine-grained material, scalloped and eroded by Martian winds and having forms reminiscent of those seen in terrestrial deserts. Rocks in the vicinity of the spacecraft exhibit great diversity in brightness, shape, and texture, and many are faceted by the wind. In contrast, the lander 2 site is generally flat with no bedrock exposures or dunes. Individual rocks are monotonous in their vesicular texture and could be part of a blanket of debris ejected from the large 100-km Mie crater that lies about 200 km to the east of the landing site.

H. J. Moore II (USGS), a member of the Physical Properties Team, reported that surface materials between the rocks at both sites are weakly cohesive (10^4 dyn/cm^2) with in-place densities near 1.6 to 1.8 g/cm^3. Drifts are less cohesive (10^3 dyn/cm^2). When surface materials are excavated by the Viking surface sampler, most of them break into clods about 4 cm across. Clods from the drifts are finer than 4 cm. Temperatures of the surface materials reach a high of a few degrees Celsius below zero in the late afternoon. Footpad 2 temperatures at sunrise are near 73°C below zero.

Priestley Toulmin III, H. J. Rose, Jr., and R. P. Christian (USGS), in conjunction with B. C. Clark (Martin Marietta Aerospace), A. K. Baird (Pomona College), Klaus Keil (University of New Mexico), and other members of the Viking Inorganic Chemical Analysis Team, reported that the chemical compositions of fine-grained surface materials at the two Viking landing sites are remarkably similar and suggest chemical weathering products of mafic rocks rather than primary igneous rock material (Toulmin and others, 1976; Clark and others, 1976a; Baird and others, 1976). The materials are very low in alkali elements and in the trace elements strontium, rubidium, yttrium, and zirconium. Aluminum is low relative to silicon and thus suggests the presence of iron-rich aluminum-poor clay minerals. Iron also appears to be present in the ubiquitous red to orange fine-grained material that imparts its characteristic color to the Martian landscape (and sky). Ferromagnetic minerals constitute 3 to 5 percent of the surface fines (Hargraves, Collinson, and Spitzer, 1976; Hargraves and others, 1976). High sulfur content apparently reflects the concentration of soluble sulfate minerals in a weakly to thoroughly cemented surface duricrust, perhaps by a mechanism related to the diurnal cyclic transfer of H_2O between the soil and the atmosphere. Results from the molecular analysis investigation (Biemann and others, 1976; also unpub. data) are consistent with the presence of hydrated minerals and carbonate minerals in the surface samples. The X-ray fluorescence instrument also confirmed the very low content of argon in the Martian atmosphere (Clark and others, 1976b).

The Viking orbiters are equipped with cameras that can photograph the surface at a resolution of approximately 100 m. M. H. Carr, Harold Masursky, and L. A. Soderblom (USGS) reported that, during 1976, the orbiters acquired approximately 7,000 pictures of Mars. They revealed that the planet is more variegated on a fine scale than investigators had supposed previously. Most of the planet has impact crater frequencies comparable to those found on the Moon. Only the large Tharsis shield volcanoes, the polar region, and some channels have significantly lower values, which suggest relatively young ages. Abundant new evidence has been acquired for massive catastrophic floods that appear to be restricted mostly to middle Martian history. Noncatastrophic fluvial activity appears to predate the era of floods for the most part. The morphology of impact crater ejecta on Mars is quite different from that on the Moon and Mercury. The ejecta appears to have moved along the surface as a debris flow after ballistic deposition, possibly as a result of the presence of water. Abundant features, particularly in the northern midlatitudes, suggest that permafrost may have played an important role in landscape evolution. Unconformities in the polar deposits and the paucity of impact craters at the poles suggest climatic changes in the geologically recent past. How these changes are related to the seemingly older climatic changes implied by the fluvial features is not understood.

A technique was developed by Soderblom for deriving a model impact flux history for a planet directly from the planetwide distribution of crater density. Application of this technique shows that the flux histories for the Moon, Mars, and Mercury have been very similar. Additionally, it shows that Mars has had a roughly continuous surface evolution throughout its history, a new surface being created at the rate of approximately 20 percent of the planet's entire surface over a billion-year period. The Moon has had a less active surface evolution (about 15 percent/b.y.), which ceased during the first 1.5 to 2 billion years of its history and has remained quiescent. Mercury has had a resurfacing history similar to that of the Moon but apparently much shorter (less than 1 billion years). These results place important constraints on the initial thermal and chemical conditions of the inner solar system.

LUNAR INVESTIGATIONS

REGIONAL GEOLOGY

STRATIGRAPHY

Chronology of light plains and maria

J. M. Boyce (1976) applied a recently developed crater morphology technique to Lunar Orbiter IV photographs to determine the relative ages of flow units on the lunar nearside maria. He concluded that (1) there were six major episodes of mare emplacement on the Moon; (2) the early model of Boyce, Dial, and Soderblom (1974), which indicated that the ages of the maria decrease westward, is generally correct; (3) three major age units, including the two youngest, were not sampled by Apollo or Luna; and (4) the history of emplacement of mare units is more complex than previously thought.

Basalt stratigraphy in the Crisium basin

J. M. Boyce, G. G. Schaber, and A. L. Dial, Jr. (1977), indicated that the basalts in Mare Crisium sampled by Luna 24 should be about 3.5 ± 0.1 billion years old. Additionally, on the basis of spectral reflectance studies, the Luna 24 basalts should have nearly the same composition as the Apollo 15 basalts.

Light plains around basins

J. M. Boyce and J. A. Watkins showed that the density of craters in the 800-m to 7-km range on upland plains units groups into at least two sets that correspond closely to the density values for the two youngest large impact basins. This work was extended to show that there are at least four upland plains ages. Boyce and Watkins showed that the four sets of plains correspond in age to the four youngest basins with diameters of >600 km. From youngest to oldest, the basins are Orientale, Imbrium, Hombold-tianum, and Nectaris.

Ring moats on mare surfaces

J. M. Boyce and G. G. Schaber (1977) analyzed lunar ring-moat structures and concluded that these features are the surface expression of buried impact craters. They showed that the preservation of ring moats (if it is assumed that the moats are as old as the mare) is inconsistent with current crate erosion models, the cratering record, and the observation that small features erode faster than larger features. Boyce and Schaber concluded that this evidence, coupled with the observation that ring moats often contain rimless pits along their outlines, suggests that these features have formed continuously since surface formation by collapse owing to compaction of blocky, cavernous, buried rim deposits.

STRUCTURE

Tectonism and volcanism on the lunar farside

D. H. Scott found that tectonic and volcanic structures are much less abundant and less prominent on the farside of the Moon than they are on the nearside. Pervasive lineaments are the most common expression of accumulated strain on the farside and follow the same trends (northeast and northwest) as those on the nearside. There is little evidence of volcanic constructs on the lunar farside, and mare basalts are relatively uncommon and confined to areas of low elevations within some craters and basins. No correlation exists between geologic structure and volcanism on the farside, as there is in places on the nearside (Scott, Diaz, and Watkins, 1975). Gravity data show no correlation with structural grids, nor is there a good correspondence between gravity anomalies and large craters and basins (Scott, Diaz, and Watkins, 1977).

Mare ridges

B. K. Lucchitta (1977) studied mare ridges and showed that they are composed of parallel, en-echelon, or branching systems. Most of the ridge segments are located along vertical offsets in the mare surface associated with scarps and monoclinal flexures, the suggestion being that ridges are of structural origin. Ridges follow distinct trends influenced by basin structures, buried craters, and the lunar grid; they are both older and younger than rilles, and secondary craters from Aristarchus and Copernicus are superposed on them.

GEOCHEMICAL AND GEOPHYSICAL REMOTE SENSING

Infrared eclipse temperatures

Exclusive of "hotspots" such as fresh craters, lunar infrared eclipse temperatures sampled along the Apollos 14, 15, and 16 bistatic-radar ground tracks are inversely correlated with albedos, according to H. J. Moore II (Moore and others, 1976). The inverse correlation is related to the thermophysical properties of the sampled surface because albedo cannot account for the temperature differences. There is also a rough direct correlation between the relative ages of surfaces and high-infrared eclipse temperatures. Bistatic-radar roughness measures correlate directly with albedo and inversely with eclipse temperatures. The combined use of these variables, if they are sampled on a Moonwide basis, could be used to subdivide the lunar surface into remote-sensing units.

Synthesis of global data

About 30 lunar scientists were involved in a synthesis of a large body of global lunar geophysical and geochemical data acquired from the Earth and from lunar orbit. L. H. Soderblom reported that the data include (1) maps of γ-ray flux in 20 energy bands used to study the distribution of elements including U, K, Th, Fe, Ti, and Mg; (2) X-ray fluorescence spectra providing maps of the distribution of aluminum, silicon, and magnesium; (3) visible and near-infrared spectral-reflectivity maps (0.4 to 0.8 μ m) providing detailed maps on the distribution of chemically distinct units; (4) maps of remanent magnetism; and (5) maps of gravity and altimetry.

This year's findings include the following:

- The eastern and western maria are generally divisible into two classes; Eastern maria are younger, lower in remanent field, and higher in radionuclides (uranium, potassium, and thorium) than western maria.
- Regional variations in iron, titanium, and magnesium seen in the eastern maria are correlated with color variations. Extremely "red" maria are high in iron, and extremely "blue" maria are likely to be high in iron and titanium.
- Variations in field strength and direction are now recognized among ancient upland provinces.

TERRESTRIAL ANALOGS AND EXPERIMENTAL STUDIES

The Ries Crater of Germany

E. C. T. Chao and J. A. Minkin proposed a model that outlines the cratering phenomenon for the multiring structure of Germany's Ries Crater. This schematic reconstruction conforms to the constraints imposed by geological, geophysical, and petrological observations made by numerous investigators (Chao, 1976) and to the postulated nature of the impacting body (El Goresy and Chao, 1976). Two key observational facts are dominant in the proposed model: (1) The shallow configuration of the geometry of the crater (depth-to-diameter ratio of 1:33), and (2) the predominance of ejecta transported nonballistically under locally high confining pressures.

Critical to the production of a shallow crater is shallow penetration by an impacting body of relatively low density—that is, a stony meteorite rather than an iron meteorite. Lateral, radially outward forces become dominant in this shallow excavation as the impacting body fragments and flows rapidly outward and as a large percentage of the target materials (estimated as 90 percent or more) becomes displaced laterally in a rolling, gliding, cascading, nonballistic motion; much mixing of the ejecta within itself and with local underlying materials takes place during transport. This nonballistic mode of ejecta transport has been named the Wagner mode by Chao in honor of the late G. H. Wagner, who first documented and properly interpreted field evidence of nonballistic ejecta transport at the Ries Crater (Wagner, 1964).

The production of a shallow basin-type crater appears to be genetically related to extensive nonballistic transport of ejecta; if evidence of large amounts of nonballistically transported ejecta is found (Chao, 1976), then the associated impact crater must be a shallow structure, and vice versa. This relationship has important implications for large multiring basins observed on planetary surfaces and is particularly interesting with respect to recent Viking photographs of Mars that show lobate flows of ejecta from impact craters (M. H. Carr, written commun., 1976).

Lonar Crater of India

Laboratory experiments show a correlation between terrestrial impact craters and lunar samples in calibrating shock pressures. India's Lonar Crater is particularly useful since it is in tholeiitic flood basalt similar to that found in the lunar maria. D. J. Milton and coworkers at the University of California (Los Angeles), the Johnson Space Center, and the Geological Survey of India found five progressively more shocked classes having distinctive features (Kieffer and others, 1976). These classes can be subdivided as follows:

- Grains that are fractured.
- Labradorite (partially to totally converted to isotropic maskelynite), pyroxene, and devitrified palagonite (showing undulatory extinction).
- Labradorite (converted to glass that shows some evidence of flow), pyroxene (granulated and appearing to contain sparse, dendritic, titaniferous magnetite crystals possibly along glass lamellae), and devitrified palagonite (partially to totally isotropic).
- Labradorite (melted to a clear, vesiculated glass that has flowed so extensively that the original lathlike shape of the grains is no longer recognizable, pyroxene (visibly melted on their edges and contain skeletal titaniferous magnetite crystals), and devitrified palagonite (isotropic, the implication being that it was revitrified by the shock).
- Labradorite and pyroxene (melted and becoming thoroughly mixed into brown glass with innumerable dendritic crystals of titaniferous magnetite that are dispersed throughout the remaining pyroxene fragments and the melt) and glass (devitrified into spherulites in places).

In samples of Lonar basalt experimentally shocked in a vacuum to pressures between 200 and 650 kbar by a 20-mm high-velocity gun, plagioclase and palagonite show deformation similar to that seen in naturally shocked rocks, but pyroxene does not show optically resolvable edge melting. Comparison of the plagioclase textures in the two sets of rocks gives the following pressures for the naturally shock metamorphosed Lonar basalts: Class 1, $P<200$ kbar; class 2, $200<P<400$ kbar; class 3, $400<P<600$ kbar; and class 4, $P>600$ kbar. Shock pressures in excess of 800 to 1,000 kbar appear necessary to totally melt nonporous basalt.

LUNAR SAMPLE INVESTIGATIONS

PETROLOGY, MINERALOGY, AND CHEMISTRY

Apollo 16 breccia

The large white boulder from which Apollo 16 samples 67455 and 67475 were collected was found by astronauts John Young and Charles Duke near the southwestern rim of North Ray Crater, which is located in the foothills of the Smoky Mountains of Descartes (Muehlberger and others, 1972). The boulder is thought to be an ejecta block that represents a major lithology of the ejecta stratigraphic section penetrated by the North Ray cratering event (Hodges, Muehlberger, and Ulrich, 1973). An interdisciplinary consortium study under the leadership of E. C. T. Chao characterized the suite of major lithic types in this breccia boulder, their relative abundances, and their temperature and pressure histories in order to obtain clues to the source basin and the probable age of the event that transported the boulder to the Apollo 16 site.

Mineralogic and petrologic studies conducted by Chao, Minkin, and Thompson (1977) determined that sample 67455 is a feldspathic breccia whose dominant source materials appear to be anorthositic rocks that contain relatively iron-rich pyroxenes and olivines. The iron-to-magnesium ratios determined by Lindstrom and others (1977) in several subsamples of 67455 are higher than those reported for most other Apollo 16 breccias. The fact that no glass spherules have been observed in this sample supports the assumption that the breccia is probably part of an ejecta rather than a regolith deposit. The composition of the boulder as represented by sample 67455 is distinctive with respect to its high aluminum and calcium contents and the presence of iron-rich olivine (about FO_{50}); thus, it is unlikely that sample 67455 was derived from a source such as Orientale or Imbrium (Chao and others, 1975). Nectaris is therefore suggested as the possible source basin, in agreement with Krahenbuhl and others (1973), who interpreted Nectaris as the likely source of the Apollo 16 cataclastic anorthosites. Of extreme importance in confirming or rejecting this Nectaris hypothesis will be radiometric age determinations made on unannealed glassy clasts found in sample 67455. These glasses are believed to be impact melts formed during the event that placed sample 67455 material as ejecta at the Apollo 16 site.

Apollo 17 breccia

After the Apollo 17 samples were returned, a consortium of investigators from 12 different fields was established under the leadership of O. B. James (USGS) to study an especially significant lunar breccia—sample 73215. The breccia was chosen for such concentrated and coordinated study because superficial examination suggested that it formed as an aggregate of melt and clasts produced during a major impact event, that it cooled rapidly after aggregation, and that it was never significantly reheated. Thus, it appeared that a study of the breccia might afford an opportunity to date a major impact event and to look back through the effects of that event at the nature of the preimpact lunar crust. The results of studies conducted by the consortium confirmed these early tentative suppositions. The major results of all sample 73215 studies as of March 1976 were summarized by James and Blanchard (1976), and the most important results of the petrologic studies carried out in 1976 are outlined below.

Sample 73215 is lithologically heterogeneous, but the various materials that it contains can be divided into two basic categories: (1) Gray-to-black rock and (2) physically separable clast material. Aphanitic rock makes up the bulk of the breccia and encloses the clasts; this aphanite has been termed "matrix" (James and Blanchard, 1976; James, 1976). Similar aphanite also forms distinct clastlike bodies within matrix aphanite and within granulated clastic material. These aphanites all consist of abundant small lithic and mineral fragments set in a very fine grained crystalline intergrowth—termed groundmass—that crystallized from melt (James and others, 1975; James, 1976). The petrologic studies (James, 1976) suggested that the aphanite "clasts" are not true fragments of preexisting rocks but instead are cogenetic with matrix aphanite. The results of Rb-Sr studies (Compston, Foster, and Gray, 1977) and major- and rare-earth-element analyses (Blanchard and others, 1976) supported this interpretation, and James is currently engaged in a collaborative age-dating study with H. W. Muller and O. A. Schaeffer (State University of New York at Stony Brook) to confirm this hypothesis.

The petrologic studies were also used to set limits on the cooling history of the bulk breccia (James, 1976). The bulk aggregate of melt and clasts equilibrated immediately after mixing at a temperature of $\leq$1,000°C (a limit set by the presence of unmelted clasts of granitic composition). Clasts of magnesian olivine show marginal iron enrichment caused by diffusive exchange of iron and magnesium with melt-derived groundmass during postaggregation cooling. From the nature of the compositional gradients, it can be calculated that, if the zoning formed at a constant temperature of 1,000°C, the time required to form the zoning would have been 5 weeks. Since the zoning probably formed during cooling from a maximum temperature of 1,000°C, the 5-week time is a minimum estimate for postconsolidation cooling.

Detailed petrologic studies are now in progress on four lithic clasts extracted from the breccia for consortium study. Preliminary results were reported by James (1977). Three of these clasts are of anorthositic gabbros—typical of the dominant type of lithic clast in the breccia—and the fourth clast is of felsite (lunar "granite"). The three anorthositic gabbro clasts have similar mineralogies, and their textures form a gradational series, an indication that their parent rocks were genetically related. The data indicate that the rock textures were formed during a high-temperature igneous-metamorphic episode. Age-dating studies conducted by other consortium members (Compston, Foster and Gray, 1977; Jessberger, Kirsten, and Staudacher, 1976) suggested that the date of this episode may be about 4.24 billion years. The felsite consists of fragments of crystalline felsite (a quartz-plagioclase-potassium-feldspar intergrowth) veined and enclosed by brown felsic glass. The petrologic data suggest that the crystalline felsite formed by crystallization of residual liquid in a differentiated igneous body. The brown glass formed by melting of the crystalline felsite just prior to or during the breccia-forming event and was molten during the event. The results of Rb-Sr studies (Compston and others, 1977) and $^{40}Ar/^{39}Ar$ age-dating studies (Staudacher, Jessberger, and Kirsten, 1977) yield an age of 3.90 to 3.92 billion years; this age probably represents the date of the breccia-forming event, possibly the south Serenitatis basin-forming impact (James and Blanchard, 1976).

James is participating in a collaborative age-dating study with Muller and Schaeffer to define more precisely the ages of events in the history of the bulk breccia and its clasts. This study uses the laser-probe $^{40}Ar/^{39}Ar$ method, which permits dating of very small volumes of material located with a petrographic microscope. The first results were reported by Muller and others (1977). This method has dated the melt-derived groundmass separately from the small clasts that it contains at 4.01 billion years. This figure represents an upper limit to age of the breccia-forming event because the groundmass may contain tiny irresolvable clasts that were not completely outgassed. Plagioclase clasts on the order of 0.3 mm across generally show older ages (from 4.10 to 4.17 billion years) and demonstrate that such clasts clearly were not completely outgassed when they were incorporated in the breccia.

Melt inclusions and mare basalt relationships

P. W. Weiblen (University of Minnesota) and Edwin Roedder (USGS) (1976) reported that their analyses of silicate melt inclusions in lunar olivine and chromian ulvospinel showed that the mare basalts are not significantly differentiated relative to the possible compositions defined by the melt-inclusion data. These relationships were shown by computer-derived plots of the inclusion data, normalized to a terrestrial lava composition (that of the 1976 Makaopuhi lava lake in Hawaii) by means of a normalization method similar to the one used in rare-earth-element studies. Such plots were found to be very useful in illustrating variations between major elements in melt-inclusion and bulk-rock compositions, in distinguishing mare basalt types, and in showing the nature of the fractionation needed to obtain, for example, one type of basalt from another.

Distribution coefficients for iron and magnesium partitioning between trapped melt and host olivine and ilmenite were also calculated and show a range of probable equilibrium values. It is suggested that the crystallization sequence (in part metastable?) olivine-ilmenite-plagioclase-pyroxene, defined by the melt-inclusion data, may be the actual sequence that obtained generally for Apollo 11 and 17 mare basalts just prior to eruption.

Reduction of lunar magma by carbon

Motoaki Sato evaluated various proposed theories on the origin of metallic iron in lunar basalts on the basis of measured fo_2 values, Fe^0 and FeO activities, computed gaseous fugacities, textural relations, phase relations involving metallic iron and nickel, and the results of melting experiments under controlled fo_2. He concluded that isochemical models such as valency-exchange models and exsolution from sulfide-metal liquid could be viable only if the lunar magmas had been reduced sufficiently prior to extrusion and would be significant only near the solidus temperature. The isochemical models all fail to explain the origin of metal spherules trapped in early phenocrysts.

Various volatiles-loss models were examined in terms of fugacities of volatile species supposed to have been lost and to have caused reduction. Sato concluded that reduction by carbon is probably the most easily acceptable model, since the fugacity of CO, generated by the reaction of carbon with the melt, could exceed a few hundred atmospheres. Thus, reduction could have been initiated even in a shallow magma chamber. The presence of carbon also would make the sulfur-loss model viable by forming COS, the fugacity of which exceeds that of sodium metal. Otherwise, the loss of sodium vapor and the resulting oxidation of the magma would supercede the loss of sulfur as sulfide and its reduction effect.

Early lunar melting

Recent data obtained by a number of workers suggested that the source region of mare basalts became compositionally closed at 4.42 billion years, presumably some 170 million years after the Moon accreted. Thermal history models indicate that the outer part of the Moon could not have cooled to temperatures low enough to cause closure unless only the outer few hundred kilometers were initially molten. Robin Brett concluded that a total early lunar differentiation is prohibited. The bulk of the Moon was therefore pristine and undifferentiated at the time of mare basalt formation.

ISOTOPIC SYSTEMATICS

KREEP basalt age

Mitsunobu Tatsumoto used a tandem mass spectrometer equipped with an ion-counting system, which was constructed for microsample analyses in the last year, and performed a mineral-grain U-Th-Pb analyses for the quartz monzodiorite clast 15405,88 taken from a boulder at Station 6a during the Apollo 15 mission.

Many, but not all, U-Pb data for lunar rocks fall on a 3.93- to 4.42-billion-year chord on a U-Pb evolution diagram when the Pb data are corrected for meteorite primordial lead. This phenomenon was first observed by Tera and Wasserburg (1972) for P-Pb data obtained from mineral separates of impact-melt rocks 14053 and 14310. They proposed that this 4.42-billion-year age corresponds to the Moon's primary differentiation (Tera and Wasserburg, 1974) and that the 3.9-billion-year age corresponds to a metamorphic event caused by cataclysmic planetesimal bombardments. These ages are valid only if (1) the lead data are correct for the proper initial lead isotopic composition (if the $^{238}U/^{204}Pb$ ratio of the Moon from ~4.57 to 4.42 billion years was low, so that lead could not evolve significantly during this time interval) and (2) the U-Th-Pb systems of the samples evolved simply as two stages and have not been severely affected by more recent events.

Since the 3.9- to 4.42-billion-year chord is clearly defined by Apollo 14, 15, and 17 rocks having a high KREEP component, the 4.42- and 3.9-billion-year concordia intercepts thus appear to represent the genesis of the KREEP parent material and the crystallization time of KREEP rocks, respectively. The study of a quartz-monzodiorite clast in rock 15405 indicates that the rock has had a complex history since its formation. The U-Pb data indicate that rock 15405 has suffered at least two U-Pb system disturbances during the interval 0.6 to 1.5 billion years. These recent events obscure the rock-formation age. If the assumption that the U-Pb systems of multigrained samples were closed during all but one of the recent disturbances is valid, the U-Pb data would indicate that the quartz-monzodiorite clast formed 4.0 ± 0.1 billion years ago. Although the 4.0 ± 0.1-billion-year age is rather poorly defined because of later disturbances, the age is considered to be more realistic than the 4.45-billion-year upper-intercept age of this clast on a U-Pb evolution diagram that has been corrected for an initial meteoritic contribution.

REMOTE SENSING AND ADVANCED TECHNIQUES

EARTH RESOURCES OBSERVATION SYSTEMS PROGRAM

The Earth Resources Observation Systems (EROS) program supports and coordinates research in remote-sensing applications and conducts demonstrations of these applications within Bureaus and Offices of the Department of the Interior. Significant improvements were made at the EROS Data Center in Sioux Falls, S. Dak., in production scheduling and in reproducing images obtained from aircraft and satellites, as well as in applications assistance and training programs that offer workshops and orientation sessions tailored to needs of foreign and domestic users from various disciplines. The EROS program also operates five other facilities in the United States and the Canal Zone, where assistance in searching for and ordering data via computer terminal and access to data-manipulation equipment and basic remote-sensing literature are available to the public.

The Data Analysis Laboratory at the EROS Data Center serves as a national and international center where Earth scientists and representatives of user organizations can participate in training and applications demonstrations and evaluate techniques for advanced digital image analysis. Techniques of grid sampling and measurements of the accuracy of analysis results were developed, and installation of the preprocessor hardware-software system for the maximum likelihood classifier was completed.

IMAGE PROCESSING TECHNOLOGY

High-resolution film recording system

George Harris, Jr., reported that the EROS Data Center has acquired a laser-beam recording system for the production of images from digital tapes. The recording system, built by the Goodyear Aerospace Corporation in Litchfield Park, Ariz., uses 22-cm-wide black-and-white roll film as much as 76 m long. Two tape recorders are available to input specially formatted CCT's containing image and annotation data. Digital radiance values from the tapes are converted to analog voltages that vary the intensity of an argon laser as it scans an image line. The film is exposed on the surface of a capstan roller on which the normally curved surface of focus is converted to a plane by a special field-flattening lens. A digital lookup table permits the user to specify almost any relationship between digital input value and film density. The laser recorder system now produces a small number of Landsat film images (two to three scenes per day).

Experimental digital enhancement of Landsat images and CCT's

George Harris, Jr., reported that the EROS Data Center is producing a new digitally processed Landsat film product with improved image contrast, finer detail rendition, and greatly reduced striping in comparison with conventional photographically processed images. Digital data entered from a standard Landsat CCT into a Univac 90/30 computer system are first organized into a band-sequential format and then corrected to compensate for the effects of Earth-rotation skew and nonuniform velocity of the sensor's scanning mirror. Image striping is reduced by making digital corrections for the unequal response characteristics of the six Landsat detectors. Corrections are based on the statistics of the whole scene rather than only on the spacecraft calibration data. By using the Image 100 analysis system, the highest and lowest digital radiance values are determined in the scene; to increase the visibility of the significant detail, the digital values are altered by an intensity transformation that stretches the values over the full digital range. An additional operation, known as edge enhancement, is performed to increase the visibility of fine detail in the image. Edge enhancement is achieved by adding a high-pass-filtered image onto the original image. This addition enhances the edge contours of features in the image. Information from the completely processed digital tape is then fed into a laser-beam recorder to generate 1:1,000,000-scale film products.

STUDIES USING COMPUTER-ENHANCED LANDSAT DATA

Computer enhancement of Landsat data for geologic applications

J. V. Taranik (USGS) and C. M. Trautwein (Technicolor Graphic Services, Inc.) (1977) reported that a methodology has been developed for computer enhancement of Landsat MSS data for geologic applications. Analysis of a 1972 Landsat scene of the Goldfield, Nev., area by an interactive multispectral minicomputer determined that parts of playa lakes and snow cover could be assigned maximum brightness levels without significant loss of geologic information. The contrast-enhancement parameters determined through analysis with an interactive computer were used in a general-purpose computer together with algorithms to linearly expand the brightness range of the data to match a 1.6 optical density range of film. Algorithms were also used in the computer process to reduce radiometric striping caused by variations in MSS detector gain and offset and to enhance boundaries between landscape features. A laser-recorder system was used to produce black-and-white first-generation positive transparencies of MSS bands 4, 5, and 7 on 241-mm film; second-generation color-composite transparencies were then produced from the black-and-white images.

More geologic information can be extracted from these second-generation color transparencies by manual image analysis than can be extracted from the sixth-generation standard color products produced from the 70-mm negatives currently furnished to the USGS by NASA. Expansion of the brightness range reduced the effects of atmospheric scattering and permitted closer discrimination of geologic units having subtle variations in reflectance. Reduction in striping permitted better evaluation of landscape features and delineation of smaller patterns. Edge enhancement produced sharper delineation of drainage and landforms but destroyed some of the radiometric uniformity within cover types.

Strip-mine monitoring from computer-enhanced images

J. V. Taranik (USGS), J. R. Lucas (Technicolor Graphic Services, Inc.), and F. C. Billingsley (NASA) reported that both digital and photographic procedures must be used with Landsat data to correctly display a coal strip-mined area in Iowa. Land cover patterns related to strip mining can be lost when the contrasts in Landsat data are enhanced only by an automatic 1- or 2-percent truncation of histograms depicting the frequency of occurrence of brightness values. Multispectral analysis with an interactive computer system must be used to determine which digital numbers may be assigned minimum and maximum brightness values without such loss. A lookup table is then used to distribute the computer-enhanced data evenly over the range of digital numbers that limit the discrete density levels that can be recorded on Kodak 2474 film.

Forest defoliation mapping and damage assessment

W. G. Rohde and G. R. Johnson (Technicolor Graphic Services, Inc.) reported that digital image-processing techniques were used to enhance Landsat CCT data showing hardwood forest defoliation caused by the fall cankerworm (*Alsophila pometaria*), the gypsy moth (*Porthetria dispar*), and the variable oak leaf caterpillar (*Heterocampa manteo*). The enhanced data were printed on film with a film-recording device and interpreted manually. In addition, Rohde and Johnson successfully demonstrated, on the Interactive Display Image Manipulation System at the EROS Data Center, an interactive, controlled clustering technique for deriving, from Landsat CCT data, training-set signatures for use with a maximum likelihood classifier. A procedure to evaluate the likelihood values of each pixel classified was implemented in order to determine how well the training data described the spectral variability of the data. Areas characterized by low likelihood values were identified in the original image. Additional training was performed in these areas, and the revised statistics file was used to classify the data a second time. Pixels from each computer class were then randomly sampled and their geographic location calculated; finally, an interpretation was made to evaluate classification performance. By using this technique, the percentage of correct classifications, standard error, and confidence limits associated with performing a classification on Landsat CCT data were estimated.

VISUAL INTERPRETATIONS OF LANDSAT IMAGERY

Targeting ground-water exploration

J. V. Taranik (USGS) and C. M. Trautwein (Technicolor Graphic Services, Inc.) (1976) reported a methodology for using multidate Landsat images to target ground-water exploration in an area near Tucson, Ariz. Landsat band-7 imagery acquired in December was selected because low-sun-angle (28°) illumination enhances the delineation of bedrock areas, linear features, and drainage texture. A Landsat color composite taken in April was also analyzed because phreatophytic vegetation can be easily identified at that time of year. An interpretation of geohydrologic conditions in the Tucson basin was made from an analysis of these landscape features, and an exploration plan was developed from a geohydrologic model that partially explains surface-water movement and ground-water recharge, flow, storage, and discharge.

Geologic investigation in the Black Hills

J. V. Taranik (USGS) and K. L. Pan (University of Iowa) completed a preliminary geologic interpretation of the Black Hills of South Dakota and Wyoming from an analysis of landforms, drainage, and cover types on Landsat images at a 1:250,000 scale. Four geomorphic units were identified: asymmetric ridges, a peripheral valley, a peripheral plateau, and a central irregular surface. Twenty-one landform subunits were delineated on the basis of differences in tone, texture, and shape. The analysis of drainage revealed that the Precambrian core has angular drainage patterns and a relatively low drainage density, while the areas surrounding the core have subparallel to dendritic patterns and a higher drainage density. Two major types of vegetative cover are present in the Black Hills: coniferous forest and grassland. Grassland is present in areas where coniferous forest cannot develop because either soil moisture is lacking or surface materials are unstable.

Five major lineaments displayed on the images were interpreted as zones of major structural weakness, which may have localized mineral deposits. The azimuths of 800 linear features mapped in Precambrian and Phanerozoic rocks can be divided into three groups. The first group trends dominantly north-south, the second trends N. 45° E., and the third trends N. 15° W.

A brief field trip to the Pringle area of South Dakota revealed an extensive zone of fracturing and solution-collapse features in Paleozoic limestones along the lineament trend, although the vertical displacement was minor. Linear features mapped from images of Precambrian terrane east of the Pringle area are alined with the general trend of lineaments in the Pringle area itself.

Late Wisconsinan deglaciation of the northern Midwest

J. R. Lucas (Technicolor Graphic Services, Inc.) and J. V. Taranik (USGS) (1977) determined that Landsat images taken in late April and early May best display landscape patterns resulting from continental glaciation in the Midwest. A false-color mosaic of 75 springtime scenes covering North and South Dakota, Nebraska, Minnesota, Iowa, Wisconsin, and parts of Montana and Illinois was constructed at a 1:1,000,000 scale. The most striking features displayed on this mosaic were arcuate patterns formed by hill and valley topography, stream drainages, differences in unconsolidated material and vegetative cover, and chains of lakes. Some of the larger lakes were elongate in shape and paralleled the trend of the arcuate patterns. Mapping of three arcuate patterns indicates that they form larger patterns of lobes. These lobate patterns may be nested, and the most prominent show a noticeable periodicity in their decrease in size.

The nested series of lobate patterns suggests stillstands of the last continental ice mass that receded from the north-central United States beginning about 14,000 years ago. At least 17 major cycles of retreat must have occurred between Des Moines, Iowa, and the northern end of the Prairie Coteau—a distance of 550 km—and 11 more cycles occurred between the northern end of the Prairie Coteau and the Canadian border. The spacing of the nested lobate patterns suggests periodic climatic variations in temperature and precipitation.

In two areas in Iowa where lobate patterns were difficult to map, the largest pattern was extrapolated along an arcuate trend across what has been mapped as the Iowan surface and Tazewell Drift. Apparently, Wisconsinan materials were deposited in this area during the last major ice advance but were later stripped away by fluvial erosion that exposed older glacial deposits. An understanding of the positions of the stillstands of the continental ice mass as it retreated from the north-central Midwest is pertinent to the targeting of exploration for deposits of sand and gravel and for ground water.

COMPLEMENTARY USE OF LANDSAT DATA AND AERIAL PHOTOGRAPHY

Pacific Northwest Demonstration Project

D. R. Hood reported that the Pacific Northwest Regional Commission, NASA, and the USGS are cooperating in a five-phase project to determine the usefulness of Landsat data for regional resource inventory, planning, and management in Oregon, Washington, and Idaho. Approximately 90 State and local personnel are involved in the project, which represents about 45 State agencies, regional councils, and local units of government. Work on Phases I and II has been completed; work on Phase III is about 60 percent complete.

During Phase I, a set of map overlays for the entire area was produced at scales of 1:250,000, 1:500,000, and 1:1,000,000 displaying (1) land use and land cover obtained by photointerpretation of Landsat imagery; (2) soils information at a level consistent with the Level I land use and land cover data; (3) drainage basin location and extent; (4) private, State, and Federal land ownership; and (5) energy-related features (for example, major ports and refineries, petroleum and natural gas pipelines, and powerline corridors).

Phase II of the project introduced interested State and local personnel to the use of remotely sensed data acquired by aircraft and satellites. The combination of formal classroom training and actual examples of remote-sensing products from selected test sites allowed regional personnel to determine whether further involvement in the project was desirable.

Phase III is the primary demonstration technology-transfer phase of the project (Gaydos and Newland, 1976; Nichols and others, 1976; Aggers and Kelly, 1976; Packer, 1976; Draeger, 1976). Digital analysis of Landsat data is being conducted to determine its usefulness to disciplines such as agriculture, forestry, rangeland management, urban planning, and noxious weed control.

South Dakota Cooperative Land Use Demonstration Project

The South Dakota State Planning Bureau and the EROS Data Center are cooperating in a project to incorporate statewide land use inventory data into a geographic system being developed by the State. System and user documentation was prepared for the State's Landsat digital analysis and mapping system (Tessar and others, 1976; Tessar, 1976a). High-altitude aircraft images of selected urban areas were acquired and are being used to verify the results of digital analysis of Landsat data and to extend the land cover inventory to Level III in the urban areas. Operational applications of the system to date include a surface-water inventory and a map of the Cheyenne River Indian Reservation in South Dakota which are providing information that will increase the carrying capacity of grazing lands, and the incorporation of soil survey, terrain, and census data for two counties into the State's geographic-information system. These data are being used by the District Planning Office for a variety of projects, including Section 208 Water Quality Planning (Tessar and Eidenshink, 1976; Tessar, 1976b).

Red River flood analysis

J. V. Taranik and G. K. Moore (USGS) completed an analysis of the 1975 Red River flood using USGS stream-gaging data in conjunction with images obtained from aircraft and satellites. The boundary of overbank flood inundation was mapped at a 1:24,000 scale on USGS 7.5-min quadrangle maps by using stream-gage readings taken on July 10 and 14, 1975, along the Maple, Sheyenne, and Red Rivers in North Dakota and Minnesota. Boundaries of inundation mapped from images obtained from aircraft and satellites coincided with flood boundaries shown on the maps in areas where natural drainage was not disrupted by manmade structures. Where the boundaries did not coincide, either (1) the natural drainage was disrupted, (2) the main tributaries had well-developed natural levees adjacent to an underfit stream in the ancient glacial lake bed, or (3) the mapped boundaries were complex because of low-stream gradients and subtle topographic differences in the lake bottom. This preliminary analysis showed that the distribution of effects of the flood on crops depended for the most part on the location and amount of rainfall that occurred during the flood.

W. G. Rohde (Technicolor Graphic Services, Inc.), J. V. Taranik, and C. A. Nelson (Technicolor Graphic Services, Inc.) (1976) reported that interactive digital multispectral analysis techniques were used to inventory and map the effects of flooding on agriculture. Landsat CCT data for an area covering 609,208 ha in the Red River Valley of North Dakota and Minnesota were analyzed.

In order to classify the Landsat data, a controlled clustering technique was used to derive training-set statistics for use with a maximum likelihood classification algorithm. Evaluation of initial results indicated that the classification of older residential areas had been confused with the classification of agricultural land that was partially inundated. Fallow agricultural fields and fields recently plowed and planted were also misclassified as inundated. The Landsat image was then manually analyzed to delineate three environmental strata: urban areas, crop land affected by flooding, and crop land not affected by flooding. Data were stratified in order to minimize multispectral variations related to land cover and flood inundation. Strata boundaries were plotted on USGS 1:24,000-scale maps, digitized, and subsequently registered to the Landsat CCT data. Thirty-five control points were selected to develop a transformation that registered the digitized strata boundaries to the Landsat CCT data with a mean residual error of less than 0.5 pixel. The maximum likelihood classification algorithm was again used to classify all pixels within each stratum. Evaluation of the classification accuracy of the Landsat analysis indicated that stratification prior to classification increased classification accuracy by 5 to 10 percent.

A multiphase sampling design based on double sampling with regression was used to estimate the number of hectares of agricultural land affected by flood conditions. A sample unit grid with each sample unit equal to 725 ha was superimposed on the classification results. An estimate of the sample size was based on the expected correlation between measurements made at each phase and the cost ratio of obtaining an estimate at each phase. To achieve an estimate with an accuracy of plus or minus 10 percent at the 0.95 probability level, 200 Landsat plots and 30 photographic plots were selected for measurement. The measurements made on the photographic plots were used to develop a regression coefficient to adjust the estimates made from the Landsat classification. By using this procedure, it was estimated that 379,167 ha (sampling error, 4 percent) of agricultural land were affected by flood conditions—236,835 ha of crops were completely destroyed (sampling error, 6 percent) and 148,020 ha of crops were partially destroyed (sampling error, 5 percent).

This procedure was developed to assist in the rapid assessment of flood damage to agricultural lands for Federal disaster assistance and crop insurance programs.

Impact of strip mining on range resources and wildlife habitat

D. M. Carneggie (USGS) demonstrated the usefulness of remote sensing for assessing the impact of phosphate strip mining in southeastern Idaho on wild-land vegetation resources (D. M. Carneggie and C. S. Holm, 1976). Vegetation cover maps were prepared for the Upper Blackfoot watershed (1,035 km^2) by applying manual analysis techniques to small-scale (1:120,000) color-infrared aerial photographs and a Landsat color-composite image. Nine cover types, including seven vegetation categories, were mapped on the Landsat image and verified by using the small-scale color-infrared aerial photographs, an effort requiring only 1 man-day. Thirteen cover types suggested by the Idaho State Department of Fish and Game were mapped by using enlarged color-infrared aerial photographs. Seven man-days were required for verification of the mapping. Because of the high resolution of the aerial photographs, they were very useful in assessing the impacts of strip mining, such as the disturbance of plant communities, the presence of existing or potential erosion, the construction of settling ponds, the building of pits and dumps, and the jeopardizing of aquatic environments. Aerial photographs taken on four dates between 1963 and 1975 were used to monitor the rate of disturbance and the type and location of areas disturbed by strip mining.

Digital analysis of Landsat CCT's was used to generate cover maps and to detect changes caused by strip mining. By applying ratioing techniques to Landsat data obtained on two different dates, new roads, recently clear-cut forest, and new pits and waste dumps were readily detected. It was concluded that Landsat CCT's provide an efficient means for detecting the location of changed features; however, high-resolution photography or ground surveys are still required to verify the types of change and their impacts on the environment.

Analysis of Landsat images of Claunch, New Mexico, and vicinity

W. A. Fischer began a multidisciplinary study of a relatively unexplored area near Claunch, N.Mex., whose geologic setting suggests undiscovered water and mineral resources. Landsat imagery, high-altitude aerial photography, aeromagnetic data, and existing geologic information are being used to assess the area's potential. Fifty-six multidate Landsat images of the area were recorded on the ISI–170 image analysis system at the EROS Data Center to make a time-lapse movie showing 4 years of temporal changes and surface dynamics. An image representation of the aeromagnetic data is being prepared in the USGS laboratory in Flagstaff, Ariz., for visual integration with Landsat data to provide a composite view of the surface and subsurface as an aid in mineral exploration.

Natural-resource and land use inventory of the Grand Valley project

The EROS program is supporting a study being done by R. L. Hansen (Bureau of Reclamation) to establish an in-house capability for a computer-assisted resource analysis of the Grand Valley project in the Grand Junction area of western Colorado. Data available include regular ground measurements of selected training fields at the time of Landsat overflights, large-scale color-infrared aerial photography, multidate Landsat CCT's, and ground reference data available from the Bureau of Reclamation's Irrigation Management Services study. These data will be used to conduct a crop inventory of irrigated lands using interactive hardware provided by the University of California. Analysis and reporting of results of the Grand Valley inventory have begun.

Interactive computer hardware and software needs were based on recommendations made by the University of California. The Department of the Interior has approved the purchase of a complete interactive computer system for image analysis, which will be used in a wide variety of resource surveys at the Bureau of Reclamation's Engineering and Research Center in Denver, Colo.

Geological and geophysical remote sensing in Iceland

As part of a research project to establish that remotely sensed data from aircraft and satellites can be used effectively to monitor dynamic environmental phenomena, R. S. Williams, Jr., reported that Landsat images of Iceland's Vatnajökull icecap, computer-enhanced by the California Institute of Technology Jet Propulsion Laboratory (JPL), were prepared using contrast-stretch and ratioing techniques to delineate very subtle topographic features on the surface of the icecap. The fall image (sun angle of 25°), under the JPL enhancement technique, is similar to the winter image (sun angle of 7°).

Additional research was done on the analysis of aerial thermography, aerial photography, and satellite imagery (Landsat and NOAA) of the geothermal areas of Iceland. A comprehensive bibliography of the geological and geophysical literature on Iceland is nearly complete.

Research on the use of Landsat CCT's to map the vegetative cover of Iceland produced mixed results. Although gross patterns of vegetative cover and some species delineation could be achieved with the Image 100 analysis system, the variation in substrate and percentage of vegetative cover made the use of spectral parameters as a basis for classification rather ambiguous. It was also determined that herbage must occupy an entire Landsat pixel or approximately 15 percent of an aerial photograph in order to be mapped. Thus, an area could be mapped as barren even though herbage is present in as much as 5 percent of the total area.

DIGITAL ANALYSIS OF LANDSAT DATA

Integrated mapping of terrain

C. J. Robinove investigated the feasibility of integrated mapping of terrain using Landsat images of Australia and the United States. A report on the Australian studies (Robinove, unpub. data, 1976) indicated that land systems maps of part of Queensland can be made largely by digital classification of Landsat images. The Australian philosophy of land systems mapping and the use of Landsat images are now being extended to terrain mapping in the eastern Mojave Desert of California.

Inventorying and mapping kelp and eelgrass, Oregon and Washington coasts

In an EROS-funded project, R. O. Weaver (U.S. Fish and Wildlife Service) used Landsat imagery, digital data, and the facilities of the Data Analysis Laboratory at the EROS Data Center to locate, map, and inventory eelgrass and kelp along the Oregon and Washington coasts. The initial effort included the use of the Image 100 analysis system, but identification of kelp was difficult, primarily because only small areas of kelp were exposed and, hence, available for training purposes. Eelgrass was readily identified when it was present above tidewater but not when it was submerged. However, sparsely and densely populated eelgrass beds could be differentiated from each other, and preliminary comparisons of Image 100 data with information provided by ground transects are encouraging.

Landsat investigation of mineral resources of the Andes Mountains

Evaluation of the application of Landsat imagery to geologic mapping and studies of temporal phenomena by W. D. Carter and W. S. Kowalik focused mainly on the salars of the Andes Mountains, primarily in northern Chile and southern Bolivia. Automated analyses of CCT's on the Image 100 analysis system were successful in subdividing the features of the Salar de Coposa of northern Chile into general surface reflectance classes, which matched geologic maps prepared earlier by G. E. Stoertz and G. E. Ericksen from surface mapping and aerial photography. These classes were further subdivided on the basis of spectral differences. Of special significance was the successful separation of saline and gypseous deposits.

Features of the Salar de Uyuni, which covers over 10,000 km^2 of southern Bolivia, were subdivided into nine spectral classes ranging from deep water, water underlain by salt, salt with thin layers of water, to three classes of dry salt having different surface roughness characteristics that appeared to correlate with their degree of maturation. These features were documented and sampled in the field. Two brine samples collected by Carter revealed the presence of high concentrations of lithium and potassium. More detailed sampling by Ericksen and J. D. Vine confirmed initial results and demonstrated that these elements are more widespread than originally presumed.

Repetitive Landsat images of the Salar de Uyuni demonstrated the highly variable nature of the salt and water surfaces. Images taken 18 days apart on March 5 and 23, 1975, showed water coverage of the surface ranging from more than 65 percent during the rainy season (early March) to as little as 20 percent. This dramatic change, caused by rapid evaporation, indicates the dynamic nature of the climatic forces affecting the region.

DATA-COLLECTION PLATFORMS

Multispectral radiance measurements of crop canopy using Landsat DCS platforms

The Exotech Model 100–A ground-truth radiometer was tested by H. D. Newkirk (Bureau of Reclamation) in a study funded by the EROS program. The purpose of the study was to monitor multispectral reflectance from an irrigated crop and to relay the data through the Landsat Data-Collection System (DCS). The radiometer was mounted on a tower 6 m above a furrow-irrigated cornfield. Reflected energy values in each of the wavelength bands covered by Landsat, as well as global radiation, were relayed daily from a DCS platform from the time the corn emerged until just before harvest (June to November). Reflectance measurements are being compared with field measurements of plant conditions to determine whether spectral reflectance in the various bands can be correlated with plant physiology and irrigation practices.

Monitoring meteorological parameters for the High Plains Cooperative Program

A. M. Kahan (Bureau of Reclamation) reported that the design, development, construction, and testing of two Automatic Surface Observation Platforms (AESOP) were completed. Further testing of the platforms under winter conditions in the High Sierra Mountains is in progress to determine their suitability to support wintertime weather-modification research projects.

The two completed AESOP configurations are intended for operational use at the municipal airports of Broadus and Jordan, Mont., to measure atmospheric pressure, temperature, relative humidity, precipitation, and wind direction and speed. As was the case during previous tests, AESOP reports to GOES on an hourly basis to coincide with the National Weather Service and the Federal Aviation Administration surface-network reporting times.

A third AESOP is being constructed for operational use at Bonny Reservoir, the Kansas High Plains Cooperative Program site.

DATA FROM WEATHER SATELLITES

Monitoring and predicting cloud growth in the High Plains Cooperative Program

A. M. Kahan (Bureau of Reclamation) reported that satellite images were received in real time from GOES and SMS-2 at the High Plains Cooperative Program (HIPLEX) field site at Miles City, Mont. These data were used to make significantly improved local forecasts for project operations. Images were received in photographic form every 30 min, 12 min after the satellites scanned the HIPLEX operations area, and proved valuable to field scientists for making synoptic, mesoscale, and convective analyses.

The images were sent to Denver, where they were used to classify the weather at each of the three HIPLEX sites according to mesoscale types and their location and cloud types for local-noon and late-afternoon conditions during the program's operating season, May 1 to September 30. Monthly and seasonal frequency distributions prepared from these data aided in planning operations and provided stratifications of days for statistical analysis of other HIPLEX data, including radar, rain-gage, and aircraft observations. These analyses, used in concert with digital images, reduce the scientific uncertainties of beneficial and acceptable management of precipitation from summer convective clouds.

The Sierra Cooperative Pilot Project to augment winter precipitation is using laserfax imagery to examine the structure of convective bands and to develop techniques to aid in their analysis and prediction.

DATA FROM AIRBORNE INSTRUMENTS

Thermographic mosaic of Yellowstone National Park

R. S. Williams, Jr., reported that an uncontrolled thermographic mosaic (U.S. Geological Survey, 1976) of about 85 percent (7,800 km^2) of the area of Yellowstone National Park was compiled from 13 individual thermal-infrared images obtained from a nighttime aerial survey flown at an altitude of 5.5 km. Recording aerial thermographic data on videotape improves the accuracy of mosaics because postmission electronic processing of the videotape record can rectify the nadir line to a topographic map base, correct for velocity/height variations in adjacent flight lines and yaw distortions, and rectify distortions caused by pitch or produced by nonlinearity of the sidewise scan.

Analysis of the mosaic indicated that, in at least two areas, previously unmapped faults may be present. New or more extensive areas of geothermal emission were also noted in several places, such as the Hot Spring Basin area south of White Lake and the south shore of Shoshone Lake in Wyoming (Williams and others, 1976). The techniques used in the preparation of this mosaic can be applied to the preparation of other regional thermographic mosaics of geothermal and volcanic areas and to other types of environmental investigations such as pollution studies of large water bodies where a precise planimetric image is not critical.

Luminescence studies using the Fraunhofer line discriminator

Phosphate rocks.—The Fraunhofer line discriminator (FLD) is an airborne electro-optical device that operates as a nonimaging radiometer and permits detection of solar-stimulated luminescence several orders of magnitude below the intensity detectable by the human eye. Measurements made by R. D. Watson using a laboratory fluorescence spectrometer showed that the luminescence of phosphate rocks collected near Santa Barbara and Paso Robles, Calif., and also in Baja California in Mexico is on the lower end of the luminescence scale for phosphates; Santa Barbara and Paso Robles phosphate rocks range from 0.37 to 1.05 ppb and 0.62 to 1.24 ppb rhodamine WT dye equivalence, respectively (R. D. Watson and W. R. Hemphill, 1976). The luminescence of background rocks in both areas ranges from 0.25 to 0.30 ppb. The luminescence of phosphate rocks from Baja California is typically 0.25 ppb. To assess the application of the FLD in prospecting for phosphate rocks from a fixed-wing aircraft the FLD was placed on the USGS Cessna 337 aircraft and flown over the Sespe Creek area near Santa Barbara at altitudes of 500, 1,000, and 2,000 m at a speed of 90 kn. The phosphate rock was detected from all altitudes.

Stressed vegetation.—In an experiment to assess the FLD as a detector of stressed vegetation, R. D. Watson, in cooperation with scientists from EPA and the USDA Agricultural Research Laboratories, measured the luminescence of selected plots of alfalfa and cotton near Phoenix, Ariz., under varying degrees of moisture stress. Measurements from the airborne FLD indicated that cotton is a better indicator species than alfalfa for correlating luminescence with moisture. Cotton has an average gradient (ratio of percent luminescence change to percent moisture change) of 0.33; alfalfa has an average gradient of 0.15. In similar experiments on geochemically stressed juniper trees near Gardnerville, Nev., the gradient averaged 0.69 when luminescence was correlated with the molybdenum content in juniper ash (R. D. Watson and W. R. Hemphill, 1976).

Extent of oil spill.—R. D. Watson (USGS) and Craig McFarlane (EPA) conducted a joint experiment to map the distribution of oil from an oil-well blowout near Vermillion Point, La. (McFarlane and Watson, 1977). Laboratory measurements on the Vermillion Point oil indicated an optimum Fraunhofer wavelength of 589.0 nm and a rhodamine WT equivalent dye concentration of 9.7 ppb, well within the sensitivity limits of the FLD. FLD measurements made from a helicopter at Vermillion Point showed that the oil was distributed over a larger area than anticipated. Luminescence ranged from 0.25 to 8.2 ppb rhodamine WT dye equivalence. An oil-pollution-concentration map prepared from the airborne FLD data correlated extremely well with an EPA map produced from samples collected in the spill area.

Manganese-enriched rocks.—R. D. Watson, W. R. Hemphill, and T. J. Donovan conducted a series of airborne FLD experiments to measure the luminescence of manganese-enriched rocks against background luminescence carbonate-cemented rocks located in and near known oilfields in south-central Oklahoma. Field laboratory measurements of the fluorescence and the atomic absorption of selected rocks from each oilfield permitted preliminary determination of the correlation between luminescence and manganese content. Measurements on a small number of samples indicated that 656.3 nm was the optimum Fraunhofer wavelength for FLD measurements and that the correlation coefficient between manganese content and luminescence ranges from 0.7 in relatively unweathered surfaces to 0.3 in heavily weathered surfaces. FLD measurements made from a fixed-wing aircraft, obtained at an altitude of 500 m and a speed of 120 kn over the Cement, Okla., field, indicated positive correlation of luminescence with manganese highs.

APPLICATIONS TO GEOLOGIC STUDIES

Heat discharge estimates from thermal surveys

Reconstruction of the 1972 surface thermal regime of Sherman Crater and the Dorr Fumarole Field of Mount Daker, Washington, based on seven aerial infrared surveys (1970-73) and on Landsat DCP thermistor measurements by J. D. Friedman and D. G. Frank, provided an assessment of Mount Baker's heat exchange with the atmosphere before the 1975 increase in thermal emission. Calibrated infrared images obtained in November 1972, contoured for apparent radiometric temperature and corrected for atmospheric absorption and surface emissivity, indicate a differential radiant-flux value of 1.0 MW for Sherman Crater. A total heat discharge of 13 MW from the Crater, which included > 8 MW from fumarolic emission and advective loss, was estimated by using, in addition to other methods, a modified two-point differential geothermal-flux model based on heat balance of the ground surface and surface-air temperature data. (The model was adapted for use with infrared scanner output.) Similar calculations applied to 1975 infrared images and field data yielded a differential radiant flux of 5 MW and a total heat discharge of 93 MW, which included advective losses of 41 MW from ice melt and melt-water drainage and 38 MW from fumaroles and vapor plumes. Heat loss by radiation represented 8 percent of the total discharge in 1972 and 3 percent in 1975. The Bowen ratio, R, linking heat loss by conduction and turbulence to heat loss by evaporation, was 0.31. The estimated net energy yield in 1975 exceeded that in 1972 by 2.5×10^{15} J yr^{-1} (Friedman and Frank, 1976).

Expression of lineaments within the Mississippi embayment

Two distinct terrains, with distinct kinds of lineaments, were recognized in the Mississippi embayment by D. W. O'Leary and S. L. Simpson. A relatively well-dissected terrain of moderate relief typifies the embayment east of the Mississippi River. The embayment rises gradually to a low cuesta in the vicinity of the Tennessee River; and along the northern border of the embayment, between Cape Girardeau, Mo., and Paducah, Ky., it consists of discrete blocky segments. A stream-scarred alluvial plain constitutes the embayment terrain west of the Mississippi River. Crowley's Ridge, a subdued remnant of an older upland, is an inlier within the alluvial plain.

Two types of remote-sensing data have been used to detect lineaments in the two terrains: SLAR effectively depicts lineaments in the uplands, and microwave radiometry records lineaments in the alluvial plain. In the uplands, pronounced patterns of narrow ravines and first-order streams are mapped as sets of short, straight, parallel lineaments with consistent angular relationships. Superimposed on these sets are long, anomalous stream courses, scarps, and valleys that are generally broadly and irregularly curved. These features are mapped as long, locally discontinuous lineaments of varied and complex topographic expression. The former type is assumed to represent mainly joints; the latter type is assumed to represent faults. An example of a lineament that is defined by a terrain boundary and that probably represents a fault-line scarp is located at Tatumville in Alexander County, Illinois. It trends N. 35° E. and has a relief of over 30 m. Its origin is suggested by its straightness, truncated spurs, and lack of alluvial buildup along debouching streams.

Airborne microwave surveys made by A. W. England and G. R. Johnson over two areas within the alluvial plain indicated the presence of lineaments defined by soil moisture anomalies. More interesting results came from a survey made between Ridgely and Reelfoot Lake, Tenn. Here a major lineament, striking N. 32° E., lies 0.5 to 1 km east of the projected trace of the Ridgely fault (Moore, 1965), which strikes N. 40° E. The alinement of these features is improved when the average flightline bearing of N. 92° E. is taken into account. The positions of two other emission-defined lineaments are not consistent with projected faults, but their strikes (N. 12° E.) coincide with the general strike of the Reelfoot Lake faults (Krinitzsky, 1950) located just north of the survey area.

Landscape patterns and structure of the Maine coastal region

The Maine costal region, from Portland to the eastern side of Penobscot Bay and inland to about 70 km, was examined by D. W. O'Leary and S. L. Simpson using Landsat images and selected RB-57 high-altitude color infrared photographs. Four distinct terrains or landscapes were defined, each bounded by a major lineament or alinement except for a boundary that is a flexure axis extending southeast from about 12 km west of Dover-Foxcraft to the vicinity of Sebasticook Pond. Within each terrain, smaller lineaments and general physiographic features constitute distinctive landscape patterns. The lineaments are themselves defined by alined landforms and stream courses. The southwesternmost of the major lines, the Lewiston line, extends northeast from the northern side of Sebago Lake through Lewiston, up along the northwestern shore of Messalonskee Lake to the Kennebec River. Southeast of this line the topographic grain is strongly oriented in a N. 35°-40° E. direction manifested by ridges, valleys, ponds, and small streams such as tributaries to the Androscoggin and Kennebec Rivers. The Merrymeeting lineament extends northeast from Merrymeeting Bay, along the Sheepscot River to the northern side of Frye Mountain, parallel to the Lewiston line further west. Northeast-oriented linear trends are strongly developed southeast of the Merrymeeting lineament, but they become gradually diminished to the north between Camden and Belfast.

The northeast-trending strike-controlled landforms characteristic of south-central coastal Maine bend from N. 35°-40° E. to about N. 70° E. near Dover-Foxcroft and die out. The Dover-Foxcroft orocline marks the axis of this bend and more or less defines the western edge of the Penobscot River basin, a broad lowland with no pronounced terrain pattern.

The Penobscot lineament follows a broad curve from the head of Penobscot Bay northeast past the northern side of Sebao Mountain to the southern tip of Grand Lake. This line is the most significant major line in the study area because it separates the pluton-dominated terrane of the bays of Maine sequence from the relatively intact metasedimentary units to the southwest.

So far, the structural nature of the lineaments is not clear. There is fragmentary evidence that the Penobscot lineament represents a zone of shearing; along its northern part it is certainly coincident with mapped fault segments. The Merrymeeting lineament is coincident for part of its length with a high-angle postmetamorphic fault and for most of its length with a contact between the Cushing Formation and the Cape Elizabeth Formation (Hussey and Pankwiskyj, 1975). No good structural control presently exists for the Lewiston line or the Dover-Foxcroft line.

Detection of hydrothermally altered rocks from remote-sensor images

Evaluation of Landsat Multispectral Scanner (MSS) images and Skylab and high-altitude color and color-infrared photographs of four Nevada and Utah study areas by L. C. Rowan and R. P. Ashley (USGS) and Alex Goetz (Jet Propulsion Laboratory) showed that MSS color-ratio composites are the most effective and practical means for detecting and mapping limonitic hydrothermally altered rocks. The basis for this approach is the distinctive spectral reflectance of iron-oxide minerals (limonite) in the MSS response range. The study areas—the Virginia Range southeast of Reno, Nev.; Battle Mountain and the Shoshone Range in Nevada; and the Tintic Mountains in Utah—provide a variety of geologic and environmental problems not found in the initial south-central Nevada study area (Rowan and others, 1974) and hence are suitable for further evaluations of this technique.

One of the most serious limitations to the present technique is the fact that limonitic altered rocks cannot be distinguished from limonitic unaltered rocks on the basis of their MSS spectral radiances, as both have intense ferric-iron absorption bands. Those altered rocks that are not limonitic are not distinctive in MSS color-ratio composite images.

Preliminary analyses of approximately 1,000 in situ reflectance spectra in the range 0.45 to 2.5 μm, compared with representative mineralogical data, indicate that spectral radiance in the 2.2- and the 1.6-μm regions is critical for the discrimination of most altered and unaltered limonitic rocks and for the detection of nonlimonitic hydrous altered rocks. The importance of the 2.2-μm region in most altered rock spectra stems from the presence of an intense absorption band caused by the presence of hydrous phases (alunite, pyrophyllite, and clay minerals). This absorption band is absent or weakly expressed in most unaltered rocks; important exceptions include shale, argillaceous siltstone, and intensely weathered rocks.

Another important limitation is that more than 50- to 55-percent coverage of desert shrubs obscures limonitic rocks in MSS color-ratio composite images. High spatial resolution is important for alleviating this problem.

Passive and active microwave techniques in remote-sensing geophysics

Soil moisture maps produced by microwave radiometry reveal linear moisture anomalies in areas where buried faults are thought to occur. In an area near Bakersfield, Calif., A. W. England and G. R. Johnson found that linear moisture anomalies, shown as emissivity lows on the soil moisture map, are apparently caused by buried stream channels. The relationship between these channels and buried fault structure is not yet known (Johnson and England, 1976), but the linear aspect of the channels suggests a control of some sort. At two survey areas, near New Madrid, Mo., soil moisture maps reveal a series of linear emissivity anomalies, many of which have the same orientation as local faults and fractures. These lineaments are thought to be surface expressions of buried fault structures.

Mineral exploration research in Iran using Landsat data

A combination of computer processing and color compositing of Landsat data was used by H. A. Pohn to locate areas of iron-oxide stain in the mineral belt west of Kerman, Iran.

The technique, which is based on a system developed by Rowan and others (1974), is one of computer enhancement of small visible and near-infrared reflectivity differences between rock types as they appear in the various Landsat bands. Multispectral scanner bands are stretched and ratioed, picture element by picture element, and are printed in each of three colors, a diazo process being used to produce the individual color sheets. The color combinations used in the study were cyan for the ratio of band 4 to band 5, yellow for band 5 to band 6, and magenta for band 6 to band 7. In the composite, areas of iron-oxide stain are represented in green.

The color composite was compared to 1:100,000-geologic maps to evaluate the usefulness of the technique in locating mineral deposits. Of 122 green areas on the composite, 17 were found to be sites of known copper deposits; 3 of these 17 were sites of copper mines. Included among the copper mines was the Sar Cheshmeh deposit, one of the largest copper mines in the world.

The areas that appeared green on the composite are not apparent on any of the individual bands or on false-color-infrared composites.

Enhanced images for lineament mapping

Comparison of lineament maps of areas in Brazil, Texas, and Wyoming, made from unenhanced Landsat images and from computer-enhanced images, showed that 2 to 5 times more linear topographic features longer than 4 km could be defined by using the enhanced images. The enhancement evaluated by T. W. Offield, is scene dependent (a function of such things as topographic relief, vegetation cover, lineament pattern, and sun azimuth and elevation), but the basic advantage of the computer images stems from the much larger dynamic range of the digital-tape data compared to the range of the normal photographic products.

Remote sensing for uranium exploration

T. W. Offield's continuing study of Landsat data for the southern Powder River basin in Wyoming demonstrated that the texture and mineralogy of sandstones are reflected in vegetation habit and surface character as discerned in Landsat images. New image-processing techniques have resulted in sharper definition of reddish altered ground commonly observed behind uranium roll fronts. Further analysis of aircraft thermal-infrared images of the Freer-Ray Point uranium area in southern Texas involved production of day-night temperature-difference maps (using a new image-registration technique developed by D. L. Sawatzky). The data reveal many anomalously warm areas that may be possible exploration-target channel fills within the Catahoula Tuff, outliers of younger Oakville Sandstone, or silicified fault zones. Available aeroradioactivity data can be used to distinguish channel fills from outliers and thus to identify remotely the anomalous materials; the thermal images in turn permit improved interpretation of aeroradioactivity maps.

Interpretation of thermal-infrared images

Thermal-infrared images provide information about the near-surface physical state of geologic materials, particularly density, water content, and heat-transfer mechanisms.

Interpretation of thermal images is complicated by the various types of physical processes involved and commonly requires an assessment of many different factors, including direct and diffuse solar radiation, emitted radiation between the sky and the ground, convective heat transfer between the atmosphere and the ground surface, conductive heat transfer in the ground, and evapotranspiration. A simple theoretical model was developed by Kenneth Watson to provide quantitative assessment of these factors, to predict optimum times for acquiring thermal data, and to determine quantitative values of various properties of terrain.

Studies conducted by Watson at various scales from satellite and aircraft have been useful for monitoring effusive volcanism, delineating areas of steaming altered ground and hot-spring activity, detecting fractures expressed hydrologically and topographically, and for distinguishing a variety of geologic materials. Two geologic applications have been studied in some detail: geothermal mapping and thermal-inertia mapping. Initial results indicate that both techniques have considerable potential as mapping tools, especially in reconnaissance studies. These data were acquired under optimal meteorological conditions and at sites (Mill Creek, Okla.; Raft River, Idaho; and Oman) where the geologic materials were well exposed.

New porphyry copper prospect located using digital classification of Landsat-1 data

Two new porphyry copper-type alteration zones in Pakistan, one of which appears to indicate a copper prospect and has been named for the late M. G. White, were located by R. G. Schmidt, working in cooperation with NASA and the Government of Pakistan (Resource Development Corporation). The discovery was made during a field check of possible alteration sites selected by digital classification of Landsat data in the Chagai District of Pakistan.

The Max G. White prospect was indicated as one of 50 spectrally anomalous areas in a 1974 evaluation of the region through use of digitally processed Landsat multispectral reflectance data. This prospect did not show up well on standard enhancements and false-color composites of Landsat images and was not selected to be checked in a first visit to the area. A continued study using a new digital classification method indicated that only 16 localities were significantly altered and potentially mineralized. Field inspection has revealed seven of these sites to be porphyry alteration systems (five were found in the 1974 remote-sensing work, and two, including the White prospect, were found in the present study).

The roughly elliptical quartz-sericite zone at the White prospect is about 1,500×1,200 m. Most of this zone occupies a broad drywash pediment surface; bedrock exposures are low and small but sufficient for roughly outlining the alteration. A well-developed propylitic zone also is present. Intense leaching of all outcrops at the prospect makes recognition of potassic alteration difficult, but what appeared to be secondary biotite was found in some of the outcrops. Fresh sulfide was seen within the propylitic zone but not in the quartz-sericite zone, although there is abundant evidence that much has been leached. Stockworks of fine quartz veinlets were particularly abundant in two outcrop areas. "Live limonite," a dark-red alteration product, possibly after secondary chalcocite, was seen at several places.

The association of widespread porphyry-type mineralization with extensive exposures of intrusive porphyry and the abundance of "live limonite" suggest that the Max G. White prospect deserves careful further investigation. The possibility of the presence of a zone of secondary enrichment is excellent.

APPLICATIONS TO HYDROLOGIC STUDIES

The use of remote sensors to obtain hydrologic information is increasing as analysis, classification, interpretation, and measurement techniques are developed and perfected. Thus, a correlation of wetland vegetation types with water depths in the Florida Everglades permitted a calculation of total surface-water volume in Conservation Area 3A. Also, satellite-relayed data on streamflow and water content of snow in Arizona were used on an almost routine basis for reservoir regulation. Research continued on the classification and hydrologic significance of land cover types, on the remote measurement of the chemical content of water, and on the interpretation of ground-water occurrence.

Landsat data used to calculate water volume in the Florida Everglades

Previous work in the Florida Everglades showed a good correlation between wetland vegetation type and average depth of surface water. Similarly, the ability to classify water depths and vegetation types by using Landsat data was established. A. L. Higer, E. H. Cordes, and A. E. Coker reported that October 1974 Landsat data were categorized into nine open-water and vegetation classes representing 1 cm to 1 m of water depth. The areas of all classes of water depth were tabulated, and the total surface-water volume in Conservation Area 3A (a water-management area) was calculated. This calculation gave the amount of water available (aquifer recharge) for man's use on Florida's eastern coast and the amount that can be diverted into Everglades National Park.

Pine trees are common in the area and are associated with other types of vegetation in almost all classes. Water-level measurements in shallow wells showed that pine trees are well adapted to a wide range of water-table conditions and fluctuations.

Remote sensing of water quality

An evaluation of available technology in the field of laser-Raman spectroscopy led M. C. Goldberg and E. R. Weiner to the conclusion that a TV-type detector, a single monochromator with a holographic grating, an entrance slit filter to block Rayleigh-scattered light, and a pulsed laser coupled to signal-averaging electronics is the best combination of commercial equipment that is presently available for use in assembling a water-quality remote sensor. Such a sensor would be capable of measuring oxyanions in water at concentrations ranging from 10 to 50 mg/L at distances from ground level to 30 m above a sample. Interferences by ambient light, bioluminescence, and natural fluorescence would be minimized by the signal-generating and readout capabilities contained in this equipment package.

Ground-water information inferred from Landsat-image data

A study by G. K. Moore showed that general principles of photographic interpretation can be applied to Landsat data to (1) recognize landforms, drainage and cover patterns, and geologic lithologies and structures that are favorable for ground-water occurrence; (2) delineate some of the limits of surface and shallow aquifers; and (3) study some phases of aquifer operation, such as recharge and discharge. Landsat data thus may be used to supply information on regional aquifers, to aid in solving specific problems such as water supply and pollution, and to plan or minimize fieldwork.

Characteristic shapes, forms, and patterns have the highest relative confidence as indicators of shallow aquifers; image tones and textures have the lowest relative confidence. Time of year is critical for obtaining maximum geologic and hydrologic information from images. Many features are enhanced by low-sun-elevation angles in early winter, but other features are most apparent in the spring when soil moisture is high.

Satellite-data relay used for reservoir regulation in Arizona

An unusual series of storms over central Arizona in April 1976 threatened to necessitate major changes in the Salt River Project's operating plan for reservoirs on the Verde River above Phoenix. Using information on snow-water content and streamflow rates furnished in near-real time by the Landsat data-collection system, H. H. Schumann determined that changes in the reservoir operating plan would not be necessary.

Vegetation mapping in Volusia County, Florida

Because well fields in central Volusia County, Florida, will be needed to supply water to coastal cities in the future, it is necessary to determine the effects of pumpage from the Floridan aquifer on water tables in shallow aquifers and the possible resulting effects of water-table declines on vegetation. P. W. Bush reported that a study of wetlands vegetation was begun in order to document the present conditions.

Vegetation was divided into 6 main classes and 17 subclasses on the basis of field reconnaisance and interpretation of low-altitude aerial color photographs. Digital processing of Landsat data showed that eight classes of vegetation can be detected from satellite data.

Tennessee wetland classification and mapping

V. P. Carter reported that 15 wetland-classification maps were completed for four sites in western Tennessee by using a classification system developed for the Tennessee Valley region by the USGS in cooperation with the Tennessee Valley Authority (TVA). NASA high-altitude color-infrared photographs were used to identify 12 wetland classes and adjacent land use on 1:24,000-scale overlays on existing USGS 7½-min quadrangle maps. A stage-duration curve referenced to the seasonal photographs was placed on the map collars to supply information relating the wetland-class boundaries to water-level fluctuations. The State of Tennessee and the TVA are using the maps to supply management information. The maps are also being used for evaluating wetland classifications based on Landsat digital data (V. P. Carter, Alan Voss, Donald Malone, and William Godsey, 1977).

National wetland-classification system

The USGS is cooperating with the U.S. Fish and Wildlife Service to develop a new national wetland-classification system for the current U.S. Fish and Wildlife Service National Wetlands Inventory. According to V. P. Carter, remotely sensed data will be the basic-data source for the inventory. Wetland-habitat type, the lowest level of the new system, is based on vegetation, soils, and hydrology. The final version of the classification system will be published after wetland plant and soil lists are completed. The system will allow countrywide comparison of inventory data by ecological system, by physiographic region, and by wetland class and subclass.

In cooperation with the Jet Propulsion Laboratory in Pasadena, Calif., and the U.S. Fish and Wildlife Service, the USGS is testing the potential of Landsat digital data for future updates of the present National Wetlands Inventory and for the present inventory in areas such as Alaska where very little aerial photography has been done.

Vegetative-cover mapping of the Great Dismal Swamp

V. P. Carter reported that a 1:100,000-scale vegetative-cover map (V. P. Carter and P. T. Gammon, 1976) and two 1:24,000-scale vegetative-cover maps of the Great Dismal Swamp of Virginia and North Carolina were prepared from seasonal color-infrared photographs obtained by NASA. Black-and-white photographs for 1937–38, 1953, and 1971 were used to make 1:24,000-scale overlays showing changes in vegetative composition as a result of clear-cutting or fire. These maps are being correlated with climatic and biological data to give information on successional patterns within the swamp (V. P. Carter, M. K. Garrett, Lurie Shima, and P. T. Gammon, 1977; M. K. Garrett and V. P. Carter, 1977).

Geometrically corrected and registered Landsat data are being used to classify the swamp vegetation in order to provide a basis for monitoring future vegetative trends in response to various management practices (P. T. Gammon and V. P. Carter, 1976). Information obtained from color-infrared photographs was used to select sites for 31 shallow ground-water observation wells. Water-level data for these wells are being analyzed with reference to surface vegetation to correlate vegetative cover with water availability. These data may also prove useful for predicting the pattern of vegetative regeneration following fires or timber-cutting operations.

APPLICATIONS TO CARTOGRAPHIC STUDIES

In FY 1977, NASA, the EROS program of the Department of the Interior, and the USGS continued research in the cartographic applications of space imagery and high-altitude photographs. As Landsat–2 continued its third year of operation and Landsat–1 ended its fifth, the demonstrated possibilities of operational applications became increasingly significant, particularly for areas not yet adequately mapped even at the small scales of 1:500,000 or 1:1,000,000. The shallow seas, for example, have been charted more or less adequately for navigation but not adequately for the resource exploration and development underway worldwide.

SATELLITE IMAGE MAPS

Eleven 1:500,000-scale color image maps were printed with Landsat–1 multispectral scanner imagery for most of the State of Florida. Each map was prepared from a single Landsat scene in image format and printed with a 20,000–m Universal Transverse Mercator grid fitted to selected image points.

Unlike the other maps, which were conventionally processed by photographic methods and printed with yellow and magenta plates for band 5 and a cyan plate for band 7, the Florida Keys map was prepared from an image enhanced by computer processing at the Jet Propulsion Laboratory (JPL) (Pasadena, Calif.) to preserve underwater details. It was printed with the magenta plate for bands 4 and 5, the yellow plate for band 4, and the cyan plate for band 7. The result is improved depiction of shallow-sea areas near the Florida Keys.

In FY 1977, the following satellite-image maps of areas of Florida were printed at 1:500,000 scale: (1) Florida Keys, (2) The Everglades, (3) Sanibel Island, (4) Charlotte Harbor, (5) Lake Okeechobee, (6) Lake George, (7) Gulf Hammock, (8) Okefenokee Swamp, (9) Apalachee Bay, (10) Lake Seminole, and (11) Pensacola Bay. In addition, a Landsat image of the Vatnajökull Glacier area of Iceland that was taken in the fall season was also prepared and printed as a satellite-image map at 1:500,000 scale.

HARTFORD 1:250,000-SCALE IMAGE MAP

A gridded 1:250,000-scale image map of the Hartford area of Connecticut was printed from a mosaic prepared from enlarged photographs (11.2×) taken by the S-190A multispectral camera on Skylab Mission 3. In processing this image map, which covers the 1°×2° format of the Hartford quadrangle, two sets of four photographs were used. One set was exposed with red-sensitive film, and one set was exposed with infrared-sensitive film. Yellow and magenta plates printed the red image, and a cyan plate printed the infrared image.

PARAMETERS FOR AN OPERATIONAL LANDSAT

On the basis of results of investigations and experiments with satellite and high-altitude aircraft

Parameter	Proposed specifications
Sensor type	Multispectral Linear Arrays
Wavebands:	
Blue-green (water penetration)	0.47–0.57 μm[1]
Green-red (boundary delineation)	0.57–0.70 μm[1]
Near infrared (water, vegetation, and cultural delineation)	0.76–1.05 μm[1]
Spatial frequency (resolution) or picture element (pixel) in terms of ground coverage:	
Band 1 (blue-green)	60–90 m[1,2]
Band 2 (green-red)	30–40 m[1,2]
Band 3 (near infrared)	60–90 m[1,2]
Quantizing level (radiometric sensitivity)	64–256 levels (6–8 bits)[1]
Sampling frequency	1.4 times/pixel[3]
Data rate	Approximately 15 megabits per second (capability of Landsat reception stations)
Sensor weight (estimated)	40 kg
Sensor power requirement (estimated	40 W
Expected sensor life	6–10 years
Satellite orbit	Circular Sun-synchronous at 919 km[3]
Ground coverage	185-km swath[3]
Orbital position and attitude stability and determination	Improved over landsat-1, Landsat-2, and Landsat-C—perhaps by an order magnitude.
Data storage capability	Equal to or better than Landsat-1, Landsat-2, and Landsat-C.

[1] Subject to adjustment based on engineering tests for final design.
[2] Similar to Landsat-1, Landsat-2, and Landsat-C.
[3] Same as Landsat-1, Landsat-2, and Landsat-C.

images and the indicated needs of users of satellite data worldwide, an operational Landsat that retains the basic parameters of Landsat-1 and Landsat-2 has been defined. This action does not recommend an end to the experimental program but merely recommends a separation of the operational function from the experimental and thereby assures continuity in the data flow from the Landsat missions.

LANDSAT MAPPING AND CHARTING OF THE SHALLOW SEAS

Although the USGS is not actively engaged in either hydrographic surveying or nautical charting, other bureaus of the Department of the Interior and such industries as oil, mining, utilities, and fisheries are concerned with offshore mapping. Consequently, the EROS program has sponsored studies of water penetration and arranged for objective tests and exhibits of high-gain, enhanced Landsat images of areas in the Caribbean Sea and the Indian Ocean. In the Caribbean, investigations showed that with suitable clear-water and bottom conditions and with appropriate calibration data, water depths to 22 m could be determined radiometrically with root-mean-square errors of only 10 percent. In the Chagos Archipelago area, images indicated dramatic changes in the positions and shapes of reefs as depicted on current nautical charts, as well as the existence of a previously uncharted reef. This information led to immediate revision of published nautical chart 61610 by the Defense Mapping Agency (DMA) Hydrographic Center.

LANDSAT INVESTIGATIONS

Two Landsat follow-on experiments were pursued in cooperation with NASA:

Overall evaluation of Landsat (ERTS) follow-on imagery for cartographic application (No. 23960).— This study concerns the activities of all cartographers trying to apply Landsat data and to report significant problems and results to NASA. During the past year, the following conclusions were reported:

- Landsat is a valuable source of data that can greatly improve nautical charting, with large economic benefits. This improvement also leads to the effective mapping of the shallow seas for other than navigational purposes.
- Landsat is a valuable source of data for both aeronautical charting and small-scale mapping.
- Landsat image maps were prepared in enhanced form, and further improvements in displaying the cartographic potential of Landsat in image form were developed.
- Detailed geometric analysis of Landsat images indicated systematic anomalies that can largely be corrected before printing.

Processing of Landsat imagery for dissemination purposes (No. 23650)—This investigation concerns two fundamental problems of processing Landsat imagery for publication:

- Determination of when and how to convert from digital to analog form.
- Determination of specific enhancement procedures that will make Landsat imagery optimal for general distribution.

Experimentation with various band treatments and enhancements (both digital and analog) determined that:

- Enhancement of band 4 shows both growing and dormant vegetation.
- Edge-enhancement and other techniques demonstrated by IBM, JPL, the EROS Data Center, and others increase feature contrast and therefore information content.
- Combination of Landsat imagery with higher resolution radar imagery produces a composite that displays information not readily discernible in either of the original images. This significant result questions whether multispectral systems should obtain records of equal resolution. Tests and theory indicate that one properly selected high-resolution band can effectively increase the resolution of Landsat imagery without the quantum increase in data that results from increased resolution in all bands.

NIGHTTIME IMAGES

Under USGS contract, the Stanford Research Institute (Stanford, Calif.) analyzed nighttime satellite images to assess such phenomena as the burning of resources. The initial phase was limited to assessing nighttime images obtained by the Air Force Defense Meteorological Satellite Program (DMSP) and will produce an atlas of the nighttime Earth depicted by DMSP images that will be valuable to many investigators. The report also indicates the complementary role that Landsat can play in obtaining nighttime images of the Earth.

SPACE OBLIQUE MERCATOR PROJECTION

The Space Oblique Mercator (SOM), as defined by the USGS, has been adopted by the NASA Data Processing Facility. Consultations with NASA, DMA, and NOAA scientists are intended to assure the most efficient methods of defining the rigorous mathematical elements of the projection. Financial support is being provided for John Junkins (University of Virginia) to complete the mathematical formulation and to write the basic computer program for transformation to and from the SOM.

When it is fully adopted, Landsat processing based on the SOM projection should provide for automated production of maps and should deliver them, if necessary, in a matter of days.

LAND USE AND ENVIRONMENTAL IMPACT

MULTIDISCIPLINARY STUDIES IN SUPPORT OF LAND USE PLANNING AND DECISIONMAKING

Many new products have arisen from programs that provide scientific and engineering data collected by the USGS and the Department of the Interior in support of land use and resource planning and decisionmaking at all levels of government and in the private sector. Some of these products are highlighted in the following sections.

SAN FRANCISCO BAY REGIONAL STUDIES

A critical evaluation of city and county use of the 87 Earth-science products prepared as part of the USGS-HUD San Francisco Bay Region Environment and Resources Planning Study (SFBRS) was completed by W. J. Kockelman (1975, 1976).

Inventories of three discrete user groups—91 cities, 8 county planning departments, and 8 county flood-control and water-conservation districts—in the bay region were conducted. The inventories were designed not only to document applications of SFBRS products but also to evaluate the extent of those applications and to suggest ways to achieve greater and more effective use of Earth-science information.

From the inventories and responses to interviews, Kockelman concluded that the cities and counties in the bay region are very familiar with, have made frequent use of, and will continue to use SFBRS products for a wide range of city and county planning activities.

Seventeen selected examples of applications of the products to various county planning and decisionmaking activities are discussed and illustrated by Kockelman (1976, p. 44-127). Some of the activities selected are:

- Seismic zoning based on geologic units and their re sponse to shaking.
- Evaluating waste-disposal zones.
- Land use planning related to seismic risks, steep slopes, inadequate water supplies, and sewage disposal.
- Open-space planning related to geologic hazards and steep slopes.
- Seismic safety plans based on known potential earthquake hazards.
- Administering land use and land development ordinances.
- Developing official geological hazard maps that are itegrated into subdivision, building, and grading ordinances.
- Developing and administering an innovative zoning district that computes the number of dwelling units per acre permitted on the basis of steepness of slopes, probability of flooding, presence of active faults, and landslide susceptibility.
- Preparing environmental impact reports.
- Conducting public information programs.

COLORADO FRONT RANGE URBAN CORRIDOR

Mapping of the relative amounts of soil and bedrock in the mountainous western part of the greater Denver area has been largely completed as part of the Colorado Front Range Urban Corridor Project. These maps are used by the Jefferson County geologist, county planners, and the county health department in reviewing applications for mountain development, defining areas of constraint on development, and flagging areas of potential hazard. Other users include soil-conservation and water-resource personnel in government agencies.

Data on the chemical and physical quality of lake water, and the distribution, size, and biology of lakes, were given on a recently published map (D. B. Adams, 1976) of the Colorado Springs-Castle Rock area. These data not only document the character of lake water but also the threat of general deterioration of lake water caused by changes in lake and land use.

Two other maps resulting from this project delineated natural and historic landmarks (B. N. Petrie, 1976) and historic trails (G. R. Scott, 1976). These maps received broad popular acceptance and should serve as guides for the preservation of valuable historic and geologic features during future development of the Denver metropolitan area.

Additionally, the project has continued to produce maps that delineate flood-prone areas. These maps are designed to aid local planners in mitigating flood hazards through land use planning.

GEOTECHNICAL AND GEOHYDROLOGICAL STUDIES IN FAIRFAX COUNTY, VIRGINIA

Three reports pertaining to engineering and hydrology in the Franconia area of Fairfax County, Virginia—the location of a new 1,000-acre planned housing development—were released to open file last year (R. H. Johnston and J. D. Larson, 1976; S. F. Obermeir and A. J. Froelich, 1976; S. F. Obermier and Curt Hollocher, 1976). Integrated geologic, engineering, and hydrologic studies in this area defined Earth-related constraints and opportunities for development and provided county officials with a scientific basis for modifying the plans for the development.

The application of multidisciplinary studies has also shed light on local planning and development problems in other parts of the county. In the Coastal Plain region, an evaluation of ground-water resources was made. Surface geologic studies (lithologic mapping of channel-fill sands and gravels and the contrasting overbank silts and clays, studies of crossbedding) and subsurface hydrologic studies (sand thickness and distribution, potentiometric surface and transmissivity variations) of the Potomac aquifer indicated that localized, buried, east-trending channels have the greatest potential for ground-water development. Additionally, comparison of the potentiometric surfaces measured in 1960 and 1976 indicates that water levels have risen locally as much as hundred meters as a result of decreased pumpage.

Another study result with direct application to the county's planning needs is an interpretive map entitled, "Map showing mineral resources of Fairfax County, Virginia—Availability and planning for future needs" (Froelich, 1976). The map is being used by members of the county planning staff as a basis for reexamining natural-resource policy.

PUGET SOUND REGION ESA PROJECT

The first set of topographic maps in the Far West using the new all-metric 1:100,000 scale were produced as part of the Puget Sound Region Earth Sciences Applications (ESA) Project. One map, that of King County, Washington, has been published in a 1-deg by 30-min quadrangle format; several other maps are being published in the same format. The first in a new series of land use and land cover maps using a classification system based on the interpretation of remotely sensed data has been compiled using these topographic maps as a base. The categories shown on these maps are based on the "Level II" classification level described in USGS Professional Paper 964 (Anderson and others, 1976). The maps are being prepared under the direction of Eugene Napier and when published will be sold as copies on paper or transparent film.

Howard Gower (unpub. data, 1976) compiled a tectonic map of the Puget Sound region of Washington summarizing information on bedrock faults and on the locations of large-scale deformation in Quaternary deposits. The map shows the locations of known faults and major inferred fault zones in the bedrock and indicates the relative direction of fault movement and the age of the movement. The map also shows where large-scale deformation occurs in the Quaternary sediments overlying the bedrock of the Puget Sound Lowland. The map is an up-to-date summary of known and inferred tectonic activity in the region and will help define critical areas for future detailed studies and for evaluation of sites for new facilities.

James Yount and Kim Marcus (unpub. data, 1976) prepared a report on the Puget Sound Lowland that summarizes available information on carbon-14 dates. The report consists of a map that shows where the samples for carbon-14 analysis were taken and a table that describes the samples and their stratigraphic significance. The compilation brings together for the first time information on many carbon-14 dates that heretofore has been widely scattered throughout many professional journals. The report will greatly assist in correlating rock units in the Puget Sound Lowland and thereby contribute to many activities that require the application of geologic and ground-water data.

G. C. Bortleson, R. T. Wilson, and B. L. Foxworthy (1976) analyzed the effects of the recent volcanic activity at Mount Baker, Wash., on the quality of local streams and of Baker Lake. Boulder Creek, which is about 5 percent of the total drainage to the lake, carried increased loads of acid and dissolved minerals from the mountain to the lake during 1975; however, measured concentrations in the stream water remained below dangerous levels throughout this period of increased activity. The lake would be able to assimilate almost indefinitely the acid and mineral loads measured in 1975; the concrete dam that impounds the lake was not endangered by the acid water.

RESOURCE AND LAND INVESTIGATIONS PROGRAM

Environmental impacts and western coal

Benjamin Schlesinger and Douglas Daetz (Stanford University) (1975) described a general method for quantifying probable environmental impacts by using a matrix of interrelationships to predict the cumulative effect of direct and higher order impacts. Cross-impact and related matrix algebra methods were used. The MITRE Corporation (1975a) describe, in a companion report, the secondary and higher order impacts associated with Western coal development. The impact forecasting technique was tested by applying it to coal development in Campbell County, Wyoming. A scenario generation process was used. Computer models simulated the allocation of coal for alternate uses or transport (for example, mine-mouth powerplants, slurry lines, unit trains and gasification plants). Primary and higher order impacts were forecast for quantities of coal allocated according to these alternatives. Impacts on air quality forecast by a dispersion model were also included in the analysis. All computer programs used in the test are available on the INFONET system under a contract between Computer Sciences Corporation, Arlington, Va., and the General Services Administration.

E. T. Smith (1976) described the impact forecasting method at the Summer Computer Simulation Conference, held in July 1976 in Washington, D.C., and at a workshop for regional planners from the States of Colorado, Montana, New Mexico, North Dakota, Utah, Wyoming, and the Navajo Nation, held in December 1976 in Denver, Colo.

Surface mining and land use planning

E. A. Imhoff and T. O. Friz (USGS) and J. R. LaFevers (Argonne National Laboratory) (1976) examined State statutes relating to the reclamation of surface mined lands and summarized them in matrix form. Administrative requirements vary from State to State, but a general trend toward requiring the integration of land use planning and mine planning was noted. Local government involvement is also increasing.

Imhoff (1976a, b) reviewed State laws in Colorado and Florida as they relate to mineral-resource management and surface mining; he found that Florida exhibits the most complete spectrum of planning legislation among the 50 States and has developed a broad array of planning and management tools. In Colorado, most land use control has been delegated to local governments. Several local governments, notably those of Weld County and the City of Boulder, have responded with plans and implementation devices to guide private concerns in mining, reclaiming, and eventually converting mined land to other productive uses.

Environmental statistics and indicators

The Environmental Statistics and Indicators project, now in its second year, is a cooperative undertaking of the Resource and Land Investigations Program, the Council on Environmental Quality, and the Environmental Protection Agency. Its objective is to describe the environment of the Nation by summary statistics that cover all significant aspects (for example, environmental quality, natural resources, housing, and economics). The first-year report (MITRE Corporation, 1975b) consisted of about 200 tables showing data as of May 1975. Data are by State, where possible, and, in some cases, trends showing variations over a period of years are presented.

Selected data and tables from the second-year report were extracted for use in the annual report of the Council on Environmental Quality (1976).

South Florida environment

In 1968, the Dade County Port Authority proposed the construction of an international jetport in the Big Cypress Swamp area of south Florida. Federal interests were involved, and several studies were made on the impact of the jetport. In 1970, the Department of the Interior expanded the scope of the studies to include the total ecological environment of south Florida. The National Park Service was in charge of the project, and, between 1971 and 1974, 51 studies were produced by the USGS, the National Park Service (NPS), the Fish and Wildlife Service (FWS), the Bureau of Outdoor Recreation, the Bureau of Indian Affairs, and the National Marine Fisheries Service. B. F. McPherson (USGS), G. Y. Hendrix (NPS), Howard Klein (USGS), and H. M. Tyus (FWS) (1976) summarized these 51 studies in a popular form useful to land and resource decisionmakers.

Integrated surface mine reclamation and land use planning

E. A. Imhoff, W. J. Kockelman, and J. T. O'Connor (unpub. data, 1977) reviewed the concept of integrated planning for mined-area reclamation and related land use. They found that the concept has been used more by some mineral industries than others but has been overlooked by most governmental agencies. The structure of a general program was developed from segments in current use, and a model procedure was suggested on which effective reclamation programs could be built.

Surface mining control in a changing environment

J. T. O'Connor, T. N. V. Karlstrom, and R. L. Sutton (unpub. data, 1977) examined the geologic and climatic setting of the Black Mesa area of Arizona and outlined the potential environmental problems related to surface coal mining. Legislative attempts to protect this environment failed to consider the effects of coal development on climate and the benefits of land use planning in environmental protection.

Onshore facilities associated with Outer Continential Shelf energy development

A report by the New England River Basins Commission (1976a), prepared for the Resource and Land Investigations Program, described the characteristics, siting requirements, operation, and impacts of onshore facilities associated with offshore oil and gas operations. These facilities include service bases, platform and pipeline support bases, repair and maintenance yards, pipelines and landfalls, marine terminals, partial processing facilities, natural gas processing and treatment plants, refineries, platform fabrication yards, and pipecoating yards. The impact of site alterations, construction, and vehicle air and noise emissions are also described.

A second report by the New England River Basins Commission (1976b) described a scenario technique that relates the offshore activities to the onshore facilities required to support development. The scenarios are applicable to the New England-Georges Bank area and include high, medium, and no-find situations.

The DEROCS (Development of Energy Resources of the Outer Continental Shelf) computer program, developed by P. A. Marcus and E. T. Smith (USGS) and S. R. Robertson and A. T. Wong (Data Technology Industries, Inc.), applies the scenario technique. The program user specifies the number, timing, and amounts of offshore oil and natural gas finds and multiplier relationships for onshore service requirements. The program determines schedules of platform installation, drilling, production, and well workover and calculates the requirements and impacts of onshore service facilities on a yearly basis.

Coastal area activities

A directory of USGS programs in the coastal areas (P. A. Marcus, 1976) describes 16 activity categories and lists each program and project within these activities. It provides information on the Earth science and natural-science investigations in which the USGS is currently engaged and which are capable of supporting coastal zone planning.

DIGITAL SYSTEMS TECHNOLOGY

In May 1975, the International Geographical Union Commission on Data Sensing and Processing was awarded a grant by the Land Information and Analysis Office and the Topographic Division for a cooperative study of digital spatial data systems technology and digital spatial data activity in the USGS. An inventory of computer software listed 296 computer programs used in North America, western Europe, Australia, and New Zealand. The programs included manipulation routines such as arc to polygon, display programs such as choropleth mapping, contouring, or three-dimensional display, modeling programs such as network and demographic models, and comprehensive geographic information systems.

Fifty-four USGS digital spatial data systems were also described. A data volume of 1.37 terra bits has been projected through 1980, at which time the largest (digital geographic) systems will come on line. This document points out the extent to which the USGS is changing from an organization that stores its data in map or text form to one that collects, stores, and transmits massive amounts data in digital form.

The two documents mentioned above were used as background material for a spatial data systems seminar in which 26 USGS data managers or technical personnel participated. On the basis of this seminar, the International Geographical Union made a report to USGS management summarizing USGS spatial data handling activities, problems, and the technological state of the art and recommending changes and new initiatives.

LAND USE AND LAND COVER MAPS AND DATA AND OTHER GEOGRAPHIC STUDIES

Land use and land cover mapping and data compilation and related research being carried out by the Geography Program of the Land Information and Analysis Office can be divided into the following major activities:

- Compilation and release of land use and land cover maps and associated maps at scales of 1:250,000 or 1:100,000, depending on the availability of the new 1:100,000-scale maps at the time of publication.
- Experimentation with and demonstration of land use and land cover mapping at scales larger than 1:100,000 for specific applications.
- Experimentation with Landsat data to test for consistent mapping results and measurement of spatial and temporal changes in land use and land cover.
- Research on and development of a Geographic Information Retrieval and Analysis System (GIRAS) for handling land use and land cover data in conjunction with environmental, socioeconomic, demographic, and other data.
- Analytical and interpretative studies on land use patterns, problems, and trends.

Land use and land cover and associated maps

The USGS has undertaken a program to provide land use and land cover and associated maps for the entire United States. This program, initiated in 1975, is beginning to satisfy a long-standing need for a consistent level of detail, standardization of classification categories, and scales of compilation for land use and land cover maps and data. No baseline or benchmark land use and land cover maps and data have ever been compiled for the entire Nation. The initial nationwide mapping is scheduled for completion by 1982, and systematic revision is to begin in 1979.

Land use and land cover categories used on the USGS maps are described by J. R. Anderson, E. E. Hardy, J. T. Roach, and R. E. Witmer (1976).

Land use and land cover and associated maps are being compiled at a scale of approximately 1:125,000 and then reduced and keyed to the combined black and blue color-separation plates of the standard USGS 1:250,000-scale topographic sheets. As the new 1:100,000-scale map series becomes available, it will be used as a base for compilation, and the land use and land cover and associated maps will be published at the 1:100,000 scale. The minimum mapping unit for all urban or built-up areas, water areas, confined feeding operations, other agricultural land, and strip mines, quarries, and gravel pits is 4 ha. All other categories of land use and land cover are delineated with a minimum unit of 16 ha. Federal land holdings are shown for tracts of 16 ha or larger.

The compilation of these map sets is being done through the USGS Topographic Division regional mapping centers. Scheduling, specifications, quality control, and accuracy checks to insure standardization and consultation on program development are provided by the Geography Program.

By the end of December 1976, land use and land cover maps were compiled for about 2,000,000 km^2 of the United States; 86 map sets were completed and placed on open file for public use and reference (fig. 5).

Land use and land cover and associated map data are digitized in a polygon format in order to provide graphic and statistical displays quickly by use of computers. Conversion of land use and land cover polygons to grid cells of varying sizes can be made when desired so that demographic, socioeconomic, soil, and slope data may be compared.

The land use and land cover and associated maps are placed on open file at the USGS regional mapping center that has responsibility for the mapped areas. Reproductions of particular maps may be obtained at a nominal cost from the same regional mapping centers. Open-file copies of these maps are also available for reference use in the mapping centers.

Statistical data on land use and land cover are published for each State as mapping is completed and are presented by counties, hydrologic units, census county subdivisions and tracts, and federally owned land. Magnetic tapes containing these data are available for sale about 9 months after the mapping is completed. Documentation for use of these computer-generated data is also available.

During 1976, a study was begun to test the accuracy of the data contained on the land use and land cover maps at scales of 1:250,000, 1:100,000, and 1:24,000. The research method used to determine the accuracy of the land use and land cover maps was to apply a systematic stratified unalined point sampling technique to determine the percent of correctly mapped points. In 1976, the land use and land cover maps for the Atlanta area of Georgia were chosen as the first in a series of maps to be tested for accuracy. Points on the map were selected for field verification, and comparison of map data with data from high-altitude photography was begun. As part of a regional assessment of mapping problems, the problem of identifying categories of land use or land cover that merge gradually into adjacent categories and the problem of identifying certain unique categories in the mountains of southern California were examined in the field.

Cooperative land use and land cover maps and data projects

During 1976, land use and land cover and associated maps were compiled to fulfill terms of cooperative agreements between the USGS and the States of Alabama, Florida, Georgia, Missouri, Pennsylvania, and West Virginia and with the Ozarks Regional Commission for the State of Kansas. Land

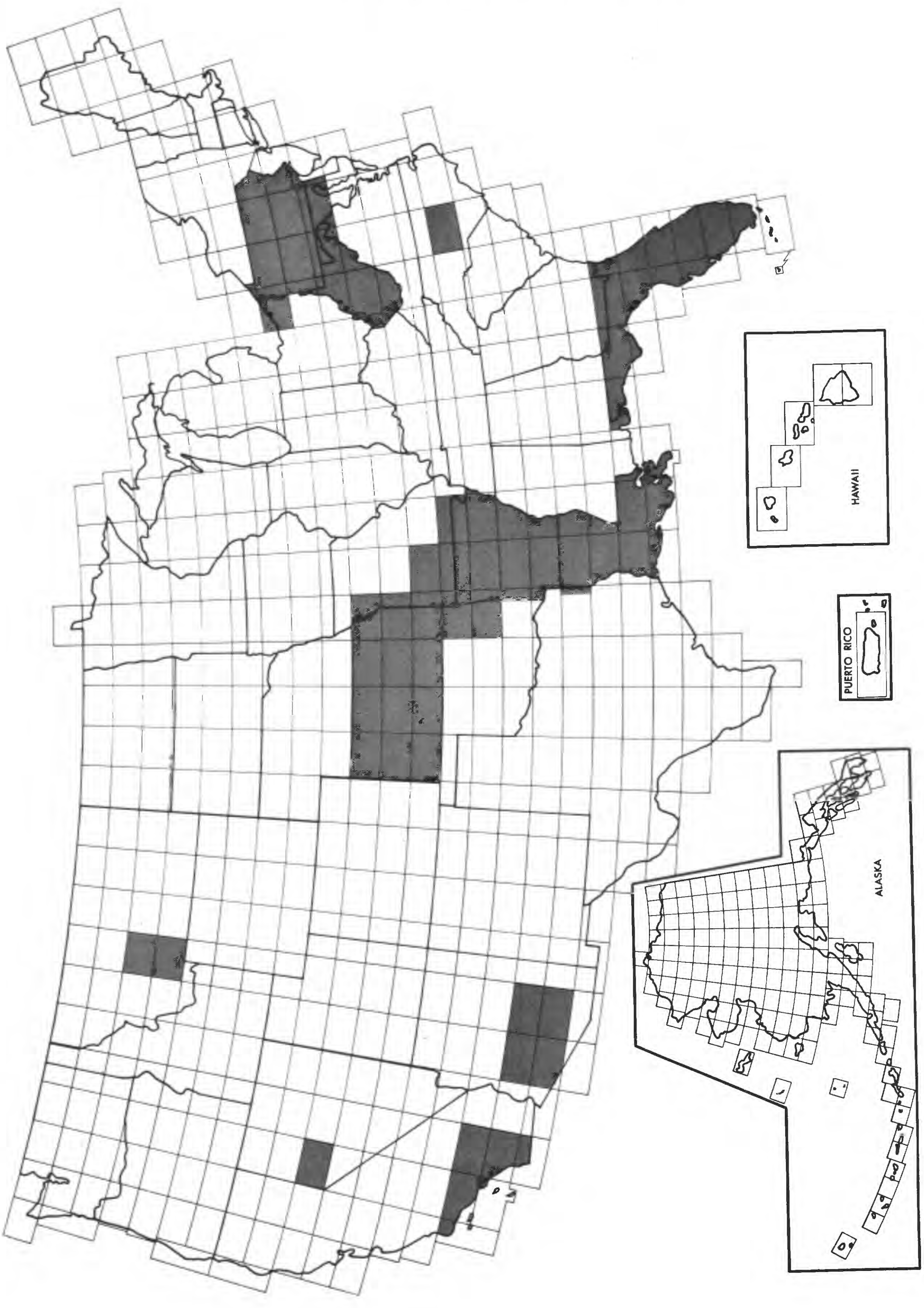

FIGURE 5.—Land use and land cover and associated map sets released to the open file as of December 31, 1976.

use and land cover, political units, hydrologic units, census county subdivisions, and Federal ownership maps were prepared under these agreements. In addition, the location of State-owned lands in the States of Florida, Missouri, and Pennsylvania were mapped. The States of Arkansas and Louisiana had previously been completely and uniformly mapped. In September 1976, a cooperative agreement with the State of North Carolina was signed. Under this agreement, the USGS will complete land use and land cover and associated maps for the State.

As an example of the usefulness of these maps, the State of Pennsylvania is using them to prepare an environmental impact statement on a proposed steel plant in the northwestern section of the State. The State of Florida also has distributed these maps to various State and local offices to supply information and fulfill the data needs of Environmental Protection Agency Section 208 projects.

Central Atlantic Regional Ecological Test Site Project

The basic assumption of the Central Atlantic Regional Ecological Test Site (CARETS) Project is that there is a measurable environmental impact associated with land use and land use change that can be determined with remotely sensed data; therefore, such data provide regional planners and other users with an understanding of the environmental changes occurring in their areas. Research and evaluation of the usefulness of remotely sensed data as sources of information on land use and land cover and land use changes is jointly funded by NASA and the USGS under this project. Ten of the 13 volumes of this report have been completed and forwarded to NASA and to the National Technical Information Service of the Department of Commerce for public information and distribution.

Several research reports dealing with a land use climatology segment of the CARETS Project have been completed and are in the review process. Among these research reports is a study of the relationship between aerodynamic roughness and land use in Baltimore, Md., by F. W. Nicholas and J. E. Lewis, Jr. In this study, aerodynamics roughness, an important surface parameter in urban climate simulation modeling, was estimated from obstacle element descriptions acquired from 324 hectare-sized samples in Baltimore. In a second report, C. B. Jenner used Washington, D.C., as a test site for the development of a method to predict the effects of land use on the urban temperature field. Jenner used time spans ranging from 1 day to 1 month in his simulation experiment.

R. W. Pease is nearing completion of a third report on the impact of land use on climate and mapping of energy-exchange phenomena using remotely sensed data. Pease demonstrated two new tools for land use climatology research: (1) The interpretation of energy-exchange processes from space-surface characteristics and (2) the simulation of a complex of energy transfers by numerical computer models. These techniques are useful for understanding the relationship of climate to land use and for predicting alterations of climate resulting from alterations of the land surface.

Accuracy tests of the land use maps prepared for the CARETS project and published at 1:100,000 scale and experimental maps published at scales of 1:24,000 and 1:250,000 revealed that accuracy decreases as scale decreases. Field verification of 760 stratified-sampling points located in 43 randomly selected areas yielded accuracy percentages of 85 percent at a 1:24,000 scale, 77 percent at a 1:100,000 scale, and 73 percent at a 1:250,000 scale. The unit area costs of mapping also decrease as scale decreases.

During 1976, the Canada Geographic Information System (CGIS) completed its contract to digitize CARETS maps of land use and correlative data. These data were found to be comparable with those from conventional sources of areal data. Comparisons of the costs of digitizing the maps reveal that the costs are basically proportional to the density of the polygon data. CGIS data-summary tapes of land use by county in the Washington, D.C., Standard Metropolitan Statistical Area and summary tapes for the entire area were used by the Metropolitan Washington Council of Governments for examining the usefulness of the CARETS land use data in regional planning processes.

An evaluation of the Skylab S-190A and S-190B cameras and the S-192 multispectral scanner, a separate research effort within the CARETS project, demonstrated that a Skylab-type sensor platform could effectively aid land use mapping and the surveying of urban microclimatological conditions. A final report, by R. H. Alexander, J. E. Lewis, Jr., H. F. Lins, Jr., C. B. Jenner, S. I. Outcalt, and R. W. Pease (1976) was forwarded to NASA.

Land use and land cover change mapping of urban areas

In the past few years, the Geography Program has been engaged in research on the use of remotely sensed data from high-altitude aircraft and satellites in preparing maps of land use and land cover changes for selected urban areas of the United States.

A fourth experimental map of the Washington, D.C., metropolitan area at a scale of 1:100,000 showing land use changes from 1970 to 1972 was completed and published (U.S. Geological Survey, 1976c).

A 44-sheet set of maps covering the nine-county San Francisco Bay region showing (1) land use change from 1970 to 1972 in areas 4 ha or larger; (2) census tract boundaries, numbers, and centroids; (3) the UTM grid at 5-km intervals; (4) geographic grid at 5-min intervals; and (5) the 1970–72 boundaries of the urban area, was placed on open file for public reference at the USGS Public Inquiries Office in San Francisco, Calif., and the USGS library in Menlo Park, Calif. These maps complement an earlier set showing Level II land use at the time of the 1970 census.

Two sets of land use and land cover maps of the six-county greater Pittsburgh region of Pennsylvania were compiled at a scale of 1:50,000 and released to the open file. One set of 26 sheets shows a 1-km UTM grid and 1970 census tract boundaries, numbers, and centroids on a topographic map base. A second set of 26 sheets shows 1973 Level II land use and land cover data derived by manual interpretation of high-altitude color-infrared aerial photographs and some conventional photographs. Seven sheets show land use changes in Allegheny County from 1969 to 1973.

Land use and land cover change—a framework for monitoring

Land use and land cover maps and statistical data need to be kept current in order to provide useful information for land use planning, management, and research. Many different types of updating are needed by users of land use and land cover data. An analysis of the need for updating land use and land cover maps (Anderson, 1977) demonstrate that rates of change in land use and land cover vary greatly from place to place, and some types of change occur in a much shorter time frame than others.

The rapidly developing technology of remote sensing offers an efficient and timely approach to the mapping and collection of basic land use and land cover data. To a large number of users, the potential value of Landsat data for use in the consistent mapping and measuring of spatial and temporal changes in land use and land cover has yet to be fully demonstrated. However, the need for a remote sensor capable of periodically scanning extensive areas for such changes is becoming more obvious as the costs and problems of collecting information about land use and land cover by enumeration, ground surveys, and low-altitude high-resolution aerial photography continue to mount.

Land use and land cover data analysis for the Chattahoochee River Quality Assessment

Land use and land cover data-collection activities related to the Chattahoochee River Quality Assessment project were completed in FY 1976. The primary purpose of the project is to demonstrate products containing information that can guide management in making meaningful decisions on the basic development and future uses of the Chattahoochee River in Georgia. Maintenance and improvement of the water quality are prime requisites of the project.

An important focus of this study is the relationship between the results of a spatial analysis of land use and land cover data and sediment yield and pollution of the Chattahoochee River from its headwaters to the West Point Dam, approximately 320 km downstream.

Land cover mapping from Landsat digital data

The Geography Program has undertaken research to find ways to generate land cover information and to monitor land use and land cover changes by direct computer-aided interpretation of multitemporal and multispectral data acquired from Landsat.

New digital land cover maps were prepared for the Washington, D.C., urban area; the Puget Sound region of Washington; Portland, Oreg.; Boise and the Teton Dam-eastern Snake River plain of Idaho; San Jose, Calif.; and Williston, N. Dak. In addition, a map of land cover change, derived by machine-processing multitemporal data, was prepared for a portion of the growing edge of the Phoenix urban area of Arizona. The work in Idaho, Oregon, and Washington was performed as part of the Pacific Northwest Demonstration Project, jointly undertaken with NASA and the Pacific Northwest Regional Commission. One objective of USGS participation in this work was not only to learn how others use this digital technology but also to learn how to use Landsat digital data in conjunction with other data sources in the national land use and land cover mapping and data analysis program.

To this end, the USGS has made use of the ILLIAC-IV parallel-processing computer at NASA Ames Research Center, Moffitt Field, Calif., and other facilities on the Advanced Research Projects Agency (ARPA) network. The digital land cover map of the Washington, D.C., urban area was reproduced by a computer directly onto the color separation negatives from which the map was lithoprinted. The negatives were prepared to densities specified by the USGS Publications Division staff to insure legible color symbols under black map overprint when only four ink colors are used on the USGS printing press. The negatives were prepared to specifications by Mead Technology, Inc., using a laser-beam-exposing technique. A random dot matrix that can be repeated for all of the 775,000 data cells on the map was produced.

Purdue University's Laboratory for Applications of Remote Sensing (LARS), under contract with the USGS, fitted digitized census tract boundaries in the Washington, D.C., urban area onto a digitized land cover base derived from Landsat data. LARS then counted the number of Landsat picture elements (pixels) in each land cover category and census tract. Because all Landsat pixels are equal in size (0.464 ha or 1.14 acre), the area of each land cover category within census tracts was easily computed. These results demonstrate that digitized land cover data from Landsat can meet the polygon digitizing requirements of the USGS geographic information system for the land use and land cover mapping and that the areas of land cover categories within jurisdictional tracts defined in the geographic information system data base may be computed.

Geographic information system research and development

The Geography Program is conducting research on and developing a geographic information system to input, edit, store, retrieve, manipulate, and analyze digital spatial data collected from the land use and land cover mapping activities of the program. System processing includes (1) digitization of maps of land use and land cover and other environmental data, (2) editing and updating of the geographic data base, (3) retrieval and manipulation of the spatial data in order to perform area measurements, grid compositing, and statistical and other computer-aided analyses, and (4) display of graphics, and output of statistics.

Production digitizing of 76 land use and land cover maps and 286 associated maps were done under a contract with the I/O Metrics Corporation using a SWEEPNIK laser scanner. Editing and correcting of the data are two of the important functions of the Geographic Information Retrieval and Analysis System (GIRAS). The GIRAS procedures insure the production of clean or logically correct data files and include (1) converting data files to a standard GIRAS format, (2) data reduction, (3) converting data to a standard orientation and scale, (4) splitting data sets into sections for editing, (5) automatic editing and error detecting for arc or line data, (6) manual batch or interactive editing of arc data, (7) merging of labeled polygon points with the arc data to enable polygon formation through an arc-to-polygon program, (8) manual batch or interactive editing of polygon files, and (9) edge matching of each map section with neighboring map sections.

GIRAS I, the initial version of GIRAS, is a batch-oriented system with emphasis on editing and correcting digitized land use and associated data bases. Areal data and associated attributes are transformed to a fixed grid system that produces simple composites of graphic data and simple tabular listings.

A strong interest in GIRAS I was shown over the past year by Federal agencies and State cooperative users. The Fish and Wildlife Service and the National Park Service are both interested in geographic information system development; the Forest Service is developing interface procedures that will permit the direct input of Geography Program digital data into their analytical packages. All 10 States that have cooperative agreements with the USGS have requested computer programs, documentation, and digital data, and other States that also need to analyze digital spatial data have expressed a desire to obtain the GIRAS system.

In response to the need of State and Federal users of this data, conversion of GIRAS I to an interactive, time-sharing computer system, GIRAS II, began during 1976. The implementation of GIRAS II not only will mark the conversion of geographic information system production from the batch-editing of digital spatial data to interactive editing using remote graphics terminals linked to the computer but also will mark the transition of the current production-oriented data-storage system to a user-oriented geographic information system.

The Geography Program initiated and participated in the sponsorship of sixteen 1-day seminars on spatial data handling held in the National Center at Reston, Va., during the summer of 1976. Twenty-six USGS staff members who are directly involved with the design or management of spatial data handling techniques in the USGS participated in these seminars, which were organized and conducted by 12 members of the International Geographical Union (IGU) Commission on Geographical Data Sensing and Processing.

The seminars examined characteristics of USGS spatial digital data, digitizing, data encoding options, computer hardware, special output hardware, data manipulation techniques, software, and file structures and data base management systems.

A final report resulting from an earlier grant to the IGU Commission on Geographic Data Sensing and Processing (1976) examined five major data-handling techniques currently used for nongraphic storage and computer-aided manipulation of environmental data.

ENVIRONMENTAL IMPACT STUDIES

The Environmental Impact Analysis (EIA) Program provides an integrated USGS response to the

National Environmental Policy Act requirements for the preparation and review of environmental impact statements (EIS's). The program supplies direction, coordination, and expertise in the preparation of EIS's for which the USGS has lead or joint-lead responsibility; furnishes technical information and expertise to support the preparation of EIS's to which the USGS is a contributor; provides technical analysis, review, and comment on EIS's prepared by the USGS and other agencies; and stimulates, promotes, and conducts environmental research related to EIS's and the anticipated needs of the program.

During FY 1977, EIA administered the USGS lead or joint-lead responsibility with State or other Federal agencies for 17 EIS's; 16 of these were energy related (13 concerned coal, 1 oil and gas, 1 oil shale, and 1 uranium), and 1 concerned critical minerals. The EIS's scheduled for completion during the year involved oil-shale development in Colorado and Utah; phosphate development in Idaho; and development of the Decker coal mines and the Westmoreland coal mine in Montana; and the Eagle Butte coal mine, the Caballo coal mine, the East Gillette coal mine, the Rochelle coal mine, and the Bear Creek uranium mine in Wyoming.

The USGS participated in the preparation of 18 additional EIS's under the lead of other Federal agencies—namely, the Bureaus of Indian Affairs, ville Power Administration. Sixteen of these statements were energy related; one dealt with critical minerals, and one dealt with a land dispute. The USGS also provided technical information to the Forest Service for seven EIS's on geothermal energy resources and to the Bureau of Land Management for eight EIS's on oil and gas leasing on the Outer Continental Shelf.

EIA Program staff members reviewed and commented on more than 2,200 statements and related documents in order to support in-house environmental studies and to assist other agencies in areas of USGS jurisdiction and expertise. The quality of environmental statements continues to improve. Topically, most of the deficiencies are related to ground-water resources; there are fewer inadequacies related to surface water and geology.

The staff also conducted a seminar on task-force management and EIS preparation; completed a guidance manual, released in modular format, on preparing an EIS; collaborated with the Conservation Division on preparing guidelines for environmental and other data required from applicants wishing to begin surface coal mine development; conducted an evaluation of the effectiveness of increased contracting in support of EIS preparation; and began preparation of a prototype mini-EIS as part of the effort to reduce the bulk, time, cost, and manpower requirements of EIS's.

PRELIMINARY IDENTIFICATION OF IMPACTS IN EIS's

Environmental impacts identified in the draft environmental statements prepared in FY 1977 under USGS lead differ from one another because of the unique characteristics of each site. However, analyses reported in the EIS's commonly emphasize the following potential impacts:

- Disruption of aquifers.
- Reduction of air quality as the result of the introduction of dust from mining operations and as a result of a temporarily devegetated ground surface.
- Degradation of livestock and wildlife grazing, recreational hunting, and open-space qualities until reclamation is completed.
- Disruption of the existing land surface, vegetation, and soils.
- Reduction in the future productivity of the disturbed ground.
- Modification of socioeconomic patterns, including (1) permanent increases in population, traffic, roads, powerlines, and buildings; (2) increased employment; and (3) a need for more public services and recreational facilities.
- Increases in tax and royalty income to the State and county.

Modification of preliminary assessments is made as a result of Federal, State, and public review and comment on the draft statements and is incorporated into the final statements.

INTERNATIONAL COOPERATION IN THE EARTH SCIENCES

International cooperation in investigating geological resources, environmental and land use problems, and geologic hazards, together with assistance in strengthening geologic institutions and programs in other countries, has continued to be a significant part of USGS operations. All such cooperation is conducted on behalf of, or coordinated with, the Department of State. Most of this cooperation has been in the form of technical assistance to less developed countries or international organizations, sponsored or authorized by the U.S. Agency for International Development (USAID) in accordance with the United States Foreign Assistance Act. In recent years, the USGS has also been involved increasingly in joint scientific studies of geologic phenomena and techniques and in international commissions, committees, symposia, and other representational activities in support of U.S. policies and programs.

INTERNATIONAL RESOURCES PROGRAMS

During the past year, the growing worldwide concern over future supplies of energy, mineral, and water resources resulted in USGS participation in a number of special resource planning or program-development activities. B. F. Grossling, R. P. Sheldon, I. A. Breger, J. R. Donnell, and R. F. Meyer presented papers at a conference on Future Supply of Nature-Made Petroleum and Gas, held in Laxenburg, Austria, and cosponsored by the United Nations Institute for Training and Research and the International Institute for Applied Systems Analysis. The USGS continued to advise the Department of State concerning U.S. participation in the United Nations Revolving Fund for Natural Resources Exploration, to which the United States is now a contributor.

J. S. Cragwall, Jr., accompanied by five other USGS scientists, served as an official member of the U.S. delegation to a meeting of the World Meteorological Organization at Ottawa, Canada, in May. R. A. Cadigan, serving as team leader and program director, and accompanied by 11 other USGS scientists and specialists, attended meetings of the International Atomic Energy Agency and the Nuclear Energy Agency of the Organization for Economic Cooperation and Development and participated in the International Symposium on Exploration of Uranium Ore Deposits at Mexico City, Mex.

F. H. Wang, USGS marine resources advisor to the Coordinating Committee for Joint Prospecting for Mineral Resources in Asian Offshore Areas (CCOP), assisted in organizing an international petroleum conference and exhibition titled "Offshore Southeast Asia" held in Singapore. The conference was sponsored primarily by the Southeast Asia Petroleum Exploration Society; CCOP, the Society of Petroleum Engineers, the Society of Naval Architects of Singapore, and Petroleum News Magazine served as cosponsors.

The USGS also continued to support the Circum-Pacific Map Project and related activities of the Circum-Pacific Council on Energy and Mineral Resources. This project, which involves the participation of national and international agencies, research institutes, and private industry throughout the Pacific region, is one of the largest projects ever established for collecting, synthesizing, and interpreting geologic and resources data. USGS participation is intended partly to coordinate the work of five panels of Earth scientists and direct the publication of maps and partly to develop a better understanding of the known and possible resources of U.S. territorial areas in the Pacific region. Results of the project are to appear in a series of geographic, geologic, tectonic, and energy- and mineral-resource maps covering the northeastern, northwestern, southwestern, and southeastern quadrants of the Pacific Ocean and Antarctica at a scale of 1:10,000,000 on an equal-area projection. A sixth map at scale of 1:20,000,000 will cover the full Pacific basin and adjacent lands. M. J. Terman (1976) compiled the geology of China and Mongolia and an oil and gas map of China for the northwestern quadrant map and reported on China's oil and gas prospects.

TECHNICAL ASSISTANCE AND PARTICIPANT TRAINING

SCOPE OF ASSISTANCE ACTIVITIES

During 1976, the USGS continued to provide technical assistance in a wide range of scientific disciplines to many countries on behalf of the Department of State. In the period covered by this report, USGS scientists undertook 223 assignments in 44 countries. The subjects and scope of these assignments in each country are listed in table 6, and results of many of these projects are described in the section entitled "summary by countries."

As a part of USGS cooperative and assistance programs abroad, 91 Earth scientists, engineers, and technical personnel from 30 countries pursued academic, observation, or intern experience in the United States during the report period. Types of assistance to or exchanges of scientific experience with each country are summarized in table 6. In addition, the Water Resources Division alone assisted or consulted with more than 100 visitors from 28 countries. Under USGS guidance, a total of 1,659 participants from 98 countries have completed research, observation, academic, or intern training in the United States.

Since the beginning of technical assistance work in 1940, more than 2,415 technical and administrative documents authored by USGS personnel have been issued. Reports published from 1967 to 1974 are listed in Bulletin 1426 (Bergquist, 1976). During the report period, 33 administrative and (or) technical documents were prepared, and 29 reports and maps were published or released in open file (see table 7).

ASSISTANCE IN REMOTE-SENSING APPLICATIONS

A series of AIDSAT satellite technology programs were televised live from Goddard Space Flight Center in Greenbelt, Md., during the period August 1 to October 30, 1976. Each broadcast reached a different country; 14 members of the USGS assisted as panel members:

Host Country	*USGS Panel Member*
Argentina	W. D. Carter
Bolivia	W. D. Carter
Cameroon	M. J. Grolier
Central African Empire	R. D. Regan
Costa Rica	W. D. Carter
Ecuador	W. D. Carter
Haiti	R. S. Williams, Jr.
Ivory Coast	M. J. Grolier
Jamaica	Morris Deutsch
Jordan	G. F. Brown
Kenya	J. R. Jones
Libya	J. R. Jones
Mali	Morris Deutsch
Mano River Union (Liberia and Sierra Leone)	S. J. Gawarecki
Morocco, Conference of Arab Ministers	J. R. Balsley
Oman	G. F. Brown
Peru	W. A. Fischer
Sudan	W. F. Seitz
Surinam	W. R. Hemphill
Thailand	J. O Morgan
United Arab Emirates	G. F. Brown
Upper Volta	M. J. Grolier
Uruguay	G. C. Taylor, Jr.
Yemen	J. R. Jones

The telecasts were part of a program sponsored by USAID to demonstrate possible applications of space-age technology in developing countries.

Remote-sensing applications and training continued to occupy much of the USGS technical assistance program. In particular, data produced by Landsat and other spacecraft have had a great impact on the Earth-sciences communities of the world, and requests for cooperation and training have increased as more applications are tested and as more knowledge is disseminated concerning the use and interpretation of satellite imagery. Landsat receiving stations are active in Brazil, Canada, and Italy and are under construction in Argentina, Chile, Iran, and Zaire. Two workshops for transferring knowledge about satellite and aerial remote sensing, given at the EROS Data Center, in Sioux Falls, S. Dak., were attended by 52 participants from 22 countries. Special training programs were also presented at the Geological Survey of Iran, at the Directorate General of Mineral Resources in Saudi Arabia, and in Ethiopia, Nepal, Somalia, and Thailand in cooperation with United Nations Development Programme/Food and Agriculture Organization and (or) USAID. Other similar training programs were conducted for the Coordinating Committee for Joint Prospecting for Mineral Resources in Asian Offshore Areas (CCOP) in Thailand and in the Central Treaty Organization countries. These programs were sponsored by the cooperating countries, by the United Nations or other international organizations, or by USAID.

Examples of cooperative efforts based on satellite data are:

- The Government of the Central African Empire, in cooperation with NASA, requested that the USGS investigate a large magnetic anomaly, discovered by research of satellite (MAGSAT)

Table 6.—*Technical assistance to other countries provided by the USGS during January-October 1976*

Country	USGS personnel assigned to other countries			Scientists from other countries trained in United States	
	Number	Type	Type of activity[1]	Number	Field of Training
Latin America					
Argentina	1	Geophysicist-seismologist	C		
	1	Remote-sensing specialist	C		
	1	Geophysicist	C		
Belize	1	Geologist	C		
	1	Physical science technician	C		
Bolivia	4	Geologist	D	2	Seismology.
	1	Remote-sensing specialist	D		
	1	Hydrologist	D		
	1	Geophysicist	D		
Brazil	4	Geologist	A	1	Petrology and petrolography.
				1	Remote sensing.
Chile	1	Research geophysicist	D		
	1	Geophysicist	D		
	1	Remote-sensing specialist	D		
Columbia				3	Economic geology.
				1	Geology.
Costa Rica	1	Research geophysicist	D		
	1	Geophysicist	D		
	1	Electronics engineer	D		
	2	Geologist	D		
	1	Remote-sensing specialist	D		
Ecuador	2	Geologist	C		
	1	Geophysicist	C		
El Salvador	1	Geologist	D		
	1	Geophysicist	D		
	1	Physical science technician	D		
	1	Electronics engineer	D		
	1	Remote-sensing specialist	D		
Guatemala	18	Geologist	C, D		
	3	Geophysicist	C		
	1	Seismic engineer	C		
	2	Seismologist	C		
	2	structural engineer	C		
	1	Electronics technician	C		
	3	Civil engineer	C		
	1	Physical science technician	D		
	1	Remote-sensing specialist			
Honduras	1	Geologist	C		
	1	Physical science technician	C		
	1	Remote-sensing specialist	D		
Mexico				4	Remote sensing.
				1	Cartography.
Nicaragua	2	Geophysicist	C		
	2	Geologist	D		
Panama	2	Geologist	D		
	1	Remote-sensing specialist	D		
Peru	10	Geologist	A, C, D		
	1	Structural engineer	C		
	2	Geophysicist	D		
	1	Physical science technician	C		
	1	Remote-sensing specialist	D		
Uruguay				1	Remote Sensing.
Venezuela	1	Geophysicist	D	1	Uranium and thorium.
				2	Remote sensing.

See footnote at end of table.

Country	USGS personnel assigned to other countries			Scientists from other countries trained in United States	
	Number	Type	Type of activity[1]	Number	Field of Training
			Africa		
Algeria	3	Geologist	C, D		
	1	Remote-sensing specialist	C		
	1	Senior scientist	C		
Central African Republic	1	Geologist	D		
	1	Geophysicist	D		
Egypt	5	Geologist	A, B, C	4	Remote sensing.
	1	Cartographer	A, B	3	Cartography.
				1	Typography.
Kenya	1	Hydrologist	A		
Malagasy Republic				1	Seismology.
Morocco	2	Geologist	D		
Niger	1	Hydrologist	C		
Nigeria	3	Geologist	A		
South Africa	2	Geologist	D		
Sudan	2	Geologist	D		
			Near East and South Asia		
Afghanistan				1	Seismology.
India	1	Hydrologist	D	1	Mineral exploration.
	1	Electronics engineer	D	3	Remote sensing.
				1	Industrial minerals.
				1	Cartography.
Iran	2	Geologist	C, D	7	Remote sensing.
	1	Remote-sensing specialist	D		
Iraq				2	Remote sensing.
Oman	1	Geologist	D		
Pakistan	1	Geologist	D	1	Uranium exploration.
	1	Remote-sensing specialist	D	1	Nuclear materials.
Qatar	1	Hydrologist	D	1	Remote sensing.
Saudi Arabia	2	Administrative Officer	A, B	6	Remote sensing.
	6	Cartographer	A, B	1	Geophysics.
	2	Chemist	A, B	2	Photography.
	1	Civil Engineer	D	1	Editing and publications.
	2	Computer specialist	A, B	4	Cartography.
	1	Desalination expert	D		
	1	Drilling operator	A, B		
	2	Editor	A, B		
	1	Electronics technician	A, B		
	1	General services officer	A, B		
	1	Geochronologist	A, B		
	20	Geologist	A, B, D		
	6	Geophysicist	A, B		
	6	Hydrologist	D		
	2	Mathematrician	A, B		
	1	Photo lab chief	A, B		
	2	Photogrammetrist	A, B		
	1	Procurement specialist	A, B		
	1	Remote-sensing specialist	A, B		
	1	Rock properties specialist	A, B		
	1	Senior water resources specialist	D		
	2	Topographic engineer	A, B		
	1	Water economist	D		
Syria				1	Exploration geophysics.

See footnote at end of table.

Country	USGS personnel assigned to other countries: Number	Type	Type of activity[1]	Scientists from other countries trained in United States: Number	Field of Training
Near East and South Asia—Continued					
Turkey	4	Geologist	C, D	1	Remote sensing.
	1	Remote-sensing specialist	D		
Yemen	2	Hydrologist	A, B		
	1	Geologist	A, B		
Far East					
Burma				1	Mineral exploration and geologic mapping.
				1	Photography.
				1	Geologic education.
China, Republic of				6	Remote sensing.
				1	Irrigation and drainage.
Indonesia	1	Research chemist	D	1	Remote sensing.
Japan				2	Remote sensing.
Nepal	1	Remote-sensing specialist	D		
Philippine Islands	1	Photomosaic specialist	C	1	Remote sensing.
	1	Geologist	D		
Thailand	2	Geologist	A	1	Cartography.
	4	Remote-sensing specialist	A, C, D	2	Seismology.
	1	Chemist	D		
Other					
Australia	1	Geologist	C		Seismology.
					Remote sensing.
Austria	4	Geologist	C		
	1	Research chemist	C		
	1	Research geophysicist	C		
Belgium					Remote sensing.
Cape Verde Islands	1	Hydrologist	C		
Denmark	1	Geophysicist	C		
France	1	Geophysicist	C		Aluminum chemistry.
	1	Hydrologist	D		Remote sensing; hydrology.
French West Indies	2	Geophysicist	D		
Germany					Remote sensing.
					Volcanic rocks.
					Seismology.
Italy	1	Cartographic technician	D		
New Zealand					Seismology.
Norway					Nuclear analysis.
					Remote sensing.
Spain	1	Geologist	D		Humic substances.
Switzerland	1	Hydrologist	D		

[1] A, Broad program of assistance in developing or strengthening Earth-science institutions and cadres; B, broad program of geologic mapping and appraisal of resources; C, special studies of geologic or hydrologic phenomena or resources; D, short-range advisory help on geologic or hydrologic problems and resources.

Table 7.—*Technical and administrative documents issued during the period January through September 1976 as a result of USGS technical and scientific cooperation programs*

	Reports or maps prepared			
		Approved for publication	Published	
Country	Project and administrative reports	by counterpart agencies or USGS	In technical journals	By USGS
Argentina				1
Bangladesh				1
Bolivia	2			
Brazil	2	1		
Central African Empire	1			
Chile				1
Colombia	2	3		
Costa Rica				1
Ecuador	2			
Guatemala	1	1		1
Indonesia	1	1	3	
Iran		1		
Kenya				1
Liberia	1			
Pakistan	1			2
Qatar				1
Saudi Arabia	6	9	7	4
Taiwan	1	1		1
Uruguay		1		1
Yemen Arab Republic	9	1		1
General	4	4	2	1
Total	33	23	12	17

data, and participate in a field reconnaissance survey of geologic conditions of the area. Cooperative work is continuing toward determining the mineralogic-economic significance of the findings.

- The Governments of Costa Rica, Guatemala, Honduras, Nicaragua, and San Salvador, in cooperation with the Inter-American Development Bank, were advised on establishing and conducting programs for applying satellite and aerial remote-sensing technology to resources and environmental problems.
- Landsat and aerial data were used in support of a regional reconnaissance program for hydrologic and engineering planning in the Rio Pilcomayo basin of Argentina, Bolivia, and Paraguay in cooperation with the Organization of American States and the national governments.
- Aerial magnetic surveys are used routinely as part of the geologic mapping program being conducted by the USGS for the Government of Saudi Arabia. Landsat data also are being used in support of the mapping program and, in addition, were used effectively in a short-term preliminary geologic and hydrologic study of the Yemen Arab Republic.
- A multidisciplinary remote-sensing project in Thailand, sponsored by USAID, was successfully completed during the year. This 4-year project was designed to assist resource agencies and institutions in Thailand in applying data derived from analysis of Landsat imagery to improve development and management of Earth resources at the national level. Twenty-two organizations participated in the project, which was coordinated by the National Research Council of Thailand.
- Landsat image analysis programs conducted by Thai Government agencies since 1973 have produced data that are considered invaluable for resource management and conservation. Results obtained to date have encouraged the Royal Thai Government to intensify and broaden its national remote-sensing program; it is considering development of improved data acquisition and reproduction and computer-processing capabilities.
- Landsat data are being used to prepare a tectonic map of Thailand and to improve existing geologic maps of selected transect areas of the island-arc systems of several East Asia countries. This activity, which is being conducted in cooperation with CCOP and the International Decade of Ocean Exploration program (IDOE), will produce transect maps to supplement offshore geophysical data being gathered under the IDOE program.

ASSISTANCE TO REGIONAL ORGANIZATIONS

In addition to providing direct assistance to countries, the USGS has continued to assist certain regional organizations. F. H. Wang provided general guidance on program planning and development to the 10-nation Coordinating Committee for Joint Prospecting for Mineral Resources in Asian Offshore Areas (CCOP) headquartered in Bangkok, Thailand.

A broad range of activities was carried out by other USGS scientists serving as members of Central Treaty Organization (CENTO) Working Groups. Meetings and field programs were held by the Working Groups on Recent Tectonics, Hydrogeology, Intrusive Rocks and their Relation to Mineral Deposits, and Remote Sensing. D. F. Davidson served as U.S. delegate to the annual meeting of the CENTO Advisory Group on Mineral Development held in Karachi, Pakistan, in November 1976.

R. V. Sharp attended the meeting of the CENTO Working Group on Recent Tectonics held in Turkey, where surface fault movements associated with seismic activity were discussed. A field trip was taken along a segment of the north Anatolian fault, Turkey's most earthquake-prone fault zone. This area is important because of its comparability to the San Andreas fault in California.

SCIENTIFIC AND TECHNICAL COOPERATION

SCOPE OF COOPERATION

The USGS has a rapidly growing involvement in cooperative research and exchange activities of mutual benefit to the United States and to the cooperating countries. These activities involve studying geological or resource phenomena, testing geologic concepts and techniques, or exchanging scientific data. Some of these activities are carried out under bilateral agreements, and others involve participation in multilateral programs. Results of the bilateral activities are given in the section entitled "Summary by countries." Some of the major worldwide programs are reviewed below.

GEOLOGIC HAZARDS AND DISASTER RESPONSE

The USGS became increasingly active in the study of geologic hazards and disaster phenomena, both as an extension of its domestic research program and in response to requests from other countries channeled through USAID.

National Earthquake Information Service

The USGS National Earthquake Information Service (NEIS) maintains a 24-hour standby system in Golden, Colo., to which arrival times and amplitude data recorded at seismographs all over the world are sent by telegram and airmail as soon as possible after major shocks occur. Computers at NEIS compute earthquake origin time, geographic coordinates, depth, and magnitude and transmit the information to public safety agencies, disaster relief organizations, news media, and others who need to know. This monitoring of global seismicity requires a high degree of international cooperation. Nearly all nations of the world, including the Soviet Union and Mainland China, now contribute to this program, which annually determines the source parameters of more than 6,000 seismic events. During the communications blackouts that accompany large earthquakes, these data may be vitally important.

The USGS seismic observatories at Guam and at Newport, Wash., are part of an international network of seismographs and tide stations designed to furnish warnings in the event of a tsunami in the Pacific basin. J. N. Taggart participated in a meeting of U.S.-U.S.S.R. tsunami experts held at Novosibirsk in the U.S.S.R. Plans were made to exchange seismic data, seismic instruments, and scientific personnel during 1977 and 1978. A Soviet seismologist spent some time in Albuquerque, N. Mex., and Golden, Colo., discussing ultralong-period systems with USGS instrument specialists.

As part of a long-standing policy to foster the international exchange of seismic data, the NEIS conducts training sessions on earthquake seismology and observatory practice for foreign nationals. This instruction stresses seismic instrumentation, interpretation of seismograms, and methods of data transmission. During the past year, two members of the staff of the station at Kabul, Afghanistan, received instruction at the instrument laboratory at Albuquerque, N. Mex., and at NEIS. A similar program was carried out for a graduate student from Costa Rica.

J. W. Dewey assisted in installing and upgrading four seismograph stations in Costa Rica and, in cooperation with local seismologists, developed a simple procedure to expedite the flow of data from Costa Rica to the NEIS. Arrangements were made for Dewey to return to Costa Rica to continue developing a broad-based seismological program for that country.

Guatemalan earthquake of February 4, 1976

On February 4, 1976, a major earthquake shook Guatemala and caused an estimated 23,000 deaths and tremendous damage in a heavily populated area in the south-central part of the country. In accord with the USGS practice of investigating disasters to help develop plans and guidelines for reconstruction and to obtain scientific information about the geologic processes that caused the disasters, George Plafker and C. F. Knudson (USGS) were on the scene in Guatemala within 36 hours and were followed in a day or two by A. F. Espinosa, Raul Husid, and C. J. Langer (USGS), and K. V. Steinbrugge (Earthquake Engineering Research Institute).

The epicenter was south of Lake Izabal in the valley of the Motagua River, near the Carribbean coast and about 150 east-northeast of Guatemala City. The magnitude of the shock was 7.5 on the Richter scale, and the focal depth was about 33 km. The epicenter was close to the Motagua fault, which is one of the major faults in Central America, and has been recognized from the northeastern edge of the Central American chain of volcanoes and recent lava flows east-northeastward almost to the Carribbean coast. Ground breakage was observed along 240 km of the fault. The movement was left lateral, the northern block moving westward relative to the southern block. Maximum observed displacement was about 1.5 m but averaged 1 m for the full length of the fault. Secondary movement also took place along the Mexico fault, which marks the western edge of the north-trending graben in which Guatemala City lies. Here the movement was vertical, downdropped on the east, and amounted to about 13 m at a maximum.

Three strong aftershocks that followed over the next week, ranged in magnitude from about 4.5 to 6. Two of these were in the eastern part of Guatemala not far from the epicenter, but the strongest was near Guatemala City and close to Pacaya Volcano. This aftershock, which occurred 2 days after the initial shock, did considerable damage to structures in Guatemala City that had already been weakened by the first quake.

Seismological investigations in Costa Rica

J. W. Dewey and W. J. Strahle went to Costa Rica with the Escuela CentroAmerican de Geologia of the Universidad de Costa Rica (USR) to work on a project funded by the Organization of American States. Strahle installed or repaired instruments at San Ramon and Volcan Poás, La Lucha Farm, and San José. All four stations are now operating. Dewey worked on interpreting seismograms and using the program HYPO71. A number of local earthquakes were located by using data from the San José and La Lucha Farm stations and the seismographic stations in the northwestern part of the country, which are operated by the Instituto Costaricense Electricidad. Most earthquakes that were located occurred off the Pacific coast of Costa Rica. There is a suggestion, however, of significant seismic activity on the Candelaria fault, which strikes east and passes near La Lucha Farm. Dewey established a means of sending seismograph data from the UCR network to NEIS to be included in the global network.

Strong-motion programs in Southeast Asia

Under the sponsorship of UNESCO, R. P. Maley toured Hong Kong, Indonesia, Malaysia, the Philippine Islands, and Thailand to determine the relative need for strong-motion instrumentation programs in each area. Meetings were held in each country with earthquake engineers, public works officials, national geological organizations, and seismological agencies to determine the following: (1) Significant seismic hazards presented by strong shaking, (2) status of and plans for engineering seismology programs in each country, (3) responsibilities of various organizations, (4) fundamentals of network design and maintenance, record collection, and data processing and analysis, and (5) projected implementation of UNESCO's contribution to strong-motion programs in the five countries. Development of strong-motion programs in highly seismic areas of Southeast Asia can be a source of potential-risk data for worldwide use in earthquake engineering and engineering seismology.

INTERNATIONAL COMMISSIONS AND REPRESENTATION

V. E. McKelvey (USGS) headed the U.S. delegation to the 25th International Geological Congress (IGC) held in Sydney, Australia. A USGS exhibit arranged by D. M. Kinney (USGS) included, in addition to recently published maps, a display of Landsat imagery and images received from Viking Lander 1 on Mars. These exhibits and a preliminary copy of a geologic and tectonic map of the Caribbean area compiled by J. E. Case (USGS) attracted great attention. The Circum-Pacific Council on Energy and Mineral Resources sponsored an exhibit that consisted largely of compilations of the Circum-Pacific Map Project and that was prepared by P. W. Richards (USGS).

About 30 papers were presented by USGS scientists in the general sessions of IGC. USGS personnel also participated on various commissions and international programs and committees in conjunction with the IGC: Kinney, (Vice President for North America), P. W. Guild, (USGS) (President of the Subcommission for the Metallogenic Map of the World), and P. B. King (USGS) (consultant to the Subcommission for the Tectonic Map of the World) participated in meetings and working groups of the Commission for the Geological Map of the World. At the International Geological Correlations Program (IGCP) meeting, Guild and P. C. Bateman (USGS) participated in a review of the status of the program, including its history, proposals, projects, and committees. D. F. Davidson (USGS) served as convenor and chairman of an IGC Seminar on Data Storage and Retrieval for Developing Countries sponsored by the Committee on Storage, Automatic Processing, and Retrieval of Geological Data and the Association of Geoscientists for International Development. E. H. Bailey (USGS) summarized the successful multinational Central Treaty Organization training program, which he has directed each summer for the past 10 years.

USGS geologists have taken part in many projects under the IGCP, which is sponsored jointly by the International Union of Geological Sciences (IUGS) and the United Nations Educational, Scientific and Cultural Organization. USGS scientists serve as the leaders of three IGCP projects: (1) Circum-Pacific plutonism, (2) standards for computer applications in resource studies, and (3) remote sensing and mineral exploration.

The project on circum-Pacific plutonism, under the leadership of Bateman, is studying the petrology, distribution, and geological framework of the plutonic rocks found along continental margins around the Pacific. Joint working-group meetings and field trips have been held in Canada, Chile, Malaysia, and the United States. The project on standards for computer applications, headed by A. L. Clark (USGS), held a working-group meeting in Norway to help other countries develop and apply computerization procedures to resource assessment. The project on remote sensing, under the leadership of W. D. Carter and L. C. Rowan (USGS), involves joint study, interpretation, and exchange of data on remote-sensing interpretations of geologic features related to known mineralization.

One of the major IGCP projects in which the USGS participates is the Caledonide orogen project, which involves analysis and reconstruction of the early Paleozoic geology of the North Atlantic region. The U.S. working group for this project is led by R. B. Neuman (USGS) and includes scientists from universities and other organizations. The evolution of the orogen is being analyzed by working groups on both sides of the Atlantic through the compilation of 1:1,000,000-scale maps showing basement and basement-cover relations, plutonism, volcanism, sedimentary and faunal provinces, deformation, and metamorphism.

R. G. Coleman and W. P. Irwin (USGS) participated in a cruise of the Russian oceanographic research vessel DMITRY MENDELEEV as part of the IGCP project on ophiolites. The cruise conducted dredge sampling at sites in the Mariannas Trench and the Philippine Sea for comparative study of seafloor and land ophiolites.

Guild and H. L. James (USGS) continued to serve on IGCP scientific committees, and J. A. Reinemund (USGS) continued to serve on the IGCP Board, which coordinates and directs the program.

The USGS has accepted the lead role in a Working Group on the Precambrian under the auspices of the Subcommission on the Precambrian of the Commission on Stratigraphy of the IUGS. The Working Group has been asked to cover the United States and Mexico. The first goal of the Working Group is to prepare geologic-chronometric charts showing the state of knowledge concerning ages and correlations of all known Precambrian rock bodies. Chairman J. E. Harrison (USGS) has enlisted 15 U.S. geologists and geochronologists, and Diego Cordoba (Institute of Geology of the National University of Mexico) has appointed two representatives for Mexico. Murray Frarey (Geological Survey of Canada), Chairman of the Working Group on the Precambrian for Canada, has offered close cooperation in solving mutual problems.

R. W. Fary (USGS) represented the Department of Interior at the second meeting of the Joint U.S.-Iran Committee for Science, Technology, and Education Exchange, held in Tehran, Iran. F. E. Clarke represented the Department at the fifth meeting of the Joint U.S.-Egypt Commission on Technology, Research, and Development. Reinemund attended the Conference on Science and Technology in the Arab Countries, held in Rabat, Morocco, and headed the U.S. delegation to the meeting of the Economic and Social Commission for Asia and the Pacific (ESCAP) Committee on Natural Resources, held in Bangkok, Thailand. The committee reviewed the progress of a number of ESCAP projects, including compiling regional resource maps, stratigraphic correlation, strengthening the regional mineral development center, and establishing a regional tin research center. The committee also reviewed the progress of the Circum-Pacific Map Project within the ESCAP region and considered measures to establish coordination between the project and the Coordinating Committee for Offshore Prospecting for Mineral Resources in the South Pacific (CCOP-/SOPAC).

R. J. Dingman (USGS) presented three papers at the Symposium on Uses of Cartography in Water Resources, held at the University of San Carlos in Guatemala City, Guatemala. The symposium was sponsored by the Organization of American States, the Pan American Institute of Geography and History, and the School of Sanitary Engineering.

R. L. Miller and A. H. Chidester (USGS) attended the Third Congress of Latin American Geology, held in Acapulco, Mexico. Prior to the conference, they conferred with officials in Costa Rica, Guatemala, Mexico, and Nicaragua on current programs in the national geological agencies and institutions and visited field projects in potential geothermal areas and earthquake-damaged areas in Guatemala and Nicaragua.

R. L. Parker (USGS) and Chidester participated in the International Symposium on Carbonatites, sponsored by the Geological Society of Brazil and the International Association of Geochemistry and Cosmochemistry in Pocos de Caldas, Brazil.

Chidester and Guild attended the Third Biennial Conference of the Geological Society of Africa at the University of Khartoum in Sudan and took part in a field trip to the Ingessana Hills ultramafic complex.

For the United Nations regional meeting on Technical Cooperation among Developing Countries, held in Bangkok, Thailand, F. H. Wang (USGS) prepared background materials summarizing (1) CCOP's significant offshore surveys during the past 10 years to stimulate intensive activities of the petroleum industry, (2) CCOP's offshore tin and detrital minerals programs, and (3) current IDOE research.

RESOURCES ATTACHE AND REPORTING PROGRAM

A major responsibility of the Department of the Interior is to appraise the present and future supplies of mineral and energy raw materials in relation to the Nation's requirements. In 1975, petroleum imports represented 37 percent of consumption. The United States is dependent on foreign sources for more than 50 percent of its supplies of 21 important minerals, including manganese, chromium, asbestos, tin, and nickel. In addition, more than 25 percent of eight other minerals, including iron, gold, and silver, are imported. It is expected that the United States will be increasingly dependent on foreign sources in the future. The two Government agencies primarily involved in developing information about energy and mineral raw materials are the Bureau of Mines (present supplies and known reserves) and the USGS (undiscovered resources and future supplies). To help meet the need for data on reserves and resources in foreign countries, the Bureau of Mines and the USGS are cooperating with the Department of State in a Resources Attache and Reporting Program. The program is expanding and will ultimately include at least 20 regional Resources Attaches; of the 12 resources attache positions that have been established, 9 are staffed (Australia, Belgium, Bolivia, Brazil, India, Japan, South Africa, Thailand, and Venezuela). Information is also received from officers reporting on a part-time basis in many countries. Comprehensive reports on mineral-resource matters, received regularly from the attaches, supplement numerous published and unpublished geological and resource reports transmitted to the USGS and the Bureau of Mines through established bilateral channels.

INTERNATIONAL HYDROLOGICAL PROGRAM AND RELATED ACTIVITIES

The International Hydrological Program (IHP) and activities related to the program are the responsibility of the USGS Office of International Activities (OIA). These activities are under the general guidance of the U.S. National Committee on Scientific Hydrology (USNC/SH), which is concerned primarily with the IHP of the United Nations Educational, Scientific and Cultural Organization (UNESCO) and the hydrological activities of the World Meteorological Organization. In addition, the USNC/SH cooperates with international nongovernmental bodies in sponsoring, organizing, and otherwise encouraging international meetings. These bodies include the International Association of Hydrological Sciences (IAHS), the International Association of Hydrogeologists (IAH), the International Standardization Organization (ISO), and the Association of Geoscientists for International Development (AGID).

The OIA and USNC/SH also cooperate with other intergovernmental bodies such as the International Atomic Energy Agency, the World Health Organization, and the Food and Agriculture Organization and with nongovernmental groups such as the International Commission on Irrigation and Drainage, the International Commission on Large Dams, and the Association for Hydraulic Research. Within this part of its program, OIA also seeks to answer many inquiries from universities, local hydrological societies, and individuals. These inquiries are concerned mostly with education, publications, technical matters, research assistance, and organizational activities.

In 1976, USGS scientists participated extensively in the operations of international organizations and contributed many scientific papers. A. I. Johnson is First Vice President of IAHS, and R. F. Hadley and William Back are Vice-Chairmen of the IAHS International Commissions on Surface Water and on Water Quality, respectively. Johnson is also Chairman of the U.S. National Committee for the IAHS, and L. A. Heindl is Chairman of the U.S. National Committee for the IAH and editor of the AGID Newsletter. G. H. Davis is Treasurer of the International Water Resources Association.

International symposia and workshops organized with the assistance of the USNC/SH and the USGS included: Hydrological Problems in Karst Regions (Bowling Green, Ky., April 26-29, 1976); New Directions in Education (Sydney, Australia, August 22, 1976); International Workshop on Socio-Economic Effects of Urban Hydrology (Lund, Sweden, November 15-19, 1976); and Land Subsidence (Anaheim, Calif., December 13-17, 1976). These gatherings were among the 45 international meetings attended by participants from the Water Resources Division. The meetings included 18 scientific sessions, two working sessions connected with the IHP, 8 working sessions called for United Nations programs other than the IHP, 7 joint U.S.-Canada meetings to exchange cross-boundary data, 4 official U.S. information exchanges with countries such as the U.S.S.R. and Mexico, 14 sessions on problems of standardizing equipment, procedures, and methodologies, and 1 session on training.

Davis, D. G. Anderson, and R. H. Langford also put considerable effort into the preparation of draft thematic papers for the United Nations Water Conference held in March 1977 in Argentina.

The USNC/SH, under the chairmanship of J. S. Cragwall, Jr., contributed to the IHP by arranging for the translation into English of the Russian treatise "World Water Resources and their Future" by M. I. Lvovitch of the U.S.S.R. Academy of Sciences. In order to acquaint English-speaking hydrologists with Soviet literature in their field, Heindl and Thomas Maddock III served on the Soviet Hydrology Selections Committee of the American Geophysical Union.

The Secretariat for the U.S. National Committee on Scientific Hydrology also assisted in the National Academy of Sciences' completion and publication of three reports prepared for activities of the U.S. National Committee for the International Hydrological Decade. These included "Water in Carbonate Rocks—U.S. Progress in Perspective," "Education in Hydrology and Water Resources 1965-1974—An Overview with Recommendations," and "Snow and Ice Hydrology—the United States—Current Status and Future Directions." Contributors to these reports included Back, V. T. Stringfield, R. L. Nace, and M. F. Meier.

UNESCO published two volumes in its series on "Studies and Reports in Hydrology," for which the USNC/SH and the USGS provided data on the United States. These are "World Catalog of Very Large Floods" and "Floodflow Computation." S. E. Rantz was one of the three coeditors of the second volume.

HISTORICAL REVIEW OF HYDROLOGIC INVESTIGATIONS

G. C. Taylor, Jr. (1976), described the history of USGS activities in international water-resource investigations and institutional development as well as exchanges in scientific and applied hydrology from 1940 to 1970. The bulk of these activities was sponsored by the U.S. Department of State, USAID and its predecessors, the United Nations and its specialized agencies, and regional intergovernmental agencies.

From 1940 to 1970, USGS hydrogeologists, water chemists, engineers, and hydrologists completed 340 short- and long-term project-oriented international assignments in some 80 host countries. During the same period, 428 water scientists, engineers, and technicians from 60 countries received academic and inservice training in USGS water-resource facilities in the United States. Also, during that period, 336 technical and scientific reports resulted from water-resource projects in the U.S. bilateral program.

SUMMARY BY COUNTRIES

ARGENTINA

At the request of the Organization of American States, W. W. Hays gave a 4-week course on the "Interpretation of Gravity Data" in June and July 1976. The course was attended by 27 individuals representing 10 Argentine agencies and institutions. The course, which provided specialized training for developing Argentine natural resources, provided a basis for exchange of technical information.

BOLIVIA

Under an agreement with the World Bank, Ernest Dobrovolny acted as a consultant for proposed urban projects in the La Paz Valley of Bolivia. The sites considered required studying slope stability in relation to potential geologic hazards, landslides, and hydrology. Dobrovolny inspected 12 sites and reviewed the plans for increasing slope stability, for initiating erosion control, and for stabilizing landslides.

Harold Kirkemo visited La Paz to discuss with officials of the Ministry of Mines and Metallurgy plans for developing a fund to assist exploration in the small mines sector.

BRAZIL

In May 1976, officials of the Brazilian Ministry of Mines and Energy, the U.S. Department of the Interior, the USGS, and USAID signed a Statement of Principles for Technical Cooperation in the Earth Sciences between the Governments of Brazil and the United States.

L. S. Hilpert prepared a review of Brazil's nonferrous metallic resources exploration program and made recommendations for the exploration and assessment of selected promising mineral districts. The report was based on 3 months of fieldwork in Brazil, during which Hilpert visited more than a dozen of the more important mineral districts and conferred with officials in regional and district offices of Departamento Nacional da Producao Mineral.

CAPE VERDE

The need for water to irrigate about 600 ha of flatland and to provide additional municipal supplies for Tarrafal prompted the Government of the Republic of Cape Verde to request assistance from USAID. R. J. Dingman made a reconnaissance of water resources and related features of the northern part of mountainous Sao Tiago Island. He and other members of the USAID team suggested a plan for investigating water resources and for constructing wells and collecting galleries that will permit the development of ground water at rates greatly exceeding recharge to provide an interim water supply, pending installation of structures to retain and convey runoff from the characteristically short, intense storms. One-third of the area's annual precipitation may fall in 1 day, and, at times, it amounts to more than 250 mm in 24 hours in the high areas. Perhaps as much as 50 percent of the annual rainfall runs off into the sea.

ECUADOR

A reconnaissance appraisal of potential volcanic hazards from Cotopaxi Volcano in Ecuador was undertaken by D. R. Mullineaux and C. D. Miller at the request of the Ecuadorian Government after Cotopaxi showed signs of increased thermal activity in 1975. The study was conducted under the auspices of USAID. An appraisal based on volcanic events at Cotopaxi during historic time suggests that the chief hazards from future eruptions will include ashfalls, mudflows, and floods. Ash will chiefly affect areas west of the volcano, where fertile agricultural lands are occupied by several tens of thousands of people. Large mudflows and floods will affect the floors of valleys that head on the volcano. Future ashfalls, mudflows, and floods could have disastrous effects on people, animals, works of man, and food crops downvalley and downwind from Cotopaxi.

The historical record of Cotopaxi's eruptive activity indicates that future eruptions are a near certainty. Of the 50 eruptions reported since 1738, 20 have produced volcanic ash, lava flows, and mudflows. At least five of those eruptions resulted in the loss of many lives and much property. The historic record indicates that, during the last 238 years, eruptions have produced lava and mudflows on an average of about once every 12 years. At the present time (1976), Cotopaxi has been inactive for at least 34 years and perhaps as long as 72 years.

GUATEMALA

Earthquake of February 4, 1976

Under an agreement sponsored by USAID, A. F. Espinosa and Raul Husid (USGS) and Antonio Quesada (Organization of American States) (1976) made engineering and geologic studies of the February 4, 1976, earthquake in Guatemala. The earthquake caused extensive damage in Guatemala and in metropolitan Guatemala City. Data gathered in the field and analyzed consisted of questionnaires and damage photographs. The isoseismal pattern in Guatemala suggests that the shaking intensity was greatest in the western part of the country. This intensity distribution suggests a fault propagation rupture from east to west. Statistics on casualties and damage were collected for each Department (State) of the country. Information from Guatemala City and the area along the Motagua fault delineates the distribution of Modified Mercalli intensities, damage to adobe-type structures, strong motion, and other related phenomena.

Landslides

M. G. Bonilla and Ernest Dobrovolny, at the request of the Inter-American Development Bank, investigated a possible landslide area adjacent to the right abutment or Guatemala's Pueblo Viejo damsite in September 1976. On the basis of earlier work and helicopter-supported field examination, they reported that the Cuilco-Chixoy-Polochic fault could generate an earthquake that could produce a strike-slip displacement of 3.5 m and that could cause substantial sliding near the power tunnel intake. Bonilla and Dobrovolny concluded that the designated landslide area is not a single landslide and that, whereas a landslide probably would not harm the reservoir and dam, it could have a serious effect on the access road being constructed. The construction of the road could cause additional sliding if runoff from the road enters the slide or if the cut and fill decrease the stability of the slide.

INDIA

R. J. Burt (USGS) and S. V. Allison (World Bank), who served as hydrologists on a World Bank Foodgrains Review Mission to Assam, India, concluded that farmers living on the plain of the Brahmaputra River is Assam State inhabit an "earth platform" about 3 m above one of the major aquifers of the world. Farmland is irrigated only for brief periods in the relatively short dry season. The area is ideal for irrigation (1) because moderate temperatures, high humidity, and light winds during the irrigation season contribute to low rates of water use by plants and (2) because large quantities of water of good chemical quality are available at shallow depths. Burt and Allison recommended a program for development and monitoring of ground water.

INDONESIA

D. J. Grimes was assigned to Indonesia in March 1976 under the sponsorship of USAID to assist with the installation and testing of emission spectrographic instruments at the Geological Survey of Indonesia (GSI) in Bandung. The instruments were purchased on the basis of recommendations made by Grimes following previous assignment to Indonesia. When the instruments were set up, Grimes spent 1 week making emission spectrographic analyses of geologic materials for 30 elements to test the instruments under normal laboratory workload. Lectures on the theory, operation, and practical application of emission spectroscopy were also given to new GSI employees.

At the completion of Grimes' assignment, the emission spectrographic laboratory at GSI was completely operational, and two analysts trained in spectroscopy as well as a spectrographic apprentice were assigned to full-time spectrographic work. The present workload capacity of the laboratory is approximately 200 samples per week for 30 elements each, or about 6,000 determinations per week.

IRAN

A group of craters 12 km southeast of Kerman, Iran, the largest of which is 1,200 m across and 300 m deep, was studied by D. J. Milton at the request of the Geological Survey of Iran. Originally, the craters were thought to be meteorite craters, but they proved to be typical maars—excavated depressions with rims of bedded pyroclastic debris. Most of the crater rims are composed entirely of country rock clasts, but the largest crater yields tephrite, which is composed of phenocrysts of phlogopite, clinopyroxene, and olivine in a groundmass of anorthoclase, analcime, hauyne, clinopyroxene, and magnetite, and a cumulate of phlogopite and clinopyroxene with highly potassic glass. The occurrence of hauyne as a groundmass mineral is a rare or unique feature. The maar field lies on the projection to the north of the Nayband fault and, with some flows near that fault, represents a province of Quaternary alkali basalt volcanism.

KENYA

N. E. McClymonds reported that the USGS, in cooperation with the Kenyan Ministry of Water Development, continued the program of reconnaissance ground-water studies in Kenya's North Eastern Province and investigated one district of the Coast Province to further range and ranch water-development efforts. Two of the six test holes drilled were completed as production wells because of their high yields and good water quality.

MEXICO

A U.S. National Science Foundation-Consejo Nacional de Ciencia y Technologia of Mexico project is staffed by scientists from the USGS, the Secretaria de Recursos Hidraulicos (SRH), the University of New Orleans, and the University of Kansas.

In a study to determine the geomorphic significance of geochemical reactions in developing coastline morphology, William Back, B. B. Hanshaw, and Neil Plummer (USGS) and Thomas Pyle (University of South Florida) and A. E. Weidie (University of New Orleans) determined the amount of ground-water discharge and the rate of limestone solution in a lagoon on the eastern coast of the Yucatan Peninsula.

Models were developed to evaluate the role of mixing freshwater with ocean water and the role of other geochemical processes, such as degassing of CO_2 and solution or precipitation of calcium carbonate. The model that best described the observed field conditions was a mixing model of a system open to CO_2 in which calcite may dissolve or precipitate. The investigators' conclusion, based in part on these models, was that the lagoon was formed primarily by solution along fractures and required about 25,000 years to attain its present size and shape. The eastern coast of the Yucatan Peninsula is characterized by (1) crescent-shaped beaches that are indicative of the advanced stages of the solution processes that cause the formation of lagoons and (2) elongated and transverse solution channels that are incipient geomorphic features of lagoon formation.

In another study of the Yucatan Peninsula, Back and Juan Lesser (SRH) concluded that the Yucatan's water resources are critically vulnerable to climatic, chemical, and geologic conditions, which include (1) the presence of an extensive saltwater body at a shallow depth; (2) widespread and long-term pollution, which results in part from the lack of a fine-grained sediment cover to serve as a filtration purifier; (3) the limestone's abnormally high transmissivity, which permits rapid discharge and precludes development of enough head to provide adequate storage; (4) uneven seasonal distribution of rainfall, which often occurs in heavy downpours with a simultaneous discharge to the sea; and (5) the absence of rivers.

In northern Mexico, Back and Lesser identified an unusual relationship between tectonic activity and the formation of an aquifer. In the valley of Saltillo, the Parras Formation, a black Cretaceous shale, is a productive aquifer with yields large enough to support irrigation. As they are in most black shales, the primary porosity and transmissivity are extremely low. However, an orogeny (near the end of the Mesozoic) formed many doubly plunging anticlines and thus caused intense shattering of the Parras Formation on the flanks of these folds, which thereby created secondary permeability.

NEW ZEALAND

Ivan Barnes reported that the USGS cooperated with New Zealand's Department of Scientific and Industrial Research in a study that showed that all of the warm springs of South Island, New Zealand, are supersaturated with the zeolite mineral laumontite and saturated with prehnite. The waters, in general, have the potential to dissolve albite and calcite and yield laumontite at temperatures as low as 40°C; calcium-alumino-silicate precipitates were found in two springs.

Studies revealed that the carbon dioxide springs of North Island, are similar to springs rich in carbon dioxide (soda springs) that commonly issue from eugeosynclinal rocks in California (Ivan Barnes, W. P. Irwin, and H. A. Gibson, 1975).

Barnes and Irwin prepared a world map that shows seismicity and carbon dioxide occurrences; in general, the two occur together and are probably related.

PHILIPPINE ISLANDS

From July to November 1976, D. J. Kitrinas (USGS) was assigned, under the sponsorship of USAID, to advise the Government of the Philippine Islands on implementing a nationwide land-tenure improvement program. The program is designed to provide eligible tenants an opportunity to become owners of the land that they are now cultivating. To expedite this program, the Philippine Government is using aerial photography to identify, measure, and code tenanted rice and corn lands affected by the program. Under the Agrarian Reform Project, a special activity produces semicontrolled photomosaic maps. Kitinas advised the Bureau of Lands and the Department of Agrarian Reform on increasing their technical capability to produce improved rectified photoprints from which to prepare semicontrolled photomosaics that will give optimum resolution and imagery when they are enlarged. These mosaics are expected to improve the quality and accuracy of the program as well as its rate of implementation.

SAUDI ARABIA

Paleontologic collection

Large bones collected by D. L. Schmidt and C. T. Madden from lakebeds in the Taif region of the Jabal 'In quadrangle in western Saudi Arabia were identified by F. C. Whitmore, Jr., as representing the primitive crocodilian suborder Mesosuchia. This group, widespread in Mesozoic time, was known from the Jurassic and (or) Cretaceous of Europe, East Asia, Madagascar, and North America and South America. It was only in Africa that these crocodiles were previously known to have survived into the Tertiary. They are known from the Montian (Paleocene) of Landana, Angola; the lower Eocene of Sokoto, Nigeria; the Ypresian (lower Eocene) of Morocco and southern Tunisia; and the Lutetian (middle Ecocene) of Libya. From the field relations observed by Schmidt, it appears that the Mesosuchia also survived into the Tertiary in the Arabian Peninsula. It is Schmidt's opinion that these sediments were probably contiguous with beds in the Jiddah-Mecca area of Saudi Arabia prior to the uplift of the Red Sea escarpment. Also, *Ceratodus,* a lungfish that was widespread in the Mesozoic and that survived into the Paleocene in Africa, was collected along with many teeth and some tail spines of stingrays. Mesosuchia and *Ceratodus* are associated in the Senonian (Upper Cretaceous) of the Republic of Niger.

Ceratodus is an important paleoenvironment indicator because the lungfish are able to survive in climates of seasonal aridity by burrowing into the bottom mud and estivating during the dry season. They inhabit freshwater exclusively. Rays are also known to live in freshwater.

Geologic mapping

F. S. Simons (USGS) reported that 1976 was largely a year of report writing, but geologic mapping on two whole and four partial 30-min quadrangles was begun. Status of mapping of 30-min quadrangles at 1:100,000 scale since September 1969 is as follows:

- 44 quadrangles mapped (plus 10 mapped prior to September 1969).
- 16 quadrangle maps printed in color by the Directorate General of Mineral Resources (3 by Saudi geologists).
- 11 quadrangle maps published as open-file reports (3 by Saudi geologists).
- 15 quadrangle maps in press or almost ready (2 by Saudi geologists).
- 12 quadrangle maps being prepared by authors.

A regional compilation project begun in 1975 continued through 1976. The study involves compiling all USGS mapping south of lat 21° 30′ N. and the regional correlation of Precambrian layered units. The initial compilation is being done on a Landsat image base at a scale of 1:250,000 for a final compilation scale of 1:1,000,000.

A study of the petrogenesis of the Precambrian acid plutonic rocks of the Arabian Shield continued through 1976. This work mainly involved a study of upper Precambrian granites and gabbros of the southeastern shield and a reconnaissance traverse across the width of the central shield that was tied to geochronologic sampling. An interactive computerized data base for silicic plutonic rocks has been designed and will be used for a synthesis study of the whole shield.

A cooperative project initiated in conjunction with H. W. Blodgett (NASA) is developing ratio-enhanced color Landsat imagery to aid in geologic mapping. The imagery enhances the spectral differences between various rock types. Initial results appear very encouraging, and this imagery is now being field tested as an aid to quadrangle mapping.

Mineral deposits in the southern Arabian Shield

Base- and precious-metal deposits in the southern Arabian Shield were mapped and geochemically sampled by C. W. Smith. Most deposits are parallel to bedding in pyroclastic volcanic and sedimentary rocks of the Jiddah Group, but locally some are in shear zones. The principal host rock is a quartz-bearing rock that in places is bedded and may be a pyroclastic rock but in other places forms hypabyssal intrusive bodies. Interbedded marble layers, generally sheared and brecciated, and graphitic beds are associated with mineralized zones in many of the deposits. The sulfide minerals occur largely in the quartz-bearing rock, but, at Farah Garan, the host rock is marble that is locally replaced by sulfide minerals along fissures. Deposits in the area generally are volcanogenic in origin, but some may be syngenetic, and some may be epigenetic.

Geochronology

Genetic types of Precambrian and Cenozoic mineral deposits in Saudi Arabia are being studied by lead isotopic methods by B. R. Doe and M. N. Delevaux in collaboration with R. J. Roberts. The Precambrian deposits comprise several kinds of massive sulfide bodies: Syngenetic iron and copper sulfide, dual syngenetic and epigenetic base metals, and epigenetic base metals. Leads in Precambrian gold- and silver-bearing quartz veins also have been isotopically analyzed. The Cenozoic rocks include lead-bearing barite veins, zinc-lead in Miocene rocks, and metalliferous deposits in the Red Sea. The lead isotopic ratios in the Precambrian deposits indicate that the leads are primitive and were derived directly from the mantle or through leaching of mantle materials about 900 million years ago. The ratios plot in two distinct fields: Those of the massive sulfide deposits in one and those of the veins in the other. The vein deposits tend to be more radiogenic than the massive sulfide deposits, and they are also demonstrably younger. Their radiogenic ratios are thought to be the result of additional generation of radiogenic lead through radioactive decay since the massive sulfide deposits formed. This theory implies that lead from the massive sulfide deposits and from preexisting rocks was mobilized into the veins during metamorphism and deformation. Isotopic ratios in leads from the Cenozoic deposits resemble those of the Red Sea brines (Delevaux, Doe, and Brown, 1967) and may have been derived from mantle sources.

Laboratory analysis

Mineralogic studies conducted in areas of anomalous radioactivity by J. J. Matzko (USGS) and M. I. Maqvi (Directorate General of Mineral Resources) revealed that the anomalies are in the Wajid Sandstone and Tabuk Formation, in a pluton, and in some veins. The Wajid Sandstone of Cambrian and Ordovician age contains as much as 0.0007 percent chemical uranium mainly in goethitic cement. Thorium is found in the detrital minerals monazite, sphene, zircon, epidote, and apatite. Samples from the lower part of the Tabuk Formation of Early Ordovician age at Al Qassim in northeastern Saudi Arabia contain zircon, monazite, xenotime, huttonite, allanite, and sphene. No uranium minerals were identified, although neutron activation analyses show as much as 22 ppm U. Two kinds of zircons are recognized: Radiation-damaged nonfluorescent zircon and colorless zircon that fluoresces bright orange under ultraviolet light (2,536 A). A radioactive albite granite pluton at Al Ghurayyah in northwestern Saudi Arabia contains the following maximum amounts of trace elements in drill cores: 0.18 percent Nb and 0.024 percent Ta by X-ray fluorescence, and 720 ppm Th by semiquantitative spectrographic analysis. An outcrop sample shows by semiquantitative spectrographic analysis that it contains up to 1,600 ppm Nb and also contains anomalous amounts of Ce, Hf, Nb, Pb, Zn, and Zr. Chromatographic analyses show as much as 40 ppm U. Thorite, pyrochlore, columbite, fergusonite, thorogummite, columbite-tantalite, zircon, sphalerite, galena, and pyrite have been identified by microscopic and X-ray methods.

Veins that cut the Halaban Group in the Hail area were studied by X-ray and alpha plate methods. The veins contain niobium-bearing minerals and minor amounts of uranium in brecciated quartz-hematite-goethite vein filling.

Rubidium-strontium age determinations made by R. J. Fleck on plutonic rocks of the Arabian Shield range from less than 550 to over 900 million years and represent three major rock types. The oldest group, now strongly deformed gneissic bodies, ranges in composition from hornblende diorite to trondjhemite and forms large batholiths in the western part of the shield. Ages of these bodies range from about 780 to 900 million years. Host rocks for the batholiths are sedimentary and volcanic rocks, some of which are older than 1,150 million years, but others are only slightly older than the intrusive rocks. Two-mica granitic gneiss domes represent the second group of rocks. These bodies are foliated parallel to thietheir contacts with wall rocks and commonly are surrounded by broad contact-metamorphic aureoles. Ages of these bodies range from 665 to 765 million years, but the majority cluster about the older end of the time span. The youngest rock types are later post-orogenic granodiorite to granite plutons, emplaced between 580 and 650 million year. Ages obtained from bodies within each group appear to decrease gradually from west to east across the shield. This trend parallels an increase in both SiO_2 and K_2O and may represent a migration of the axis of the orogen with time.

Mining geophysics

Geophysical exploration at the Kutam prospect, now a part of the Noranda Exploration Concession, began in 1974 and was completed in 1975. Five different prospecting methods were used: Self-potential (SP), induced polarization (IP) (dipole-dipole and mise-a-la-masse), gamma-ray spectrometry, and total intensity magnetics. In addition, three drill holes were logged for self-potential and electrical resistivity. The combined data clearly delineate the mineral deposit mined in ancient Kutam workings—and hence the drilled orebody—as an SP and IP anomaly having a strike length about 400 m and width of 100 to 150 m. In the absence of Turam anomalies over the workings, the orebody is inferred to be poorly conductive. The principal Turam, SP, and IP anomalies together delineate a shear zone that trends about N. 40° W. and that probably contains an internal en-echelon fabric at about N. 20° W. If mineralization is principally localized by intersections of these two trends, the resulting orebodies might have steep-plunging rodlike forms, as the equidimensional character of many of the associated IP anomalies suggests. In the absence of IP anomalies associated with linear Turam anomalies of the shear zone, the Turam anomalies are interpreted as ionic conductors, that is, as wet shears. The remaining Turam and IP anomalies are believed to have no economic significance, but their origins are not well understood.

The zone of sheared and altered chlorite-sericite schist and silicified quartz porphyry that contains the ore mineralization at Kutam is conspicuous on the magnetic anomaly map as a relatively "quiet" zone lacking strong magnetic contrasts, particularly where pyritization and oxidation are most intense. The magnetic character of predominantly quartz porphyry terrane south of the Kutam ore deposit is markedly different from that of predominantly metamorphic terrane to the north and northwest, owing both to stronger anomalies and to the stronger influence of structures oriented east-west and north-south. Pronounced east-west elongation of a negative IP anomaly at the apparent southern termination of the Kutam orebody may be related to an east-west magnetic lineament of a set generally attributed to relatively late Precambrian shearing, and hence such a shear may have had a role in localization of mineralization. Alternatively, the possibility of a sudden steepening of plunge or downfaulting of the Kutam orebody in this vicinity cannot be discounted entirely.

Production wells for King Khalid Military City

H. R. Anderson was detailed to the U.S. Army Corps of Engineers in connection with the development of water supplies for King Khalid Military City, now being constructed near Al Batin. His mission was to observe drilling operations, analyze pumpimg-test data, and advise on well-completion procedures. Two wells were drilled to depths of 1,000 and 1,300 m in the Wasia Sand aquifer, and three wells were drilled to depths of 300 m in limestone of the Umm er Radhuma Formation.

Water-resources advisory services

An earlier review of the operations of the Water Resources Development Department of the Ministry of Agriculture and Water for the U.S.-Saudi Arabian Joint Commission on Economic Cooperation resulted in an agreement to establish an interdisciplinary advisory group of hydrology specialists to work closely with local Ministry counterparts. Arrangements to staff two of the five positions in the group were completed, and prospective program elements were being discussed at the d of the year.

Alternative sources of water supplies for Ar Riyāḑ

Under the auspices of the U.S.-Saudi Arabian Joint Commission on Economic Cooperation, a multidisciplinary team led by S. S. Papadopulos made a detailed technical and economic study of several developmental options for providing water supplies to meet the future needs of Ar Riyāḑ. Preliminary results were obtained from simulation modeling (by digital computer) of the effects of developing two potential aquifer systems and of the conveyance of desalinated Red Sea Water.

SENEGAL, MALI, AND MAURITANIA

H. M. Babcock was the ground-water hydrologist on a team provided by the U.S. Bureau of Reclamation to assist in the preparation of a development plan for the Senegal River basin on behalf of USAID. He found that considerable information is available for parts of the basin, although, generally, it is not compiled in a form that can be conveniently used. At places, the river flood plain and adjacent areas are potential sources of irrigation water, but careful compilation and synthesis of existing data are needed before these areas can be developed. Babcock suggested that assembly and review of data, maps, and reports should be followed by an irrigation feasibility study with limited test drilling rather than massive program of test drilling on the flood plain in both Senegal and Mauritania.

SPAIN

Marine geology

Final interpretations of high-resolution continuous seismic-reflection profiles indicated a complex Quaternary history for the coastal part of Almeria Province in Spain. Sedimentary features observed in the profiles appear to be the result of several transgressions and regressions of the sea during Pleistocene time. During late Pleistocene and early Holocene time, a large amount of sediment was supplied to the Campo de Dalias region of the coast, and a wide progradational shelf developed.

Intermediate-penetration (25 km) seismic-reflection profiles suggest that structures that may contain oil and gas exist in the Almeria offshore area. Both the Almeria and the Cabode Gata marginal basins are filled with moderately thick Tertiary sediments (generally more than 1 km thick). Stratigraphic traps probably are present along the flanks of the basins, and structural traps occur along faults and anticlines or antiforms produced by post-Miocene tectonics.

TURKEY

The Government of Turkey, through the Maden Tetkik ve Arama Enstitusu (MTA) of the Ministry of Energy and Natural Resources, has undertaken a project to establish a data bank for energy and mineral data to aid MTA in exploration and policymaking activities. S. M. Cargill was assigned, through the United Nations Development Programme, to determine the effort required and the applicability of present data to MTA objectives. Cargill recommended the initiation of the proposed data bank and provided a schedule and suggestions for implementation.

VENEZUELA

The Venezuelan Government invited A. F. Espinosa to advise the Venezuelan Foundation on Seismic Studies (FUNVISIS) and to deliver a series of lectures at the Universidad Simon Bolivar in Caracas, Venezuela. Graduate students from Universidad Simon Bolivar and Universidad Central and a number of professional engineers and architects attended this intensive 2 week, 3-hours-a-day lecture course. The course dealt with topics in seismic zoning and ground-motion studies, in particular with methodologies in microzonation and seismic zoning, theoretical seismic amplification studies, dynamic simulation of ground displacements, response spectra, methodology of response spectra simulation, integration of strong ground-motion recordings, instrumental intensity studies, and field studies of damaging earthquakes.

YEMEN ARAB REPUBLIC

Ground-water survey

The USGS, in cooperation with the Ministry of Agriculture and the Mineral and Petroleum Authority of the Yemen Arab Republic, continued the test-drilling program in the Amran Valley. According to G. J. Tibbits, Jr., several test holes were completed as observation wells and were logged and tested, and two production wells were completed and tested. Although present production is from zones at depths of less than 100 m, test drilling to depths of more than 300 m indicated the possibility of alluvial aquifers at depths of about 150 to 200 m. A number of sites in the central and southern part of the republic were visited to provide advice on drilling locations in support of another USAID project.

Despite increased withdrawals of ground water through newly dug and drilled irrigation wells, water levels in the Amran Valley declined only slightly. By contrast, water levels in the Sanaa Basin declined at rates that locally exceed 1 m/yr. Especially alarming is the rapid decline of water levels in the northwestern part of the basin, the site of the planned well field for the municipal supply of Sanaa. Present withdrawals from this part of the basin are small. In the city of Sanaa, many wells were abandoned because of declining levels.

Training

Seven third-year geology students from Sanaa University were given on-the-job field and laboratory training during their summer vacation. These students served as student assistants for project operations.

Intepretation of characteristics of wadis

M. J. Grolier visited the Yemen Arab Republic in February and again in July to obtain ground and aerial data in order to interpret the hydrologic characteristics of a number of the country's wadis.

As a result of a field reconnaissance in May and a study of the few available stream-discharge data, H. C. Riggs (1977) proposed qualitative procedures for estimating the mean flow and flood-frequency characteristics of about a dozen large wadis and for estimating ground-water recharge. He proposed a streamflow data-collection program to verify the procedures and to meet the needs of project plans and designs.

YUGOSLAVIA

Four Special Foreign Currency Program (SFCP) projects continued in Yugoslavia: (1) Research on the applicability of geophysics to defining permeability in karstic terrane, (2) research on light-metal and rare-earth mineral provinces in some Yugoslav granitoid massifs, (3) research on crustal structure in relation to earthquakes, intrusives, and metallogenic provinces, and (4) research on geologic and hydrologic factors affecting urbanization and economic development.

ANTARCTIC PROGRAMS

During the 1976-77 austral summer, USGS personnel carried out geologic and geophysical studies in the Pensacola Mountains and geologic studies in the Shackleton Range of Antarctica (see index map). Fieldwork in the Pensacola Mountains continued studies on the Dufek intrusion, one of the world's largest known layered igneous complexes. This work focused on the lower exposed part of the body in the western end of the Dufek Massif and on the unexposed basal part underlying ice adjacent to the massif. A. B. Ford's field work in the Shackleton Range was conducted in cooperation with the

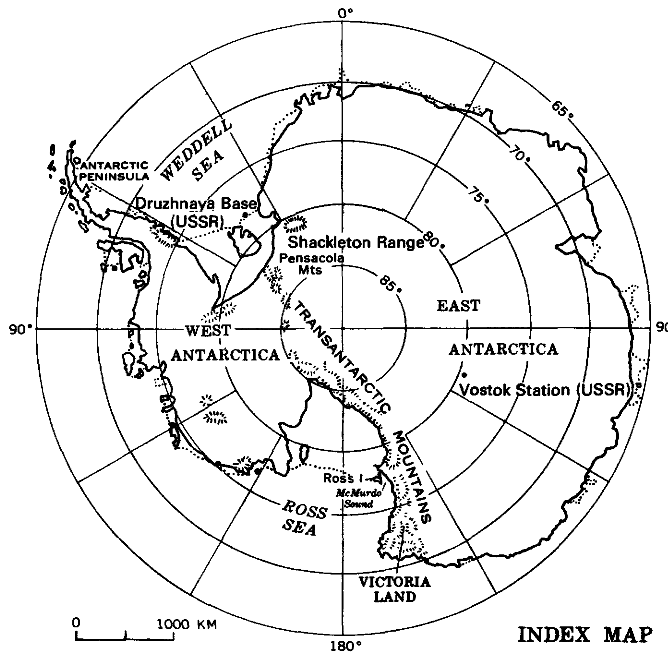

INDEX MAP

U.S.S.R. as part of the 22d Soviet Antarctic Expedition. The USGS also carried out year-round geophysical studies at the Soviet Vostok Station on the high ice plateau of interior east Antarctica, a site where the world's lowest-recorded temperature (-88.3°C) was measured in 1960. J. D. Wood coordinated the U.S.-Soviet scientist-exchange program at Vostok. R. N. Johnson, the 1976 U.S. exchange scientist at the Soviet station, collected data for a USGS ULF program, a Stanford University VLF program, a NOAA riometry program, and a University of Alaska magnetic micropulsation program. These activities, as well as laboratory and office work done on material collected during earlier expeditions to the Pensacola Mountains and southern Antarctic Peninsula, are part of the U.S. Antarctic Research Program of the National Science Foundation's Division of Polar Programs.

The USGS supports the operation of the Worldwide Standardized Seismograph Network station at the South Pole. Because of its unique location, this station provides essential azimuth control for many epicenter solutions in southern latitudes. The personnel at Antarctica normally rotate on an annual basis. During their Antarctic tour of duty, these observers keep the South Pole seismographs in working order, determine earthquake arrival times and amplitudes, and report their readings to Golden, Colo., via radiotelegraph.

Geophysical studies of the Dufek intrusion

Basal parts of layered complexes of the Dufek type commonly contain ultramafic cumulates consisting of minerals that crystallized early from the parent magma. Separation of these minerals from the melt is one of the principal factors controlling chemical changes in the residual magma. The basal part of this body is not exposed, and so whether basal ultramafic cumulates are present is a major uncertainty in interpreting fractionation trends of the exposed cumulate stratigraphy. Such basal cumulates are commonly associated with a wide variety of mineral deposits in bodies of this type elsewhere in the world. Although diamond drilling is needed to investigate this part of the body and to assess accurately its mineral-resource potential, useful clues to its nature can be provided indirectly by geophysical methods. Geophysical studies were therefore begun in ice-covered areas near the lowest exposed part of the body, at the western end of Dufek Massif. The objectives of this work, carried out by A. W. England, assisted by W. H. Nelson, Christine Carlson, G. K. Czamanske, A. B. Ford, and C. J. Nutt, were to determine the boundaries of the intrusion and the thickness of the unexposed basal part.

Nearly 80 km of traverse lines were surveyed at 300-m intervals across ice surfaces northwest and southwest from Dufek Massif. Gravity, measured by means of a LaCoste instrument, and ice thickness, measured by means of ice-sounding radar equipment, were determined at 600-m intervals along the traverse lines. Preliminary analysis of the data suggests that the boundary of the Dufek intrusion lies much closer to Dufek Massif on the north than 10 km, the distance that was originally estimated. The boundary beneath the 15-km wide Jaburg Glacier on the south lies about 10 southwest of Dufek Massif.

Mafic cyclic units in the Dufek intrusion

The presence of cyclic units in mafic cumulate sections of the layered Dufek intrusion seems to be indicated by pyroxene compositional trends (Himmelberg and Ford, 1976). The units were not accurately defined during the 1965–66 USGS reconnaissance mapping of the complex (Schmidt and Ford, 1969), and, therefore, more detailed mapping (1:25,000 scale) and sampling of sections containing the cyclic units were undertaken by A. B. Ford, W. H. Nelson, G. K. Czamanske, C. J. Nutt, and Christine Carlson. The nearly 4 km of exposed stratigraphic thickness of mostly mafic cumulates in Dufek Massif and the Forrestal Range are characterized by an abundance of well-defined layering (Ford, 1976). Layer thicknesses range from a few millimeters to many tens of meters. Many major layers are of the "mineral-graded" variety that show sharp bases and gradational tops. Basal parts of many of them consist of single-mineral cumulates made up of settled plagioclase, pyroxene, or magnetite. Those layers showing evidence of lateral current action, such as channels or sharply alined xenoliths, are believed to represent distinct cyclic units. They were sampled at closely spaced stratigraphic intervals for study of compositional variation. Whereas cyclic units of certain other layered intrusions are postulated to be related to introduction of fresh batches of magma into the chamber, presently available evidence suggests that the cyclic units in the Dufek intrusion are more likely related to processes internal to the chamber, such as convection or other current activity.

Fractionation trends in cumulus oxide minerals of the Dufek intrusion

Iron-titanium oxide minerals are major cumulus phases in the upper part of the layered Dufek intrusion exposed in the Forrestal Range (Ford, 1976). Model amounts of these minerals—ferrian ilmenite and titaniferous magnetite—generally range from 2 to 12 percent, although much greater concentrations are known to occur in local thin layers and lenses on the order of 1 cm to 1 m thick. Other major cumulus phases, such as augite and inverted pigeonite, show compositional trends closely relatable to stratigraphic height and thus to stages of magma fractionation. Compositions of oxide minerals, accordingly, also might be expected to show fractionation trends. However, titanium and iron contents of these minerals, determined by electron-microprobe analysis by G. R. Himmelberg (University of Missouri), are largely controlled by subsolidus recrystallization and thus do not show any regular variation with stratigraphic height. On the other hand, contents of the minor elements vanadium and aluminum in ilmeno-magnetites generally decrease with stratigraphic height and thus are useful indicators of fractionation trends during the stage of oxide-mineral crystallization.

Geologic comparison of the Pensacola Mountains with the Shackleton Range

Upper Precambrian to Permian sedimentary rocks, mapped by USGS field parties in 1962–66, are exposed throughout the 500-km long belt of the Pensacola Mountains (Schmidt and Ford, 1969). The stratigraphy and record of tectonic events in this area compare closely with those in other ranges of the Transantarctic Mountains in the direction of the Ross Sea. However, comparisons with the nearby Shackleton Range have been more poorly known. Mapping by British parties in 1957–71 showed the range to consist chiefly of crystalline metamorphic rocks belonging to part of the Antarctic Shield and to be locally overlain by upper Precambrian to Cambrian(?) low-rank metasedimentary rocks (Turnpike Bluff Group) and Cambrian(?) to Ordovician(?) sandstone and conglomerate (Blaiklock Glacier Group). The only fossils found were inarticulate brachiopods of probable Cambrian to Ordovician age that occur in morainal erratics near Mount Provender.

Geologic studies of the Shackleton Range have been continued by Soviet parties working from Druzhnaya Base, a temporary summer-only station established in 1975 on the edge of Filchner Ice Shelf at the southern end of the Weddell Sea. The program at this base has included extensive aerial photographic mapping and aeromagnetic surveying of the Shackleton Range and nearby regions. These studies will be expanded in future years to include other coastal parts of the Weddell Sea.

A. B. Ford's participation in the 22d Soviet Antarctic Expedition at Druzhnaya Base provided the first opportunity for firsthand geologic comparison of the Pensacola Mountains and the Shackleton Range. Geologic mapping was carried out by ski and motor toboggan traverses from tent camps in the Read Mountains and La Grange Nunataks and by MI-8 helicopters and AN-2 biwing skiplanes as auxiliary support to reach distant nunataks and mountains. At different localities, the Turnpike Bluff Group and the Blaiklock Glacier Group were found to lie with angular unconformity on high-rank shield-type garnetiferous metamorphic rocks that locally contain staurolite, kyanite, and (or) coarse sillimanite. The contact between the two younger groups was not observed. The basement metamorphic rocks have no correlatives exposed in the Pensacola Mountains, in which the oldest rocks are strongly folded upper Precambrian metasandstone and slate (Patuxent Formation) of greenschist-facies rank. Style and degree of deformation and metamorphism of the Turnpike Bluff Group and the Patuxent Formation are generally similar, but the two units show many lithologic differences, (chiefly, a comparatively much greater abundance of quartzite in the Turnpike Bluff and of slaty interbeds in the Patuxent) and the common presence of mafic volcanics and of graded bedding and sole markings in the Patuxent that are not found in the Turnpike Bluff. Although the two units are probably correlatives, their sedimentary environments obviously differed greatly, from a stable shelf in the Shackleton Range area to a volcanically active eugeosyncline in the Pensacola Mountains. The Blaiklock Glacier Group is lithologically similar to units of the Neptune Group (lower to middle Paleozoic) in the Pensacola Mountains, but exact correlation is precluded by the poorly fossiliferous nature of the rocks. A strong folding event of probable Triassic age in the Pensacola Mountains was not apparently recorded in the Shackleton Range, where the Blaiklock Glacier Group (lower Paleozoic?) is only gently tilted.

TOPOGRAPHIC SURVEYS AND MAPPING

FIELD SURVEYING

INERTIAL POSITIONING SYSTEM

USGS and DMA used an Inertial Positioning System (IPS) mounted in a Chevrolet Blazer to control several mapping projects in northern Maine. The IPS was on the project a total of 34 days—22 spent on production, 6 spent on testing, and 6 lost because of system or vehicle malfunctions. The IPS operated for 140 hours (not counting travel time to and from the work area), traversed 2,744 km, and established control on 328 image points. In addition to mapping control, positions were determined for 175 town-line/road crossings. These points, obtained while traversing to required control points, will be valuable in positioning town lines on standard quadrangle maps.

Closures indicate a surveying accuracy (standard error) of 1:20,000 in distance and 43″ in azimuth. With the IPS, 245 control points were established in addition to the 83 points required to aerotriangulate the project. Approximately 20 percent or 66 of these points were obtained to strengthen the geometry of the IPS survey net. Discounting the latter points, the cost per control point was 9 man-hours. The cost using conventional methods (paneling and electronic traverse) was estimated at 15 man-hours per control point. In spite of well-above-average rainfall (200 percent above normal for the period), no days were lost to inclement weather as would have been the case with conventional control methods.

METAL DETECTOR EVALUATION

A bench mark recovery course was installed on the grounds of the USGS National Center in the summer of 1976. Adjacent to a previously established standard monument (included in the course as a control station), 16 subsurface stations were set. The stations represented bench marks of various materials and configurations. The relative recoverability of the experimental stations demonstrated the performance of five types of metal detecting instruments.

The evaluated detectors are the Schonstedt Models *GA*-32 and *GA*-22, the Garrett Hunter, the Aqua Magnetic Locator, and the Teledyne Gurley L^2 Locator. All models are magnetic locators and, except for the Garrett Hunter, are thus limited to ferrous metal detection. The Garrett Hunter is sensitive to all refined metals as well as ferrous metals and ores. All instruments, except the Aqua Magnetic Locator, generate an audio signal by a battery-powered oscillator in the locator. The Aqua Magnetic Locator does not require electrical power since it registers a mechanical response by a metered magnetic dip needle. Approximate costs of the instruments are: Schonstedt GA-32, $450; Schonstedt GA-22, $410; Garrett Hunter, $240; Aqua Magnetic Locator, $45; and Teledyne Gurley, $350.

None of the various metal wire-ring bench mark configurations significantly increased recoverability. However, the response improved at all stations with magnets. Thus a magnet should be installed as part of permanent bench mark monuments where difficult recovery is likely. Time saved in recovering the station would offset the cost of the magnet.

The Aqua Magnetic Locator appears to be the most sensitive and reliable of the instruments tested. It responded to the buried magnets as did the others; however, its response to the bench marks with wire rings was consistently higher. The simple mechanical-magnetic design of the Aqua Magnetic Locator provides high performance at the lowest cost.

MAPPING STANDARDS

Since July 1, 1975, the USGS accuracy testing program identified failure of one horizontal and two vertical accuracy tests to meet accuracy standards. This fact, plus the upward creep in RMSE, show the importance of the testing program, especially when new techniques are used.

The Crownpoint, N. Mex., orthophotoquad (OQ) project was evaluated. The 91 OQ's were made for the Bureau of Indian Affairs (BIA) with USGS publication. The investigation determined (1) that the public land net from published line maps would fit the OQ imagery reasonably well and (2) that the OQ's probably meet National Map Accuracy Standards. Three formal accuracy tests made in the early 1960's were applied to the OQ's as part of the evaluation.

Some problems in matching Landsat images to maps and in fitting and testing gridded images led to development of procedures to measure their scales and study their geometry. The scales were measured along the four sides of each image and across each diagonal.

Examination showed (1) scale variation across the image in both alongtrack and crosstrack directions and (2) maximum scale differences alongtrack versus crosstrack and between diagonals. Eight scenes, and up to seven separate images of each, were studied. Images processed by IBM and the new EROS Digital Image Enhancement System (EDIES) were also analyzed. Distortions were large enough to indicate a need for systematic quality control of Landsat image processing.

CONTROL

In October 1976 the USGS established a special network of 43 control stations at Crows Landing Naval Auxiliary Landing Field, Calif. The project provided precise azimuths and elevations to support NASA's testing of microwave landing systems.

A new evaluation of Landsat images for mapping remote areas, particularly outside the United States, was completed. A strip of 14 Landsat MSS images was selected for the project. It extended from northern North Dakota and Minnesota to southern Texas and New Mexico and adjoined a 15-image strip previously triangulated. Control points were features identifiable on both large-scale maps and the Landsat imagery, and a sufficient number were obtained to control each Landsat frame with 10 to 15 points. The points common to adjoining frames and others common to the two strips were selected and marked. The ground coordinates of control points were measured on the maps with a coordinatograph and then transformed to an oblique Mercator projection oriented to the Landsat track. Image coordinates were measured on a two-plate stereocomparator. The strips were fitted to minimum control by a linear transformation to weed out bad data and then adjusted to each other and controlled as a block. The adjustment was repeated with various control configurations.

The results substantiate the findings of previous projects (the Florida ERTS mosaic and the ERTS strip triangulation) showing that simultaneous adjustment of the two strips is no more accurate than independent adjustment of each strip with the point values averaged. However, the two-strip block did provide more latitude in the selection of ground control for bridging.

USGS surveyors at the South Pole Station have been recording Doppler data from U.S. Navy navigational satellites continuously since 1971 in support of scientific and geodetic studies. These observations have shown that the South Polar ice cap has the mobility of a glacier whose vector movement is quite regular. It has also shown that the Amundsen-Scott South Pole Station (U.S.) is some 500 m from the true geographic South Pole and is moving toward it at the rate of 8 to 11 m/yr.

Doppler data obtained in the Antarctic Peninsula during the 1975-76 austral summer will be used to adjust isolated independent traverses established by United States and United Kingdom survey teams over the past decade into a common reference system. The older traverses were based on astronomic observations. These data resulting from the 1975-76 cooperative effort of the British Antarctic Survey (BAS) and the USGS have been shared with BAS and will be incorporated into a geodetic data base of control in the Antarctic Peninsula.

All available field observations for precise level lines in Georgia, Maine, Maryland, Massachusetts, New York, North Carolina, South Carolina, and Virginia were evaluated. Some 25 profiles covering 4,000 km of leveling were compiled and transmitted to the Branch of Eastern Environmental Geology to be used with other data to study the Earth's crustal movement and to aid in locating suitable nuclear reactor sites.

Releveling that began in 1975 in Yellowstone National Park was completed to determine crustal movement resulting from a major earthquake near Norris, Wyo., In 1976, 170 km of second-order leveling was run according to first-order class II procedures.

Under first-order specifications a 1942 USGS line at Oroville, Calif., was releveled a second time. The 26-km line was first releveled after the Oroville earthquake of August 1, 1975 (magnitude 5.7). The second releveling was needed to provide geologists with comparison values for determining vertical creep along the fault line.

In September 1976 an annual releveling program began. Several monitor lines in southern California are being leveled to first-order class I specifications. Also included in the program is Geodolite measurement of trilateration strain nets. This work began in

November 1976 and will continue at least through May 1977. The trilateration nets extend along the San Andreas fault from northern California to the Mexican border and along the Sierra Nevada fault in the Owens Valley area of central California. The project requires monumentation of about 30 new stations—each built to accommodate the La Coste-Romberg plate on which the gravity meter will rest. Monumentation is complete, and the first level line is nearly finished.

To monitor subsidence, 72 km of first-order leveling was run near Tucson, Ariz. The leveling, extending from Tucson, was a continuation of 1975 leveling within the city. Results are expected to provide a more accurate measurement of subsidence in the area.

Surveys were conducted to define the high-water profile of the flood area from Teton Dam to American Falls Dam, Idaho. Because of the destruction of transportation routes and inaccessibility of some areas, helicopter transportation assisted the crews.

Elevations were obtained by fly levels (to third-order standards) on 284 high-water points. Planetable elevations were established on 45 points on the canyon walls near the dam, and 23 cross sections, ranging in length from 0.8 to 9.6 km were run and plotted on 1:24,000-scale topographic maps. The data will be used to define flood-damaged areas and to help calibrate a one-dimensional model of unsteady flow that can be used to predict the effect of a large flood.

Two 17.7-km monitor lines were established for the Bureau of Land Management (BLM) across the Centennial Wash, 63.4 km west of Wickenburg, Ariz. These lines are being established to help determine conditions which might have led to a dam failure across the wash. For both lines two tablets were set in the mountain bedrock on each side of the valley. Intermediate tablets were placed from 0.8 to 1.6 km apart on driven copperweld rod. About half of the marks have a cement collar for lateral stability, for horizontal as well as vertical measurements.

The USGS is furnishing horizontal and vertical information for 322 cross sections along the channels of the Cimarron and Salt Fork Rivers of Oklahoma and Kansas to the Corps of Engineers, Tulsa District. The information is to be generated by semianalytical control extension from available photographs and control. Resulting data will define the horizontal and vertical positions of points along cross sections of the flow channel of the rivers. The points will be located to define slope changes where elevations differ by 0.3 m or more. The cross-section information is to be used in backwater studies of the river basins.

Fieldwork was completed on blocks covering 3,900 km^2 and including 422 1:4,800-scale quadrangles between Medford and Eugene, Oreg. The work for BLM consisted in establishing supplemental vertical control points and locating section corners at 2-mi intervals. Control and corners were identified by paneling or by using natural images on compilation photographs.

EQUIPMENT

A JMR-1 Doppler Survey set including Microprocessor (JMR-1MP) was leased for 3 months during the 1976-77 Antarctic austral summer for operational testing in the Antarctic environment on the Ross Ice Shelf Project. The JMR-1MP operates as an accessory to the JMR-1 Doppler Survey Set and provides a one-pass real-time output position (latitude/longitude) of the occupied site. Both units are battery operated, compact, weatherproof, and rugged. For remote locations the equipment shows considerable utility for navigating and obtaining mapping control in Antarctica.

Six field-mapping vans were custom-fitted to provide mobile work stations for revision, interpretation, and completion surveys. Seated at the light-table in the van, the surveyor can scribe corrections and additions on either line or image bases. Scribing onsite is more advantageous than penciling and later scribing in the office. The table also serves as convenient space for stereoscopic viewing of photographs. The only adverse comments concern cramped quarters and glare.

The USGS purchased two Texas Instruments SR-52 programable calculators for field horizontal-control assignments. The calculators have 224 program storage locations with 20 addressable memory registers. An add-on printout is optional. Programs were written and are being used in the field for Polaris and Sun observations and geodetic inverse solutions. The programs enable control parties to compute the observed data quickly and reobserve any questionable directions before leaving the site.

PHOTOGRAMMETRY

CAMERA CALIBRATION

The USGS optical-calibration laboratory has received 70 aerial mapping cameras for calibration from private contractors, State highway departments, a university, USFS, NASA-JSC, NOS, USAETL, a company in Guam, the Kingdom of Saudi Arabia, and the UN Geneva Division of Narcotic Drugs.

Two master grid plates, a high-definition resolution test plate and associated calibration data were provided to USGS mapping centers. The plates were made on Kodak high-resolution emulsion on micro-flat glass. The resolution plates contain an array of 17 USAF standard resolution charts. The resolution range is 1 to 203 cycles/mm in a $\sqrt[6]{2}$ progression, high contrast, clear lines on dark background.

The optical lab also compared an image motion compensation (IMC) camera system with standard commercial cameras, such as the Wild RC 8 and RC 10 and the Zeiss RMK A 15/23. There is now a considerable body of data comparing IMC cameras and f/4-lens cameras that use faster shutter speeds with maximum aperture to reduce image motion in the focal plane.

The camera-calibration data bank now contains 400 camera-magazine calibrations. A total of 90 of the calibration data sets are suitable for fully analytical aerotriangulation, and 110 additional sets contain data on fiducial-mark coordinates, lens resolution, and model flatness. The data include owner, manufacture, number, lens type, lens number, magazine and (or) platen number, calibration date, and number of fiducial marks.

ANALYTICAL AEROTRIANGULATION

High-altitude (6,600-m) super-wide-angle (SWA) photographs that were obtained 3 years ago for the Louisburg, N.C., project were reprocessed with the image-coordinate refinement (ICR) program and the new technique of grid modeling the combined radial lens distortion and platen deformation. The refinement greatly improved the quality of the aerotriangulation adjustment by the direct geodetic constraint (DGC) aerotriangulation program. The block consisted of 28 quad-centered photographs taken on north-south flights.

A statistical analysis of residuals on known points produced the following results:

	Horizontal			*Vertical*		
	Held	*Test*	*Total*	*Held*	*Test*	*Total*
Points	7	2	9	85	88	173
RMSE (ft)	3.7	5.2	4.1	2.7	3.9	3.4

Medium-altitude (3,300 m) SWA photographs taken with the same camera were similarly processed for radial distortion refinement and with the DGC program. The block contained 94 photographs taken on east-west flights. Nearly all of the same points were adjusted in both the medium- and high-altitude blocks. The statistical results from the medium-altitude photographs of the Louisburg area are as follows:

	Horizontal			*Vertical*		
	Held	*Test*	*Total*	*Held*	*Test*	*Total*
Points	6	8	14	90	116	206
RMSE (ft)	2.1	4.5	3.6	1.2	1.8	1.6

While the difference in vertical results correlates with the ratio of the flight heights (2:1), the horizontal RMSE for the two blocks does not. The high-altitude photographs would easily satisfy the horizontal requirements for 1:24,000-scale mapping and the vertical requirements for the 5-m contour interval but would not satisfy the vertical requirement for 2-m contours. (Note: The contour-interval sequence adopted for metric maps is 1, 2, 5, 10, 20, and 50 m.)

PHOTOGRAMMETRIC TECHNIQUES

Orientation parameters computed from aerotriangulation data are being supplied to stereocompilers. The data include: (1) airbase (in ground feet and millimeters at model scale), (2) differential elevation of the two exposure stations (in feet), and (3) ω and ϕ grad tilts tailored for any of the instruments used. The data are derived from relative orientation elements from aerotriangulation plotters or from analytical models in conjunction with absolute orientation elements determined by block adjustment of independent models. If properly calibrated, PG 2 and B 8 plotters (and the PPO 8 orthophoto printer) can use the data directly. Other plotters need a millimeter scale, a stick for measuring projection distance, and a graduated level trivet.

Initial results of numerical orientation with Kelsh plotters are favorable. Numerical orientation is within two floating-mark diameters of Y parallax, 13 m in scale, and 0.001 times the flying height in level. About 25 percent of the models needed no touchup. Time for numerical orientation and refinement varies from 15 to 35 min, two to four times faster than empirical methods.

Research is underway to determine whether elevations established from SWA photographs by fully analytical aerotriangulation are sufficiently accurate and economical for vertical control extension for topographic mapping with a 2-m contour interval. Varied control configurations and production procedures are being evaluated for adequacy, cost effectiveness, and potential for vertical control extension in mapping at the 2-m contour interval.

Major problems were primarily camera related. Maximum lens distortion was much higher than recommended, and there was a significant time between camera calibration and photography.

Preliminary results show that vertical data established from 2,670-m aerial photographs are inadequate for controlling maps with 2-m contour intervals. However, control extension by the same system for compilation with a 10-ft interval is feasible and allows flexible selection of control configurations. The final report will include a recommendation for testing at lower flight heights.

NISQUALLY GLACIER SPECIAL MAP

The latest in a series of topographic maps of Nisqually Glacier in Mt. Rainier National Park, Wash., is underway. The maps are used to evaluate ice motion and volume for studies by NPS and USGS. The map has been revised on a 5-year cycle. Aerial photographs were taken, and aerotriangulation is complete for the latest revision. After an analytical aerotriangulation adjustment, the map was compiled on a Kern PG 2 at 1:10,000 scale with a 10-m contour interval.

RELATIVE ACCURACY TESTING

Many older topographic maps in the Eastern United States are being evaluated for horizontal accuracy by a photogrammetric method in which relative horizontal accuracy is checked by comparing stereomodel positions from high-altitude photographs with corresponding positions on the map base. If the rejection criterion of either 2.4 m standard error for graticules or 10.5 m RMSE for planimetry is exceeded, the quadrangles are recommended for remapping rather than standard revision.

VIKING II PROJECT

Four AS-11A operators and two computer programers were assigned to an AS-11A stereoplotter for mapping possible Viking landing sites on Mars. The AS-11A had only recently been updated with a new computer and computer-plotter interface so that considerable debugging was necessary.

PHOTOIMAGE MAPPING

ORTHOPHOTO AND SATELLITE PRODUCTS

The USGS experimentally scaled orthophotographs of the Cleburne-Van Buren, Ark., project to available bases rather than scaling by normal aerotriangulation. To confirm the feasibility of the process, eight quadrangles were tested for accuracy. In addition to the necessary field control, positions were obtained for two additional points needed for aerotriangulation if the scaling process failed. The orthophotos were scanned on T-64 and T-61 Orthophotoscopes and then scaled. Camera negatives at 1:24,000 scale are being prepared photographically. When they are complete, the maps will be tested to determine whether the orthophotographs meet National Map Accuracy Standards.

A Wild PPO 8 orthoscanning instrument was installed in 1975. Since then there have been several breakdowns, but more than 1,900 quadrangles were scanned through January 1977 (3,500 models). Scanning time varies with both the size of the exposure slot, determined by the amount of relief, and the scanning speed, variable from 1 to 12 mm/s.

QUAD-CENTERED PHOTOGRAPHS FOR VERTICAL CONTROL

The USGS has developed production procedures and specifications to generate elevations from quad-centered 1:80,000 photographs to control lower altitude photographs used for 5-m contouring. Two blocks were used in the test, each with quad-centered photographs taken at 4,500 m and field control established for 5-m contour intervals. The objectives were realized when stringent limits on a number of production variables were used. Of 158 test points, 13 failed to be +1.5 m (maximum = ± 2.4 m) with no apparent cause other than random errors. Thus, 92 percent of the test points are within ± 0.25 times the contour interval (±1.5 m). The RMSE of the test points is 1.2 m, which satisfies National Map Accuracy Standards.

The USGS is attempting to obtain high-altitude photographs of sufficient resolution for compilation of standard 7.5-min quadrangle maps with a 20-ft contour interval. Previous research indicates that quad-centered photographs can be used for 5-m contour-interval mapping if the resolution can be improved. NASA took the photos for the test in September 1976 with two Zeiss RMK A 15/23 cameras. Bar targets were placed on the Poncha Springs, Colo., quadrangle, which contains a variety of topographic features. One camera contained Kodak 2402 film; the other contained SO-022. The films were inspected and accepted and are being used for stereocompilation that is being compared with standard compilation.

There is expanded use of orthophotoimage bases for compiling standard topographic maps. The procedure combines all compilation and color-separation phases into one operation so that map content is scribed only once. All map features except contours are scribed directly on color-separation guides containing the orthophotoimage. In this operation compilers refer to field-annotated photographs. Contours and any planimetric detail not discernible on the image guides are stereocompiled.

The contours are final-scribed, and the stereocompiled planimetric features are transferred to the culture guide for final scribing. More than 3,400 km^2 of 7.5-min quadrangle mapping have been completed thus far by this procedure, which saved about 10 percent of the cost of earlier procedures.

The Atlanta area orthophotomosaic, a companion product to the completed regional line map, is in final mosaicking for lithographic printing. The 1:100,000-scale orthophotomosaic covers an area of 1.5° long by 1° lat. Orthophotoquads at 1:24,000 scale were reduced in three steps by processes aimed at eliminating sunspots, flares, haze, and image-tone mismatches due to photography at different times. Initial mosaics were made in blocks by the photomontage method of alternate masking and exposure. The Atlanta area will eventually be covered by topographic maps, orthophotoquads, and land use maps at 1:24,000 scale and a topographic map, an orthophotomosaic, a slope map, and a land use map at 1:100,000 scale.

The 1:500,000-scale Idaho State map is being revised. Landsat paper prints covering the State and quad-centered photographs were obtained for transfer of detail to the map. In the areas with sufficient planimetry, transfer was made directly with a Bausch & Lomb Zoom Transfer Scope. In areas of light planimetry, the transfer was made to the Landsat imagery. The Landsat imagery was then scaled to the State map, and the linework was transferred to the imagery.

A Cibachrome color 1:1,000,000 Landsat mosaic of Alaska was aerotriangulated for the Regional Alaskan Mineral Assessment Program. In the north, excessive distortion in the Lambert conformal projection (standard parallels 55° N. and 65° N.) requires scene rectification (assuming projection distortion is partially compensated by tilt deformation). The GIANT (General Integrated Analytical Triangulation) program was used to determine the fictitious tilt and to aerotriangulate corner cross positions for mosaic control. Image coordinates from 1:250,000-scale maps were held as control points.

Because of insufficient overlap for conventional adjustment, all elevations were constrained to sea level—a unique application of analytical adjustment programs. A simultaneous horizontal (only) linear adjustment was used for the remainder of the State with procedures similar to those of previous Landsat mosaic projects. In both cases, the adjustment RMSE is about 400 m on control and 250 m on tie points, which indicates significant affine systematic distortions in scenes from northern latitudes.

In the north, 70-mm prints of bands 4, 5, and 7 are being rectified into 1:1,000,000 scenes. A private photolab will contact-print the rectified scenes in the northern area and enlarge 70-mm scenes elsewhere. The USGS will prepare mosaics by using templets showing positions of the corner crosses of each scene.

The USGS is cooperating with NASA and RCA in the geometric calibration of the RBV camera system for Landsat-C. The system will provide panchromatic Earth images with twice the ground resolution of the Landsat-1 and Landsat-2 multispectral RBV systems. The system for Landsat-C contains two identical cameras that operate in the spectral band from 0.50 to 0.75 μm. Calibration of the cameras is essential for register and cartographic referencing of high-resolution photoimage maps.

The reseau pattern of 81 crosses is on the inside of the RBV faceplate. The method used for calibration includes establishing a coordinate reference system and adjusting the measured coordinates to best fit this system. A copy of the reseau coordinates and a report for each RBV tube are available on request.

Image-format maps were prepared as byproducts of the 1:500,000-scale satellite image mosaic of Florida. Of the 16 nominal scenes 11 were printed at 1:500,000 scale as individual maps, each with a UTM grid, marginal text, a National Atlas insert, and reference coordinates of the graticule. Ten of the image maps were made from copies of bands 5 and 7 of the original images enlarged for the Florida mosaic. The image for the Florida Keys map was digitally enhanced in bands 4, 5, and 7 to accentuate underwater detail.

An individual UTM grid was computed and plotted to the imagery of each map in a curved configuration to minimize ground-coordinate errors for points measured from the grid. The Florida Keys grid fit was somewhat more complicated so that an undistorted UTM grid was used although the resulting RMSE of positions as determined from the grid exceeds 200 m.

Two widely separated geographic areas with differing vegetation were selected for investigation—the southeast quarter of the Vancleave, Miss., 15-min quadrangle (a flood plain with wetland vegetation) and the Goldwin, N. Dak., 7.5-min quadrangle (a prairie pothole area). All photographs covering the areas have been obtained, including 3,700-m CIR photographs of the Goldwin area taken on April 21 and July 21, 1976. The April photographs were valuable in mapping high water lines, and the July photographs taken at or near the peak of the growing season facilitated mapping of critical vegetation.

Compilation of the Goldwin area was completed with a PG 2 plotter. It appears that 1:12,000 is the smallest scale practical for mapping the rather narrow circular bands of wetland features associated with prairie potholes. CIR is the most effective film for wetland mapping. As expected, the 3,700-m photographs provided more clearly defined wetland data than higher altitude photographs.

To determine whether there are significant differences in the ability of operators to define and compile certain wetland features, a different operator has recompiled high water lines, normal water lines (assuming water levels were normal on the July photographs), and wetland perimeters within an area equal to half a test model. Also, the July photographs were used to recompile the April wetland perimeters to determine if the season is significant in mapping wetlands from CIR photographs. Comparison of the compilations is in progress.

Three versions of an image wetland map of the Auburndale 7.5-min quadrangle in Lakeland County, Fla., were prepared as part of a research project on inland (nontidal) wetland mapping. The objectives of the project were (1) to test the feasibility of mapping and classifying inland wetlands on USGS 7.5-min quadrangles in more detail than is now shown, (2) to develop or identify a standard definition and classification system for use by USGS, and (3) to prepare sample products for user evaluation. Each version represents a different wetland classification system (Martin and others, 1953; Anderson and others, 1975; and L. M. Cowardin and V. Carter, written commun., 1975).

Available SWA black-and-white photographs at 1:20,000 scale and quad-centered 1:76,000-scale CIR photographs were used to interpret and delineate the wetland boundaries and classes. The 1:24,000-scale photoimage bases were made from the CIR photographs by overprinting a yellow scribecoat with a rectified black-and-white transparency. The three wetland classifications were then compiled from the aerial photographs on the photoimage bases. Ozalid copies of the three image wetland maps were prepared for distribution to selected users.

TECHNIQUES

Clean-room technology is being applied to photogrammetric and photographic processes to eliminate visible blemishes caused by particles in the air and other contaminate transfer. Contamination of film and plates can obliterate photographic detail and introduce false imagery.

Laminar-flow air modules are being adapted to instruments and equipment to provide class 100 air to critical areas. Class 100 air is defined by Federal Standard 209B as limiting the number of particles 0.5 μm or larger to 100/ft^3 or 3.5/L. The mechanical filters used in the laminar flow modules are the high-efficiency particulate air (HEPA) type, 99.97 percent effective in removing particles as small as 0.3 μm.

Use of modules is unique for the varied applications in USGS. System flexibility permits selective distribution of clean air through laminar flow, nonlaminar flow, and general room purging, and results in a clean environment at minimum cost.

An economical method of producing 1:24,000-scale rectified photographs in quadrangle format has been developed for BLM. The quad-centered photographs are rectified to map points on the best available maps, usually 7.5-min quadrangles. A special mask was made with a 1-in overedge with a 133-line screen, a negative copy of the marginal data, and a small clear window through which the quadrangle name and coordinates are printed. With the map-control graphic on the rectifier easel, the photograph is fitted to the map points, and the mask is spaced evenly around the quadrangle corners. The map-control graphic is then removed, and lithographic film is inserted under the mask and exposed. Marginal information is exposed separately with a boxed light source. The finished product, made in one photographic step, is a screened positive with minimal collar information suitable for making diazo prints.

A Fairchild KC-6A and a Wild RC 10 camera were used to take 3,600-m-altitude photographs of a 3-bar resolution target array on the roof of the National Center in Reston, Va. Several different films were used, and the photographs were taken with and without the image-motion compensation available in the KC-6A. In addition to the resolution targets, many horizontal and vertical control marks in the area were paneled to evaluate the geometric fidelity of the KC-6A. Simultaneous photographs were taken on Kodak 2402 film with the two cameras. Kodak 3414 film, a very slow film with high definition, was also exposed in the KC-6A camera using image-motion compensation. An AWAR of 29 l/mm was determined for the 3414 film, and the photos taken on 2402 film with the RC 10 had an AWAR of 37.8 l/mm. This project also showed that for this flight height, slightly better resolution can be obtained with an f/8 aperture setting rather than f/4 in the RC 10.

A project is being conducted to determine the feasibility of using Landsat imagery to revise medium- and small-scale (1:63,360 and 1:250,000) maps along the Alaska pipeline route. Results to date have been negative because of low resolution. Revision already done is being compared with the new compilations and is being evaluated for content and accuracy in interpretation and delineation of cultural and hydrographic features.

FILM MOSAICKING

Research is continuing in the use of a dodging printer for film mosaicking orthophotos. A prototype was built with a 196-light bank with three-way switches on each light and overall voltage control. The exposure variation of the printer appears adequate to produce a uniform tonal match across the join line of two orthophoto positives and to correct tonal imbalances throughout the image area. Several single-join mosaics were produced with excellent results.

Further research and testing is continuing with the prototype printer to produce a better tonal join between orthophotoquads by providing greater control of exposure variation. Two additional units with 225 bulbs are being built.

QUALITY CONTROL

In a calibration program to standardize all USGS and participating contractors' densitometers, a master step wedge is being used to test and identify each densitometer's characteristics. Those in which readings vary from the master more than 0.02 density unit are earmarked for recalibration. Interim tables with weighted values to adjust readings to the master scale will be used until those densitometers are recalibrated. The program will help standardize density values in each of the USGS mapping centers.

Various negatives scanned with the Optronics rotating drum density reader were analyzed. Dodged and undodged and IR and panchromatic aerial negatives were scanned for comparison. Scanning breaks the contrast range of the gray scale into proportional steps for quantitative analysis. For each scanned negative, an impression curve is drawn with the visual uncertainties in tones plotted against tones as represented in successive ratios of white to black. The area under the curve is taken to represent the logical decision required to visually assess the tones for contrast and thus needed to extract information from the photograph. The aim of the research is to develop an objective means of assessing information content of photoimages with different tones made for orthophotoquads.

Tests were performed during the year to determine the usefulness of the Itek VEMC for evaluating mapping photographs. Matrixes for Kodak 2402 and 2405 film were recently acquired for use with the VEMC to determine resolution values for aerial photographs. However, specific density and contrast data for the two matrixes were not provided and could not be obtained from the manufacturer. Therefore, a study was made to determine the densitities and the contrast value of each matrix element. Measurements established that the contrast of all elements ranged from 1.3 to 1 in row 1 to a high of 7 to 1 in row 8 and that the contrast change between rows of elements was not constant, as might be expected. The contrast difference between rows varied from 0.03 to 0.17, and the variations were similar for both matrixes.

Several image edges on nine photos of the Fort Huachuca area of Arizona were measured with the VEMC to determine the effects of using the magnifications 25X, 40X, and 100X. Results indicate that (1) consistent and relatively accurate contrast measurements can be made with any of the three magnifications, (2) different magnifications have little effect on measurement accuracy, and (3) 40X was the easiest for VEMC measurements on the project photographs.

The project "A Study of the Influence of Ground Reflectance on Film Density and Resolution for Kodak 2402 and 2405 Film" was completed. Results indicate that contrast of photoimages of various objects are normally less than the actual ground contrast of the objects and that the amount of contrast change from ground targets to film images can vary considerably. Resolution for different photographs of the same scene also varied considerably from photo to photo, although the measurements were made on identical ground targets with the same contrast. The following table shows the ranges of image contrast and resolution obtained for several photographs of the same scene.

Film type	*Ground contrast at target*	*Photoimage contrast at target*	*Resolution (1/mm)*
2402 _______	6:1	2.5:1 to 6.3:1	32 to 41
2402 _______	16:1	5.1:1 to 7.2:1	26 to 33
2405 _______	16:1	8.2:1 to 10:1	38 to 33

In addition to the report on this project, four more reports cover related studies (C.F. Kirsch, unpub. data, 1976).

One cause for rejection of aerial photographs has been the failure of contractors to properly expose aerial film where scene reflectance varied greatly. In the future, such areas will be identified beforehand, and some flight lines will be broken so that exposures can be corrected. Different film may be used on other flight lines to accommodate extreme contrast variation.

One result of the twin-camera projects (in which simultaneous exposures were made in Texas and along the Canadian border) has been to alert contractors to the potential of this method. The images made from black-and-white film and filter combinations can be used to produce a color-image map suitable for land use and environmental control studies. The films can also satisfy photographic needs of conventional mapping. USGS has lithographed 1:24,000-scale color image maps by assigning colors to two bands of black-and-white film. The technique was used previously to produce 1:500,000-scale satellite image maps (such as the Florida mosaic) from two or more bands of imagery recorded by the Landsat MSS.

In aerial photography, two high-altitude photographs are simultaneously exposed in two synchronized, vertically oriented mapping cameras—one containing black-and-white panchromatic film filtered to record the visible spectrum and the other containing black-and-white IR film filtered to record the near-infrared spectrum. Negatives of the two images are rectified, scaled to 1:24,000, and processed for the optimum density range of 0.4 to 1.4. Halftone positives are made by screening the negatives for various combinations of yellow, magenta, cyan, and black, depending on the color rendition desired. Negatives made from the halftone positives are used to generate the printing plates. An additional negative is prepared for marginal information and the UTM grid. The final product is a 1:24,000-scale color-image map that exhibits sharper tonal contrast and better resolution than an equivalent map produced from conventional color or CIR film.

Color image maps or color orthophotoquads are excellent complements to line maps of the same area. If two-camera imagery could be incorporated into orthophotomap production, three new image maps could be available to the user in addition to the standard black-and-white orthophotoquad prepared from the panchromatic image: (1) A black and white orthophotoquad prepared from the IR image; (2) a simulated natural color rendition of the combined panchromatic and IR images, and (3) a simulated CIR rendition of the combined images.

At present, the major drawback for two-camera photography is the lack of commercially available high-altitude aircraft equipped with two mapping cameras. Until they become available, production of color image maps or color orthophotoquads will likely remain experimental.

CARTOGRAPHY AND DESIGN

METRIC MAPPING

The policy for metric mapping is flexible enough to deal with most user concerns identified in a recent survey. In general, the plan is for new maps and complete revisions. All-metric maps will be produced for States that agree, and partially metric maps will be produced for States preferring a gradual change. Metrication is being deferred in States that insist on waiting until complete 1:24,000-scale coverage is available. Maps prepared in the metric system will be at 1:25,000, 1:50,000, 1:100,000, 1:250,000, 1:500,000, and 1:1,000,000 scale. Puerto Rico maps remain at 1:20,000 scale. Contour intervals for the various scales are 1, 2, 5, 10, 20, 50, and 100 m.

Metric maps at 1:25,000 scale are being prepared of Alaska, Florida, Nevada, New York, North Carolina, and South Dakota. Projects where metric contours are planned, and where planning has already been completed for foot contours, were reviewed to determine if the requested flight height and the vertical control will meet metric specifications. During the transition period, flight heights and vertical control will be planned to accommodate contour intervals in either system.

LARGE-SCALE MAPPING

The pilot program was virtually completed, including user evaluations of individual projects covering San Francisco, Calif.; Chicago, Ill.; Fort Wayne, Ind.; Frederick, Md.; and Charleston, S.C. A draft of the Large-Scale Mapping Handbook was distributed to about 100 communities throughout the country and a number of Federal and State agencies for comments. The comments and suggestions have been evaluated and incorporated into the final version of the book.

INTERMEDIATE-SCALE MAPPING

Under the new National Mapping Program, intermediate-scale mapping has been expanded. Maps in the 1:100,000-scale series are derived from published topographic maps and, as required, are updated without field checking from new aerial photographs and other sources. The new information is extracted either monoscopically or stereoscopically, depending on the amount of relief.

The 1:100,000-scale content is compiled on feature separates to provide a wide range of products to map users. Map features are delineated by single-line symbols to facilitate future digitization. Present plans are for planimetric bases only, with metric contours to be added later.

Because of the great demand for these maps, BLM is producing some of the quadrangles, using USGS monitors and specifications. Quadrangles prepared entirely by USGS will have hypsographic detail and will be printed as a standard series.

To satisfy the immediate needs of various users, maps are compiled both in quadrangle and county format. Since the established series is in quadrangle format, all compilation for county format is extracted and used for producing the standard quadrangle, eliminating dual compilation.

A study is in progress to determine the feasibility of compiling all intermediate-scale map data at 1:75,000 on the premise that map-user needs can be better satisfied and USGS can be more responsive to them by converting the original compilation to any scale from 1:50,000 to 1:100,000. Content is being feature separated to conform to any derived scale within these limits. The study includes determining the desired line weight, type size, collar information, content, and accuracy—the desirability of showing some features only at certain scales is also being studied.

SLOPE MAPPING

USGS has developed four techniques of producing slope maps from negatives of contour plates. The first is an orbiting-light system in which contours are expanded and exposed in negative form by a rotating light source.

The second technique is a type of sandwich in which clear Mylar is placed between the film and the contour negative. Varying the thickness of the Mylar sandwich controls the amount of line spread.

The third technique uses an orbiting lens system on a cartographic camera to make a 1:1 ratio copy and can produce greater line spreads than the first two techniques.

The fourth technique uses an orbiting table with a clear vacuum plate that holds the contour negative 3 mm above an opaque vacuum film platen. The film platen can be rotated in a controlled orbit for various line spreads. This technique also has a 1:1 ratio and can produce wide line spreads.

COASTAL MAPPING

Experimental coastal maps of Beaufort, N.C., and Fort Pierce, Fla., have led the way for a series of coastal zone maps incorporating data shown on USGS topographic maps, NOS bathymetric maps, and BLM OCS resource management maps. The maps are designed to give users a complete picture of the physical environment in a given area.

Topographic/bathymetric editions of the Los Angeles and Wilmington 1:250,000-scale quadrangles were published, and 250 others are in progress. In selected areas topographic/bathymetric maps are being prepared at 1:24,000 and 1:100,000 scale. The entire Georgia coast is being mapped at the scale of 1:100,000. The five quadrangles will have a land-contour interval of 2 m. Bathymetric data will also be depicted at the 2-m interval, with 1-m supplemental contours where necessary. Other projects are underway in Texas and California. In addition, 29 topographic/bathymetric orthophotomaps of a portion of the Georgia coastline are being completed at the scale of 1:24,000.

On topographic/bathymetric maps the bathymetric data and shoreline (MHW line) compiled by NOS are combined with USGS topographic map plates. Also combined with the topographic plates are data from BLM's official OCS protraction diagrams.

Comments from State and Federal agencies about the Coastal Zone Mapping Handbook were evaluated and incorporated in the final copy. Information in the Handbook will help State and local coastal planners develop mapping programs to support their projects.

SPECIAL MAPPING PROJECTS

Nineteen maps at 1:7,500,000 scale were published for the Committee on Commerce and the Interior and Insular Affairs Committee of the U.S. Senate. The maps are incorporated in a report on U.S. energy transportation systems that was compiled by the Congressional Research Service, Library of Congress. The maps portray the magnitude and direction of energy movement through the various transporation systems. Where appropriate, energy deposits, mining, processing, and production facilities, and consumption data were also added to the maps. Companion color overlays were prepared for Senate committee hearings.

A special map of Pictured Rocks National Lakeshore, Mich., was prepared for the National Park Service (NPS). It was published at 1:62,500-scale with a contour interval of 6 m. It is a derivative of four 15-min and six 7.5-min standard quadrangle maps on 67.5x105-cm paper. Paneling and scribing were at publication scale. To save scribing time, complete topographic information is shown only within the park limits. Outside the proclamation boundary only a skeletal network of roads is shown. This outer area is covered with a screened brown tint. NPS requested that their actual ownership boundary be shown in addition to the proclamation limits, and to emphasize that boundary, the 95 percent woodland green tint is shown only within these limits. Because of the importance of the few improved roads within the park, county road shields were added where appropriate.

Work is in progress on a set of maps at 1:50,000 scale for Pueblo County, Colo., including a line map, a land use map based on the USGS classification system, a land use map based on the Colorado system, and an orthophotomosaic of the county. The line map is in the USGS/Colorado cooperative county mapping program. The orthophotomosaic was assembled from 1:24,000-scale orthophotos prepared as part of a cooperative project with SCS. The land use overlay for the Colorado system of classification was provided by the State.

A preliminary edition of the map of Federal Lands Subject to Mineral Restrictions was published at 1:7,500,000 scale. Prepared in the National Atlas format, the map is printed in two sheets—Alaska is separate. The map provides an overview of Federal lands affected by current regulations, emphasizing restrictions against mineral development. While no statement is made to identify the type of restriction, the color sequence and legend order present an implied order of decreasing severity based on current USGS mineral policy. The Federal lands depicted fall into three general categories: (1) Those to be preserved in their natural state, (2) those specifically excluded from the provisions of the Mining Law of 1872, the Mineral Leasing Act of 1920, the Acquired Lands Act of 1947, the Geothermal Steam Act of 1970, and the Materials Sales Act of 1947 as Amended, and (3) others principally under the administration of BLM or the Forest Service. Delineation of the lands shown is limited by map scale. All Federal lands to be preserved in their natural state are shown, symbolized where necessary. Generally other areas less than 22,500 acres are not shown.

Crater Lake was included in the 11,700-m altitude quad-centered photographs for the Klamath Falls orthophotoquad project. The lake is almost centered on the line between two 7.5-min quadrangles (Prospect 1 NE and NW). One 7.5-x 15-min quadrangle was made to include the entire lake. The north and south halves of the two 7.5-min qudrangles were scanned on the Wild PPO 8 at the scale of 1:45,000. The four scans were enlarged to 1:24,000 scale and mosaicked by the standard film montage method to bring the two halves of Crater Lake together on one sheet. The mosaic was retouched so that the four join lines that intersect in the middle of the lake cannot be seen. The negative was combined with a base containing grid lines and a title block.

Compilation and editing were completed on the Dry Valley, Antarctica, project, and the maps are being prepared for printing. The project consists of eight quadrangles, each covering 1° of longitude and 15′ of latitude and an area of 5,418 km^2. The contours were stereocompiled on a Kelsh plotter and scribed at 1:50,000 scale, with a basic interval of 50 m and a supplemental interval of 25 m. The planimetric features were compiled by a combination of stereoscopic and monoscopic procedures from an orthophotoimage base. Delineation of the snow, glaciers, exposed areas, and other features peculiar to this terrain and climate required special considerations and treatment.

MAP INDEXES

State map indexes for Pennsylvania and Ohio are in preparation. They are a new design similar to that of Virginia, which served as the prototype. To improve readability and economy of maintenance, the design features a black and red color scheme, bolder titling type, reduced base detail, large-scale quadrangle names oriented to town symbols, and insets explaining small-scale and special map coverage.

POCKET MAPS

Two experimental folded map projects were completed to improve the utility of USGS topographic maps for outdoor recreationists, naturalists, and tourists. Yosemite Valley, in Yosemite National Park, Calif., is a 1:24,000-scale standard topographic map folded with a tipped-on cover printed in four colors. Contemporary graphics, featuring a full-color photograph of Yosemite Valley Falls, provide an attractive display.

Twenty-two 7.5-min, 15-min, and various Alaskan quadrangles were folded and packaged in waterproof and dustproof reusable plastic pouches. A unique feature of the pouches is standard folding, packaging, and titling that do not require customizing each map in the series.

DRAFTING MEDIA

Two new pieces of equipment purchased in 1976 complete in-house facilities for testing bid samples of scribecoat and peelcoat material used in mapmaking. A Dillon Model ML universal tester measures tensile strength of the polyester base. A Tenney Ten Model TTRS temperature-humidity test chamber is used to determine thermal and hygroscopic coefficients of expansion, and shrinkage. About 20 tests are performed on the bid samples, covering physical characteristics of the base material and engraving stratum and scribing and photographic processing qualities.

LANDSAT IMAGERY FOR 1:250,000-SCALE MAPPING

USGS is experimenting with Landsat imagery (1) to investigate the feasibility of equidensity contouring, or density slicing, for theme extraction of open water, vegetation, and natural shaded-relief information from the imagery, (2) to use available 1:100,000-scale material and the theme extractions to prepare a 1:250,000-scale experimental map for evaluating the economic, factual, and visual effectiveness of the application, and (3) to assess the effectiveness of reducing 1:100,000-scale material to make the 1:250,000-scale base.

The area selected for the experiment is covered by the published 1:250,000-scale Wenatchee, Wash., quadrangle. Research was divided into separate preparation of linework and imagery. A new 1:250,000-scale base of drainage and roads was prepared from reductions of the 1:100,000-scale linework. Images of open water, vegetation, and natural shaded relief were extracted from the imagery, and preliminary fits were made to the linework. Results indicate that (1) drainage detail can be salvaged nearly intact by reduction from 1:100,000 to 1:250,000 (cultural features might be salvaged if clearance is not important) and (2) editing of roads and trails (using other maps) is desirable to emphasize the maintained transportation network.

Use of an open-water plate for this quadrangle was not warranted from the economic, factual, or visual standpoints. A handmade plate could be made in about 5 hours by using peelcoat, a process that is cheaper than photography.

Apparently some of the smaller lakes were lost because ice and snow caused reflectance. (The date of the project imagery was July 4; imagery recorded later in the year showed overlapping water surfaces.) Some reservoirs were not full at image date so that the water images did not touch all of the compiled shorelines. Extraction of open water from Landsat imagery seems best suited to areas having a large number of natural water bodies that are full, unfrozen, and situated on relatively flat ground so that terrain shadows do not interfere.

The vegetation plate is useful economically, factually, and visually, but it has limitations. The symbol is a green tint standing for trees and shrubs. Since IR picks up anything with a high chlorophyll content, field crops and natural grass must be edited out, a step that has not been tried. The image appears to represent small patches of timber better than generalized compiled outlines and thus yields not only a better picture of the vegetation but also more information about the geology.

The shaded-relief plate is effective economically, factually, and visually. However, the one obvious visual weakness is that shadows are cast away from the viewer, which can cause an impression of pseudo-relief. Much of the success of this plate depends on the landforms and the angle of their axes to the Sun. If a slope is entirely in shadow, its irregularities tend to be lost. At 1:250,000 scale, heavy timber does not appear to soften underlying structures unduly.

THE HOTINE OBLIQUE MERCATOR PROJECTION APPLIED TO LANDSAT MAPPING

A feasibility study has shown that the Hotine oblique Mercator projection will map Landsat images satisfactorily provided that new latitude zones and new projection constants are selected at intervals. Five zones are required for the north-south half of the orbit. The same zones can be applied to the south-north half of the orbit with projection constants reversed. The projection program is available to NASA-GSC for use in their image processing system.

DIGITAL APPLICATIONS

The new Gestalt Photo Mapper II (GPM-2) orthophoto-producing system became operational in June 1976. Several projects comprising more than 200 7.5-min quadranges were scanned. The average scan time is about 4 hours per quadrangle for all types of imagery and relief. At this level of production, 1,000 quadrangles can be produced each year by using two shifts arranged to allow four employees to operate the GPM-2 nearly 20 hours each day.

For quad-centered high-altitude photographs, the output is fixed at 1:80,000 scale, requiring mosaicking and enlarging to produce the standard orthophotoquads at 1:24,000 scale. With a fixed-ratio enlarger, two methods have been used: (1) Enlarging to 1:24,000 scale before mosaicking and (2) mosaicking at 1:80,000 scale before enlarging. The latter method is now used, and tests indicate that it is more accurate and less expensive. Most projects scheduled for the GPM-2 are areas of high relief. A contour plot of the model area is printed on film at the same time the image is exposed. The contour interval is usually set to record 30-m contours. Moreover, from 500 to 2,400 elevations per scanning patch, or more than 1 million points for each quadrangle, are recorded on the magnetic tape in unjoined patch format. Computer programs are to be written for joining these patches to form digital elevation models. After they are joined and the data stored back on tape, terrain data can be retrieved from the tape at any desired interval of meters or feet. Future improvements in the system include electronic masking of the scan area, stereomate printing, double-model scanning to eliminate mosaicking, and general software improvements.

The AS-11A analytical stereoplotters, which have been fitted with modern minicomputers, are to be modified with new servosystems for all stage and coordinatograph axes and with a new computer interface. The servosystems will be controlled by microprocessors. The application software for the AS-11A's is being modified.

The USGS purchased six Altek AC189 Data Acquisition Systems. These are electronic accessory components attached to encoders mounted on the axial shafts of PG 2, B 8, C 5, Topocart, and other stereoplotting instruments with optical trains. The AC189 features operator control of both point and stream recording modes, independent scaling and translation of each axis, and both thumbwheel and keyboard entry of identification information. These attachments can be used to record contour, profile, hydrographic, and planimetric digital data directly from the stereomodel during map compilation. The data are stored on 9-track 800-bpi magnetic tape.

A Voice Data Entry Terminal System (VDETS) was purchased for engineering test and evaluation. This system comprises a microphone, voice analyzer, minicomputer, magnetic cassette tape unit, and other input-output devices compatible with standard interface logic. As an operator speaks into the microphone, the system analyzes the power spectrum of the words and either stores them as part of a reference vocabulary or compares them to the vocabulary already stored. An operator trains VDETS by reading the selected vocabulary into memory and recording it on cassette tape. Because all speakers have unique voiceprints, each operator records a separate tape of the vocabulary.

In operation VDETS compares the spoken words with the stored vocabulary. When it finds a match, it responds according to the programed instructions or commands. Responses range from reading and recording data to controlling mechanical motions. Experimental projects for which VDETS has been programed include obtaining and recording geographic name information, and adding feature codes and other descriptive information to digital data acquired during map compilation.

Several Omnitext Model 1500 word processing systems were purchased for use in phototypesetting. Each system comprises a core-memory microcomputer, CRT display, paper-type reader/punch, and typographic keyboard. Operators can key in text and typesetting commands, view the data on the display screen, edit or correct the data, and then produce a punched paper tape. The data tapes are used, either directly or after transmission from remote locations, to control the Merganthaler VIP Phototypesetter at Reston, Va., which produces the map type on transparent film. The new systems have significantly reduced the turnaround time for obtaining map type.

INFORMATION

GEODETIC CONTROL TRANSFER

The USGS is fulfilling an agreement to transfer geodetic control data to NGS. Emphasis is on a filing system that insures inclusion of all relevant control in the data base. Upon receipt of the specified formats after a Geodetic Workshop in May, the actual recomputation and submission of data began. Observation data for four projects were recomputed, coded for the data base, and analyzed. The descriptive data for three of these jobs were also coded and submitted.

HP-65 PROGRAM LIBRARY

A library of programs has been compiled for the HP-65 programable pocket calculator. Each program has a complete coding listing, user instructions, and documentation in addition to a programed magnetic card. The library contains programs to convert geographic coordinates to State plane coordinates and vice versa, a worldwide UTM-coordinate and zone-number computation from geographics that will operate overedge, and all the Hewlett-Packard package programs. More programs are being added as requested.

MAP MICROFILMING

The National Cartographic Information Center (NCIC) is well into a program of copying 130,000 topographic maps on 35-mm black-and-white microfilm. The microfilming follows selection of the best copy from three separate map libraries and thus insures a nearly complete high-quality file.

Coding is alphabetical by State, on rolls, and in an increasing scale sequence so that the smallest-scale, earliest map appears first and the most recent, 1:24,000-scale map appears last. A 30-m roll of film contains about 500 map images reduced 20X and will be for sale at $20. A large State such as Texas requires 10 rolls for full historical coverage. Smaller States require as little as two rolls.

The current series, a major subset of this full series, is also being similarly microfilmed into roll form. These are the most recent maps of a State, including partials, currently available. The coding is also alphabetical, and the price per roll will be $20, including partial rolls.

GEOGRAPHIC NAMES INFORMATION SYSTEM

Information files enlarged or added to the Geographic Names Information System (GNIS) include data about names in the State of Rhode Island and Providence Plantations (1,800 records), a doubling of the storage file of decisions by the Board on Geographic Names (20,000 records), and the completion of a file to coordinate and standardize names that identify the 1:100,000-scale quadrangle maps (1,800 records) currently being compiled through joint efforts of USGS, BLM, and SCS.

The Rhode Island data were delineated on current 1:24,000-scale maps, and general textual data was input to General Information Processing System (GIPSY) records with an IBM communicating magcard terminal. The name records were then completed by adding geographic coordinates recorded by the Gradicon digitizing system. Completion of the project was a major step toward increasing the usefulness of outside files that can be converted to the GNIS format. For example, 32,000 name records have been compiled and recorded in machine language by the State of Virginia.

Total input of the file of decisions from 1890 through 1959 by the Board on Geographic Names is completed and is now being edited. Data from this file and all other GNIS files (Massachusetts, Alaska, Rhode Island, and quadrangle names) were selectively written in various formats of 9-track magnetic tape and reproduced on 21- × 28-cm paper directly through the Zerox 1200 printer. The formatted data are available on request, or other formats can be queried directly from terminals communicating with Reston.

Additional research included (1) data entry experimentation with VDETS, a procedure that will be tested with data from gazetteers of Hawaii and the Trust Territory of the Pacific Islands that were originally compiled and printed by the Board on Geographic Names, (2) plotting data recovered directly from the GIPSY file onto a map overlay by means of the Cartographic Automatic Mapping (CAM) program, and (3) construction of a test model of a 1:100,000-scale quadrangle map names index of Texas.

AUTOMATED SYSTEM FOR LOCATING AERIAL PHOTOGRAPHY PROJECTS

The automated Aerial Photography Summary Record System (APSRS) was developed as a means of quickly collecting and disseminating information on available or planned photography projects. Each summary record includes the agency name, date of coverage, photo scale, film type, extent of coverage to the nearest 7.5-min quadrangle or by State and county, agency project code, and status (planned, in progress, or complete). Output from the system is designed to show, at a glance, areas covered by aerial photographs obtained by particular agencies. The potential customer must contact the indicated agency to make sure that the film meets his requirements before placing an order.

A preliminary computerized system developed during 1975 for handling APSRS is now operational. The system was designed for data input by the agency that holds the film and thus places responsibility for accuracy on the agency most familiar with the product.

EROS USER RESEARCH FACILITY

As part of the EROS Program, the USGS maintains a user research facility at the National Center (room 2A223-B, telephone 703- 860-6271) for government-agency, university, and industry investigators with approved projects. There is no charge for use of the facility, but investigators must provide their own materials and complete their own projects. Limited instructions on the use of equipment are provided, and use is restricted to qualified operators.

Available equipment includes:

- Bendix Datagrid Digitizer with a 48×60-in light-table, a Besseler CB-7 enlarger for projecting 70-mm-format film transparencies, and magnetic tape or typewriter output
- Spatial Data Systems Datacolor model 703
- A Joyce-Loebl Mark III-C microdensitometer with reflective optics attachment
- Richards light-tables with takeup reels for film sizes to 9.5 in wide
- Bausch & Lomb zoom microscopes with magnification to 60X and stereo capability for 70-mm format film only
- Bausch & Lomb Zoom Transfer Scope with magnification to 14X and anamorphic correction
- Wild M 5 stereomicroscope with 6X to 50X magnification and trinocular viewing capability
- Zeiss point maker

Reference materials include a comprehensive file of 470 EDC-selected Landsat color prints covering the conterminous United States and a selection of Skylab images obtained with the S190A and S190B cameras on missions 2, 3, and 4.

EROS TECHNICAL MEMORANDUMS

The EROS Cartography Coordinator distributes technical memorandums on subjects related to cartographic applications of satellite data. The following were distributed in the past year:

- EC-39-Landsat—Solid-state linear arrays as a candidate Landsat imager
- EC-40-Landsat—Photographic imagery and shallow-seas bathymetry by remote sensing
- EC-41-Landsat—Distribution of recent papers relative to Landsat cartographic applications
- EC-42-Landsat—Reports on scale differences and scale variation on Landsat images
- EC-43-Landsat—Developments in shallow-seas mapping application of Landsat
- EC-44-Landsat—Technical notes on EROS Digital Image Enhancement System (EDIES)

COMPUTER TECHNOLOGY

With its scientists engaged in research into every existing and potential source of energy, the USGS is increasingly charged with providing direction to both government and industry in all phases of energy-related exploration, development, and production. Concomitantly, USGS requirements for increased computational capacity accelerated in FY 1977. The Computer Center Division (CCD) continued its expansion of computational facilities to meet the needs of the USGS scientific community. An example of this growth pattern is the recent addition to the existing batch-processing methods of sophisticated interactive processing methods using time-sharing computer systems.

TIME-SHARING SYSTEMS

To provide automatic data-processing support to its energy program and related activities, the USGS procured three fully compatible time-sharing-oriented computers. A contract was awarded in August 1976 to Honeywell Information Systems, Inc., for three Multics time-sharing systems. The first computer was installed at Denver, Colo., in November 1976; the second was installed at Menlo Park, Calif., in December 1976; and the third was installed at Reston, Va., in January 1977. All three computers are accessed by numerous terminals. Several data bases are maintained on the computers. Image-manipulation techniques using cathode-ray-tube graphic devices and minicomputers monitoring scientific instrumentation are used in support of scientific computations.

EROS DATA CENTER

The EROS Data Center in Sioux Falls, S. Dak., completed the first-year phase of a three-year effort to optimize the inquiry, order, and account-processing system. This phase is the first attempt to fully computerize the complete customer-accounting and order-processing system. Also, development was completed for a low-throughput digital-image enhancement. This procedure uses algorithms developed by USGS personnel in Flagstaff, Ariz., and is the forerunner of a full-scale high-throughput digital-image-processing system scheduled for installation in January 1978. This system will use a SEL (Systems Engineering Laboratory) 32/55 computer system and will provide, for the first time, a means of enhancing Landsat satellite imagery to customer specifications.

IMAGE PROCESSING

The approach to image processing in the Flagstaff, Ariz., facility is to remove noise from spatial data, which can then be enhanced for presentation as images for scientific interpretation.

The purposes of the facility include:

- Providing cartographic digital-image enhancements of spacecraft pictures to photographic interpreters to support preparation of geologic base maps.
- Providing custom enchancements of Landsat pictures containing areas of special geologic interest to investigators in the USGS and other agencies.
- Conducting basic research in image-processing methods.
- Providing general computational support to investigators at the Flagstaff Field Center.
- Providing custom enhancements of nonimage digital data sets by digital-image-processing methods. These data sets are reconstituted as televisionlike images in which data point values, or their derivatives are represented as "brightness" values in an image roster. Examples are sets of terrain, magnetic, gravity, or similar data represented as shaded-relief, stereoscopic, or three-color images.

Actual processing does not require elaborate central processing unit capacity. Two independent computer systems are used—a DEC (Digital Equipment

Computer) PDP 11/20 and a DEC PDP 11/45. An Electrak 100 digitizing system is used offline in the development of data sets for experimental work. Optronics Photowrite P-1500 devices are used to convert magnetic tape images to film.

Selected products are delivered to the EROS Data Center, where copies are available to the general public for a nominal charge.

U.S. GEOLOGICAL SURVEY PUBLICATIONS

PUBLICATIONS PROGRAM

Books and maps

Results of research and investigations conducted by the USGS are made available to the public through professional papers, bulletins, water-supply papers, circulars, miscellaneous reports, and several map and atlas series, most of which are published by the USGS. Books are printed by the Government Printing Office, and maps are printed by the USGS; both books and maps are sold by the USGS.

All books, maps other than topographic quadrangle maps, and related USGS publications are listed in the catalogs "Publications of the Geological Survey, 1879-1961" and "Publications of the Geological Survey, 1962-1970" and in yearly supplements, available on request, that keep the catalogs up to date.

New publications, including topographic quadrangle maps, are announced monthly in "New Publications of the Geological Survey." A free subscription to this list may be obtained on application to the *U.S. Geological Survey, 329 National Center, Reston, VA 22092.*

State list of publications on geology and hydrology

"Geologic and Water-Supply Reports and Maps, [State]," a series of booklets, provides a ready reference to these publications on a State basis. The booklets also list libraries in the subject State where USGS reports and maps may be consulted; these booklets are available free on request to the USGS.

Surface-water, quality-of-water, and ground-water-level records

Surface-water records through water year 1970 were published in a series of water-supply papers titled "Surface-Water Supply of the United States"; through water year 1960, each volume covered a single year, but the period 1961–70 was covered by two 5-year volumes (1961-65 and 1966–70).

Quality-of-water records through water year 1970 were published in an annual series of water-supply papers titled "Quality of Surface Waters of the United States."

Both surface-water and quality-of-water records for water years 1971-74 were published in a series of annual reports titled "Water Resources Data for [State]." Some of these reports contained both types of data in the same volume, but others were separated into two parts, "Part 1: Surface-Water Records" and "Part 2: Water-Quality Records." Limited numbers of these reports were printed, as they were intended for local distribution only. Since the data in these reports will not be republished in the water-supply paper series, reports will be sold by the National Technical Information Service.

Records of ground-water levels in selected observations wells through calendar year 1974 were published in the series of water-supply papers titled "Ground-Water Levels in the United States." Through 1955, each volume covered a single year, but, during the period 1956–74, most volumes covered 5 years.

Starting with water year 1975, records for surface water, quality of water, and levels of ground-water-observation wells are all published under one cover in a series of annual reports issued on a State-boundary basis. Reports for water year 1975 and subsequent water years will appear in a series that will carry an identification number consisting of a two-letter State abbreviation, the last two digits of the water year, and the volume number. These reports are titled "Water-Resources Data for [State]"; they are sold by the *National Technical Information Service, U.S. Department of Commerce, Springfield, VA 22161.*

State hydrologic unit maps

State hydrologic unit maps, which are overprints of the 1:500,000-scale State base maps, show culture in black, hydrography in blue, hydrologic subdivision boundaries and codes in red, and political (FIPS county) codes in green. The Alaska State maps are at 1:2,500,000 scale, and Puerto Rico maps are at 1:240,000 scale. All river basins having drainage areas greater than 700 mi^2 are delineated on the maps. The hydrologic boundaries depict (1) water-resources regions, (2) water-resources subregions, (3) National Water-Data Network accounting units, and (4) cataloging units of the USGS "Catalog of Information on Water Data." These maps are available for every State and Puerto Rico.

State water-resource investigations folders

A series of folders entitled "Water-Resources Investigations in [State]" is a project of the Water Resources Division to inform the public about its current programs in the 50 States and Puerto Rico, the U.S. Virgin Islands, Guam, and American Samoa. As the programs change, the folders are revised. The folders are available free on request to the *U.S. Geological Survey, 439 National Center, Reston, VA 22092* or to the Water Resources Division district offices listed on p. 355 .

Open-file reports

Open-file reports, which consist of manuscript reports, maps, and other preliminary material, are made available for public consultation and use. Arrangements generally can be made to reproduce them at private expense. Since May 1974, all reports and maps released only in the open files have been listed monthly in "New Publications of the Geological Survey," which also lists places of availability for consultation. Reports issued before May 1974 were listed annually in the circular series. Most open-file reports are placed in one or more of the three USGS libraries: Room 4A100, National Center, 12201 Sunrise Valley Drive, Reston, VA 22092; 1526 Cole Boulevard at West Colfax Avenue, Golden, Colo. (mailing address: Stop 914, Box 25046, Federal Center, Denver, CO 80225); and 345 Middlefield Road, Menlo Park, CA 94025. Other depositories may include one or more of the USGS offices listed on p. 350 and interested State agencies. Many open-file reports are superseded later by formally printed publications.

Journal of Research of the U.S. Geological Survey

The "Journal of Research of the U.S. Geological Survey" is a bimonthly periodical designed to provide relatively rapid publication of short scientific papers by USGS personnel. It replaces the short-papers chapters of the annual "Geological Survey Research" series of professional papers, issued from 1960 through 1972.

Earthquake publications

The "Earthquake Information Bulletin" is published bimonthly by the USGS to provide information on earthquakes and seismological activities of interest to both general and specialized readers. It also lists pertinent publications and selected future professional meetings of Earth-science groups.

The USGS National Earthquake Information Service locates most earthquakes above magnitide 5.0 on a worldwide basis. A chronological summary of location and magnitude data for each located earthquake is published in the monthly listing "Preliminary Determination of Epicenters."

"Earthquakes in the United States" is published quarterly as a USGS circular. The circulars supplement the information given in the monthly listing "Preliminary Determination of Epicenters" to the extent of providing detailed felt and intensity data as well as isoseismal maps for U.S. earthquakes.

"United States Earthquakes" is published annually in cooperation with NOAA. This is a sourcebook on earthquakes occurring in the United States and gives location, magnitude, and intensity data. Other information such as strong-motion data fluctuations in well-water levels, tsunami data, and a list of principal earthquakes of the world is also given.

PUBLICATIONS ISSUED

During FY 1977, the USGS published 7,719 maps comprising some 23,506,107 copies:

Kind of map printed	*Number*
Topographic	6,837
Geologic and hydrologic	736
Maps for inclusions in book reports	35
Miscellaneous (including maps for other agencies)	111
Total	7,719

In addition, 6 issues of the "Journal of Research" comprising about 37,600 copies, 6 issues of the "Earthquake Information Bulletin" comprising about 42,200 copies, 179 technical book reports, and 306 leaflets and maps of flood-prone areas were published.

At the beginning of FY 1977, more than 95.1 million copies of maps and book reports were on hand in the USGS distribution centers. During the year, 664,951 copies of maps, including 685,169 index maps, were distributed. Approximately 5.7 million maps were sold, and $5,005,223 was deposited to Miscellaneous Receipts in the U.S. Treasury.

The USGS also distributed 262,139 copies of technical book reports, without charge and for official use, and 1,693,355 copies of booklets, free of charge, chiefly to the general public; 274,789 copies of the monthly publications announcements and 261,200 copies of a sheet showing topographic map symbols were sent out.

The total distribution resulted from receipt of 552,448 individual orders. The following table compares USGS map and book distribution (including booklets but excluding map-symbol sheets and monthly announcements) during FY 1976 and FY 1977:

Number of maps and books distributed

Distribution points	*Fiscal year 1976*	*1977*	*Change (percent)*
Eastern (Arlington, Va.)	7,204,608	5,277,689	-27
Central (Denver, Colo.)	4,812,543	4,549,576	-5
Alaska (Fairbanks)	148,344	157,285	+6
Other USGS offices	782,792	803,760	+3
Total	12,948,287	10,788,310	-17

HOW TO OBTAIN PUBLICATIONS

OVER THE COUNTER

Book reports

Book reports (professional papers, bulletins, water-supply papers, "Topographic Instructions," "Techniques of Water-Resources Investigations," and some miscellaneous reports) can be purchased from the *Branch of Distribution, U.S. Geological Survey, 1200 South Eads Street, Arlington, Va 22202,* and from the USGS Public Inquiries Offices listed on p. 354 (authorized agents of the Superintendent of Documents).

Some book publications that can no longer be obtained from the Superintendent of Documents are available for purchase from the above authorized agents of the Superintendent of Documents.

Maps and charts

Maps and charts may be purchased at the following USGS offices:

1200 South Eads Street, Arlington, Va.
1400 Independence Road, Rolla, Mo.
Building 41, Federal Center, Denver, Colo.
345 Middlefield Road, Menlo Park, Calif.
310 First Avenue, Fairbanks, Alaska
Public Inquiries Offices listed on p. 354 .

USGS maps are also sold by some 1,650 commercial dealers throughout the United States. Prices charged are generally higher than those charged by USGS offices.

Indexes showing topographic maps published for each State, Puerto Rico, the U.S. Virgin Islands, Guam, American Samoa, and Antarctica are available free on request. Publication of revised indexes to topographic mapping is announced in the monthly "New Publications of the Geological Survey." Each index also lists special and U.S. maps, as well as USGS offices and commercial dealers from which maps may be purchased.

Maps, charts, folios, and atlases that are out of print can no longer be obtained from any official source. They may be consulted at many libraries, and some can be purchased from secondhand-book dealers.

BY MAIL

Book reports

Technical book reports and some miscellaneous reports can be ordered from the *Branch of Distribution, U.S. Geological Survey, 1200 South Eads Street, Arlington, VA 22202.* Prepayment is required and should be made by check or money order in U.S. funds payable to the U.S. Geological Survey. Postage stamps are not accepted; please do not send cash. On orders of 100 copies or more of the same report sent to the same address, a 25-percent discount is allowed. Circulars, publications of general interest (such as leaflets, pamphlets, and booklets), and some miscellaneous reports may be obtained free from the Branch of Distribution.

Maps and charts

Maps and charts, including folios and hydrologic atlases, are sold by the USGS. Address orders to *Branch of Distribution, U.S. Geological Survey, 1200 South Eads Street, Arlington, VA 22202* for maps of areas east of the Mississippi River, including Minnesota, Puerto Rico, and the U.S. Virgin Islands, and to *Branch of Distribution, U.S. Geological Survey, Box 25286, Federal Center, Denver, CO 80225* for maps of areas west of the Mississippi, including Alaska, Hawaii, Louisiana, Guam, and American Samoa. Residents of Alaska may also order maps of their State from the *Alaska Distribution Section, U.S. Geological Survey, 310 First Avenue, Fairbanks, AK 99701.*

Prepayment is required. Remittances should be by check or money order in U.S. funds payable to the U.S. Geological Survey. On an order amounting to $300 or more at the list price, a 30-percent discount is allowed. Prices are quoted in lists of publications and in indexes to topographic mapping for individual States. Prices include the cost of surface transportation.

Journal of Research, Earthquake Information Bulletin, and Preliminary Determination of Epicenters

Subscriptions to the "Journal of Research of the U.S. Geological Survey," the "Earthquake Information Bulletin," and the "Preliminary Determination of Epicenters" are by application to the *Superintendent of Documents, Government Printing Office, Washington, DC 20402.* Payment is by check payable to the Superintendent of Documents or by charge to your deposit account number. Single issues may be purchased from the *Branch of Distribution, U.S. Geological Survey, 1200 South Eads Street, Arlington, VA 22202.*

Advance material from mapping

Advance material available from current topographic mapping is indicated on individual State index maps, which are issued quarterly. This material, which includes such items as aerial photography, geodetic control data, and maps in various stages of preparation and editing, is available for puchase. Requests for the indexes or inquiries concerning the availability of advance material should be directed to the *National Cartographic Information Center, U.S. Geological Survey, 507 National Center, Reston, VA 22092.*

EROS Data Center materials

USGS aerial photography, NASA aircraft photography and imagery, Landsat (formerly ERTS) imagery, and Skylab imagery and photography are sold by the USGS, as are copies of the photography and imagery produced on 16-mm browse film, which are designed for prepurchase evaluation. Landsat data in digital form and Landsat Standard Catalogs are also sold. Address requests for price list, additional information, and orders to *EROS Data Center, U.S. Geological Survey, Sioux Falls, SD 57198.* Prepayment is required for orders. Remittances should be made payable in U.S. funds to the U.S. Geological Survey.

National Technical Information Service

Some USGS reports, including computer programs, data and information supplemental to map or book publications, and data files, are released through the National Technical Information Service (NTIS). These reports, available either in paper copies or microfiche or sometimes on magnetic tapes, can be purchased only from the *National Technical Information Service, U.S. Department of Commerce, Springfield, VA 22161.* USGS reports that are released through NTIS, together with their NTIS order numbers and prices, are announced in the monthly "New Publications of the Geological Survey."

REFERENCES CITED

Aggers, L. W., and Kelley, E. B., 1976, Douglas County forest cover condition mapping and forest volume inventory: Am. Cong. Surveying and Mapping, Seattle, Wash., 1976, Proc.

Aki, K., and Lee, W. H. K., 1976, Jour. Geophys. Research, 81, 4400-4406.

Anderson, J. R., 1977, Land use and land cover changes—a framework for monitoring: U.S. Geol. Survey Jour. of Research, vol. 5, no. 1, p. 143-153.

Anderson, J. R., Hardy, E. E., Roach, J. T., and Witmer, R. E., 1975, A land use and land cover classification system for use with remote sensor data: U.S. Geol. Survey Prof. Paper 96 , 28 p.

Asting, Neil, Goldberg, M. C., and Weiner, E. R., 1976, Examination of aqueous suspensions by Fraunhofer diffraction spectroscopy [abs.]: Rocky Mtn. Spectroscopy Conf., 18th, Denver, Colo., August 1976, Program, p. 12.

Bailey, E. H., Blake, M. C., Jr., and Jones, D. L., 1970, On-land Mesozoic oceanic crust in California Coast Ranges: U.S. Geol. Survey Prof. Paper 700-C, p. C70-C81.

Bailey, R. A., Dalrymple, G. B., and Lanphere, M. A., 1976, Volcanism, structure, and geochronology of Long Valley caldera, Mono County, California: Jour. Geophys. Research, v. 81, no. 5, p. 725-744.

Baird, A. K., Toulmin, Priestley III, Clark, B. C., Rose, H. J. Jr., Keil, Klaus, Christian, R. P., Gooding, J. L., 1976, Mineralogic/petrologic implications of Viking geochemical results from Mars—interim report: Science, v. 194, p. 1288-1293.

Bamber, E. W., and Waterhouse, J. B., 1971, Carboniferous and Permian stratigraphy and paleontology, northern Yukon Territory, Canada: Alberta Soc. Petroleum Geologists Bull., v. 19, n. 1, p. 29-250.

Barnes, Ivan, Irwin, W. P., and Gibson, H. A., 1975, Geologic map showing springs rich in carbon dioxide or chloride in California: U.S. Geol. Survey open-file map, 1 sheet, scale 1:500,000.

Barraclough, J. T., Robertson, J. B., and Janzer, V. J., 1976, Hydrology of the solid waste burial ground, as related to the potential migration of radionuclides, Idaho National Engineering Laboratory, *with a section on* Drilling and sample analyses *by* L. G. Saindon: U.S. Geol. Survey open-file rept. 76-471, 199 p.

Bartells, J. H., and Hubbard, L. L., 1976a, Teton Dam flood of June 1976, Rose quadrangle, Idaho: U.S. Geol. Survey Hydrol. Inv. Atlas HA-578, 1 sheet, scale 1:24,000.

———1976b, Teton Dam flood of June 1976, Blackfoot quadrangle, Idaho: U.S. Geol. Survey Hydrol. Inv. Atlas HA-579, 1 sheet, 1:24,000 scale.

Bateman, P. C., and Eaton, J. P., 1967, Sierra Nevada Batholith: Science, 158, 1407-1417.

Beikman, H. M., 1974a, Preliminary geologic map of the southwest quadrant of Alaska: U.S. Geol. Survey Misc. Field Studies Map MF-611, 2 sheets, scale 1:1,000,000.

———1974b, Preliminary geologic map of the southeast quadrant of Alaska: U.S. Geol. Survey Misc. Field Studies Map MF-612, 2 sheets, scale 1:1,000,000.

Beikman, H. M., 1975a, Preliminary geologic map of southeastern Alaska: U.S. Geol. Survey Misc. Field Studies Map MF-673, 2 sheets, scale 1:1,000,000.

———1975b, Preliminary geologic map of the Alaska Peninsula and the Aleutian Islands: U.S. Geol. Survey Misc. Field Studies Map MF-674, 2 sheets, scale 1:1,000,000.

Beikman, H. M., and Lathram, E. H., 1976, Preliminary geologic map of northern Alaska: U.S. Geol. Survey Misc. Field Studies Map MF-789, 2 sheets, scale 1:1,000,000.

Bennison, A. P., and Milton, Charles 1954, Preliminary geologic map of the Fairfax, Va., and parts the Seneca, Md.-Va. quadrangles: U.S. Geol. Survey open-file map, scale 1:62,500.

Benson, D. G., 1974, Geology of the Antigonish Highlands, Nova Scotia: Geol. Survey of Canada Mem. 376.

Berg, H. C. 1972, Geologic map of Annette Island, Alaska: U.S. Geol. Survey Misc. Geol. Inv. Map I-684, scale 1:63,360.

Berg, H. C., Elliott, R. L., Smith, J. G. Pittman, T. L., and Kimball, A. L., 1977, Mineral resources of the Granite Fiords Wilderness Study Area, Alaska: U.S. Geol. Survey Bull. 1403. [In press.]

Berg, H. C., Jones, D. L., and Richter, D. H., 1972, Gravina-Nutzotin belt—tectonic significance of an Upper Mesozoic sedimentary and volcanic sequence in southern and southeastern Alaska, *in* Geological Survey Research 1972: U.S. Geol. Survey Prof. Paper 800-D, p. D1-D24.

Bergquist, W. E., 1976, Bibliography of reports resulting from U.S. Geological Survey Technical cooperation with other countries: U.S. Geol. Survey Bull. 1426, 68 p.

Bertram, J. G., and Erdmann, C. E., 1935, Natural Gas in Montana, *in* Geology of natural gas: Am. Assoc. Petroleum Geologists [June], p. 245-276.

Bethke, P. M., Barton, P. B., Jr., Lanphere, M. A., and Steven, T. A., 1976, Environment of ore deposition in the Creede mining district, San Juan Mountains, Colorado—Age of Mineralization. Econ. Geology v. 71, p. 1006-1011.

Beuttner, E. C., 1972, Reverse gravitative movement on earlier overthrusts, Lemhi Range, Idaho: Geol. Soc. America Bull., v. 83, no. 3, p. 839-846.

Biemann, Klaus, Oro, John, Toulmin, Prestley III, Orgel, L. E., Nier, A. O., Anderson, D. M., Simmonds, P. G., Flory, D., Diaz, A. R., Rushneck, D. R., and Biller, J. A., 1976, Search for organic and volatile inorganic compounds in two surface samples from the Chryse Planitia region of Mars: Science, v. 194, p. 72-76.

Bigelow, H. B., and Sears, Mary, 1935, Studies of the waters on the Continental Shelf, Cape Cod to Chesapeake Bay—Part II—Salinity: Mass. Inst. Technol. Papers, Phys. Oceanography and Meteorology, v. 4, no. 1. 94 p.

Blanchard, D. P., Jacobs, J. W., Brannon, J. C., and Haskin, L. A., 1976, Major and trace element compositions of matrix and aphanitic clasts from consortium breccia 73215: Proc. 7th Lunar Sci. Conf., v. 2, p. 2179-2187.

Blixt, J. E., 1941, Cut Bank oil and gas field, Glacier County, Montana, *in* Levorsen, A. I., ed., Stratigraphic type oil fields: Am. Assoc. Petroleum Geologists [Dec.], p. 327-381.

Blomeke, J. O. and Kee, C. W., 1976, Projections of wastes to be generated: Internat. Symposium on the Management of Wastes from the LWR Fuel Cycle, Denver, Colorado, July 11-16, 1976, Proc., p. 96-117.

Bohor, B. F., Hatch, J. R., and Hill, D. J., 1976, Altered volcanic ash partings as stratigraphic mer beds in coals of the Rocky Mountain region [abs.]: Am. Assoc. Petroleum Geologists Bull., v. 60, no. 4, p. 651.

Bortleson, G. C., Wilson, R. T., and Foxworthy, B. L., 1976, Water-quality effects on Baker Lake of recent volcanic activity at Mount Baker, Washington: U.S. Geol. Survey open-file rept. 45 p.

Bowin, Carl, 1976, Caribbean gravity field and plate tectonics: Geol. Soc. America Spec. Paper 167, 79 p.

Boyce, J. M., 1976, Relative ages of flow units in the lunar nearside maria based on Lunar Orbiter IV photographs: Proc. Seventh Lunar Sci. Conf., Geochim et. Cosmochim. Acta, Suppl. 7, v. 3, p. 2717-2728.

Boyce, J. M., Dial, A. L., and Soderblom, L. A., 1974, Relative age of lunar nearside plains and maria: Proc. Fifth Lunar Sci. Conf., Geochim. et. Cosmochim, Acta, suppl. 5, v. 1, p. 11-23.

Boyce, J. M., and Schaber, G. G., 1977, Ring-moats on the lunar maria: buried impact craters and their implication to crater erosion models [abs.], *in* Lunar Science VIII: Houston, Texas, Lunar Sci. Inst., p. 133.

Boyce, J. M., Schaber, G. G. and Dial, A. L., Jr., 1977, Age of the Luna 24 mare basalts based on crater studies: Nature, v. 265, no. 5589, p. 38-39.

Brew, D. A., and Ford, A. B., 1977, Preliminary geologic and metamorphic-isograd map of the Juneau B-1 quadrangle, Alaska: U.S. Geol. Survey Misc. Field Studies Map MF-846, scale 1:31,680.

Brew, D. A., Grybeck, D., Johnson, B. R., and Nutt, C. J., 1976, Glacier Bay National Monument mineral-resource studies recommenced, *in* Cobb, E. H., ed., U.S. Geological Survey in Alaska; accomplishments during 1975: U.S. Geol. Survey Circ. 733, p. 58-59.

Brew, D. A., Johnson, B. R., Nutt, C. J., Grybeck, Donald, and Ford, A. B., 1977, Newly discovered granitic and gabbroic bodies in the Fairweather Range, Glacier Bay National Monument, Alaska, *in* Blean, K. M., ed., The U.S. Geological Survey in Alaska: accomplishments during 1976: U.S. Geol. Survey Circ. 751-B, p. 112.

Brew, D. A., Loney, R. A., and Muffler, L. J. P., 1966, Tectonic history of southeastern Alaska, *in* A sysium on tectonic history and mineral deposits of the western Cordillera in British Columbia and neighbouring parts of the United States: Canadian Inst. Mining Metallurgy Spec., v. 8, p. 149-170.

Brew, D. A., and Ovenshine, A. T., 1974, Summary of recent studies in Glacier Bay National Monument, Alaska, *in* Carter, Claire, ed., U.S. Geological Survey Alaska Program, 1974: U.S. Geol. Survey Circ. 700, p. 53-54.

Brock, M. R., and Singewald, Q. D., 1968, Geologic map of the Mount Tyndall quadrangle, Custer County, Colorado: U.S. Geol. Survey Geol. Quad. Map GQ-596, 2 sheets, 1:24,000 scale.

Brooks, C., Hart, S. R., Hoffmann, A., and James, D. E., 1976, Rb-Sr mantle isochrons fcom oceanic regions: Earth and Planetary Sci. Letters, v. 32, p. 51-61.

Brown, D. W., 1976, The adsorption of lead from solution on streambed sediment: Hayward, Calif., California State University, M.S. Thesis, 102 p.

Brown, D. W., and Roberson, C. E., 1977, Solubility of natural fluorite at 25°C: U.S. Geol. Survey Jour. Research. [In press.]

Brown, J. S., Emery, J. A., Meyer, P. A., Jr., 1954, Explosion pipe in test well on Hicks Dome, Hardin, County, Illinois: Econ. Geol. v. 49, p. 891-902.

Brown, R. D., Jr., Ward, P. L., and Plafker, George, 1973, Geologic and seismic aspects of the Managua, Nicaragua, earthquakes of December 23, 1972: U.S. Geol. Survey Prof. Paper 838, 34 p.

Buddington, A. F., and Chapin, T., 1929, Geology and mineral deposits of southeastern Alaska: U.S. Geol. Survey Bull. 800, 398 p.

Bufe, C. G., Harsh P. W., and Burford R. O., 1977, Steady state seismic slip—a precise recurrence model, Geophys. Research Letters, v. 4, p. 91-94.

Burkham, D. E., Kroll, C. G., and Porterfield, George, 1976, A guide for application of the computer program for the modified Einstein method of computing total sediment discharge (MODEIN): U.S. Geol. Survey Computer Contr., 138 p.

Burns, A. W., and Weeks, J. B., 1976, Simulated effects of the proposed Narrows Reservoir on the water-table aquifer along the South Platte River, Morgan County, Colorado: U.S. Geol. Survey open-file rept. 76-379, 15 p.

Cacchione, D. A., Drake, D. E., Winant, C. D., Dingler, John, and Olson, J. R., 1976, Observations of sediment movement by surface and internal waves off San Diego, California: EOS (Am. Geophys. Union Trans.), v. 58, no. 5, p. 307.

Calbeck, J. M., 1975, Geology of the central Wise River valley, Pioneer Mountains, Beaverhead County, Montana: Missoula, Mont., Montana Univ., M.S. thesis, 89 p.

Calkins, F. C., 1930, The granitic rocks of the Yosemite region, *in* Matthes, F. C., Geologic history of the Yosemite Valley: U.S. Geol. Survey Prof. Paper 160, p. 120-129.

Campbell, J. A., 1976, Depositional environments of the uranium-bearing Cutler Formation, eastern Utah [abs.]: Geol. Soc. America Abs. with Programs, v. 8, no. 6, p. 801 -802.

Campbell, R. H., 1975, Soil slips, debris flows, and rainstorms in the Santa Monica Mountains and vicinity, southern California: U.S. Geol. Survey Prof. Paper 851, 51 p.

Cannon, W. F., and Klasner, J. S., 1976, Phosphorite and other apatite-bearing sedimentary rocks in the Precambrian of northern Michigan: U.S. Geol. Sucvey Circ. 746, 6 p.

Carneggie, D. M., and Holm, C. S., 1976, Remote sensing techniques for monitoring impacts of phosphate mining in southeastern Idaho [abs.]: W. T. Pecora Memorial Symp., 2nd, Am. Soc. Photogramm., Sioux Falls, S. Dak., 1976, Proc. [In press.]

Carothers, W. W., 1976, Aliphatic acids and stable carbon isotopes of oil-field waters in the San Joaquin Valley, California: San Jose State Univ., M.S. Thesis, 68 p.

Case, J. E., and Donnelly, T. W., 1976, Gravitational evidence for crustal structure in central Guatemala [abs.]: Trans. Amer. Geophys. Union, EOS, v. 57, p. 948-949.

Casteel, R. W., Adam, D. P., and Sims, J. D., 1977, Late-Pleistocene and Holocene remains of *Hysterocarpus traski* (Tule perch) from Clear Lake, California, and inferred Holocene temperature fluctuations: Quaternary Research, v. 7, no. 1, p. 133-143.

Castle, R. O., Church, J. P., and Elliott, M. R., 1976, Aseismic uplift in southern California: Science, v. 192, p. 251-253.

Carr, W. J., and Dickey, D. D., 1977, Cenozoic tectonics of eastern Mojave Desert, *in* Geological Survey Research 1976: U.S. Geol. Survey Prof. Paper 1000, p. 75.

Carter, V. P., and Gammon, P. T., 1976, Vegetative cover map of the Great Dismal Swamp: U.S. Geol. Sucvey open-file map 76-615.

Carter, V. P., Garrett, M. K., Shima, Lurie, and Gammon, P. T., 1977, The Great Dismal Swamp: Management of a hydrologic resource with the aid of remote sensing: Am. Water Resources Assoc. Bull. [In press.]

Carter, V. P., Voss, Alan, Malone, Donald, and Godsey, William, 1977, Classification and mapping of wetlands in western Tennessee: 2d Ann. William T. Pecora Symposium, Sioux Falls, S. Dak., 1976, Proc. [In press.]

Chao, E. C. T., 1976, Mineral-produced high-pressure striae and clay polish—key evidence for nonballistic transport of ejecta from Ries Crater: Science, v. 194, no. 4265, p. 615-618.

Chao, E. C. T., Hodges, C. A., Boyce, J. M., and Soderblom, L. A., 1975, Origin of lunar light plains: U.S. Geol. Survey Jour. Research, v. 3, no. 4, p. 379-392.

Chao, E. C. T., Minkin, J. A., and Thompson, C. L., 1977, Petrology of consortium sample 67455, from a white-matrix breccia boulder near the rim of North Ray Crater, Descartes [abs.], *in* Lunar science VIII Abstracts: Houston, Tex., Lunar Sci. Inst., p. 166.

Chappell, John and Polach, H. A., 1976, Holocene sea-level change and coral-reef growth at Huon Peninsula, Papua New Guinea: Geol. Soc. America Bull. v. 87, p. 235-240.

Chatterjee, N. D., and Wilhelm Johannes, 1974, Thermal stability and standard thermodynamic properties of synthetic $2M_1$ muscovite $KA_2 (AlSi_3O_{10}(OH)_2$: Contr. Mineralogy and Petrology, v. 48, p. 89-114.

Chayes, Felix, 1960, On corelation between variables of constant sum: Jour. Geophys. Research, v. 65, no. 15, p. 4185-4193.

Chayes, Felix, and Kruskal, W. B., 1966, An approximate statistical test for correlations between proportions: Jour. Geology, v. 74, no. 5, pt. 2, p. 692-702.

Christ, C. L., 1960, Crystal chemistry and systematic classification of hydrated borate minerals: Am. Mineral., v. 45, p. 334-340.

Clark, B. C., Baird, A. K., Rose, H. J. Jr., Toulmin, Priestley III, Keil, Klaus, Castro, A. J., Kelliher, W. C., Rowe, C. D., and Evans, P. H., 1976a, Inorganic analyses of Martian surface samples at the Viking landing sites: Science, v. 194, p. 1283-1288.

Clark, B. C., Toulmin, Priestley III, Baird, A. K., Keil, Klaus, Rose, H. J. Jr., 1976b, Argon content of the Martian atmosphere at the Viking landing site: Analysis by X-ray fluorescence spectroscopy: Science, v. 193, p. 804-805.

Clark, T. H., 1923, New fossils from the vicinity of Boston: Boston Soc. Nat. History Proc., v. 36, p. 473-485.

Claypool, G. E., and Reed, P. R., 1976, Thermal-analysis technique for source-rock evaluation; quantitative estimate of organic richness and effects of lithologic variation: Am. Assoc. Petroleum Geologists Bull., v. 60, no. 4, p. 608-612.

Coats, R. R., 1950, Volcanic activity in the Aleutian Arc: U.S. Geol. Survey Bull. 947-B, p. B35-B49.

Coats, R. R., and Riva, John, 1976, Eastward obduction of early Paleozoic eugeosynclinal sediments, and early Mesozoic transverse thrusting resulting fcom southward movement of a compressed Paleozoic sedimentary pile, northeastern Great Basin, Nevada, U.S.A. [abs.]: Internat. Geol. Cong., 25th, 1976, v. 1, no. 25, p. 80.

Cobb, J. C., and Russell, S. J., 1976, Sphalerite mineralization in coals of the Illinois Basin [abs.]: Geol. Soc. America Bull., v. 8, no. 8, p. 816.

Cobban, W. A., 1945, Marine Jurassic formations of Sweetgrass arch, Montana: Am. Assoc. Petroleum Geologists Bull., v. 29, no. 9, p. 1262-1303.

——— 1955, Cretaceous rocks of northwestern Montana: Geol. Soc. America, 6th Ann. Conf., Sweetgrass arch-Disturbed belt, Montana, 1955, Billings guidebook, p. 107-119.

Colby, B. R., and Hembree, C. H., 1955, Computations of total sediment discharge, Niobrara River near Cody, Nebraska: U.S. Geol. Survey Water-Supply Paper 1593, 187 p.

Coleman, R. G., Ghent, E. D., and Fleck, R. J., 1973, The Jabal Shayi layered gabbro in southwestern Saudi Arabia: U.S. Geol. Survey Saudi Arabian project rept. 159, 93 p.

Collins, F. R., and Robinson, F. M., 1967, Subsurface stratigraphic, structural, and economic geology, northern Alaska: U.S. Geol. Survey open-file rept., 252 p., 16 pls., 19 figs., 2 tables.

Compston, W., Foster, T. J., and Gray, C. M., 1977, RB-SR systematics in clasts and aphanites from consortium breccia 73215 *in* Lunar science VIII: Houston, Tex. Lunar Sci. Inst., p. 199-201.

Conant, L. C., and Swanson, V. E., 1961, Chattanooga Shale and related rocks of central Tennessee and nearby areas: U.S. Geol. Survey Prof. Paper 357, 91 p.

Connor, J. J., Keith, J. R., and Anderson, B. M., 1976, Trace-metal variation in soils and sagebrush in the Powder River basin, Wyoming and Montana: Jour. Research, U.S. Geol. Survey, v. 4, p. 49-59.

Cornwall, H. R., 1966, Nickel deposits of North America: U.S. Geol. Survey Bull. 1223, 62 p.

Council on Environmental Quality, 1976, Environmental quality, seventh annual report of the Council on Environmental Quality: Washington, D.C., 378 p.

Cowardin, L. M., Carter, V. P., Golet, F. C., and LaRoe, E. T., 1976, Interim classifications of wetlands and aquatic habitats of the United States, *in* Sather, H. J., ed., Proceedings of the National Wetland and Inventory Workshop, July 20-23, 1975: U.S. Fish and Wildlife Service, addendum, 110 p.

Crawford, M. L., 1966, Composition of plagioclase and associated minerals in some schists fcom Vermont, U.S.A., and South Westland, New Zealand, with inferences about the peristerite solvus: Contr. Mineralogy and Petrology v. 13, p. 269-294.

Cunningham, Kirk, Goldberg, M. C., and Weiner, E. R., 1977, Investigations of the detection limits for dissolved solutes in water measured by Laser-Raman spectroscopy: Anal. Chemistry, v. 49, no. 1, p. 70-75.

Damon, P. E., Shafiqullah, M., and Leventhal, J. S., 1974, K-Ar chronology for the San Francisco volcanic field rate of erosion of the Little Colorado River, *in* Karlstrom, T. N. V., and others, eds., Geology of northern Arizona, with notes on archaeology and paleoclimate, Pt. II: Geol. Soc. America Rocky Mtn. Sec. Mtg. Guidebook, p. 221-235.

Davidson, M. J., 1963, Geochemistry can help find oil if properly used: World Oil, p. 94-107.

Davis, G. H., Counts, H. B., and Holdahl, S. R., 1977, Further examination of subsidence, Savannah, Georgia, 1955-1975: Internat. Assoc. Sci. Hydrologists, Internat. Symposium on Land Subsidence, 2d, Anaheim, Calif., Dec. 1976, Proc. [In press.]

Davis, J. R., 1976, The influence of drainage basin area upon the distribution of lithium in playa sediments, *in* Vine, J. D., ed., Lithium resources and requirements by the year 2000: U.S. Geol. Survey Prof. Paper 1005, p. 105-109.

Davis, S. N., and Hall, F. R., 1958, Late Cenozoic history of northeastern San Joaquin Valley, California [abs.]: Geol. Soc. America Bull., v. 69, no. 12, pt. 2, p. 1552.

Day, H. W., 1973, The high temperature stability of muscovite plus quartz: Am. Mineralogist, v. 58, p. 255-262.

Dean, W. E., Jr., and Schreiber, B. C., 1976, Authigenic barite in the eastern north Atlantic, Leg 41, Deep Sea Drilling Project [abs.]: Geol. Soc. America Abs. with Programs, v. 8, p. 830-831.

Delevaux, M. N., Doe, B. R., and Brown, G. F., 1967, Preliminary lead isotope investigations of brine from the Red Sea, galena from the Kingdom of Saudi Arabia, and galena from United Arab Republic (Egypt): Earth and Planetary Sci. Letters, v. 3, no. 2, p. 139-144.

Detterman, R. L., 1968, Recent volcanic activity on Augustine Island, Alaska: U.S. Geol. Sucvey Prof. Paper 600-C, p. C126-C129.

Detterman, R. L., Plafker, George, Tysdal, R. G., Hudson, Travis, 1976, Geology and surface features along part of the Talkeetna segment of the Castle Mountain-Caribou fault system, Alaska: U.S. Geol. Survey Misc. Field Studies Map MF-738, scale 1:63,360.

Dixon, H. R., and Lundgren, L. W., Jr., 1968, Structure of eastern Connecticut, *in* Zen, E-an, White, W. S., Hadley, J. B., and Thompson, J. B., Jr., eds., Studies in Appalachian geology—Northern and Maritime: New York, Interscience Publishers, p. 219–229.

Donnelly, J. M., Goff, F. E., Thompson, J. M., and Hearn, B. C., Jr., 1976, Implications of thermal water chemistry in The Geysers-Clear Lake area: Program, Geothermal-Environmental Seminar-76, Oct. 27-29, Lake County, Calif., 6 p.

Donovan, T. J., 1974, Petroleum microseepage at Cement, Oklahoma; evidence and mechanism: Am. Assoc. Petroleum Geologists Bull., v. 58, no. 3, p. 429–446.

Douglas, R. J. W., Gabrielse, H., Wheeler, J. O., Stott, D. F., and Belyea, H. R., 1970, Geology of western Canada, *in* Douglas, R. J. W., ed., Geology and economic minerals of Canada: Geol. Survey Canada Econ. Geology Rept. 1, p. 365–488.

Draeger, W. C., 1976, Monitoring irrigated land acreage using Landsat imagery—an application example: U.S. Geol. Sucvey open-file rept. 76–630, 25 p.

Duckworth, J. P., Jump, M. J., and Knight, B. E., 1974, Low-level radioactive waste management research project final report: West Valley, N.Y., Nuclear Fuels Services, Inc., 57 p.

Duffield, W. A., 1975, Late Cenozoic ring faulting and volcanism in the Coso Range area of California: Geology, v. 3, p. 335–338.

Eakin, H. M., 1918, The Cosna-Nowitna region, Alaska: U.S. Geol. Survey Bull. 667, 54 p.

Eaton, G. P., Prostka, H. J., Oriel, S. S., and Pierce, K. L., 1976, Cordilleran thermotectonic anomaly—pt. I—Geophysical and geological evidence of coherent Late Cenozoic intraplate magmatism and deformation [abs.]: Geol. Soc. America Abs. with Programs, v. 8, no. 6, p. 850.

Eberlein, G. D., and Churkin, Michael, Jr., 1970, Paleozoic stratigraphy in the northwest coastal area of Prince of Wales Island, southeastern Alaska: U.S. Geol. Survey Bull. 1284, 67 p.

Eddy, R. M., 1976, The effect of point-source discharges on the diversity of benthic invertebrates of the Yampa River, Steamboat Springs to Hayden, colorado, September 1975: U.S. Environmental Protection Agency, Surveillance and Analysis Div., Tech. Inv. Branch, Region VIII, Rept. S&A/TIB-30, 42 p.

Eggers, D. E., 1976, Application of borehole geophysics to the selection and monitoring of nuclear waste disposal sites: U.S. Symposium on Rock Mechanics, 17th, Snowbird, Utah, Aug. 25-26, 1976, Proc., p. 4B3-1-4B3-7.

El Goresy, A., and Chao, E. C. T., 1976, Evidence of the impacting body of the Ries Crater—the discovery of Fe-Cr-Ni veinlets below the crater bottom: Earth Planetary Sci. Letters, v. 31, p. 330–340.

Elliott, R. L., Smith, J. G., and Hudson, Travis, 1976, Upper Tertiary high-level plutons of the Smeaton Bay area, southeastern Alaska: U.S. Geol. Survey open-file rept. 76–507, 15 p.

Ellsworth, W. L., 1976, Preliminary evaluation of teleseismic travel time residuals preceding the Hawaiian earthquake of 29 November 1975 [Abs.]: EOS (Am. Geophys. Union Trans.), v. 57, p. 288.

Emmett, W. W., 1975, The channels and waters of the Upper Salmon River Area, Idaho: U.S. Geol. Survey Prof. Paper 870-A, 116 p.

———1976, Bedload transport in two large gravel-bed rivers, Idaho and Washington, *in* Proceedings of the Third Federal Interagency Sedimentation Conference, 1976: Water Resources Council, pt. 4, p. 101–114.

Emmett, W. W., Druffel, L. A., Schneider, V. R., and Skinner, J. V., 1976, Laboratory hydraulic calibration of the Helley-Smith bedload sampler: U.S. Geol. Survey open-file rept. 76–752, 63 p.

Emerson, B. K., 1917, Geology of Massachusetts and Rhode Island: U.S. Geol. Survey Bull. 597, 289 p.

Emmons, W. H., and Calkins, F. C., 1913, Geology and ore deposits of the Philipsburg quadrangle, Montana: U.S. Geol. Survey Prof. Paper 78, 271 p.

Engdahl, E. R., and Lee, W. H. K., 1976, Jour. Geophys. Research, v. 81, p. 4400–4406.

Englund, K. J., 1968, Geology and coal resources of the Elk Valley Area, Tennessee and Kentucky: U.S. Geol. Survey Prof. Paper 512.

———1971, Displacement of the Pocahontas Formation by the Russell Fork Fault, Southwest Virginia, U.S. Geol. Survey Prof. Paper 750-B, p. B13-B16.

Englund, K. J., and Roen, J. B., 1962, Origin of the Middlesboro Basin, Kentucky: U.S. Geol. Survey Prof. Paper 405-B, p. E20-E22.

Englund, K. J., Roen, J. B., and DeLaney, A. O., 1964, Geology of the Middlesboro North quadrangle, Kentucky: U.S. Geol. Survey Quad. Map GO-300, scale 1:24,000.

Epstein, A. G., Epstein, J. B., and Harris, L. D., 1977, Conodont color alteration—an index to organic metamorphism: U.S. Geol. Survey Prof. Paper 995, 27 p.

Erdmann, C. E., Beer, William, Nordquist, J. W. and Davis, N. A., 1946, Preliminary structure contour map of the Cut Bank-West Kevin-Border districts, Glacier, Toole, and Pondera Counties, Montana: U.S. Geol. Survey open-file map, scale 1:126,720.

Erdman, J. A., and Ebens, R. J., 1976, Molybdenum in sweetclover growing on mine spoils *in* Geochemical Survey of the Western Energy Regions: U.S. Geol. Survey open-file rept. 76 -729, p. 4–9.

Erdman, J. A., and Tourtelot, H. A., 1976, Denver liquid sewage sludge—its agricultural benefits and its effect on the metal composition of wheat grown at the Watkins Test Site, Adams County, Colorado: U.S. Geol. Survey open-file rept. 76 -810, 29 p.

Epsinosa, A. F., ed., 1976. The Guatemalan earthquake of February 4, 1976, a preliminary report: U.S. Geol. Survey Prof. Paper 1002, 90 p.

Espinosa, A. F., Husid, R., and Quesada, A., 1976, Intensity distribution and source parameters from field observations, *in* The Guatemalan earthquake of February 4, 1976, a preliminary report: U.S. Geol. Survey Prof. Paper 1002, p. 52–66.

Evernden, J. F., and Kistler, R. W., 1970, Chronology of emplacement of Mesozoic batholithic complexes in California and western Nevada: U.S. Geol. Survey Prof. Paper 623, 42 p.

Eychaner, J. H., 1976, Estimating runoff volumes and flood hydrographs in the Colorado River basin, southern Utah: U.S. Geol. Survey Water-Resources Inv. 76–102, 23 p.

Fabbi, B. P., and Elsheimer, H. N., 1976, Evaluation and application of an automatic fusion technique to major element XRF analysis of silicate rocks: Third Annual Meeting, Federation of Analytical Chemists and Spectroscopical Society, Philadelphia, Pa.

Fabiano, E. B., and Jones, W. J., 1976, Magnetic horizontal intensity—United States-Epoch 1975.0: U.S. Geol. Survey, Misc. Inv. Ser. Map I-913, 2 sheets, scale 1:5,000,000.

Fabiano, E. B., Peddie, N. W., and Jones, W. J., 1976, Magnetic total intensity—Epoch 1975.0, U.S. Geol. Survey: Misc. Inv. Ser. Map I-915, 2 sheets, scale 1:20,000.

Faul, Henry, Stern, T. W., Thomas, H. H., and Elmore, P. L. D., 1963, Ages of intrusion and metamorphism in the Northern Appalachians: Am. Jour. Sci., v. 261, p. 1-19.

Faulkner, G. L., 1976, Short-term storage of freshwater in saline-water aquifers in Florida—A potential solution to water shortage [abs.]: EOS (Am. Geophys. Union Trans.), v. 57, no. 12, p. 917.

Faulkner, G. L., and Pascale, C. A., 1975, Monitoring regional effects of high pressure injection of industrial waste water in a limestone aquifer: Ground Water, v. 13, no. 2, p. 197-208.

Field, M. T., 1975, Bedrock geology of the Ware area, central Massachusetts: Contrib. No. 22, Geology Dept., Amherst, Mass., Univ. of Massachusetts, 186 p.

Fish, R. E., and Yotsukura, N., 1976, Water-temperature chunges downstream from a major reservoir at Cannonsville, New York: Am. Soc. Civil Engineers, Environmental Aspects of Irrigation and Drainage, Speciality Conf., Ottawa, Canada, July 1976, Proc., p. 481-496.

Flanigan, V. J., 1976, Geophysical survey of uranium mineralization in Alaskite rocks, eastern Washington: U.S. Geol. Sucvey open-file rept. 76-679, 25 p.

Fogelman, R. P., 1976, Descriptions and chemical analyses for selected wells in the central Sacramento Valley, California: U.S. Geol. Survey open-file rept. 76-472, 71 p.

Forbes, R. B., and Engels, J. C., 1970, K^{40}/Ar^{40} age relations of the Coast Range batholith and related rocks of the Juneau icefield area: Alaska Geol. Soc. America Bull., v. 81, p. 579-584.

Force, E. R., Lipin, B. R., and Smith, R. E., 1976, Map showing heavy mineral resources in Pleistocene sand of the Port Leyden quadrangle. Southwestern Adirondack Mountains, New York: U.S. Geol. Survey Misc. Field Studies Map MF-728-B.

Ford, A. B., 1976, Stratigraphy of the layered gabbroic Dufek instrusion, Antarctica: U.S. Geol. Survey Bull. 1405-D, p. D1-D36.

Ford, A. B., and Brew, D. A., 1973, Preliminary geologic and metamorphic-isograd map of the Juneau B-2 quadrangle, Alaska: U.S. Geol. Survey Misc. Field Studies Map MF-527.

Ford, A. B., and Brew, D. A., 1977a, Chemical nature of Cretaceous greenstone near Juneau, Alaska, suggests tholeiitic ocean-floor volcanism, *in* Blean, K. M., ed., The U.S. Geological Survey in Alaska; accomplishments during 1976: U.S. Geol. Survey Circ. 751-B, 112 p.

———1977b, Preliminary geologic and metamorphic-isograd map of northern parts of the Juneau A-1 and A-2 quadrangles, Alaska: U.S. Geol. Sucvey Misc. Field Studies Map MF-847, Scales 1:250,000 and 1:31,680.

Ford, D. E., 1976, Water-temperature dynamics of dimictic lakes—analysis and predictions using integral energy concepts: Minneapolis, Minn., Univ. Minnesota, Ph. D. dissert., 438 p.

Fournier, R. O., Sorey, M. L., Mariner, R. H., and Truesdell, A. H., 1976, Geochemical prediction of quaifer temperatures in the geothermal system at Long Valley, California: U.S. Geol. Survey open-file rept. 76-469, 34 p.

Foster, J. B., and Goolsby, D. A., 1972, Construction of waste-injection monitor wells near Pensacola, Florida: Florida Dept. Nat. Resources, Bur. Geology, Inf. Circ. 74, 34 p.

Foster, R. J., 1960, Tertiary geology of a portion of the Central Cascade Mountains, Washington: Geol. Soc. Amer. Bull., v. 71, no. 2, p. 99-125.

Fraser, G. D., and Waldrop, H. A., 1972, Geologic map of the Wise River quadrangle, Silver Bow and Beaverhead Counties, Montana: U.S. Geol. Survey Geol. Quadrangle Map GQ-988, scale 1:24,000.

Friedman, J. D. and Frank, D. G., 1976, Thermal surveillance of active volcanoes using the Landsat-1 data collection system, Part 2, Infrared surveys, radiant flux and total heat discharge from Mount Baker volcano, Washington: U.S. Geol. Survey Admin. Rept. to NASA.

Froelich, A. J., 1976, Map showing mineral resources of Fairfax County, Virginia—availability and planning for future needs: U.S. Geol. Survey open-file map 76-660, scale 1:48,000.

Gammon, P. T. and Carter, V. P., 1976, Comparison of vegetation classes in the Great Dismal Swamp using two individual Landsat images and a temporal composite [abs.]: Purdue-/LARS Symposium on Machine Processing of Remotely Sensed Data, Proc. p. 3B-1.

Gard, L. M., Jr., 1976, Geology of the north end of the Salt Valley anticline, Grand County, Utah: U.S. Geol. Survey open-file rept. 76-303, 35 p.

Gardner, J. V., 1975, Late Pleistocene carbonate dissolution cycles in the eastern equatorial Atlantic, *in* Sliter, W. V., Be, A. W. H., and Berger, W. H., eds., Dissolution of deep-sea carbonates: Cushman Found. for Foraminiferal Research, Spec. Publ. 13, p. 129-141.

Gardner, J. V., and Hays, J. D., 1976, The eastern equatorial Atlantic—sea-surface temperature and circulation responses to global climatic change during the past 200,000 years, *in* Cline, R. M., and Hays, J. D., eds., Investigations of Late Quaternary Paleo-oceanography and Paleoclimatology: Geol. Soc. America Mem. 145.

Garrett, M. K., and Carter, V. P., 1977, Application of remotely sensed data to habitat evaluation and management of a highly altered ecosystem, *in* Proceedings of the 42d North American Wildlife and Natural Resources Conf., March 5-9, 1977, 20 p. [In press.]

Gaydos, L. J., and Newland, W. L., 1976, Preparation of maps and statistical summaries of land use and land cover for the Puget Sound region using Landsat digital imagery—a multi-agency regional project: Am. Cong. Surveying and Mapping Seattle, Wash., 1976, Proc.

Geological Society of London, 1964, The Phanerozoic time-scale; a symposium: Geol. Soc. London Quart. Jour., v. 120, supp., p. 260-262.

Gilbert, G. K., 1917, Hydraulic-mining debris in the Sierra Nevada: U.S. Geol. Survey Prof. Paper 105, 154 p.

Glaeser, J. D., 1966, Provenance, dispersal, and depositional environments of Triassic sediments in the Newark-Gettysburg Basin: Pennsylvania Geol. Survey Bull. G43, 168 p.

Glover, Lynn III, 1971, Geology of the Coamo area, Puerto Rico, and its relation to the volcanic arc-trench association: U.S. Geol. Survey Prof. Paper 636, 102 p.

Glover, Lynn III, and Mattson, P. H., 1967, The Jacaguas Group in central-southern Puerto Rico: U.S. Geol. Survey Bull. v. 1254-A, p. A29-38.

———1973, Geologic map of the Rio Descalabrado quadrangle, Puerto Rico: U.S. Geol. Survey Misc. Geol. Inv. Map I-735, 1 sheet, scale 1:20,000.

Goerlitz, D. F., 1976, Determination of volatile organohalides in water and treated sewage effluents: U.S. Geol. Survey open-file rept. 76-610, 15 p.

Goldberg, M. C., 1976, Reactions in the aqueous environment of low molecular weight organic molecules: The Science of the Total Environment, v. 5, no. 3, p. 277-294.

Goldsmith, Richard, 1963, Geologic sketch map of eastern Connecticut: U.S. Geol. Survey open-file rept.

Goodwin, C. R., 1977, Circulation patterns for historical, existing and proposed channel configurations in Hillsborough Bay, Florida: Internat. Navigation Congress, PIANC, 24th Leningrad, 1977, Proc. [In press.]

Goolsby, D. A., 1971, Hydrogeochemical effects of injection wastes into a limestone aquifer near Pensacola, Florida: Ground

Water, v. 9, no. 1, p. 13-19.

Goolsby, D. A., 1972, Geochemical effects and movement of injected industrial waste in limestone aquifer, *in* Cook, T. D., ed., Underground waste management and environmental implications: Am. Assoc. Petroleum Geologists Mem. 18, p. 355-368.

Gore, R. Z., 1976, Ayer crystalline complex at Ayer, Harvard, and Clinton, Massachusetts, *in* Studies in New England Geology: Geol. Soc. of Amer. Mem. 146, pp. 103-124.

Goudarzi, G. H., Rooney, L. F., and Shaffer, G. L., 1976, Supply of nonfuel minerals and materials for the United States energy industry 1975-90: U.S. Geol. Survey Prof. Paper 1006-B.

Granger, H. C., and Warren, C. G., 1969, Unstable sulfur compounds and the origin of roll-type uranium deposits: Econ. Geology, v. 64, no. 2, p. 160-171.

———1974, Zoning in the altered tongue associated with roll-type uranium deposits, *in* Formation of uranium ore deposits: Internat. Atom. Energy Agency, Vienna, 1974, p. 185-199.

Greenland, L. P., and Campbell, E. Y., 1977, Variation q Se,Te,In,Tl & Zn with differentiation of tholeiitic magma, N. Jb. Miner. Mh., H. 3, p. 112-118.

Grew, E. S., Mamay, S. H., and Barghoorn, E. S., 1970, Age of plant fossils from the Worcester coal mine, Worcester, Massachusetts: Am. Jour. Sci., v. 268, p. 113-126.

Grimes, D. J., and Earhart, R. L., 1976, A geological and geochemical evaluation of the mineral resources of the Scotchman Peak wilderness study area, Lincoln and Sanders Counties, Montana, and Bonner County, Idaho: U.S. Geol. Survey open-file rept. 76-706, 136 p.

Grow, J. A., Bowin, C. O., Hutchinson, D. R., and Kent, K. M., 1976, Preliminary free-air gravity anomaly map along the Atlantic continental margin between Virginia and Georges Bank: U.S. Geol. Survey Misc. Field Studies Map MF-795, 1 sheet, scale 1:1,200,000.

Grozier, R. U., McCain, J. F., Lang, L. F., and Merriman, D. C., 1976, The Big Thompson River flood of July 31-August 1, 1976, Larimer County, Colorado: Colorado Water Conservation Board, Flood Inf. rept., 78 p.

Gumerman, G. J., and Euler, R. C., 1976, Black Mesa retrospect and prospect, *in* Gumerman, G. J., and Euler, R. C., eds., Papers on the archaeology of Black Mesa, Arizona: Southern Illinois Univ. Press, Carbondale and Edwardsville, Illinois, p. 162-170.

Hadley, D. M., and Kanamori, H., 1976, Seismic structure of the Transverse Ranges, Calif.: EOS, (Am. Geophys. Union Trans.), v. 57, p. 899.

Hadley, R. F., and Shown, L. M., 1976, Relation of erosion to sediment yield, *in* Proceedings of the Third Federal Interagency Sedimentation Conference 1976: Water Resources Council, pt. 1, p. 132-139.

Hallet, Bernard, 1976, Deposits formed by subglacial precipitation of $CaCO_3$: Geol. Soc. America Bull., v. 87, no. 7, p. 1003-1015.

Hamilton, W., 1969, Mesozoic California and the underflow of Pacific mantle: Geol. Soc. America Bull., 80, p. 2409-2430.

Hanson, R. L., and Dawdy, D. R., 1976, Accuracy of evapotranspiration rates determined by the water-budget method, Gila River flood plain, southeastern Arizona: U.S. Geol. Survey Prof. Paper 655-L, 36 p.

Harenberg, W. A., and Bigelow, B. B., 1976a, Teton Dam flood of June 1976, Moody quadrangle, Idaho: U.S. Geol. Survey, Hydrol. Inv. Atlas, HA-568, 1 sheet.

———Teton Dam flood of June 1976, Rexburg quadrangle, Idaho: U.S. Geol. Survey, Hydrol. Inv. Atlas, HA-569, 1 sheet.

Hargraves, R. B. Collinson, D. W., Arvidson, R. E., and Spitzer, C. R., 1976, Viking magnetic properties investigation—further results: Science, v. 194, p. 1303-1309.

Hargraves, R. B., Collinson, D. W., and Spitzer, C. R., 1976, Viking magnetic properties investigation—preliminary results: Science, v. 194, p. 84-86.

Harlow, D. H., 1976, Instrumentally recorded seismic activity prior to the main event, *in* The Guatemalan earthquake of February 4, 1976, a preliminary report: U.S. Geol. Survey Prof. Paper 1002, 90 p.

Harrill, J. R., and Nowlin, J. O., 1976, Ground-water data near the northwest shore of Topaz Lake, Douglas County, Nevada: U.S. Geol. Survey open-file rept. 76-90, 12 p.

Harrison, J. E., 1972, Precambrian Belt Basin of Northwestern United States—its geometry, sedimentation, and copper occurrences: Geol. Soc. America Bull., v. 83, p. 1215-1240.

Harshman, E. N., 1972, Geology and uranium deposits, Shirley Basin area, Wyoming: U.S. Geol. Survey Prof. Paper 745, 82 p.

Hatch, J. R., Gluskoter, H. J., and Lindahl, P. C., 1976, Sphalerite in coals from the Illinois Basin: Econ. Geology, v. 71, no. 3, p. 613-624.

Hathaway, J. C., Schlee, J. S., Poag, C. W., Valentine, P. C., Weed, E. G. A., Bothner, M. H., Kohout, F. A., Manheim, F. T., Schoen, Robert, Miller, R. E., and Schultz, D. M., 1976, Preliminary summary of the 1976 Atlantic margin coring project of the U.S. Geological Survey: U.S. Geol. Survey open-file rept. 76-844, 217 p.

Hawkinson, R. O., Ficke, J. F., and Saindon, L. G., 1977, Quality of rivers of the United States, 1974 water year—based on the National Stream Quality Accounting Network (NASQAN): U.S. Geol. Survey open-file rept. 77-151, 158 p.

Hawley, C. C., and Clark, A. L., 1973, Geology and mineral deposits of the Chutlitna-Yentna mineral belt, Alaska: U.S. Geol. Survey Prof. Paper 758-A, 10 p.

Hawley, C. C., and Clark, A. L., 1974, Geology and mineral deposits of the Upper Chulitna district, Alaska: U.S. Geol. Survey Prof. Paper 758-B, 47 p.

Heinrich, E. W., and Dahlem, D. H., 1966, Carbonatites and alkalic rocks of the Arkansas River area, Fremont County, Colorado: Mineral Soc. of India, IMA volume, et. Naidu, PRT., p. 37-44.

Helm, D. C., 1976, One-dimensional simulation of aquifer-system compaction near Pixley, California—pt. 2—stress-dependent parameters: Water Resources Research, v. 12, no. 3, p. 375-391.

———1977, Estimating parameters of compacting fine-grained interbeds within a confined aquifer system by a one-dimensional simulation of field observations: Internat. Assoc. Sci. Hydrologists, Internat. Symposium on Land Subsidence, 2d, Anaheim, Calif., Dec. 1976, Proc. [In press.]

Herz, Norman, 1958, Bedrock geology of the Cheshire quadrangle, Massachusetts: U.S. Geol. Survey Geol. Quad. Map GQ-108.

Hewitt, C. H., 1959, Geology and mineral deposits of North Big Burro Mountains-Redrock area, Grant County, New Mexico: New Mexico Bur. of Mines and Mineral Resources, New Mexico Institute of Mining and Technology, 151 p.

Higgins, M. W., 1973, Petrology of Newberry Volcano, central Oregon: Geol. Soc. America Bull., v. 84, p. 455-488.

Hildreth, Wes, 1976, The Bishop Tuff—compositional zonation in a silicic magma chamber without crystal settling: Geol. Soc. America Abs. with Programs, v. 8, no. 6, p. 818.

Hillier, D. E., Brogden, R. E., and Schneider, P. A., Jr., 1977, Hydrology of the Arapahoe aquifer in the Englewood-Castle Rock area south of Denver, Denver Basin, Colorado: U.S. Geol. Survey Misc. Inv. Map I-1043. [In press.]

Hills, F. A., Gast, P. W., Houston, R. S., and Swainbank, I. G., 1968, Precambrian geochronology of the Medicine Bow Mountains, southeastern Wyoming: Geol. Soc. America Bull., v. 79, no. 12, p. 1757-1783.

Himmelberg, G. R., and Ford, A. B., 1976, Pyroxenes of the Dufek instrusion, Antarctica: Jour. Petrology, v. 17, pt. 2, p. 219-243.

Hindall, S. M., 1976, Prediction of sediment yeilds in Wisconsin streams, *in* Proceedings of the Third Federal Interagency Sedimentation Conference 1976: Water Resources Council, pt. 1, p. 205-218.

Hintze, L. F., 1976, Attenuation faulting in the Fish Springs and House Ranges, western Utah [abs.]: Geol. Soc. America Abs. with Programs, v. 8, no. 6, p. 918-919.

Hjalmarson, H. W., 1977, Delineation of flood hazards in the Cave Creek quadrangle, Maricopa County, Arizona: U.S. Geol. Survey Misc. Inv. Ser. Map I-843-B. [In press.]

Hodges, C. A., Muehlberger, W. R., and Ulrich, G. E., 1973, Geologic setting of Apollo 16, in Lunar Sci. Conf., 4th Proc.: Geochim. Cosmochim. Acta., Suppl. 4, v. 1, p. 1-25.

Holcomb, R. T., 1976, Complexity and hazards of Hawaiian shield volcanoes [abs.]: Geol. Soc. America Abs. with Programs, v. 8, no. 6, p. 920-921.

Hopson, C. A., 1964, The crystalline rocks of Howard and Montgomery Counties, *in* The geology of Howard and Montgomery Counties: Baltimore, Md., Maryland Geol. Survey, p. 27-215.

Hoyt, C. L., 1961, The Hammond sill—an instrusion in the Yakima Basalt near Wanachee, Washington: Northwest Sci., v. 35, no. 2, p. 58-64.

Hubbard, L. L., and Bartells, J. H., 1976a, Teton Dam flood of June 1976, quadrangle, Idaho: U.S. Geol. Survey, Hydrol. Inv. Atlas, HA-577, 1 sheet.

———Teton Dam flood of June 1976, Moreland quadrangle, Idaho: U.S. Geol. Survey, Hydrol. Inv. Atlas, HA-580, 1 sheet.

———Teton Dam flood of June 1976, Pingree quadrangle, Idaho: U.S. Geol. Survey, Hydrol. Inv. Atlas, HA-581, 1 sheet.

Hudson, J. H., Shinn, E. A., Halley, R. B. and Lidz, B. H., 1976a, Autopsy of a dead coral reef [abs.]: AAPG-SEPM Annual Meeting, New Orleans, La., p. 76.

Hudson, J. H., Shinn, E. A., Halley, R. B., and Lidz, B. H., 1976b, Sclerochronology—a tool for interpreting past environments: Geology, v. 4, no. 6, p. 361-364.

Hudson, Travis, Plafker, George, and Lanphere, M. A., 1977, Intrusive rocks of the Yakutat-St. Elias area, south-central Alaska: U.S. Geol. Survey Jour. Research, v. 5, n. 2, p. 155-172.

Huebner, J. S., Lipin, B. R., Wiggins, L. B., 1976, Partitioning of chromium between silicate crystals and melts: Lunar Sci. Conf., 7th, Proc. p. 1195-1220.

Hussey, A. M. III, 1971, Geologic map of the Portland quadrangle, Maine: Maine Geol. Survey, GM-1, scale 1:62,500.

Hussey, A. M. II, and Pankwiskyj, K. A., 1975, Preliminary geologic map of southwestern Maine: Maine Geol. Survey open-file map 1976-1, scale 1:62,500.

Hutchison, W. W., 1970, Metamorphic framework and plutonic styles in the Prince Rupert region of the Central Coast Mountains, British Columbia: Canadian Jour. Earth Sci., v. 7, p. 376-405.

Hyndman, D. W., Talbot, J. L., and Chase, R. B., 1975, Boulder batholith—a result of emplacement of a block detached from the Idaho batholith infrastructure?: Geology, v. 3, no. 7, p. 401-404.

Imhoff, E. A., 1976a, An analysis of selected laws and governmental programs in Florida, as related to mineral resource management and surface mining: U.S. Geol. Survey open-file rept., 41 p.

———1976b, A review of selected laws and governmental programs in Colorado, as related to mineral resources management and surface mining: U.S. Geol. Survey open-file rept., 48 p.

Imhoff, E. A., Friz, T. O., and LaFevers, J. R., 1976, A guide to State programs for the reclamation of surface mined areas: U.S. Geol. Survey Circ. 731, 33 p.

INTERCOMP Resource Development and Engineering, Inc., 1976, A model for calculating effects of liquid waste disposal in deep saline aquifers: U.S. Dept. Commerce, Natl. Tech. Inf. Service, PB-256 903/AS, 253 p.

International Geographic Union, Commission on Geographic Data Sensing and Processing, 1976, Computer handling of geographical data—an examination of selected geographic information systems: Washington, D.C., Internat. Geog. Union, — p.

Irvine, T. N., 1973, Bridget Cove Volcanics, Juneau area, Alaska; possible parental magma of Alaskantype ultramafic complexes: Carnegie Inst. Washington Yearbook 72, p. 478-491.

Irvine, T. N., 1975, Axelgold layered gabbro intrusion, McConnell Creek map-area, British Columbia: Geol. Survey Canada Paper 75-1, p. B, p. 81-88.

James, O. B., 1976, Petrology of aphanitic lithologies in consortium breccia 73215, *in* Lunar science VII: Houston, Tex., Lunar Sci. Inst., p. 420-422.

———1977, Petrology of four clasts from consortium breccia 73215, *in* Lunar science VIII: Houston, Tex., Lunar Sci. Inst., p. 502-504.

James, O. B. and Blanchard, D. P., 1976, Consortium studies of light-gray breccia 73215—introduction, subsample distribution data, and summary of results: Proc. 7th Lunar Sci. Conf., v. 1, p. 2131-2143.

James, O. B., Brecher, A., Blanchard, D. P., Jacobs, J. W., Brannon, J. C., Korotev, R. L., Haskin, L. A., Higuchi, H., Morgan, J. W., Anders, E., Silver, L. T., Marti, K., Braddy, D., Hutcheon, I. D., Kirsten, T., Kerridge, J. F., Kaplan, I. R., Pillinger, C. T. and Gardiner, L. R., 1975, Consortium studies of matrix of light gray breccia 73215: Proc. 6th Lunar Sci. Conf., v. 1, p. 547-577.

Jessberger, E. K., Kirsten, T., and Staudacher, Th., 1976, Argon-argon ages of consortium breccia 73215: Proc. 7th Lunar Sci. Conf., v. 2, p. 2201-2215.

Jobson, H. E., 1973, The dissipation of excess heat from water systems: Am. Soc. Civil Engineers Proc., Jour. Power Div., v. 99, p. 89-103.

Johnson, C. G., and Tasker, G. D., 1974, Flood magnitude and frequency of Massachusetts streams: U.S. Geol. Survey open-file rept. 74-131, 41 p.

Johnson, G. R., and England, A. W., 1976, Microwave radiometric survey of the San Joaquin Nuclear Project site Kern County, California: U.S. Geol. Survey Jour. Research, v. 5, no. 4, p. 431-435.

Johnson, M. J., 1976, Geology and mineral deposits of Pershing County, Nevada: Nevada Bur. of Mines and Geology Bull. [In press.]

Johnston, R. H., and Larson, J. D., 1976, Preliminary appraisal of ground water in the Franconia area, Virginia: U.S. Geol. Survey open-file rept. 76-400.

Jones, C. L., Cooley, M. E., and Bachman, G. O., 1973, Salt deposits of the Los Medanos area, Eddy and Lea Counties, New Mexico: U.S. Geol. Survey open-file rept., 67 p.

Jones, H. P., and Speers, R. G., 1976, Permo-Triassic reservoirs of Prudhoe Bay field, North Slope, Alaska, *in* Braunstein, Jules, ed., North American oil and gas fields: Am. Assoc. Petroleum Geologists Mem. 24, p. 23-50.

Jones, W. J. and Fabiano, E. B., 1976, Magnetic vertical intensity in the United States-Epoch 1975.0: U.S. Geol. Survey, Misc. Inv. Ser. Map I-914, scale 1:5,000,000.

Keefer, T. N., and McQuivey, R. S., 1974, Multiple linerization flow routing model: Am. Soc. Civil Engineers Proc., Jour. Hydraulics Div., v. 100, no. HY 7, p. 1031-1046.

Kharaka, Y. K., Callender, Edward, and Carothers, W. W., 1977, Geochemistry of geopressured geothermal waters of the northern Gulf of Mexico basin—pt. I—Brazona and Galveston

Counties, Texas: Internat. Symposium on Water/Rock Interaction, 2d, Strasbourg, France, Aug. 1977, Proc. [In press.]
Kieffer, S. W., Schaal, R. B., Gibbons, R., Horz, F., Milton, D. J., and Dube, A., 1976, Shocked basalt from Lonar Impact Crater, India, and experimental analogues: Lunar Sci. Conf., 7th, Proc. p. 1391-1412.
Kilpatrick, F. A., and Davis, G. H., 1976, Water demand as related to increased coal utilization in the United States, *in* Wasserwirtschaft und Gewinnung Fossiler Energieträger, Internationales Symposium, Düsseldorf, Bundesrepublik Deutschland, 7-8 September, 1976: Düsseldorf, Germany, Deutsches Komitee der IWRA im Deutschen Verband für Wasserwirtschaft e.V. (DVWW) rept. 14, 15 p.
Kistler, R. W., 1966, Geologic map of the Mono Craters Quadrangle, Mono and Tuolumne Counties, California: U.S. Geol. Survey Quad. Map, GQ-462, scale 1:62,500.
Knebel, H. J., Conomos, T. J., and Commeau, J. A., 1977, Clay-mineral variability in the suspended sediments of the San Francisco Bay system: Jour. Sed. Petrology, v. 47, no. 1, p. 229-236.
Kockelman, W. J., 1975, Use of USGS Earth-science products by city planning agencies in the San Francisco Bay region, California: U.S. Geol. Survey open-file rept. 75-276, 110 p.
———1976, Use of USGS Earth-science products by county planning agencies in the San Francisco Bay region, California: U.S. Geol. Survey open-file rept. 76-547, 186 p.
Kolessar, J., 1970, Geology and copper deposits of the Tyrone district: New Mexico Geol. Soc. Guidebook of the Tyrone-Big Hatchet Mountains-Florida Mountains region, 21st Field Conference, p. 127-132.
Krähenbuhl, U., Ganapathy, R., Morgan, J. W., and Anders, E., 1973, Volatile elements in Apollo 16 samples—implications for highland volcanism and accretion history of the Moon, *in* Lunar Sci. Conf., 4th, Proc.: Geochim. et Cosmochim. Acta., supp. 4, v. 2, p. 1325-1348.
Krinitzsky, E., 1950, Geological investigation of faulting in the lower Mississippi valley: U.S. Corps of Engineers, Waterways Experimental Station, Tech. Memo. no. 3-311, 91 p.
Krushensky, R. D., and Monroe, W. H., 1975, Geologic map of the Ponce quadrangle, Puerto Rico: U.S. Geol. Survey Mics. Geol. Inv. Map I-863, scale 1:20,000.
Lachenbruch, A. H., Sass, J. H., Munroe, R. J., and Moses, T. H., Jr., 1976, Geothermal setting and simple heat conduction models for the Long Valley caldera: Jour. Geophys. Research, v. 81, no. 5, p. 769-784.
LaFehr, T. R., 1965, Gravity, isostasy, and crustal structure in the southern Cascade Range: Jour. Geophys. Research, v. 70, no. 22, p. 5581-5597.
Langbein, W. B., 1964, Geometry of river channels: Am. Soc. Civil Engineers Proc. Jour. Hydraulics Div., no. HY2 v. 90, p. 301-312.
Langer, C. J., Hopper, M. G., Algermissen, S. T., and Dewey, J. W., 1974, Aftershocks of the Managua, Nicaragua earthquake of December 23, 1972: Bull. Seismol. Soc. America Bull., v. 64, p. 1005-1016.
Langer, C. J., Iriarte, J. C., Barnhard, T. P., and Henrisey, R. F., 1976, Locations of aftershocks of the Guatemalan earthquake of February 4, 1976, from local network data [abs.]: EOS (Am. Geophys. Union Trans.) v. 57, p. 950.
Larson, S. P., Mann, W. B. IV, Steele, T. D., and Susag, R. H., 1976, Graphic and analytical methods for assessment of stream-water quality—Mississippi River in the Minneapolis-St. Paul Metropolitan area, Minnesota: U.S. Geol. Survey Water-Resources Inv. 76-94, 55 p.
Leenheer, J. A., and Huffman, E. W. D., Jr., 1976, Classification of organic solutes in water using macroreticular resins: U.S. Geol. Survey Jour. Research, v. 4, no. 6, p. 737-751.
Leopold, L. B., and Emmett, W. W., 1976, Bedload measurements, East Fork River, Wyoming: Natl. Acad. Sci. Proc., v. 73, no. 4, p. 1000-1004.
Lindstrom, M. M. Nava, D. F., Winzer, S. R., Lindstrom, D. J., Lum, R. K. L., Schuhmann, P. J. Schuhmann, S., and Philpotts, J. A., 1977, Geochemical studies of the white breccia boulders at North Ray Crater, Descartes Highlands [abs.], *in* Lunar science VIII, Abstracts: Houston, Tex., Lunar Sci. Inst., p. 583.
Lineback, J. A., 1970, Stratigraphy of the New Albany Shale in Indiana: Indiana Geol. Survey Bull. 44, 73 p.
Lofgren, B. E., 1977, Hydrogeologic effects of subsidence, San Joaquin Valley, California: Internat. Assoc. Sci. Hydrologists, Internat. Symposium on Land Subsidence, 2d, Anaheim, Calif., Dec. 1976, Proc. [In press.]
Long, W. A., and Porter, S. C., 1968, Revision of the Alpine glacial sequence in the Leavenworth area, Washington [abs.], *in* Abstr. for 1967: Geol. Soc. America Spec. Paper 115, p. 338.
Love, J. D., 1970, Cenozoic geology of the Granite Mountains area, central Wyoming: U.S. Geol. Survey Prof. Paper 495-C, 154 p.
Lovering, T. S., 1930, The New World or Cooke City mining district, Park County, Montana: U.S. Geol. Survey Bull. 811-A, p. 1-87.
Lucas, J. R., and Taranik, J. V., 1977, Late Wisconsinan deglaciation of the northern Midwest interpreted from a springtime Landsat color mosaic [abs.]: Int. Symp. Remote Sensing of Environment, 11th, Ann Arbor, Mich., 1977, Proc.
Lucchitta, B. K., 1977, Mare ridges topography and structure in southern Imbrium and northern Procellarum, *in* Lunar Science VIII: Houston, Tex., Lunar Sci. Inst., p. 595-660.
Ludwig, W. J., Murauch, S., Den, N., Ewing, M. Hotta, H., Houtz, R. E., Yoshii, T., Asanuma, T., Hagiwara, K., Saito, T., and Ando, S., 1971, Structure of Bowers Ridge, Bering Sea: Jour. Geophys. Research, v. 76, p. 6350-6366.
Luoma, S. N., and Jenne, E. A., 1976, Factors affecting the availability of sediment-bound cadmium to the estuarine, deposit-feeding clam, *Macoma balthica, in* Cushing, C. E., ed., Radioecology and energy resources: Stroudsberg, Penn., Dowden, Hutchinson, and Ross, Inc., Ecol. Soc. of America, Spec. Pub. 1, p. 283-290.
Macintyre, I. G. and Glynn, P. W., 1976, Evolution of modern Caribbean fringing reef, Galeta Point, Panama: Am. Assoc. Petroleum Geologists Bull. v. 60, no. 7, p. 1054-1072.
MacKevett, E. M., Jr., Brew, D. A., Hawley, C. C., Huff, L. C., and Smith, J. G., 1971, Mineral resources of Glacier Bay National Monument, Alaska: U.S. Geol. Survey Prof. Paper 632, 90 p.
Maclay, R. W., and Small, T. A., 1976, Progress report on geology of the Edwards aquifers, San Antonio area, Texas, and preliminary interpretation of borehole geophysical and laboratory data on carbonate rocks: U.S. Geol. Survey open-file rept. 76-627, 65 p.
Malde, H. E., and Scott, A. G., 1977, Observations of contemporary arroyo cutting near Santa Fe, New Mexico, U.S.A.: Earth Surface Processes, v. 2, no. 1, p. 39-54.
Marcus, P. A., ed., 1976, Directory to U.S. Geological Survey program activities in coastal areas 1974-76: U.S. Geol. Survey Bull. 1428, 145 p.
Marinenko, John, 1976, Spectrophotometric determination of trivalent manganese in the presence of divalent iron with possible application to the analysis of manganese bearing ferrospinels: Anal. Letters, v. 9, p. 775-780.
Martin, A. C., Hotkiss, N., Uhler, F. M., and Bourn, W. S., 1953, Classification of wetlands of the United States: U.S. Fish and Wildlife Service Spec. Sci. Rept. Wildl. 20, 14 p.
Matthai, H. F., and Ray, H. A., 1976, Teton Dam flood of June 1976, Woodville quadrangle, Idaho: U.S. Geol. Survey, Hydrol. Inv.

Atlas, HA-576, 1 sheet, scale 1:24,000.
Mattson, P. H., 1960, Geology of the Mayaguez area, Puerto Rico: Geol. Soc. America Bull., v. 71, no. 3, p. 319-362.
———1966, Unconformity between Cretaceous and Eocene rocks in central Puerto Rico, *in* Caribbean Geol. Conf. 3rd, Kingston, Jamaica, 1962, Trans: Jamaica Geol. Survey Pub., 95, p. 49-53.
———1967, Cretaceous and lower Tertiary stratigraphy in west-central Puerto Rico: U.S. Geol. Survey Bull. 1254-B, p. B1-35.
———1968a, Geologic map of the Jayuya quadrangle, Puerto Rico: U.S. Geol. Survey Misc. Geol. Inv. Map I-520, scale 1:20,000.
———1968b, Geologic map of the Adjuntas quadrangle, Puerto Rico: U.S. Geol. Survey Misc. Geol. Inv. Map I-519, scale 1:20,000.
———1973, Middle Cretaceous nappe structures in Puerto Rican ophiolites and their relation to the tectonic history of the Greater Antilles: Geol. Soc. American Bull., v. 84, no. 1, p. 21-38.
Matumoto, T., Ohtake, M., and Latham, G., 1976, Crustal structure in Central America [abs.]: Abstracts 71st Ann. Mtg. Seismol. Soc. America, Earthquake Notes, v. 47, no. 2, p. 25-26.
Maxwell, J. C., 1974, Anatomy of an orogen: Geol. Soc. America Bull., v. 85, p. 1195-1204.
McFarlane, Craig, and Watson, R. D., 1977, Fluorescence detection and mapping of oil deposited on marsh vegetation: Oil Spill Conference, New Orleans, La., 1977, Proc. [In press.]
McIntyre, D. H., 1975, Geologic map of the Maricao quadrangle, Puerto Rico: U.S. Geol. Survey Misc. Geol. Inv. Map I-918, scale 1:20,000.
McIntyre, D. H., Aaron, J. M., and Tobsich, O. T., 1970, Cretaceous and lower Tertiary stratigraphy in northwestern Puerto Rico: U.S. Geol. Survey Bull. 1294-D, p. D1-16.
McKee, E. H., and Burke, D. B., 1972, Fission track age bearing on the Permian-Triassic boundary and time of the Sonoma Orogeny in north-central Nevada: Geol. Soc. America Bull., v. 83, no. 7, p. 1949-1952.
McKelvey, V. E., 1939, Stream and valley sedimentation in the Coon Creek drainage basin: Madison, Wis., Univ. Wisconsin, M.S. thesis, 122 p.
McKenzie, D. J., 1976, Injection of acidic industrial waste into the Floridan aquifer near Belle Glade, Florida—upward migration and geochemical interactions 1973-75: U.S. Geol. Survey open-file rept. 76-626, 64 p.
McNair, A. H., 1951, Paleozoic stratigraphy of part of northwestern Arizona: Am. Assoc. Petroleum Geologists Bull., v. 35, no. 3, p. 503-541.
McPherson, B. F., Hendrix, G. Y., Klein, Howard, and Tyus, H. M., 1976, The environment of South Florida—a summary report: U.S. Geol. Survey Prof. Paper 1011, 82 p.
Merewether, E. A., Cobban, W. A., and Spencer, C. W., 1976, The Upper Cretaceous Frontier Formation in the Kaycee-Tisdale Mountain area, Johnson County, Wyoming: Wyoming Geol. Assoc. Guidebook, Ann. Field Conf., 28th, Powder River Basin, Wyo., 1976, p. 33-44.
Miesch, A. T., 1976, Interactive computer programs for petrologic modeling with extended *Q*-mode factor analysis: Computers and Geosciences, v. 2, no. 4.
———1976, Sampling designs for geochemical surveys-Syllabus for a short course: U.S. Geol. Survey open-file rept. 76-772, 138 p.
Miller, F. K., 1970, Geologic map of the Quartzsite quadrangle, Yuma County, Arizona: U.S. Geol. Survey Geol. Quad. Map GQ-841, scale 1:62,500.
Miller, T. P., Elliott, R. L., Finch, W. I., and Brooks, R. A., 1976, Preliminary report on uranium-, thorium-, and rare-earth-bearing rocks near Golovin, Alaska: U.S. Geol. Survey open-file rept. 76-710, 13 p.
Miller, W. R., and Ficklin, W. H., 1976, Molybdenum mineralization in the White River National Forest, Colorado: U.S. Geol. Survey open-file rept. 76-711, 29 p.
MITRE Corp., 1975 Resource and Land Investigations (RALI) program—An approach to environment assessment with application to western coal development: Prepared for USGS by MITRE Corp., McLean, Va., Tech. rept. MTR-6988, 616 p.
———1975b, National environmental statistical report: Prepared for the Council on Environmental Quality and the Resource and Land Investigations program, USGS, by the MITRE Corp., McLean, Va., Tech. rept. MTR-6957, 241 p.
Mixon, R. B., and Newell, W. L., 1976, Preliminary investigation of faults und folds along the inner margin of the Coastal Plain in northeastern Virginia: U.S. Geol. Survey open-file rept. 76-330, scale 1:24,000.
Moench, A. F., 1976a, Simulation of steam transport in vapor-dominated geothermal reservoirs: U.S. Geol. Survey open-file rept. 76-607, 43 p.
———1976b, Steam transport in porous media, *in* Kruger, P., and Ramey, H. J., Jr., eds, Proc.: Second Workshop on Geothermal Reservoir Engineering, Dec. 1-3, 1976, Stanford Calif. Stanford University. [In press.]
Montgomery, Arthur, 1953, Precambrian geology of the Picuris Range, north-central New Mexico: New Mexico Bur. Mines and Mineral Resources Bull. 30, 89 p.
Moorbath, S., Hurley, P. M., and Fairbairn, H. W., 1967, Evidence for the origin and age of some mineralized Laramide intrusives in the southwestern United States from strontium isotope and rubidium-strontium measurements: Econ. Geol., v. 62, no. 2, p. 228-236.
Moore, D. O., 1976, Estimating peak discharges from small drainages in Nevada according to basin areas within elevation zones: Nevada Highway Dept., Hydrol. Rept. 3, 17 p.
Moore, D. W., and Boyles, J. M., 1976, A map of environmental values as an aid to planning reclamation of surface-mined areas—the Gap quadrangle, Wyoming: U.S. Geol. Survey open-file rept. 76-434, 11 p.
Moore, G. K., 1965, Geology and hydrology of the Clairborne Group in western Tennessee: U.S. Geol. Survey Water Supply Paper 1809 F, 44 p.
Moore, H. J., Tyler, G. L., Boyce, J. M., Shorthill, R. W., Thompson, T. W., Wilhelms, D. E., Wu, S. S. C., and Zisk, S. H., 1976, Correlation of photogeology and remote sensing data along the Apollo 14, 15, and 16 bistatic-radar ground track—pt. II—a working compendium: U.S. Geol. Survey open-file rept. 76-298, 101 p.
Morey, G. B., and Sims, P. K., 1976, Boundary between two Precambrian *W* terranes in Minnesota and its geologic significance: Geol. Soc. America Bull., v. 87, p. 141-152.
Morgridge, D. L., and Smith, W. B., 1972, Geology and discovery of Prudhoe Bay field, eastern Arctic Slope, Alaska, *in* King, R. E., ed., Stratigraphic oil and gas fields: Am. Assoc. Petroleum Geologists Mem. 16, p. 489-501.
Morris, G. B., R. W. Raitt, and G. G. Shor, Jr., 1969, Velocity anisotropy and delay-time maps of the mantle near Hawaii, Jour. Geophys. Research v. 14, 4300-4316.
Morris, H. T., and Lovering, T. S., 1.61, Stratigraphy of the East Tintic Mountains, Utah: U.S. Geol. Survey Prof. Paper 361, 145 p.
Muehlberger, N. R. and others, 1972, Preliminary geologic investigation of the Apollo 16 landing site, in Apollo 16 preliminary science report: U.S. Natl. Aeronautics and Space Admin. SP-315, p. 6-1 to 6-81.
Muffler, L. J. P., and Williams, D. L., 1976, Geothermal investigations of the U.S. Geological Survey in Long Valley, California 1972-1973: Jour. Geophys. Research, v. 81, no. 5, p. 721-724.

Muller, H. W., Plieninger, T., James, O. B., and Schaeffer, O. A., 1977, Laser probe ^{40}Ar-^{39}Ar dating of materials fcom consortium breccia 73215: *in* abs., Lunar science VIII, Hqouston, Tex., Lunar Sci. Inst. p. 697.

Mullineaux, D. R., 1976, Preliminury map of volcanic hazards in the 48 conterminous United States: U.S. Geol. Survey Misc. Field Studies Map MF-786, scale 1:7,500,000.

Murray, C. R., and Reeves, E. B., 1972, Estimated use of water in the United States in 1970: U.S. Geol. Survey Circ. 676, 37 p.

Myers, W. B., 1952, Geology and mineral deposits of the northwest quarter Willis quadrangle and adjacent Brown's Lake area, Beaverhead County, Montana: U.S. Geol. Survey open-file rept. 147, 46 p.

Naldrett, A. J., and Cabri, L. J., 1976, Ultramafic and related mafic rocks; their classification and genesis with special reference to the concentration of nickel sulfides and platinum group metals: Econ. Geology, v. 71, p. 1131-1158.

National Academy of Sciences, 1973, Water quality criteria, 1972: Washington, D.C., Environmental Protection Agency rept. EPA-R3-73-033, 594 p.

Nauman, J. W., and Kernodle, D. R., 1975, The effect of a fuel oil spill on benthic invertebrates and water quality on the Alaskan Arctic Slope, Happy Valley Creek near Sagwon, Alaska: U.S. Geol. Survey Jour. Research, v. 3, no. 4, p. 495-500.

Nelson, A. E., and Tobisch, O. T., 1968, Geologic map of the Bayaney quadrangle, Puerto Rico: U.S. Geol. Survey Misc. Geol. Inv. Map I-525, scale 1:20,000.

Nelson, W. H., and Dobell, J. P., 1961, Geology of the Bonner quadrangle, Montana: U.S. Geol. Survey Bull: 1111-F, p. 189-235.

New England River Basins Commission, 1976a, Onshore facilities related to offshore oil and gas development, factbook: Prepared for the Resource and Land Investigations program, USGS, by the New England River Basins Commission, Boston, MA 538 p.

———1976b, Onshore facilities related to offshore oil and gas development, estimates for New England: Prepared for the Resource and Land Investigations Program, USGS, by the New England River Basins Commission, Boston, MA 338 p.

Nichols, F. H., 1977a, Infaunal biomass and production on a mudflat, San Francisco Bay, California, *in* Coull, B. C., ed., Ecology of marine benthos: Belle W. Baruch Library in Marine Sci., v. 6, p. 339-358.

———1977b, Dynamics and production of *Pectinaria koreni* (Malmgren) in Kiel Bay, West Germany: 11th Europ. Symp. Marine Biol., Galway, Ireland, 1976, Proc. [In press.]

Nichols, J. D., Harding, R. A., Scott, R. B., and Edwards, J. R., 1976, Forest inventory of western Washington by satellite multi-stage sampling: Am. Cong. Surveying and Mapping, Seattle, Wash., 1976, Proc., p. 180-217.

Nichols, K. M., 1974, Coextensive supratidal dolomite and underlying secondary dolomite in the Triassic of north-central Nevada: Jour. Sed. Petrology, v. 44, no. 3, p. 783-789.

Nichols, T. C., Jr., and Savage, W. Z., 1976, Rock strain recovery-factor in foundation design, *in* Rock engineering for foundations and slopes: Proc. of a Specialty Conf. sponsored by Geotechnical Engineering Div. of Am. Soc. Civil Engineers, Boulder, v. 1, p. 34-54.

Nobel, R. D., 1976, Prediction of natural temperatures in rivers: Davis, Calif., Univ. Calif. Ph. D. dissert., 233 p.

Nockolds, S. R., 1947, The relation between chemical composition and paragenesis in biotite micas in igneous rocks: Am. Jour. Sci., v. 245, p. 401-420.

Noel, J. A., 1956, The geology of the east end of the Anaconda Range and adjacent areas, Montana: Univ. Indiana, Ph. D. thesis, University Microfilms no. 17971, 74 p.

Nord, G. L., Zen, E-an, and Hamarstrom, J., 1976, Metastable crystallization and spinodal decomposition in sodic plagioclase from southwest Massachusetts: Geol. Soc. America Abst. with Programs, v. 8, p. 1030.

Nowlin, J. O., 1976, A preliminary evaluation of the chemical character of water near the northwest shore to Topaz Lake, Douglas Co., Nevada: U.S. Geol. Survey open-file rept. 76-419, 14 p.

Nunes, P. D., Tatsumoto, M., and Unruh, D. M., 1974 U-Th-Pb and Rb-Sr systematics of Apollo 17 Boulder 7 from the north massif of the Taurus-Littrow Valley: Earth and Planetary Sci. Letters, v. 23, p. 445-452.

Obermeier, S. F., and Froelich, A. J., 1976, Preliminary geologic and engineering review of the Franconia area, Fairfax County, Virginia. U.S. Geol. Survey open-file rept. 76-273, 11 p.

Obermeier, S. F., and Hollocher, Curt, 1976, Map of landslides in Coastal Plain deposits of the Franconia area, Fairfax County, Virginia: U.S. Geol. Survey open-file rept., 79-589, 15 p.

Osborn, E. F., 1959, Role of oxygen pressure in the crystallization and differentiation of basaltic magma: Amer. Jour. Sci., v. 257, p. 609-647.

Packer, Murland, 1976, Developing operational techniques for the use of Landsat data in identifying irrigated agriculture in Idaho: Am. Cong. Surveying and Mapping, Seattle, Wash., 1976, Proc., p. 267-272.

Page, B. M., 1939, Multiple glaciation in the Leavenworth area, Washington: Jour. Geology, v. 47, p. 787-815.

Parker, R. L., and Sharp. W. N., 1970, Mafic-ultramafic rocks and associated carbonatities of the Gem Park Complex, Customer and Fremont Counties, Colorado: U.S. Geol. Survey Prof. Paper 649, 24 p.

Pascale, C. A., 1975, Hydrogeologic data collected during the construction of a deep-well waste-injection system, Santa Rosa County, Florida: U.S. Geol. Survey open-file rept. FL-75011, 34 p.

Pavlides, Louis, 1976, Guidebook for field trips 1 and 4—Piedmont geology of the Fredericksburg, Virginia area and vicinity: Arlington, Va., Geol. Soc. America, Northeast-Southeast Mtg., 44 p.

Pearce, J. A., 1975, Basalt geochemistry used to investigate past tectonic environments on Cyprus: Tectonophysics, v. 25, p. 41-67.

Pearce, J. A., and Cann, J. R., 1973, Tectonic setting of basic volcanic rocks determined using trace elements: Earth and Planet. Sci. Letters, v. 19, p. 290-300.

Pearce, T. H., Gorman, B. E., and Birkett, T. C., 1975, The TiO_2-K_2O-P_2O_5 diagrama method of discriminating between oceanic and nonoceanic basalts: Earth and Planet. Sci. Letters, vol. 24, p. 419-426.

Pease, M. H. Jr., and Briggs, R. P., 1960, Geology of the Comerio quadrangle, Puerto Rico: U.S. Geol. Survey—Misc. Geol. Inv. Map I-320, scale 1:20,000

Peddie, N. W., Jones, W. J., and Fabiano, E. B., 1976, Magnetic inclination in the United States—Epoch 1975.0: U.S. Geol. Survey: Misc. Inv. Map I-912, scale 1:5,000,000.

Peterman, Z. E., Zartman, R. E., and Sims, P. K., 1976, Old Precambrian W gneisses in northern Michigan [abs.]: Proc. Twenty-Second Ann. Inst. on Lake Superior Geology, Jour. Geol., v. 4, no. 4, p. 46.

Peterson, D. H., Festa, J. F., and Conomos, T. J., 1977, Numerical simulation of dissolved silica in the San Francisco Bay: Estuarine and Coastal Marine Sci. [In press.]

Petrie, B. N., 1976, Map showing outstanding natural and historic landmarks in the greater Denver area, Front Range Urban Corridor, Colorado: U.S. Geol. Survey Misc. Inv. Map I-856F, scale 1:100,000.

Plafker, George, 1976, Tectonic aspects of the Guatemala earthquake of 4 Feb. 1976; Science v. 193, p. 1201-1208.

Plafker, George Bonilla, M. G., and Bonis, S. B., 1976, Geologic effects, *in* the Guatemalan earthquake of February 4, 1975, a preliminary report: U.S. Geol. Survey Prof. Paper 1002, 90 p.

Plafker, George, Jones, D. L., Hudson, Travis, and Berg, H. C., 1976, The Border Ranges fault system in the Saint Elias Mountains and Alexander Archipelago, *in* Cobb, E. H., ed., United States Geological Survey in Alaska; accomplishments during 1975: U. S. Geol. Survey Circ. 733, p. 14-16.

Plafker, George, and MacKevett, E. M., Jr., 1970, Mafic and ultramafic rocks from a layered pluton at Mount Fairweather, Alaska: U.S. Geol. Survey Prof. Paper 700-B, p. B21-B26.

Plouff, Donald, 1976, Gravity and magnetic fields of polygonal prisms and application to magnetic terrain corrections: Geophysics, v. 41, no. 4, p. 727-741.

Plouff, Donald, Robbins, S. L., and Holden, K. D., 1976, Principal facts for gravity observations in the Charles Sheldon Antelope Range, Nevada-Oregon: U.S. Geol. Survey open-file rept. 76-601, 22 p.

Pojeta, John, Jr., and Palmer, T. J., 1976, The origin of rock boring in mytilacean pelecypods: Alcheringa, v. 1, no. 1, p. 167-180, 5 figs.

Poland, J. F., 1977, Land subsidence stopped by artesian-head recovery, Santa Clara Valley, California: Internat. Assoc. Sci. Hydrol. Internat. Symposium on Land Subsidence, 2d, Anaheim, Calif., Dec. 1976, Proc. [In press.]

Poore, R. Z., 1976, Microfossil correlation of California lower Tertiary sections—comparison: U.S. Geol. Survey Prof. Paper 743-F, 8 p., 2 pls., 5 figs.

Porter, S. C., 1969, Pleistocene geology of the east-central Cascade Range, Washington: Pacific Coast Friends of the Pleistocene Field Conf. Guidebook, 54 p.

———1976, Pleistocene glaciation in the southern part of the North Cascade Range, Washington: Geol. Soc. America Bull., v. 87, p. 61-75.

Post Austin, 1975, Preliminary hydrography and historic terminal changes of Columbia Glacier, Alaska: U.S. Geol. Survey Hydrol. Inv. Atlas HA-559, 3 sheets.

Prescott, W. H., and Lisowski, M., 1976, Deformation at Middleton Island, Alaska, during the decade after the Alaska earthquake of 1964 [abs.]: EOS (Am. Geophysical Union Trans.), v. 57, p. 1013.

Prescott, W. H., and Savage, J. C., 1976, Strain accumulation on the San Andreas fault near Palmdale, California: Jour. Geophys. Research, v. 81, p. 4901-4908.

Price, H. S., and Coats, H. K., 1974, Direct methods in reservoir simulation. Soc. Petroleum Engineers Jour., v. 14, no. 3, p. 295-308.

Price, W. E., Jr., 1976, A random-walk simulation model of alluvial-fan deposition *in* Merriam, D. F., Random processes in geology: Springer-Verlag, p. 55-62.

Prowell, D. C., O'Connor, B. J., and Rubin, M., 1975, Preliminary evidence for Holocene movement along the Belair fault zone near Augusta, Ga.: U.S. Geol. Survey open-file rept. 75-680, 12 p.

Raitt, R. W., Shor, Jr., T. J. G. Francis, and G. B. Morris, 1969, Anisotropy of the Pacific upper mantle: Jour. Geophys. Research, v. 74, p. 3095-3109.

Ray, H. A., Bennett, C. M., and Records, A. W., 1976, Teton Dam flood of June 1976, Deer Parks quadrangle, Idaho: U.S. Geol. Survey, Hydrol. Inv. Atlas, HA-571, 1 sheet, scale 1:24,000.

Ray, H. A., and Bigelow, B. B., 1976a, Teton Dam flood of June 1976, Rigby quadrangle, Idaho: U.S. Geol. Survey, Hydrol. Inv. Atlas, HA-572, 1 sheet, scale 1:24,000.

Ray, H. A., and Bigelow, B. B., 1976b, Teton Dam flood of June 1976, Lewisville quadrangle, Idaho: U.S. Geol. Survey Hydrol. Inv. Atlas, HA-573, 1 sheet, Scale 1:24,000.

Ray, H. A., and Matthai, H. F., 1976a, Teton Dam flood of June 1976, Idaho Falls North quadrangle, Idaho: U.S. Geol. Survey Hydrol. Inv. Atlas, HA-574, 1 sheet, scale 1:24,000.

Ray, H. A., and Matthai, H. F., 1976b, Teton Dam flood of June 1976, Idaho Falls South quadrangle, Idaho: U.S. Geol. Survey, Hydrol. Inv. Atlas, HA-575, 1 sheet, scale 1:24,000.

Ray, H. A., Matthai, H. F., and Thomas, C. A., 1976, Teton Dam flood of June 1976, Newdale quadrangle, Idaho: U.S. Geol. Survey, Hydrol. Inv. Atlas, HA-565, 1 sheet, scale 1:24,000.

Reed, B. L., and Hemley, J. J., 1966, Occurrence of pyrophyllite in Kekiktuk Conglomerate, Brooks Range, northeastern Alaska, *in* Geological Survey Research 1966: U.S. Geol. Survey Prof. Paper 500-C, p. C162-C166.

Reed, B. L., and Lanphere, M. A., 1973, The Alaska-Aleutian Range batholith: Geochronology, chemistry, and relation to circum-Pacific plutonism: Geol. Soc. America Bull., v. 84, p. 2583-2610.

Reed, P. B., and Monger, J. W. H., 1975, Operation St. Elias, Yukon Territory; the Mush Lake Group and Permo-Triassic rocks in the Kluane Ranges: Geol. Survey Canada Paper 75-1, pt. A, p. 55-59.

Regan, R. D., Cain, J. C., and Davis, W. M., 1975, A global magnetic anomaly map: Jour. Geophys. Research., v. 80, no. 5, p. 794-802.

Reimer, G. M., 1976, Design and assembly of a portable helium detector for evaluation as a uranium exploration instrument: U.S. Geol. Survey open-file rept. 76-398, 18 p.

Reimer, G. M., and Otton, J. K., 1976, Helium in soil-gas and well water in the vicinity of a uranium deposit, Weld County, Colorado: U.S. Geol. Survey open-file report. 76-699, 10 p.

Richter, D. H., Singer, D. A., and Cox, D. P., 1975, Mineral resources map of the Nabesna quadrangle, Alaska: U.S. Geol. Survey Misc. Field Studies Map MF-655K, scale 1:250,000.

Riggs, H. C., 1976, Effects of man on low flows: Am. Soc. Civil Engineers, Environmental Aspects of Irrig. and Drainage Speciality Conf., Ottawa, Canada, July 1976, Proc., p. 306-314.

———1977, A brief investigation of the surface-water hydrology of Yemen Arab Republic: U.S. Geol. Survey open-file rept. 77-150, 35 p.

Riggs, H. C., and Harenberg, W. A., 1976, Flood characteristics of streams in Owyhee County, Idaho: U.S. Geol. Survey Water-Resources Inv. 76-88, 14 p.

Roberson, C. E., and Barnes, R. B., 1977, Stability of fluoride complex with silica and its distribution in natural water systems: Chem. Geology. [In press.]

Robertson, J. B., 1976, Numerical modeling of subsurface radioactive solute transport from waste seepage ponds at the Idaho National Engineering Laboratory: U.S. Geol. Survey open-file rept. 76-717, 59 p.

Robie, R. A., Hemingway, B. S., and Wilson, W. H., 1976, The heat capacities of Calorimetric Conference copper and of muscovite $KAl_2(AlSi_3)O_{10}(OH)_2$, pyrophyllite $Al_2Si_4O_{10}(OH)_2$, and illite $K_3(Al_7Mg)(Si_{14}Al_2)O_{40}(OH)_8$ between 15 and 275K and their standard entropies at 298.15K: U.S. Geol. Survey Jour. Research 4, p. 631-644.

Roedder, Edwin, 1971, Fluid inclusion studies on the porphyry-type ore deposits at Bingham, Utah, Butte, Montana, and Climax, Colorado: Econ. Geology, v. 66, p. 98-120.

Roedder, Edwin, and Skinner, B. J., 1968, Experimental evidence that fluid inclusions do not leak: Econ. Geology, v. 63, p. 715-730.

Roddick, J. A. and Hutchison, W. W., 1974, Setting of the Coast Plutonic Complex, British Columbia: Pacific Geology, v. 8, p. 91-108.

Rodis, H. G., and Land, L. F., 1976, The shallow aquifer—A prime freshwater resource in eastern Palm Beach County, Florida: U.S. Geol. Survey Water-Resources Inv. 76-21, NTIS Rept. PB-254 393/AS, 15 p.

Rohde, W. G., and Taranik, J. V., and Nelson, C. A., 1976, Flood analysis using digital processing techniques and statistical analysis: W. T. Pecora Symp., 2nd, Am. Soc. Photogramm., Sioux Falls, S. Dak., 1976, Proc. [In press.]

Rosasco, G. J., and Roedder, Edwin, 1976, Application of a new laser-excited Raman spectrometer to non-destructive analysis of sulfate in individual phases in fluid inclusions in minerals [extended abs.]: Internat. Geol. Congress, 25th, Abs., v. 3, p. 812–813.

Rosasco, G. J., Roedder, Edwin, and Simmons, J. H., 1975; Science, v.. 190, p. 557-560.

Rossman, D. L., 1963a, Geology of the eastern part of the Mount Fairweather quadrangle, Glacier Bay, Alaska: U.S. Geol. Survey Bull. 1121-K, 57 p.

———1963b, Geology and petrology of two stocks of layered gabbro in the Fairweather Range, Alaska: U.S. Geol. Survey Bull. 1121-F, 50 p.

Rowan, L. C., Wetlaufer, P. H., Goetz, A. F. H., Billingsley, F. C., and Stewart, J. H., 1974, Discrimination of rock types and detection of hydrothermally altered areas in south-central Nevada: U.S. Geol. Survey Prof. Paper 883, 35 p.

Rubin, D. M., and McCulloch, D. S., 1976, Bedform dynamics in San Francisco Bay, California [abs.]: Geol. Soc. America Abs. with Programs, v. 8, no. 6, p. 1079.

Ruch, R. R., Gluskoter, H. J., Shimp, N. F., and others, 1974, Occurrence and distribution of potentially volatile trace elements in coal—a final report: Illinois Geol. Survey Environmental Geology Note 72, Urbana, Ill., 96 p.

Ruppel, E. T., 1976, Medicine Lodge thrust system, east-central Idaho and southwest Montana: U.S. Geol. Survey open file rept. 76–366, 25 p.

Sandberg, C. A., and Gutschick, R. C., 1977, Paleotectonic, biostratigraphic, and economic significance of Osagean to early Meramecian starved basin in Utah: U.S. Geol. Survey open-file rept. 77-121, 16 p., 5 figs.

Sanford, Samuel, 1913, The underground water resources of the Coastal Plain province of Virginia: Virginia Geol. Survey Bull. 5., 361 p.

Schlesinger, B., and Daetz, D., 1975, Development of a Procedure for forecasting long-range environmental impacts: Prepared for USGS by Stanford University, Dept. of Industrial Engineering, technical rept. 75–3, 137 p.

Schmidt, D. L., and Ford, A. B., 1969, Geologic map of the Pensacola and Thiel Mountains *in* Geologic maps of Antarctica: New York, Am. Geog. Soc., sheets, scale 1:1,000,000.

Schneider, V. R., Board, J. W., Colson, B. E., Lee, F. N., and Druffel, L. A., 1977, Computation of backwater and discharge at width constrictions of heavily-vegetated flood plains: U.S. Geol. Survey Water-Resources Inv., 76–129, 87 p.

Schneider, V. R., and Smoot, G. F., 1976, Development of a standard rating for the Price pygmy current meter: U.S. Geol. Survey Jour. Research, v. 4, no. 3, p. 293–397.

Scholle, P. A., Editor, 1977, Geological studies on the COST No. B-2 Well, U.S. Mid-Atlantic Outer Continental Shelf area: U.S. Geol. Survey Circ. 750, 71 p.

Schwartz, D. P., 1976, Pre-earthquake displacement: Motagua fault zone, Guatemala [abs.] EOS (Am. Geophys. Union Trans.), N. 57, no. 12, p. 949.

Scott, D. H., Diaz, J. M., and Watkins, J. A., 1975, The geologic evaluation and regional synthesis of metric and panoramic photographs: Lunar Sci. Conf., 6th, Proc. p. 2531-2540.

———1977, Lunar farside tectonics and volcanism: *in* Lunar science VIII: Houston, Tex., Lunar Sci. Inst., p. 863.

Scott, G. R., 1976, Historic trail map of the Greater Denver area, Colorado: U.S. Geol. Survey Misc. Inv. Map I-856G, scale 1:100,000.

Scott, W. B., Land, L. F., and Rodis, H. G., 1977, Saltwater intrusion in the shallow aquifer in Martin and Palm Beach Counties, Florida: U.S. Geol. Survey Water-Resources Inv. 76–135.[In press.]

Shaler, N. S., 1889, On the occurrence of fossils of the Cretaceous age on the Island of Martha's Vineyard, Mass.: Bull. Mus. Comparative Zoology, v. 16, no. 5, p. 89–97.

Shawe, D. R., and Parker, R. L., 1967, Mafic-ultramafic layered intrusion at Iron Mountain, Fremont County, Colorado: U.S. Geol. Survey Bull. 1251-A, 28 p.

Shepherd, R. G., 1976, Sedimentary processes and structures of ephemeral-stream point bars, Rio Puerco near Albuquerque, New Mexico [abs.]: Geol. Soc. of America Abs. with Programs, v. 8, no. 6, p. 1103.

Shinn, E.A., Halley, R. B., Hudson, J. H., and Lidz, B. H., 1977, Limestone compaction; an enigma: Geology, v. 5, no. 1, p. 21–24.

Silberman, M. L., Shawe, D. R., Koski, R. A., and Goddard, B. B., 1975, K-Ar ages of mineralization at Round Mountain and Manhattan, Nye County, Nevada: Isochron/West, no. 13, p. 1–2.

Simon, F. O., and Rollinson, C. L., 1976, Chromium in rocks and minerals from the southern California Batholith: Chem. Geology, v. 17, p. 73–88.

Simpson, R. G., 1976, Determination of channel capacity of the Scaramento River between Ordbend and Glenn, Butte and Glenn Counties, California: U.S. Geol. Survey open-file rept. 76–526, 48 p.

Sims, J. D., 1975, Determining earthquake recurrence intervals from deformational strucuures in young lacustrine sediments: Tectonophysics, v. 29, p. 141–152.

Sims, P. K., 1976a, Precambrian tectonics and mineral deposits, Lake Superior region: Econ. Geology, v. 71, p. 1092–1118.

———1976b, Middle Precambrian age of volcanogenic massive sulfide deposits in northern Wisconsin [abs.]: 22nd Ann. Inst. on Lake Superior Geology, Minneapolis, Minn., Proc. p. 57.

Sims, P. K., and Morey, G. B., 1973, A geologic model for the development of early Precambrian crust in Minnesota: Geol. Soc. America, Abs. with Programs, v. 5, no. 7, p. 812.

Sims, P. K., and Peterman, Z. E., 1976, Geology and Rb-Sr ages of reactivated Precambrian gneisses and granite in the Marenisco-Watersmeet area, northern Michigan: U.S. Geol. Survey, Jour. Research, v. 4, no. 4, p. 405–414.

Singer, D. A., 1975, Mineral resource models and the Alaskan mineral resource assessment program, *in* Vogely, W. A., ed., Mineral materials modeling: Washington, DC, Resources for the Future, p. 370–382.

———1976, Area of influence of exploratory drill holes under conditions of errors of recognition, *in* Weiss, Alfred, ed., World mining and metals technology—Proceedings of the Joint MMIJ-AIME Meeting, Denver, Colo., U.S.A., Sept. 1-3, 1976· New York, Am. Inst. Mining Metall. Petroleum Engineers, v. 2, p. 1037-1048.

Singer, D. A., Curtin, G. C., and Foster, H. C., 1976, Mineral resources map of the Tanacross quadrangle, Alaska: U.S. Geol. Survey Misc. Field Studies Map MF-767E, scale 1:250,000.

Singer, D. A., and MacKevett, E. M., 1976, Mineral resources map of the McCarthy quadrangle, Alaska: U.S. Geol. Survey Misc. Field Studies Map MF-767C, scale 1:250,000.

Skipp, B. A., 1976, Eastward bulge of the Antler Highland across the Snake River Plain [abs.]: Geol. Soc. America Abs. with Programs, v. 8, no. 6, p. 1109–1110.

Sklar, C. B., 1958, The Preston gabbro and the associated metamorphic gneisses, New London County, Connecticut: Connecticut Geol. and Nat. History Survey Bull. 88, 131 p.
Slack, J. R., and Smith, R. A., 1976, An oilspill risk analysis for the South Atlantic Outer Continental Shelf lease area: U.S. Geol. Survey open-file rept., 54 p.
Slack, L. J., 1975, Hydrologic environmental effects of sprayed sewage effluent, Tallahassee, Florida: U.S. Geol. Survey Water Resources Inv. 55-75, 73 p.
Sleep, N. H., 1971, Thermal effects of the formation of Atlantic continental margins by continental break-up: Royal Astron. Soc. Geophys. Jour., v. 24, no. 4, p. 325-350.
Sleep, N. H., and Snell, N. S., 1976, Thermal contraction and flexture of mid-continent and Atlantic margin basins: Royal Astron. Soc. Geophys. Jour., v. 45, no. 1, p. 125-154.
Smith, B. D., Cady, J., Campbell, D., Daniels, J., and Flanigan, V., 1976, A case for "other" geophysical methods, *in* Exploration for uranium ore deposits: Internat. Atomic Energy Agency, Vienna, 1976, p. 337.
Smith, E. T., 1976, Computer simulation of environmental impact, *in* Proceedings: Summer Computer Simulation Conference, Washington, D.C., July 12-14, 1976, Simulation Councils, Inc., LaJolla, CA., p. 939-942.
Smith, J. G., 1975, K-Ar evidence on timing of metamorphism and plutonism in the Coast Mountains near Ketchikan, Alaska [abs.], *in* Intrusive rocks and related mineralization of the Canadian Cordillera: Geol. Assoc. Canada, Cordilleran Sec., Vancouver, B. C., Feb. 1975, Program and Abs., p. 21.
Smith, M. A., Amato, R. V., Furbush, M. A., Pert, D. M., Nelson, M. E., Hendrix, J. S., Tamm, L. C., Wood, Jr., G., and Shaw, D. R., 1976, Geological and operational summary, COST No. B-2 well, Baltimore Canyon trough area, Mid-Atlantic OCS: U.S. Geol. Survey, open-file rept. 76-774, 79 p.
Smith, R. A., Slack, J. R., and Davis, R. K., 1976a, An oilspill risk analysis for the North Atlantic Outer Continental Shelf lease area: U.S. Geol. Survey open-file rept., 38 p.
Smith, R. A., Slack, J. R., and Davis, R. K., 1976b, An oilspill risk analysis for the Mid-Atlantic Outer Continental Shelf lease area: U.S. Geol. Survey open-file rept., 34 p.
Smith, R. L. and Bailey, R. A., 1966, The Bandelier Tuff, a study of ash-flow eruption cycles fcom zoned magma chambers: Bull. Volcanologique, v. 29, p. 83-104.
Snavely, P. D., Jr., MacLeod, N. M., Wagner, H. C., Rau, W. W., 1976, Geologic map of the Cape Foulweather and Euchre Mountain Quadrangles, Oregon: U.S. Geol. Survey Map I-868, Scale 1:62,500.
Souther, J. G., Brew, D. A., and Okulitch, A. V., 1974, Iskut River, British Columbia geological map (scale 1:1,000,000): Canada Geol. Survey open-file rept. 214, scale 1:1,000,000.
Staudacher, T. H. Jessberger, E. K., Kirsten, T., 1977, ^{40}Ar-^{39}Ar age systematics of consortium breccia 73215. II, *in* Lunar science VIII: Houston, Tex., Lunar Sci. Inst., p. 896-898.
Steele, T. D., 1976, Coal-resource development alternatives, residuals management, and impact on the water resources of the Yampa River basin, Colorado and Wyoming, *in* Wasserwitschaft und Gewinnung Fossiler Energieträger, Internationales Symposium, Düsseldorf, Bundesrepublik Deutschland, 7-8 September, 1976: Düsseldorf, Germany, Deutsches Komitee der IWRA im Deutschen Verband fur Wasserwirtschaft e.V. (DVWW), Rept. 28, 18 p.
Steele, T. D., Bauer, D. P., Wentz, D. A., and Warner, J. W., 1976, An environmental assessment of impacts of coal development on the water resources of the Yampa River basin, Colorado and Wyoming—Phase I work plan: U.S. Geol. Survey open-file rept. 76-367, 38 p.
Steele, T. D., James, I. C., II, Bauer, D. P., 1976, An environmental assessment of impacts of coal development on the water resources of the Yampa River Basin, Colorado and Wyoming—Phase II work plan: U.S. Geol. Survey open-file rept. 76-368, 33 p.
Steeples, D. W., and Pitt, A. M., 1976, Microearthquakes in and near Long Valley: Jour. Geophys. Research, v. 81, no. 5, p. 841-847.
Stephenson, L. W., 1936, Geology and paleontology of the Georges Bank Canyons, pt. II, Upper Cretaceous fossils from Georges Bank: Geol. Soc. America, Bull., v. 47, p. 367-410.
Stettler, A., Eberhardt, P., Geiss, J., and Grogler, N. 1974, ^{39}AR-^{40}Ar ages of samples from the Apollo 17 station 7 boulder and implication for its formation: *Earth Planetary Sci. Letters* 23, p. 453-461.
Steven, T. A., and Eaton, G. P., 1975, Environment of ore deposition in the Creede mining district, San Juan Mountains, Colorado:—I—Geologic, hydrologic and geophysical setting: Econ. Geology, v. 70, p. 1023-1037.
Steven, T. A., and Friedman, I., 1968, The source of travertine in the Creede formation, San Juan Mountains, Colorado, *in* Geological Survey Research 1968: U. S. Geol. Survey Prof. Paper 600-B, p. B29-B36.
Stewart, J. H., Moore, W. J., and Zietz, Isidore, 1977, East-west patterns of Cenozoic igneous rocks, aeromagnetic anomalies, and mineral deposits, Nevada and Utah: Geol. Soc. America Bull., v. 88, no. 1, p. 67-77.
Stone, B. D., and Randall. A. D., 1975, Surficial Geologic Map of the Plainfield quadrangle, Windham and New London Counties, Connecticut: U.S. Geol. Survey open-file map 75-327, scale 1:24,000.
Stuckless, J. S.., and Ferreira, C. P., 1976, Labile uranium in granitic rocks, *in* Exploration for Uranium Ore Deposits: Internat. Atomic Energy Agency, Vienna, 1976, p. 717-728.
Stuckless, J. S., Millard, H. T., Jr., Bunker, C. M. Nkomo, I. T., Rosholt, J. N., Bush, C. A., Huffman, Claude, Jr., and Keil, R. L., 1977, A comparison of some analytical techniques for determining uranium, thorium, and potassium in granitic rocks: U.S. Geol. Survey Jour. Research, v. 5, p. 83-91.
Sun, R. J., 1976, Possibility of triggering earthquakes by injection of radioactive wastes in shale at Oak Ridge National Laboratory, Tennessee: U.S. Geol. Survey Jour. Research, v. 5, no. 2, p. 253-262.
Swanson, V. E., Medlin, J. H., Hatch, J. R., Coleman, S. L., Wood, G. H., Jr., Woodruff, S. D., and Hildenbrand, R. T., 1976, Collection, chemical analysis, and evaluation of coal samples, 1975: U.S. Geol. Survey open-file rept. 76-468, 503 p.
Swetland, P. J., and Clayton, J. L., 1976, Source beds of petroleum in the Denver basin: U.S. Geol. Survey open-file rept. 76-575, 23 p.
Taranik, J. V., and Trautwein, C. M., 1976, Integration of geological remote-sensing techniques in subsurface analysis: U.S. Geol. Surv. open-file rept. 76-402, 60 p.
———1977, EROS Data Center Landsat digital enhancement techniques for geologic applications [abs.]: Am. Assoc. Pet. Geol. Conf. on Exploration Data Synthesis, Tucson, Ariz., Mar. 1977, p. 2.
Taylor, G. C., Jr., 1976, Historical review of the international water-resources program of the U.S. Geological Survey 1940-70: U.S. Geol. Survey Prof. Paper 911, 146 p.
Tera, F., and Wasserburg, G. J., 1972, U-Th-Pb systematics in three Apollo 14 basalts and the problem of initial Pb in lunar rocks; Earth Planetary Sci. Letters., v. 14, no. 3, p. 281-304.
Tera, F., and Wasserburg, G. J., 1974, U-Th-Pb systematics on lunar rocks and inferences about lunar evolution and the age of the moon: Lunar Sci. Conf., 5th, Proc., p. 1571-1599.
Terman, M. J., 1976, Geological Constraints on Chinese petroleum

development (summary) *in* China's energy policies and resource development, report of a Seminar June 2-3, 1976: Stanford Calif., Stanford Univ. U.S.-China relations rept. 1, p. 28-34.

Tessar, P. A., 1976a, LIMAP Landsat imagery analysis package, system user documentation, version 3.1: S. Dak. State Planning Bur., 95 p.

———1976b, Applications of digital remote sensing and natural resource information to land and water resource planning in South Dakota: Remote Sensing for Land and Resource Management in the South and Southwest, Texas A & M Univ., College Station, Tex., 1976, Proc. p. 152-166.

Tessar, P. A., and Eidenshink, J. C., 1976, The Landsat imagery analysis package: Automated land use classification and multidimensional geographic analysis: W. T. Pecora Memorial Symp., 2d, Am. Soc. Photogramm., Sioux Falls, S. Dak., 1976, Proc. [In press.]

Tessar, P. A., Miller, R. L., and Eidenshink, J. C., 1976, LIMAP Landsat imagery analysis package, system documentation, version 3.1: S. Dak. State Planning Bur., 105 p.

Thatcher, W. R., 1976, Episodic strain accumulation in southern California: *Science,* v. 194, p. 691-695.

Thomas, C. A., and Ray, H. A., 1976, Teton Dam flood of June 1976, Parker quadrangle, Idaho: U.S. Geol. Survey, Hydrol. Inv. Atlas, HA-567, 1 sheet, Scale 1:24,000.

Thomas, C. A., Ray, H. A., and Harenberg, W. A., 1976, Teton Dam flood of June 1976, Menan Buttes quadrangle, Idaho: U.S. Geol. Survey, Hydrol. Inv. Atlas, HA-570, 1 sheet, scale 1:24,000.

Thomas, C. A., Ray, H. A., and Matthai, H. F., 1976, Teton Dam flood of June 1976, St. Anthony quadrangle, Idaho: U.S. Geol. Survey, Hydrol. Inv. Atlas, HA-566, 1 sheet, scale 1:24,000.

Thomas, D. M., 1976, Flood frequency—expected and unexpected probabilities: U.S. Geol. Survey open-file rept. 76-755, 12 p.

Thompson, J. B., Jr., and Norton, S. A., 1968, A Paleozoic regional metamorphism in New England and adjacent areas, *in* Zen, E-an, and others, eds., studies of Appalachian geology northern and maritime: New York and London, Interscience Pub., p. 319-327.

Thompson, M. L., 1954, American Wolfcampian Fusulinids: Kansas Univ. Paleont. Contr. No. 14 Protozoa, art. 5., 225 p.

Tidball, R. R., and Ebens, R. J., 1976, Regional geochemical baselines in soils of the Powder River basin, Montana-Wyoming: Wyo. Geol. Assoc. Guidebook, 28th Ann. Field Conf., p. 299-310.

Tilling, R. I., Koyanagi, R. Y., Lipman, P. W., Lockwood, J. P., Moore, J. G., and Swanson, D. A., 1976, Earthquake and related catastrophic events, Island of Hawaii, November 29, 1975, a preliminary report: U.S. Geol. Survey Circ. 740, 33 p.

Toulmin, Priestley III, Clark, B. C., Baird, A. K., Keil, Klaus, Rose, Harry J. Jr., 1976, Preliminary results from the Viking X-ray fluorescence experiment: The first sample from Chryse Planitia, Mars: Science, v. 194, p. 81-84.

Tourtelot, H. A., and Meier, A. L., 1976, Lithium in clayey rocks of Pennsylvanian age, western Pennsylvania, *in* Vine, J. D., ed., Lithium resources and requirements by the year 2000: U.S. Geol. Survey Prof. Paper 1005, p. 128-136.

Trace, R. D., 1960, Significance of unusual mineral occurrences at Hicks Dome, Hardin County, Illinois: U.S. Geol. Survey Prof. Paper 400B, p. B63-B64.

Tracey, J. I., Jr., and Ladd, H. S., 1974, Quaternary history of Eniwetok and Bikini Atolls, Marshall Islands: Internat. Coral Reef Symposium, 2d, Great Barrier Reef Comm., Brisbane Proc., v. 2, p. 537-550.

Trescott, P. C., 1975, Documentation of finite-difference model for simulation of three-dimensional ground-water flow: U.S. Geol. Survey open-file rept. 75-438, 32 p.

Trescott, P. C. and Larson, S. P., 1976, Documentation of finite-difference model for simulation of three-dimensional groundwater flow: U.S. Geol. Survey open-file rept. 76-591, 21 p.

Trescott, P. C., Pinder, G. F., and Larson, S. P., 1976, Finite-difference model for aquifer simulation in two dimensions with results of numerical experiments, *in* Automated data processing and computation: U.S. Geol. Survey Techniques of Water-Resource Inv. Book 7, chap. 1, 116 p.

Trimble, S. W., 1976, Sedimentation in Coon Creek Valley, Wisconsin, *in* Proceedings of the Third Federal Interagency Sedimentation Conference, 1976: Water Resources Council, pt. 5, p. 100-112.

Truhlar, J. F., Jr., 1976, Determining suspended-sediment loads from turbidity records, *in* Proceedings of the Third Federal Interagency Sedimentation Conference, 1976: Water Resources Council, pt. 7, p. 65-74.

Tschudy, R. H., 1976, Pollen changes near the Port Union-Wasatch boundary, Powder River basin, *in* Lauden, R. B. ed., Geology and Energy resources of the Powder River basin: Guidebook Annual Field Conference, 28th Wyoming Geol. Assoc., p. 73-81.

Tweto, O. L., 1976, Preliminary geologic map of Colorado: U.S. Geol. Survey Misc. Field Studies Map MF-788, 2 sheets, scale 1:500,000.

Upton, J. W., Jr., Combs, J., Duffield, W. A., and Austin, C. F., 1976, The Coso geothermal project, Combs, J., ed.: Tech. Rept. no. 1, May 1976, ERDA Prime contract E(45-1)-1830, 18 p.

U.S. Geological Survey, 1972, Aeromagnetic map of the Vya and part of the McDermitt 1° × 2° quadrangles, Nevada: U. S. Geol. Survey open-file map, scale 1:250,000.

———1975. Geological Survey research 1975: U.S. Geol. Survey Prof. Paper 975, 373 p.

———1976a, Geothermal investigations of the U.S. Geological Survey in Long Valley, California 1972-1973: Jour. Geophys. Research v. 81, p. 721-860, 1527-1532.

———1976b, Geochemical survey of the Western Energy Regions (formerly Geochemical survey of the Western Coal Regions), Third Annual Progress Report, July, 1976: U.S. Geol. Survey open-file rept. 76-729.

———1976c, Land use change map, 1970-1972, Washington urban area, D.C., Md., and Va. 1975 (1976). U.S. Geol. Survey Misc. Geol. Inv. Map I-890, 1 sheet, scale 1:100,000.

———1976d, Thermographic mosaic of Yellowstone National Park, Wyoming, Idaho, and Montana: EROS Data Center, Sioux Falls, S. Dak., Accession no. E-17-2235BN.

U.S. Geological Survey and Colorado Geological Survey, 1977, Energy resources map of Colorado: U.S. Geol. Survey Misc. Investigations Map I-1039, scale 1:500,000.

U.S. Water Resources Council, 1976, Guidelines for determining flood flow frequencies: U.S. Water Resources Council Bull., no. 17, 26 p.

Van Alstine, R. E., 1969, Geology and mineral deposits of the Poncha Springs NE quadrangle, Chaffee County, Colorado: U.S. Geol. Survey Prof. Paper 626, 52 p.

Wagner, G. H., 1964, Kleintektonische Untersuchuungen im Gebiet des Nördlinger Rieses: Geol. Jahrb., v. 81, p. 519-600.

Wallace, R. E., Tatlock, D. B., and Silberling, N. J., 1960, Intrusive rocks of Permian and Triassic age in the Humboldt Range, Nevada: U.S. Geol. Survey Prof. Paper 400-B, p. B291-B293.

Waller, R. M., 1976, Surficial geologic map of the Black River basin, New York: U.S. Geol. Survey Misc. Field Studies Map 728A, scale 1:125,000.

Wanless, H. R., 1946, Pennsylvanian geology of a part of the southern Appalachian coal field; Geol. Soc. of America Mem. 13.

———1975, Appalachian region, *in* Paleotectonic investigations of the Pennsylvanian System in the United States—pt. I—Introduction and regional analyses of the Pennsylvanian System: p. 17-62.

Ward, F. N., and Fishman, M. J., 1976, Analytical methods for the determination of lead, *in* Lovering, T. G., ed., Lead in the environment: U.S. Geol. Survey Prof. Paper 957, p. 81.

Ward, P. L., Gibbs, James, Harlow, David, and Aburto, Q. Arturo, 1974, Aftershocks of the Manuagua, Nicaragua, earthquake and the tectonic significance of the Tiscapa fault: Seismol. Soc. America Bull., v. 64, p. 1017-1029.

Watson, R. D., and Hemphill, W. R., 1976, Use of an airborne Fraunhofer line discriminator for the detection of solar stimulated luminescence: U.S. Geol. Survey open file rept. 76-202, 110 p.

Weiblen, P. W., and Roedder, Edwin, 1976, Compositional interrelationships of mare basalts from bulk chemical and melt inclusion studies: Lunar Sci. Conf., 7th, Proc., p. 1449-1466.

Weimer, R. J., 1959, Jurassic-Cretaceous boundary, Cut Bank area, Montana, *in* Billings Geol. Soc. Guidebook 10th Ann. Field Conf., Sawtooth-Disturbed belt area, 1959: p. 84-88.

Wershaw, R. L., Pickney, D. J., and Booker, S. E., 1977, The chemical structure of humic acids—Part I—A generalized structural model: U. S. Geol. Survey Jour. Research, v. 5, no. 5. [In press.]

White, D. E., 1968, Environments of generation of some base-metal ore deposits: Econ. Geol., v. 63, p. 301-335.

White, D. E., Fournier, R. O., Muffler, L. J. P., and Truesdell, A. H., 1975, Physical results of research drilling in thermal areas of Yellowstone National Park: U.S. Geol. Survey Prof. Paper 892, 70 p.

White, D. E., Thompson, J. M., and Fournier, R. O., 1976, Lithium contents of thermal and mineral waters, *in* Vine, J. D., ed., Lithium resources and requirements by the year 2000: U.S. Geol. Survey Prof. Paper 1005, p. 58-60.

Wilcox, R. E., 1954, Petrology of Paricutin volcano, Mexico: U.S. Geol. Survey Bull. 965-C, p. 281-353.

Williams, Howel, 1935, Newberry Volcano of central Oregon: Geol. Soc. America Bull., v. 46, p. 253-304.

Williams, R. S., Jr., Hasell, P. G., Jr., Sellman, A. N., and Smedes, H. W., 1976, Thermographic mosaic of Yellowstone National Park: Photogramm. Eng. and Remote Sensing, v. 42, no. 10, p. 1315-1324.

Willrich, Mason, 1976, Radioactive waste management and regulation: Cambridge, Mass., M.I.T.: Energy Laboratory rept. MIT-EL 76-011, p. 2-16 to 2-20.

Winner, M. D., Jr., and Simmons, C. E., 1977, Hydrology of the Creeping Swamp watershed, North Carolina, with reference to the potential effects of stream channelization: U.S. Geol. Survey Water-Resources Inv., NC 71-050, 91 p.

Winter, T. C., 1976, Numerical simulation analysis of the interaction of lakes and ground water: U.S. Geol. Survey Prof. Paper 1001, 45 p.

Wintsch, R. P., 1976, Lithologic control of thrusting in eastern Connecticut [abs.]: Geol. Soc. America, Abs. with Programs, v. 8, no. 2, p. 303.

Wones, D. R., 1974, Igneous petrology of some plutons in northern part of the Penobscot Bay area, *in* Osberg, P. H., ed., Guidebook for field trips in east central and north-central Maine: Orono, Maine, Maine Univ., p. 99-125.

Wright, F. E., and Wright, C. W., 1908, The Ketchikan and Wrangell mining districts, Alaska: U.S. Geol. Survey Bull. 347, 210 p.

Yates, R. G., 1968, The trans-Idaho discontinuity, *in* Internat. Geol. Cong., 23d, Prague, 1968, Proc., Sec. 1, Upper mantle (geological processes): Prague, Academia, p. 117-123.

Zand, S. M., 1976, Indexes associated with information theory in water quality: Water Pollution Control Federation Jour. v. 48, no. 8, p. 2026-2031.

Zen, E-an, 1967, Time and space relationships of the Taconic allochthon and autochthon: Geol. Soc. America, Spec. Paper 97, 107 p.

Zen, E-an, 1969, Petrographic evidence for polymetamorphism in the western part of the northern Appalachians and a possible regional chronology: Geol. Soc. America, Abs. with Programs, v. 1 pt. 7, p 297-299.

Zwart, H. J., and others, 1967, A scheme of metamorphic facies for the cartographic representation of regional metamorphic belts: Internat. Union Geol. Sci. Newsletter, v. 1967, no. 2, p. 57-72.

U.S. GEOLOGICAL SURVEY OFFICES

HEADQUARTERS OFFICES

[National Center. 12201 Sunrise Valley Dr., Reston, Va. 22092]

Official and (or) office	*Name and telephone number*	*Address*
Director	V. E. McKelvey (703 860-7411)	101 National Center.
Associate Director	W. A. Radlinski (703 860-7411)	102 National Center.
Senior Scientist	Frank E. Clarke (202 343-3888)	Rm. 4441, Interior Bldg., Washington, DC 20240.
Assistant Director, Research	James R. Balsley (703 860-7488)	104 National Center.
Assistant Director, Programs	Dale D. Bajema (acting) (703 860-7435).	105 National Center.
Assistant Director, Environmental Conservation.	Henry W. Coulter (703 860-7491)	106 National Center.
Assistant Director, Administration	Edmund J. Grant (703 860-7201)	201 National Center.
Assistant Director	Montis R. Klepper (703 860-7481)	171 National Center.
Chief, Office of Land Information and Analysis.	James R. Balsley (703 860-7488)	104 National Center.
Earth Resources Observation Systems Program.	John M. DeNoyer (703 860-7881)	1925 Isaac Newton Sq. East, Reston, VA 22090.
Earth Sciences Applications Program.	Donald R. Nichols (703 860-6961)	720 National Center.
Environmental Impact Analysis	Daniel B. Krinsley (703 860-7455)	760 National Center.
Geography Program	James R. Anderson (703 860-6344)	710 National Center.
Resource and Land Investigations Program.	J. Ronald Jones (703 860-6717)	750 National Center.
Chief, Administrative Division	Edmund J. Grant (703 860-7201)	201 National Center.
Chief, Computer Center Division	Carl E. Diesen (703 860-7106)	801 National Center.
Chief, Conservation Division	Russell G. Wayland (703 860-7524)	600 National Center.
Chief, Geologic Division	Richard P. Sheldon (703 860-6531)	911 National Center.
Office of Mineral Resources	George E. Becraft (acting) (703 860-6562).	913 National Center.
Office of International Geology	John A. Reinemund (703 860-6418)	917 National Center.
Office of Energy Resources	Charles D. Masters (703 860-6431)	915 National Center.
Office of Marine Geology	Charles D. Masters (acting) (703 860-6431).	915 National Center.
Office of Environmental Geology	John C. Reed, Jr. (703 860-6411)	908 National Center.
Office of Geochemistry and Geophysics	Robert I. Tilling (acting) (703 860-6584).	906 National Center.
Office of Earthquake Studies	Robert M. Hamilton (703 860-6472)	905 National Center.
Office of Scientific Publications	Walter P. Ketterer (acting) (703 860-6575).	904 National Center.
Chief, Publications Division	Harry D. Wilson, Jr. (703 860-7181)	341 National Center.
Chief, Topographic Division	Robert H. Lyddan (703 860-6231)	516 National Center.
Chief, Water Resources Division	Joseph S. Cragwall, Jr. (703 860-6921).	409 National Center.

PRINCIPAL FIELD OFFICES

Official and (or) office	*Name and telephone number*	*Address*
Assistant Director, Eastern Region	William B. Overstreet (703 860-7414).	109 National Center, 12201 Sunrise Valley Dr., Reston, VA 22092.

Official and (or) office	Name and telephone number	Address
Assistant Director, Central Region	Thad G. McLaughlin (303 234-4630)	P.O. Box 25046, Federal Center, Denver, CO 80225.
Assistant Director, Western Region	Joel M. Johanson (415 323-2711)	345 Middlefield Rd., Menlo Park, CA 94025.

SELECTED FIELD OFFICES IN THE UNITED STATES AND PUERTO RICO

[Temporary offices are not included; list is current as of February 1977. Correspondence to the following offices should be addressed to the Post Office box, if one is given]

COMPUTER CENTER DIVISION

Location	Official in charge and telephone number	Address
Arizona, Flagstaff 86001	James E. Crawforth (602 774-1312)	601 E. Cedar Ave.
California, Menlo Park 94025	James L. Mueller (415 323-2661)	345 Middlefield Rd.
Colorado, Denver 80225	Frederick B. Sower (303 234-4810)	Stop 801, Federal Center.
Missouri, Rolla 65401	Glenn A. Ridgeway (314 364-6985)	Stop 817, 1400 Independence Rd.
South Dakota, Sioux Falls 57198	Ralph J. Thompson (605 594-6511, ext. 555).	EROS Data Center.

CONSERVATION DIVISION

REGIONAL OFFICES

Location	Official in charge and telephone number	Address
Central Region: Denver, CO 80225	George H. Horn, Regional Conservation Manager (303 234-2855).	P.O. Box 25046, 609 Federal Center; Villa Italia, Wadsworth and Alameda.
Eastern Region: Washington, DC 20244	George F. Brown, Regional Conservation Manager (202 254-3137).	Suite 204-C, 1725 K St., NW.
Gulf of Mexico Outer Continental Shelf Operations: Metairie, LA 70011	A. Dewey Acuff, Conservation Manager (504 680-9381).	P.O. Box 7944; 336 Imperial Office Bldg., 3301 N. Causeway Blvd.
Western Region: Menlo Park, CA 94025	Hillary A. Oden (acting), Regional Conservation Manager (415 467-2093).	345 Middlefield Rd.

AREA AND DISTRICT OFFICES

Location	Official in charge and telephone number	Address
Alaska, Anchorage 99510	Rodney A. Smith, Robert H. McMullin (907 265-4376).	P.O. Box 259; 212 Skyline Bldg., 218 E St.
Arizona, Phoenix 85004	Hall F. Susie (602 261-3766)	Rm. 208, Post Office Bldg., 522 N. Central Ave.
California, Los Angeles 90012	Fred J. Shambeck, Keith A. Yenne (213 798-2846).	Rm. 7744, Federal Bldg., 300 N. Los Angeles St.
Bakersfield 93301	Donald F. Russell (805 984-1186)	Rm. 309, Federal Bldg., 800 Truxtun Ave.
Menlo Park 94025	Leo H. Saarela (415 467-2874)	701 Laurel St.
	Henry L. Cullins, Jr. (415 467-3011).	345 Middlefield Rd.
	Reid T. Stone (415 467-2841)	701 Laurel St.
Sacramento 95825	Robert D. Morgan (acting) (916 484-4219).	Rm. W-2231, Federal Bldg., 2800 Cottage Way.
Ventura 93003	Michael F. Reitz (805 648-5131)	Suite 202, 145 N. Brent St.

Location	*Official in charge and telephone number*	*Address*
Colorado, Denver 80225	Gary L. Prost (303 234-4751), Daniel A. Jobin, John P. Storrs (303 234-4435).	P.O. Box 25046, 602 Federal Center.
	Gale Lutz (acting) (303 234-5042).	P.O. Box 25046, 607 Federal Center.
Durango 81301	Jerry W. Long (303 247-5144)	P.O. Box 1809; 125 W. 10th St.
Grand Junction 81501	Peter A. Rutledge, James W. Hager (303 322-0281).	Suite 300, 131 N. 6th St.
Idaho, Pocatello 83201	John T. Skinner (208 554-6262)	P.O. Box 1610; Federal Bldg., 150 S. Arthur St.
Louisiana, Houma 70360	John D. Borne (504 863-4033)	P.O. Box 1269.
Lafayette 70501	Elmo G. Hubble (318 232-6037)	P.O. Box 52289; 223 Bendel Rd.
Lake Charles 70601	Robert H. Darrow (318 478-6440)	P.O. Box 6088, Drew Station.
Metairie 70011	J. Rogers Pearcy (504 680-9381), Donald W. Solanas (504 680-9333), Jake B. Lowenhaupt (504 680-9251).	P.O. Box 7944; 336 Imperial Office Bldg., 3301 N. Causeway Blvd.
	Charles B. Mullins (504 680-9301).	P.O. Box 7966.
Mississippi, Jackson 39201	Thomas E. Godfrey (601 490-4405)	505 Unifirst Federal Savings & Loan Bldg.
Missouri, Rolla 65401	C. V. Collins (314 276-8411)	P.O. Box 936; 400 Main St.
Montana, Billings 59103	Albert F. Czarnowsky (406 585-6181), Jim S. Hinds (406 585-6185), Virgil L. Pauli (406 585-6367).	P.O. Box 2550; 3 7th St. W.
Nevada, Reno 89502	Don C. Jones (702 598-5676)	Suite 102, McCarthy Bldg., 63 Keystone.
New Mexico, Albuquerque 87102	James W. Sutherland (505 474-2841)	Suite 815, 505 Marquette Ave. NW., Western Bank Bldg.
Artesia 88210	James A. Knauff (505 746-9838)	Drawer U; 105 S. 4th St.
Carlsbad 88220	David R. Stewart (505 885-6454)	P.O. Box 1716; Federal Bldg., 114 S. Halagueno St.
Farmington 87401	J. E. Fassett, Philip T. McGrath (505 325-4572).	P.O. Box 959; 407 Petroleum Club Plaza, 3535 E. 30th St.
Hobbs 88240	Arthur R. Brown (505 393-5146)	P.O. Box 1157; 205 N. Linam St.
Roswell 88201	Donald M. VanSickle, Carl C. Traywick (505 476-9257).	Drawer 1857; Federal Bldg. and U.S. Courthouse, Richardson Ave. at 5th St.
Oklahoma, McAlester 74502	Alexander M. Dinsmore (918 423-5030).	P.O. Box 816; 509 S. 3d St.
Oklahoma City 73118	Charley W. Nease (405 736-4806)	Suite 404, 50 Penn Pl.
Tulsa 74135	Edward L. Johnson (918 736-7638), Floyd L. Stelzer (918 736-7631).	6136 E. 32d Pl.
Oregon, Portland 97208	Jesse L. Colbert, Ted H. Hudson (503 429-4796).	P.O. Box 2967; 830 NE. Holladay St.
	Dick Cramer-Borneman (503 429-5357).	P.O Box 2967; Bldg. 100, 1425 NE. Irving St.
Texas, Freeport 77541	Jack C. Sandridge (713 233-2604)	P.O. Box 2006; 2007 Brazosport Blvd. (Hwy. 28).
Utah, Salt Lake City 84138	Donald C. Alvord (801 524-5643), Edgar Guynn (801 588-5650), Jackson W. Moffit (801 588-5646).	Rms. 8422, 8240, and 8426, Federal Bldg., 125 S. State St.
Washington, D.C. 20244	Edward M. Rodgers (202 254-5856)	Suite 214, 1725 K St., NW.
	Harry A. Dupont (202 634-6654)	Suite 402, 1725 K St., NW.
	John A. Lees (202 634-1550)	Suite 316-F, 1825 K St., NW.
	Dwayne Hull (202 254-7870)	Suite 208-B, 1725 K St., NW.
	Bruce Wamsley (202 254-7870)	Suite 208-A, 1725 K St., NW.

Location	Official in charge and telephone number	Address
Wyoming, Casper 82602	Charles J. Curtis (307 265-5405), James W. Shelton (acting) (307 328-5247), Elmer M. Schell (307 328-5421).	P.O. Boxes 2859 and 2372; Rms. 2002, 2225, and 2001, Federal Bldg. and Post Office, 100 E. B St.
Newcastle 82701	Glenn E. Worden (307 746-2737)	P.O. Box 219; Suite 201, 110½ W. Main St.
Rock Springs 82901	John A. Fraher (307 362-6422), Arne A. Mattila (307 362-7350).	P.O. Box 1170; Rm. 201, First Security Bank Bldg., 502 S. Front St.
Thermopolis 82443	George Kinsel (307 864-3477)	P.O. Box 590; Rm. 202, Federal Bldg.

EARTH RESOURCES OBSERVATION SYSTEMS PROGRAM

Location	Official in charge and telephone number	Address
Mississippi, Bay St. Louis 39521	Frank D. Beatty (acting) (601 688-3541).	Bldg. 1100, National Space Technology Laboratories.
South Dakota, Sioux Falls 57198	Allen H. Watkins (605 594-6123)	EROS Data Center.

GEOLOGIC DIVISION

REGIONAL OFFICES

Location	Official in charge and telephone number	Address
Central Region: Denver, CO 80225	William R. Keefer, Regional Geologist (303 234-3624).	P.O. Box 25046, Federal Center.
Eastern Region: Reston, VA 22092	Eugene H. Roseboom, Jr., Regional Geologist (703 860-6631).	953 National Center, 12201 Sunrise Valley Dr.
Western Region: Menlo Park, CA 94025	George Gryc, Regional Geologist (415 323-2214).	345 Middlefield Rd.

PUBLICATIONS DIVISION

REGIONAL OFFICES

Office	Official in charge and telephone number	Address
Central Region: Denver, CO 80225	John L. Heller, Regional Publications Manager (303 234-4974).	P.O. Box 25046, Federal Center.
Eastern Region: Reston, VA 22092	Lewis D. Brown, Regional Publications Manager (703 860-6761).	328 National Center, 12201 Sunrise Valley Dr.
Western Region: Menlo Park, CA 94025	Fred Kunkel, Regional Publications Manager (415 323-2537).	345 Middlefield Rd.

PUBLIC INQUIRIES OFFICES

[Each of the following offices provides over-the-counter sales service for Survey book reports and geologic and topographic maps relating to its geographic area and for selected Survey reports of general interest]

Location	Official in charge and telephone number	Address
Alaska, Anchorage 99501	Margaret I. Erwin (907 277-0577)	Rm. 108, Skyline Bldg., 508 2d Ave.
California, Los Angeles 90012	Lucy E. Birdsall (213 688-2850)	Rm. 7638, Federal Bldg., 300 N. Los Angeles St.
San Francisco 94111	Jean V. Molleskog (415 556-5627)	Rm. 504, Custom House, 555 Battery St.
Colorado, Denver 80294	Alice M. Coleman (303 837-4169)	Rm. 1012, Federal Bldg., 1961 Stout St.
Washington, D.C. 20244	Bruce A. Hubbard (202 343-8073)	Rm. 1028, General Services Bldg., 19th and F Sts., NW.
Texas, Dallas 75202	Jimmie L. Wilkinson (acting) (214 749-3230).	Rm. 1C45, Federal Bldg., 1100 Commerce St.
Utah, Salt Lake City 84138	Wendy R. Hassibe (801 524-5652)	Rm. 8105, Federal Bldg., 125 S. State St.
Virginia, Reston 22092	A. Ernestine Jones (703 860-6167)	Rm. 1C402, National Center, 12201 Sunrise Valley Dr.
Washington, Spokane 99201	Eula M. Thune (509 456-2524)	Rm. 678, U.S. Courthouse, W. 920 Riverside Ave.

DISTRIBUTION CENTERS

[Survey maps are distributed by mail and over the counter from the following centers]

Location	Official in charge and telephone number	Address
Virginia, Arlington 22202 [1, 2]	John J. Curry (703 557-2781)	1200 S. Eads St.
Colorado, Denver 80225 [3]	Dwight F. Canfield (303 234-3832)	P.O. Box 25286, Federal Center.
Alaska, Fairbanks 99701 [4]	Natalie A. Cornforth (907 452-1951, ext. 174).	310 First Ave.

TOPOGRAPHIC DIVISION

Location	Official in charge and telephone number	Address
California, Menlo Park 94025	Dean T. Edson (acting) (415 467-2411).	345 Middlefield Rd.
Colorado, Denver 80225	Albert E. Letey (303 234-2351)	P.O. Box 25046, 510 Federal Center.
Missouri, Rolla 65401	Lawrence H. Borgerding (acting) (314 276-9111).	1400 Independence Rd.
South Dakota, Sioux Falls 57198	Allen H. Watkins (605 784-7123)	EROS Data Center.
Virginia, Reston 22090	Roy E. Fordham (703 860-7760)	1925 Isaac Newton Sq. East.
Reston 22092	Peter F. Bermel (703 860-6352)	567 National Center, 12201 Sunrise Valley Dr.

[1] For maps of areas east of the Mississippi River (including Minnesota).
[2] Also provides mail and over-the-counter distribution for Survey book reports.
[3] For maps of areas west of the Mississippi River (including Louisiana).
[4] For residents of Alaska.

WATER RESOURCES DIVISION

REGIONAL OFFICES

Location	*Official in charge and telephone number*	*Address*
Northeastern Region: Reston, VA 22092	Joseph T. Callahan, Regional Hydrologist (703 860-6985).	433 National Center, 12201 Sunrise Valley Dr.
Southeastern Region: Atlanta, GA 30309	Leslie B. Laird, Regional Hydrologist (404 881-4395).	Suite 200, 1459 Peachtree St. NE.
Central Region: Denver, CO 80225	Alfred Clebsch, Jr., Regional Hydrologist (303 234-3661).	P.O. Box 25046, 406 Federal Center.
Western Region: Menlo Park, CA 94025	William H. Robinson, Regional Hydrologist (415 323-8111).	345 Middlefield Rd.

DISTRICT OFFICES

Location	*Official in charge and telephone number*	*Address*
Alabama, Tuscaloosa 35486	William J. Powell (205 752-8104)	P.O. Box V; Rm. 202, Oil and Gas Board Bldg., Univ. of Alabama.
Alaska, Anchorage 99501	Harry Hulsing (907 277-5526, 5527)	Skyline Bldg., 218 E St.
Arizona, Tucson 85701	Horace M. Babcock (602 792-6671)	Federal Bldg., 301 W. Congress St.
Arkansas, Little Rock 72201	Richard T. Sniegocki (501 378-5246, 5247).	Rm. 2301, Federal Office Bldg., 700 W. Capitol Ave.
California, Menlo Park 94025	Lee R. Peterson (415 323-8111, exts. 2326, 2327, 2465, 2466).	855 Oak Grove Ave.
Colorado, Denver 80225	James E. Biesecker (303 234-5092)	P.O. Box 25046, 415 Federal Center.
Connecticut, Hartford 06101	Vacant (203 244-2528)	Rm. 235, 135 High St.
Delaware	Walter F. White, Jr. (301 828-1535)	See Maryland District Office.
District of Columbia	do	Do.
Florida, Tallahassee 32303	Clyde S. Conover (904 386-1118)	Suite F-240, 325 John Knox Rd.
Georgia, Doraville 30360	John R. George (404 221-4858)	Suite B, 6481 Peachtree Industrial Blvd.
Hawaii, Honolulu 96815	Frank T. Hidaka (808 955-0251)	1833 Kalakaua Ave.
Idaho, Boise 83724	E. E. Harris (208 384-1750)	P.O. Box 036; Rm. 365, Federal Bldg., 550 W. Fort St.
Illinois, Champaign 61820	Lawrence A. Martens (217 359-3918)	P.O. Box 1026; 605 N. Neil St.
Indiana, Indianapolis 46202	Vacant (317 269-7101)	1819 N. Meridian St.
Iowa, Iowa City 52240	Sulo W. Wiitala (319 338-0581, ext. 521).	P.O. Box 1230; Rm. 269, Federal Bldg., 400 S. Clinton St.
Kansas, Lawrence 66045	Joseph S. Rosenshein (913 864-4321).	1950 Ave. "A"—Campus West, Univ. of Kansas.
Kentucky, Louisville 40202	P. A. Emery (502 582-5241)	Rm. 572, Federal Bldg., 600 Federal Pl.
Louisiana, Baton Rouge 70806	Albert N. Cameron (504 387-0181, ext. 281).	P.O. Box 66492; 6554 Florida Blvd.
Maine	John A. Baker (617 223-2822)	See Massachusetts District Office.
Maryland, Towson 21204	Walter F. White, Jr. (301 828-1535)	208 Carroll Bldg., 8600 La Salle Rd.
Massachusetts, Boston 02114	John A. Baker (617 223-2822)	Suite 1001, 150 Causeway St.
Michigan, Okemos 48864	T. Ray Cummings (517 372-1910, ext. 561).	2400 Science Parkway, Red Cedar Research Park.
Minnesota, St. Paul 55101	Charles R. Collier (612 725-7841, 7842).	Rm. 1033, Post Office Bldg.
Mississippi, Jackson 39206	Lamar E. Carroon (601 969-4600)	430 Bounds St.
Missouri, Rolla 65401	Vacant (314 364-3680)	Stop 200, 1400 Independence Rd.

Location	Official in charge and telephone number	Address
Montana, Helena 59601	George M. Pike (406 449-5263)	P.O. Box 1696; Rm. 421, Federal Bldg., 316 N. Park Ave.
Nebraska, Lincoln 68508	Kenneth A. MacKichan (402 471-5082).	Rm. 406, Federal Bldg. and U.S. Courthouse, 100 Centennial Mall N.
Nevada, Carson City 89701	John P. Monis (702 882-1388)	Rm. 227, Federal Bldg., 705 N. Plaza St.
New Hampshire	John A. Baker (617 223-2822)	See Massachusetts District Office.
New Jersey, Trenton 08607	Harold Meisler (609 989-2162)	P.O. Box 1238; Rm. 420, Federal Bldg., 402 E. State St.
New Mexico, Albuquerque 87125	William E. Hale (505 766-2246)	P.O. Box 26659; Rm. 815, 505 Marquette NW., Western Bank Bldg.
New York, Albany 12201	Robert J. Dingman (518 472-3107)	P.O. Box 1350; Rm. 343, U.S. Post Office and Courthouse.
North Carolina, Raleigh 27602	Ralph C. Heath (919 755-4510)	P.O. Box 2857; Rm. 436, Century Station Post Office Bldg.
North Dakota, Bismarck 58501	Walter R. Scott (701 255-4011, exts. 227, 228).	P.O. Box 778; Rm. 332, New Federal Bldg., 3d St. and Rosser Ave.
Ohio, Columbus 43212	James F. Blakey (614 469-5553)	975 W. 3d Ave.
Oklahoma, Oklahoma City 73102	James H. Irwin (405 231-4256)	Rm. 621, 201 NW. 3d St.
Oregon, Portland 97208	Stanley F. Kapustka (503 234-3361, exts. 4776, 4777).	P.O. Box 3202; 830 NE. Holladay St.
Pennsylvania, Harrisburg 17108	Norman H. Beamer (717 782-3468)	P.O. Box 1107; 4th Floor, Federal Bldg., 228 Walnut St.
Puerto Rico, San Juan 00934	Ernest D. Cobb (809 783-4660)	P.O. Box 34168; Bldg. 652, Fort Buchanan.
Rhode Island	John A. Baker (617 223-2822)	See Massachusetts District Office.
South Carolina, Columbia 29201	John S. Stallings (803 765-5966)	Suite 200, 2001 Assembly St.
South Dakota, Huron 57350	John E. Powell (605 352-8651, ext. 258).	P.O. Box 1412; Rm. 231, Federal Bldg.
Tennessee, Nashville 37203	Stanley P. Sauer (615 749-5424)	Rm. A-413, Federal Bldg. and U.S. Courthouse.
Texas, Austin 78701	I. Dale Yost (512 397-5766)	Rm. 649, Federal Bldg., 300 E. 8th St.
Utah, Salt Lake City 84138	Theodore Arnow (801 524-5663)	Rm. 8002, Federal Bldg., 125 S. State St.
Vermont	John A. Baker (617 223-2822)	See Massachusetts District Office.
Virginia, Richmond 23220	William E. Forrest (804 782-2427)	Rm. 304, 200 W. Grace St.
Washington, Tacoma 98402	Vacant (206 593-6510)	Suite 600, 1201 Pacific Ave.
West Virginia, Charleston 25301	David H. Appel (304 343-6181, exts. 310, 311).	Rm. 3303, Federal Bldg. and U.S. Courthouse, 500 Quarrier St. E.
Wisconsin, Madison 53706	W. W. Barnwell (608 262-2488)	Rm. 200, 1815 University Ave.
Wyoming, Cheyenne 82001	Samuel W. West (307 778-2220, ext. 2111).	P.O. Box 2087; 4020 House Ave.

OFFICES IN OTHER COUNTRIES

WATER RESOURCES DIVISION

Location	Officer in charge	Address
Kenya, Nairobi	Neal E. McClymonds	USAID/Nairobi, U.S. Department of State, Washington, DC 20521.
New Zealand, Wellington	Ivan K. Barnes	c/o A. J. Ellis, DSIR Chemical Division, Private Bag, Petone, New Zealand.
Saudi Arabia, Riyadh	David W. Greenman	USREP/JECOR, APO New York 09038.
Yemen, San'a'	G. Chase Tibbitts, Jr.	U.S. Geological Survey, USAID/San'a', Agency for International Development, Washington, DC 20521.

INVESTIGATIONS IN PROGRESS IN THE GEOLOGICAL SURVEY

Investigations in progress during fiscal year 1977 are listed below together with the names and headquarters of the individuals in charge of each. Headquarters at main centers are indicated by NC for the National Center in Reston, Va., D for Denver, Colo., and M for Menlo Park, Calif.; headquarters in other cities are indicated by name (see list of offices, p. 354, for addresses). Inquiries regarding projects for which no address is given in the list of offices should be directed to the appropriate Division of the Geological Survey, National Center, 12201 Sunrise Valley, Dr., Reston, Va. 22092. The lowercase letter after the name of the project leader shows the Division technical responsibility: c, Conservation Division; l, Land Information and Analysis; w, Water Resources Division; no letter, Geologic Division.

The projects are classified by principal topic. Most geologic-mapping projects involve special studies of stratigraphy, petrology, geologic structure, or mineral deposits but are listed only under "Geologic mapping" unless a special topic or commodity is the primary justification for the project. A reader interested in investigations of volcanology, for example, should look under the heading "Geologic mapping" for projects in areas of volcanic rocks, as well as under the heading "Volcanology." Likewise, most water-resource investigations involve special studies of several aspects of hydrology and geology but are listed only under "Water Resources" unless a special topic—such as floods or sedimentation—is the primary justification for the project.

Areal geologic mapping is subdivided into mapping at scales smaller than 1:62,500 (for example, 1:250,000) and mapping at scales of 1:62,500 or larger (for example, 1:24,000).

Abstracts. *See* Bibliographies and abstracts.

Aluminum:
- Resources of the United States (S. H. Patterson, NC)

Analytical chemistry:
- Activation analysis (J. J. Rowe, NC)
- Analytical methods:
  - Textural automatic image analyzer research (M. B. Sawyer, D)
  - Water chemistry (M. J. Fishman, w, D)
- Analytical services and research (J. I. Dinnin, NC; Claude Huffman, Jr., D; C. O. Ingamells, M)
- Assessment of neutron activation methods (V. J. Janzer, w, D)
- Mineral deposits, characteristic analysis (J. M. Botbol, NC)
- Natural organic macromolecules in water (R. L. Wershaw, w, D)
- Organic geochemistry and infrared analysis (I. A. Berger, NC)
- Plant laboratory (T. F. Harms, D)
- Radioactivation and radiochemistry (H. T. Millard, D)
- Reactor support (G. P. Kraker, Jr., w, D)
- Rock chemical analysis:
  - General (D. R. Norton, D)
  - Rapid (Leonard Shapiro, NC)
- Services (L. B. Riley, D)
- Trace analysis methods, research (F. N. Ward, D)
- Ultratrace analysis (H. T. Millard, D)
- X-ray spectrometer for Viking lander (Priestley Toulmin III, NC)
- *See also* Spectroscopy.

Arctic engineering geology (Reuben Kachadoorian, M)

Artificial recharge:
- Artificial recharge methods (W. F. Lichtler, w, Lincoln, Nebr.)
- Fort Allen recharge (J. R. Diaz, w, Fort Buchanan, P.R.)
- Nassau County recharge (T. M. Robinson, w, Mineola, N.Y.)
- Recharge, Bijou Creek (R. K. Livingston, w, D)
- Subsurface storage, waste heat (J. D. Bredehoeft, w, NC)
- Subsurface waste disposal (R. W. Davis, w, Louisville, Ky.)

Barite:
- Geology, geochemistry, and resources of barite (D. A. Brobst, NC)

Base metals. *See base-metal names.*

Bibliographies and abstracts:
- Lunar bibliography (J. H. Freeberg, M)
- Outer Continental Shelf onshore impact assessment (M. L. Pattison, l, NC)

Borates:
- California (M):
  - Furnace Creek area (J. F. McAllister)
  - Searles Lake area (G. I. Smith)

Chromite. *See* Ferro-alloy metals.

Clays:
- Bentonite, resource evaluation in Rocky Mountain region (C. A. Wolfbauer, D)
- *State:*
- Georgia, kaolin investigations (S. H. Patterson, NC)

Coal:
- Geochemistry of United States coal (V. E. Swanson, D)
- National Coal Resources Data System (M. D. Carter, NC)
- *States:*
- Alaska:
  - Bering River coal field (c, Anchorage)
  - Cape Beaufort-Corwin Bluff coal field (J. E. Callahan, c, Casper, Wyo.)

Coal—Continued
States—Continued
Alaska—Continued
Coal sample collection and mapping in Alaska and entry of data into the National Coal Resources Data System (C. N. Conwell, College; M. D. Carter, NC)
Nenana (Clyde Wahrhaftig, M)
Arizona, collection of coal samples for analysis (R. T. Moore, Tucson; V. E. Swanson, D)
Colorado (c, D, except as otherwise noted):
Buckhorn Lakes quadrangle (R. G. Dickinson)
Citadel Plateau (G. A. Izett)
Courthouse Mountain quadrangle (R. G. Dickinson)
Denver basin, Tertiary coal zone (P. E. Soister)
Disappointment Valley, eastern (D. E. Ward, D)
Douglas Creek Arch area (B. E. Barnum)
Grand Mesa coal field (G. P. Eager)
North Park area (D. J. Madden)
Savery quadrangle (C. S. V. Barclay)
Smizer Gulch and Rough Gulch quadrangles (W. J. Hail, D)
Washboard Rock quadrangle (R. G. Dickinson)
Watkins and Watkins SE quadrangles (P. E. Soister)
Idaho, collection of coal samples in Idaho (C. R. Knowles, Moscow; V. E. Swanson, D)
Illinois, coal sampling, analysis and National Coal Resources Data System (H. J. Gluskoter, Urbana; M. D. Carter, NC)
Kentucky (D):
Adams quadrangle (D. E. Ward)
Blaine quadrangle (C. L. Pillmore)
Louisa quadrangle (R. M. Flores)
Richardson quadrangle (P. T. Hayes)
Sitka quadrangle (P. T. Hayes)
Missouri, coal data collection and transfer to the National Coal Resources Data System (C. E. Robertson, Rolla; M. D. Carter, NC)
Montana:
Birney SW quadrangle (S. P. Buck, c, Casper, Wyo.)
Black Butte quadrangle (W. L. Rohrer, c, Casper, Wyo.)
Coal mechanics in northen Powder River basin (J. M. White, c, Billings)
Collection of coal samples in Montana (R. E. Matson, Butte; V. E. Swanson, D)
Decker quadrangle (B. E. Law, c, D)
Girard field (M. A. Soule, c, Billings)
Holmes Ranch quadrangle (N. E. Micklich, c, Casper, Wyo.)
Jordan quadrangle (G. D. Mowat, c, Billings)
McCone County lignite (H. C. Taylor, c, Billings)
Monarch quadrangle (B. E. Barnum, c, D)
Pearl School quadrangle (G. L. Galyardt, c, Casper, Wyo.)
Sidney coal field (M. J. Carnevale, c, Washington, D.C.)
Spring Gulch quadrangle (N. E. Micklich, c, Casper, Wyo.)
Subsidence of spoil piles, Colstrip (R. A. Farrow, D; J. M. White, c, Billings)
Taintor Desert quadrangle (S. P. Buck, c, Casper, Wyo.)

Coal—Continued
States—Continued
Montana—Continued
Tongue River Dam quadrangle (Juliana Waring, c, Casper, Wyo.)
Nevada, collection of coal samples in Nevada (J. A. Schilling, Reno; V. E. Swanson, D)
New Mexico:
Alamosa Mesa West quadrangle (D. B. Umshler, c, Roswell)
Collection of coal samples in New Mexico (F. E. Kottlowski, Socorro; V. E. Swanson, D)
Gallup East quadrangle (E. D. Patterson, c, Roswell)
Gallup West quadrangle (J. E. Fassett, c, Farmington)
Manuelito quadrangle (J. E. Fassett, c, Farmington)
Ojo Encino Mesa quadrangle (D. B. Umshler, c, Roswell)
Pueblo Alto Trading Post quadrangle (R. W. Jentgen, c, Farmington)
Samson Lake quadrangle (J. E. Fassett, c, Farmington)
Star Lake quadrangle (J. E. Fassett, c, Farmington)
Tanner Lake quadrangle (D. B. Umshler, c, Roswell)
Twin Butte quadrangle (M. L. Millgate, c, Farmington)
Western Raton field (C. L. Pillmore, D)
North Dakota (c, Billings, Mont., except as otherwise noted):
Adams, Bowman, and Slope Counties lignite resources (R. C. Lewis)
Clark Butte 15-minute quadrangle (G. D. Mowat)
North Almont quadrangle (H. L. Smith, c, D)
West-central North Dakota lignite resources (E. A. Rehbein)
Williston area lignite resources (J. M. Spencer)
Oklahoma (c, Tulsa, except as otherwise noted):
Blocker quadrangle (E. H. Hare, Jr.)
Collection of coal samples in Oklahoma (S. A. Friedman, Norman; V. E. Swanson, D)
Hackett quadrangle (E. H. Hare, Jr.)
Panama quadrangle (E. H. Hare, Jr.)
Spiro quadrangle (E. H. Hare, Jr.)
Pennsylvania (NC, except as otherwise noted):
Collection of coal samples for analysis (W. E. Edmunds, Pennsylvania State Geological Survey, Harrisburg; M. J. Bergin)
Northern anthracite field (M. J. Bergin)
Southern anthracite field (G. H. Wood, Jr.)
Utah (c, D, except as otherwise noted):
Basin Canyon quadrangle (Fred Peterson)
Big Hollow Wash quadrangle (Fred Peterson)
Blackburn Canyon quadrangle (Fred Peterson)
Butler Valley quadrangle (W. E. Bowers)
Canaan Peak quadrangle (W. E. Bowers)
Collet Top quadrangle (H. D. Zeller)
East-of-the-Navajo quadrangle (H. D. Zeller)
Fourmile Bench quadrangle (W. E. Bowers)
Horse Flat quadrangle (H. D. Zeller)
Horse Mountain quadrangle (W. E. Bowers)
Jessen Butte quadrangle (E. M. Schell, c, Casper, Wyo.)
Needle Eye Point quadrangle (H. D. Zeller)

Coal—Continued
States—Continued
Utah (c, D, except as otherwise noted)—Continued
Pete's Cove quadrangle (H. D. Zeller)
Ship Mountain Point quadrangle (H. D. Zeller)
Sunset Flat quadrangle (H. D. Zeller)
Virginia and West Virginia, central Appalachian Basin (K. J. Englund, NC)
Washington:
Coal resources of Washington (W. H. Lee, c, M)
Collection of coal samples for analysis (V. E. Livingston, Jr., Olympia; V. E. Swanson, D)
West Virginia:
Formatting coal data for National Coal Resources Data System (M. C. Behling, Mogantown; M. D. Carter, NC)
Louisa quadrangle (C. W. Connor, D)
Wyoming (c, D, except as otherwise noted):
Acme quadrangle (B. E. Barnum)
Appel Butte quadrangle (G. L. Galyardt)
Bailey Lake quadrangle (M. L. Schroeder)
Beaver Creek Hills quadrangle (E. I. Winger, c, Casper)
Betty Reservoir NE quadrangle (F. B. Kistner, c, Casper)
Browns Hill quadrangle (C. S. V. Barclay)
Cottonwood Rim quadrangle (C. S. V. Barclay)
Coyote Draw quadrangle (G. L. Galyardt)
Deer Creek quadrangle (M. L. Schroeder)
Eagle Rock quadrangle (S. P. Buck, c, Casper)
Fortin Draw quadrangle (B. E. Law)
Four Bar-J Ranch quadrangle (G. L. Galyardt)
Gillette East quadrangle (B. E. Law)
Gillette West quadrangle (B. E. Law)
Greenhill quadrangle (S. P. Buck, c, Casper)
Grieve Reservoir quadrangle (C. S. V. Barclay)
Hilight quadrangle (W. J. Purdon, c, Casper)
Hultz Draw quadrangle (E. I. Winger, c, Casper)
Kemmerer area (M. L. Schroeder)
Ketchum Buttes quadrangle (C. S. V. Barclay)
Little Thunder Reservoir quadrangle (G. C. Martin, c, Casper)
Monarch quadrangle (B. E. Barnum)
Moyer Springs quadrangle (B. E. Law)
Neil Butte quadrangle (S. P. Buck, c, Casper)
North Star School NE quadrangle (S. P. Buck, c, Casper)
North Star School NW quadrangle (S. P. Buck, c, Casper)
North Star School SW quadrangle (W. J. Purdon, c, Casper)
North Star School SE quadrangle (W. J. Purdon, c, Casper)
Open A Ranch quadrangle (G. C. Martin, c, Casper)
Oriva quadrangle (B. E. Law)
Pickle Pass quadrangle (M. L. Schroeder)
Pine Mountain-Oil Mountain area (G. J. Kerns, c, Casper)
Piney Canyon NW quadrangle (G. C. Martin, c, Casper)
Piney Canyon SW quadrangle (J. E. Goolsby, c, Casper)
Pleasantdale quadrangle (S. L. Grazis)
Rawlins coal field (C. S. V. Barclay)
Reid Canyon (G. J. Kerns, c, Casper)

Coal—Continued
States—Continued
Wyoming (c, D, except as otherwise noted)—Continued
Reno Junction quadrangle (W. J. Purdon, c, Casper)
Reno Reservoir quadrangle (G. C. Martin, c, Casper)
Rock Springs uplift (P. J. LaPoint)
Rough Creek quadrangle (S. P. Buck, c, Casper)
Saddle Horse Butte quadrangle (S. L. Grazis)
Savery quadrangle (C. S. V. Barclay)
Scaper Reservoir quadrangle (S. L. Grazis)
Sheridan quadrangle (E. I. Winger, c, Casper)
Sheridan Pass quadrangle (W. L. Rohrer, c, Casper)
Square Top Butte quadrangle (G. J. Kerns, c, Casper)
Teckla quadrangle (J. E. Goolsby, c, Casper)
Teckla SW quadrangle (J. E. Goolsby, c, Casper)
The Gap quadrangle (G. L. Galyardt)
The Gap SW quadrangle (S. L. Grazis)
Tullis quadrangle (C. S. V. Barclay)
Turnercrest NE quadrangle (G. C. Martin, c, Casper)
Weston SW quadrangle (R. W. Jones, c, Casper)

Construction and terrain problems:
Areal slope stability analysis, San Francisco Bay region (S. D. Ellen, M)
Electronics instrumentation research for engineering geology (J. B. Bennetti, D)
Engineering geology laboratory (R. A. Farrow, D)
Fissuring-subsidence research (T. L. Holzer, M)
Geotechnical measurements and services (H. W. Olsen, D)
Reactor hazards research (K. L. Pierce, D)
Reactor site investigations (R. H. Morris, D)
Research in rock mechanics (F. T. Lee, D)
Sino-Soviet terrain (L. D. Bonham, l, NC)
Soil engineering research (T. L. Youd, M)
Special intelligence (L. D. Bonham, l, NC)
Volcanic hazards (D. R. Crandell, D)
States:
California (M, except as otherwise noted):
Feasibility of tunneling for rapid transit, Los Angeles area (R. F. Yerkes)
Geologic environmental maps for land use planning (E. H. Pampeyan)
Geology and slope stability, western Santa Monica Mountains (R. H. Campbell)
Los Angeles County Cooperative (R. H. Campbell)
Pacific Palisades landslide area, Los Angeles (J. T. McGill, D)
California and Colorado, regional stability studies (D. H. Radruch-Hall, M)
Colorado (D):
Coal mine deformation studies, Somerset mining district (C. R. Dunrud)
Engineering geology mapping research, Denver region (H. E. Simpson)
Massachusetts, sea-cliff erosion studies (C. A. Kaye, Boston)
Nevada:
Geologic and geomechanical investigations (J. R. Ege, D)
Seismic engineering program (K. W. King, Las Vegas)
Surface effects of nuclear explosions (R. P. Snyder, D)
Utah, coal-mine bumps (F. W. Osterwald, D)
See also Urban geology; Land use and environmental impact; Urban hydrology.

Copper:
- United States and world resources (D. P. Cox, NC)
- *States:*
- Alaska, southwest Brooks Range (I. L. Tailleur, M)
- Arizona (M):
  - Jerome and Bagdad districts (C. M. Conway)
  - Ray porphyry copper (H. M. Cornwall)
- California, Shasta districts (C. M. Conway, M)
- Maine-New Hampshire, porphyry, with molybdenum (R. G. Schmidt, NC)
- Michigan (NC):
  - Greenland and Rockland quadrangles (J. W. Whitlow)
  - Michigan copper district (W. S. White)
- Virginia, massive sulfides (J. E. Gair, NC)

Crustal studies. *See* Earthquake studies; Geophysics, regional.

Directories:
- Department of the Interior information services (E. T. Smith, 1, NC)

Earthquake studies:
- Active fault analysis (R. E. Wallace, M)
- Automatic earthquake data processing (S. W. Stewart, M)
- Comparative elevation studies (R. O. Castle, M)
- Computer fault modeling (J. H. Dieterich, M)
- Computer operations and maintenance (T. C. Jackson, M)
- Crustal strain (J. C. Savage, M)
- Crustal studies (ARPA) (Isidore Zietz, NC)
- Dynamic soil behavior (A. T. F. Chen, M)
- Earth structure studies (J. H. Healy, M)
- Earthquake field studies (W. J. Spence, C. J. Langer, J. N. Jordan, M)
- Earthquake-induced ground failures (T. L. Youd, M)
- Earthquake-induced landslides (E. L. Harp, M)
- Earthquake-induced sedimentary structures (J. D. Sims, M)
- Earthquake recurrence and history (R. D. Nason, M)
- Eastern United States (R. K. McGuire, D)
- Experimental liquefaction potential mapping (T. L. Youd, M)
- Fault-zone tectonics (J. C. Savage, M)
- Fluid injection, laboratory investigations (J. D. Byerlee, Louis Peselnick, M)
- Geologic and geotechnical factors in ground-motion analysis (R. C. Wilson, M)
- Geologic parameters of seismic source areas (F. A. McKeown, D)
- Ground-motion modeling and prediction (W. B. Joyner, M)
- Ground-motion studies (R. D. Borcherdt, R. P. Maley, M)
- Microearthquake data analysis (W. H. K. Lee, M)
- National Earthquake Information Service (A. C. Tarr, D)
- National Strong-Motion Instrumentation Network (R. B. Matthiesen, M)
- Nicaragua, Central America, technical assistance in establishing center for earthquake hazard reduction (P. L. Ward, M)
- Plate-tectonic studies (E. D. Jackson, M)
- Precursory phenomena (P. L. Ward, M)
- Prediction, animal behavior studies (P. A. Reasenberg, M)
- Recurrence intervals along Quaternary faults (K. L. Pierce, D)
- Relative activity of multiple fault strands (M. G. Bonilla, M)
- Seismic-risk studies (S. T. Algermissen, D)

Earthquake studies—Continued
- Seismic-source studies (W. R. Thatcher, M)
- Seismic studies for earthquake prediction (C. G. Bufe, M)
- Seismicity and Earth structure (J. N. Taggart, D)
- Seismicity patterns in time and space (C. G. Bufe, M)
- Seismological research observatories (J. R. Peterson, Albuquerque, N. Mex.)
- Soil engineering research (T. L. Youd, M)
- Stress studies (C. B. Raleigh, M)
- Synthetic strong-motion seismograms (W. B. Joyner, M)
- Tectonic studies (W. B. Hamilton, D)
- Theoretical seismology (A. F. Espinosa, D)
- Worldwide Network of Standard Seismographs (J. R. Peterson, Albuquerque, N. Mex.)
- *States:*
- Alaska:
  - Earthquake hazards:
    - Anchorage (Ernest Dobrovolny, D)
    - Coastal communities (R. W. Lemke, D)
    - Juneau (R. D. Miller, D)
    - Sitka (L. A. Yehle, D)
    - Southern part (George Plafker, M)
  - Microearthquake studies (R. A. Page, M)
  - Turnagain Arm sediments (A. T. Ovenshine, M)
- California (M, except as otherwise noted):
  - Basement rock studies along San Andreas fault (D. C. Ross)
  - Central California microearthquake studies (C. G. Bufe)
  - Continental Shelf fault studies (S. C. Wolf)
  - Depth of bedrock in the San Francisco Bay region (R. M. Hazlewood)
  - Earthquake hazards:
    - San Francisco Bay region (E. E. Brabb)
    - Southern part (D. M. Morton, Los Angeles)
  - Geodetic strain (W. H. Prescott)
  - Geophysical studies, San Andreas fault (J. H. Healy)
  - Measurement of seismic velocities for seismic zonation (J. F. Gibbs, R. D. Borcherdt, T. E. Fumal)
  - Microearthquake studies:
    - Central part (J. H. Pfluke)
    - New Melones (J. C. Roller)
    - Southern part (D. P. Hill)
  - Recency of faulting:
    - Coastal California Desert (E. H. Pampeyan)
    - Eastern Mojave Desert (W. J. Carr)
  - Tectonics:
    - Central and northern part (W. P. Irwin)
    - Central San Andreas fault (D. B. Burke, T. W. Dibblee, Jr.)
    - Salton Trough tectonics (R. V. Sharp)
    - Southern part (M. M. Clark)
  - Theory of wave propagation in anelastic media (R. D. Borcherdt)
- Colorado, Rangely (C. B. Raleigh, M)
- Idaho, active faults, Snake River Plain (S. S. Oriel, D)
- Missouri, New Madrid fault-zone geophysics (M. F. Kane, D)
- Montana, Yellowstone National Park, microearthquake studies (A. M. Pitt, M)
- Nevada, tectonics, west-central (E. B. Ekren, D)

Earthquake studies—Continued
- New Mexico, seismotectonic analysis, Rio Grande rift (E. H. Baltz, Jr., D)
- South Carolina, microearthquake studies (A. C. Tarr, D)
- Washington (M):
  - Earthquake hazards, Puget Sound region (H. D. Gower, P. D. Snavely, Jr.)
  - Hanford microearthquake studies (J. H. Pfluke)

Engineering geologic studies. *See* Construction and terrain problems; Urban geology.

Environmental assessment:
- Amax Eagle Butte mine (J. D. Unger, l, NC)
- Carter Oil Caballo mine (F. J. Anderson, l, NC)
- Decker mines (N. J. King, w, D)
- Guidelines for administration and management of EIS task forces (K. E. Vanlier, J. W. Allingham, l, NC)
- Guidelines for preparation of EIS's (K. E. Vanlier, J. W. Allingham, l, NC)
- Kerr-McGee East Gillette mine (F. J. Anderson, l, NC)
- Methodology for monitoring impacts of phosphate development, Idaho (L. G. Marcus, l, NC)
- Northern Great Plains, methodological guidebook (B. B. Hanshaw, w, NC)
- Oil-shale supplement (D. L. Schleicher, l, D)
- Peabody Rochelle mine (F. J. Anderson, l, NC)
- Powder River basin uranium (E. S. Santos, D)
- Review of environmental impact statements (L. D. Bonham, l, NC)
- South Florida environment (B. F. McPherson, w, Miami)
- Westmoreland mine (C. W. Lane, w, D)

Environmental geology:
- Quaternary dating applications—overview map (K. L. Pierce, D)
- *States:*
- Montana:
  - Butte region (H. W. Smedes, D)
  - Environmental study of the Big Fork-Avon area (I. J. Witkind, D)
  - Land resources, Helena region (R. G. Schmidt, NC; G. D. Robinson, M)
- Utah, Kaiparowits Plateau coal basin (K. A. Sargent, D)
- *See also* Construction and terrain problems; Land use and environmental impact; Urban geology.

Evapotranspiration:
- Evapotranspiration (F. A. Branson, w, D)
- Evapotranspiration data analyses (T. E. A. van Hylckama, w, Lubbock, Tex.)
- Evapotranspiration theory (O. E. Leppanen, w, Phoenix, Ariz.)
- Mechanics of evaporation (G. E. Koberg, w, D)
- Vegetation ecohydrology (R. M. Turner, w, Tucson, Ariz.)

Extraterrestrial studies:
- Lunar analog studies:
  - Explosion craters (D. J. Roddy, Flagstaff, Ariz.)
- Lunar data synthesis:
  - Imbrium and Serenitatis Basins (J. F. McCauley, Flagstaff, Ariz.)
  - Sample petrology and stratigraphy (H. G. Wilshire, M)
  - Synoptic lunar geology (D. E. Wilhelms, M)

Extraterrestrial studies—Continued
- Lunar sample investigations:
  - Chemical and X-ray fluorescence analysis (H. J. Rose, Jr., NC)
  - Impact metamorphism (E. C. T. Chao, NC)
  - Lunar igneous-textured rocks (O. B. James, NC)
  - Major lunar breccia types (E. C. T. Chao, NC)
  - Mineralogical analyses (R. B. Finkelman, NC)
  - Oxygen fugacities and crystallization sequence (Motoaki Sato, NC)
  - Petrologic studies (Edwin Roedder, NC)
  - Pyroxenes (J. S. Huebner, NC)
- Planetary analog studies, mass movements (E. C. Morris, Flagstaff, Ariz.)
- Planetary investigations:
  - Geologic mapping of Mars (D. H. Scott, J. F. McCauley, Flagstaff, Ariz.)
  - Geologic synthesis of Mars (Harold Masursky, Flagstaff, Ariz.)
  - Image-processing studies (L. A. Soderblom, Flagstaff, Ariz.)
  - Mariner Jupiter-Saturn (L. A. Soderblom, Flagstaff, Ariz.)
  - Mariner Venus-Mercury TV (N. J. Trask, NC)
  - Mars mineralogy and chemistry, Viking lander (Priestley Toulmin III, H. J. Rose, Jr., NC)
  - Mars topographic synthesis (S. S. C. Wu, Flagstaff, Ariz.)
  - Planetary cartography (R. M. Batson, Flagstaff, Ariz.)
  - Radar applications (G. G. Schaber, Flagstaff, Ariz.)
  - Viking mission:
    - Lander (E. C. Morris, Flagstaff, Ariz.)
    - Orbiter TV (M. H. Carr, M)
    - Physical properties of Mars (H. J. Moore, M)
    - Site analysis (Harold Masursky, Flagstaff, Ariz.)

Ferro-alloy metals:
- Chromium:
  - Geochemistry (B. A. Morgan III, NC)
  - Resource studies (T. P. Thayer, NC)
- Molybdenum-rhenium resource studies (R. U. King, D)
- *States:*
- North Carolina, tungsten in Hamme district (J. E. Gair, NC)
- Oregon, John Day area (T. P. Thayer, NC)
- Pennsylvania, State Line district (B. A. Morgan III, NC)

Flood discharge from small drainage areas:
- Colorado (R. K. Livingston, w, D)
- Connecticut (M. D. Thomas, w, Hartford)
- Delaware (R. H. Simmons, w, Dover)
- Florida (W. C. Bridges, w, Tallahassee)
- Maryland (D. H. Carpenter, w, College Park)
- Massachusetts (J. S. Wandle, w, Boston)
- Virginia (E. M. Miller, w, Richmond)

Flood-hazard mapping:
- Alabama (C. O. Ming, w, Montgomery)
- Arizona (B. N. Aldridge, w, Tucson)
- Arkansas (M. S. Hines, w, Little Rock)
- California (J. R. Crippen, w, M)
- Florida (S. D. Leach, w, Tallahassee)
- Connecticut (M. A. Cervione, Jr., w, Hartford)
- Georgia (McGlone Price, w, Doraville)
- Hawaii (C. J. Ewart, w, Honolulu)

Flood-hazard mapping—Continued

Idaho (W. A. Harenberg, w, Boise)
Illinois (B. J. Prugh, w, Champaign)
Indiana (J. B. Swing, w, Indianapolis)
Iowa (O. G. Lara, w, Iowa City)
Kansas (D. B. Richards, w, Lawrence)
Louisiana (A. S. Lowe, w, Baton Rouge)
Maine (R. A. Morrill, w, Augusta)
Massachusetts (S. W. Wandle, Jr., w, Boston)
Michigan (R. L. Knutilla, w, Okemos)
Minnesota (L. C. Guetzkow, w, St. Paul)
Mississippi (K. V. Wilson, w, Jackson)
Missouri (L. D. Hauth, w, Rolla)
Montana (M. V. Johnson, w, Helena)
Nebraska (G. G. Jamison, w, Lincoln)
Nevada (D. O. Moore, w, Carson City)
New Hampshire (S. W. Wandle, Jr., w, Boston, Mass.)
New Jersey (R. E. Gatton, Jr., w, Trenton)
North Carolina (R. W. Coble, w, Raleigh)
North Dakota (O. A. Crosby, w, Bismarck)
Ohio (D. K. Roth, w, Columbus)
Oklahoma (W. B. Mills, w, Oklahoma City)
Oregon (D. D. Harris, w, Portland)
Pennsylvania (L. V. Page, w, Harrisburg)
Puerto Rico (E. D. Cobb, w, San Juan)
South Carolina (W. T. Utter, w, Columbia)
Tennessee (C. R. Gamble, w, Nashville)
Texas (J. D. Bohn, w, Austin)
United States (G. W. Edelen, w, NC)
Vermont (S. W. Wandle, Jr., w, Boston, Mass.)
Virginia (E. M. Miller, w, Richmond)
Washington (E. G. Nassar, w, Tacoma)
West Virginia (G. S. Runner, w, Charleston)
Wisconsin (C. L. Lawrence, w, Madison)
Wyoming (J. F. Wilson, Jr., w, Cheyenne)

Flood-insurance studies:

Alabama (C. O. Ming, w, Montgomery)
Arizona (B. N. Aldridge, w, Tucson)
Arkansas (A. H. Ludwig, w, Little Rock)
California (J. R. Crippen, w, M)
Colorado (R. C. Christensen, w, D)
Connecticut (M. A. Cervione, Jr., w, Hartford)
Florida (S. D. Leach, w, Tallahassee)
Georgia (McGlone Price, w, Doraville)
Idaho (W. A. Harenberg, w, Boise)
Illinois (A. W. Noehre, w, DeKalb)
Indiana (D. H. Rapp, w, Indianapolis)
Iowa (A. J. Heinitz, w, Iowa City)
Kansas (D. B. Richards, w, Lawrence)
Kentucky (C. H. Hannum, w, Louisville)
Louisiana (F. N. Lee, Baton Rouge)
Maine (R. M. Morrill, w, Augusta)
Massachusetts (L. A. Swallow, w, Boston)
Michigan (R. L. Knutilla, w, Okemos)
Minnesota (L. C. Guetzkow, w, St. Paul)
Missouri (L. D. Hauth, w, Rolla)
Montana (M. V. Johnson, w, Helena)
Nebraska (G. G. Jamison, w, Lincoln)
Nevada (C. V. Schroer, w, Carson City)
New Hampshire (L. A. Swallow, w, Boston, Mass.)
New Jersey (R. D. Schopp, w, Trenton)
New Mexico (L. P. Denis, w, Albuquerque)
New York (R. T. Mycyk, w, Albany)

Flood-insurance studies—Continued

North Carolina (N. N. Jackson, w, Raleigh)
Ohio (D. K. Roth, w, Columbus)
Oklahoma (T. L. Huntzinger, w, Oklahoma City)
Oregon (D. D. Harris, w, Portland)
Pennsylvania (Andrew Voytik, w, Harrisburg)
Puerto Rico (J. R. Harkins, w, San Juan)
Rhode Island (L. A. Swallow, w, Boston, Mass.)
South Carolina (B. H. Whetstone, w, Columbia)
Texas (J. D. Bohn, w, Austin)
Virginia (J. R. Mohler, w, Marion)
Washington (C. H. Swift, w, Tacoma)
Wisconsin (C. L. Lawrence, w, Madison)

Flood investigations:

Countermeasures, scour and erosion (J. C. Bruce, w, M)
Documentation of extreme floods (H. H. Barnes, Jr., w, NC)
Model bridge-site report (H. H. Barnes, w, NC)
States:
Alabama, floods, bridge-site studies (C. O. Ming, w, Montgomery)
Arkansas (M. S. Hines, w, Little Rock)
California:
- Hydraulic techniques—HUD studies (D. E. Burkham, w, Sacramento)
- Lake Playa flood study (M. W. Busby, w, Laguna Niguel)

Colorado (w, D):
- Flood data for Colorado (J. F. McCain)
- Flood-plain mapping (J. F. McCain)
- Mountain rainfall floods (J. F. McCain)

Florida (w, Tampa):
- Flood-hazard evaluation, Myakka River (W. R. Murphy, Jr.)
- Regional flood-frequency study (J. F. Turner)

Georgia, Atlanta flood characteristics (E. J. Inman, w, Doraville)
Idaho (W. A. Harenberg, w, Boise)
Illinois:
- Flood flows in small basins (G. W. Curtis, w, Champaign)
- Urban floods in northeastern Illinois (H. E. Allen, Jr., w, DeKalb)

Indiana, flood frequency (L. G. Davis, w, Indianapolis)
Iowa (w, Iowa City):
- Flood data for selected bridge sites (O. G. Lara)
- Flood profiles, statewide (O. G. Lara)
- Flood information, Linn County (O. G. Lara)

Kentucky, small-area flood hydrology (J. N. Sullivan, Jr., w, Louisville)
Louisiana, bridge site computations (F. N. Lee, w, Baton Rouge)
Minnesota, flood-plain studies (L. C. Guetzkow, w, St. Paul)
Mississippi (w, Jackson):
- Hydraulic performance of bridges (B. E. Colson)
- Multiple-bridge hydraulics (B. E. Colson)

Nebraska, magnitude and frequency of floods (E. W. Beckman, w, Lincoln)
Nevada (w, Carson City):
- Environmental study, western Nevada (P. A. Glancy)
- Flood investigations (Lynn Harmsen)

Flood investigations—Continued
States—Continued
New Jersey, flood peaks and flood plains (S. J. Stankowski, w, Trenton)
New Mexico, flood analysis (A. G. Scott, w, Santa Fe)
New York, peak discharge of ungaged streams (Bernard Dunn, w, Albany)
Oklahoma, small watersheds (W. O. Thomas, Jr., w, Oklahoma City)
South Carolina (w, Columbia):
Flood frequency statewide (B. H. Whetstone)
Hydraulic site reports (B. H. Whetstone)
Tennessee (W. J. Randolph, w, Nashville)
Virginia:
Hydrology, Wytheville fish hatchery (J. R. Hendrick, w, Marion)
Statewide (E. M. Miller, w, Richmond)
Washington (w, Tacoma):
Flood-inundation mapping (J. H. Bartells)
Chehalis water resources (K. L. Walters)
Wisconsin (w, Madison):
Dane County, flood-inundation study (R. C. Grant)
Digital model of floodflow in Rock River (W. R. Krug)
Flood-control effects on Trout Creek (R. S. Grant)
Maximum flood at Chippewa Flowage (W. R. Krug)
St. Croix scenic river waste study (R. S. Grant)
Wyoming, flood investigations (G. S. Craig, w, Cheyenne)

Fluorspar:
Colorado, Bonanza and Poncha Springs quadrangles (R. E. Van Alstine, NC)
Illinois-Kentucky district, regional structure and ore controls (D. M. Pinckney, D)

Foreign nations, geologic investigations:
Brazil, mineral resources and geologic training (S. A. Stanin, Rio de Janeiro)
Poland:
Characteristics of coal basins (K. J. Englund, NC)
Geochemistry of coal and computerization of coal data (V. E. Swanson, D)
Saudi Arabia, crystalline shield, geologic and mineral reconnaissance (F. S. Simons, Jiddah)
Spain, marine mineral resources (P. D. Snavely, Jr., M)
Thailand, remote-sensing program (J. O. Morgan, Bangkok)

Foreign nations, hydrologic investigations. *See* Water resources, foreign countries.

Fuels, organic. *See* Coal; Oil shale; Petroleum and natural gas.

Gas, natural. *See* Petroleum and natural gas.

Geochemical distribution of the elements:
Basin and Range granites (D. E. Lee, D)
Botanical exploration and research (H. L. Cannon, D)
Coding and retrieval of geologic data (T. G. Lovering, D)
Data of geochemistry (Michael Fleischer, NC)
Data systems (R. V. Mendes, D)
Element availability:
Soils (R. C. Severson, D)
Vegetation (L. P. Gough, D)
Light stable isotopes (J. R. O'Neil, M)
Phosphoria Formation, organic carbon and trace element distribution (E. K. Maughan, D)

Geochemical distribution of the elements—Continued
Sedimentary rocks, chemical composition (T. P. Hill, D)
Selenium, tellurium, and thallium, geochemical exploration (H. W. Lakin, D)
Statistical geochemistry and petrology (A. T. Miesch, D)
Tippecanoe sequence, Western Craton (L. G. Schultz, D)
Trace elements in oil shale (W. E. Dean, Jr., D)
Urban geochemistry (H. A. Tourtelot, D)
Western coal regions:
Geochemical survey of rocks (R. J. Ebens, D)
Geochemical survey of soils (R. R. Tidball, D)
Geochemical survey of vegetation (J. A. Erdman, D)
Geochemical survey of waters (G. L. Feder, D)
States:
California, Sierra Nevada batholith, geochemical study (F. C. W. Dodge, M)
Colorado, Mt. Princeton igneous complex (Priestley Toulmin III, NC)
Pennsylvania, greater Pittsburgh region, environmental geochemistry (R. P. Biggs, Carnegie)

Geochemical prospecting methods:
Application and evaluation of methods of chemical analysis to diverse geochemical environments (J. G. Viets, D)
Application of silver-gold geochemistry to exploration (H. W. Lakin, D)
Botanical exploration and research (H. L. Cannon, D)
Development of effective on-site methods of chemical analysis for geochemical exploration (W. L. Campbell, D)
Elements in organic-rich material (F. N. Ward, D)
Gamma-ray spectrometry (J. A. Pitkin, D)
Geochemical characterization of metallogenic provinces and mineralized areas (G. J. Neuerburg, D)
Geochemical exploration:
Glaciated areas (H. V. Alminas, D)
Research in arctic, alpine, and subalpine regions (J. H. McCarthy, D)
Techniques:
Alpine and subalpine environments (G. C. Curtin, D)
Arid environments (M. A. Chaffee, D)
Gold compositional analysis in mineral exploration (J. C. Antweiler, D)
Instrumentation development (R. C. Bigelow, D)
Jasperoid, relations to ore deposits (T. G. Lovering, D)
Lateritic areas, southern Appalachian Mountains (W. R. Griffitts, D)
Mercury, geochemistry (A. P. Pierce, D)
Mineral exploration methods (G. B. Gott, D)
Mineralogical techniques in geochemical exploration (Theodore Botinelly, D)
New mineral storage and identification program (George Van Trump, Jr., D)
Ore-deposit controls (A. V. Heyl, Jr., D)
Pattern recognition and clustering methods for the graphical analysis of geochemical data (J. B. Fife, D)
Research in methods of spectrographic analysis for geochemical exploration (E. L. Mosier, D)
Sulfides, accessory in igneous rocks (G. J. Neuerberg, D)
Surface and ground water in geochemical exploration (G. A. Nowlan, D)

Geochemical prospecting methods—Continued
Volatile elements and compounds in geochemical exploration (M. E. Hinkle, D)
States:
Alaska, geochemical exploration techniques (G. C. Curtin, D)
New Mexico, Basin and Range part, geochemical reconnaissance (W. R. Griffitts, D)

Geochemistry, experimental:
Environment of ore deposition (P. B. Barton, Jr., NC)
Experimental mineralogy (R. O. Fournier, M)
Fluid inclusions in minerals (Edwin Roedder, NC)
Fluid zonation in metal deposits (J. T. Nash, M)
Geologic thermometry (J. S. Huebner, NC)
Hydrothermal alteration (J. J. Hemley, NC)
Impact metamorphism (E. C. T. Chao, NC)
Kinetics of igneous processes (H. R. Shaw, NC)
Late-stage magmatic processes (G. T. Faust, NC)
Mineral equilibria, low-temperature (E-an Zen, NC)
Neutron activation (F. E. Senftle, NC)
Oil shale:
Colorado, Utah, and Wyoming (W. E. Dean, Jr., D)
Organic geochemistry (R. E. Miller, D)
Organic geochemistry (J. G. Palacas, D)
Organometallic complexes, geochemistry (Peter Zubovic, NC)
Solution-mineral equilibria (C. L. Christ, M)
Stable isotopes and ore genesis (R. O. Rye, D)
Statistical geochemistry (A. T. Miesch, D)

Geochemistry, water:
Chemical constituents in ground water, spatial distribution (William Back, w, NC)
Chemical reactions at mineral surfaces (J. D. Hem, w, M)
Computer modeling of rock-water interactions (J. L. Haas, Jr., NC)
Elements, distribution in fluvial and brackish environments (V. C. Kennedy, w, M)
Factors determining solute transfer in the unsaturated zone (Jacob Rubin, w, M)
Gases, complexes in water (D. W. Fischer, w, NC)
Geochemistry of geothermal systems (Ivan Barnes, w, M)
Geochemistry of San Francisco Bay waters and sediments (D. H. Peterson, w, M)
Geothermal trace-element reactions (E. A. Jenne, w, M)
Hydrologic applications of quantitative mineralogy (Robert Schoen, w, NC)
Hydrosolic metals and related constituents in natural water, chemistry (J. D. Hem, w, M)
Interaction of minerals and water in saline environments (B. F. Jones, w, NC)
Mineralogic controls of the chemistry of ground water (B. B. Hanshaw, w, NC)
Organic geochemistry (R. L. Malcolm, w, D)
Trace-element partitioning (E. A. Jenne, w, M)
Western coal regions, geochemical survey of waters (G. L. Feder, D)
See also Quality of water.

Geochemistry and petrology, field studies:
Basalt, genesis (T. L. Wright, NC)
Basin and Range granites (D. E. Lee, D)
Epithermal deposits (R. G. Worl, D)
Geochemical studies in southeastern States (Henry Bell III, NC)

Geochemistry and petrology, field studies—Continued
Geochemistry of diagenesis (K. J. Murata, M)
Geochemistry of Tippecanoe Sequence, Western Craton (L. G. Schultz, D)
Inclusions in basaltic rocks (E. D. Jackson, M)
Layered Dufek intrusion, Antarctica (A. B. Ford, M)
Layered intrusives (N. J. Page, M)
Mercury, geochemistry and occurrence (A. P. Pierce, D)
Niobium and tantalum, distribution in igneous rocks (David Gottfried, NC)
Organic petrology of sedimentary rocks (N. H. Bostick, D)
Rare-earth elements, resources and geochemistry (J. W. Adams, D)
Regional geochemistry (W. E. Dean, Jr., D)
Regional metamorphic studies (H. L. James, M)
Residual minor elements in igneous rocks and veins (George Phair, NC)
Solution transport of heavy metals (G. K. Czamanske, M)
Submarine volcanic rocks, properties (J. G. Moore, M)
Syngenetic ore deposition (C. M. Conway, M)
Thermal waters, origin and characteristics (D. E. White, M)
Trace elements in oil shale (W. E. Dean, Jr., D)
Trondhjemites, major and minor elements, isotopes (Fred Barker, D)
Ultramafic rocks, petrology of alpine types (R. G. Coleman, M)
Uranium, radon, and helium—gaseous emanation detection (G. M. Reimer, D)
Western coal regions:
Geochemical survey of rocks (R. J. Ebens, D)
Geochemical survey of soils (R. R. Tidball, D)
Geochemical survey of vegetation (J. A. Erdman, D)
States:
Alaska (M):
La Perouse layered intrusion (R. A. Loney)
Metasedimentary and metaigneous rocks, southwestern Brooks Range (I. L. Tailleur)
Arizona (M):
Ray program:
Mineral Mountain (T. G. Theodore)
Silicate mineralogy, geochemistry (N. G. Banks)
Stocks (S. C. Creasey)
California:
Geochemistry of sediments, San Francisco Bay (D. S. McCulloch, M)
Granitic rocks of Yosemite National Park (D. L. Peck, NC)
Kings Canyon National Park (J. G. Moore, M)
Long Valley caldera-Mono Craters volcanic rocks (R. A. Bailey, NC)
Sierra Nevada xenoliths (J. P. Lockwood, M)
Colorado:
Petrology of Mt. Princeton igneous complex (Priestley Toulmin III, NC)
Tertiary-Laramide intrusives (E. J. Young, D)
Hawaii, ankaramites (M. H. Beeson, M)
Idaho, WoodRiverdistrict (W. E. Hall, M)
Idaho-Montana-Wyoming, petrology of the Yellowstone Plateau volcanic field (R. L. Christiansen, M)

Geochemistry and petrology, field studies—Continued

Montana:

Diatremes, Missouri River Breaks (B. C. Hearn, Jr., NC)

Geochronology, north-central Montana (B. C. Hearn, Jr., NC; R. F. Marvin, R. E. Zartman, D)

Wolf Creek area, petrology (R. G. Schmidt, NC)

Nevada, igneous rocks and related ore deposits (M. L. Silberman, M)

Pennsylvania, geochemistry of Pittsburgh urban area (H. A. Tourtelot, D)

South Dakota, Keystone pegmatite area (J. J. Norton, Rapid City)

Geochronological investigations:

Carbon-14 method (Meyer Rubin, NC)

Geochronology and rock magnetism (G. B. Dalrymple, M)

Geochronology of uranium ores and their host rocks (K. R. Ludig, D)

Igneous rocks and deformational periods (R. W. Kistler, M)

Lead-uranium, lead-thorium, and lead-alpha methods (T. W. Stern, NC)

Magnetic chronology, Colorado Plateau and environs (D. P. Elston, E. M. Shoemaker, Flagstaff, Ariz.)

Quaternary dating techniques, numerical and relative-age (K. L. Pierce, D)

Radioactive-disequilibrium studies (J. N. Rosholt, D)

San Francisco volcanic field (P. E. Damon, University of Arizona)

States:

Alaska, K-Ar dates, southwest Brooks Range (I. L. Tailleur, M; R. B. Forbes, D. L. Turner, Fairbanks)

Colorado, geochronology of Denver area (C. E. Hedge, D)

See also Isotope and nuclear studies.

Geologic mapping:

Map scale smaller than 1:62,500:

Antarctica, Dufek Massif and Forrestal Range, Pensacola Mountains (A. B. Ford, M)

Belt basin study (J. E. Harrison, D)

Columbia River basalt (D. A. Swanson, M)

States:

Alaska (M):

Ambler River and Baird Mountains quadrangles (I. L. Tailleur)

Charley River quadrangle (E. E. Brabb)

Craig quadrangle (G. D. Eberlein, Michael Churkin, Jr.)

Delong Mountains quadrangle (I. L. Tailleur)

Geologic map (H. M. Beikman)

Glacier Bay National Monument (D. A. Brew)

Hughes-Shungnak area (W. W. Patton, Jr.)

Iliamna quadrangle (R. L. Detterman)

Juneau and Taku River quadrangles (D. A. Brew)

Metamorphic facies map (D. A. Brew)

Natural landmarks investigation (R. L. Detterman)

St. Lawrence Island (W. W. Patton, Jr.)

Arizona (Flagstaff):

North-central part (D. P. Elston)

Phoenix 2-degree quadrangle (T. N. V. Karlstrom)

Shivwits Plateau (Ivo Lucchitta)

Geologic mapping—Continued

Map scale smaller than 1:62,500—Continued

States—Continued

Arkansas (B. R. Haley, Little Rock)

California (M):

Tectonic studies, Great Valley area (J. A. Bartow, D. E. Marchand)

Environmental maps for land use planning (E. H. Pampeyan)

Colorado (D):

Colorado Plateau geologic map (D. D. Haynes)

Denver 2-degree quadrangle (B. H. Bryant)

Geologic map (O. L. Tweto)

Greeley 2-degree quadrangle, western half (W. A. Braddock)

Leadville 2-degree quadrangle (O. L. Tweto)

Montrose 2-degree quadrangle (W. J. Hail, Jr.)

Pueblo 2-degree quadrangle (G. R. Scott)

Sterling 2-degree quadrangle (G. R. Scott)

Idaho (D):

Challis Volcanics (D. H. McIntyre)

Dubois 2-degree quadrangle (D. L. Schleicher)

Idaho Falls 2-degree quadrangle (D. L. Schleicher)

Preston 2-degree quadrangle (S. S. Oriel)

Snake River Plain, central part, volcanic petrology (H. E. Malde)

Snake River Plain region, eastern part (S. S. Oriel)

Missouri, Rolla 2-degree quadrangle, mineral-resource appraisal (W. P. Pratt, D)

Montana, White Sulphur Springs 2-degree quadrangle (M. W. Raynolds, D)

Nevada:

Elko County:

Central (K. B. Ketner, D)

Countywide (R. A. Hope, M)

Western (R. R. Coats, M)

Geologic map (J. H. Stewart, M)

Lincoln County, Tertiary rocks (G. L. Dixon, D)

New Mexico (D):

North Church Rock area (A. R. Kirk)

Sanostee (A. C. Huffman, Jr.)

Santa Fe 2-degree quadrangle, western half (E. H. Baltz, Jr.)

Socorro 2-degree quadrangle (G. O. Bachman)

North Carolina, Charlotte 2-degree sheet (Richard Goldsmith, NC)

South Carolina, Charlotte 2-degree sheet (Richard Goldsmith, NC)

South Carolina-Georgia-North Carolina, Greenville 2-degree quadrangle (A. E. Nelson, NC)

Utah (M):

Delta 2-degree quadrangle (H. T. Morris)

Tooele 2-degree quadrangle (W. J. Moore)

Washington, Wenatchee 2-degree sheet (R. W. Tabor, R. B. Waitt, Jr., V. A. Frizzell, Jr., M)

Wyoming:

Geologic map (J. D. Love, Laramie)

Preston 2-degree quadrangle (S. S. Oriel, D)

Teton Wilderness (J. D. Love, Laramie)

Geologic mapping—Continued

Map scale 1:62,500, and larger:

States and territories:

Alaska:

- Anatuvuk Pass (G. B. Shearer, c, Anchorage)
- Anchorage area (Ernest Dobrovolny, D)
- Bering River coal field (R. B. Sanders, c, Anchorage)
- Cape Beaufort-Corwin Bluffs coal field (J. E. Callahan, c, Anchorage)
- Geology and mineral resources of the Ketchikan quadrangle (H. C. Berg, M)
- Juneau area (R. D. Miller, D)
- Kukpowruk River coal field (J. E. Callahan, c, Anchorage)
- Nelchina area, Mesozoic investigations (Arthur Grantz, M)
- Nenana coal investigations (Clyde Wahrhaftig, M)
- Nome area (C. L. Hummel, M)
- Utukok River and Kokolik River coal field (J. E. Callahan, c, Anchorage)

Arizona:

- Bowie zeolite area (L. H. Godwin, c, NC)
- Cummings Mesa quadrangle (Fred Peterson, c, D)
- Hackberry Mountain area (D. P. Elston, Flagstaff)
- Mt. Wrightson quadrangle (H. D. Drewes, D)
- Ray district, porphyry copper (H. R. Cornwall, M)
- Sedona area (D. P. Elston, Flagstaff)
- Western Arizona tectonic studies (Ivo Lucchitta, Flagstaff)

California (M, except as otherwise noted):

- Coast Range, ultramafic rocks (E. H. Bailey)
- Condrey Mountain and Hornbrook quadrangles (P. E. Hotz)
- Long Valley caldera (R. A. Bailey, NC)
- Malibu Beach and Topanga quadrangles (R. F. Yerkes)
- Merced Peak quadrangle (D. L. Peck, NC)
- Northern Coast Ranges (K. F. Fox, Jr.)
- Palo Alto, San Mateo, and Montara Mountain quadrangles (E. H. Pampeyan)
- Peninsular Ranges (V. R. Todd, La Jolla)
- Point Dume and Triunfo Pass quadrangles (R. H. Campbell)
- Regional fault studies (E. J. Helley, D. G. Herd, B. F. Atwater)
- Ryan quadrangle (J. F. McAllister)
- Santa Lucia Range (V. M. Seiders)
- Searles Lake area (G. I. Smith)
- Sierra Nevada batholith (P. C. Bateman)
- The Geysers-Clear Lake area (R. J. McLaughlin)
- Western Santa Monica Mountains (R. H. Campbell)

Colorado (D, except as otherwise noted):

- Aspen 15-minute quadrangle (B. H. Bryant)
- Barcus Creek quadrangle (W. J. Hail)
- Barcus Creek SE quadrangle (W. J. Hail)
- Bonanza quadrangle (R. E. Van Alstine, NC)

Geologic mapping—Continued

Map scale 1:62,500 and larger—Continued

States and territories—Continued

Colorado (D, except as otherwise noted)—Continued

- Buckhorn Lakes quadrangle (R. G. Dickinson, c, D)
- Central City area (R. B. Taylor)
- Citadel Plateau (G. A. Izett, c, D)
- Coal mine deformation studies, Somerset mining district (C. R. Dunrud)
- Cochetopa area (J. C. Olson)
- Courthouse Mountain quadrangle (R. G. Dickinson, c, D)
- Denver basin, Tertiary coal zone (P. E. Soister, c, D)
- Denver metropolitan area (R. M. Lindvall)
- Disappointment Valley, geology and coal resources (D. E. Ward)
- Front Range, northeastern part, Fort Collins area (W. A. Braddock)
- Northern Park Range (G. L. Snyder)
- Poncha Springs quadrangle (R. E. Van Alstine, NC)
- Rangely NE quadrangle (R. S. Garrigues, c, D)
- Rocky Mountain National Park (W. A. Braddock)
- Rough Gulch quadrangle (W. J. Hail)
- Rustic quadrangle (K. L. Shaver)
- Savery quadrangle (C. S. V. Barclay, c, D)
- Smizer Gulch quadrangle (W. J. Hail)
- Strasburg SW quadrangle (P. E. Soister, c, D)
- Thornburgh quadrangle (M. J. Reheis, c, D)
- Ward and Gold Hill quadrangles (D. J. Gable)
- Washboard Rock quadrangle (R. G. Dickinson, c, D)
- Watkins and Watkins SE quadrangles (P. E. Soister, c, D)

Connecticut:

- Cooperative mapping program (M. H. Pease, Jr., Boston, Mass.)
- Taconic sequence (E-an Zen, NC)

Idaho (D, except as otherwise noted):

- Bayhorse area (S. W. Hobbs)
- Black Pine Mountains (J. F. Smith, Jr.)
- Boulder Mountains (C. M. Tschanz)
- Goat Mountain quadrangle (M. H. Staatz)
- Grouse quadrangle (B. A. Skipp)
- Hawley Mountain quadrangle (W. J. Mapel)
- Malad SE quadrangle (S. S. Oriel)
- Montour quadrangle (H. E. Malde)
- Palisades Dam quadrangle (D. A. Jobin, c, D)
- Patterson quadrangle (E. T. Ruppel)
- Strevell quadrangle (J. F. Smith)
- Upper and Lower Red Rock Lake quadrangles (I. J. Witkind)
- Wood River district (W. E. Hall, M)
- Yellow Pine quadrangle (B. F. Leonard)

Kentucky, cooperative mapping program (E. R. Cressman, Lexington)

Maine:

- Blue Hill quadrangle (D. B. Stewart, NC)
- Castine quadrangle (D. B. Stewart, NC)
- Orland quadrangle (D. R. Wones, NC)

Geologic mapping—Continued

Map scale 1:62,500 and larger—Continued

States and territories—Continued

Maine—Continued

- Rumford quadrangle (R. H. Moench, D)
- The Forks quadrangle (F. C. Canney, D)

Maryland (NC):

- Delmarva Peninsula (J. P. Owens)
- Northern Coastal Plain (J. P. Minard)
- Western Maryland Piedmont (M. W. Higgins)

Massachusetts:

- Boston and vicinity (C. A. Kaye, Boston)
- Cooperative mapping program (M. H. Pease, Jr., Boston)
- Taconic sequence (E-an Zen, NC)

Michigan, Gogebic Range, western part (R. G. Schmidt, NC)

Minnesota, Vermilion greenstone belt (P. K. Sims, D)

Montana:

- Birney SW quadrangle (S. P. Buck, c, Casper, Wyo.)
- Cooke City quadrangle (J. E. Elliott, D)
- Craig quadrangle (R. G. Schmidt, NC)
- Crazy Mountains Basin (B. A. Skipp, D)
- Decker quadrangle (B. E. Law, c, D)
- Elk Park quadrangle (H. W. Smedes, D)
- Holmes Ranch quadrangle (N. E. Micklich, c, Casper, Wyo.)
- Jordan quadrangle (G. D. Mowat, c, Billings)
- Lemhi Pass quadrangle (M. H. Staatz, D)
- Melrose phosphate field (G. D. Fraser, c, D)
- Northern Pioneer Range, geologic environment (E-an Zen, NC)
- Pearl School quadrangle (G. L. Galyardt, c, Casper, Wyo.)
- Spring Gulch quadrangle (N. E. Micklich, c, Casper, Wyo.)
- Taintor Desert quadrangle (S. P. Buck, c, Casper, Wyo.)
- Tongue River Dam quadrangle (Juliana Waring, c, Casper, Wyo.)
- Wolf Creek area, petrology (R. G. Schmidt, NC)

Nebraska, McCook 2-degree quadrangle (G. E. Prichard, D)

Nevada:

- Austin quadrangle (E. H. McKee, M)
- Bellevue Peak quadrangle (T. B. Nolan, NC)
- Carlin region (J. F. Smith, Jr., D)
- Jordan Meadow and Disaster Peak quadrangles (R. C. Greene, M)
- Kobeh Valley (T. B. Nolan, NC)
- Midas-Jarbidge area (R. R. Coats, M)
- Round Mountain and Manhattan quadrangles (D. R. Shawe, D)
- Spruce Mountain 4 quadrangle (G. D. Fraser, c, D)

New Hampshire, cooperative mapping program, surficial (Carl Koteff, Boston, Mass.)

New Mexico:

- Acoma area (C. H. Maxwell, D)
- Alamosa Mesa West quadrangle (D. B. Umshler, c, Roswell)
- Church Rock-Smith Lake (C. T. Pierson, D)
- Cretaceous stratigraphy, San Juan basin (E. R. Landis, D)
- Gallup East quadrangle (E. D. Patterson, c, Roswell)
- Gallup West quadrangle (J. E. Fassett, c, Farmington)
- Hillsboro quadrangle (D. C. Hedlund, D)
- Iron Mountain (A. V. Heyl, Jr., D)
- Manuelito quadrangle (J. E. Fassett, c, Farmington)
- Manzano Mountains (D. A. Myers, D)
- Ojo Encino Mesa quadrangle (D. B. Umshler, c, Roswell)
- Pinos Altos Range (T. L. Finnell, D)
- Pueblo Alto Trading Post quadrangle (R. W. Jentgen, c, Farmington)
- Raton coal basin, western part (C. L. Pillmore, D)
- Samson Lake quadrangle (J. E. Fassett, c, Farmington)
- Star Lake quadrangle (J. E. Fassett, c, Farmington)
- Tanner Lake quadrangle (D. B. Umshler, c, Roswell)
- Twin Butte quadrangle (M. L. Millgate, c, Farmington)
- Valles Mountains, petrology (R. L. Smith, NC)

New York (NC):

- Pope Mills and Richville quadrangles (C. E. Brown)
- Taconic sequence (E-an Zen)

North Carolina, central Piedmont (A. A. Stromquist, D)

North Dakota:

- Clark Butte 15-minute quadrangle (G. D. Mowat, c, Billings, Mont.)
- North Almont quadrangle (H. L. Smith, c, D)

Pennsylvania (NC):

- Northern anthracite field (M. J. Bergin)
- Southern anthracite field (G. H. Wood, Jr.)
- Wind Gap and adjacent quadrangles (J. B. Epstein)

Puerto Rico (R. D. Krushensky, NC)

South Dakota:

- Black Hills Precambrian (J. A. Redden, Hill City)
- Keystone pegmatite area (J. J. Norton, Rapid City)

Texas, Tilden-Loma Alta area (K. A. Dickinson, D)

Utah (c, D, unless otherwise noted):

- Basin Canyon quadrangle (Fred Peterson)
- Big Hollow Wash quadrangle (Fred Peterson)
- Blackburn Canyon quadrangle (Fred Peterson)
- Butler Valley quadrangle (W. E. Bowers)
- Canaan Peak quadrangle (W. E. Bowers)
- Coal mine bumps, Sunnyside mining district (F. W. Osterwald, D)
- Collet Top quadrangle (H. D. Zeller)
- Confusion Range (R. K. Hose, M)
- Crawford Mountains (W. C. Gere, c, M)

Geologic mapping—Continued
Map scale 1:62,500 and larger—Continued
States and territories—Continued
Utah (c, D, unless otherwise noted)—Continued
East-of-the-Navajo quadrangle (H. D. Zeller)
Fourmile Bench quadrangle (W. E. Bowers)
Horse Flat quadrangle (H. D. Zeller)
Horse Mountain quadrangle (W. E. Bowers)
Jessen Butte quadrangle (E. M. Schell, c, Casper, Wyo.)
Matlin Mountains (V. R. Todd, M)
Needle Eye Point quadrangle (H. D. Zeller)
Oak City area (D. J. Varnes, D)
Ogden 4 NW quadrangle (R. J. Hite)
Pete's Cove quadrangle (H. D. Zeller)
Salt Lake City and vicinity (Richard VanHorn, D)
Sheeprock Mountains, West Tintic district (H. T. Morris, M)
Ship Mountain Point quadrangle (H. D. Zeller)
Sunset Flat quadrangle (Fred Peterson)
Wah Wah Summit quadrangle (L. F. Hintze, Salt Lake City)
Wasatch Front surficial geology (R. D. Miller, D)
Willard Peak area (M. D. Crittenden, Jr., M)
Virginia (NC):
Culpeper basin (K. Y. Lee)
Delmarva Peninsula (J. P. Owens)
Northern Blue Ridge (G. H. Espenshade)
Rapidan-Rappahannock (Louis Pavlides)
Washington:
Chewelah No. 4 quadrangle (F. K. Miller, M)
Glacier Park area (F. W. Cater, Jr., D)
Northern Okanogan Highlands (C. D. Rinehart, M)
Olympic Peninsula, eastern part (W. M. Cady, D)
Stevens County (R. G. Yates, M)
Togo Mountain quadrangle (R. C. Pearson, D)
Wisconsin, Black River Falls and Hatfield quadrangles (Harry Klemic, NC)
Wyoming (c, D, unless otherwise noted):
Acme quadrangle (B. E. Barnum)
Albany and Keystone quadrangles (M. E. McCallum, D)
Alkali Butte quadrangle (M. W. Reynolds, D)
Appel Butte quadrangle (G. L. Galyardt)
Badwater Creek (R. E. Thaden, D)
Bailey Lake quadrangle (M. L. Schroeder)
Beaver Creek Hills quadrangle (E. I. Winger, c, Casper)
Betty Reservoir NE quadrangle (F. B. Kistner, c, Casper)
Browns Hill quadrangle (C. S. V. Barclay)
Cottonwood Rim quadrangle (C. S. V. Barclay)
Coyote Draw quadrangle (G. L. Galyardt)
Crawford Mountains (W. C. Gere, c, M)
Deer Creek quadrangle (M. L. Schroeder)
Devils Tooth quadrangle (W. G. Pierce, M)
Eagle Rock quadrangle (S. P. Buck, c, Casper)
Fortin Draw quadrangle (B. E. Law)
Four Bar-J Ranch quadrangle (G. L. Galyardt)
Gillette East quadrangle (B. E. Law)

Geologic mapping—Continued
Map scale 1:62,500 and larger—Continued
States and territories—Continued
Wyoming (c, D, unless otherwise noted)—Continued
Gillette West quadrangle (B. E. Law)
Grand Teton National Park (J. D. Love, Laramie)
Greenhill quadrangle (S. P. Buck, c. Casper)
Grieve Reservoir quadrangle (C. S. V. Barclay)
Gros Ventre Range (F. S. Simons)
Hilight quadrangle (W. J. Purdon, c, Casper)
Hultz Draw quadrangle (E. I. Winger, c, Casper)
Ketchum Buttes quadrangle (C. S. V. Barclay)
Little Thunder Reservoir quadrangle (G. C. Martin, c, Casper)
Monarch quadrangle (B. E. Barnum)
Moyer Springs quadrangle (B. E. Law)
Neil Butte quadrangle (S. P. Buck, c, Casper)
North Star School NE quadrangle (S. P. Buck, c, Casper)
North Star School NW quadrangle (S. P. Buck, c, Casper)
North Star School SW quadrangle (W. J. Purdon, c, Casper)
North Star School SE quadrangle (W. J. Purdon, c, Casper)
Open A Ranch quadrangle (G. C. Martin, c, Casper)
Oriva quadrangle (B. E. Law)
Pickle Pass quadrangle (M. L. Schroeder)
Pine Creek quadrangle (D. A. Jobin)
Pine Mountain-Oil Mountain area (G. J. Kerns, c, Casper)
Piney Canyon NW quadrangle (G. C. Martin, c, Casper)
Piney Canyon SW quadrangle (J. E. Goolsby, c, Casper)
Pleasantdale quadrangle (S. L. Grazis)
Reid Canyon quadrangle (G. J. Kerns, c, Casper)
Reno Junction quadrangle (W. J. Purdon, c, Casper)
Reno Reservoir quadrangle (G. C. Martin, c, Casper)
Rough Creek quadrangle (S. P. Buck, c, Casper)
Saddle Horse Butte quadrangle (S. L. Grazis)
Savery quadrangle (C. S. V. Barclay)
Scaper Reservoir quadrangle (S. L. Grazis)
Sheridan quadrangle (E. I. Winger, c, Casper)
Sheridan Pass quadrangle (W. L. Rohrer, c, Casper)
Square Top Butte quadrangle (G. J. Kerns, c, Casper)
Teckla quadrangle (J. E. Goolsby, c, Casper)
Teckla SW quadrangle (J. E. Goolsby, c, Casper)
The Gap quadrangle (G. L. Galyardt)
The Gap SW quadrangle (S. L. Grazis)
Tullis quadrangle (C. S. V. Barclay)
Turnercrest NE quadrangle (G. C. Martin, c, Casper)
Wapiti quadrangle (W. G. Pierce, M)
Weston SW quadrangle (R. W. Jones, c, Casper)

Geomagnetism:
External geomagnetic-field variations (W. H. Campbell, D)

Geomagnetism—Continued
- Geomagnetic-data analysis (C. O. Stearns, D)
- Geomagnetic observatories (J. D. Wood, D)
- Geomagnetic secular variation (L. R. Alldredge, D)
- Magnetic-field analysis and U.S. charts (E. B. Fabiano, D)
- World magnetic charts and analysis (E. B. Fabiano, D)

Geomorphology:
- Channel adjustment, Cochiti Dam (J. D. Dewey, w, Albuquerque, N. Mex.)
- Forest geomorphology, Pacific coast (R. J. Janda, w, M)
- Morphology, provenance, and movement of desert sand (E. D. McKee, D)
- Quaternary landforms and deposits interpreted from Landsat–1 imagery, Midwest and Geat Plains (R. B. Morrison, D)
- Stream channelization (J. C. Brice, w, M)
- Studies of erosion control (N. J. King, w, M)
- *States:*
- Arizona, post-1890 A.D. erosion features interpreted from Landsat–1 imagery (R. B. Morrison, D)
- Idaho, surficial geology of eastern Snake River Plain (W. E. Scott, M. D. Hait, Jr., D)
- Massachusetts, sea-cliff erosion studies (C. A. Kaye, Boston)
- New Mexico, Chaco Canyon National Monument (H. E. Malde, D)
- Wyoming (D):
  - Wind River Mountains, Quaternary geology (G. M. Richmond)
  - Yellowstone National Park, glacial and postglacial geology (G. M. Richmond)
- *See also* Sedimentology; Geochronological investigations.

Geophysics, regional:
- Airborne and satellite research:
  - Aeromagnetic studies (M. F. Kane, D)
  - Electromagnetic research (F. C. Frischknecht, D)
  - Regional studies (Isidore Zietz, NC)
- Antarctica, Pensacola Mountains, geophysical studies (J. C. Behrendt, Woods Hole, Mass.)
- Basin and Range geophysical studies (W. E. Davis, M)
- Crust and upper mantle:
  - Aeromagnetic interpretation of metamorphic rocks (Isidore Zietz, NC)
  - Aeromagnetic studies of the United States (Isidore Zietz, NC)
  - Analysis of traveltime data (J. C. Roller, M)
  - Seismicity and Earth structure (J. N. Taggart, D)
  - Seismologic studies (J. P. Eaton, M)
- Engineering geophysics (H. D. Ackermann, D)
- Florida Continental Shelf, gravity studies (H. L. Krivoy, NC)
- Gravity surveys:
  - Dona Ana, Otero, Lincoln, Sierra, and Socorro Counties, New Mexico (D. L. Healey, D)
  - Maryland cooperative (D. L. Daniels, NC)
- Ground-water geophysics (W. D. Stanley, D)
- Magnetic chronology, Colorado Plateau and environs (D. P. Elston, E. M. Shoemaker, Flagstaff, Ariz.)
- Mobile magnetometer profiles, Eastern United States (M. F. Kane, D)
- New England, magnetic properties of rocks (Andrew Griscom, M)

Geophysics, regional—Continued
- Program and systems development (G. I. Evenden, W. L. Anderson, D)
- Rainier Mesa (J. R. Ege)
- Rocky Mountains, northern (D. L. Peterson, M. D. Kleinkopf, D)
- Southeastern States geophysical studies (Peter Popenoe, NC)
- Southwestern States geophysical studies (D. L. Peterson, NC)
- Ultramafic rocks, geophysical studies, intrusions (G. A. Thompson, M)
- United States, aeromagnetic surveys (E. R. King, NC)
- *States and territories:*
- Alaska, Ambler River and Baird Mountains quadrangles, gravity studies (D. F. Barnes, M)
- California, Sierra Nevada, geophysical studies (H. W. Oliver, M)
- Idaho, Snake River Plain (D. L. Peterson, D)
- Massachusetts, geophysical studies (M. F. Kane, NC)
- Minnesota (NC):
  - Keweenawan rocks, magnetic studies (K. G. Books)
  - Southern part, aeromagnetic survey (E. R. King)
- Nevada, engineering geophysics, Nevada Test Site (R. D. Carroll, D)
- New Mexico, Rio Grande graben (L. E. Cordell, D)
- Pennsylvania, magnetic properties of rocks (Andrew Griscom, M)
- Puerto Rico, seismicity of Puerto Rico (A. C. Tarr, D)

Geophysics, theoretical and experimental:
- Earthquakes, local seismic studies (J. P. Eaton, M)
- Elastic and inelastic properties of Earth materials (Louis Peselnick, M)
- Electrical properties of rocks (R. D. Carroll, D)
- Electrical resistivity studies (A. A. R. Zohdy, D)
- Experimental rock mechanics (C. B. Raleigh, M)
- Gamma-ray spectrometry for uranium exploration in crystalline terranes (J. A. Pitkin, D)
- Geomechanical studies, in-situ stress (J. R. Ege, D)
- Geophysical data, interpretation using electronic computers (R. G. Henderson, NC)
- Ground-motion studies (J. H. Healy, M)
- Infrared and ultraviolet radiation studies (R. M. Moxham, NC)
- Magnetic and luminescent properties (F. E. Senftle, NC)
- Magnetic Properties Laboratory (M. E. Beck, Jr., Bellingham, Wash.)
- Microwave studies (A. W. England, D)
- Paleomagnetism, Precambrian and Tertiary chronology (D. P. Elston, Flagstaff, Ariz.)
- Remanent magnetization of rocks (C. S. Grommé, M)
- Resistivity interpretation (A. A. R. Zohdy, D)
- Rock behavior at high temperature and pressure (E. C. Robertson, NC)
- Seismicity patterns in time and space (C. G. Bufe, M)
- Stress studies (C. B. Raleigh, M)
- Thermodynamic properties of rocks (R. A. Robie, NC)
- Ultramafic intrusions, geophysical studies (G. A. Thompson, M)
- Volcano geophysics (E. T. Endo, M)
- *States:*
- California, mass properties of oil-field rocks (L. A. Beyer, M)

Geophysics, theoretical and experimental—Continued
States—Continued
Nevada (D):
Nevada Test Site:
Interpretation of geophysical logs (R. D. Carroll)
Seismic velocity measuring techniques (R. D. Carroll)
Vermont, in-situ stress in a granite quarry (G. E. Brethauer, D)

Geotechnical investigations:
Geotechnical measurements and services (H. W. Olsen, D)
In-situ stress, reactor hazards research (T. C. Nichols, Jr., D)
Electronics instrumentation research for engineering geology (J. B. Bennetti, Jr., D)
Miscellaneous landslide investigations (R. W. Fleming, D)
Open-pit slope stability (F. T. Lee, D)
Research in rock mechanics (F. T. Lee, D)
Soil engineering research (T. L. Youd, M)
States:
Colorado, coal mine deformation at Somerset (C. R. Dunrud, D)
Utah, coal mine bumps (F. W. Osterwald, D)
Virginia, Reston (S. F. Obemeier, NC)
Western United States, engineering geology investigations in Powder River basin (F. W. Osterwald, D)

Geothermal investigations:
Broad-band electrical surveys (Mark Landisman, University of Texas)
Convection and thermoelastic effects in narrow vertical fracture spaces:
Analytical techniques (Gunnar Bodvarsson, Oregon State University)
Numerical techniques (R. P. Lowell, Georgia Institute of Technology)
Colorado Plateau, potential field methods (R. R. Wahl, D)
Development of first-motion holography for exploration (Keiiti Aki, Massachusetts Institute of Technology)
Electrical and electromagnetic methods in geothermal areas (D. B. Jackson, D)
Evaluation of intermediate-period seismic waves as an exploration tool (D. M. Boore, Stanford University)
Evaluation of noble gas studies in exploration (Emanuel Mazor, Weizmann Institute of Science, Rehovot, Israel)
Exploration and characterization from seismic activity (E. A. Page, ENSCO, Inc.)
Geochemical exploration (M. E. Hinkle, D)
Geochemical indicators (A. H. Truesdell, M)
Geochemistry of geopressured systems (Y. K. Kharaka, w, M)
Geophysical characterization of young silicic volcanic centers, eastern Sierran Front (W. F. Isherwood, D)
Geothermal geophysics (D. R. Mabey, D)
Geothermal hydrologic reconnaissance (F. H. Olmsted, w, M)
Geothermal reservoirs (Manuel Nathenson, M)
Geothermal studies (A. H. Lachenbruch, M)
Gravity variations as a monitor of water levels (J. M. Goodkind, University of California, San Diego)

Geothermal investigations—Continued
Heat flow (J. H. Sass, A. H. Lachenbruch, M)
Isotopic and chemical studies of geothermal gases (Harmon Craig, University of California, San Diego)
Long Valley hydrothermal system (M. L. Sorey, w, M)
Low-frequency electromagnetic prospecting system (J. Clarke and H. F. Morrison, University of California, Berkeley)
Mercury geochemistry as a tool for geothermal exploration (P. R. Buseck, Arizona State University)
Oxygen isotopes (J. R. O'Neil, M)
Physics of geothermal systems (W. H. Diment, M)
Radioactivity series isotopic disequilibrium (J. K. Osmond and J. B. Cowart, Florida State University)
Regional geoelectromagnetic traverse (J. F. Hermance, Brown University)
Regional volcanology (R. L. Smith, NC)
Remote sensing (Kenneth Watson, D)
Rio Grande geothermal (P. H. Jones, w, Bay St. Louis, Miss.)
Rock-water interactions (R. O. Fournier, M)
Seismic exploration (P. L. Ward, M)
Signal processing methods for magnetotellurics (W. C. Hernandez, ENSCO, Inc.)
Statistical characteristics of geothermal resources, Basin and Range province (W. F. Isherwood, D)
Thermal waters (D. E. White, M)
States:
Alaska, geothermal reconnaissance (T. D. Miller, M)
Arizona, San Francisco volcanic field (E. W. Wolfe, Flagstaff)
California:
Coso area, passive seismology (P. A. Reasenberg, M)
Geology of Long Valley-Mono basin (R. A. Bailey, NC)
Imperial Valley geothermal area (J. J. French, w, Garden Grove)
Long Valley:
Active seismology (D. P. Hill, M)
Hydrology (R. E. Lewis, w, Laguna Niguel)
Microearthquake monitoring:
Imperial Valley (D. P. Hill, M)
The Geysers-Clear Lake (C. G. Bufe, M)
Mercury in soils of geothermal areas (R. W. Klusman, Colorado School of Mines)
Simulation model, Raft River basin (W. D. Nichols, w, Sacramento)
The Geysers area:
H_2S (C. A. Brook, c, M)
Seismic noise (H. M. Iyer, M)
The Geysers-Clear Lake (B. C. Hearn, Jr., NC)
The Geysers-Clear Lake area, pre-Tertiary geology (R. J. McLaughlin, M)
Colorado:
Colorado geothermal (R. E. Moran, w, D)
Geochemical and hydrological parameters of geothermal systems (R. H. Pearl, Colorado Geological Survey)
Geothermal resources (G. L. Galyardt, c, D)
Relationship between geothermal resources and ground water (J. C. Romero, Colorado Geological Survey)

Geothermal investigations—Continued

States—Continued

Georgia, heat flow and radioactive heat generation studies in Southeastern United States (D. L. Smith, University of Florida)

Hawaii, Kilauea Volcano, potential field methods for subsurface magma mapping (C. J. Zablocki, D)

Idaho, test drilling, Raft River valley (E. G. Crosthwaite, Boise)

Montana:

Geothermal investigations in Montana (R. B. Leonard, w, Helena)

Geothermal reconnaissance in southwestern Montana (R. A. Chadwick, Montana State University)

Nevada, geothermal reconnaissance (R. K. Hose, M)

New Mexico, evaluation of geothermal potential of the Basin and Range province (G. P. Landis, University of New Mexico)

Oregon:

Geophysical investigation of the Cascade Range (R. W. Couch, Oregon State University)

Geophysical investigations of the Vale-Owyhee geothermal region (R. W. Couch, Oregon State University)

Geothermal hydrology and geochemistry of Klamath Falls (J. W. Lund, Oregon Institute of Technology)

Geothermal reconnaissance (N. S. MacLeod, M)

Hydrologic reconnaissance of geothermal areas (E. A. Sammel, w, M)

Newberry Caldera (W. H. Lee, c, M)

Utah:

Geothermal reconnaissance in Utah (F. E. Rush, w, Salt Lake City)

Geothermal resources (G. L. Galyardt, c, D)

Petrology and geochronology of late Tertiary and Quaternary volcanic rocks (W. P. Nash, University of Utah)

Regional heat flow and geochemical studies (S. H. Ward, University of Utah)

West Virginia, eastern Warm Springs (W. A. Hobba, Jr., w, Morgantown)

Wyoming, Yellowstone thermal areas, geology (L. J. P. Muffler, M)

Glaciology:

Glaciological research, International Hydrological Decade (M. F. Meier, w, Tacoma, Wash.)

Ice dynamics (W. J. Campbell, w, Tacoma, Wash.)

Water, ice, and energy balance of mountain glaciers and ice physics (M. F. Meier, w, Tacoma, Wash.)

World Data Center A—Glaciology (A. S. Post, w, Tacoma, Wash.)

State:

Alaska (L. R. Mayo, w, Fairbanks)

Gold:

Composition related to exploration (J. C. Antweiler, D)

Great Lakes region (D. A. Seeland, D)

States:

Alaska, Seward Peninsula, nearshore (D. M. Hopkins, M)

California, Klamath Mountains (P. E. Hotz, M)

Montana (D):

Cooke City quadrangle (J. E. Elliott)

Ore deposits, southwestern part (K. L. Wier)

Gold—Continued

States—Continued

Nevada (M, except as otherwise noted):

Aurora and Bodie districts, Nevada-California (F. J. Kleinhampl)

Carlin mine (A. S. Radtke)

Comstock district (D. H. Whitebread)

Dun Glen quadrangle (D. H. Whitebread)

Goldfield district (R. P. Ashley)

Round Mountain and Manhattan districts (D. R. Shawe, D)

New Mexico, placer deposits (Kenneth Segerstrom, D)

North Carolina, Gold Hill area (A. A. Stromquist, D)

Oregon-Washington, nearshore area (P. D. Snavely, Jr., M)

South Dakota, Keystone area (W. H. Raymond, D)

Wyoming, northwestern part, conglomerates (J. C. Antweiler, D)

See also Heavy metals.

Ground water-surface water relations:

Bank storage reconnaissance (W. D. Simons, w, M)

States:

California, confined aquifer, San Bernardino (W. H. Hardt, w, Laguna Niguel)

Florida (w, Miami, except as otherwise noted):

Biscayne aquifer analog model (E. H. Cordes)

Hydrologic base, Dade County (J. E. Hull)

Miami Canal infiltration (F. W. Meyer)

Well fields, west-central Florida (E. R. Close, w, Tampa)

Idaho (w, Boise):

Hydrology:

Island Park-Henrys Lake (R. L. Whitehead)

Weiser Basin (H. W. Young)

Missouri, hydrology of Ozarks Basin (John Skelton, w, Rolla)

Nebraska, Platte Basin water resources (E. G. Lappala, w, Lincoln)

New Mexico, Pecos River, miscellaneous (G. E. Welder, w, Roswell)

North Carolina, effect of channel improvement on hydrologic conditions in Creeping Swamp (M. D. Winner, w, Raleigh)

Ohio, Franklin County digital model (R. E. Fidler, w, Columbus)

Washington, water, Yakima Reservation (R. D. MacNish, w, Tacoma)

Wisconsin (w, Madison):

Hydrology:

Cedar Lake (R. S. McLeod)

Nederlo Creek (P. A. Kammerer, Jr.)

Wetlands (R. P. Novitzki)

Heavy metals:

Appalachian region:

Mineral resources, Connecticut-Massachusetts (J. P. D'Agostino, NC)

South-central (A. A. Stromquist, D)

Hydrogeochemistry and biogeochemistry (T. T. Chao, D)

Mineral paragenesis (J. T. Nash, M)

Regional variation in heavy-metals content of Colorado Plateau stratified rocks (R. C. Cadigan, D)

Rocky Mountain region, fossil beach placers (R. S. Houston, Laramie, Wyo.)

Heavy metals—Continued
Solution transport (G. K. Czamanske, M)
Southeastern States, geochemical studies (Henry Bell III, NC)
States:
Alaska (M):
Gulf of Alaska, nearshore placers (Erk Reimnitz)
Hogatza trend (T. P. Miller)
Southeastern part (D. A. Brew)
Southern Alaska Range (B. L. Reed)
Southwestern part (J. M. Hoare)
Yukon-Tanana Upland (H. L. Foster)
Idaho, Washington Peak quadrangle (D. A. Seeland, D)
Nevada:
Aurora and Bodie districts, Nevada-California (F. J. Kleinhampl, M)
Basin and Range (D. R. Shawe, D)

Hydraulics, ground water:
Computer analysis, ground-water problems (S. S. Papadopulos, w, NC)
Transient phenomena in ground-water flow (C. E. Mongan, w, Boston, Mass.)
Transport processes in fluid flows (Akio Ogata, w, Honolulu, Hawaii)

Hydraulics, surface flow:
Dispersion by turbulent flow in open channels (Nobuhiro Yotsukura, w, NC)
Time-of-travel studies, New York (L. A. Wagner, w, Albany, N.Y.)
Unsteady flow and saline intrusions in rivers and estuaries (R. A. Baltzer, w, NC)
See also Hydrologic instrumentation.

Hydrologic data collection and processing:
Data file for well records (R. S. McLeod, w, Madison, Wis.)
Hydrologic probability models (W. H. Kirby, w, NC)
Runoff cycle simulation (D. R. Dawdy, w, M)
Store-retrieve hydrologic data (D. E. Vaupel, w, Mineola, N.Y.)
See also Hydrologic instrumentation.

Hydrologic instrumentation:
Analog model unit (S. M. Longwill, w, NC)
Drilling techniques (Eugene Shuter, w, D)
GOES data collecton (A. L. Higer, w, Miami, Fla.)
Ground water, quality of water monitors (R. L. Whitehead, w, Boise, Idaho)
Instrumentation and environmental studies (G. E. Ghering, w, D)
Instrumentation research, water (F. C. Koopman, w, Bay St. Louis, Miss.)
Interagency sedimentation project (J. V. Skinner, w, Minneapolis, Minn.)
Laboratory research, instruments, water (G. F. Smoot, w, NC)
Laser spectroscopy (M. C. Goldberg, w, D)
Optical current meter design (Winchell Smith, w, M)
Remote sensing in karst terrane (J. H. Williams, w, Rolla, Mo.)
Satellite data relay project (R. W. Paulson, w, NC)
Suspended solids sensors (J. V. Skinner, w, Minneapolis, Minn.)
Susquehanna Landsat-DCS test (J. V. Funt, w, Harrisburg, Pa.)

Hydrologic instrumentation—Continued
Techniques of flood-plain mapping (G. W. Edelen, Jr., w, NC)
Telemetry evaluation program (J. F. Turner, w, Tampa, Fla.)
See also Hydrologic data collection and processing.

Hydrology, ground water:
Alluvial fan deposition (W. E. Price, Jr., w, NC)
Appalachian Basin, waste storage (P. M. Brown, w, Raleigh, N.C.)
Aquifer systems:
Field research (B. E. Lofgren, w, Sacramento, Calif.)
Theoretical aspects (D. C. Helm, w, Sacramento, Calif.)
Borehole geophysics (W. S. Keys, w, D)
Consultation and research (C. V. Theis, w, Albuquerque, N. Mex.)
Digital modeling, ground-water flow (S. P. Larson, w, NC)
Geopressured-geothermal resources (R. H. Wallace, w, Bay St. Louis, Miss.)
Geothermal modeling (J. W. Mercer, w, NC)
Ground-water geophysics research (A. A. R. Zohdy, w, D)
Ground-water staff functions (S. W. Lohman, w, D)
Ground-water tracer studies (R. J. Sun, w, NC)
Gulf Coast hydrodynamics (P. C. Trescott, w, NC)
Hydrologic laboratory (F. S. Riley, w, D)
Hydrology of the Madison aquifer (E. M. Cushing, w, D)
Hydrology of Wilcox Formation with reference to liquid waste emplacement in the Gulf Coastal Plain (R. H. Wallace, Jr., w, Bay St. Louis, Miss.)
Impact of mining on aquifers (N. J. King, w, D)
In-situ stress measurements (J. D. Bredehoeft, w, NC)
Liaison, U.S. Geological Survey-Bureau of Land Management (F. W. Giessner, w, D)
Limestone hydraulic permeability (V. T. Stringfield, w, NC)
Microbes in ground water (G. G. Ehrlich, w, M)
Modeling of geothermal systems (M. L. Sorey, w, M)
Recharge feasibility factors (Jacob Rubin, w, M)
Regional ground-water-studies coordination (E. M. Cushing, w, NC)
Role of confining clays (R. G. Wolff, w, NC)
Tropical carbonate aquifers (William Back, w, NC)
States and territories:
Alabama, water management, Madison County (J. R. Avrett, w, University)
Alaska (w, Anchorage):
Data summary, Cook Inlet (G. W. Freethey)
Ground-water appraisal, Alaska region (Chester Zenone)
Arizona:
Ground water to Colorado River (O. J. Loeltz, w, Yuma)
Southern Apache County (T. W. Anderson, w, Flagstaff)
Special site studies (H. M. Babcock, w, Tucson)
Water supply, Lake Mead area (R. L. Laney, w, Phoenix)
Arkansas, ground water, lower Mississippi region (J. E. Terry, Jr., w, Little Rock)
California (w, Laguna Niguel, except as otherwise noted):
Cahuilla Indian Reservation water resources (W. R. Moyle, Jr.)

Hydrology, ground water—Continued
States and territories—Continued
California (w, Laguna Niguel, except as otherwise noted) —Continued
Emergency water, Santa Clara County (J. J. Akers, w, M)
Geohydrology, southwestern San Bernardino County (D. H. Schaefer)
Ground-water appraisal, Ocotillo basin (J. A. Skrivan)
Ground water, Beale Air Force Base (R. W. Page, w, Sacramento)
Ground water:
Hollister area (K. S. Muir, w, M)
Monterey Bay (K. S. Muir, w, M)
Napa County (J. P. Akers, w, M)
Imperial Valley geothermal model (R. E. Miller)
United States Marine Corps Twentynine Palms (D. H. Schaefer)
Updating ground-water information in the Eureka area (M. J. Johnson, w, M)
Water resources, Upper Coachella (L. A. Swain)
Water resources, Vandenberg AFB (C. E. Lamb)
Colorado (w, D):
Aquifer testing (F. A. Welder)
Ground water, Denver basin (D. E. Hillier)
Connecticut (w, Hartford):
Farmington ground-water potential (R. L. Melvin)
Newtown ground-water potential (F. P. Haeni)
Florida:
Aquifer characteristics in southwest Florida (R. M. Wolansky, w, Tampa)
Aquifer maps, Southwest Florida Water Management District (Anthony Buono, w, Tampa)
Broward County (C. B. Sherwood, Jr., w, Miami)
Dade City ground water (Warren Anderson, w, Winter Park)
Deep well injection, Ft. Lauderdale (C. B. Sherwood, Jr., w, Miami)
Freshwater in saline aquifers (F. W. Meyer, w, Miami)
Freshwater resources, Big Pine Key (C. E. Hanson, w, Miami)
Geohydrology, citrus irrigation (W. E. Wilson III, w, Tampa)
Hydrology of Lake Tsala Apopka (A. T. Rutledge, w, Winter Park)
Injecting wastes in saline aquifers (F. W. Meyer, w, Miami)
New well fields, Dade County (Howard Klein, w, Miami)
Palm Beach County flatlands (A. L. Knight, w, Miami)
Potentiometric maps in Southwest Florida Water Management District (P. D. Ryder, w, Tampa)
Sarasota disposal well, phase 1 (Horace Sutcliffe, Jr., w, Sarasota)
Shallow aquifer ,Jacksonville (L. V. Causey, w, Jacksonville)
Springs of Florida (J. C. Rosenau, w, Ocala)
Storage of storm waters (J. J. Hickey, w, Tampa)
Water for desalting Florida Keys (F. W. Meyer, w, Miami)
Water resources, Clay County (C. B. Bentley, w, Jacksonville)

Hydrology, ground water—Continued
States and territories—Continued
Florida—Continued
Technical support, ground water (P. D. Ryder, w, Tampa)
Water resources, Everglades (A. L. Higer, w, Miami)
Water resources, Lake Worth (L. F. Land, w, Miami)
Water resources, St. Lucie County (W. L. Miller, w, Miami)
Water supply, Temple Terrace (J. W. Stewart, w, Tampa)
Winter Haven lakes study (R. E. Reichenbaugh, w, Tampa)
Georgia, ground water, Atlanta region (C. W. Cressler, w, Doraville)
Hawaii (w, Honolulu):
Ground-water appraisal, Hawaii region (K. J. Takasaki)
Honolulu basal aquifer (R. H. Dale)
Indiana (w, Indianapolis):
Ground-water appraisal, Great Lakes basin (W. G. West)
Ground water near Carmel (D. C. Gilles)
Ground water, Upper West Fork of the River basin (William Meyer)
Jennings County fracture trace (William Meyer)
Newton County ground water (William Meyer)
Vincennes ground-water study (William Meyer)
Iowa (w, Iowa City):
Ground water, Muscatine Island (R. E. Hansen)
Hydrology of glaciated carbonate terranes (W. L. Steinhilber)
Kansas:
Arbuckle Group:
Liquid waste (A. J. Gogel, w, Lawrence)
Southeastern Kansas (K. M. Keene, w, Lawrence)
Geohydrologic maps, southwestern Kansas (E. D. Gutentag, w, Garden City)
Geohydrology for planning in western Kansas (E. D. Gutentag, w, Garden City)
Great Bend Prairie (S. W. Fader, w, Lawrence)
Greeley and Wichita Counties (S. E. Slagle, w, Garden City)
Ground water, Rush County (J. M. McNellis, w, Lawrence)
Hydrologic data base, Ground Water Management District 3 (D. H. Lobmeyer, w, Garden City)
Water resources, Ness County (E. D. Jenkins, w, Garden City)
Kentucky, Pennyrile Plain potentiometric map (T. W. Lambert, w, Louisville)
Louisiana (w, Baton Rouge):
Red River navigation study (J. F. Rogers)
Washington Parish ground water (H. L. Case)
Maine (w, Augusta):
Androscoggin ground water (G. C. Prescott, Jr.)
Ground water in southwestern Maine (G. C. Prescott, Jr.)
Maryland (w, Towson):
Environmental geohydrologic studies (E. G. Otton)
Maryland Aquifer Studies III (I. J. Kantrowitz)
Massachusetts (w, Boston):
Coal hydrology, Massachusetts and Rhode Island (M. H. Frimpter)

Hydrology, ground water—Continued
States and territories—Continued
Massachusetts (w, Boston)—Continued
Ground water:
Cape Cod (J. H. Guswa)
Martha's Vineyard (D. F. Delaney)
Nantucket (E. H. Walker)
Minnesota (w, St. Paul):
Ground water:
Four-county area (G. F. Lindholm)
Souris-Red-Rainy region (H. O. Reeder)
Twin Cities tunnel-system hydrology (E. L. Madsen)
Water resources, Buffalo River (E. L. Madsen)
Mississippi (w, Jackson):
Water:
Central Delta (G. J. Dalsin)
Developing areas (J. M. Bettandorff)
Southwest-central Mississippi (J. M. Bettandorff)
Missouri, water in southeastern Missouri lowlands (E. J. Harvey, w, Rolla)
Montana:
Geohydrologic maps, Madison aquifer (R. D. Feltis, w, Billings)
Ground water, Swan-Avon Valleys (K. R. Wilke, w, Helena)
Pumpkin Creek (J. D. Stoner, w, Billings)
Tongue River inflow (R. D. Hutchison, w, Helena)
Nevada (w, Carson City):
Fort McDermitt ground water (J. R. Harrill)
Ground-water levels, Topaz Lake (J. O. Nowlin)
Pumping effects on Devil's Hole (J. D. Larson)
Storage depletion:
Las Vegas (J. R. Harrill)
Pahrump Valley (J. R. Harrill)
Well-site evaluations, Bureau of Land Management (J. R. Harrill)
New Hampshire, ground water in Lamprey River basin (J. E. Cotton, w, Concord)
New Jersey (w, Trenton):
Digital model, Potomac-Raritan-Magothy aquifer system (J. E. Luzier)
Geohydrology, east-central New Jersey (G. M. Farlekas)
Pumpage inventory (William Kam)
New Mexico (w, Albuquerque, except as otherwise noted):
Effects of development in northwest New Mexico (F. P. Lyford)
Elephant Butte Irrigation District well-field evaluation (C. A. Wilson, w, Las Cruces)
Geothermal hydrology, Jemez Mountains (F. W. Trainer)
Lower Rio Grande valley (C. A. Wilson)
Navajo Indian Health Service (W. L. Hiss)
Northern High Plains (E. G. Lappala)
Roswell Basin, quantitative (G. E. Welder, w, Roswell)
Sandia-Manzano Mountains (J. B. Cooper)
Water resources:
Mimbres Basin (J. S. McLain)
Santa Fe (W. A. Mourant)
Water supply, Tijeras Canyon (J. D. Hudson)

Hydrology, ground water—Continued
States and territories—Continued
New York:
Buried-channel aquifers, Albany (R. M. Waller, w, Albany)
Hydrologic environment, Salina Group (O. J. Cosner, w, Ithaca)
North Carolina, ground water, Blue Ridge Parkway (M. D. Winner, w, Raleigh)
North Dakota (w, Bismarck, except as otherwise noted):
Ground water:
Adams and Bowman Counties (M. B. Croft)
Emmons County (C. A. Armstrong)
Griggs and Steele Counties (J. S. Downey)
McHenry County (P. G. Randich)
McIntosh County (R. L. Klausing)
Ground-water availability, Fort Union coal (M. G. Croft)
Hydrology of Madison Group (D. J. Ackerman, w, Grand Forks)
Mining and reclamation, Mercer County (J. S. Downey)
Ohio (w, Columbus):
Dayton digital model (R. E. Fidler)
Piketon investigation (S. E. Norris)
Subsurface mines as source of water (J. O. Helgesen)
Oklahoma (w, Oklahoma City):
Arbuckle aquifer (R. W. Fairchild)
Ogallala model, Texas County (R. B. Morton)
Oregon (w, Portland):
Dalles-Monmouth ground-water study (J. B. Gonthier)
Ground water, Clackamas County (A. R. Leonard)
Myrtle Creek ground-water study (F. J. Frank)
Water resources, lower Santiam (A. R. Leonard)
Pennsylvania (w, Harrisburg, except as otherwise noted):
Geology and ground water, Pike County (L. D. Carswell)
Ground water, central Columbia County (O. B. Lloyd, Jr.)
Hydrogeology:
Erie County (G. R. Schiner, w, Meadville)
Great Valley (A. E. Becher)
Hydrology of Gettysburg Formation (C. R. Wood)
Water levels and quality monitoring (W. C. Roth)
Puerto Rico:
Ground-water appraisal, Caribbean (J. E. Heisel, w, San Juan)
Water-resources appraisal of St. Croix, Virgin Islands (H. J. McCoy, w, Fort Buchanan)
Rhode Island, ground water in Pawcatuck River basin (H. E. Johnston, w, Providence)
South Carolina (w, Conway, except as otherwise noted):
Assessment of ground-water resources (A. L. Zack)
Capacity use study (A. L. Zack)
Low country capacity use study (L. R. Hayes, w, Columbia)
Study of geohydrologic problems (A. L. Zack)
South Dakota:
Hydrology of the Madison Group (L. W. Howells, w, Huron)
Water resources, Walworth County (Jack Kume, w, Vermillion)

Hydrology, ground water—Continued

States and territories—Continued

Tennessee (w, Nashville):

Availability of water resources (D. R. Rima)

Ground-water appraisal, Tennessee region (P. A. Zurawski)

Texas, ground water, Palo Duro Creek Basin (P. L. Rettman, w, San Antonio)

Utah (w, Salt Lake City:)

Bonneville Salt Flats (G. C. Lines)

Hydrology:

Beaver Valley (R. W. Mower)

Tooele Valley area (A. G. Razem)

Navajo Sandstone:

Ground water (R. M. Cordova)

Southwestern Utah (R. M. Cordova)

Reconnaissance, Dugway and Government Creeks (J. C. Stephens)

Spanish Valley ground-water model (J. H. Eychaner)

Vermont, ground water in Rutland area (R. E. Willey, w, Montpelier)

Virginia, Fairfax County urban-area study (R. H. Johnston, w, Fairfax)

Washington (w, Tacoma, except as otherwise noted):

Colville, No Name Creek study (D. R. Cline)

Fort Madison study (B. W. Drost)

Kitsap Peninsula study (A. J. Hansen, Jr.)

Port Gamble water resources (B. W. Drost)

Spokane ground-water quality (I. V. Tracy, w, Spokane)

Water data for coal mining (F. A. Packard)

West Virginia (w, Charleston):

Guyandotte River study (J. S. Bader)

Migration of saltwater (J. W. Borchers)

Wisconsin (w, Madison):

Ground water, Dodge County (R. W. Devaul)

Horsehead Lake hydrology (H. L. Young)

Hydrologic maps of southeastern Wisconsin (M. G. Sherrill)

Wyoming (w, Cheyenne):

Bighorn Basin aquifers (M. E. Cooley)

Paleozoic hydrology, Powder River basin (W. G. Hodson)

Tertiary aquifers, Laramie County (M. A. Crist)

Hydrology, surface-water:

Atchafalaya River basin model (M. E. Jennings, w, Bay St. Louis, Miss.)

Evaluation of low-flow runoff (W. D. Simons, w, M)

Hydrology defined by rainfall simulation (G. C. Lusby, w, D)

Modeling principles (J. P. Bennett, w, NC)

Runoff simulation (R. W. Lichty, w, NC)

Water-quality-model development and implementation (R. A. Baltzer, w, NC)

States:

Alabama (w, Tuscaloosa):

Environmental study, Birmingham (R. H. Bingham)

Small-stream studies (D. A. Olin)

Travel-time studies (E. R. German)

Alaska, water resources of fish sites (G. A. McCoy, w, Anchorage)

Arizona, flood hydrology of Arizona (B. N. Aldridge, w, Tucson)

Hydrology, surface-water—Continued

States—Continued

California (w, Sacramento, except as otherwise noted):

Flood hydrology, Butte Basin (R. G. Simpson)

Low-flow study of selected streams (R. N. Oltmann)

Special studies (L. R. Peterson, w, M)

Tidal River discharge computation (R. N. Oltmann)

Colorado (w, D):

Colorado streamflow statistics (J. F. McCain)

Jackson County, surface water (R. K. Livingston)

Delaware, Delaware River master activity (F. T. Schaefer, w, Milford, Pa.)

Florida:

Hillsborough River basin water supply (C. L. Goetz, w, Tampa)

Hydrograph simulation studies (J. F. Turner, Jr., w, Tampa)

Jumper Creek investigation (Warren Anderson, w, Orlando)

Low flows in northwestern Florida (R. P. Rumenik, w, Tallahassee)

Volusia wetlands delineation (P. W. Bush, w, Winter Park)

Georgia (w, Doraville):

Hydrology of Upper Flint Basin (R. F. Carter)

Seasonal low flow (T. R. Dyar)

Small-area flood hydrology (H. G. Golden)

Indiana, coal mine lakes (M. A. Hardy, w, Indianapolis)

Kansas (w, Lawrence):

Flood investigations (H. R. Hepl, Jr.)

Sediment-active geometry (W. R. Osterkamp)

Soldier Creek (W. J. Carswell)

Streamflow characteristics (C. V. Burns)

Kentucky, Green River model study (T. W. Hale, w, Louisville)

Louisiana (w, Baton Rouge):

Characteristics of streams (M. J. Forbes, Jr.)

Small-stream flood frequency (A. S. Lowe)

Maine, drainage areas (D. J. Cowing, w, Augusta)

Minnesota (w, St. Paul):

Bridge site, project reports (L. C. Guetzkow)

Movement and dispersion of solutes (K. L. Lindskov)

Mississippi, documentation of bridge backwater (B. E. Colson, w, Jackson)

Montana (w, Helena):

Bridge-site investigations (M. V. Johnson)

Peak flow, small drainage areas (M. V. Johnson)

Nevada, Fire Mountain flood-hazard study (Otto Moosburner, w, Carson City)

New Jersey, low-flow frequency (R. D. Schopp, w, Trenton)

New Mexico, runoff from channel geometry (A. G. Scott, w, Santa Fe)

New York, low-flow study (B. B. Eissler, w, Albany)

North Carolina (w, Raleigh):

Channelization effects, Chicod Creek (C. P. Humphreys)

Nonpoint pollution (C. E. Simmons)

Stream-system modeling (F. E. Arteaga)

Ohio (w, Columbus):

Flood hydrology, small areas (E. E. Webber)

Hydraulics of bridge sites (R. I. Mayo)

Low flow of Ohio streams (R. I. Mayo)

Time-of-travel studies of Ohio streams (A. O. Westfall)

Hydrology, surface-water—Continued
States—Continued
Oklahoma, coal field hydrology (J. S. Havens, w, Oklahoma City)
Oregon, Oregon lakes and reservoirs (D. D. Harris, w, Portland)
Pennsylvania (w, Harrisburg):
Flow routing:
Lower Susquehanna Basin (J. T. Armbruster)
Susquehanna River (D. L. Bingham)
Low-flow regionalization (H. N. Flippo)
Streamflow characteristics (Andrew Voytik)
South Carolina (w, Columbia):
Data reports, flood forecasting (C. S. Bennett)
Low-flow characteristics (W. M. Bloxham)
South Dakota (w, Huron):
Flood-frequency study (L. D. Becker)
Small-stream flood frequency (L. D. Becker)
Tennessee (w, Nashville, except as otherwise noted):
Memphis urban flood frequency (C. W. Boning, w, Memphis)
Metro urban development alternatives (H. C. Wibben)
Small-stream modeling (H. C. Wibben)
Tennessee bridge scour (W. J. Randolph)
Texas (w, Austin, except as otherwise noted):
Hydrology of small drainage areas (E. E. Schroeder)
Small watersheds (R. D. Hawkinson)
Trinity River time-of-travel studies (R. H. Ollman, w, Fort Worth)
Washington (w, Tacoma):
Anadromous fish hydraulics (C. H. Swift III)
Low flow (P. J. Carpenter)
Lower Elwha project (K. L. Walters)
Makah project (K. L. Walters)
Nisqually Indian Reservation study (K. L. Walters)
Ozette Lake study (G. C. Bortelson)
West Virginia, drainage area study (J. L. Chisholm, w, Charleston)
Wisconsin (w, Madison):
Flood-frequency study (D. H. Conger)
Low-flow study (W. A. Gebert)
Mean monthly flow determination (B. K. Holstrom)
Water-quality control (B. K. Holstrom)
Wisconsin River low flow (W. A. Gebert)
See also Evapotranspiration; Flood investigations; Marine hydrology; Plant ecology; Urbanization, hydrologic effects.

Industrial minerals. *See specific minerals.*

Iron:
Resource studies, United States (Harry Klemic, NC)
States:
Michigan, Gogebic County, western part (R. G. Schmidt, NC)
Wisconsin, Black River Falls (Harry Klemic, NC)

Isotope and nuclear studies:
Instrument development (F. J. Jurceka, D)
Interface of isotope hydrology and hydrogeology (I. J. Winograd, w, NC)
Isotope fractionation (T. B. Coplen II, w, NC)
Isotope ratios in rocks and minerals (Irving Friedman, D)
Isotopes in hydrology (C. T. Rightmire, w, NC)

Isotope and nuclear studies—Continued
Isotopic hydrology (F. J. Pearson, w, NC)
Lead isotopes and ore deposits (R. E. Zartman, D)
Mass spectrometry and isotopic measurements (J. S. Stacey, D)
Nuclear irradiation (G. M. Bunker, D)
Nuclear reactor facility (G. P. Kraker, Jr., w, D)
Radioisotope dilution (L. P. Greenland, NC)
Stable isotopes and ore genesis (R. O. Rye, D)
Upper mantle studies (Mitsunobu Tatsumoto, D)
See also Geochronological investigations; Geochemistry, water; Radioactive-waste disposal.

Land resources analysis:
Idaho, eastern Snake River Plain region (S. S. Oriel, D)

Land subsidence:
Geothermal subsidence research (B. E. Lofgren, w, Sacramento, Calif.)
Land subsidence studies (B. E. Lofgren, w, Sacramento, Calif.)
States:
New Mexico, land subsidence in the Known Potash Leasing Area (M. L. Millgate, c, Roswell)
Texas, Johnson Space Center artificial recharge (Sergio Garza, w, Austin)

Land use and environmental impact:
Central Atlantic Regional Ecological Test Site (CARETS) Project (R. H. Alexander, l, NC)
Comparative urban land use analysis studies (J. R. Wray, l, NC)
Demonstration land use mapping (R. E. Witmer, l, NC)
Geographic Information Retrieval and Analysis System (GIRAS) (W. B. Mitchell, l, NC)
Geographic Information Systems software development (W. B. Mitchell, l, NC)
Hazard prediction and warning, socioeconomic and land use planning implications (R. H. Alexander, l, Boulder, Colo.)
Impact of the oil and gas industry on the Louisiana coast (D. W. Davis, J. L. Place, l, NC)
Impact of Outer Continental Shelf development on coastal land and environmental resources (H. F. Lins, l, NC)
Land use analysis for Chattahoochee River quality assessment (J. L. Place, l, NC)
Land use and land cover:
Compilation and interpretation research (G. L. Loelkes, l, NC)
Input and output processing of cover maps and data (W. B. Mitchell, l, NC)
Map accuracy determination (R. E. Witmer, l, NC)
Mapping and data compilation (G. L. Loelkes, l, NC)
Land Use Data and Analysis Program and other geographic studies (G. L. Loelkes, R. E. Witmer, l, NC)
Land use impact on solar-terrestrial energy systems (R. W. Pease, l, NC)
Land use patterns related to selected environmental problems (J. L. Place, l, NC)
Mid-Atlantic land information and analysis study (R. H. Alexander, l, NC)
Review and analysis of USGS spatial data handling (Olaf Kays, l, NC)

Land use and environmental impact—Continued
Multidisciplinary studies:
Earth-science information for decisionmakers (R. D. Brown, Jr., M)
Use of Earth-science maps in land and water planning (G. D. Robinson, M; A. M. Spieker, w, M)
States:
Colorado, environmental and resource demonstration study, Front Range urban corridor (W. R. Hansen, D)
Virginia, Earth-science applications study in Fairfax County (A. J. Froelich, NC)
See also Construction and terrain problems; Urban geology; Urban hydrology.

Lead, zinc, and silver:
Lead resources of United States (C. S. Bromfield, D)
Zinz resources of United States (Helmuth Wedow, Jr., Knoxville, Tenn.)
States:
Alaska, southwest Brooks Range (I. L. Tailleur, M)
Colorado (D):
San Juan Mountains:
Eastern, reconnaissance (W. N. Sharp)
Northwestern (F. S. Fisher)
Illinois-Kentucky district, regional structure and ore controls (D. M. Pinckney, D)
Nevada (M):
Comstock district (D. H. Whitebread)
Silver Peak Range (R. P. Ashley)
Utah, Park City district (C. S. Bromfield, D)

Limnology:
Hydrology of lakes (G. C. Bortleson, w, Tacoma, Wash.)
Impoundment water quality (D. R. Williams, w, Harrisburg, Pa.)
Interrelations of aquatic ecology and water quality (K. V. Slack, w, M)
Oxygen cycle in streams (R. E. Rathbun, w, Bay St. Louis, Miss.)
Relation of ground water to lakes (T. C. Winter, w, D)
Water quality of impoundments (J. L. Barker, w, Harrisburg, Pa.)
States and territories:
Colorado, lake reconnaissance (D. A. Wentz, w, D)
Maine, limnological study of lakes (D. J. Cowing, w, Boston, Mass.)
Massachusetts, Hager Pond nutrient study (W. D. Silvey, w, Boston)
Ohio, limnology of selected lakes (R. L. Tobin, w, Columbus)
Pennsylvania, stream health in Chester County (B. W. Lium, w, West Chester)
Puerto Rico (w, San Juan):
Quality of water:
Lago Carraizo (Ferdinand Quinoñes-Marquez)
Laguna Tortuguero (Ferdinand Quinoñes-Marquez)
Wisconsin, hydrology of lakes (R. W. Devaul, w, Madison)
See also Quality of water.

Lunar geology. *See* Extraterrestrial studies.

Manganese. *See* Ferro-alloy metals.

Marine geology:
Atlantic Continental Shelf:
Environmental impact of petroleum exploration and production (H. J. Knebel, Woods Hole, Mass.)
Geophysics studies (J. C. Behrendt, Woods Hole, Mass.)
Magnetic chronology (E. M. Shoemaker, D. P. Elston, Flagstaff, Ariz.)
New England coastal zone (R. N. Oldale, Woods Hole, Mass.)
Site surveys (W. P. Dillon, Woods Hole, Mass.)
Stratigraphy (J. C. Hathaway, Woods Hole, Mass.)
Stratigraphy and structure (J. S. Schlee, Woods Hole, Mass.)
Caribbean and Gulf of Mexico:
Coastal environments (H. L. Berryhill, Corpus Christi, Tex.)
Estuaries (C. W. Holmes, Corpus Christi, Tex.)
Mississippi delta studies (L. E. Garrison, Corpus Christi, Tex.)
Natural resources and tectonic features (R. G. Martin, Jr., Corpus Christi, Tex.)
Oil migration and diagenesis of sediments (C. W. Holmes, Corpus Christi, Tex.)
Tectonics, Caribbean (J. E. Case, Corpus Christi, Tex.)
Tectonics, gulf (L. E. Garrison, Corpus Christi, Tex.)
Marine mineral resources, worldwide (F. H. Wang, M)
Pacific coast sedimentology (H. E. Clifton, M)
Pacific Ocean, biostratigraphy, deep ocean (J. D. Bukry, La Jolla, Calif.)
Pacific reef studies (J. I. Tracey, Jr., NC)
Spanish Continental Margin (Almeria Province) (P. D. Snavely, Jr., H. G. Greene, H. F. Clifton, W. P. Dillon, J. M. Robb, M)
Volcanic geology, Mariana and Caroline Islands (Gilbert Corwin, NC)
World offshore oil and gas (T. H. McCulloh, Seattle, Wash.)
States and territories:
Alaska (M, except as otherwise noted):
Arctic coastal marine processes (Erik Reimnitz)
Beaufort-Chuckchi Sea Continental Shelf (Arthur Grantz)
Beaufort Sea environment studies (P. W. Barnes)
Bering Sea:
General study (D. W. Scholl)
Northern:
Environmental geologic studies (C. H. Nelson)
Sea floor (C. H. Nelson)
Coastal environments (A. T. Ovenshine)
Continental Shelf resources (D. M. Hopkins)
Cook Inlet (L. B. Magoon III)
Gulf of Alaska (B. F. Molnia)
Seward Peninsula, nearshore (D. M. Hopkins)
Tectonic history (R. E. von Huene, NC)
California (M):
Borderlands:
Geologic framework (A. E. Roberts)
Southern part (G. W. Moore)
Continental Margin, central part (E. A. Silver)
La Jolla marine geology laboratory (G. W. Moore)
Monterey Bay (H. G. Greene)

Marine geology—Continued
States and territories—Continued
California (M)—Continued
San Francisco Bay:
General study (D. S. McCulloch)
Geochemistry of sediments (D. H. Peterson)
Oregon, land-sea transect, Newport (P. D. Snavely, Jr., M)
Oregon-California, black sands (H. C. Clifton, M)
Oregon-Washington, nearshore (P. D. Snavely, Jr., M)
Puerto Rico, cooperative program (J. V. A. Trumbull, Santurce)
Texas, barrier islands (R. E. Hunter, Corpus Christi)
Marine hydrology:
Hydrologic-oceanographic studies (F. A. Kohout, w, Woods Hole, Mass.)
States and territories:
Maryland, effects of water-quality changes on biota in estuaries (R. L. Cory, w, NC)
North Carolina, flow of Chowan River (C. C. Daniel, w, Raleigh)
Puerto Rico, San Juan lagoons (S. R. Ellis, w, San Juan)
See also Hydrology, surface water; Quality of water; Geochemistry, water; Marine geology.
Mercury:
Geochemistry (A. P. Pierce, D)
Mercury deposits and resources (E. H. Bailey, M)
State:
California, Coast Range ultramafic rocks (E. H. Bailey, M)
Meteorites. *See* Extraterrestrial studies.
Mine drainage and hydrology:
Assessment of reclaimed areas (S. E. Eikenberry, w, Indianapolis, Ind.)
Deep-mine collapse hydrology (W. H. Hobba, w, Charleston, W. Va.)
Metals and buffering in mine stream (W. L. Shampine, w, Indianapolis, Ind.)
Water from coal mines (D. S. Mull, w, Louisville, Ky.)
Western Middle anthracite hydrology (D. J. Growitz, w, Harrisburg, Pa.)
States:
Kentucky (w, Louisville):
Coal-mining effects:
Grapevine Creek (K. L. Dyer)
Kentucky River (K. L. Dyer)
Pennsylvania, coal hydrology of Big Sandy Creek (D. L. Bingham, w, Harrisburg)
Montana, East Trail Creek (W. R. Hotchkiss, w, Helena)
Mineral and fuel resources—compilations and topical studies:
Application massive sulfides, Virginia deposits (J. E. Gair, NC)
Arctic mineral-resource investigations (W. P. Brosgé, M)
Basin and Range, geologic studies (F. G. Poole, D)
Colorado Plateau (R. P. Fischer, D)
Information bank, computerized (J. A. Calkins, NC)
Mineral-resource surveys:
Minerals for energy production (L. F. Rooney, NC)
Primitive and Wilderness Areas:
Bob Marshall Wilderness Area, Montana (R. L. Earhart, D)
Citico Creek, Tennessee (E. R. Force, NC)
Craggy Mountain, North Carolina (F. G. Lesure, NC)
Cranberry, West Virginia (F. G. Lesure, NC)
Mineral and fuel resources—compilations and topical studies —Continued
Mineral-resource surveys—Continued
Primitive and Wilderness Areas—Continued
Elkhorn Wilderness Study Area, Montana W. R. Greenwood, D)
Flint Creek Range Study Area, Montana (G. E. Ericksen, NC)
Gates of the Mountains Wilderness Area, Montana (M. W. Reynolds, D)
Glacier Bay National Monument Wilderness Area, Alaska (D. A. Brew, M)
John Muir Wilderness, California (N. K. Huber, M)
Pecos Wilderness, New Mexico (R. H. Moench, D)
Rainbow Lake, Flynn Lake, and Round Lake, Wisconsin (W. F. Cannon, NC)
Rawah Wilderness Area and nearby study areas, Colorado (R. C. Pearson, D)
Selway-Bitterroot Wilderness, Idaho and Montana (W. R. Greenwood, D)
Snowy Range Wilderness Study Area, Wyoming (R. S. Houston, D)
Superstition Wilderness, Arizona (D. W. Peterson, D)
Wambau Swamp, South Carolina (F. G. Lesure, NC)
Washakie Wilderness, Wyoming (J. C. Antweiler, D)
Nonmetallic deposits, mineralogy (B. M. Madsen, M)
Oil and gas resources:
Central and northern California Continental Shelf (C. W. Spencer, D)
Petroleum potential of southern California borderland appraised (C. W. Spencer, D)
Resource analysis, economics of mineral resources (J. H. DeYoung, Jr., NC)
Wilderness Program:
Geochemical services (D. J. Grimes, D)
Geophysical services (M. F. Kane, D)
States:
Alaska (M):
AMRAP program (J. E. Case)
Mineral resources (E. H. Cobb)
Southwestern Brooks Range (I. L. Tailleur)
Colorado, Summitville district, alteration study (R. E. Van Loenen, D)
Missouri, Rolla 2-degree quadrangle, mineral-resource appraisal (W. P. Pratt, D)
Nevada, igneous rocks and related ore deposits (M. L. Silberman, M)
United States:
Central States, mineral-deposit controls (A. V. Heyl, Jr., D)
Iron-resources studies (Harry Klemic, NC)
Lightweight-aggregate resources (A. L. Bush, D)
Metallogenic maps (P. W. Guild, NC)
Northeastern States, peat resources (C. C. Cameron, NC)
Southeastern States, mineral-resource surveys (R. A. Laurence, Knoxville, Tenn.)
Wisconsin, northern, mineral-resource survey (C. E. Dutton, Madison)
See also specific minerals or fuels.

Mineralogy and crystallography, experimental:
Crystal chemistry (Malcolm Ross, NC)
Crystal structure, sulfides (H. T. Evans, Jr., NC)
Electrochemistry of minerals (Motoaki Sato, NC)
Mineralogical crystal chemistry (J. R. Clark, M)
Mineralogic services and research (R. C. Erd, M)
Mineralogy of heavy metals (F. A. Hildebrand, D)
Planetary mineralogical studies (Priestley Toulmin III, NC)
Research on ore minerals (B. F. Leonard, D)
See also Geochemistry, experimental.
Minor elements:
Geochemistry (George Phair, NC)
Niobium:
Colorado, Wet Mountains (R. L. Parker, D)
Niobium and tantalum, distribution in igneous rocks (David Gottfried, NC)
Phosphoria Formation, stratigraphy and resources (R. A. Gulbrandsen, M)
Nonpegmatic lithium resources (J. D. Vine, D)
Rare-earth elements, resources and geochemistry (J. W. Adams, D)
Trace-analysis methods, research (F. N. Ward, D)
Model studies, geologic and geophysical:
Computer modeling:
Rock-water interactions (J. L. Haas, Jr., NC)
Tectonic deformation (J. H. Dieterich, M)
Model studies, hydrologic:
Alluvial fan deposition (W. E. Price, w, NC)
Digital model, aquifer system (A. F. Robertson, w, Tampa, Fla.)
Ground-water hydrology, strip-mining areas (D. D. Knochenmus, w, Columbus, Ohio)
Hydrodynamics of a tidal estuary (R. T. Cheng, w, M)
Linear models (T. N. Keefer, w, Bay St. Louis, Miss.)
Miocene aquifer study (E. T. Baker, Jr., w, Austin, Tex.)
Modeling organic solute transport (J. B. Robertson, w, M)
Numerical simulation (V. C. Lai, w, NC)
Operation models, surface-water systems (M. E. Jennings, w, Bay St. Louis, Miss.)
Physical modeling (V. R. Schneider, w, Bay St. Louis, Miss.)
Runoff simulation (P. H. Carrigan, w, NC)
Simulation of hydrogeologic systems (R. L. Cooley, w, D)
Streamflow models (P. R. Jordan, w, Lawrence, Kans.)
Surface-water-quality modeling (S. M. Zand-Yazdani, w, M)
Systems Analysis Laboratory (N. C. Matalas, w, NC)
Transport in ground water (L. F. Konikow, w, D)
Water-quality modeling (D. B. Grove, w, D)
Watershed modeling (J. F. Turner, w; Tampa, Fla.)
States:
California:
Barstow quality-of-water model (S. G. Robson, w, Laguna Niguel)
Salinas ground-water model (T. J. Durbin, w, M)
Colorado, Rocky Mountain Arsenal DIMP contamination (S. G. Robson, w, D)
Florida:
Ground water, Ft. Lauderdale (C. B. Sherwood, Jr., w, Miami)
Impact phosphate mining, Mid-Peace (W. E. Wilson, w, Tampa)
Loxahatchee River basin model (G. W. Hill, w, Miami)

Model studies, hydrologic—Continued
States—Continued
Indiana, Logansport ground-water study (D. C. Gillies, w, Indianapolis)
Kansas, ground water-surface water, north-central Kansas (D. G. Jorgensen, w, Lawrence)
Maryland, small basin modeling (L. J. Nutter, w, Towson)
Minnesota, evaluation of quality-of-water data for management (M. S. McBride, w, St. Paul)
Nebraska (w, Lincoln):
Irrigation districts in southwestern Nebraska (E. G. Lappala)
Willow Creek dam site (E. G. Lappala)
New Jersey, Englishtown Formation (W. D. Nichols, w, Trenton)
New York:
Hydrologic modeling, phase 2 (A. W. Harbaugh, w, Mineola)
Tioughnioga River ground water (O. J. Cosner, w, Albany)
Pennsylvania (w, Harrisburg):
Delaware River streamflow model (J. O. Shearman)
Flow simulation, Juniata River (J. T. Armbruster)
South Dakota, water resources of Big Sioux Valley (N. C. Koch, w, Huron)
Tennessee, Memphis ground-water model (J. V. Brahana, w, Nashville)
Washington (w, Tacoma):
Columbia River basalt model (J. V. Tracy)
Ground water-surface water model (E. A. Prych)
Wisconsin, digital streamflow model, Rock River (W. R. Krug, w, Madison)
Wyoming, hydrology of Sweetwater Basin (W. B. Borchert, w, Cheyenne)
Molybdenum. *See* Ferro-alloy metals.
Moon studies. *See* Extraterrestrial studies.
Nickel. *See* Ferro-alloy metals.
Nuclear explosions, geology:
Engineering geophysics, Nevada Test Site (R. D. Carroll, D)
Environmental effects (P. P. Orkild, D)
Geologic investigations:
Computer-stored physical properties data (J. R. Ege, D)
Nevada Test Site:
Nevada Test Site (P. P. Orkild, D)
Northern Yucca Flat and Pahute Mesa (W. D. Quinlivan, D)
Pahute Mesa and central and southern Yucca Flat (G. L. Dixon, D)
Geomechanical investigations, Nevada Test Site (J. R. Ege, D)
Nuclear explosions, hydrology:
Nuclear-explosive underground engineering, hydrology (J. E. Weir, Jr., w, D)
States:
Alaska, hydrology of Amchitka Island Test Site (D. D. Gonzalez, w, D)
Nevada (w, D):
Nevada Test Site:
Central, hydrology (G. A. Dinwiddie)
Hydrology (W. W. Dudley, Jr.)

Nuclear site studies:
- Geohydrologic study, Argonne Laboratory (M. G. Sherrill, w, Madison, Wis.)

Oil shale:
- Organic geochemistry (R. E. Miller, D)
- Oil shale and associated minerals (J. L. Renner, c, D)
- Petrology (J. R. Dyni, D)
- Regional geochemistry (W. E. Dean, Jr., D)
- Trace elements (W. E. Dean, Jr., D)
- *States:*
- Alaska, Anatuvuk Pass (G. B. Shearer, c, Anchorage)
- Colorado (D):
  - Lower Yellow Creek area (W. J. Hall)
  - Piceance Creek basin:
    - East-central (R. B. O'Sullivan)
    - Experimental mining (R. P. Snyder)
    - General (J. R. Donnell)
- Colorado-Wyoming, Eocene rocks (H. W. Roehler, D)
- Colorado-Utah-Wyoming, geochemistry (W. E. Dean, Jr., D)
- Utah (W. B. Cashion, Jr., D)

Paleobotany, systematic:
- Diatom studies (G. W. Andrews, NC)
- Floras:
  - Cenozoic:
    - Pacific Northwest (J. A. Wolfe, M)
    - Western United States and Alaska (J. A. Wolfe, M)
  - Devonian (J. M. Schopf, Columbus, Ohio)
  - Paleozoic (S. H. Mamay, NC)
- Fossil wood and general paleobotany (R. A. Scott, D)
- Plant microfossils:
  - Mesozoic (R. H. Tschudy, D)
  - Paleozoic (R. M. Kosanke, D)

Paleoecology:
- Faunas, Late Pleistocene, Pacific coast (W. O. Addicott, M)
- Foraminifera, ecology (M. R. Todd, NC)
- Ostracodes, Recent, North Atlantic (J. E. Hazel, NC)
- Paleoenvironmental studies, Miocene, Atlantic Coastal Plain (T. G. Gibson, NC)
- *Tempskya*, Southwestern United States (C. B. Read, Albuquerque, N. Mex.)
- Vertebrate faunas, Ryukyu Islands, biogeography (F. C. Whitmore, Jr., NC)

Paleontology, invertebrate, systematic:
- Brachiopods:
  - Carboniferous (Mackenzie Gordon, Jr., NC)
  - Ordovician (R. B. Neuman, NC; R. J. Ross, Jr., D)
  - Upper Paleozoic (J. T. Dutro, Jr., NC)
- Bryozoans, Ordovician (O. L. Karklins, NC)
- Cephalopods:
  - Cretaceous (D. L. Jones, M)
  - Jurassic (R. W. Imlay, NC)
  - Upper Cretaceous (W. A. Cobban, D)
  - Upper Paleozoic (Mackenzie Gordon, Jr., NC)
- Chitinozoans, Lower Paleozoic (J. M. Schopf, Columbus, Ohio)
- Conodonts, Devonian and Mississippian (C. A. Sandberg, D)
- Corals, rugose:
  - Mississippian (W. J. Sando, NC)
  - Silurian-Devonian (W. A. Oliver, Jr., NC)

Paleontology, invertebrate, systematic—Continued
- Foraminifera:
  - Fusuline and orbitoline (R. C. Douglass, NC)
  - Cenozoic (M. R. Todd, NC)
  - Cenozoic, California and Alaska (P. J. Smith, M)
  - Mississippian (B. A. Skipp, D)
  - Recent, Atlantic shelf (T. G. Gibson, NC)
- Gastropods:
  - Mesozoic (N. F. Sohl, NC)
  - Miocene-Pliocene, Atlantic coast (T. G. Gibson, NC)
  - Paleozoic (E. L. Yochelson, NC)
- Graptolites, Ordovician-Silurian (R. J. Ross, Jr., D)
- Mollusks, Cenozoic, Pacific coast (W. A. Addicott, M)
- Ostracodes:
  - Lower Paleozoic (J. M. Berdan, NC)
  - Upper Cretaceous and Tertiary (J. E. Hazel, NC)
  - Upper Paleozoic (I. G. Sohn, NC)
- Pelecypods:
  - Inoceramids (D. L. Jones, M)
  - Jurassic (R. W. Imlay, NC)
  - Paleozoic (John Pojeta, Jr., NC)
  - Triassic (N. J. Silberling, M)
- Trilobites, Ordovician (R. J. Ross, Jr., D)

Paleontology, stratigraphic:
- Cenozoic:
  - Diatoms, Great Plains, nonmarine (G. W. Andrews, NC)
  - Foraminifera, smaller, Pacific Ocean and islands (M. R. Todd, NC)
  - Mollusks:
    - Atlantic coast, Miocene (T. G. Gibson, NC)
    - Pacific coast, Miocene (W. O. Addicott, M)
  - Pollen and spores, Kentucky (R. H. Tschudy, D)
  - Vertebrates:
    - Pleistocene (G. E. Lewis, D)
    - Atlantic coast (F. C. Whitmore, Jr., NC)
    - Pacific coast (C. A. Repenning, M)
    - Panama Canal Zone (F. C. Whitmore, Jr., NC)
- Mesozoic:
- Pacific coast and Alaska (D. L. Jones, M)
  - Cretaceous:
    - Alaska (D. L. Jones, M)
    - Foraminifera:
      - Alaska (H. R. Bergquist, NC)
      - Atlantic and Gulf Coastal Plains (H. R. Bergquist, NC)
      - Pacific coast (R. L. Pierce, M)
    - Gulf Coast and Caribbean (N. F. Sohl, NC)
    - Molluscan faunas, Caribbean (N. F. Sohl, NC)
    - Western interior United States (W. A. Cobban, D)
  - Jurassic, North America (R. W. Imlay, NC)
  - Triassic, marine faunas and stratigraphy (N. J. Silberling, M)
- Paleozoic:
  - Devonian and Mississippian conodonts, Western United States (C. A. Sandberg, D)
  - Fusuline Foraminifera, Nevada (R. C. Douglass, NC)
  - Mississippian biostratigraphy, Alaska (A. K. Armstrong, M)
  - Onesquethaw Stage (Devonian), stratigraphy and rugose corals (W. A. Oliver, NC)
  - Paleobotany and coal studies Antarctica (J. M. Schopf, Columbus, Ohio)

Paleontology, stratigraphic—Continued
- Paleozoic—Continued
  - Palynology of cores from Naval Petroleum Reserve No. 4 (R. A. Scott, D)
  - Subsurface rocks, Florida (J. M. Berdan, NC)
  - Ordovician:
    - Bryozoans, Kentucky (O. L. Karklins, NC)
    - Stratigraphy and brachiopods, Eastern United States (R. B. Neuman, NC)
    - Western United States (R. J. Ross, Jr., D)
  - Silurian-Devonian:
    - Corals, northeastern United States (W. A. Oliver, Jr., NC)
    - Upper Silurian-Lower Devonian, Eastern United States (J. M. Berdan, NC)
  - Mississippian:
    - Stratigraphy and brachiopods, northern Rocky Mountains and Alaska (J. T. Dutro, Jr., NC)
    - Stratigraphy and corals, northern Rocky Mountains (W. J. Sando, NC)
  - Pennsylvanian:
    - Fusulinidae:
      - Alaska (R. C. Douglass, NC)
      - North-central Texas (D. A. Myers, D)
    - Spores and pollen, Kentucky (R. M. Kosanke, D)
  - Permian, floras, Southwestern United States (S. H. Mamay, NC)
  - Upper Paleozoic, Western States (Mackenzie Gordon, Jr., NC)

Paleontology, vertebrate, systematic:
- Artiodactyls, primitive (F. C. Whitmore, Jr., NC)
- Pinnipedia (C. A. Repenning, M)
- Pleistocene fauna, Big Bone Lick, Kentucky (F. C. Whitmore, Jr., NC)
- Tritylodonts, American (G. E. Lewis, D)

Paleotectonic maps. *See* Regional studies and compilations.

Petroleum and natural gas:
- Automatic data-processing system for field and reservoir estimates (K. A. Yenne, c, Los Angeles, Calif.)
- Borehole gravimetry, application to oil exploration (J. W. Schmoker, D)
- Catagenesis of organic matter and generation of petroleum (N. H. Bostick, D)
- Devonian black shale, Appalachian Basin:
  - Borehole gravity study (J. W. Schmoker, D)
  - Clay mineralogy (J. W. Hosterman, NC)
  - Conodont maturation (A. G. Harris, NC)
  - Data storage and retrieval system
  - Geochemical study (G. E. Claypool, D)
  - Stratigraphy (J. B. Roen, NC)
  - Structural studies (L. D. Harris, NC)
  - Uranium and trace-element study (J. S. Leventhal, D)
- Methods of recovery (F. W. Stead, D)
- Oil and gas map, North America (W. W. Mallory, D)
- Oil and gas resource appraisal methodology and procedures (B. M. Miller, D)
- Organic geochemistry (J. G. Palacas, D)
- Origin and distribution of natural gases (D. D. Rice, D)
- Origin, migration, and accumulation of petroleum (L. C. Price, D)
- Petroleum prospecting with helium detector (A. A. Roberts, D)

Petroleum and natural gas—Continued
- Rocky Mountain States, seismic detection of stratigraphic traps (R. T. Ryder, D)
- Tight gas sands (D. D. Rice, D)
- Western Interior Cretaceous studies (C. W. Spencer, D)
- Western United States:
  - Devonian and Mississippian (C. A. Sandberg, D)
  - Devonian and Mississippian flysch source-rock studies (F. G. Poole, D)
  - Properties of reservoir rocks (R. F. Mast, D)
  - Source rocks of Permian age (E. K. Maughan, D)
- *States:*
- Alaska (M):
  - Cook Inlet (L. B. Magoon III)
  - North Slope, petroleum geology (R. D. Carter)
- California:
  - Carpenteria and Hondo-Santa Ynez field reserves, OCS (D. G. Griggs, c, Los Angeles)
  - Eastern Los Angeles basin (T. H. McCulloh, Seattle, Wash.)
  - Salinas Valley (D. L. Durham, M)
  - Southern San Joaquin Valley, subsurface geology (J. C. Maher, M)
- Colorado (c, D, except as otherwise noted):
  - Citadel Plateau (G. A. Izett)
  - Denver Basin, Tertiary coal zone and associated strata (P. A. Soister)
  - Grand Junction 2-degree quadrangle (W. B. Cashion, Jr., D)
  - Savery quadrangle (C. S. V. Barclay)
- New Mexico, San Juan Basin (E. R. Landis, D)
- Utah (c, D, except as otherwise noted):
  - Canaan Peak quadrangle (W. E. Bowers)
  - Collet Top quadrangle (H. D. Zeller)
  - Grand Junction 2-degree quadrangle (W. B. Cashion, Jr., D)
- Wyoming:
  - Browns Hill quadrangle (C. S. V. Barclay, c, D)
  - Lander area phosphate reserve (W. L. Rohrer, c, D)
  - Pine Mountain-Oil Mountain area (G. J. Kerns, c, Casper)
  - Reid Canyon quadrangle (G. J. Kerns, c, Casper)
  - Savery quadrangle (C. S. V. Barclay, c, D)
  - Square Top Butte quadrangle (W. H. Laraway, c, Casper)
  - Stratigraphy, lower Upper Cretaceous formations (E. A. Merewether, D)
- Wyoming-Montana-North Dakota-South Dakota, Williston Basin (C. A. Sandberg, D)

Petrology. *See* Geochemistry and petrology, field studies.

Phosphate:
- Phosphoria Formation, stratigraphy and resources (R. A. Gulbrandsen, M)
- *States:*
- Alaska, Anatuvuk Pass (c, Anchorage)
- Idaho:
  - Palisades Dam quadrangle (D. A. Jobin, c, D)
  - Phosphate resources (Peter Oberlindacher, c, M)
- Montana, Melrose phosphate field (G. D. Fraser, c, D)
- Nevada:
  - Phosphate resources (E. A. Johnson, c, M)
  - Spruce Mountain 4 quadrangle (G. D. Fraser, c, D)
- United States, southeastern, phosphate resources (J. B. Cathcart, D)

Phosphate—Continued
States—Continued
Utah:
Crawford Mountains (W. C. Gere, c, M)
Ogden 4 NW quadrangle (R. J. Hite, c, D)
Wyoming:
Crawford Mountains phosphate deposits (W. C. Gere, c, M)
Pickle Pass quadrangle (M. L. Schroeder, c, D)
Pine Creek quadrangle (M. L. Schroeder, c, D)
Plant ecology:
Element availability:
Soils (R. C. Severson, D)
Vegetation (L. P. Gough, D)
Vegetation and hydrology (R. S. Sigafoos, w, NC)
Periodic plant-growth phenomena and hydrology (R. L. Phipps, w, NC)
Western coal regions, geochemical survey of vegetation (J. A. Erdman, D)
See also Evapotranspiration; Geochronological investigations; Limnology.
Platinum:
Mineralogy and occurrence (G. A. Desborough, D)
States:
Montana, Stillwater complex (N. J Page, M)
Wyoming, Medicine Bow Mountains (M. E. McCallum, Fort Collins, Colo.)
Potash:
Arizona, Patagonia area (J. A. Crowley, c, M)
Colorado and Utah, Paradox basin (O. B. Raup, D)
Nevada, alunite (J. A. Crowley, c, M)
New Mexico, Carlsbad, potash and other saline deposits (C. L. Jones, M)
Primitive areas. *See under* Mineral and fuel resources—compilations and topical studies, mineral-resource surveys.
Public and industrial water supplies. *See* Quality of water; Water resources.
Quality of water:
Adsorption process models (J. D. Hern, w, M)
Bedload samplers (D. W. Hubbell, w, D)
Chemistry of New Zealand waters (I. K. Barnes, w, M)
Development of biological methods (B. W. Lium, w, Atlanta, Ga.)
Geochemical kinetics studies (H. C. Claassen, w, D)
Geochemistry, Western coal region (G. L. Feder, w, D)
Heat transfer (H. E. Jobson, w, Bay St. Louis, Miss.)
Methods coordination (M. W. Skougstad, w, D)
Modeling mineral-water reactions (L. N. Plummer, w, NC)
Natural water quality (D. A. Rickert, w, Portland, Oreg.)
Organic substances in streams (R. E. Rathbun, w, Bay St. Louis, Miss.)
Organics in oil-shale residues (J. A. Leenheer, w, D)
Pesticide monitoring network (R. J. Pickering, w, NC)
Radioanalytical methods (L. L. Thatcher, w, D)
Radiochemical network (R. J. Pickering, w, NC)
Stream-temperature patterns (E. J. Pluhowski, w, NC)
Temperature modeling in natural streams (A. P. Jackman, w, M)
Thermal pollution (G. E. Harbeck, Jr., w, D)
Toxic substances in aquatic ecosystems (H. V. Leland, w, M)
Trace-element availability in sediments (S. N. Luoma, w, M)

Quality of water—Continued
Transport in ground water (L. F. Konikow, w, D)
Water-quality-data evaluation (W. H. Doyle, Jr., w, Salt Lake City, Utah)
States and territories:
Alabama:
Water problems in coal-mine areas (J. G. Newton, w, University)
Water resources in oil fields (W. J. Powell, w, Tuscaloosa)
Arkansas (w, Little Rock):
Soil Conservation Service watershed studies (T. E. Lamb)
Waste-assimilation capacity (C. T. Bryant)
California:
Ground-water quality, Barstow (J. L. Hughes, w, Laguna Niguel)
Hydrology, Sagehen Creek (R. G. Simpson, w, Sacramento)
Merced River water quality (R. J. Hoffman, w, Sacramento)
Nitrate and nitrogen isotope study (J. M. Klein, w, Laguna Niguel)
Quality of water, California streams (W. S. Bradford, w, M)
Santa Maria water quality (J. L. Hughes, w, Laguna Niguel)
Thermograph network evaluation (J. T. Limerinos, w, M)
Colorado (w, D, except as otherwise noted):
Aquatic biology of Piceance Creek (K. J. Covay, w, Meeker)
Feedlots, effects on ground water (S. G. Robson)
Northwestern Colorado water quality (T. R. Ford, w, Meeker)
Quality of water in metal-mine drainage (D. A. Wentz)
Quality of water in underground coal mines (D. A. Wentz)
Sludge, effects on ground water (S. G. Robson)
Statewide ground-water quality (Robert Brennan)
Yampa Valley ground-water reconnaissance (W. E. Hofstra)
Florida:
Contaminants, Broward County (B. G. Waller, w, Miami)
Deep-well waste injection (C. A. Pascale, w, Tallahassee)
Environmental studies, statewide (G. A. Irwin, w, Tallahassee)
Injection wells, Santa Rosa County (C. A. Pascale, w, Tallahassee)
Lakes Faith, Hope, and Charity (A. G. Lamonds, Jr., w, Winter Park)
Subsurface waste storage (G. L. Faulkner, w, Tallahassee)
Water quality:
Broward County (C. B. Sherwood, Jr., w, Miami)
South New River Channel (B. G. Waller, w, Miami)
Storm water, south Florida (H. C. Mattraw, Jr., w, Miami)

Quality of water—Continued
States and territories—Continued
Georgia (w, Doraville):
Quality of water, northern coal region (J. B. McConnell)
Storm runoff, greater Atlanta area (J. B. McConnell)
Hawaii, surface-water-quality monitoring network (J. S. Yee, w, Honolulu)
Illinois (w, Champaign):
Mine drainage in Illinois (L. G. Toler)
Sludge irrigation hydrology (R. F. Fuentes)
Indiana (w, Indianapolis):
Ground water, Indiana dunes (W. G. Weist)
Landfill monitoring, Marion County (J. R. Marie)
Stream-temperature study (W. J. Shampine)
Kansas (w, Lawrence):
Ground-water-quality network evaluations (A. M. Diaz)
Quality of water in mined areas in southeast (A. M. Diaz)
Saline discharge, Smoky Hill River (J. B. Gillespie)
South Fork, Ninnescah River basin (A. M. Diaz)
Kentucky, effects of coal mining, Kentucky River (K. L. Dyer, w, Louisville)
Louisiana (w, Baton Rouge):
Pollution capacity of streams (R. F. Martien)
Quality of water:
Atchafalaya Basin (F. C. Wells)
Lower Mississippi River (F. C. Wells)
Minnesota, water quality of highway runoff (M. R. Have, w, St. Paul)
Missouri, water quality in Joplin area (J. H. Barks, w, Rolla)
Montana, environmental impact statement, Youngs Creek Mine (C. W. Lane, w, D)
Nebraska, ground-water quality (R. A. Engberg, w, Lincoln)
Nevada (w, Carson City):
Ground-water contamination by explosives wastes (A. S. Van Denburgh)
Ground-water-quality monitoring network (J. O. Nowlin)
Pond seepage, Weed Heights (A. S. Van Denburgh)
Topical quality-of-water studies (J. P. Monis)
New Hampshire, eutrophication, Lake Winnisquam (W. D. Silvey, w, Concord)
New Jersey, waste-water reclamation (William Kam, w, Trenton)
New Mexico:
Malaga Bend evaluation (C. C. Cranston, w, Carlsbad)
Quality-of-water monitor in Chaco River basin (Kim Ong, w, Albuquerque)
New York (w, Albany):
Biology of landfill leaching (T. A. Ehlke)
Public water supply, New York State (D. F. Farrell)
Sediment nutrient dynamics (J. T. Turk)
Transport of heavy metals at Waterford (J. T. Turk)
Westchester County waste management (R. J. Archer)
North Dakota, mining effects, Gascoyne area (M. G. Croft, w, Bismarck)

Quality of water—Continued
States and territories—Continued
Ohio (w, Columbus):
Acid-mine drainage characterization (C. G. Angelo)
Rattlesnake Creek water quality (K. F. Evans)
Oklahoma (w, Oklahoma City):
Saltwater infiltration (J. J. D'Lugosz)
Zinc mine water quality (J. D. Stoner)
Oregon (w, Portland):
GOES water-data system (G. L. Gallino)
Portland:
Harbor study (S. W. McKenzie)
Water-quality study (S. W. McKenzie)
Pennsylvania (w, Harrisburg):
Anthracite mine discharge (D. J. Growitz)
Lakes, eastern Pennsylvania (J. L. Barker)
Water quality in Tioga River basin (J. R. Ward)
Puerto Rico (w, Fort Buchanan):
Pesticide monitoring (Fernando Gomez-Gomez)
Solid-waste study (Fernando Gomez-Gomez)
South Carolinia (w, Columbia):
Fluoride in ground water, coastal plain (J. M. Rhett)
Savannah River plant (D. I. Cahal)
Tennessee:
Burial-ground studies at Oak Ridge National Laboratory (D. A. Webster, w, Knoxville)
Pesticide migration study (Craig Sprinkle, w, Nashville)
Texas, Colorado River salinity (Jack Rawson, w, Austin)
Utah (w, Salt Lake City):
Reconnaissance of Utah coal fields (K. M. Waddell)
Surface-water quality:
Dirty Devil River basin (J. C. Mundorff)
Duchesne River basin (J. C. Mundorff)
Virginia (w, Richmond):
Quality of ground water (S. M. Rogers)
Watershed water quality (S. M. Rogers)
Washington (w, Tacoma):
Ground-water-quality network (M. O. Fretwell)
Lake Wilderness nutrients (N. P. Dion)
Sulphur Creek program (P. R. Boucher)
Waste effects, coastal waters (W. L. Haushild)
West Virginia, effects of deep mining (J. L. Chisholm, w, Charleston)
Wisconsin (w, Madison):
Ground-water quality, Waukesha County (M. G. Sherrill)
Irrigation and ground-water quality (S. M. Hindall)
Nederlo Creek biota (P. A. Kammerer, Jr.)
Stream reaeration (R. S. Grant)
Wyoming, North Platte reservoirs (S. J. Rucker IV, w, Cheyenne)
See also Geochemistry; Hydrologic instrumentation; Hydrology, surface water; Limnology; Marine hydrology; Sedimentology; Water resources.
Quicksilver. *See* Mercury.
Radioactive materials, transport in water. *See* Geochemistry, water.
Radioactive-waste disposal:
Hydrology of nuclear landfill (A. D. Randall, w, Albany, N.Y.)
Hydrology of salt domes (R. L. Hosman, w, Baton Rouge, La.)
National Overview Atlas (J. P. Ohl, D)

Radioactive-waste disposal—Continued
Pierre Shale (G. W. Shurr, D)
Radioactive byproducts in salt (J. W. Mercer, w, Albuquerque, N. Mex.)
Radioactive-waste burial (George DeBuchananne, w, NC)
Radioactive-waste-burial study (J. M. Cahill, w, Columbia, S.C.)
Radiohydrology technical coordination (George DeBuchananne, w, NC)
Sheffield site investigation (J. B. Foster, w, Champaign, Ill.)
Waste-disposal sites (L. A. Wood, w, NC)
Waste emplacement, crystalline rocks in conterminous United States (H. W. Smedes, D)
States:
Idaho, National Reactor Testing Station, hydrology of subsurface waste disposal (J. T. Barraclough, w, Idaho Falls)
Kentucky, Maxey Flats investigation (H. H. Zehner, w, Louisville)
New Mexico (D):
Eddy and Lea Counties, exploratory drilling (C. L. Jones)
Southeastern, waste emplacement (C. L. Jones)
Utah (D):
Paradox Basin (L. M. Gard)
Salt Valley anticline (L. M. Gard)
See also Geochemistry, water.
Rare-earth metals. *See* Minor elements.
Regional studies and compilations, large areas of the United States:
Basement rock map (R. W. Bayley, M)
Paleotectonic map folios:
Devonian System (E. G. Sable, D)
Mississippian System (L. C. Craig, D)
Pennsylvanian System (E. D. McKee, D)
Physiography of Southeastern United States (J. T. Hack, NC)
Volcanic rocks of the Appalachians (D. W. Rankin, NC)
Remote sensing:
Geologic applications:
Airborne and satellite research:
Aeromagnetic studies (M. F. Kane, D)
Development of an automatic analog earthquake processor (J. P. Eaton, M)
Electromagnetic research (F. C. Frischknecht, D)
Fraunhofer line discriminator studies (R. D. Watson, D)
Geochemical plant stress (F. C. Canney, D)
Geothermal resources (Kenneth Watson, D)
Infrared surveillance of volcanoes (J. D. Friedman, D)
Interpretation studies (R. H. Henderson, NC)
National aeromagnetic survey (J. R. Henderson, D)
Remote-sensing geophysics (Kenneth Watson, D)
Satellite magnetometry (R. D. Regan, NC)
Surficial and thematic mapping (T. N. V. Karlstrom, Flagstaff, Ariz.)
Terrain mapping from Skylab data (H. W. Smedes, D)

Remote sensing—Continued
Geologic applications—Continued
Airborne and satellite research—Continued
Urban geologic studies (T. W. Offield, D)
Volcanic gas monitoring (Motoaki Sato, NC)
High-resolution film recording system (George Harris, l, Sioux Falls, S. Dak.)
Landsat experiments:
Analysis of porphyry copper prospects from Landsat digital data (R. G. Schmidt, NC)
Computer mapping of terrain using multispectral data, Yellowstone National Park (H. W. Smedes, D)
Evaluation of Great Plains area (R. B. Morrison, D)
Experimental digital enhancement of Landsat images and CCT's (George Harris, l, Sioux Falls, S. Dak.)
Geologic mapping, South America (W. D. Carter, l, NC)
Geological and geophysical remote sensing of Iceland (R. S. Williams, Jr., l, NC)
Geostructures of the continental crust (E. H. Lathram, M)
Iron-absorption band analysis for the discrimination of iron-rich zones (L. C. Rowan, NC)
Linear features of the conterminous United States (W. D. Carter, l, NC)
Luminescence studies (R. D. Watson, l, Flagstaff, Ariz.)
Morphology, provenance, and movement of desert and seas in Africa, Asia, and Australia (E. D. McKee, D)
Optimum Landsat spectral bands (G. L. Raines, D)
Prototype volcano surveillance network (J. P. Eaton, M)
Structural, volcanic, glaciologic, and vegetation mapping, Iceland (R. S. Williams, Jr., l, NC)
Study of multispectral imagery, northwestern Saudi Arabia (A. J. Bodenlos, NC)
Suspended particulate matter in nearshore surface waters, northeast Pacific Ocean and the Hawaiian Islands (P. R. Carlson, M)
Synthetic stereo in Landsat imagery (Gordon Swann, Flagstaff, Ariz.)
Targeting of mineral exploration effort (J. V. Taranik, l, Sioux Falls, S. Dak.)
Tectonic and mineral-resource investigations, Andes Mountains, South America (W. D. Carter, l, NC)
Thermal surveillance of active volcanoes (J. D. Friedman, NC)
Skylab/EREP studies:
Evaluation of Great Plains area (R. B. Morrison, D)
Marine and coastal processes on the Puerto Rico-Virgin Islands Platform (J. V. A. Trumbull, Santurce, P.R.)
Remote-sensing geophysics (Kenneth Watson, D)

Remote sensing—Continued
Geologic applications—Continued
Skylab/visual observations:
Desert sand seas (E. D. McKee, D; C. S. Breed, Flagstaff, Ariz.)
Volcanologic features (J. D. Friedman, D)
Time-lapse satellite data for monitoring dynamic hydrologic phenomena (Morris Deutsch, S. Serebreny, l, NC)
States:
Alaska (M):
Beaufort Sea, inner shelf and coastal sedimentation environment (Erk Reimnitz)
Remote sensing of permafrost and geologic hazards (O. J. Ferrians, Jr.)
Arizona:
Arizona Regional Ecological Test Site:
North-central (D. P. Elston, Flagstaff)
Post-1890 A.D. episode erosion (R. B. Morrison, D)
Basin and Range-Colorado Plateau boundary investigation (D. P. Elston, Ivo Lucchitta, Flagstaff)
Colorado, effects of atmosphere on multispectral mapping of rock types by computer, Cripple Creek-Canon City (H. W. Smedes, D)
Colorado-Wyoming, analysis of Cortez-Uinta mineralized areas from Landsat digital data (L. C. Rowan, NC)
New Mexico, analysis of Landsat images of Claunch and vicinity (W. A. Fischer, l, NC)
Texas, monitoring changing geologic features, Texas Gulf Coast (R. B. Hunter, Corpus Christi)
Hydrologic applications:
Aircraft and spacecraft observations of Arctic sea ice (W. J. Campbell, w, Tacoma, Wash.)
Antarctic sea-ice model (W. J. Campbell, w, Tacoma, Wash.)
Application of hydrometeorological model to Sierra Nevades (L. A. Rasmussen, W. V. Tangborn, w, Tacoma, Wash.)
Arctic Ice Dynamics Joint Experiment (W. J. Campbell, w, Tacoma, Wash.)
Flood and flood-plain analysis (J. V. Taranik, l, Sioux Falls, S. Dak.)
High Plains Cooperative Program:
Cloud-formation monitoring (G. A. Thorley, (A. M. Kahan, l, NC)
Meterological-parameter monitoring with Landsat DCS (G. A. Thorley, A. M. Kahan, l, NC)
Method of correcting distortion in SLAR imagery due to curvature of flight path (C. H. Ling, L. A. Rasmussen, W. J. Campbell, w, Tacoma, Wash.)
Microwave remote sensing (G. K. Moore, w, Bay St. Louis, Miss.)
Optical and computer processing and interpretation techniques for Landsat hydrologic and environmental applications (Morris Deutsch, l, NC)
Polar-ice remote sensing (W. J. Campbell, w, Tacoma, Wash.)
Remote-sensing techniques (E. J. Pluhowski, w, NC)
Remote sensing, wetlands (V. P. Carter, w, NC)

Remote sensing—Continued
Hydrologic applications—Continued
States:
Arizona (w, Phoenix):
Arizona Test Site (H. H. Schumann)
Snow-cover mapping (H. H. Schumann)
Connecticut, Connecticut River estuary (F. H. Ruggles, Jr., w, Hartford)
Florida, southern, Landsat (A. L. Higer, w, Miami)
Pennsylvania, GOES, Juniata basin (C. D. Kauffman, w, Harrisburg)
South Dakota, hydrologic remote sensing (G. K. Moore, w, Sioux Falls)
Tennessee, Landsat digital processing of Duncan Flats quadrangle (A. L. Higer, A. E. Coker, w, Miami, Fla.)
Image processing technology:
Experimental digital enhancement of Landsat images and computer-compatible tapes (George Harris, Jr., l, Sioux Falls, S. Dak.)
High-resolution film recording system (George Harris, Jr., l, Sioux Falls, S. Dak.)
Land-resource applications:
Agricultural inventory demonstration project (W. H. Anderson, l, Sioux Falls, S. Dak.)
Applications of Landsat imagery to land systems mapping, Australia (C. J. Robinove, l, NC)
CARETS, a prototype regional environmental information system (R. H. Alexander, l, NC)
Colorado River natural resources and land use data inventory (G. A. Thorley, R. L. Hansen, l, NC)
Development of automatic techniques for land use mapping from remote-sensor data (J. R. Wray, l, NC)
Forest defoliation mapping and damage assessment (W. G. Rohde, Technicolor Graphics, Inc.)
Forest land classification and assessment of forest succession (W. G. Rohde, Technicolor Graphics, Inc.)
Impact of strip mining on range resources and wildlife habitat (D. M. Carneggie, l, Sioux Falls, S. Dak.)
Investigation of remote-sensing techniques to assess agricultural drainage (G. A. Thorley, W. A. Lidester, l, NC)
Landsat imagery for aiding objectives of the IFYGL (Morris Deutsch, A. Falconer, l, NC)
Land systems mapping with digital Landsat data (C. J. Robinove, l, NC)
Multispectral crop canopy radiance measurement using Landsat DCS platforms (G. A. Thorley, H. D. Newkirk, l, NC)
Pacific Northwest Demonstration Project (D. R. Hood, l, Sioux Falls, S. Dak.)
Skylab/EREP investigation, census cities (J. R. Wray, !, NC)
Urban and regional land use analysis, CARETS and census cities experiment (R. H. Alexander, l, NC)
States:
Oregon-Washington, inventorying and mapping kelp and eelgrass on the coasts using Landsat digital data (G. A. Thorley, R. O. Weaver, l, NC)

Remote sensing—Continued
States—Continued
South Dakota, Cooperative Land Use Demonstration Project (D. R. Hood, l, Sioux Falls)
Reservoirs. *See* Evapotranspiration; Sedimentology.
Resource and land investigations:
Council of State Governments, communication of data needs (J. T. O'Connor, l, NC)
Designation of critical environmental areas (J. T. O'Connor, l, NC)
Environmental planning and Western coal development (E. T. Smith, l, NC)
Implementing critical resource area programs (E. A. Imhoff, l, NC)
Methodology for siting onshore facilities associated with OCS development in the New England region (W. W. Doyel, l, NC)
Mined-area reclamation and related land use planning (E. A. Imhoff, l, NC)
National Environmental Indicators report (E. T. Smith, l, NC)
State land inventory systems (Olaf Kays, l, NC)
State programs on wild, scenic, and recreational rivers (M. L. Pattison, l, NC)
States:
California, Redwoods National Park (J. T. O'Connor, l, NC)
Washington, Colville Indian Reservation, case study on land use planning (E. T. Smith, l, NC)
Rhenium. *See* Minor elements; Ferro-alloy metals.
Saline minerals:
Mineralogy (B. M. Madsen, M)
States:
Colorado and Utah, Paradox Basin (O. B. Raup, D)
New Mexico, Carlsbad potash and other saline deposits (C. L. Jones, M)
Wyoming, Sweetwater County, Green River Formation (W. C. Culbertson, D)
Saltwater intrusion. *See* Marine hydrology; Quality of water.
Sedimentology:
Arctic fluvial processes, landforms (K. M. Scott, w, Laguna Niguel, Calif.)
Bedload-transport research (W. W. Emmett, w, D)
Channel morphology (L. B. Leopold, w, Berkeley, Calif.)
Coon Creek morphology (S. W. Trimble, w, Los Angeles, Calif.)
Estuarine intertidal environments (J. L. Glenn, w, D)
Measurement of sediment-laden flows (A. G. Scott, w, NC)
Petrology Laboratory (L. G. Schultz, D)
Sediment-hillside morphology (G. P. William, w, D)
Sediment movement in rivers (R. H. Meade, Jr., w, D)
Sediment transport phenomena (D. W. Hubbell, w, D)
Transport processes (C. F. Nordin, w, D)
States:
Alabama, hydrology of Warrior coal field (J. G. Newton, w, University)
Alaska, coastal environments (A. T. Ovenshine, M)
California (w, M):
San Francisco Bay, circulation (T. J. Conomos)
Santa Margarita Reservoir sediment (J. M. Knott)
Sediment, Feather River (George Porterfield)

Sedimentology—Continued
States—Continued
Hawaii, peak flow-sediment discharge relations (B. L. Jones, w, Honolulu)
Idaho, Snake and Clearwater Rivers, sediment (W. W. Emmet, w, D)
Kansas (w, Lawrence):
Estimation of sediment yield (P. R. Jordan)
Fluvial sediment in northeastern Kansas (C. D. Albert)
Sediment and geometry of channels (W. R. Osterkamp)
Kentucky, sediment yields (W. F. Curtis, w, Pikesville)
Louisiana, sediment in Lake Verret basin (L. D. Fayard, w, Baton Rouge)
Minnesota, red clay sediment and quality-of-water evaluation (E. G. Giacomini, w, St. Paul)
Pennsylvania (w, Harrisburg):
Highway erosion-control measures (L. A. Reed)
Predicting sediment flow (L. A. Reed)
Study of cobble bed streams (J. R. Ritter)
Tennessee, coal-mining study, New River (R. S. Parker, w, Nashville)
Washington (w, Tacoma):
Quileute project (M. O. Fretwell)
Sediment characteristics (L. M. Nelson)
Wisconsin (w, Madison):
Nemadji River sediment study (S. M. Hindall)
Red clay sedimentation (S. M. Hindall)
White River reservoir study (S. M. Hindall)
See also Geochemistry, water; Geochronological investigations; Hydraulics, surface flow; Hydrologic data collection and processing; Stratigraphy and sedimentation; Urbanization, hydrologic effects.
Selenium. *See* Minor elements.
Silver. *See* Heavy metals; Lead, zinc, and silver.
Soil moisture:
Grazing exclusion, effects on soil moisture (G. C. Lusby, w, D)
Infiltration and drainage (Jacob Rubin, w, M)
Vegetation changes, effects on soil moisture (G. C. Lusby, w, D)
See also Evapotranspiration.
Spectroscopy:
Mobile spectrographic laboratory (D. J. Grimes, D)
Spectrographic analytical services and research (A. W. Helz, NC; A. T. Myers, D; Harry Bastron, M)
X-ray spectroscopy (H. J. Rose, Jr., NC; Harry Bastron, M)
Stratigraphy and sedimentation:
Antler flysch, Western United States (F. G. Poole, D)
East coast Continental Shelf and margin (R. H. Meade, Jr., Woods Hole, Mass.)
Middle and late Tertiary history, Northern Rocky Mountains and Great Plains (N. M. Denson, D)
Pennsylvania System stratotype section (G. H. Wood, Jr., NC)
Permian, Western United States (E. K. Maughan, D)
Phosphoria Formation, stratigraphy and resources (R. A. Gulbrandsen, M)
Rocky Mountains and Great Basin, Devonian and Mississippian conodont biostratigraphy (C. A. Sandberg, D)

Stratigraphy and sedimentation—Continued
Sedimentary structures, model studies (E. D. McKee, D)
Tight gas sands (D. D. Rice, D)
States:
Alabama-Florida, stratigraphy (J. A. Miller, w, Raleigh, N.C.)
Alaska, Cretaceous (D. L. Jones, M)
Arizona:
Hermit and Supai Formations (E. D. McKee, D)
Magnetic chronology, Colorado Plateau and environs (D. P. Elston, E. M. Shoemaker, Flagstaff)
Arizona-New Mexico, paleomagnetic correlation, Colorado Plateau (J. D. Strobell, Flagstaff, Ariz.)
California, southern San Joaquin Valley, subsurface geology (J. C. Maher, M)
Colorado, Jurassic stratigraphy (G. N. Pipiringos, D)
Louisiana, Continental Shelf (H. L. Berryhill, Jr., Corpus Christi, Tex.)
Montana, Ruby Range, Paleozoic rocks (E. T. Ruppel, D)
Montana-North Dakota-South Dakota-Wyoming, Williston basin (C. A. Sandberg, D)
Nebraska, central Nebraska basin (G. E. Prichard, D)
Nevada, Indian Trail Formation, abandonment of name (G. L. Dixon, D)
New Mexico, western and adjacent areas, Cretaceous stratigraphy (E. R. Landis, D)
Oregon-California (M):
Black sands:
Geologic investigations (H. E. Clifton)
Hydrologic investigations (P. D. Snavely, Jr.)
Utah, Promontory Point (R. B. Morrison, D)
Wyoming (D):
Lamont-Baroil area (M. W. Reynolds)
South-central part, Jurassic stratigraphy (G. N. Pipiringos)
See also Paleontology, stratigraphic; *specific areas under* Geologic mapping.

Structural geology and tectonics:
Contemporary coastal deformation (R. O. Castle, M)
Rock behavior at high temperature and pressure (E. C. Robertson, NC)
Structural studies, Basin and Range (F. G. Poole, D)
States:
Arizona, southeastern, tectonics (Harold Drewes, D)
California-Nevada, transcurrent fault analysis, western Great Basin (R. E. Anderson, D)
Nevada, central, east-trending lineaments (G. L. Dixon, D)
See also specific areas under Geologic mapping.

Talc:
New York, Pope Mills and Richville quadrangles (C. E. Brown, NC)

Tantalum. *See* Minor elements.

Thorium:
Analytical support (C. M. Bunker, D)
Investigations of thorium in igneous rocks (M. H. Staatz, D)
States:
Colorado (D):
Cochetopa area (J. C. Olson)
Wet Mountains, thorium resources appraisal (T. J. Armbrustmacher)
Wyoming, Bear Lodge Mountains (M. H. Staatz, D)

Tungsten. *See* Ferro-alloy metals.

Uranium:
Exploration techniques:
Geochemical techniques (R. A. Cadigan, D)
Geochemical techniques of halo uranium (J. K. Otton, D)
Morrison Formation (L. C. Craig, D)
Uranium in streams as an exploration technique (K. J. Wenrich-Verbeek, D)
Ore-forming processes (H. C. Granger, D)
Paleomagnetism applied to uranium exploration (R. L. Reynolds, D)
Precambrian sedimentary and metasedimentary rocks (F. A. Hills, D)
Radium and other isotopic distintegration products in springs and subsurface water (R. A. Cadigan, J. K. Felmlee, D)
Resources of radioactive minerals (A. P. Butler, Jr., D)
Resources of United States and world (W. I. Finch, D)
Southern High Plains (W. I. Finch, D)
United States:
Eastern:
Appalachian Basin, Paleozoic rocks (A. F. Jacob, D)
Basin analysis as related to uranium potential in Triassic sedimentary rocks (C. E. Turner, D)
Uranium vein deposits (R. I. Grauch, D)
Southwestern, basin analysis related to uranium potential in Permian rocks (J. A. Campbell, D)
Western:
Relation of diagenesis and uranium deposits (M. B. Goldhaber, D)
Vein and disseminated deposits of uranium (J. T. Nash, D)
Uranium daughter products in modern decaying plant remains, in soils, and in stream sediments (K. J. Wenrich-Verbeek, D)
Volcanic source rocks (R. A. Zielinski, D)
States:
Arizona (R. E. Thaden, D)
Arizona-Colorado-New Mexico-Utah (D):
Colorado Plateau:
Basin analysis of uranium-bearing Jurassic rocks (Fred Peterson)
Tabular deposits (R. A. Brooks)
Arizona-Nevada-Utah, uranium potential of Basin and Range province (J. E. Peterson, D)
Colorado (D):
Cochetopa Creek uranium-thorium area (J. C. Olson)
Marshall Pass uranium (J. C. Olson)
Schwartzwalder mine (E. J. Young)
Uranium-bearing Triassic rocks (R. D. Lupe)
Colorado-New Mexico-Texas-Utah-Wyoming, organic chemistry of uranium (J. S. Leventhal, D)
New Mexico (D):
Acoma area (C. H. Maxwell)
Church Rock-Smith Lake (C. T. Pierson)
North Church Rock (A. R. Kirk)
San Juan Basin uranium (M. W. Green)
Sanostee (A. C. Huffman, Jr.)

Uranium—Continued
- *States—Continued*
  - Texas:
    - Coastal Plain, geophysical and geological studies (D. H. Eargle, Austin)
    - Tilden-Loma Alta area (K. A. Dickinson, D)
    - Uranium disequilibrium studies (F. E. Senftle, NC)
  - Texas-Wyoming, roll-type deposits (E. N. Harshman, D)
  - Utah-Colorado (D):
    - Moab quadrangle (A. P. Butler, Jr.)
    - Uinta and Piceance Creek basin (L. C. Craig)
  - Wyoming (D):
    - Badwater Creek (R. E. Thaden)
    - Crooks Peak quadrangle (L. J. Schmitt, Jr.)
    - Granite as a source rock of uranium (J. S. Stuckless, D)
    - Northeastern Great Divide Basin (L. J. Schmitt, Jr.)
    - Powder River basin (E. S. Santos)
    - Sagebrush Park quadrangle (L. J. Schmitt, Jr.)
    - Stratigraphic analysis of Tertiary uranium basins of Wyoming (D. A. Seeland)
    - Stratigraphic analysis of Western Interior Cretaceous uranium basins (H. W. Dodge, Jr.)

Urban geology:
- Alaska (D):
  - Anchorage area (Ernest Dobrovolny)
  - Juneau area (R. D. Miller)
  - Sitka area (L. A. Yehle)
  - Small coastal communities (R. W. Lemke)
- Arizona, Phoenix-Tucson region resources (T. G. Theodore, M)
- California (M, except as otherwise noted):
  - Coastal geologic processes (K. R. Lajoie)
  - Flatlands materials and their land use significance (E. J. Helley)
  - Geologic factors in open space (R. M. Gulliver)
  - Hillside materials and their land use significance (C. M. Wentworth, Jr.)
  - Malibu Beach and Topanga quadrangles (R. F. Yerkes)
  - Quaternary framework for earthquake studies, Los Angeles Basin (J. C. Tinsley III)
  - Regional slope stability (T. H. Nilsen)
  - San Francisco Bay region, environment and resources planning study:
    - Bedrock geology (M. C. Blake)
    - Marine geology (D. S. McCulloch)
    - Open space (C. S. Danielson)
    - San Andreas fault:
      - Basement studies (D. C. Ross)
      - Basin studies (J. A. Bartow)
      - Regional framework (E. E. Brabb)
      - Tectonic framework (R. D. Brown)
    - San Mateo County cooperative (H. D. Gower)
    - Sargent-Berrocal fault zone (R. J. McLaughlin, D. H. Sorg)
    - Seismicity and ground motion (W. B. Joyner)
  - Southern:
    - Eastern part (D. M. Morton, Riverside)
    - Western part (R. F. Yerkes)
- Colorado (D):
  - Denver-Front Range urban corridor, remote sensing (T. W. Offield)

Urban geology—Continued
- *States—Continued*
  - Colorado (D)—Continued
    - Denver metropolitan area (R. M. Lindvall)
    - Denver mountain soils (P. W. Schmidt)
    - Denver urban area, regional geochemistry (H. A. Tourtelot)
    - Denver urban-area study:
      - Geologic maps:
        - Boulder-Fort Collins-Greeley area (R. B. Colton)
        - Colorado Springs-Castle Rock area (W. R. Hansen)
        - Greater Denver area (D. E. Trimble)
      - Land use classification, Colorado Front Range urban corridor (W. R. Hansen, L. B. Driscoll)
    - Engineering geology mapping research, Denver region (H. E. Simpson)
    - Terrain mapping from Skylab data (H. W. Smedes)
  - Maryland, Baltimore-Washington urban-area study (J. T. Hack, NC)
  - Massachusetts, Boston and vicinity (C. A. Kaye, Boston)
  - Montana, geology for planning, Helena region (R. G. Schmidt, NC)
  - New Mexico, geology of urban development (H. E. Malde, D)
  - Pennsylvania (NC, except as otherwise noted):
    - Coal-mining features, Allegheny County (W. E. Davies)
    - Geochemistry of Pittsburgh urban area (H. A. Tourtelot, D)
    - Susceptibility to landsliding:
      - Allegheny County (J. S. Pomeroy)
      - Beaver, Butler, and Washington Counties (J. S. Pomeroy)
  - Utah, Salt Lake City and vicinity (Richard VanHorn, D)
  - Virginia, geohydrologic mapping of Fairfax County (A. J. Froelich, NC)

Urban hydrology:
- Geohydrology, urban planning (H. G. O'Connor, w, Lawrence, Kans.)
- Urban-area reconnaissance (W. E. Hale, w, Albuquerque, N. Mex.)
- Urban runoff networks (H. H. Barnes, Jr., w, NC)
- Urban sedimentology (H. P. Guy, w, NC)
- *States:*
- Alabama, Jefferson County floodway evaluation (R. H. Bingham, w, Tuscaloosa)
- Arizona, Tucson-Phoenix urban-area pilot study (E. S. Davidson, w, Tucson)
- California:
  - Morphology, San Francisquito (J. R. Crippen, w, M)
  - Perris Valley (M. W. Busby, w, Laguna Niguel)
  - Poway Valley (M. W. Busby, w, Laguna Niguel)
- Colorado:
  - Climatological atlases, Colorado Front Range urban corridor (W. R. Hansen, D)
  - Flood frequency, urban areas (R. K. Livingston, w, D)
  - Front Range urban corridor (D. E. Hillier, w, D)
  - Storm runoff quality, Denver (S. R. Ellis, w, D)

Urban hydrology—Continued
- *States—Continued*
- Connecticut, Connecticut Valley urban pilot study (R. L. Melvin, w, Hartford)
- Florida:
  - Bay Lake (A. L. Putnam, w, Winter Park)
  - Riviera Beach investigations (A. L. Knight, w, Miami)
  - Tampa Bay region (G. E. Seaburn, w, Tampa)
- Hawaii, hydrology, sediment in Mauna Loa (C. J. Ewart, w, Honolulu)
- Illinois, quality-of-water monitoring, Bloomington-Normal (B. J. Prugh, Jr., w, Champaign)
- Iowa, flow models, Walnut Creek (O. G. Lara, w, Iowa City)
- Kansas, urban runoff, Wichita (D. B. Richards, w, Lawrence)
- Kentucky (w, Louisville):
  - Hydraulics of bridge sites (C. H. Hannum)
  - Water use and availability (D. C. Griffin)
- Mississippi, bridge-site investigations (K. V. Wilson, w, Jackson)
- Missouri, stream hydrology, St. Louis (T. W. Alexander, w, Rolla)
- New Mexico, urban flood hydrology, Albuquerque (A. G. Scott, w, Santa Fe)
- North Carolina, urban hydrology, Charlotte (W. H. Eddins, w, Raleigh)
- Ohio (R. P. Hawkinson, w, Columbus)
- Oregon (w, Portland):
  - Bear Creek water-quality study (S. W. McKenzie)
  - Portland rainfall-runoff study (Antonius Laenen)
- Pennsylvania (w, Harrisburg):
  - Philadelphia (T. G. Ross)
  - Storm-water measurements (T. G. Ross)
- South Carolina, hydraulic-site reports (B. H. Whetstone, w, Columbia)
- Texas (w, Forth Worth, except as otherwise noted):
  - Austin (M. L. Maderak, w, Austin)
  - Dallas County urban study (B. B. Hampton)
  - Dallas urban study (B. B. Hampton)
  - Fort Worth urban study (R. M. Slade, Jr.)
  - Houston urban study (E. L. Johnson, w, Houston)
  - San Antonio urban study (R. D. Steger, w, San Antonio)
- Washington, Puget Sound urban-area studies (B. L. Foxworthy, w, Tacoma)
- Wisconsin, simulation of urban runoff (R. S. Grant, w, Madison)

Urbanization, hydrologic effects:
- North Carolina, effect on flood flow, Charlotte area (W. H. Eddins, w, Raleigh)

Vegetation:
- Element availability:
  - Soils (R. C. Severson, D)
  - Vegetation (L. P. Gough, D)
- Elements in organic-rich material (F. N. Ward, D)
- Plant geochemistry, urban areas (H. A. Tourtelot, D)
- Western coal regions, geochemical survey of vegetation (J. A. Erdman, D)
- *See also* Plant ecology.

Volcanic-terrane hydrology. *See* Artificial recharge.

Volcanology:
- Cascade volcanoes, geodimeter studies (D. A. Swanson, M)
- Cauldron and ash-flow studies (R. L. Smith, NC)
- Columbia River basalt (D. A. Swanson, M)
- Regional volcanology (R. L. Smith, NC)
- Volcanic-ash chronology (R. E. Wilcox, D)
- Volcanic hazards (D. R. Crandell, D)
- *States*
- Arizona, San Francisco volcanic field (J. F. McCauley, M)
- Hawaii:
  - Hawaiian Volcano Observatory (Hawaii National Park)
  - Seismic studies (P. L. Ward, M)
  - Submarine volcanic rocks (J. G. Moore, M)
- Idaho (D):
  - Central Snake River Plain, volcanic petrology (H. E. Malde)
  - Eastern Snake River Plain region (P. L. Williams, H. J. Prostka)
  - Snake River basalt (P. L. Williams, H. J. Prostka)
- Montana, Wolf Creek area, petrology (R. G. Schmidt, NC)
- New Mexico, Valles Mountains, petrology (R. L. Smith, NC)
- Wyoming, deposition of volcanic ash in the Mowry Shale and Frontier Formation (G. P. Eaton, D)

Water resources:
- Central Region field coordination (J. L. Poole, w, D)
- CENTO working group on hydrogeology (J. R. Jones, w, NC)
- Chattahoochee intensive river quality (R. N. Cherry, w, Atlanta, Ga.)
- Columbia-North Pacific ground water (B. L. Foxworthy, w, Tacoma, Wash.)
- Comprehensive studies, Pacific Northwest (L. E. Newcomb, w, M)
- Dams, weirs, and flumes (H. J. Tracy, w, Atlanta, Ga.)
- Data coordination, acquisition, and storage:
  - NAWDEX Project (M. D. Edwards, w, NC)
  - Water Data Coordination (R. H. Langford, w, NC)
- East Triassic waste-disposal study (G. L. Bain, w, Raleigh, N.C.)
- Effects of vegetation changes (G. C. Lusby, w, D)
- Environmental impact analyses support (G. H. Davis, w, NC)
- Environmental impact statement, Idaho phosphate (W. J. Schneider, w, Pocatello, Idaho)
- Evaluation of land treatment (R. F. Hadley, w, D)
- Foreign assistance:
  - PL 80–402 (J. R. Jones, w, NC)
  - Section 607 (J. R. Jones, w, NC)
- Foreign countries:
  - Canada, gas pipeline (V. K. Berwick, w, Anchorage, Alaska)
  - India, ground-water investigations in states of Madhya Pradesh, Gujarat, Maharashtra, and Mysore (J. R. Jones, w, NC)
  - Kenya, range water resources (N. E. McClymonds, w, Nairobi)
  - Nepal, hydrogeology of Tera region (G. C. Tibbitts, Jr., w, Katmandu)

Water resources—Continued
Foreign countries—Continued
Saudi Arabia:
Saudi Arabian advisory services (J. T. Callahan, w, NC)
Source of Riyadh water supply (J. R. Jones, w, NC)
Yemen, northern, water and mineral survey, (J. R. Jones, w, NC)
General hydrologic research (R. L. Nace, w, Raleigh, N.C.)
Ground-water appraisal, New England region (Allen Sinnott, w, Trenton, N.J.)
Ground water, Missouri Basin (O. J. Taylor, w, D)
Hydrology of Dismal Swamp (P. E. Ward, w, NC)
Infiltration and drainage (Jacob Rubin, w, M)
Intensive river-quality assessment (D. A. Rickert, w, Portland, Oreg.)
Intermediate-depth drilling (L. C. Dutcher, w, M)
Modeling principles (J. P. Bennett, w, NC)
Network design (M. E. Moss, w, NC)
Northeastern Region field coordination (J. W. Geurin, w, NC)
Northwest water-resources data center (N. A. Kallio, w, Portland, Oreg.)
Powell arid lands centennial (R. F. Hadley, w, D)
Quality-of-water accounting network (R. J. Pickering, w, NC)
Rating extensions (K. L. Wahl, w, NC)
Rehabilitation potential, energy lands (L. M. Shown, w, D)
Reservoir bank storage study (T. H. Thompson, w, M)
Southeastern Region field coordination (C. L. Holt, w, Atlanta, Ga.)
State aid, miscellaneous (J. R. Jones, w, NC)
Subsurface waste emplacement potential (P. M. Brown, w, Raleigh, N.C.)
Water-resource activities (J. R. Carter, w, D)
Waterway treaty engineering studies (J. A. Bettendorf, w, NC)
Western Region field coordination (G. L. Bodhaine, w, M)
Yellowstone level B study (H. H. Hudson, w, D)
States and territories:
Alabama:
Cretaceous aquifer simulation (R. A. Gardner, w, Montgomery)
Drainage areas (J. C. Scott, w, Montgomery)
Low flows of Alabama streams (W. J. Powell, E. C. Hayes, w, Tuscaloosa)
Plans, reports, and information (W. J. Powell, w, Tuscaloosa)
Alaska (w, Anchorage, except as otherwise noted):
Alaska water assessment (G. O. Balding)
Arctic resources (J. M. Childers)
Coal resources study (D. R. Scully)
Hydrology:
Anchorage area (Chester Zenone)
Hydrologic environment of the trans-Alaska pipeline system (TAPS) (J. M. Childers)
Municipal water supply (G. S. Anderson)
National park proposal studies (A. J. Feulner)
North Slope study (G. L. Nelson, w, Fairbanks)
North Star project (G. L. Nelson, w, Fairbanks)
TAPS construction hydrology (C. E. Sloan)

Water resources—Continued
States and territories—Continued
Arizona:
Black Mesa hydrologic study (R. M. Myrick, w, Tucson)
Black Mesa monitoring program (G. W. Levings, w, Flagstaff)
Channel loss study (T. W. Anderson, w, Phoenix)
Coconino Sandstone water budget, Navajo County (L. J. Mann, w, Flagstaff)
Copper Basin study (B. W. Thomsen, w, Phoenix)
Ground-water appraisal, Lower Colorado River (E. S. Davidson, w, Tucson)
Sedona ground-water availability (G. W. Levings, w, Flagstaff)
Verde Valley water resources (G. W. Levings, w, Flagstaff)
Arkansas (w, Little Rock):
Bayou Bartholomew systems study (M. E. Broom)
Cache River aquifer-stream system (M. E. Broom)
Characteristics of streams (M. S. Hines)
Investigations and hydrologic information (R. T. Sniegocki)
Time-of-travel study (T. E. Lamb)
California:
Ground water:
Antelope Valley:
Antelope Valley area (F. W. Geissner, w, Laguna Niguel)
Ground-water model (T. J. Durbin, w, Laguna Niguel)
City of Modesto, ground-water planning (R. W. Page, Sacramento)
Death Valley (C. E. Lamb, w, Laguna Niguel)
Geohydrology, Round Valley (K. S. Muir, w, M)
Indian Wells Valley (J. H. Koehler, w, Laguna Niguel)
Joshua Tree (D. J. Downing, w, Laguna Niguel)
Madera area, ground-water model (W. D. Nichols w, Sacramento)
Redlands nitrate study (L. A. Eccles, w, Laguna Niguel)
Sacramento Valley (R. M. Bloyd, Jr., w, Sacramento)
Santa Barbara-San Luis Obispo (F. W. Geissner, w, Laguna Niguel)
Santa Cruz (K. S. Muir, w, M)
Southern California (C. E. Lamb, w, Laguna Niguel)
Indian reservations (J. W. Wark, w, M)
Quality of water:
Ground-water quality, Suisun Bay (Chabot Kilburn, w, M)
Lakes and reservoirs (R. C. Averett, w, M)
Trace-metals control, Sacramento (R. F. Ferreira, w, Sacramento)
Surface water:
Floods, small drainage areas (A. O. Waananen, w, M)
Sediment, Redwoods National Park (J. M. Knott, w, M)
Urbanization, Santa Clara County (J. M. Knott, w, M)

Water resources—Continued

States and territories—Continued

Colorado (w, D, except as otherwise noted):
- Areawide water-quality inventory (L. J. Britton)
- Coal rehabilitation (G. H. Leavesley)
- Evaporation, Colorado lakes (D. B. Adams)
- Ground water:
  - High Plains of Colorado (R. G. Borman)
  - Potentiometric surface mapping (F. A. Welder)
  - Southern Ute lands (R. E. Brogden)
  - Southwestern Colorado (R. E. Brogden)
  - U.S. Bureau of Mines prototype mine (J. B. Weeks)
- Hydrology:
  - Arkansas River basin (R. L. Livingston, w, Pueblo)
  - El Paso County (R. E. Fidler, w, Pueblo)
  - Naval Oil Shale Reserve No. 1 (G. H. Leavesley)
  - Parachute-Roan Creek Basin (G. H. Leavesley)
  - San Luis Valley (R. E. Fidler, w, Pueblo)
  - South Platte River basin, Henderson to State line (R. T. Hurr)
- Quality of water:
  - Boulder County (D. C. Hall)
  - Geochemical investigations (S. G. Robson)
  - Hydrology of Jefferson County (D. C. Hall)
  - Sediment yield, Piceance Basin (V. C. Norman)
  - West slope aquifers (T. F. Giles)
- Spring hydraulics (G. J. Saulnier)
- Water resources, Park-Teller County (K. E. Goddard, w, Pueblo)
- Yampa River basin assessment (T. D. Steele)

Connecticut (w, Hartford):
- Hydrogeology, south-central Connecticut (R. L. Melvin)
- Part 7, Upper Connecticut River basin (R. B. Ryder)
- Part 8, Quinnipiac River basin (D. L. Mazzaferro)
- Part 9, Farmington River basin (H. R. Anderson)
- Part 10, Lower Connecticut River basin (L. A. Weiss)
- Short-term studies (F. H. Ruggles, Jr.)

Delaware, aquifer-model studies (R. H. Johnston, w, Dover)

Florida:
- Annual hydrologic report, southwestern Florida (K. W. Causseaux, w, Tampa)
- Bridge-site studies (W. C. Bridges, w, Tallahassee)
- Broward County (C. B. Sherwood, Jr., w, Miami)
- Ground water:
  - Aquifer mapping, south Florida (Howard Klein, w, Miami)
  - Coastal springs (W. C. Sinclair, w, Miami)
  - Hallandale area (H. W. Bearden, w, Miami)
  - Hollywood area (H. W. Bearden, w, Miami)
  - Hydrogeology, middle Peace basin (W. E. Wilson III, w, Tampa)
  - Hydrology:
    - Cocoa well field (J. B. Holly, w, Winter Park)
    - Manatee County (D. P. Brown, w, Sarasota)
    - Sarasota County (Horace Sutcliffe, Jr., w, Sarasota)
  - Ochlockonee River basin investigation (C. A. Pascale, w, Tallahassee)

Water resources—Continued

States and territories—Continued

Florida—Continued
- Ground water—Continued
  - Potentiometric surface, St. Petersburg-Tampa (C. B. Hutchinson, w, Tampa)
  - Recharge, Orange County (P. W. Bush, w, Winter Park)
  - Saltwater intrusion, Fernandina (R. W. Fairchild, w, Jacksonville)
  - Sand-gravel aquifer, Pensacola (Henry Trapp, w, Tallahassee)
  - Santa Fe River basin (J. D. Hunn, w, Tallahassee)
  - Sewage effluent disposal, irrigation (L. J. Slack, w, Tallahassee)
  - Shallow aquifer, Brevard County (J. M. Frazee, Jr., w, Winter Park)
  - Shallow aquifers, Alafia and Peace Rivers (C. B. Hutchison, w, Tampa)
  - Technical assistance, Hillsborough County (J. W. Stewart, w, Tampa)
  - Technical assistance, south Florida (Howard Klein, w, Miami)
  - Urban hydrology, Englewood area (Horace Sutcliffe, Jr., w, Sarasota)
  - Verna well field (Horace Sutcliffe, Jr., w, Sarasota)
  - Water resources:
    - Duval and Nassau Counties (G. W. Leve, w, Jacksonville)
    - Martin County (R. A. Miller, w, Miami)
    - Tequesta (A. L. Knight, w, Miami)
  - Water-supply potential, Green Swamp (H. F. Grubb, w, Winter Park)
- Hydrogeologic maps, Seminole County (W. D. Wood, w, Winter Park)
- Hydrogeology, Osceola Forest (P. R. Seaber, w, Tallahassee)
- Hydrologic suitability study (L. V. Causey, w, Jacksonville)
- Hydrology, Volusia County (P. W. Bush, w, Winter Park)
- Lee County (D. H. Boggess, w, Ft. Myers)
- Mapping, Green Swamp (B. F. McPherson, w, Miami)
- Palm Beach County (A. L. Knight, w, Miami)
- Quality of water:
  - Estuarine hydrology, Tampa Bay (C. R. Goodwin, w, Tampa)
  - Landfill and water quality (J. E. Hull, w, Miami)
  - Solid waste, Hillsborough County (Mario Fernandez, Jr., w, Tampa)
  - Solid waste, St. Petersburg (Mario Fernandez, Jr., w, Tampa)
  - Subsurface disposal, Pinellas County (J. J. Hickey, w, Tampa)
  - Technical assistance, Department of Environmental Regulation (G. A. Irwin, w, Tallahassee)
- Special studies, statewide (C. S. Conover, w, Tallahassee)

Water resources—Continued
States and territories—Continued
Florida—Continued
Surface water:
Hydrology study, Fakahatchee Strand (L. J. Swayze, w, Miami)
Lakes in southwest Florida (R. C. Reichenbaugh, w, Tampa)
Manasota technical assistance (Horace Sutcliffe, Jr., w, Sarasota)
Technical assistance:
Northwest Florida Water Management District (W. B. Mann, w, Tallahassee)
Suwanee River Water Management District (J. C. Rosenau, w, Tallahassee)
Tri-county investigation (C. B. Bentley, w, Jacksonville)
Waccasassa Basin hydrology (G. F. Taylor, w, Winter Park)
Water atlas (S. D. Leach, w, Tallahassee)
Water resources, Hendry County (T. H. O'Donnell, w, Miami)
Water resources, Orange County (C. H. Tibbals, w, Winter Park)
Western Collier County (W. J. Haire, w, Miami)
Georgia (w, Doraville):
Cretaceous (L. D. Pollard)
Hydrology of the Albany area (R. E. Krause)
Information system (J. R. George)
Northwest Georgia geology and water (C. W. Cressler)
Valdosta hydrology (R. E. Krause)
Hawaii (w, Honolulu):
Data management, Guam (C. J. Huxel, Jr.)
Kauai water-resource survey (R. J. Burt)
Regional study (B. L. Jones)
Topical studies (F. T. Hidaka)
Idaho (w, Boise):
Flow in Silver Creek, Idaho (J. A. Moreland)
Geohydrology of Bruneau Plateau (H. W. Young)
Ground-water-quality assessment (H. R. Seitz)
Kootenai Board—WWT (E. E. Harris)
Streamflow evaluation, Upper Snake River (C. A. Thomas)
Illinois, water-quality appraisal (L. G. Toler, w, Champaign)
Indiana, ground water near Fort Wayne (Michael Planert, w, Indianapolis)
Iowa (w, Iowa City):
Bedrock mapping (R. E. Hansen)
Cambrian-Ordovician aquifer (W. L. Steinhilber)
East-central (K. D. Wahl)
Low flow, Iowa streams (O. G. Lara)
National eutrophication survey (I. L. Burmeister)
Sediment data (J. R. Schuetz)
South-central (J. W. Cagle, Jr.)
Kansas (w, Lawrence, except as otherwise noted):
Kansas-Oklahoma Arkansas River Commission (E. R. Hedman)
Miscellaneous investigations (H. G. O'Connor)
Numerical modeling (J. C. Halepaska)
Report processing (H. E. McGovern)
Saline ground-water resources (K. M. Keene)

Water resources—Continued
States and territories—Continued
Kansas (w, Lawrence, except as otherwise noted) —Continued
Saline water from Permian rocks (D. R. Albin)
Water supply in droughts (F. C. Foley)
Kentucky (w, Louisville):
Covington-Lexington-Louisville triangle (D. S. Mull)
Ground water, Ohio River valley (J. M. Kernodle)
London-Corbin area (R. W. Davis)
Somerset hydrology (R. W. Davis)
Louisiana (w, Baton Rouge):
Baton Rouge area (C. D. Whiteman, Jr.)
New Orleans area (D. C. Dial)
Ground water:
Gramercy area (G. T. Cardwell)
Kisatchie Forest area (J. E. Rogers)
Terrace aquifer, central Louisiana (J. T. Snider)
Reports on special topics (M. F. Cook)
Site studies (R. L. Hosman)
Southwestern part (D. J. Nyman)
Surface water:
Flood hydraulics and hydrology (B. L. Neely, Jr.)
Velocity of Louisiana streams (A. J. Calandro)
Tangipahoa-Tchefuncte River basins (D. J. Nyman)
Maine, public inquiries (C. R. Wagner, w, Augusta)
Maryland, (w, Towson, except as otherwise noted):
Baltimore-Washington urban hydrology (W. F. White)
Ground-water resources, urbanization, Hartford County (L. J. Nutter)
Low-flow studies (W. J. Herb)
Special studies, ground water (C. G. Richardson)
Trap efficiency, Rock Creek (T. H. Yorke, Jr., College Park)
Massachusetts (w, Boston):
Coastal southeastern Massachusetts, Wareham to Seekonk (G. D. Tasker)
Connecticut River lowlands (E. H. Walker)
Deicing chemicals, ground water (L. G. Toler)
Nashua River basin (R. A. Brackley)
Northeast:
Coastal basins (F. B. Gay)
River basins (R. A. Brackley)
Public inquiries (J. A. Baker)
Michigan (w, Okemos, except as otherwise noted):
Erosion in St. Joseph Basin (T. R. Cummings)
Geohydrology, environmental planning (F. R. Twenter)
Ground water:
Models, Muskegon County (W. B. Fleck)
West Upper Peninsula (C. J. Doonan, w, Escabana)
Minnesota (w, St. Paul):
Ground water in Park Rapids area (J. O. Helgesen)
Impact of copper-nickel mining (P. G. Olcott)
Twin Cities level B study (C. R. Collier)
Upper Mississippi and Souris-Red-Rainy Rivers (V. J. Latkovich)
Water budget, Shagawa Lake (D. W. Ericson)

Water resources—Continued

State and territories—Continued

Mississippi (w, Jackson):
- Ground water:
  - Aquifer maps for Mississippi (E. H. Boswell)
  - Ground-water use (J. A. Callahan)
  - Hydrology, Tennessee-Tombigbee (A. G. Lamonds)
  - Water, subcoastal Mississippi (G. T. Dalsin)
- Waste assimilation (J. K. Arthur)
- Water use (J. A. Callahan)

Missouri (w, Rolla):
- Ground-water resources, Springfield area (L. F. Emmett)
- Water quality, scenic riverways (J. H. Barks)

Montana (w, Helena, except as otherwise noted):
- Ground water:
  - Fort Belknap (R. D. Feltis)
  - Fort Union Formation (W. B. Hopkins, w, Billings)
  - Hydrology, lower Flathead (A. J. Boettche)
  - Mined lands reclamation (W. R. Hotchkiss)
  - Powder River valley:
    - Central (W. R. Miller, w, Billings)
    - Southern (W. R. Miller, w, Billings)
  - Quality of water near Libby (A. J. Boettcher)
  - "Saline seeps" (R. G. McMurtrey)
  - Special investigations (D. L. Coffin)
  - Water availabliity, Madison (W. R. Miller, w, Billings)
  - Water supplies for national parks, monuments, and recreation areas (D. L. Coffin)
- Mining effects, shallow water (R. S. Roberts)

Nebraska (w, Lincoln):
- Hydrogeology of southwest Nebraska (E. G. Lappala)
- Movement of nitrogen into aquifers (L. R. Petri)
- Time-of-travel data (L. R. Petri)

Nevada (w, Carson City):
- Aquifers in the Fallon area (P. A. Glancy)
- Topical studies (J. P. Monis)
- Water supply:
  - Cold Spring Valley (A. S. Van Denburgh)
  - Mining districts (H. A. Shamberger)

New Hampshire (w, Concord):
- Ground-water reconnaissance, river basins (J. E. Cotton)
- Public inquiries (C. E. Hale)

New Jersey (w, Trenton):
- Automatic processing of ground-water data (William Kam)
- Base-flow studies (E. G. Miller)
- Miscellaneous Federal work (Harold Meisler)
- Problem river studies (J. C. Schornick, Jr.)
- Quantification nonpoint pollution (J. C. Schornick, Jr.)
- Short-term studies (Harold Meisler)
- Test drill geophysical logging (J. E. Luzier)
- Water resources, Wharton Tract (William Kam)

New Mexico (w, Albuquerque):
- Bureau of Indian Affairs water-supply investigations (F. P. Lyford)
- Cimarron Basin analysis (P. L. Soule)

Water resources—Continued

States and territories—Continued

New Mexico (w, Albuquerque)—Continued
- Coal-lease areas, northwest New Mexico (Kim Ong)
- Ground water:
  - Capitan Reef (W. L. Hiss)
  - Harding County (F. D. Trauger)
  - Miscellaneous activities, State Engineer (W. A. Mourant)
  - White Sands Missile Range, water levels and pumpage (H. D. Hudson)
- New Mexico data bank (D. R. Possan)
- Rio Grande Commission (P. L. Soule)
- Surface water, Pojoaque River analyses (G. A. Hearne)
- Water resources, Acoma and Laguna Reservations (F. P. Lyford)

New York (w, Mineola, except as otherwise noted):
- Basin recharge with sewage effluent (R. C. Prill)
- Column-basin studies (M. S. Garber)
- Hydrogeology of southeast Nassau County (H. F. H. Ku)
- Long Island water quality (S. E. Ragone)
- Management modeling (G. E. Kimmel)
- Nassau County, ground-water-system study (Chabot Kilburn)
- Short-term studies (R. J. Dingman, w, Albany)
- Suffolk County:
  - Hydrologic conditions (H. M. Jensen)
  - Water-quality observation well program (Julian Soren)
- Supplemental recharge by storm basins (D. A. Aronson)
- Water resources, South Fork, Long Island (Bronius Nemickas)

North Carolina (w, Raleigh):
- Ground water:
  - Automatic data processing program (C. C. Daniel)
  - Blue Ridge Parkway (M. D. Winner)
- Hydrology of Albermarle-Pamlico area (C. C. Daniel)
- Public water supplies (T. M. Robison)
- Surface water:
  - Hydrology of estuaries (G. L. Geisse)
  - Requests for data (H. G. Hinson)

North Dakota (w, Bismarck, except as otherwise noted):
- Ground water:
  - Billings-Golden Valley Slope (L. O. Anna)
  - Dickey-Lamoure (J. S. Downey)
  - Dunn County (R. L. Klausing)
  - Grant and Sioux Counties (P. G. Randich)
  - Hydrologic changes due to mining (O. A. Crosby)
  - Morton County (P. G. Randich)
  - Ramsey County (R. D. Hutchinson, w, Grand Forks)
  - Ransom-Sargent (C. A. Armstrong)
  - Special investigations (Q. F. Paulson)
- National eutrophication survey (O. A. Crosby)

Ohio, water inventory, hydrologic studies (D. D. Knockhenmus, w, Columbus)

Water resources—Continued
States and territories—Continued
Oklahoma (w, Oklahoma City):
Ground water:
Antlers Sand (D. L. Hart, Jr.)
Vamoosa Formation (J. J. D'Lugosz)
Requests, special investigations (J. H. Irwin)
Oregon (w, Portland):
Ground water:
Coos Bay, dune aquifers (J. H. Robison)
Near Winston (J. H. Robinson)
Newberg area (F. J. Frank)
Umatilla Reservation water (J. B. Gonthier)
Pennsylvania (w, Harrisburg, except as otherwise noted):
Geohydrology of Berks County (C. R. Wood)
Geology and ground-water resources of Monroe County (L. D. Carswell, w, Philadelphia)
Ground water:
Chester County (L. J. McGreevy, w, West Chester)
Cumberland Valley (A. E. Becher)
Ground-water resources of the Williamsport area (O. B. Lloyd)
Quality of water:
Highway construction effects on streams (J. F. Truhlar, Jr.)
Sediment from highway construction (L. A. Reed)
Western Pennsylvania (G. R. Schiner)
Puerto Rico (w, San Juan):
Contingent requests (E. D. Cobb)
Ground water, North Coast model (J. E. Heisel)
Hydrologic systems modeling (M. A. Lopez)
Surface water, floods investigation program (E. D. Cobb)
Rhode Island, public inquiries (H. E. Johnston, w, Providence)
South Carolina (w, Columbia):
Cooper River rediversion (P. W. Johnson)
Reconnaissance of estuaries (F. A. Johnson)
South Dakota (w, Huron, except otherwise noted):
Cheyenne and Standing Rock Indian Reservations (L. W. Howells)
Clark County (L. J. Hamilton)
Deuel and Hamlin Counties (Jack Kume, w, Vermillion)
Ground water, Hand and Hyde Counties (N. C. Koch)
McPherson, Edmunds, and Faulk Counties (L. J. Hamilton)
Water resources:
Aurora and Jerauld Counties (L. J. Hamilton)
Miner County (Jack Kume, w, Vermillion)
Tennessee (w, Nashville, except as otherwise noted):
Flow characteristics (R. L. Gold)
Hydrogeology of linear features (D. R. Rima)
Memphis area (J. H. Criner, Jr.)
Terrace-deposits study (W. S. Parks, w, Memphis)
Water for Murfreeseboro (D. R. Rima)
Wetlands delineation (E. F. Hollyday)
Texas:
Ground water:
Artificial recharge research (E. P. Weeks, w, Lubbock)
El Paso (W. R. Meyer, w, El Paso)

Water resources—Continued
States and territories—Continued
Texas—Continued
Ground water—Continued
Galveston County continuing quantitative studies (R. K. Gabrysch, w, Houston)
Houston (R. K. Gabrysch, w, Houston)
Model study, Chicot and Evangeline aquifers (D. G. Jorgensen, w, Houston)
Orange County (G. D. McAdoo, w, Houston)
Rio Grande environmental study (J. S. Gates, w, El Paso)
Salt encroachment at Houston (D. G. Jorgensen, w, Houston)
San Antonio (R. D. Reeves, w, San Antonio)
Hydrologic investigations:
Drainage-area determinations (P. H. Holland, w, Austin)
Limestone hydrology study (R. W. Maclay, w, San Antonio)
Quality of water, bays and estuaries (D. C. Hahl, w, Austin)
Trust territory, water-resource information (D. A. Davis, w, Honolulu, Hawaii)
Utah (w, Salt Lake City, except as otherwise noted):
Environmental impacts (Donald Price)
Ground water:
Cedar City and Parawon (L. J. Bjorklund, w, Cedar City)
Oil-shale hydrology (F. K. Fields)
Statewide ground-water conditions (J. C. Stephens)
Navajo Sandstone, southeastern Utah (J. W. Hood)
Program enhancement (Theodore Arnow)
Quality of water, Flaming Gorge Reservoir (E. L. Bolke)
Surface water:
Canal-loss studies (R. W. Cruff)
Inflow to Great Salt Lake (J. C. Mundorff)
Mined lands rehabilitation (G. W. Sandberg, w, Cedar City)
Vermont:
Ground water, Upper Winooski Basin (A. L. Hodges, Jr., w, Montpelier)
Public inquiries (R. E. Willey, w, Montpelier)
Water quality, Black River (W. D. Silvey, w, Boston, Mass.)
Virginia (w, Richmond):
Coastal plain studies (H. T. Hopkins)
Ground water:
Geohydrologic data (R. L. Wait)
Hydrology of Prince William Forest (H. T. Hopkins)
South of James River (O. J. Cosner)
Service work (H. T. Hopkins)
Surface water, project planning and public inquiries (P. M. Frye)
Washington (w, Tacoma):
Ground water:
Long Beach (J. V. Tracy)
Special hydrologic problems (B. L. Foxworthy)
Spokane Basin water resources (H. H. Tanaka)

Water resources—Continued
States and territories—Continued
Washington (w, Tacoma)—Continued
Ground water—Continued
Swinomish (K. L. Walters)
Test drillings (K. L. Walters)
Model simulation for water management (R. D. MacNish)
Real-time data collection (R. R. Adsit)
Surface-water network reevaluation (W. L. Haushild)
Tulalip water resources (B. W. Drost)
West Virginia (w, Charleston):
Coal River study (J. S. Bader)
Quantitative mine-water studies (G. G. Wyrick)
Salt water (J. B. Foster)
Small drainage areas (G. S. Runner)
Studies for unforeseen needs (G. G. Wyrick)
Wisconsin (w, Madison):
Ground water:
Columbia County (C. A. Harr)
Washington and Ozaukee Counties (H. L. Young)
Low flow of small streams (S. J. Field)
Quality of water:
Ground-water-quality monitoring (C. A. Harr)
Menomonee River sediment study (E. R. Zuehls)
Pine River basin (P. A. Kammerer, Jr.)
Washington County sediment study (S. M. Hindall)
Surface water:
Drainage areas (E. W. Henrich)
Recreation reservoirs (B. K. Holstrom)
Water resources (R. D. Cotter)
Wyoming (w, Cheyenne):
Arikaree Formation, Lusk (M. A. Crist)
Effluent monitor, national parks (E. R. Cox)
Green River basin water supply (H. W. Lowham)
Hanna Basin water resources (K. D. Peter)
Water resources, Powder River basin (M. E. Lowry)

Water use:
United States, water use in 1975 (C. R. Murray, w, NC)
States:
Florida:
Ground-water use, Peace basin (A. D. Duerr, w, Tampa)
Water use, statewide (S. D. Leach, w, Tallahassee)
Hawaii, water-use data (R. H. Nakahara, w, Honolulu)

Water use—Continued
States—Continued
Louisiana, water use, 1975 (G. C. Cardwell, w, Baton Rouge)

Waterpower classification:
Washington, water use (G. G. Parker, w, Tacoma)
Alaska (c, Portland, Oreg.):
Barrier Glacier and its effect on Chakachamna Lake potential powersite (J. B. Dugwyler, Jr.)
Chakachatna River, review of withdrawals (J. B. Dugwyler, Jr.)
California (c, Sacramento):
Mokelumne River basin, examination of pumped storage sites (D. E. Wilson)
Owens River basin, review of withdrawals:
George Creek to Olancha Creek (R. D. Morgan)
Westside tributaries (R. D. Morgan)
Colorado, Dolores River basin, review of withdrawals (Ralph Smith, c, D)
Oregon (c, Portland):
Review of withdrawals:
Clackamas River basin (L. O. Moe)
Coquille River basin (S. R. Osborne)
Nestucca River basin (K. J. St. Mary)
North Umpqua River (K. J. St. Mary)
South Umpqua River (L. O. Moe)
Washington (c, Portland, Oreg.):
Blanca Lake and Troublesome Creek pumped storage site, Skykomish River (J. B. Dugwyler, Jr.)
Columbia River, vicinity of developed Wells Project, review of withdrawals (J. B. Dugwyler, Jr.)
Wood Plateau-Coyote Creek and John Day pool pumped storage site, Columbia River (J. B. Dugwyler, Jr.)
Wyoming (c, D):
Shoshone River, review of withdrawals (G. A. Lutz)
Wind River basin, review of withdrawals (Ralph Smith)

Wilderness Program. *See* Primitive and Wilderness Areas *under* Mineral and fuel resources—compilations and topical studies, mineral-resources surveys.

Zeolites:
Arizona, Bowie area (L. H. Godwin, c, NC)
California (southeastern), Oregon, and Arizona (R. A. Sheppard, D)
Idaho (southwestern) and Oregon (southeastern) (W. H. Lee, c, M)

Zinc. *See* Lead, zinc, and silver.

SUBJECT INDEX

Page

A

Aeromagnetic maps. *See* individual States.
Africa:
  Cyclic deposition 145
  Senegal, Mali, and Mauritania, ground-water development 310
AIDJEX 217
Alabama-New York:
  lineament 58
Alaska:
  ages of copper and molybdenum deposit 83
  batholithic complex, metamorphic zonation pattern 89
  blue amphiboles 85
  calving rate, Portage Glacier 191
  carboniferous volcanic rocks 80
  Changes in mass velocity and volume, Black Rapids Glacier 191
  Chitistone limestone 201
  Coast Range megalineament 87
  Complex shelf topography 144
  Continental shelf permafrost, Beaufort Sea 81
  Continental slope 143
  Displacement, Nikolai Greenstone Triassic in McCarthy 153
  Earthquake recurrence interval 75
  Evolution, tin-granite complex and Seward Peninsula 119
  Ferruginous bauxite deposit 81
  Galena 79
  Geochemical anomalies 82
  Geochronology, Wrangell Mountains 35
  Geologic map 92
  Geothermal studies 35
  Glacier retreat 120
  Granitic and gabbroic bodies, Glacier Bay National Monument 87
  Ground-water/stream flow relationship, Ship Creek 130
  Greenstone, tholeitic ocean-floor Volcanism, Juneau 90
  History, Yukon River Delta 84
  Iceberg drift, Columbia Glacier 152
  Kyanite, Big Delta C-4 Quadrangle 82
  Land fill site 127
  Metamorphic facies 78
  Metamorphosed trondhjemite 85
  Microfacies 206
  Molybdenite deposit investigation 86
  New mineral occurrences 9
  New petroleum targets 81
  Paleozoi or Precambrian age of rocks, Glacier Bay National Monument 87
  Porphyry copper potential 84
  Potential geothermal source 100
  Praguian Age faunas, Heceta Island 89
  Pre-Ordovician unconformity 81
  Reservoir and source-rock parameters 85
  Reservoir characteristics of sandstone 80
  Surface-water data, coal-resource areas 120
  Stability of Columbia Glacier, Alaska 151
  Streamflow/ground-water relationship, Ship

Page

Alaska—Continued
  Creek 120
  Rare earth 28
  Thorium 28
  Till, pre-Delta age 84
  Trans-Alaska pipeline 119
  Uranium 28
  Uranium studies 33
  Volcanic hazards, Cook Inlet 84
  Water-resource study, Fairbanks 119
  Water resources, North Slope 120
  Winter hydrologic reconnaissance 120
  Zoned chromium 110
  Alaskan-Arctic Investigations: slope instability, tectonics 142
Alexander terrane 85
Allochthonous sequences 89
Aluminum 1
Alunite 1
Ammonoosuc Volcanics 47
Amphiboles 85,90
Analytical chemistry:
  Analytical techniques for uranium, thorium, potassium 218
  Chlorium determination 219
  Emission spectroscopy 218
  Minicomputer-based emission spectrographic analysis 218
  Neutron activation 219
  Organic materials characterization in organic-rich rocks 220
  Part per million level determinations 218
  Thin and polished sections 220
  Trivalent Mangranis determined, spectrophotometric method 217
  X-ray fluorescence 219
  Atomic absorption spectrophotometric method 13
  Chemical dissolution technique 13
  Solvent extraction: liquid ion-exchange process 14
  Spectrochemical determination of tungsten 14
  Sulfide minerals, chemical dissolution 13
  Titanium, x-ray determination of 14
Animal productivity, microfaunal invertebrate species 148
Anomalies, geochemical 10,11
Antarctic programs:
  Dufek intrusion:
    Geophysical studies 311
    Mafic cyclic units 312
Antarctic programs:
  Fractionation trunks, cumulus oxide minerals, Dufek intrusion 312
  Geologic comparison, Pensacola Mountains with Schackleton Range 312
Antiformal folds 55
Antigorite 122
Appalachian Mountains:
  Dissolved gases, warm springs 208
Appalachian Mountains:
  Landslides 236
Aquifer 96, 115, 118, 121, 125, 192, 193, 194, 210, 211

Page

Aquifer rocks 118
Aquifer studies:
  Cyclic water storage modeling 195
  Differential aquifer development, Fort Payne Chert 197
  Glacial-outwash, South Dakota 116
Lignite 116
  Liquid storage, saline-water aquifers 194
  Paving effects on aquifer recharge 194
  Saline-water and freshwater relationship 197
  Trace studies for aquifer evaluation 196
Argentina, natural resource development course 304
Arkansas, Ground-water flow, Crowleys Ridge 198
Arizona:
  Cenozoic structure, stratigraphy, volcanism 70
  Flood mapping 250
  Geochemical study, copper deposit 110
  Past and future climate, Black Mesa 146
  Permian rocks 71
  Precambrian thrusting 68
  Reservoir regulation, satellite-data relay 279
  Tectonic style 64
  Tertiary lead-silver mineralization 68
  Volcanic field 35
Arizona-California:
  Tectonic zone, Mojave Desert 70
Arizona-New Mexico:
  Distal zone of Cow Springs sandstone 32
Asia, Southeast:
  Strong-motion programs 301
Astrogeology:
  Basalt stratigraphy 262
    Global data synthesis 263
    Infrared eclipse temperatures 263
    KREEP basalt age 266
    Light plains and maria 262
    Lunar melting 266
    Magma reduction by carbon 266
    Mare ridges 263
    Melt inclusions and mare basalt relationships 266
    Ring moats 262
    Tectonism and volcanism 263
  Lunar investigations:
    Appollo 16 breccia 264
    Appollo 17 breccia 265
  Planetary studies 262
  Terrestrial analogs and experimental studies:
    Lonar Crater, India 264
    Ries Crater, Germany 263
Atlantic Coastal Plain:
  Cenozoic faults 237, 238
  Stratigraphic correlation 56
Antigonite 28

B

Baltic Sea 148
Barite 8
Basalt 119, 130, 131, 146
Basalt volcanism 113
Basaltic rocks 114
Basement rocks,
  Lake Superior region 60

Page
Batholith ... 61, 76
Bathymetric charts ... 137
Bauxite ... 1, 81
Bayer process ... 1
Bedrock terraces ... 59
Benthic community,
fair weather influence ... 148
Bentonite ... 43
Bioelectric cell ... 20
Biomass distribution ... 148
Biostratigraphy ... 205
Bolivia, urban projects ... 304
Borate minerals ... 109
Brazil, mineral assessment ... 304
Breccia ... 7, 91, 264, 265
Breccia pipes:
Uranium-copper enrichment zone ... 32
Bryozoa ... 205

C

Cadmium ... 123
Calcite ... 149
Calcium tantulum-niobium oxide ... 110
Caldera ... 37, 67, 100
Caliche rinds ... 133, 238
California:
Ancient volcanism ... 117
Aquatic biology assessment ... 214
Aquifer response model ... 121
Aquifer temperatures ... 120
Areal/temporal water-quality variations, San Lorenzo River basin ... 121
Artificial-recharge program ... 121
Benthic organisms ... 215
Chemical evolution, Long Valley magma chamber ... 116
Chemical quality of groundwater, Sacramento Valley ... 121
Chromium in batholith ... 219
Clay-mineral variability ... 148
Climatic history, late Cenozoic ... 74
Deep-sea Navy-Fan ... 141
Depositional environment, Santa Cruz Mountains ... 142
Distribution coefficients, zinc and cadmium in stream water and seawater ... 123
Earthquake recurrence intervals ... 75
Fault, Melones ... 72
Flood-flow capacity of Sacramento River ... 250
Fossils, Clear Lake ... 145
Geochronology ... 72
Geophysical studies, Cosogeothermal area ... 36
Geotechnical data problems, Los Angeles ... 75
Granite rocks, Yosemite National Park ... 120
Ground-water basin, Merced area ... 122
Ground-water basin, well-response Model ... 122
Ground-water modeling, Salinas Valley ... 122
Hydrogeologic changes in subsidence area ... 258
Hydrologic and solute-transport models ... 122
Infaunal biomass and production, San Francisco Bay Mudflat ... 148
Land subsidence, artesian-head recovery ... 259
Lateral movement of fault, San Gregorio ... 74
Lithium in Searles Lake ... 41
Long Valley caldera ... 37
Mafic plutonic rocks ... 76
Magmatic cycles, Coso Range ... 117
Magnetization of Mount Shasta ... 100
Metavolcanic rocks, Sierra Nevada ... 73
Migration of Sacromento River ... 121
Mining debris effects ... 140
Offsets along faults ... 76
Overdraft, Koehn Lake area ... 122
Paleomagnetism, Great Valley sequence, Sacramento Valley ... 153
phosphorite, potential for phosphate ... 42
Pleistocene climate ... 202
Potential geothermal field ... 36
Sedimentary record, San Joaquin Valley ... 147
Silica, numerical simulation ... 148

Page
California—Continued
Soil development and age ... 238
Subsurface chemical movement ... 119
Thrust fault ... 73
Volcanism, Devonian island-arc ... 117
Water-level decline, Twentynine Palm Marine Corps Base ... 121
Well-response model ... 122
Cape Fox pluton ... 86
Cape Verde, water-resource reconnaissance ... 305
Carbon ... 141, 266
Carbonate rocks ... 70
Carbonates, composition variation ... 6
Carbonatites ... 31
Cartography and design ... 322
Catalog of Information on Water Data ... 125
Central Atlantic Regional Ecological Test Site (CARETS) Project ... 290
Central Laboratories System ... 132
Central Region, geologic investigation ... 58
Chalks ... 24
Chemical Resources. *See* specific mineral.
Chemical study, intrusive rocks, Montana ... 64
Chloride ... 103, 113
Chromite:
Refractory, supply problems by 1985 ... 2
Chromium ... 106
Chrysotile ... 122
Clastic wedges ... 23
Clay-mineral variability ... 148
Climatology:
Fair weather influence on benthic community ... 148
Glaciers reflect former climate ... 148
Coal ... 16, 7, 18, 96, 114, 118, 121, 131, 140, 155
Coal resources, Known recoverable areas ... 151
Coal-bed characteristics, Ancient environments ... 18
Coal-bed correlation:
Tonstein identification ... 18
Coal exploration ... 96
Coal gasification ... 131
Coal liquefaction ... 131
Coastal geology:
Nearshore studies, Beaufort Sea ... 144
Coastal hydrology:
Baltic Sea ... 148
Clay/mineral in suspended sediments, San Francsco Bay ... 148
Dissolved silica, numerical simulation ... 148
Littoral drift, Bering Sea coast ... 144
Colorado:
Contaminated wells, Park County ... 111
Creede:
Carbonate composition variation ... 6
Ore deposits, hydrologic history of ... 5
Early Eocene age rocks ... 201
Effects of reservoir on adjacent aquifer ... 109
Energy-resources map ... 241
Erosion reduced ... 112
Flood-mapping ... 250
Genesis of uranium veins ... 31
Geologic map ... 92
Geothermal systems ... 38
Green River formation:
Marlstone tongues ... 26
Ground water, Front Range ... 111
Gunnison County:
Precambrian sulfide deposits ... 6
Hydrology of aquifer ... 111
Large-scale gravitational spreading, Crested Butte area ... 234
Long-lived mineralization ... 131
Oil origin ... 22
Peat deposits ... 19
Petrology of carbonatites, West Mountains ... 31
Petrophysics Laboratory established, Denver 155
Poncho Hot Springs:
Fluorspar mineralization ... 6
Hydrothermal circulation ... 6
Rocks favorable for uranium, Piceance Basin ... 32
Saline waters distribution, computer model ... 208

Page
Colorado—Continued
Sawatch Quartzite outcrop ... 62
Shallow water table, Arkansas River Valley ... 110
Spring-water flow ... 112
Storm runoff, chemical quality ... 110
Surface-water-quality inventory ... 109
Thorium content of carbonatites, Wet Mountains ... 31
Thorium veins, Powder horn and Wet Mountains ... 29
Total sulfur in oil shale ... 26
Trace elements in Colorado Plateau uranium deposits ... 31
Water quality, Boulder County ... 111
Water quality, Colorado River ... 110
Water quality, Jefferson County ... 110
Water-level changes, High Plains ... 109
Water-resource appraisal, Mountain Valley ... 112
Wet Mountains, Alkalic complexes ... 27
Zircon-dated gravels ... 63
Colorado-Wyoming:
Water-quality study, Yampa River basin ... 132
Computer technology:
EROS Data Center ... 329
Conglomerates ... 56, 63
Connecticut:
Deglaciation of Hamburg quadrangle ... 45
Fault, Honey Hill ... 51
Ground-water availability, Farmington ... 96
Intrusion, gneiss ... 51
Land-use planning, drainage-area maps ... 96
Petrography of Preston Gabbro ... 50
Stratified drift aquifer:
Pootatuck River valley ... 96
Quinnipiac River basin ... 96
Water-quality assessment, Farm River basin ... 90
Computer technology:
Image processing ... 329
Time-sharing systems ... 329
Conodont studies:
Praguianage faunas, Karheen Formation ... 89
Conterminous United States:
Geologic map ... 92
Continental drift ... 135
Continental margin facies ... 81
Continental shelf:
Beaufort Sea permafrost ... 81
Copper ... 4, 9, 10, 11, 83, 84, 100, 104, 105
Copper sulfide deposits ... 83
Corals ... 140, 148, 205
CORRAN ... 128
Costa Rica:
Seismological investigations ... 301
CRIB ... 14
Crossbedded sands ... 142
Crystal chemistry:
Hydrated borate minerals ... 109
Crystallization ... 106
Crystallography:
Crystal chemical studies ... 108
Structure, scandium-lithium protoenstatite ... 108
Cyanide ... 220

D

Data base:
Geothermal ... 14
Oil-shale and saline-mineral ... 26
Data, biogeochemical ... 12
Data file:
National atlas ... 15
Data system:
National coal resources ... 16
Decollement, Idaho ... 65
Delaware:
Piney Point aquifer, Kent County ... 97
Dendroclimatic studies ... 207
Depositional environments ... 63
Diatoms ... 140
Dinoflagellates ... 203
Dolomite ... 69

Page

DOMES 145
Drumlins 49
Dry Tortugas 140

E

Earth Resources Observation Systms (EROS) program 268
Earthquake studies:
Crustal deformation 225
Crustal stress 225
Crust and upper mantle structure 226
Fault activity 228
Ground motion 231
Hazards 228
Precursors 224
Seismicity 222, 227
Seismic network studies 230
Earthquake studies:
Seismic risk analysis 232
Seismic studies for prediction 223
Earthquakes 38, 75, 99, 143
See also under individual States and countries.
Eastern United States:
Fault system 57
Ecuador, volcanic hazard appraisal 305
Electromagnetic studies. *See* Geophysics.
Embayment 59
Energy 23, 131
Energy Mineral Rehabilitation Inventory and Analysis program 17
See also under individual States.
Energy studies:
Coal-basin studies, Kaiparowitz 240
Energy resources map 241
Foreign mining methods 241
Geochemical survey of western energy regions 255
Mapping potential surface-mind lands reclamation 240
Mined-land reclamation, climatic constraints 242
Molybdenosis, ruminant problem 240
Nonmineral resources evaluation 240
Energy studies:
Powder River basin, remotely sensed 241
Trace element geochemistry, coal usage and disposal 241
Engineering geology:
Field measurement techniques research 234
Geologic hazards research 233
Slope stability research 233
Soils engineering research 233
Tunneling research 232
Eniwetak atoll 146
Environmental geochemistry:
Oil-shale geochemistry 256
Saprolite vertical variation 257
Survey of western energy regions 255
Urban geochemistry 256
Erbium 108
Erosion 112, 147
Estuarine hydrology:
Alaska 172
Atlantic Coast 147
Baltic sea 148
Fair weather influence on benthic community, Kiel Bay, Germany 148
Gulf coast 147
Pacific Coast 147
Sedimintation, Tillamook Estuary, Oregon 148
Evapotranspiration, water-budget estimates 212

F

Fault breccia 91
Fault zones 46, 55, 99
Faulting 53, 55, 56, 58,
Federal and Indian lands, natural resource
Fe-Mn ratios 11
Ferromanganese 123
Flood-frequency studies:

Page

Flood-frequency studies—Continued
Arizona streams 248
California 100-year flood 248
Flood depths, rigid-boundary channels 250
Floodflow characteristics of small streams 249
Flood-hydrograph synthesis and peak-discharge reduction, Colorado River basin 250
Frequency and magnitude estimation 249
Tatum Sawgrass dikes effects, Myakka
Ungaged sites, streams in Minnesota 249
Flood mapping:
Accuracy of flood-prone area maps 250
Flood-flow capacity, california 250
Flood-prone areas:
Arizona 250
Minnesota 250
Inundation maps, Teton Dam, Idaho 251
Mannings roughness coefficient, floodflow prediction in urban areas 250
Floods:
Colorado, 1976, Big Thompson River 248
Idaho, 1976, Teton Dam failure 247
Maine coastal flood, 1976 247
Maine, Penobscot River 95
Outstanding 247
Florida:
Adequacy of water resources 103
Aquifer system 104
Botany of freshwater peat 207
Carbonate source rocks 23
Computer model, Floridan aquifer 103
Connector-well experiment, Orange County 195
Corals, climate and environmental indicators 140
Calculating water volume by Landsat data, Everglades 279
Flood-frequency study 249
Geohydrology of Tamiami Formation 104
Ground water, supplemental 103
Lake-aquifer connection 210
Leachate movement to groundwater, Broward County 105
Macronutrient concentrations 213
Phosphate resources 43
Remote sensing, vegetation mapping 279
Resources and Land Investigations Program 286
Saltwater intrusion 104
Spray irrigation, sewage effluent 103
Suwannee Limestone, Chloride concentration 103
Waste-injection zone 104
Water resources, Palm Beach County 104
Water resources, St. Lucie County 104
Water supplies, Withlacoochee and Week: Wachee Rivers 104
Florida Keys:
Search for water 105
Fluorite 127
Folds 55, 65
Freshwater interface 102
Fusulinids 205

G

Gabbro 50, 87, 90
Galena 79
Gamma rays 98
Garnets 48
Gas analyses:
Burning culm banks 20
Genesis:
Uranium, Colorado 31
Geochemical anomalies 82, 129
Geochemical studies:
Alaska uranium 33
Magnetic susceptibility, erbium and ytterbium-doped zircon 108
Uranium potential of Snowy Range Wilderness 30
Geochemistry:
Amorphous silica solubility, high tem-

Page

Geochemistry—Continued
peratures and pressures 103
Basaltic rocks 114
Cation distribution, lunar orthepyroxene 108
Chemical changes, Watchung Basalt 115
Chemical evolution, Long Valley magona chamber 116
Chemical rock weathering in forested watersheds 128
Chlorite-sulfide phase relations 103
Crystals and melts, chromium partitioning 106
Diagenetic studies 122
Experimental 101
Evolution, silicic magma chambers 116
Geochemical correlations 128
Geochemical kinetics 126
Guide to uranium mobility, secondary silica dating 118
Geopressured geothermal waters 127
Heat capacities, minerals 102
Hot spring deposits, isotopic evidence 130
Hydrothermal alteration, ophiolites 115
Ion-ratio maps, ground-water-flow systems 125
Iron-silicic acid complexes evidence 103
Isotope and nuclear 130
Lead in oceanic basalts, isotopic composition 130
Lunar orthopyroxene, thermal history indicator 108
Modeling, high-pressure processes 105
Organic 23
Solubility, natural fluorite 127
Spinel crystallization, chromium effect 106
Stable isotope, copper sulfide deposits 83
Statistical 128
Sulfide globules, Mid-Atlantic Ridge basalts 114
Thermodynamic data, minerals 101
Thermodynamic data, muscovite 102
Trace elements 90
Volcanic sediment in alkaline lake 122
Water and sediments 122
Geochronology 30, 33, 35, 53, 60, 63, 64, 67, 72, 73, 74, 82, 83, 84, 87, 88, 89, 90, 133, 135, 146
Geochronometry:
Ancient sialic terraine 132
Kimberlite diatreme dating 131
Long-lived mineralization, Colorado 131
Ore sources, lead isotope indicator 134
Samarium-neodymium chronology 134
Thermoluminescence dating silicic volcanic rocks 132
Geohydrology 104
Geologic hazards:
Aseismic faulting 239
Fossils, amino-acid dating 238
Rock stress, foundation design 239
Geologic investigations:
Stratigraphic framework of onshore wells 136
Uranium potential of Snowy Range Wilderness 30
Geologic Maps 58, 82, 91
See also under individual States
Geologic principles, processes, and techniques 153
Geologic structure 116
Geology:
Massachusetts:
Pepperell and Shirley, quadrangles 47
Lowell-Ayer region 49
Pre-Triassic, Massachusetts 46
Geology and climate:
Arroyo cutting, New Mexico 146
Coral growth lands 148
Erosion rates, growth rings in tree roots 147
Fossil plants and fish scale growth investigation 145
Glaciers reflect former climate 148
Past and future climate, Arizona 146
Sedimentary record, San Joaquin Valley 147
Subglacially precipitated calcite 149
Weathering rinds 150
Geomagnetism 95, 154

Page
Geophysical studies ------------------ 36, 38, 65, 140
Geophysics:
Aeromagnetic and gravity data,
Bob Marshall Wilderness area --------------99
Airborne gamma ray data --------------------98
Geophysical techniques:
Characteristics of uranium deposits ------------94
Gravity variations, Kilauea Volcano ----------94
Geophysics:
Crustal blocks, Central America --------------99
Current loop models, geomagnetic field --------154
Discovery of caldera, Nevada ----------------100
Electromagnetic measurements, controlled
source ------------------------------------97
Electrical properties of oil shale ---------------95
Geoelectric structure, Kilauea Iki lava lake ----101
Geomagnetic observations --------------------154
Geomagnetic soundings -----------------------96
Gravity exploration, gold-bearing gravels ------95
Gravity and magnetic modeling ----------------97
Gravity surveys, coal exploration --------------96
Long-wavelength anomalies, Main field ------154
Magnetization, Mount Shasta ----------------100
Magnetic charts, US 1975.0 ----------------1954
Magnetic surveys ----------------------------154
Magnetism of Mount Shasta -------------------100
Schlumberger sounding -----------------------99
Soil moisture, self-potential ------------------100
Underground conductors -----------------------95
Wave pressure, bottom-motion response ------139
Geophysics, experimental, rock magnetism --------153
Georgia:
Bauxite and koalin resources ------------------1
Belair fault zone investigations ----------------55
Borehole traverses made in municipal well,
Albany ----------------------------------196
Ground-water availability ---------------------105
Ground-water data, minicomputer processing --106
Ground-water quality, Cretacous aquifers ----105
High-yield wells ----------------------------106
Kaolin deposits --------------------------------1
Low-flow analyses, regulated streams --------106
Storm runoff, quality -------------------------105
Subsidence ---------------------------------259
GOETHERM ----------------------------------14
Geothermal assessment -------------------------39
Geothermal field, California -------------------36
Geothermal resources ---------------------------35
Geothermal source -----------------------------100
Geothermal Steam Act, 1970 --------------------151
Goethermal studies ------------------35, 37, 39, 127
See also under individual States.
Geothermal systems:
Boiling and dilution effects on isotopic
compostion of thermal waters --------------138
Effects of vertical flow on temperature
distribution in geothermal
reservoirs --------------------------------136
Elastic wave velocities in granite ------------138
Geothermal well logging ----------------------137
Hydraulic fracture models, shallow
geothermal fields --------------------------136
Low-temperature, chemical and physical
characteristics -----------------------------38
Passive seismic exploration ------------------136
Thermodynamic properties of complex brines --137
Two-phase, finite-difference modeling,
geothermal reservoirs ----------------------136
Germany:
Ries Crater, investigation ----------------------263
Ghana, gold, Tarkwa ----------------------------5
Glacial melt-water deposits ------------------------46
Glacial outwash ---------------------------------101
Glacial readvance --------------------------------51
Glacial studies:
Mass change, South Caseade Glacier, 1970
and 1976 ----------------------------------151
Stability of Columbia Glacier, Alaska --------151
Surging glaciers, Pamirs, USSR inventory ----191
Temperate glaciers, thickness measurements --191
United States glacial fluctuations, 1970 to

Page
Glacial studies—Continued
1975 ------------------------------------150
Glaciology -------------------------51, 52, 119, 191
Glauconite --5
GLOMAR CHALLENGER Deap Sea
Drilling Project ------------------------------145
GLOMAR CONCEPTION -----------------135, 137
Gneiss ----------------------------45, 46, 51, 132
Gold ---12, 95
Granite -----------------------------------119, 138
Granite bodies ------------------------------------87
Granite rocks -------------------------------------120
Granitie terranes, uranium exploration ------------33
Graptolitic shales ----------------------------------89
Gravity --94
Gravity studies: *See* Geophysics.
Great Basin, Ordovician rock temperatures --------68
Great Dismal Swamp ----------------------------207
Greenstone -------------------------------------76, 90
Guatemala:
Earthquake, 1976 ----------------------300, 305
Other earthquakes -----------------226, 227, 228
Gulf Coast and Caribbean Sea --------------------138
Gulf of Mexico:
Bottom stability -----------------------------139
Seismic survey, common-depth-point ----------138
Guyana, Mud accumulation ----------------------23

H

Hawaii:
Earthquakes ---------------------------------38
Geoelectric structure, Kilauea Iki lava lake ----101
Gravity variations, Kilauea Volcano ----------94
Ground-water appraisal ----------------------123
Ground-water problems ----------------------123
Magona chambers and volcano structure --------38
Mauna Loa continues to inflate --------------111
Shield volcanoes -----------------------------112
Volcanic chain, revisedage -------------------112
Helium ---------------------------------------24, 34
Humic acid --------------------------------------208
Hydrocarbons -------------------------------------142
Hydrogeologic systems, mathematical
simulation ----------------------------------192
Hydrogeology ------------------------------------114
Hydrologic modeling -----------------------------127
Hydrologic studies: *See also under individual States.*
Arapahoe aquifer, Colorado -------------------111
Artificial-recharge program -------------------121
Borehole geophysics, ground water ------------196
Characteristics of Gallup Sandstone ----------115
Data coordination, acquisition, and storage ----124
Differential aquifer development, Fort Payne
Chert -------------------------------------197
Disposal and storage -------------------------194
Effects of land clearing and drainage ----------106
Estuarine -----------------------------------147
Energy development --------------------------108
Facotrs in reclaiming coal lands --------------114
Federal Plan, Acquisition of Water-Data ------125
Geopressured geothermal waters --------------127
Ground water --------------------------------192
Ground-water pollution ----------------------127
High peak flows, storms ---------------------127
History of Creede, Colo., ore deposits ------------5
Hydraulic and hydrologic characteristics,
Limestone aquifer --------------------------108
National water-quality programs --------------132
New instruments and techniques -------------216
Rainfall intensities --------------------------127
Recharge studies, basin sewage effluent ------194
Stream-aquifer systems, saline-water and
freshwater relationship --------------------197
Stream flow model ----------------------------112
Strippable lignite deposits --------------------116
Surface water --------------------------------198
Test drilling, preglacial river valleys,
New York ---------------------------------197
Texas coastal plain ---------------------------117
Urban-hydrology program ---------------------127

Page
Hydrologic studies—Continued
Water budget, watershed --------------------107
Water-data acquisition, National Handbook --125
Wisconsin wetland --------------------------211
Wyoming, Arikaree Formation --------------118
Hydrologic principles, processes, techniques --------153
Hydrology ----------------------114, 115, 120, 123
Hydrothermal alteration studies ------------------40

I

Iceland:
Remote sensing, geological and
geophysical ------------------------------272
Ice lobe --46
Idaho:
Aquatic biology, Salmon River ----------------214
Belt and pre-belt rocks near bathelith ----------61
Disharmonic folds ----------------------------65
Faults, Black Pine Mountains -----------------69
Geophysical model of Snake River Plain --------65
Geothermal area, Raft River -----------------38
Geothermal potential, Sugar City -------------39
Ground-water resources, Mountain Home
plateau ----------------------------------123
Ground-water/surface relationships, Silver
Creek area -------------------------------123
Ore targets ----------------------------------10
Phosphoria formation ------------------------63
Radioactive burial ground --------------------245
Rock, thrust-plate origin, Lemhi Range --------65
Rocks, Mississippian --------------------------63
Stratigraphy ---------------------------------65
Teton Dam flood -----------------------------119
Teton Dam, inundation maps ----------------251
Water resources, Henrys Fork basin ----------123
Igneous rocks ----------------------------33, 71, 99
Igneous studies ----------------------------------64
Illinois:
Deposition, Fox Chain-of-Lakes ---------------141
Flood frequency and magnitude estimation
on small streams --------------------------249
Ground-water movement at radioactive-waste
disposal site -------------------------------246
Hicks Dome:
Breccia minerals ---------------------------7
Illinois Basin:
Zinc distribution --------------------------------2
India:
Lonar Crater, investigations ------------------264
Major world aquifer --------------------------305
Indiana:
Lineament mapping, limestone terrane --------97
Saline ground-water, Vineinnes ---------------97
Simulated leachate movement ----------------97
Indonesia, emission spectrographic
instruments --------------------------------306
Inlier, Precambrian metamorphosed greenstone
and feldspathic arenacious rock ----------------56
International cooperation:
Antarctic programs ---------------------------311
Hydrologic investigations, historical
review ------------------------------------304
International commissions and
presentations -----------------------------301
International Hydrolo gical Program ----------303
Resources Attache and Reporting Program ----303
Resources programs --------------------------294
Scientific and technical cooperation ----------300
Technical assistance and participant
training -----------------------------------295
Intersitial water studies ---------------------------137
Intrusive ------------------------------104, 107, 134
Intrusive center, Utah ----------------------------71
Intrusion, gabbro --------------------------------90
Intrusive rocks -----------------------------------64
Iran:
Craters study -------------------------------306
Mineral exploration research -----------------277

Page

Isotopes:
  Other studies ---- 8, 24
  Sulfur ---- 33
  Trace studies ---- 130

Iron ---- 11
Iron-titanium oxide ---- 30
Irrigation ---- 100, 103, 107, 128, 196

J

"Journal of Research of the U.S. Geological Survey" ---- 334

K

Kansas:
Depletion of aquifer ---- 112
  Liquid-waste disposal ---- 196
  Streamflow studies ---- 112
Kaolin ---- 1
Kentucky:
  Abandoned coal mines ---- 106
  Bryozoa ---- 205
  Cryptoenplosion structure, Middlesboro ---- 58
  Fusulinid-bearing limestone ---- 59
  Geologic mapping ---- 58
Kenya, reconnaissance ground-water studies ---- 306
Kettle holes ---- 46
Kyanite ---- 46, 82

L

Laccolith ---- 71
Lake Superior region, geologic investigation ---- 60
Land classification ---- 151
Land snails ---- 204
Land subsidence. *See* Subsidence.
Land use and environmental impact:
  Environmental impact studies ---- 292, 293
  Land use and land cover maps and data:
    Analysis, Chattahoochee River Quality Assessment ---- 291
    Central Atlantic Regional Ecological Test Site Project ---- 290
    Change, monitoring framework ---- 291
    Change, urban areas ---- 290
    Data projects ---- 288
  Digital systems technology ---- 287
    Geographic information system research and development ---- 292
    Mapping from Landsat digital data ---- 291
  Multidisciplinary studies:
    Colorado Front Range Urban Corridor ---- 284
    Geotechnical and geohydrological, Fairfax County, Virginia ---- 285
    Puget Sound Region ESA Project ---- 285
    San Francisco Bay Regional ---- 284
  Resource and Land Investigations Program:
    Coastal area activities ---- 287
    Integrated surface mine reclamation and land use planning ---- 286
    Onshore facilities, Outer Continental Shelf energy development ---- 287
    South Florida environment ---- 286
  Statistics and indicators ---- 286
    Surface mining control ---- 287
    Surface mining and land use planning ---- 286
    Western coal, environmental impact ---- 286

Landsat: *See* Remote sensing.
Landslides:
  Inventory, Rocky Mountain ---- 236
  Regional slope-stability studies ---- 234
  Slope failure types ---- 236
Landslides. *See also under individual States.*
Land-use studies:
  Drainage-area maps ---- 96
Leachate analyses, burning culm banks ---- 20
Leachates ---- 97, 105
Lead ---- 127, 130, 131
Leasing areas:
  Known for potassium, phosphate, sodium ---- 151
Lignite ---- 116
Limestone ---- 24, 59, 69, 108, 117, 140, 201, 211
Limnology:
  Aquatic ecosystems quantification ---- 216
  Benthie organisms ---- 215
  Biogensis-chemical stratified-lake model ---- 123
  Distribution coefficents, zinc and cadmium in stream water ---- 123
  Lake-reconnaissance ---- 212
  Lake and reservoir dissolved oxygen depletion ---- 213
  Lake temperature simulation model ---- 213
  Rio Ojo Caliente ---- 31
  Salmon streamflow preference ---- 215
  Stream relocation effects on aquatic habitat ---- 215

Lineament, magnetic ---- 58
Lithium:
  Cenozoic alluvium distribution ---- 42
  Exploration limited ---- 42
  High-temperature waters ---- 41
  Pennsylvania and Maryland flint clays ---- 42
  Sedimentary environments ---- 42
  Tin and oil-shale deposits ---- 42
Lithology ---- 62, 64, 136,
Lithostratigraphy ---- 57
Louisiana:
  Alluvial aquifer ---- 113
  Compaction, land subsidence ---- 258
  Ground-water resource appraisal ---- 113
  Red River water quality ---- 255
  Seasonal water-quality changes ---- 113
  Terrace aquifer, chloride contamination ---- 113
Lunar investigations. *See* Astrogeology.
Lunar plagioclase ---- 110

M

Magnetic anomalies ---- 134, 154
Magnetic field ---- 154
Magnetic studies. *See* Geophysics.
Magnetite, litanifeous:
  Composition ---- 8
  Curie temperature ---- 8
Maine:
  Fault zone ---- 46
  Kyanite in schists ---- 46
  Landscape patterns and structure ---- 276
  Middle Paleozoic unconformity in bedded rocks ---- 45
Manganese ---- 11
Maps:
  Aeromagnetic, Nevada ---- 69
  Alaska, metamorphic facies ---- 78
  Drainage-area, Connecticut ---- 96
Marine geology:
  Atlantic Coast ---- 134
  Continental shelves, boundary layers and sediment transport ---- 141
  Corals, climatic and enviromental indicators ---- 140
  Holocene rates of reaf growth, Einewetak atoll ---- 146
  Inner shelf development, Massachusetts ---- 135
  Littoral drift, Being Sea coast ---- 144
  Mantle refractions ---- 143
  Slumps ---- 143

Marine geology—Continued
  Structural and geophysical studies, Atlantic Continental Margin ---- 134
  Tidal point bars ---- 142
  Wave pressure, bottom-motion response ---- 139
Maryland:
  Aquifer, Manokin ---- 98
  Ground-water availability ---- 97
  Saltwater monitoring ---- 98
  Two-dimensional model, Piney Point ---- 98
Maryland-New Jersey:
  Statigraphic correlation ---- 56
Maryland-Pennsylvania:
  Lithium in flint clays ---- 42
Massachusetts:
  Age of Belchertown penton ---- 121
  Ammonoosuc Volcanies ---- 47
  Cambrianage rocks ---- 51
  Deep drilling, Martha's Vineyard ---- 99
  Drumlin cores, rhythmic laminations ---- 49
  Floodflow characteristics of small streams ---- 249
  Garnets, Worcester coal mine ---- 48
  Geology, Lowell-Ayer region ---- 49
  Geology of Pepperell and Shirley quadrangles ---- 47
  Glacial and glaciofluvial sedimentation ---- 52
  Glacial readvance, Boston Basin ---- 51
  Ground-water assessment, Shawsheen River basin ---- 98
  Ground-water chloride concentrations ---- 255
  Ground-water exploration ---- 98
  Ground-water quality, Cape Cod ---- 99
  Ice lake, Connecticut Valley ---- 46
  Inner shelf development ---- 135
  Mollusks ---- 203
  Plutomic rocks ---- 52
  Pre-Triassic rocks ---- 46
  Structure in Oxford ---- 48
  Thrust faults ---- 49
  Water quality, Martha's Vineyard ---- 99
  Water resources, Nantucket Island ---- 99
Megalineament ---- 87
Mercury ---- 35, 270
Metallogenesis, Mesozoic-Cenozoic ---- 4
Metallogeny:
  Western United States ---- 4
Metamorphic facies ---- 78
Metamorphic processes:
  Fluid inclusion evidence, sedimentary diagenesis ---- 124
  Origin, natural gas; shales ---- 124
  Petrology, age of Belchertown pluton ---- 121
  Sedimentary diagenesis, marine ferromanganese deposits ---- 123
  Stability relations, antigorite and chrysotile ---- 122
Metamorphic rocks ---- 50, 54, 61, 74, 99
Metamorphic zone pattern ---- 89
Metavolcanic rocks ---- 73
Methane hydrate ---- 146
Methods and techniques:
  Digital simulation model, alluvial-fan deposition ---- 193
  Direct solution algorithm, two-dimensional ground-water-flow simulator ---- 192
  Computer composite mapping ---- 5
  Computer modeling processes forming uranium ---- 29
  Computer simulation, compositional data ---- 128
  Conceptual model, hydrothermal system ---- 38
  Crossbedding dip direction analysis of sandstone flavial dispersal pattern ---- 29
  Digital model, leachate movement simulated ---- 97
  Electromagnetic method, uranium exploration ---- 35
  Gamma-ray spectrometry ---- 33
  Gas chromatography ---- 29
  Ground-water data, minicomputer processing ---- 106
  Helium surveys, truck-mobile detector ---- 34
  Hybrid computational system, multiaquifer problems ---- 193

Page

Methods and techniques—Continued
Mathematical simulation, hydrogeologic systems 192
Pyrolysis 29
Petrologic and sulfur isotope studies 33
Pyrite oxidation 32
Q-mode factor analysis 179
Resistivity study 34
Self-contained tripod-mounted instrument package, bottom boundary layer and sediment transport 141
Three-dimensional flow model application to large models 193
Unconfined aquifer simulation 194
Well-logging system 34
X-ray analysis, clay-size fraction 53
Mexico, ground-water studies 306
Microfacies 206
Michigan:
Precambrian phosphorite 43
Relationship, land use and erosion 100
Mid-Atlantic Continental Shelf, environmental condition 136
Mineral assessment:
Indian lands 4
Mineral belts 12
Mineral exploration, New Mexico 10
Mineral identification, in polished coal mounts 20
Mineralization, lead-silver 68
Mineral lands, classification and evaluation 150
Mineral Leasing Act, 1920 151
Mineral leasing, supervisor 151
Mineralogy:
Experimental 101
Lead isotope composition, minerals from basalt 131
Long-lived mineralization, Colorado 131
New calcium tantutum-niobium oride 110
Oxygen frigacity, mantle environment 106
Sorting and source effects 142
Stability of phlogopite 102
Zoned chromium, iron-spinel, Alaska 110
Mineral Resource Assessment Program, Alaska 78
Mineral resource studies:
Cooling history, lunar plagioclase 110
Discovery loan program 9
Energy related studies 16
Iron-titanium oxide 30
Leasing provisions and laws 151
Mineral and water resources, Federal and Indian lands 150

Mining. *See mineral names, as well as under individual States.*
Minnesota:
Aquifer, surface resistivity delimiting 101
Copper exploration 10
Effects of copper and nickel mining 100
Flood-frequency relations, ungaged sites on streams 249
Flood-prone areas 250
Glacial Lake Agassiz 3
Ground-water, Park Rapids 100
Ground-water irrigation 100
Nickel exploration 10
Peat resources 3
Streamflows, record lows 101
Surface resistively 101
Unconfmed aquifers 100
Water-quality analysis 100
Miogeosyncline 68, 74
Mississippi:
Bridges, maintenance problems 106
Embayment, Upper Tertiary bedrock terraces 59
Lineaments expression 276
Mississippi River, pre-Pleistocene evidence 60
Missouri:
Aquifer, excharge of water between limestone and dolomite 113
Irrigation water-use increase 131
Tracer experiment 211
Commodities 16
Mollusks 203
Molybdenum 8, 83, 86
Molybdenum mineralization 12
Montana:
Age of Kootenai Formation 201
Bentonites, Bearpaw shale 43
Cenozoic tectonics 66
Depositional environments, Eagle Sandstone 63
Environmental study, Big Fork-Avon area 234
Evaluation, hydrologic factors in reclaiming coal lands 114
Fault connections 66
Geophysical studies, Bob Marshall Wilderness area 99
Great Bear Wilderness study area: mineral potential 3
Ground-water resources study 113
Igneous studies, layered sequence 64
Intrusive centers 64
Large-scale gravitational spreading of mountain ridges 235
Natural radioactivity thermal waters 208
Pioneer Mountains:
Tungsten distribution 7
Sapphire thrust belt 66
Scotchman Peak Wilderness study area:
Stratabound copper-silver deposit 4
Monazite:
Indicator of ore deposits 12
Mud 23
Muscovite 102

N

Nannoplankton 203
NASQAN 132
National Earthquake Information Service 300
National security:
Geology and hydrology related 242
Natural gas:
Origin, shales 124
Natural resources 150
NAWDEX 125
Nebraska:
Ground-water recharge, interfluvial areas 114
Ground-water recharge 114
Ground-water-quality atlas 114
Nevada:
Aeromagnetic maps 68
Barite deposits 8
Carbonate rocks, Mississippi 70
Esmeralda County:
Geology of Cuprite mining district 7
Geochronometry, Rochester mining district 67
Geophysical characterization of lithium-brine deposits 41
New England:
Geologic investigations 45
Granitic plutons 45
New Hampshire, Kettle hole significance 46

O

Oceanic studies:
Nodule and sediment distribution and chemistry, North Pacific Ocean 145
Ohio:
Glacial-outwash aquifer study 101
Oil and gas resources:
Evaluation of Naval Petroleum Reserve 20
Known geologic structures 151
Lease sales, Outer Continental Shelf 152
Seepage mechanisms 25
Oil exploration 21
Oil shale 26, 95
Oil-shale resources:
Data base, oil shale and saline mineral 26
World 26
Oil spill 25
Oklahoma:
Ground water, confined and unconfined, Vamoosa aquifer 116
OMB guidelines 124
OME program 9
Ophiolite 74, 115
Oregon:
Estuarine sedimentation 148
Geothermal assessment, Newberry volcano 39
Greenstone 76
Groundwater, Winston 124
Paleogeography 76
Peak runoff from storms 127
Uranium in mercury deposits 35
Volcanic rocks, geochemical anomalies 10
Water-quality diel fluctuations 216
Water-quality, storm runoff 209
Oregon-Washington:
Shallow structures, Outer Continental Shelf 141
Organic chemistry:
Uranium ores 29
Organohalides, volatile 220
Outer Continental Shelf:
Lease areas 25
Outer Contenental Shelf:
Lease sales, oil and gas 152
Outer Continental Shelf:
Oregon-Washington, shallow structures 141
Outer Continental Shelf 143, 287
Oxygen fugacity 106

P

Paleogeography 76
Paleomagnetic anomely 153
Paleontology:
Age of Kootenai Formation 201
Age of Sarten Formation and Colorado Formation, New Mexico 201
Age of Skonun Formation, Canada 202
Chitistone limestone, Alaska 201
Dinoflagellates 203
Early Escene age rocks, Colorado 201
Mesozaic and Esnozaic studies 200
Mollusks 203
Nannoplankton 203
Planktonic foraminifers 202
Pleistocene climates, California 202
Upper Oligecene rocks, North Carolina and Arizona 202
Paleozoic rocks 87
Paleozoic studies:
Biostratigraphy 205
Bryozoa 205
Cambrian-Ordovician boundary, North America 204
Coral biostratigraphy 205
Devonian-Mississippian boundary 206
Fusulinids 205
Land snails 204
Palladium 7
Peat 3
Pegmatites, soil & stream sediments 41
Pelecypods 204
Pennsylvania:
Highway construction effects on small area 140
Resistivity study Gettysburg Basin 34
Water-quality studies 101

Page

Pennsylvania-Maryland:
  Lithium in flint clays ---- 42
Pennsylvania-New Jersey:
  Uranium mineralization ---- 28
Periphyton growth ---- 215
Peristerite ---- 50
Permafrost ---- 81
Permafrost clay ---- 155
Permian rocks ---- 71, 80
Petrography ---- 50, 64
Petology: ---- 31, 33, 121
  Experimental ---- 107
  Geochemical correlations ---- 128
  Igneous, Q-mode factor analysis ---- 129
  Oxygen fugacity, Skaergaard intrusive ---- 107
  Reconnaissance, uranium studies ---- 33
  Stability phegopite ---- 102
Petroleum ---- 24, 81, 97, 138
Petrophyscis:
  Laboratory establishment ---- 155
  Nonlinear complex resistivity ---- 154
  Permafrost clay, complex resistivity nonlinear ---- 155
  Petroleum exploration, deep-well seismic measurements ---- 97
  Spectral studies ---- 155
Philippine Islands, nationwide land tenure improvement program ---- 307
Phlogopite ---- 102
Phosphate ---- 42, 150
Phosphorite ---- 43
Photogrammetry ---- 316
Photoimage mapping ---- 318
Phytoplankton ---- 140
Planktonic foraminifers ---- 202
Plant ecology:
  Botany of Florida Everglades freshwater peat ---- 207
  Growth rings date alluvial deposition ---- 207
  Nutrient dynamics ---- 207
Plate tectonic model ---- 89
Pleistocene sand ---- 2
Plutonic rocks ---- 76
Plutonic rocks and magmatic processes:
  Evolution, tin-granite complex ---- 119
  Granite fusion, basalt ---- 119
Plutons ---- 45, 52, 85, 86, 88, 121, 135
Potamology:
  Mississippi River water quality ---- 214
  Salmon River aquatic biology ---- 214
Potassium ---- 33, 150
Powerplant ---- 131
Precambrian rocks ---- 87
Puerto Rico:
  Artesian water-pressure drop in limestone aquifer ---- 107
  Daguao formation source ---- 91
  Late Cretaceous and early Tertiary unconformity ---- 91
  Molybdenum distribution ---- 8
  Offshore sand resources ---- 140
  Sewage efficient, irrigation, and recharge ---- 107
Pyrite oxidation ---- 32
Publications, how to obtain:
  By mail ---- 333
  Over the counter ---- 333
Publications issued ---- 332
Publications program, USGS:
  Books and maps ---- 331
  Earthquake publications ---- 332
  Journal of Research ---- 332
  Open-file reports ---- 332
  Records, surface-water, quality-of-water, and ground-water-level ---- 331
  State hydrologic unit maps ---- 331
  State list, geology and hydrology ---- 331
  State water-resource investigations

Publications program, USGS—Continued
  folder ---- 332
Q-mode factor analysis ---- 12, 129
Quartzite outcrops ---- 62

R

Radioactive material ---- 13
Radioactivity:
  Burial ground, Idaho ---- 245
  Gamma spectrometry ---- 245
  Grout injection disposal ---- 246
  Hydrogeologic investigation, Maxey Flats ---- 244
  Hydrologic aspects of nuclear-waste storage ---- 246
  Natural, thermal waters ---- 208
  Nevada Test Site, potential repositories ---- 244
  Pierre Shale, waste repositories ---- 244
  Pierre Shale, potential waste-disposal sites ---- 247
  Pond waste supage simulated ---- 246
  Potential waste isolation pilot plant ---- 243
  Radioactive-waste burial evaluation ---- 245
  Waste landfill ---- 245
  Waste relation to environment ---- 243
Radiometric studies:
  Age of *Monograptus cyphus* zone ---- 89
  Subdivision of Ordovician and Silurian time seale ---- 89
  Uranium in Alaska ---- 33
Radiometry. *See* Radiometric studies.
Radium ---- 13
Rainfall intensities ---- 127
Rare earths ---- 28
Remote sensing:
  Airborne instruments data:
    Luminescence studies, Fraunhafer line discriminator ---- 274
  Thermographic mosaic, Yellowstone National Park ---- 274
  Cartographic studies applications to:
    Landsat investigations ---- 281
    Landsat mapping and charting of shallow seas ---- 281
    Hartford 1:250,000-scale image map ---- 281
    Nighttime images ---- 282
    Space Oblique Mercator projection ---- 283
    Operational Landsat parameters ---- 281
    Satellite image maps ---- 280
  Computer-enhanced Landsat data:
    Forest defoliation mapping and damage assessment ---- 269
    Geologic appreciations ---- 269
    Strip-mine monitoring ---- 269
  EROS program ---- 268
  Geochemical and geophysical, lunar investigations ---- 263
  Geologic studies, applications to:
    Enhanced images for lineament mapping ---- 277
    Heat discharge ---- 275
    Hydrothermally altered rock detection ---- 277
    Landscape patterns and structure, Maine ---- 276
    Lineaments expression, Mississippi ---- 276
    Mineral exploration research, Iran ---- 277
    Passive and active microwave techniques, geophysics ---- 277
    Porphyry copper prospect located, Landsat-/data ---- 278
    Thermal-infrared images interpretation ---- 278
    Uranium exploration ---- 278
  Hydrologic studies, application to:
    Calculating water volume,

Remote sensing—Continued
  Hydrologic studies—Continued
    Florida Everglades ---- 179
    Ground-water information ---- 279
    National wetland-classification system ---- 280
    Reservoir regulation, satellite-data relay ---- 279
    Vegetative-cover mapping, Great Dismal Swamp ---- 280
    Vegetation mapping ---- 279
    Water quality ---- 279
    Wetland classification, Tennessee ---- 280
  Image processing:
    High-resolution film recording system ---- 268
    Landsat images, digital enhancement ---- 268
  International cooperation in applications ---- 295
  Landsat:
    Deglaciation, late Wisconsinan ---- 270
    Geologic investigation, Black Hills ---- 270
    Targeting ground-water exploration ---- 269
  Landsat data and aerial photography:
    Geological and geophysical remote sensing, Iceland ---- 272
    Grand Valley project inventory, Natural resource and land use ---- 272
    Landsat image analysis ---- 272
    Pacific Northwest Demonstration Project ---- 270
    Red River flood analysis ---- 271
    Strip-mining impact, range resources and wildlife habitat ---- 272
    South Dakota cooperative land use demonstration project ---- 271
  Landsat data-collection platforms:
    Crop canopy multispectral radiance measurements ---- 273
    Meteorological parameters monitored ---- 274
  Landsat data digital analysis:
    Integrated terrain mapping ---- 273
    Kelp and eelgrass mapping and inventorying ---- 273
    Mineral resources of Andes Mountains ---- 273
  Weather satellites data:
    Cloud growth ---- 274
Resource and Land Investigations Program (RALI) ---- 286
Resource assessment:
  Regional minerals ---- 15
  Techniques, geochemical and geophysical ---- 9
Resource information bank, computerized ---- 14
Resource model studies:
  Discovery rate ---- 15
  Resource appraisal ---- 15
  Weighted characteristic analyses ---- 15
Rift, Rio Grande, New Mexico ---- 65
Risk analyses, oil spill ---- 25
R-mode factor analysis, Stream sediment and water samples ---- 13
Rock magnetism ---- 153
Rocks, Permian and Triassic ---- 80
Rock temperatures, Ordovician ---- 68
Rocky Mountains, landslides ---- 236

S

Saline waters ---- 208
Saline-water interface ---- 102
Saltwater injection ---- 116
Saltwater intrusion ---- 104
Sandstones ---- 80
Sandstone, uranium-bearing ---- 30
Sapphire ---- 66
Saudi Arabia:
  Alternative water supply sources, Ar Riyad ---- 309
  Geochronology ---- 308
  Geologic mapping ---- 307
  Laboratory analysis ---- 308

Page
Saudi Arabia—Continued
Mineral deposits 308
Mining geophysics 309
Paleontologic collection 307
Production wells 309
Water-resources advisory services 309
Scandium-lithium protenslatite 108
Schists 46
Sea floor, methane hydrate 146
Sea-in studies:
AIDJEX 217
Aircraft and spacecraft observation 217
Seawater 123
Sediment transport 141
Sedimentary rocks 140
Sedimentary structures:
Point-bar sequences, ephemeral streams 144
Stratigraphy model, shallow water deposits 144
Sedimentation 52, 148, 140, 155
Sediment-discharge modeling:
Arid regions 143
Highway-construction sites 142
Modified Einstein procedure 142
Wisconsin streams 143
Sediment-measuring techniques:
Bedload samples 142
Suspended solids 142
Turbidity recording 142
Sedimentology:
Coal 18
High sediment yields impact 139
Organic carbon on bottom materials 141
Sediment diagenesis 123
Sedimentary diagenesis, fluid inclusion evidence 124
Sedimentary record, California 147
Sediment chemistry and trace contaminants 141
Sediment study, Amazon River 140
Streambed sediment lead adsorption 127
Transport and deposition 140
Transport, steam power 141
Seismic data 134
Seismic refraction 52
Seismicity 138, 143
Seismic studies. *See also* Earthquake *studies as well as under individual States.*
Shale 5, 59, 124
Silica 103, 118, 148
Silicoflagellates 146
Sills 113
Silver 4, 11
Slumps 143
Sodium 150
Soil gases 12
Soil moisture 100
South America, iron-ore assessment 2
South Atlantic Continental Shelf, shallow structure 138
South Carolina:
Fault, Charleston 53
Geochemical anomalies 11
Limestone aquifer 108
Seismic refraction, Charleston 52
South Dakota:
Aquifer, buried river channel 116
Aquifers, Clark County 117
Grand Aquifer 117
Radioactive Precambrian conglomerate 30
Southeastern United States, late tectonic uplift 56
Spain:
Marine geology 310
Porosity in reefs 200
Spectrometry:
Infrared spectral behavior, particulate solids 155
Spectral signatures of minerals 155
Spectroscopy 218
Sphalerite, epigenetic 2
Spilite 90

Page
Stamukhi zone 144
Statistical analyses:
Computer simulation, compositional data 128
Steam power 141
Storm runoff 209
Stratigraphy 23, 47, 56, 57, 59, 61, 63, 65, 68, 69, 70, 75, 77, 85, 91, 117, 135, 136, 139, 143, 262
Streamflow 101, 118, 120
Stream water. *See* Limenology.
Structure studies 68, 70
Subsidence:
Faulting, ground-water extration 260
Ground-water discharge, New York 258
Hydrogeologic changes, California 258
Land subsidence, artesian-head recovery, California 259
Land subsidence, Texas 258
Model application 259
Open-pit and underground mining effects 257
Sulfide 27, 33, 90
Sulfur 19, 26, 33, 104
Sulfur isotopes, history of roll deposits 33
Surface water. *See* Water, surface, Limnology, Potamology, *as well as under individual States.*

T

Tectonic uplift 56
Tectonic zone 70
Tectonics 65, 66, 77
Temperature surveys 39
Tennessee:
Glauconitic sandstone 5
Remote sensing, wetland classification 280
Tennessee-Kentucky, Stratigraphic marker in shale 59
Test hole, Clubhouse Crossroads Core Hole no. 1 53
Texas:
Availability of ground water 117
Environmental studies, Outer Continental Shelf 139
Grond water, westernmost basins 117
Hydrology for coastal plain 117
Land subsidence 258
Nannoplankton 203
Pore structure, Edwards Limestone 117
Stratigraphy for coast plain 117
Suspended sediments, Corpus Christi Bay 140
Thermal history, miogeosyncline 68
Thermoelectric powerplant cooling 131
Thermal waters 808
Thermodynamics: *See* Geochemistry.
Thorium 28, 29, 31, 33
Thrust belt 66
Thurst faults 49, 73
Thrust plate 69
Thrusting 69
Till 84
Titanium 2, 14
Topographic surveys and mapping:
Analytical aerotriangulation 317
Camera calibration 316
Coastal mapping 323
Control 315
Digital applications 325
Drafting media 324
Equipment 316
EROS technical memorandums 327
Film mosaicking 320
Geodetic control transfer 326
Geographic Names Information System 327
Hotline Oblique Mercator projection 325
HP-65 program library 326
Inertial positioning system 314
Intermediate-scale mapping 322
Landsat imagery, 1:250,000-scale mapping 324
Large-scale mapping 322

Page
Topographic surveys and mapping—Continued
Map indexes 324
Map microfilming 326
Mapping standards 314
Metal detector evaluation 314
Metric mapping 322
Nisqually Glacier special map 318
Orthophoto and satellite products 318
Photogrammetric techniques 317, 320
Pocket maps 324
Quad-centered photographs 318
Quality control 321
Relative accuracy testing 318
Slope mapping 323
Special mapping projects 323
Viking II project 318
Topography:
Complex shelf in Alaska 144
Trace element analysis 219
Trace elements 18, 31
Transpiration and evaporation 212
Triassic rocks 80
Trondhjemite pluton 85
Tuffaceous rocks 125
Tungsten 14
Turbidity 139
Turkey, energy and mineral data bank 310

U

Ulexite 109
Uranium 13, 27, 28, 31, 35, 94, 118, 131
Uranium exploration:
Electromagnetic methods 35
Mobile helium detector 34
Well-logging system 34
Uranium studies:
Chemistry of organs, uranium-associated materials 29
Colorado, Piceance Basin 32
Conifer needles 29
Depositional environments, eastern Utah 34
Genesis, veins in Schwartzwalder Mine 31
Geochemical exploration in granitic terranes 33
Granite rocks 30
Guide to mineralization 28
Ore formation, pyrite oxidation 32
Rocks favorable for 32
Roll-type ore 29
Sedimentary environments, Utah 32
Snowy Range Wilderness study area 30
Trace elements, Colorado Plateau 31
Triassic and Jurassic lacustrine basin 27
Triassic rocks, Utah 33
Uranium-copper:
Enrichment zones in breccia papers 32
Uranium-series dating 238
USSR, surging glaciers inventory, Panirs 191
Utah:
Caldera, Tushar Mountains 67
Crude oil link to oil-shale rocks 22
Depositional environments 34
Devonian-Mississippian boundary 206
Fusulinids 205
Geochemical anomalics 10
Great Basin, metalliferous shales 5
Ground-water model 118
Intrusive center, Keg Mountains 71
Keg Mountains, instrusive center 9
Landslide, Manti Canyon 234
Mississippian oil exploration 21
Petroleum source beds 21
Radioactive storage, Paradox Basin 244
Stratigraphy and structure of House Range 69
Streamflow, coal-mining impact 118
Trace elements, Phosphoria Formation 21
Uranium, sedimentary environments 32
Uranium, Triassic rocks 33

Page

Utah—Continued
Water quality, Dirty Devil River basin ---118

V

Venezuela, seismic zoning and ground-motion studies ---310
Vermont, aquifers, sand-and-gravel deposits ---101
Virginia:
Antiformal folds ---55
Faults and folds ---55, 56
Freshwater-saline water interface ---102
Greenstone conglomerate ---56
Lithostratigraphy, Oak Grove Core ---57
Metamorphic rocks ---54
Precambrian inlier ---56
Upper Oligocence rocks in Coastal Plain ---202
Vegetative-cover mapping, Great Dismal Swamp 280
Volcanic hazards ---84, 239
Volcanic rocks ---80, 118, 132, 135, 141
Volcanic ash beds ---64
Volcanic rocks and processes:
Columbia Plateau studies ---113
Hawaiian volcano studies ---111
Volcanic sediment ---122
Volcanism ---70, 90, 113, 117
Volcanoes ---111, 112

W

Washington:
Faults, Olympic-Wallapa Lineament ---78
Fumarolic activity ---119
Gamma-ray measurements ---98
Glacial sequence, Wenatchee and Yakima Valleys ---77
Hydrocarbons in sediments, Willapa Bay ---142
Hydrology, Pullman-Moscow basin ---124
Invasive sills ---113
Streamflow-data network design ---124
Swauk stratigraphy and age ---77
Tectonic framework, Olympic Peninsula ---77
Tidal point bar sequences, Willapa Bay ---142
Volcanic activity effects ---216
Washington-Oregon:
Shallow structures, Outer Continental Shelf ---141
Water, analysis ---220
Water, chemical, physical, and biological properties ---93, 208
Water chemistry:
Geologic controls ---125
Water, dissolved solutes, remote sensing ---22
Water, ground:
Aquifer model studies ---192
Assessment, Shawsheen River basin, Massachusetts ---98
Availability in Texas ---117
Borehole geophysics ---196
Budget ---211
Canal leakage ---114
Cape Code exploration, Massachusetts ---98
Chloride concentrations, Massachusetts ---255
Chloride and nitrate ion concentrations, New York glacial aquifer ---255
Cycle water storage modeling ---195
Decomposition, organic compounds ---126
Development plan, Senegal, Mali, and Mauritania ---310
Digital model evaluation ---97
Direct solution algorithm, two-dimensional ground-water-flow simulator ---192
Disposal and storage studies ---194
Effects of copper and nickel mining ---100
Faulting caused by extraction ---260

Page

Water, ground—Continued
Flow, Arkansas ---198
Geochemical sampling ---125
Injection-recovery tests ---195
Landsat targeting exploration ---269
Liquid-waste disposal ---196
Mississippi region ---198
Movement and quality ---115
Movement at radioactive-waste disposal, Illinois ---246
Nitrate contamination abatement ---254
Oklahoma, Vamoosa aquifer ---116
Organics solutes modeling ---253
Paving effects on aquifer recharge ---194
Pollution potential, landfill site ---127
Quality, Cape Cod, Massachusetts ---99
Recharge by farming, practice ---114
Recharge studies ---194
Sludge effects on quality ---254
Subsidence related to discharge, New York ---258
Surface-water relationship ---210
Unconfined aquifer ---100
USGS water-supply paper ---95
Waste-water irrigation effects ---196
Withdrawal for industrial use ---129
Yemen Arab Republic survey ---310
Water, organic materials distribution ---209
Water, organic solutes separation ---221
Water, quality:
Analysis, well water ---99
Assessment, Connecticut Farm River basin ---96
Chemical qaulity of storm runoff ---110
Diel fluctuations ---216
Ground water, California ---121
Landfill leachate migration ---254
Liquid industrial waste underground disposal ---251
Mining effects ---252
Mississippi River investigations ---214
Nantucket Island, Massachusetts ---99
National programs ---132
National Stream Quality Accounting Network 132
New Mexico ---115
Organic solutes separation ---253
Parameter relationship, storm runoff ---209
Pollutant effects ---251
Red clay sediment, Minnesota ---100
Red River, Louisiana ---255
Saltwater injection ---116
Solute-transport modeling ---132
Surface water data storage and retreival ---127
Trans-Alaska pipeline effects ---253
Urban ---254
Variation from land use, climate, physiography, Susquehanna River basin ---255
Yampa River basin study ---132
Water-resource development:
Preservation of reservoir sites ---151
Water power classification ---151
Water-resource programs ---124, 132
Water resources:
Central region ---108
Investigations ---93
Nantucket Island ---99
Northeastern region ---95
Regional studies. *See individual states.*
Southeastern region ---102
Western region ---119
Water, surface:
Computer applications ---199
Effects of copper and nickel mining ---100
Flow and channel processes ---198
Flood-frequency analyses ---200
Ground-water relationship ---210
Lake-level fluctuation ---211
Low flows ---200
Macronutrient concentrations ---213

Page

Water, surface—Continued
Open-channel hydraulics ---199
Quality data evaluation ---209
Semiarid regions, flood characeristics ---199
USGS water-supply papers ---94
See also under individual States.
Water, treatment of acid mine ---20
Water use:
Coal-mining consumption ---131
Estimate of withdrawals ---127
Estimate, U.S. 1975- ---127
Irrigation consumption ---130
Irrigation, Missouri ---131
Power production consumption ---131
Public-supply withdrawals ---128
Thermoelectric powerplant cooling ---131
Water-data indexing ---126
Water-data search assistance ---126
Water-data sources ---126
Water-data storage system ---125
Watersheds ---107, 128, 207
Weathering profile ---53,54
Western United States:
Subsidence, Cordilleran-miogeocline ---68
Thermal history, Cordilleran miogeocline ---68
Wetlands:
National classification system ---280
Tennessee classification and mapping ---280
Wilderness Act, investigations ---3
Wisconsin:
Copper exploration ---9
Glauconitic sandstones ---5
Ground-water budget ---211
Ground-water quality ---102
Sedimentation in Coon Creek Valley ---139
Sediment-discharge moedling ---143
Water-level stabilization, Chippewa Flowing ---102
Wetland hydrology ---211
Aquifer digital model ---211
Chemical-quality and temperature modeling ---209
Coal strip-mine area pondo ---210
Geochronometry, kimberlite diatreme dating ---131
Geologic map ---92
Guide to uranium mineralization ---28
Hydrology, Arikaree Formation ---118
Hydrothermal alteration studies ---40
Medicine Bow Mountains, uranium potential ---30
Secondary silica dating ---118
Sediment yield, coal strip-mine area ---140
Stratigraphy of lower Upper Cretaceous rock ---22
Stratigraphic traps and source rocks ---23
Test drilling, Madison aquifer ---118
Uranium-bearing sandstones, fluvial dispersal patterns ---29
Uranium ore ages ---27
Volcanic ash localities ---64

X

X-ray analysis. *See* Methods and techniques.

Y

Yemen Arab Republic:
Ground-water survey ---310
Wadis characteristics ---311
Ytterbium-doped zircon ---108
Yugoslavia:
Special foreign Currency Program projects ---311

Z

Zinc ---2, 123
Zircon ---2, 63, 108

INVESTIGATOR INDEX

Page

A

Adam, D. P 187
Adams, D. B 284
Adams, J. W 7
Addicott, W. O 200, 202
Albert, C. D 252
Alexander, C. C 164
Alexander, R. H 290
Algermissen, S. T 232
Alldredge, L. R 153
Allen, R. V 227
Allison, S. V 305
Alminas, H. V 10
Altschuler, Z. S 19, 207
Anders, D. E 22
Anderson, B. M 256
Anderson, D. G 304
Anderson, G. S 120
Anderson, H. R 309
Anderson, J. R 287, 288
Anderson, R. C 23
Anderson, W. L 157
Angelo, C. G 252
Anna, L. O 115
Antweiler, J. C 12
Apgar, M 176
Applegate, L. H 207
Armbruster, J. T 199
Armbrustmacher, T. J 27, 31
Armstrong, A. K 200, 201, 206
Armstrong, C. A 65, 115
Armstrong, R. L 65
Ashley, R. P 7, 277
Ashwal, L. D 172
Asting, N. J 185
Averett, R. C 214, 215

B

Bachman, G. O 243
Back, W 176, 306
Bacon, C. R 170
Baedecker, M. J 176
Baedecker, P. A 219
Bailey, E. H 73, 301
Bailey, K. A 143
Bailey, R. A 37, 169, 301
Baird, A. K 261
Baker, C. P 207
Baker, E. T., Jr 117
Balch, A. H 157, 244
Ballance, W. C 241, 242
Baltz, E. H 62, 229
Barker, F 170
Barker, J 79
Barker, R. A 124
Barker, R. M 45
Barnes, I 176, 307
Barnes, P. W 144
Barnes, R. B 176
Barraclough, J. T 245
Barton, P. B., Jr 5
Bateman, P. C 301

Page

Bauer, D. P 132
Bayer, K. C 136
Baysinger, J. P 23, 24, 136
Beard, M. M 252
Bearden, H. W 105
Beeson, M. H 40
Beetem, W. A 132
Behrendt, J. C 134
Beikman, H. M 92
Bell, H 11
Bence, A. E 50
Bennetti, J. B., Jr 234
Benson, D. A 217
Berg, H. C 78, 85
Berryhill, H. L., Jr 139
Bethke, P. M 5
Beverage, J. P 217
Bigelow, H. B 99
Billingsley, F. C 269
Bingham, R. H 248
Bird, K. J 20
Bischoff, J. L 145
Bisdorf, R. J 145, 158
Blake, M. C., Jr 73, 76
Blakely, R. J 159
Blodgett, H. W 308
Board, J. W 199
Bodenlos, A. J 19
Boettcher, A. J 113
Bohannon, R. G 42
Bohor, B. F 18
Bolke, E. L 213
Bolm, J. G 85
Bonham, S 243
Bonilla, M. G 230, 305
Boning, C. W 127
Bonis, S. B 230
Booker, S. E 208
Booth, J. S 139
Borcherdt, R. D 231
Borman, R. G 109
Bortleson, G. C 212, 216, 285
Botbol, J. M 15
Bothner, M. H 135, 136, 137
Bouma, A. H 142
Bowles, C. G 32
Bowser, C. J 173
Boyce, J. M 262
Boyd, E. L 111
Boyles, J. M 240
Brabb, E. E 74, 202
Brabets, T. P 185
Bradford, W. L 176, 207
Bradley, J. A 157
Breger, I. A 175, 294
Brett, R 266
Brew, D. A 79, 87, 90
Brice, J 121
Britton, L. J 109, 215
Brogden, R. E 111
Brooks, R. A 31
Broom, M. E 198
Brosgé, W. P 79, 80, 81
Brown, C. S 190

Page

Brown, D. W 176
Brunner, R. L 24
Bryant, C. T 198
Bucknam, R. C 229, 230
Bukry, J. D 146
Buller, W 255
Bunker, C. M 218
Burford, R. O 224
Burkham, D. E 186, 250
Burns, A. W 109
Burt, R. J 305
Busby, M. W 248
Bush, C. A 197
Bush, P. W 195, 279, 280
Butler, H. M 223
Butman, B 135, 136
Bybell, L. M 53
Byerlee, J. D 224
Byerly, G. R 167

C

Cacchione, D. A 141, 144
Cadigan, R. A 13, 294
Cady, J. W 157
Cahill, J. M 245
Cain, D. L 110, 111
Cain, J. C 154
Calk, L. C 119
Calkins, J. A 14, 171
Callender, E 176
Cameron, C. C 3
Campbell, D. L 34, 156
Campbell, E. Y 219
Campbell, J. A 34
Campbell, W. J 217
Campbell, W. L 12
Cannon, W. F 43
Cargill, S. M 16
Carey, M. A 1
Carlson, C 312
Carlson, G. H 250
Carlson, M. A 222
Carlson, R. R 8, 235
Carneggie, D. M 272
Carothers, W. W 176
Carr, M. H 262
Carr, W. J 70, 71
Carrara, P. E 188
Carroll, R. D 243
Carter, C 81, 89
Carter, L. D 84
Carter, R. D 20
Carter, R. F 106
Carter, V. P 279, 320
Carter, W. D 273, 302
Case, III, H. L 113, 301
Case, J. E 158
Castell, R. W 187
Castle, R. O 230
Cathcart, J. B 43
Cathrall, J. B 10, 12
Causey, L. V 103
Chaffee, M. A 10

	Page
Chang, T. C	217
Chao, E. C. T	263, 264
Chao, T. T	11, 13, 14
Chapman, R. M	81, 82
Chemerys, J. C	208
Chen, C	199
Chidester, A. H	302
Childers, J. M	120, 199
Childs, J. R	143
Chleborad, A. F	233
Christ, C. L	165
Christensen, C. M	116, 117
Christian, R. P	261
Christiansen, R. L	159
Churkin, Jr., M	81, 89
Claassen, H. C	175
Clague, D. A	167
Clark, A. L	302
Clark, B. C	261
Clark, J. C	74, 164, 165
Clark, J. R	109
Clark, M. M	228
Clark, S	46
Clarke, F. E	302
Claypool, G. E	22, 136
Clayton, J. L	22
Clifton, H. E	142
Coats, R. R	69
Cobb, J. C	2
Cobban, W. A	22, 201
Cofer, H. E	1
Coker, A. E	279
Coleman, R. G	168, 302
Collins, C. A	124
Collins, D. B	13, 31
Colman, S. M	190
Colson, B. E	199
Colton, R. B	236
Commeau, J. A	147
Connor, C. W	18
Connor, J. J	256
Conomos, T. J	147, 148
Cooley, M. E	64, 243
Cooley, R. L	193
Coonrad, W. L	85
Cooper, A. K	143
Cooper, M	2
Cordell, L. E	65
Cordes, E. H	216, 279
Cordiviola, S	106
Counts, H. B	259
Covay, K. J	121
Covington, H. R	39
Cowardin, L. M	320
Cox, D. C	83
Cox, D. P	8
Cragwall, Jr., J. S	294, 304
Craig, L. C	32
Cran, C. E	222
Creager, J. S	84
Cress, L. D	229
Cressler, C. W	105, 106
Crist, M. A	118
Crosthwaite, E. G	39
Csejtey, B., Jr	82, 84
Culbertson, W. C	17
Cummings, T. R	99
Cunningham, M. J	221, 243
Curet, A. F	90, 91
Curtin, G. C	9, 84
Curtis, G. W	249
Cushing, E. M	118
Czamanske, G. K	90, 165, 168, 312

D

	Page
Daetz, D	286
Dalrymple, G. B	35, 167, 170
Dalziel, M. C	24
Daniel, C. C	106
Daniels, J. J	156
Darton, N. H	201
Davidson, D. F	299, 301
Davies, W. E	236
Davis, G. A	73
Davis, G. H	131, 259, 303
Davis, J. R	42
Davis, R. E	252
Davis, S. N	230
Dawdy, D. R	127, 212
Dean, J	187
Dean, W. E., Jr	145, 256
Dearborn, L. L	127
deForest, A. V	49
Deike, R. G	173
Delaney, D. F	98, 99
Delevaux, M. N	308
DeLong, L. L	209
Dempsey, W. J	243
Derr, J. S	222
Desborough, G. A	5, 174, 220
Detterman, R. L	80, 84
Devaul, R. W	211
Dewey, J. D	184
Dewey, J. W	300, 301
De Young, J. H., Jr	16
Dial, A. L., Jr	262
Díaz, J. R	107, 252
Dickey, D. D	70, 71
Dillon, W. P	135, 136, 138
Diment, W. H	37, 38
Dingman, R. J	302, 305
Dinwiddie, G. A	241, 242
Dion, N. P	212
Dixon, H. R	48, 50
D'Lugosz, J. J	116
Dobrovolny, E	234, 304
Dodge, F. C. W	160, 171
Dodge, H. W., Jr	28
Doe, B. R	177, 308, 332
Doell, R. R	153
Donaldson, D. E	120
Donnell, J. R	26, 294
Donnelly, J. M	36
Donovan, T. J	25, 275
Doty, G. C	241
Douglass, R. C	59, 205
Doyle, P. F	199
Drake, A. A., Jr	54
Drake, D. E	141, 144
Drasnow, M	175
Drew, L. J	15
Drewes, H. D	64
Druffel, L. A	195, 199, 217
Dudley, Jr., W. W	241, 242
Duffield, W. A	169
Duke, C	264
Duncan, R. A	146
Dunrud, C. R	257
Dupre, W. R	84, 143
Durbin, T. J	122
Dutro, J. T., Jr	80, 81, 205
Duval, J. S	158
Dyni, J. R	26
Dysart, J. E	103

E

	Page
Eakin, H. M	81
Earhart, R. L	3, 4
Ebaugh, W. F	233, 234
Ebens, R. J	240, 256
Eberlein, G. D	82, 89
Eccles, L. A	255
Eddy, R. M	132
Edelen, G. W., Jr	251
Edsall, D. W	138
Egbert, R. M	85
Eggers, D. E	196, 245
Ehrlich, G. G	210, 253
Ellen, S. D	236
Elliott, J. E	64
Elliott, R. L	33, 85, 86
Ellis, S. R	110
Ellis, W. L	243
Elsheimer, H. N	219
Emmett, L. F	113
Emmett, W. W	185, 217
Engberg, R. A	114
England, A. T	191
England, A. W	276, 277, 312
Erdman, J. A	240, 256
Erdmann, D. E	220
Ericksen, G. E	273
Ericson, D. W	100
Espinell, N	140
Espinosa, A. F	230, 232, 300, 305, 310
Espos, L. F	219
Evans, H. T., Jr	164
Evans, K. F	101
Eychaner, J. H	118, 250

F

	Page
Fabbi, B. P	219
Fabiano, E. B	154
Fahey, R. J	57
Faizi, S	243
Farrow, R. A	234
Fary, R. W	302
Faulkner, G. L	195, 251
Faust, C. R	181
Faust, G. T	168
Felmlee, J. K	13
Ferreira, R. F	215
Festa, J. F	148
Ficke, J. F	132
Ficklin, W. H	12
Field, M. E	144
Field, M. T	47
Finkelman, R. B	20
Firek, F	140
Fish, R. E	198
Fishel, D. K	101
Fischer, W. A	272
Fisher, D. W	176, 208
Fishman, M. J	220
Fitterman, D. V	157
Flanigan, V. J	35
Fleck, R. J	73, 309
Fleck, W. B	196
Fleming, R. W	234
Flores, R. M	18
Fogelman, R. P	121
Folger, D. W	135, 136
Foord, E. E	165
Foose, M. P	2
Force, E. R	2
Ford, A. B	87, 90, 311, 312, 313
Ford, D. E	213
Ford, T. R	110
Foster, H. L	82, 84
Foster, J. B	245, 251
Fouch, T. D	21
Fournier, R. O	37, 41, 161
Fox, J. E	80
Foxworthy, B. L	285
Frank, D. G	275
Freckleton, J. R	122
Freethey, G. W	120
Friedman, I	178, 189

	Page
Friedman, J. D	275
Frimpter, M. H	99
Frischknecht, F. C	156, 157
Friz, T. O	286
Frizzell, V. A	77
Froelich, A. J	53, 285
Frost, L. R., Jr	213, 255
Fuis, G. S	226
Fumal, T. E	231

G

Gabrysch, R. K	258
Galloway, J. P	84
Gammon, P. T	280
Gard, L. M., Jr	244
Gardner, J. V	145
Garrett, M. K	280
Garrison, L. E	139
Gates, J. S	117
Gay, F. B	98, 99
Gerrild, P. M	22
Giacomini, E. G	100
Gibbs, J. F	231
Gibson, H. A	307
Gilbert, G. K	184
Giles, T. F	110
Gillespie, J. B	196
Ging, T. G	136
Ginsburg, R. N	23
Girard, Jr., O. W	136
Glanzman, V. M	241, 242
Glenn, J. L	148
Glenn, M. W	17
Gloersen, P	217
Goddard, K. E	110, 111
Godsy, E. M	210
Goerlitz, D. F	202, 220, 253, 255
Goff, F. E	36
Gogel, A. J	196
Gohn, G. S	53
Goldberg, M. C	185, 209, 221, 279
Goldhaber, M. B	30, 33
Gonthier, J. B	124
Gonzalez, J. R	107
Goodwin, C. R	147
Goolsby, D. A	251
Gore, R. Z	49
Goter, E. R	146
Gott, G. B	10, 12
Gottfried, D	53
Granger, H. C	
Grant, R. S	198
Grason, D	96
Grauch, R. I	27
Greeman, T. K	97
Greenland, L. P	219
Griffitts, W. R	41
Grimes, D. J	14, 306
Grolier, M. J	311
Grommé, S. C	87
Grossling, B. F	294
Grove, D. B	195
Grow, J. A	134
Growitz, D. J	252
Grozier, R. U	248
Grybeck, D	87
Guetzkow, L. C	249, 250
Guild, P. P. W	4, 301
Gunard, K. T	250
Guswa, J. H	98
Gutentag, E. D	113
Gutschick, R. C	22, 206

H

	Page
Haas, J. L., Jr	159, 182
Hack, J. T	56
Hackman, R. L	236
Hadley, R. F	184, 186, 303
Haeni, F. P	96
Hail, W. J	26
Hait, M. H., Jr	63, 65, 216, 229
Hall, D. C	110, 111
Hall, R. B	1
Hall, W. E	178
Hallet, B	189
Halley, R. B	24, 140
Hamilton, L. J	116, 117
Hamilton, M. S	16
Hammarstrom, J. M	7, 50
Hammett, K. M	249
Hampton, M. A	142
Hanshaw, B. B	189, 306
Hanson, C. E	105
Hanson, R. L	212, 272
Happ, S. C	183, 184
Harden, J. W	238
Hardt, W. F	122, 255
Hardy, E. E	287, 288
Harenburg, W. A	199
Harlow, D. H	210
Harp, E. L	230
Harrill, J. R	124, 131
Harris, A. G	68
Harris, G., Jr	268
Harrison, J. E	61, 302
Harsh, J. F	255
Harshman, E. N	170
Hassemer, J. R	11
Hatch, D. R	17
Hatcher, R. D	57
Haushild, W. L	124
Hawkinson, R. O	132
Hayes, L. R	108
Hayes, P. T	18, 71
Hays, W. W	232
Hazlewood, R. M	231
Healy, J. H	225
Hearn, B. C., Jr	36
Hearne, G. A	193
Heath, R. C	200
Hedge, C. E	72
Hedlund, D. C	71
Heindl, L. A	303
Heisel, J. E	107
Hejl, H. R., Jr	250
Helgesen, J. O	99
Helley, E. J	228
Helm, D. C	259
Helm, R. E	184
Helz, R. L	162
Hemley, J. J	172
Hemphill, P. F	114
Hemphill, W. R	275
Hendrix, G. Y	286
Hepburn, J. C	48
Herd, D. G	55, 228
Heropoulos, C	218
Hess, A. E	182
Hess, G. R	141
Hewitt, C. H	71
Heyl, A. V	8
Hickey, J. J	104
Higer, A. L	279
Higgins, B. B	53
Hildenbrand, T. G	229
Hill, D. P	227
Hill, G	139
Hillier, D. E	111
Hillhouse, J. W	153
Hilpert, L. S	304
Himmelberg, G. R	90, 312
Hindall, S. M	102, 186
Hinkle, M. E	12
Hintze, L. F	69
Hirsch, R. M	131
Hite, R. J	244
Hjalmarson, H. W	250
Hoare, J. M	85
Hobbs, R. G	17
Hodge, S. M	191
Hoffman, R. J	215
Hoggan, R. D	65
Hoggatt, W. C	237
Holcomb, R. P	229
Holcomb, R. T	166
Holden, K. D	159
Hollocher, C	285
Holm, C. S	272
Holm, R. F	35
Holmes, C. W	139
Holzer, T. L	239, 260
Holzhausen, G. R	181
Hood, D. R	270
Hook, S. C	201
Hoose, S. M	233
Hoover, D. B	159
Hoover, D. L	244
Hopkins, D. M	81
Hopkins, H. T	102
Horak, W. F	116
Hosman, R. L	198, 246
Hotchkiss, W. R	114
Houston, R. S	30
Howell, D. G	57, 140
Hubbell, D. W	185
Hudson, J. H	24, 140, 188
Hudson, L	171
Hudson, T. L	86
Huebner, J. S	162, 163, 164
Huffman, C., Jr	218
Huffman, E. W. D., Jr	220, 253
Hull, J. E	254
Hunt, G. R	155
Hunter, R. E	143
Hunter, R. N	223
Husid, R	230, 232, 300, 305
Hutchinson, C. B	104, 122
Hutchison, E. C	111

I

Ierley, D. L	207
Imhoff, E. A	286
Irwin, W. P	72, 302, 307
Ito, J	164
Iwatsubo, R. T	176, 207, 214
Iyer, H. M	36

J

Jachens, R. C	225
Jackman, A. P	198
Jackson, D. B	37
Jackson, N. M., Jr	200
James, H. L	302
James, I. C., II	132
James, O. B	265
Jarrett, R. D	250
Jenne, E. A	185
Jenner, C. B	290
Jennings, M. E	200
Jobson, H. E	131
Jochim, C. L	80
Johnson, A. I	303
Johnson, B. R	87, 89
Johnson, F. A	147
Johnson, G. R	269, 276, 277
Johnson, J. G	205
Johnson, M. G	76
Johnson, R. B	234
Johnson, R. N	311

	Page
Johnston, M. J	224
Johnston, R. H	53, 285
Jones, B. F	173
Jones, C. L	243
Jones, D. L	72
Jordon, P. R	112

K

	Page
Kahan, A. M	274
Kam, W	254
Kane, M. F	122, 229
Kapple, G. W	122
Karklins, O. L	205
Karlstrom, K	30
Karlstrom, T. N. V	187, 287
Kaye, C. A	57, 203
Keefer, T. N	199
Keighin, C. W	26
Keil, K	261
Keith, J. R	256
Keith, T. E. C	40
Keith, W. J	68
Kehn, T. M	59
Kennedy, V. C	174, 216
Kepferle, R. C	59
Kernodle, D. R	215, 253
Keys, W. S	182, 196, 225, 245
Kharaka, Y. K	176
Kilpatrick, F. A	131
King, B. W	219
King, C. Y	181, 224
King, E. R	58
King, P. B	301
Kinney, D. M	301
Kirby, S. H	226
Kirkemo, H	304
Kirsch, C. F	321
Kistler, R. W	87, 172
Kitely, L. W	22
Kitrinas, D. J	307
Klasner, J. S	43
Klausing, R. L	116
Klein, F. W	38
Klein, H	254, 286
Klein, J. M	111
Klemic, H	2, 8
Klepper, M. R	66
Klitgord, K. D	134, 135
Klusman, R. W	256
Knebel, H. J	84, 136, 147
Knight, R. J	170
Knott, J. M	127
Knudson, C. F	300
Koch, R. D	85, 86
Kockelman, W. J	284
Koehler, J. H	122
Kohout, F. A	137
Kolessar, J	71
Konikow, L. F	195
Konnert, J. A	164
Kopf, R. W	205
Kork, J. O	177
Koteff, C	46
Kowalik, W. S	273
Krause, R. E	106, 197
Krimmel, R. M	189, 190, 191
Kroll, C. G	186
Krug, W. R	102
Krushensky, R. D	90, 91
Ku, D. N	106
Kume, J	117
Kuntz, M. A	237
Kvenvolden, K. A	142

L

	Page
Laenen, A.	127
LaFevers, J. R	286
Lahr, J. C	230
Lai, C	199
Lajoie, K. R	228, 238
Lambert, P. W	80
Land, L. F	104, 200
Landing, E	204
Landis, E. R	17, 18, 201
Lang, L. F	248
Langbein, W. B	199
Langer, C. J	300
Langford, R. H	304
Lanphere, M. A	35, 82, 89, 167
Lappala, E. G	114
Larsen, F. D	47
Larson, J. D	285
Larson, L. R	209
Larson, S. P	192, 193, 209
Leahy, P. P	97
Leap, D. I	197
Learned, R. E	8, 11
LeBlanc, D. R	98
Lee, F. N	199
Lee, F. T	233, 238
Lee, K. Y	56
Lee, M. W	157
Lee, R. W	175
Leeman, W. P	177
Leenheer, J. A	220, 253
Leinz, R. W	14
Leo, G. W	172, 257
Leon, G. B	182
Leonard, R. B	208
Lesser, J	306
Leve, G. W	103
Leventhal, J. S	29
Lewis, B. D	175
Lewis, J. E., Jr	290
Lewis, R. E	38
Liddicoat, J. C	153
Lidz, B. H	24, 140
Lindh, A. G	223
Lindholm, G. F	100
Lindskov, K. L	101, 198
Ling, C. H	217
Lins, H. F., Jr	290
Lipin, B. R	2, 162
Livingston, R. K	111, 112
Lockner, D. A	224
Loferski, P. J	8
Lofgren, B. E	239, 258, 260
Londquist, C. J	112
Loney, R. A	87, 90
Longwill, S. M	193
Love, J. D	92
Lowham, H. W	209
Lubeck, C. M	136
Lucas, J. R	269, 270
Lucchitta, B. K	263
Lucchitta, I	70
Luckey, R. R	113, 131
Luoma, S. N	185
Lupe, R. D	33
Lyford, F. P	114
Lyle, W. M	85
Lystrom, D. J	255
Lyttle, P. T	238

M

	Page
Mabey, D. R	65
Mack, F. K	97
MacKevett, E. M., Jr	201
Maclay, R. W	117
MacLeod, N. S	39
Madden, C. T	307
Madsen, E. L	232
Magoon, L. B., III	85
Main, R. J., Jr	154
Major, T. J	109
Malde, H. E	188
Maley, R. P	301
Mamet, B. L	206
Mandle, R. J	97
Manheim, F. T	137
Mankinen, E. A	153
Mann, W. B., IV	209
Manteuffel, T. A	193
Mantis, C. E	223
Mapel, W. J	17
Maqvi, M. I	308
Marchand, D. E	74, 188, 236, 238
Marcus, K	285
Marcus, P. A	287
Marinenko, J. W	218
Mariner, R. H	37
Marks, L. Y	3
Marlow, M. S	143
Marrs, R. J	241
Martien, R. F	255
Martin, R. G	138
Marvin, R. F	72
Masursky, H	262
Matthews, A	83
Mattick, R. E	136
Mattraw, H. C., Jr	254
Matuska, D	193
Matzko, J. J	308
Maughan, E. K	21, 58
Maxwell, C. H	8
May, F. E	203
May, R. J	179
Mayo, L. R	191
Mays, R. E	218
Mazzaferro, D. L	96
McCain, J. F	248
McCallum, M. E	178
McCammon, R. B	15
McCarthy, R. P	223
McClymonds, N. E	306
McConnell, J. B	105
McCulloch, D. S	147
McDonald, M. G	196
McFarlane, C	275
McGregor, E. E	233
McGuire, R. K	232
McKee, E. D	186
McKee, E. H	167
McKelvey, V. E	183, 301
McKenzie, D. J	195
McKenzie, S. W	209, 216
McLaughlin, R. J	73, 74
McLean, J. S	115
McPherson, B. F	286
McQuivey, R. S	199
Meade, R. H., Jr.	184
Meckel, J. C	120
Meier, M. F	189, 304
Melvin, R. L	96
Mercer, J. W	181
Merewether, E. A	22
Merriam, C. W	205, 248
Merriman, D. C	255
Meyer, F. W	105, 195
Meyer, R. F	294
M'Gonigle, J. W	91
Miesch, A. T	177
Millard, H. T., Jr	170, 218
Miller, C. D	305
Miller, C. H	233, 234
Miller, D. R	239
Miller, F. K	76
Miller, R. E	137, 302
Miller, T. P	33, 35
Miller, W. L	104
Miller, W. R	12, 30

	Page
Mills, L. R	104
Milton, D. J	146, 264, 306
Minard, J. P	56
Minkin, J. A	263
Minsch, J. H	222
Mitchell, C. M	157
Mixon, R. B	55
Moench, A. F	182
Moore, D. O	199
Moore, D. W	240
Moore, G. K	271, 279
Moore, H. J., II	261, 263
Moore, J. G	168
Moore, R. B	35
Moore, W. J	10, 68
Moran, M. S	197
Moran, R. E	38
Morehouse, J. M	85
Moreland, J. A	123
Morey, G. B	61
Morgan, B. A., III	72, 181
Morgan, C. O	122
Morill, R. A	247
Morris, E. C	261
Morris, H. T	205
Mortensen, C. E	224
Morton, D. M	76
Morton, J. L	83
Moss, M. E	124
Mrose, M. E	165
Mudge, M. R	3
Muffler, L. J. P	40, 180
Mull, C. G	20
Mull, D. S	106
Mullineaux, D. R	239, 305
Mundorff, J. C	118
Muniz, J	140
Murphy, W. R., Jr	249
Murray, C. R	127
Myers, W. B	5, 241

N

Nace, R. L	304
Naeser, C. W	63, 171, 178
Nakamura, N	180
Nash, J. T	29, 30
Nason, R. D	232
Nathenson, M	181, 183
Nauman, J. W	120, 215, 253
Nelson, C. A	271
Nelson, C. H	144
Nelson, G. L	119, 120
Nelson, W. H	82, 312
Neuerburg, G. J	12
Neuman, R. B	302
Newell, W. L	55
Newkirk, H. D	274
Nicholas, F. W	290
Nichols, F. H	148
Nichols, T. C	239
Nichols, W. D	194
Nichols, W. J	255
Niem, A. R	77
Nilsen, T	144
Nissenbaum, A	80
Niven, D. W	80
Noble, R. D	198
Nord, G. L	50, 166
Nordin, C. F., Jr	184
Normark, W. R	141
Norvitch, R. F	232
Novitzki, R. P	211
Nowlin, J. O	124, 131
Nutt, C. J	87, 312

O

Oaksford, E. T	194
Obermeier, S. F	53, 54, 257, 258
Obradovich, J. D	179
O'Connor, J. T	286
O'Donnell, T. H	104, 213
Offield, T. W	278
O'Hara, C. J	135
Ohlmacher, G. C	236
Olcott, P. G	100
Oldale, R. N	135
O'Leary, D. W	276
Olhoeft, G. R	155, 156
Olin, D. A	248
Olive, W. W	59
Oliver, H. W	156
Oliver, W. A., Jr	205
Olmsted, F. H	38, 39
Olsen, A. B	236
Olsen, H. W	234
Olson, A. C	16
Olson, E. P	234
Olson, J. C	62
O'Neill, J. M	62
Ong, K	115
Oriel, S. S	39
Osberg, P. H	46
Osterwald, F. W	234, 257
Outcalt, S. I	290

P

Packard, F. A	252
Page, N. J	8
Palacas, J. G	23
Palmer, I. F	85
Pampeyan, E. H	237
Pan, K. L	270
Papadopulos, S. S	310
Parker, R. L	302
Pascale, C. A	103, 195, 251
Patrick, L. D	120
Patterson, J. M	23
Patterson, S. H	1, 81
Patton, W. W., Jr	81, 82
Pavich, M. J	54, 257
Pavlides, L	55
Payne, G. A	101
Pearl, J. E	77
Pearson, F. J., Jr	208
Pease, M. H., Jr	51
Pease, R. W	290
Peck, D. L	172
Peddie, N. W	154
Peper, J. D	52, 57
Perkins, D. M	232
Person, W. J	223
Peselnick, L	182, 226
Pessagno, E. A., Jr	72, 74
Peterman, Z. E	61, 179
Peterson, D. H	148
Peterson, F	32
Pettijohn, R. A	97
Phelps, G. G	103
Phipps, R. L	207
Pickney, E. J	208
Pierce, K. L	64, 180, 190, 238
Piper, D. Z	145
Pitkin, J. A	158
Pitman, J. K	26, 80
Pitt, A. M	36
Plafker, G	230, 300
Playton, S. J	252
Plouff, D	159
Plummer, L. N	208, 306
Poag, C. W	136
Pohn, H. A	277
Pojeta, J., Jr	204
Poland, J. F	259
Pollard, L. D	105
Pollock, S. J	255
Pomerov, P. W	222
Pomeroy, J. S	47
Poole, F. G	5, 8, 21, 70, 71
R. Z. Poore	202
Popp, R. K	161
Porterfield, G	184, 186
Posson, D. R	193
Post, A	191
Potter, D. B	49
Potter, P. E	59
Potter, R. W., II	83, 182
Prescott, W. H	225
Price, L. C	23
Price, W. E., Jr	193
Prill, R. C	194
Prostka, H. J	39
Provo, L. J	59
Prowell, D. C	55
Prudic, D. E	245
Prugh, B. J., Jr	254
Pyle, T	306

R

Rachlin, J	243
Radbruch-Hall, D. H	234
Ram, N. M	210
Randall, A. D	245
Randich, P. G	116
Rantz, S. E	304
Rapp, J. B	142
Rasmussen, L. A	217
Ratcliffe, N. M	49
Rathbun, R. E	198
Ray, H. A	247
Raymond, W. H	6
Reasenberg, P. A	181
Reed, B. L	81
Reed, L. A	186
Reeves, E. B	127
Reimer, G. M	34
Reimnitz, E	144
Reinemund, J. A	302
Reinhardt, J	55, 57
Reiser, H. N	80, 81
Reynolds, M. W	66
Reynolds, R. L	30, 33
Rhodehamel, E. C	136
Rice, C. L	58, 59
Rice, D. D	3, 201
Richards, P. W	301
Richmond, G. M	92
Richter, D. H	35, 83
Riggs, H. C	199, 200, 311
Ringen, B. H	184
Ringrose, C. D	256
Ritter, J. R	185
Roach, J. T	288
Robb, J. M	135
Robbins, E. I	136
Robbins, S. L	159
Roberson, C. E	176
Roberts, A. A	24
Roberts, A. E	42
Roberts, R. J	308
Robertson, J. B	246, 253
Robertson, S. R	287
Robinove, C. J	273
Robinson, G. R., Jr	47
Robinson, P	47
Robison, J. H	124
Robson, S. G	208
Rodis, H. G	104
Roedder, E. W	161, 174, 266
Roeske, R. H	248
Rogers, A. M	231, 232, 244
Rogers, J. E	212
Rogers, S. M	102

Page

Rohde, W. G 269, 271
Rollinson, C. L 219
Rosasco, G. J 161
Rose, H. J., Jr 261
Rosenblum, S 12
Rosholt, J. N., Jr 179, 238
Ross, D. C 74
Rowan, L. C 277, 302
Rowe, J. J 161, 219
Ruane, P. J 236, 243
Rubin, D. M 147
Rumen, L. L 23
Rutledge, A. T 211
Ryder, P. D 104
Ryder, R. T 23, 157
Rye, R. O 58, 33, 183
Ryer, T. A 17
Rymer, M. J 187, 202
Rynerson, B. F 165
Rynerson, E. B 165
Rynerson, F. J 166
Rytuba, J. J 35

S

Saboe, C. W 250
Saindon, L. G 132
Sallenger, A. H 137, 143
Sanchez, D. J 18
Sandberg, C. A 22, 206
Sando, W. J 22, 63
Sanzolone, R. F 11, 13
Sardo, W. J 206
Sargent, K. A 240
Sarnecki, J. C 19
Sato, M 163, 266
Saulnier, G. J., Jr 112, 208
Savage, J. C 225
Savage, N 89
Savage, W. Z 233, 235, 238
Schaber, G. G 262
Schaefer, D. H 120
Schlee, J. S 134, 136
Schlesinger, B 286
Schmidt, D. L 307
Schmidt, R. G 229, 278
Schmidt, P. W 248
Schneider, G. B 17, 18
Schneider, J. J 104
Schneider, P. A., Jr 111
Schneider, V. R 199, 216, 217
Schoen, R 137
Scholl, D. W 143
Scholle, P. A 136
Schornick, J. C 101, 210
Schultz, D. M 136, 137
Schumann, H. H 279
Schurr, G. R 244
Schuster, R. L 234
Scott, A. G 188
Scott, D. H 263
Scott, G. R 284
Scott, R. A 136
Scott, W. B 104
Scott, W. E 136, 229, 247
Scully, D. R 120
Sears, M 99
Sebetich, M. J 216
Seeland, D. A 26, 29
Seeley, J. L 218
Segerstrom, K 235
Senftle, F. E 157, 164
Shaffer, G. L 16
Sharp, R. V 228, 230, 299
Sharps, J. A 241
Shaw, H. R 169
Shawe, D. R 8, 69
Shearman, J. O 200
Shedlock, R. J 97, 173

Page

Sheldon, R. P 294
Shely, R 220
Shepherd, R. G 186
Sheridan, D. M 6
Sherill, M. G 246
Shideler, G. L 139, 140
Shima, L 280
Shinn, E. A 24, 140
Shoemaker, E. M 55
Shown, L. M 184, 186
Shroba, R. R 248
Shurr, G. W 247
Sigafoos, R. S 207
Signor, D. C 217
Silberling, N. J 80
Silberman, M. L 67, 83
Simmon, J. H 161
Simmons, C. E 107
Simon, F. O 219
Simons, F. S 307
Simpson, H. E 234
Simpson, R. G 250
Simpson, S. L 276
Sims, J. D 75, 187
Sims, P. K 61, 179
Sinclair, W. C 104
Singer, D. A 84
Sisler, F. D 20
Skelton, J 211
Skinner, J. V 217
Skipp, B. A 63, 65
Slack, K. V 214
Slack, L. J 103
Slack, J. R 25, 96
Slagle, S. E 175
Sloan, C. E 120, 215, 253
Small, T. A 117
Smith, B. D 35
Smith, C. C 203
Smith, C. L 41
Smith, C. W 308
Smith, E. T 286, 287
Smith, G. I 189
Smith, J. C 10
Smith, J. G 85, 86
Smith, R. A 25
Smith, R. L 35, 96, 169
Smith, W. K 233
Smoot, G. F 216
Snavely, P. D., Jr 77, 141, 200, 202
Snider, J. L 113
Snyder, G. L 63
Snyder, R. P 244
Soderblom, L. A 262
Soderblom, L. H 263
Sohl, N. F 203
Soister, P. E 201
Sorey, M. L 37, 38
Spence, W. J 223
Spencer, C. W 22
Spieth, M. A 226
Spiker, E. G 176
Spirakis, C. S 28
Staatz, M. H 28
Stacey, J. S 180
Stanley, W. D 117
Steele, T. D 132, 209
Steinbrugge, K. V 300
Stern, T. W 72, 120, 135, 172, 181
Stevens, H. H., Jr 185
Stewart, D. B 47
Stewart, J. H 68
Stewart, R. M 182, 226
Stoertz, G. E 273
Stone, B. D 49, 52
Stone, J. R 46
Stoner, J. D 114
Stoufer, R 176
Stover, C. W 222

Page

Strahle, W. J 301
Stringfield, V. T 304
Stuart, W. D 224
Stuart-Alexander, D. E 236
Stuckless, J. S 218
Suhayda, J. N 139
Sun, R. J 197, 246
Susag, R. H 209
Sutton, R. L 287
Swain, L. A 122
Swanson, D. A 78, 167
Swanson, J. A 14
Swift, III, C. H 215
Sylvester, M. A 121
Szabo, B. J 147

T

Tabor, R. W 77, 237
Taggart, J. N 300
Takasaki, K. J 122
Tanghorn, W. V 189
Taranik, J. V 269, 270, 271
Tarr, A. C 231
Tatsumoto, M 87, 178, 180, 266
Taylor, D. J 136
Taylor, F 234
Taylor, G. C., Jr 304
Taylor, M. E 204
Taylor, T. A 196, 245
Terbeek, C. L 252
Terry, G. R 239
Terry, J. E., Jr 198
Thatcher, W. R 225
Thayer, T. P 2
Theodore, T. G 8, 68
Thomas, C. P 218
Thomas, D. M 200
Thomas, M. P 96
Thompson, J. M 36, 41
Thorman, C. H 64
Thorpe, A. N 164
Tibbals, C. H 194
Tibbits, G. J., Jr 310
Tilley, L. J 214
Tinsley, J. C 75
Todd, V. R 76, 237
Toimil, L. J 144
Toulmin, J., III 261
Tourtelot, E. B 42
Tourtelot, H. A 42, 256
Toy, T. J 242
Trabant, D. C 191
Tracey, J. I., Jr 146
Trautwein, C. M 269
Trescott, P. C 193, 196
Trimble, S. W 183
Tripp, R. B 9
Truesdell, A. H 37, 183
Truhlar, Jr., J. F 185
Tschudy, R. H 60, 201
Tucker, R 47
Turk, J. T 213
Turner, J. F., Jr 200, 249
Tweto, O. L 92
Tyus, H. M 286

U

Ueblacker, H 241
Ulrich, G. E 35
Unruh, D. M 178
Urban, T. C 37, 38

V

Valentine, P. C 136
Valenza, M 163
Van Alstine, R. E 6

	Page
Van Driel, J. N	53
Van Horn, R	237
Van Schaack, J. R	227
Vance, J. A	77
Varnes, D. J	234
Vedder, J. G	140
Venuti, P. E	8
Verbeek, E. R	239
Viets, J. G	14
Vikre, P	67
Vine, J. D	42, 273
Vorhis, R. C	105

W

Waddell, K. M	118
Wagner, G. H	264
Waitt, R. B., Jr	77, 237
Walcott, C. D	69
Walker, E. H	99
Wallace, C. A	66
Waller, R. M	197, 258
Walter, A. W	36
Wandle, S. W., Jr	249
Wang, F. H	294, 299, 303
Wangsness, D. J	210
Ward, D. E	18
Ward, F. N	29
Ward, J. R	102, 186
Warner, J. W	132
Warrick, R. E	233
Watkins, J. A	262
Watts, K. C	11
Watts, R. D	156
Watts, R. W	191
Watson, D. E	155
Watson, K	278
Watson, R. D	274
Weaver, C. S	36
Weaver, R. O	272, 273
Weeks, J. B	109
Weeks, R. A	15
Wehmiller, J. F	238
Weiblen, P. W	266
Weidie, A. E	306
Weigle, J. M	96
Weiner, E. R	185, 221, 279
Weis, P. L	5
Welder, G. E	115
Wells, F. C	214
Wenrich-Verbeek, K. J	13, 31
Wentz, D. A	132, 252
Wershaw, R. L	208
Wetlaufer, P. H	5, 6
Wetzel, K. L	186
Whelan, J. F	177
Whetten, J. T	237
White, A. F	175
White, D. E	37, 40, 41, 117
White, W. S	9
Whitebread, D. H	69
Whitehead, R. L	123
Whiteman, C. D., Jr	258
Whitfield, M. S., Jr	113
Whitmore, F. C., Jr	307
Widhelm, S. C	230
Wieczorek, G. F	230
Wier, K. E	55
Wiggins, L. B	163
Wilcox, D	120
Wilheit, T. T	217
Willey, R. E	102
Williams, G. P	199
Williams, J. F	98
Williams, R. S., Jr	272, 274
William, H. B	60
Wills, J. C	83
Wilson, K. V	106
Wilson, L. R	154
Wilson, R. T	285
Winkler, G. R	81
Winner, M. D., Jr	107
Winter, T. C	210
Winterhalder, E. C	237
Witkind, I. J	234
Witmer, R. E	288
Wolf, R. J	101
Wolfbauer, C. A	43
Wolfe, E. W	35
Wolfe, J. A	202
Wones, D. R	45, 46, 160
Wong, A. T	287
Wood, J. D	154, 311
Wood, M. D	225
Wood, S. H	232
Wright, D. S	238
Wright, N. A	1, 15
Wright, T. L	78, 162, 167
Wu, C. H	80
Wyant, T. S	25, 96
Wynn, J. C	10, 156

Y

Yerkes, R. F	232
Yochelson, E. L	204, 205
Yotsukura, N	198
Youd, T. L	233
Young, E. J	31
Young, H. L	211
Young, H. W	123
Young, J	264
Yount, J	285

Z

Zablocki, C. J	159
Zand, S. M	216
Zartman, R. E	45, 50, 179
Zehner, H. H	244
Zellweger, G. W	174
Zen, C. S	19, 207
Zen, E	7, 50, 66, 160
Zielinski, R. A	170, 171
Zietz, I	58, 68
Zoback, M. D	225
Zohdy, A. A. R	158
Zubovic, P	241
Zwelly, H. J	196

☆U.S. GOVERNMENT PRINTING OFFICE: 1978 O—261-221/21